Outer Continental Shelf Environmental Assessment Program

Final Reports of Principal Investigators

Volume 48 **November 1986**

U.S. DEPARTMENT OF COMMERCE
National Oceanic and Atmospheric Administration
National Ocean Service
Office of Oceanography and Marine Assessment
Ocean Assessments Division
Alaska Office

U.S. DEPARTMENT OF THE INTERIOR
Minerals Management Service
OCS Study, MMS 86-0065

"Outer Continental Shelf Environmental Assessment Program Final Reports of Principal Investigators" ("OCSEAP Final Reports") continues the series entitled "Environmental Assessment of the Alaskan Continental Shelf Final Reports of Principal Investigators."

It is suggested that sections of this publication be cited as follows:

Hampton, M. A. 1983. Geotechnical Framework Study of the Kodiak Shelf, Alaska. U.S. Dep. Commer., NOAA, OCSEAP Final Rep. 48(1986):1-94

Lee, H. J. and W. C. Schwab. 1983. Geotechnical Framework, Northeast Gulf of Alaska. U.S. Dep. Commer., NOAA, OCSEAP Final Rep. 48(1986):95-547

OCSEAP Final Reports are published by the U.S. Department of Commerce, National Oceanic and Atmospheric Administration, National Ocean Service, Office of Oceanography and Marine Assessment, Ocean Assessments Division, Alaska Office, Anchorage, and primarily funded by the Minerals Management Service, U.S. Department of the Interior, through interagency agreement.

Requests for receipt of OCSEAP Final Reports on a continuing basis should be addressed to:

NOAA-OMA-OAD
Alaska Office
701 C Street
P.O. Box 56
Anchorage, AK 99513

OUTER CONTINENTAL SHELF
ENVIRONMENTAL ASSESSMENT PROGRAM

FINAL REPORTS OF PRINCIPAL INVESTIGATORS

Volume 48

November 1986

U.S. DEPARTMENT OF COMMERCE
National Oceanic and Atmospheric Administration
National Ocean Service
Office of Oceanography and Marine Assessment
Alaska Office

U.S. DEPARTMENT OF THE INTERIOR
Minerals Management Service
Alaska OCS Region
OCS Study, MMS 86-0065

Anchorage, Alaska

The facts, conclusions, and issues appearing in these reports are based on research results of the Outer Continental Shelf Environmental Assessment Program (OCSEAP), which is managed by the National Oceanic and Atmospheric Administration, U.S. Department of Commerce, and funded (wholly or in part) by the Minerals Management Service, U.S. Department of the Interior, through an Interagency Agreement.

Mention of a commercial company or product does not constitute endorsement by the National Oceanic and Atmospheric Administration. Use for publicity or advertising purposes of information from this publication concerning proprietary products or the tests of such products is not authorized.

Content of these reports has not been altered from that submitted by the Principal Investigators. In some instances, minor grammatical, spelling, and punctuation errors have been corrected to improve readability; some figures, charts, and tables have been enhanced to improve clarity in reproduction.

Outer Continental Shelf Environmental Assessment Program

Final Reports of Principal Investigators

VOLUME 48 NOVEMBER 1986

CONTENTS

GEOTECHNICAL FRAMEWORK STUDY OF THE KODIAK SHELF, ALASKA

by

Monty A. Hampton

U.S. Department of the Interior
Geological Survey

Final Report
Outer Continental Shelf Environmental Assessment Program
Research Unit 589

1983

TABLE OF CONTENTS

LIST OF FIGURES

LIST OF TABLES

INTRODUCTION

Environmental geologic studies have been conducted on the Kodiak Shelf, Gulf of Alaska, to evaluate the potential impact and constraints that geology can impose on offshore industrial operations (Fig. 1; Hampton 1982a,b). As part of these studies, cores were taken from the diverse suite of compositionally distinct and areally restricted sedimentary deposits on the shelf and upper continental slope. Physical property measurements were made on samples from the cores, and geotechnical methods were employed in order to broadly characterize the behavior of the sedimentary deposits under conditions of static and dynamic loading. The data and conclusions are meant as a guide for detailed and site-specific studies that accompany resource regulation and development activities.

GEOLOGIC SETTING

The Kodiak Shelf consists of a series of flat banks, generally less than 100 m deep, separated by transversely trending troughs (Fig. 1). Most of the seafloor is flat to gently inclined; steep slopes are uncommon (Fig. 2).

The banks are largely covered by coarse gravelly debris, typically less than 100 m thick, although there are broad areas of bedrock outcrop at the seafloor (Fig. 3). Local thin deposits rich in shells or volcanic ash are also present. The troughs contain relatively fine-grained deposits, but sediment composition is different in each. Stevenson Trough contains terrigenous sand deposits that are molded into large sand waves, as well as deposits of terrigenous mud and volcanic ash. The floor of Chiniak Trough is covered with sediment composed predominantly of volcanic ash, with local outcrops of a terrigenous mud deposit that evidently underlies the surficial ash-rich material. Kiliuda Trough is blanketed almost entirely by a mixture of fine-grained volcanic ash, diatom tests, and minor terrigenous material. Samples from Sitkinak Trough contain terrigenous gravelly and sandy mud (Hampton, 1981).

Most of the unconsolidated sediment was originally emplaced by glacial processes. Glaciers are believed to have covered the shelf during parts of Pleistocene time, depositing a cover of till and outwash (Karlstrom, 1964; Thrasher, 1979). During the Holocene, no major input of terrigenous sediment has been made, but volcanic eruptions have spread ash across the seafloor, and biologic activity has produced carbonate and siliceous shell material (Hampton, 1981, 1982a, b). Marine currents have reworked the surficial sediment and created a segregation of sediment types. Fine-grained sediment particles have been winnowed from the banks and redeposited in the troughs. The composition of deposits in the individual troughs depends on the locally available material, with sand-size volcanic ash from the 1912 Katmai eruption being abundant near Chiniak Trough and finer ash and diatoms near Kiliuda Trough. Stevenson and Sitkinak Troughs have had essentially pure terrigenous material accessible to them.

Much reworking of shelf sediment probably was accomplished by waves during the Holocene marine transgression. The present-day shelf environment does not include strong geostrophic or tidal currents (Muench and Schumacher, 1980), and sediment reworking probably occurs only occasionally when large storm waves traverse the shelf.

Convergence of the North America and Pacific lithospheric plates a few kilometers seaward of the Kodiak Shelf causes strong compressional forces that have warped and faulted the seafloor. Strong earthquakes are frequent (Pulpan and Kienle, 1979). They range in excess of magnitude 8 and cause strong ground accelerations.

METHODS

Geotechnical measurements were made on sediment cores obtained on four cruises from 1977 to 1980. Cores could only be recovered from four physiographic areas: Chiniak Trough, Kiliuda Trough, Sitkinak Trough, and the upper continental slope (Fig. 4; Table 1). Sedimentary deposits in other areas are too stiff or coarse-grained to be collected with our coring devices.

Both gravity cores and vibracores were collected in 8.5-cm diameter plastic liners. Most cores were obtained principally for geological purposes. Upon retrieval they were cut into 1.5-m-long sections and then split lengthwise into replicate halves. Geotechnical index properties were measured on these core halves. On some, vane shear tests were made at regular intervals down-core to give measures of undrained shear strength. Subsamples were taken for determination of water content, bulk sediment density, grain specific gravity, and plasticity in the shore-based laboratory.

Several cores were taken expressly for geotechnical testing. Onboard ship, these cores were cut into 1- or 1.5-m lengths, and the ends were capped. Then each section was wrapped in cheesecloth and covered with microcrystalline wax in order to prevent moisture loss, and then stored upright in a refrigerator to retard decay of organic matter. These cores were later subjected to a suite of geotechnical tests in laboratories at the USGS and at a commercial testing company.

One-dimensional consolidation tests were run on subsamples from geotechnical cores to determine sub-failure deformational properties. Tests were run on an oedometer in a stress-controlled mode (Lambe, 1951). The consolidation tests measure change in volume with change in applied load. The results are typically expressed in plots of void ratio (e = volume of voids/volume of solids) versus the logarithm of effective (buoyant) vertical stress (p'). Two useful parameters are derived from these curves. The compression index (C_c) is the slope of the straight-line, virgin compression portion of the e-log p' curve and indicates the amount of compression produced by a particular increase in load. The maximum past pressure σ'_{vm} is the greatest effective overburden stress that the sediment has ever been exposed to and is determined by a simple graphical construction (Casagrande, 1936). The ratio of σ'_{vm} to the calculated effective overburden stress at the time of sampling σ'_{vo} is the overconsolidation ratio (OCR), which can be, for example, a measure of unloading that the sediment may have experienced by erosion. A third parameter, the coefficient of consolidation (c_v), is determined for each load increment of the one-dimensional consolidation test and defines the rate of consolidation.

Static triaxial tests were run on cylindrical samples 3.6-cm diameter and 7.6-cm long in order to determine strength properties of the sediment. Tests were run under undrained conditions with pore pressure measurements (Bishop and Henkel, 1964). Most samples were consolidated isotropically prior to testing, but some were consolidated anisotropically.

Dynamically loaded triaxial tests were also run on some cores, with the axial stress on samples varied sinusoidally at 0.1 Hz. Both compression and tension were applied at a predetermined percentage of the static strength. These tests can be used to evaluate the failure conditions of sediment under repeated loading, such as by earthquakes and waves.

Early triaxial tests were run on sediment samples that were consolidated to somewhat arbitrary stress levels. However, the later testing program followed the normalized stress parameter (NSP) approach (Ladd and Foott, 1974), whereby consolidation stresses are chosen on the basis of maximum past pressure (σ'_{vm}), as determined from the one-dimensional consolidation tests. Typically, the triaxial test specimen was consolidated to four times σ'_{vm}, which eliminates some of the disturbance effects associated with coring. Overconsolidation was artificially induced in some samples by rebounding to lower stress levels before applying the triaxial load. Measured values of undrained shear strength (S_u) are normalized with respect to effective overburden stress (σ'_{vm}). A premise of the NSP method is that the ratio s_u/σ'_v is constant for a particular sediment at a particular value of OCR. Moreover, a relation exists between s_u/σ'_v and OCR that allows prediction of sediment strength at confining stresses that exceed those at the level of sampling (Mayne, 1980).

RESULTS

Lithology of sediment cores is fairly uniform in each physiographic area, with a few exceptions, but major differences exist amongst the various areas (Table 1). Inspection of the geotechnical data gives consonant results; physical properties are by-and-large similar within areas, except where atypical lithology is found, and dissimilar from area to area (Figs. 5-11; Tables 1-5). Therefore, geotechnical characterization is possible for each area. That is, representative values of physical properties can be deduced, and general statements can be made about soil deformation in one area relative to others.

Index properties: Figure 5 presents index properties for sediment cores. Individual values are shown graphically at the depths they were measured. Summary values are also given, as averages for properties that are depth-independent and as linear-regression estimates at 1 m from the top of the core for those properties that vary with depth (Fig. 5, Table 2).

Water content is the weight of water relative to the weight of solids, expressed as a percent and corrected for salt content. Values in excess of 100% are possible; they indicate a greater weight of water than sediment. Water content typically decreases with depth in a uniform sedimentary deposit. This is the case for most sediment cores collected from the Kodiak Shelf, although some increases with depth occur.

Water content is highest for cores from Kiliuda Trough, followed by slightly lower values in Chiniak Trough, then by substantially lower values in Sitkinak Trough and on the upper continental slope. Water in the terrigenous sediment of the latter two areas is interparticulate; that is, it exists in the interstices between grains. But, the ash grains and diatom tests in Chiniak and Kiliuda troughs accommodate significant amounts of intraparticle water within voids and recesses in grains. The coarse ash particles abundant in Chiniak Trough include pumice shards with thin, pipe-shaped vesicles (Hampton and others, 1978). Most silt- and clay-size ash particles are flat to curved plates. Diatom tests are perforate and spherical- to basket-shaped. These nonterrigenous grains, because of their irregular morphology, would be expected to pack loosely, in addition to accommodating intraparticle water. Therefore, the high water contents in Chiniak and Kiliuda Troughs are related principally to sediment composition.

Note that anomalously low values of water content were measured in one core each from Chiniak Trough (station 582) and Kiliuda Trough (station 351). Cores from both stations are of terrigenous composition, and their water content is similar to the other terrigenous cores.

Values of other index properties also can be explained in terms of composition. Grain specific gravity is low in samples from Chiniak and Kiliuda Troughs because the amorphous silica that constitutes the volcanic ash is of low density (~ 2.4 gm/cm^3) as is the hydrous silica (~ 2.1 gm/cm^3) that constitutes the diatom tests. Isolated internal vesicles within the coarse pumice shards in Chiniak Trough might explain the exceptionally low values of grain specific gravity there. The values of grain specific gravity in Sitkinak Trough and on the upper continental slope are in accord with the density of common terrigenous minerals (2.6 - 2.8 gm/cm^3).

Bulk density is calculated from porosity (water content) and grain specific gravity. In normal terrigenous marine sediment, differences in bulk density mainly reflect differences in water content, because the range of grain specific gravity is relatively small. But, the exceptionally low bulk density values in Chiniak and Kiliuda Troughs reflect not only high water content but also the unusually low values of grain specific gravity.

Atterberg limits are used in this study as a measure of the plasticity of remolded sediment. The plastic limit (PL) is the water content below which the sediment deforms as a semi-solid when remolded, whereas the liquid limit is the water content above which the sediment behaves as a liquid. The range of water content between these limits, where the sediment deforms plastically, is defined as the plasticity index (PI). The liquidity index (LI) refers to the relative position of the natural water content (w) to the plastic limit and the liquid limit. A negative value (w < PL) implies that the remolded sediment will act as a semi-solid, a value between 0 and 1 (PL < w < LL) indicates plastic behavior, and a value greater than 1 (w > LL) indicates liquid behavior.

Ash-rich sediment from Chiniak Trough is nonplastic; i.e., it is noncohesive and does not exhibit plastic behavior at any water content. Therefore, Atterberg limits cannot be determined for this material. The sediment in Kiliuda Trough has high values of plastic and liquid limits relative to terrigenous cores. This may be somewhat misleading, because any intraparticle water that is present probably is passive with respect to plastic behavior but is measured in plastic- and liquid-limit tests. However, the high values of plasticity index, which do not reflect intraparticle water, show that this sediment is generally more plastic than the terrigenous sediment. The high plasticity indices might be a reflection of clay mineralogy. Mitchell (1976, p. 173) presents data that indicate a higher liquid limit and plasticity index for illite than for chlorite. Hein and others (1977, 1979, and unpublished data) report that sediment from Chiniak and Kiliuda Troughs contains somewhat larger proportions of illite and less chlorite and kaolinite than sediment from Sitkinak Trough and the upper continental slope. Smectite abundance is similar in all areas. However, because the clay content in Kiliuda Trough sediment is minor and the variation in clay mineral populations is small, this mineralogy factor may not account for all the differences. Variation in organic matter, which was measured in a few seafloor sediment samples and is slightly greater than 1% in Kiliuda Trough and on the order of a few tenths of a percent in Sitkinak Trough and on the continental slope, is another possible cause.

A plot of liquid limit versus plasticity index, called a plasticity chart, can be used to categorize fine-grained sediment types according to the Unified Soil Classification System (Casagrande, 1948). Figure 6 shows that the terrigenous sediment from the upper continental slope covers a range of sediment types designated as CL to CH (low to high plasticity clay to silty or sandy clay). The two samples from Sitkinak Trough and the one terrigenous sample from Chiniak Trough plot similarly to some upper continental slope sediment, classified as CL and borderline ML (silt, very fine sand, or sandy mud). The Kiliuda Trough data plot in an entirely separate region of the chart, as MH (diatomaceous silt and volcanic ash). Comparison is favorable between the visual sediment descriptions in Table 1 and the classification according to physical properties in Figure 6. Casagrande notes that samples from the same sedimentary deposit typically fall in a linear zone parallel to the A-line (an empirical boundary between sediment types). The upper continental slope data agree well with this concept, whereas the Kiliuda Trough data are rather dispersed.

Consolidation properties: Table 3 is a listing of the consolidation properties as determined from laboratory tests. Most sediment from Chiniak and Kiliuda Troughs shows high maximum past pressure (σ'_{vm}) relative to the insitu overburden stress (σ'_{vo}), with consequent high values of OCR. The implication drawn from traditional theory is that substantial unloading of the sediment has occurred, by erosion perhaps, but there is no supporting geological evidence. Instead, the high OCR values might reflect initial cementation or grain interlocking. Hence, the term "false overconsolidation" might be appropriate. Terrigenous cores show lower OCR, and in fact some from the upper continental slope have values less than 1.0, which indicates underconsolidation, a condition whereby the sediment has not compacted to an equilibrium state with the overburden load and some excess pore water pressure exists. Underconsolidation usually results from high sedimentation rates and low sediment permeability and can imply low sediment strength.

Compression index (C_c) spans a wide range of values ($0.06<C_c<1.06$), beyond the limits computed by Richards (1962) for several marine sediments ($0.20 < C_c < 0.87$). The ash-rich sandy core (station 433) from Chiniak Trough appears to be highly incompressible (low C_c), as are many of the terrigenous cores (Chiniak Trough and upper continental slope). In contrast, the fine-grained ash and diatom-rich sediment in Kiliuda Trough and the terrigenous sediment from Sitkinak Trough are moderately to highly compressible.

Skempton (1944) demonstrated a relation between compression index and liquid limit:

$$C_c = 0.009\ (LL-10).$$

A plot of the Kodiak Shelf data shows a general agreement with this relation, but with significant scatter (Fig. 7).

The e-log p' plots for consolidation tests of sediment from station 433 in Chiniak Trough continue to curve downward at high load levels, whereas common sediment behavior yields a straight-line segment (termed the virgin compression curve) for loads greater than σ'_{vm} (Fig. 8). A likely explanation for this curvature, which indicates greater than normal settlement under high loads, is crushing of fragile, void-rich ash grains. Consolidation of most sediment types involves rearrangement of grains and expulsion of pore water, with minor grain crushing.

Coefficient of consolidation (c_v) is variable both within and between cores, but is generally high compared to reported values for other marine sediment (Richards, 1962). High c_v implies that the sediment is permeable enough to permit rapid pore water escape and fast consolidation. A value of c_v is calculated in a consolidation test at each load increment from plots of deformation versus time. The sediment at station 433 consolidated so fast immediately after loads were applied that the proper construction for calculating c_v could not be made. The obvious implication is high c_v and consequent rapid consolidation.

Static strength properties: Sediment properties derived from static triaxial strength tests are listed in Table 4. The primary measured property is the undrained shear strength (S_u). It is the maximum sustainable shear stress within a sample subjected to a particular consolidation stress (σ_c'). S_u acts along a plane inclined at 45° to the axial load. The arcsine of S_u divided by the effective normal stress across this plane is the effective angle of internal friction (ϕ'), whose magnitude is an indication of the strength behavior of the sediment under slow (drained) loading conditions. In comparison, the ratio s_u/σ_c' gives an indication of the strength behavior during rapid (undrained) loading conditions. The difference in drained and undrained strength behavior depends on the pore water pressure generated in response to the tendency for volume change when the sediment is axially loaded. If a sediment has a high tendency for volume change, the difference in strength between rapid and slow loading can be substantial.

The terrigenous sediment samples from the upper continental slope, Sitkinak Trough, and station 582 in Chiniak Trough have values of ϕ' mostly in the 30° - 40° range, common values for marine sediment. The ash- and diatom-rich sediment in Kiliuda Trough has higher values of ϕ', 40° - 50°, whereas the ash-rich core from station 433 in Chiniak Trough has values to greater than 60°. The ash-rich sediment apparently is stronger under drained static loading conditions than the terrigenous sediment at equal confining stress.

Lambe and Whitman (1969, p. 307) present a relation between ϕ' and liquid limit for normally consolidated soil. The comparative plot of the Kodiak Shelf data in Fig. 9 shows that the terrigenous samples fall within the range of variability of Lambe and Whitman's data, whereas the ash- and diatom-rich sediment from Kiliuda Trough does not. The drained strength behavior of this sediment appears to be atypical. It is relatively strong for sediment with such high plasticity.

The values of s_u/σ_c' are highly variable and require some judgement in order to characterize the sediment types. The tests run at low levels of σ_c' seem to be the most erratic; these are the tests most likely to incorporate disturbance effects associated with coring. Other tests, except those at station 433, show fairly consistent values of S_u/σ_c' between 0.4 and 1.0 for OCR = 1, and higher values for OCR = 6. At station 433, S_u/σ_c' has significantly higher values of 3.8 (OCR = 1) and 16.1 (OCR = 5.8). Relatively high strength under conditions of undrained loading (because of low pore pressure response) is indicated for the ash-rich sandy material at this station. Somewhat surprisingly, the finer ash- and diatom-rich sediment in Kiliuda Trough exhibits undrained loading behavior similar to the terrigenous sediment.

Figure 10 is a plot of the static triaxial data according to the NSP approach. The slope Λ of the line for each sample is an indication of the change in strength with OCR. The ash-rich cores from both Chiniak and Kiliuda Troughs have similar values of Λ, 0.80-0.84. The terrigenous sediment from station 445 in Sitkinak Trough has a value of $\Lambda = 0.68$, which is near the average of $\Lambda = 0.64$ for numerous triaxial data compiled by Mayne (1980). An implication of the data in Figure 10 is that the ash-rich sediment would retain a larger portion of its strength after unloading compared to the terrigenous sediment.

S_u/σ_v' values were calculated from the vane shear data (Table 2). The magnitude of strength increase with effective overburden pressure is greater for the ash-rich sediment from Kiliuda Trough than for the terrigenous sediment from Sitkinak Trough. This may be related to higher OCR and Λ for the ash-rich sediment compared to the terrigenous sediment (Table 3, Fig. 10) and does not necessarily conflict with the S_u/σ_v' values derived from the triaxial data (Table 4).

Dynamic strength properties: The data from cyclic triaxial strength tests are given in Table 5. The quantity τ_{cyc}/S_u is the cyclic stress level: the average value of shear stress (τ_{cyc}) applied sinusoidally at 0.1 Hz as a percentage of the static undrained shear strength (S_u). Pore water pressure and strain accumulate with repeated application of τ_{cyc}. At some point, the pore water pressure approaches the confining stress, strain increases abruptly, and the sediment fails. In our tests, failure was not a discrete event, and was arbitrarily defined at 20% strain.

Samples typically fail in fewer cycles at progressively higher stress levels. Figure 11 shows the number of cycles to failure versus stress level for Kodiak Shelf samples. All except the sandy ash deposit from Chiniak

Trough (station 433) fall in a range that shows low to moderate dynamic strength degradation. For example, after 10 cycles of loading (as might be imparted by an earthquake), these sediments will not fail unless the applied stress level is at least from 70% to nearly 100% of their static strength. Tests on terrigenous sediment from other geographic areas have shown similar results (Lee and others, 1981; Anderson and others, 1980).

In contrast, the ash-rich sediment from Chiniak Trough is highly suseptible to failure under cyclic loading. Its dynamic strength at 10 cycles is only about 12% of its static strength. Recall that the static undrained strength of this material is relatively high, but under repeated loading it becomes highly suseptible to liquefaction-type failure.

DISCUSSION

Three sediment types have been tested in this study: 1) muddy terrigenous sediment collected throughout Sitkinak Trough, along the upper continental slope, and at one station each in Chiniak and Kiliuda Troughs, 2) muddy ash- and diatom-rich sediment with minor amount of terrigenous minerals from Kiliuda Trough, and 3) ash-rich sandy mud with a minor amount of terrigenous minerals from Chiniak Trough. Each has a distinctive set of physical properties, and some differences in deformational behavior can be expected.

The terrigenous sediment cores have physical properties that by and large are within normal ranges measured on terrigenous sediment elsewhere, except that several samples exhibit low compressibility. This implies relatively small settlement when subjected to sub-failure loads. The reason for this behavior is not evident.

Steep seafloor slopes exist in Sitkinak Trough and along the upper continental slope, so, given the geotechnical properties and the tectonic activity, slumping of the terrigenous sediment is possible. Large slumps have in fact been observed in seismic-reflection profiles along the upper continental slope, and a geotechnical analysis by Hampton and others (1978) indicates that earthquakes and removal of support by faulting are the likely triggering mechanisms. Seismic profiles in Sitkinak Trough have not revealed large slumps, but the existence of steep slopes warrants concern. Static stability can be crudely evaluated by performing a simple factor of safety calculation:

$F=(S_u/\sigma_v') / (\sin\gamma \cdot \cos\gamma)$ where F is the factor of safety and γ is the slope angle of the seafloor. F= 1.0 indicates incipient instability, whereas higher values indicate stability.

The steepest slopes in Sitkinak Trough are on the order of 50% (27°) (Fig. 2). From Table 4, a minimum value of S_u/σ_v' is about 0.4, which will give F=1 at a slope of 18.4°. This implies that steep slopes are statically unstable under conditions of undrained loading if underlain by the weakest sediment. Under conditions of drained loading, the critical slope angle is equal to ϕ', which is 26° - 37° and greater than slope angles likely to be encountered in the trough.

The effects of earthquake loading can be evaluated for a simplified two-dimensional model by the method developed by Lee and others (1981):

$$k=(\gamma'/\gamma)\ (A_C A_D S_u/\sigma_v' - \sin\gamma \cdot \cos\gamma)/\cos^2\gamma$$

where k is the pseudo-static horizontal acceleration (expressed as a percent of gravity) required to cause failure, A_C is a correction factor for the strength difference between isotropic (laboratory) versus anisotropic (field) confining pressure, A_D is a correction factor for cyclic strength degredation, and γ'/γ is the ratio of buoyant total to bulk densities.

The core from station 445 has enough data for analysis. An anisotropically consolidated triaxial test was run at a horizontal to vertical stress ratio of 2, which models the field confining-stress conditions. The ratio of static strength (51.8 kPa) determined in this test to the static strength (58.4 kPa) determined for a sample consolidated isotropically to the same stress level, gives a value of 0.89 for A_C. From Figure 11, the cyclic strength degredation is seen to be slight; it is about 0.98 of the static strength at 10 cycles (a reasonable number of load applications by an earthquake). Using the bulk density at 1-m depth from Table 2, $\gamma'/\gamma = 0.45$.

Determination of k for several values of seafloor slope are given in Table 6. Using the data from Seed and others (1975), the distances ($d_{6.5}$) from an earthquake of magnitude 6.5 that would experience accelerations equal to k can be estimated (Table 6).

The above analysis of dynamic loading involves many simplifications and works best where k values can be calculated for an area of known instability and compared to k values from a nearby area of potential instability (Lee and others, 1981; Winters and Lee, 1982). Moreover, a state of overconsolidation was measured in oedometer tests at station 445 (Table 3). If this condition continues with depth, greater stability than calculated above would exist. On the other hand, the cyclic strength degredation is exceedingly small, and values of 0.60 to 0.80 are more typical for terrigenous sediment. Stability would be reduced as a consequence of greater cyclic degredation.

Both static and dynamic analysis indicate potential instability in the steepest areas of Sitkinak Trough. The fact that no large sediment slides have been observed points to the need for further study.

The fine-grained sediment in Kiliuda Trough, which is composed of volcanic ash, siliceous diatom tests, and a minor quantity of terrigenous minerals, plots with sediment of similar composition on a plasticity chart (Fig. 6; Casagrande, 1948). It has high water content and, because of the low grain specific gravity, a low bulk sediment density. This indicates a low increase of overburden stress with depth and a consequent low increase of dependent properties such as consolidation state and shear strength. However, values of compression index (C_c) are the highest measured on the Kodiak Shelf (Table 3), which implies relatively large amounts of settlement under a given load.

The sediment is highly plastic (Fig. 5) and, compared to other sediment of similarly high plasticity, it is relatively strong under conditions of drained loading. Its undrained static loading behavior is similar to the terrigenous samples that were tested (Table 4). In dynamic, undrained triaxial tests, the Kiliuda Trough sediment has somewhat more strength degradation at low numbers of cycles than terrigenous samples, but is by no means unusually susceptible to repeated loading.

The sandy, ash-rich sediment from Chiniak Trough (station 433) is different in most respects from the other sediment types. Clay content is low, so the sediment classifies as noncohesive according to plasticity tests. Its water content is lower than that of the sediment from Kiliuda Trough, but due to low grain specific gravity, the bulk density is comparable (Table 2). In contrast to the samples from Kiliuda Trough, station 433 material is highly incompressible, similar to the underlying terrigenous material sampled at station 582 (Table 3). But, the downward concavity of the virgin compression curve (Fig. 8) suggests that excessive settlement (perhaps due to grain crushing) occurs under high loads. Rapid consolidation also is indicated by oedometer tests.

High static strength was measured in triaxial tests on samples from station 433 for both drained and undrained conditions (Table 4). However, dynamic loading causes severe strength degredation, to 12% of the static undrained strength at 10 cycles (Fig. 11). Earthquake-induced sediment slides are not likely, because the seafloor is generally horizontal where the ash-rich sediment occurs. However, loss of bearing capacity due to liquefaction is possible, which could cause sinking and failure of pipelines.

Ash-rich material covers most of the floor of Chiniak Trough (Table 1; Hampton, 1981), but the deposit pinches out near the trough margins and may only be several meters thick. Seismic-reflection profiles show that the terrigenous core at station 582 is near the lateral edge of the trough sediment fill and probably represents a sedimentary deposit that underlies the surficial ash deposit and extends a few tens of meters to deeper, presumably strong and stable glacial material. The ash was erupted in 1912 from Mt. Katmai on the Alaska peninsula (Hampton and others, 1979), and the fine-grained terrigenous section as sampled at station 582 may represent the normal Holocene sedimentary environment in Chiniak Trough. Buried ash deposits from earlier volcanic eruptions may be present.

The ash-rich sediment from both Chiniak and Kiliuda Troughs has similar values of the normalized strength parameter Λ (0.80 to 0.84) (Fig. 10). The one terrigenous sample for which determination could be made has a more normal value of $\Lambda = 0.68$. Overconsolidated ash-rich sediment would strengthen more than the terrigenous sediment would. Oedometer tests indicate various levels of overconsolidation for ash-rich sediment, but there is no geologic evidence that unloading has occurred. Perhaps the overconsolidation is only present at shallow depths, or it may reflect a physical phenomenon other than unloading.

It is evident from the geotechnical framework study of Kodiak Shelf that a variety of fine-grained sediment types with different physical properties exists. The deposits cover a minor area of the shelf when compared to the extent of coarse-grained glacial deposits and sedimentary bedrock that probably have favorable geotechnical properties. But, where the fine-grained sediment is encountered, it can present special engineering concern.

REFERENCES

Anderson, K.H., Pool, J.H., Brown, S.F., and Rosenbrand, W.F., 1980, Cyclic and static laboratory tests on Drammen clay. Journal of the Geotechnical Engineering Division, ASCE, v. 106, p. 499-529.

Bishop, A.W., and Henkel, D.J., 1964, The Measurement of Soil Properties in the Triaxial Test. London, Edward Arnold Ltd., 228 p.

Casagrande, A., 1936, The determination of the pre-consolidation load and its practical significance. Proceedings 1st International Conference on Soil Mechanics and Foundation Engineering, v. 3, p. 60-64.

Casagrande, A., 1948, Classification and identification of soils. Transactions ASCE, p. 901-930.

Hampton, 1981, Grain size and composition of seafloor sediment, Kodiak Shelf, Alaska. U.S. Geological Survey Open-File Report 81-659, 78 p.

Hampton, M.A., 1982a, Synthesis report: Environmental geology of Kodiak Shelf, Alaska. U.S. Geological Survey Open-File Report 82-59, 76 p.

Hampton, M.A., 1982b, Geology of the Kodiak Shelf, Alaska: Environmental considerations for resource development. Continental Shelf Research, in press.

Hampton, M.A., Bouma, A.H., Carlson, P.R., Molnia, B.F., Clukey, E.C., and Sangrey, D.A., 1978, Quantitative study of slope stability in the Gulf of Alaska. Proceedings 10th Offshore Technology Conference, p. 2308-2318.

Hampton, M.A., Bouma, A.H., Frost, T.P., and Colburn, I.P., 1979, Volcanic ash in surficial sediments of the Kodiak Shelf - An indicator of sediment dispersal patterns. Marine Geology, v. 29, p. 347-356.

Hein, J.R., Bouma, A.H., and Hampton, M.A., 1977, Distribution of clay minerals in lower Cook Inlet and Kodiak Shelf sediment, Alaska. U.S. Geological Survey Open-File Report 77-581, 18 p.

Hein, J.R., Bouma, A.H., Hampton, M.A., and Ross, C.R., 1979, Clay mineralogy, fine-grained sediment dispersal, and inferred current patterns, lower Cook Inlet and Kodiak Shelf, Alaska. Sedimentary Geology, v. 24, p. 291-306.

Karlstrom, T.N.V., 1964, Quaternary geology of the Kenai Lowland and glacial history of the Cook Inlet region, Alaska. U.S. Geological Survey Professional Paper 443.

Ladd, C.C., and Foott, R., 1974, New design procedure for stability of soft clays. Journal of the Geotechnical Engineering Division, ASCE, v. 100, p. 763-786.

Lambe, T.W., 1951, Soil Testing for Engineers. New York, John Wiley and sons, 165 p.

Lambe, T.W., and Whitman, R.V., 1969, Soil Mechanics. New York, John Wiley and Sons, 553 p.

Lee, H.J., Edwards, B.D., and Field, M.E., 1981, Geotechnical analysis of a submarine slump, Eureka, California. Proceedings 13th Offshore Technology Conference, p. 53-65.

Mayne, P.W., 1980, Cam-clay predictions of undrained strength. Journal of the Geotechnical Engineering Division, ASCE, v. 106, p. 1219-1242.

Mitchell, J.K., 1976, Fundamentals of Soil Behavior. New York, John Wiley and Sons, Inc., 422 p.

Muench, R.D., and Schumacher, J.D., 1980, Physical oceanographic and meteorologic conditions in the northwest Gulf of Alaska. NOAA Technical Memorandum ERL PMEL-22, 147 p.

Pulpan, H., and Kienle, J., 1979, Western Gulf of Alaska seismic risk. Proceedings 11th Offshore Technology Conference, p. 2209-2218.

Richards, A.F., 1962, Investigation of deep-sea sediment cores, II. Mass physical properties. U.S. Navy Hydrographic Office Technical Report 106, 146 p.

Seed, H.B., Murarka, R., Lysmer, J., and Idriss, I.M., 1975, Relationships between maximum acceleration, maximum velocity, distance from source and local site conditions for moderately strong earthquakes. Berkeley, University of California, Earthquake Engineering Research Center, EERC Report No. 75-17.

Skempton, A.W., 1944, Notes on the compressibility of clays. Geological Society of London, Quarterly Journal, v. 100, p. 119-135.

Thrasher, G.P., 1979, Geologic map of the Kodiak outer continental shelf, western Gulf of Alaska. U.S. Geological Survey Open-File Report 79-1267, 1:500,000.

Winters, W.J., and Lee, H.J., 1982, Evaluation of geotechnical properties and slope stability of a calcareous ooze on the south-west slope off Oahu, Hawaii. U.S. Geological Survey Open-File Report 82-468B, 274 p.

TABLES

Table 1. Locations of sampling stations and descriptions of sediment types.

Physiographic area	Station number	North latitude	West longitude	Sediment type
Chiniak Trough	329	57° 38.95'	151° 58.03'	sandy mud with ash and terrigenous minerals
	432	57° 25.50'	151° 23.43'	sandy mud with ash and terrigenous minerals
	434	57° 26.71'	151° 25.26'	muddy sand with ash and terrigenous minerals
	582	57° 29.7'	151° 38.6'	sandy mud with terrigenous minerals; ash-rich only at top of core.
Kiliuda Trough	343	56° 39.37'	153° 04.72'	mud with ash and terrigenous minerals
	344	56° 39.47'	153° 05.63'	mud with terrigenous minerals and ash
	347	56° 36.76'	153° 17.92'	mud with terrigenous minerals and ash
	348	56° 37.66'	153° 18.89'	mud with terrigenous minerals and ash
	349	56° 38.24'	153° 19.80'	mud with ash and terrigenous minerals
	351	56° 46.86'	153° 11.02'	gravelly sandy mud with terrigenous minerals and mud
	439	56° 08.13'	154° 17.33'	mud with ash and terrigenous minerals
	440	56° 39.15'	153° 06.36'	mud with ash and terrigenous minerals
	441	56° 39.50'	153° 04.62'	mud with ash and terrigenous minerals
	578	56° 39.5'	153° 05.2'	mud with ash and terrigenous minerals

Table 1 (continued)

Physiographic area	Station number	North latitude	West longitude	Sediment type
Kiliuda Trough (continued)	579	56° 54.9'	152° 32.6'	mud with terrigenous minerals and ash
Sitkinak Trough	355	56° 08.53'	153° 29.41'	gravelly sandy mud with terrigenous minerals
	356	56° 05.55'	153° 31.28'	gravelly muddy sand with terrigenous minerals
	357	56° 07.56'	153° 38.46'	muddy sand with terrigenous minerals
	445	56° 11.17'	153° 17.28'	sandy mud with terrigenous minerals
	455	56° 12.44'	152° 58.36'	mud with terrigenous minerals
Upper Continental Slope	224	56° 46.3'	151° 34.5'	mud with terrigenous minerals
	225	56° 47.5'	151° 37.5'	mud with terrigenous minerals
	226	56° 48.3'	151° 40.9'	mud with terrigenous minerals
	239	57° 50.7'	149° 07.4'	mud with terrigenous minerals
	240	57° 48.3'	149° 05.4'	mud with terrigenous minerals
	336	57° 46.60'	149° 02.08'	mud with terrigenous minerals
	340	57° 17.48'	150° 24.92'	sandy mud with terrigenous minerals
Upper Continental Slope	450	55° 56.06'	154° 14.13'	sandy mud with terrigenous minerals

Table 2. Summary values of index physical properties. (Replicate cores taken at some stations.)

Physiographic area	Station number	Water Content at 1 m (% dry weight)	Bulk density at 1 m (gm/cm^3)	Average plastic limit	Average liquid limit	Average plasticity index	Liquidity index at 1 m	Average grain specific gravity	Vane shear strength at 1 m (kPa)	S_u/σ_v'
Chiniak Trough	329	93	1.39	np	np			2.26		
	432	81/86	1.47/1.45					2.32/2.30		
	433	67	1.52					2.30		
	582	32	1.95	18	30	13		2.74		
Kiliuda Trough	343	105	1.43					2.56	19.69	4.67
	344	123	1.37	68	118	50		2.53	16.71	4.61
	347	99	1.44					2.59	14.10	3.27
	348	122	1.34	56	114			2.59	12.00	3.60
	349	132	1.38	52	104	52		2.63	3.50	0.94
	351	37	1.89					2.75	30.27	3.47
	439	133/99	1.37/-	67/-	110/-	43/-	1.31/-	2.57/2.52	10.12/-	
	440	100						2.52		
	441	97						2.60		
	578	122		60	102	42	1.47		15.90	

Table 2. Cont'd

Physiographic area	Station number	Water Content at 1 m (% dry weight)	Bulk density at 1 m (gm/cm^3)	Average plastic limit	Average liquid limit	Average plasticity index	Liquidity index at 1 m	Average grain specific gravity	Vane shear strength at 1 m (kPa)	S_u/σ'_v
	579	91/100	1.48/-	54/-	87/-	33/-		2.64/-	-/13.63	
Sitkinak Trough	355	35	1.88					2.75	5.11	0.59
	356	36	1.86					2.70		
	357	36	1.86					2.65	7.44	0.88
	445	40	1.83	22	31	10	1.82	2.71	19.80	2.43
	455	45	1.77	23	36	12	1.24	2.69	15.23	2.02
Upper Continental Slope	224	45	1.76	24	53	29	1.19	2.75		
	225	33	1.92	18	30	12	1.17	2.72		
	226	38	1.85	17	32	15	1.30	2.74		
	239	32	1.91	17	32	15		2.72		
	240	36	1.87	20	48	27	1.17	2.79		
	336	48	1.74	29	60	29		2.69		
	340		1.91					2.71	11.29	1.27
	450	21		19	20	4				

Table 3. Consolidation test results.

Physiographic area	Station number	Depth in core (cm)	σ'_{vo} (kPa)	σ'_{vm} (kPa)	C_c	$c_v \times 10^{-2}$ (cm^2/sec) from	to	OCR
Chiniak Trough	433	42	2.2	190.0	0.12	*	*	8
		92	5.2	150.0	0.07	*	*	29
	582	103	9.5	21.0	0.10	0.13	0.68	2.2
		194	21.5	40.0	0.06	0.52	2.27	1.9
Kiliuda Trough	439	66	2.3	24.0	1.06	0.33	1.65	10.4
	578	82	3.2	60.0	0.50	0.35	2.19	18.8
		180	7.2	118.0	0.48	1.24	3.51	16.4
		244	9.8	100.0	0.42	0.76	2.09	10.2
	579	51	2.0	110.0	0.43	0.21	2.27	55.0
		119	6.0	67.0	0.43	0.47	3.99	11.2
	579	176	9.6	80.0	0.37	0.71	4.54	8.3

Table 3 (continued)

Physiographic area	Station number	Depth in core (cm)	σ'_{vo} (kPa)	σ'_{vm} (kPa)	C_c	$c_v \times 10^{-2}$ (cm^2/sec) from	to	OCR
Sitkinak Trough	445	12	0.6	3.4	0.73	0.10	1.06	5.7
	455	18	3.9	14.8	0.32	0.11	1.60	3.8
		102	8.4	89.0	0.30	0.11	0.31	10.6
Upper Continental Slope	224	25	1.3	3.8	0.55	0.01	0.29	2.9
		155	13.2	65.0	0.18	0.21	1.10	4.9
		395	47.0		0.16	0.07	0.50	
	225	135	13.0	9.0	0.10	0.10	2.05	0.7
	226	25	2.4	8.3	0.12	0.09	1.12	3.5
	239	165	15.2	9.2	0.16	0.05	2.27	0.6
		287	29.0	22.0	0.12	0.02	0.26	0.8
	240	45	7.2	6.3	0.38	0.02	0.32	0.9
	450	53	5.3	96.0	0.15	0.18	1.74	18.1

*c_v could not be determined from the data, but consolidation was extremely fast.

Table 4. Static triaxial strength test results.

Physiographic area	Station number	Depth in core (cm)	σ'_c (kPa)	Induced OCR	S_u (kPa)	s_u/σ'_c	ϕ' (degrees)
Chiniak Trough	433	100	0.7	-	1.9	2.9	<62
		114	353.3	1	1325.3	3.8	46
		124	60.4	5.8	974.4	16.1	<53
	582	41	1.4	-	9.4	6.7	33
		63	6.9	-	17.8	2.6	43
		113	48.2	1	52.4	1.1	34
		142	8.0	6	30.7	3.8	31
		155	165.4	1	56.2	0.3	47
		183	35.8	-	45.9	1.3	36
Kiliuda Trough	439	94	291.2	1	256.9	0.9	43
		118	194.2	1	110.8	0.6	45
	578	49	244.8/62.0	1	98.2	0.4	45
		148	241.2	1	109.4	0.4	41

Table 4 (continued)

Physiographic area	Station number	Depth in core (cm)	σ'_c (kPa)	Induced OCR	S_u (kPa)	s_u/σ'_c	ϕ' (degrees)
Kiliuda Trough	578	190	75.8	6	122.3	1.6	44
(continued)		205	130.9	3	157.7	1.2	44
		219	1.0	-	22.9	22.9	50
		233	11.7	-	32.9	2.8	50
	579	61	68.9	6	151.0	2.2	45
		103	248.1	1	122.6	0.5	43
		151	1.0	-	22.3	22.3	54
		165	910	-	2.3	0.3	45
Sitkinak Trough	445	37	141.2	1	58.4	0.4	35
		37	141.0/68.4	1	51.8	0.4	36
		46	30.7	5.9	42.9	1.4	<34
		46	60.4	3	42.6	0.7	<30
		95	294.2	1	180.4	0.6	37
		107	194.0	1	128.5	0.7	30

Table 4 (continued)

Physiographic area	Station number	Depth in core (cm)	σ_c' (kPa)	Induced OCR	S_u (kPa)	s_u/σ_c'	ϕ' (degrees)
Sitkinak Trough (con't)	445	119	97.1	1	73.6	0.8	26
	455	110	103.0	1	105.9	1.0	32
		122	199.1	1	155.9	0.8	37
Upper Continental Slope	224						35
	225						35
	226						37
	239						30
	450	62	289.3	1	294.1	1.0	40
		74	103.9	1	207.9	2.0	38

Table 5. Dynamic triaxial strength test results.

Physiographic area	Station number	Depth in core (cm)	σ_c' (kPa)	Induced OCR	τ_{cyc}/S_u (%)	Cycles to failure
Chiniak Trough	433	76	347.2	1	12	12
		85	344.2	1	6	230
	582	77	165.3	1	74	14
		92	165.3	1	53	58
Kiliuda Trough	578	55	241.0	1	77	1
		68	75.8	6	60	21
		84	75.8	6	41	520
		135	241.0	1	50	35
	579	75	248.1	1	75	9
		89	248.1	1	45	242
Sitkinak Trough	445	60	137.8	1	93	16
		60	134.1	1	51	410

Table 6. Values of variables in dynamic slope stability analysis.

α	k	$d_{6.5}$ (km)
1°	0.15	28
5°	0.12	34
10°	0.08	51
15°	0.05	80
20°	0.014	240

FIGURES

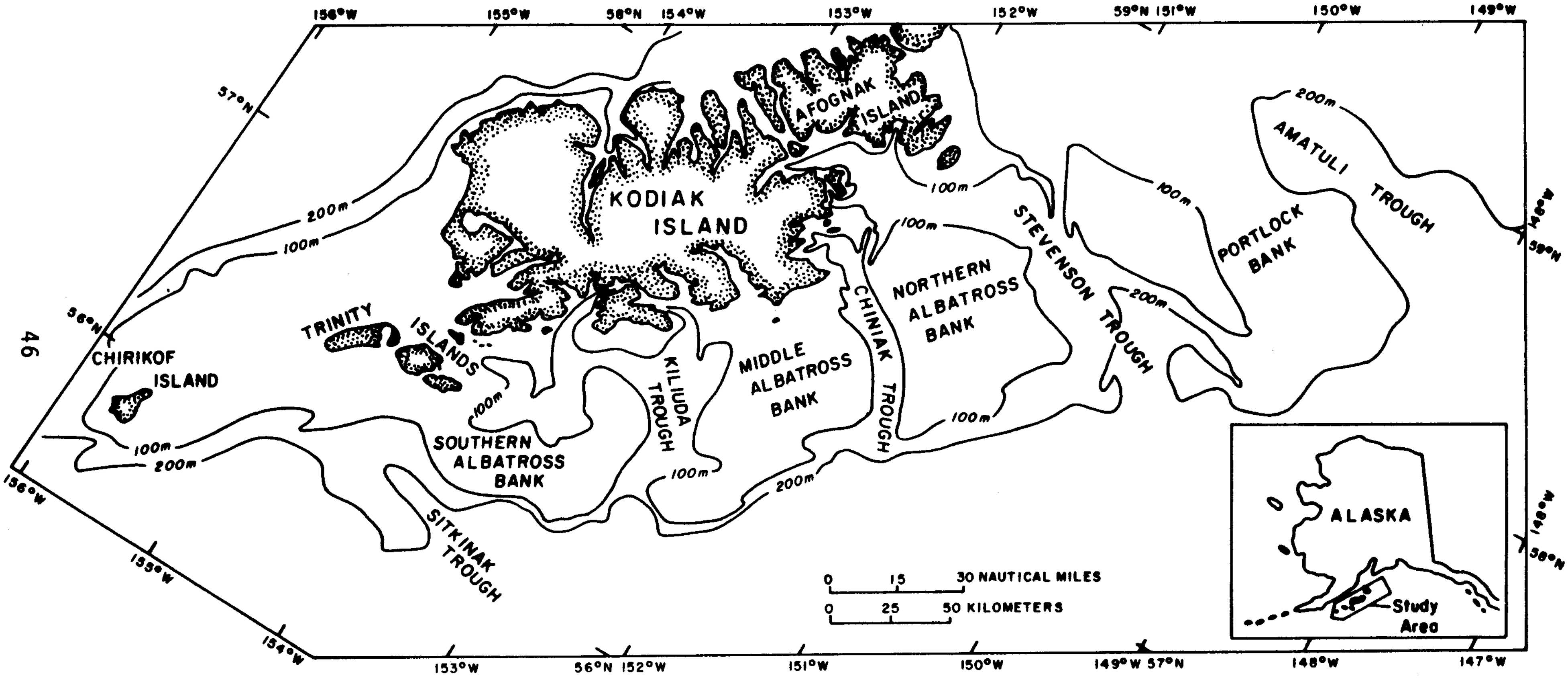

Figure 1. Location map of the Kodiak Shelf, Alaska, showing physiographic features and bathymetry.

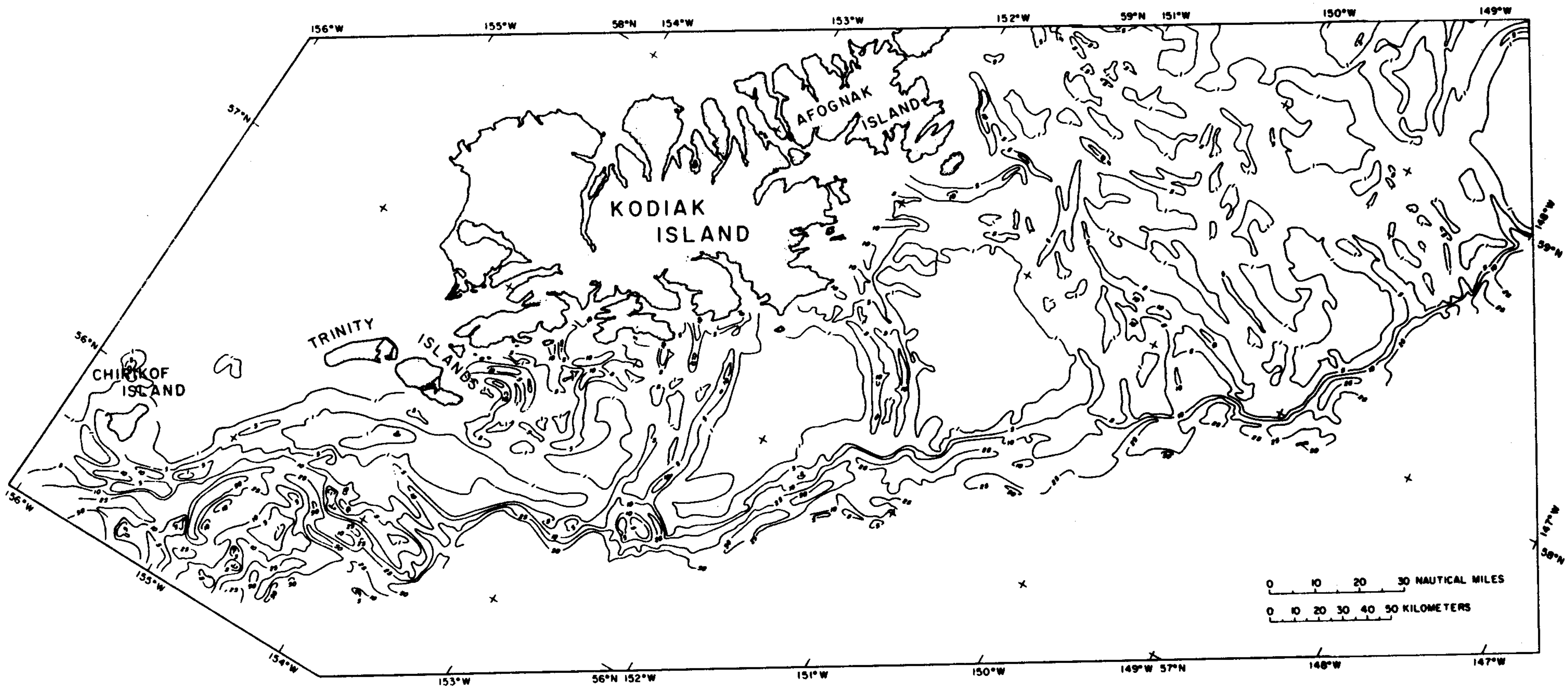

Figure 2. Map of seafloor slopes. Coverage extends from 3-mile limit to 100 m water depth. Contours in percent.

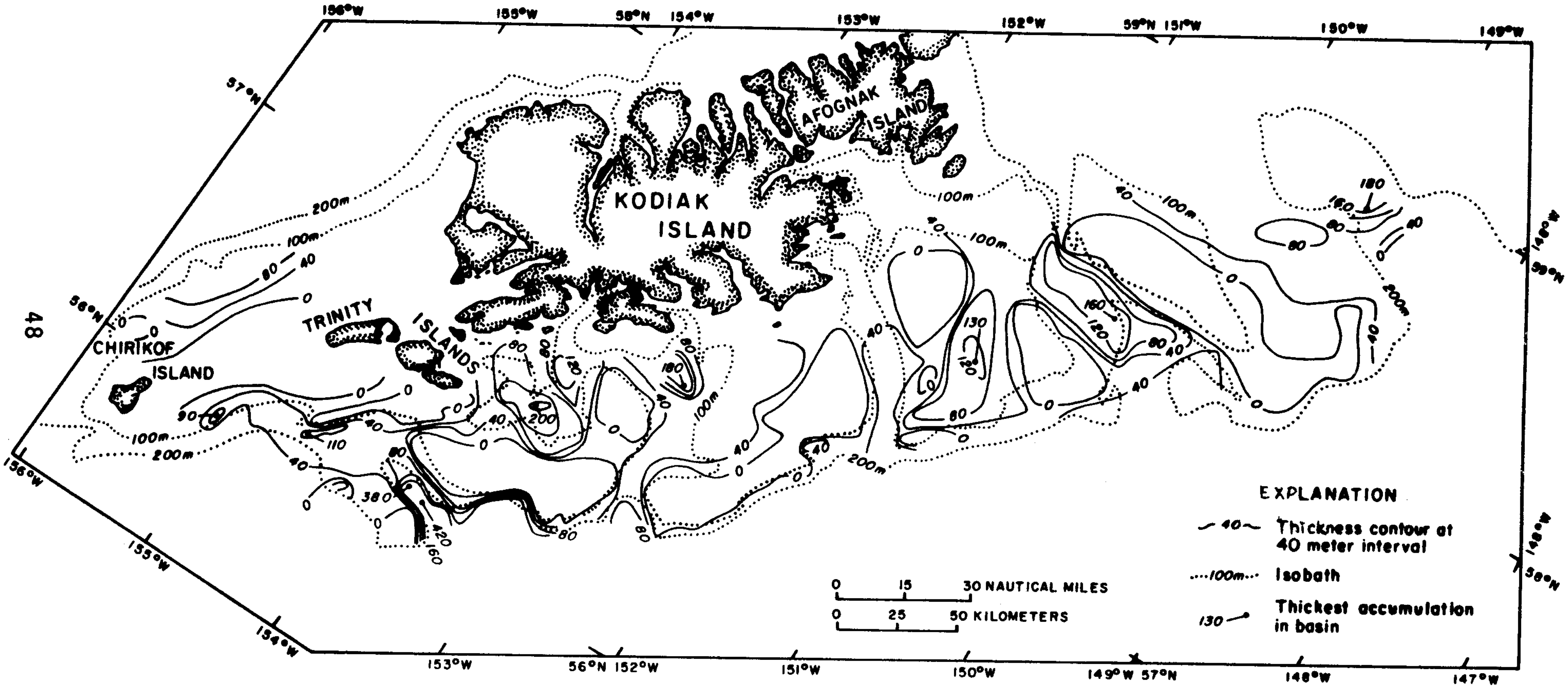

Figure 3. Generalized thickness map of unconsolidated sedimentary deposits. Contours in meters.

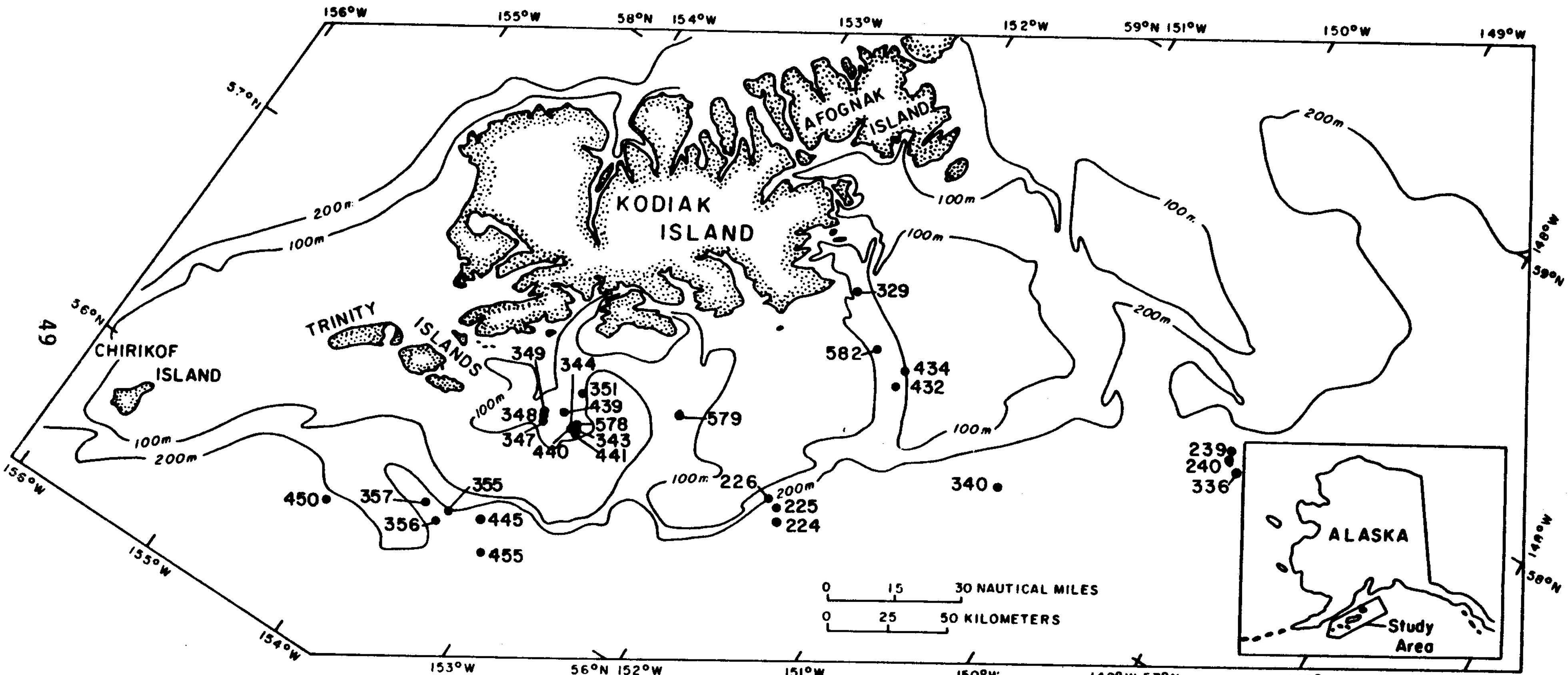

Figure 4. Locations of sediment sample stations. (See Table 1.)

Figure 5. Index physical properties of sediment samples. (page 50 to 88)

Station 224 Physiographic area Upper Continental Slope

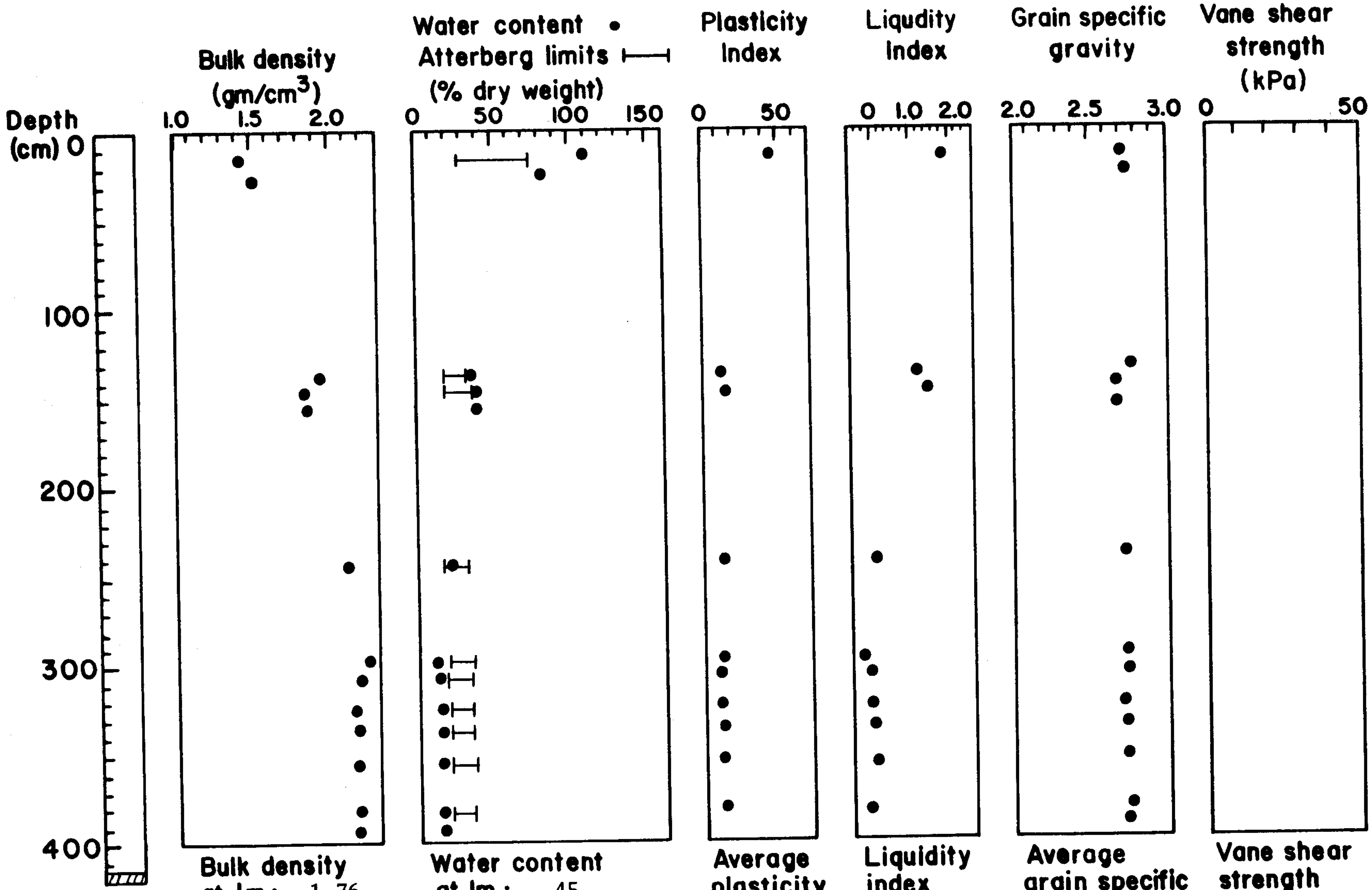

Bulk density at lm.: 1.76

Water content at lm.: 45

Average plastic limit: 24

Average liquid limit: 53

Average plasticity index: 29

Liquidity index at lm.: 1.19

Average grain specific gravity: 2.75

Vane shear strength at lm.: ______

Station 225 Physiographic area Upper Continental Slope

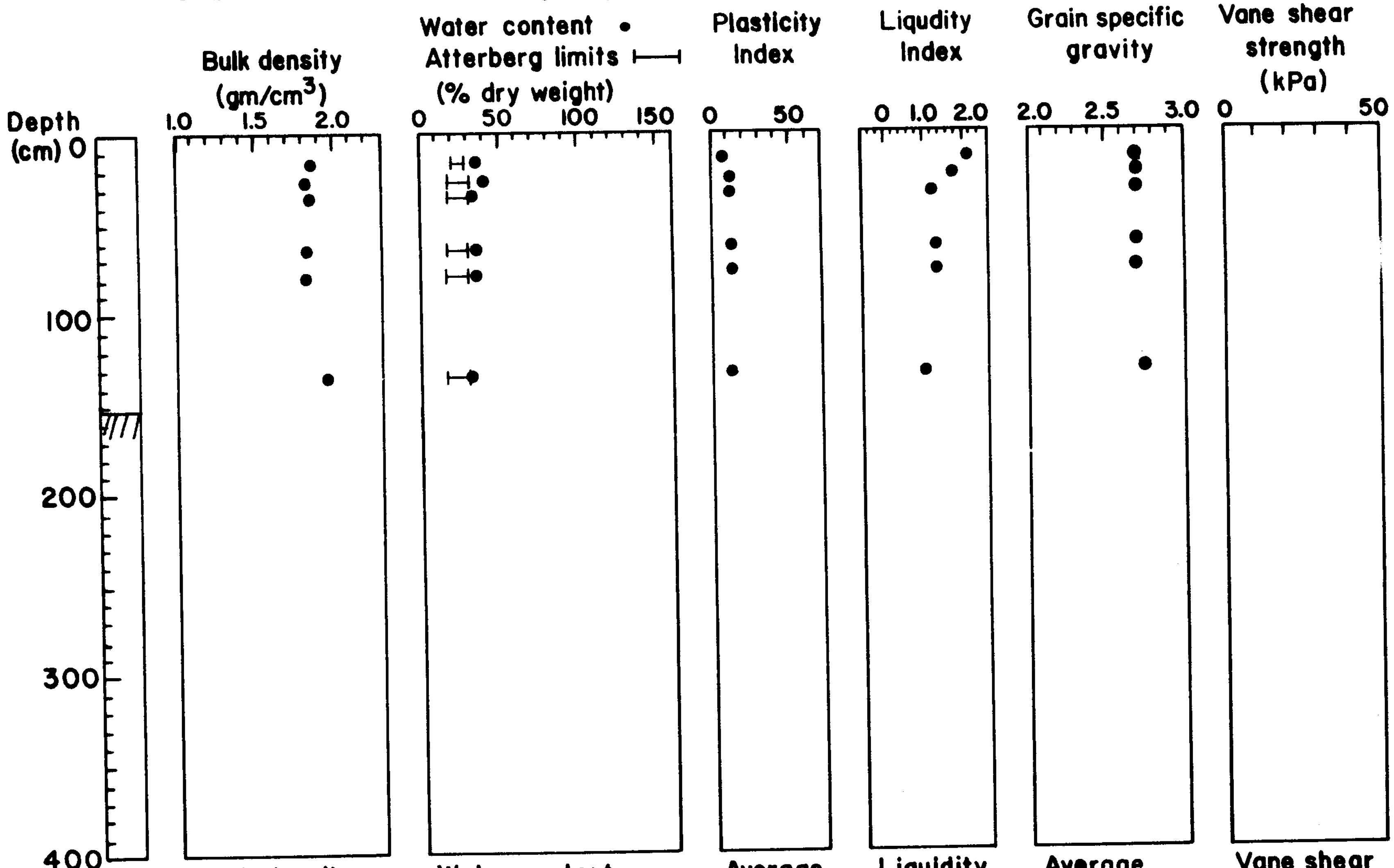

Bulk density at lm.: 1.92

Water content at lm.: 33

Average plastic limit: 18

Average liquid limit: 30

Average plasticity index: 12

Liquidity index at lm.: 1.17

Average grain specific gravity: 2.72

Vane shear strength at lm.: ______

Station 226 Physiographic area Upper Continental Slope

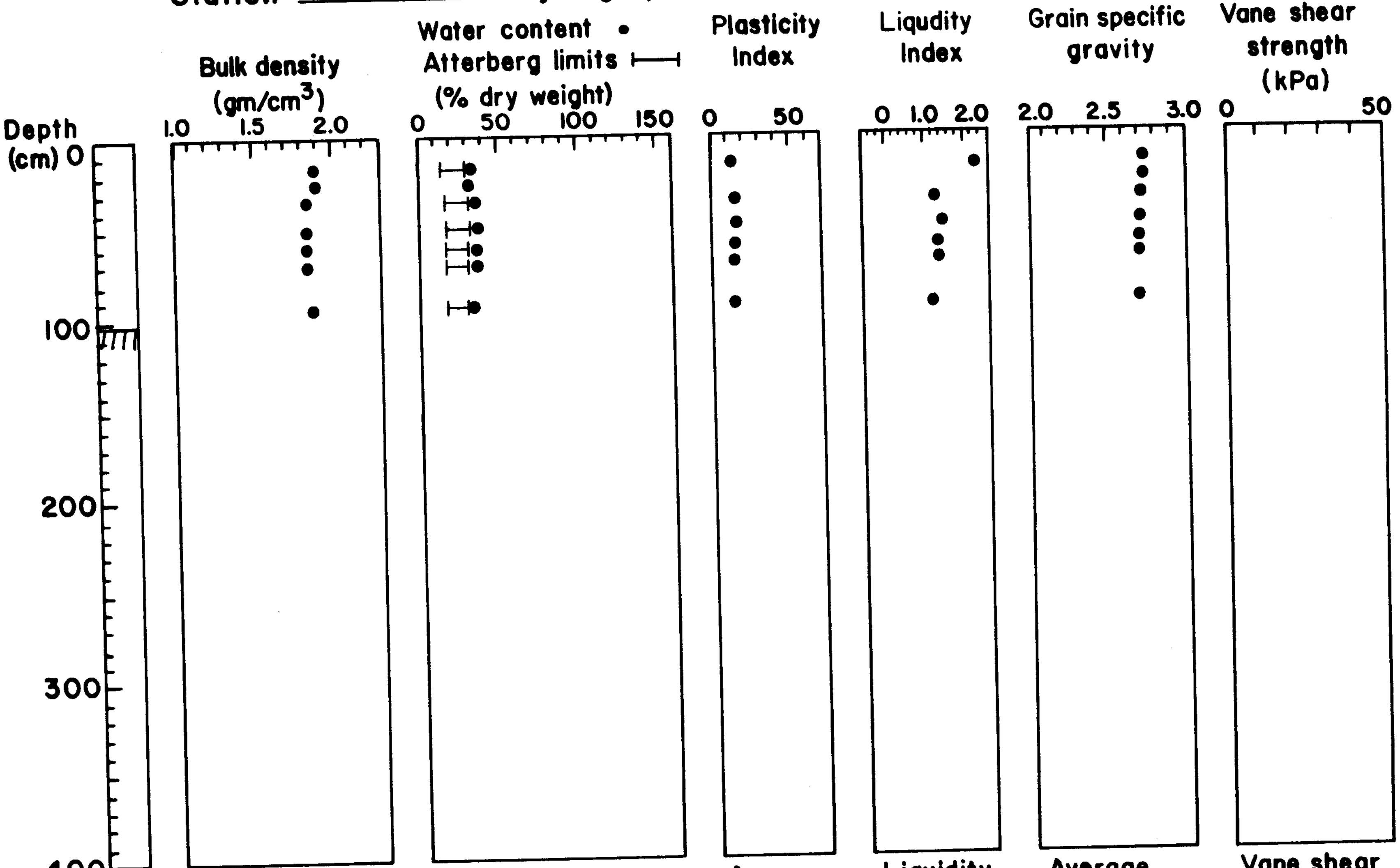

Bulk density at lm.: 1.85

Water content at lm.: 38

Average plastic limit: 17

Average liquid limit: 32

Average plasticity index: 15

Liquidity index at lm.: 1.30

Average grain specific gravity: 2.74

Vane shear strength at lm.:

Station 239 Physiographic area Upper Continental Slope

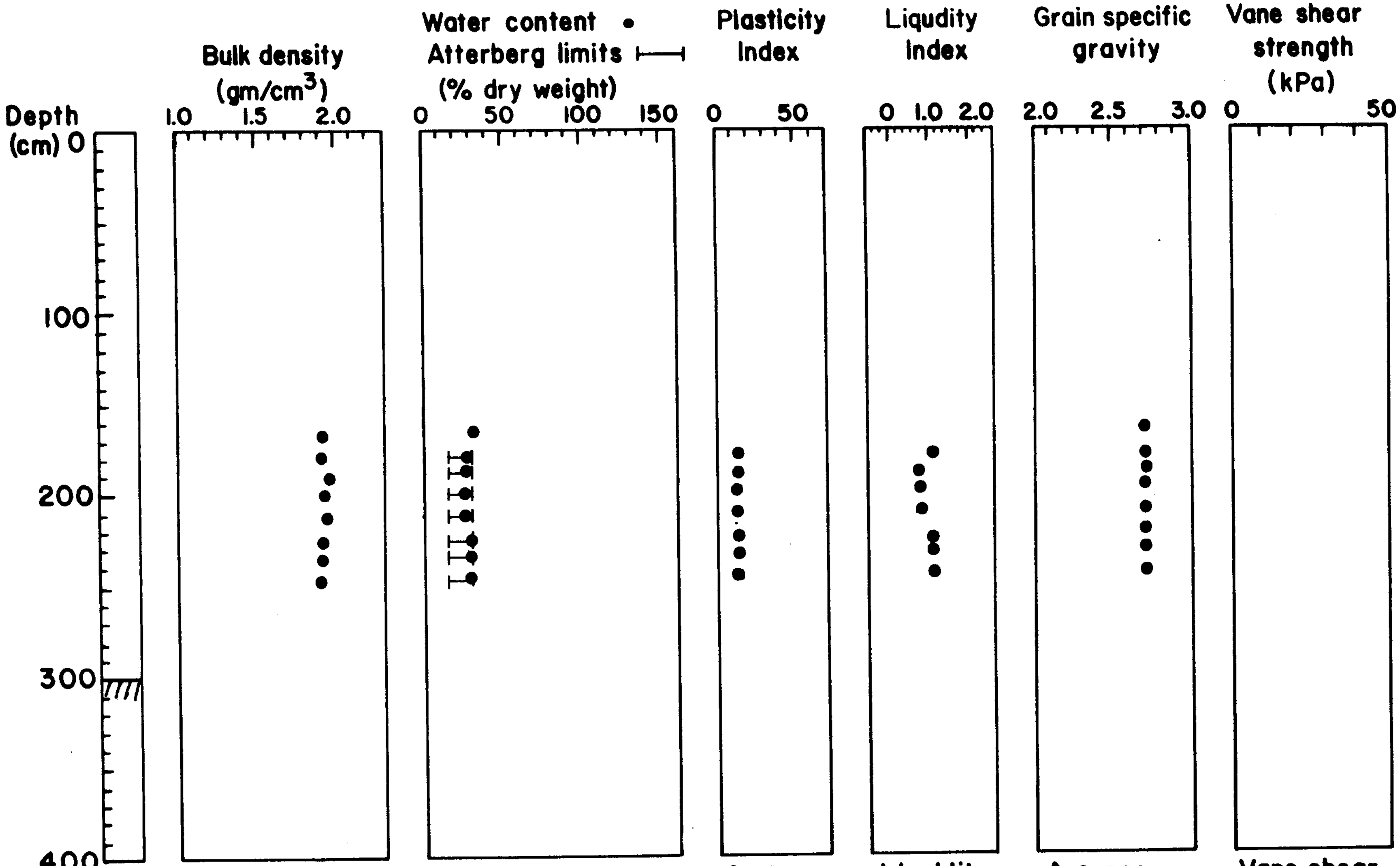

Bulk density at lm.: 1.91

Water content at lm.: 32

Average plastic limit: 17

Average liquid limit: 32

Average plasticity index: 15

Liquidity index at lm.: ______

Average grain specific gravity: 2.72

Vane shear strength at lm.: ______

Station 240 Physiographic area Upper Continental Slope

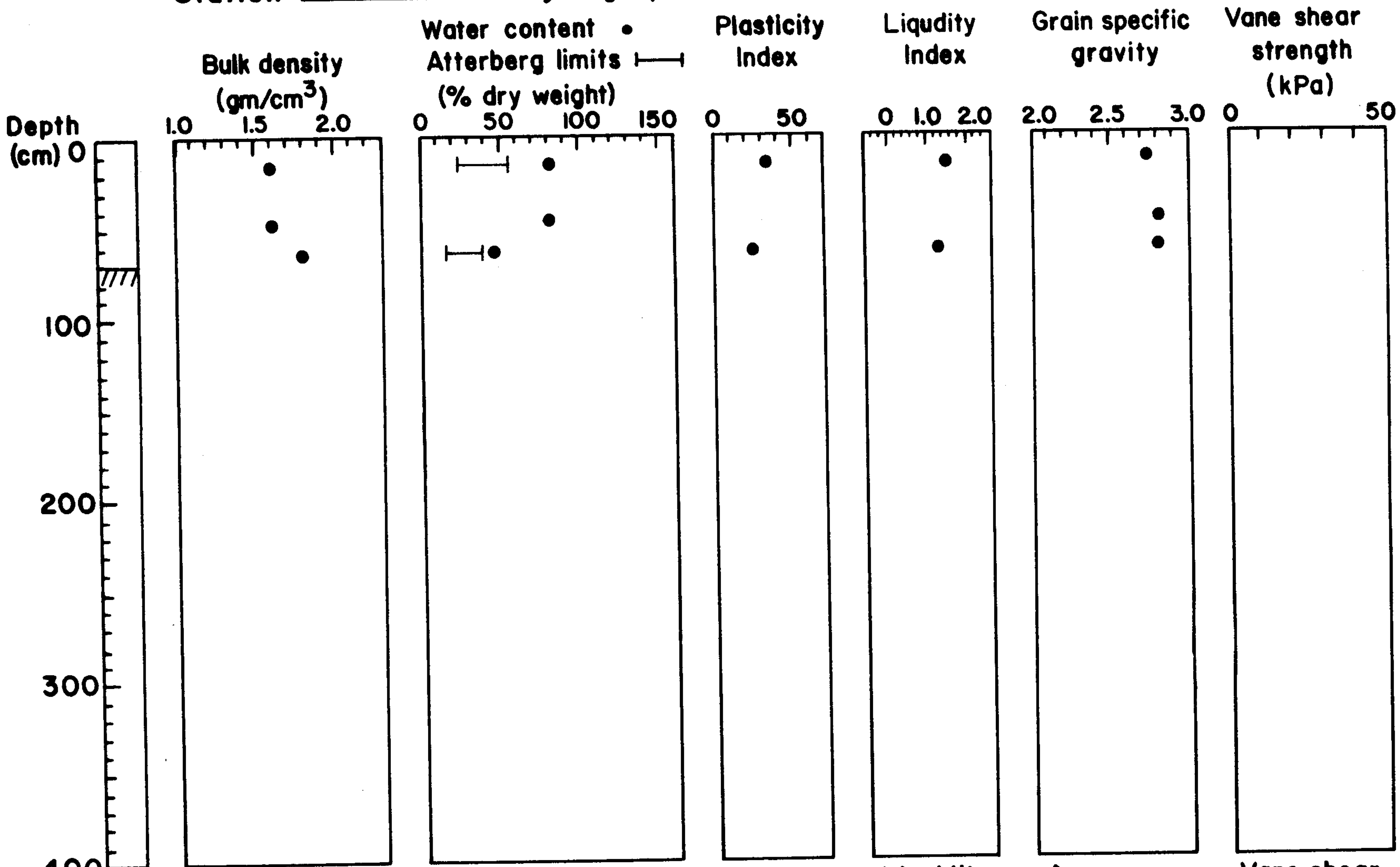

Bulk density at lm.: 1.87

Water content at lm.: 36

Average plastic limit: 20

Average liquid limit: 48

Average plasticity index: 27

Liquidity index at lm.: 1.17

Average grain specific gravity: 2.79

Vane shear strength at lm.:

Station 329 Physiographic area Chiniak Trough

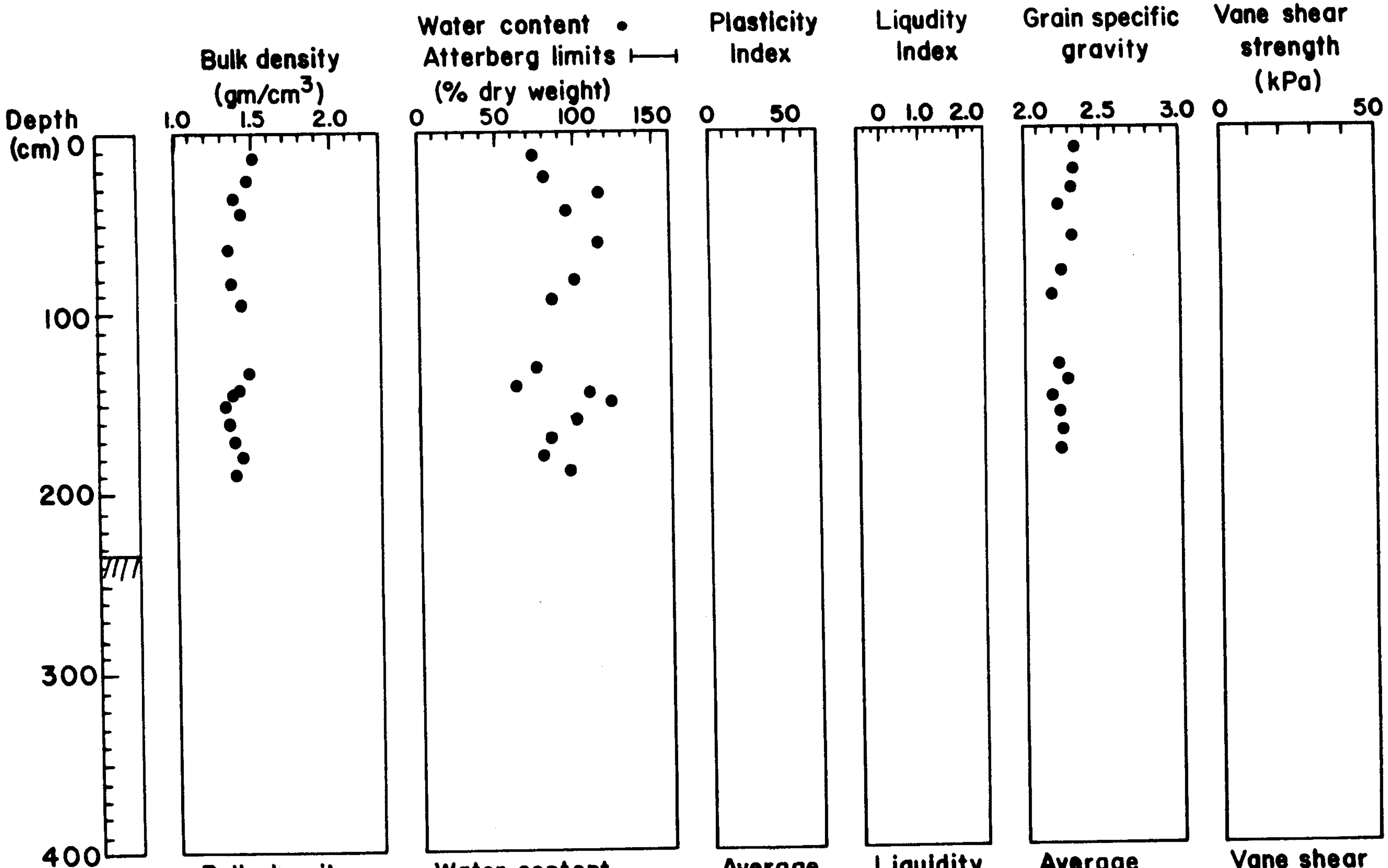

Bulk density at lm.: 1.39

Water content at lm.: 93

Average plastic limit: ______

Average liquid limit: ______

Average plasticity index: np

Liquidity index at lm.: ______

Average grain specific gravity: 2.26

Vane shear strength at lm.: ______

Station 336 Physiographic area Upper Continental Slope

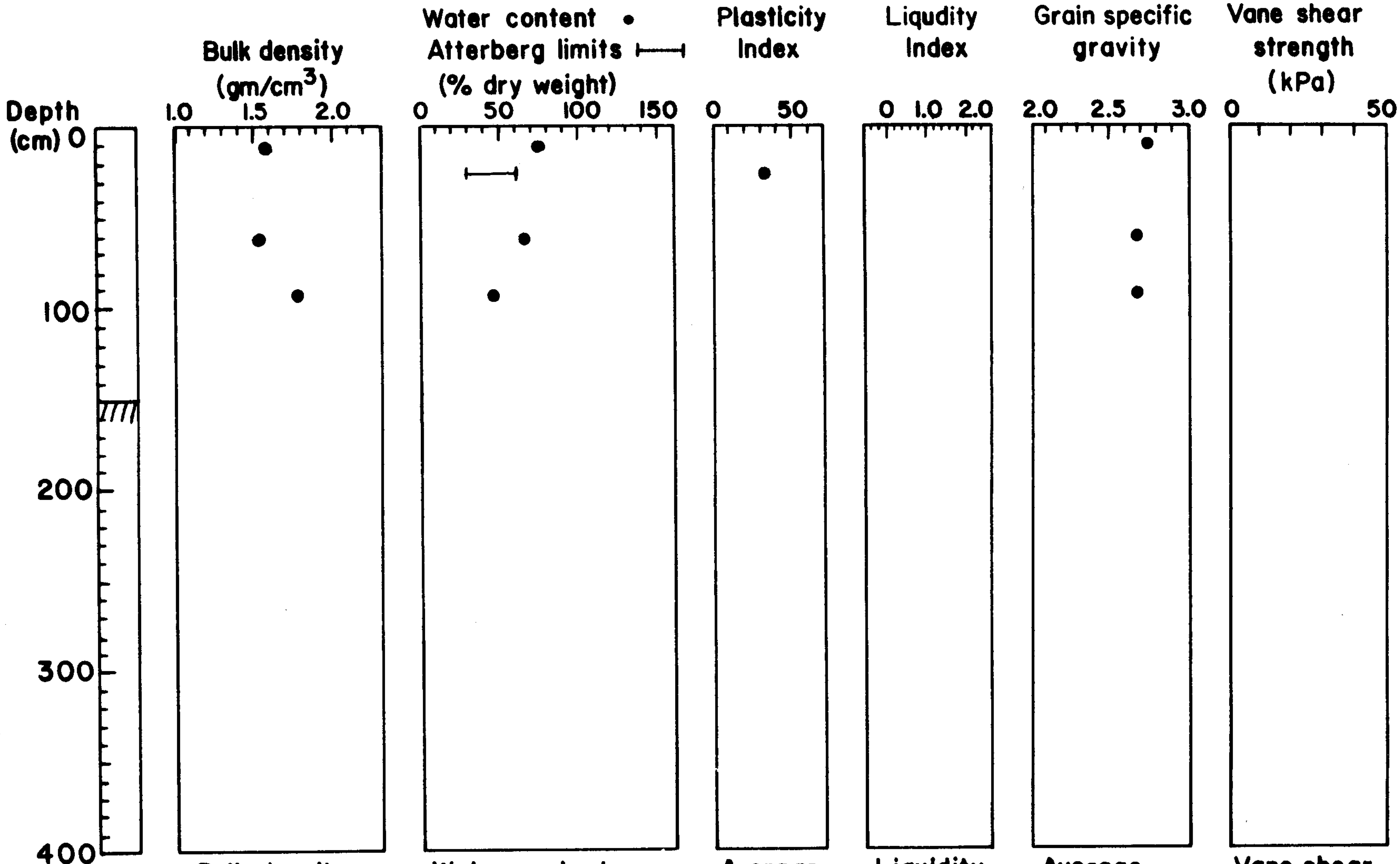

Bulk density at lm.: 1.74

Water content at lm.: 48

Average plastic limit: 29

Average liquid limit: 60

Average plasticity index: 29

Liquidity index at lm.: ______

Average grain specific gravity: 2.69

Vane shear strength at lm.: ______

Station 340 Physiographic area Upper Continental Slope

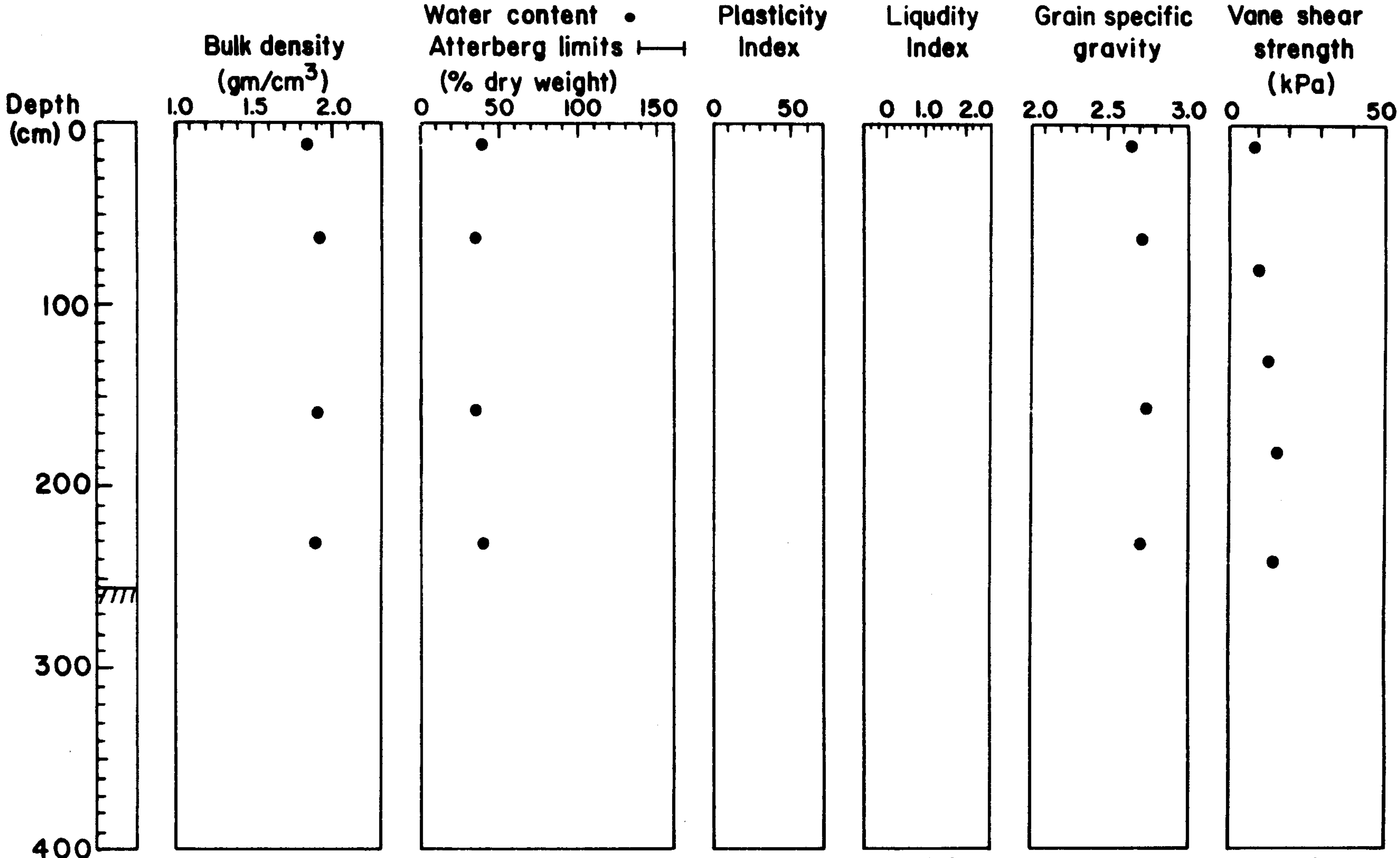

Bulk density at lm.: 1.91

Water content at lm.: 33
Average plastic limit: ______
Average liquid limit: ______

Average plasticity index: ______

Liquidity index at lm.: ______

Average grain specific gravity: 2.71

Vane shear strength at lm.: 11.29

Station 343 Physiographic area Kiliuda Trough

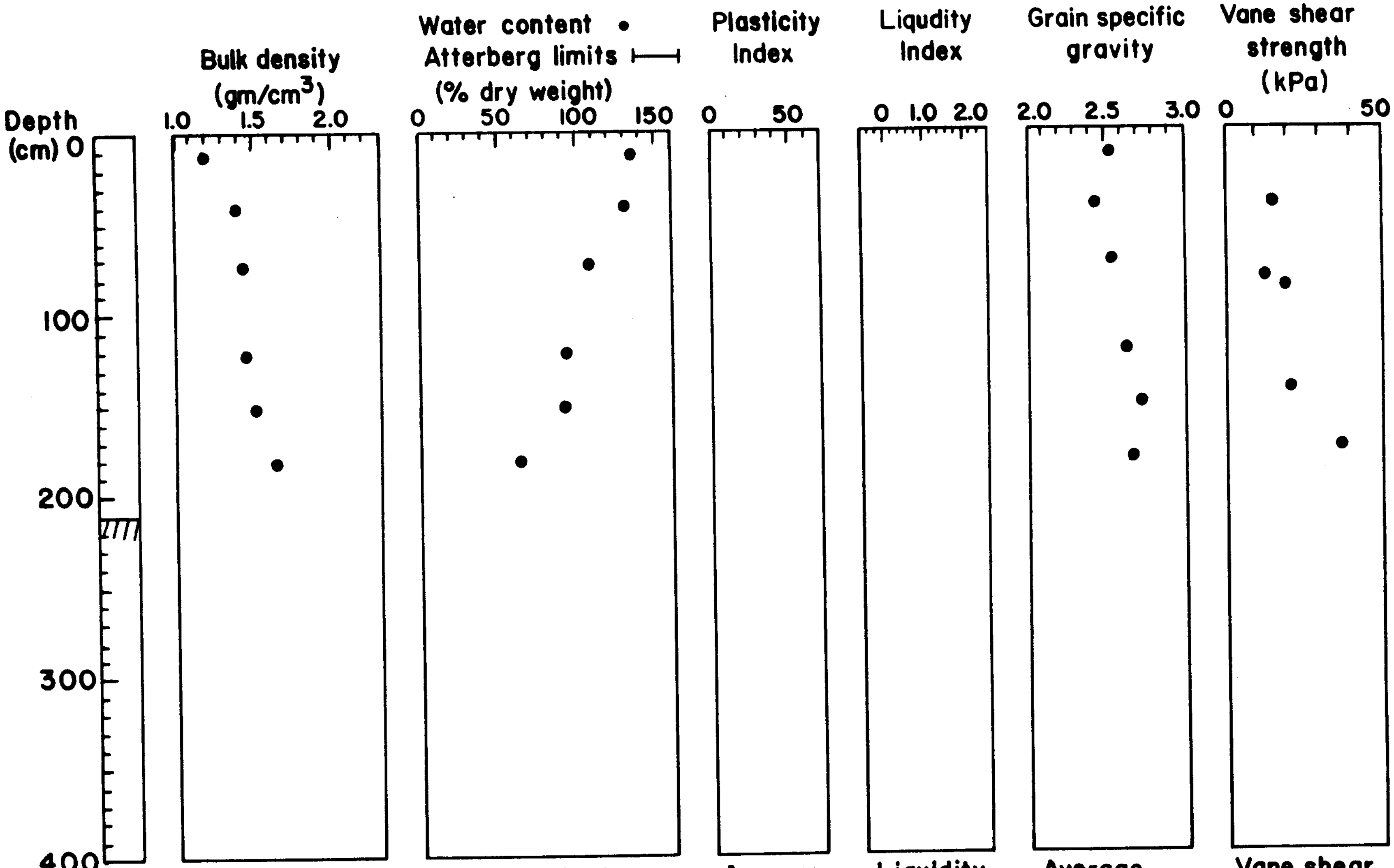

Bulk density at lm.: 143

Water content at lm.: 105

Average plastic limit: ______

Average liquid limit: ______

Average plasticity index: ______

Liquidity index at lm.: ______

Average grain specific gravity: 2.56

Vane shear strength at lm.: 19.69

Station 344 Physiographic area Kiliuda Trough

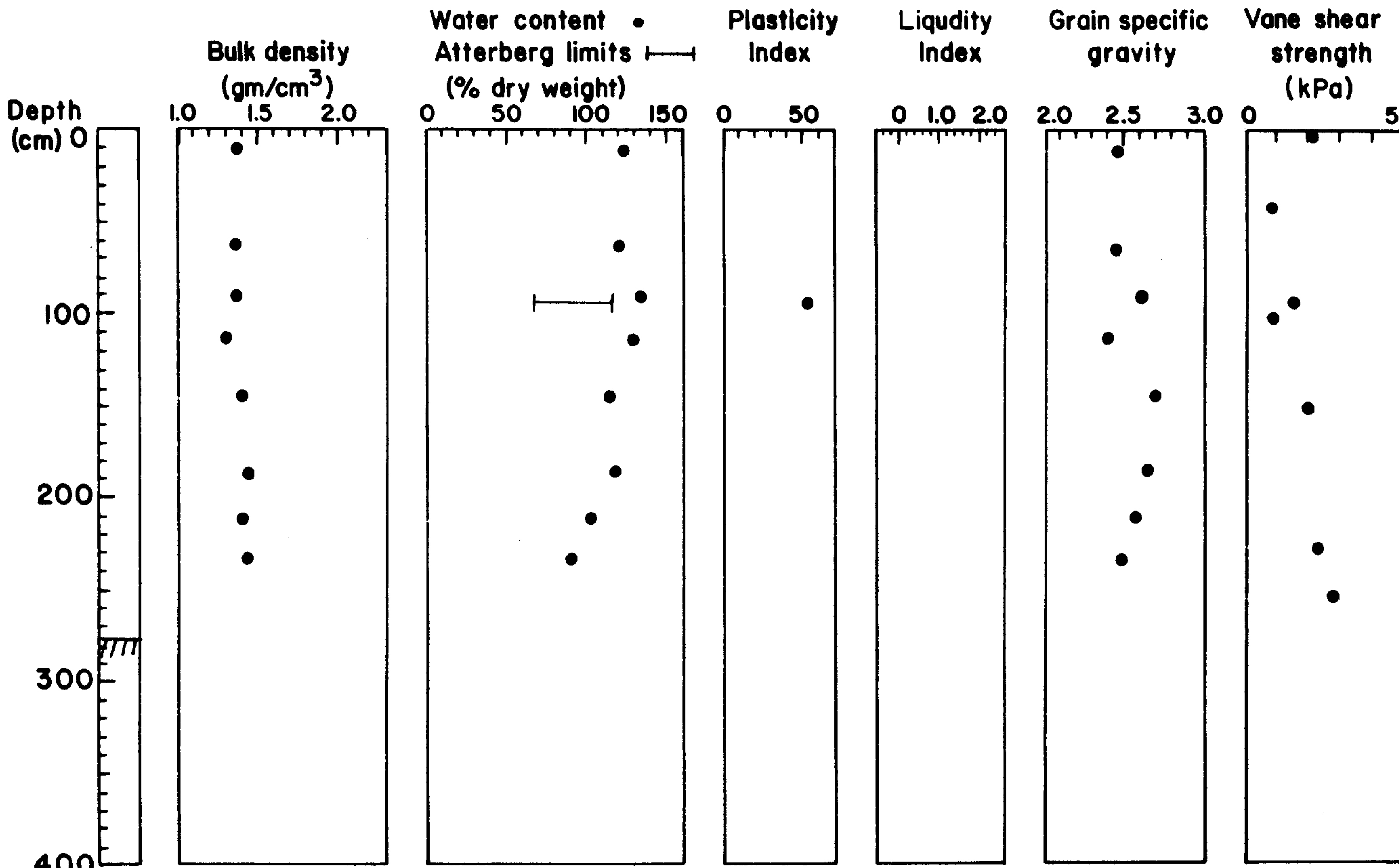

Bulk density at lm.: 1.37

Water content at lm.: 123

Average plastic limit: 68

Average liquid limit: 118

Average plasticity index: 50

Liquidity index at lm.:

Average grain specific gravity: 2.53

Vane shear strength at lm.: 16.71

Station 345 Physiographic area Kiliuda Trough

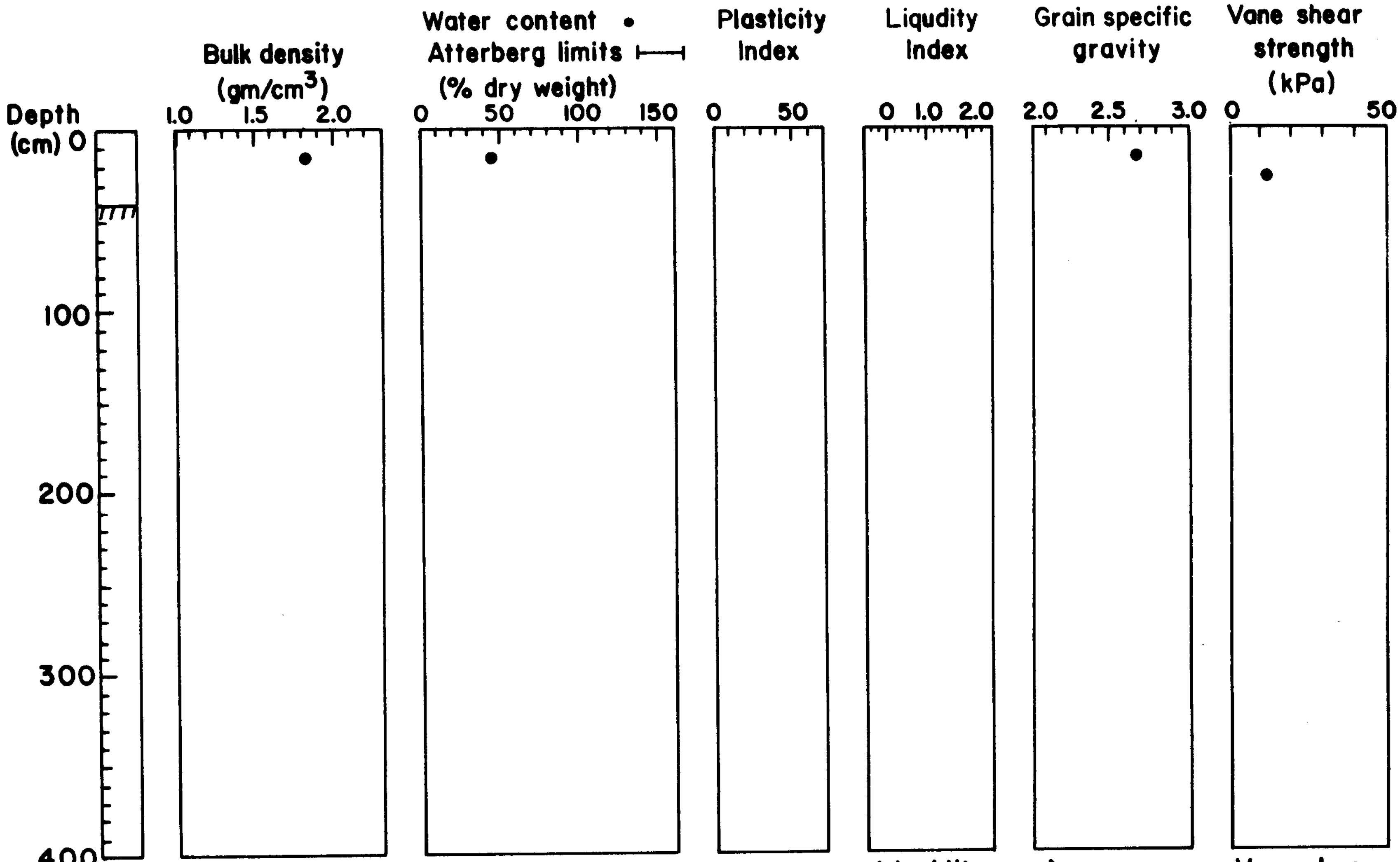

Bulk density at lm.: ________

Water content at lm.: ________
Average plastic limit: ________
Average liquid limit: ________

Average plasticity index: ________

Liquidity index at lm.: ________

Average grain specific gravity: ________

Vane shear strength at lm.: ________

Station 347 Physiographic area Kiliuda Trough

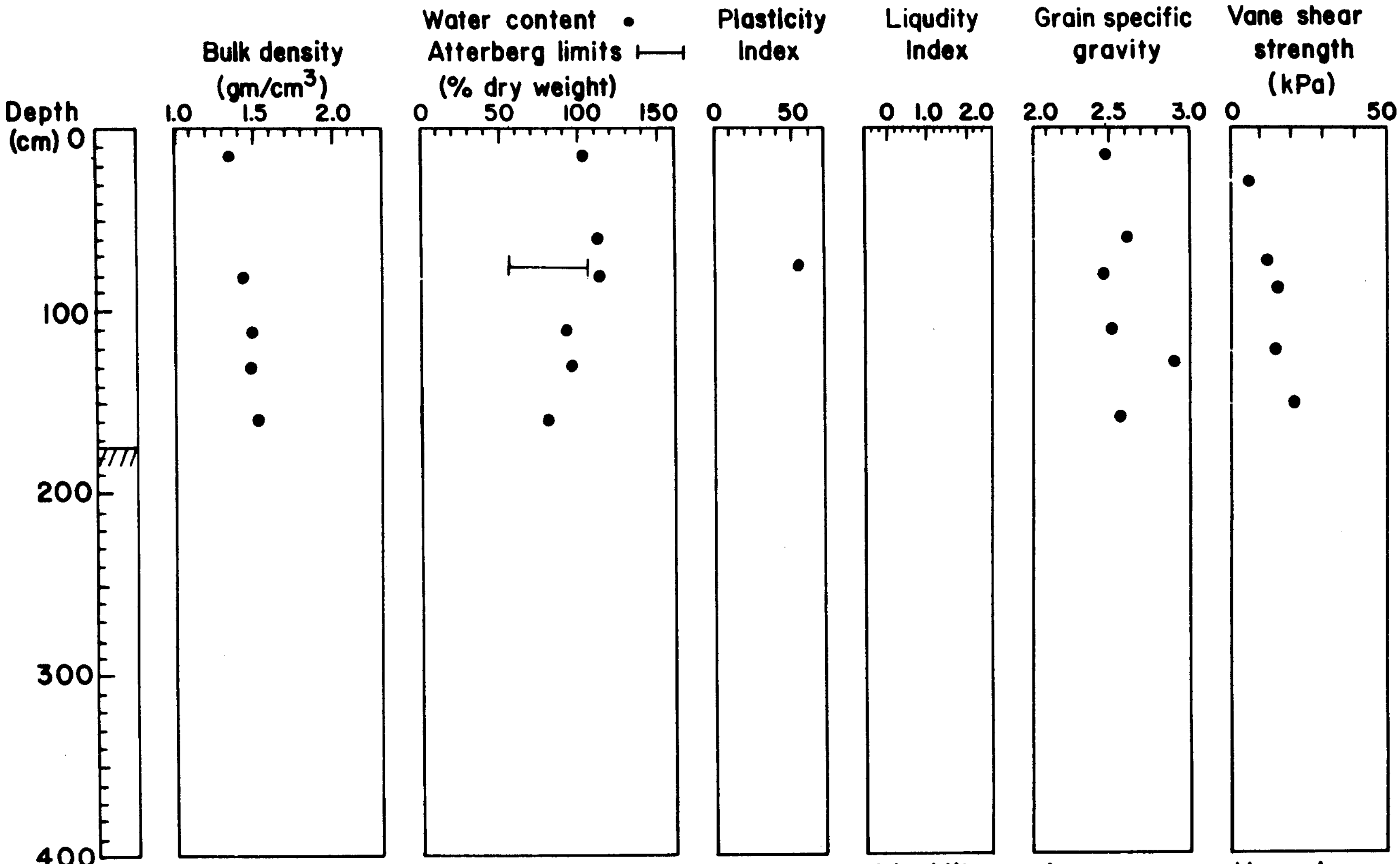

Bulk density at lm.: 1.44

Water content at lm.: 99

Average plastic limit:

Average liquid limit:

Average plasticity index:

Liquidity index at lm.:

Average grain specific gravity: 2.59

Vane shear strength at lm.: 14.10

Station 348 Physiographic area Kiliuda Trough

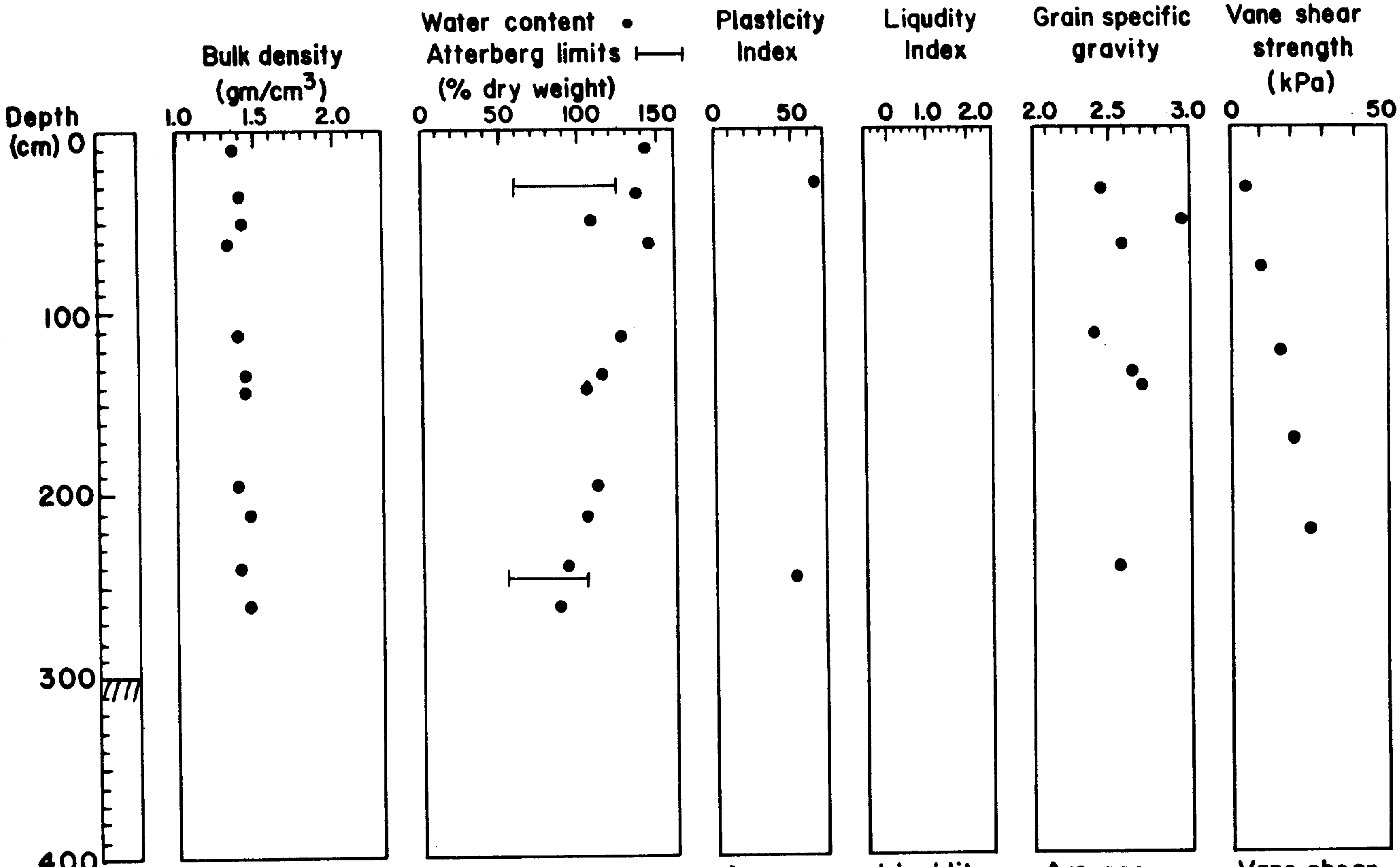

Bulk density at lm.: 1.34

Water content at lm.: 122

Average plastic limit: 56

Average liquid limit: 114

Average plasticity index: 58

Liquidity index at lm.: ____

Average grain specific gravity: 2.59

Vane shear strength at lm.: 12.00

Station 349 Physiographic area Kiliuda Trough

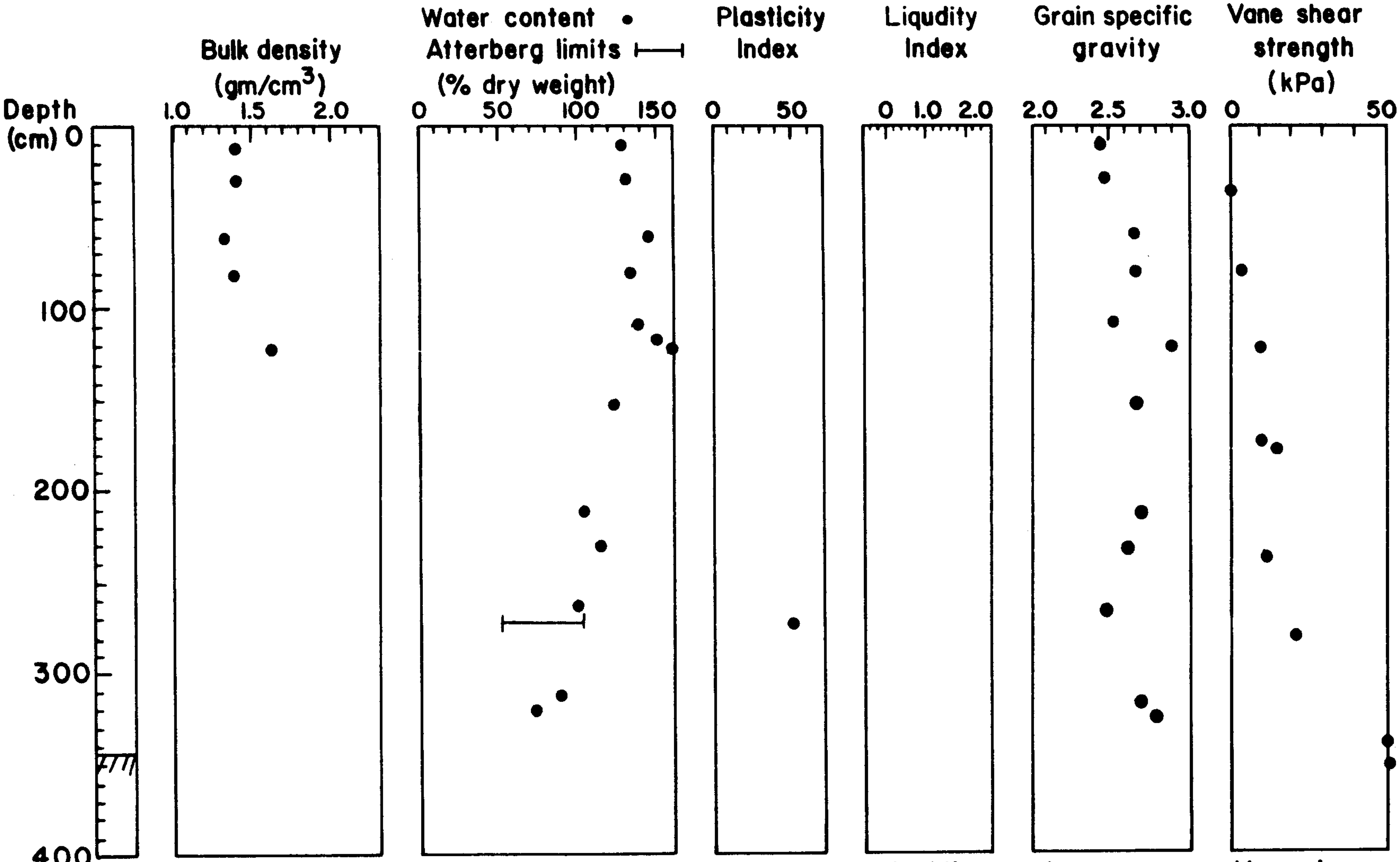

Bulk density at lm.: 1.38

Water content at lm.: 132

Average plastic limit: 52

Average liquid limit: 104

Average plasticity index: 52

Liquidity index at lm.:

Average grain specific gravity: 2.63

Vane shear strength at lm.: 3.50

Station 350 Physiographic area Kiliuda Trough

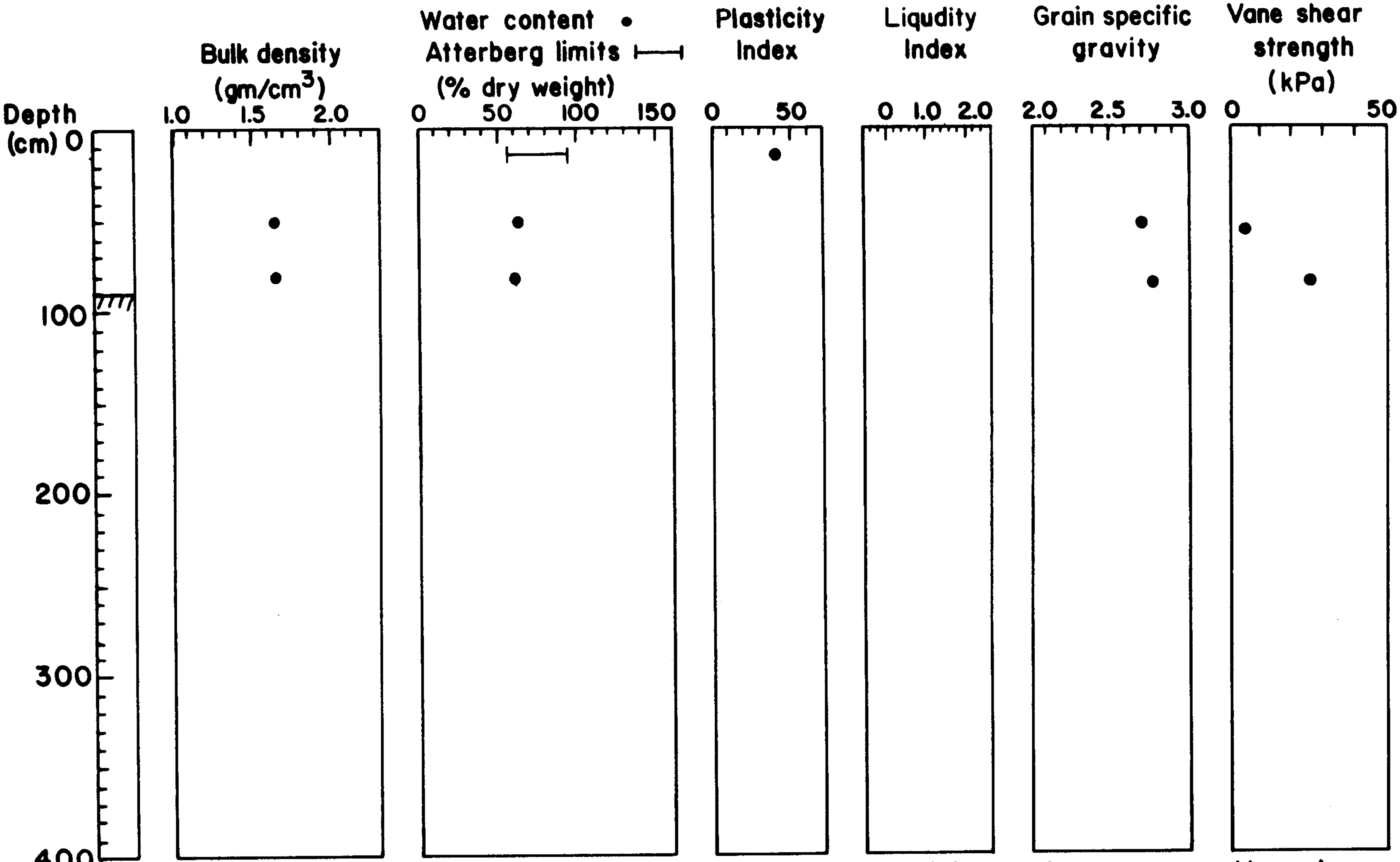

Bulk density at lm.: ______

Water content at lm.: ______

Average plastic limit: ______

Average liquid limit: ______

Average plasticity index: ______

Liquidity index at lm.: ______

Average grain specific gravity: 2.75

Vane shear strength at lm.: ______

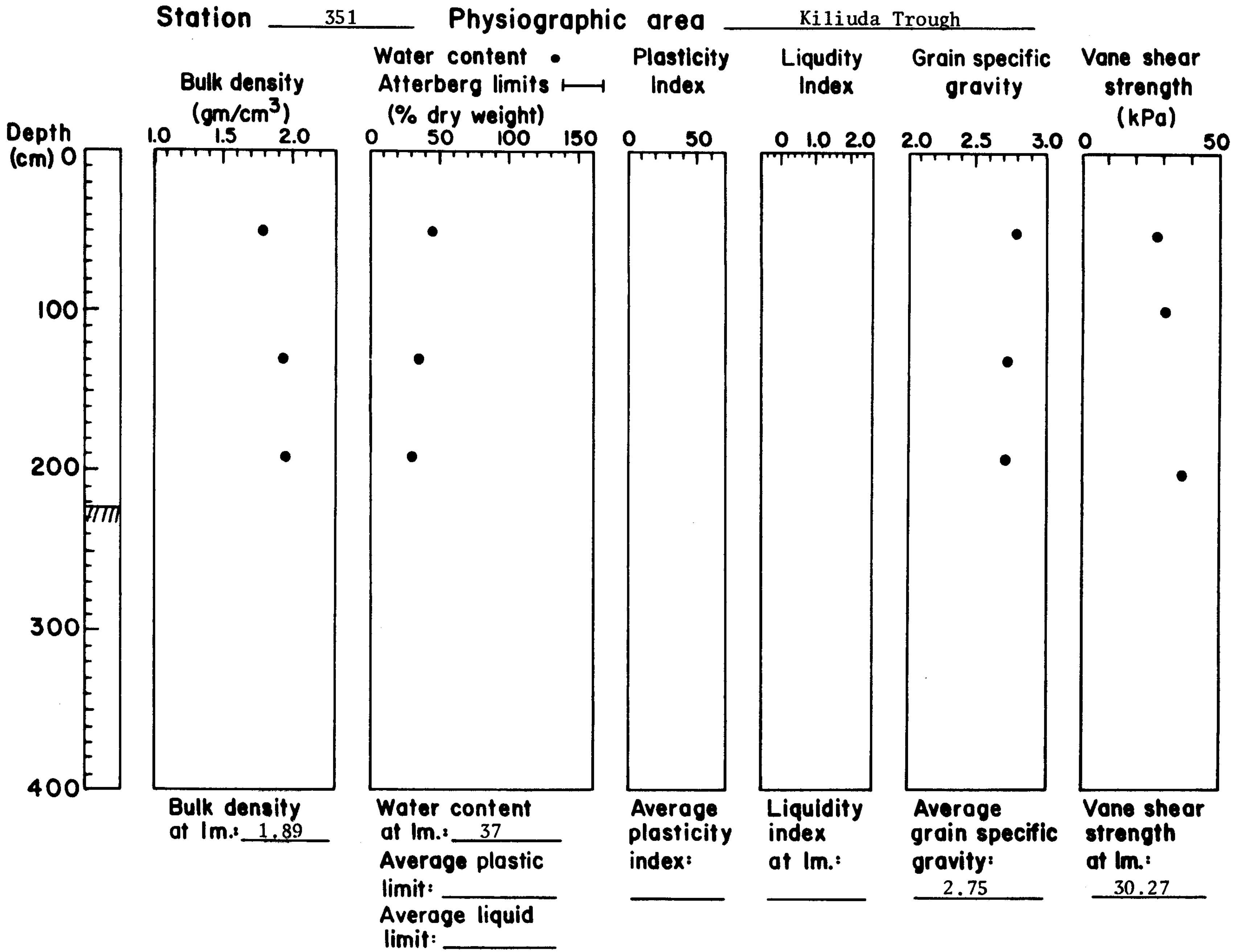
Station 351 Physiographic area Kiliuda Trough
Depth (cm)
0
100
200
300
400
Bulk density (gm/cm3)
1.0 1.5 2.0
Water content •
Atterberg limits ⊢⊣
(% dry weight)
0 50 100 150
Plasticity Index
0 50
Liqudity Index
0 1.0 2.0
Grain specific gravity
2.0 2.5 3.0
Vane shear strength (kPa)
0 50
Bulk density at lm.: 1.89
Water content at lm.: 37
Average plastic limit:
Average liquid limit:
Average plasticity index:
Liquidity index at lm.:
Average grain specific gravity: 2.75
Vane shear strength at lm.: 30.27

Station 355 Physiographic area Sitkinak Trough

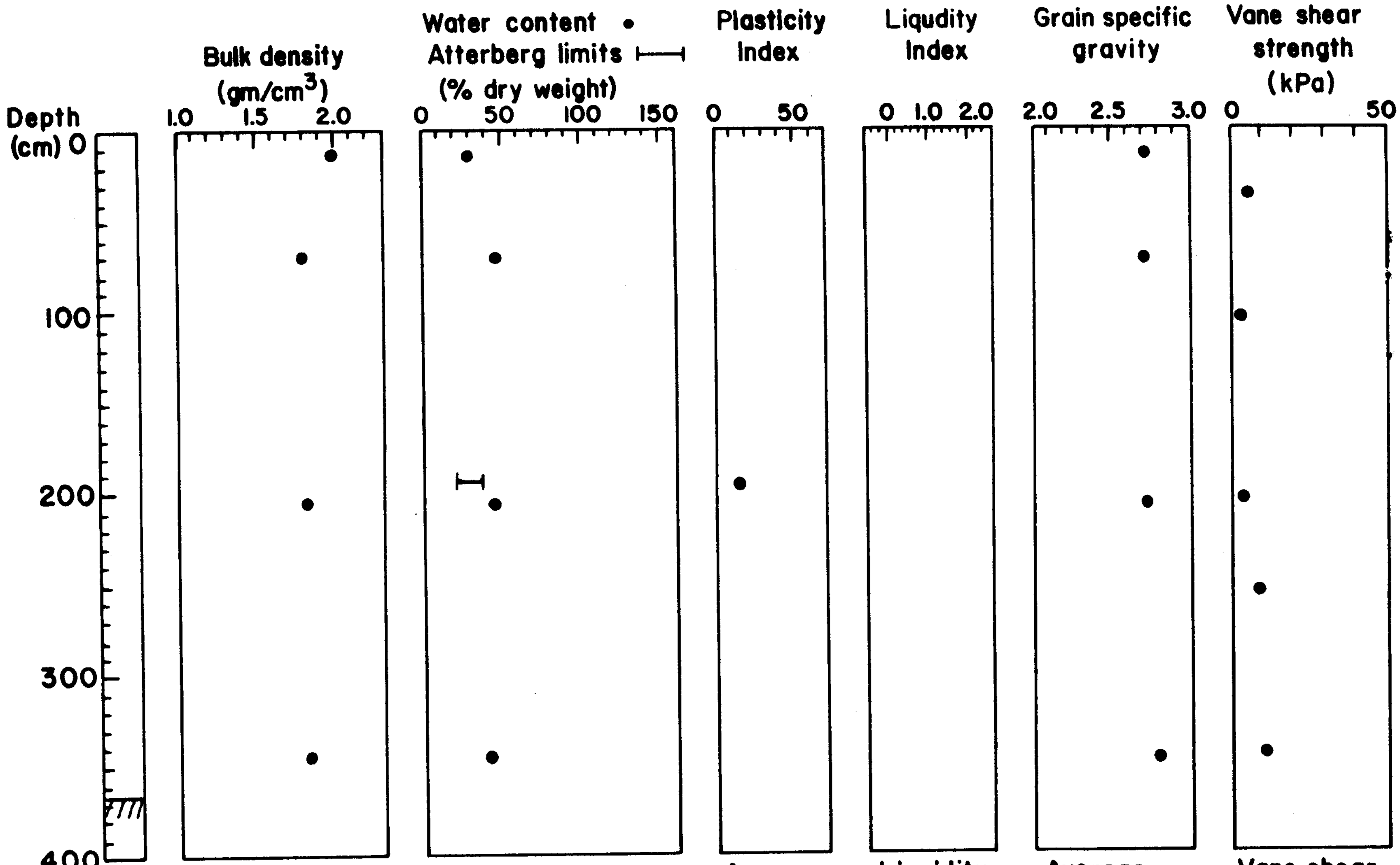

Bulk density at lm.: 1.88

Water content at lm.: 35

Average plastic limit: ____

Average liquid limit: ____

Average plasticity index: ____

Liquidity index at lm.: ____

Average grain specific gravity: 2.75

Vane shear strength at lm.: 5.11

Station 356 Physiographic area Sitkinak Trough

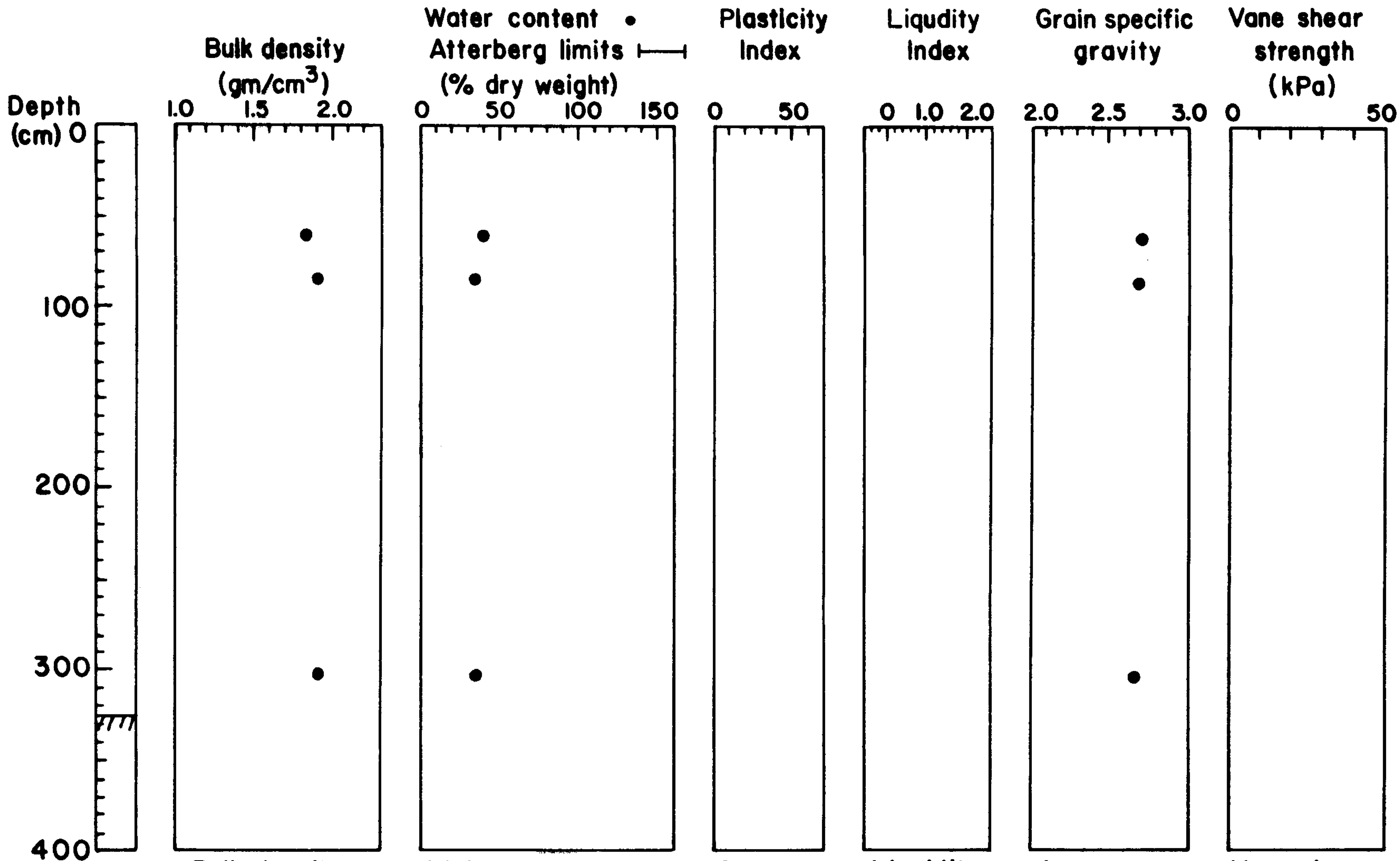

Bulk density at lm.: 1.86

Water content at lm.: 36

Average plastic limit:

Average liquid limit:

Average plasticity index:

Liquidity index at lm.:

Average grain specific gravity: 2.70

Vane shear strength at lm.:

Station 357 Physiographic area Sitkinak Trough

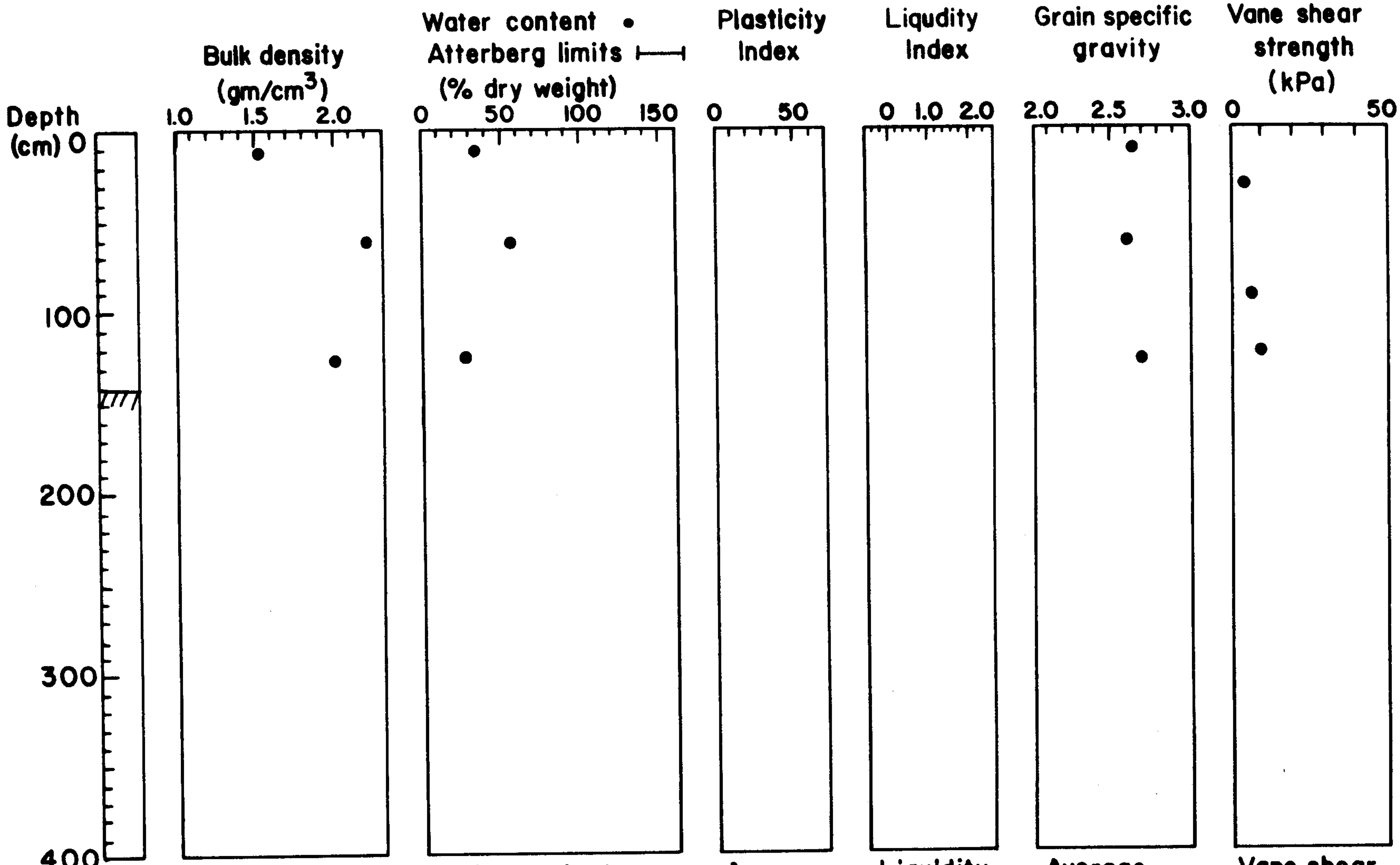

Bulk density at lm.: 1.86

Water content at lm.: 36

Average plastic limit: ____

Average liquid limit: ____

Average plasticity index: ____

Liquidity index at lm.: ____

Average grain specific gravity: 2.65

Vane shear strength at lm.: 7.44

Station 432 Physiographic area Chiniak Trough

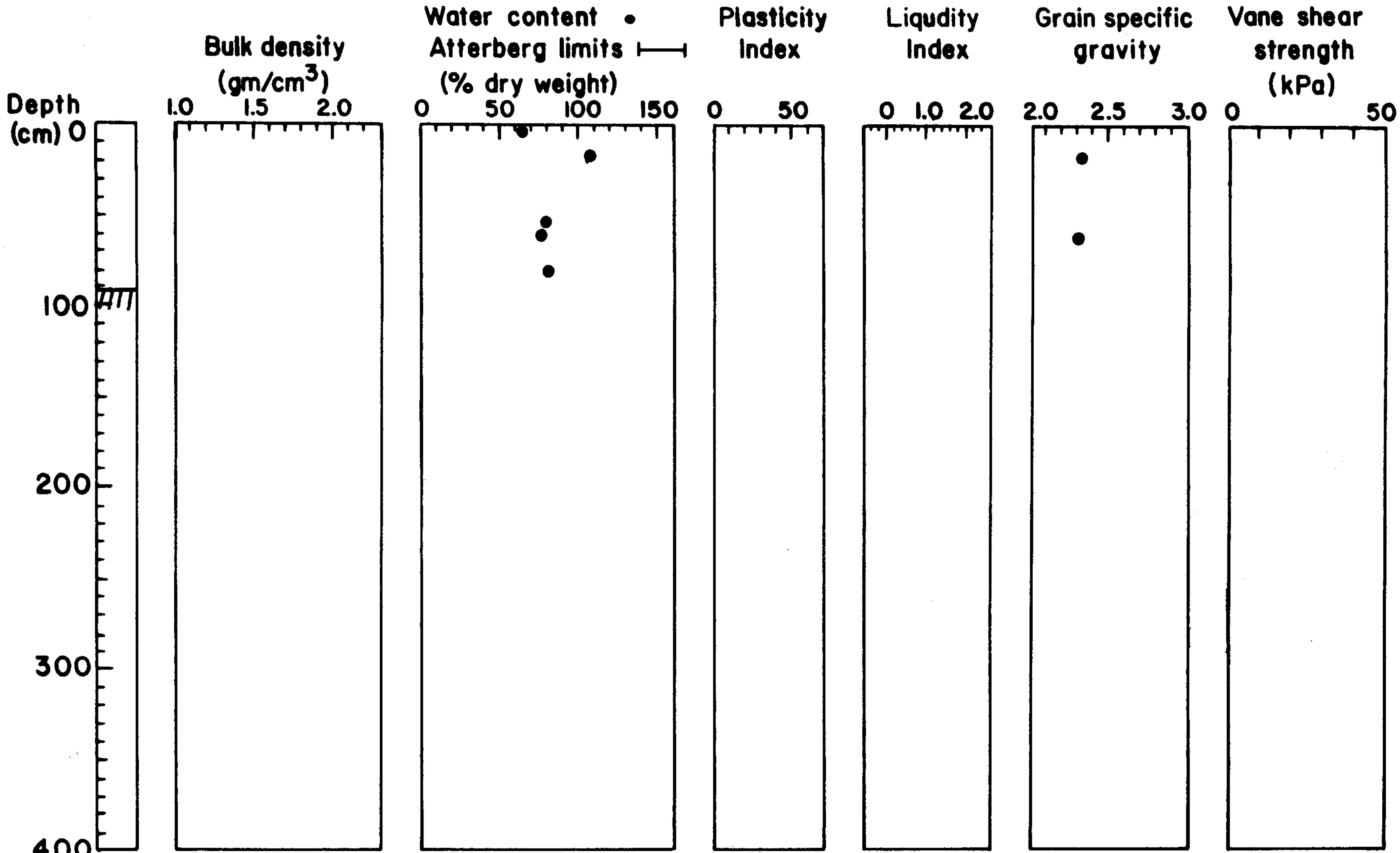

Bulk density at lm.: 1.47

Water content at lm.: 81

Average plastic limit: ______

Average liquid limit: ______

Average plasticity index: ______

Liquidity index at lm.: ______

Average grain specific gravity: 2.32

Vane shear strength at lm.: ______

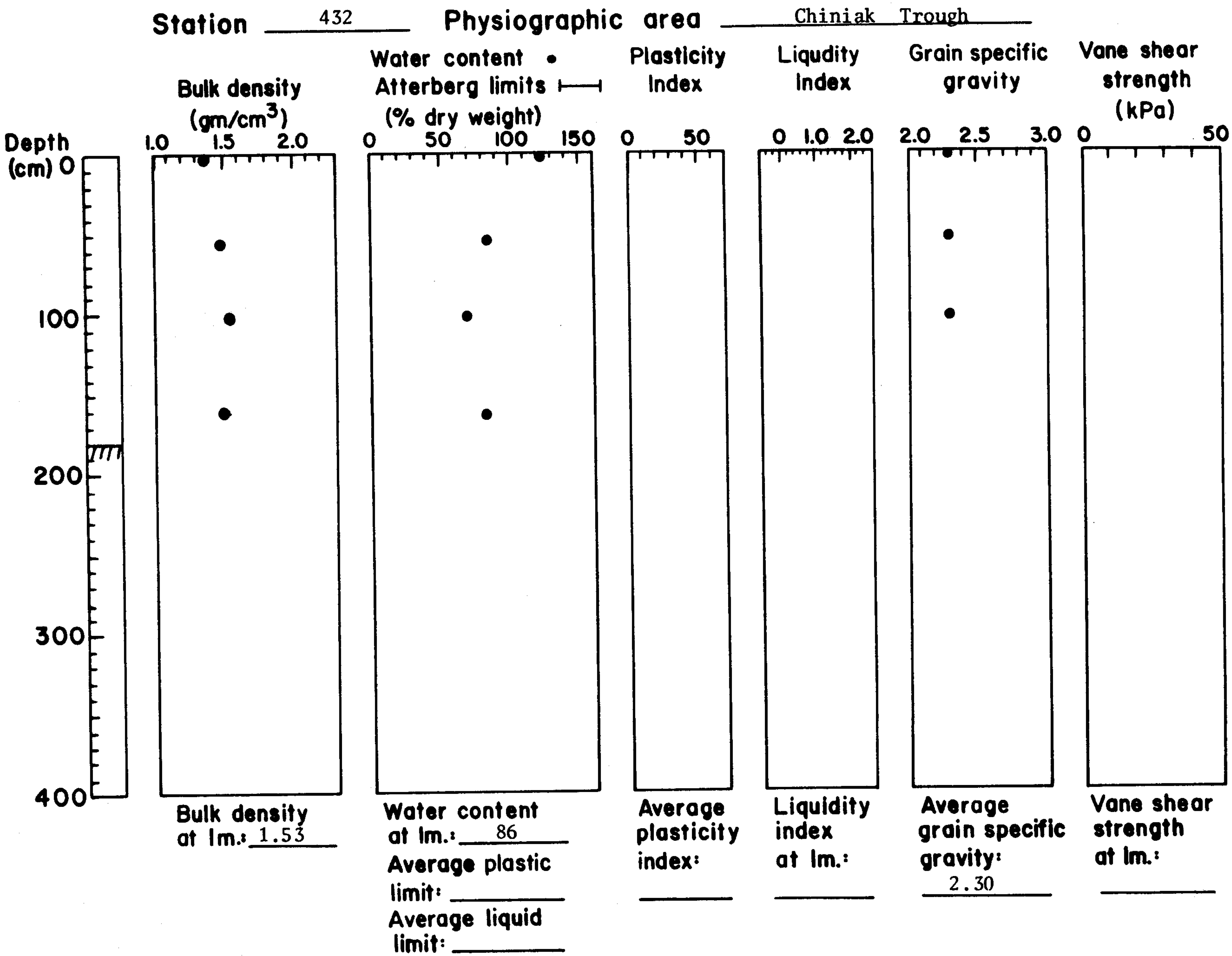

Station 432 Physiographic area Chiniak Trough
Depth (cm)
0
100
200
300
400
Bulk density (gm/cm3)
1.0 1.5 2.0
Water content •
Atterberg limits ⊢—⊣
(% dry weight)
0 50 100 150
Plasticity index
0 50
Liqudity index
0 1.0 2.0
Grain specific gravity
2.0 2.5 3.0
Vane shear strength (kPa)
0 50
Bulk density at lm.: 1.53
Water content at lm.: 86
Average plastic limit:
Average liquid limit:
Average plasticity index:
Liquidity index at lm.:
Average grain specific gravity: 2.30
Vane shear strength at lm.:

Station 433 Physiographic area Chiniak Trough

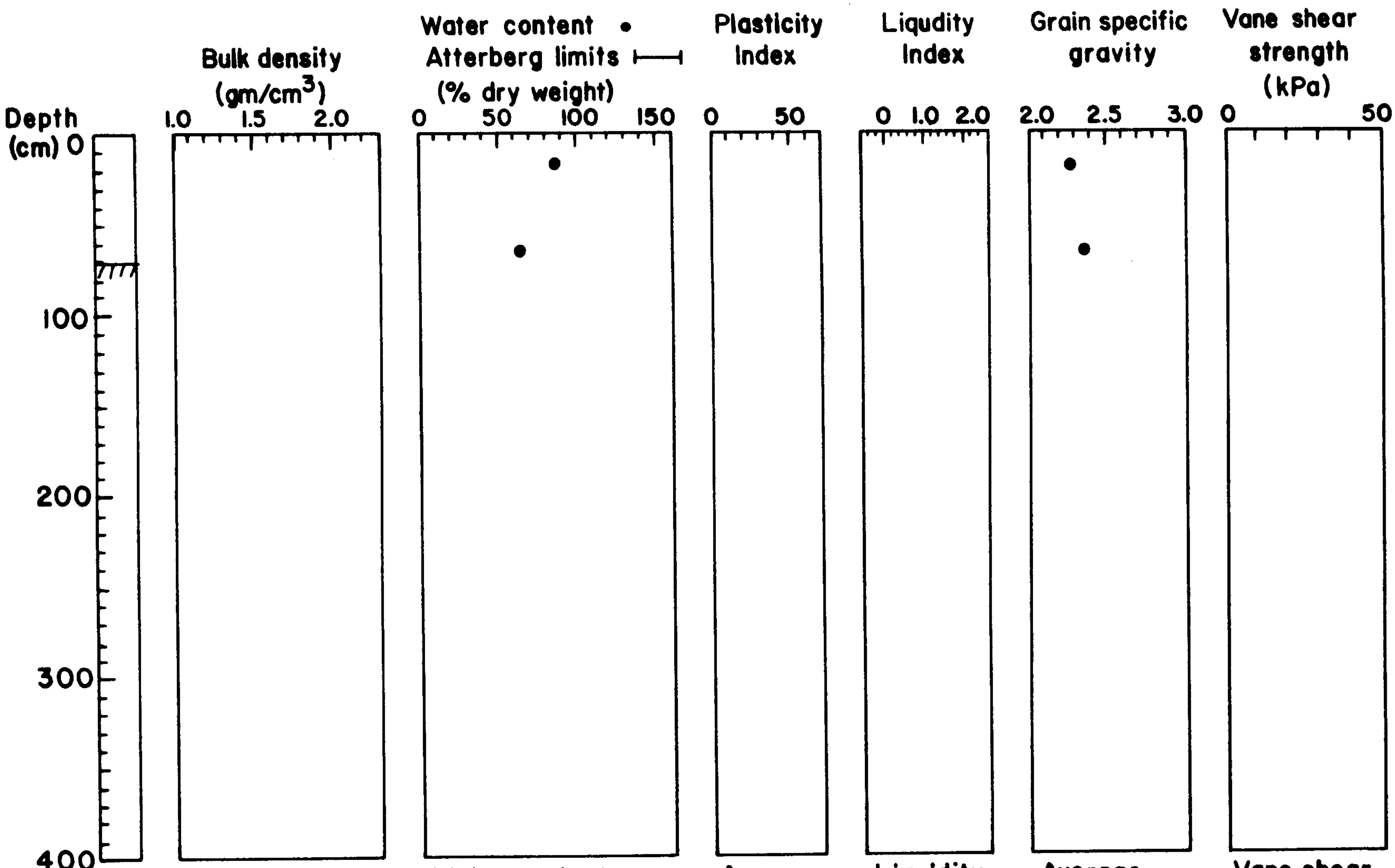

Bulk density at lm.: ______

Water content at lm.: 67

Average plastic limit: ______

Average liquid limit: ______

Average plasticity index: ______

Liquidity index at lm.: ______

Average grain specific gravity: 2.30

Vane shear strength at lm.: ______

Station 433 Physiographic area Chiniak Trough

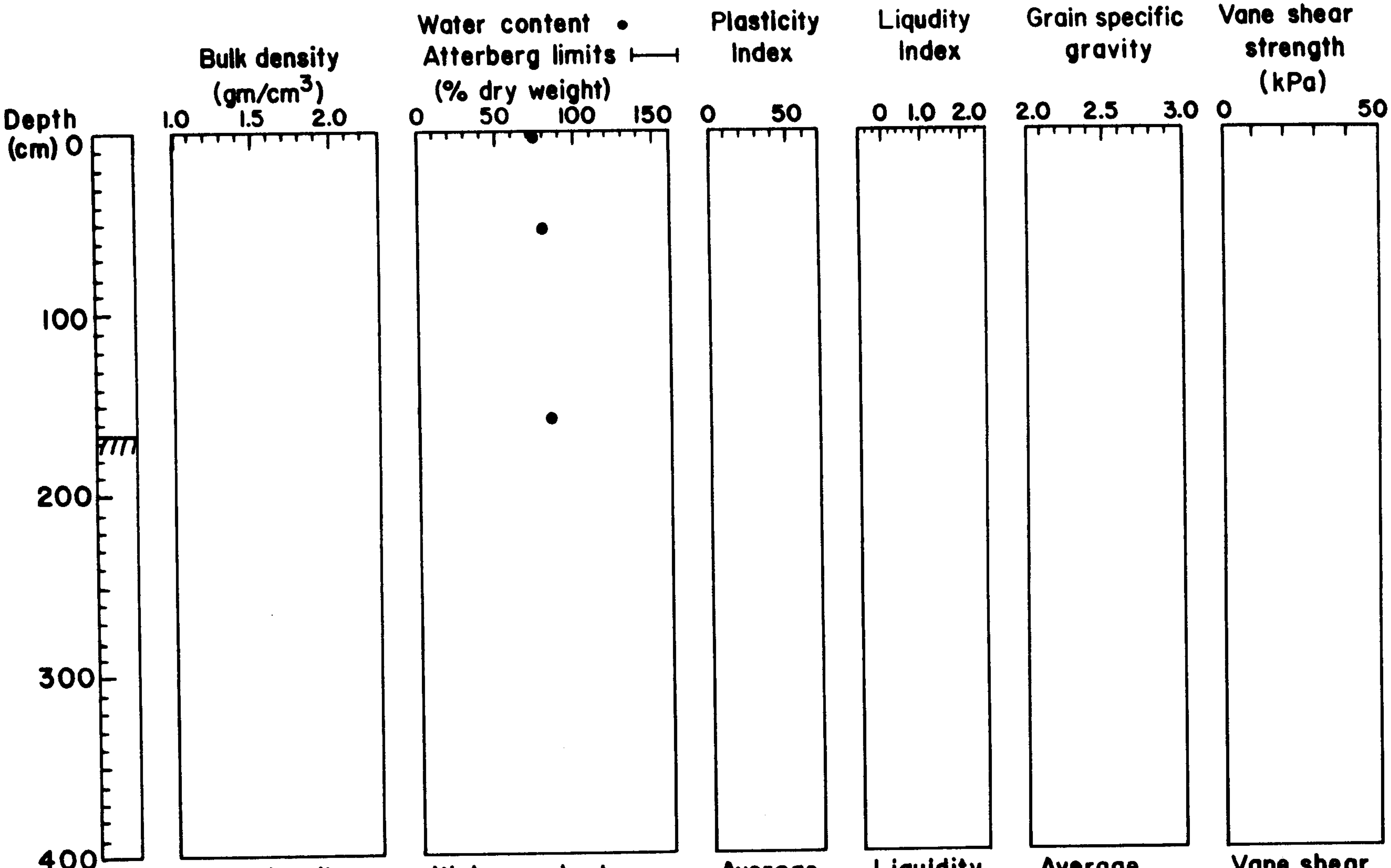

Bulk density at lm.: ______

Water content at lm.: 67

Average plastic limit: ______

Average liquid limit: ______

Average plasticity index: ______

Liquidity index at lm.: ______

Average grain specific gravity: 2.31

Vane shear strength at lm.: ______

Station 434 Physiographic area Chiniak Trough

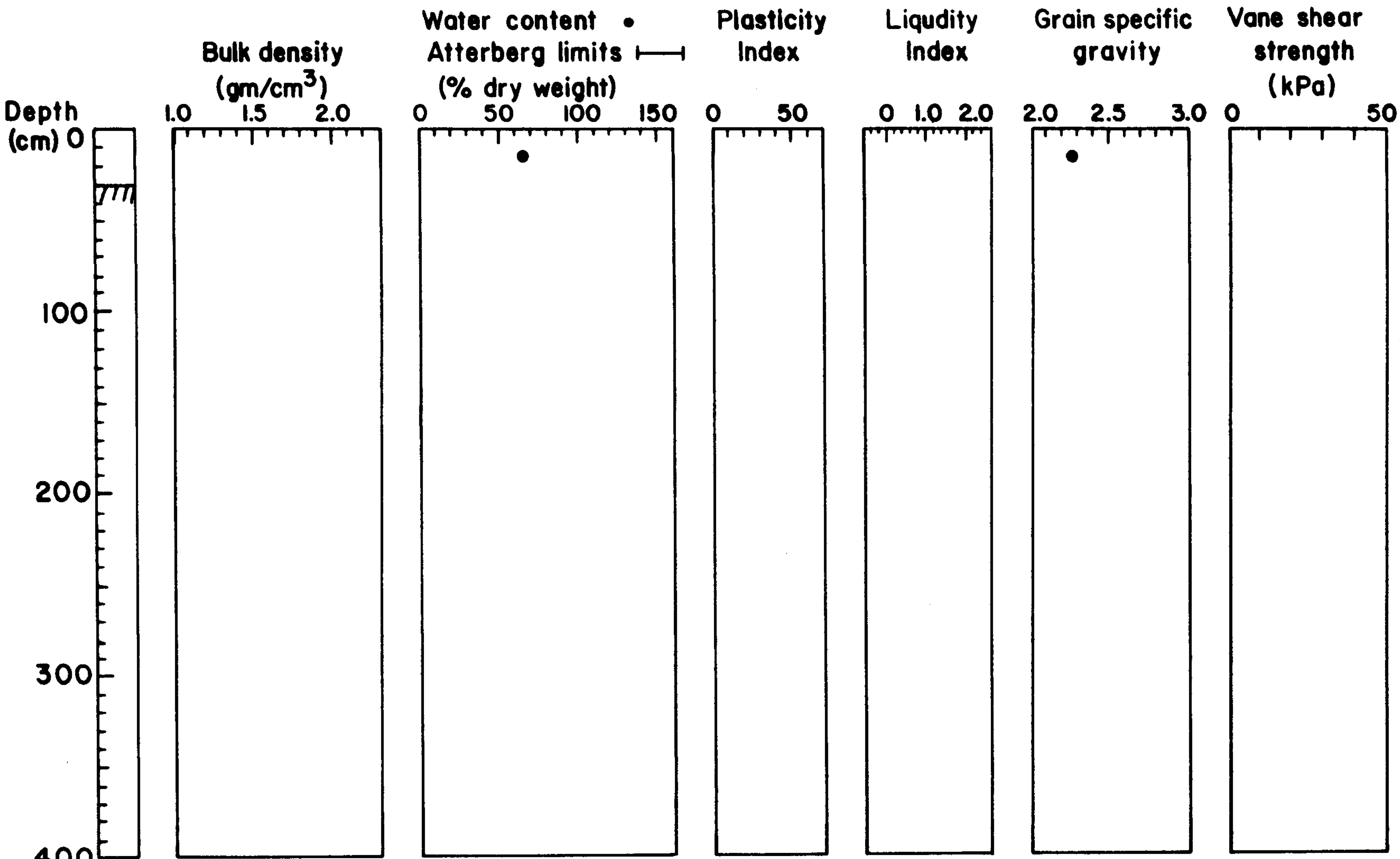

Bulk density at lm.: ______

Water content at lm.: ______

Average plastic limit: ______

Average liquid limit: ______

Average plasticity index: ______

Liquidity index at lm.: ______

Average grain specific gravity: ______

Vane shear strength at lm.: ______

Station 435 Physiographic area Chiniak Trough

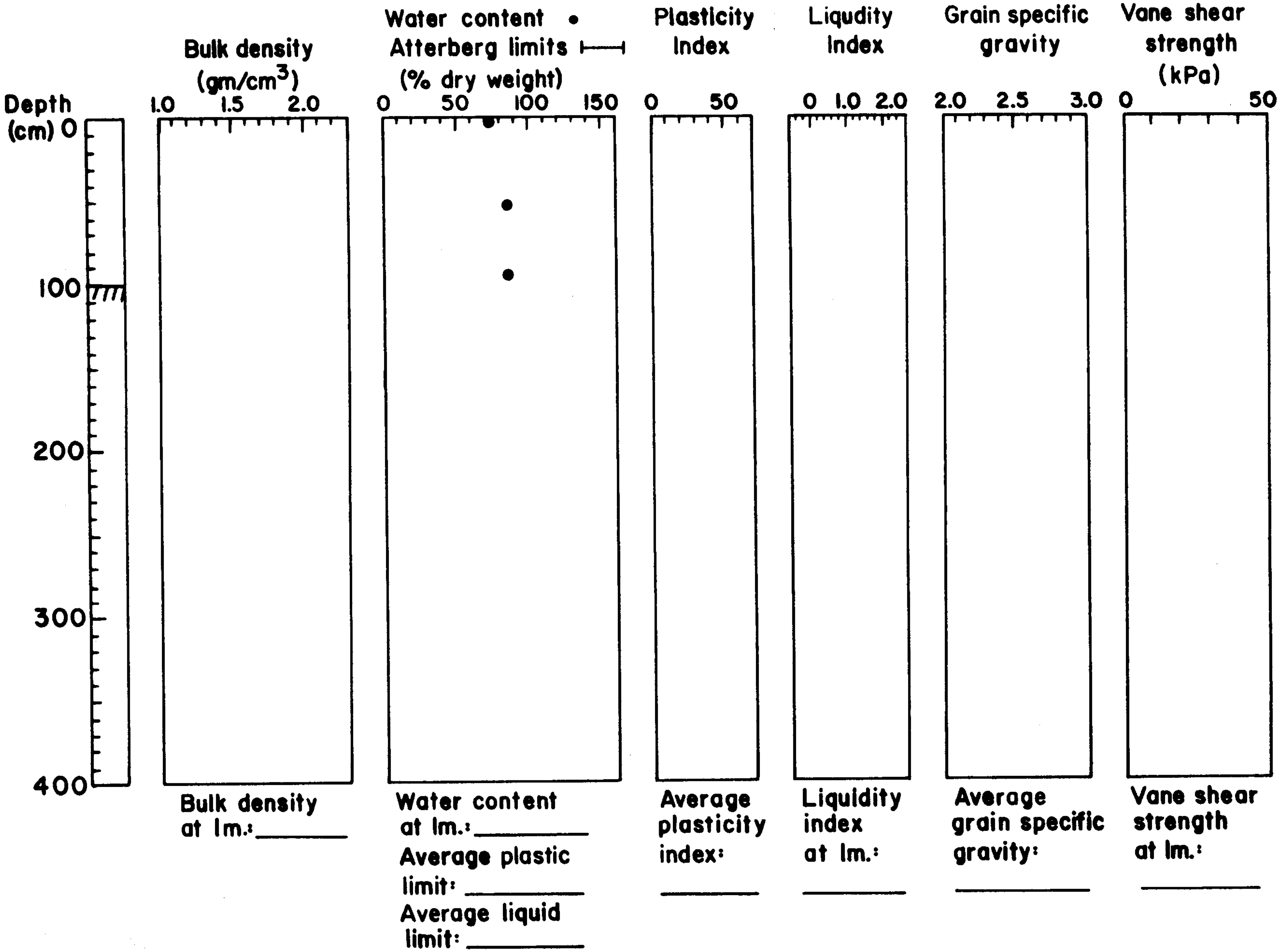

Station 439 **Physiographic area** Kiliuda Trough

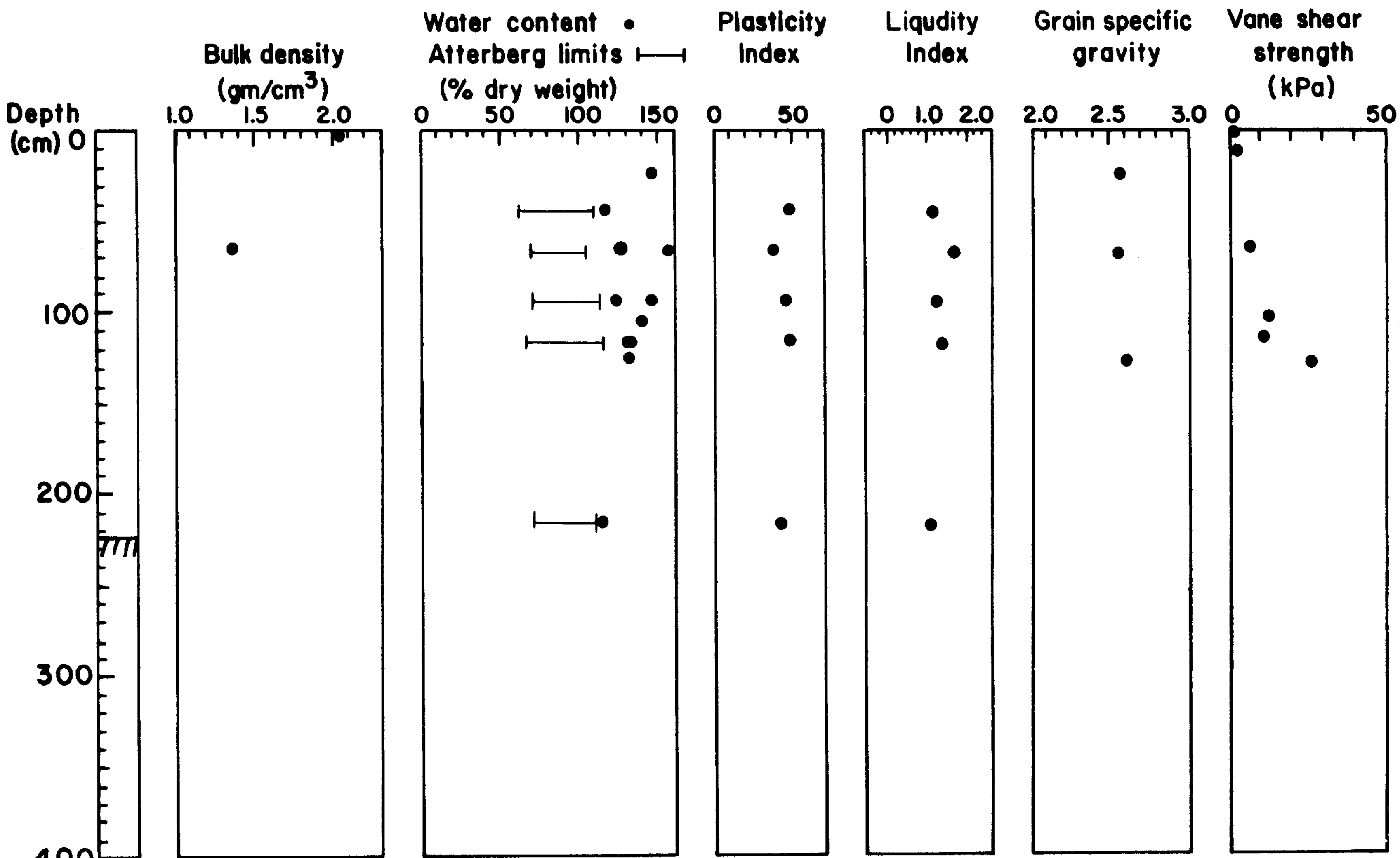

Bulk density at lm.: 1.37

Water content at lm.: 133

Average plastic limit: 67

Average liquid limit: 110

Average plasticity index: 43

Liquidity index at lm.: 1.31

Average grain specific gravity: 2.57

Vane shear strength at lm.: 10.12

Station 439 Physiographic area Kiliuda Trough

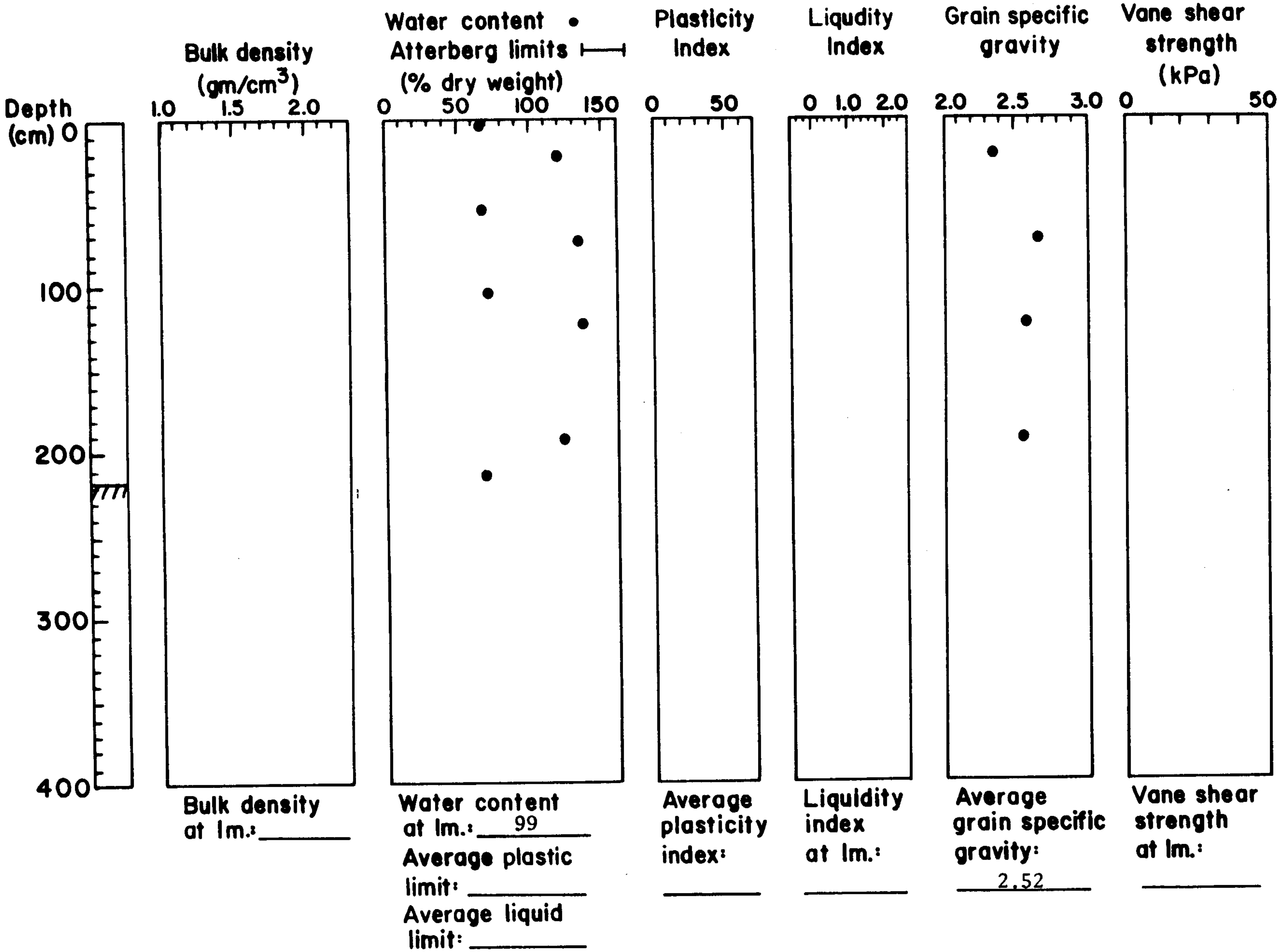

Station 440 Physiographic area Kiliuda Trough

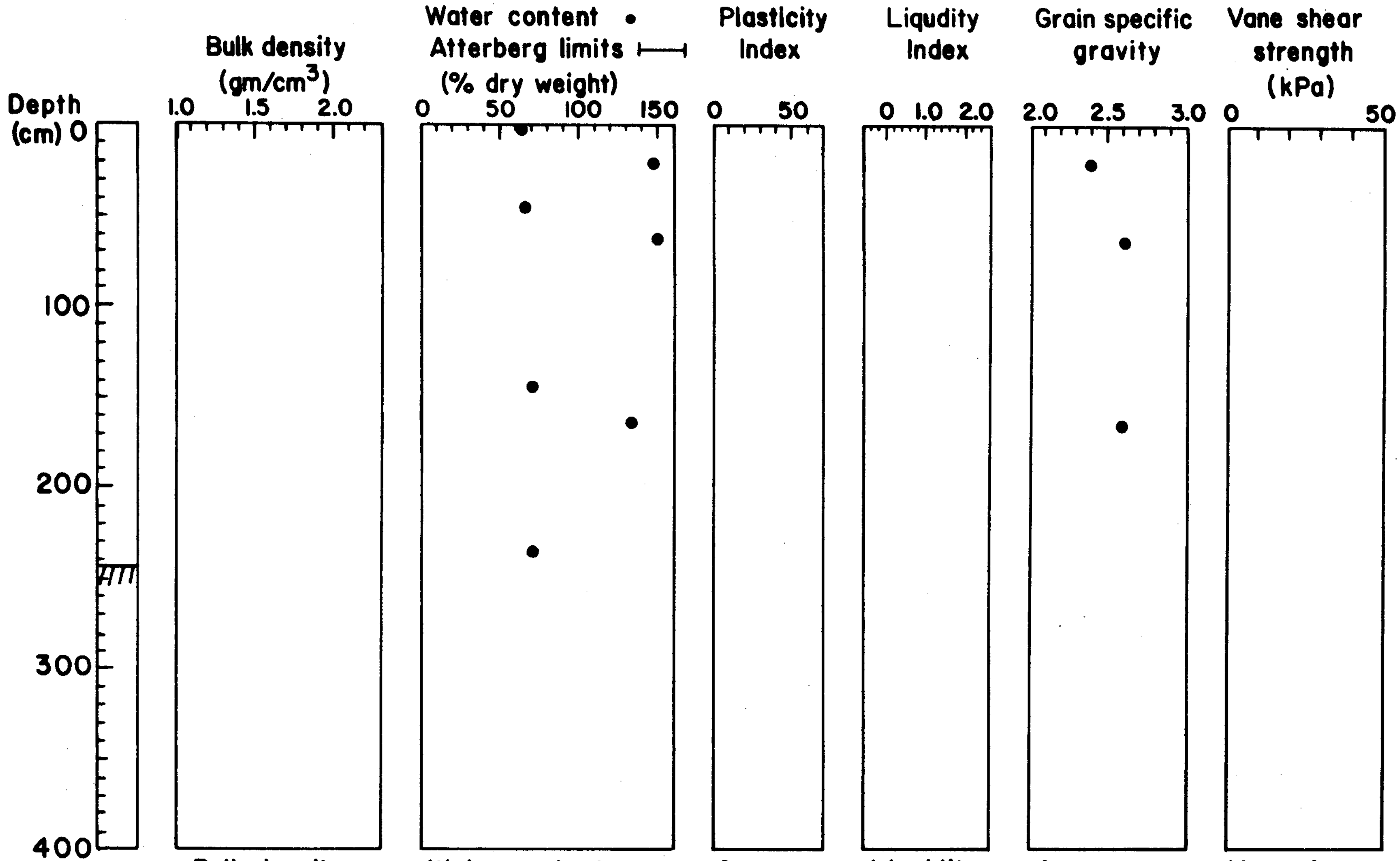

Bulk density at lm.: ______

Water content at lm.: 100

Average plastic limit: ______

Average liquid limit: ______

Average plasticity index: ______

Liquidity index at lm.: ______

Average grain specific gravity: 2.52

Vane shear strength at lm.: ______

Station 441 Physiographic area Kiliuda Trough

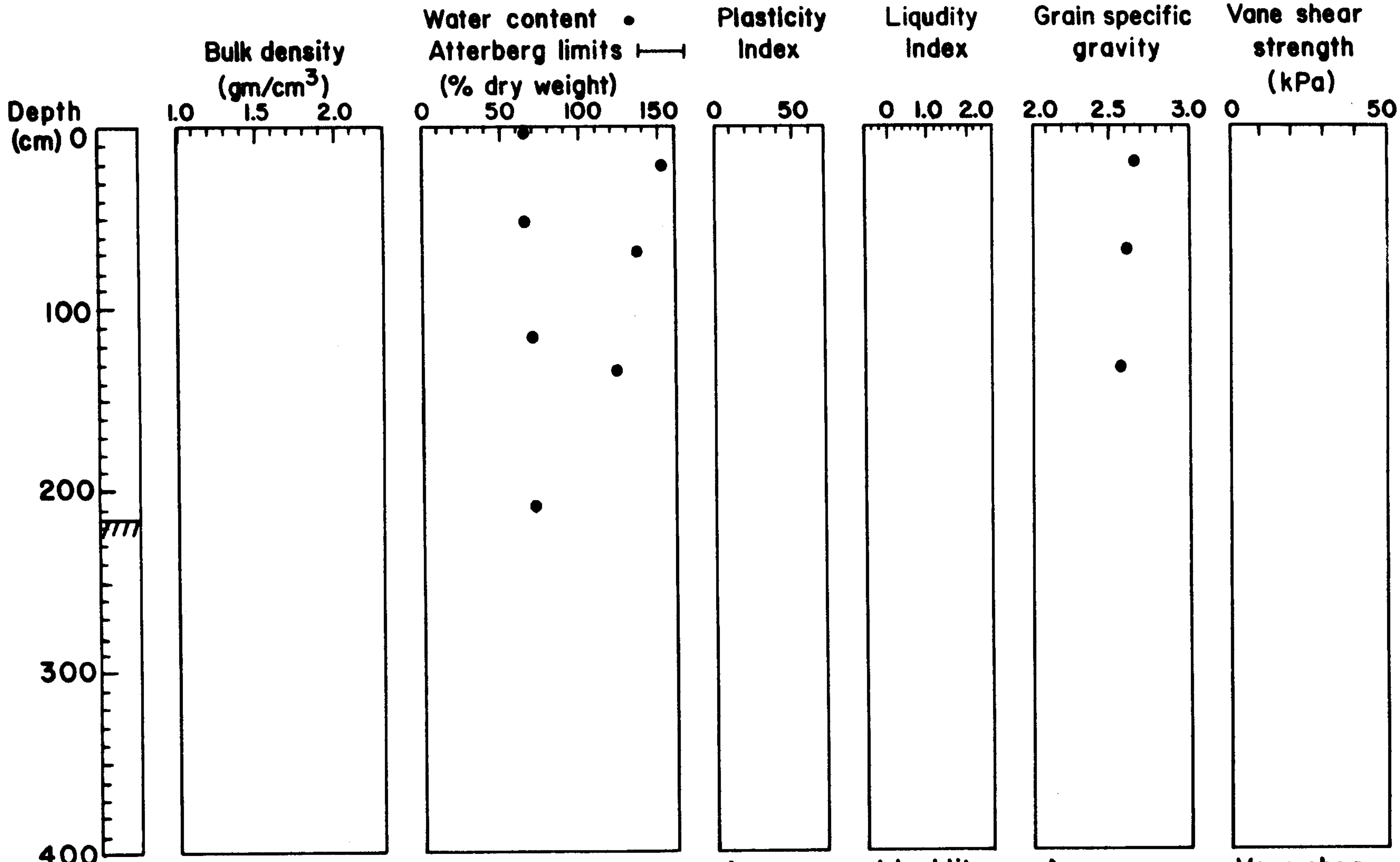

Bulk density at lm.: ______

Water content at lm.: 97

Average plastic limit: ______

Average liquid limit: ______

Average plasticity index: ______

Liquidity index at lm.: ______

Average grain specific gravity: 2.60

Vane shear strength at lm.: ______

Station 442 Physiographic area Kiliuda Trough

Bulk density (gm/cm^3) | Water content • Atterberg limits ⊢⊣ (% dry weight) | Plasticity Index | Liqudity Index | Grain specific gravity | Vane shear strength (kPa)

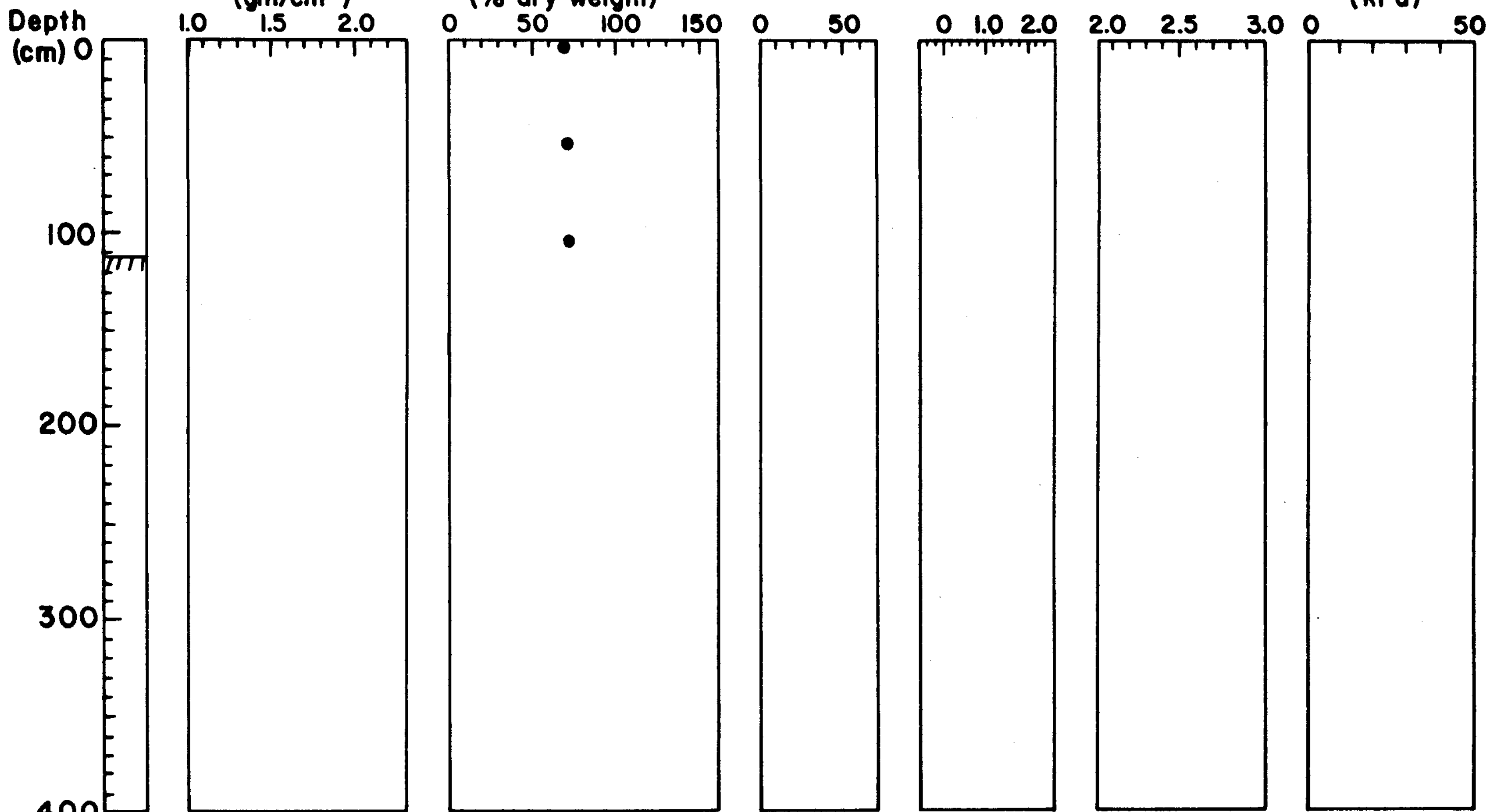

Bulk density at lm.: ______

Water content at lm.: 70

Average plastic limit: ______

Average liquid limit: ______

Average plasticity index: ______

Liquidity index at lm.: ______

Average grain specific gravity: ______

Vane shear strength at lm.: ______

Station 445 Physiographic area Sitkinak Trough

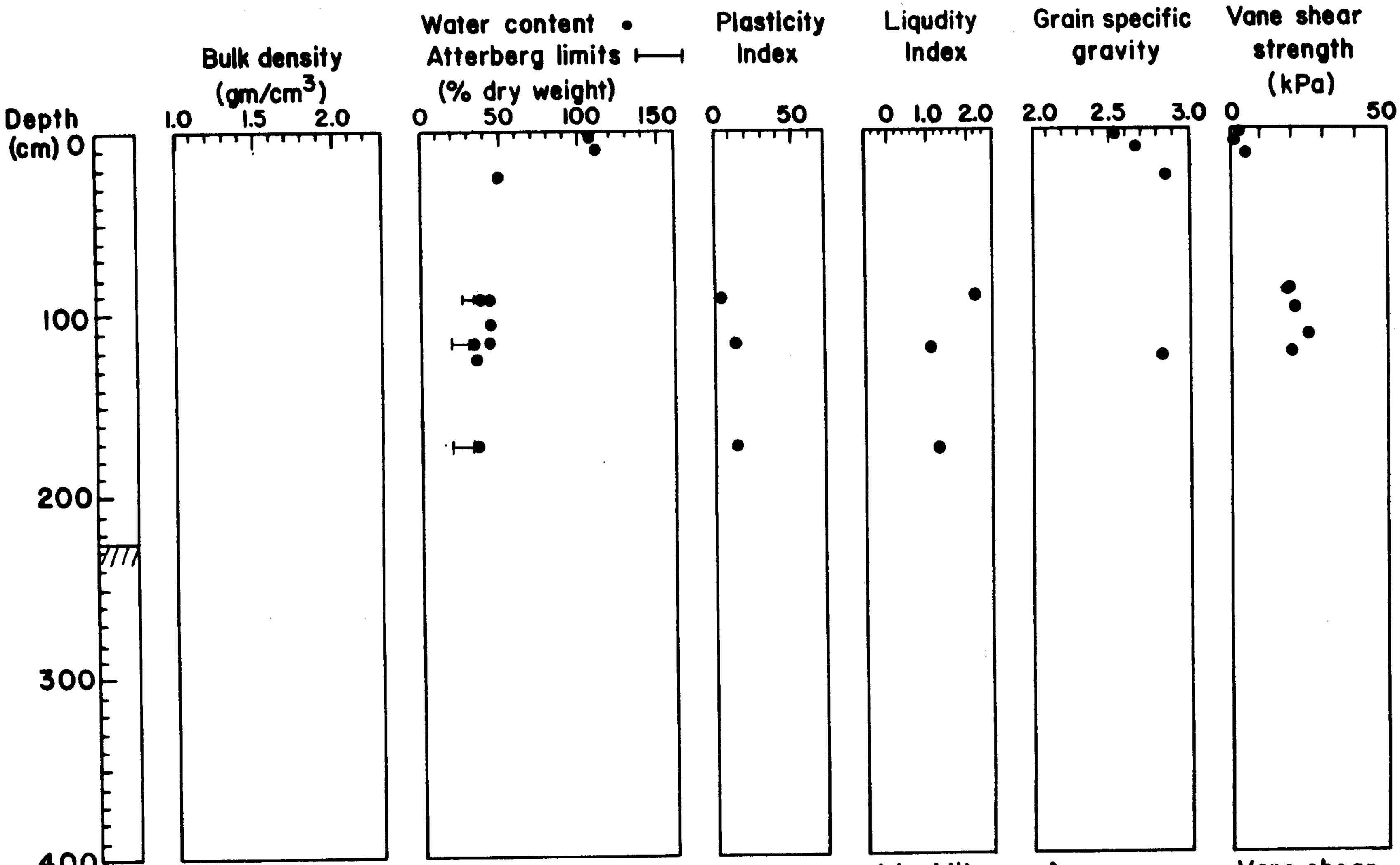

Bulk density at lm.: 1.83

Water content at lm.: 40

Average plastic limit: 22

Average liquid limit: 31

Average plasticity index: 10

Liquidity index at lm.: 1.82

Average grain specific gravity: 2.71

Vane shear strength at lm.: 19.08

Station 450 Physiographic area Upper Continental Slope

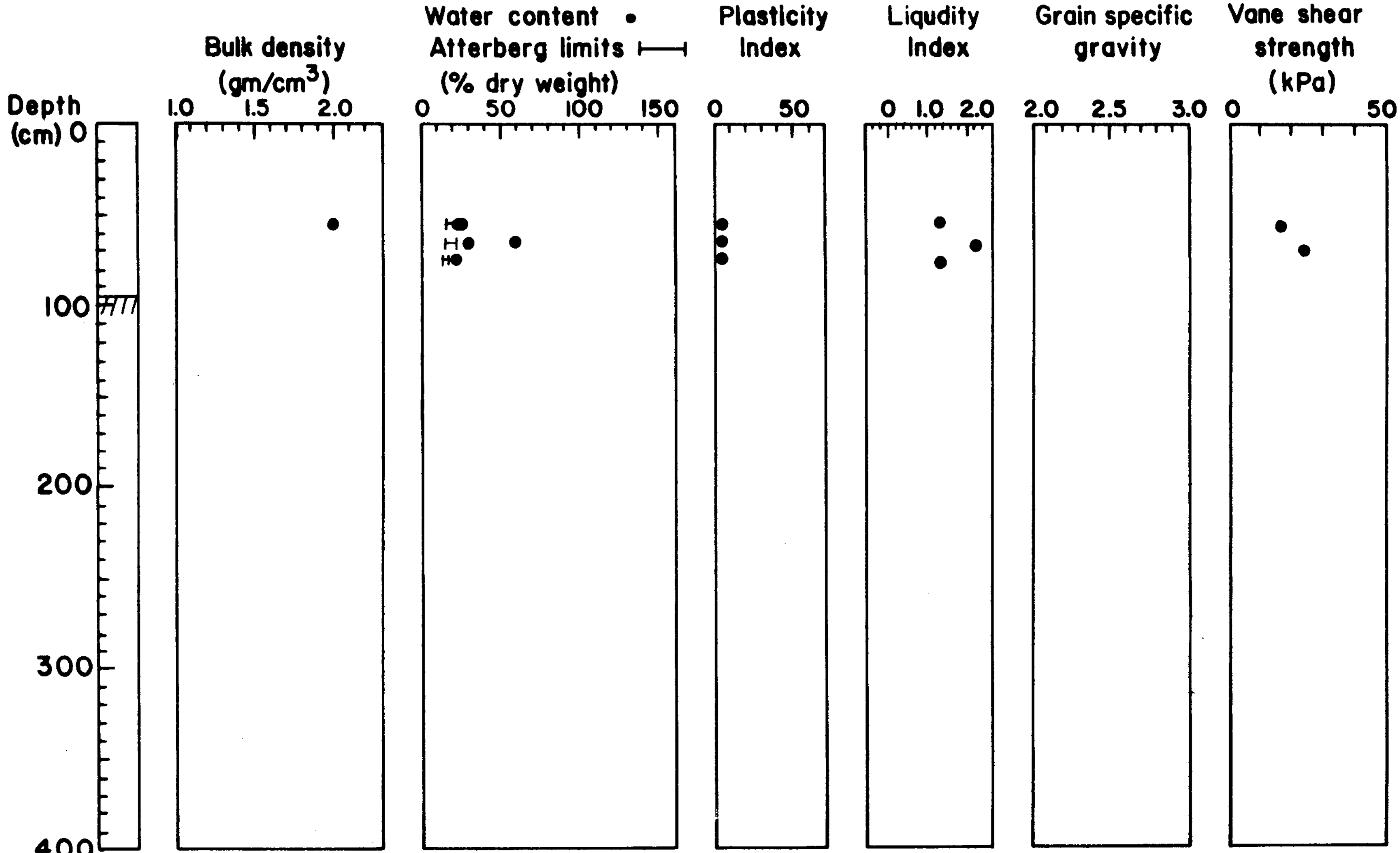

Bulk density at lm.: ______

Water content at lm.: 21

Average plastic limit: 19

Average liquid limit: 20

Average plasticity index: 4

Liquidity index at lm.: ______

Average grain specific gravity: ______

Vane shear strength at lm.: ______

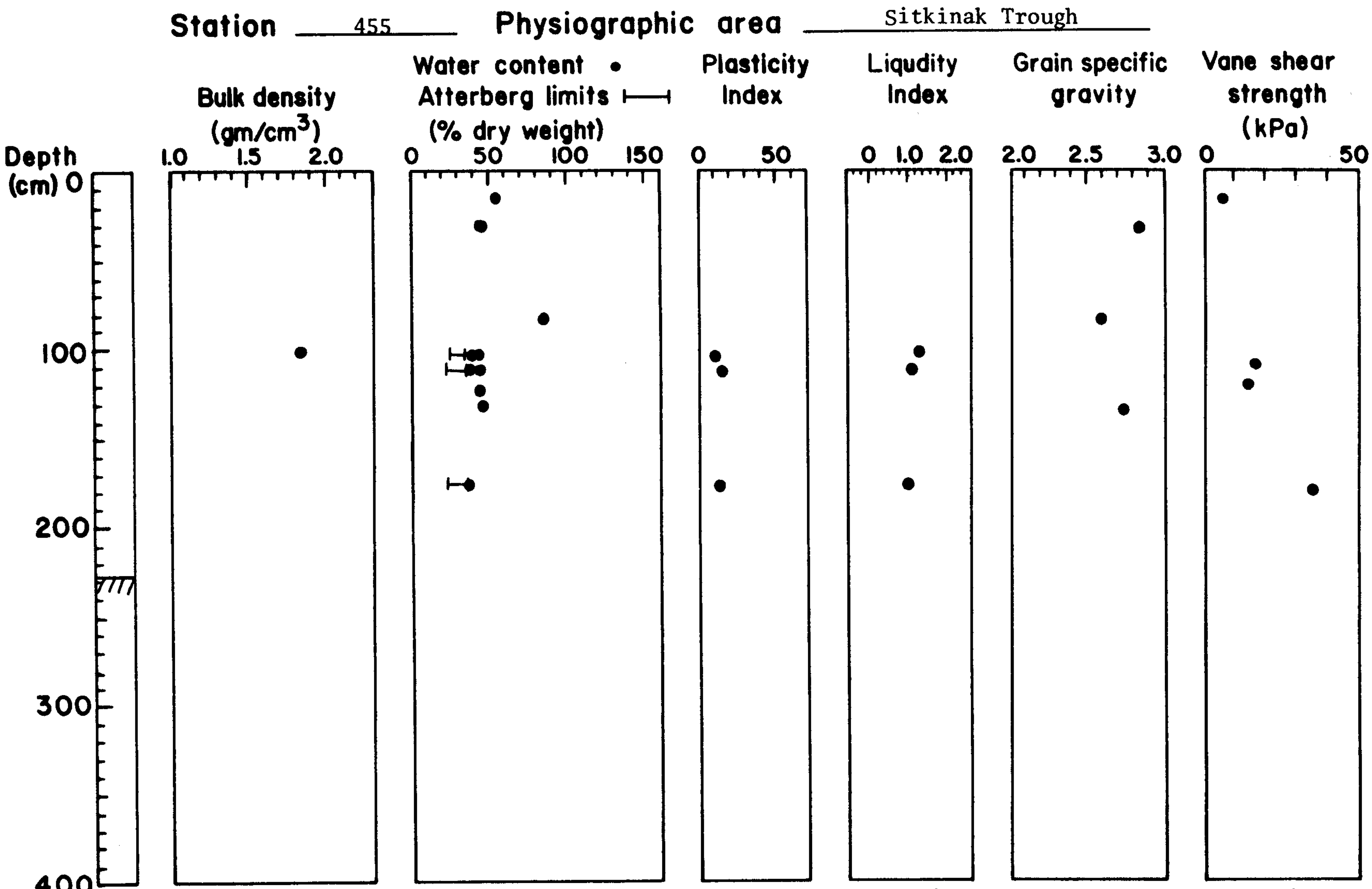

Bulk density at lm.: 1.77

Water content at lm.: 45

Average plastic limit: 23

Average liquid limit: 36

Average plasticity index: 12

Liquidity index at lm.: 1.24

Average grain specific gravity: 2.69

Vane shear strength at lm.: 15.23

Station 578 Physiographic area Kiliuda Trough

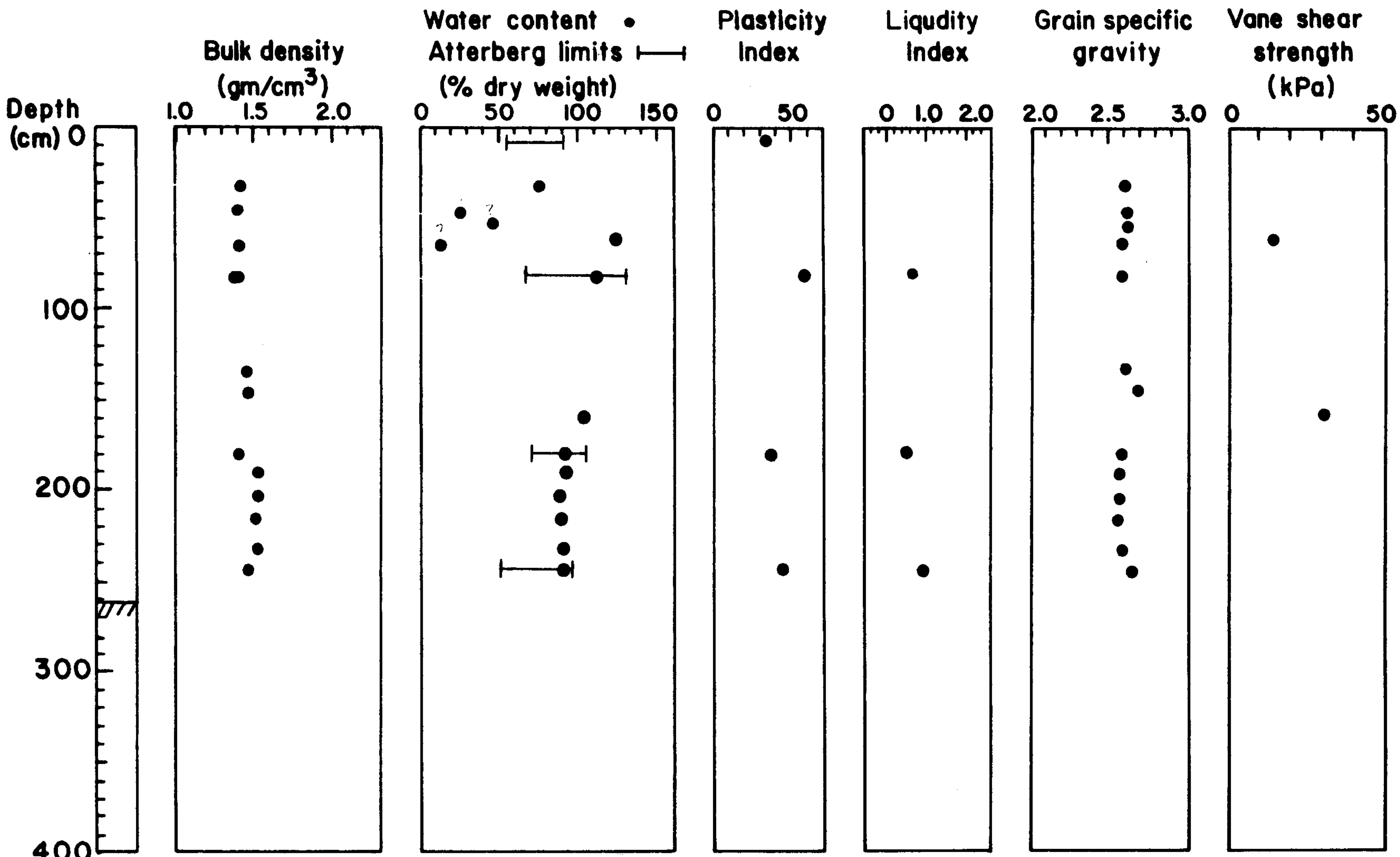

Bulk density at lm.: 1.39

Water content at lm.: 105

Average plastic limit: 64

Average liquid limit: 106

Average plasticity index: 42

Liquidity index at lm.: 0.6

Average grain specific gravity: 2.58

Vane shear strength at lm.: 15.90

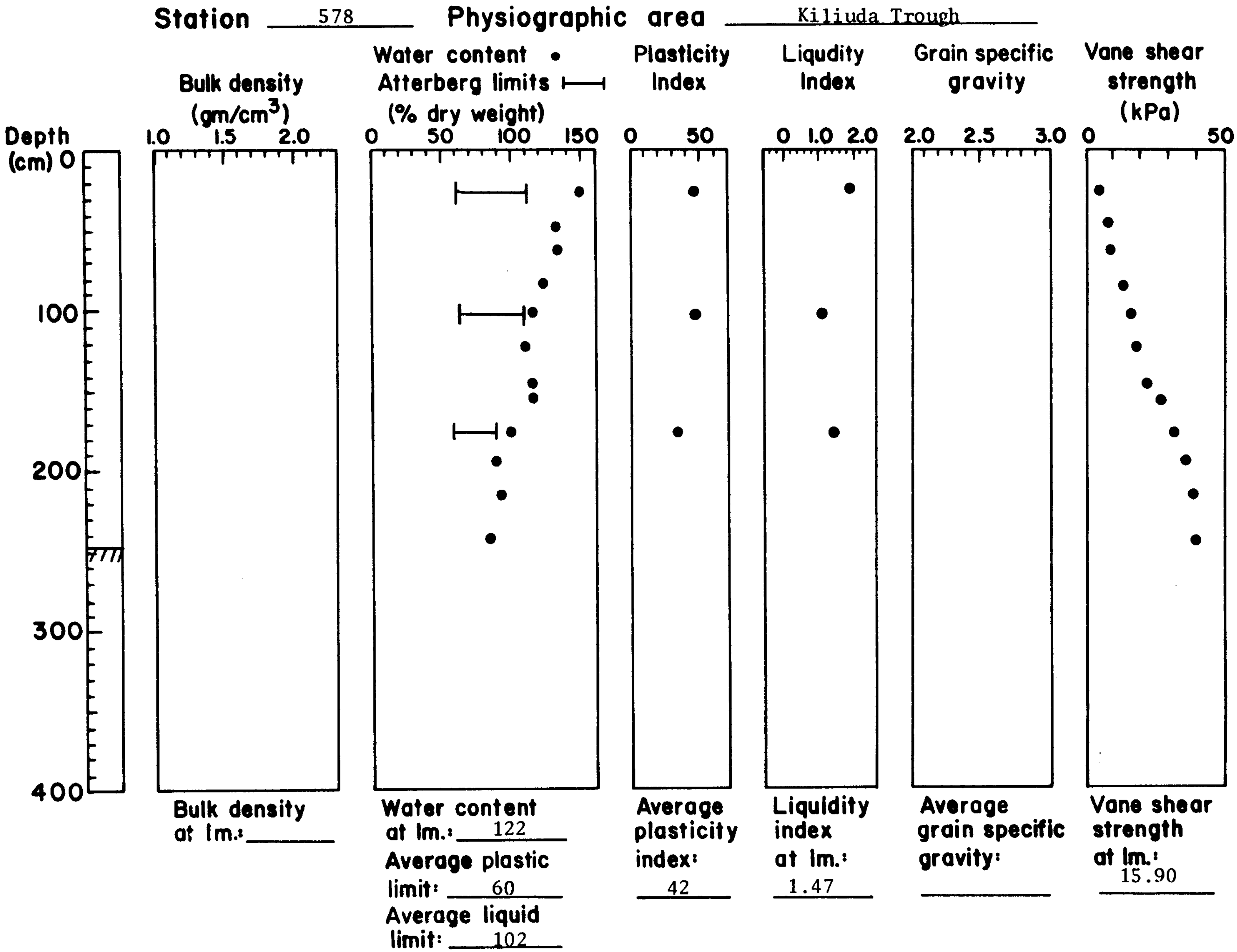

Station 578
Physiographic area Kiliuda Trough
Depth (cm)
0
100
200
300
400
Bulk density (gm/cm3)
1.0 1.5 2.0
Water content •
Atterberg limits
(% dry weight)
0 50 100 150
Plasticity Index
0 50
Liqudity Index
0 1.0 2.0
Grain specific gravity
2.0 2.5 3.0
Vane shear strength (kPa)
0 50
Bulk density at lm.:
Water content at lm.: 122
Average plastic limit: 60
Average liquid limit: 102
Average plasticity index: 42
Liquidity index at lm.: 1.47
Average grain specific gravity:
Vane shear strength at lm.: 15.90

Station 579 Physiographic area Kiliuda Trough

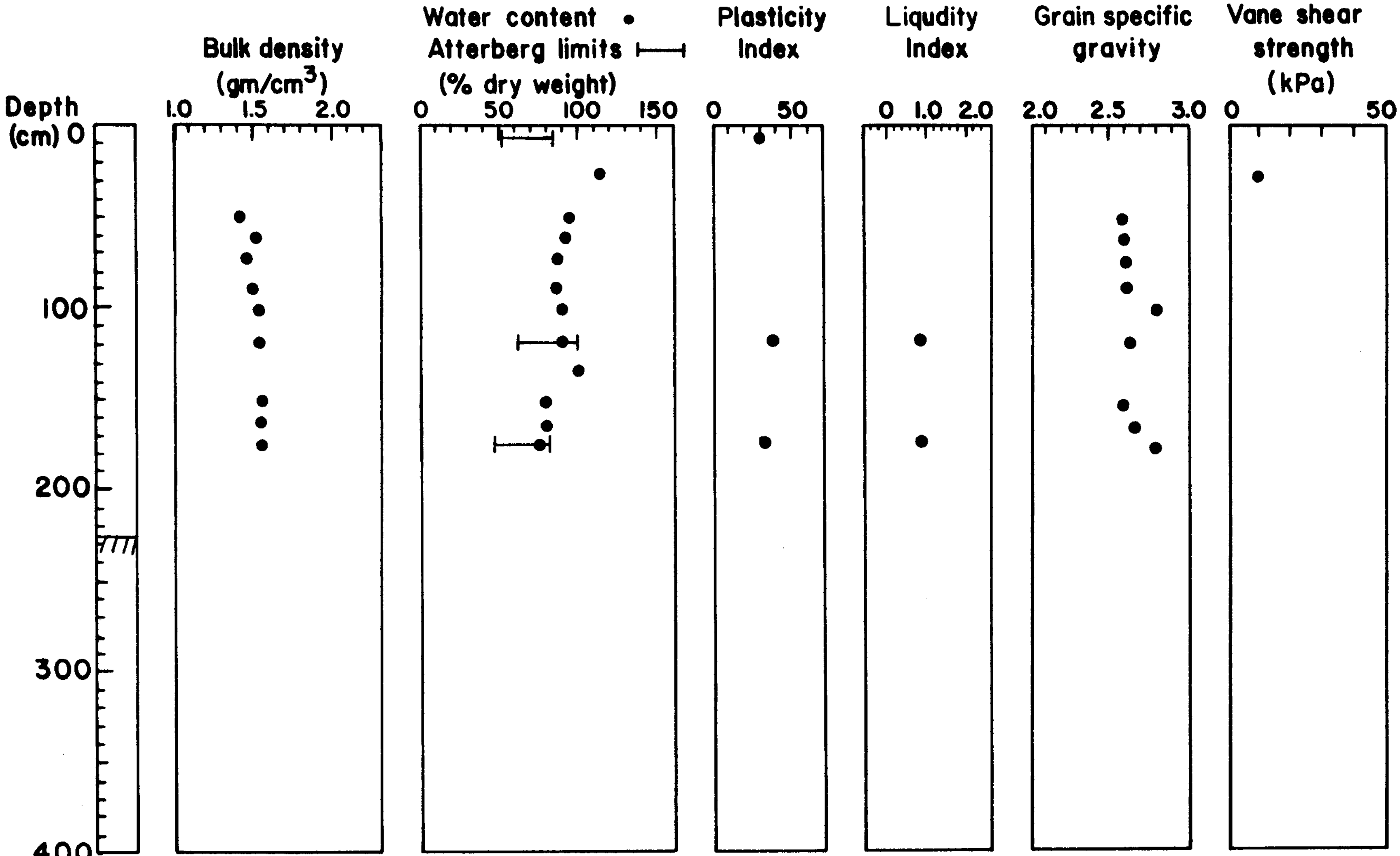

Bulk density at lm.: 1.48

Water content at lm.: 91

Average plastic limit: 54

Average liquid limit: 87

Average plasticity index: 33

Liquidity index at lm.: 0.8

Average grain specific gravity: 2.64

Vane shear strength at lm.:

Station 579 **Physiographic area** Kiliuda Trough

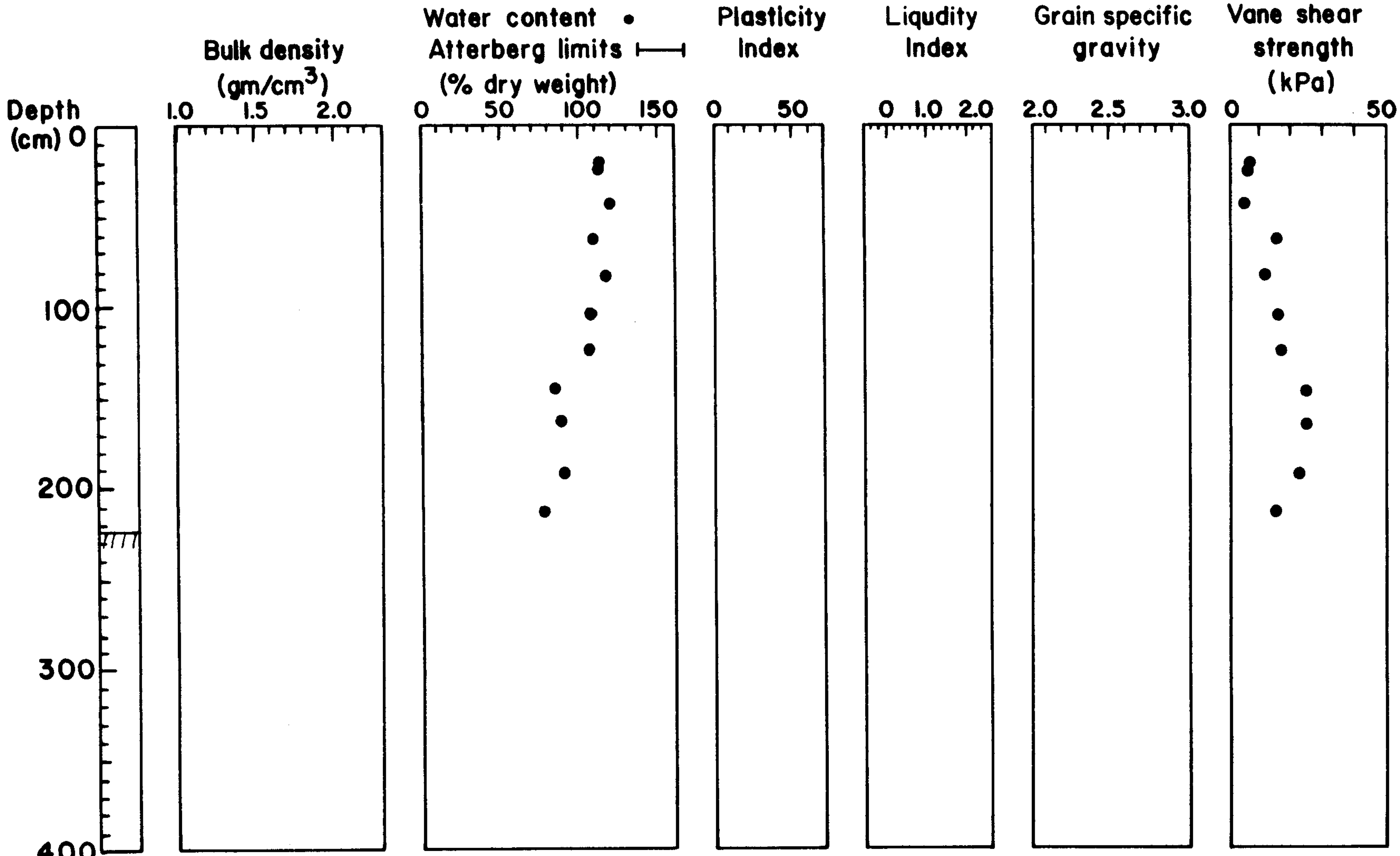

Bulk density at 1m.: ______

Water content at 1m.: 100

Average plastic limit: ______

Average liquid limit: ______

Average plasticity index: ______

Liquidity index at 1m.: ______

Average grain specific gravity: ______

Vane shear strength at 1m.: 13.63

Station 582 Physiographic area Chiniak Trough

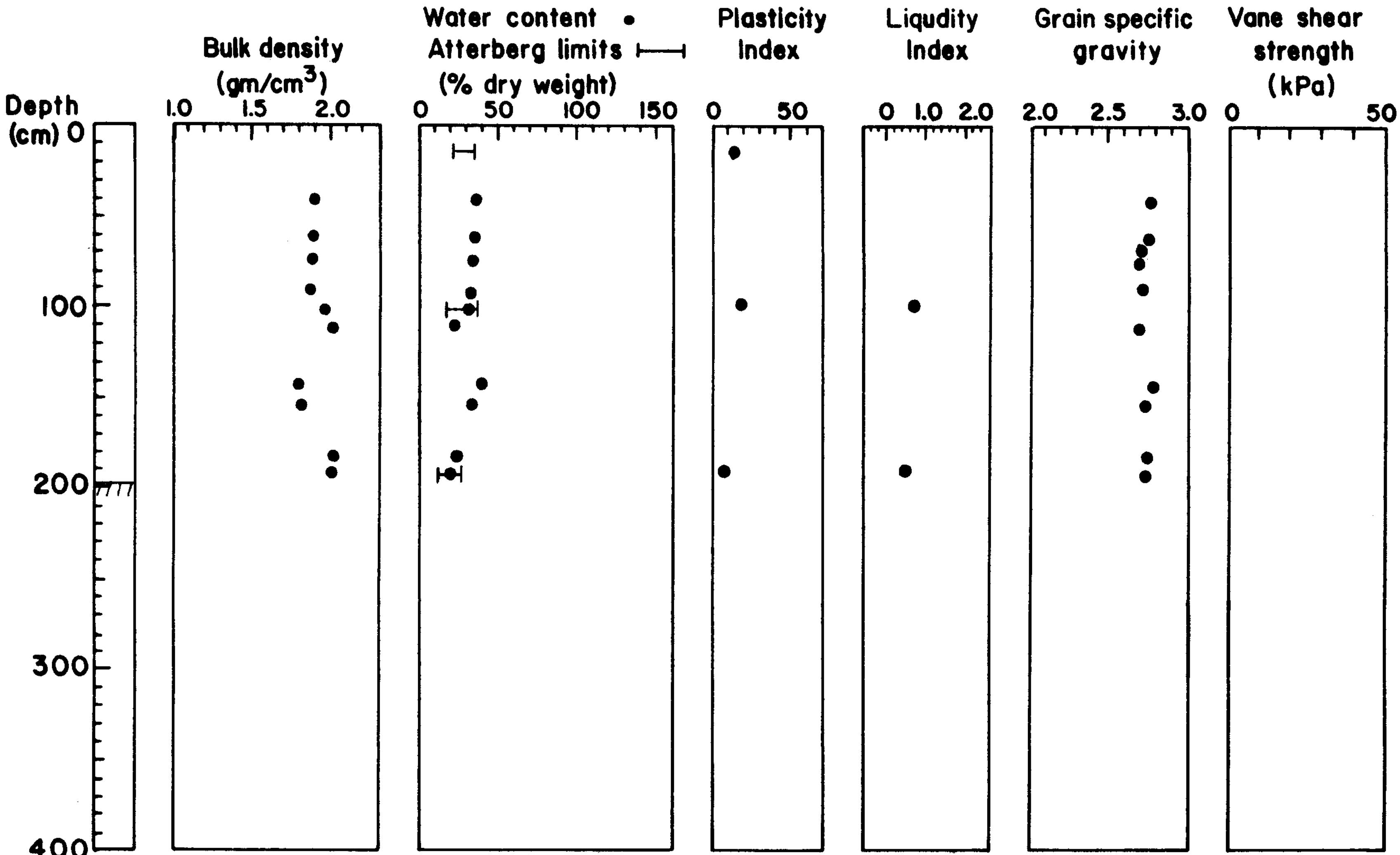

Bulk density at lm.: 1.95

Water content at lm.: 32

Average plastic limit: 18

Average liquid limit: 30

Average plasticity index: 13

Liquidity index at lm.: 0.67

Average grain specific gravity: 2.74

Vane shear strength at lm.: ______

Station 582 Physiographic area Chiniak Trough

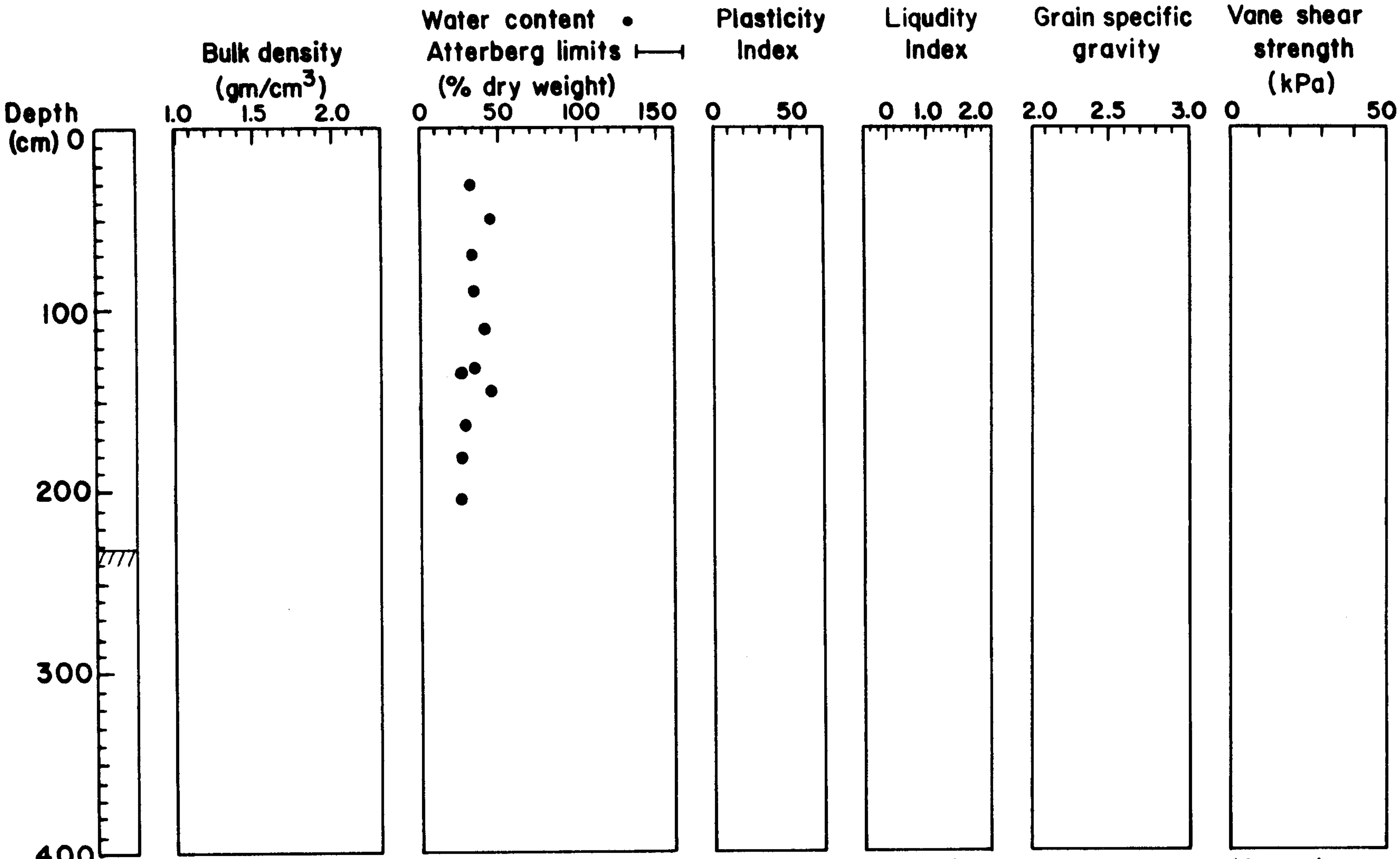

Bulk density at lm.: ______

Water content at lm.: 32

Average plastic limit: ______

Average liquid limit: ______

Average plasticity index: ______

Liquidity index at lm.: ______

Average grain specific gravity: ______

Vane shear strength at lm.: ______

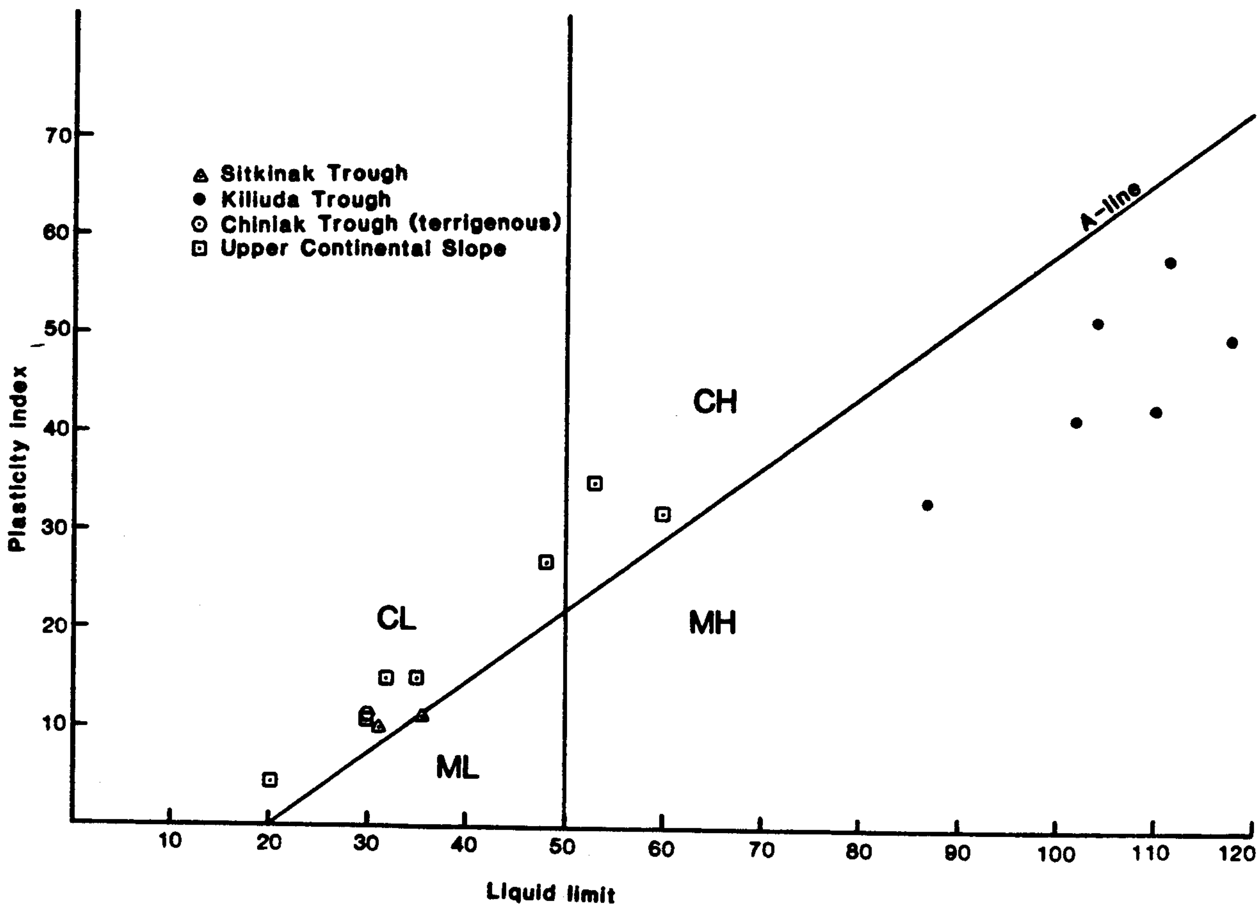

Figure 6. Plasticity chart and sediment classification according to the Unified Soil Classification System. (See Casagrande, 1948.)

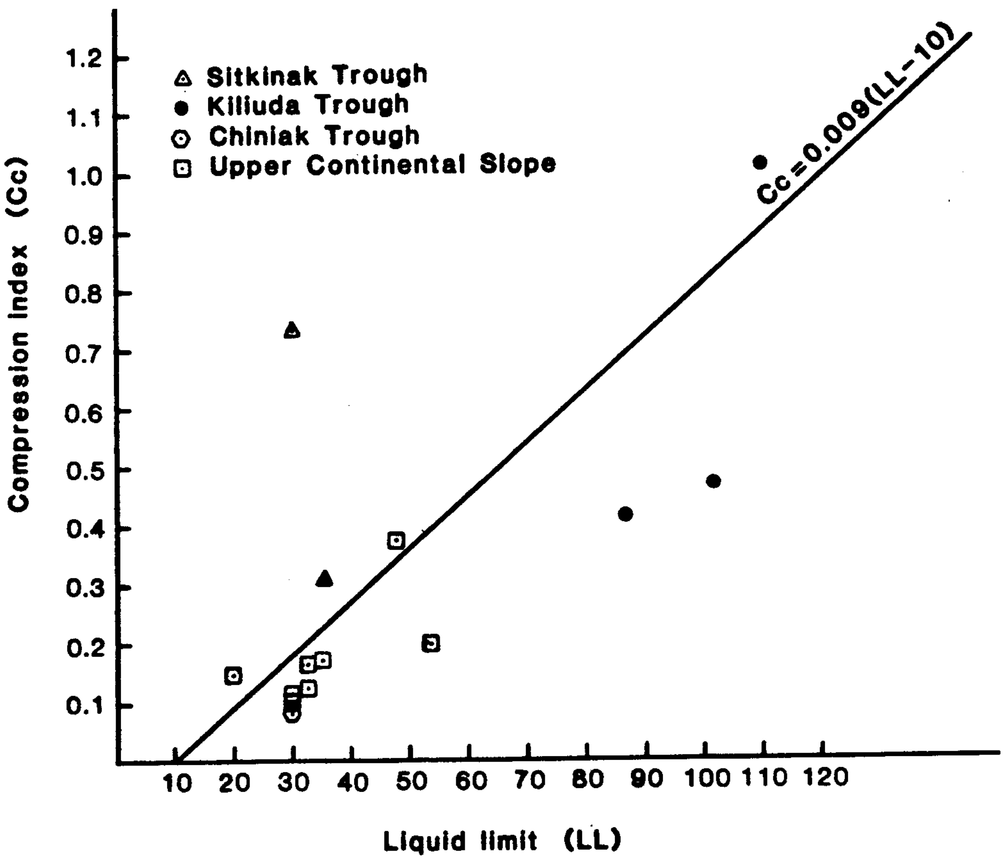

Figure 7. Compression index versus liquid limit for Kodiak Shelf sediment samples. Empirical relation derived by Skempton (1944) is shown for reference.

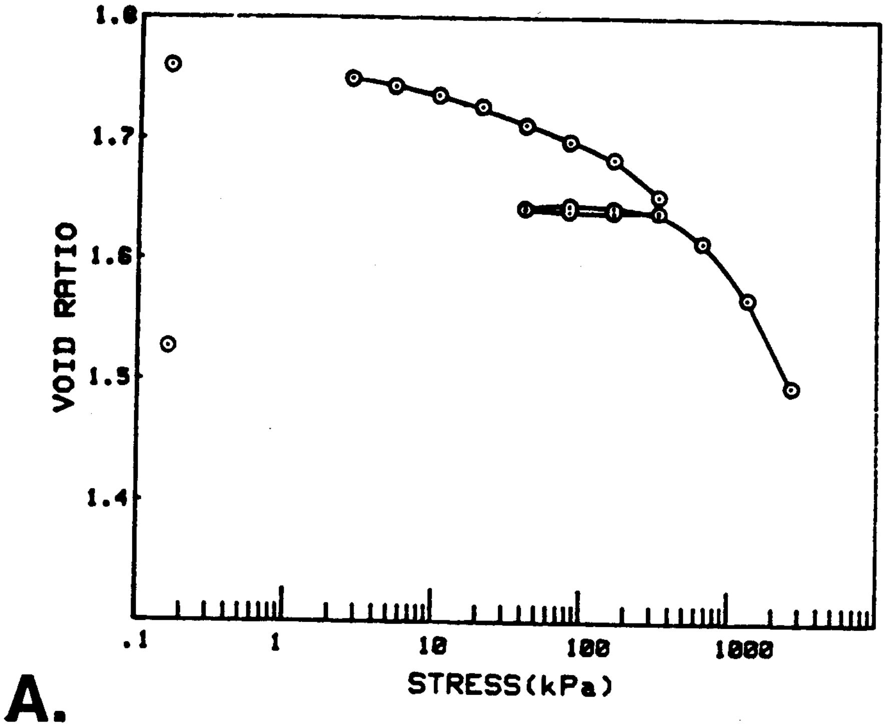

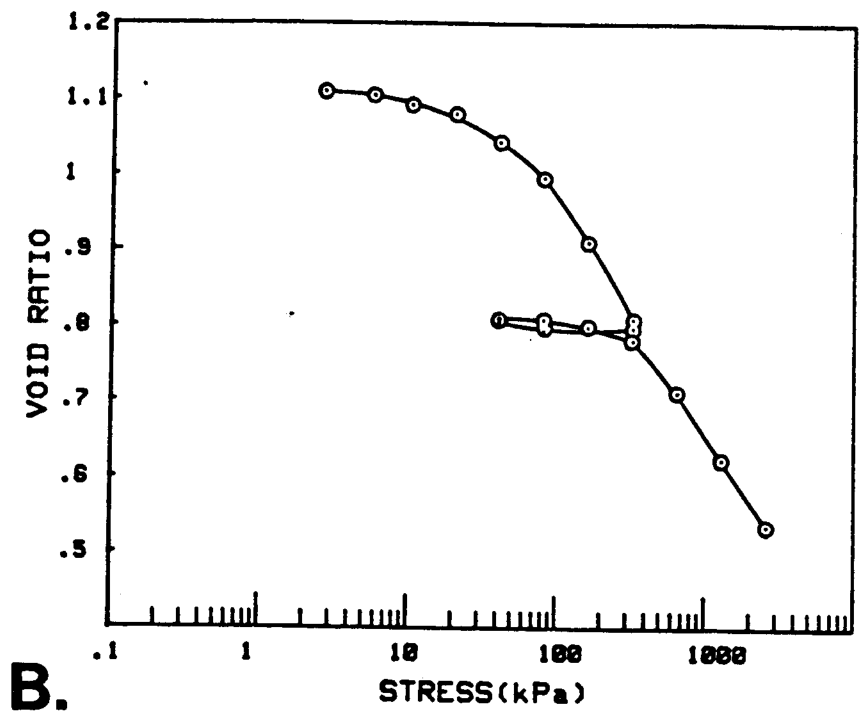

Fig. 8

Figure 8. Oedometer consolidation test results, plotted as logarithm of the effective consolidation stress versus void ratio: (Note that unload-reload cycle was performed once during each oedometer test.) A) Station 433, showing continuous downward curvature of loading curve; B) Normal loading curve, showing straight-line relation between void ratio and effective consolidation stress at loads exceeding approximately 100 kPa.

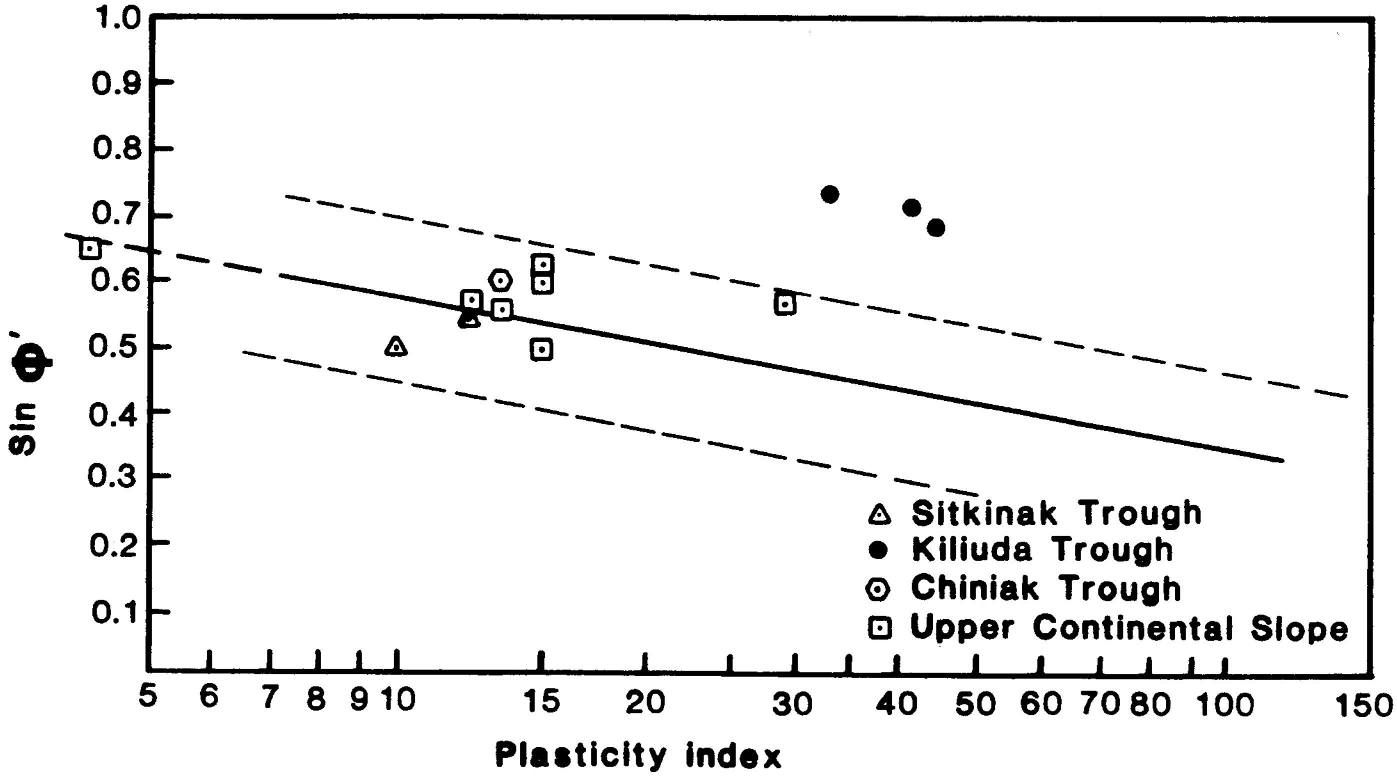

Figure 9. Effective angle of internal friction versus plasticity index. Center line is the empirical relation derived by Lambe and Whitman (1969), and upper and lower lines show range of variation of their data.

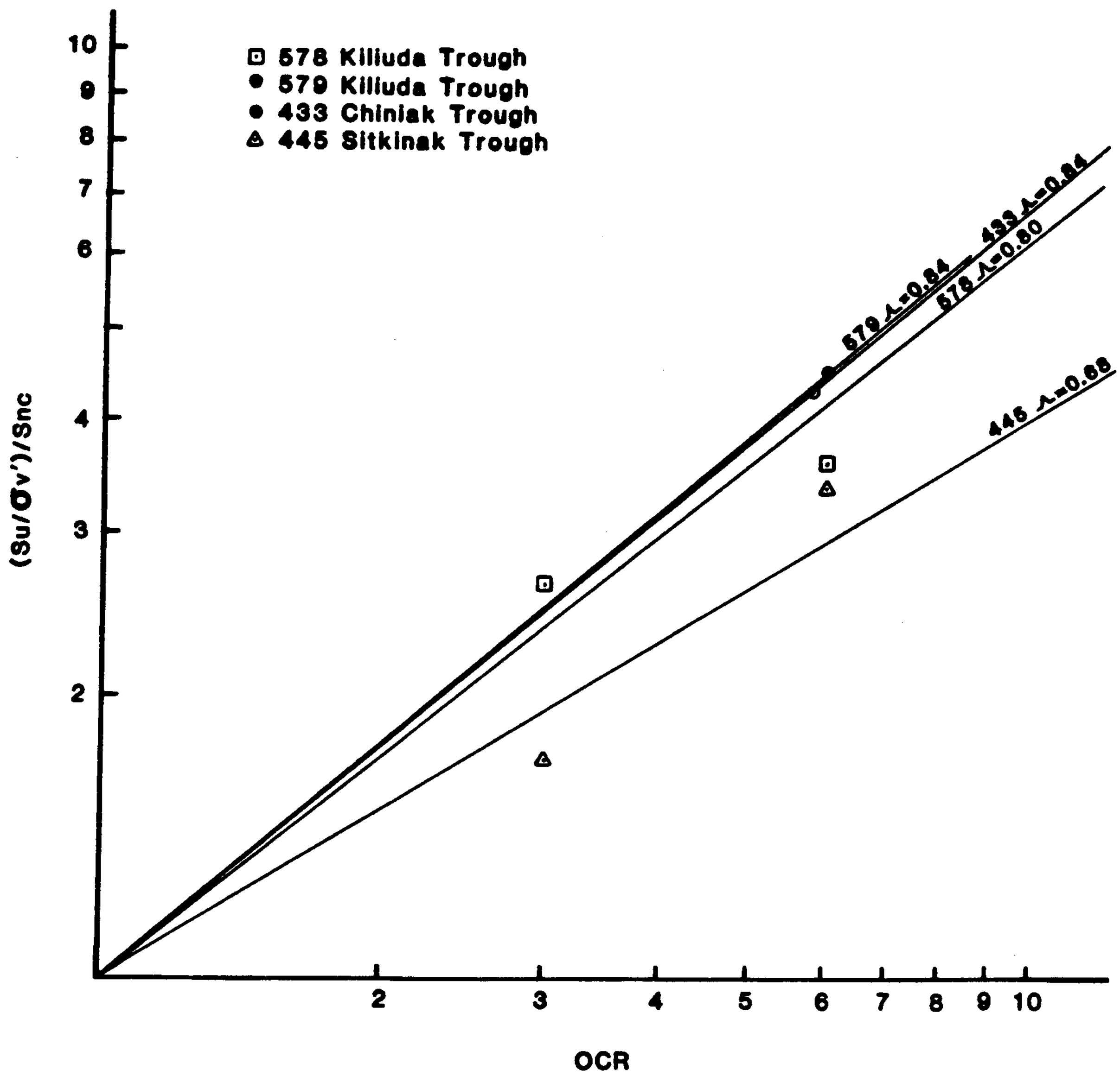

Figure 10. Normalized strength versus overconsolidation ratio. (See Mayne, 1980.)

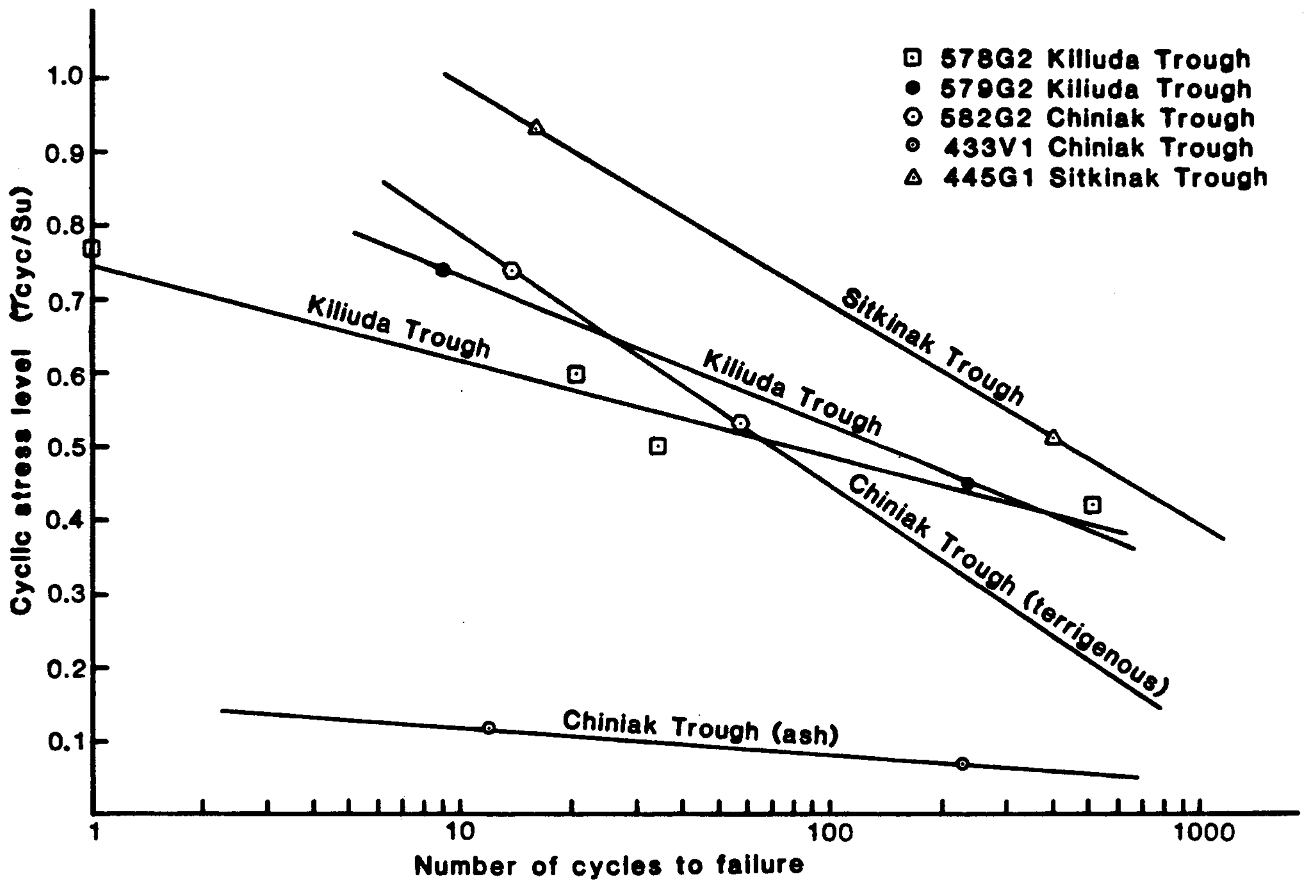

Figure 11. Stress level versus number of cycles to failure.

GEOTECHNICAL FRAMEWORK, NORTHEAST GULF OF ALASKA

by

Homa J. Lee
William C. Schwab

U.S. Department of the Interior
Geological Survey

Final Report
Outer Continental Shelf Environmental Assessment Program
Research Unit 589

1983

TABLE OF CONTENTS

TABLE OF CONTENTS (Continued)

LIST OF FIGURES

LIST OF TABLES

INTRODUCTION

The U.S. Geological Survey began a systematic study of sediment distribution, depositional environments, and shallow structure of the northeast Gulf of Alaska in 1974. The objective of the study was primarily to evaluate seafloor hazards on a regional basis in preparation for possible offshore petroleum development. The study was extended to include an extensive sediment sampling program in 1975 when approximately 400 samples of continental shelf sediments were collected (Carlson and others, 1977). Systematic measurement of geotechnical properties was started in 1977 (Carlson and others, 1978).

Detailed geologic study of seismic reflection records and sediment samples in areas of sediment instability, although valuable for specifying the types and extents of different past hazardous conditions, leave unanswered questions. For example, they often do not specify causes of failures, provide information on the safety of apparently unfailed areas, suggest whether existing slide bodies will fail again or enlarge, or predict the implications of certain earthquake or storm events.

The quantitative methods of geotechnology have the potential for answering some of these questions. A vast amount of previously unpublished geotechnical data, primarily derived from tests on core samples but supplemented with a few in situ tests, has been accumulated on the continental shelf between Montague Island and Cross Sound (Fig. 1). The primary objective of this report is to make these data available with a consistent format. A secondary objective is to provide preliminary quantitative analyses of some of the geologic hazards.

SETTING

Geologic Setting. Glaciation is the most important process contributing sediment to the northeast Gulf of Alaska continental shelf. In Miocene time, glaciation was restricted to the onshore area but by early to middle Pleistocene, a large ice sheet had spread across the continental shelf (Molnia and Carlson,1978; Molnia and Sangrey, 1979; Carlson and others, 1982). Today glaciers in the Gulf of Alaska region are restricted to the onshore areas (Fig. 1). As recently as 75 years ago, however, a glacier filled Icy Bay and extended 5 km or 6 km onto the continental shelf (Molnia, 1979).

The complex Quaternary history of the northeast Gulf of Alaska has generated a variety of sedimentary deposits. Four major sedimentary units (Fig. 1) are defined on the basis of seismic reflection and sedimentologic data (Carlson and Molnia, 1975; Molnia and Carlson, 1975, 1980; Carlson and others, 1977, Molnia and Sangrey, 1979; Molnia and Carlson, 1980). These units are: A. Holocene glacial-marine sediment; B. Holocene end moraine deposits; C. Quaternary glacial deposits; and D. Pleistocene and older lithified sedimentary rocks. Holocene end moraine deposits, Quaternary glacial-marine sediment, and Pleistocene and older lithified sedimentary rocks are predominantly dense and hard, reflecting diagenesis or glacial ice loading. These compacted deposits are probably not susceptible to instability on the continental shelf (Lee and Schwab, 1982). Therefore, Geotechnical studies have been directed almost exclusively toward investigating Holocene glacial-marine sediment.

Fine sand and clayey silt of the Holocene glacial-marine unit cover most of the inner shelf, reaching a maximum thickness of about 350 m seaward of the Copper River, about 200 m seaward of Icy Bay (Carlson and Molnia, 1975), and about 260 m seaward of the Alsek River. This sediment is glacially derived from the Gulf of Alaska Tertiary province and bordering rocks of Mesozoic and older age, then fluvially transported to the gulf as rock flour (Molnia and Carlson, 1980). The Mesozoic and older age rocks are highly deformed, locally metamorphosed sedimentary and volcanic rocks that are commonly intruded by igneous plutons, whereas the Tertiary Province is a compound continental margin basin made up almost entirely of terrigenous clastic rocks with minor coal. For a summary of the onshore geology of the Gulf of Alaska the reader is referred to Plafker (1971), Bruns (1979), and Bruns and Plafker (1982).

West of Kayak Island, the Copper River is the primary source of Holocene sediment, carrying a sediment load of 107×10^9 kg/yr (Reimnitz, 1966). East of Kayak Island, major sediment sources are streams draining the larger ice fields (Malaspina and Bering Glaciers) and the Alsek River. Accumulation rates of the Holocene glacial-marine unit on the continental shelf range from 0 to 29 mm/yr (Molnia and others, 1980). Accumulation rates of Holocene glacial-marine sediment in coastal embayments are thought to be as high as 2 to 3.75 m/yr (Molnia, 1979).

The largest deposits of sand in the Holocene glacial-marine unit occur along the barrier islands at the mouth of the Copper River, along the nearshore zone both adjacent to and west of the Malaspina Glacier (Carlson and others, 1977), and along the nearshore zone between the Alsek River and Yakutat Bay (Fig. 1). The moderately well sorted, mineralogically immature sand (containing about equal parts of quartz and metamorphic rock fragments) is mostly found in water depths less than 50 m indicating an environment subject to high wave and current energy. Storm waves and longshore currents resuspend the fine silt and clay particles or maintain them in suspension and the Alaska Current transports them offshore and westward (Molnia and Carlson, 1980).

Large deposits of Holocene glacial-marine clayey silt occur seaward of the Copper River and seaward of the Malaspina and Bering Glaciers (Carlson and others, 1977). The mean grain size of Gulf of Alaska Holocene glacial-marine sediment generally decreases with distance from shore and is largely glacial rock flour which is dominated by the silt fraction (Carlson and others, 1977).

<u>Offshore Geologic Hazards</u>. Seafloor gelogic hazards in the northeast Gulf of Alaska are summarized by Carlson and Schwab (1982) and have been described by Carlson and others (1975), Carlson and Molnia (1977), Molnia and others (1977), Carlson (1978), and Carlson and others (1980). The hazards include shallow faults, buried channels, gas-charged sediment, and submarine slides and flows.

Active faulting is well documented using conventional geophysical techniques (Bruns 1979; 1982; Bruns and Schwab, 1982; Carlson and Schwab, 1982). Buried channels involve sediment and sedimentary rocks that are too deeply buried to be sampled with conventional coring equipment and therefore have not been studied except with geophysical profiling.

Bubble phase gas charging, although present in the northeastern Gulf of Alaska, is not widespread. Of the hydrocarbon gases, only methane is present in concentrations that may exceed the saturation of interstitial water (Appendix A). Anomalously high concentrations of methane suggesting the presence of bubble phase gas in place and potentially unstable sediment, were found in only two areas: a fault zone southeast of Kayak Island (sample concentration of 14,000 µl/l), and an area east of Dry Bay (sample concentration of 32,8000 µl/l). Other locations had significant amounts of methane but the amounts measured in samples were insufficient to indicate that the sediment in situ was, indeed, charged with bubble-phase gas. No correlation between the occurrence of seismic reflection anomalies and the presence of gas-charged sediment is apparent, except for the sediment southeast of Kayak Island. The sampling and analytical techniques needed to quantitatively assess gas-charged sediment as a geologic hazard have not been fully developed.

Geotechnical studies have been directed almost exclusively toward investigating slides and flows in the Holocene glacial-marine sediment. Holocene morainal sediments, Quaternary glacial-marine sediment and Pleistocene and older lithified sedimentary rocks are predominantly dense and hard, reflecting diagenesis or glacial ice loading. These compacted deposits are probably not susceptible to sliding on the continental shelf. In contrast, the Holocene glacial marine sediment is weak. In this area of frequent earthquakes and large storm waves, the Holocene glacial marine sediment is susceptible to slope failure under cyclic loading (Lee and Schwab, 1982).

Morphology of Submarine Slides and Flows. Numerous slides and slumps have been identified from seismic profiles of an 8 by 100 km area seaward of the mouth of the Copper River (Hampton and others, 1978; Carlson and Schwab, 1982) (Fig. 4). Some disrupted reflectors on a few of the profiles may indicate the presence of gas-charged sediment (Fig. 5). The disrupted reflectors occur beneath a slope of about 0.5° and appear to outline individual slump "blocks" that range in height from 1 m to 5 m and in length from 0.3 km to 1.0 km. The slump structures appear to be developed to a depth in the sediment of 20 m to 40 m in water depths of 40 m to 125 m.

A spectacular example of a large submarine slide is located in Kayak Trough (Carlson and Molnia, 1977; Molnia and others, 1977; Hampton and others, 1978) (Fig. 4). This slide has a length of 17 km, a maximum width of 12 km, and a maximum thickness of 115 m (estimated volume is approximately 5.9 km^3). The slide occurred on a 1° slope. Seismic profiles over the Kayak Trough slide typically show disrupted internal reflectors and irregular surface morphology. This slide has a fairly well-preserved pull-apart scarp with a relief of about 10 m and a well-developed toe that is 20 m thick about 2 km from the distal end (Fig. 6). Apparently there was enough momentum to carry the toe of the slide past the thalweg of the trough (Carlson and Molnia, 1977).

The largest known slide on the continental shelf east of Kayak Island is the Icy Bay-Malaspina slump (Carlson, 1978), located seaward of the Malaspina Glacier (Slide A, Fig. 7). Here a process of en echelon slumping of Holocene clayey silt is taking place in water depths of 70 m to 150 m on a slope of less than 0.5° (Fig. 8). These slump structures extend over an area of about

1080 km^2. The slump blocks are about 0.5 km long and have reliefs of 2 m to 5 m. The slip surfaces extend to a depth of 15 m to 40 m beneath the sea floor. The volume of the entire slump is about 32 km^3.

Four smaller slides have been mapped in the nearshore zone east of the Icy Bay-Malaspina slump, all of which begin in water shallower than 100 m (Carlson and others, 1980) (Slide B, Fig. 7). One slide southwest of Yakutat Bay begins on the north wall of Yakutat Sea valley and extends across most of the valley floor. This slide covers an area of 350 km^2 and incorporates the upper few meters of clayey silt. This slide appears to fit into Varnes (1978) classification as a mudflow that failed due to lateral spreading (Carlson and others, 1980).

The second of the four smaller slides, the Yakutat slide, begins 4 km seaward of the coastline between Yakutat Bay and the Dangerous River. It is about 40 km in width, and about 260 km^2 in area (Carlson and others, 1980) (Slide C. Fig. 7). The slope of the upper part of the slide is about 1° and decreases to about 0.5° at the seaward edge of the slide. This slide mass is characterized by a series of clayey silt blocks undergoing rotational slump movement. The steplike surfaces of the blocks have a tread length of about 100 m and a riser height of 3 to 4 m (Fig. 9). The slip surfaces extend 10 m below the sea floor and the volume of slumped material is nearly 3 km^3.

The third smaller slide is located southeast of the Dangerous River in clayey silt (Carlson and others, 1980) (Slide D, Fig. 7). This slide begins about 2 km offshore in water depths less than 20 m. This area of seafloor instability is thought to be associated with gas-charged sediment interpreted from acoustic anomalies in high resolution seismic profiles, and water column gas plumes visible on side-scan sonographs (Carlson and others, 1980) (Fig. 10).

The fourth of the smaller slides is just seaward of the Alsek River (Alsek River Prodelta) (Slide E, Fig. 7) and has an area of 150 km^2. The shoreward edge of the slide is in sand and sandy mud less than 2 km offshore. Water depths are around 35 m and the slope is about 0.5°. This slide is thought to have moved down the headwall of the Alsek Sea Valley (1.3° slope) possibly as far offshore as the floor of the valley (Slide F, Fig. 7) where it offsets the clayey silt to a depth of 10 m to 20 m (Carlson and others, 1980). A detailed picture of the sea floor in a 10 x 2 km area within the Alsek River prodelta was made by assembling 21 speed corrected, digitally processed, side-scan sonographs (Molnia and Rappeport, 1980). Typical side-scan sonographs of the Alsek River slide are presented in Figures 11, 12, and 13. Molnia and Rappeport (1980) suggest that the principal factor for causing the Alsek Prodelta slope failures is saturation of the sediment by biogenic methane gas. Carlson and others (1980) also mapped this failure as an area of gas-charged sediment.

In addition to the slides and flows in the nearshore zone, other slides have been mapped within the Yakutat and Alsek Sea Valleys (Carlson and others, 1980) (Fig. 7). These slides all appear to be mud flows affecting the upper 10 m to 20 m of clayey silt.

Numerous areas of slides and slumps have been mapped on the continental slope (Fig. 7) (Carlson and others, 1980). Although most of these slides are immediatly seaward of the valleys, sliding appears to be a common mechanism for transporting sediment down the continental slope in the entire Gulf of Alaska (Hampton and others, 1978; Carlson, 1979). Many of these slides are longer than 5 km and occur on slopes with gradients of 3° to 6°. The slides range from discrete mudflows, thinner than 50 m, to complex zones of mass transport several hundred meters thick consisting of multiple slides, such as in the area southeast of Yakobi Sea Valley (Carlson and others 1980; Carlson and Schwab, 1982). The sediment contained in these slides is primarily a pebbly mud that was deposited by glaciers on the shelf during parts of the Pleistocene (Carlson and others, 1980).

GEOTECHNICAL APPROACH

General Methodology. The critical sediment geotechnical property measured for use in geologic hazards evaluations is the shearing strength. It must be exceeded by environmental loads for most types of failure to occur. Index properties (grain size, water content, bulk density, Atterberg limits and grain density) are measured as well because they aid in classifying the sediment and can be correlated with both strength parameters and sedimentary processes. Also, they are not strongly affected by coring disturbance. Compression or consolidation properties are measured because the consolidation state (relative degree of compaction) correlates well with relative shearing strength (Ladd and Foott, 1974), and reflects earlier geologic events (for example preloading by glaciers or erosion of overburden).

The usefullness of most of our geotechnical data are limited by the short length of cores (typically 1 m to 10 m) and by core disturbance. Because many failure features have basal shearing planes that are much deeper (50 m or more) than conventional coring devices penetrate, the sediment involved in failure may not have the same properties as that sampled. Coring disturbance, generated by the thick walled samplers that are commonly used, alters the engineering properties of the sampled sediment from the properties of the sediment in place. Both of these limitations, core shortness and disturbance, are serious and capable of greatly reducing the validity of any geotechnical study.

A methodology for partially overcoming these limitations is provided by the normalized soil parameter (NSP) approach (Ladd and Foott, 1974, Mayne, 1980). The NSP approach is based on empirical results that show certain engineering properties of certain sediments to be constant if normalized by appropriate consolidation stresses. For example, in a normally consolidated sediment profile (one in which no removal of sediment or preloading has occurred), the ratio of undrained shearing strength to overburden effective stress is often constant. If this ratio is known, a strength profile can be constructed by multiplying the ratio by values of overburden effective stress (sub-bottom depth times the average submerged density). If the sediment is overconsolidated, that is, if it has been preloaded by glaciers or other sediment that has since been eroded, a different ratio of strength to overburden stress will result. This ratio of strength to overburden stress is constant as long as the degree of overconsolidation, expressed as the overconsolidation ratio (OCR), is constant. The ratio of strength to overburden stress typically varies with the OCR raised to the power Λ_o, where Λ_o is a sediment constant (Mayne, 1980). If the variation of OCR with depth in the sediment column is known, a prediction of the strength variation can be made. If the sediment is normally or underconsolidated, as the Holocene glacial-marine sediment appears to be in most locations, the value of Λ_o is irrelevant.

One advantage of the NSP approach lies in its ability to provide parameters that are independent of consolidation stress and depth in the sediment column. In a sense, therefore, the limitation imposed by short samples is at least partially removed, particularly in large depositional environments where the type of sediment being deposited at a given location is fairly constant over a long period of time (i.e., to a significant depth). The northeast Gulf of Alaska is probably such a large depositional environment. A second advantage of the NSP approach is that normalized parameters can be made somewhat independent of coring disturbance by conducting all strength tests at greatly increased consolidation stresses (Ladd and Foott, 1974). That is, a disturbed sample and a nearly undisturbed sample would produce almost the same normalized strength parameters if both are consolidated (in a triaxial or direct simple shear cell) to a high stress level before testing for shear. Once the normalized strength parameters have been measured at the high stress levels, they can be applied to any stress level including the low level that the sample originally experienced in place.

The NSP approach cannot handle all offshore geotechnical conditions. Ladd and Foott (1974) warn against applying it in cases of naturally cemented clays. Offshore sediments often display "psuedo-overconsolidation"; that is, most aspects (low surface strength, no obvious hiatus, steady increase of strength with depth) point to normal consolidation but consolidation tests indicate a moderate degree of overconsolidation. If "psuedo-overconsolidation" results from a form of interparticle cementation, the NSP approach would predict strengths that are too low.

The presence of significantly different sediment below the level of sampling or the presence of undetermined environmental factors that might alter the consolidation state also cannot be handled by the NSP approach. Bubble phase gas might be an example of the latter. Highly varied or stratified sediment might also produce complications.

Cyclic Strength Degradation and Test Type Effects. Excess pore water pressures that develop during episodes of cyclic loading from earthquakes or storm waves effectively reduce the ability of the sediment to resist shear. This effect on shearing resistance can be expressed as a strength degradation factor, A_D. If this factor is multiplied by the static shearing strength obtained by the NSP approach, an estimate of the strength remaining in the sediment after dynamic loading will result. The degradation factor, A_D, varies with the type and magnitude of cyclic loading. If the loading is wave induced and the sediment is fairly pervious, an effective stress approach with allowance for partial pore pressure dissipation may be required for accurate modeling. For this situation a worst case (lower bound of strength) model can be provided by using a strength degradation parameter, A_D corresponding to no drainage. For earthquakes the duration of cyclic loading is short and a simple, undrained approach can be taken.

Another factor affecting measured sediment strength is the type of strength test performed. A reported value of shearing strength is not independent of test type because of initial consolidation conditions, shearing rate, stress inhomogeneities, variations in stress orientations and many other potential differences. A parameter that relates the strength corresponding to the mode and rate of stress application that would exist during failure in the field to the strength of the same material measured in a field or laboratory test is needed. In the present studies most strengths were obtained through isotropically consolidated triaxial shear tests. Because field consolidation conditions are typically anisotropic, a correction factor, A_c, is applied to correct strength values for these consolidation effects.

Summary of NSP Strength Determination. A summary of the normalized soil parameter approach as it has been applied in the northeastern Gulf of Alaska is given by the following equation:

$$S_u/\sigma_v' = A_C A_D (OCR)^{\Lambda_o} S_{nc} \qquad (1)$$

Where S_u = The undrained shearing strength applicable to the mode of failure under consideration

σ_v' = overburden effective stress = $U\gamma'z$

U = degree of consolidation

= 1 for complete normal or over-consolidation

γ' = average submerged density

z = sub-bottom depth

A_C = Test type correction factor

A_D = Cyclic strength degradation factor

OCR = Overconsolidation ratio

= σ_{vm}' / σ_v'

σ_{vm}' = Maximum past effective stress

Λ_o = A normalized strength exponent that is constant for a given sediment

S_{nc} = the ratio of static undrained shearing strength to isotropic consolidation stress for normally consolidated conditions.

A program that involves a family of triaxial test types has been developed to obtain the parameters needed to evaluate Equation 1. The specific procedures are described under TEST PROCEDURES. Not that all of these properties relate to undrained conditions. For earthquake loading and wave loading of relatively impervious sediment, the undrained assumption is valid. For long term gravitational loading and wave loading of pervious sediment, a drained or partially drained analysis would be required.

Other shearing strength tests have been conducted that do not follow the NSP methodology directly. These include laboratory vane shear, field vane shear and static cone penetration, and certain types of triaxial shearing tests. The field tests were conducted to establish a level of ground truth and provide a basis for judging the quality of subsequent laboratory data. Also, some field penetration tests were conducted in sandy deposits and provide the only reliable geotechnical data for these deposits. Laboratory vane tests were conducted onboard the ship immediately following sample recovery. They typically provide a lower bound estimate of the in place undrained shearing strength (Lee, 1979). The triaxial tests that did not follow the NSP methodology involved samples consolidated to the in situ effective overburden stress or lower. These types of tests typically produce an upper bound estimate of the in place undrained shearing strength (Ladd and Lambe, 1963).

Quantitative Evaluation of Offshore Stability. Some of these geotechnical results can be readily used to evaluate geologic hazards or provide a means of mapping relative stability. The three major offshore downslope driving forces are gravity, earthquake shaking and storm wave loading. By writing a simplified equation for each driving force and setting it equal to the estimated, in place undrained shearing strength, we can determine the level of force needed to achieve failure. For example, it can be shown (Lee and others, 1981) that the approximate shearing stress developed under combined earthquake and gravitational loading is given by the simplified equation:

$$\tau = \gamma' z \sin\alpha + k\gamma z \qquad (2)$$

Where:
- τ = mobilized shearing stress at depth z
- α = slope angle
- k = horizontal pseudo-static earthquake acceleration (in g's)
- γ = average total density of sediment (unit weight in air)

This relation was derived from Morgenstern's (1967) infinite-slope pseudo-static, earthquake-influenced slope stability analysis. It is valid only for small slope angles (α less than about 10°). The pseudo-static approach assumes that an earthquake can be modeled by a constant horizontal acceleration. The infinite slope approach assumes that the seafloor is smooth and has the same slope over a large area. Failure occurs on a plane parallel to the surface of the slope and movement takes the form of a sliding sheet. At failure the driving force will equal the resisting force. Substituting τ from Equation 2 for S_u in Equation 1 and solving for k yields:

$$k = (\gamma/\gamma')U\, A_C A_D (OCR)^{\Lambda_o} S_{nc} - (\gamma'/\gamma)\sin\alpha \qquad (3)$$

The resulting critical acceleration, k, derived from Equation 3 is the pseudo-static acceleration needed to induce failure given all of the conditions and assumptions present in the derivation. It is a function of sediment and site parameters. Lower values of the critical acceleration would correspond to areas that are more vulnerable to seismically induced sliding, given a uniform degree of seismicity over the region being investigated. The value of this approach is increased if known failures are sampled. Critical accelerations from a known failure area indicate the level of shaking required to cause failure and provide a value by which the significance of other measured critical accelerations can be judged.

A similar approach could be followed to evaluate relative stability with respect to storm wave-induced shearing stresses. However, as shown in Appendix B, the magnitude of peak wave-induced stresses exceeds that of peak earthquake-induced stresses only in relatively shallow water (water depth less than 35 to 76 m). In these depths the sediment is primarily sand which might allow nearly full dissipation of excess pore water pressures during storms. If full dissipation did not occur, a condition similar to liquefaction might develop under certain combinations of density, wave height and permeability (Clukey and others, 1980). This situation is unlikely and not considered in this report. For other conditions, earthquake loading dominates and Equation (3) can serve as the critical equilibrium relation.

TEST PROCEDURES

Geotechnical testing was conducted in conjunction with four cruises to the Gulf of Alaska: three from the R/V DISCOVERER in 1977, 1980 and 1981 (DC1-77-EG, DC2-80-EG and DC1-81-EG) and one from the R/V SEA SOUNDER in 1977 (S8-77-EG). Many different USGS individuals were involved in planning and conducting these tests in-house, and three outside laboratories conducted additional tests on four separate contracts (Geotechnical Engineers, Incorporated (GEI), 1977 cores, University of California, Berkeley, 1977 cores and Law Engineering Testing Company (LETCO), 1977 cores and 1980 cores). As a result, not all of the procedures followed in determining each property were identical throughout the test program. In the following discussion, major differences in procedure are listed whenever significant.

Shipboard Sampling and Testing. Most core samples were taken with gravity corers weighing between 2 and 10 kNt. A few samples were obtained with piston samplers or a vibratory corer similar to the Alpine Vibracore sampler described by Tirey (1972). All cores were contained within a plastic liner. Once aboard ship the core liners were sectioned into 1 or 1.5 m lengths. At most sites replicate cores were obtained; one was split, described and subsampled on shipboard (stratigraphy-sedimentology core), while the other was sealed with cheesecloth and microcrystalline wax and preserved under refrigeration for shore laboratory testing (geotechnical core). One of the split core sections was subsampled for water content determiniation.

Most vane shear testing was conducted on split cores sections. A miniature four-bladed vane (typically 1.22 x 1.22 cm) was inserted perpendicular to the split face so that it was at least 1.2 cm below the surface. The vane was rotated by a motor-driven device through a calibrated spring on the 1977 cruises and through a torque cell on the 1980 and 1981 cruises. The top of the torque cell or spring rotated at 90°/minute, a rate relayed directly to the vane by the stiff torque cell. With the more flexible springs, the true vane rotation rate was less than 90°/minute before failure and greater after failure. The peak torque was measured and used to calculate the sample undrained shearing strength (ASTM, 1982 standard D 2573-72).

In Place Testing. In place vane shear and cone penetration tests were conducted during the 1980 cruise. The Multi-purpose in situ testing system (MITS) was leased from Woodward-Clyde Consultants, Plymough Meeting, PA, and deployed at seven locations in the eastern Gulf of Alaska. The device is a tethered, bottom-supported platform capable of conducting static cone penetration and vane shear tests to a depth of 6 m below the seafloor. The device weighs 27 kNt (2.7 metric tons) in water. The ultimate cone penetration depth at a few locations was limited because of insufficient reaction force. The static cone penetrometer tip has a standard 10 cm^2 base area and a 60° tip angle. The load on the cone was measured by a full-bridge strain gage load cell mounted directly above the cone. The shear vane sensor consisted of a torque cell mounted above the vane blade. The vane was rotated by a pressure compensated electric motor at a rate of 60°/min and the shearing strength was calculated from the same formula as that used for laboratory vane shear measurements. Both the cone and the vane were driven into the seafloor by a sliding drive head coupled to a drill rod. The drive head was moved at 1 m/minute by an electric motor and a chain and sprocket assembly. The sub-bottom depth to the cone or vane was measured by a 360° potentiometer connected to the sprocket assembly. A tilt indicator mounted on the base sensed the attitude of the frame to determine whether the maximum deadweight reaction was exceeded or if lateral loads on the tether line were pulling the device over. All electrical signals were carried to shipboard recorders through a shielded cable.

The MITS system was deployed from the R/V DISCOVERER from a two-point mooring. Typically the system was assembled in the cone penetrometer mode on its first deployment at a site. After a penetrometer record was obtained, the device was returned to the ship and rigged to perform a vane shear test. The size of vane and torque cell as well as sub-bottom locations for vane shear tests were selected based on the cone penetration resistance. The device was redeployed and the vane was driven in to the predetermined depths. At each depth the vane was rotated to obtain a peak torque and thus a measure of in place undrained shearing strength. At some depths the vane was rotated in the opposite direction (following an initial undisturbed strength determination) to obtain a measure of the remolded strength and the sediment sensitivity.

Shore Laboratory Testing. Water contents were obtained using drying and weighing techniques (ASTM, 1982 standard D2216-80). A correction was made to the weights to account for dried salts (assuming a salinity of 35 ppt).

Atterberg limits were obtained using ASTM standards (D 423-66, D 424-59 and wet preparation technique, D 2217-66) with the exception that the Casagrande grooving tool was used instead of the ASTM tool. Salt corrections identical to those described above were applied to both the liquid and plastic limits. The grain density was obtained using a Beckman air comparison pycnometer at the USGS laboratory and by ASTM Standard D 854-58 for the tests conducted by contractors. Grain size distributions and parameters were obtained using pipette analysis (Carver, 1971) at the USGS and by the hydrometer technique (ASTM Standard D 422-63) at the contractor laboratories.

Consolidation testing followed ASTM Standard D 2435-70 with these exceptions:

(a) In two early contracts (GEI and LETCO testing of 1977 cores), calculated and plotted void ratios corresponded to the end of a stress increment time period. In later testing the plotted void ratios corresponded to 100% consolidation.
(b) In all contracted tests the coefficient of consolidation (c_v) was calculated using the square root of time method. For the tests conducted at the USGS, c_v was obtained using the log of time method.
(c) In the LETCO testing of 1980 samples, about half of the tests were conducted with a pneumatically controlled Anteus consolidometer while the remainder were conducted with a dead weight oedometer.
(d) Some of the tests conducted by the USGS on 1980 and 1981 samples were performed in a back pressured triaxial cell using the constant rate of strain technique (Wissa and others, 1971).

In all cases the results were used to estimate the maximum past vertical stress, σ'_{vm}, using the Casagrande (1936) construction and to obtain other consolidation parameters.

Static triaxial testing roughly followed the procedures given by Bishop and Henkel (1957). Cylindrical samples (3.6 cm in diameter by about 9 cm in height) were hand-trimmed from larger core sections extruded from the plastic liner. Filter strips were attached and the sample was enclosed in a thin rubber/latex membrane in a triaxial cell. Differential pressures between cell and sample fluids were applied and full drainage was allowed. These consolidation stresses were applied in increments until a final value was reached. In some tests conducted by the USGS and LETCO on 1980 and 1981 samples, final consolidation was set to a level of about four times the maximum past stress. This was followed by a reduction in differential pressure and full drainage. In this way, an induced state of overconsolidation with a known value of OCR was generated. A few samples were consolidated anisotropically with the horizontal consolidation stress equal to about 0.5 times the vertical consolidation stress.

Most samples were sheared without drainage by increasing the axial load at a constant rate of strain, typically 0.03% to 0.16% per hour. Some of the LETCO testing of 1977 cores involved constant rate of stress application. Excess pore water pressures developed in the samples during undrained shear were measured using electronic pressure transducers. Axial loads were measured with strain gage type load cells and axial deformations were obtained with linearly variable differential transformers (LVDT's). Testing was continued until about 20% axial strain was obtained. Stresses and strains were calculated using standard procedures but without membrane or filter strip corrections. The static undrained shearing strength was obtained from the peak axial load measured over the full 20% axial strain range of the test.

Three types of static triaxial tests were performed:

(a) Consolidation to a stress level less than three times the estimated maximum past stress without rebound.
(b) Consolidation to a stress level greater than three times the estimated maximum past stress with a subsequent rebound to a lower final consolidation stress. A known induced overconsolidation ratio is obtained.
(c) Consolidation to a stress level greater than three times the estimated maximum past stress without rebound.

Type (a) tests produce strength values that may be less than, equal to or greater than the in place shearing strength, depending on the details of the consolidation stresses. The approach does not provide parameters that can be used in the NSP approach. The value of this type of test would be in obtaining upper and lower bound values of strength and in studying naturally cemented sediment for which the NSP approach is not applicable.

Type (b) and (c) tests yield strength values for use in the NSP approach. Type (c) is used to obtain the ratio of strength to consolidation stress for normal consolidation, S_{nc}, while type (b) yields the parameter Λ_o required for Equation 1.

Specimens for cyclic triaxial tests were prepared and consolidated in the same way as specimens for static tests (b) and (c) above. Because the static test for each consolidation condition was performed first on an adjacent sample, an estimate of the static strength of the cyclic specimen could be made. Cyclic stresses less than the estimated static strength were then applied and the number of cycles needed to cause a predetermined one-directional strain was measured. Nearly full stress reversal (tensile and compressive stresses approximately equal) was developed. Loading was sinusoidal with a frequency of 0.1 Hz. The results were graphed on a plot of relative stress level (maximum average one-directional cyclic stress/estimated static strength) versus the log of number of cycles to 20% one-directional strain. A straight line connecting the data points was drawn and the stress level required for failure in 10 cycles was estimated by interpolation or extrapolation. Because 10 cycles is a characteristic number of significant cycles for a major earthquake (Seed and Peacock, 1971), this stress level was used for A_D in Equations 1 and 3 for earthquake analysis. The parameter A_D for storm-wave-induced instability would correspond to a larger number of cycles.

RESULTS

Study Areas and Core Locations. To simplify locating core sample and in place data, the region has been divided into eight study areas. Many of the study areas are associated with the major failure features discussed previously. Proceeding from west to east the eight study areas are (Figure 14):

(A) Copper River
(B) Kayak Trough
(C) Bering Trough
(D) Icy Bay
(E) Icy Bay-Malaspina
(F) Yakutat Bay
(G) Yakutat
(H) Alsek River

A ninth category, "other", includes a few sampling and in place stations that fall outside the regular areas.

Core and in place test location maps for each study area are given in Figures 15 through 21. The coordinates for these locations are given in Table 1.

Organization of Laboratory Test Data Presentation. All of the index property data are provided on summary plots in Appendix C. These data include water content, Atterberg limits, vane shear, grain size and grain density. Downcore locations of samples on which consolidation and triaxial tests were performed are also shown. The nature of these tests is indicated by a coded test number. The code for the test numbering system is as follows:

First two letters:
(a) OE - Oedometer test
(b) CE - Constant rate of strain (CRS) consolidation test
(c) TE - Static triaxial test
(d) TC - or D - Cyclic triaxial test

Trailing characters:
(a) No trailing characters - test performed by the USGS

(b) L1 - Test of 1977 core sample by Law Engineering and Testing Company
(c) G - Test of 1977 sample by Geotechnical Engineers, Incorporated
(d) B - Test of 1977 sample by University of California, Berkeley
(e) L2 - Test of 1980 sample by Law Engineering and Testing Company

Critical sediment geotechnical parameters from each test are summarized in Tables 2 (consolidation), 3 (static triaxial) and 4 (cyclic triaxial). Graphical presentations of the results of each test are given in Appendices D (Law Engineering testing of 1977 cores), E (Geotechnical Engineers, Incorporated testing), F (Law Engineering testing at 1980 cores) and G (USGS testing of 1980 and 1981 cores). The appendices are grouped according to the organization performing the test because of a variation in the formats followed in graphically presenting the data. Each appendix is subdivided according to test type (consolidation, static triaxial or cyclic triaxial).

For the consolidation tests, a standard plot of void ratio, e, versus vertical effective stress, σ_v', is given. These plots were used to obtain the slopes of the virgin compression and rebound curves (C_c and C_r) and the maximum past stresses, σ_{vm}', all of which are tabulated in Table 2. For some of the testing organizations, a plot is also given of the calculated coefficient of consolidation, c_v, versus the vertical effective stress.

For the static triaxial tests, plots are given of the shearing or deviatoric stress, q, versus the mean normal effective stress, p. These stress paths provide a definition of the failure envelope and indicate whether sediment behavior is of a collapsing (bend to the left) or dilitative (bend to the right) nature. Also given are plots of shearing or deviatoric stress and pore pressure change versus axial stress.

The cyclic triaxial test plots include shearing stress-axial strain curves (hysteresis loops) and shearing stress-average normal effective stress (stress path) plots for selected cycles. The stress path plots indicate roughly the failure envelope applicable for cyclic loading and the rapidity with which pore pressures develop as a result of cyclic loading. The hysteresis loops indicate damping (proportional to relative area of each loop) and degrading stiffness (proportional to average slope through each loop). For the USGS tests these results are further presented on four additional plots that show pore pressure developed, damping, stiffness (modulus) and peak strain developed as a function of cycle number.

In Place Test Data. The results of in place vane shear testing are given in Figures 22 through 26 and cone penetrometer records appear in Figures 27 through 34. The vane shear results are plots of calculated undrained shearing strength versus sub-bottom depth. The cone results are continuous plots of cone pressure versus depth. Additional information plotted on the figures is discussed in a later section.

SYNTHESIS AND DISCUSSION

Analysis of Parameters. A major goal of the geotechnical testing was to provide parameters that could be inserted into Equation 3 so that a stability-related parameter, the critical acceleration, k, could be calculated. These parameters are:

(a) S_{nc} - ratio of undrained strength to consolidation stress for normal consolidation
(b) A_C - test type correction factor
(c) A_D - cyclic strength degradation factor
(d) U - degree of consolidation
(e) OCR - overconsolidation ratio
(f) Λ_o - normalized strength exponent
(g) γ/γ' - ratio of submerged unit weight to total unit weight
(h) α - slope angle

The next few sections discuss several of these parameters and how they were obtained from the basic engineering properties given in Tables 2 through 4 and in the appendices. Most of these parameters are correlated with sediment water content. In these correlations the water content is used as an index property that is representative of more basic sediment characteristics such as clay mineralogy, grain size and plasticity. The water content is used in place of these other parameters because it is the only parameter that was measured in conjunction with every other test. Also, because more water contents were measured than any other property, correlations can be applied to any location where a water content measurement was made. The influence of in place consolidation on reducing the water content with sub-bottom depth is ignored because of the shortness of the cores and the relative incompressibility of the silty sediment. The significant down-core fluctuations in water content in many of the cores appear to be related to basic lithologic changes.

Undrained Strength to Consolidation Stress Ratio for Normal Consolidation, S_{nc}. The type (c) tests listed in Table 3 were used to obtain values of S_{nc}. The criterion used to distinguish type (c) tests was that the final consolidation stress applied in the triaxial cell needed to exceed the natural maximum past stress by at least a factor of 3. Any lower consolidation stresses, in conjunction with disturbance effects, might produce a sample with some characteristics of overconsolidation (Ladd and Foott, 1974). The ratios of strength to overburden pressure for all of the type (c) tests were obtained and are plotted versus water content in Figure 35. The correlation is fairly good, given the scatter typically involved in geotechnical measurements, and shows a trend toward decreasing S_{nc} with increasing water content. A solid line follows the trend of the tests for which the initial consolidation was isotropic. The tests for which initial consolidation was anisotropic (lateral stress about one-half of the vertical stress) are shown with circled dots. Although a limitation in the number of these points prevents the construction of a line as complete as that for isotropic consolidation, a line with values of S_{nc} that are 0.8 times the isotropic values seems to fit the data fairly well.

Test Type Correction Factor, A_C. The factor A_C ideally should relate strength under laboratory test rate, test mode and consolidation stress conditions to the strength effective in the field under natural loading conditions. Most aspects cannot be considered without a major increase in the scope of investigation. The relation between strength under laboratory consolidation (predominately isotropic) and field consolidation (predominately anisotropic) condition is straightforward and represented by the difference between the two lines in Figures 35. Because a ratio of 0.8 appeared to account for most of the variation, this value will be used for A_C. The value is similar to that obtained in an earlier study of sediment from offshore northern California. (Lee and others, 1981).

Cyclic Strength Degradiation Factor, A_D. Results of cyclic triaxial tests on fine grained sediment are typically presented on a plot of cyclic stress level (as a percent of static strength) versus number of cycles to failure (Lee and Focht, 1976). Such a presentation is dependent upon knowledge of a static strength that can be used for normalization. In the University of California, Berkeley tests, the static strength of a third sample cut from the same increment as two cyclic test samples was determined. Normalizing the cyclic stress levels by this static strength is legitimate because the cyclic samples probably would have had the same strength if failed statically. For the USGS and Law Engineering tests, however, a static strength was measured on a sample from the same core but a different depth increment from that of the cyclic tests. One method (Method I) of normalizing the cyclic stress is to divide the cyclic stress level by this measured static strength. In some cores, however, there were lithologic changes downcore and the static and cyclic tests were not run on the same material type. This problem was solved partially by estimating a static strength from the water content and consolidation stress of the cyclic sample and an estimate of the ratio of static strength to consolidation stress from Figure 35. This approach to obtaining the static strength is termed Method II. A third method of handling this problem is to eliminate the need for static strength estimation by evaluating the product $A_D\ S_{nc}$ rather than its components. Because A_D is a cyclic shear stress, τ_c, divided by a static strength, S_u, and S_{nc} is S_u divided by a consolidation stress, σ_{vc}', the product is τ_c/σ_{vc}'. This ratio can be obtained from a cyclic test alone without any static test results. The use of the ratio τ_c/σ_{vc}' is termed Method III.

Plots of relative cyclic stress levels versus number of cycles to failure are given in Figures 36 through 48. Separate figures corresponding to the three methods of analysis are given for the USGS/Law Engineering test results. The lines shown in the figures connect two or more cyclic test results and have been extended when necessary to cover the 10 cycles to failure zone. For methods I and II, the relative stress level corresponding to 10 cycles to failure was taken as A_D. For method III this value was taken as $A_D\ S_{nc}$ or τ_c/σ_{vc}'. Plots of relative stress level for failure in 10 cycles versus representative water content for the three methods of analysis are given in figures 49 through 51. Method II (Figure 50) shows a somewhat closer correlation than Method I (Figure 49); a solid line fit of the data shows an acceptable level of scatter (Figure 50). The trend shows an increase in A_D with increasing water content. That is, the lower water content coarse silts and sands are more susceptible to cyclic strength degradation than are the higher water content fine silts and clays. The product of the solid line fits for S_{nc} (Figure 35) and A_D (Figure 50) yields a solid line fit for $S_{NC}\ A_D$ versus water content (Method III, Figure 51).

Some of the University of California, Berkeley, tests were performed with a static bias (Figures 36 through 39). That is, following nearly isotropic consolidation but before cyclic shear, a static shearing stress was applied. The sinusoidal cyclic stress was then applied relative to the static bias. The level of principal stress rotation (alternating compressive and tensile stresses) is reduced as the static bias is increased. Herrmann and Houston

(1976) show that the greater the level of principal stress rotation the greater is the extent of cyclic strength degradation. In cyclic earthquake loading of nearly horizontal sediment deposits, there is considerable rotation of principal stresses with each major cycle of loading (Seed and Peacock, 1971). Therefore, the case of no static bias or full stress rotation is more realistic as well as more conservative. The tests with a significant static bias give an intermediate level of cyclic strength degradation.

Degree of Consolidation, U, Overconsolidation Ratio (OCR) and Normalized Strength Exponent, Λ_o. A critical concern in evaluating offshore stability is the relative consolidation state of the sediment. Table 2 provides some information on consolidation state in the form of two parameters: σ_e' and $\sigma_{vm}'/\gamma'z$. The parameter, σ_e' is the difference between the maximum past stress, σ_{vm}' and the submerged weight per unit area of overlying material, $\gamma'z$. The parameter is negative for underconsolidated sediment (not all submerged overburden carried by interparticle stress), zero for normal consolidation and greater than 1 for overconsolidation. The ratio $\sigma_{vm}'/\gamma'z$ is the degree of consolidation, U, for values of σ_e' less than or equal to 1 and the overconsolidation ratio (OCR) for values greater than or equal to 1. As may be seen, scattered values of both parameters were obtained with apparently underconsolidated, normally consolidated and overconsolidated sediment all present. There is little consistency among the values, however, and in only about 10% of the tests is the absolute value of σ_e' greater than 50 kPa. Because of inaccuracies present in the Casagrande procedure and coring disturbance, these small deviations from normal consolidation are probably insignificant. In later sections additional in place data and theoretical information is used to further evaluate the consolidation state of these sediments. Based on Table 2 alone, it appears that the best estimate for both U and OCR for most of the cores is 1.0 (normal consolidation).

In anticipation of at least some of the cores being overconsolidated, a few static triaxial tests of the type (b) variety (induced overconsolidation ratio) were performed. These were used to obtain estimates of the parameter Λ_o needed for Equations 1 and 3. To obtain Λ_o, one first obtains the ratio of undrained strength to consolidation stress for a specimen that has an induced overconsolidation ratio (OCR known). This ratio is divided by the ratio of strength to consolidation stress for normal consolidation, S_{nc} to obtain a shear strength that has been normalized twice. Again, S_{nc} may be obtained from a test on a different sample from the same core or estimated from Figure 35 (if the initial water content of the induced OCR sample is known). These methods are termed I and II, respectively, and are similar to Methods I and II for normalizing cyclic triaxial test data discussed previously. The parameter Λ_o is obtained by dividing the log of the twice normalized shear strength by the log of the induced OCR (Mayne, 1980). Values of Λ_o (by both Methods I and II) and the intermediate parameters required to calculate them are given in Table 5. There is considerable scatter and a few values exceed 1.0 (not physically reasonable; probably indicative of experimental error at some level). Also, there is no correlation between Λ_o and water content. The average value of 0.9 would be appropriate for overconsolidated sediment. However, in the present study, all Holocene glacial-marine silty clays tested appear to be under- or normally consolidated.

Ratio of Submerged to Total Unit Weight, γ'/γ. The ratio of submerged to total unit weight can be calculated directly from the water content by assuming 100% saturation and using the average measured grain density, 2.8 g/cm^3.

Validity of NSP Approach, Vane Shear Tests and Type (a) Triaxial Tests. One purpose of performing in place strength tests was to provide a ground truth check on values obtained in the laboratory. The locations where both in place vane shear tests were performed and cores were taken for shore geotechnical analysis offer an opportunity to check the quality of laboratory strength determination procedures. Strengths were measured in the laboratory using the miniature vane, type (a) static triaxial tests (consolidation to a low value, often near the estimated in situ overburden stress) and normalized soil property (NSP) oriented tests (types (b) and (c)). These laboratory strength determinations are shown on the same figures as the field vane shear results (Figures 22 through 26). In these comparisons the laboratory vane shear results are consistently lower than the field results. The laboratory values range between about 50 and 80% of the field values. These findings are thus in line with a value of 60% obtained for a low plasticity (PI=15%) southern California sediment (Lee, 1979). The type (a) static triaxial tests consistently yielded strengths 150 to 250% higher than the field values.

The NSP values were obtained by using measured core water contents to obtain ratios of static strength to overburden effective stresses (S_{nc}) from Figure 34. The overburden effective stresses were obtained from $\gamma' z$ (average submerged unit weight times depth) and multiplied by the S_{nc} estimates to obtain an estimated shear strength profile. An implicit assumption of normal consolidation was made. These estimated shear strength values ranged between about 60% and 140% of the measured field values for the depth range sampled (excluding the upper 1 m). Below the level of sampling, a range of estimated strengths is given, corresponding to the range of water contents measured in the core. In this deeper unsampled sediment the NSP estimated shearing strengths were about 80 to 140% of the field values.

The NSP approach appears to provide the best estimate of the in place shearing strength values while the type (a) static triaxial test (consolidation to a low stress level with no normalization) appears to provide the poorest estimate and has the lowest correlation with the in place results. The simple laboratory vane shear test is nearly as accurate as the NSP approach if measured strengths are multiplied by a correction factor of about 1.7 (1/0.6) to account for disturbance. The laboratory vane test is not suitable for extrapolation below the level of sampling or evaluating cyclic strength degradation, however.

Evaluation of Consolidation State Using Field Strength Results and Gibson's Theory. Laboratory consolidation tests showed little indication of underconsolidation but the results were fairly scattered. Another means of judging consolidation state is to compare field vane strengths with NSP generated strengths. Such a comparison (Figures 22 through 26) shows no indication of overconsolidation except possibly for the upper 3.5 m of field test MV-1. That is, the field strengths do not greatly exceed the NSP strengths calculated by assuming normal consolidation. With field test MV-1 the high field strengths are probably a result of layered sand observed in nearby vibratory cores rather than true overconsolidation.

Field tests MV-4 (Figure 25) and, to a lesser extent MV-5 (Figure 26) suggest that a state of underconsolidation exists in the sediment in the eastern portion of the Icy Bay-Malaspina study area. The field strengths are 60 to 80% of the NSP generated strengths for normal consolidation. Excluding any other errors or opportunities for variability, these values correspond directly to the degree of consolidation.

To further evaluate the potential for underconsolidation in the northeast Gulf of Alaska, we performed a simplified theoretical analysis using the method of Gibson (1958). Gibson modeled a layer of sediment deposited at a steady and continuing sedimentation rate, m, that began to be deposited at a time, t, in the past. The degree of consolidation at the base of the sediment column can be predicted (Figure 52) as a function of the dimensionless parameter, m^2t/c_v, where c_v is the coefficient of consolidation. The degree of consolidation at shallower levels is somewhat lower.

Values of c_v were measured in this study but are fairly scattered and inconsistent (Table 2). To reduce the scatter, a simplified correlation between c_v and liquid limit (Figure 53) from Lambe and Whitman (1969, p. 412) was used along with average liquid limit values for several locations. Sedimentation rates were taken from Figure 3.

By combining the results of Figures 52 and 53, we constructed lines of constant degree of consolidation on a plot of liquid limit versus m^2t (Figure 54). Using measured results, locations within the eastern Gulf of Alaska were plotted on the same figure. The position of these data points relative to the lines of constant degree of consolidation indicates the theoretical degree of consolidation of the sites. Most of the sites fall to the left of the 90% consolidation line indicating a degree of consolidation approaching 100%. All of the field vane shear tests except MV-4 (eastern Icy Bay-Malyaspina study area) correspond to sites that fall in this range. The eastern Icy Bay-Malaspina study area has a theoretical degree of consolidation of about 85%, somewhat greater than the discrepancy between NSP and field strengths (Figures 25 and 26), but in the same range. Therefore, several lines of evidence (field versus NSP strength, theory and consolidation test results) suggest a degree of underconsolidation (60 to 85% of normal consolidation) of the sediment in the eastern Icy Bay-Malaspina study area. As indicated on Figure 54, the eastern portion of the Alsek prodelta study area and Kayak Trough may also display a similar underconsolidation level. Two of the embayments, Icy Bay and Yakutat Bay, appear to be highly underconsolidated, having degrees of consolidation of 30 and near 15%, respectively. The remainder of the Holocene glacial-marine sediment sites appear to be normally consolidated.

Critical Acceleration Calculation. The critical acceleration, k, is calculated from Equation 3. If we assume normal consolidation (U=OCR=1) and horizontal surfaces (α=0), then all of the remaining parameters have been obtained as a function of water content in the sections above. Note that with a value of OCR equal to 1.0, the value of Λ_o is irrelevant. Also, with OCR equal to 1.0, the solution for k is independent of sub-bottom depth. By combining the best fits of the data using Equation 3, a plot of critical acceleration versus water content can be drawn (Figure 55). The resulting values of the critical acceleration have a broad-based minimum between water contents of 35% and 45%. On either side of this zone the acceleration increases rapidly. The existence of this minimum range indicates that certain types of sediment found in the eastern Gulf of Alaska are more susceptible to earthquake loading than others. If we assume that each location within the region has the same potential ground shaking intensity and that underconsolidation and slope effects can be ignored initially, then locations that have more of the susceptible material should have failed more often. Within the Icy Bay-Malaspina study area (Figure 56), this appears to be the case. The portion of each core with a water content between 35% and 45% has been calculated and listed by the location of the core. It appears that those cores within the observed failure feature typically have more of the susceptible sediment than do those outside the feature. The correlation is not exact but is consistent. Thus mapping of vulnerable material according to surface core water content may be viable even though the extent of underconsolidation, steepness of slope, variations in seismicity and variations in seismic response have not been considered.

The distribution of susceptible material in the Yakutat study area is shown in Figure 57. The correlation of susceptible material with the slump zone is not as good as for the Icy Bay-Malaspina area. The higher level of underconsolidation in the Icy Bay-Malaspina area may contribute to the greater extent of failure. Also, the boundaries of the Yakutat slump are poorly defined acoustically.

In the Alsek study area (Figure 58), all cores were collected within the failure zone. The majority of samples appear to consist of susceptible sediment.

Regional Variations. Most of the geotechnical properties discussed above have been tied together through a seismic-induced instability analysis. A correlation of parameters with water content has shown some consistent trends and has helped to identify a susceptible sediment type. The water content, in turn, typically increases offshore, although not consistently. Downcore variations in water content are large.

No consistent variations in the correlations of geotechnical parameters with water content were found that could be related to study area. Indeed, the differences between study areas appear to be of the same order as variations within study areas. Some differences in landslide morphology were noted in the geologic framework discussion that cannot be explained by these basic correlations. For example, the multiple, complex flows of the Alsek prodelta contrast with the massive but simple rotational slumps of the Icy Bay-Malaspina study area. One possible explanation of these morphology differences is that fundamental sedimentological parameters contribute to variations in post failure behavior. That is, certain geotechnical properties that correlate well with water content may determine the point of initial failure. Movement after failure may be controlled by other characteristics that are not properly evaluated in triaxial testing.

An example of at least one characteristic that appears to vary consistently among the study areas is plasticity. All of the Atterberg limits measurements, grouped according to geographic area, are plotted on a series of plasticity charts (plasticity index versus liquid limit, Lambe and Whitman, 1969, p. 35) in Figures 59 through 64. Least squares regression fits of each set of data were developed and displayed fairly good correlation coefficients. Figure 65 presents a summary of all of the linear regression lines. All plot above the "A-line" and fall near or within the zone generally occupied by glacial clays (Lambe, 1951, p. 27). Most sediment classifies as CL ("inorganic clays of low to medium plasticity, gravelly clays, sandy clays, silty clays, lean clays"). The regression lines are nearly parallel to each other and to the "A-line." The continental shelf study areas (Alsek prodelta, Yakutat, Icy Bay-Malaspina, Copper River) show a progressively greater distance from the "A-line" as one progresses toward the west. The Alsek prodelta slide, which has the most unusual morphology, provides data that plot closest to the "A-line." The embayments (Icy Bay, Yakutat Bay) and troughs (Bering, Kayak) show the greatest distance from the "A-line". This behavior probably relates to changes in clay mineral activity. The unusual morphology of the Alsek prodelta slides and flows may relate to these changes in index properties.

SUMMARY AND CONCLUSIONS

1. Previous studies have shown the major seafloor geologic hazards in the eastern Gulf of Alaska to be slides and flows, shallow faults, gas charged sediment and buried channels. Excluding shallow faulting, these hazards on the continental shelf are associated with Holocene glacial-marine sediment. This sediment consists primarily of sand and muddy sand in water depth less than 50 m and clayey silt at greater depths. The Holocene glacial-marine sediment is a typical glacial rock flour produced by intense mechanical weathering. Massive failure features have been identified acoustically on slopes of 0.5° to 1.3° on the continental shelf. Sediment volumes of up to 32 km^3 are involved.

2. Both underconsolidation (Hampton and others, 1978; Carlson and others, 1978; Molnia and Sangrey, 1979) and bubble-phase gas charging (Carlson and others, 1980; Hampton and others, 1978; Molnia and Rappeport, 1980) have been suggested as principal causative factors for sediment instability in the region. The present study indicated that both features are present but that their occurrence is uncommon.

3. Cyclic loading by storm waves and particularly earthquakes appears sufficient to cause the observed failure features. Gas charging and underconsolidation may facilitate failure in a few locations. Major wave induced shearing stresses exceed major earthquake induced stresses only in relatively shallow water (less than 35 to 76 m).

4. As noted by Ladd and Foott (1974), the normalized soil parameter (NSP) approach appears capable of partially overcoming the problems of coring disturbance and core shortness in obtaining valid geotechnical properties. This is illustrated in this study by good comparisons between NSP generated strength profiles and those measured with an in place vane shear device. One comparison that is not as good can be explained by underconsolidation predicted by Gibson's (1958) analysis.

5. Laboratory vane shear tests produce shearing strengths that are consistently lower than the field strengths. Triaxial specimens consolidated to near the in place overburden stress produce strengths that are erratically higher to much higher than the field strengths.

6. There is little evidence for overconsolidation in the Holocene glacial-marine sediment tested.

7. Many of the geotechnical parameters correlate well with water content, which is probably representative of more basic sediment characteristics such as clay mineralogy, grain size, and plasticity. According to laboratory tests, sediment with a water content between 35% and 45% is most susceptible to earthquake loading. Cores that contain more of this susceptible material roughly correlate with the locations of failure features.

8. Differences in failure morphology are difficult to relate to advanced geotechnical parameters but may relate to observed variations in plasticity.

ACKNOWLEDGEMENTS

These studies were supported by the U.S. Geological Survey and the Bureau of Land Management through an interagency agreement with the National Oceanic and Atmospheric Administration, under which a multiyear program responding to needs of petroleum development of the Alaskan continental shelf is managed by the Outer Continental Shelf Environmental Assessment Program (OCSEAP) office.

We wish to thank Bill Levy, Ed Clukey, Charles Fitts, Dwight Sangrey, Arnold Bouma, Bruce Molnia and Paul Carlson for their effort in acquiring the early geotechnical data presented in this report. We also wish to thank Dan Bright, Pat Spragge, Kris Johnson and Mike Torresan for performing the later geotechnical tests. Finally, we thank Monty Hampton, Bill Winters and Jim Booth for their thoughtful and helpful reviews of this manuscript.

REFERENCES

American Society for Testing and Materials (ASTM), 1982, 1982 annual book of ASTM Standards, part 19, Natural Building Stones; Soil and Rock, ASTM, Philadelphia, 710 pp.

Bea, R.G., 1976, Earthquake criteria for platforms in the Gulf of Alaska: Proceedings of the 8th Offshore Technology Conference, Houston, vol. 2., p. 657-679.

Beikman, Helen, 1974, Preliminary geologic map of the southeast quadrant of Alaska: U.S. Geological Survey Miscellaneous Field Studies Map MF-612, Scale 1:1,000,000.

Beikmann, Helen, 1975, Preliminary geologic map of southeastern Alaska: U.S. Geological Survey Miscellaneous Field Studies Map MF-673, Scale 1:1,000,000.

Bishop, A.W. and Henkel, D.J., 1957, The measurement of soil properties in the triaxial test, Edward Arnold, Ltd, London, 227 p.

Bruns, T.R., 1979, Late Cenozoic structure of the continental margin, northern Gulf of Alaska, in Sisson, Alexander, ed., The relationship of plate tectonics to Alaskan geology and resources: Alaska Geological Society 1977 Symposium Proceedings, p. I1-I30.

Bruns, T.R., 1982, Structure and petroleum potential of the continental margin between Cross Sound and Icy Bay, northern Gulf of Alaska: U.S. Geological Survey Open-File Report 82-929, 63 p.

Bruns, T.R. and Plafker, George, 1982, Geology, structure, and petroleum potential of the southeastern Alaska and northern Gulf of Alaska continental margins, in Bruns, T.R., ed., Hydrocarbon resource report for proposed O.C.S. Lease Sale 88: Southeastern Alaska, Northern Gulf of Alaska, Cook Inlet, and Shelikof Strait, Alaska, p. 11-52.

Bruns, T.R., and Schwab, W.C., 1982, Structure maps and seismic stratigraphy of the Yakataga segment of the continental margin, northern Gulf of Alaska: U.S. Geological Survey Miscellaneous Field Studies Map MF-1424, 2 sheets and 25 p., scale 1:250,000 (in press).

Carlson, P.R., 1978, Holocene slump on continental margin off Malaspina Glacier, Gulf of Alaska: American Association of Petroleum Geologists, Bulletin, vol. 62, no. 12, p. 2412-2426.

Carlson, P.R., 1979, Extensive sliding of continental slope sediments, eastern Gulf of Alaska (abs.): Geol. Soc. of America, Abstracts with Program, vol. 11, p. 398.

Carlson, P.R., Bruns, T.R., and Molnia, B.F., 1975, Submarine slides and near surface faults, northern Gulf of Alaska: U.S. Geological Survey Open-File Report 75-505, 1 map.

Carlson, P.R., Bruns, T.R., Molnia, B.F., and Schwab, W.C., 1982, Submarine valleys in the northeastern Gulf of Alaska: Characteristics and probable origin: Marine Geology, vol. 47, p. 217-242.

Carlson, P.R., Levy, W.P., Molnia, B.F. and Hampson, J.C., 1978,Geotechnical properties of sediments from the continental shelf south of Icy Bay, northeastern Gulf of Alaska: U.S. Geological Survey Open-File Report 78-1071, 29 p.

Carlson, P.R., and Molnia, B.F., 1975, Preliminary isopach map of Holocene sediments, northern Gulf of Alaska: U.S. Geological Survey Open-File Report 75-507.

Carlson, P.R., and Molnia, B.F., 1977, Submarine faults and slides on the continental shelf, northern Gulf of Alaska: Marine Geotechnology vol. 2, p. 275-280.

Carlson, P.R., Molnia, B.F., Kittelson, S.C., and Hampson, J.C., Jr., 1977, Distribution of bottom sediments on the continental shelf, northern Gulf of Alaska: U.S. Geological Survey Miscellaneous Field Studies Map MF-876, 2 sheets and 13 p., scale 1:500,000.

Carlson, P. R., Molnia, B. F., and Wheeler, M. C., 1980, Seafloor geologic hazards in O.C.S. lease area 55, eastern Gulf of Alaska: Proceedings of the 12th Offshore Technology Conference, Houston, v. 1, p. 563-603.

Carlson, P. R., and Schwab, W. C., 1982, Northern Gulf of Alaska environmental geology, in Bruns, T. R., ed., Hydrocarbon resource report for proposed OCS lease sale 88: southeastern Alaska, northern Gulf of Alaska, Cook Inlet, and Shelikof Strait, Alaska: U.S. Geological Survey Open-File Report 82-928, p. 73-86.

Carver, R. E., 1971, Procedures in sedimentary petrology: Wiley-Interscience, New York.

Casagrande, Arthur, 1936, The determination of the pre-consolidation load and its practical significance: Proceedings, 1st International Conference of Soil Mechanics and Foundation Engineering, p. 60.

Clukey, E. C., Cacchione, D. A., and Nelson, C. H., 1980, Liquefaction potential of the Yukon Prodelta, Bering Sea: Proceedings of the 12th Annual Offshore Technology Conference, Houston, vol. 1, p. 315-325.

Gibson, R. E., 1958, The progress of consolidation in a clay layer increasing in thickness with time: Geotechnique, vol. 8, p. 71-182.

Hampton, M. A., Bouma, A. H., Carlson, P. R., Molnia, B. F., Clukey, E. C., and Sangrey, D. A., 1978, Quantitative study of slope instability in the Gulf of Alaska: Proceedings of the 10th Offshore Technology Conference, Houston, vol. 4, p. 2307-2318

Herrmann, H. G., and Houston, W. N., 1976, Response of seafloor soils to combined static and cyclic loading: Proceedings of the Eighth Offshore Technology Conference, paper number OTC 2428.

Ladd, C. C., and Foott, Roger, 1974, New design procedure for stability of soft clays: American Society of Civil Engineers, Journal of the Geotechnical Engineering Division, vol. 100, no. GT7, p. 763-786.

Ladd, C. C., and Lambe, T. W., 1963, The strength of "undisturbed" clay determined from undrained tests: American Society for Testing and Materials, Standard Technical Publication 361, p. 342-371.

Lambe, T. W., 1951, Soil testing for engineers, J. Wiley and Sons, New York, 165 p.

Lambe, T. W. and Whitman, R. V., 1969, Soil Mechanics, J. Wiley and Sons, New York, 533 p.

Lee, H. J., 1979, Offshore soil sampling and geotechnical parameter determination: Proceedings of the 11th annual Offshore Technology conference, paper number OTC 3524.

Lee, H. J., Edwards, B. D., and Field, M. E., 1981, Geotechnical analysis of a submarine slump, Eureka, California: Proceedings of the 13th annual Offshore Technology Conference, paper number OTC 4121.

Lee, H. J., and Schwab, W. C., 1982, Geotechnical investigations related to geologic hazards: northern Gulf of Alaska, in, Bruns, ed, Hydrocarbon resource report for proposed O.C.S. Lease Sale 88: southeastern Alaska, northern Gulf of Alaska, Cook Inlet, and Shelikof Strait, Alaska: U.S. Geological Survey Open-File Report 82-928, p. 87-94.

Lee, K. L., and Focht, J. A., 1976, Strength of clay subjected to cyclic loading: Marine Geotechnology, vol. 1, no. 3, p. 165-186.

Mayne, Paul, 1980, Cam-clay prediction of undrained strength: American Society of Civil Engineers, Journal of the Geotechnical Engineering Division, vol. 106, p. 1219-1242.

Minster, J. B., and Jordon, T. H., 1978, Present day plate motions: Journal of Geophysical Research, vol. 83, no. B11, p. 5331-5354.

Molnia, B. F., 1979, Sedimentation in coastal embayments, northeastern Gulf of Alaska: Proceedings of the 11th Annual Offshore Technology Conference, Houston, vol. 2, p. 665-676.

Molnia, B. F., and Carlson, P. R., 1975, Surface sediment distribution, northern Gulf of Alaska: U.S. Geological Survey Open-File Report 75-505, 1 sheet.

Molnia, B. F., and Carlson, P. R., 1978, Surface sedimentary units of northern Gulf of Alaska continental shelf: American Association of Petroleum Geologists Bulletin, vol. 62, no. 4, p. 633-643.

Molnia, B. F., and Carlson, P. R., 1980, Quaternary sedimentary facies on the continental shelf of the northeastern Gulf of Alaska, in Field, M. E., Bouma, A., and Colburn, I., ed., Quaternary depositional environment of the U.S. Pacific continental margin: Society of Economic Paleontologists and Mineralogists Symposium, Pacific Section, Bakersfield, p. 157-168.

Molnia, B. F., Carlson, P. R., and Bruns, T. R., 1977, Large submarine slide in Kayak Trough, Gulf of Alaska, in Coates, D. R., ed., Landslides: Reviews in Engineering Geology, vol. 3, Geological Society of America, p. 137-148.

Molnia, B. F., Levy, W. P., and Carlson, P. R., 1980, Map showing sedimentation rates in the northeastern Gulf of Alaska: U.S. Geological Survey Miscellaneous field studies Map, MF-1170 1 sheet.

Molnia, B. F., and Rappeport, M. L., 1980, Seafloor mosaic of the Alsek pockmark, slump, and sediment failure area, northeast Gulf of Alaska (Abs.): Geol. Soc. Amer., abstracts with programs, Atlanta, p. 436.

Molnia, B. F., and Sangrey, D. A., 1979, Glacially derived sediments in the Gulf of Alaska; geology and engineering characteristics: Proceedings of the 1979 Offshore Technology Conference, Houston, vol. 1, p. 647-655.

Morgenstern, N. M., 1967, Submarine slumping and the initiation of turbidity currents: in Marine Geotechnique, A. F. Richards (ed.), University of Illinois Press, p. 189-220.

Plafker, George, 1967, Geologic map of the Gulf of Alaska Tertiary province, Alaska: U.S. Geological Survey Miscellaneous Geologic Investigations Map I-484, scale 1:500,000.

Plafker, George, 1971, Pacific margin Tertiary basin, in Future petroleum provinces of North America: American Association of Petroleum Geologists Memoir 15, p. 120-125.

Reimnitz, Erk, 1966, Late Quaternary history and sedimentation of the Copper River delta and vicinity, Alaska: University of California, San Diego, Ph.D. thesis (unpub.), 160 p.

Seed, H. B., and Peacock, W. H., 1971, Procedures for measuring soil liquefaction characteristics: American Society of Civil Engineers, Journal of the Soil Mechanics and Foundation Engineering Division, vol. 97, no. SM8, p. 1099-1119.

Seed, H. B., and Rahman, M. S., 1978, Wave-induced pore pressure in relation to ocean floor stability of cohesionless soils: Marine Geotechnology, vol. 3, no. 2, p. 123-150.

Stephens, C. D., and Page, R. A., 1982, Seismic activity in the northern Gulf of Alaska since 1974, in, Bruns, T. R., Hydrocarbon resource report for proposed O.C.S. Lease Sale 88: Southeastern Alaska, Northern Gulf of Alaska, Cook Inlet, and Shelikof Strait, Alaska, p. 115-121.

Tirey, G. B., 1972, Recent trends in underwater soil sampling methods: American Society for Testing and Materials, Standard Technical Publication 501, p. 42-54.

Varnes, D. J., 1978, Slope movement types and processes, in Schuster, R. L., ed., Landslides, analysis and control: National Research Council, Transportation Research Board Special Report 176, p. 12-23.

Wissa, A.E.Z., Christian, J. T., Davis, E. H., and Heiberg, Sigurd, 1971, Consolidation at constant rate of strain, American Society of Civil Engineers, Journal of the Soil Mechanics and Foundation Division, vol. 97, no. SM10, p. 1393-1413.

TABLES

Table 1. Core and in place test locations organized by study area

Study Area	Cruise	Core or In Place Test Number*	Latitude	Longitude
Copper River	S8-77-EG	4G	60° 15.18' N	145° 45.91' W
		6G	60° 12.94' N	145° 44.87' W
		7G	60° 12.93' N	145° 44.79' W
		8G	60° 10.64' N	145° 45.13' W
		9G	60° 10.64' N	145° 45.13' W
Kayak Trough	S8-77-EG	10G	60° 06.59' N	144° 39.06' W
		11G	60° 06.59' N	144° 39.06' W
		13G	60° 05.12' N	144° 40.44' W
		14G	60° 05.12' N	144° 40.44' W
		15G	60° 00.44' N	144° 34.55' W
		16G	60° 00.93' N	144° 40.16' W
		17G	60° 01.15' N	144° 40.7' W
		18G	59° 56.05' N	144° 39.14' W
		19G	59° 56.22' N	144° 39.24' W
		20G	59° 56.35' N	144° 39.34' W
		21G	59° 56.43' N	144° 38.27' W
Bering Trough	S8-77-EG	34G	59° 56.53' N	143° 32.36' W
		36G	59° 56.64' N	143° 35.75' W
		38G	59° 58.05' N	143° 38.00' W
Icy Bay-Malaspina	S8-77-EG	25G	59° 34.86' N	141° 58.20' W
		26G	59° 45.29' N	141° 57.17' W
		27G	59° 49.38' N	141° 55.61' W
		28G	59° 30.98' N	141° 20.73' W
		29G	59° 31.13' N	141° 20.90' W
		31G	59° 34.30' N	141° 21.04' W
		32G	59° 34.43' N	141° 20.96' W
		33G	59° 37.45' N	141° 20.18' W
	DC2-80-EG	95G	59° 36.60' N	141° 23.40' W
		96G	59° 36.60' N	141° 23.30' W
		173G	59° 38.05' N	141° 22.75' W
		175G	59° 37.25' N	141° 23.35' W
		176G	59° 37.25' N	141° 23.15' W
		178G	59° 36.10' N	141° 23.50' W
		179G	59° 36.00' N	141° 23.40' W
		181G	59° 35.30' N	141° 24.60' W
		182G	59° 35.20' N	141° 24.50' W
		184G	59° 34.40' N	141° 25.30' W
		185G	59° 34.40' N	141° 25.30' W
		187G	59° 33.30' N	141° 25.80' W
		188G	59° 33.30' N	141° 25.80' W
		190G	59° 32.50' N	141° 26.30' W
		191G	59° 32.50' N	141° 26.30' W
		193G	59° 31.20' N	141° 26.6' W
		194G	59° 31.30' N	141° 26.20' W

Table 1. Core and in place test locations organized by study area (continued)

Study Area	Cruise	Core or In Place Test Number*	Latitude	Longitude
Icy Bay-Malaspina	DC2-80-EG	196G	59° 36.50' N	141° 19.10' W
		197G	59° 36.50' N	141° 19.10' W
		MP9	59° 36.6' N	141° 23.4' W
		MP10	59° 36.5' N	140° 19.1' W
		MV4	59° 36.6' N	141° 23.4' W
		MV5	59° 36.5' N	140° 19.1' W
	DC1-81-EG	626G3	59° 35.00' N	140° 33.60' W
		627G1	59° 36.30' N	140° 45.20' W
		627G2	59° 36.35' N	140° 44.80' W
		628G2	59° 37.60' N	140° 57.00' W
		628G3	59° 37.50' N	140° 56.90' W
		630A1	59° 41.90' N	141° 20.10' W
		630A2	59° 41.70' N	141° 20.20' W
		632G1	59° 35.50' N	141° 09.50' W
		632G2	59° 35.50' N	141° 09.50' W
		633G1	59° 32.40' N	141° 06.00' W
		633G2	59° 32.40' N	141° 06.00' W
		634G1	59° 30.20' N	141° 00.00' W
		634G2	59° 30.20' N	141° 00.00' W
		635A2	59° 39.81' N	141° 09.15' W
	DC1-77-EG	709B	59° 34.30' N	141° 51.45' W
		709C	59° 34.30' N	141° 51.45' W
		710B	59° 41.50' N	141° 40.50' W
		710C	59° 41.40' N	141° 40.40' W
		711B	59° 42.60' N	141° 39.85' W
		715B	59° 36.45' N	141° 47.45' W
		715C	59° 36.45' N	141° 47.45' W
		717B	59° 39.30' N	141° 42.20' W
		717C	59° 39.30' N	141° 42.20' W
		718B	59° 38.45' N	142° 07.30' W
		719B	59° 42.60' N	142° 01.85' W
		720B	59° 45.65' N	141° 57.85' W
		721C	59° 47.00' N	141° 52.85' W
		721D	59° 48.00' N	141° 52.85' W
Icy Bay	S8-77EG	39G	60° 04.16' N	141° 23.42' W
		40G	60° 03.56' N	141° 22.27' W
		41G	60° 01.71' N	141° 21.06' W
		42G	60° 01.05' N	141° 21.31' W
		43G	59° 56.99' N	141° 26.49' W
		44G	59° 59.03' N	141° 27.94' W
Yakutat Bay	S8-77-EG	45G	59° 52.15' N	139° 41.85' W
		46G	59° 52.21' N	139° 41.81' W
		47G	59° 43.93' N	139° 42.08' W
		48G	59° 38.22' N	139° 47.93' W
Yakutat	DC2-80-EG	61G	59° 28.45' N	139° 48.16' W
		64G	59° 28.23' N	139° 48.83' W

Table 1. Core and in place test locations organized by study area (continued)

Study Area	Cruise	Core or In Place Test Number[a]	Latitude	Longitude
Yakutat	DC2-80-EG	65G	59° 28.22' N	139° 48.97' W
		66G	59° 28.20' N	139° 48.88' W
		69G	59° 28.13' N	139° 49.38' W
		72G	59° 27.83' N	139° 49.59' W
		83G	59° 28.21' N	139° 48.00' W
		84G	59° 28.21' N	139° 48.40' W
		85G	59° 27.71' N	139° 50.06' W
		87G	59° 27.49' N	139° 50.58' W
		88G	59° 27.50' N	139° 50.64' W
		MP4	59° 28.21' N	139° 48.40' W
		MP5	59° 28.63' N	139° 48.14' W
		MV2	59° 28.21' N	139° 48.40' W
		MV3	59° 28.63' N	139° 48.15' W
	DC1-81-EG	616A2	59° 28.80' N	139° 48.10' W
		617G1	59° 22.70' N	139° 48.90' W
		617G2	59° 22.90' N	139° 48.80' W
		618G1	59° 23.19' N	139° 48.45' W
		618G2	59° 23.34' N	139° 48.44' W
		619G1	59° 24.45' N	139° 48.19' W
		620G1	59° 25.59' N	139° 48.09' W
		620G2	59° 26.03' N	139° 48.20' W
		621G1	59° 26.58' N	139° 47.31' W
		621G2	59° 27.04' N	139° 47.34' W
		623A1	59° 28.70' N	139° 49.70' W
		624A1	59° 28.70' N	139° 49.10' W
		624A2	59° 28.70' N	139° 48.70' W
		625A1	59° 28.70' N	139° 47.90' W
		625A2	59° 28.50' N	139° 48.20' W
Alsek River	DC2-80-EG	MC3-22	59° 06.99' N	138° 44.31' W
		23G	59° 06.99' N	138° 44.31' W
		26G	59° 07.09' N	138° 44.19' W
		28G	59° 06.99' N	138° 43.97' W
		29G	59° 06.93' N	138° 43.85' W
		31G	59° 06.89' N	138° 43.72' W
		32G	59° 06.99' N	138° 43.72' W
		35G	59° 06.99' N	138° 43.39' W
		36G	59° 06.94' N	138° 43.44' W
		38G	59° 06.94' N	138° 43.17' W
		43G	59° 06.94' N	138° 43.09' W
		46G	59° 06.91' N	138° 42.85' W
		47G	59° 06.94' N	138° 42.79' W
		49G	59° 06.92' N	138° 42.63' W
		50G	59° 06.92' N	138° 42.67' W
		52G	59° 06.93' N	138° 42.58' W
		55G	59° 06.93' N	138° 42.10' W
		56G	59° 06.88' N	138° 42.11' W
		MP3	59° 07.00' N	138° 44.29' W
		MP6	59° 07.74' N	138° 43.85' W
Alsek River	DC2-80-EG	MP7	59° 07.74' N	138° 43.85' W
		MV1	59° 07.00' N	138° 44.31' W
	DC1-81-EG	601G2	59° 06.60' N	138° 42.20' W
		602G3	59° 06.18' N	138° 40.25' W
		603G1	59° 06.16' N	138° 39.25' W
		604G3	59° 06.02' N	138° 39.42' W
		604G4	59° 06.09' N	138° 39.57' W
		605G1	59° 05.47' N	138° 38.01' W
		605G2	59° 05.49' N	138° 38.09' W
		606G1	59° 05.50' N	138° 36.80' W
		606G2	59° 05.27' N	138° 37.13' W
		607A1	59° 07.60' N	138° 44.60' W
		607A2	59° 07.50' N	138° 44.60' W
		608A2	59° 06.90' N	138° 45.40' W
		609A1	59° 05.70' N	138° 39.60' W
		610A2	59° 05.50' N	138° 37.70' W
		611G1	59° 04.90' N	138° 38.60' W
		611G2	59° 05.10' N	138° 39.10' W
		G12G1	59° 05.60' N	138° 40.50' W
		G13G2	59° 06.20' N	138° 43.70' W
		G14G2	59° 07.00' N	138° 46.10' W
Other	S8-77-EG	1G	60° 02.21' N	147° 11.28' W
		2G	60° 02.21' N	147° 11.28' W
		23G	59° 50.75' N	144° 24.26' W
	DC2-80-EG	92G	59° 00.15' N	139° 54.03' W
		MP2	59° 18.81' N	139° 18.59' W
		MP8	59° 00.16' N	139° 54.01' W
	DC1-81-EG	615A1	58° 18.80' N	139° 19.20' W
	DC1-77-EG	700B	59° 42.15' N	142° 41.80' W
		704B	59° 55.10' N	142° 31.05' W

[a] Core or test number code
- G, B, C, or D - Gravity or piston core
- A - Vibratory core
- MP - In place cone penetration test
- MV - In place vane shear test

Table 2. Consolidation Test Results

Cruise Core #	Depth in Core, z, cm	Test Number	Study Area	$\gamma'z$, kPa[a]	σ_{vm}', kPa[b]	σ_e', kPa[c]	$\frac{\sigma_{vm}'}{\gamma'z}$[d]	C_c[e]	C_s[f]	c_v[g] (cm^2/sec) ($X10^{-3}$)	Initial Water Content, %
S8-77-BG											
1G	80-90	OE1L1	Other	6.5	7	0.5	1.08	0.20	0.015	0.5-2	45.8
	230-235	OE2L1	Other	17.8	17	-0.8	0.96	0.15	0.020	0.5-3	37.5
4G	90-100	OE1G	Copper River	7	13	6	1.86	0.13	0.027	0.8-4	47.5
	190-200	OE2G	Copper River	13	12	-1	0.92	0.20	0.023	1.1-4.4	45.3
	310-320	OE3G	Copper River	23	14(?)	-9	0.61	0.25	0.038	2.0-4.1	39.2
	400-410	OE4G	Copper River	31	40	9	1.29	0.24	0.020	4.5-5.8	36.0
	605-610	OE5G	Copper River	49	29(?)	-20	0.73	0.23	0.032	4.0-5.0	40.1
6G	30-40	OE6G	Copper River	3	10	7	3.33	0.41	0.032	0.4-2.5	61.9
	100-107	OE7G	Copper River	6	8	2	1.33	0.48	0.053	0.6-2.4	60.5
7G	850-860	OE86	Copper River	66	39(?)	-27	0.59	0.36	0.045	2.0-3.3	45.1
8G	200-210	OE9G	Copper River	12	11	-1	0.92	0.49	0.061	0.5-1.4	73.6
	350-360	OE10G	Copper River	22	20	-2	0.91	0.41	0.041	2.0-3.1	55.9
	410-420	OE11G	Copper River	26	26	0	1.00	0.71?	0.105?	1.5-3.3	58.0
	660-670	OE12G	Copper River	45	68	23	1.51	0.42	0.062	2.5-3.1	52.3
	730-740	OE13G	Copper River	51	56	5	1.10	0.37	0.039	3.8-4.8	41.7
	800-810	OE14G	Copper River	58	58	0	1.00	0.30	0.033	3.5-4.8	42.0
	860-870	OE15G	Copper River	63	56	-7	0.89	0.33	0.033	3.9-4.9	43.8
9G	85-100	OE16G	Copper River	5	11	6	2.20	0.48	0.048	1.0-3.0	77.7
	290-300	OE17G	Copper River	20	18	-2	0.90	0.25?	0.034	2.1-4.1	45.2
10G	190-200	OE3L1	Kayak Trough	13.9	27	13.1	1.94	0.17	0.015	?-2	38.9
11G	115-125	OE4L1	Kayak Trough	´1.8	?	?	?	0.17	0.02	0.2-2	28.4
	240-250	OE5L1	Kayak Trough	19.8	15	-4.8	0.76	0.15	0.015	2.6-3.5	35.7
	390-400	OE6L1	Kayak Trough	31.9	60	28.1	1.88	0.20	0.02	1-3	39.9
	545-555	OE7L1	Kayak Trough	44.2	45	0.8	1.02	0.20	0.03	2.5-8	41.2
14G	100-110	OE8L1	Kayak Trough	6.3	10	3.7	1.59	0.23	0.02	0.4-1.5	42.[illegible]
16G	10-15	OE9L1	Kayak Trough	1.1	6	4.9	5.45	0.31	0.015	?	53.9
	102-107	OE10L1	Kayak Trough	9.2	12	2.8	1.30	0.13	0.02	1-2	30.0
	190-195	OE11L1	Kayak Trough	16.9	24	7.1	1.42	0.32	0.03	0.7-1.3	50.3
18G	30-40	OE12L1	Kayak Trough	2.2	?	?	?	0.30	0.02	0.2-0.5	63.8
	180-190	OE13L1	Kayak Trough	14	7	-7	0.50	0.21	0.03	?	47.7
	250-260	OE14L1	Kayak Trough	18.2	44	25.8	2.41	0.24	0.03	1-2.5	52.5
19G	65-75	OE15L1	Kayak Trough	4.6	8	3.4	1.74	0.24	0.015	?	53.9
	160-170	OE16L1	Kayak Trough	10.9	17	6.1	1.56	0.38	0.04	0.7-1.5	57.3
	260-270	OE17L1	Kayak Trough	17.5	15	-2.5	0.86	0.20	0.03	0.5-1.8	42.3
21G	280-300	OE18L1	Kayak Trough	13.8	14	0.2	1.01	0.30	0.04	0.5-2.0	43.1
	400-410	OE19L1	Kayak Trough	19.3	35	15.7	1.81	0.25	0.02	0.03-2.5	49.7
23G	100-110	OE20L1	Other	8.6	11	2.4	1.28	0.09	0.01	1-5	29.0
25G	80-90	OE18G	Icy Bay-Malaspina	6	9	3	1.50	0.21	0.026	1.0-3.1	58.4
	290-300	OE19G	Icy Bay-Malaspina	21	44	23	2.10	0.40	0.050	0.9-2.6	53.4
26G	100-110	OE20G	Icy Bay-Malaspina	9	12	3	1.33	0.17	0.02	2.5-3.3	36.9
	200-210	OE21G	Icy Bay-Malaspina	19	14	-5	0.74	0.18	0.029	2.1-4.0	34.5
27G	190-200	OE22G	Icy Bay-Malaspina	18	37	19	2.06	0.07	0.010	2.9-5.6	26.7
29G	105-115	OE23G	Icy Bay-Malaspina	9	14	5	1.56	0.23	0.021	2.1-4.5	39.4
	185-195	OE24G	Icy Bay-Malaspina	16	14	-2	0.88	0.25	0.027	2.0-4.1	44.6

Table 2. Consolidation Test Results (continued)

Cruise Core #	Depth in Core, z,cm	Test Number	Study Area	$\gamma'z$,kPa[a]	σ_{vm}',kPa[b]	σ_e',kPa[c]	$\frac{\sigma_{vm}'}{\gamma'z}$[d]	C_c[e]	C_s[f]	c_v[g] (cm^2/sec) ($X10^{-3}$)	Initial Water Content
S8-77-EG											
29G	290-300	OE25G	Icy Bay-Malaspina	26	20	-6	0.77	0.19	0.020	2.9-4.8	35.3
31G	90-100	OE26G	Icy Bay-Malaspina	9	15	6	1.67	0.16	0.019	4.6-6.1	34.0
	180-190	OE27G	Icy Bay-Malaspina	17	12	-5	0.71	0.17	0.017	2.0-5.5	33.1
	273-283	OE28G	Icy Bay-Malaspina	21	26	5	1.24	0.18	0.028	2.1-4.2	30.5
33G	22-30	OE29G	Icy Bay-Malaspina	2	13	11	6.50	0.24	0.025	1.0-5.7	35.5
	90-100	OE30G	Icy Bay-Malaspina	9	33	24	3.67	0.13	0.019	2.8-6.1	33.1
	205-216	OE31G	Icy Bay-Malaspina	19	16	-3	0.84	0.13	0.018	2.7-5.0	29.0
	361-371	OE32G	Icy Bay-Malaspina	32	25	-7	0.78	0.21	0.025	2.3-4.9	31.6
	500-510	OE33G	Icy Bay-Malaspina	48	25	-23	0.52	0.22	0.029	2.9-4.8	34.2
	675-685	OE346	Icy Bay-Malaspina	62	66	4	1.06	0.18	0.023	2.9-5.3	30.2
	790-800	OE35G	Icy Bay-Malaspina	73	35(?)	-38	0.48	0.16	0.024	3.8-5.1	29.7
34G	60-70	OE21L1	Bering Trough	7	6	-1	0.86	0.05	0.008	1-2.5	23.0
38G	27-37	OE22L1	Bering Trough	3	6	3	2.00	0.20	0.020	0.9-1.6	46.9
40G	306-316	OE36G	Icy Bay	22	12	-8	0.55	0.020	0.23	0.3-2.0	46.4
	506-516	OE37G	Icy Bay	44	23	-21	0.52	0.43	0.081	1.8-3.2	60.4
42G	110-120	OE38G	Icy Bay	8	8	0	1.00	0.34	0.039	0.3-1.6	37.7
	270-280	OE39G	Icy Bay	20	13	-7	0.65	0.29	0.050	1.0-2.8	43.9
47G	100-110	OE23L1	Yakutat Bay	7.7	11	3.3	1.43	0.18	0.020	?	43.8
	250-260	OE24L1	Yakutat Bay	18.8	10	-8.8	0.53	0.18	0.025	0.5-3.5	41.1
DC2-80-EG											
MC3-22	86-92	OE1L2	Alsek River	7.6	22	14.4	2.89	0.20	0.023	3-28	43.0
28G	37-39	CE11	Alsek River	3.8	80	76.2	20.9	0.09	0.014	---	26.7
35G	10-13	CE7	Alsek River	1.0	19(?)	18.0	19.3	---	---	---	34.7
	40-44	CE8	Alsek River	3.2	47	43.8	14.6	0.22	0.02	---	46.4
38G	68-74	OE2L2	Alsek River	6	22	16	3.67	0.20	0.021	6-17	31.6
43G	4-8	CE4	Alsek River	.5	11(?)	10.5	23.0	0.08	0.01	---	30.0
	38-41	CE5	Alsek River	3.6	17(?)	13.4	4.7	0.09	0.01	---	31.9
46G	4-7	CE10	Alsek River	.5	42	41.5	79.6	0.12	---	---	35.8
	41-44	CE9	Alsek River	3.8	51	47.2	13.5	0.15	0.02	---	36.1
49G	64-77	OE3L2	Alsek River	5.6	30	24.4	5.4	0.16	0.037	2.6-14	41.4
55G	74-80	OE4L2	Alsek River	6.2	28	21.8	4.5	0.27	0.028	5.3-15.6	53.1
84G	14-21	OE5L2	Yakutat	1.6	12	11.4	7.5	0.18	0.035	1.5-8	37.4
	76-84	OE6L2	Yakutat	5.6	20	14.4	3.6	0.22	0.030	---	44.0
	200-210	OE7L2	Yakutat	14.4	50	35.6	3.5	0.10	0.016	5.7-23	23.8
87G	146-148	CE26	Yakutat	11.8	50	38.2	4.2	0.17	---	20-80	41.1
96G	86-96	OE8L2	Icy Bay-Malaspina	7.4	10	2.6	1.4	0.17	0.053	1.8-15.3	39.3
	263-271	OE9L2	Icy Bay-Malaspina	27.0	120	93.0	4.4	0.13	0.015	19-28	28.6
	354-261	OE10L2	Icy Bay-Malaspina	30.8	31	0.2	1.0	0.17	0.022	1.5-7.9	32.7
	374-381	OE11L2	Icy Bay-Malaspina	33.4	40	6.6	1.2	0.14	0.037	3.0-12.3	38.0
181G	33-35	CE3	Icy Bay-Malaspina	2.7	11	9.3	4.1	0.22	---	---	40.0
	116-118	CE1	Icy Bay-Malaspina	9.4	22	12.6	2.3	0.21	---	---	41.3
	196-198	CE2	Icy Bay-Malaspina	15.8	13	-2.8	0.8	0.26	---	---	44.0
190G	30-38	OE12L2	Icy Bay-Malaspina	3.2	70	65.8	21.9	0.16	0.017	19-26	31.5
	227-234	OE13L2	Icy Bay-Malaspina	18.8	45	26.2	2.4	0.21	0.028	2.1-9.3	40.7

Table 2. Consolidation Test Results (continued)

Cruise Core #	Depth in Core	Test Number	Study Area	$\gamma'z$, kPa[a]	σ_{vm}', kPa[b]	σ_e', kPa[c]	$\frac{\sigma_{vm}'}{\gamma'z}$[d]	C_c[e]	C_s[f]	c_{2v}[g] (cm^2/sec) $(X10^{-3})$	Initial Water Content	
DC2-80-EG												
190G	281-289	OE14L2	Icy Bay-Malaspina	23.2	50	26.8	2.2	0.21	0.054	2.1-6.7	38.0	
196G	142-148	OE15L2	Icy Bay-Malaspina	14.2	23	8.8	1.6	0.10	0.031	10.2-34.8	28.6	
	248-255	OE16L2	Icy Bay-Malaspina	25.2	140	114.8	5.6	0.12	0.021	14.7-21.7	25.7	
	435-439	OE17L2	Icy Bay-Malaspina	45.8	120	74.2	2.6	0.11	0.027	8.6-17.8	21.9	
DC1-81-EG												
604-G3	142	OE44	Alsek River	11.6	280(?)	268.4	24.1	0.13	0.009	10-20	32.2	
605G2	70	OE46	Alsek River	5.0	70	65	14.0	0.25	0.017	2-11	52.8	
	154	CE25	Alsek River	11.0	50	39	4.5	0.25	---	6-22	46.9	
	198	OE45	Alsek River	16.4	42	25.6	2.6	0.17	0.012	2.5-9	40.2	
618G2	62-64	CE22	Yakutat	5	31	26	6.2	0.25	---	6-25	49.7	
	106-108	OE41	Yakutat	10	250(?)	240	25.0	0.16	0.007	9-12	31.3	
	110-115	CE17	Yakutat	11	14	3	1.3	0.14	0.014	3-40	30.0	
	166-168	CE29	Yakutat	13.4	32	18.6	2.4	0.25	---	5-22	44.8	
	190-195	CE18	Yakutat	16.4	22	5.6	1.3	?	---	3-30	39.0	
620G2	71-73	CE23	Yakutat	5.8	28	22	4.3	0.26	---	5-22	43.0	
624A1	152-157	CE33	Yakutat	15.7	570	554	36.3	0.03	---	2000	27.6	sand
	210-212	CE27	Yakutat	19.5	8.4to105	-11to85	.4to5.4	0.12	---	2-40	33.6	
627G2	26-28	CE16	Icy Bay-Malaspina	2	22	20	11.0	0.21	---	3.5-15	44.2	
	32-34	CE14	Icy Bay-Malaspina	2.6	82	80	31.6	0.21	---	10-25	41.1	
	116-118	CE13	Icy Bay-Malaspina	9.4	28	18.6	3.0	0.27	0.025	4-22	40.1	
	122-124	OE40	Icy Bay-Malaspina	9	15	6	1.7	0.24	0.017	0.9-10	48.1	
	222-224	CE15	Icy Bay-Malaspina	18	28	10	1.6	0.20	---	2-10	38.7	
630A2	210	CE32	Icy Bay-Malaspina	21	1050	1029	49.3	?	---	?	26.2	Sand
632G1	77	CE31	Icy Bay-Malaspina	7	90	83	12.9	0.16	---	5-30	33.9	
634G2	47-49	CE24	Icy Bay-Malaspina	3	12	9	4.0	0.33	---	2-12	56.7	

a - Sediment submerged unit weight times embedment depth, equal to in situ overburden stress for normal- and over-consolidation

b - Maximum past stress obtained by Casagrande technique

c - Difference between σ_{vm}' and $\gamma'z$; negative values correspond to underconsolidation, near zero values to normal consolidation and postitive values to overconsolidation

d - This parameter is the overconsolidation ratio for normally or overconsolidated sediment and the degree of consolidation for normally or underconsolidated sediment

e - Slope of the laboratory virgin compression curve

f - Slope of the laboratory rebound curve

g - Coefficient of consolidation for stresses greater than σ_{vm}'

Table 3. Static Triaxial Test Results

Cruise Core #	Depth in core, z, cm	Test Number	Study Area	$\gamma' z$, kPa[a]	σ'_{vm}, kPa[b]	σ'_{vc}, kPa[c]	σ'_{hc}, kPa[d]	Test Type[e]	Induced OCR[f]	$q_f(S_u)$, kPa[g]	S_u/σ'_{vc}[h]	ϕ', degrees[i]	Initial Water Content, %
88-77-EG													
1G	117-130	TE1L1	Other	9.5	9.1	10		a		16.5	1.65		47.4
	140-150	TE4L1	Other	11.2	10.7	7		a		27.5	3.93		44.6
	163-177	TE2L1	Other	13.1	12.6	20		a		17	0.85		44.7
	190-202	TE3L1	Other	15.1	14.5	40		a		29.5	0.74		42.4
	202-214	TE7L1	Other	16.0	15.4	50		c	1	34.3	0.69	34.3	38.4
	214-225	TE6L1	Other	16.9	16.2	30		a		25.5	0.85		41.1
	225-235	TE5L1	Other	17.7	17.0	20		a		29.7	1.49		38.4
4G	210-220	TE1G	Copper River	17.1	14	15		a		16.5	1.10		42.0
	220-230	TE2G	Copper River	17.9	14.5	29		a		21.0	0.72		45.7
	230-240	TE3G	Copper River	18.7	15.0	59		c	1	35.5	0.60	36.0	41.9
	240-250	TE4G	Copper River	19.5	15.5	10	5	a		15.0	1.50		41.6
	630-640	TE5G	Copper River	50.4	29.5	34		a		39.5	1.16		39.2
	640-650	TE6G	Copper River	51.2	30.0	69		a		53.5	0.78		36.9
	650-660	TE7G	Copper River	52.0	30.5	139		c	1	63.0	0.46	34.5	43.6
	660-670	TE8G	Copper River	52.8	30.5	25	12.5	a		55.0	2.20		36.0
	670-680	TE9G	Copper River	53.6	31.0	75		a		40.5	0.54		40.5
	680-690	TE10G	Copper River	54.4	31.5	200		c	1	93.0	0.47	36.5	37.6
	690-700	TE11G	Copper River	55.2	32.0	125		c	1	76.0	0.61	34.8	36.5
7G	780-790	TE12G	Copper River	60.8	35	40		a		22	0.55		47.7
	790-800	TE13G	Copper River	61.5	36	80		a		39	0.49		46.6
	800-810	TE14G	Copper River	62.3	36	30	15	a		27	0.90		46.6
	810-820	TE15G	Copper River	63.1	37	160		c	1	73	0.46	34.8	45.9
8G	230-240	TE16G	Copper River	16.2	11	15		a		9	0.60		61.3
	240-250	TE17G	Copper River	16.9	12	30		a		16	0.53		67.8
	250-260	TE18G	Copper River	17.6	13	10	5	a		9	0.90		66.0
	260-270	TE19G	Copper River	18.3	14	23		a		23	1.00		63.3
	650-660	TE20G	Copper River	45.3	49	50		a		23	0.47		58.4
	670-680	TE21G	Copper River	46.6	51	90		a		46	0.51		50.3
	680-690	TE22G	Copper River	47.3	52	140		a		51	0.36		53.7
	790-800	TE23G	Copper River	54.9	62	160		a		80	0.50		45.4
	810-820	TE24G	Copper River	56.3	64	40		a		36	0.90		45.7
	820-830	TE25G	Copper River	57.0	64.5	80		a		54	0.68		44.3
	830-840	TE26G	Copper River	57.7	65.5	30	15	a		41	1.37		---
	260-270	TE27G	Copper River	18.4	17	30		a		11.5	0.38		63.3
	270-280	TE28G	Copper River	19.1	17.5	15		a		10.5	0.70		48.7
	270-280	TE29G	Copper River	19.1	17.5	60		c	1	24	0.40	32.4	50.8
	280-290	TE30G	Copper River	19.8	18	10		a		11	1.10		59.5
10G	120-137	TE8L1	Kayak Trough	9.2	17.8	10		a		6	0.60		46.4
	137-150	TE9L1[j]	Kayak Trough	10.3	20.0	20		a		9.5	0.48		45.0
	150-162	TE10L1	Kayak Trough	11.1	21.5	30		a		11.5	0.38		49.2
	162-174	TE11L1[j]	Kayak Trough	12.0	23.3	7		a		14.7	2.10		41.6
11G	270-284	TE12L1	Kayak Trough	22.4	27.3	35		a		21.3	0.61		38.3
	300-314	TE13L1	Kayak Trough	24.8	30.3	60		a		50.1	0.84		36.3
	354-368	TE14L1	Kayak Trough	29.2	35.6	90		a		38.2	0.42		35.8
	555-568	TE17L1	Kayak Trough	45.4	55.4	120		a		30.0	0.25		40.3

Table 3. Static Triaxial Test Results (continued)

Cruise Core #	Depth in core, z, cm	Test Number	Study Area	$\gamma'z$, kPa[a]	σ'_{vm}, kPa[b]	σ'_{vc}, kPa[c]	σ'_{hc}, kPa[d]	Test Type[e]	Induced OCR[f]	q_f(Su), kPa[g]	S_u/σ'_{vc}[h]	ϕ', degrees[i]	Initial Water Content, %
S8-77-EG													
11G	582-592	TE18L1[j]	Kayak Trough	47.4	57.8	21		a		13.8	0.66		42.1
	642-655	TE16L1[j]	Kayak Trough	52.4	63.9	60		a		19.3	0.32		35.7
	662-675	TE15L1[j]	Kayak Trough	54.0	65.9	30		a		16.8	0.56		34.0
14G	41-54	TE19L1[j]	Kayak Trough	2.9	4.6	10		a		9	0.90		70.1
	54-68	TE20L1[j]	Kayak Trough	3.7	5.9	20		a		4.7	0.24		60.3
	84-98	TE21L1	Kayak Trough	5.5	8.7	40		c	1	20	0.50	33.7	55.5
16G	120-132	TE22L1	Kayak Trough	11.1	15.2	13		a		13	1.00		29.8
	132-144	TE24L1	Kayak Trough	12.2	16.6	54		c	1	19.8	0.37	31.5	35.1
	144-156	TE25L1	Kayak Trough	12.9	17.9	7		a		20	2.86		43.6
	167-180	TE23L1	Kayak Trough	15.3	20.8	20		a		30	1.50		30.6
19G	80-94	TE26L1[j]	Kayak Trough	5.8	8.0	10		a		11.5	2.00		52.0
	94-108	TE27L1[j]	Kayak Trough	6.7	9.3	20		a		14.3	2.13		53.5
	108-122	TE28L1[j]	Kayak Trough	7.6	10.5	40		a		17.0	2.23		53.8
21G	140-160	TE29L1	Kayak Trough	10.2	14.4	20		a		11.7	0.59		56.8
	195-210	TE30L1	Kayak Trough	13.7	19.3	35		a		26.3	0.75		50.2
	210-225	TE31L1	Kayak Trough	14.8	20.9	60		c	1	25.8	0.43	34.7	45.6
23G	42-56	TE33L1	Other	4.0	6.4	20		c	1	24	1.20	33.5	31.5
	56-70	TE34L1[j]	Other	5.1	7.5	40		c	1	37	0.93	40.5	34.3
	70-84	TE35L1[j]	Other	6.3	8.9	7		a		11.3	1.61		36.4
	84-108	TE32L1[j]	Other	7.8	11.0	10		a		18.8	1.88		34.2
25G	240-250	TE31G	Icy Bay-Malaspina	18.0	35.5	15		a		11	0.73		54.3
	260-270	TE32G	Icy Bay-Malaspina	19.5	39	60		a		25.5	0.43		54.1
	270-280	TE33G	Icy Bay-Malaspina	20.2	41	10	5	a		7	0.70		55.5
	280-290	TE34G	Icy Bay-Malaspina	20.9	43	30		a		15.5	0.52		49.7
26G	90-100	TE35G	Icy Bay-Malaspina	8.5	11	10		a		11	1.10		37.6
	160-170	TE36G	Icy Bay-Malaspina	14.8	13	20		a		17.5	0.88		37.0
	170-180	TE37G	Icy Bay-Malaspina	15.7	13	40		c	1	38.5	0.96	38.5	32.8
	180-190	TE38G	Icy Bay-Malaspina	16.6	13.5	10	5	a		19	1.90		31.2
27G	50-60	TE39G	Icy Bay-Malaspina	4.9	29	10	5	a		6	0.60		52.7
	60-70	TE40G	Icy Bay-Malaspina	5.8	30	30		a		13.5	0.45		51.0
	80-90	TE41G	Icy Bay-Malaspina	7.6	31	20		a		10.5	0.53		39.7
	90-100	TE42G	Icy Bay-Malaspina	8.5	31.5	10		a		12	1.20		34.6
	140-150	TE43G	Icy Bay-Malaspina	13.0	34	25		a		23	0.92		34.7
	150-160	TE44G	Icy Bay-Malaspina	13.9	35	15		a		14.5	0.97		40.0
	180-190	TE45G	Icy Bay-Malaspina	16.5	36	40		a		25	0.63		37.7
29G	135-145	TE46G	Icy Bay-Malaspina	12.1	14	15		a		10.5	0.70		47.2
	145-155	TE47G	Icy Bay-Malaspina	13.0	14	25		a		12	0.48		43.9
	155-165	TE48G	Icy Bay-Malaspina	13.9	14.5	40		a		10	0.25		39.4
	250-260	TE49G	Icy Bay-Malaspina	22.1	18	15		a		8.5	0.57		45.0
	330-340	TE50G	Icy Bay-Malaspina	29.0	21	10		a		11.5	1.15		35.6
	340-350	TE51G	Icy Bay-Malaspina	29.9	21.5	60		a		29	0.48		41.2
	350-360	TE52G	Icy Bay-Malaspina	30.8	22	30		a		23.5	0.78		35.9
31G	150-160	TE53G	Icy Bay-Malaspina	14.4	15.5	10	5	a		10	1.0		33
	160-170	TE54G	Icy Bay-Malaspina	15.4	16	10		a		12.5	1.25		35
	170-180	TE55G	Icy Bay-Malaspina	16.3	17	20		a		27	1.35		33

Table 3. Static Triaxial Test Results (continued)

Cruise Core #	Depth in core, z, cm	Test Number	Study Area	$\gamma'z$, kPa[a]	σ'_{vm}, kPa[b]	σ'_{vc}, kPa[c]	σ'_{hc}, kPa[d]	Test Type[e]	Induced OCR[f]	$q_f(S_u)$, kPa[g]	S_u/σ_{vc}[h]	ϕ', degrees[i]	Initial Water Content, %
S8-77-EG													
31G	190-200	TE56G	Icy Bay-Malaspina	18.2	18	40		a		32.5	0.81		34
33G	290-300	TE57G	Icy Bay-Malaspina	27.4	21	10	5	a		18.5	1.85		32.4
	321-331	TE58G	Icy Bay-Malaspina	30.2	22	10	5	a		13.5	1.35		37.2
	331-341	TE59G	Icy Bay-Malaspina	31.2	22	15		a		10	0.66		31.0
	341-351	TE60G	Icy Bay-Malaspina	32.1	22.5	30		a		25	0.83		36.0
	351-361	TE61G	Icy Bay-Malaspina	33.0	23	60		a		46.5	0.78		33.3
	470-480	TE62G	Icy Bay-Malaspina	44.0	26.5	45		a		30	0.67		37.5
	480-490	TE63G	Icy Bay-Malaspina	45.0	27	75		a		33	0.44		43.8
	490-500	TE64G	Icy Bay-Malaspina	45.9	27	98		c	1	41	0.42	30.5	40.0
36G	46-60	TE37L1	Bering Trough	4.7	---	40		a		39	0.98		37.9
	60-75	TE36L1	Bering Trough	5.9	---	10		a		13.3	1.33		27.0
38G	90-110	TE38L1	Bering Trough	9.5	19	10		a		24.5	2.45		25.9
40G	340-350	TE65G	Icy Bay	23.7	14	40		a		19	0.48		49.3
	350-360	TE66G	Icy Bay	24.4	14.5	80		c	1	26.5	0.33	25.8	51.8
42G	231-245	TE67G	Icy Bay	17.9	12	20		a		18.5	0.93		41.6
	245-258	TE68G	Icy Bay	18.9	12	39		c	1	22.5	0.58	30.0	43.1
	258-270	TE69G	Icy Bay	19.9	12.5	10	5	a		13.5	1.35		42
47G	133-147	TE41L1	Yakutat Bay	10.3	12.4	50		a		58.8	1.18		42.3
	189-202	TE39L1	Yakutat Bay	14.4	14.4	20		a		24.0	1.20		42.8
	239-250	TE40L1	Yakutat Bay	18.0	?	30		a		70.5	1.45		48.6
DC2-80-EG													
MC3-22	3-13	TE1L2	Alsek River	0.5	22	1.4		a		13	9.27		35.0
	47-62	TE6L2	Alsek River	4.8	22	3.4		a		58	17.06		25.0
	62-76	TE4L2	Alsek River	6.1	22	27.6		b	3	124.4	4.51		29.4
28G	6-14	TE64	Alsek River	0.8	80	328.5	136.8	c	1	159.4	0.48	39.6	45
	25-34	TE63	Alsek River	2.6	80	56.9		b	5.7	227.1	3.99		36.2
	26-35	TE62	Alsek River	2.6	80	310.7		c	1	268.8	0.87	38.2	30.5
31G	4-11	TE65	Alsek River	0.7	60	3		a		27.2	9.08		28.7
	4-11	TE66	Alsek River	0.7	60	223.2		c	1	215.0	0.96	38.2	30.4
	11-19	TE67	Alsek River	1.4	60	251.2	126.1	c	1	146.1	0.58	33.5	32.2
35G	14-23	TE56	Alsek River	1.6	40	154.8		c	1	80.8	0.52	36.3	40.4
	14-23	TE57	Alsek River	1.5	40	24.7		b	6.2	58.4	2.36		40.4
	25-32	TE58	Alsek River	2.3	40	137.6	68.5	c	1	60.3	0.44	34.8	43.6
38G	52-64	TE3L2	Alsek River	5.4	22	27.6		b	6	86.1	3.12		31.6
43G	8-17	TE27	Alsek River	1.1	14(?)	6.5		b	5	37.4	5.74		33.9
	18-27	TE34	Alsek River	2.0	14(?)	31.3		a		79.9	2.55		32.5
	18-27	TE35	Alsek River	2.0	14(?)	31.1		a		73.9	2.38		32.9
46G	18-27	TE59	Alsek River	2.1	45	203.1		c	1	222.4	1.10	35.8	31.5
	28-37	TE60	Alsek River	2.0	45	35.7		b	6.2	166.0	4.66		33.9
	28-37	TE61	Alsek River	2.2	45	0.7		a		23.4	33.46		29.8
49G	18-28	TE5L2	Alsek River	2.24	30	169.2	61.93	c	1	89.5	0.53	40.5	35.0
	28-40	TE2L2	Alsek River	3.19	30	120.6		c	1	87.7	0.73	38.3	35.2
84G	21-33	TE11L2	Yakutat	2.45	15	103.4		c	1	64.4	0.62	36.9	33.9
	63-76	TE8L2	Yakutat	6.06	20	3.4		b	6	27.8	8.17		35.7

Table 3. Static Triaxial Test Results (continued)

Cruise Core #	Depth in core, z, cm	Test Number	Study Area	$\gamma' z$, kPa[a]	σ'_{vm}, kPa[b]	σ'_{vc}, kPa[c]	σ'_{hc}, kPa[d]	Test Type[e]	Induced OCR[f]	q_f(Su), kPa[g]	S_u/σ'_{vc}[h]	ϕ',[i] degrees	Initial Water Content, %
DC2-80-EG													
84G	100-112	TE7L2	Yakutat	9.26	20	20.7		c	1	14.6	0.70	36.9	33.2
	160-172	TE10L2	Yakutat	15.78	35	1.4		a		34.9	24.93		24.6
	176-190	TE9L2	Yakutat	17.97	35	17.2		a		78.2	4.54		21.0
87G	150-158	TE84	Yakutat	13.04	50	203.1		c	1	122.8	0.61	35.7	38.6
96G	108-124	TE17L2	Icy Bay-Malaspina	11.17	95(?)	379.3	165.8	c	1	135.8	0.36	37.3	36.4
	155-170	TE12L2	Icy Bay-Malaspina	15.27	30	1.4		a		12.1	8.71		34.4
	173-183	TE13L2	Icy Bay-Malaspina	16.74	30	35.1		a		30.1	0.85		38.8
	198-212	TE16L2	Icy Bay-Malaspina	19.28	30	30.3		b	3	61.3	2.02		32.8
	343-356	TE15L2	Icy Bay-Malaspina	34.51	35	34.8		b	4	70.4	2.02		33.3
	361-374	TE14L2	Icy Bay-Malaspina	36.11	35	139.9		c	1	71.8	0.51	31.7	34.3
181G	5-15	TE15	Icy Bay-Malaspina	0.84	15	277.7		c	1	131.5	0.47	35.9	39.2
	5-15	TE16	Icy Bay-Malaspina	0.84	15	45.0		b	6.1	105.6	2.35		39.2
	71-81	TE18	Icy Bay-Malaspina	6.16	15	39.9		c	1	23.7	0.59	39.8	42.2
	71-81	TE19	Icy Bay-Malaspina	6.16	15	5.3		b	7.3	19.0	3.57		41.9
	100-110	TE20	Icy Bay-Malaspina	8.04	15	39.4	20.3	c	1	17.6	0.45	33.6	46.5
	100-110	TE21	Icy Bay-Malaspina	8.04	15	13.1		b	3	17.4	1.33		46.2
	120-130	TE22	Icy Bay-Malaspina	11.00	15	0.5		a		8.7	18.49		36.9
	120-130	TE23	Icy Bay-Malaspina	11.00	15	9.7		a		20.9	2.15		35.7
190G	80-94	TE20L2	Icy Bay-Malaspina	7.86	50	48.2		b	6	97.8	2.03		31.9
	101-114	TE18L2	Icy Bay-Malaspina	10.38	50	62.0		a		36.1	0.58	39.8	38.8
	114-125	TE19L2	Icy Bay-Malaspina	11.44	50	96.5		b	3	80.7	0.84		42.6
	175-188	TE21L2	Icy Bay-Malaspina	17.70	50	230.6	96.4	c	1	82.6	0.36	39.0	41.0
	201-214	TE22L2	Icy Bay-Malaspina	19.74	50	1.4		a		11.0	7.86		39.4
	214-227	TE23L2	Icy Bay-Malaspina	20.6	50	16.5		a		12.7	0.77		42.2
196G	160-173	TE24L2	Icy Bay-Malaspina	17.0	100	165.2	82.8	a		99.3	0.60		32.0
	234-246	TE28L2	Icy Bay-Malaspina	24.8	100	48.2		a		48.6	1.01		30.7
	274-286	TE25L2	Icy Bay-Malaspina	29.0	100	172.3		b	3	251.8	1.46		25.9
	286-298	TE26L2	Icy Bay-Malaspina	30.3	100	1.4		a		42.4	30.29		25.9
	355-365	TE29L2	Icy Bay-Malaspina	37.6	100	55.1		b	6	184.3	3.34		26.0
	367-377	TE30L2	Icy Bay-Malaspina	38.8	100	248.1		c	1	265.9	1.07	37.2	24.0
	381-400	TE27L2	Icy Bay-Malaspina	42.0	100	320.4		c	1	256.4	0.80	37.2	25.2
DC1-81-EG													
604G3	120-127	TE114	Alsek River	11.0	280(?)	293.4		a		176.6	0.60		34.7
605G2	44-52	TE113	Alsek River	4.3	55	222.2		c	1	163.8	0.74	38.1	34.4
	141-149	TE116	Alsek River	11.1	55	0.3		a		8.4	28.07		46.8
	156-164	TE111	Alsek River	13.6	55	216.1		c	1	127.9	0.59	37.0	38.4
	156-164	TE112	Alsek River	13.6	55	35.3		b	6.2	87.6	2.48		38.4
	176-184	TE115	Alsek River	14.8	55	227.9	102.9	c	1	114.2	0.50	39.9	40.8
	186-194	TE117	Alsek River	15.4	55	71.3		b	3.1	91.0	1.28		42.0
618G2	127-132	TE87	Yakutat	10.2	35	184.7		c	1	95.6	0.52	34.2	44.2
	127-132	TE88	Yakutat	10.2	35	231.5	113.6	c	1	157.8	0.68	44.2	43.1
	149-158	TE74	Yakutat	11.9	35	0.5		a		4.6	9.28		45.9
	149-158	TE75	Yakutat	11.9	35	12.1		a		15.6	1.29		46.4
620G2	90-99	TE82	Yakutat	7.1	28	120.8		c	1	53.2	0.44	32.5	48.3

Table 3. Static Triaxial Test Results (continued)

Cruise Core #	Depth in core, z, cm	Test Number	Study Area	$\gamma'z$, kPa[a]	σ'_{vm}, kPa[b]	σ'_{vc}, kPa[c]	σ'_{hc}, kPa[d]	Test Type[e]	Induced OCR[f]	q_f(Su), kPa[g]	S_u/σ'_{vc}[h]	ϕ'[i], degrees	Initial Water Content, %
DC1-81-EG													
624A1	141-150	TE91	Yakutat	14.7	100to500	333.1		c?	1?	401.25	1.21	38.0	29.0
	141-150	TE93[k]	Yakutat	14.7	100to500	341.5		c?	1?	440.27?		34.3?	37.0
625A1	170-180	TE118	Yakutat	18.0	?	293.3		c?	1?	889.0	3.03	39.8	25.3
627G2	71-78	TE72	Icy Bay-Malaspina	6.0	25	18.6		b	5.5	44.7	2.40		42.2
	71-78	TE73	Icy Bay-Malaspina	6.0	25	31.0		b	3.1	45.9	1.48		46.4
	82-90	TE70	Icy Bay-Malaspina	7.0	25	104.7	48.7	c	1	44.4	0.42	37.1	42.3
	82-90	TE71	Icy Bay-Malaspina	7.0	25	100.1		c	1	53.2	0.53	36.1	40.7
	104-112	TE68	Icy Bay-Malaspina	8.5	25	1.6		a		2.1	1.31		45.1
	104-112	TE69	Icy Bay-Malaspina	8.5	25	10.4		a		10.4	0.99		43.4
630A2	220-229	TE89	Icy Bay-Malaspina	23.1	1050	299.9		a		561.98	1.87		24.3
	220-229	TE90[k]	Icy Bay-Malaspina	23.1	1050	295.5		a		631.95		42.9	25.9
632G1	80-89	TE92	Icy Bay-Malaspina	7.8	90	362.8		c	1	208.4	0.57	36.4	32.4
634G2	73-80	TE83	Icy Bay-Malaspina	5.3	12	57.9		c	1	23.9	0.41	33.7	56.0

a - Sediment submerged unit weight times sub-bottom depth, equal to in place overburden stress for normal - and over-consolidation

b - Sediment natural maximum past stress, interpolated or extrapolated from adjacent consolidation tests

c - final vertical consolidation stress

d - final horizontal consolidation stress, blank if same as vertical stress

e - Type (a) test has a final vertical consolidation stress less than three times the maximum past stress without rebound. Type (b) test has a maximum triaxial vertical consolidation stress greater than three times the natural maximum past stress. The sample was subsequently rebounded to a lower consolidation stress inducing a known overconsolidation ratio. Type (c) test has a final vertical consolidation stress greater than three times the maximum past stress without rebound.

f - Blank indicates a type (a) test: final level of overconsolidation is unknown. Value greater than 1 indicates a type (b) test: value given is known induced overconsolidation ratio. Value of 1 indicates a type (c) test: sample has been forced to be normally consolidated.

g - maximum shear stress over 15 or 20% strain: assumed equal to undrained shear strength, S_u.

h - Ratio of undrained shear strength to vertical consolidation stress

i - Effective friction angle assuming no cohesion intercept: given for type (c) or drained tests only

j - Stress control test

k - Drained test

Table 4. Cyclic Triaxial Test Results

Cruise Core #	Depth in Core, z, cm	Test Number	Study Area	σ_{vc}', kPa[a]	σ_{hc}', kPa[b]	Induced OCR[c]	$(q_f \text{Static})_I$[d]	$(q_f \text{Static})_{II}$[e]	Static Bias, kPa[f]	Peak Cyclic Stress, τ_c, kPa[g]	$\frac{\tau_c}{q_f \text{static}}$[h] (I)	$\frac{\tau_c}{q_f \text{static}}$[i] (II)	$\frac{\tau_c}{\sigma_{vc}'}$[j] (III)	# of Cycles to failure[k]	Strain at failure, %[l]	Initial Water Content %
S8-77-EG																
4G	485	TC1B	Copper River	34.3	29.4		27.0		11.9	18.9	0.70		0.55	5000	5	39.9
	485	TC2B	Copper River	34.3	29.4		27.0		11.9	27.5	1.02		0.80	13	12	41.5
	485	TC3B[m]	Copper River	33.3	29.4		36.8		15.5	28.0	0.76		0.84	403	11	41.5
	500	TC4B	Copper River	34.3	29.4		25.0		10.5	17.5	0.70		0.51	5000	6	42.3
	500	TC5B	Copper River	34.3	29.4		25.0		10.8	23.5	0.94		0.69	45	12	43.3
	500	TC6B[m]	Copper River	33.3	29.4		31.9		13.7	23.3	0.73		0.70	4583	8.8	43.3
	510	TC7B	Copper River	34.3	29.4		25.5		10.7	19.9	0.78		0.58	5000	7.4	44.3
	520	TC8B	Copper River	211.8	196.1	1	107.8		8.6	34.5	0.32		0.16	2493	1.4	35.6
	520	TC9B	Copper River	212.7	196.1	1	107.8		3.2	67.9	0.63		0.32	30	-8.8	38.2
	530	TC10B	Copper River	216.7	196.1	1	100.5		42.2	94.5	0.94		0.44	37	12	42.7
	545	TC11B	Copper River	217.6	196.1	1	92.6		38.0	80.6	0.87		0.37	150	12	40.7
	555	TC12B	Copper River	217.6	196.1	1	108.8		38.1	74.0	0.68		0.34	935	12	39.3
	575	TC13B	Copper River	217.6	196.1	1	93.1		37.2	70.8	0.76		0.33	5000	10	40.8
8G	495	TC14B	Copper River	216.7	196.1	1	100.0		19.0	63.0	0.63		0.29	87	12	41.4
	530	TC15B	Copper River	215.7	196.1	1	96.1		16.3	53.8	0.56		0.25	500	12	40.8
11G	420	TC16B	Kayak Trough	32.4	29.4		18.1		0.7	11.2	0.62		0.35	71	12	46.7
	450	TC17B	Kayak Trough	32.4	29.4		24.0		2.4	9.1	0.38		0.28	3994	12	39.6
	450	TC18B	Kayak Trough	32.4	29.4		24.0		2.4	10.3	0.43		0.32	2679	12	40.6
	470	TC19B	Kayak Trough	32.4	29.4		19.6		2.0	11.8	0.60		0.36	243	12	42.7
	470	TC20B	Kayak Trough	32.4	29.4		19.6		2.0	12.5	0.64		0.39	152	12	43.6
	485	TC21B	Kayak Trough	32.4	29.4		20.6		1.6	14.4	0.70		0.44	74	12	45.0
	485	TC22B	Kayak Trough	32.4	29.4		20.6		1.6	16.5	0.80		0.51	13	12	44.8
	515	TC23B	Kayak Trough	32.4	29.4		24.0		8.4	19.7	0.82		0.61	200	12	39.8
	515	TC24B	Kayak Trough	32.4	29.4		24.0		8.1	20.4	0.85		0.63	15	12	41.9
28G	20	TC25B	Icy Bay-Malaspina	32.4	29.4		27.9		0.5	10.3	0.37		0.32	391	12	35.4
	40	TC26B	Icy Bay-Malaspina	32.4	29.4		20.6		1.4	12.2	0.59		0.38	35	12	40.7
33G	550	TC27B	Icy Bay-Malaspina	32.4	29.4		26.5		9.0	16.7	0.63		0.51	5000	5.1	33.9
	550	TC28B	Icy Bay-Malaspina	32.4	29.4		26.5		8.2	20.7	0.78		0.64	175	12	35.6
	560	TC29B	Icy Bay-Malaspina	33.3	29.4		56.4		18.6	28.2	0.50		0.85	5000	4.3	26.6
	560	TC30B	Icy Bay-Malaspina	23.3	29.4		56.4		18.6	33.8	0.60		1.02	537	11	26.1
	585	TC31B	Icy Bay-Malaspina	217.6	196.1	1	98.0		16.7	61.7	0.63		0.28	21	12	33.6
	600	TC32B	Icy Bay-Malaspina	215.7	196.1	1	103.9		12.5	63.4	0.61		0.29	2	-12	34.3
	610	TC33B	Icy Bay-Malaspina	217.6	196.1	1	87.7		29.8	78.1	0.89		0.36	55	12	39.6
	620	TC34B	Icy Bay-Malaspina	217.6	196.1	1	100.5		19.1	68.3	0.68		0.31	29	12	34.8
	630	TC35B	Icy Bay-Malaspina	216.7	196.1	1	104.4		18.8	60.6	0.58		0.28	500	12	32.6
DC2-80-EG																
MC3-22	35-47	TC1L2	Alsek River	27.6		6	84.6			-23.7	0.28			35	-15	28.1
28G	15-22	TC24	Alsek River	302.6		1	268.9	226.9		115.6	0.43	0.51	0.38	4	-20	31.8
	15-22	TC25	Alsek River	297.9		1	268.9	226.9		21	0.08	0.09	0.07	1100	-20	31.8
35G	32-39	TC18	Alsek River	160.3		1	80.8	83.4		54.9	0.68	0.66	0.34	7	20	41.2
	32-39	TC19	Alsek River	154.6		1	80.8	75.8		51.6	0.64	0.68	0.33	20	20	44.8
38G	1-15	TC2L2	Alsek River	27.6		6	86.4			-38.0	0.44			3	-15	40.7
	27-38	TC3L2	Alsek River	120.6		1	88.9	63.9		-24.9	0.28	0.39	0.21	8	-15	40.9

Table 4. Cyclic Triaxial Test Results (continued)

Cruise Core #	Depth in Core, z, cm	Test Number	Study Area	σ_{vc}', kPa[a]	σ_{hc}', kPa[b]	Induced OCR[c]	$(q_f \text{Static})_I$[d]	$(q_f \text{Static})_{II}$[e]	Static Bias, kPa[f]	Peak Cyclic Stress, τ_c, kPa[g]	$\frac{\tau_c}{q_f \text{static}}$ (I)[h]	$\frac{\tau_c}{q_f \text{static}}$ (II)[i]	$\frac{\tau_c}{\sigma_{vc}}$, (III)[j]	# of Cycles to failure[k]	Strain at failure, %[l]	Initial Water Content, %
DC2-80-EG																
38G	40-52	TC4L2	Alsek River	120.6		1	87.4	74.8		-33.2	0.38	0.44	0.28	10	-15	36.0
43G	27-35	TC20	Alsek River	28.3			73.9			43.2	0.59			8	20	33.6
	27-35	TC21	Alsek River	27.2			73.9			43.2	0.62			8	20	32.5
46G	7-15	TC22	Alsek River	196.2		1	222.4	141.3		-42.4	0.19	0.30	0.22	94	20	33.1
	7-15	TC23	Alsek River	192.6		1	222.4	138.7		79	0.36	0.57	0.41	15	20	33.1
49G	6-17	TC5L2	Alsek River	120.6		1	87.1	71.2		-65.3	0.75	0.92	0.54	0.5	-15	37.4
84G	33-48	TC6L2	Yakutat	103.3		1	64.6	108.5		-23.9	0.37	0.22	0.23	80	-15	25.6
	48-63	TC7L2	Yakutat	103.3		1	64.1	72.3		-31.4	0.49	0.43	0.30	6	-15	33.0
87G	161-172	TC52	Yakutat	200.9		1	122.8	148.7		-106.3	0.87	0.71	0.53	4	-20	32.3
87G	161-169	TC53	Yakutat	194.3		1	122.8	147.7		-45.5	0.37	0.31	0.23	82	-20	31.6
96G	145-155	TC11L2	Icy Bay-Malaspina	34.5		4	70			-39.2	0.56			2	-15	35.0
	226-237	TC8L2	Icy Bay-Malaspina	137.8		1	71	107.5		-34.1	0.48	0.32	0.25	33	-15	31.2
	286-300	TC10L2	Icy Bay-Malaspina	35.1		4	70			-16.1	0.23			60	-15	35.5
	331-343	TC9L2	Icy Bay-Malaspina	137.8		1	78.7	96.5		-59.8	0.76	0.62	0.43	8	-15	33.1
181G	61-68	TC30	Icy Bay-Malaspina	30.3		1	23.7	14.5		-25	1.06	1.72	0.83	59	20	46.0
	61-68	TC31	Icy Bay-Malaspina	24.2		1	23.7	11.4		-24	1.00	2.11	0.99	12	20	46.4
	85-95	TC32	Icy Bay-Malaspina	10.4		3.5	19.0			-15	0.79			20	20	44.2
	85-95	TC33	Icy Bay-Malaspina	2.5		14.4	19.0			-15.9	0.84			10	20	47.6
190G	66-80	TC12L2	Icy Bay-Malaspina	151.6		1	88.4	86.4		-61.9	0.70	0.72	0.41	1	-15	38.2
	80-97	TC13L2	Icy Bay-Malaspina	151.6		1	87.8	87.9		-40.4	0.46	0.46	0.27	4	-15	37.5
	160-175	TC14L2[n]	Icy Bay-Malaspina	232	96.5	1	89.4		67.8	89.6	1.00			300	1.3	42.0
196G	197-213	TC15L2[n]	Icy Bay-Malaspina	166.5	83.3	1	99.3		41.6	96.8	0.97			300	0.9	26.7
	312-326	TC16L2	Icy Bay-Malaspina	53.4		6	182.1			-51.0	0.28			16	-15	23.9
	326-340	TC17L2	Icy Bay-Malaspina	53.4		6	187.7			-41.3	0.22			24	-15	25.4
	400-414	TC18L2	Icy Bay-Malaspina	320.2		1	257.0	256		-187.6	0.73	0.73	0.59	0.5	-15	24.4
	414-428	TC19L2	Icy Bay-Malaspina	320.2		1	255.5	256		-92	0.36	0.36	0.29	10	-15	24.4
DC1-81-EG																
604G3	130-137	TC99	Alsek River	297.1		1	176.6	175.3		61.5	0.35	0.35	0.21	35	-20	37.0
	130-137	D102	Alsek River	290.4		1	176.6	174.2		86.5	0.49	0.50	0.30	28	20	36.6
605G2	55-62	TC92	Alsek River	215.9		1	163.8	127.4		-55.7	0.34	0.44	0.26	26	-20	37.1
	55-62	TC93	Alsek River	204.8		1	163.8	120.8		-84.1	0.51	0.70	0.41	5	-20	37.1
	166-173	TC87	Alsek River	215.1		1	127.9	133.4		-41.8	0.33	0.31	0.15	78	-20	35.9
	166-173	TC86	Alsek River	216.3		1	127.9	125.5		-66.5	0.52	0.53	0.31	5	-20	35.9
618G2	138-145	TC58	Yakutat	184.8		1	95.6	92.4		56.2	0.59	0.61	0.30	17	-20	43.1
	138-145	TC59	Yakutat	183.9		1	95.6	86.4		44.6	0.47	0.52	0.24	42	-20	46.2
620G2	100-148	TC46	Yakutat	121.8		1	53.2	67.0		31.0	0.58	0.46	0.25	58	20	39.4
	100-108	TC47	Yakutat	117.6		1	53.2	65.9		46.1	0.87	0.70	0.39	14	20	38.6
624A1	172-179	TC60	Yakutat	338.9		1	401.3	186.4		206.6	0.51	1.11	0.61	1	-20	39.4
	172-179	TC61	Yakutat	344.7		1	401.3	186.1		-134.6	0.54	0.72	0.39	7	-20	39.8
627G2	60-71	TC36	Icy Bay-Malaspina	18.3		5.4	44.7			21.5	0.48			42	20	46.6
	60-67	TC37	Icy Bay-Malaspina	17.3		5.7	44.7			34.7	0.78			8	20	46.6
	93-104	TC34	Icy Bay-Malaspina	100.7		1	53.2	47.3		-39.4	0.74	0.83	0.39	5	20	47.6
	93-100	TC35	Icy Bay-Malaspina	99.5		1	53.2	48.8		-26.4	0.50	0.54	0.26	280	-20	44.7

Table 4. Cyclic Triaxial Test Results (continued)

Cruise Core #	Depth in Core, z, cm	Test Number	Study Area	σ_{vc}', kPa [a]	σ_{hc}', kPa [b]	Induced OCR [c]	$(q_f \text{Static})_I$ [d]	$(q_f \text{Static})_{II}$ [e]	Static Bias, kPa [f]	Peak Cyclic Stress, τ_c, kPa [g]	$\frac{\tau_c}{q_f \text{static}}$ (I) [h]	$\frac{\tau_c}{q_f \text{static}}$ (II) [i]	$\frac{\tau_c}{\sigma_{vc}'}$ (III) [j]	# of Cycles to failure [k]	Strain at failure, % [l]	Initial Water Content %
DC1-81-EG																
630A2	153-161	TC57	Icy Bay-Malaspina	297.9		1	562	259.2		162.9	0.29	0.63	0.55	>27	-20	29.3
	153-161	TC56	Icy Bay-Malaspina	301.0		1	562	295.0		120.2	0.21	0.41	0.40	>37	-20	27.4
634G2	61-69	TC48	Icy Bay-Malaspina	60.3		1	23.9	25.3		-40.6	1.70	1.60	0.67	2	-20	56.4
	61-68	TC49	Icy Bay-Malaspina	58.1		1	23.9	24.4		-31.8	1.33	1.30	0.55	6	-20	59.0
	72-79	TC54	Icy Bay-Malaspina	61.9		1	23.9	27.9		17.6	0.74	0.63	0.28	158	20	48.9
	73-80	TC55	Icy Bay-Malaspina	59.3		1	23.9	26.7		22.2	0.93	0.83	0.37	37	20	50.3

a - Final vertical consolidation stress

b - Final horizontal consolidation stress, blank if same as vertical stress

c - Induced OCR defined in Table 3.

d - Static shear strength obtained from test on sample from the same core (Method I)

e - Static shear strength obtained from water content, consolidation stress and Figure 35 (Method II)

f - A static shear stress applied under undrained conditions prior to cyclic testing. The cyclic shear stress is symmetrical about this bias level.

g - The maximum shear stress level applied during cyclic loading (may include some static bias in addition to cyclic component - negative sign indicates tension)

h - Ratio of maximum cyclic shear stress to static shearing strength estimated using Method I.

i - Ratio of maximum cyclic shear stress to static shearing strength estimated using Method II

j - Ratio of maximum cyclic shear stress to vertical consolidation stress (termed method III)

k - Number of cycles required to reach strain given in next column

l - Strain level defined as failure or strain level at which test was halted (if less than 10%)

m - Reconsolidated sample

n - Cyclic loading in compression only

Table 5. Calculation of NSP exponent, Λ_o

Cruise Core #	Depth in Core, z, cm	Test Number	Study Area	Induced[a] OCR	$(S_{nc})_I$[b]	$(S_{nc})_{II}$[c]	σ_f/σ_{vc}'[d]	$(\Lambda_o)_I$[e]	$(\Lambda_o)_{II}$[f]	Initial Water content, %
DC2-80-EG										
MC3-22	62-76	TE4L2	Alsek River	3	----	0.86	4.51	----	1.51	29.4
28	25-34	TE63	Alsek River	5.7	0.87	0.62	3.99	0.88	1.07	36.2
35	14-23	TE57	Alsek River	6.2	0.52	0.53	2.36	0.83	0.82	40.4
38	18-28	TE3L2	Alsek River	6	----	0.76	3.12	----	0.79	31.6
43	8-17	TE27	Alsek River	5	----	0.67	5.74	----	1.33	33.9
46	28-37	TE60	Alsek River	6.2	1.10	0.67	4.66	0.82	1.06	33.9
84	63-76	TE8L2	Yakutat	6	0.70	0.63	8.17	1.37	1.43	35.7
96	198-212	TE16L2	Icy Bay-Malaspina	3	0.51	0.72	2.02	1.25	0.74	32.8
	343-356	TE15L2	Icy Bay-Malaspina	4	0.51	0.70	2.02	0.99	0.76	33.3
181	5-15	TE16	Icy Bay-Malaspina	6.1	0.47	0.55	2.35	0.89	0.80	39.2
	71-81	TE19	Icy Bay-Malaspina	7.3	0.47	0.52	3.57	1.02	0.97	41.9
	100-110	TE21	Icy Bay-Malaspina	3	0.47	0.48	1.33	0.95	0.93	46.2
190	80-94	TE20L2	Icy Bay-Malaspina	6	0.58	0.75	2.03	0.70	0.91	31.9
	114-125	TE19L2	Icy Bay-Malaspina	3	0.58	0.50	0.84	0.34	0.47	42.6
196	274-286	TE25L2	Icy Bay-Malaspina	3	0.93	1.06	1.46	0.41	0.29	25.9
	355-365	TE29L2	Icy Bay-Malaspina	6	0.93	1.06	3.34	0.71	0.64	26.0
DC1-81-EG										
605G2	186-194	TE112	Alsek River	3.1	0.59	0.51	1.28	0.68	0.81	42.0
	156-164	TE117	Alsek River	6.2	0.59	0.57	2.48	0.79	0.81	38.4
627G2	71-78	TE72	Icy Bay-Malaspina	5.5	0.53	0.51	2.40	0.89	0.91	42.6
	71-78	TE73	Icy Bay-Malaspina	3.1	0.53	0.47	1.48	0.91	1.01	46.4

a - Induced OCR defined in Table 3

b - Ratio of undrained shear strength, S_u, to vertical consolidation stress, σ_{vc}', for normal consolidation obtained from test on sample from the same core (Method I)

c - Ratio of undrained shear strength, S_u, to vertical consolidation stress, σ_{vc}', for normal consolidation obtained from initial water content and Figure 35 (Method II)

d - Ratio of measured undrained shear strength to vertical consolidation stress

e - The NSP exponent, Λ_o, calculated using S_{nc} from Method I.

f - The NSP exponent, Λ_o, calculated using S_{nc} from Method II

FIGURES

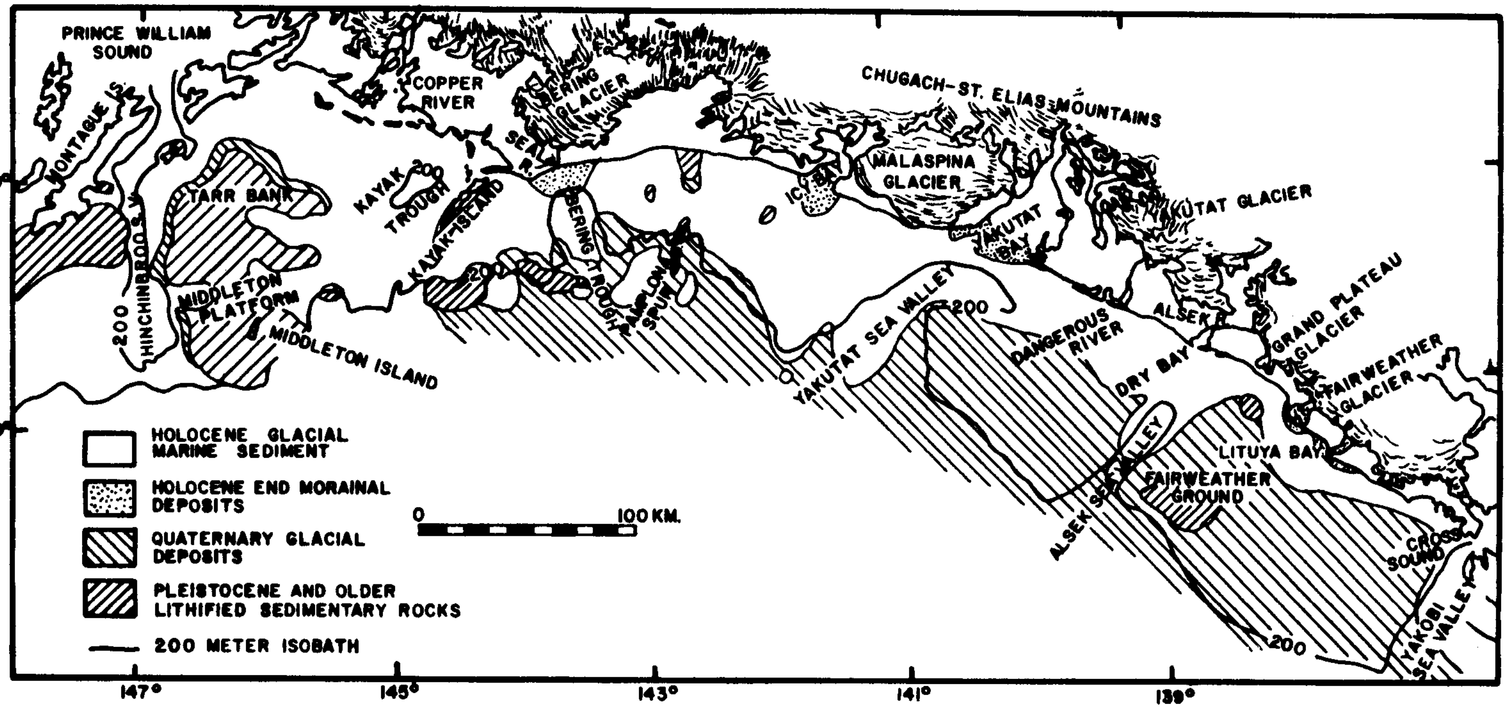

Figure 1. Distribution of four continental shelf surface sedimentary units between Cross Sound and Prince William Sound (Molnia and Carlson, 1980)

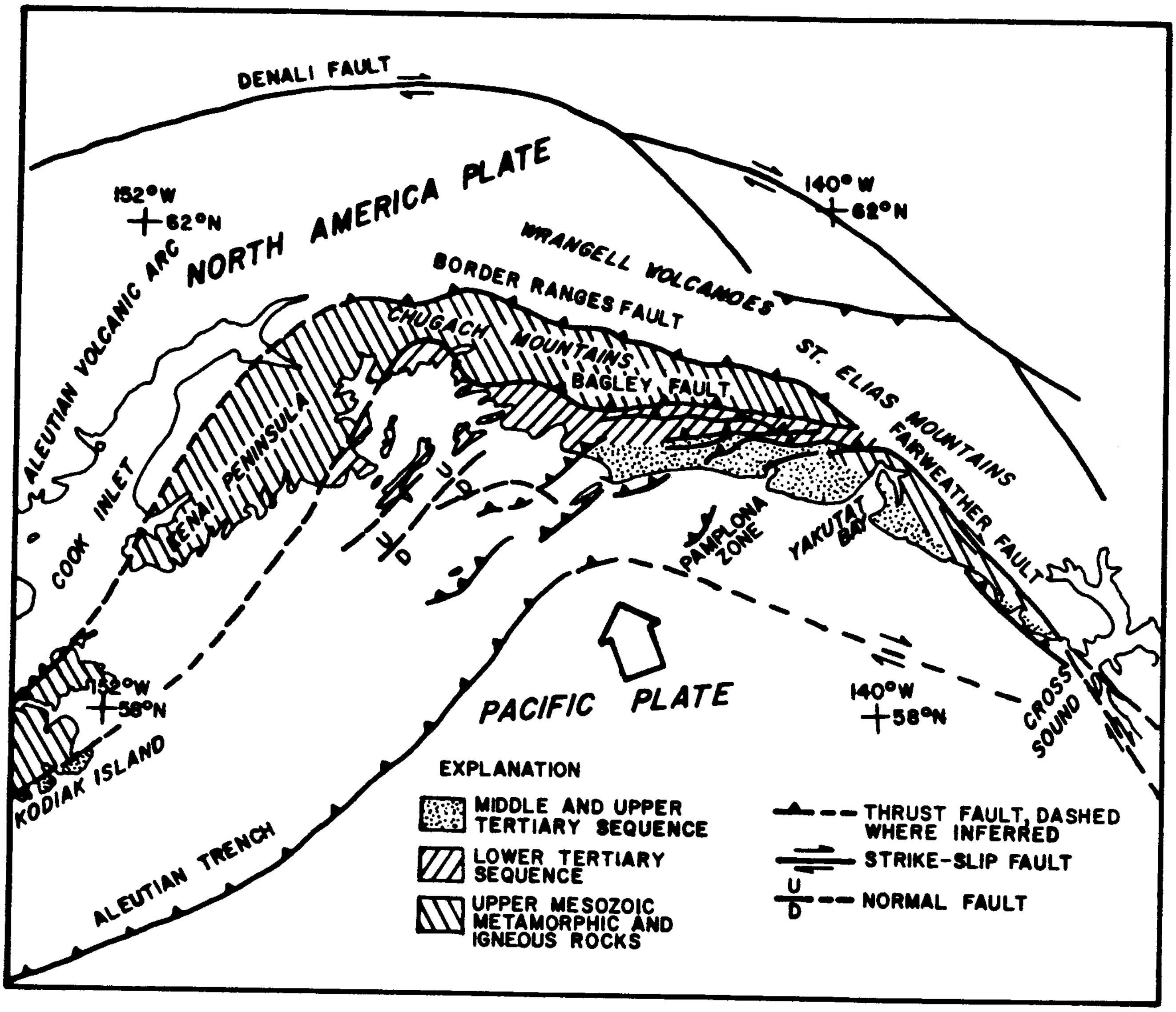

Figure 2. Simplified geologic setting of the northern Gulf of Alaska, showing general trends of Mesozoic and Cenozoic rocks (modified from Bruns, 1979). Onshore geology is from Plafker (1967), and Beikman (1974,1975). Relative convergence vector between Pacific and North American plates (large arrow) is from Minster and Jordon (1978)

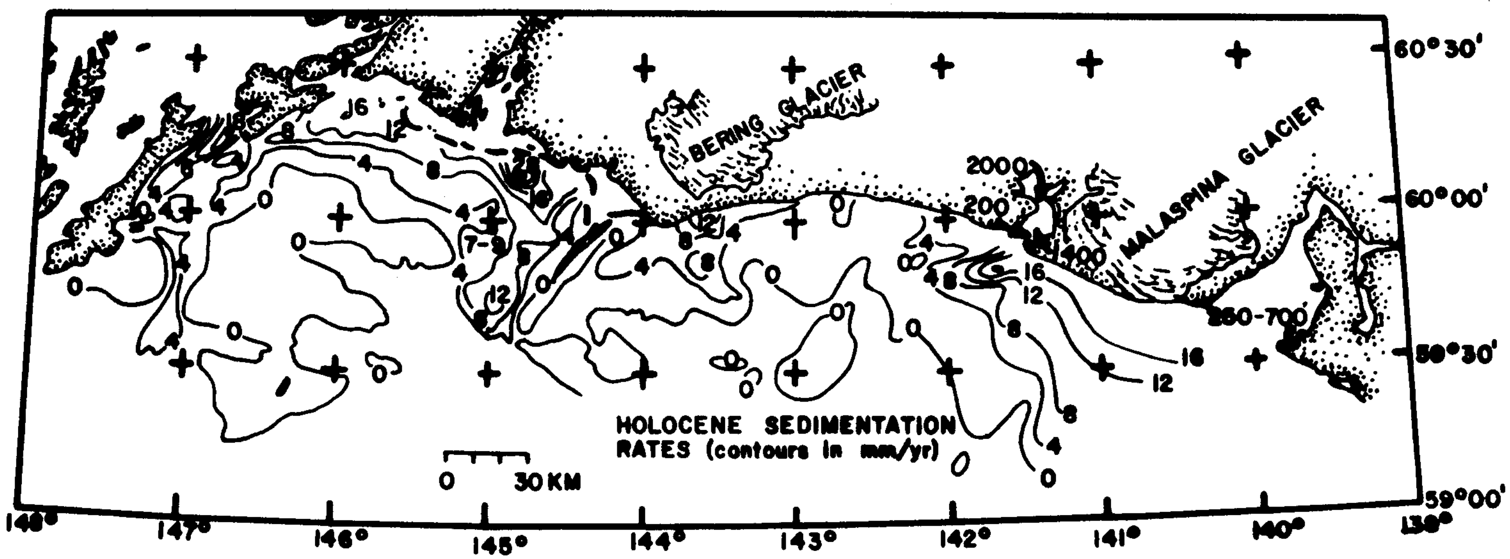

Figure 3. Holocene sedimentation rates (mm/yr) in the northeast Gulf of Alaska (Molnia and Carlson, 1980)

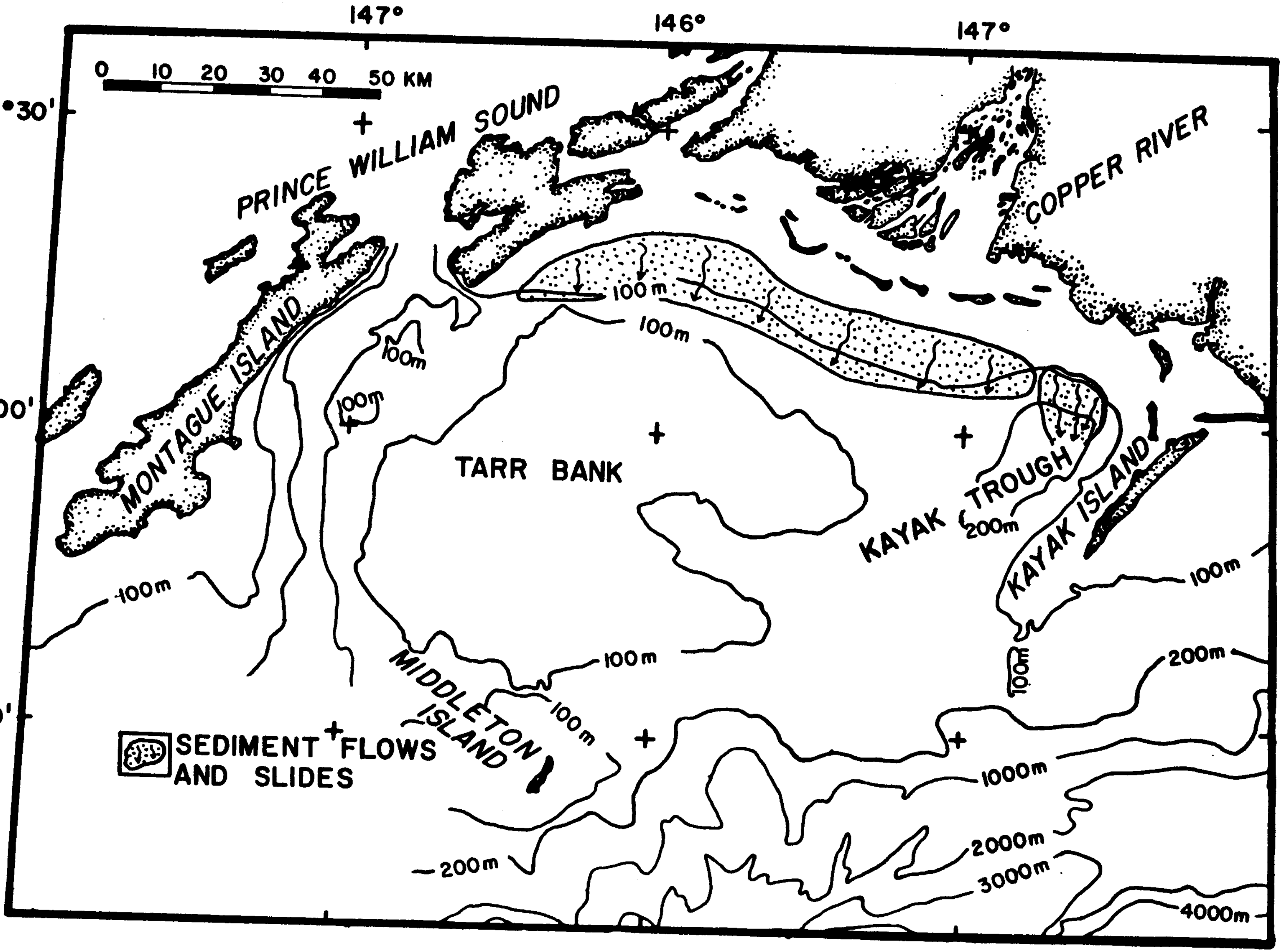

Figure 4. Location map of seafloor flows and slumps west of Kayak Island (Carlson and Schwab, 1982)

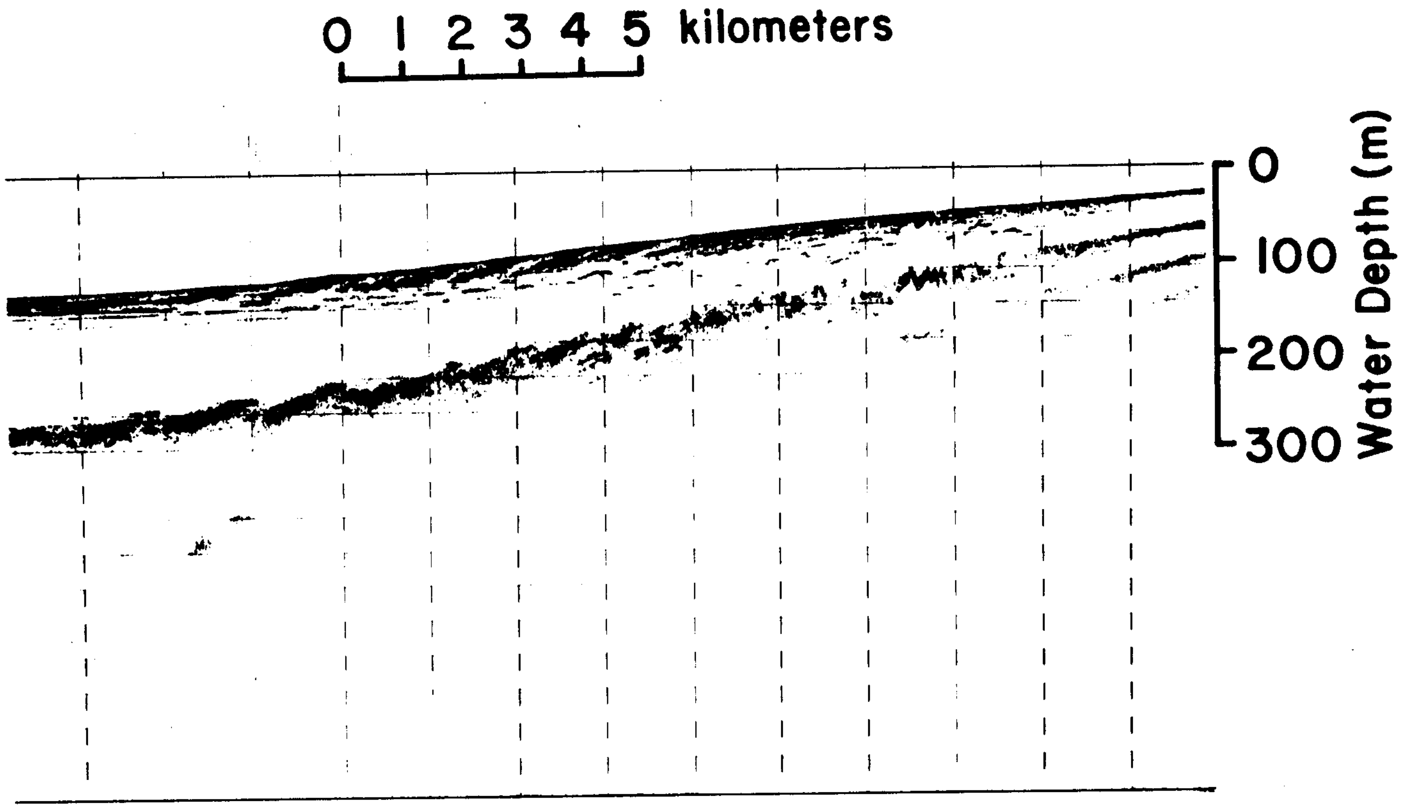

Figure 5. High resolution seismic reflection record of the sediment slide off the Copper River.

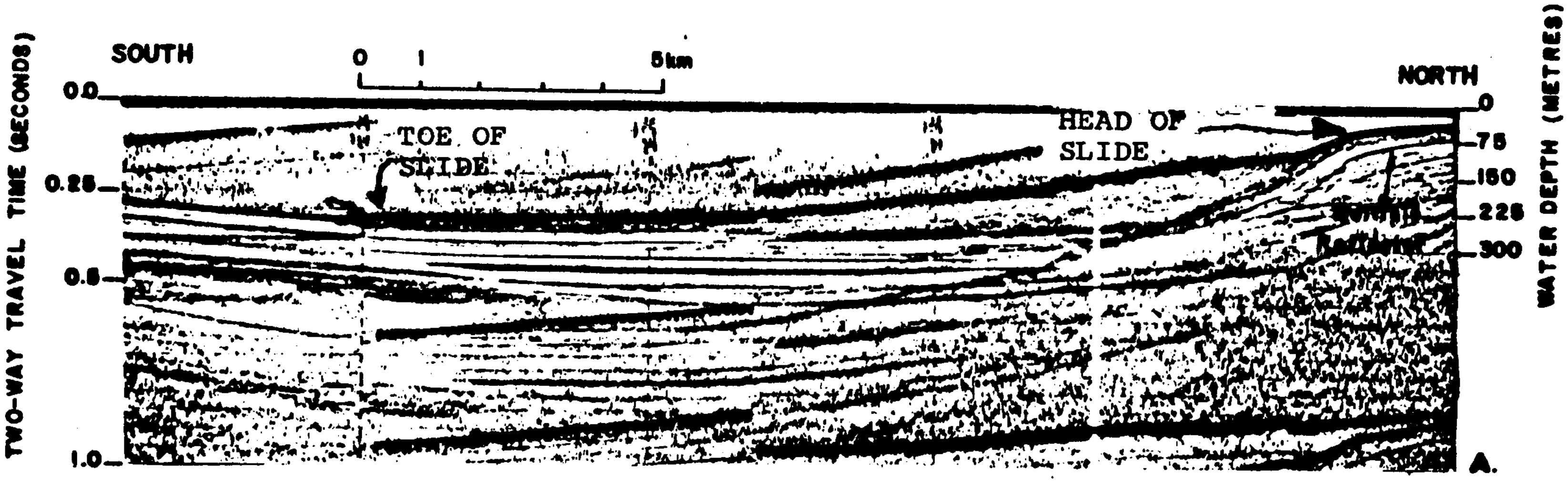

Figure 6. High resolution seismic reflection record of the submarine slide located in Kayak Trough (Hampton and others, 1978).

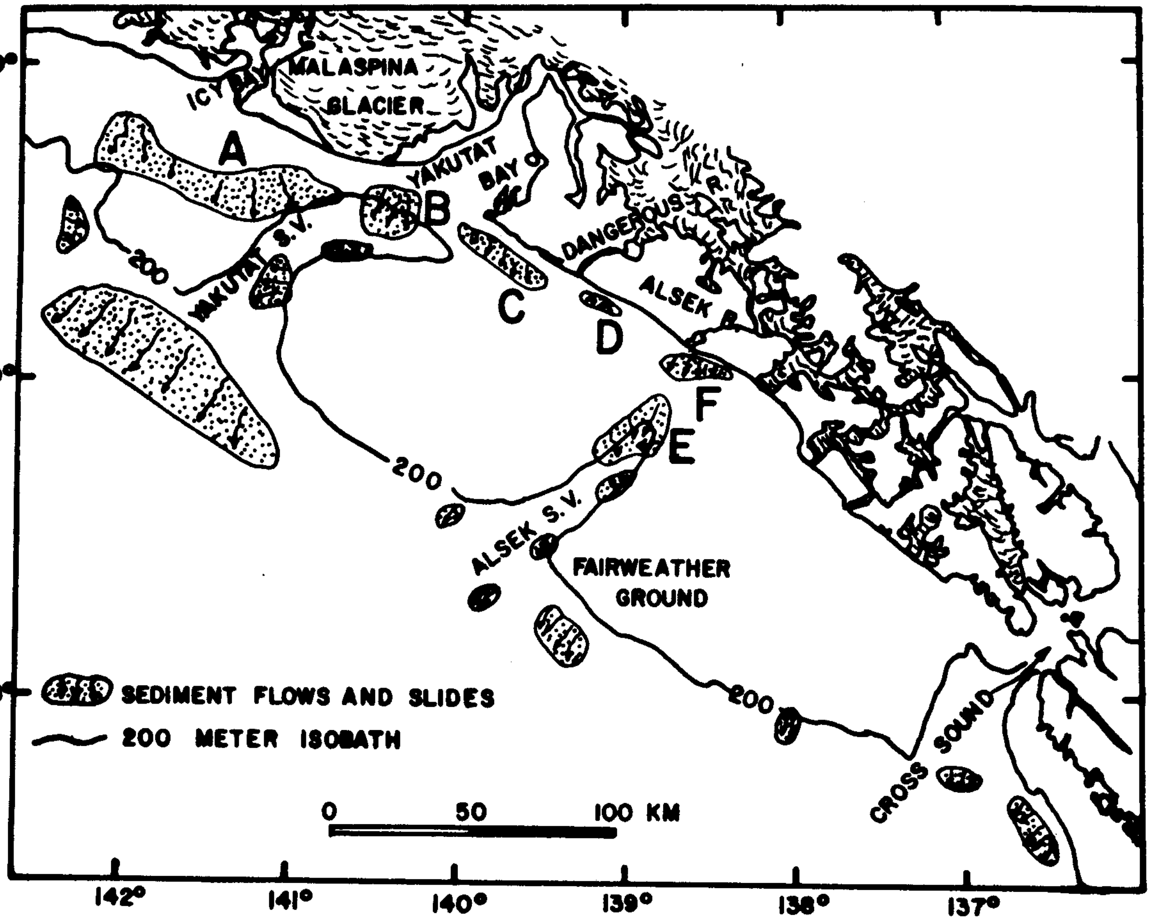

Figure 7. Location map of seafloor geologic hazards east of Icy Bay, Gulf of Alaska (modified from Carlson and others, 1980).

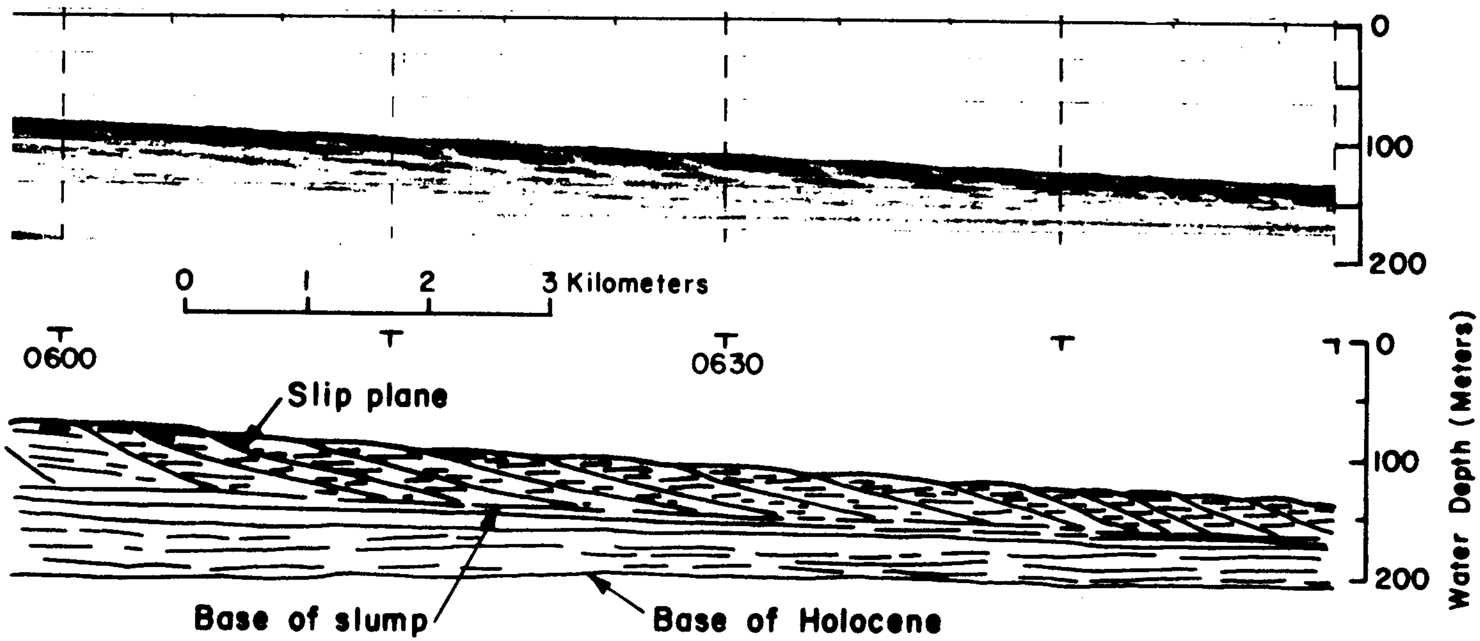

Figure 8. High resolution seismic reflection record of the Icy Bay-Malaspina Slump (Carlson, 1978).

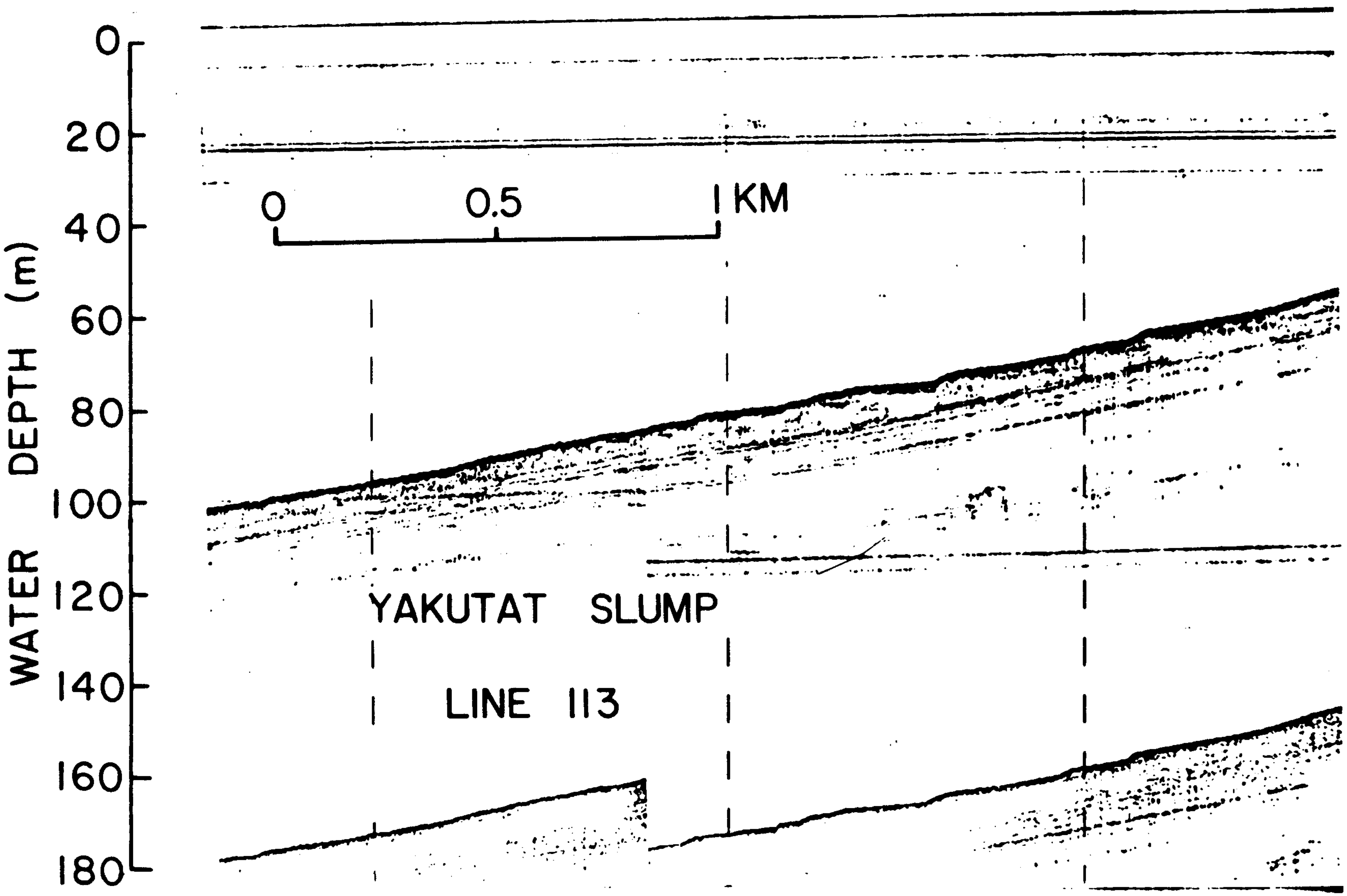

Figure 9. High resolution seismic reflection record of the Yakutat Slump.

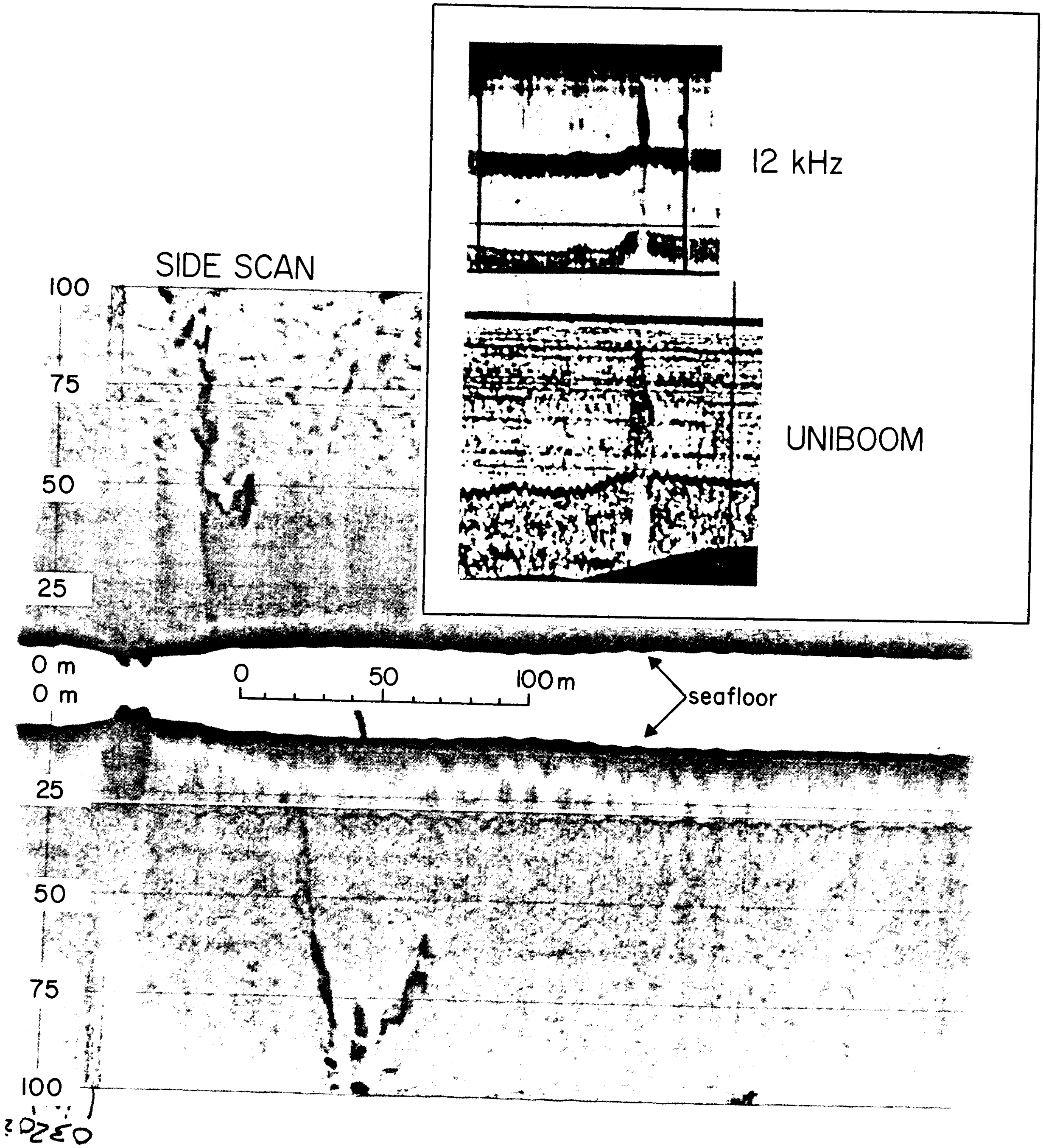

Figure 10. High resolution seismic reflection data and side scan sonographs depicting a water column gas plume southeast of the Dangerous River delta (Carlson and others, 1980).

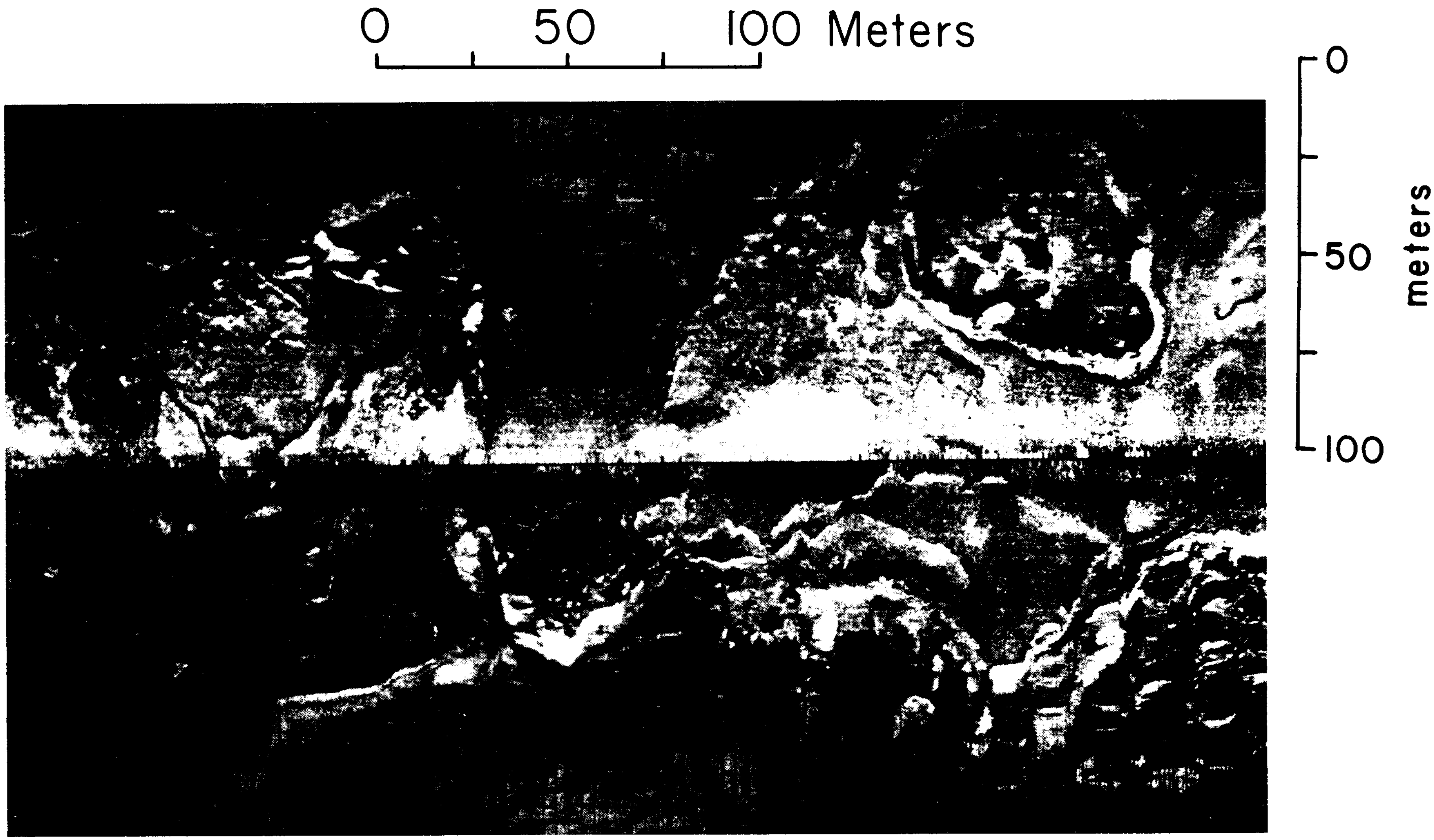

Figure 11. Side scan sonograph example of small slides and linear flows on the Alsek River prodelta (Molnia and Rappeport, 1980). Onshore direction is toward the top of the figure.

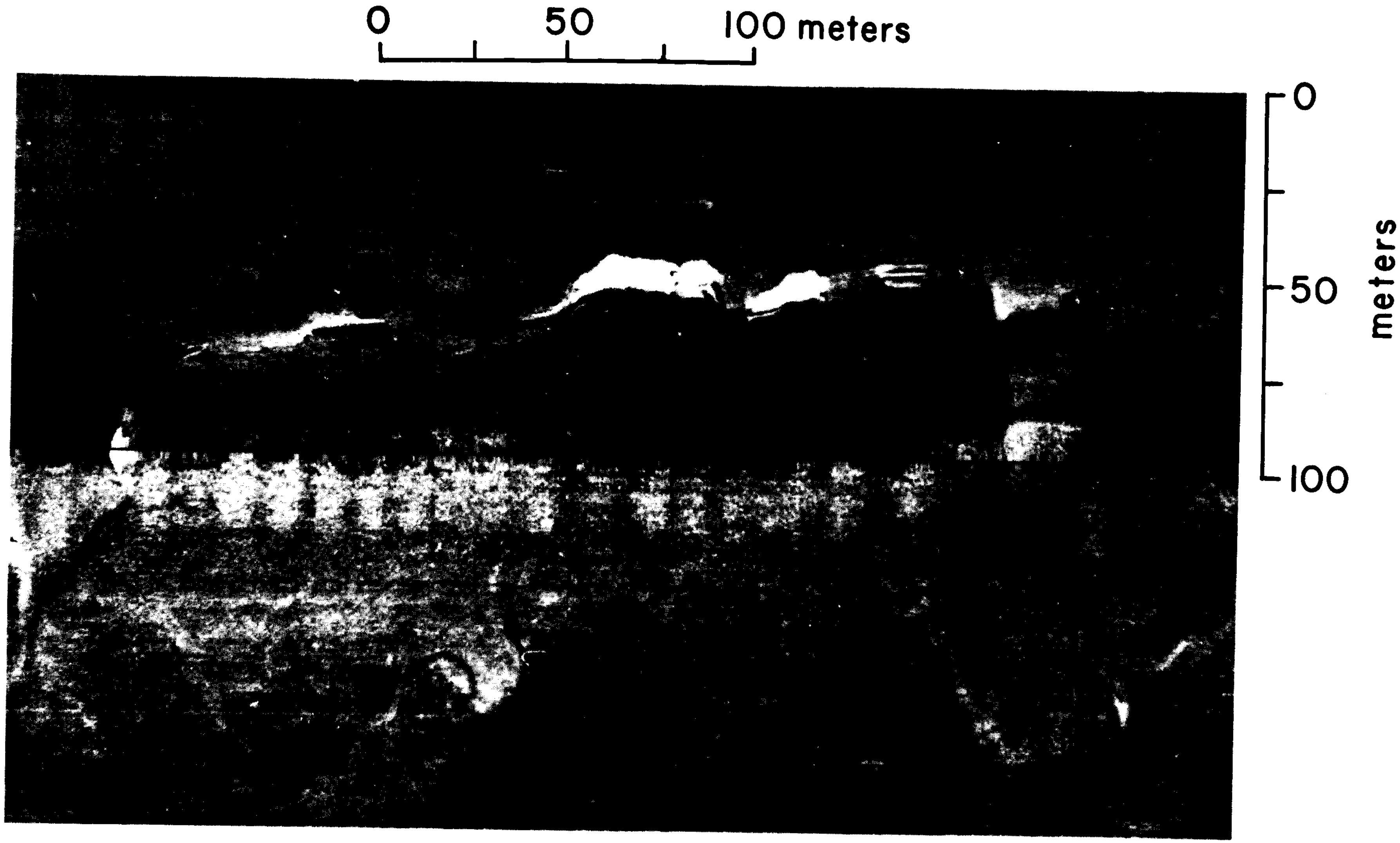

Figure 12. Side scan sonograph depicting a massive, lobate slide toe and a series of smaller slide toes on the Alsek River prodelta (Molnia and Rappeport, 1980). Onshore direction is toward the top of the figure.

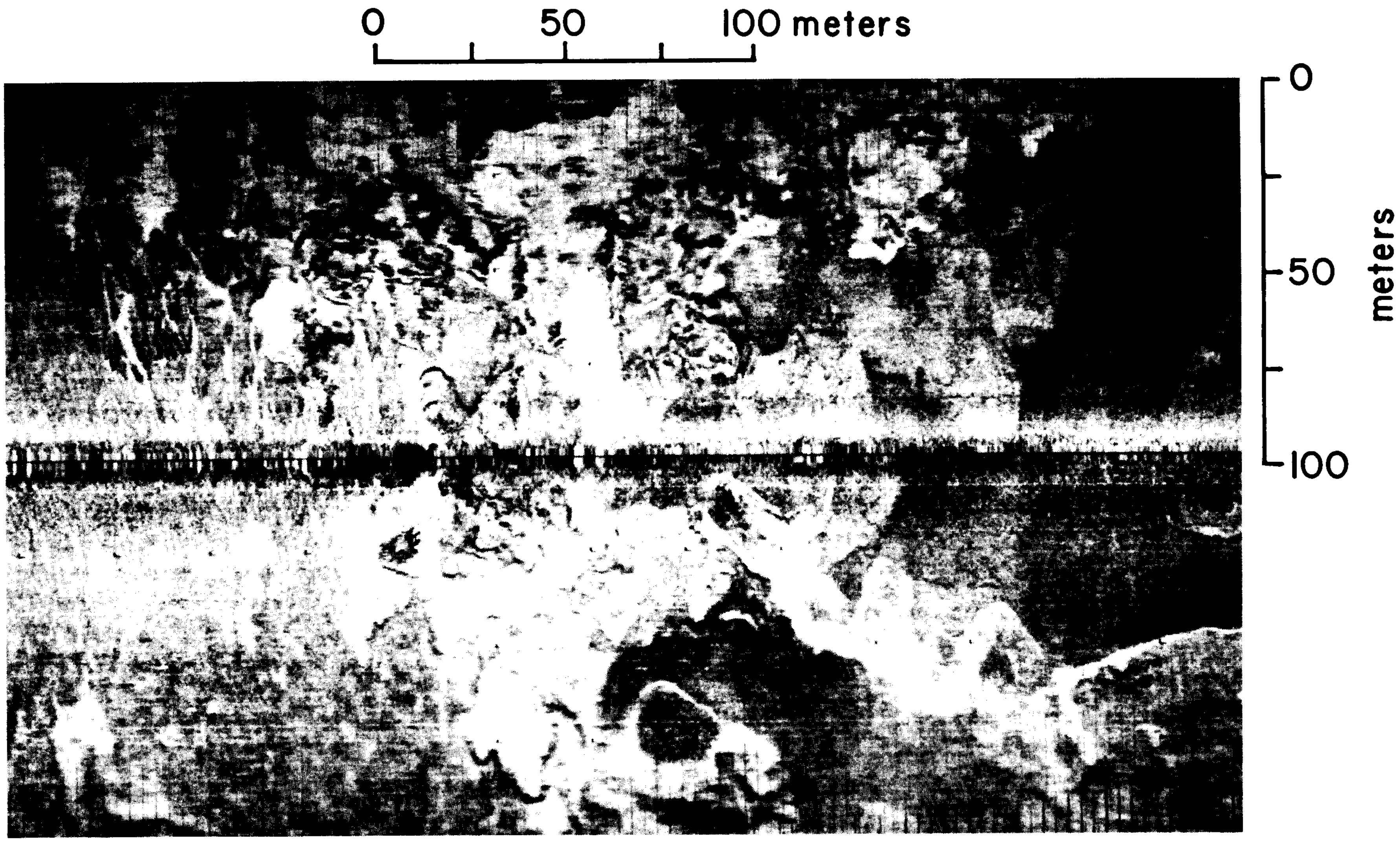

Figure 13. Side scan sonograph depicting multiple flows, slumps and slides on the Alsek River prodelta (Molnia and Rappeport, 1980).

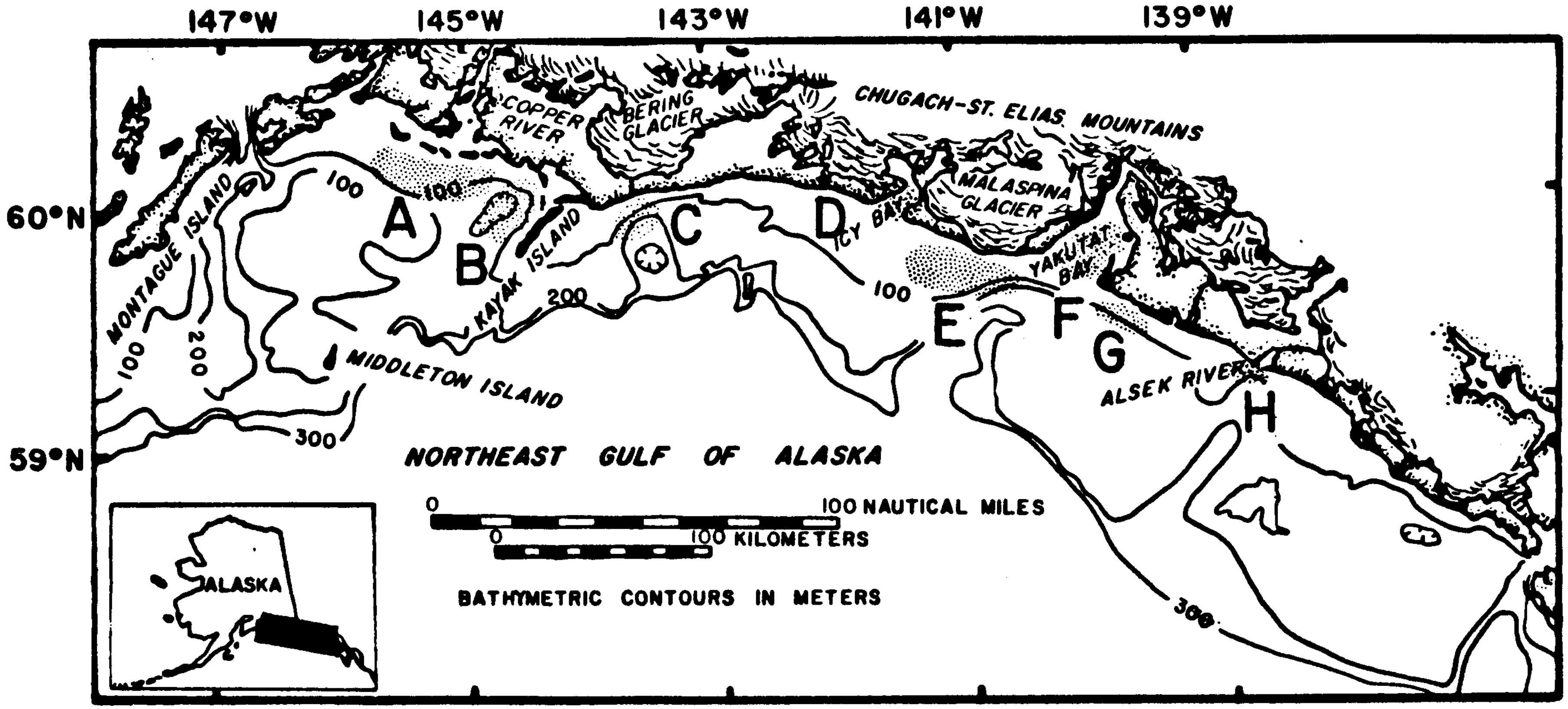

Figure 14. Locations of study areas.

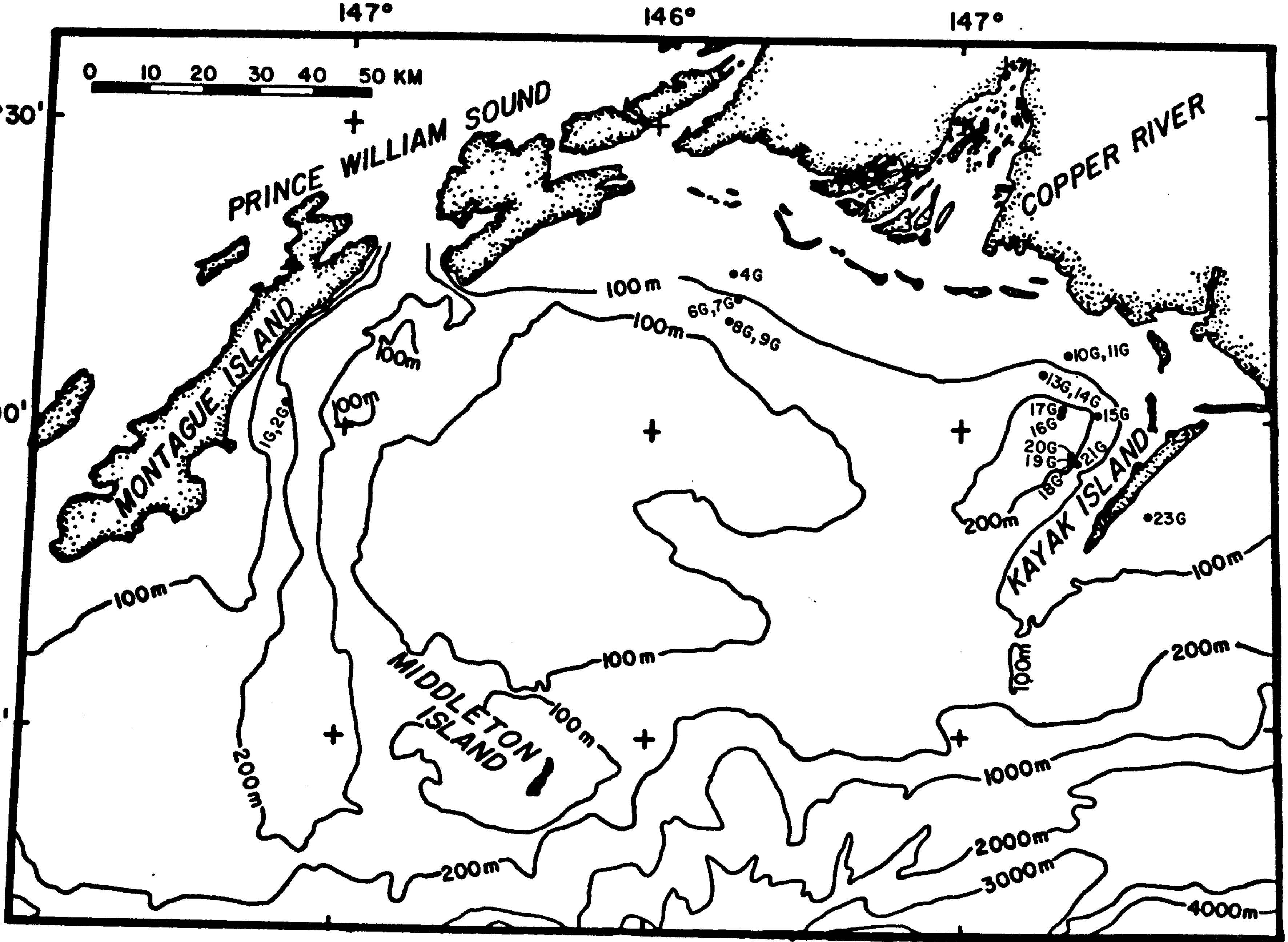

Figure 15. Core locations-Copper River Study Area (group to west) and Kayak Trough Study Area (group to east)

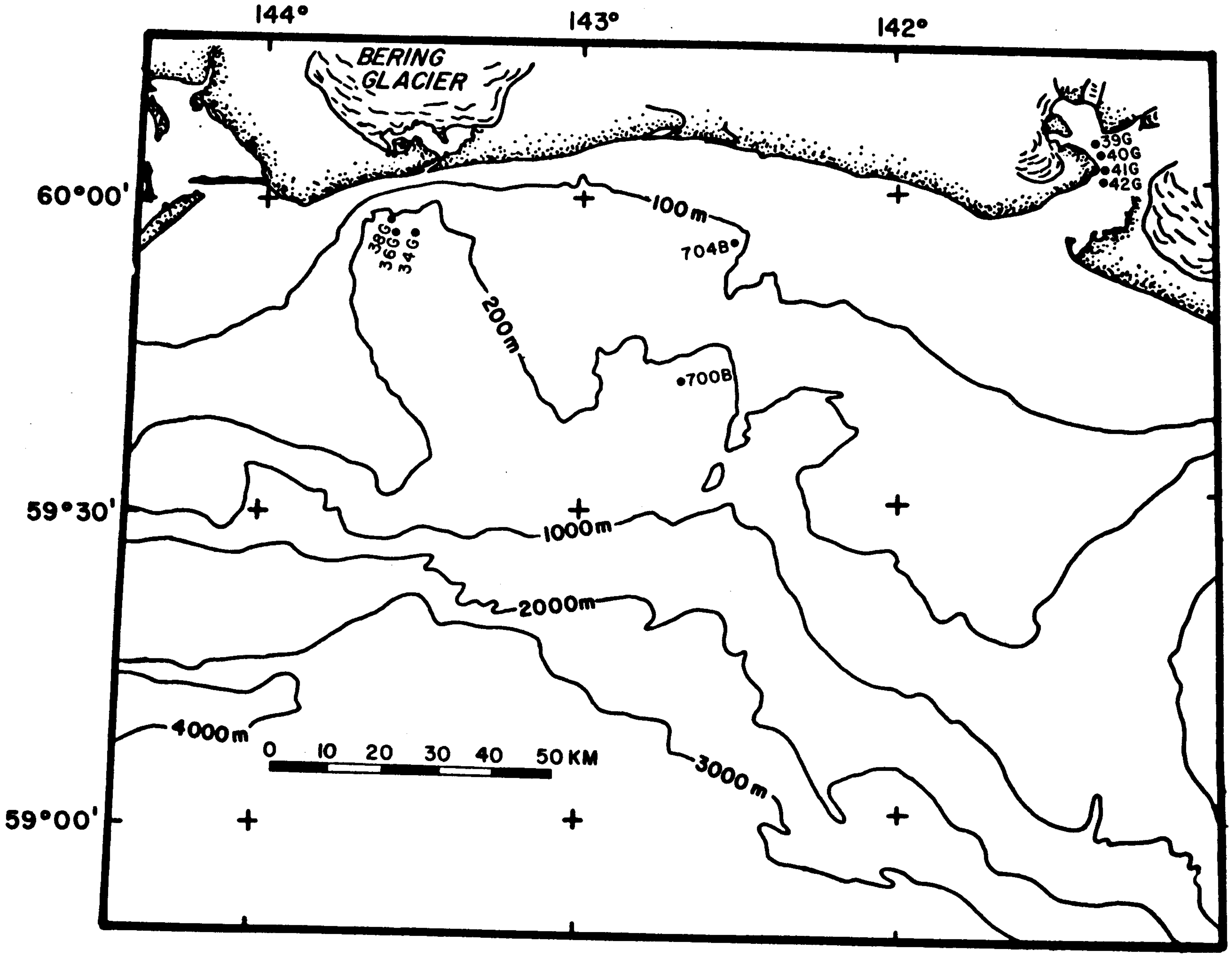

Figure 16. Core locations-Bering Trough and Icy Bay Study Areas.

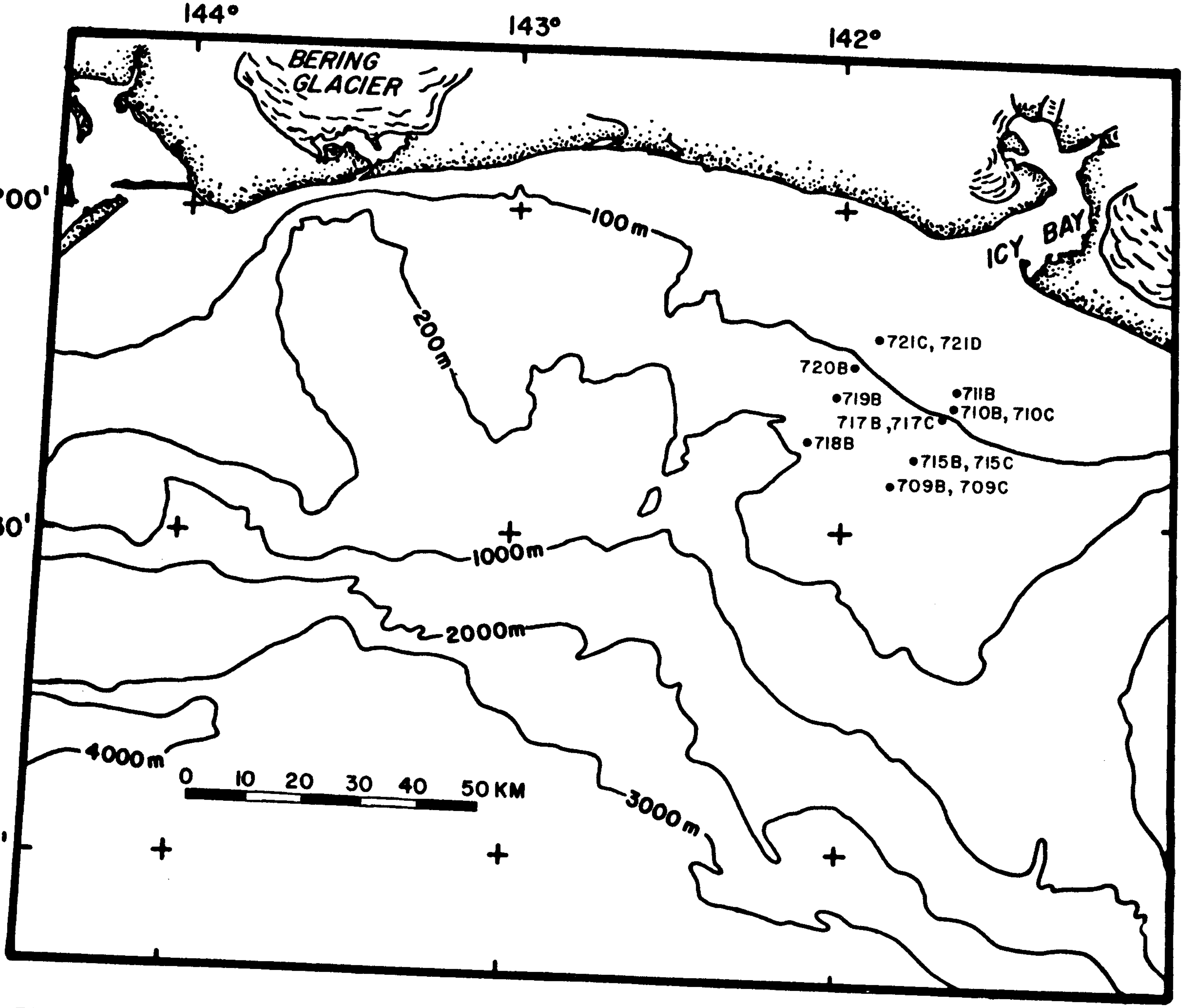

Figure 17. Core locations-Icy Bay-Malaspina Study Area (Cruise DC1-77-EG)

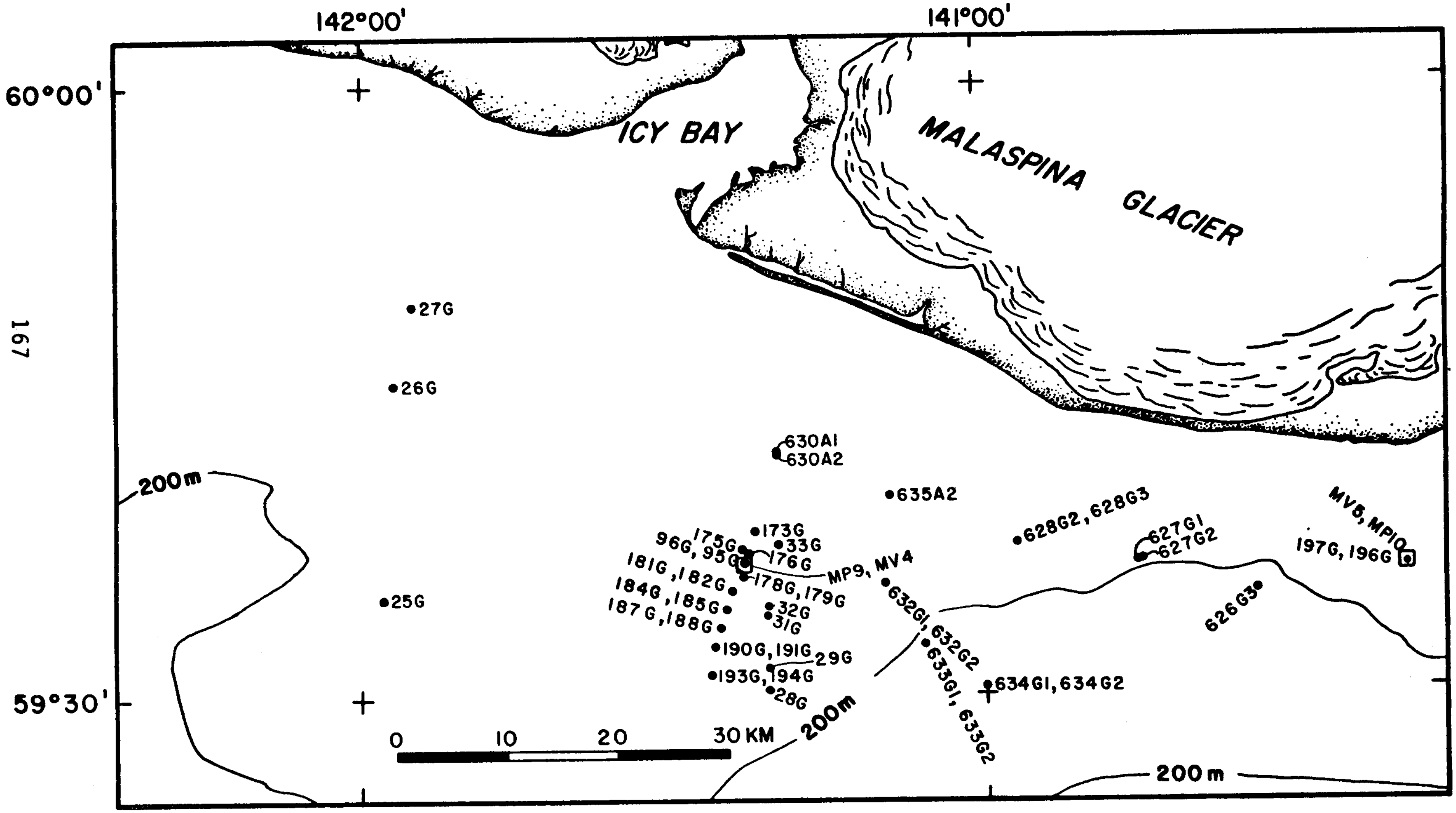

Figure 18. Core and in place test locations-Icy Bay-Malaspina Study Area (Cruises S8-77-EG, DC2-80-EG and DC1-81-EG).

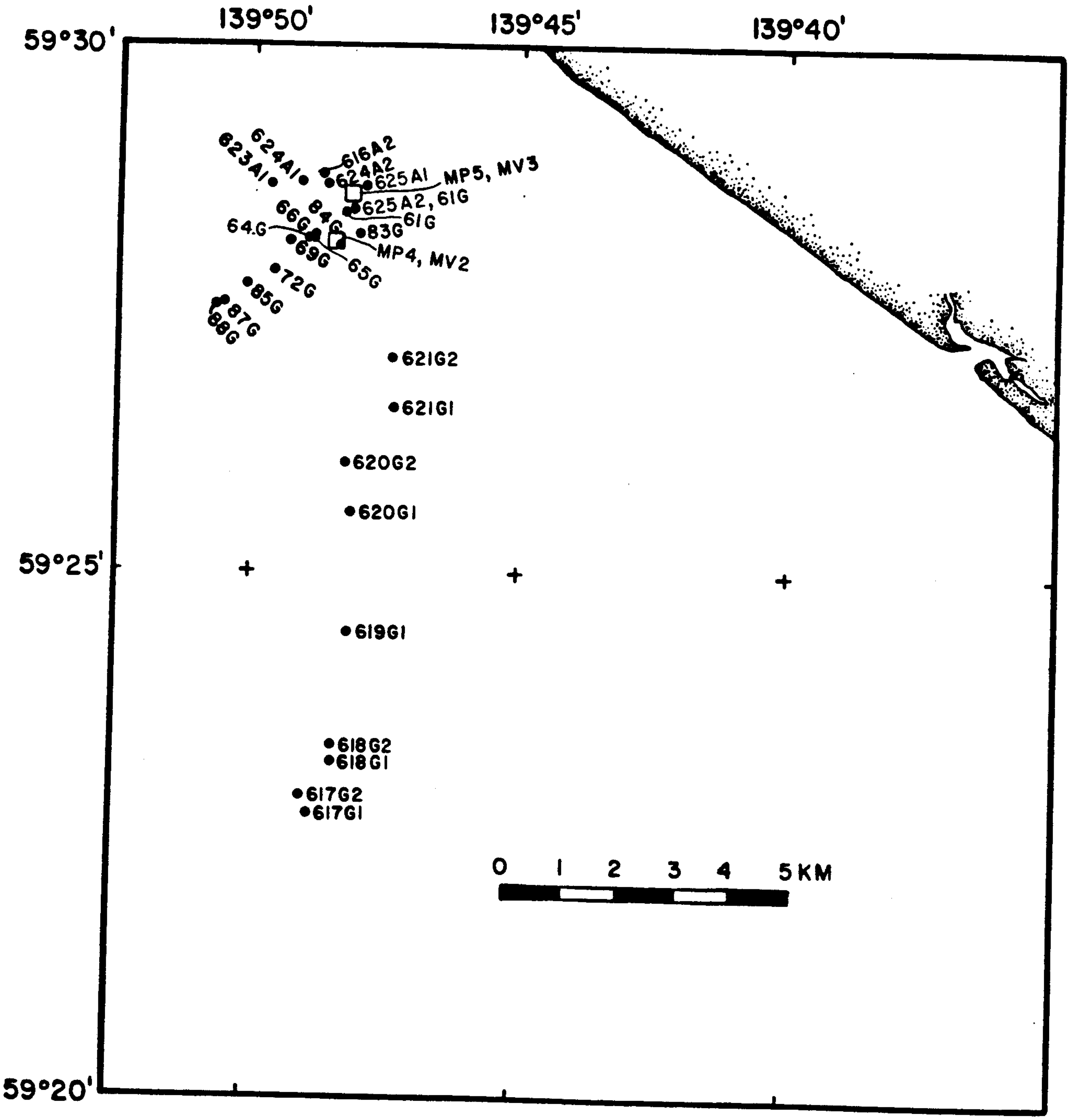

Figure 19. Core and in place test locations-Yakutat Study Area.

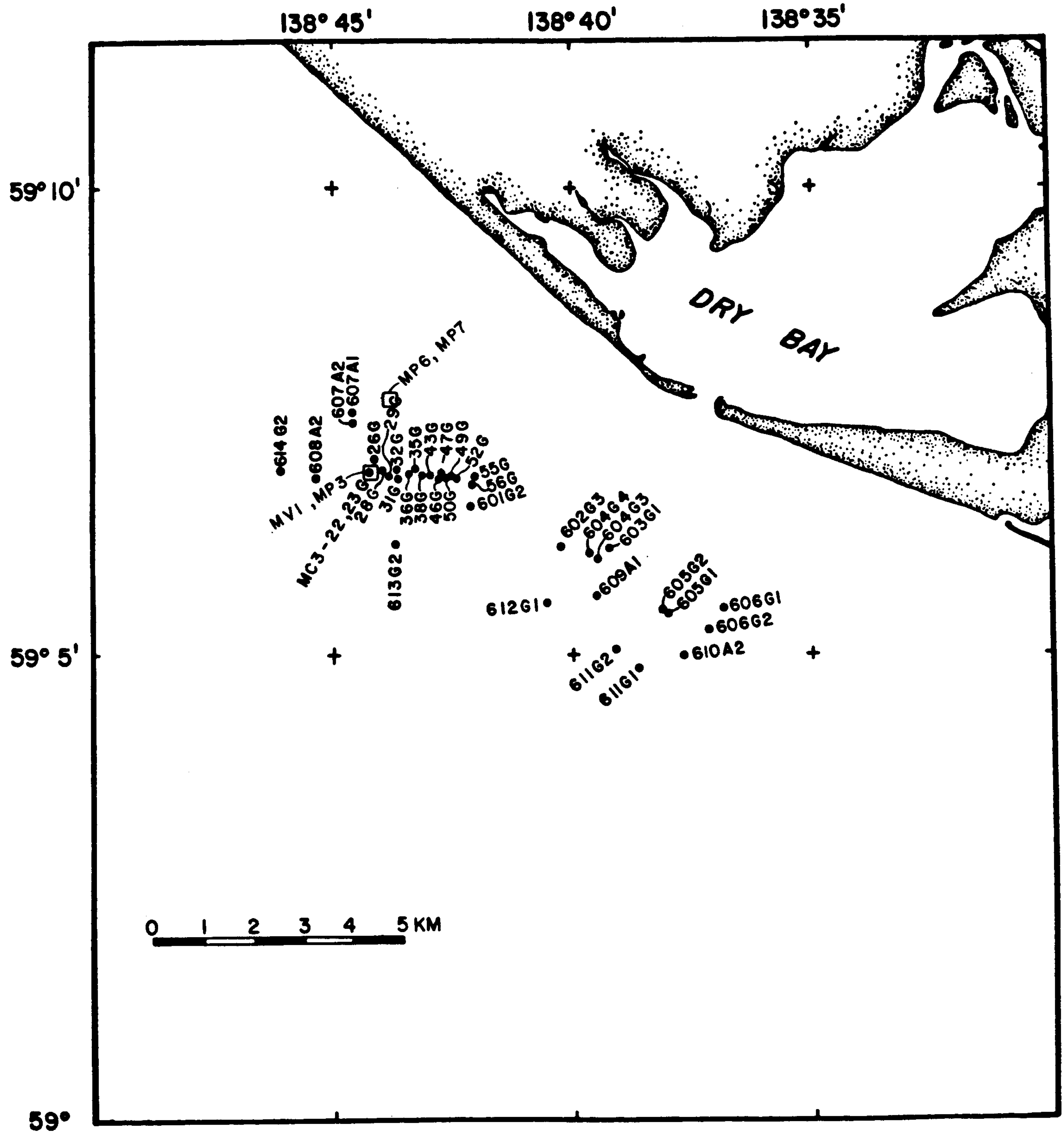

Figure 20. Core and in place test locations-Alsek River Study Area.

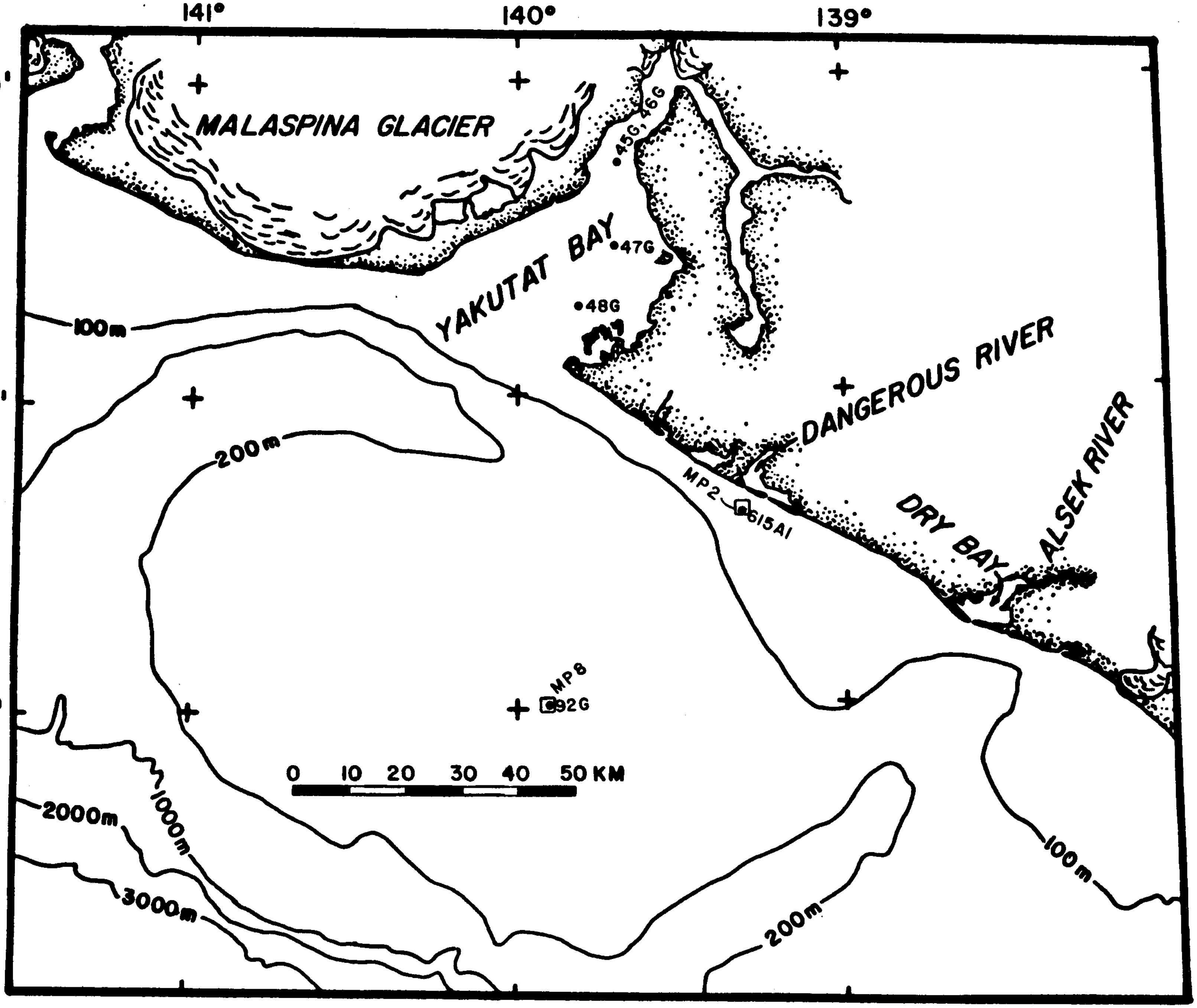

Figure 21. Core locations-Yakutat Bay Study Area and "other".

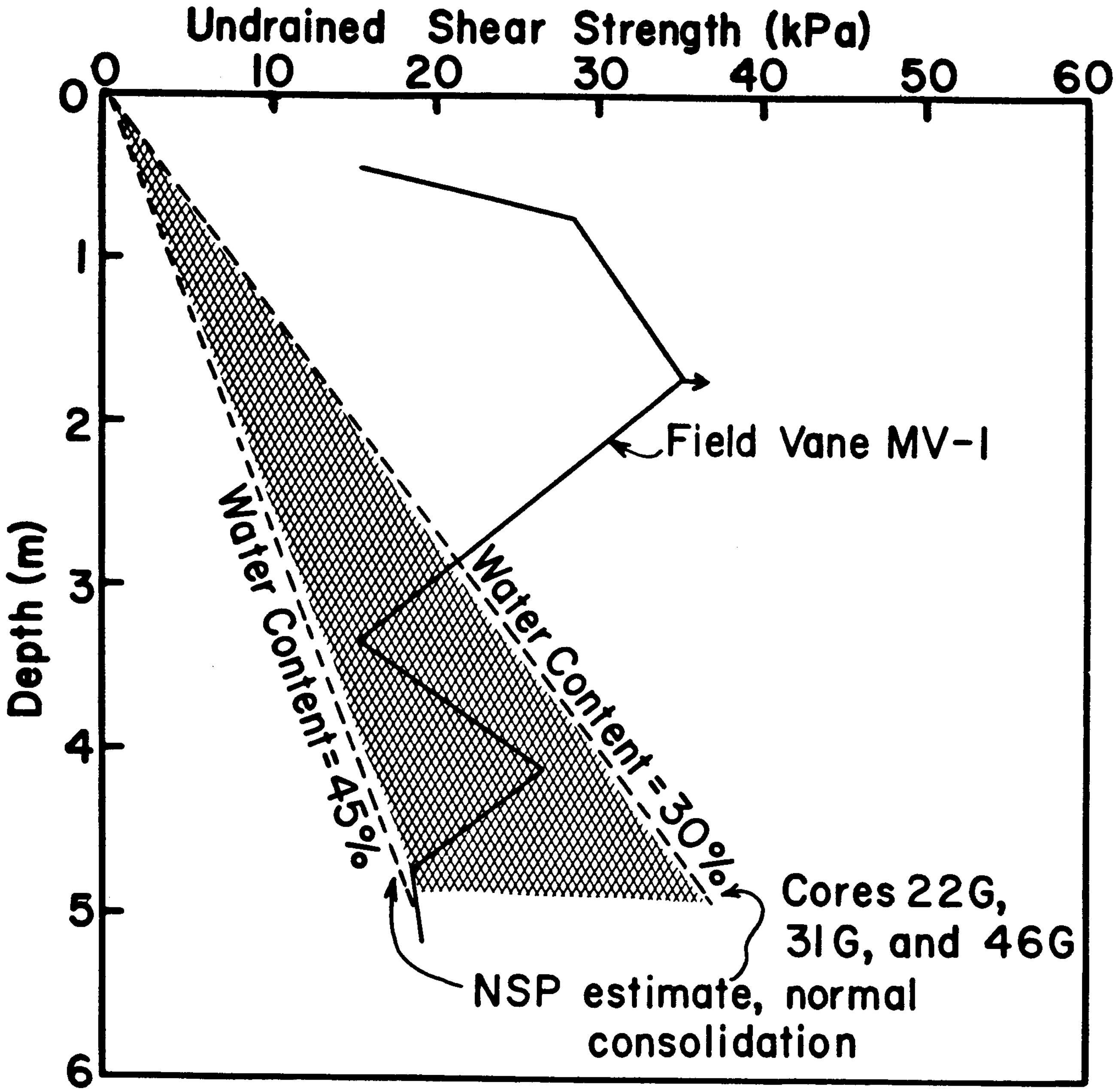

Figure 22. Results of field vane shear test MV-1 (Alsek River Study Area) compared with normalized strength parameter (NSP) estimate of undrained strength from triaxial tests.

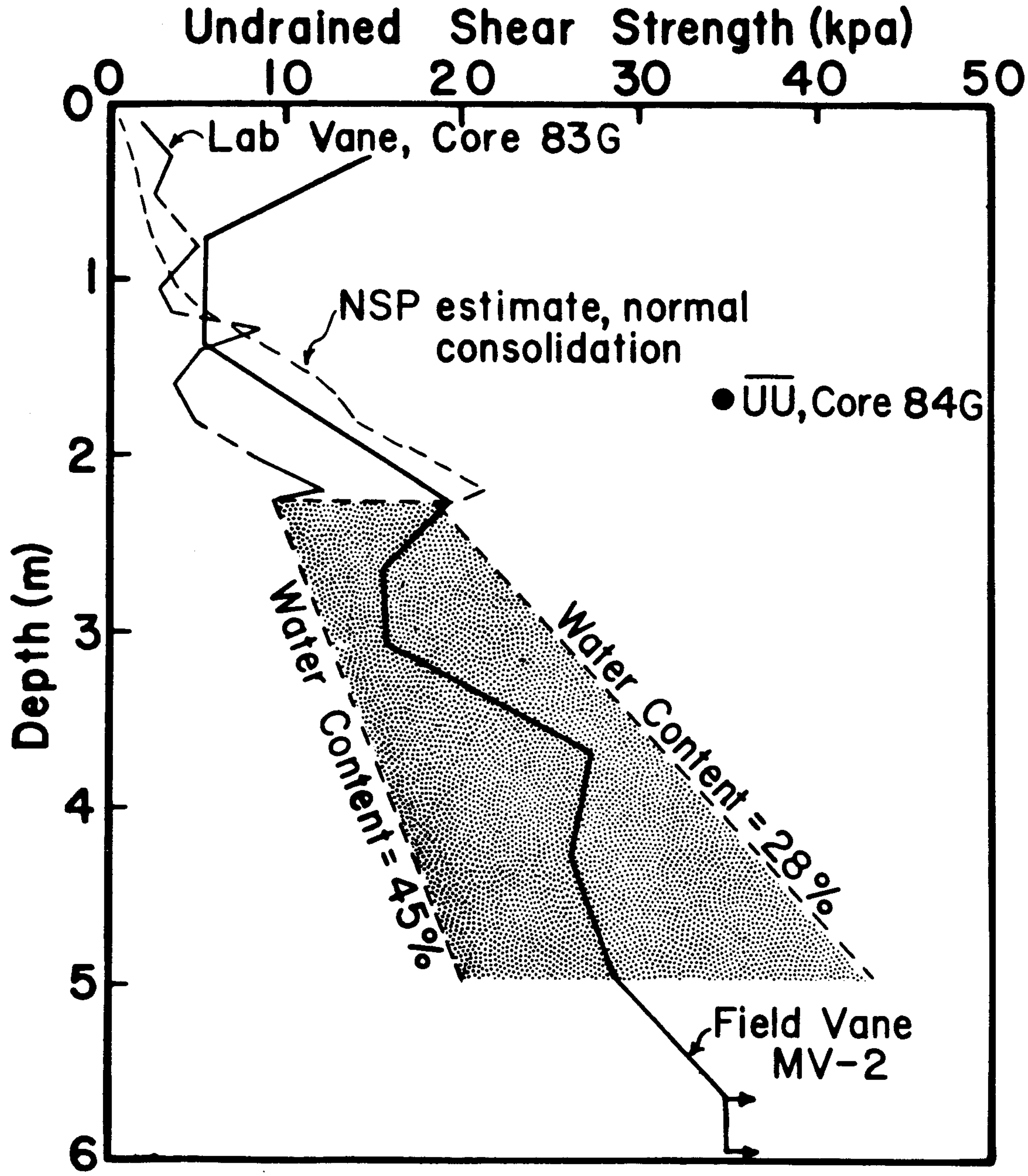

Figure 23. Results of field vane shear test MV-2 (Yakutat Study Area) compared with laboratory vane shear strengths and NSP estimates from triaxial tests. CIU and UU tests represent triaxial tests with consolidation to near the overburden stress and to nearly no stress, respectively.

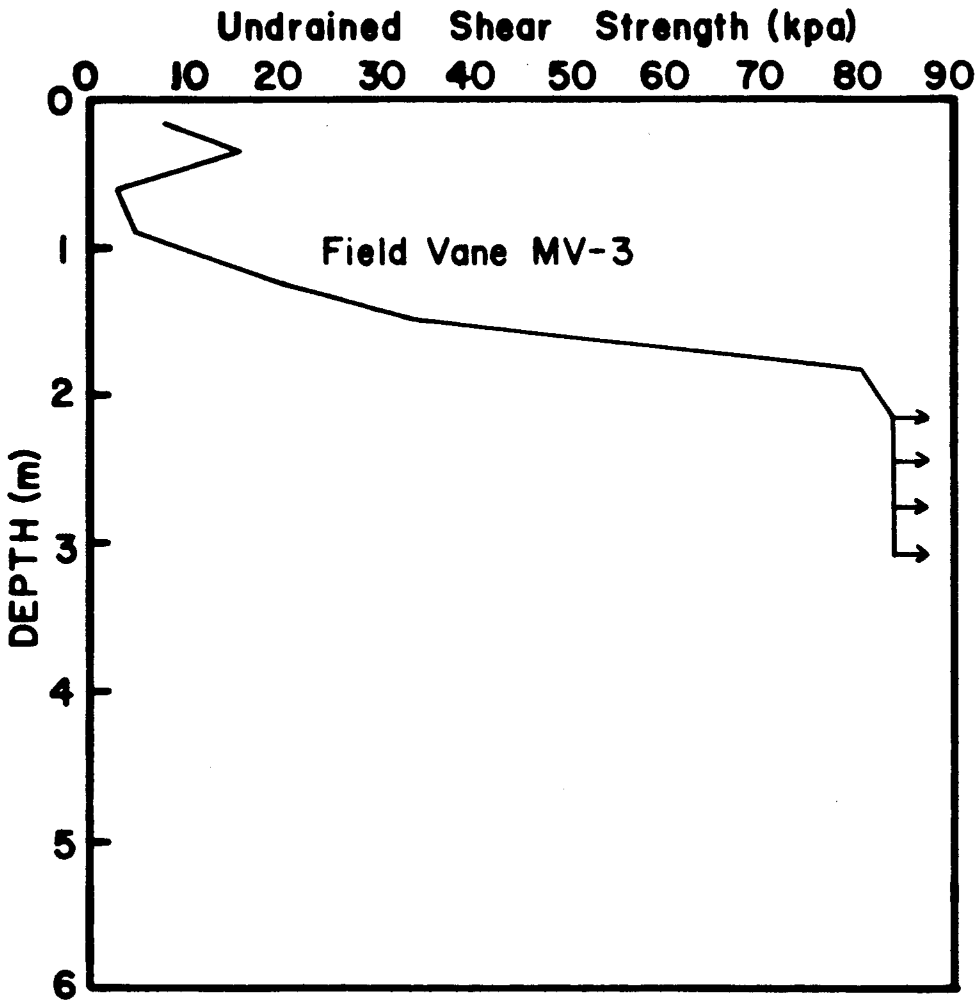

Figure 24. Results of field vane shear test MV-3 (Yakutat Study Area). Arrows indicate locations where the capacity of the field vane torque cell was reached.

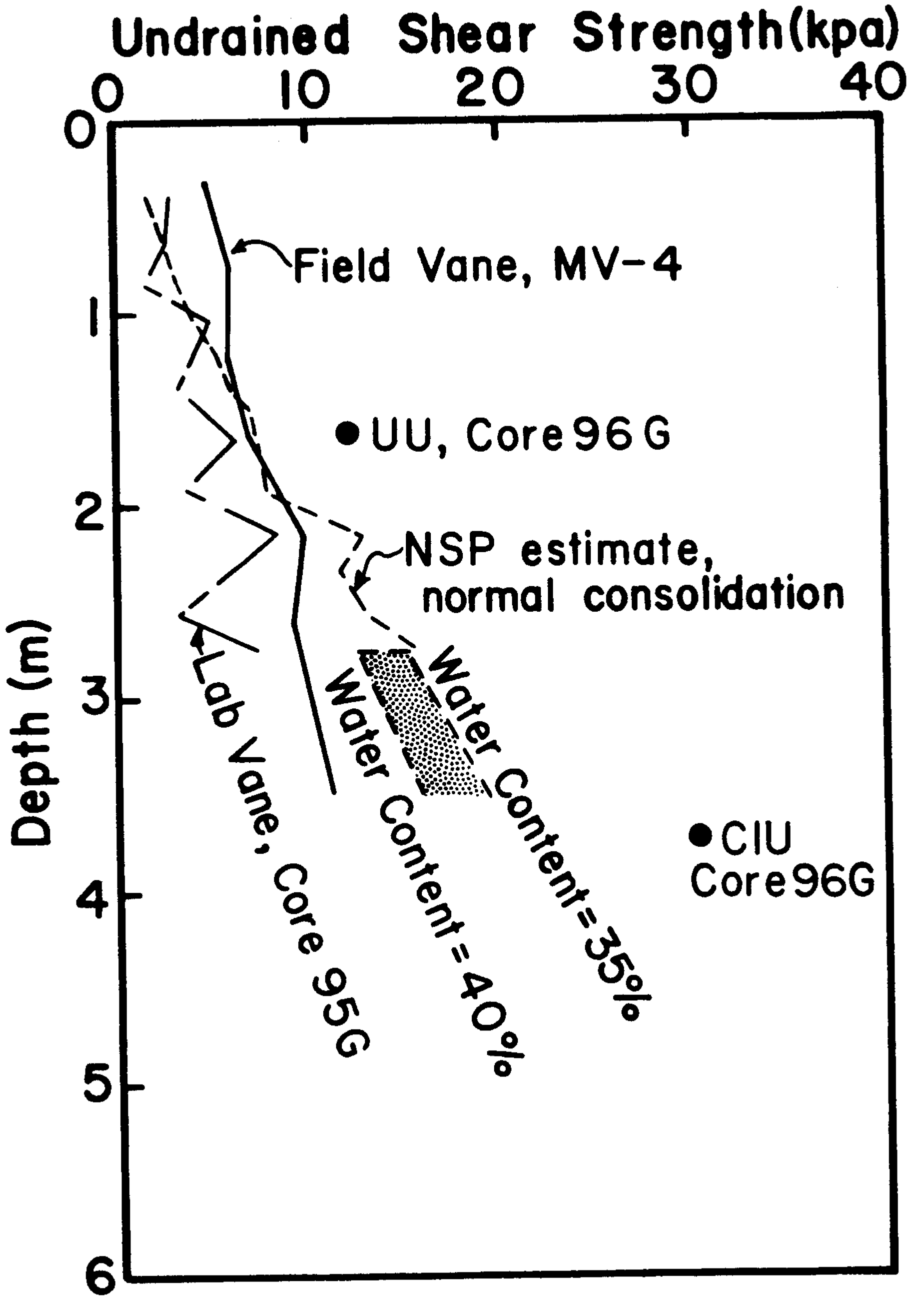

Figure 25. Results of field vane shear test MV-4 (Icy Bay-Malaspina Study Area) compared with laboratory vane shear strengths and NSP estimates from triaxial tests. CIU and UU tests represent triaxial tests consolidated to near the overburden stress and to nearly no stress, respectively.

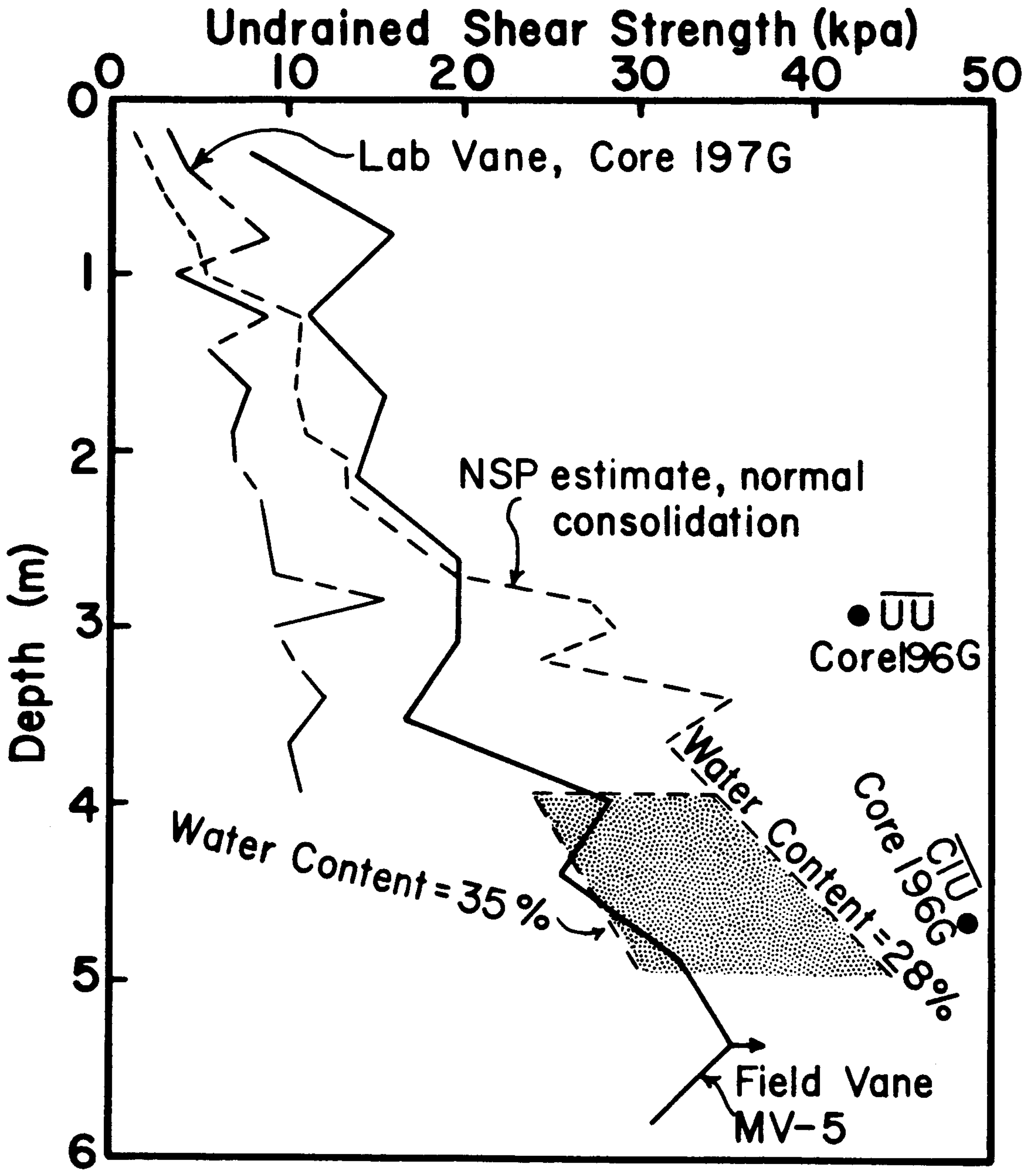

Figure 26. Results of field vane shear test MV-5 (eastern part of Icy Bay-Malaspina Study Area) compared with laboratory vane shear strengths and NSP estimates from triaxial tests. CIU and UU tests represent triaxial tests to near the overburden stress and to nearly no stress, respectively.

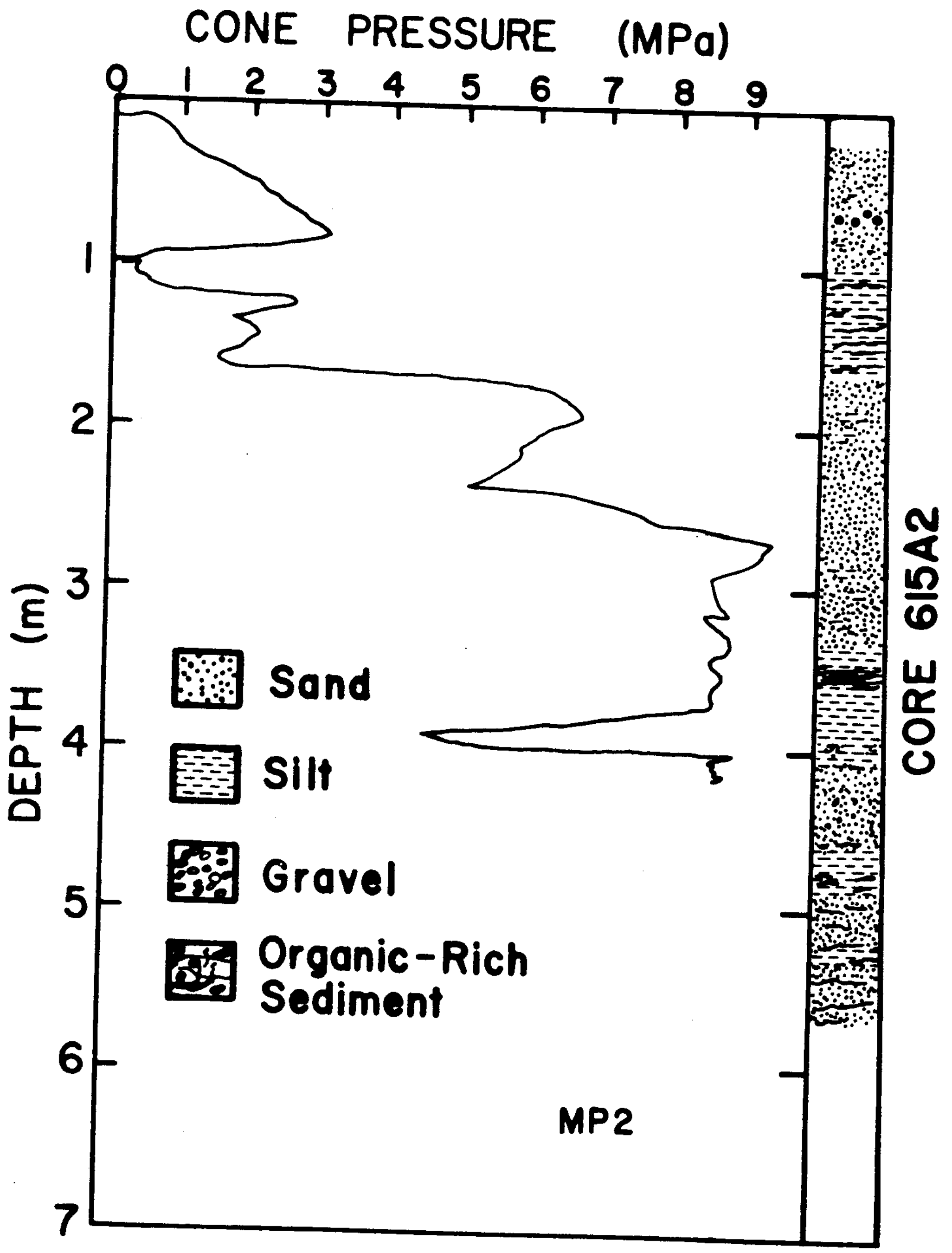

Figure 27. Results of in place cone penetration test MP-2 (off the mouth of the Dangerous River). Stratigraphy of nearby core is given at right.

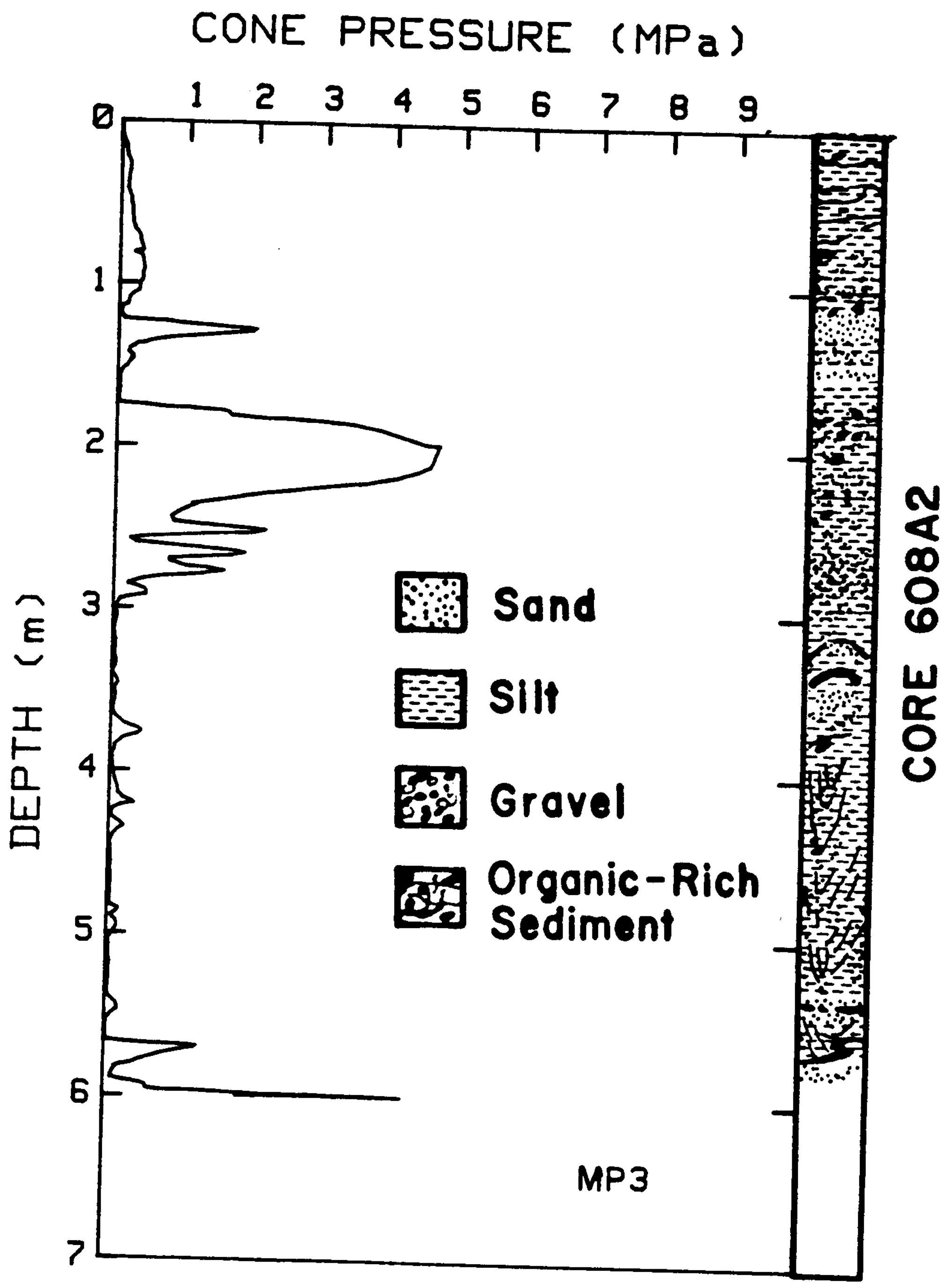

Figure 28. Results of in place cone penetration test MP-3. (Alsek River Study Area). Stratigraphy of nearby core is given at right.

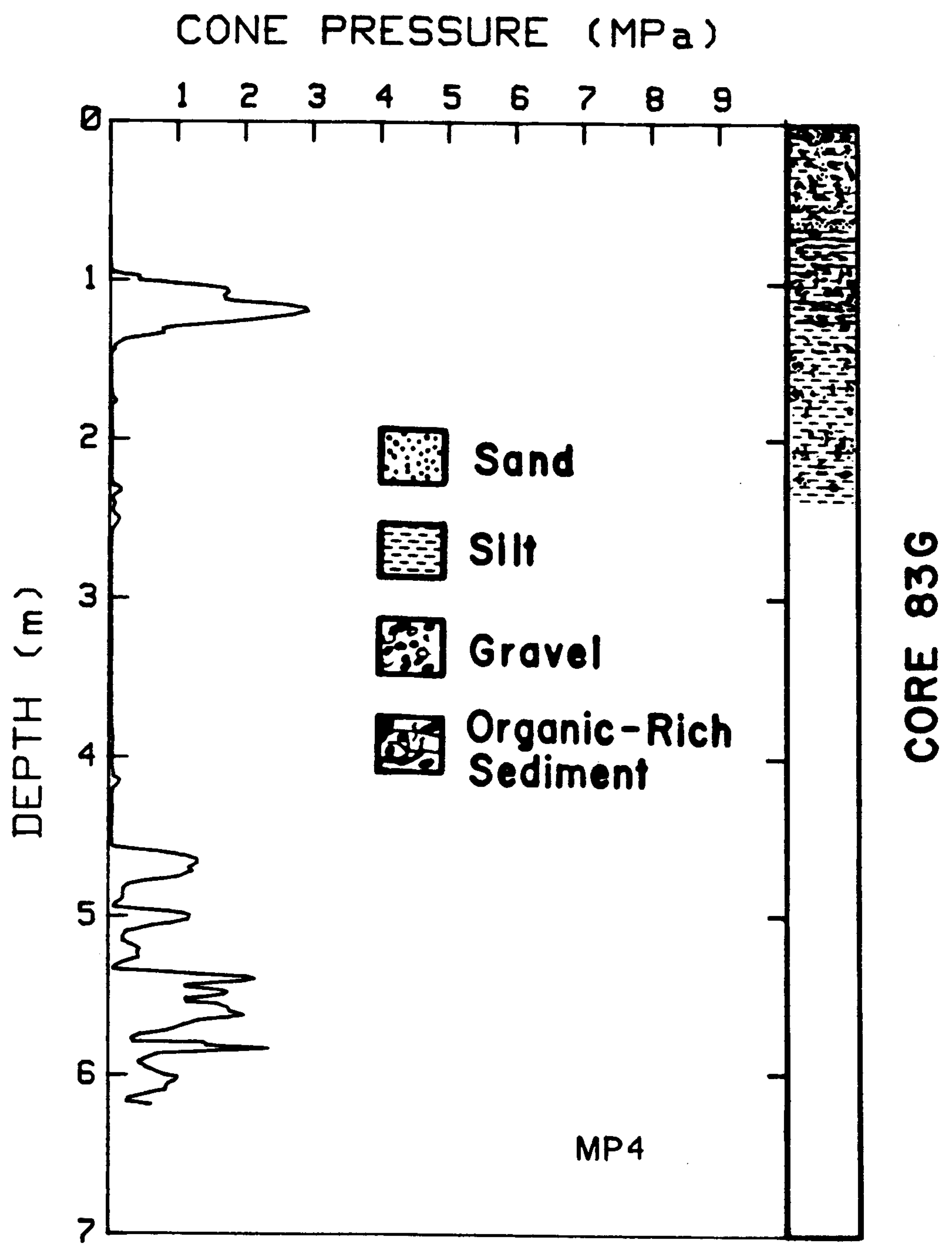

Figure 29. Results of in place cone penetration test MP-4 (Yakutat Study Area). Stratigraphy of nearby core is given at right.

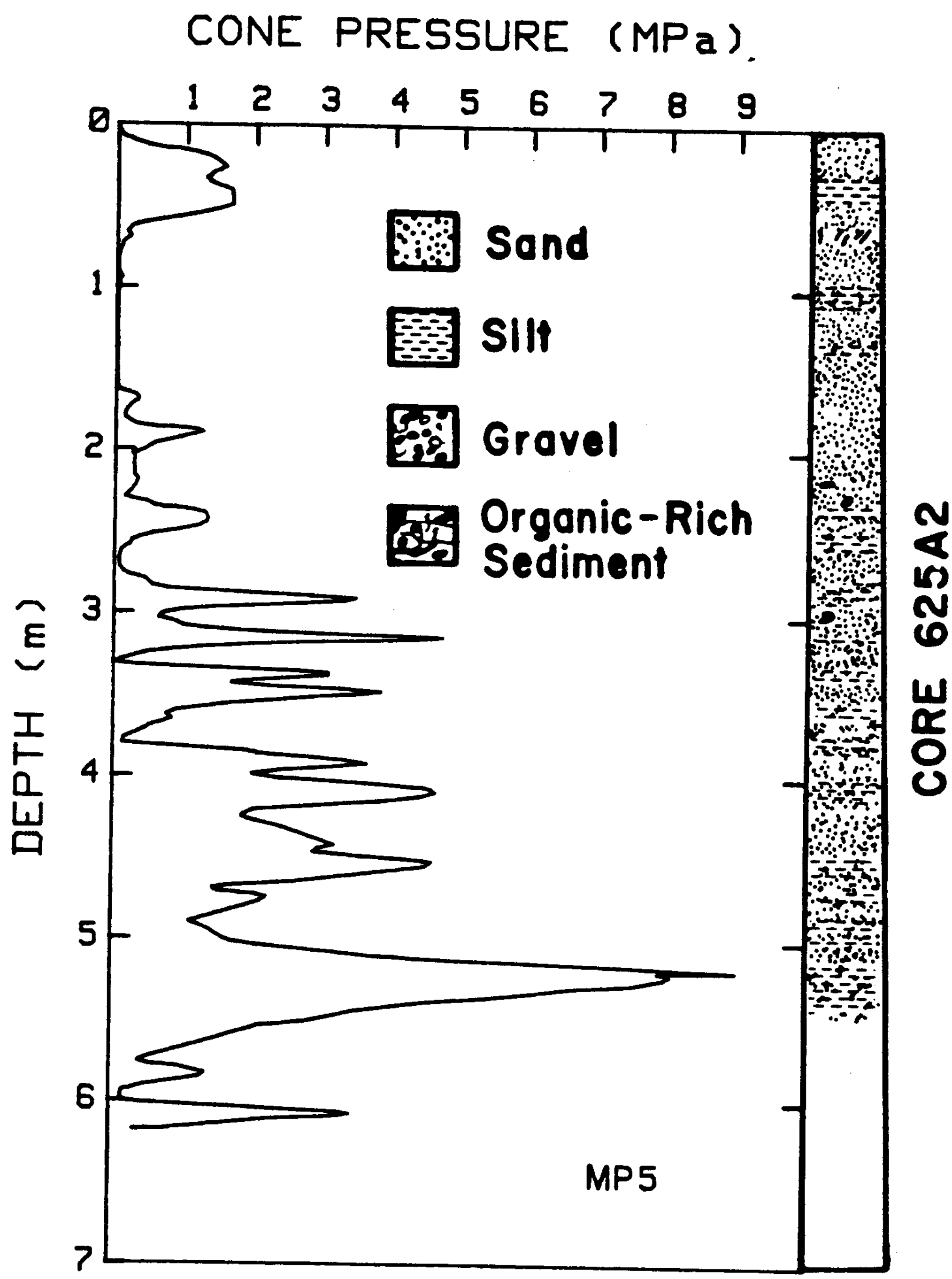

Figure 30. Results of in place cone penetration test MP-5 (Yakutat Study Area). Stratigraphy of nearby core is given at right.

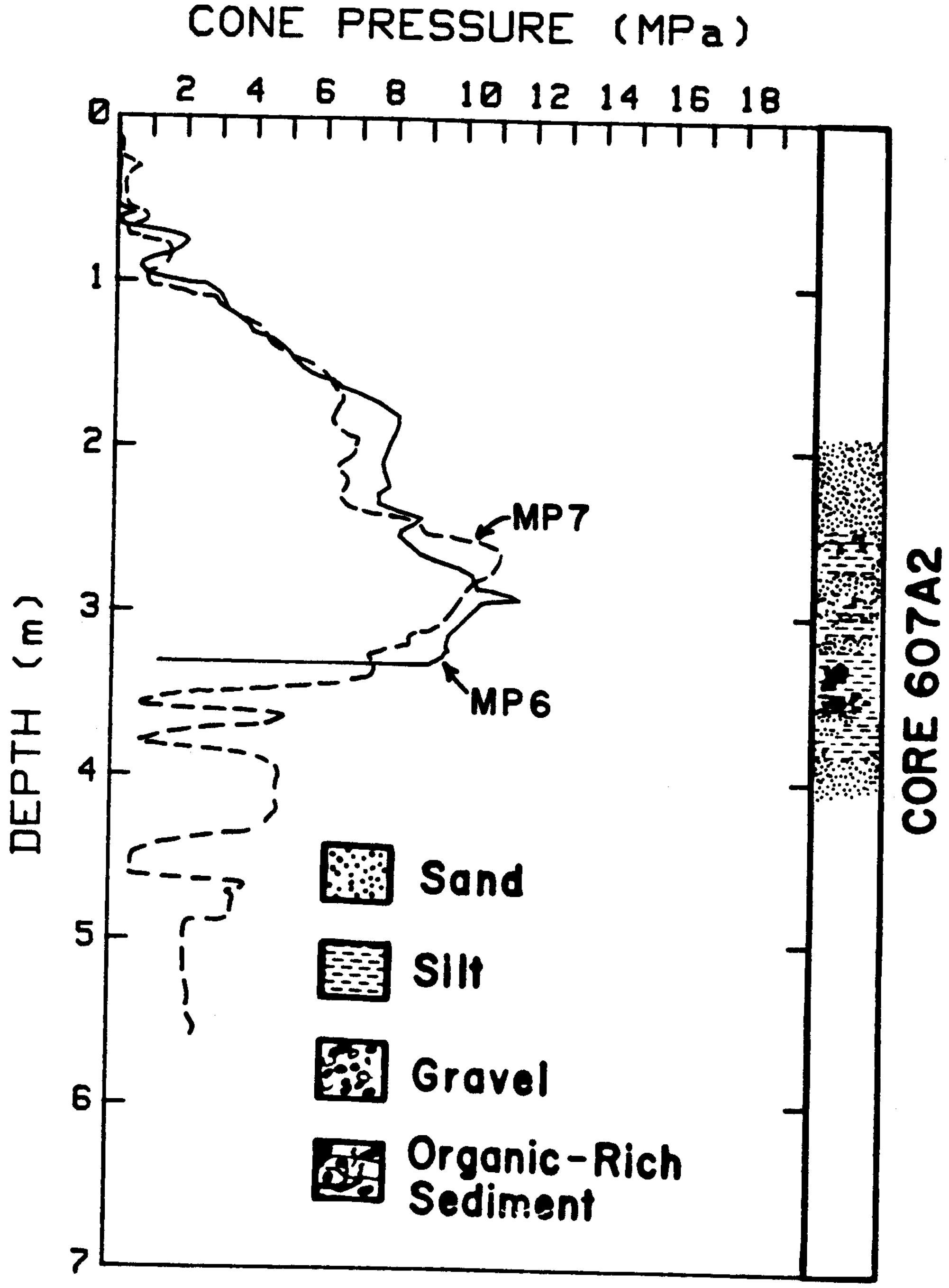

Figure 31. Results of in place cone penetration tests MP-6 and MP-7 (Alsek River Study Area). Stratigraphy of nearby core is given at right.

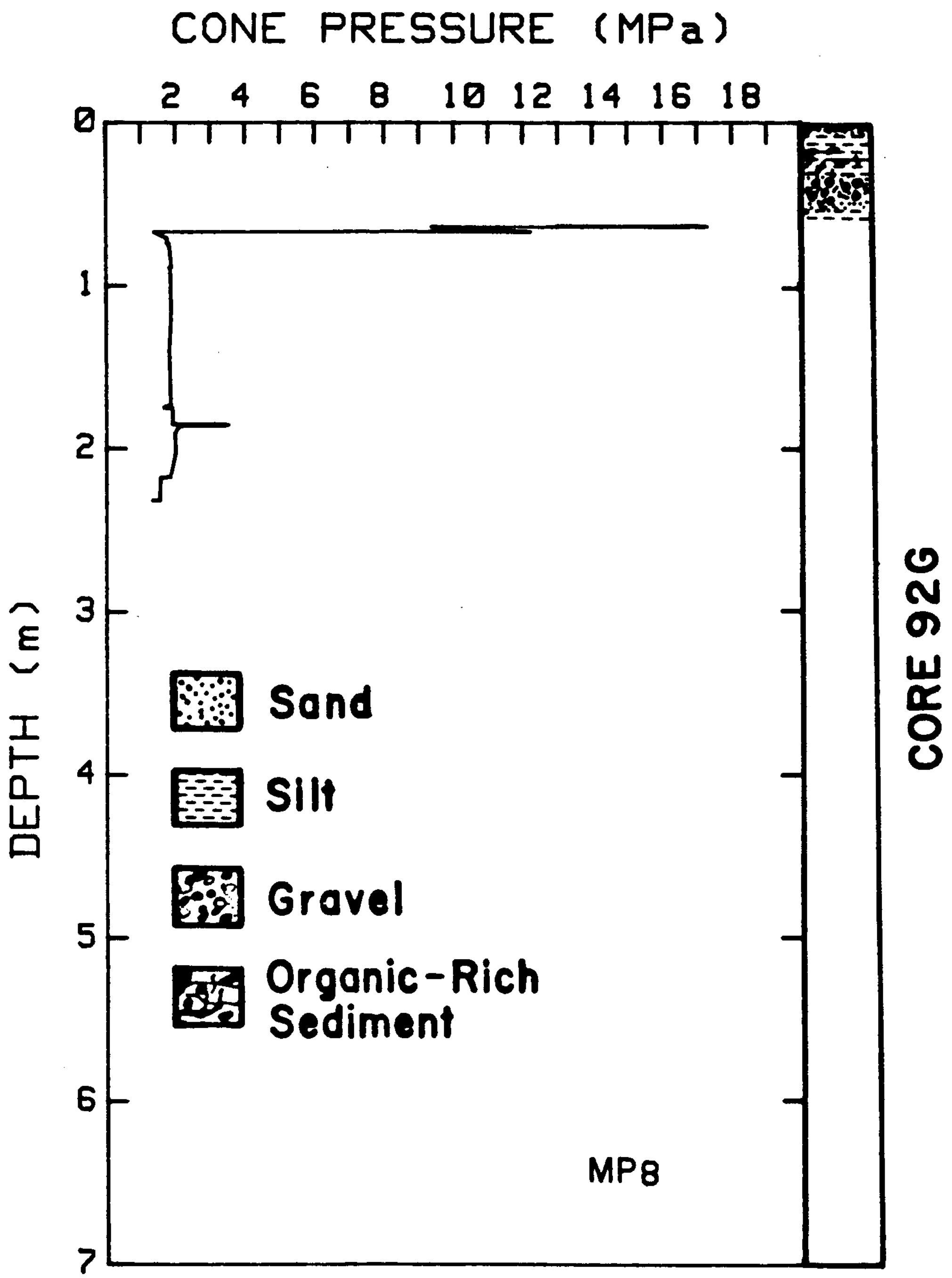

Figure 32. Results of in place cone penetration test MP-8 (Quaternary glacial deposits off Dangerous River Delta). Stratigraphy of nearby core is given at right.

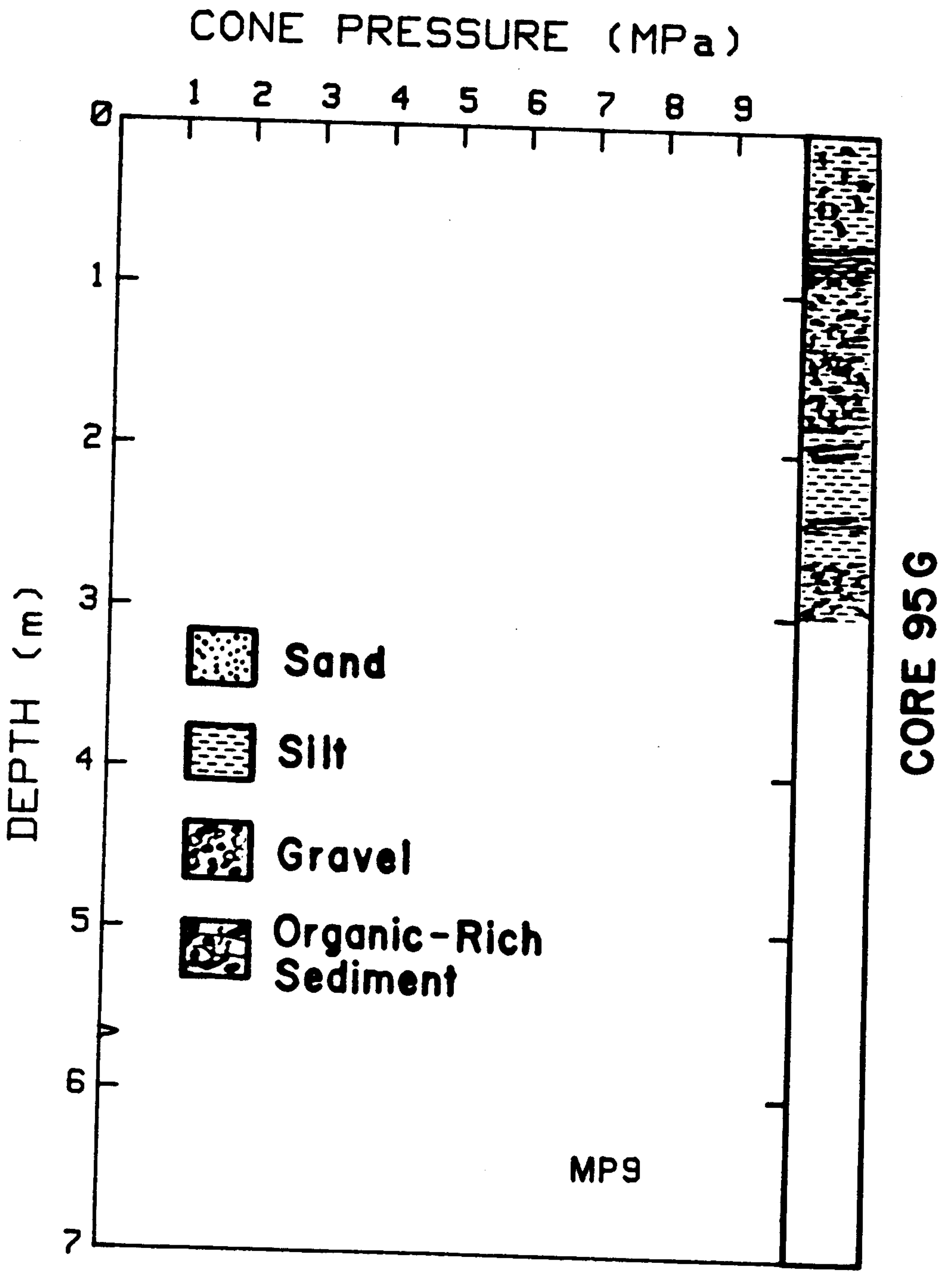

Figure 33. Results of in place cone penetration test MP-9 (Icy Bay-Malaspina Study Area). Stratigraphy of nearby core is given at right.

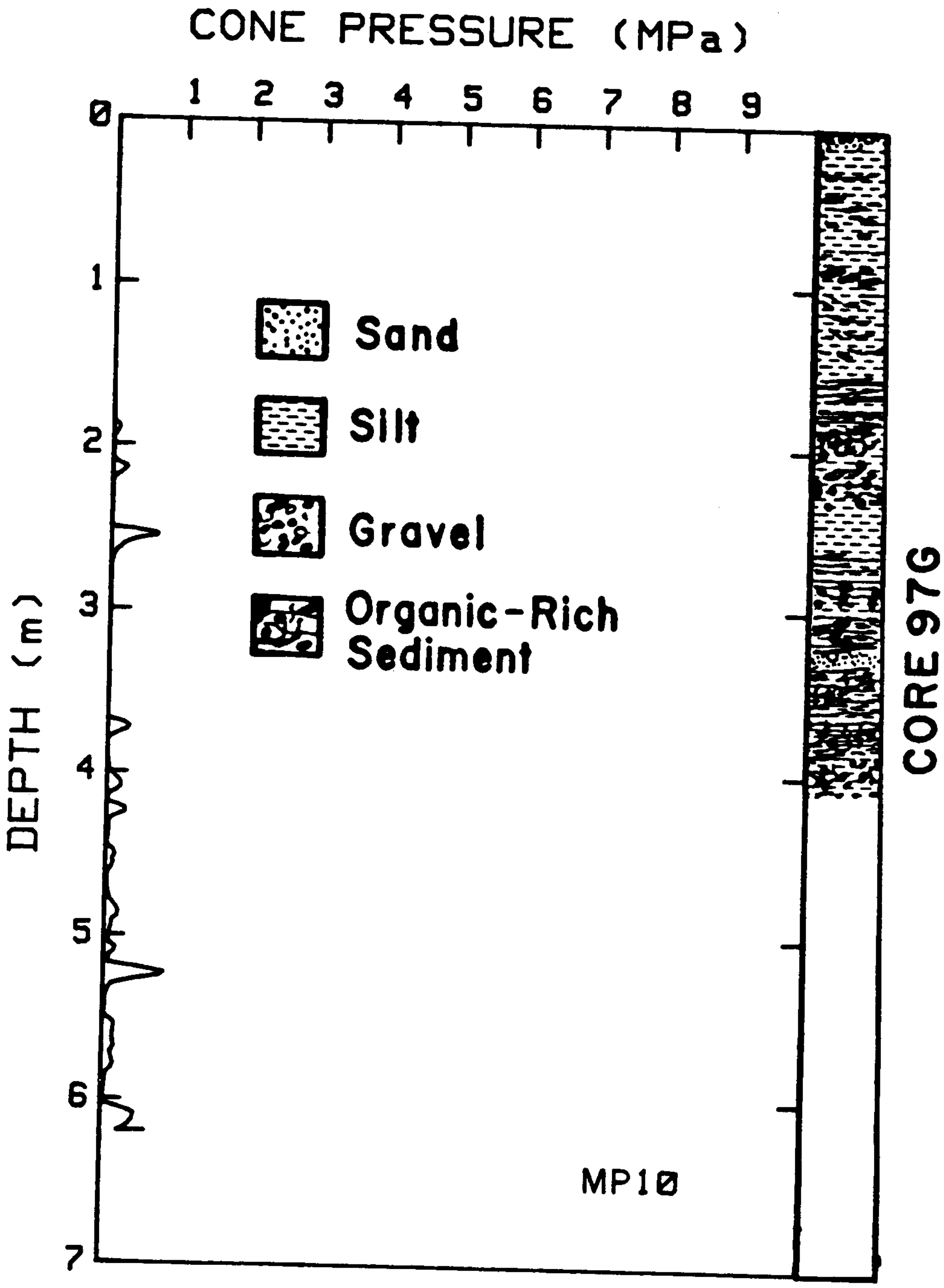

Figure 34. Results of in place cone penetration test MP-10 (eastern part of Icy Bay-Malaspina Study Area). Stratigraphy of nearby core is given at right.

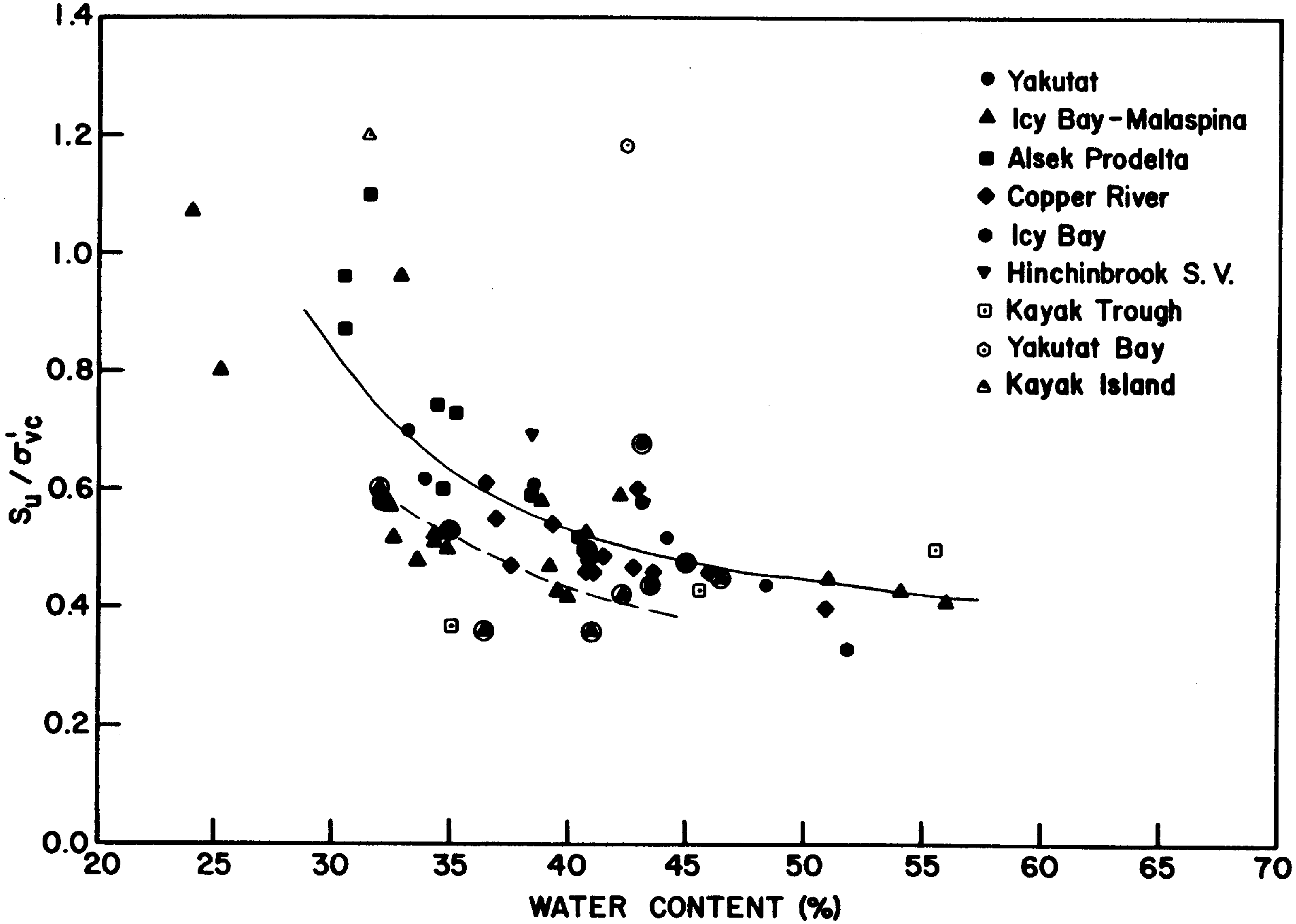

Figure 35. Correlation of ratio of undrained shearing strength, S_u, to vertical consolidation stress, σ'_{vc}, with natural water content; all type (c) static triaxial tests. Circled data points represent anisotropic consolidation. Solid line is a fit of the isotropic consolidation data points (uncircled dots). Dashed line represents 0.8 times the solid line and roughly follows anisotropic data points.

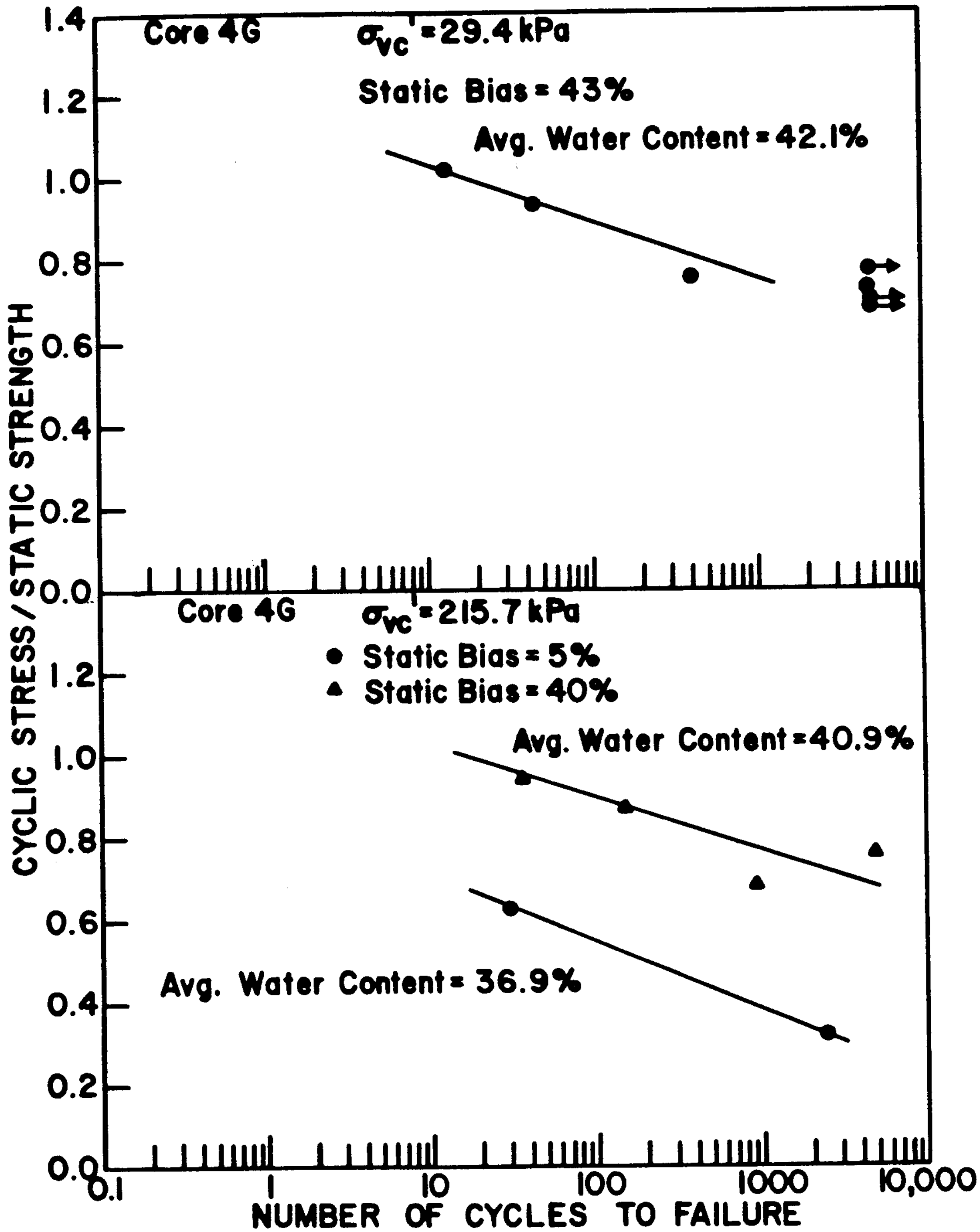

Figure 36. Relative cyclic stress level versus number of cycles to failure: Core 4G (Copper River Study area).

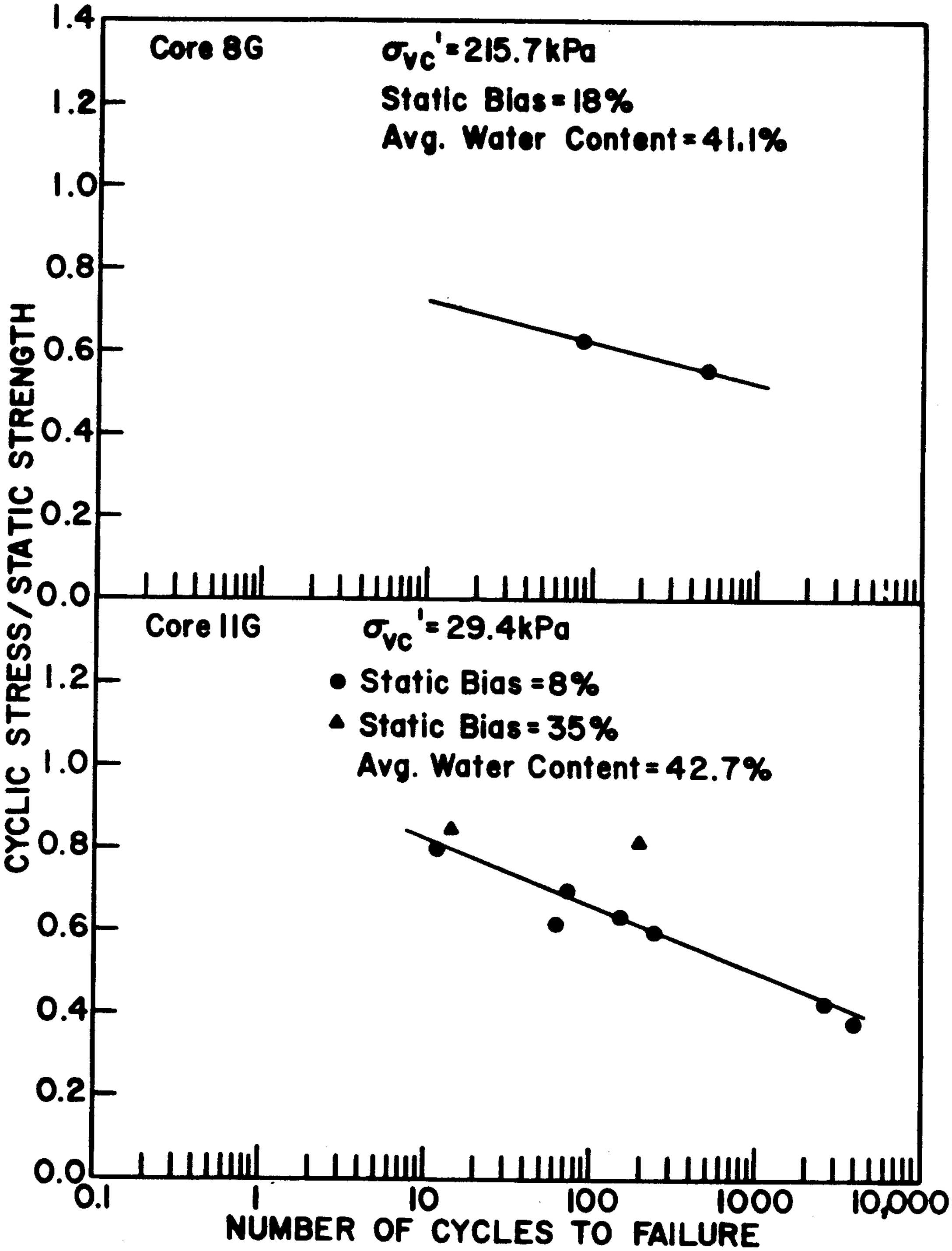

Figure 37. Relative cyclic stress level versus number of cycles to failure: Cores 8G and 11G (Copper River and Kayak Trough Study Areas).

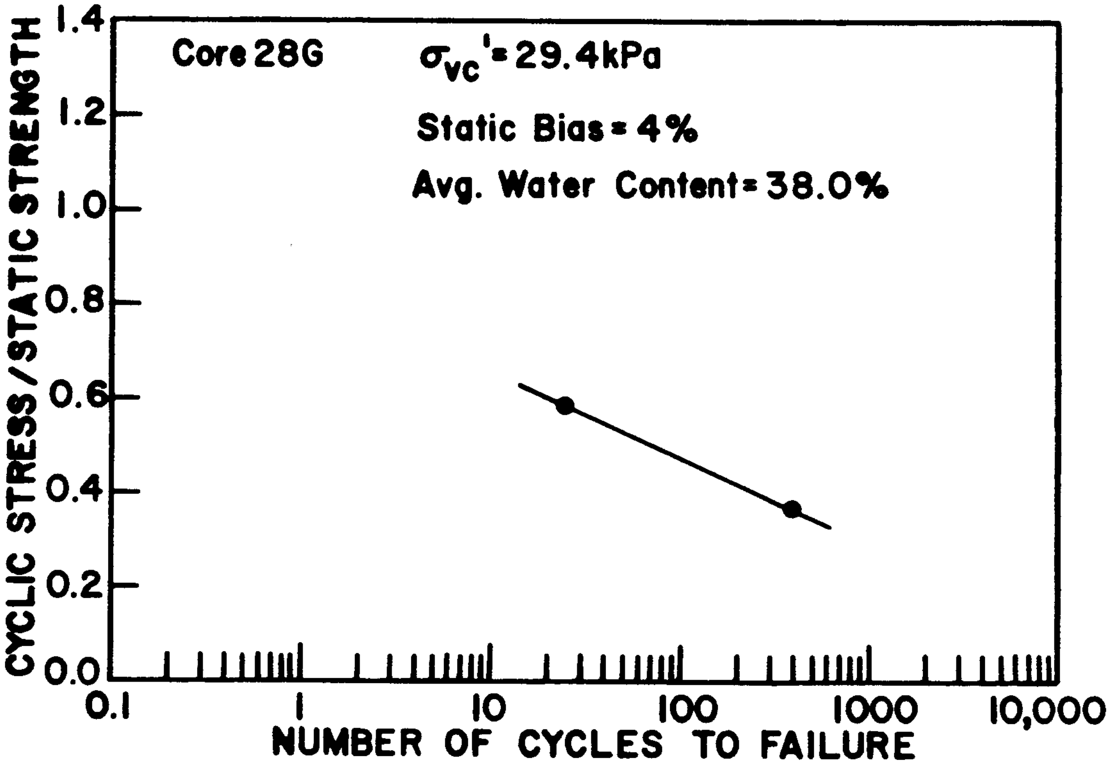

Figure 38. Relative cyclic stress level versus number of cycles to failure: Core 28G (Icy Bay-Malaspina Study Area).

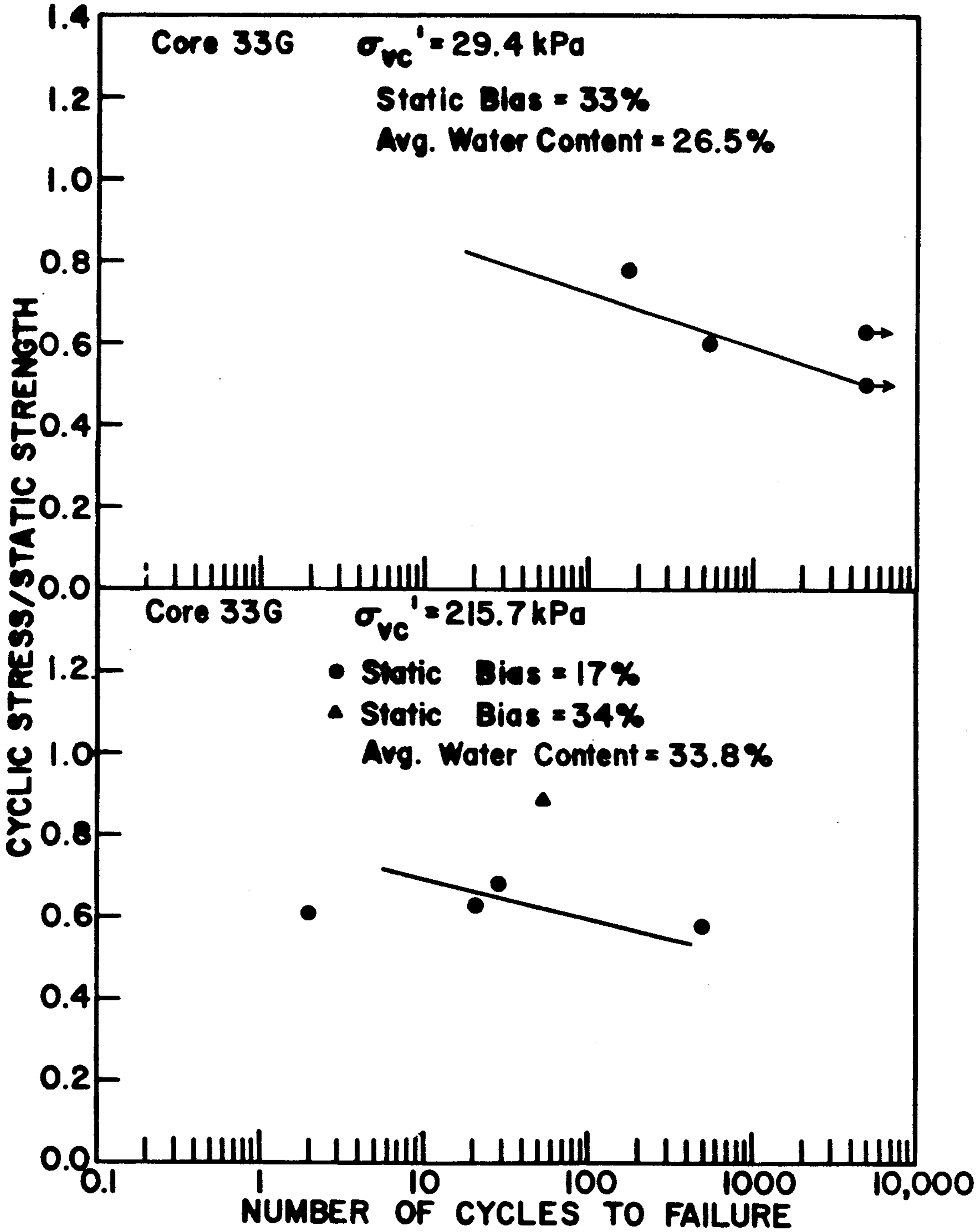

Figure 39. Relative cyclic stress level versus number of cycles to failure: Core 33G (Icy Bay-Malaspina Study Area).

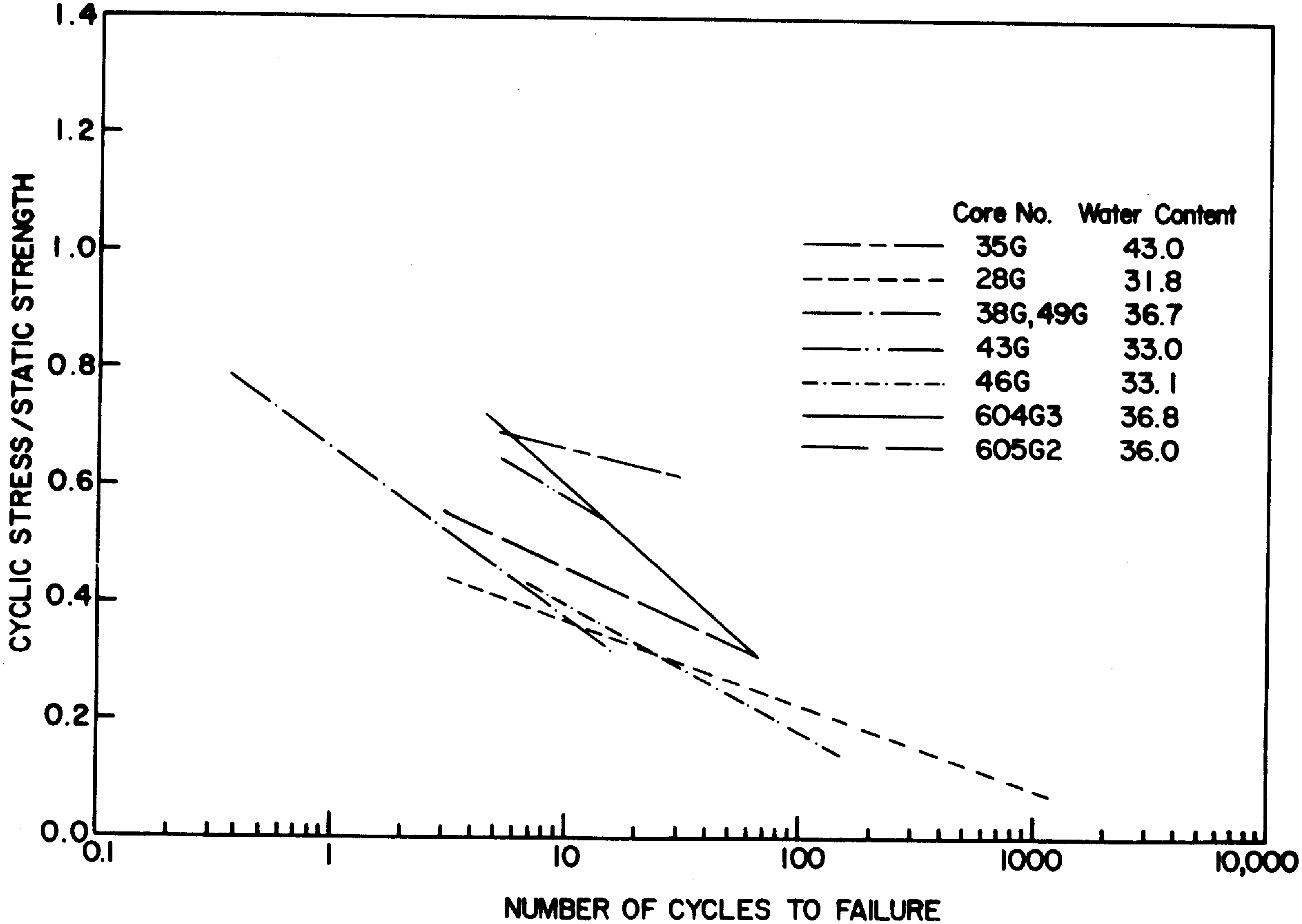

Figure 40. Relative cyclic stress level versus number of cycles to failure: Alsek River Study Area, Method I.

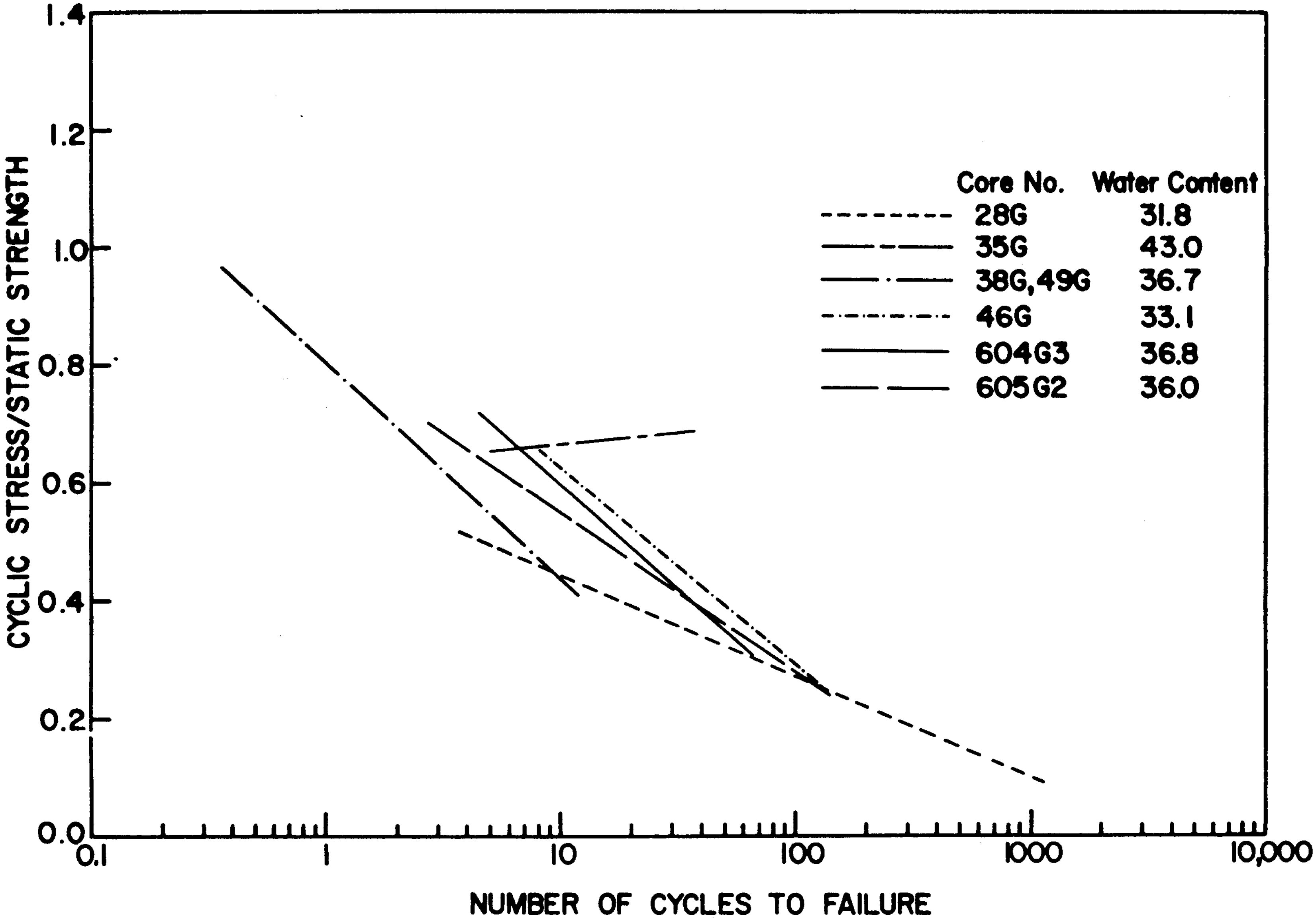

Figure 4I. Relative cyclic stress level versus number of cycles to failure: Alsek River Study Area, Method II.

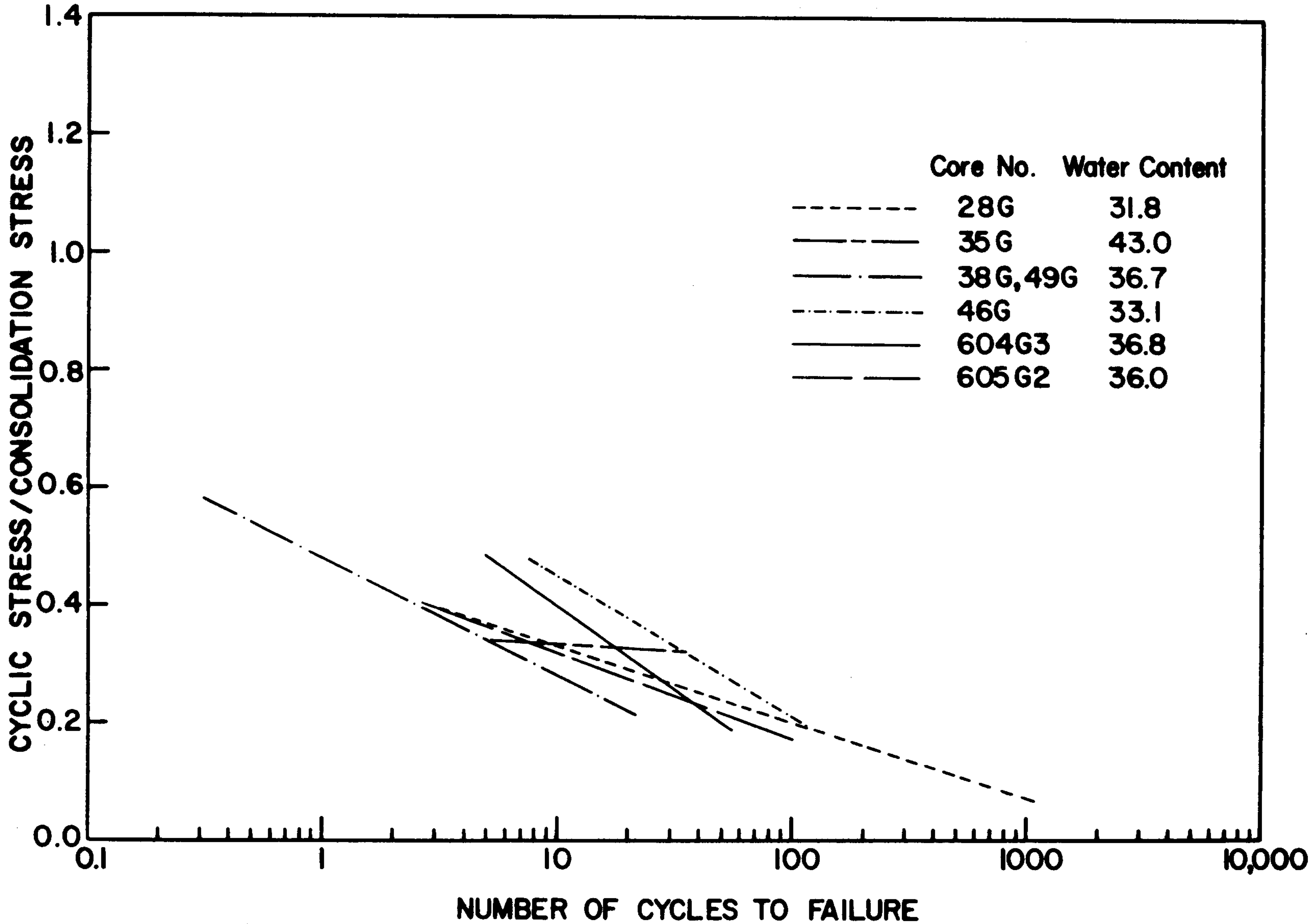

Figure 42. Relative cyclic stress level versus number of cycles to failure: Alsek River Study Area, Method III.

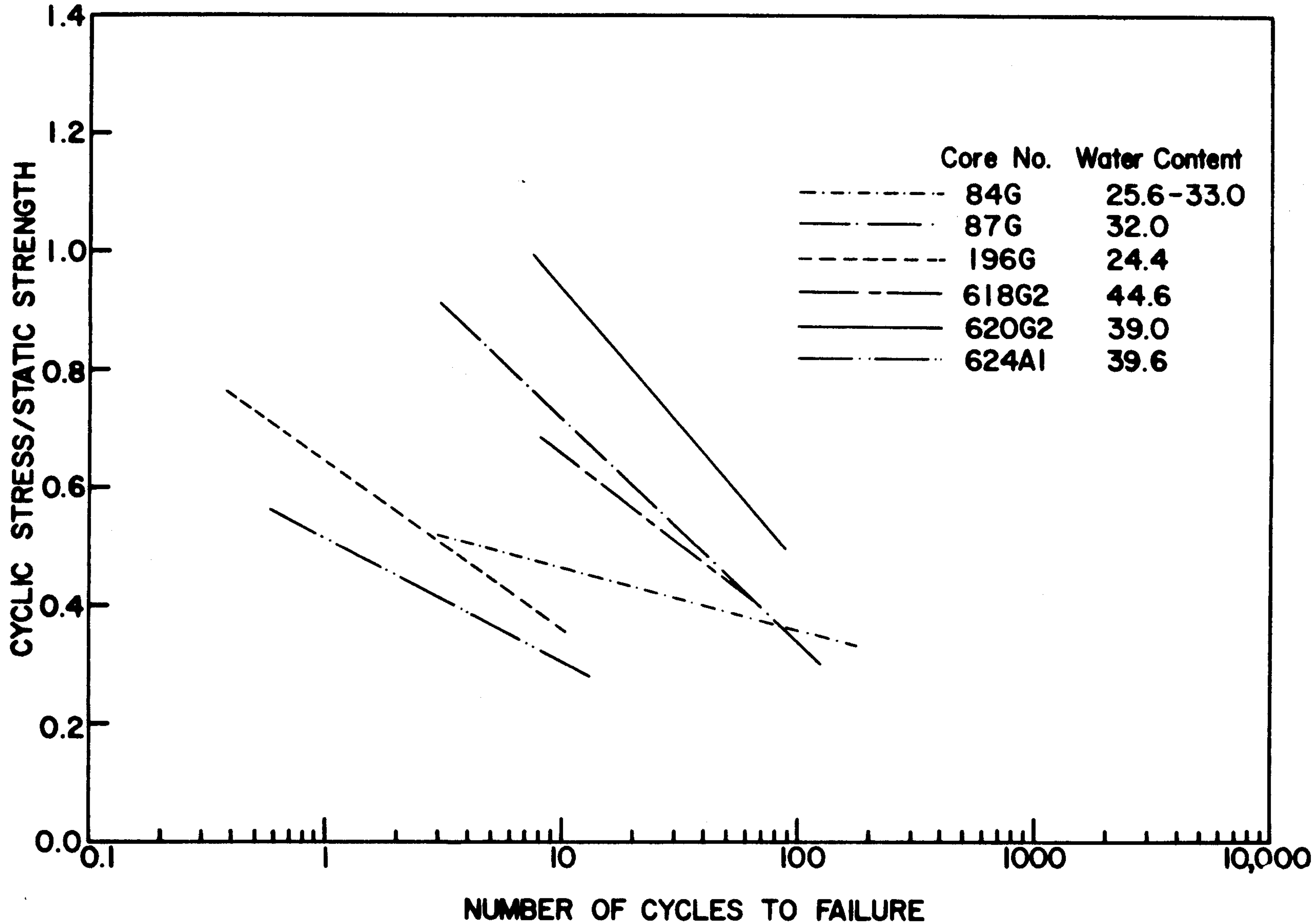

Figure 43. Relative cyclic stress level versus number of cycles to failure: Yakutat Study Area, Method I.

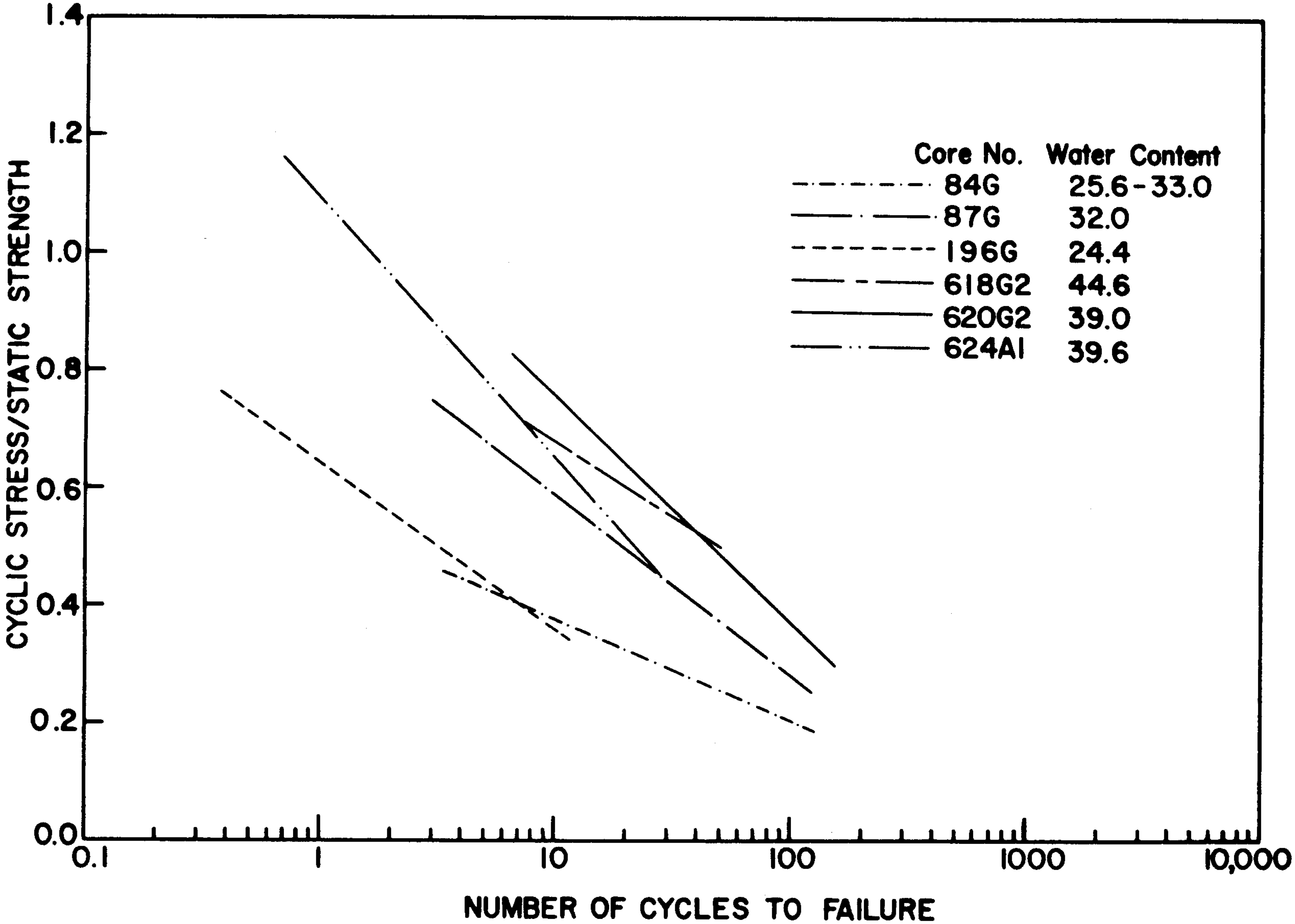

Figure 44. Relative cyclic stress level versus number of cycles to failure: Yakutat Study Area, Method II.

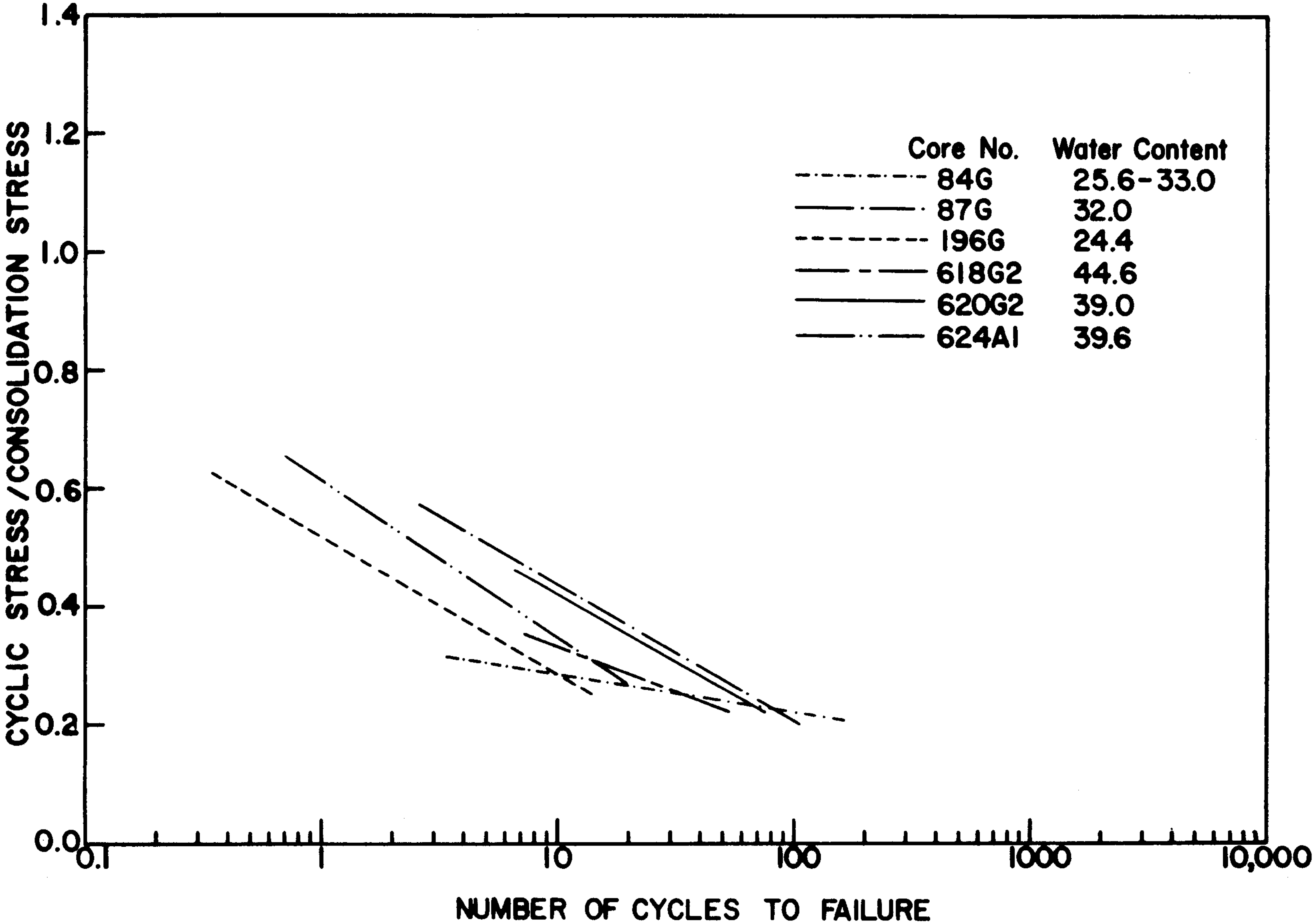

Figure 45. Relative cyclic stress level versus number of cycles to failure: Yakutat Study Area, Method III.

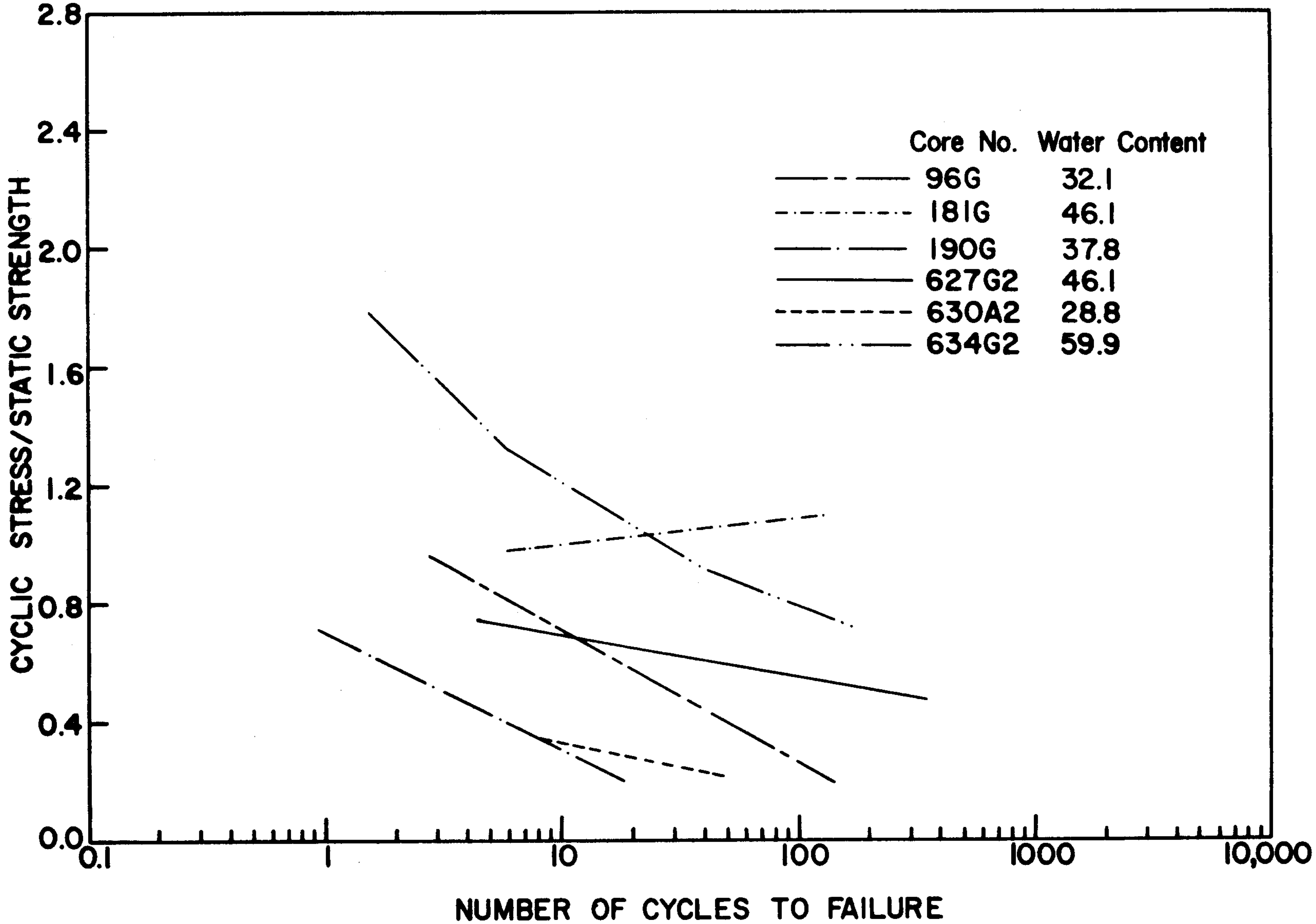

Figure 46. Relative cyclic stress level versus number of cycles to failure: Icy Bay-Malaspina Study Area (USGS testing), Method I.

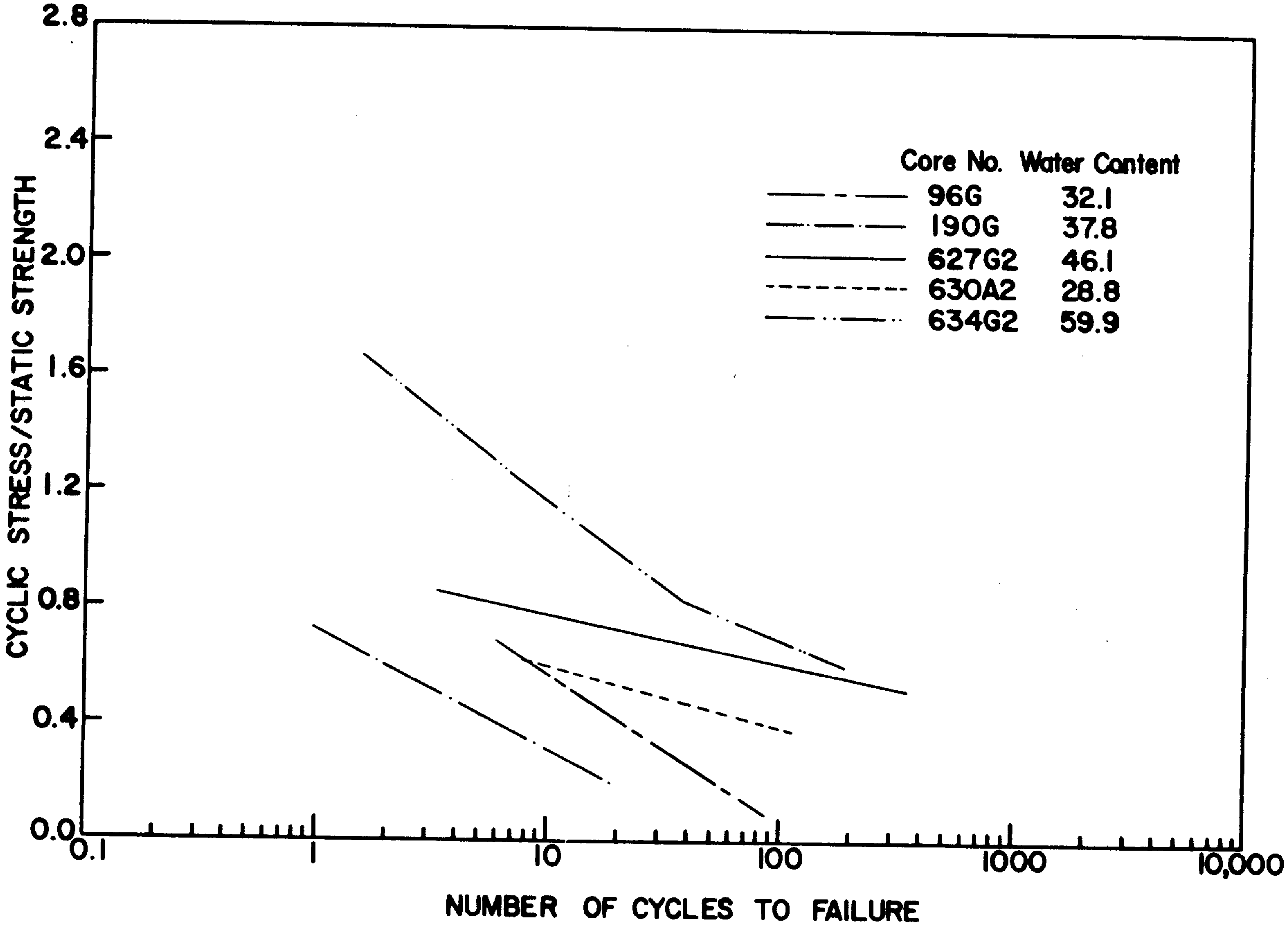

Figure 47. Relative cyclic stress level versus number of cycles to failure: Icy Bay-Malaspina Study Area (USGS testing), Method II.

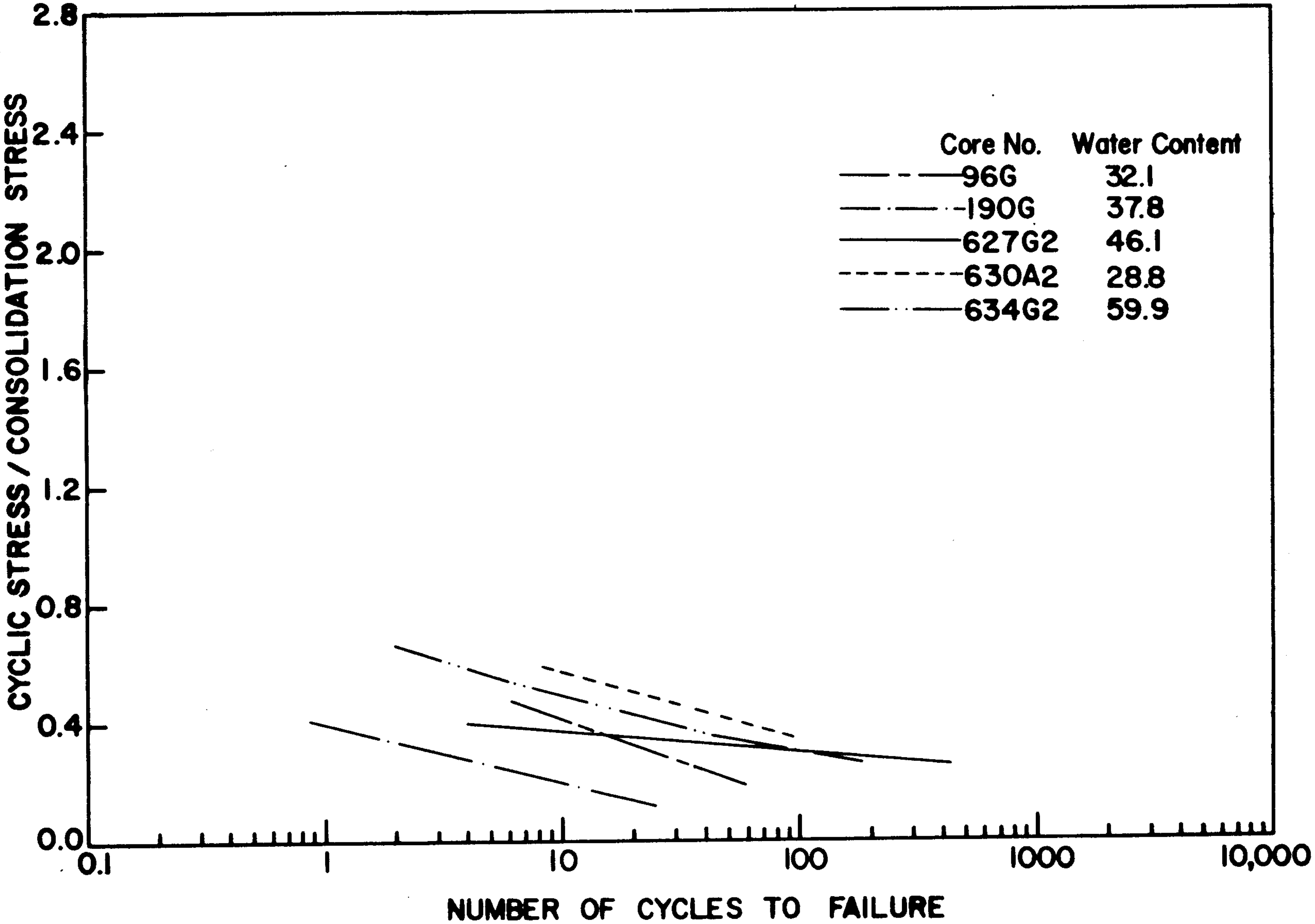

Figure 48. Relative cyclic stress level versus number of cyclics to failure: Icy Bay-Malaspina Study Area (USGS testing), Method III.

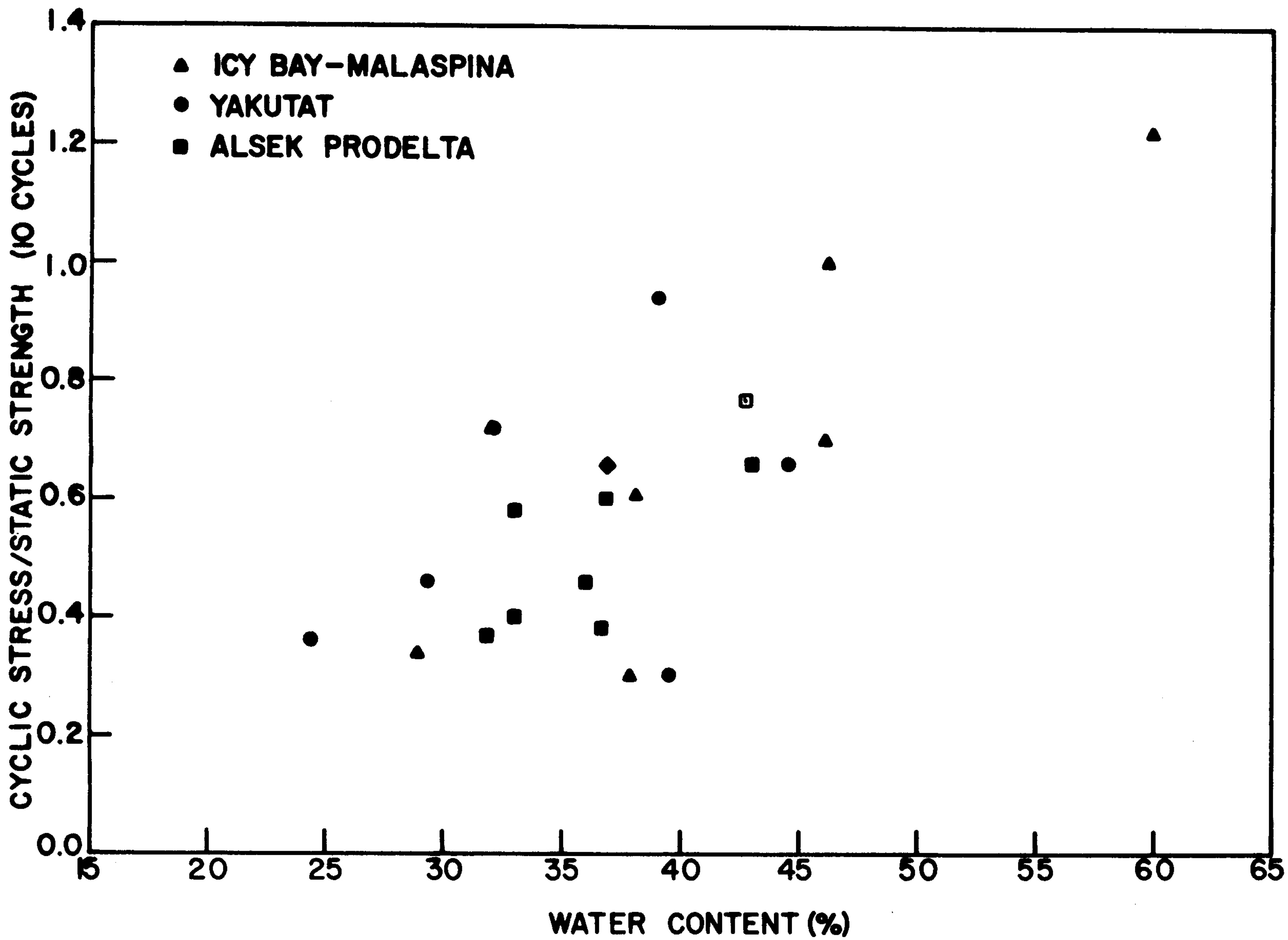

Figure 49. Relative cyclic stress level for failure in 10 cycles versus natural water content, Method I.

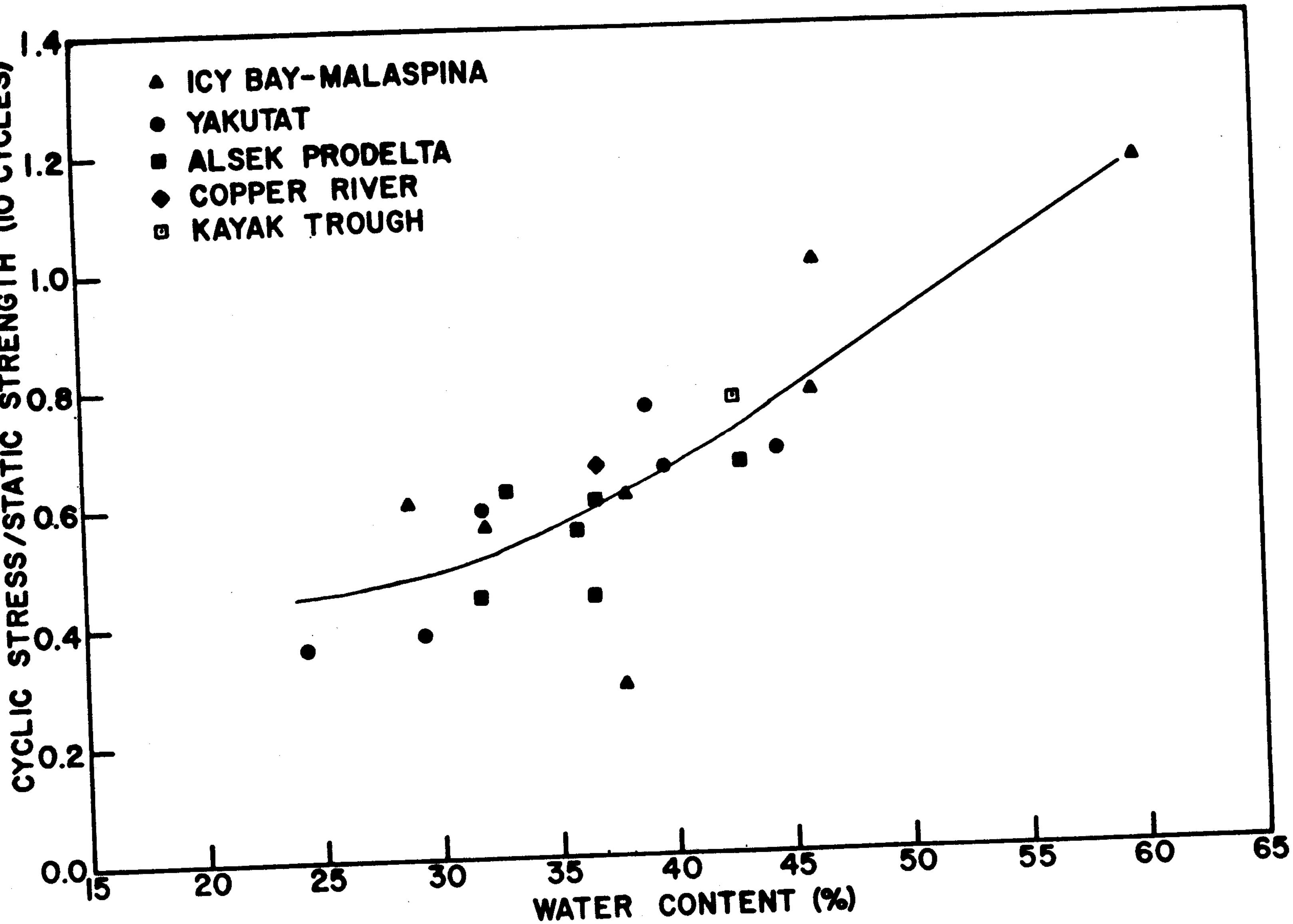

Figure 50. Relative cyclic stress level for failure in 10 cycles versus natural water content, Method II.

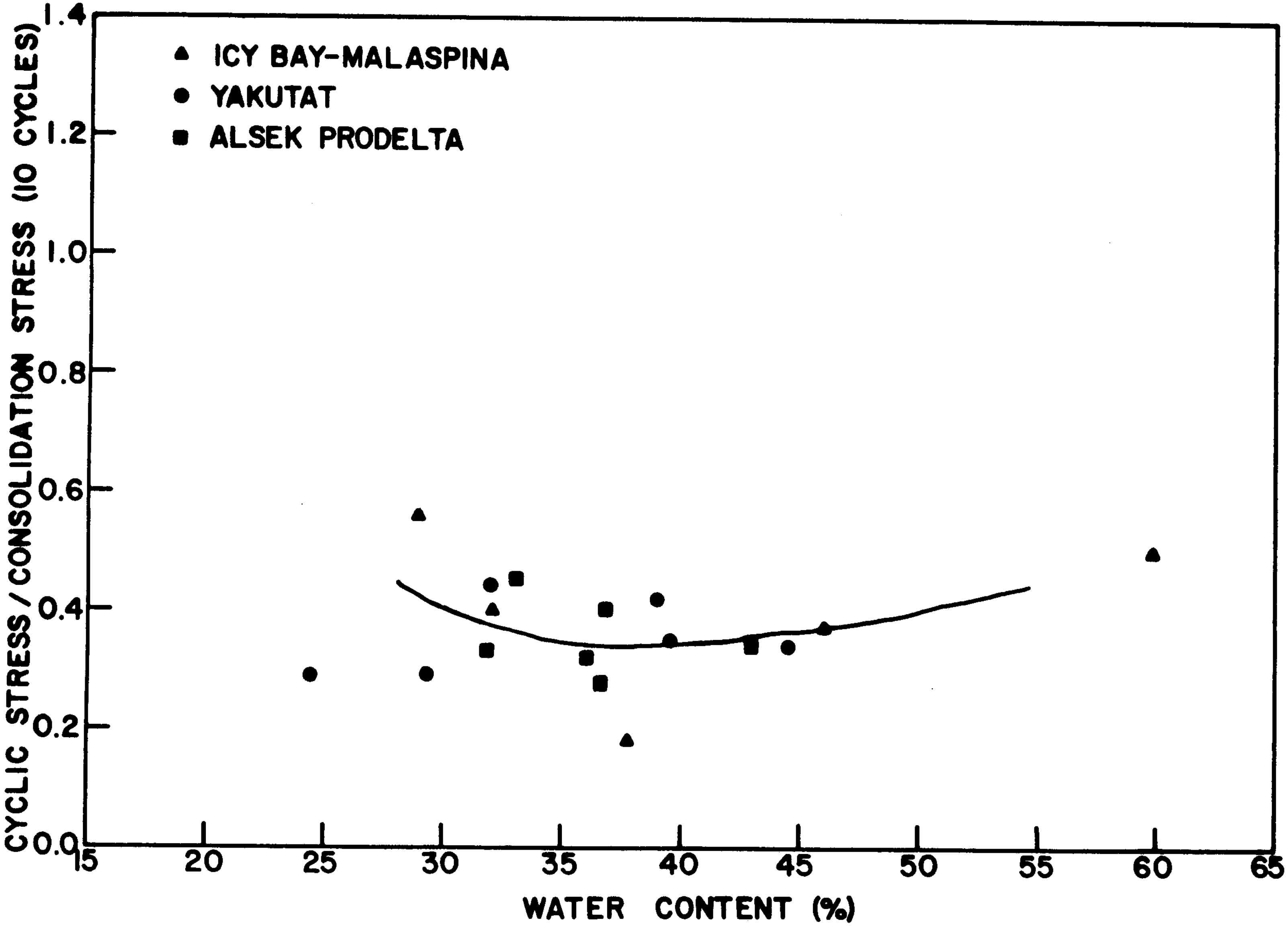

Figure 51. Relative cyclic stress level for failure in 10 cycles versus natural water content, Method III.

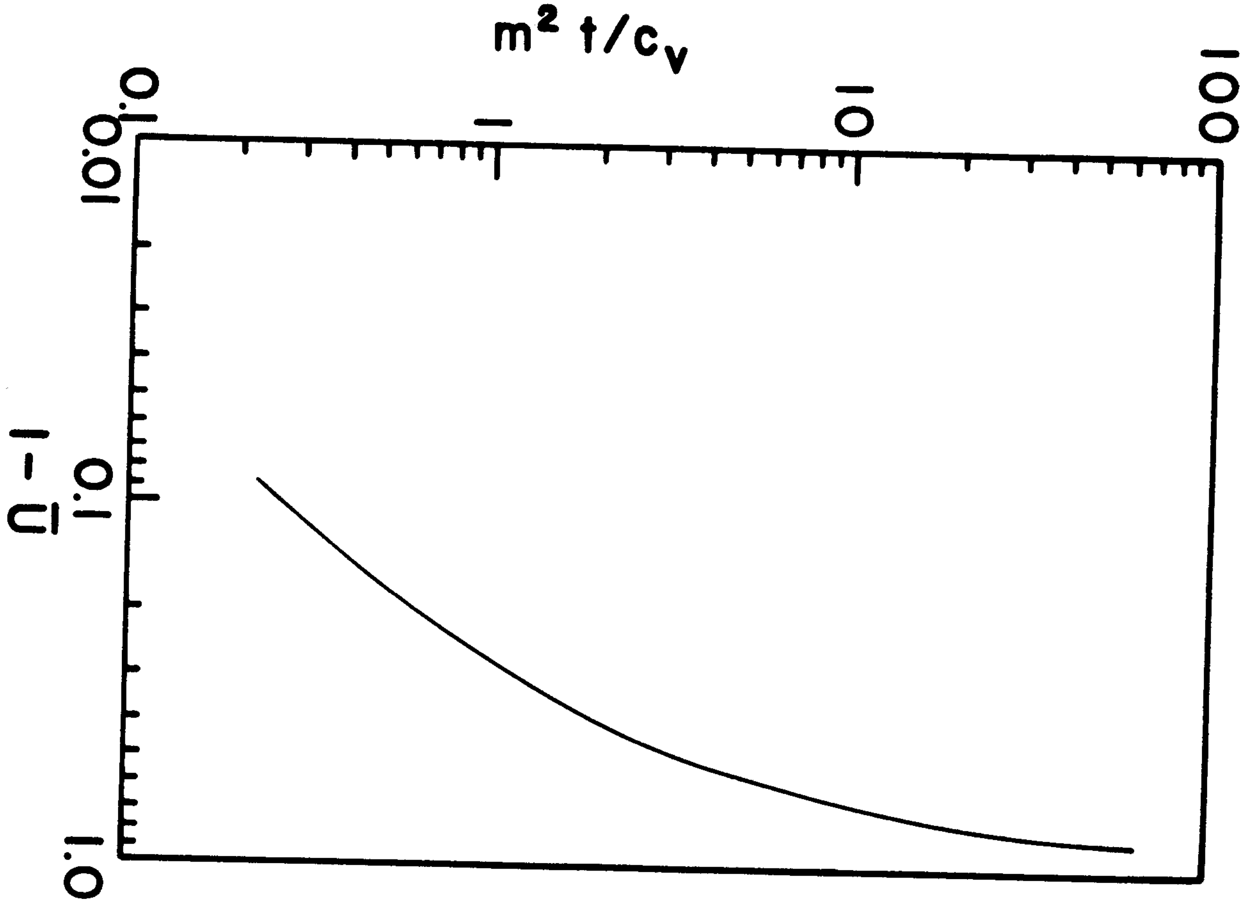

Figure 52. Predicted degree of consolidation (U) at the base of a sediment column that has been deposited at a steady rate, m, for t years (after Gibson, 1958).

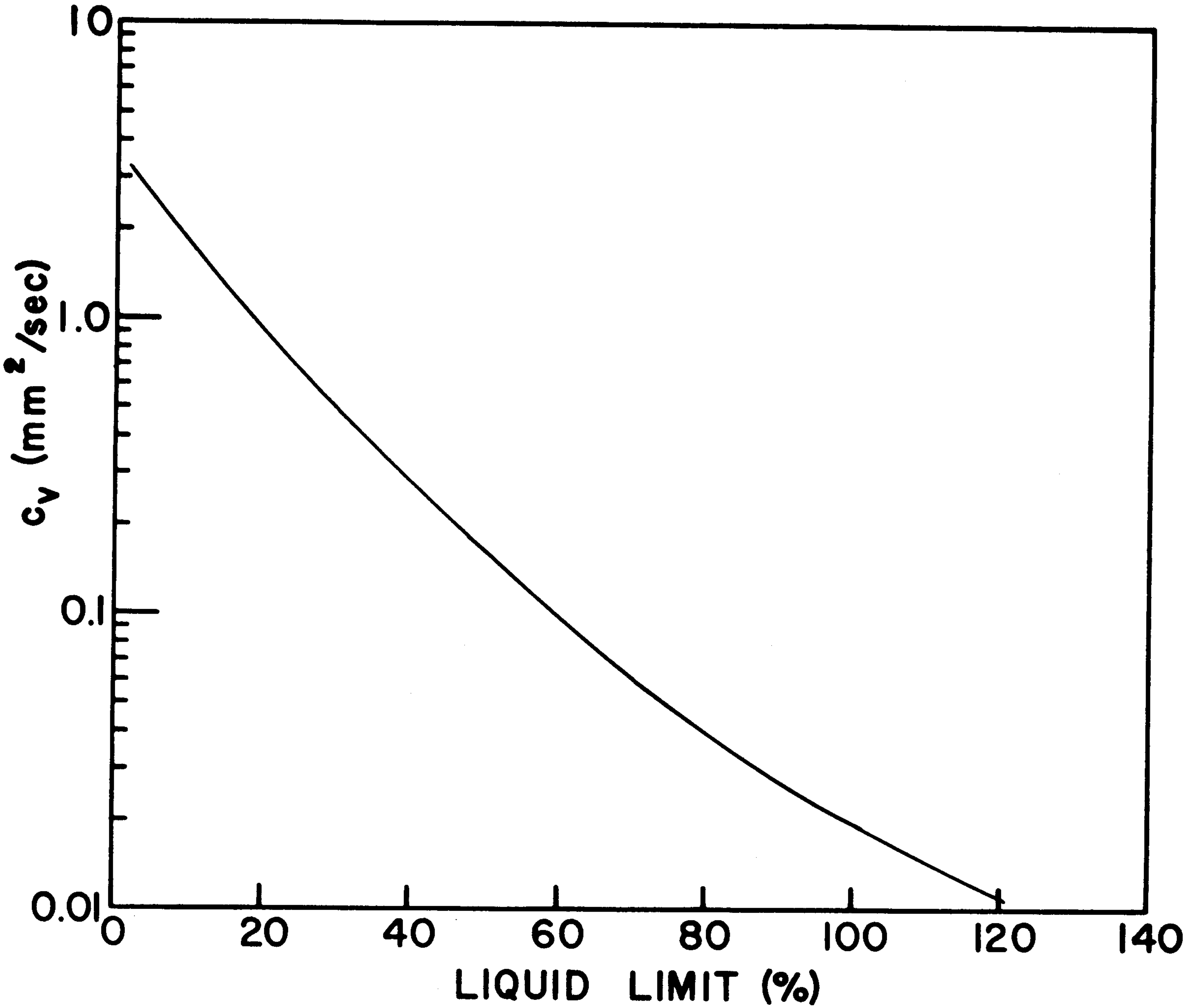

Figure 53. Correlation between coefficient of consolidation (c_v) and liquid limit (after Lambe and Whitman, 1969, p. 412).

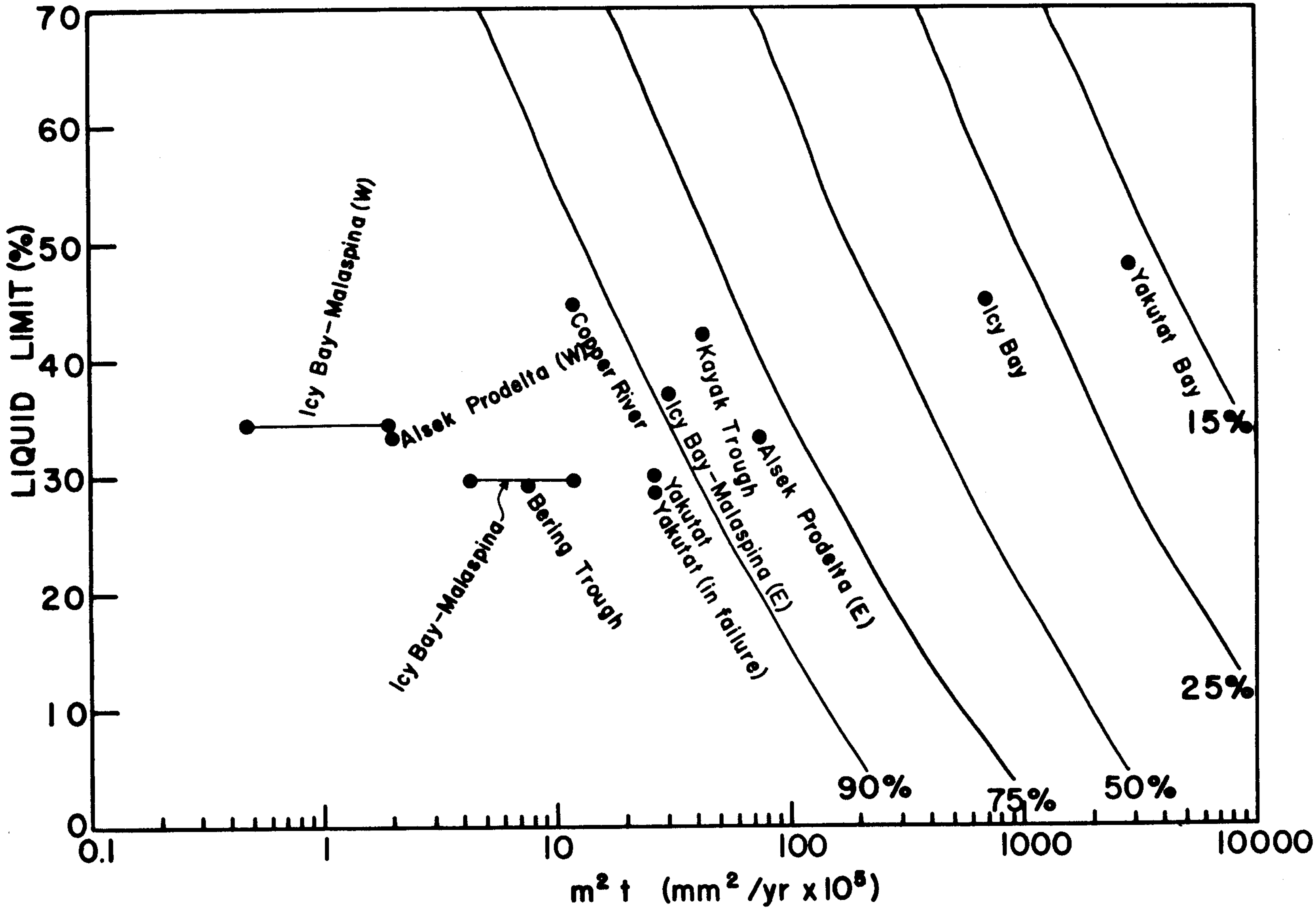

Figure 54. Solid lines represent constant degrees of consolidation, U, predicted by the Gibson (1958) technique. Selected locations in the eastern Gulf of Alaska for which the required parameters were available are shown as data points. Bars indicate a larger segment over which the sedimentation rate varies.

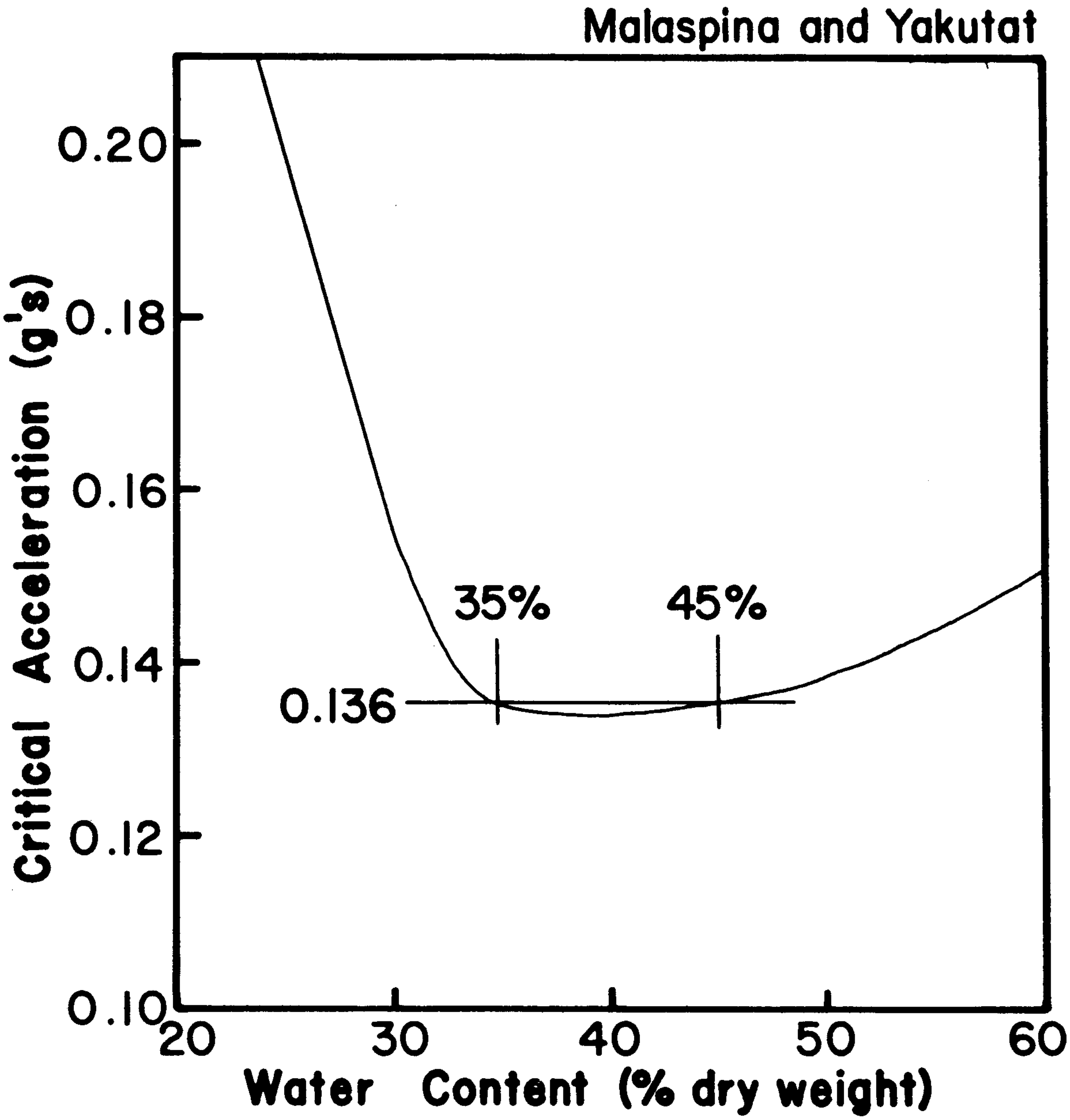

Figure 55. Estimate of critical earthquake acceleration, k, versus natural water content.

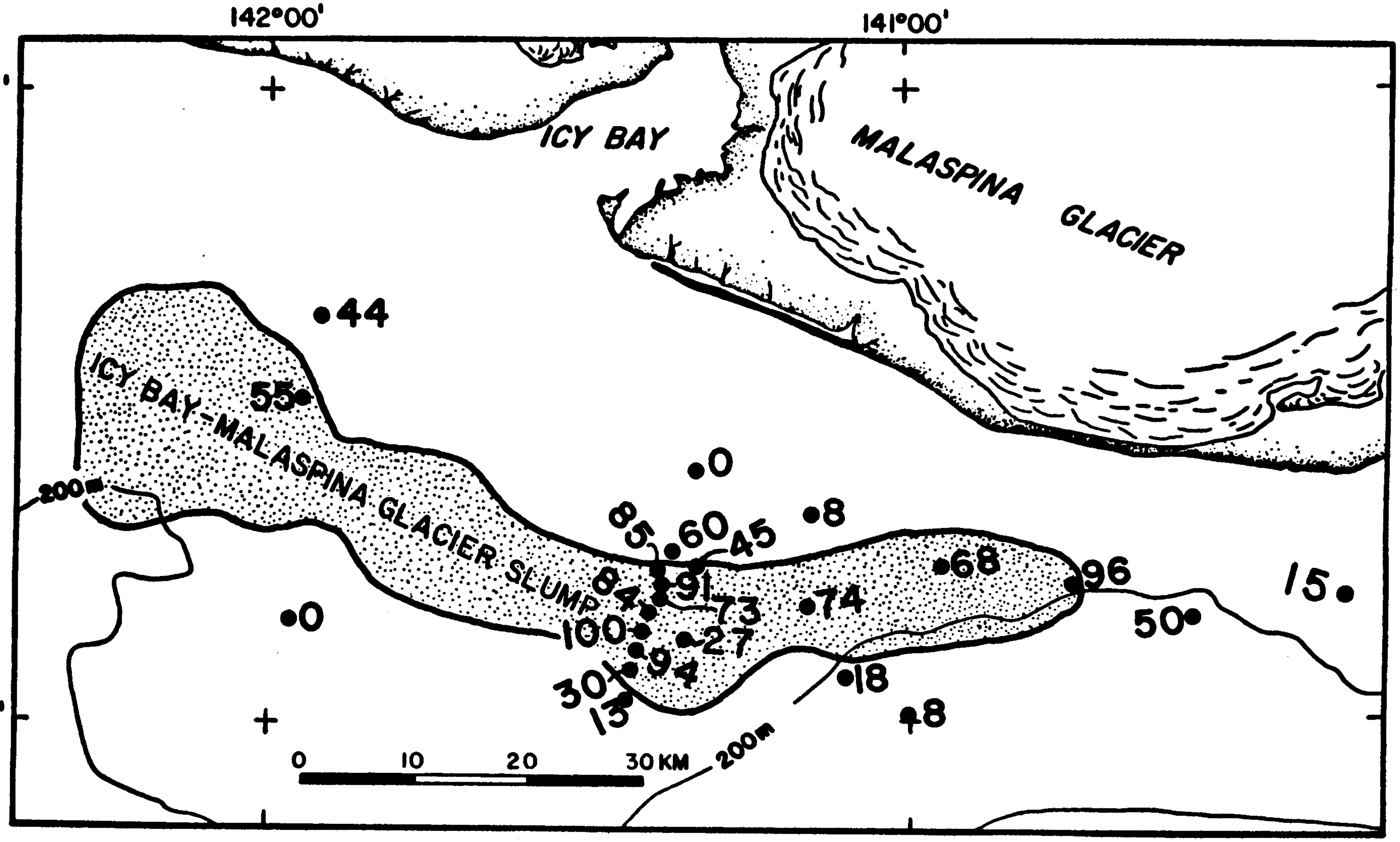

% Of Core With 35 < Water Content < 45

Figure 56. Locations of core samples within the Icy Bay-Malaspina Study Area relative to the observed slump feature. Numbers near the core locations represent the percentage of the core that has a water content in the critical 35% to 45% range.

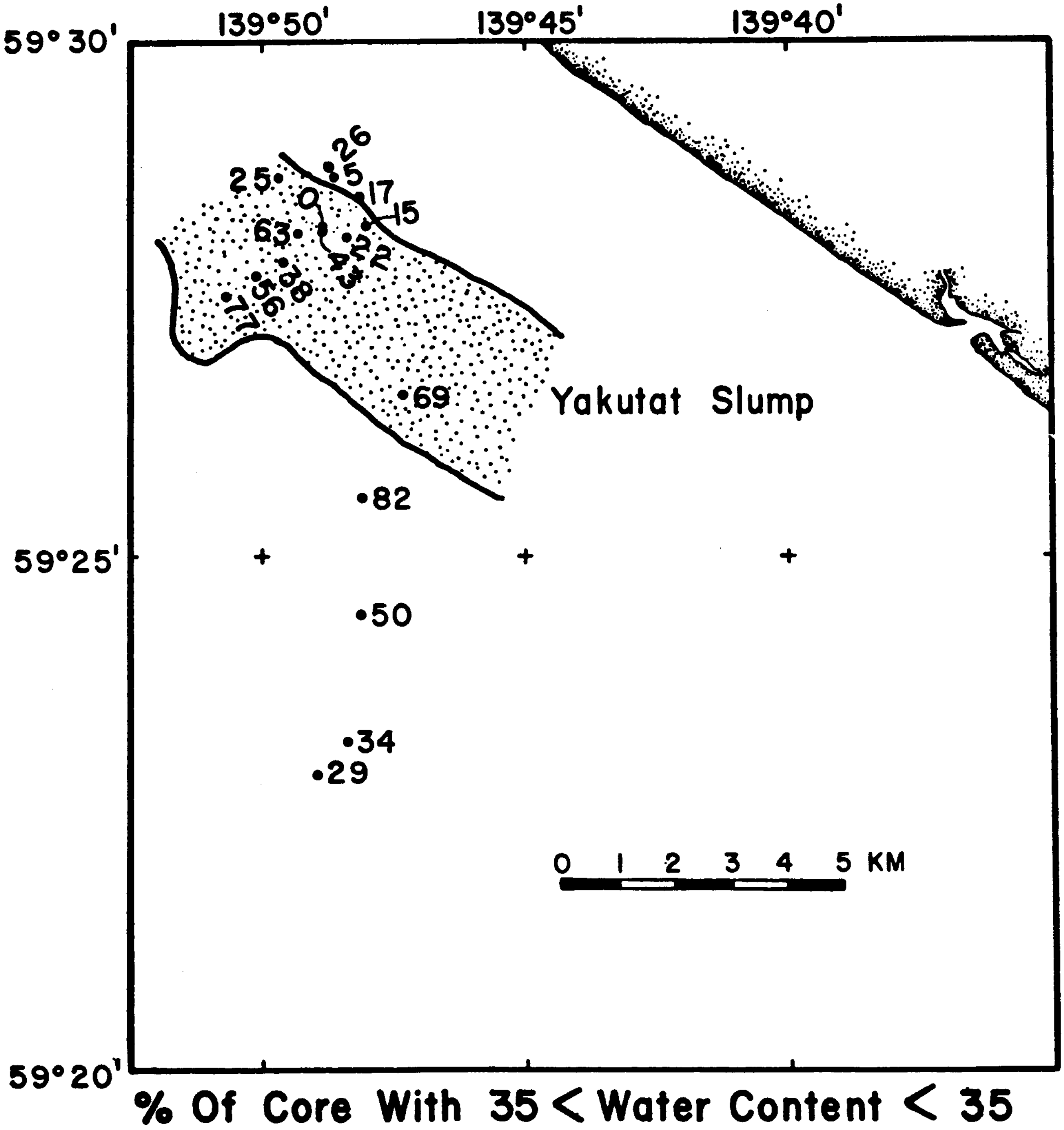

Figure 57. Locations of core samples within the Yakutat Study Area relative to the observed slump feature. Numbers near the core locations represent the percentage of the core that has a water content in the critical 35% to 45% range.

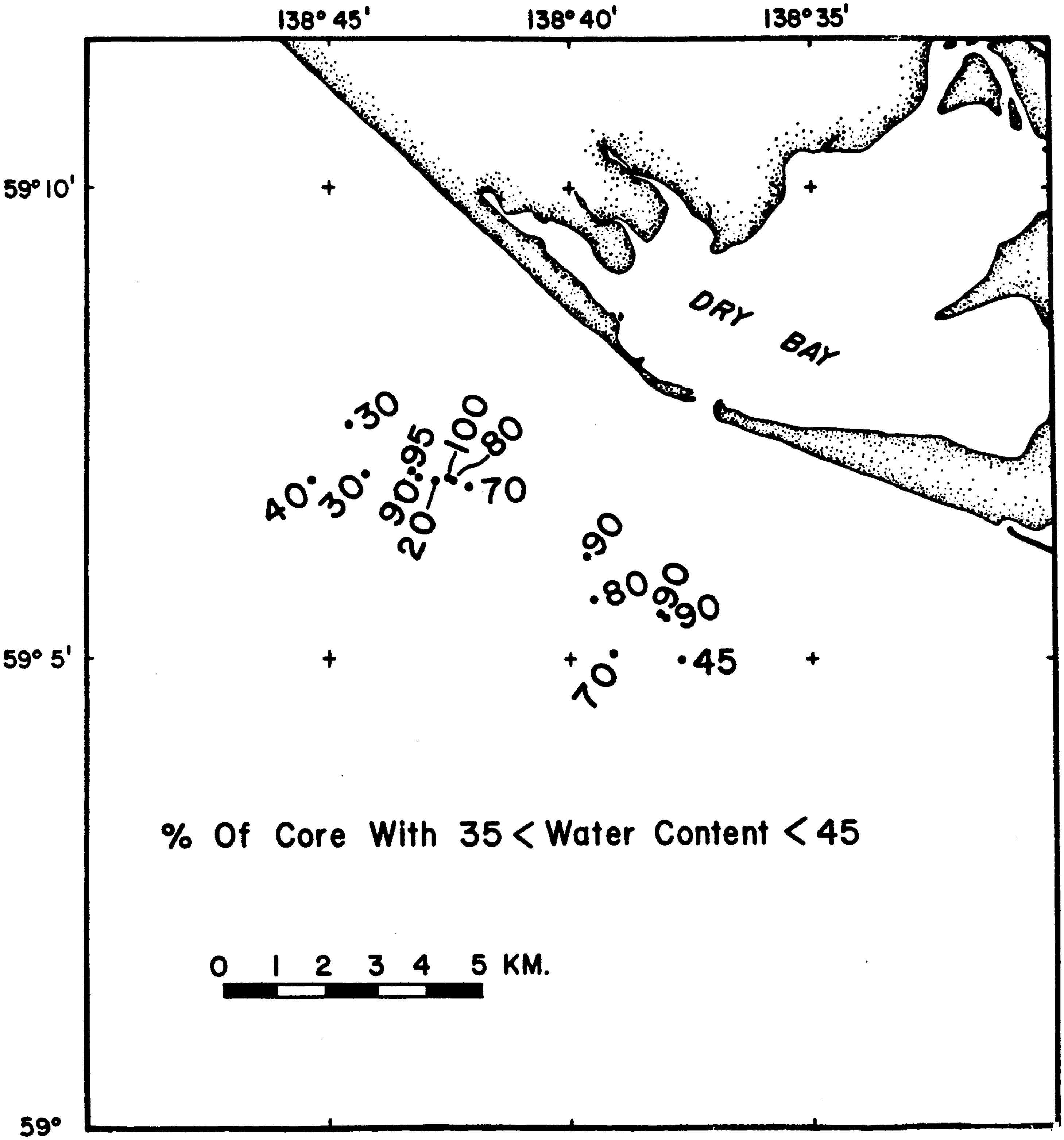

Figure 58. Locations of core samples within the Alsek River Study Area. Numbers near the core locations represent the percentage of the core that has a water content in the critical 35% to 45% range. All cores are thought to be in the failed zone.

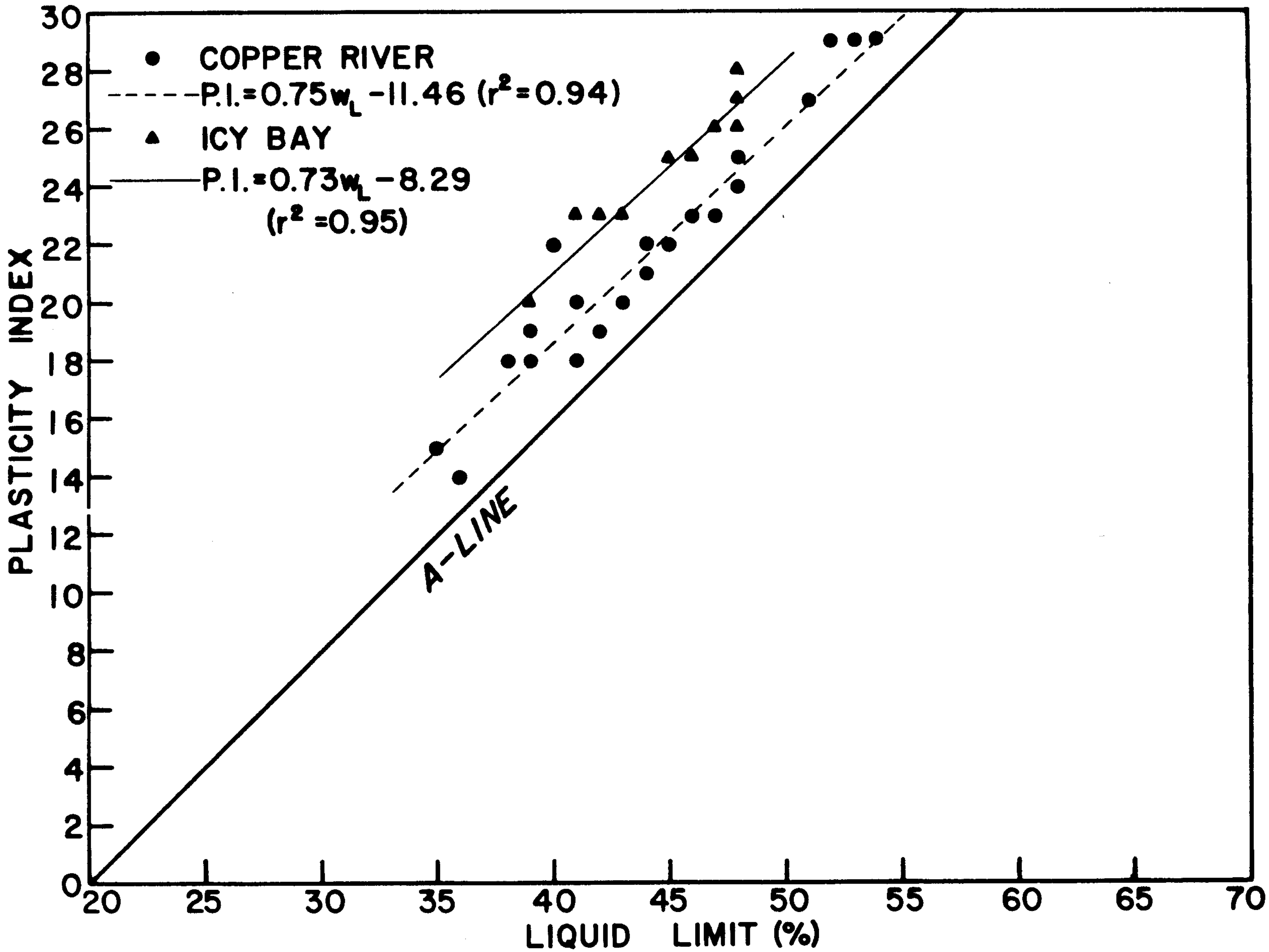

Figure 59. Plasticity chart for Copper River and Icy Bay Study Areas with least squares regression fits of the data.

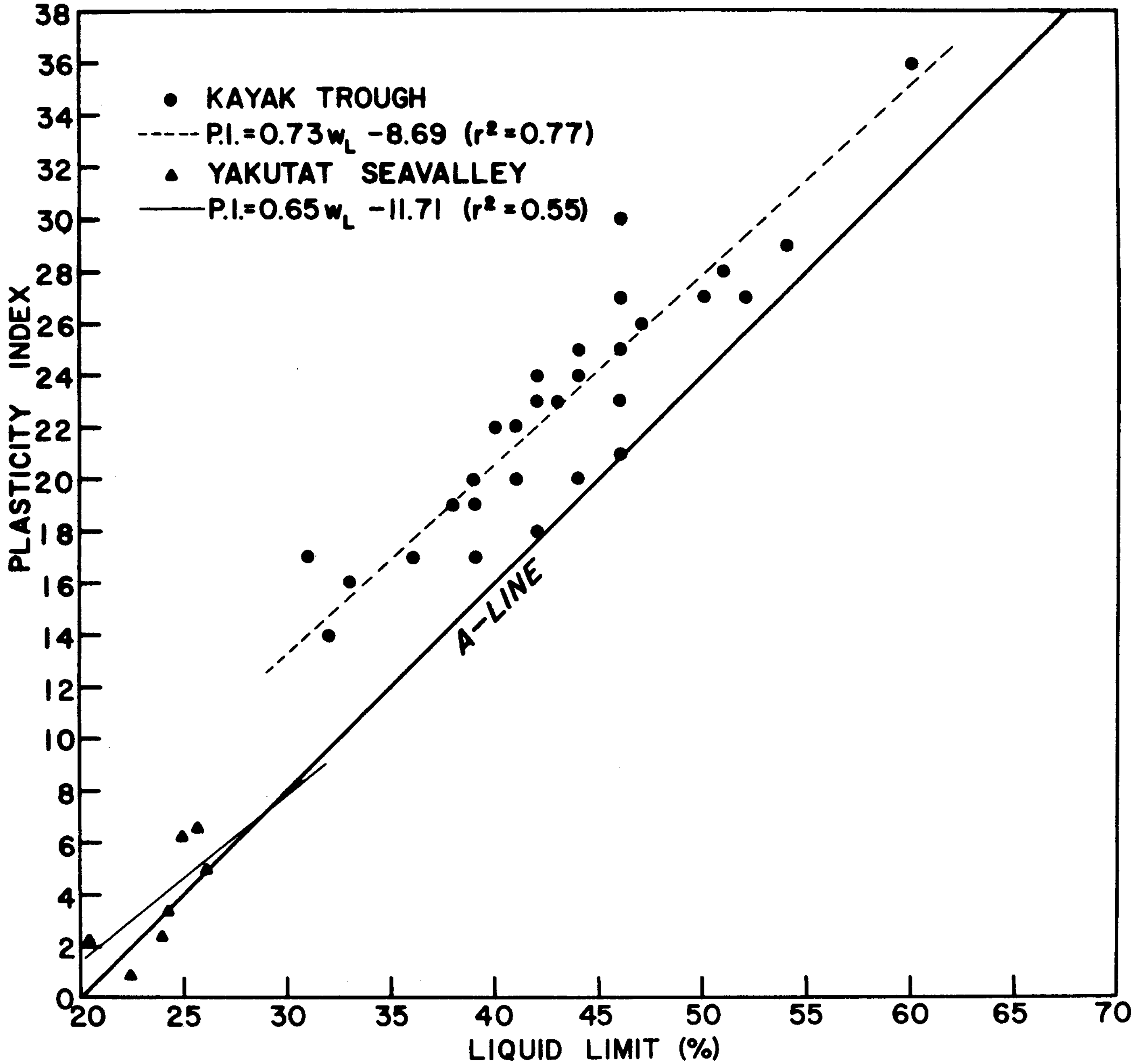

Figure 60. Plasticity chart for Kayak Trough Study Area and Yakutat Sea Valley (SE portion of Icy Bay-Malaspina Study Area) with least squares regression fits of data.

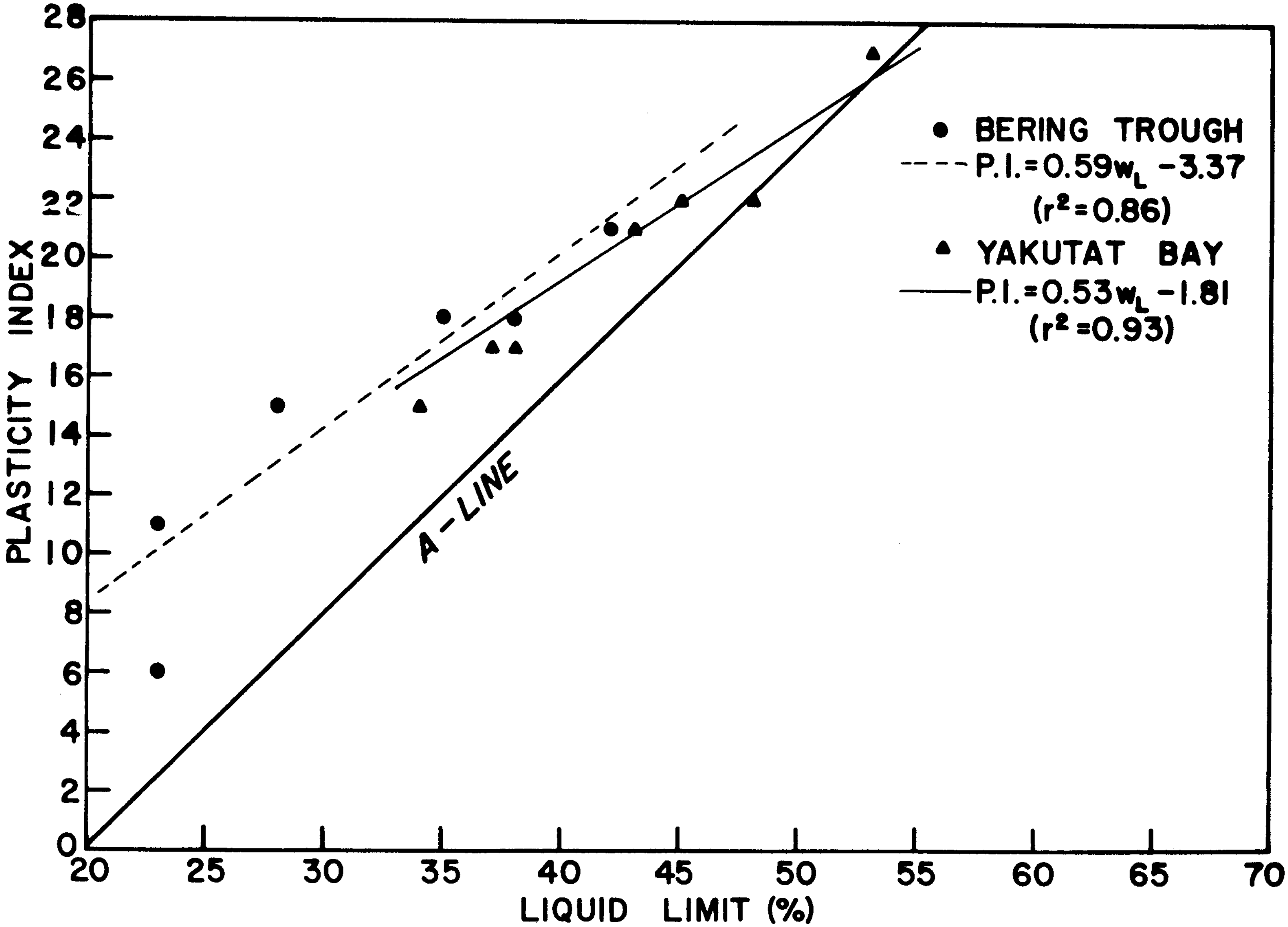

Figure 61. Plasticity chart for Bering Trough and Yakutat Bay Study Areas with least squares regression fits of data.

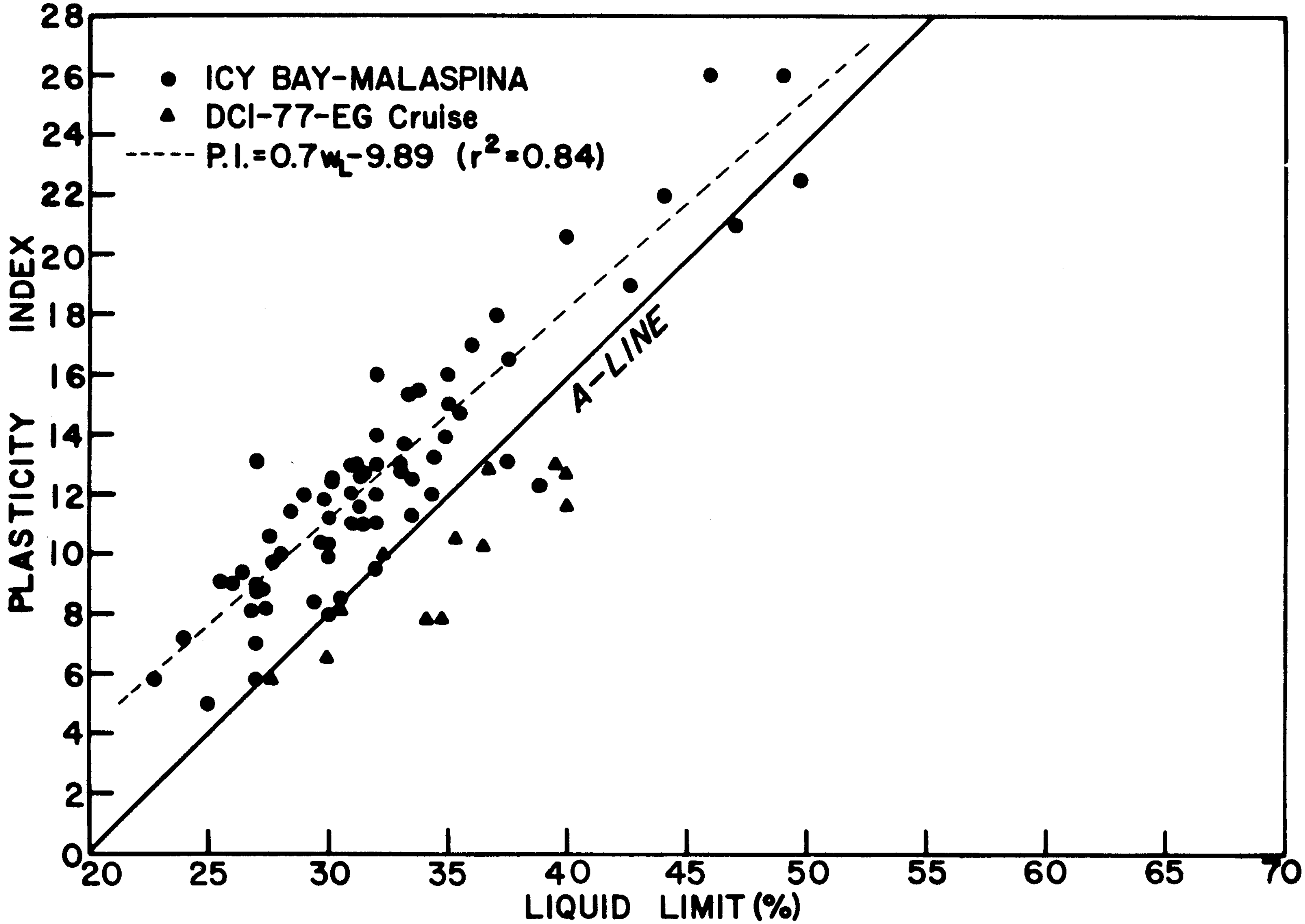

Figure 62. Plasticity chart for Icy Bay-Malaspina Study Area with least squares regression fit of the data (not including Cruise DC1-77-EG data).

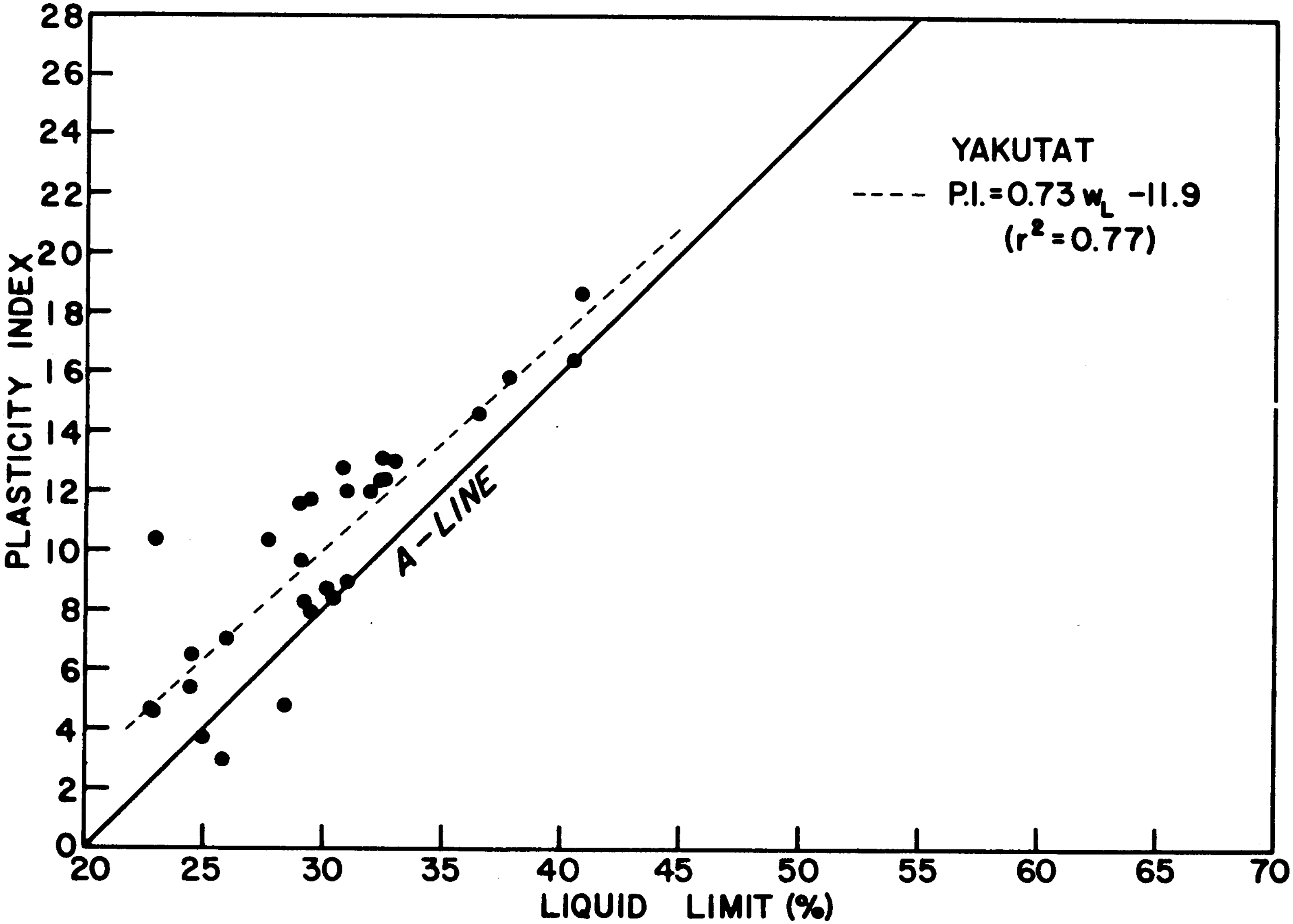

Figure 63. Plasticity chart for Yakutat Study Area with least squares regression fit of data.

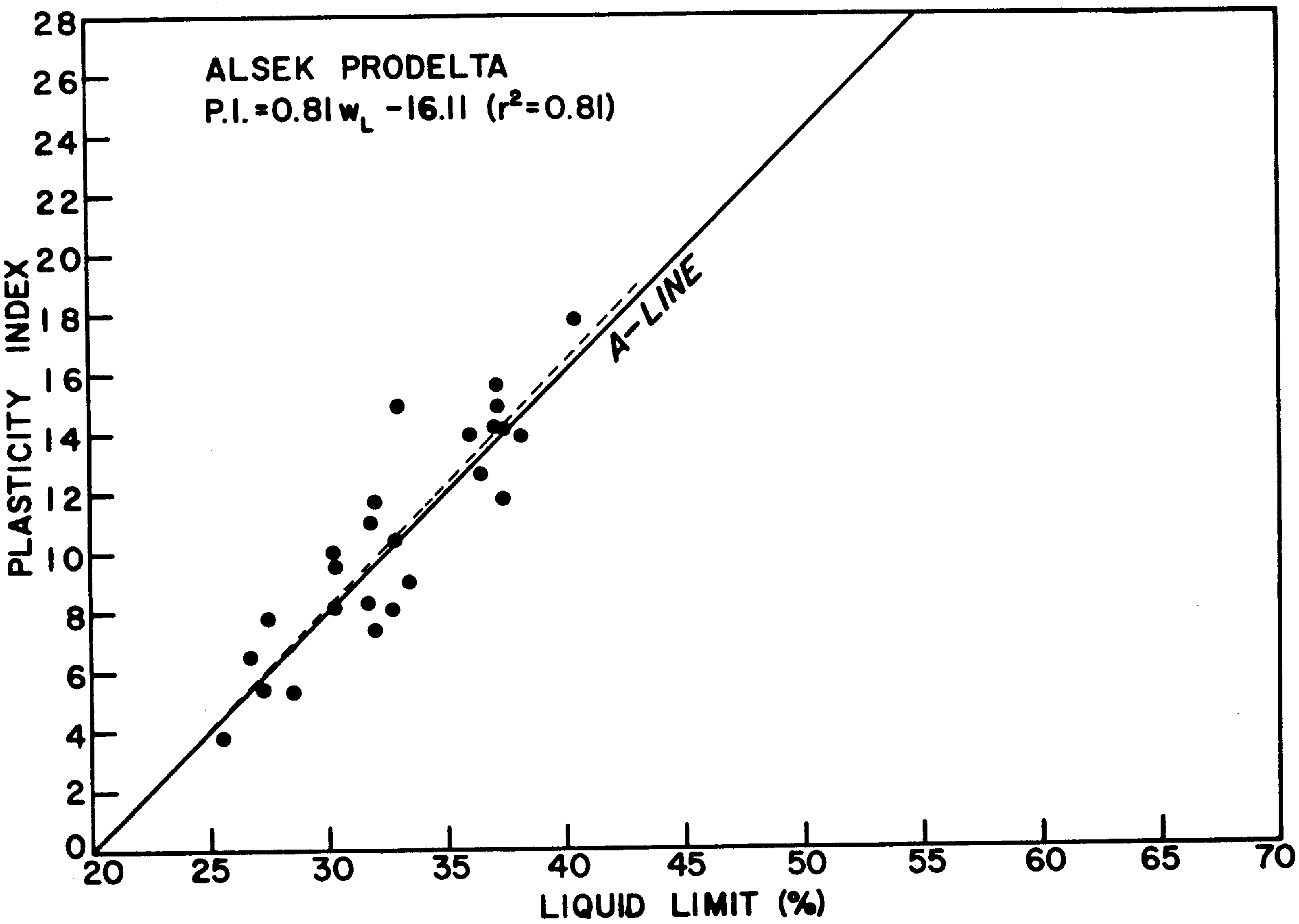

Figure 64. Plasticity chart for Alsek River Study Area with least squares regression fit of data.

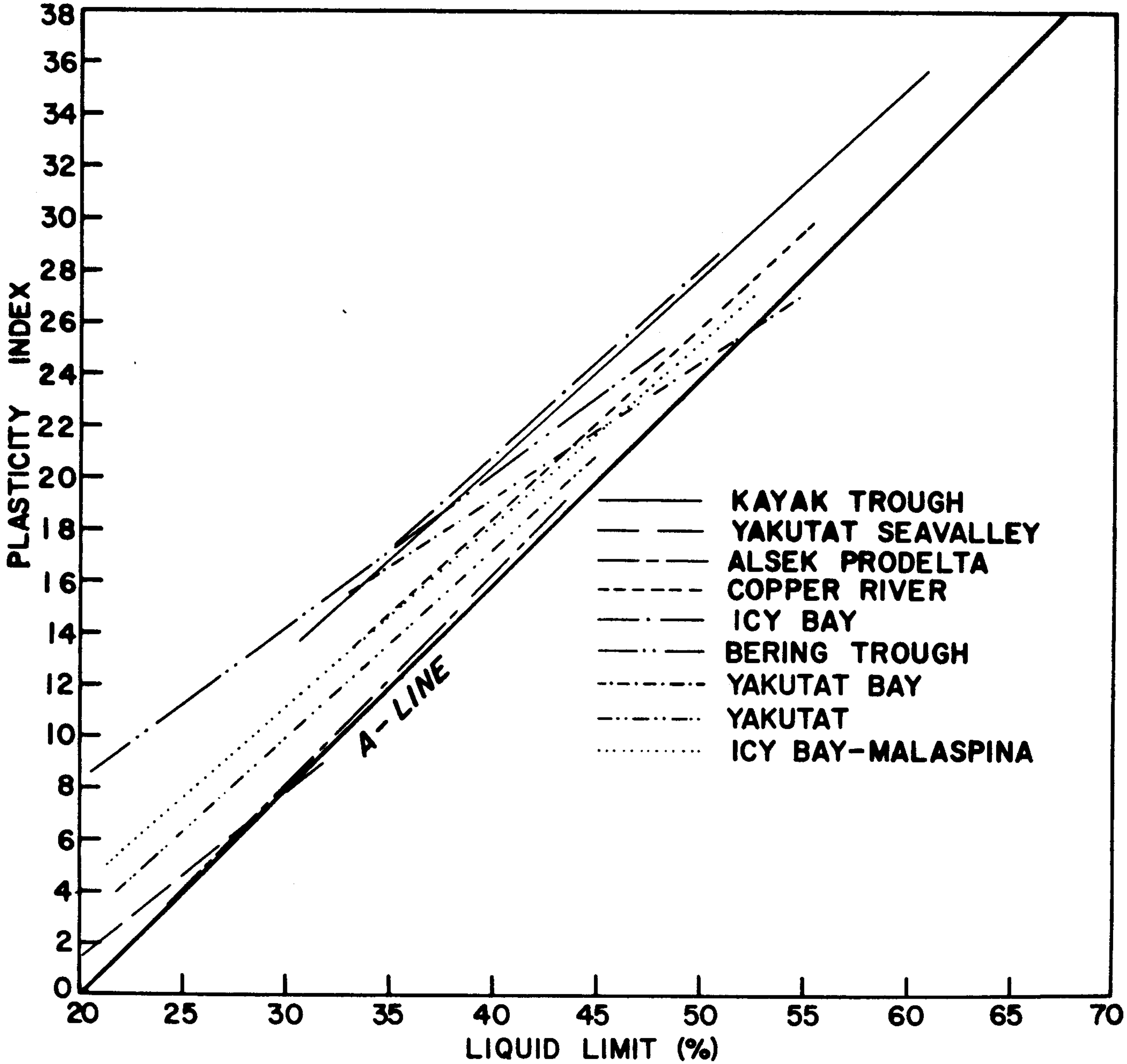

Figure 65. Summary of linear regression fits of plasticity data for the various study areas.

APPENDIX A

METHANE IN SEDIMENTS OF THE EASTERN GULF OF ALASKA

by

Marge Golan-Bac
Keith A. Kvenvolden

Because the presence of interstitial gas may have a significant effect on the stability of sediment, analysis of gas contents can be an important part of an overall hazards evaluation of an area. Accordingly, hydrocarbon gas data from four cruises in the eastern Gulf of Alaska (S1-76-EG, S8-77-EG, S6-78-EG, and S11-79-EG) may be applied to this investigation. Although the gases methane, ethane, ethene, propane, propene, iso-butane, and n-butane were analyzed, this discussion is limited to the concentrations and distributions of methane. It is the only hydrocarbon gas present in concentrations that may exceed its saturation level in the interstitial water.

During the S1-76-EG cruise, 15 samples from 12 stations were taken from Van Veen samples and gravity cores that covered a large area of the eastern Gulf of Alaska, from off the western end of the Copper River Delta to the western end of Palma Bay (geographic locations shown in Fig. 1 of the main text). Methane values ranged from the detection level to approximately 60 µl/l wet sediment. Note that these and other gas concentration values reported in this appendix are sample concentrations. The actual gas concentrations in place are probably higher. The highest concentration was found at Station 665 near the mouth of the Copper River. The next highest concentrations (approximately 30 and 40 µl/l) were at stations 658 and 659 respectively, east of the southern end of Kayak Island. Discontinuous seismic reflectors and turbid seismic returns were found in this area, suggesting that the sediments are gas-charged. The gas concentrations, although among the highest measured during this cruise, are well below saturation level (which is about 40,000 µl/l at atmospheric pressure): free gas is probably not present in the sediment. During the 1977 cruise, samples taken near these stations measured much higher concentrations of methane as discussed below. At Station 661 in the Kayak Trough Slump the methane concentration was approximately 30 µl/l. All other samples from the 1976 cruise had methane concentrations less than 10 µl/l.

The S8-77-EG cruise concentrated on recovering samples from specific geologic features located in an area from off the east coast of Montague Island to Yakutat Bay. The specific areas involved, from west to east, were: the Hinchinbrook Sea Valley, east of Montague Island; a slump in the Egg Island Trough, southwest of the Copper River Delta; a slump mass in the Kayak Trough, southeast of the Copper River Delta; a zone of faulting southeast of Kayak Island; the Bering trough, off the Bering Glacier; a large slump southwest of Icy Bay; Icy Bay; a slump off the western edge of Malaspina Glacier; Yakutat Bay. Sixty samples from 23 stations were obtained from gravity, piston and hydroplastic cores. Methane values ranged from 0.8 to 19,000 µl/l wet sediment. Most concentrations were equal to or exceeded by a factor of 2 the four highest concentrations measured during the 1976 cruise. Core 14G in the Kayak Trough Slump and Cores 36G and 38G from the Bering Trough had higher concentrations (180, 380. and 180 µl/l, respectively) than other cores in this particular area. The concentrations of methane from these samples were not high enough to indicate gas-charged sediment in place, however. At these stations the sediment may have larger concentrations of methane at depth. Core 23G from the zone of faulting southeast of Kayak Island had anomalously high concentrations of methane. This core was taken in the same area as those cores from stations 658 and 659 from the S1-76-EG cruise. However, the concentrations obtained from Core 23G were 2,100 µl/l at the surface and 14,000 µl/l at the 100 cm depth. The latter concentration begins to approach the solubility of methane in water at atmospheric conditions. Because these laboratory values represent a lower bound for the in place concentrations, the concentration of methane at this station in place may in fact have reached or exceeded its solubility. These anomalously high methane values correlate with acoustic anomalies attributed to gas-charged sediments; the presence of gas may affect the stability of the sediment southeast of Kayak Island.

The S6-78-EG cruise recovered 17 samples from Van Veen samplers and gravity cores. The area covered included 5 main localities: Icy Bay and a slump off the western edge of the Malaspina Glacier, both areas covered during the S8-79-EG cruise; off the Dangerous River and just east of Dry Bay, both areas which were later covered during the S11-79-EG cruise; and an area beyond the 200 m bathymetric contour situated southwest of Lituya Bay, that was not sampled during any other cruise. These methane values ranged from about 1 to 48 μl/l wet sediment from sediments up to a depth of 296 cm. Core 13A in Icy Bay represents the upper limit of this range and is similar to the concentrantions obtained in 1977. Four cores (8A, 8B, 9B, and 12B) from off the western edge of Malaspina Glacier ranged from 21 to 40 μl/l wet sediment, which is also similar to the concentrations obtained in the 1977 cruise. Three cores off the Dangerous River (3, 4, and 5) had low concentrations of methane, averaging 1.4 μl/l wet sediment. The S11-79-EG cruise the next year confirmed these low concentration levels in 4 cores (3, 5, 6, and 26) which averaged 7.0 μl/l wet sediment. Core 1 just east of Dry Bay indicated a very low concentration of methane (1.4 μl/l) similar to 7 of 8 cores taken in that area on the S11-79-EG cruise. The concentrations averaged 12 μl/l wet sediment. Two cores (10A and 11A) were taken beyond the 200 m bathymetric level southwest of Lituya Bay and averaged 3.0 μl/l wet sediment.

The S11-79-EG cruise concentrated on 3 main localities: off the Dangerous River, off Dry Bay and just east of Dry Bay. Thirty-seven samples were obtained from 17 vibracores and gravity cores. Methane concentrations ranged from just detectable to 33,000 μl/l. In eight cores (1, 2, 11, 16, 20, 21, 26 and 30) the amount of methane was greater than 10 but less than 64 μl/l, a range of values similar to those observed on the S1-76-EG and S6-78-EG cruises. Except for one core the methane concentrations at the other stations were less than 10 μl/l. Core 14 at a site just east of Dry Bay was anomalous. At the 80-90 cm depth interval, the concentration of methane was approximately 32,800 μl/l wet sediment, a value which nearly equals the solubility of methane in the interstitial water at atmospheric conditions. This high concentration of methane may indicate gas-charging which would affect the stability of the sediments.

Anomalously high concentrations of methane suggesting the presence of gas-charged and, therefore, unstable sediments, were found in only two areas: a fault zone southeast of Kayak Island and east of Dry Bay. Sediments from near the mouth of the Copper River, from the Kayak Trough, and from east of Kayak Island had significant amounts of methane, but the amount measured was insufficient to indicate that the sediments in place were, indeed, gas-charged. Deeper sediments in the area may be gas-charged, however. There appears to be no good correlation between the occurrence of seismic anomalies and the possible presence of sampled gas-charged sediment except for the sediment southwest of Kayak Island.

Methane in Sediments of the Eastern Gulf of Alaska-Sample Locations.

Cruise	Sample or station	Latitude	Longitude
S1-76-EG	658B	59°47.19'N	144°28.83'W
	659B	59°49.40'N	144°28.03'W
	661	60°06.20'N	144°40.30'W
	665	60°08.20'N	145°00.00'W
S8-77-EG	14G	60°05.12'N	144°40.44'W
	23G	59°50.75'N	144°24.26'W
	36G	59°56.64'N	143°35.75'W
	38G	59°58.05'N	143°38.00'W
S6-78-EG	1	59°02.70'N	138°22.80'W
	3	59°17.70'N	139°16.60'W
	4	59°17.35'N	139°15.90'W
	5	59°16.95'N	139°14.30'W
	8A	59°36.50'N	140°55.50'W
	8B	59°36.20'N	140°56.00'W
	9B	59°37.40'N	140°55.70'W
	10A	57°55.01'N	138°04.89'W
	11A	57°55.36'N	138°04.19'W
	12B	59°36.80'N	140°55.80'W
	13A	59°55.97'N	141°32.27'W
S11-79-EG	1	59°06.08'N	138°42.36'W
	2	59°06.00'N	138°42.17'W
	3	59°16.33'N	139°12.29'W
	5	59°17.49'N	139°16.10'W
	6	59°17.74'N	139°17.31'W
	11	59°03.53'N	138°25.32'W
	14	59°02.21'N	138°25.50'W
	16	59°05.95'N	138°38.97'W
	20	59°05.81'N	138°42.01'W
	21	59°02.45'N	138°25.38'W
	26	59°17.27'N	139°16.03'W
	30	58°59.84'N	138°43.51'W

APPENDIX B

RELATIVE IMPORTANCE OF SEISMIC AND STORM WAVE LOADING

The Gulf of Alaska is susceptible to both high seismicity (Stephens and Page, 1982) and large storm waves (Bea, 1976). This appendix provides a brief discussion of the factors influencing cyclic loading dominance and develops a quantitative estimate of the water depth separating storm wave and earthquake control.

One way of separating earthquake and wave control is to determine the water depth at which the shearing stresses developed by peak storm waves equal the shearing stresses developed by a critical earthquake. Modifying Equation (2) from the main text for a horizontal bottom, we obtain:

$$\tau/\sigma_v'=k\gamma/\gamma' \quad \text{(B-1)}$$

where τ is the shearing stress generated by an earthquake with a critical acceleration, k.

As shown in the main text, the critical acceleration corresponding to many of the failure features (including the Icy Bay-Malaspina slump in water depths ranging from 75 to 175 m) is 0.136g (Figure 55). Assuming that failures in relative deep water are earthquake induced, this critical value of k can be used to estimate a representative level of shearing stress developed by major earthquakes in the area. For typical sediment densities (γ=1.8 g/cm^3 and γ'=0.8 g/cm^3), Equation (B-1) yields $\tau/\sigma_v'=0.306$ for major earthquakes.

Seed and Rahman (1978) provide the following equation for shearing stresses near the seafloor surface produced by large storm waves:

$$\tau/\sigma_v'=[\pi\gamma_w H]/[\cosh(2\pi d/L)\gamma' L] \quad \text{(B-2)}$$

where γ_w=unit weight of water
d=water depth
H=wave height
L=wave length

The maximum probable storm wave for the area (Bea, 1976) is 37 m, corresponding to a very limited number of waves. For a longer series of waves, we assumed 30 m as a more realistic maximum wave height. Because the solution is fairly independent of wave length, any reasonable choice of wave length is satisfactory. We assumed a representative value of 300 m. Inserting these values into Equation B-2 and solving for the water depth, d, necessary to produce shearing stresses comparable to those produced by earthquakes (τ/σ_v'=0.306 from Fig. 35 in the main text) yields a critical water depth of 35 m. Therefore, in water depths shallower than 35 m, major storms would produce shearing stresses greater than major earthquakes would induce. In greater water depths earthquakes would produce the greater stresses.

Equating stress levels does not completely determine the level at which the influence of major earthquakes and waves is equal. Waves produce a much larger number of critical cycles than earthquakes and would cause a greater level of strength degradation under completely undrained conditions. That is, waves might cause the same damage at a lower stress level than that produced by an earthquake. Judging by the extensive data base of Lee and Focht (1976), the strength degradation factor, A_D, might be reduced by up to 50% if 1000 cycles were considered rather than 10. Under fully undrained conditions and a major storm with 1000 cycles, the stress level required to cause the same damage as the representative major earthquake for the area would be only one-half as much as that induced by the earthquake. That is, a value of $\tau/\sigma_v'=(0.5)(0.306)=0.153$ would be needed. The water depth at which earthquakes and waves would cause the same level of damage would drop to 76 m, as calculated from Equation (B-2).

The 76 m level is the deepest for which storm waves and earthquakes could be equivalent. The water depth at which earthquakes and waves would cause the same level of failure is probably shallower because some drainage of pore pressures during a storm would be expected (Seed and Rahman, 1978). If enough drainage were to occur, the level of equivalence could even be shallower than the 35 m calculated for equivalent stresses. Because the glacial marine sediment is silty and drains fairly easily, the 35 m level is probably a good estimate of the depth of equivalent damage; the depth could drop to as deep as 76 m under special circumstances.

APPENDIX C

INDEX PROPERTIES

APPENDIX C. INDEX PROPERTIES

This Appendix presents downcore profiles of all the index property measurements. The profiles are organized by study area ordered from west to east. Within study areas the profiles are ordered by core number. The measurements include laboratory original and remolded vane shear strength, natural water content, liquid and plastic limits, grain density, and grain size (as percent sand, silt, and clay). Also shown are locations of consolidation or triaxial tests. The identification number indicates the type of test and the testing organization. The nature of these tests is indicated by a coded test number. The code for the test numbering system is as follows:

First two letters:
(a) OE - Oedometer test
(b) CE - Constant rate of strain (CRS) consolidation test
(c) TE - Static triaxial test
(d) TC - or D - Cyclic triaxial test

Trailing characters:
(a) No trailing characters - test performed by the USGS
(b) L1 - Test of 1977 core sample by Law Engineering and Testing Company
(c) G - Test of 1977 sample by Geotechnical Engineers, Incorporated
(d) B - Test of 1977 sample by University of California, Berkeley
(e) L2 - Test of 1980 sample by Law Engineering and Testing Company

These consolidation and triaxial test results are presented in Appendices D through G and are grouped according to the organization performing the test.

The water contents from Cruise DC1-77-EG (Carlson and others, 1978) appear to have been calculated incorrectly, possibly through a faulty computer program. The error is indicated in Figure 62 in which the Atterberg limits for DC1-77-EG plot in a distinctly different section of the plasticity chart from that in which the results of tests from other cruises to the same area plot. Because of this discrepancy, water contents from DC1-77-EG were not shown in Figure 56.

COPPER RIVER STUDY AREA

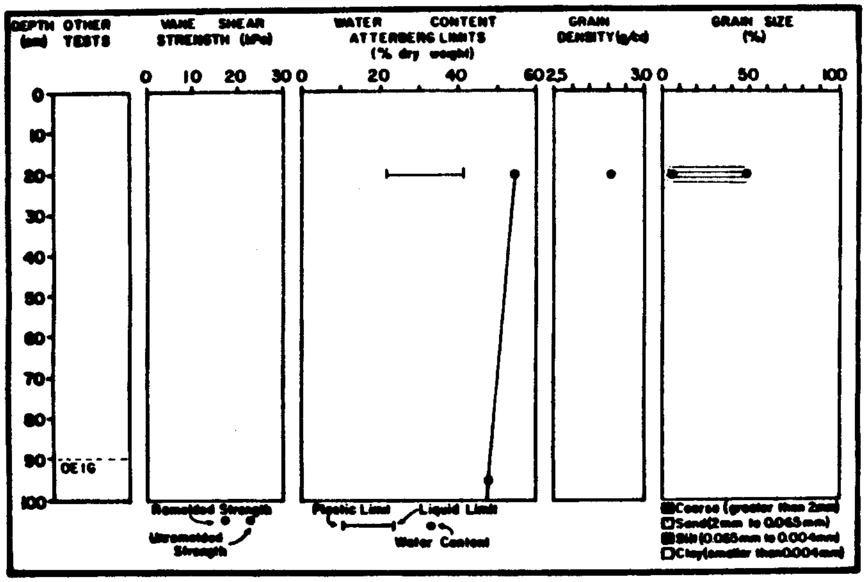

CRUISE: S8-77-EG CORE: 4G

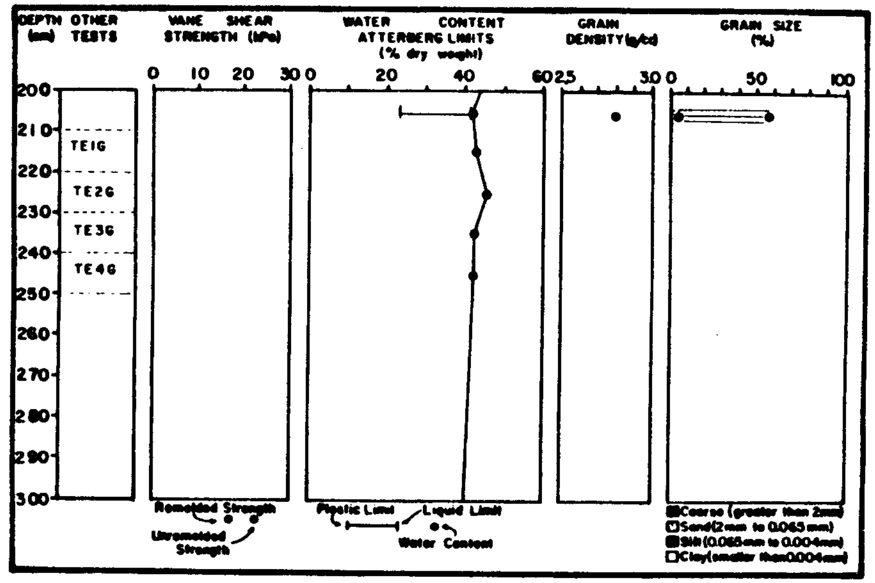

CRUISE: S8-77-EG CORE: 4G

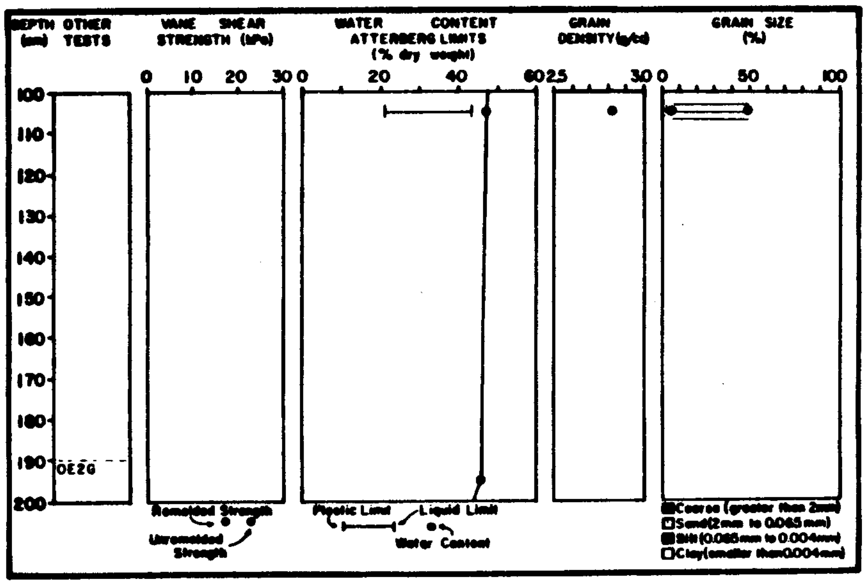

CRUISE: S8-77-EG CORE: 4G

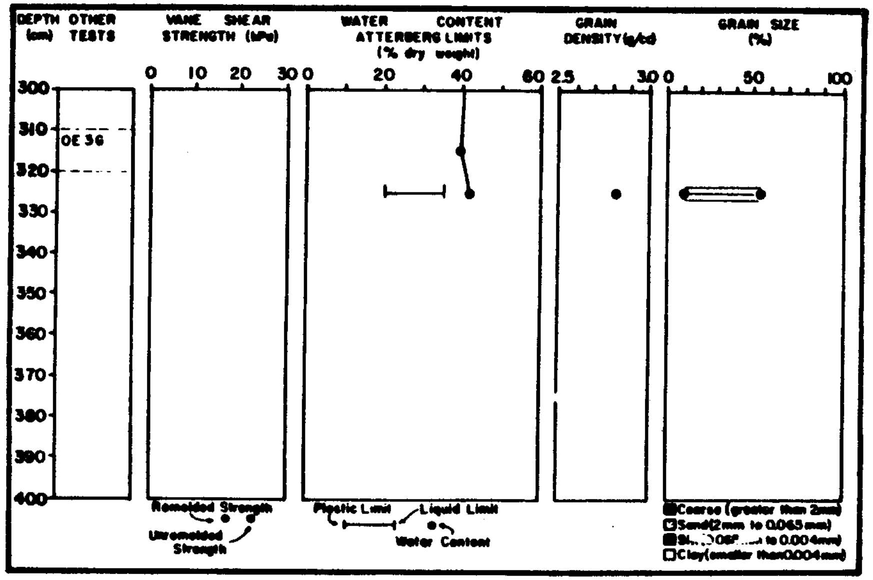

CRUISE: S8-77-EG CORE: 4G

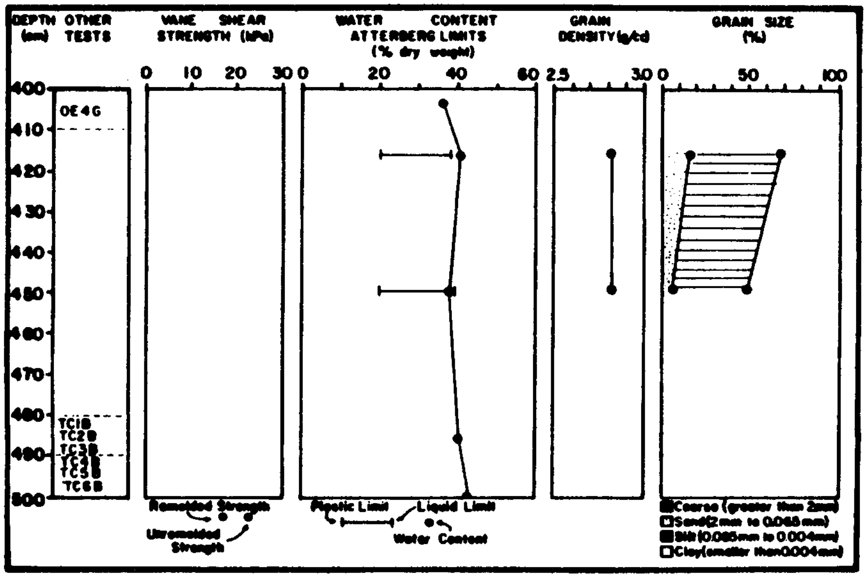

CRUISE: S8-77-EG CORE: 4G

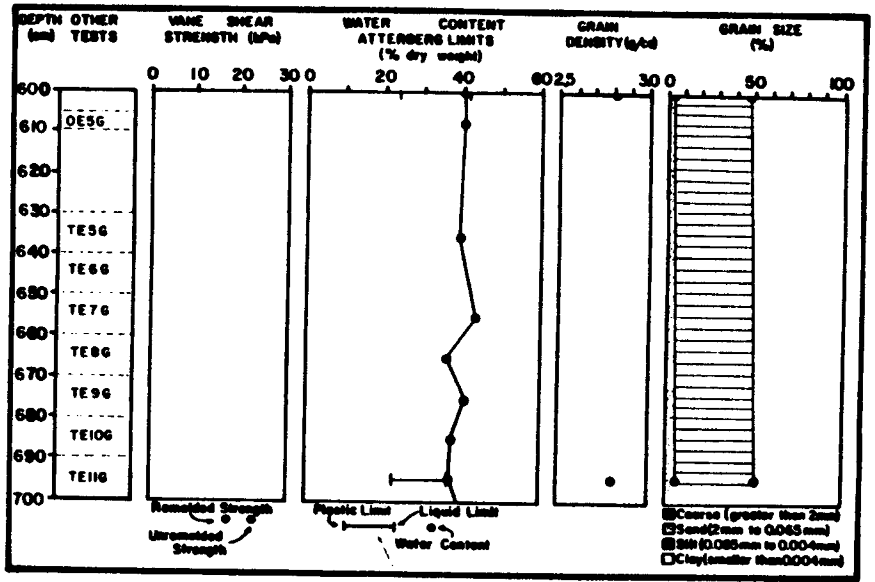

CRUISE: S8-77-EG CORE: 4G

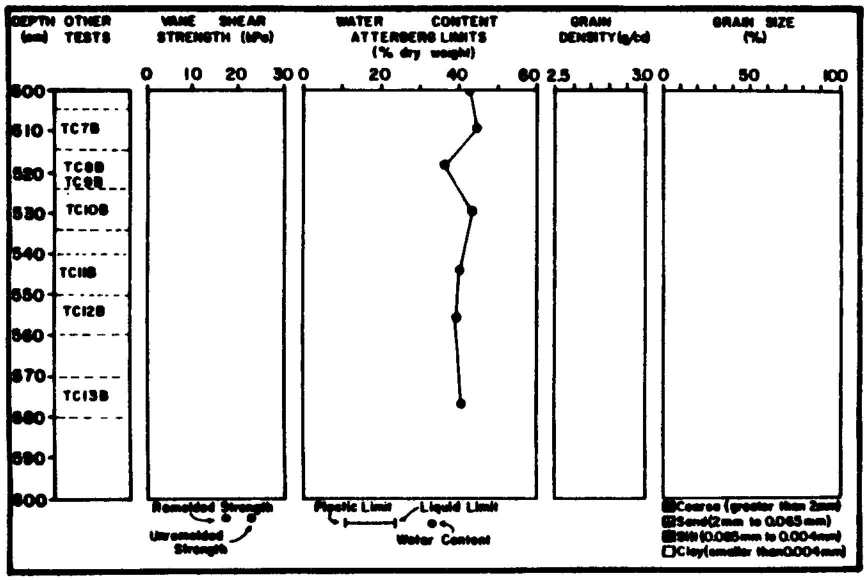

CRUISE: S8-77-EG CORE: 4G

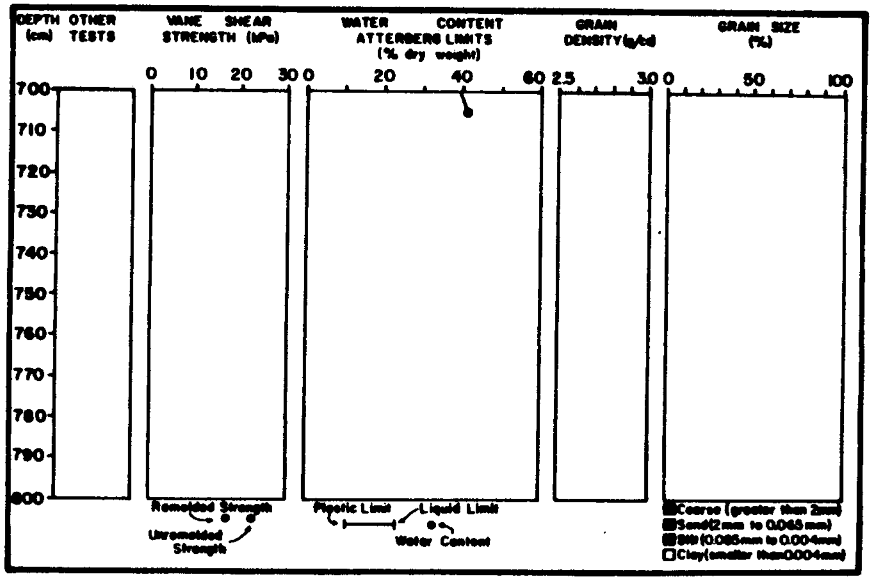

CRUISE: S8-77-EG CORE: 4G

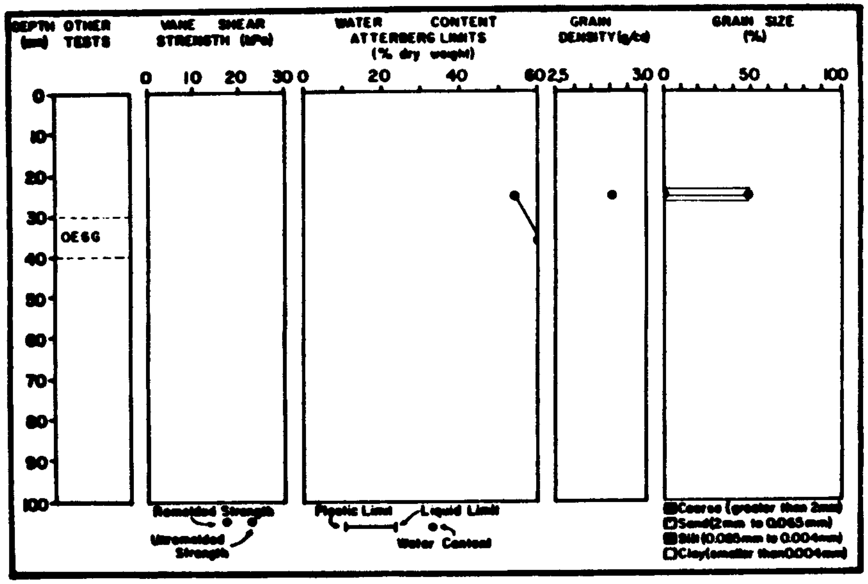

CRUISE: S8-77-EG CORE: 6G

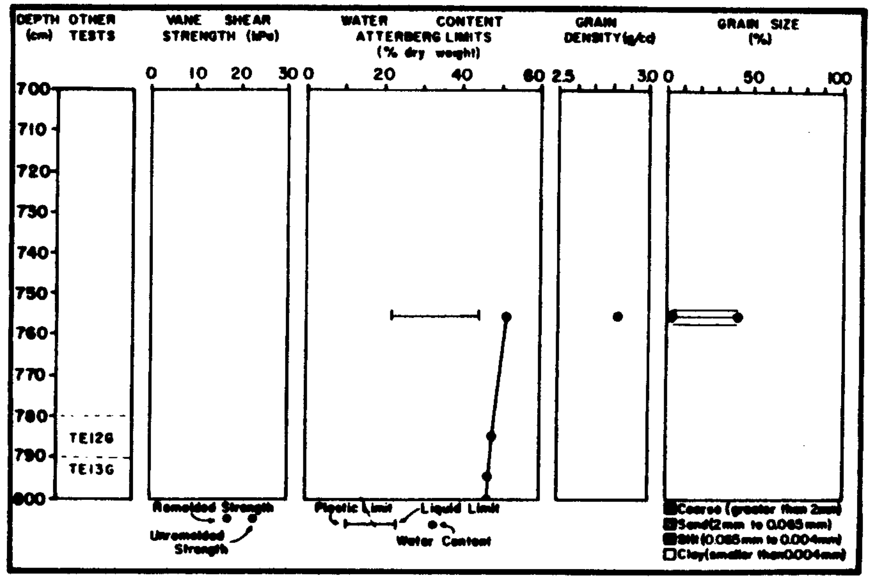

CRUISE: S8-77-EG CORE: 7G

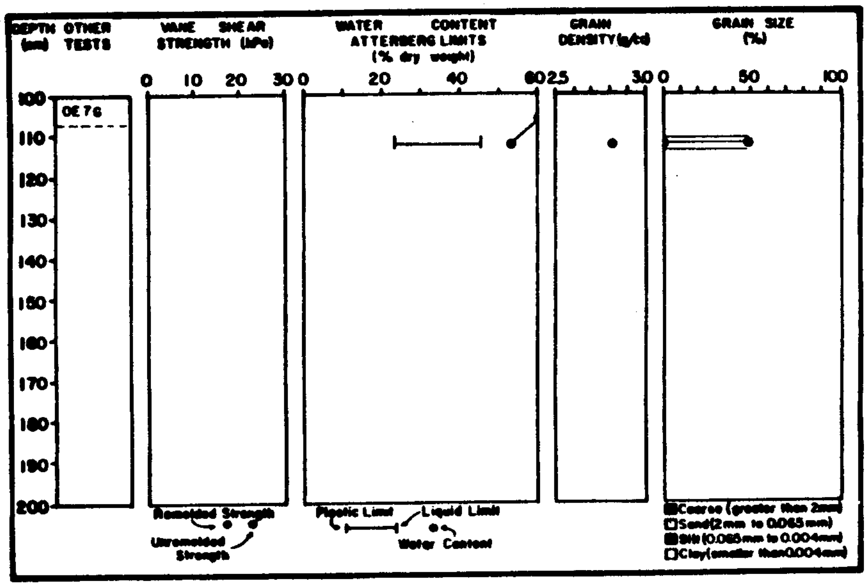

CRUISE: S8-77-EG CORE: 6G

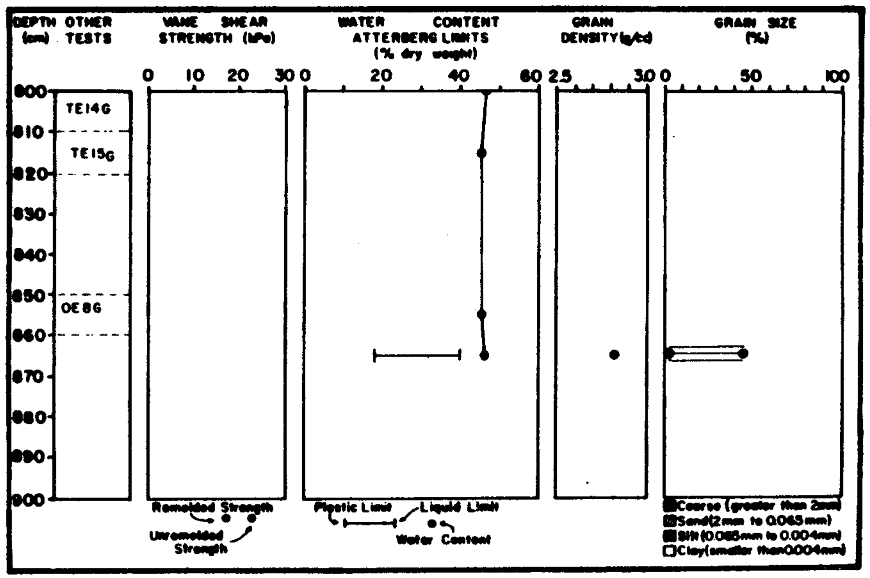

CRUISE: S8-77-EG CORE: 7G

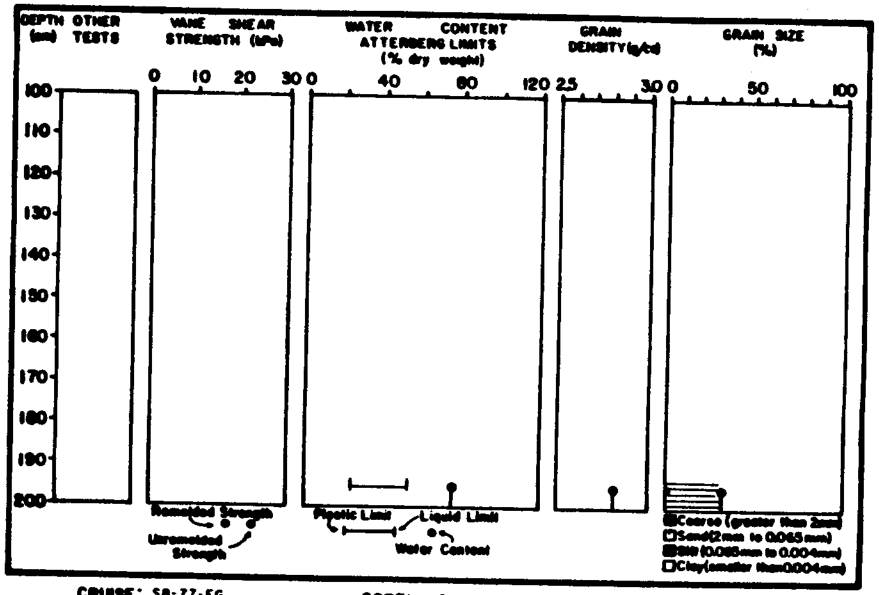

CRUISE: 58-77-EG CORE: 8G

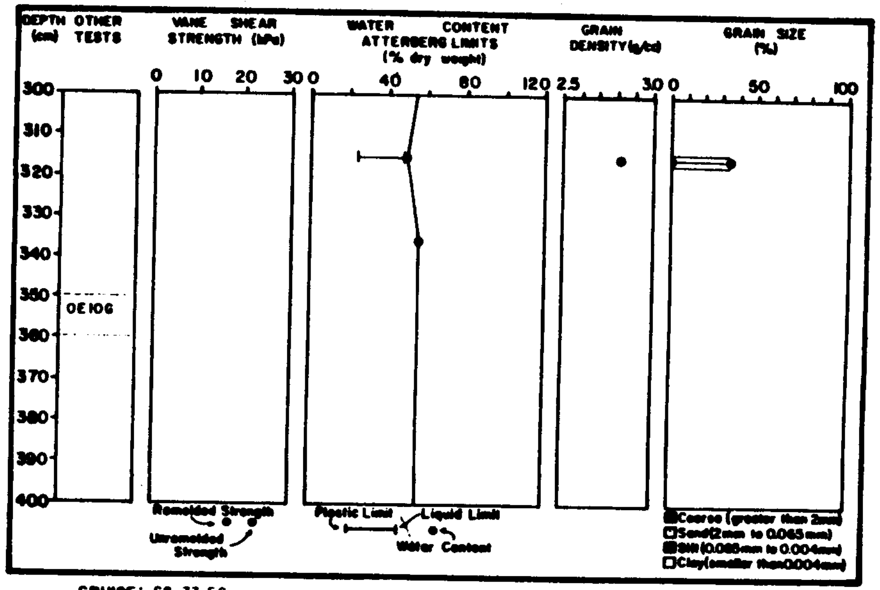

CRUISE: 58-77-EG CORE: 8G

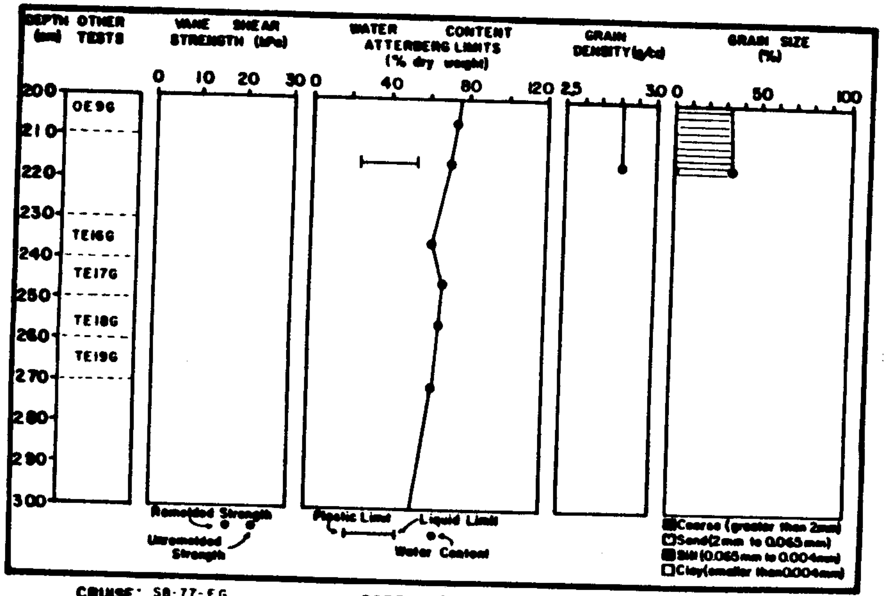

CRUISE: 58-77-EG CORE: 8G

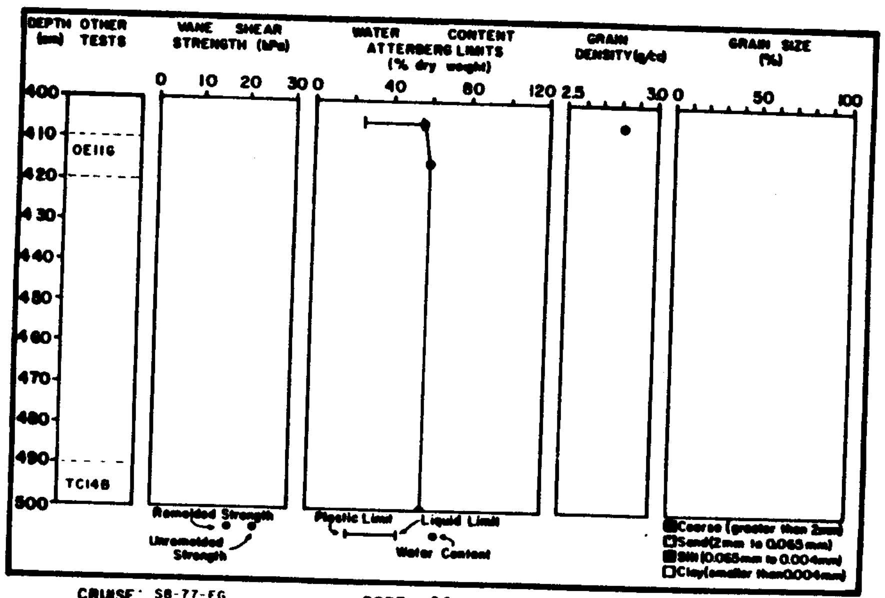

CRUISE: 58-77-EG CORE: 8G

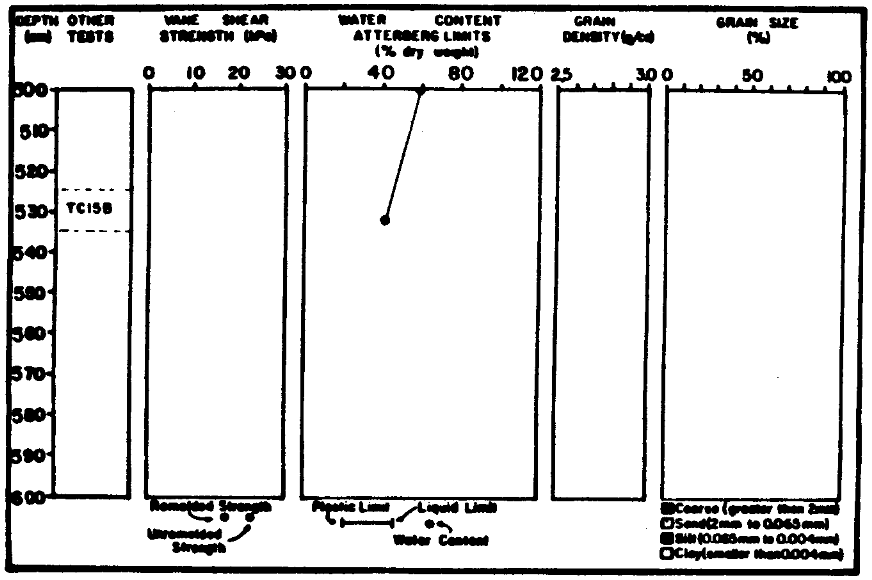

CRUISE: S8-77-EG CORE: 8G

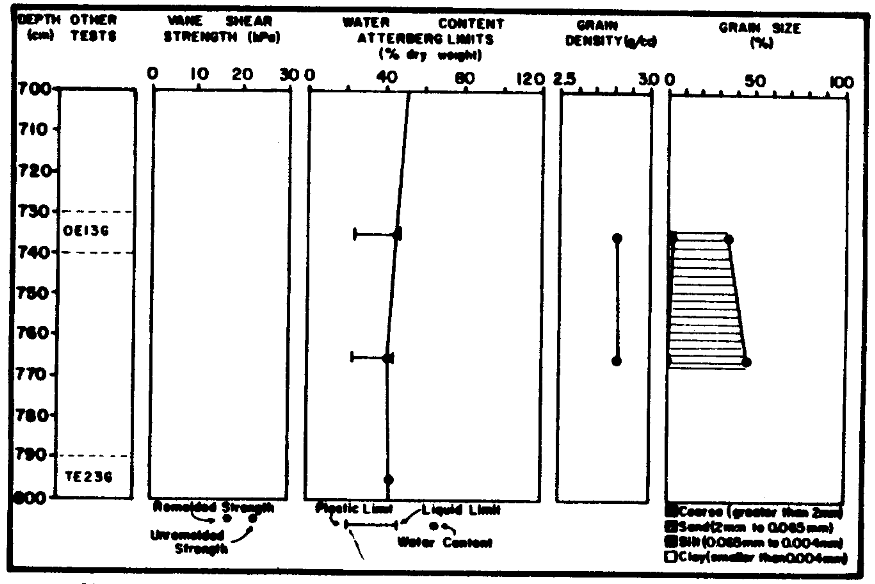

CRUISE: S8-77-EG CORE: 8G

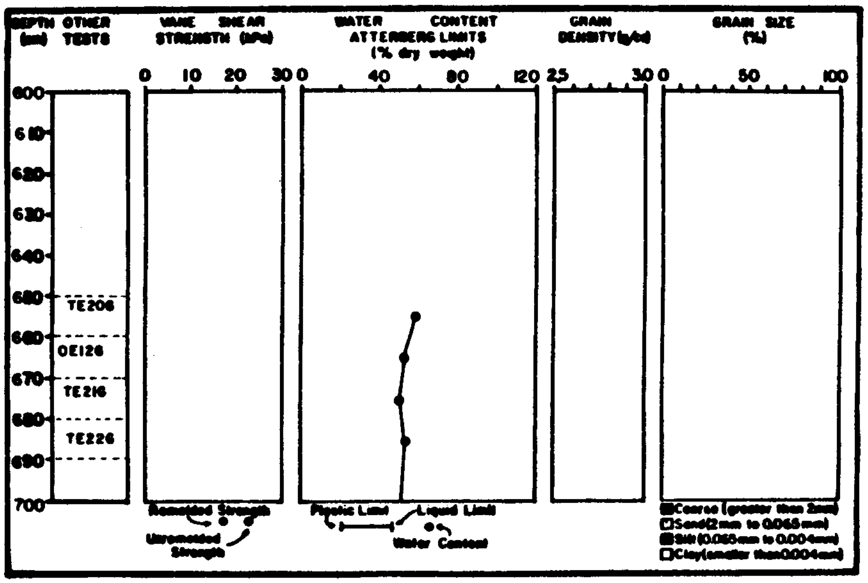

CRUISE: S8-77-EG CORE: 8G

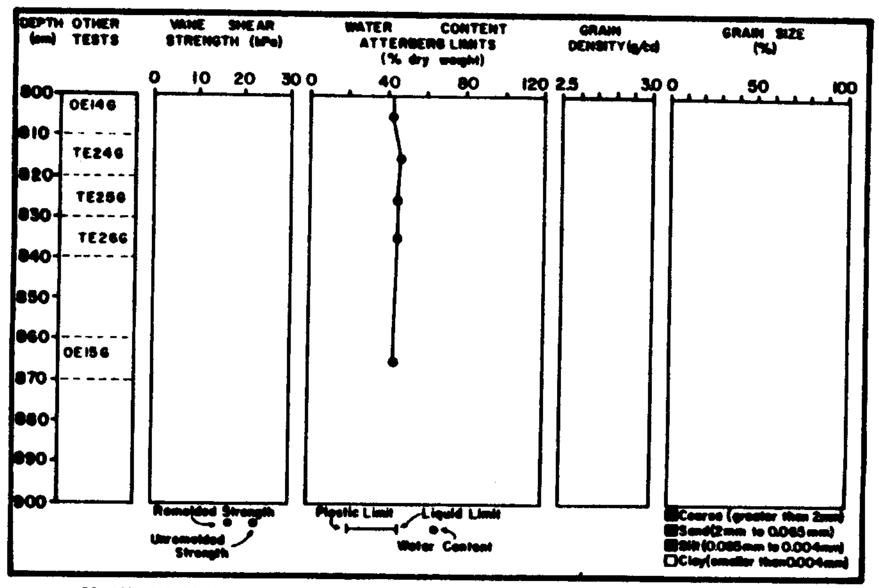

CRUISE: S8-77-EG CORE: 8G

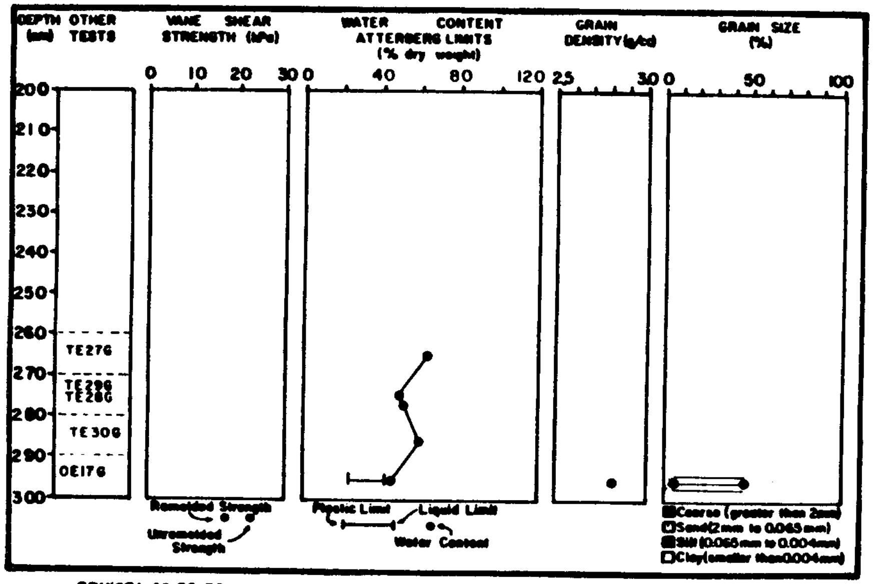

CRUISE: S8-77-EG CORE: 9G

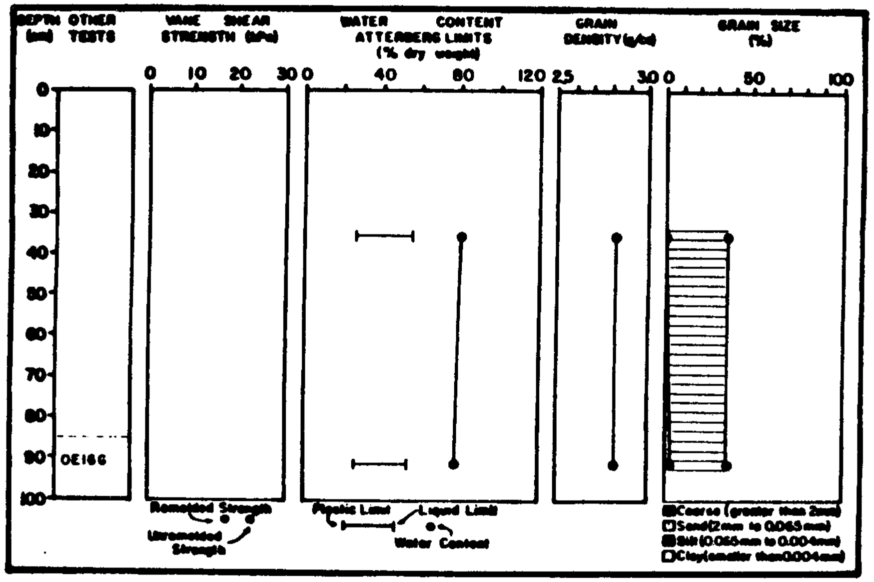

CRUISE: S8-77-EG CORE: 9G

KAYAK TROUGH STUDY AREA

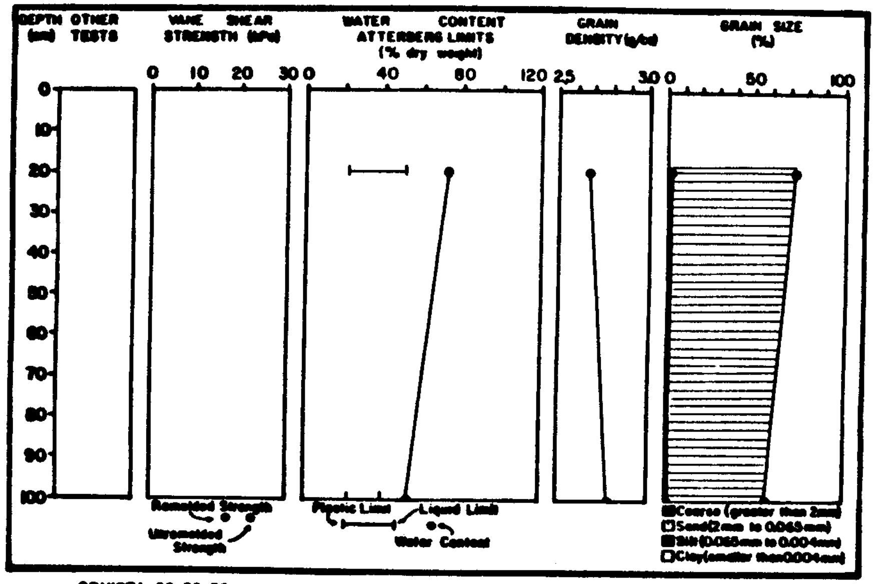

CRUISE: 58-77-EG CORE: 10G

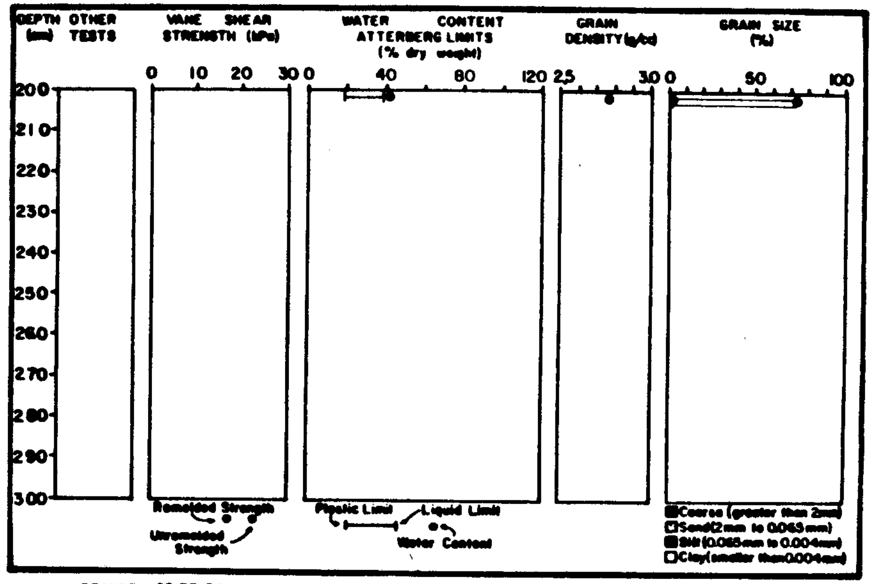

CRUISE: 58-77-EG CORE: 10G

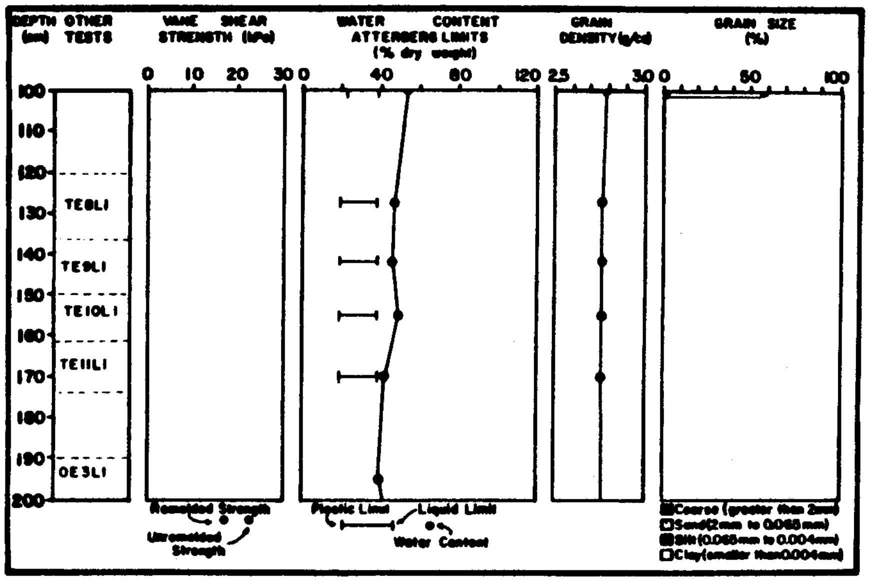

CRUISE: 58-77-EG CORE: 10G

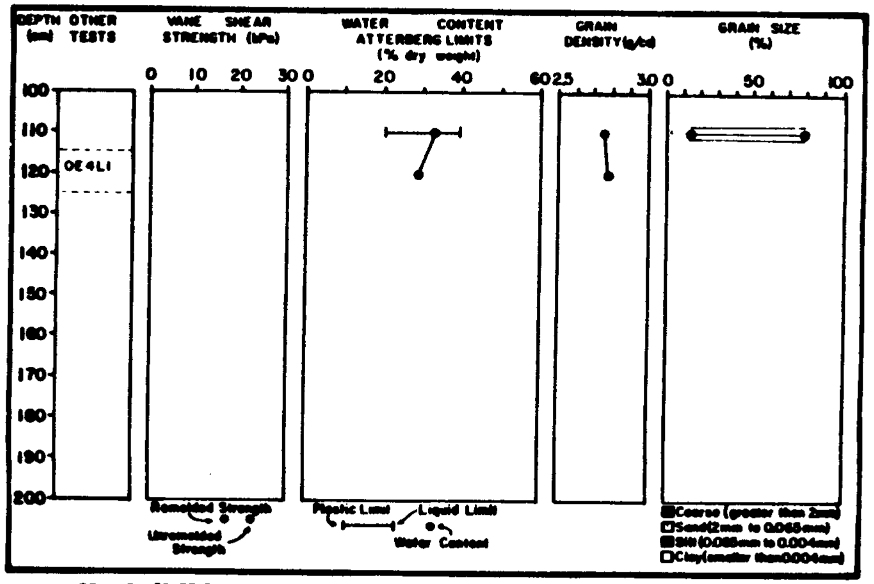

CRUISE: S8-77-EG CORE: 116

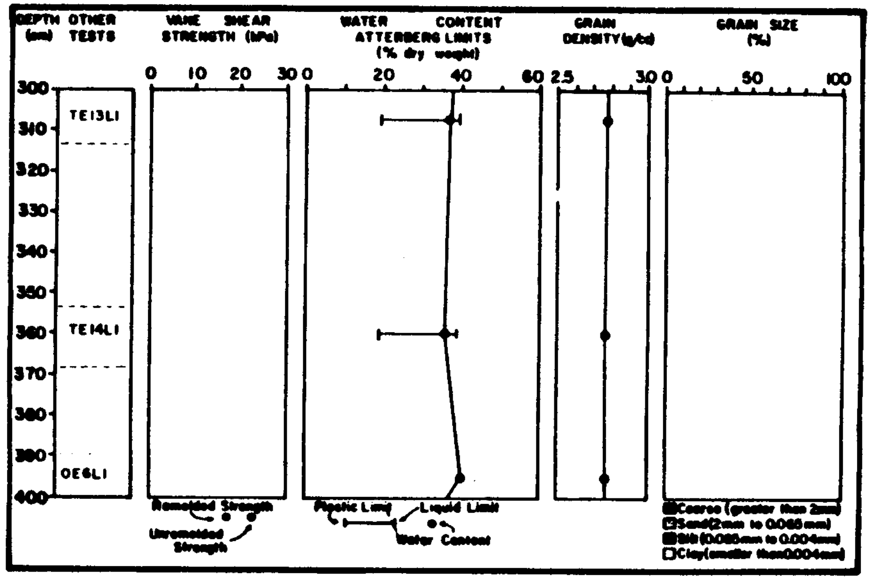

CRUISE: S8-77-EG CORE: 116

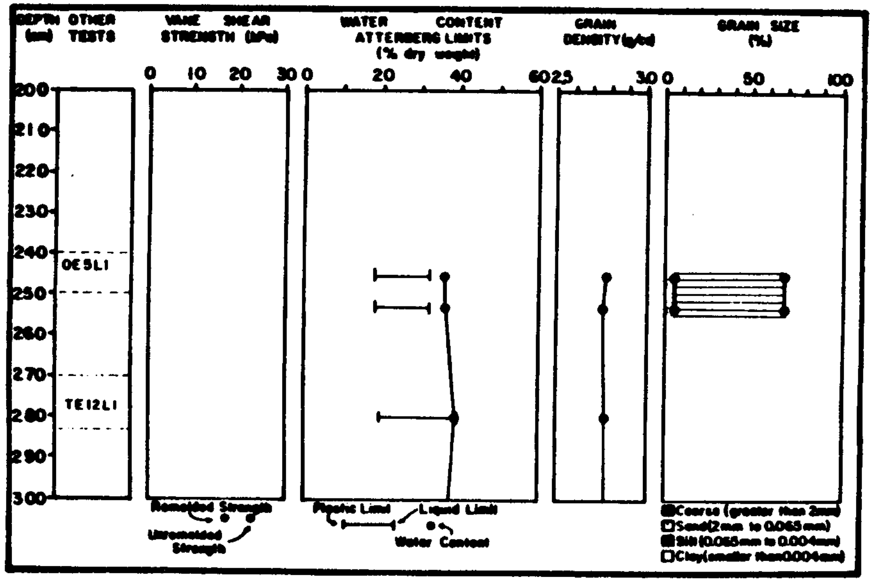

CRUISE: S8-77-EG CORE: 116

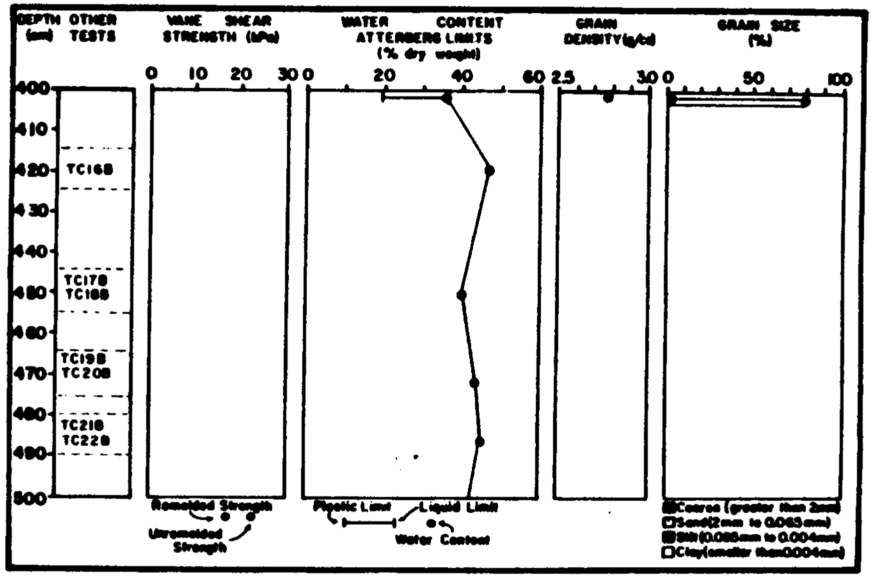

CRUISE: S8-77-EG CORE: 116

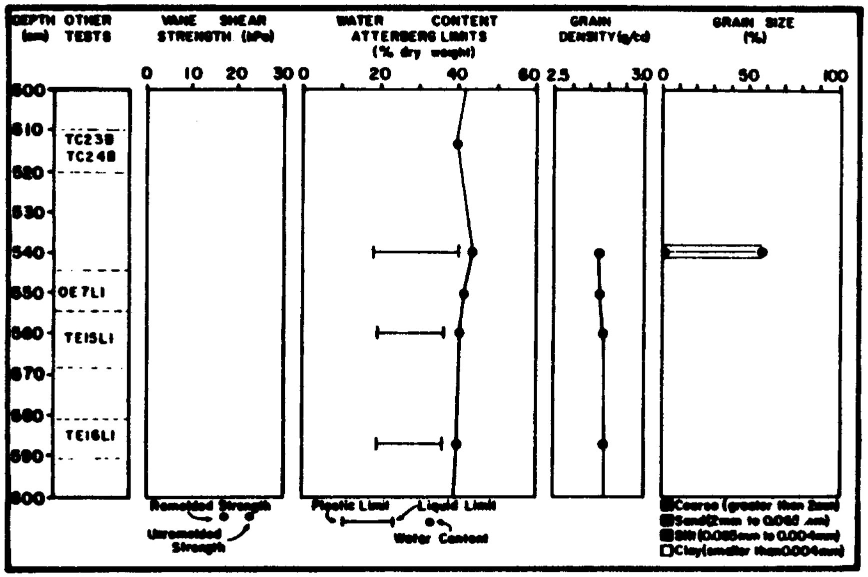

CRUISE: S8-77-EG CORE: 11G

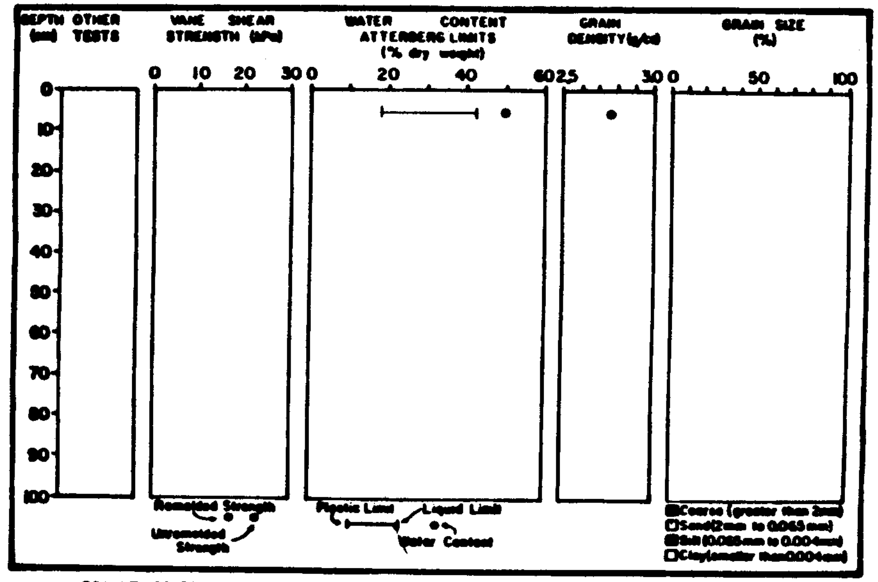

CRUISE: S8-77-EG CORE: 13G

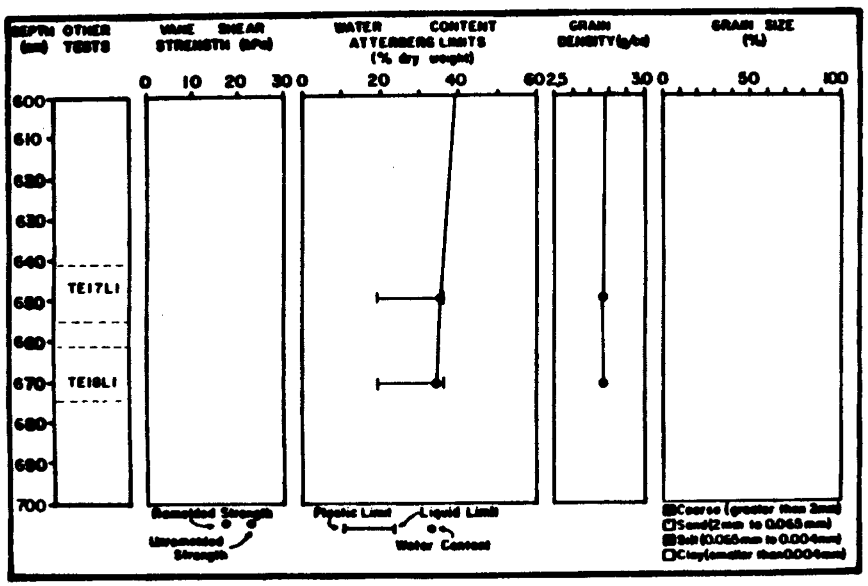

CRUISE: S8-77-EG CORE: 11G

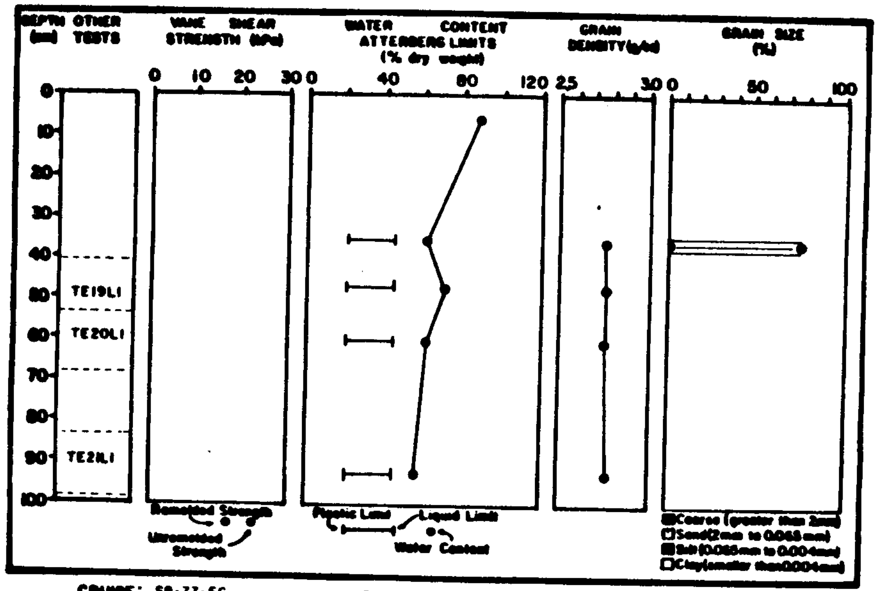

CRUISE: S8-77-EG CORE: 14G

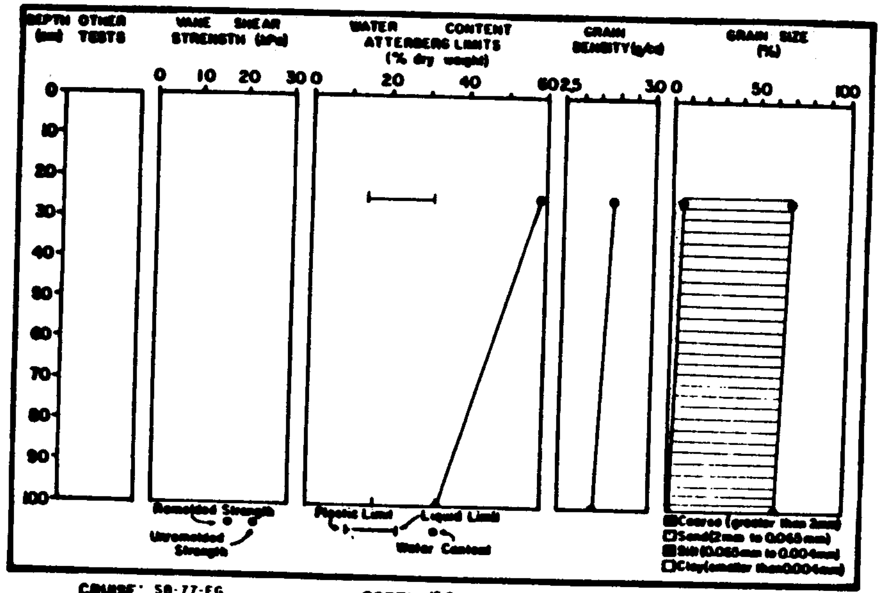

CRUISE: S8-77-EG CORE: 15G

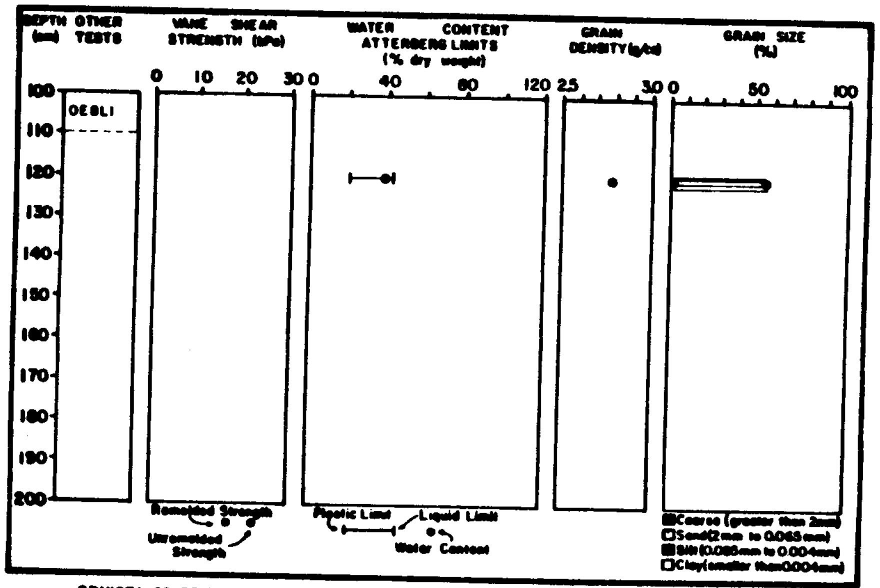

CRUISE: S8-77-EG CORE: 14G

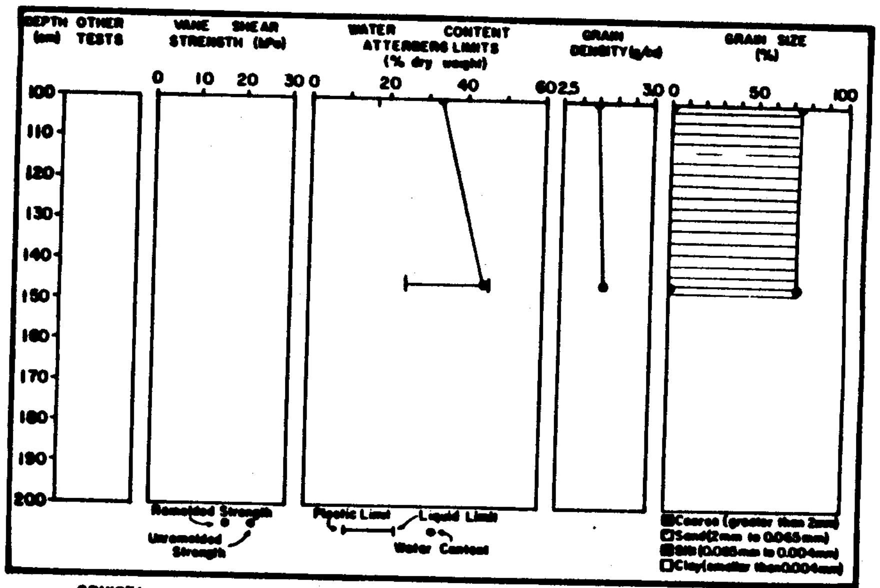

CRUISE: S8-77-EG CORE: 15G

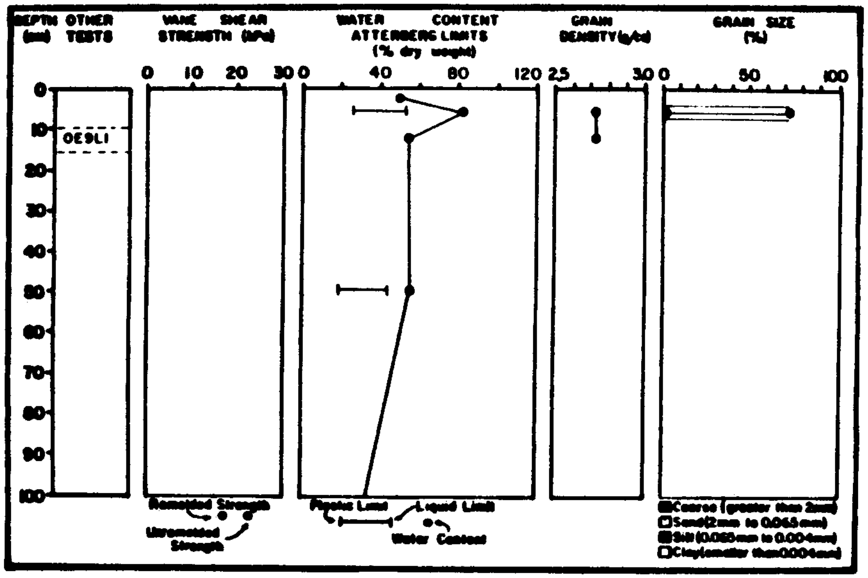

CRUISE: S8-77-EG CORE: 16G

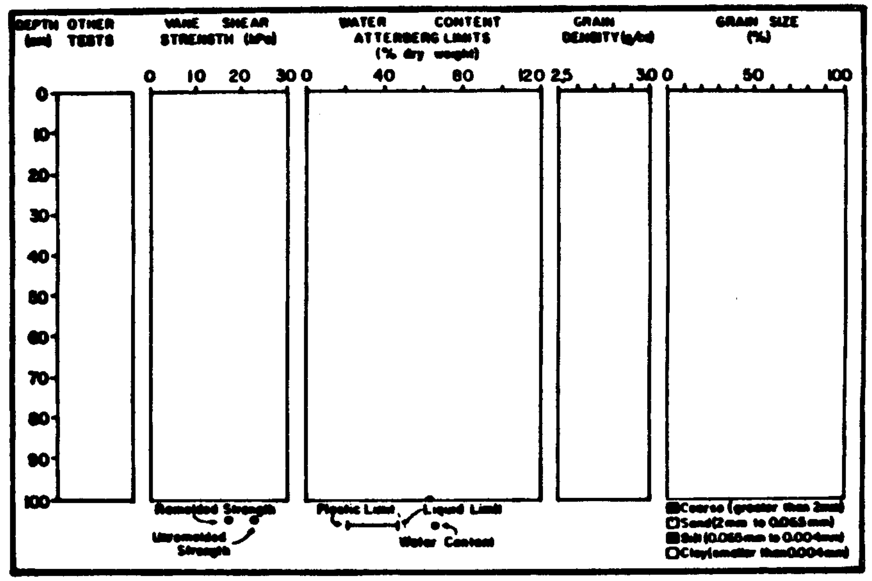

CRUISE: S8-77-EG CORE: 17G

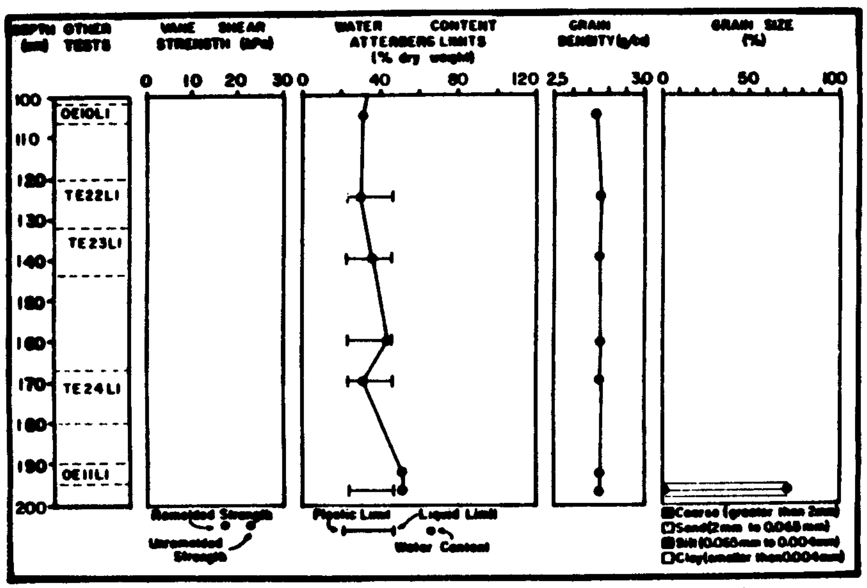

CRUISE: S8-77-EG CORE: 16G

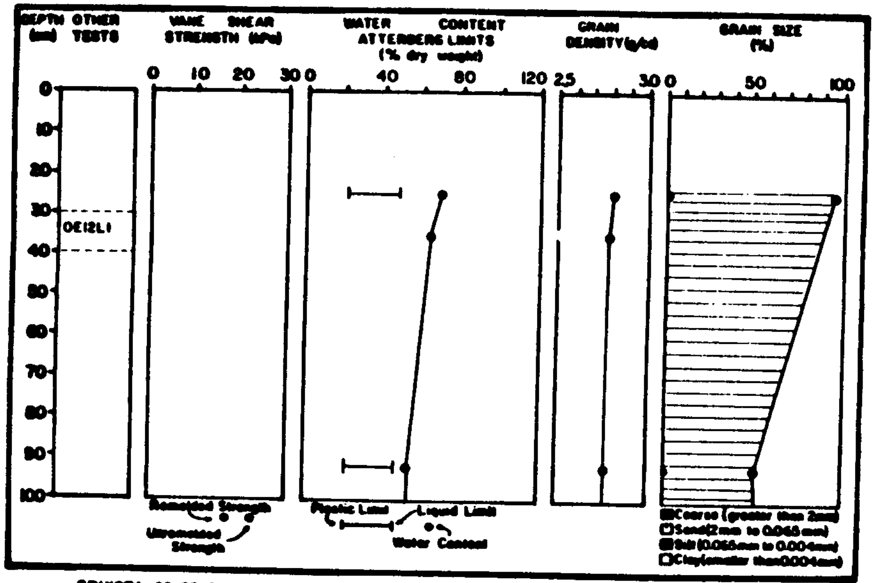

CRUISE: S8-77-EG CORE: 18G

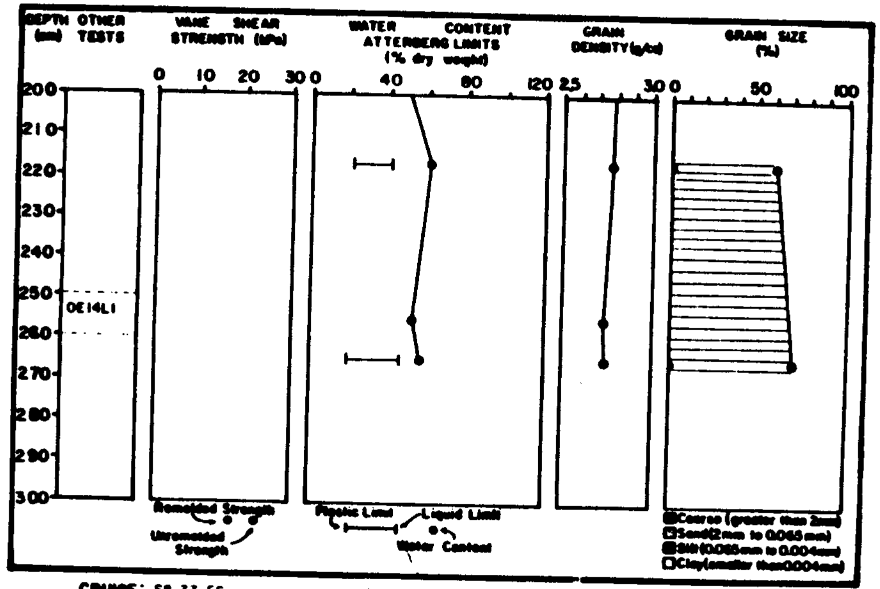

CRUISE: S8-77-EG CORE: 18G

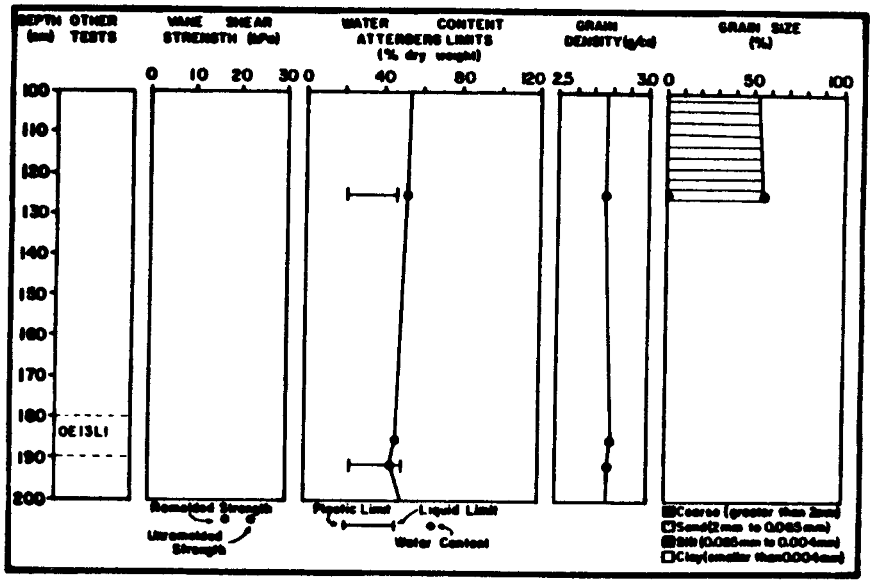

CRUISE: S8-77-EG CORE: 18G

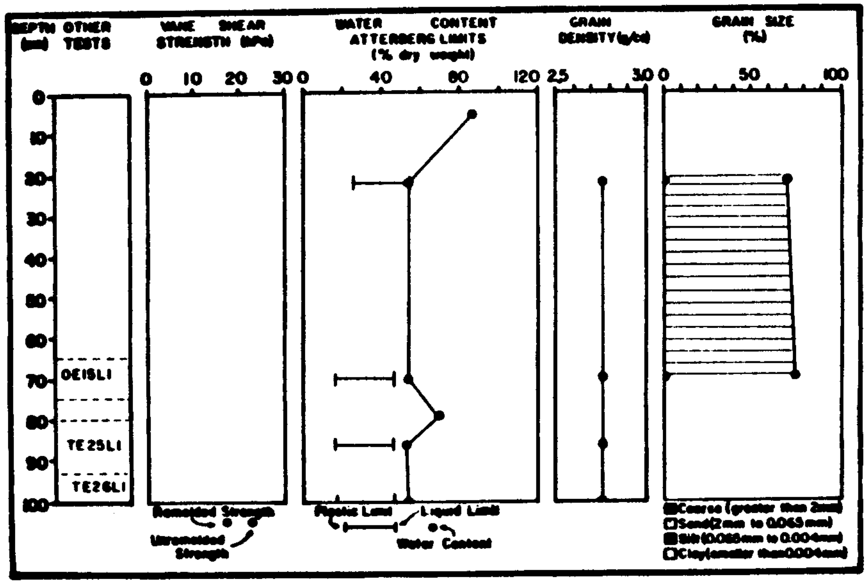

CRUISE: S8-77-EG CORE: 19G

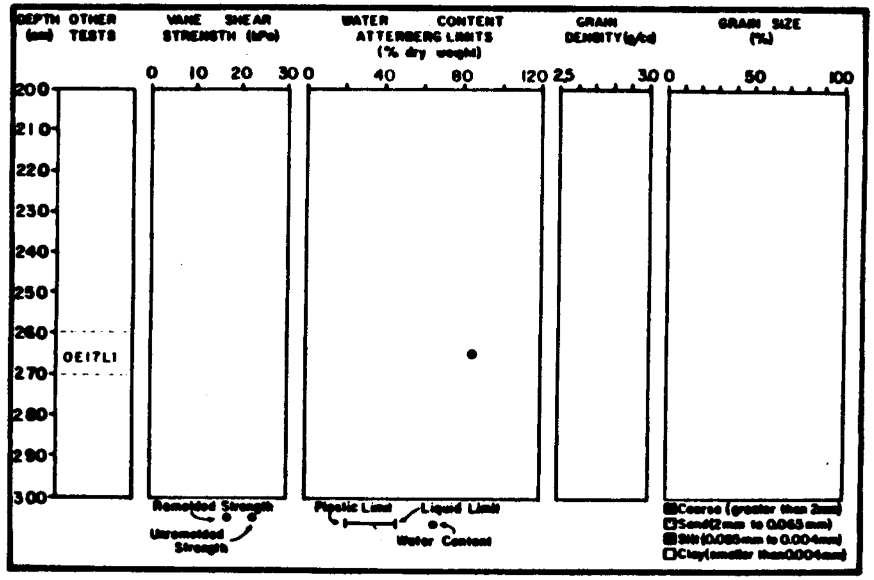

CRUISE: S8-77-EG CORE: 19G

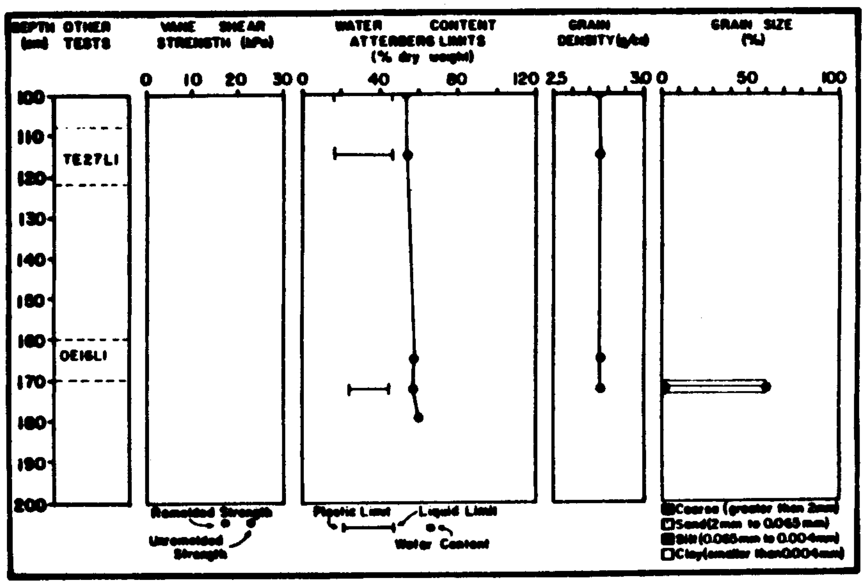

CRUISE: S8-77-EG CORE: 19G

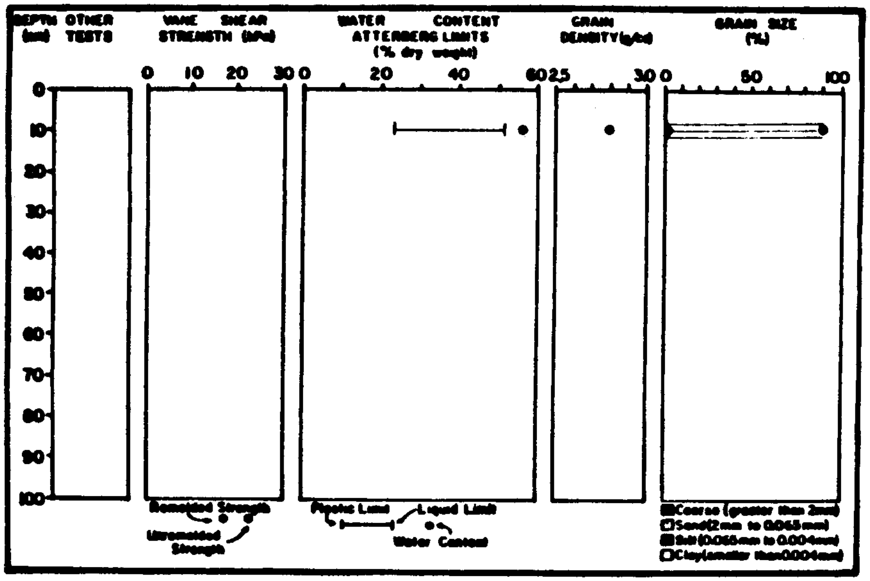

CRUISE: S8-77-EG CORE: 21G

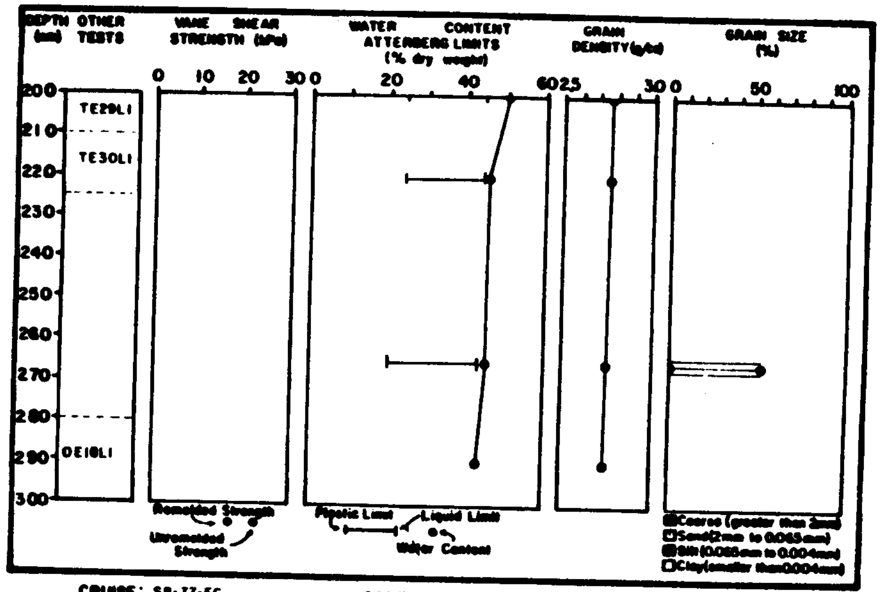

CRUISE: S8-77-EG CORE: 21G

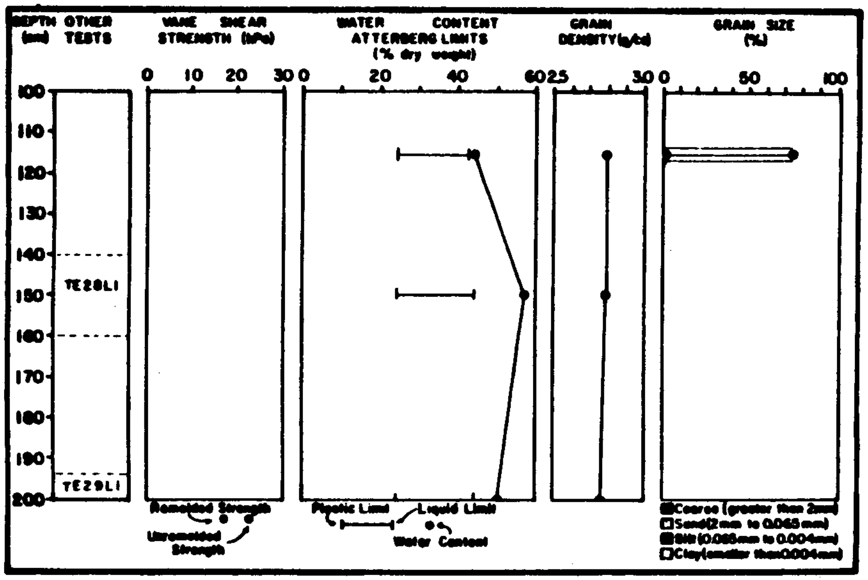

CRUISE: S8-77-EG CORE: 21G

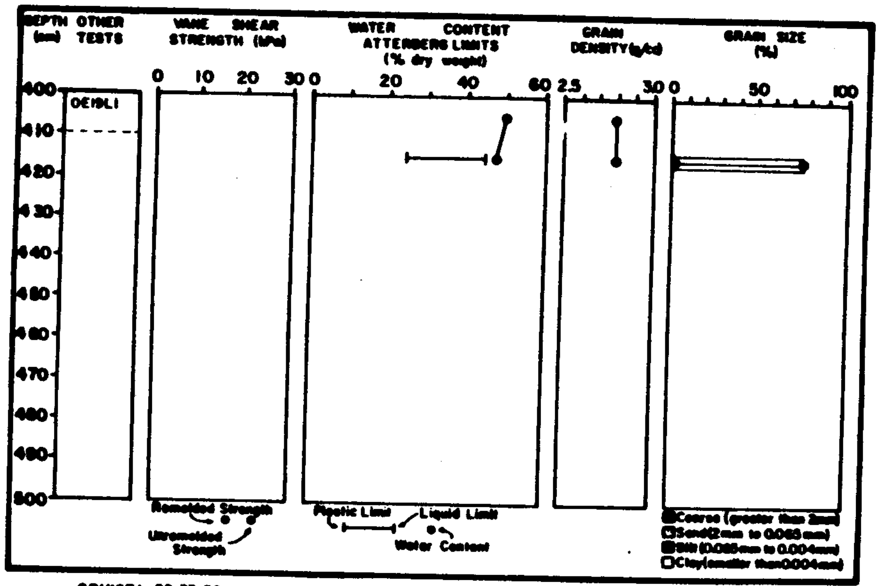

CRUISE: S8-77-EG CORE: 21G

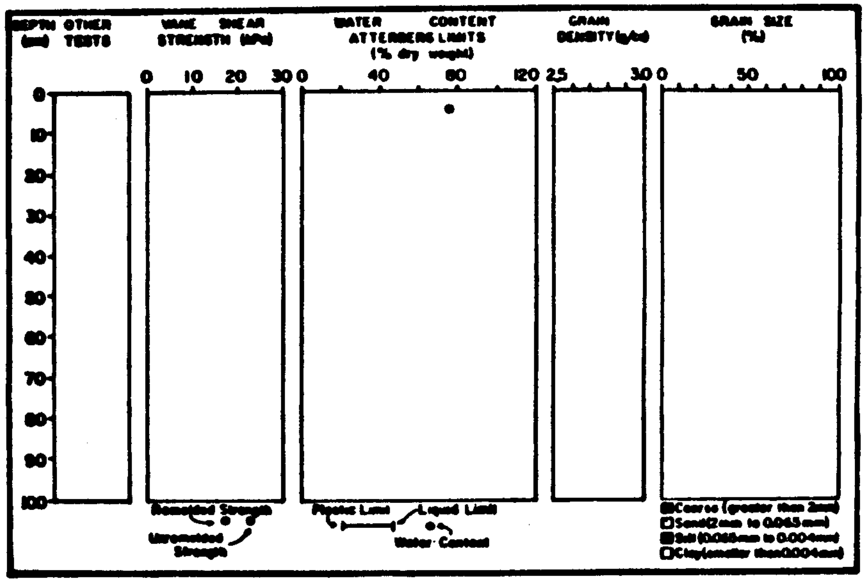

CRUISE: 58-77-EG CORE: 206

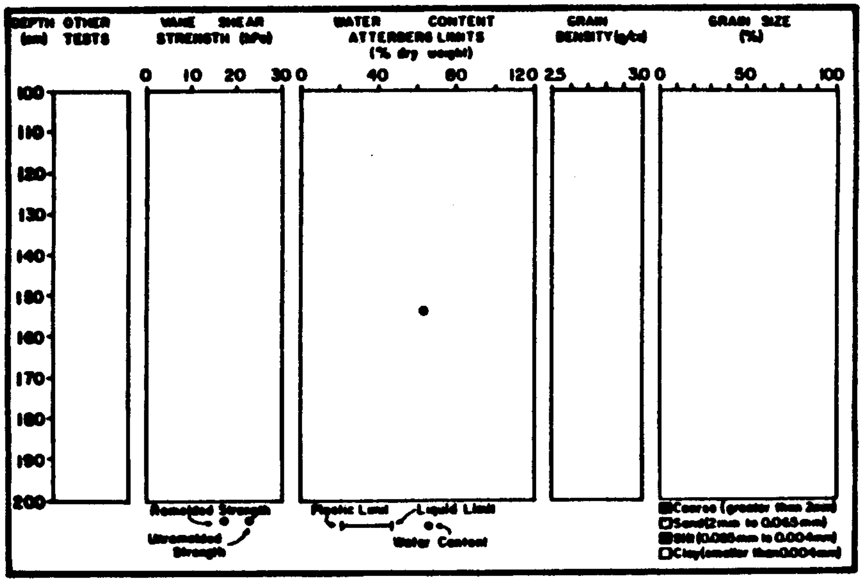

CRUISE: 58-77-EG CORE: 206

BERING TROUGH STUDY AREA

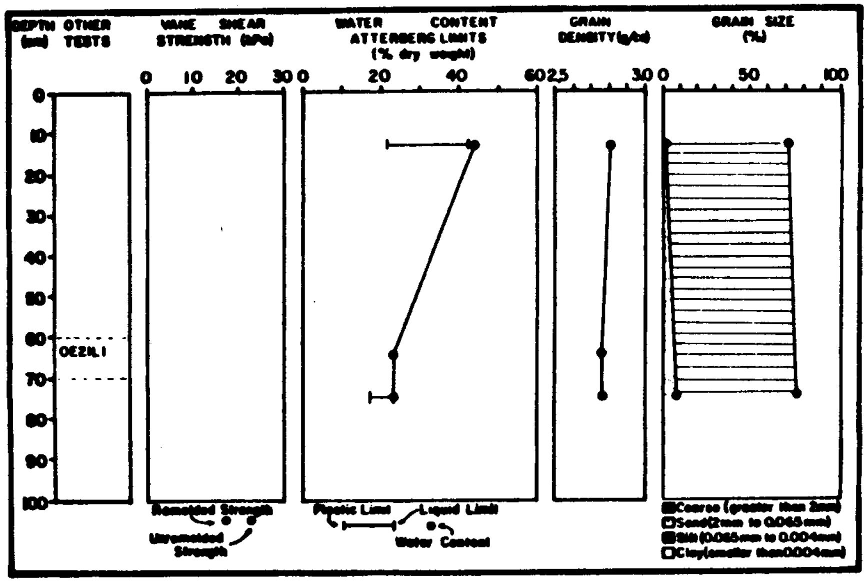

CRUISE: S8-77-EG CORE: 34G

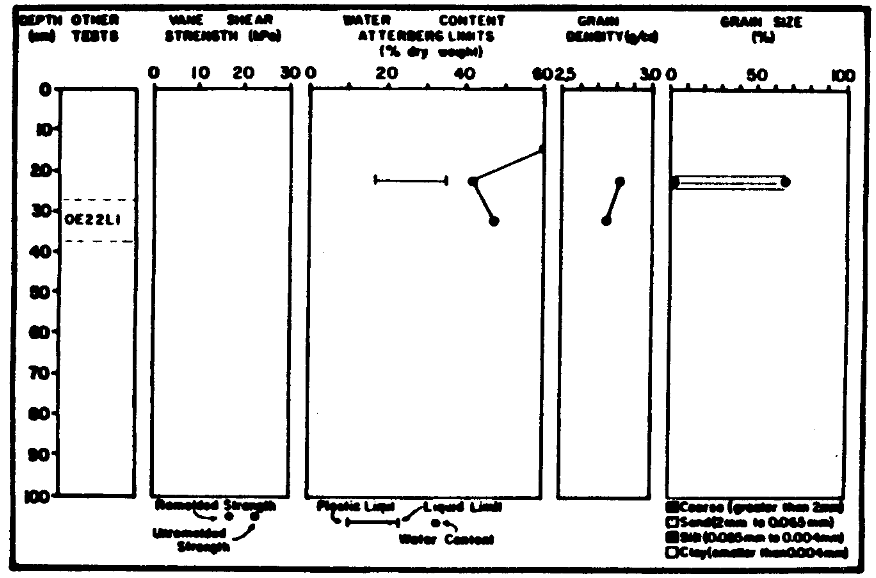

CRUISE: S8-77-EG CORE: 38G

250

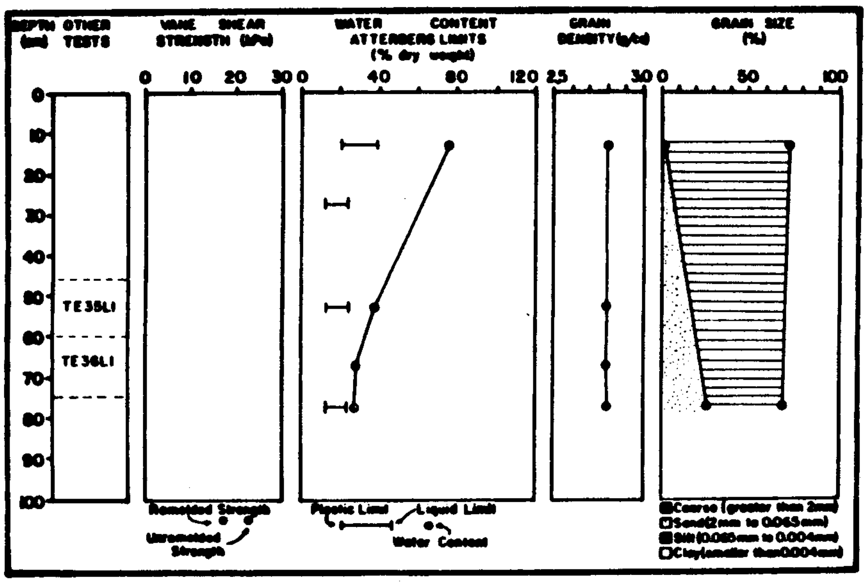

CRUISE: S8-77-EG CORE: 36G

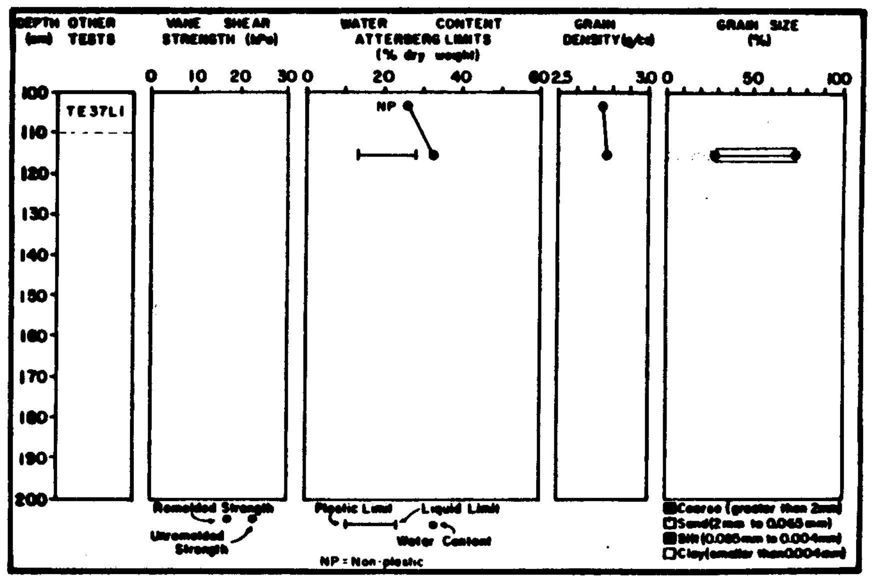

CRUISE: S8-77-EG CORE: 38G

ICY BAY-MALASPINA STUDY AREA

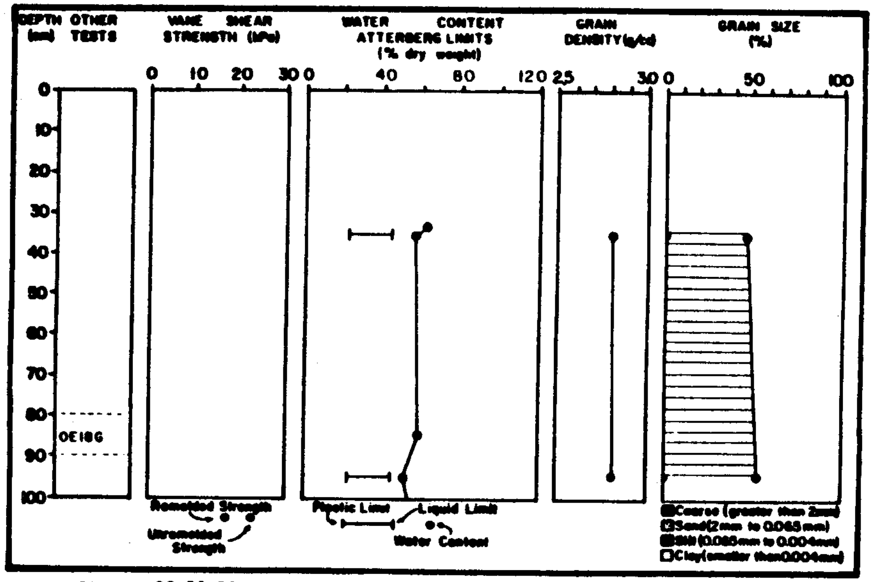

CRUISE: SB-77-EG CORE: 25G

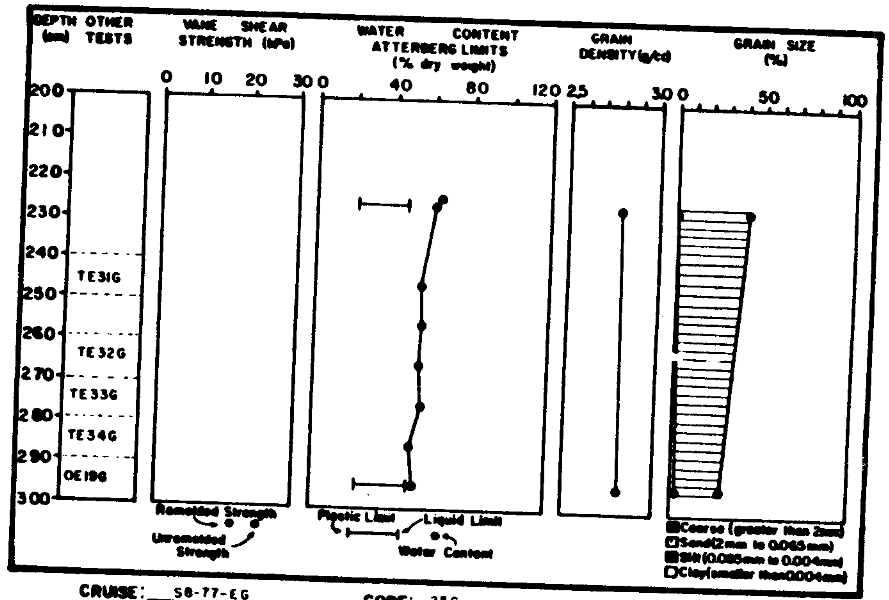

CRUISE: SB-77-EG CORE: 25G

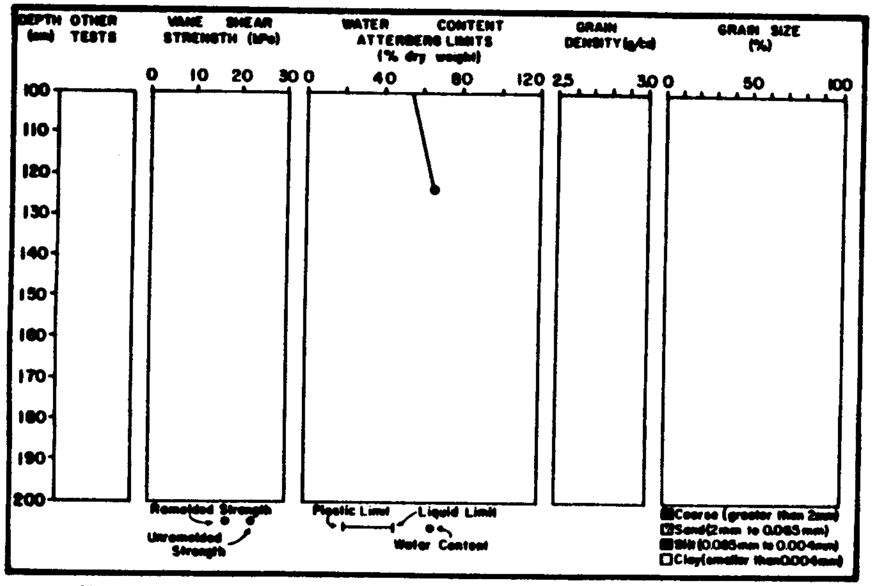

CRUISE: SB-77-EG CORE: 25G

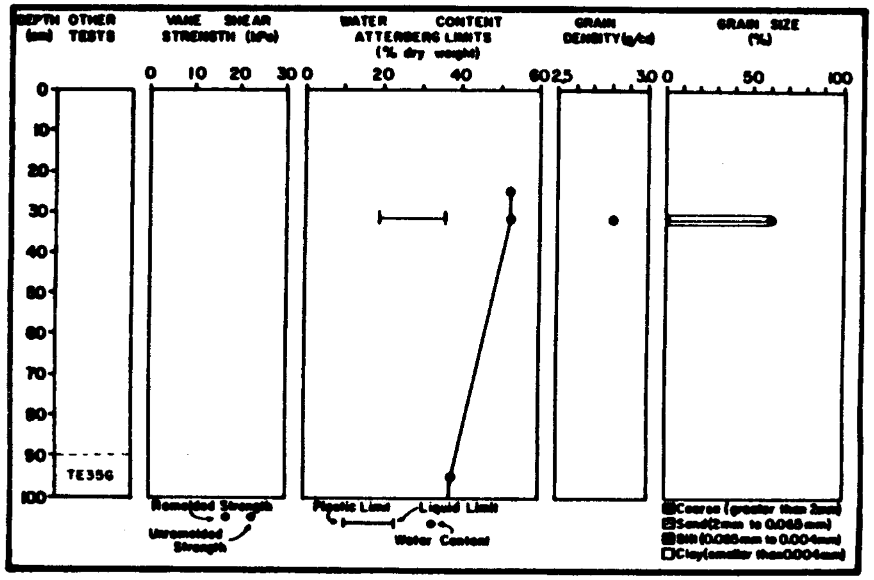

CRUISE: S8-77-EG CORE: 26G

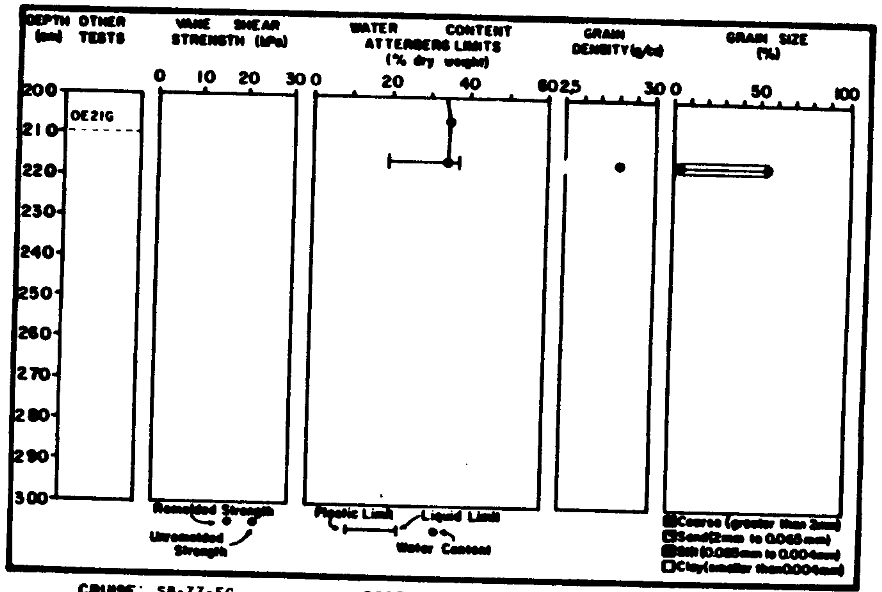

CRUISE: S8-77-EG CORE: 26G

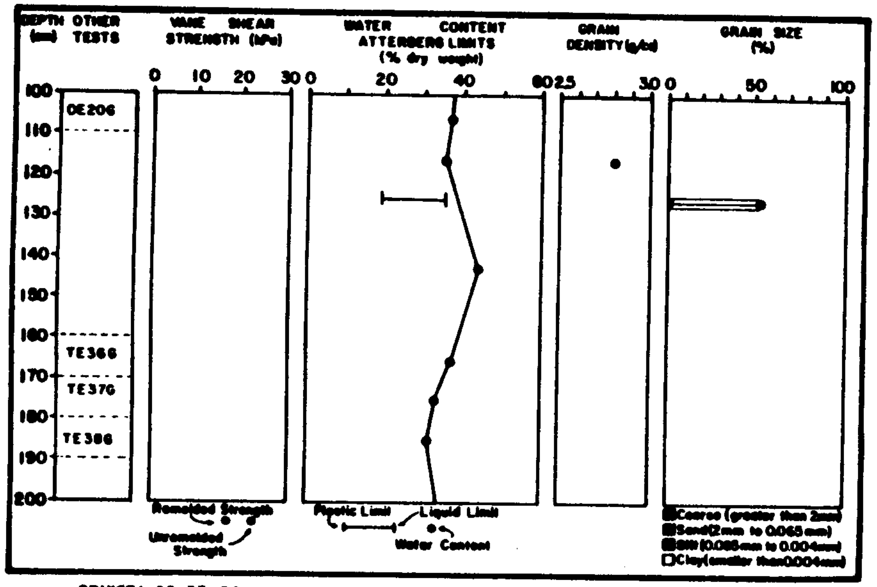

CRUISE: S8-77-EG CORE: 26G

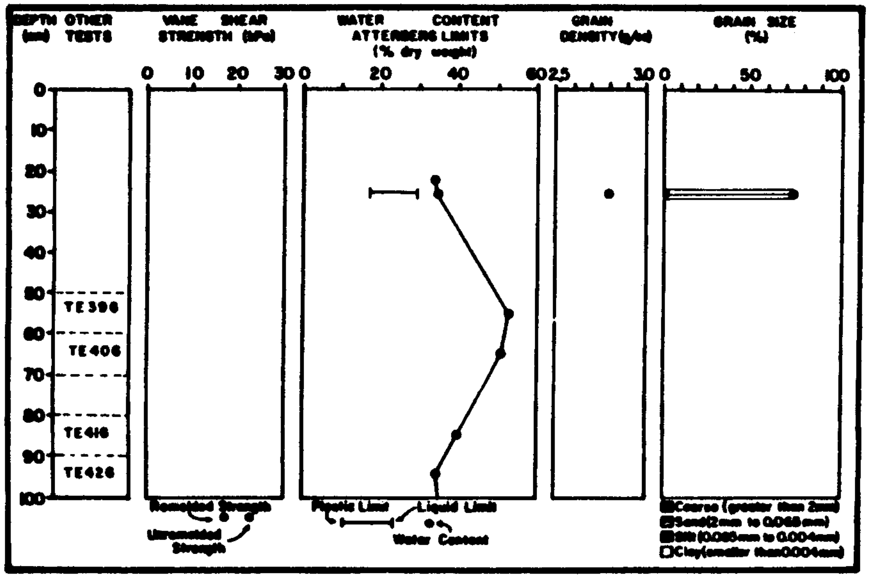

CRUISE: S8-77-EG CORE: 27G

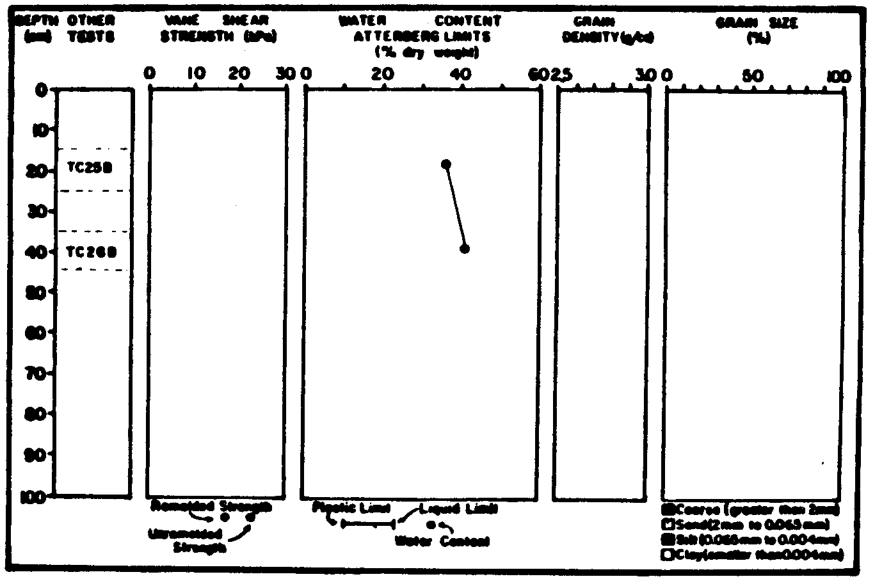

CRUISE: S8-77-EG CORE: 28G

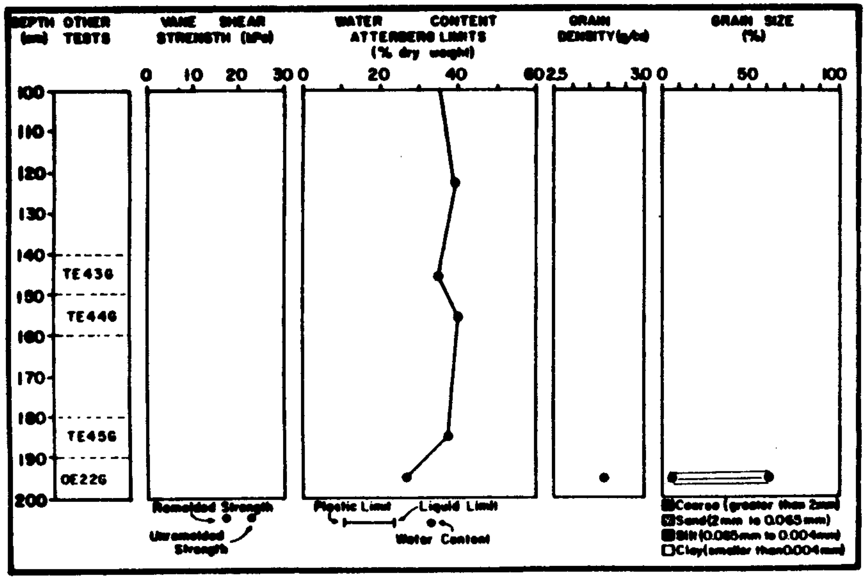

CRUISE: S8-77-EG CORE: 27G

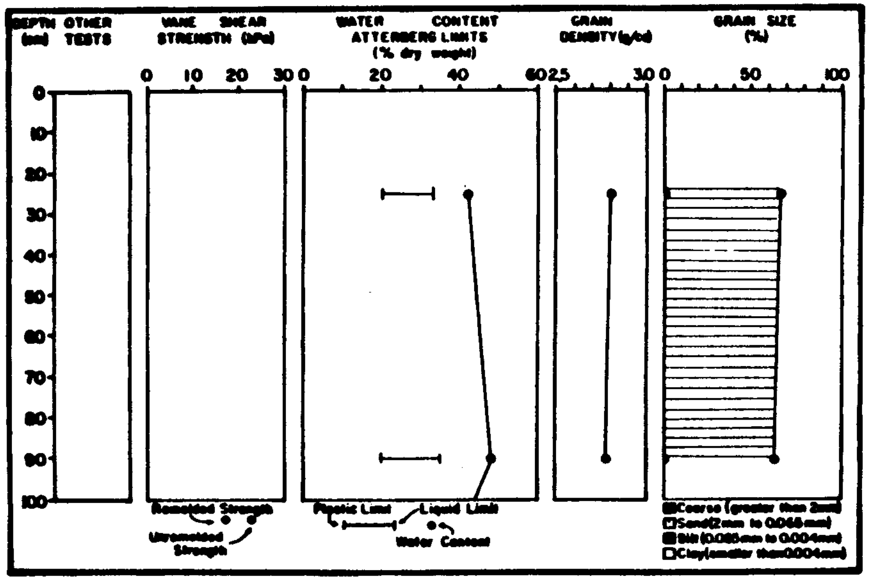

CRUISE: 58-77-EG CORE: 29G

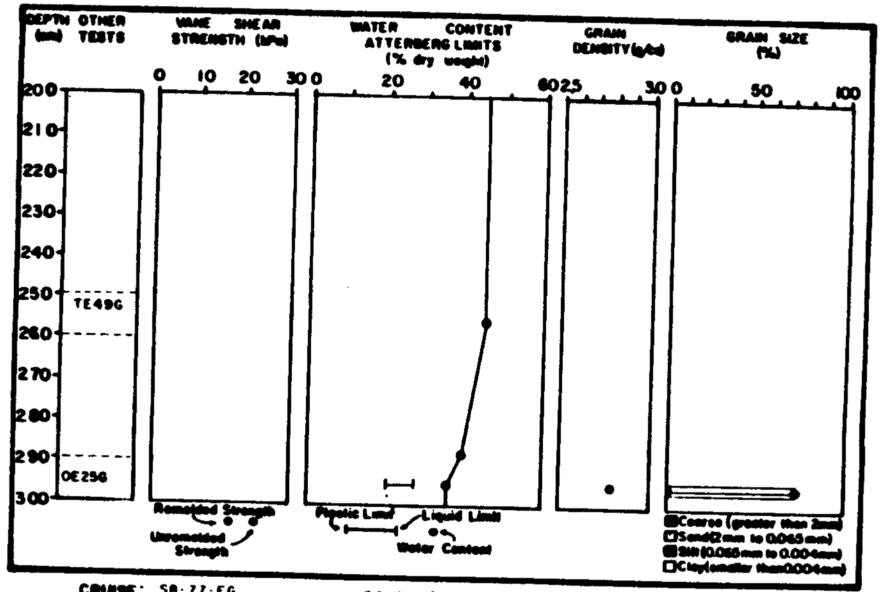

CRUISE: 58-77-EG CORE: 29G

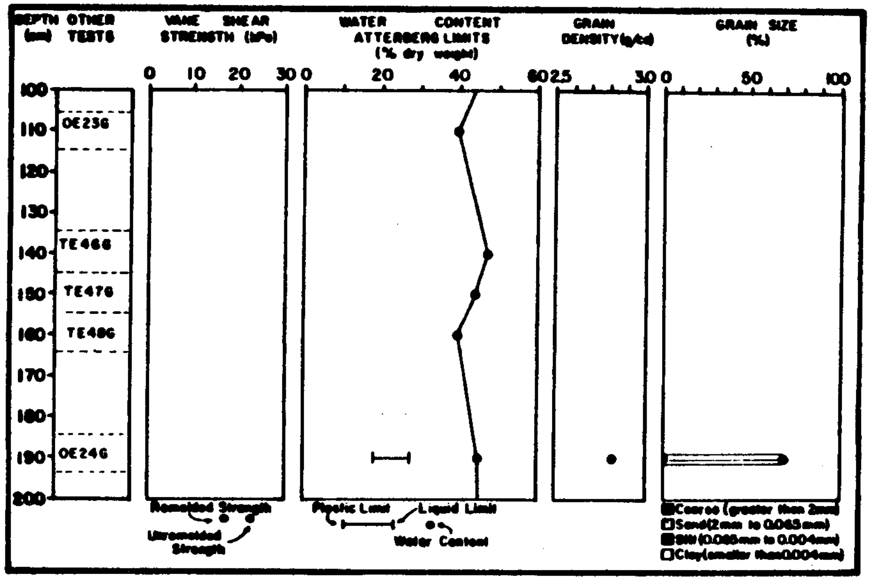

CRUISE: 58-77-EG CORE: 29G

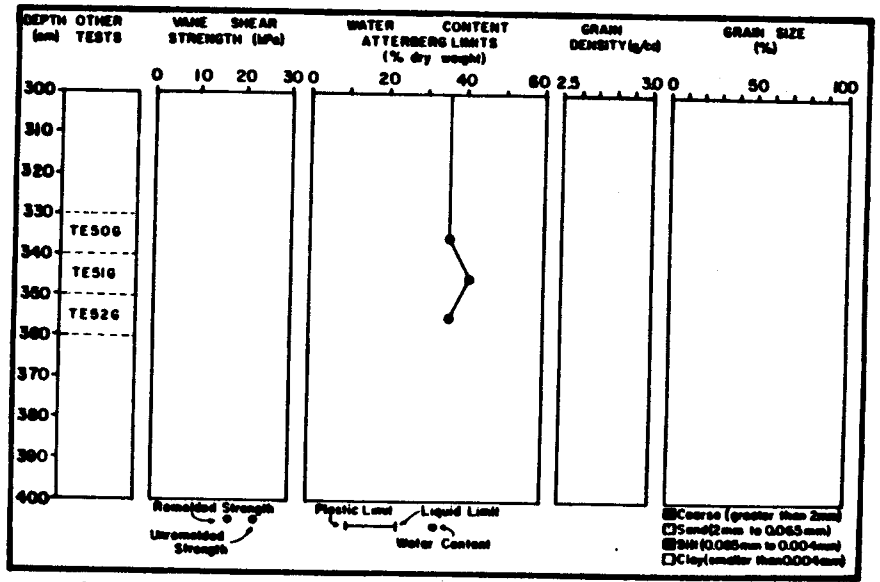

CRUISE: 58-77-EG CORE: 29G

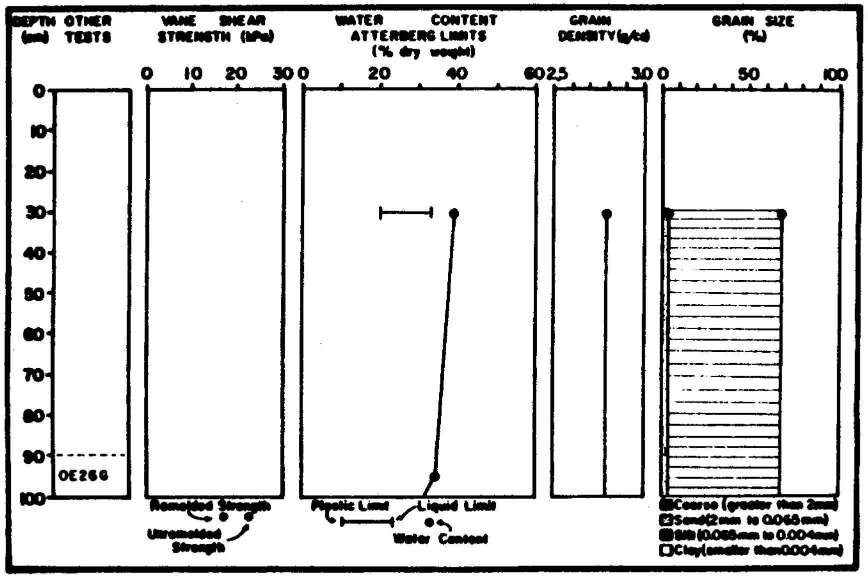

CRUISE: S8-77-EG CORE: 31G

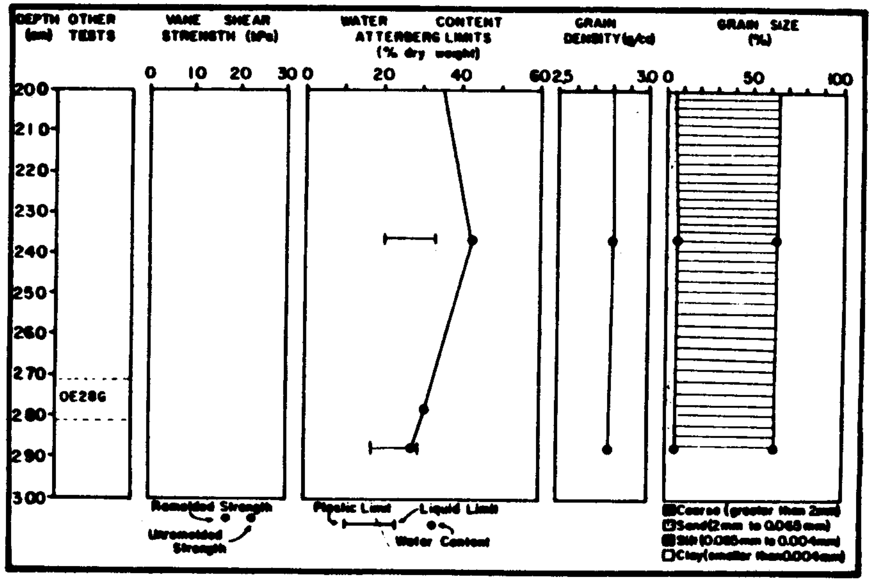

CRUISE: S8-77-EG CORE: 31G

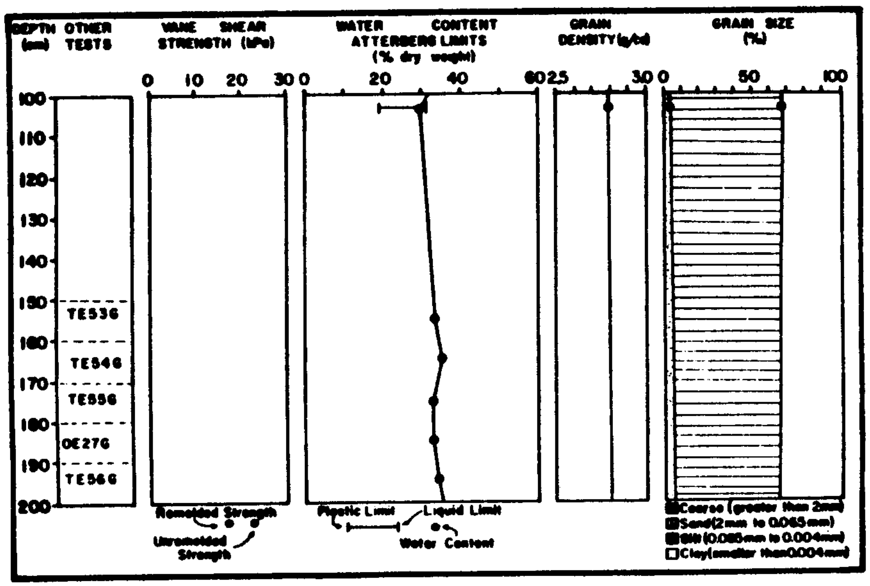

CRUISE: S8-77-EG CORE: 31G

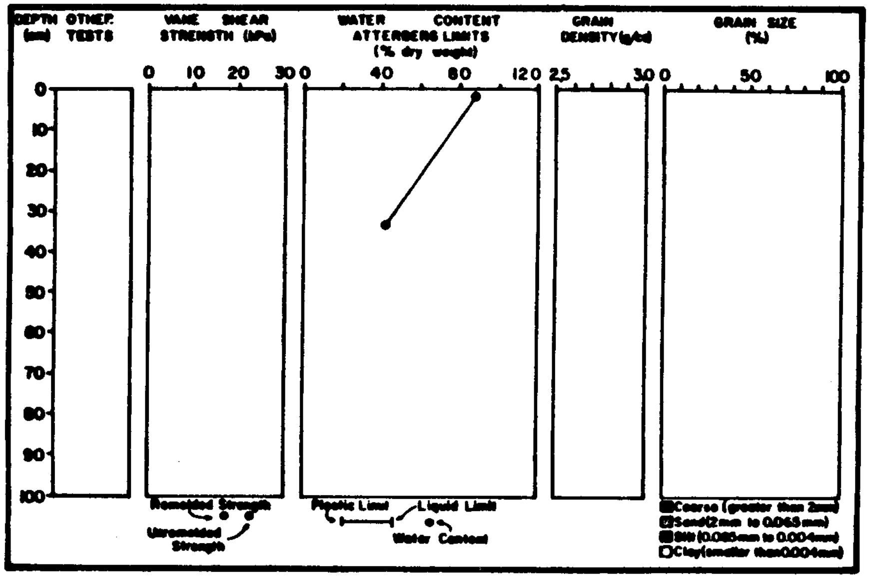

CRUISE: S0-77-EG CORE: 32G

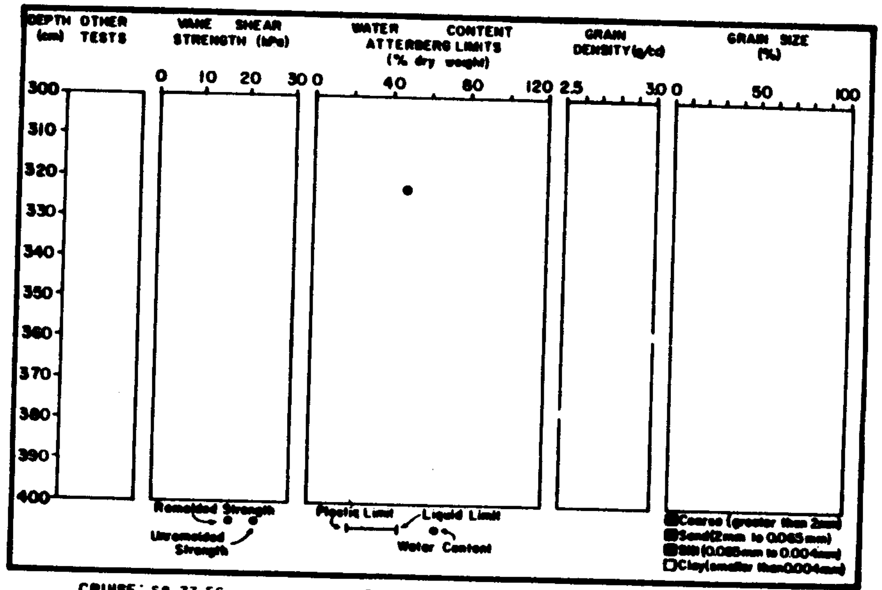

CRUISE: S0-77-EG CORE: 32G

257

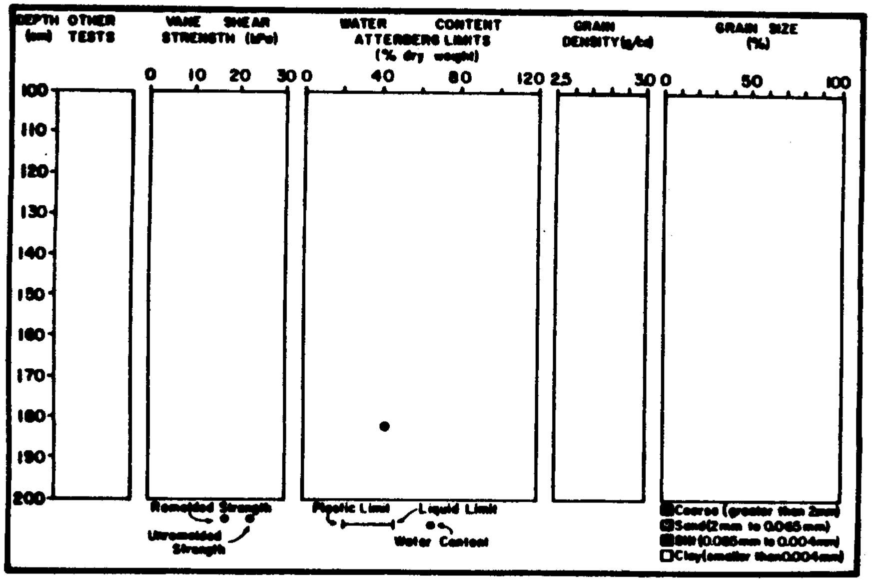

CRUISE: S0-77-EG CORE: 32G

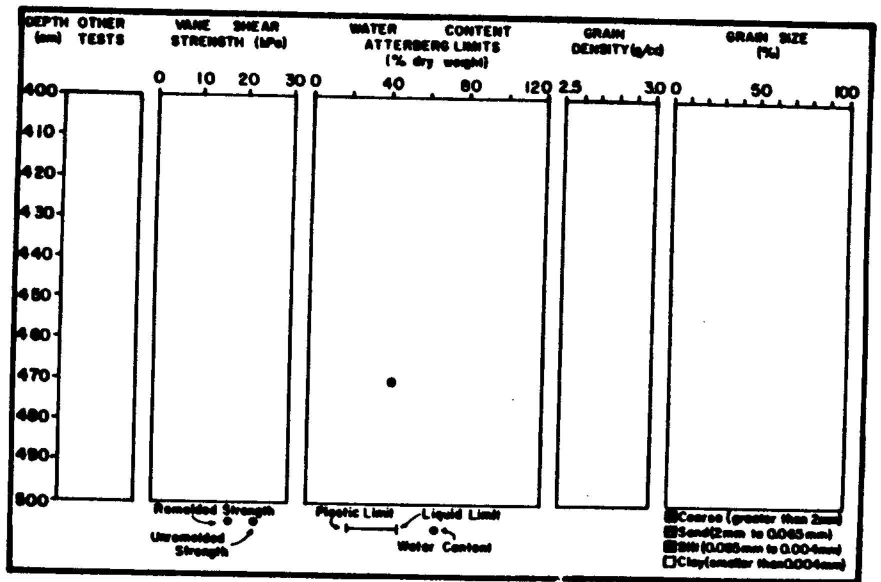

CRUISE: S0-77-EG CORE: 32G

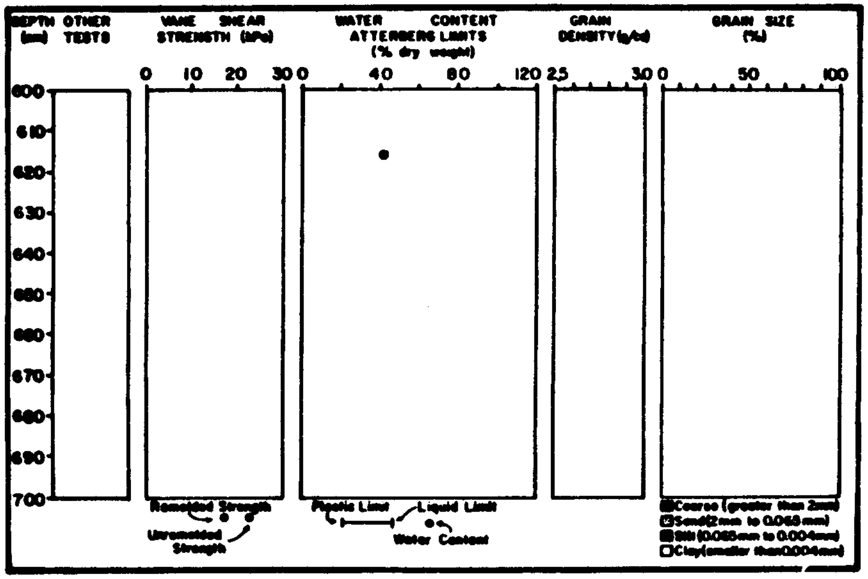

CRUISE: S0-77-EG CORE: 32G

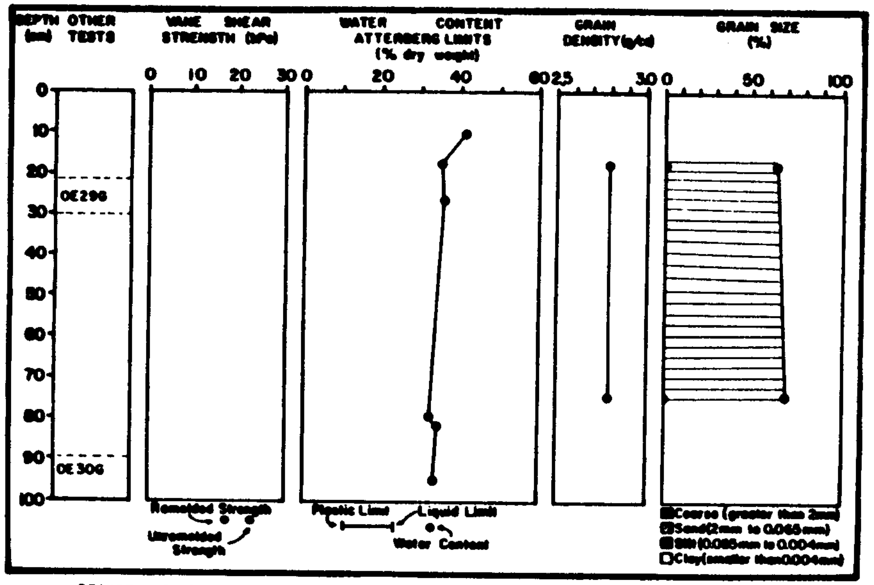

CRUISE: S8-77-EG CORE: 33G

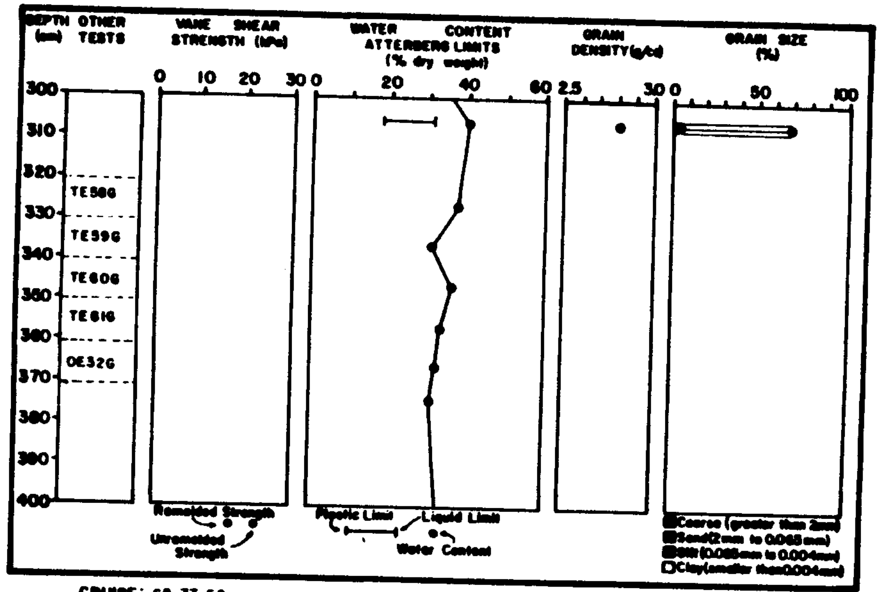

CRUISE: S8-77-EG CORE: 33G

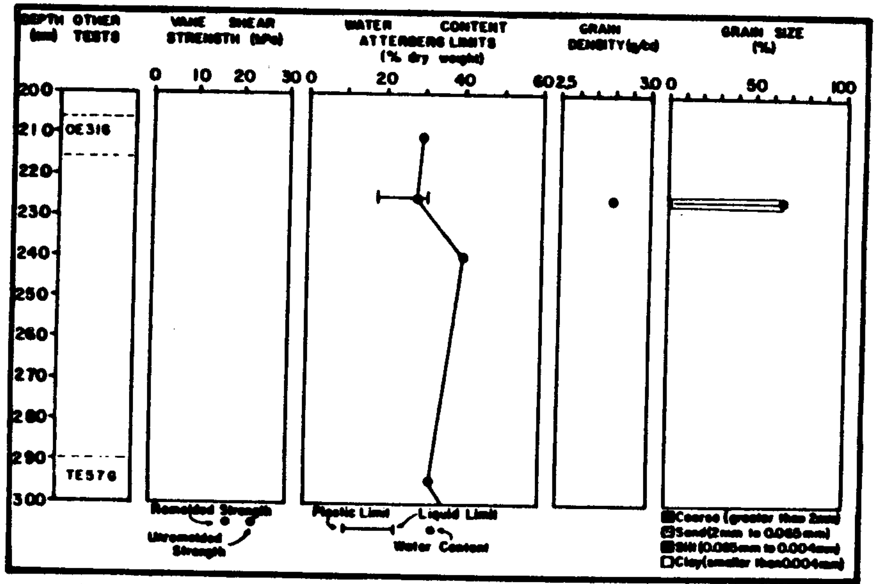

CRUISE: S8-77-EG CORE: 33G

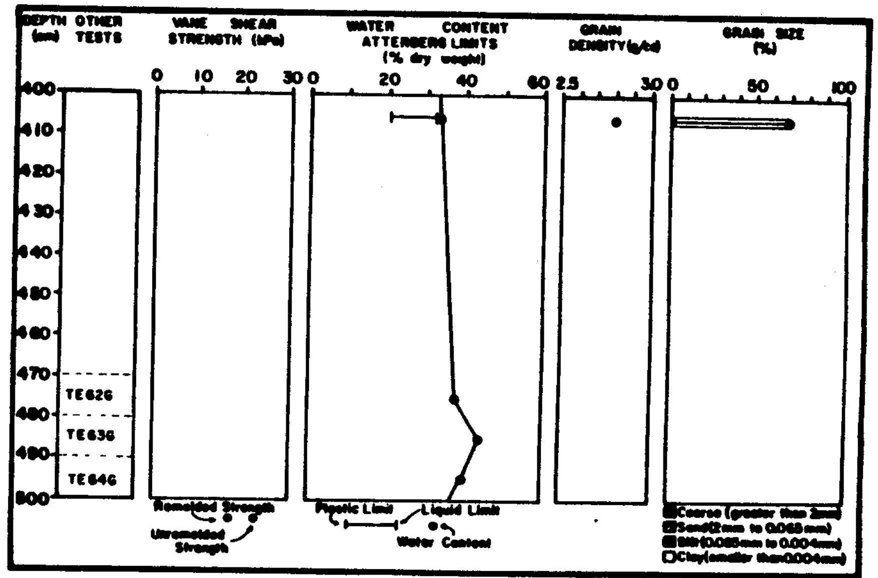

CRUISE: S8-77-EG CORE: 33G

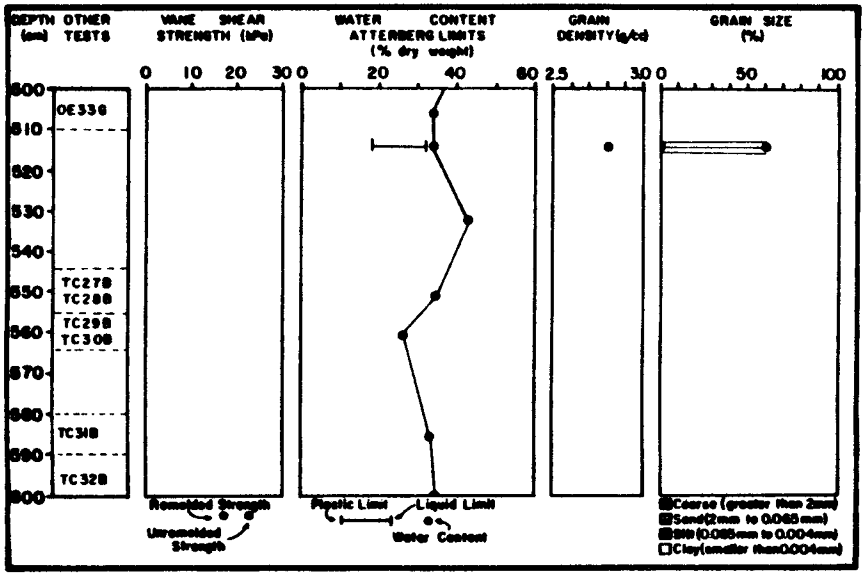

CRUISE: S8-77-EG CORE: 33G

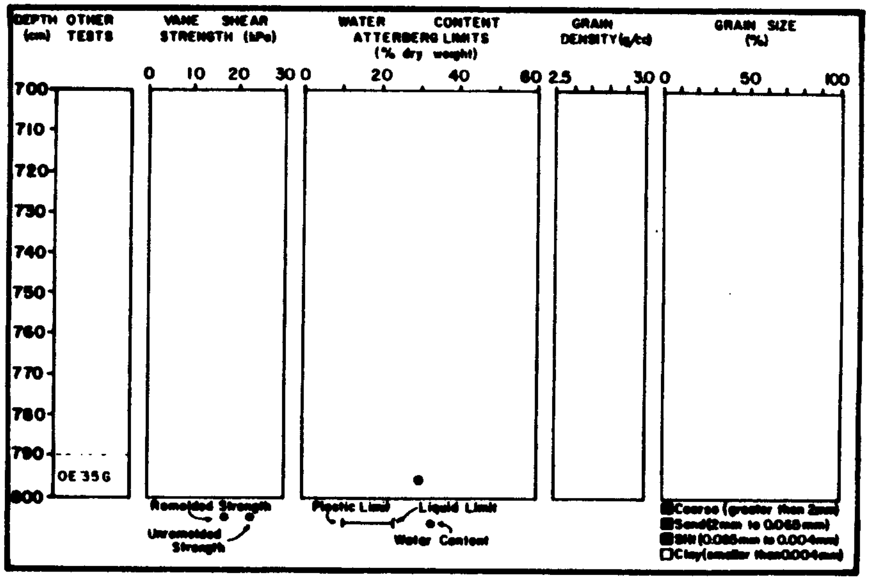

CRUISE: S8-77-EG CORE: 33G

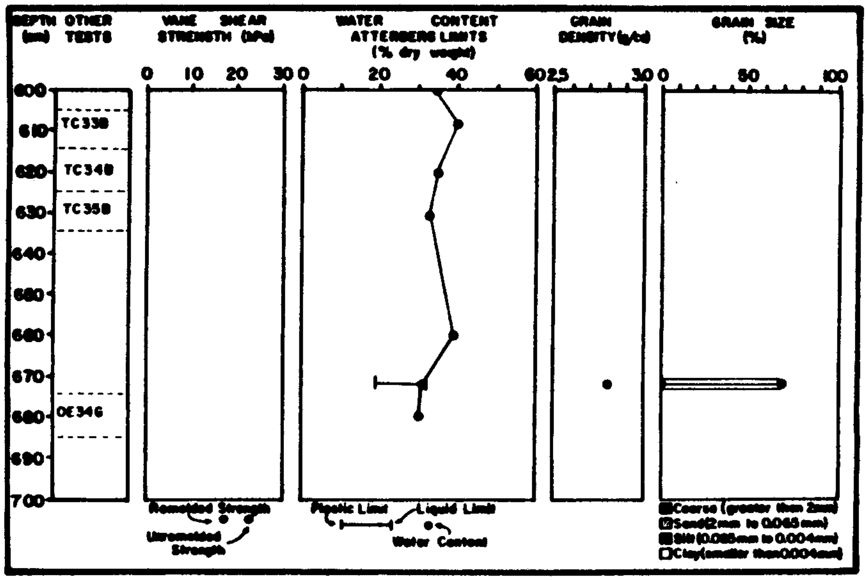

CRUISE: S8-77-EG CORE: 33G

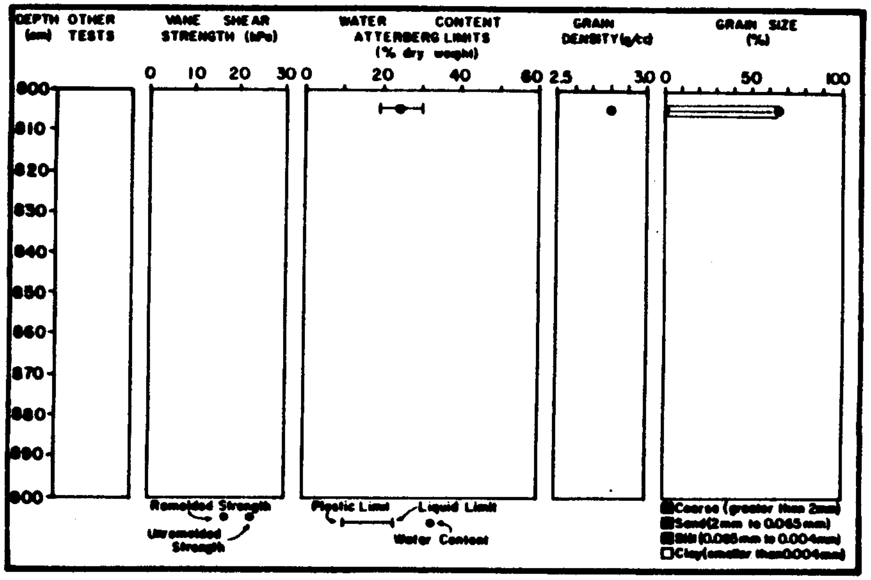

CRUISE: S8-77-EG CORE: 33G

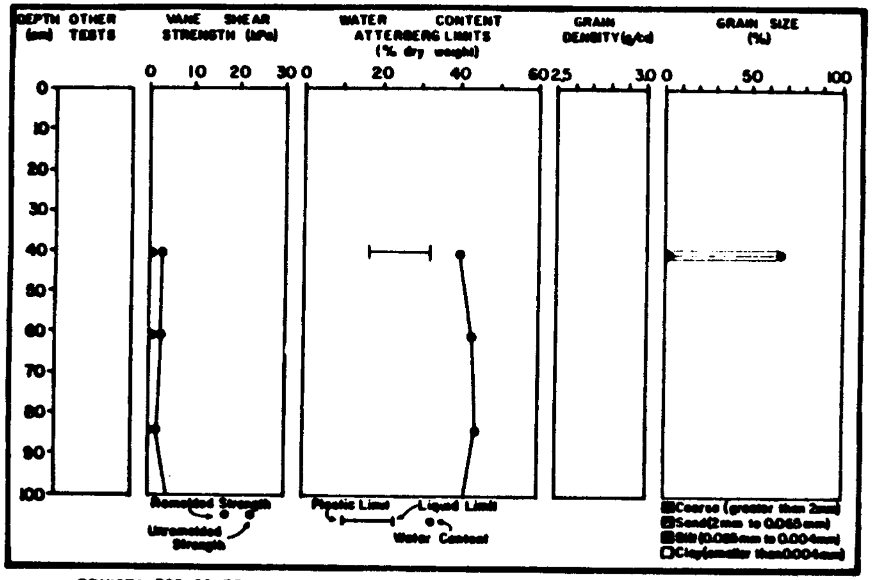

CRUISE: DC2-80-EG CORE: 956

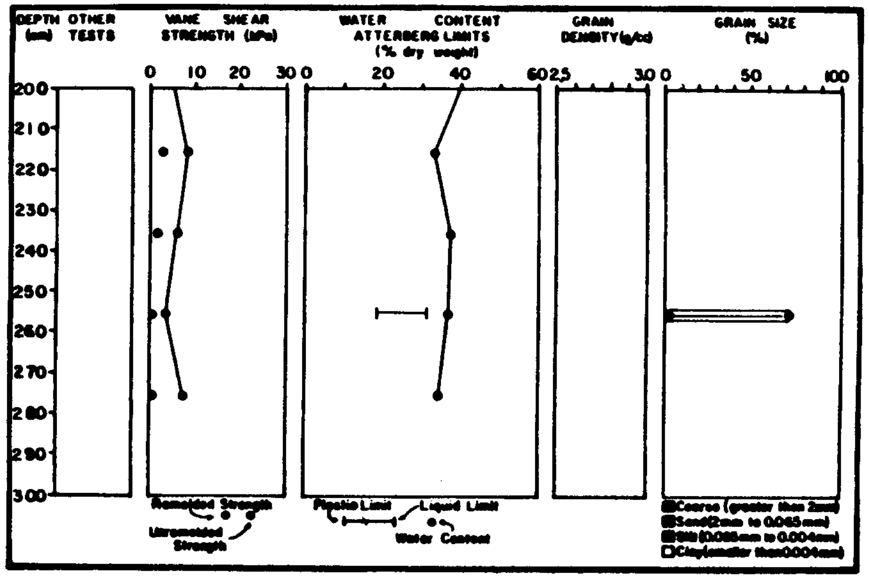

CRUISE: DC2-80-EG CORE: 956

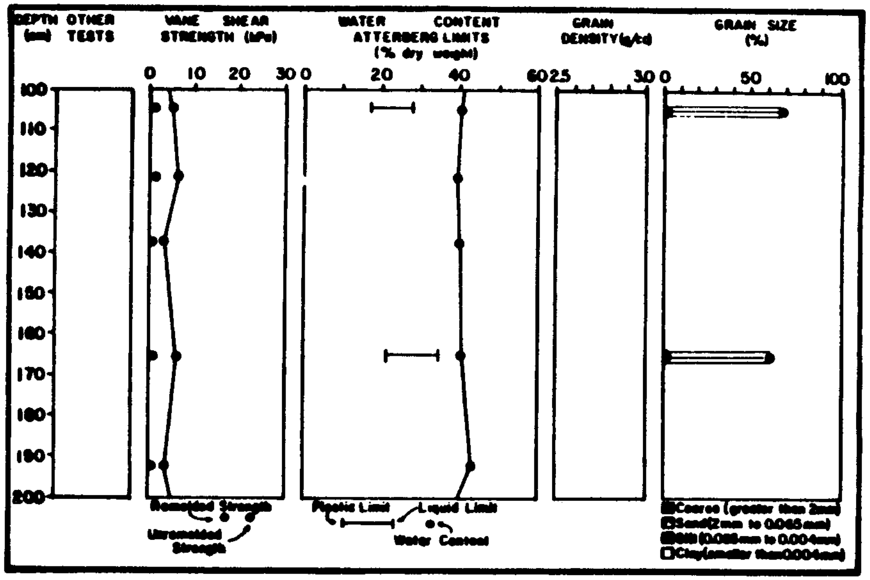

CRUISE: DC2-80-EG CORE: 956

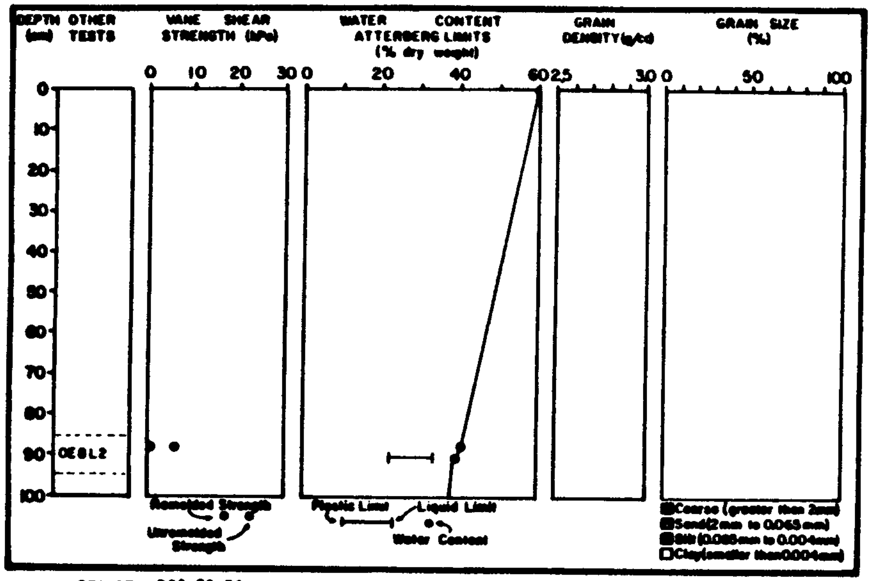

CRUISE: DC2-80-EG CORE: 96G

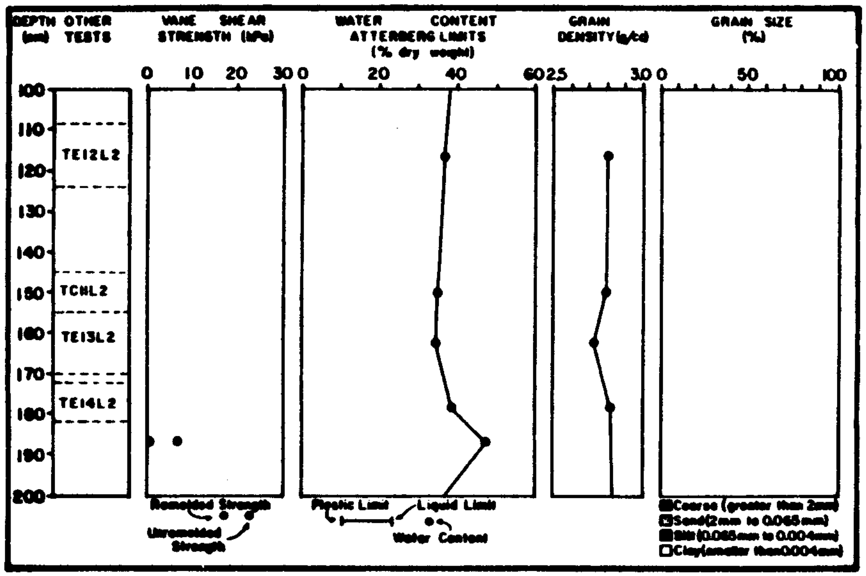

CRUISE: DC2-80-EG CORE: 96G

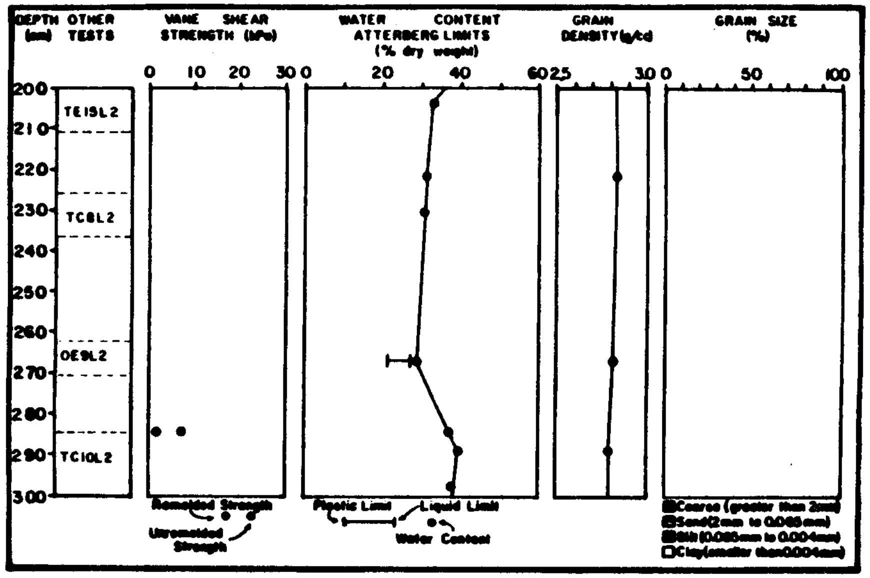

CRUISE: DC2-80-EG CORE: 96G

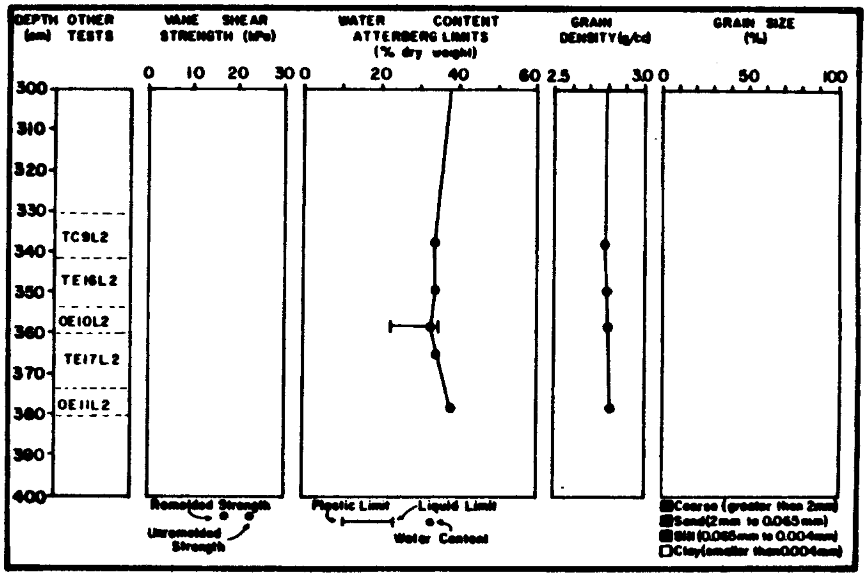

CRUISE: DC2-80-EG CORE: 96G

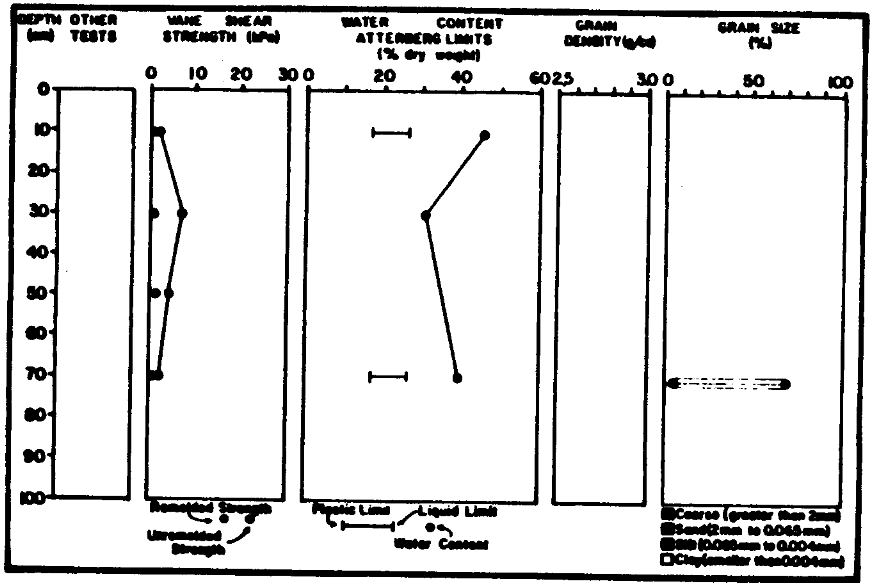

CRUISE: DC2-80-EG CORE: 173G

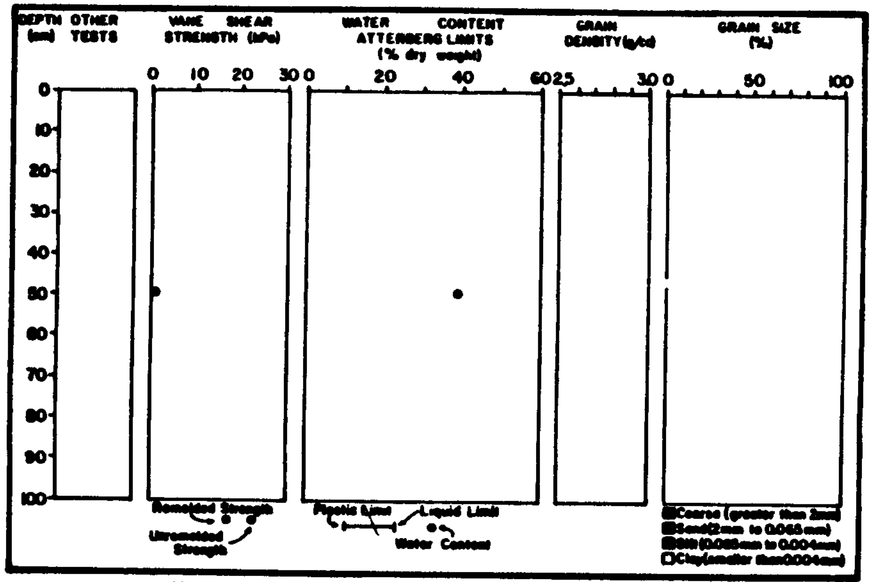

CRUISE: DC2-80-EG CORE: 175G

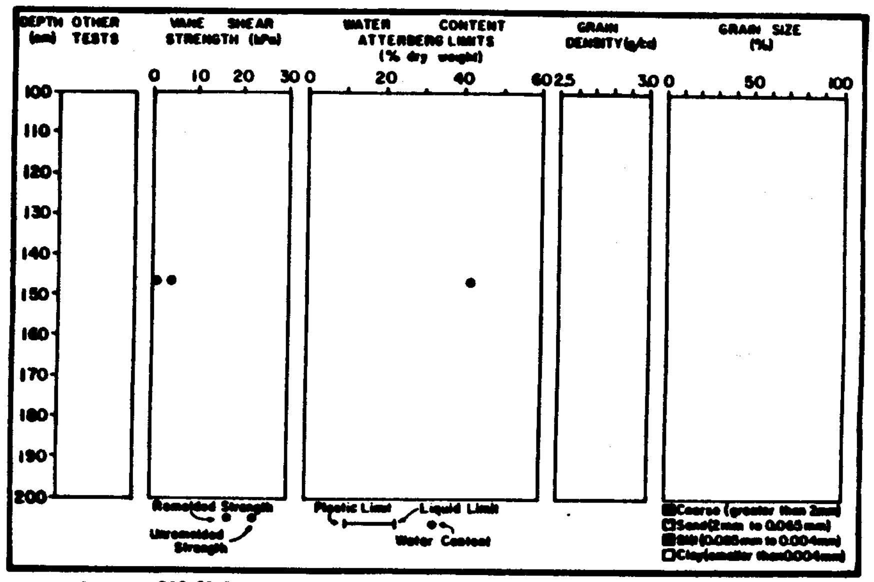

CRUISE: DC2-80-EG CORE: 175G

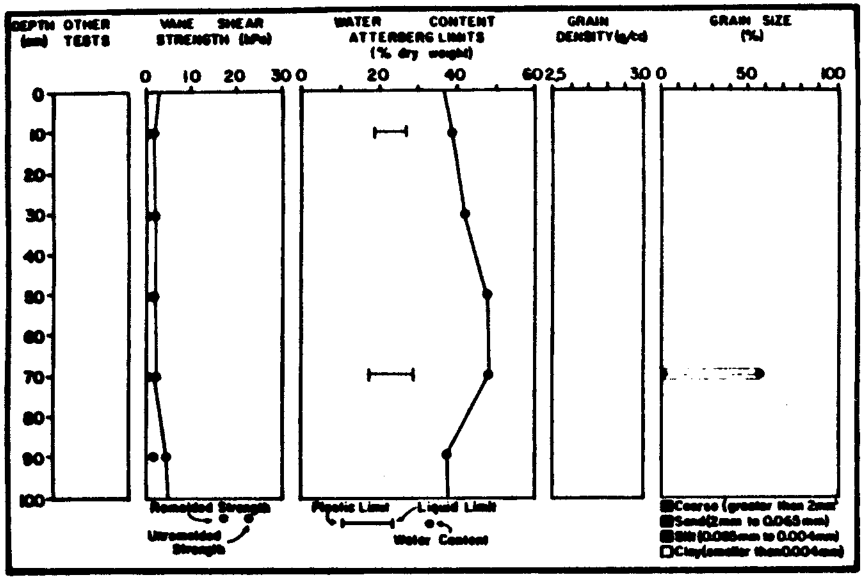

CRUISE: DC2-80-EG CORE: 176G

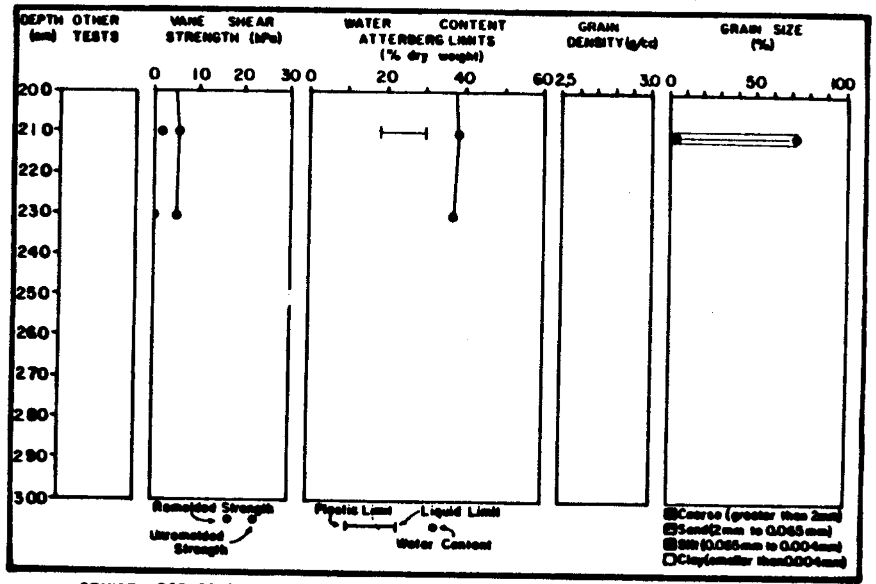

CRUISE: DC2-80-EG CORE: 176G

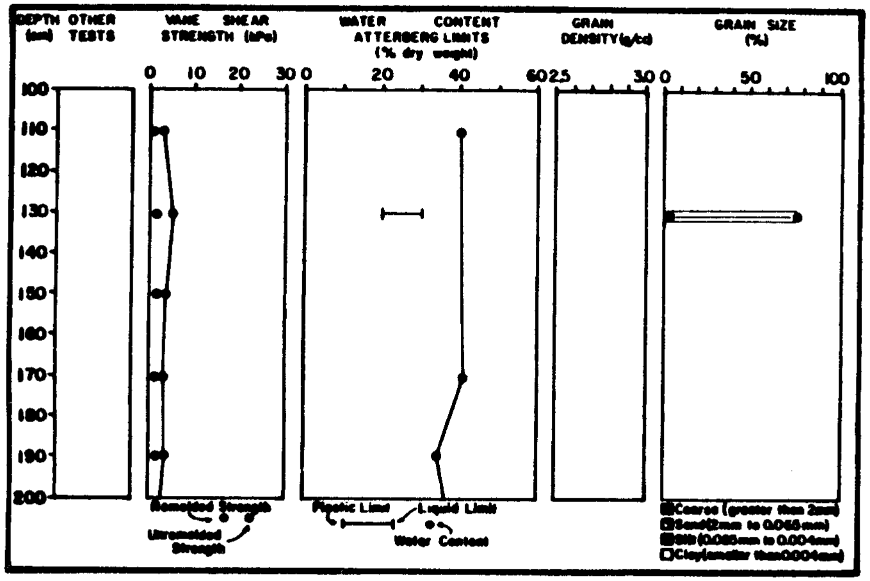

CRUISE: DC2-80-EG CORE: 176G

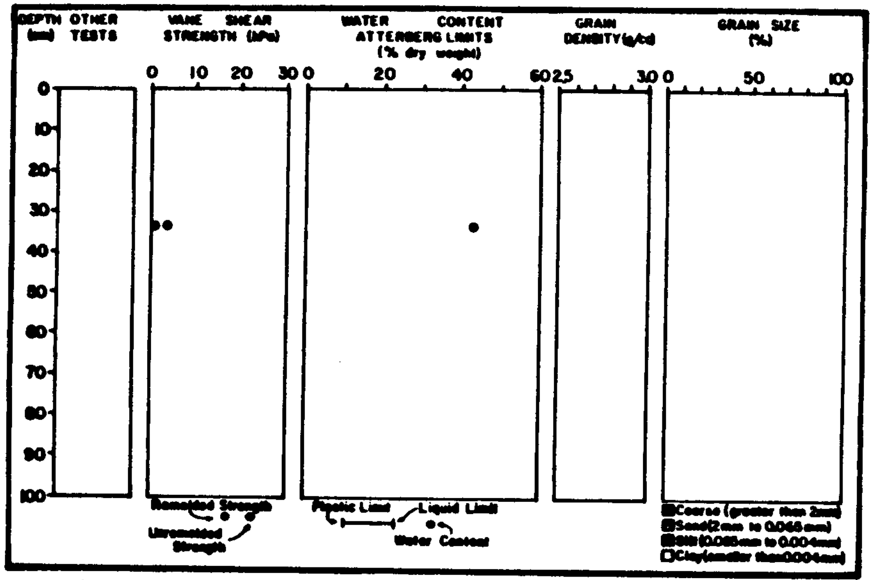

CRUISE: DC2-80-EG CORE: 178G

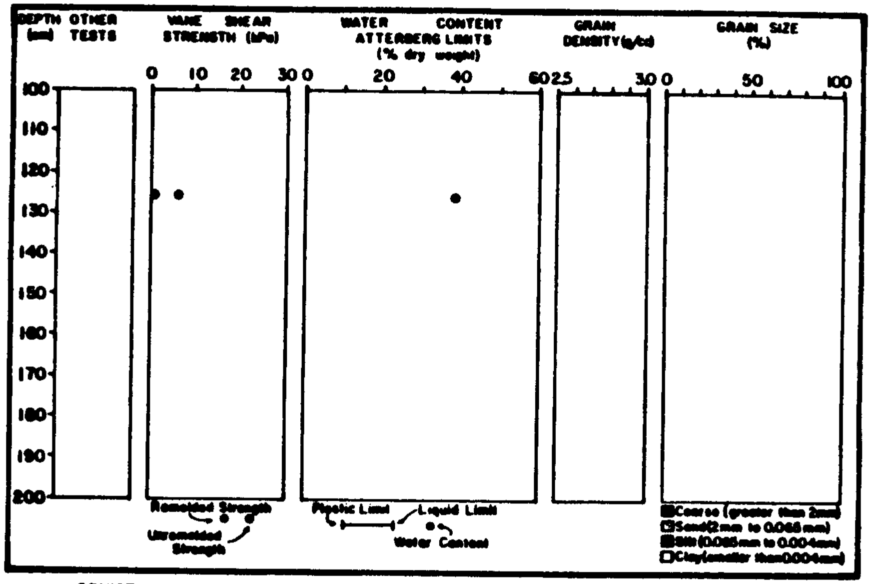

CRUISE: DC2-80-EG CORE: 178G

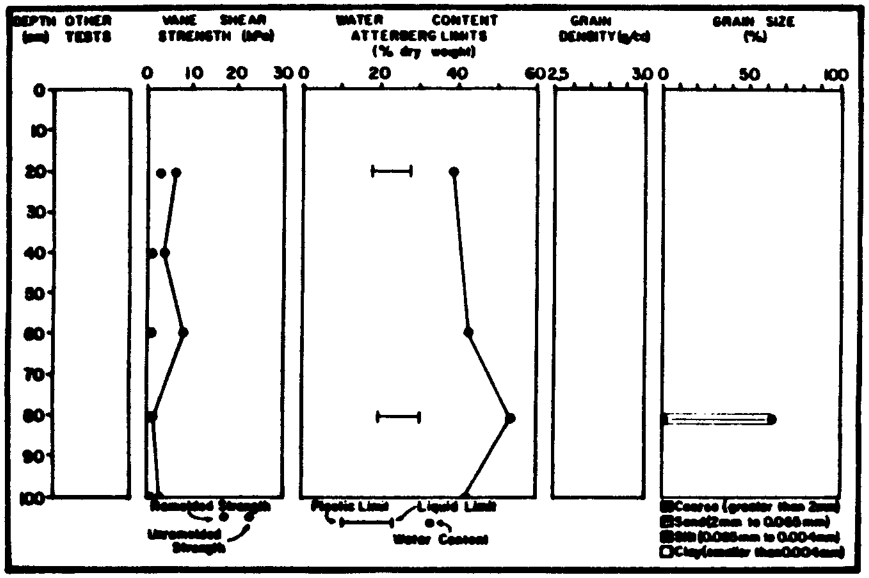

CRUISE: DC2-80-E6 CORE: 1796

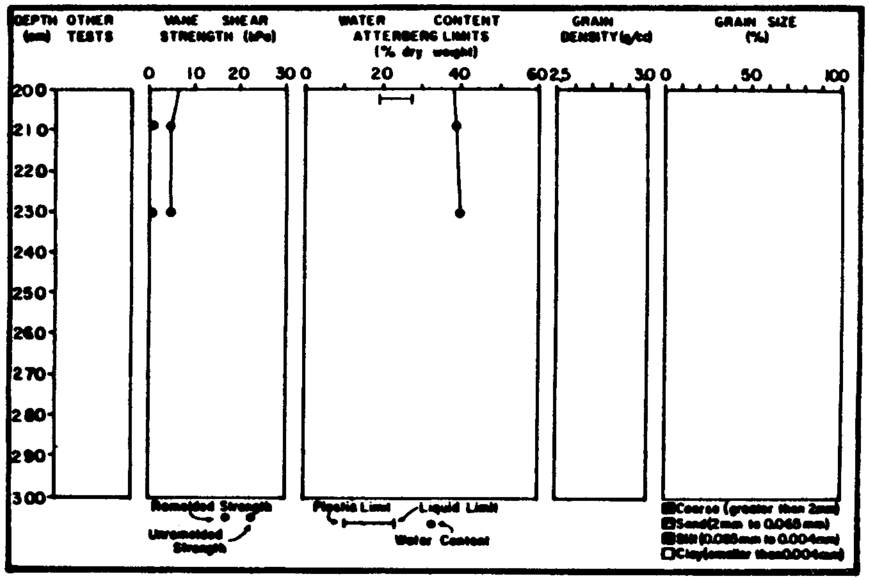

CRUISE: DC2-80-E6 CORE: 1796

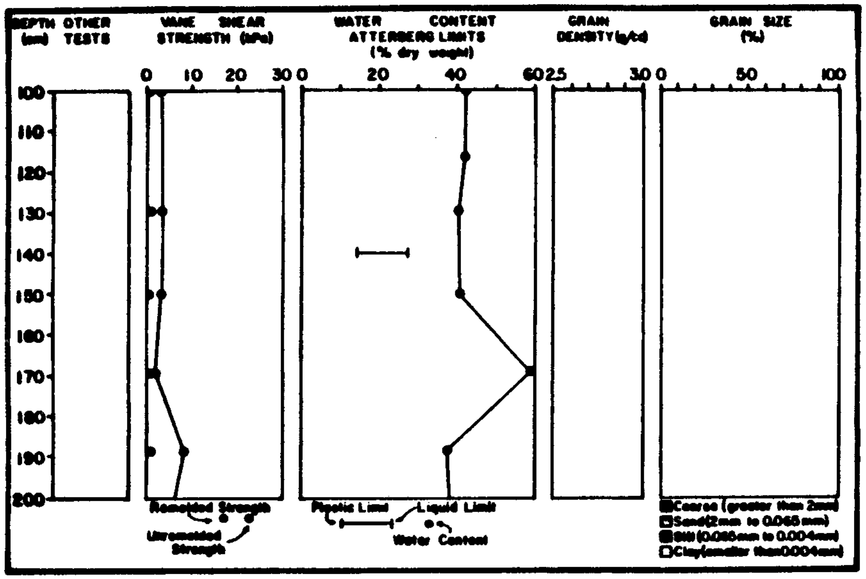

CRUISE: DC2-80-E6 CORE: 1796

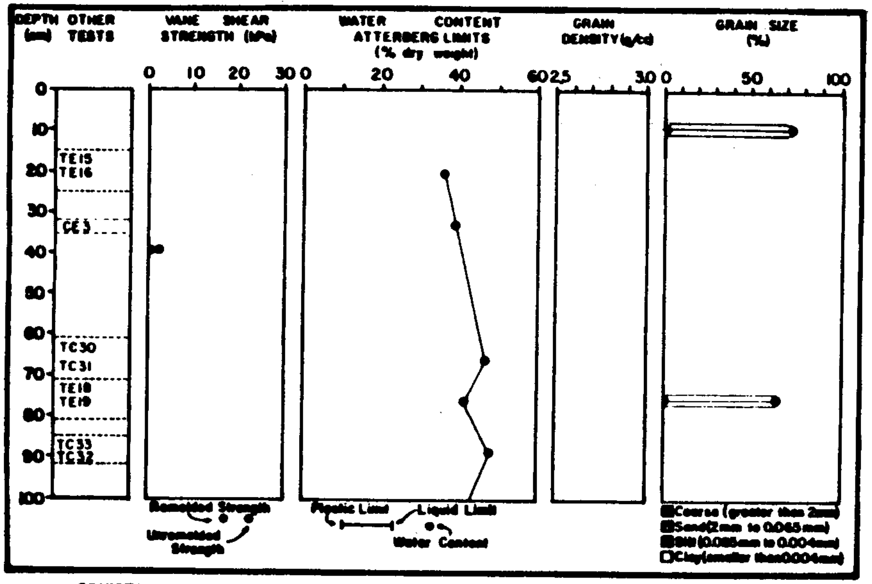

CRUISE: DC2-80-EG CORE: 181G

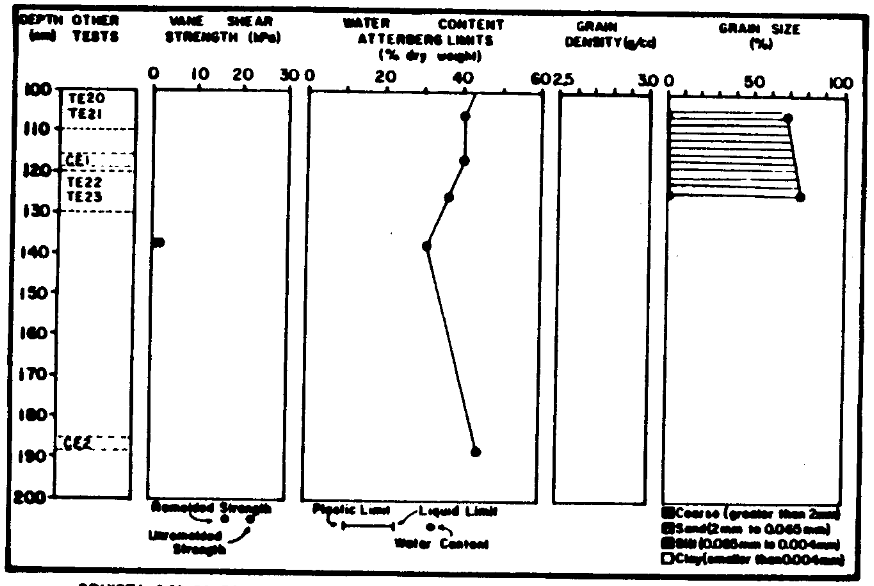

CRUISE: DC2-80-EG CORE: 181G

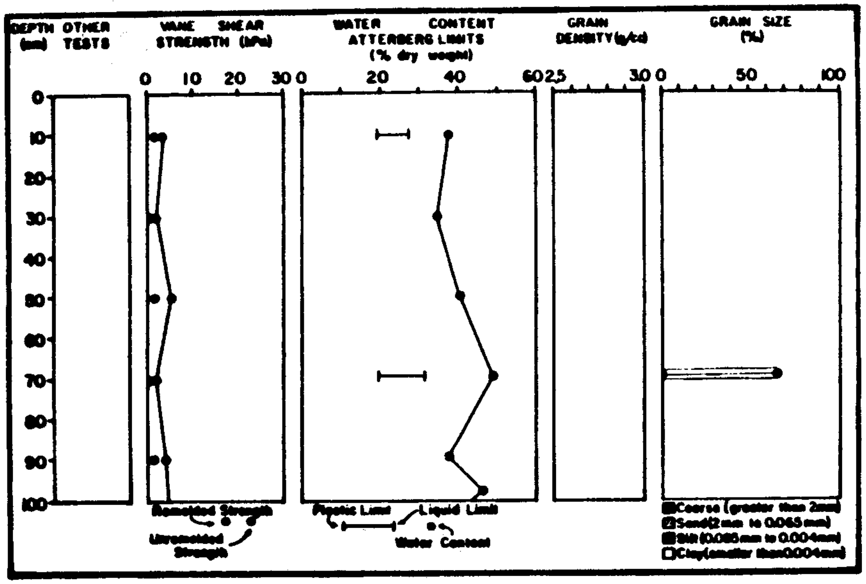

CRUISE: DC2-80-E6 CORE: 1826

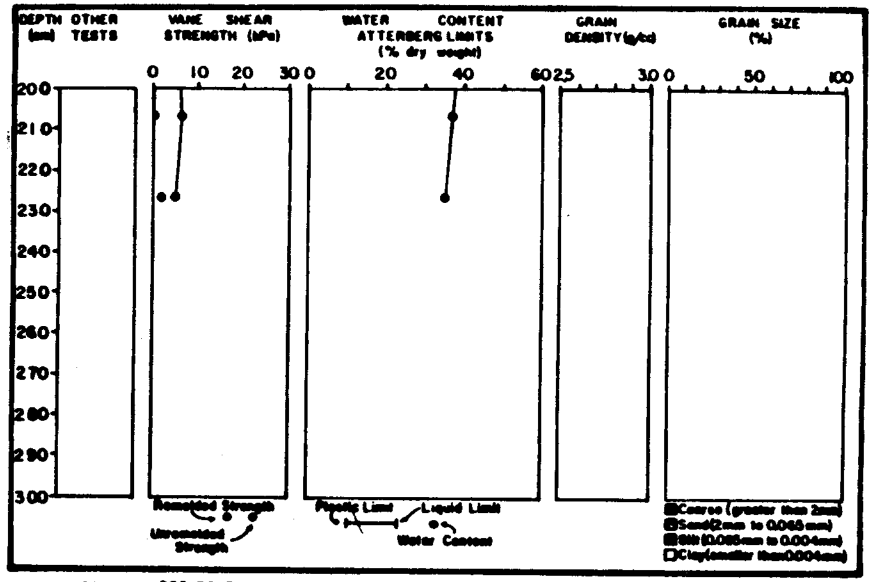

CRUISE: DC2-80-E6 CORE: 1826

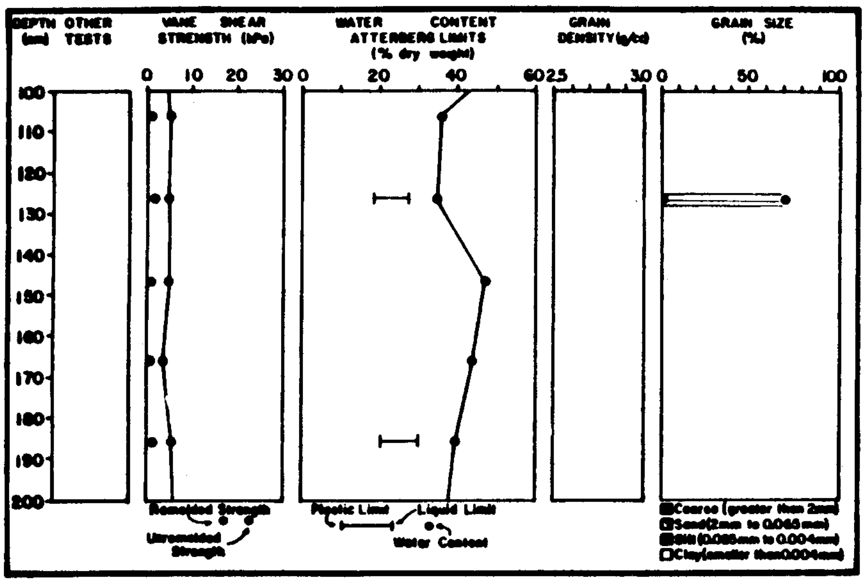

CRUISE: DC2-80-E6 CORE: 1826

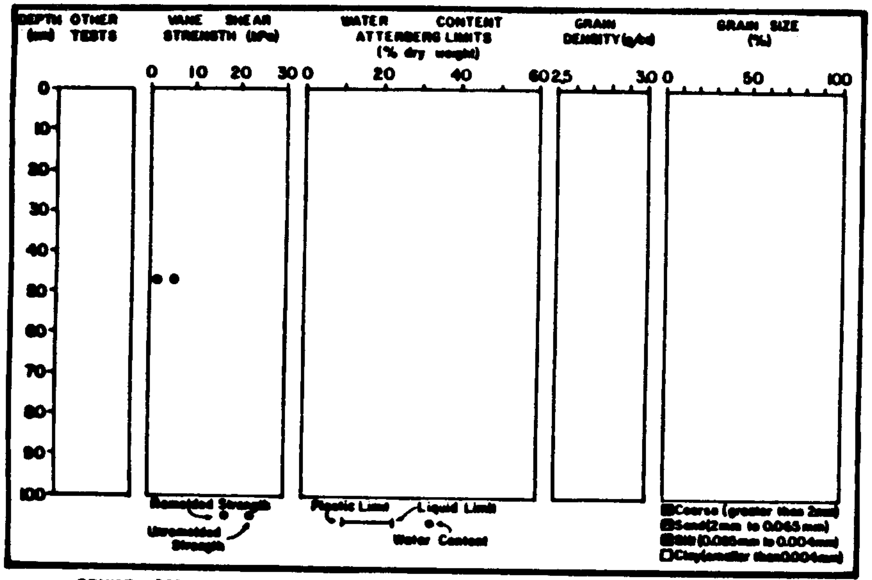

CRUISE: DC2-80-EG CORE: 184G

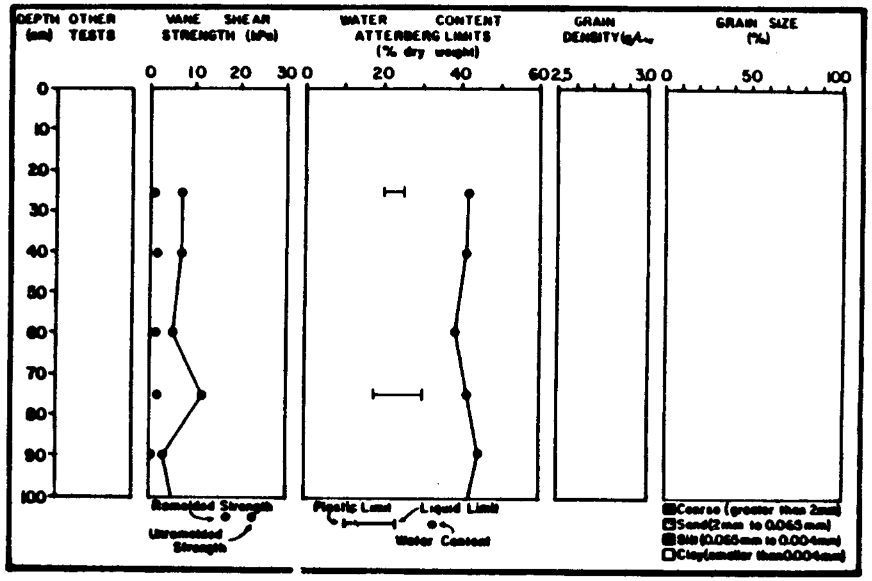

CRUISE: DC2-80-EG CORE: 185G

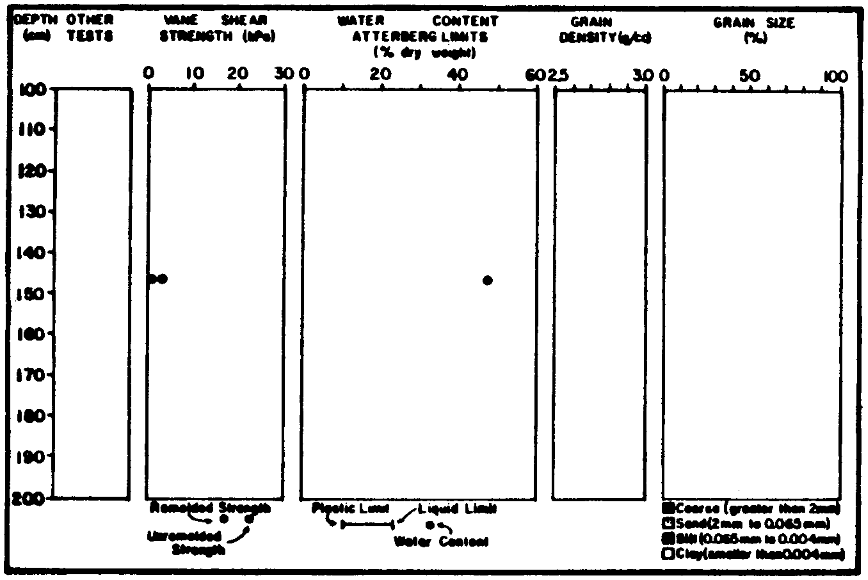

CRUISE: DC2-80-EG CORE: 184G

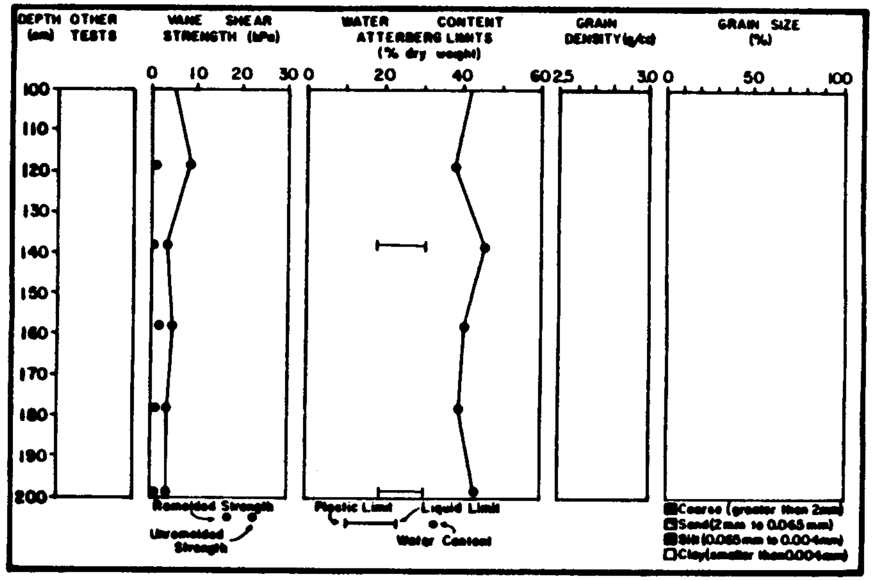

CRUISE: DC2-80-EG CORE: 185G

270

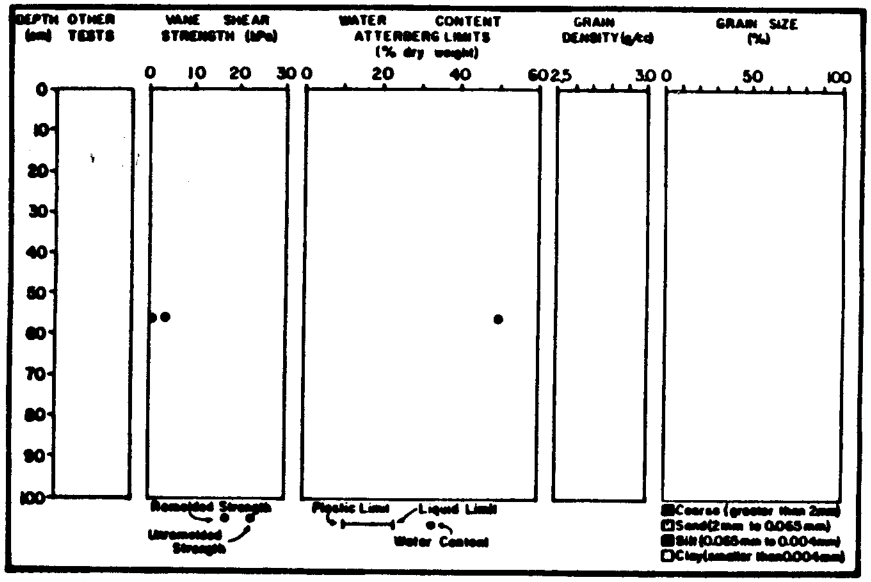

CRUISE: DC2-80-EG CORE: 187G

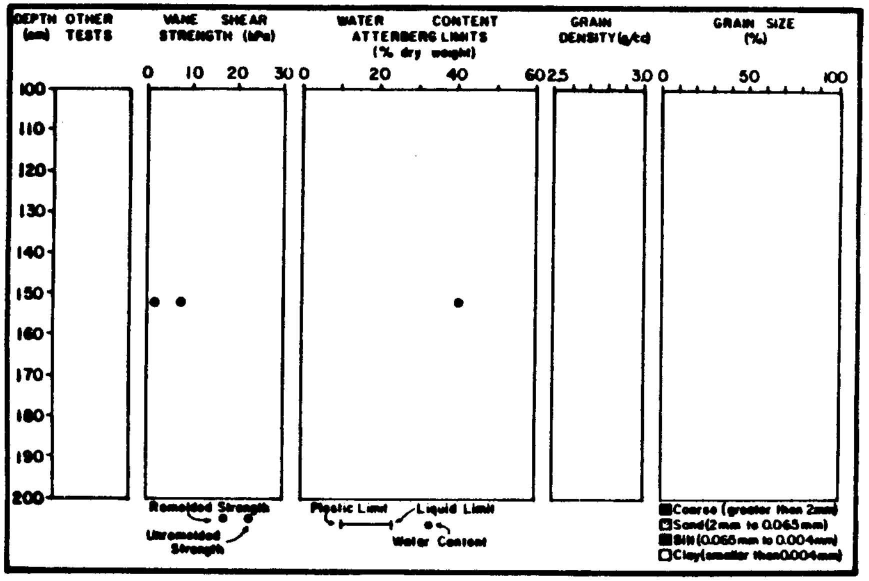

CRUISE: DC2-80-EG CORE: 187G

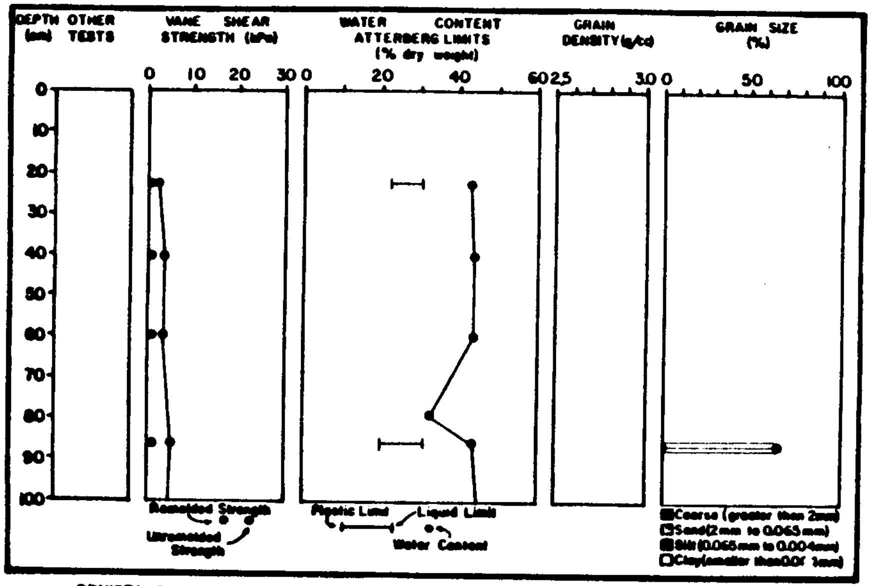

CRUISE: DC2-80-EG CORE: 186G

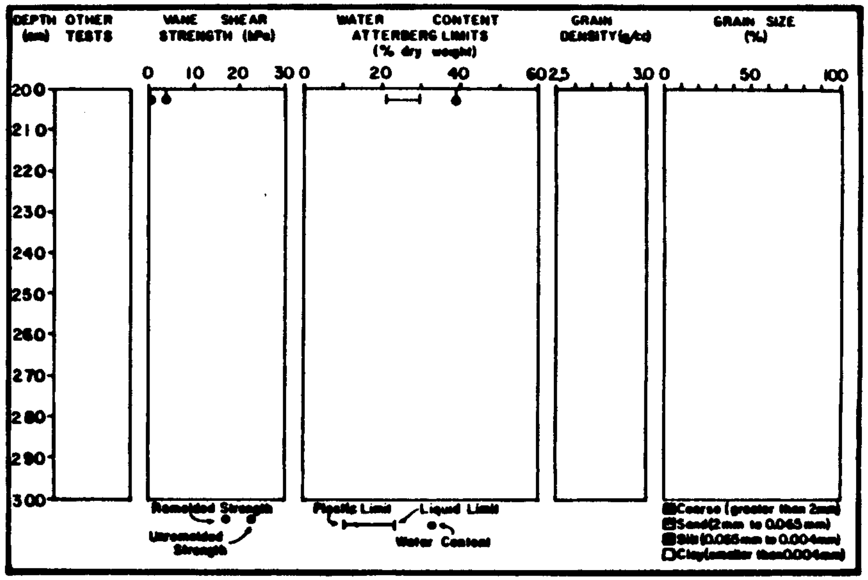

CRUISE: DC2-80-EG CORE: 186G

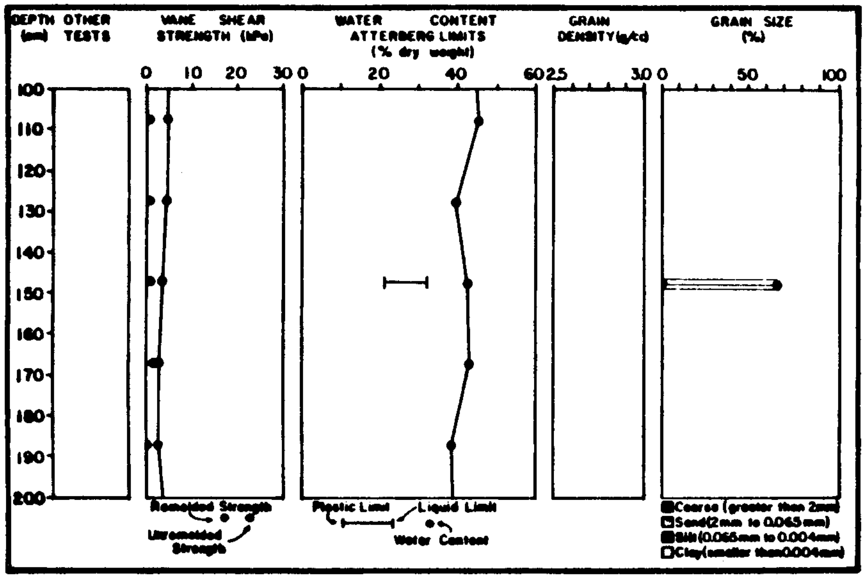

CRUISE: DC2-80-EG CORE: 186G

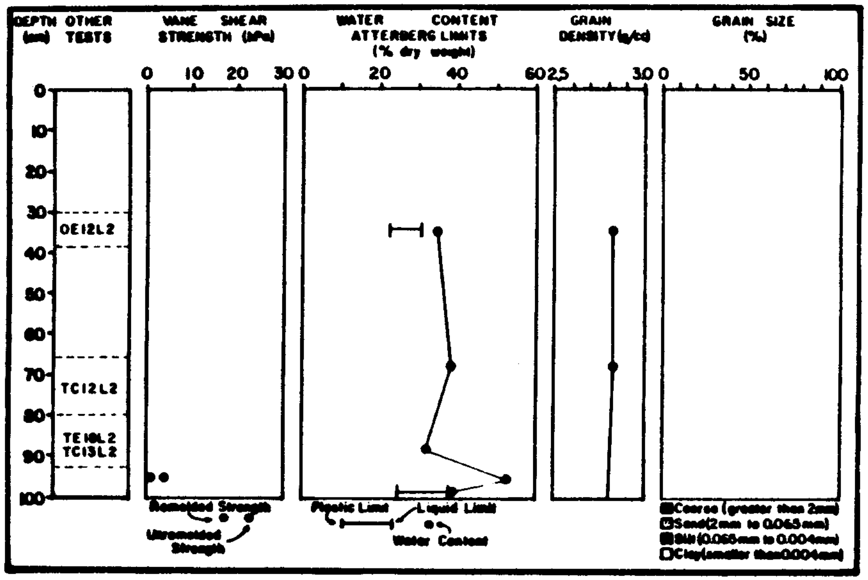

CRUISE: DC2-80-EG CORE: 1906

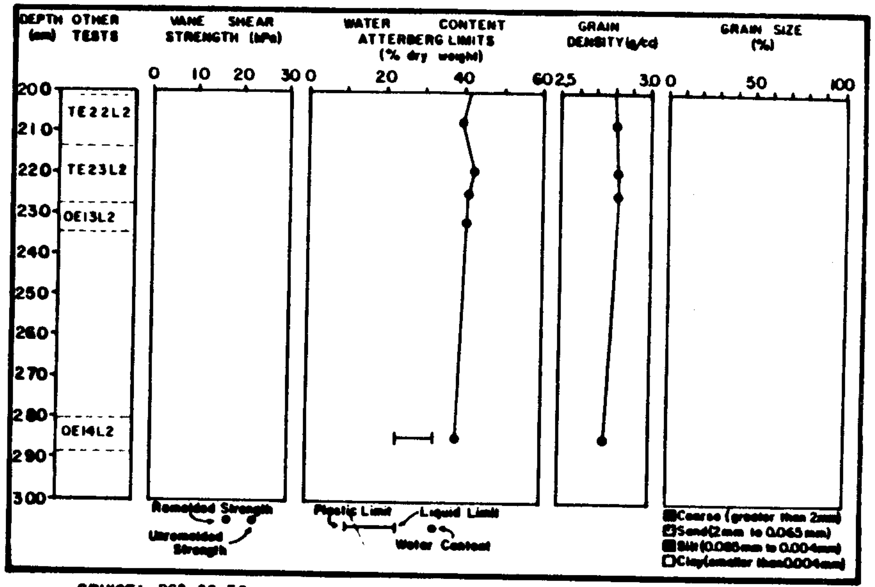

CRUISE: DC2-80-EG CORE: 1906

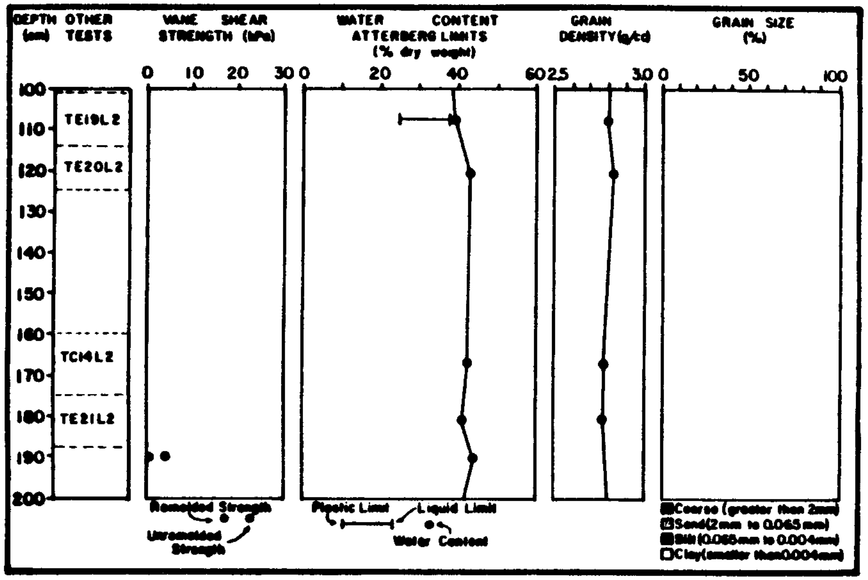

CRUISE: DC2-80-EG CORE: 1906

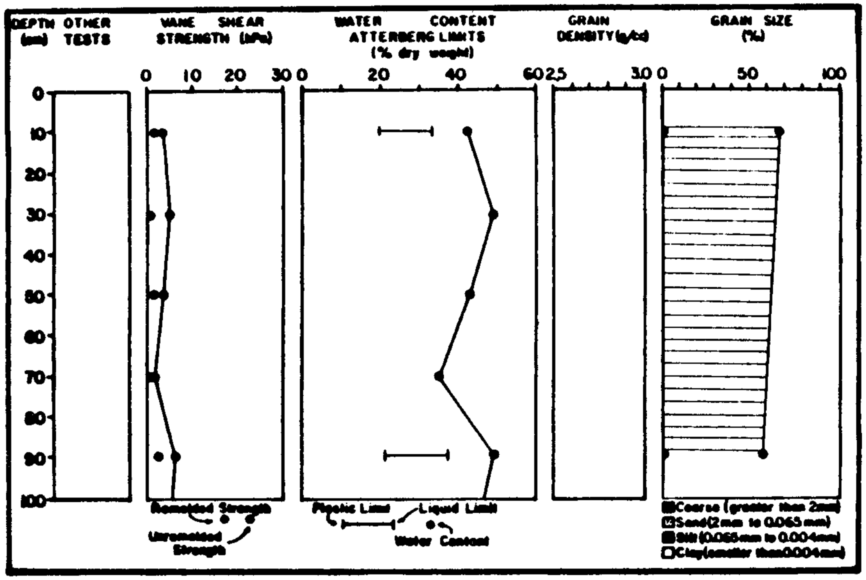

CRUISE: DC2-80-EG CORE: 191G

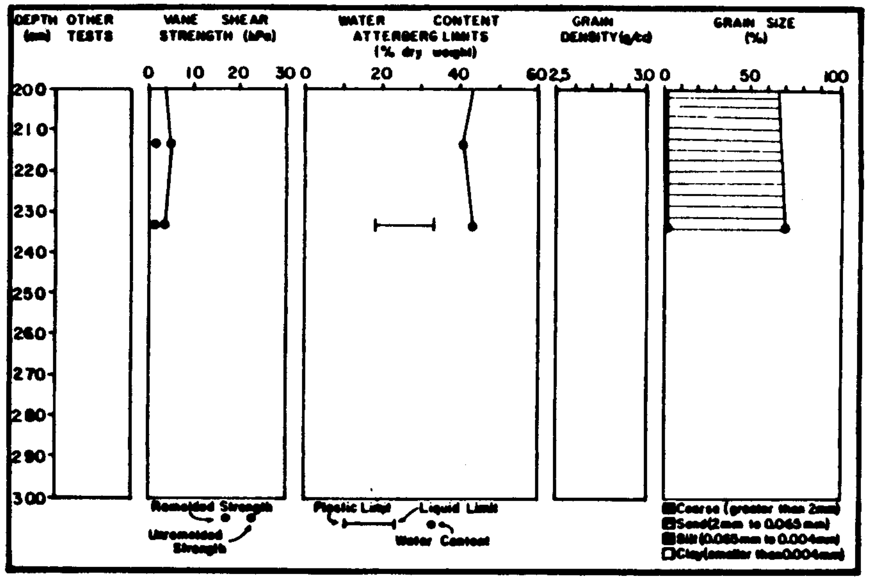

CRUISE: DC2-80-EG CORE: 191G

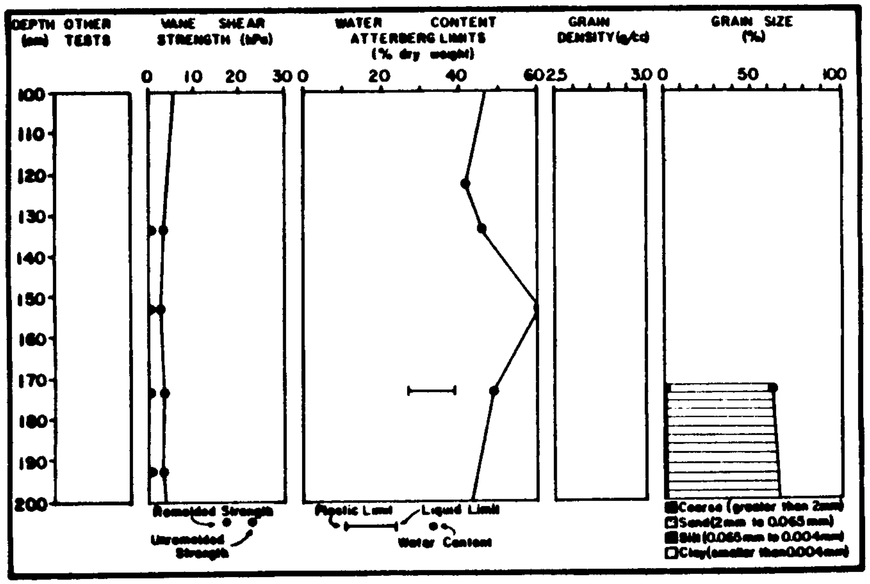

CRUISE: DC2-80-EG CORE: 191G

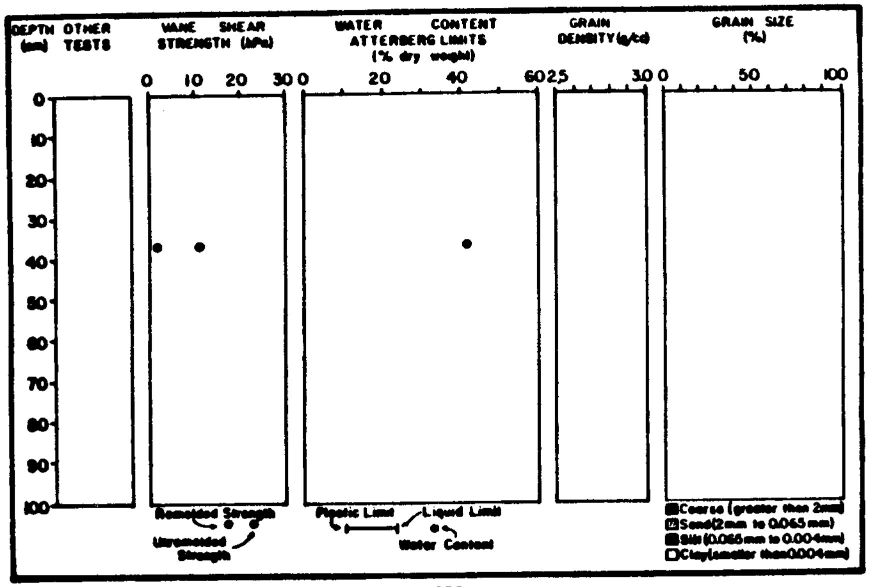

CRUISE: DC2-80-EG CORE: 193G

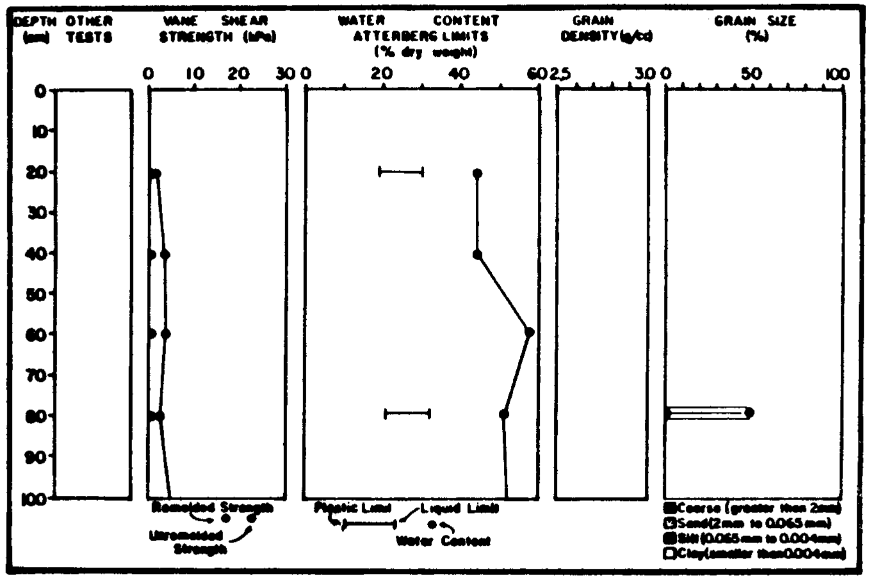

CRUISE: DC2-80-EG CORE: 194G

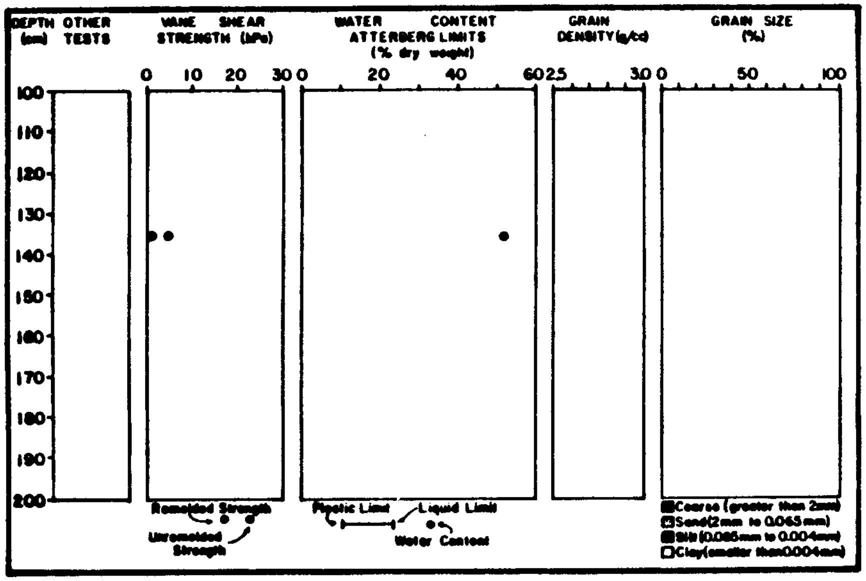

CRUISE: DC2-80-EG CORE: 193G

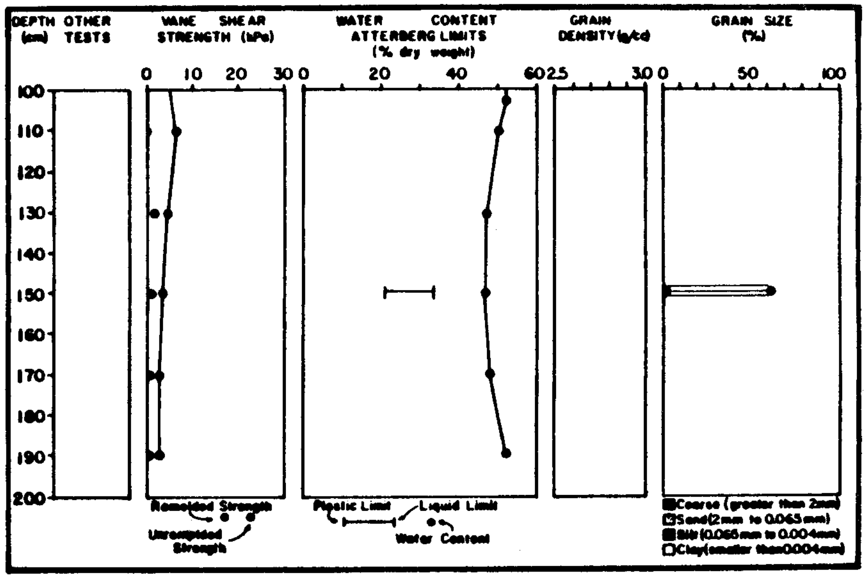

CRUISE: DC2-80-EG CORE: 194G

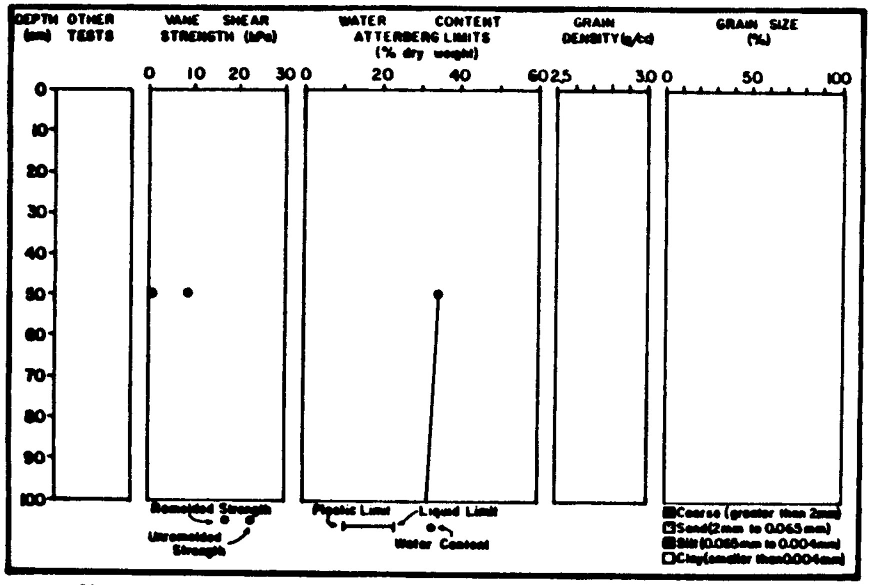

CRUISE: DC2-80-EG CORE: 1966

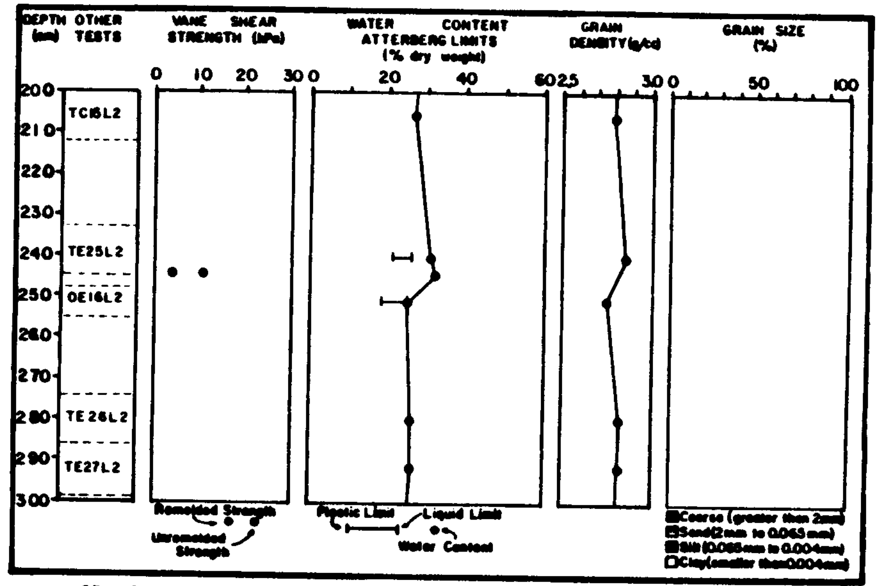

CRUISE: DC2-80-EG CORE: 1966

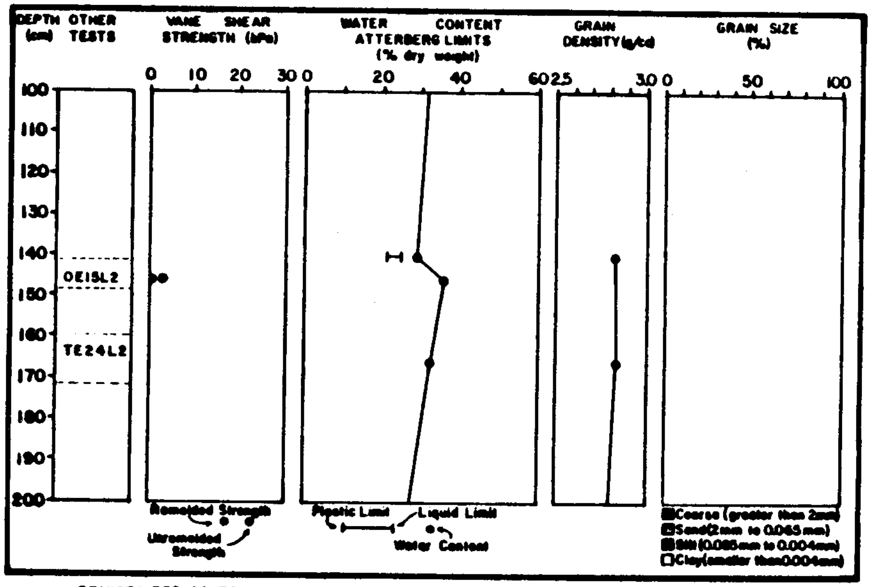

CRUISE: DC2-80-EG CORE: 1966

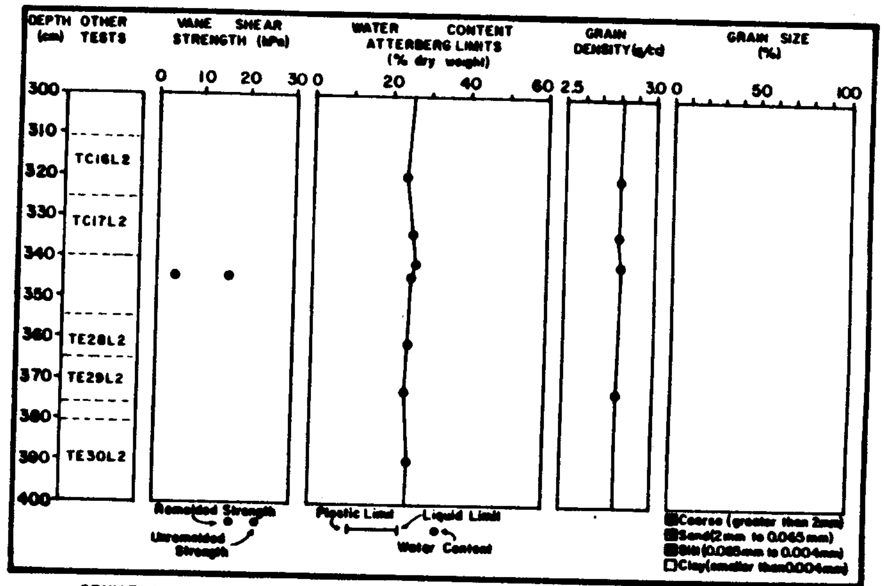

CRUISE: DC2-80-EG CORE: 1966

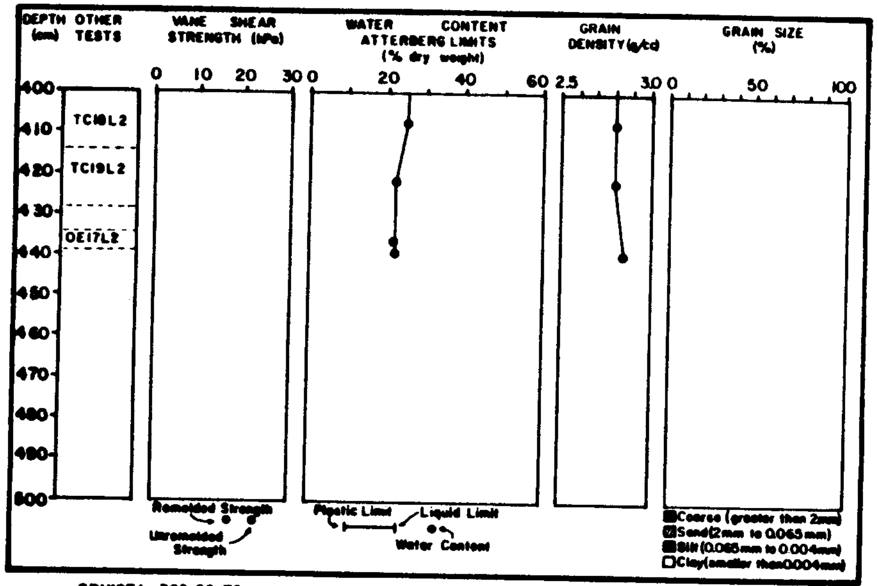

CRUISE: DC2-80-E8 CORE: 1966

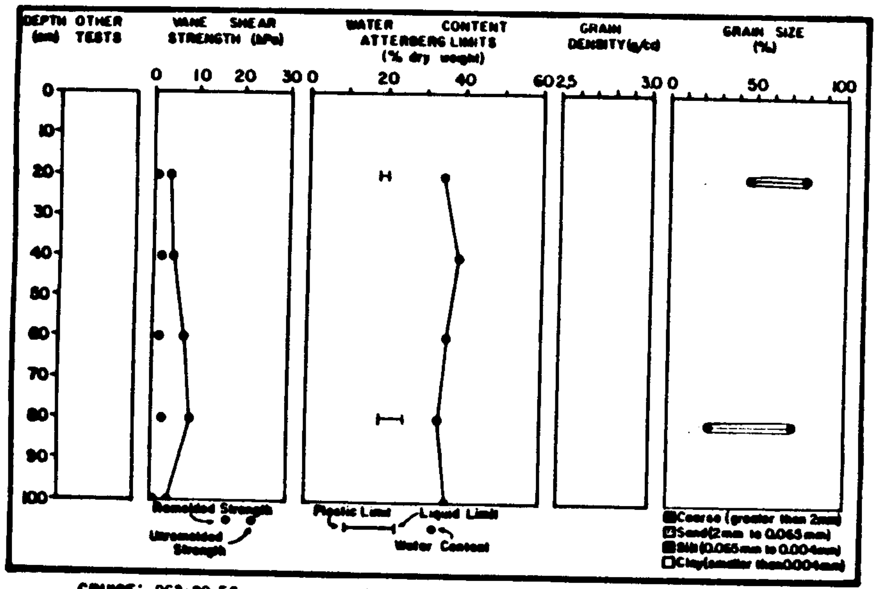

CRUISE: DC2-80-EG CORE: 197G

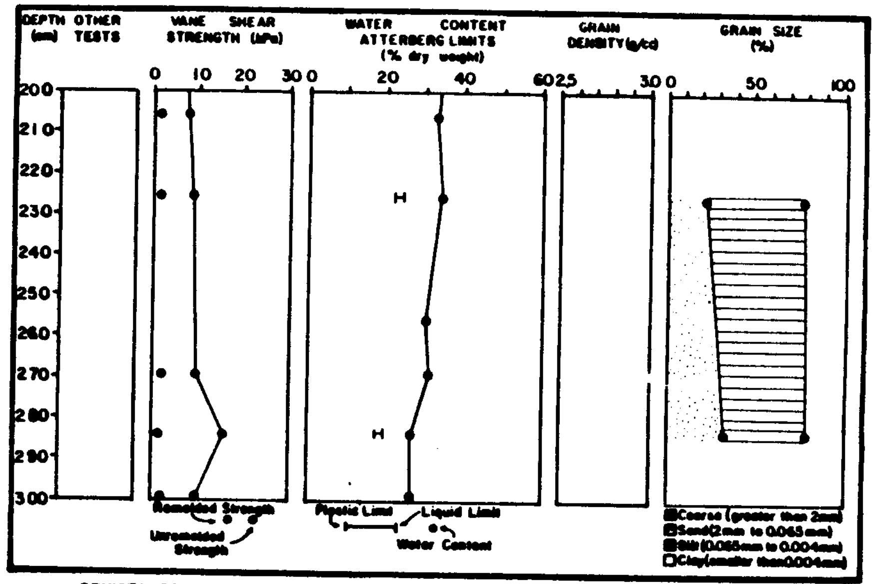

CRUISE: DC2-80-EG CORE: 197G

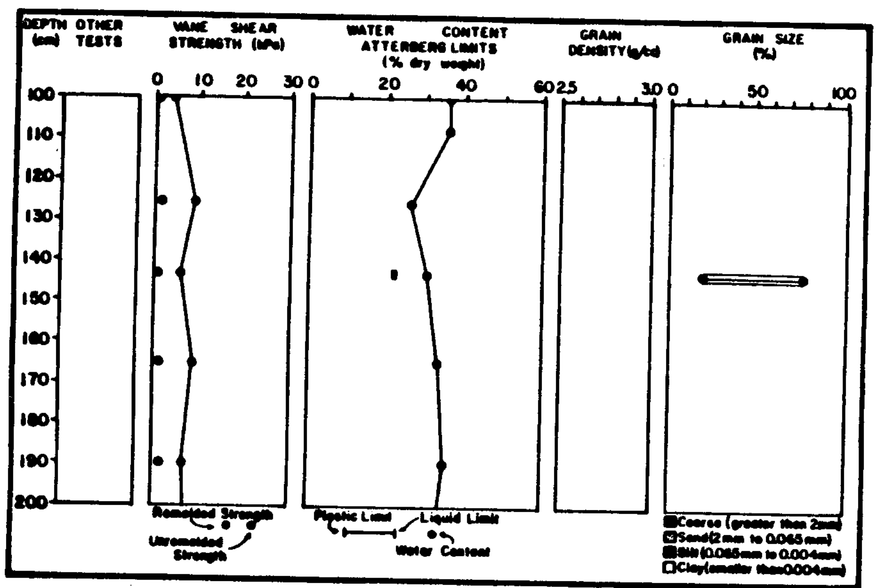

CRUISE: DC2-80-EG CORE: 197G

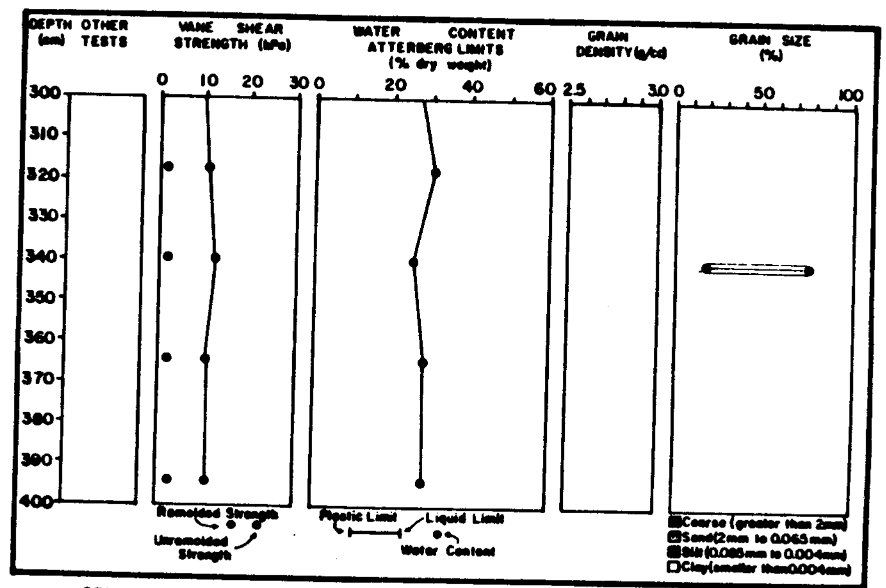

CRUISE: DC2-80-EG CORE: 197G

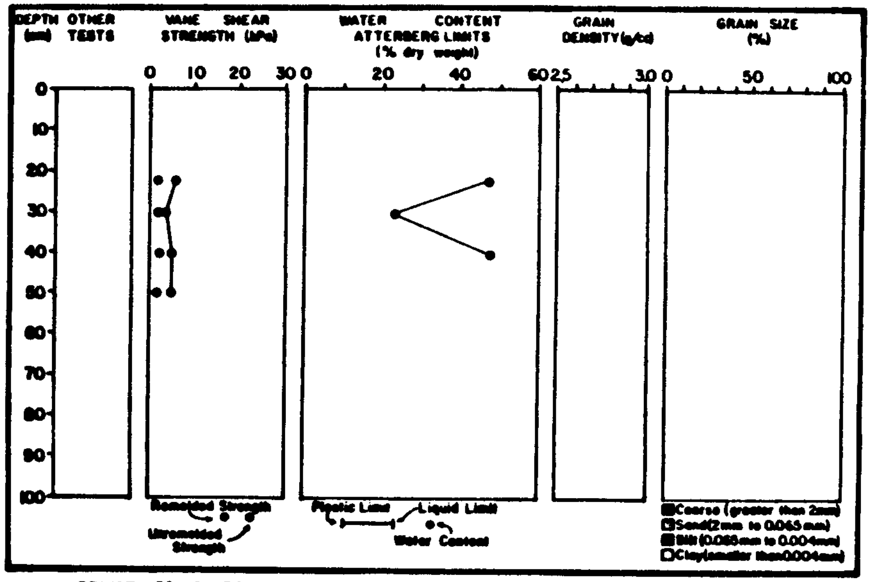

CRUISE: DCI-81-EG CORE: 626G3

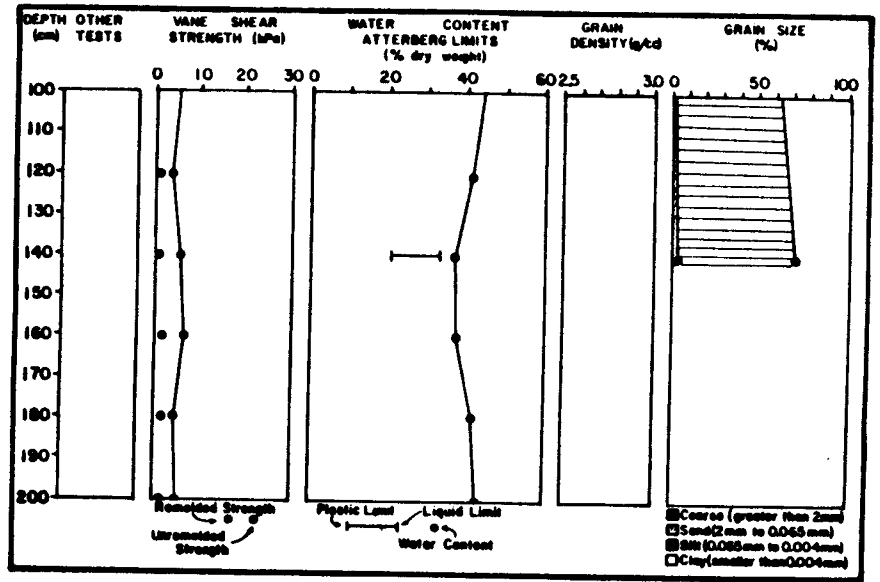

CRUISE: DCI-81-EG CORE: 627G1

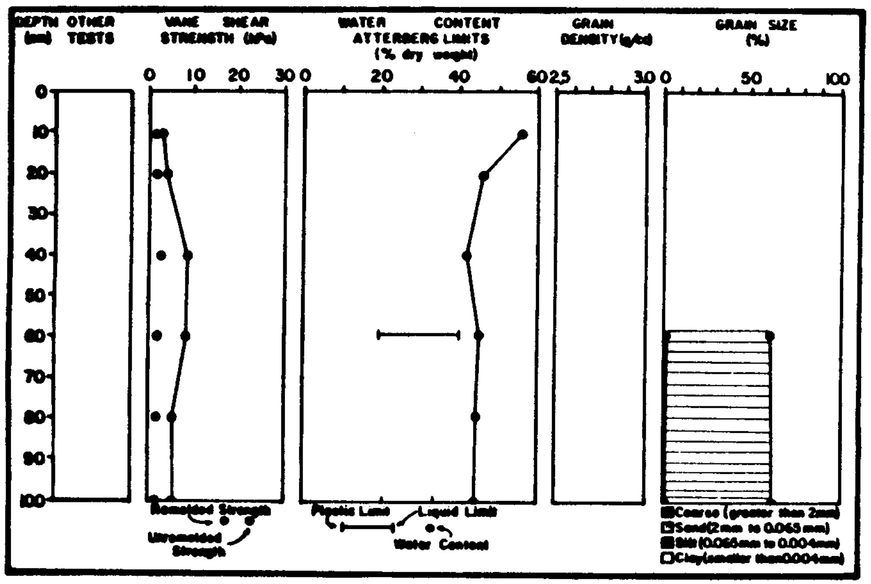

CRUISE: DCI-81-EG CORE: 627G1

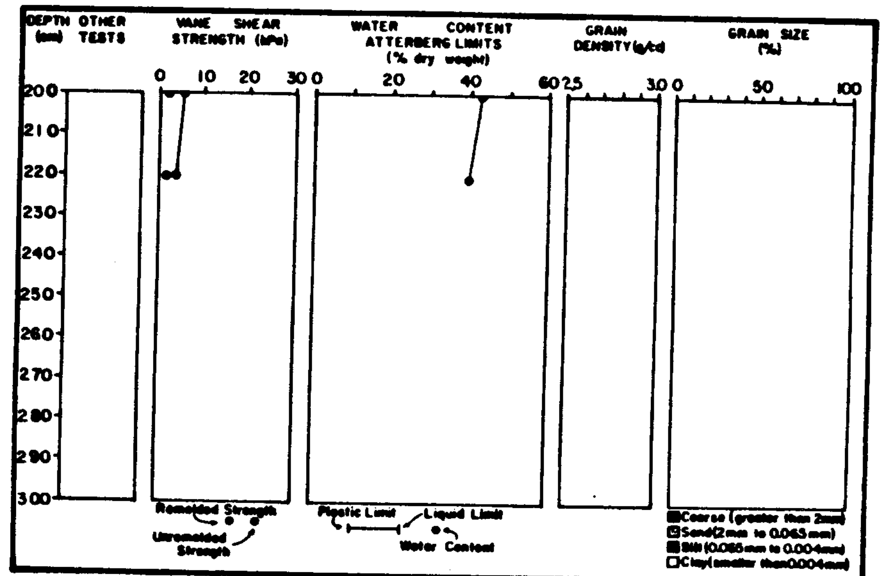

CRUISE: DCI-81-EG CORE: 627G1

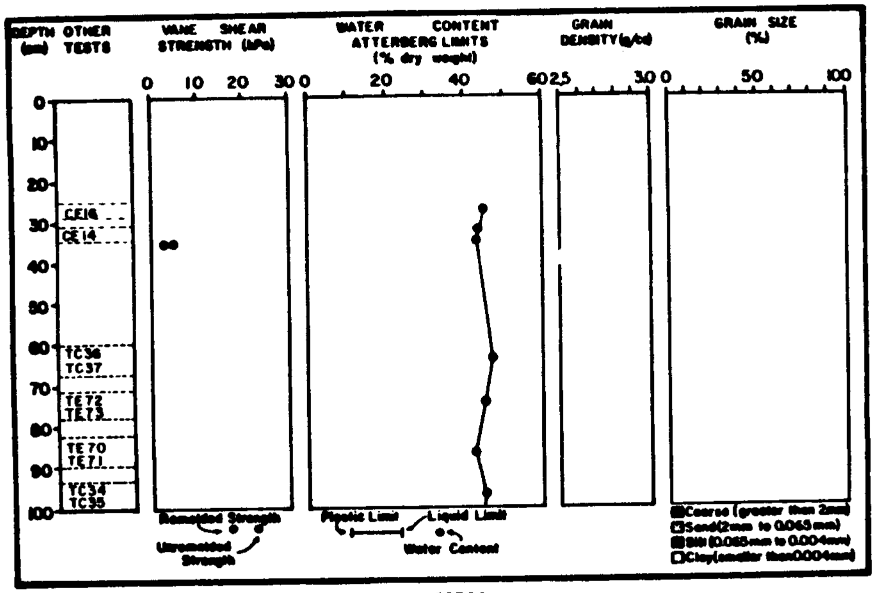

CRUISE: DCI-81-EG CORE: 627G2

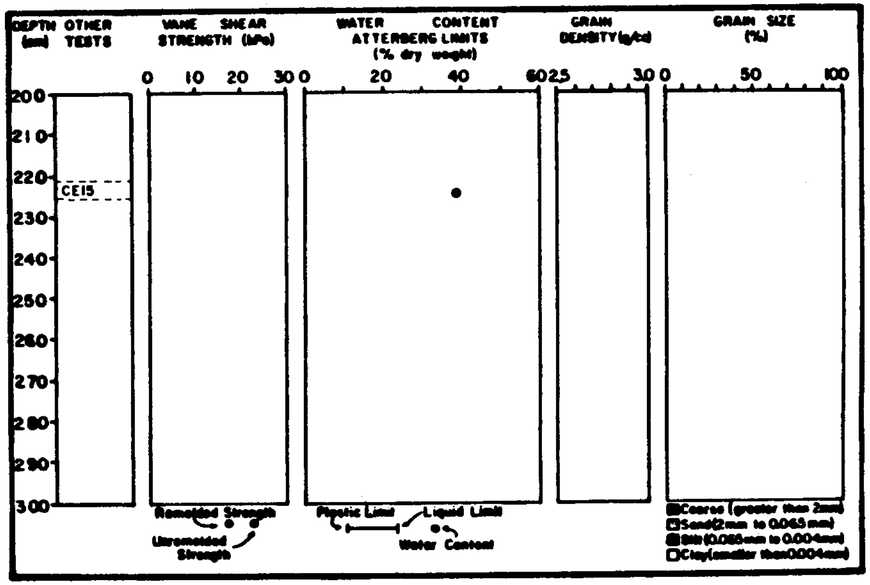

CRUISE: S DCI-81-EG CORE: 627G2

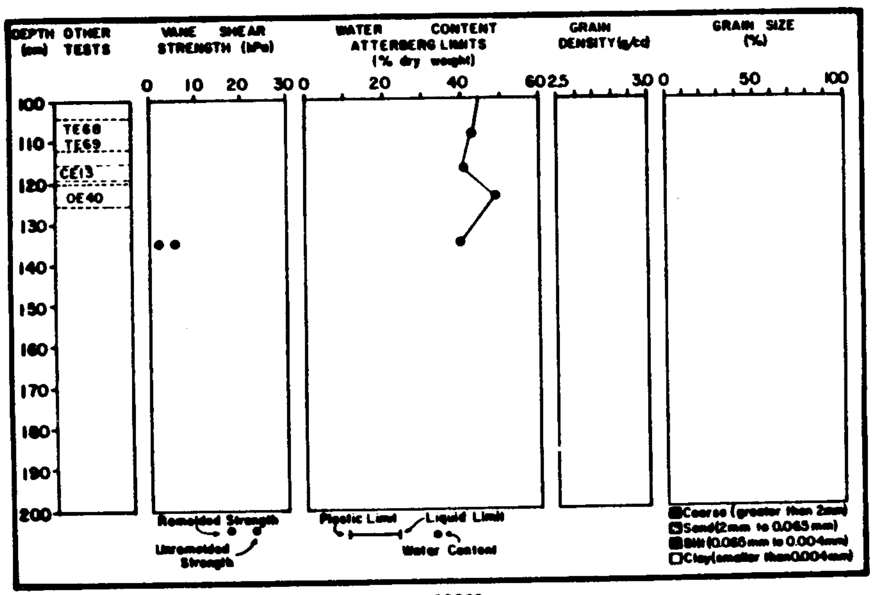

CRUISE: DCI-81-EG CORE: 627G2

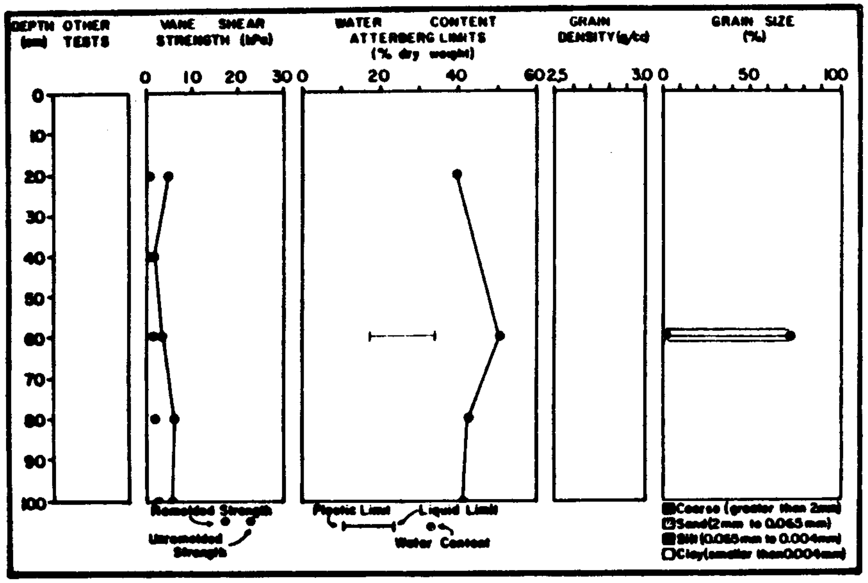

CRUISE: DCI-81-EG CORE: 628G2

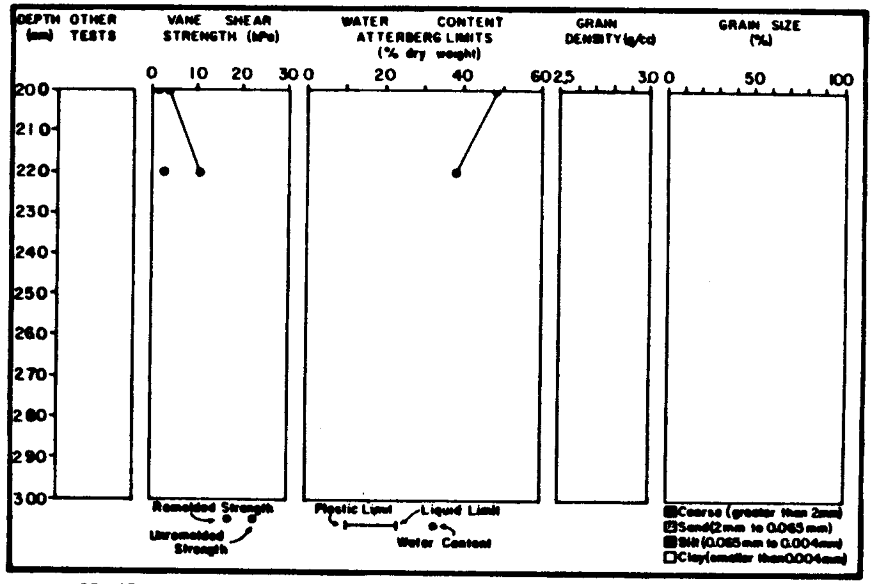

CRUISE: DCI-81-EG CORE: 628G2

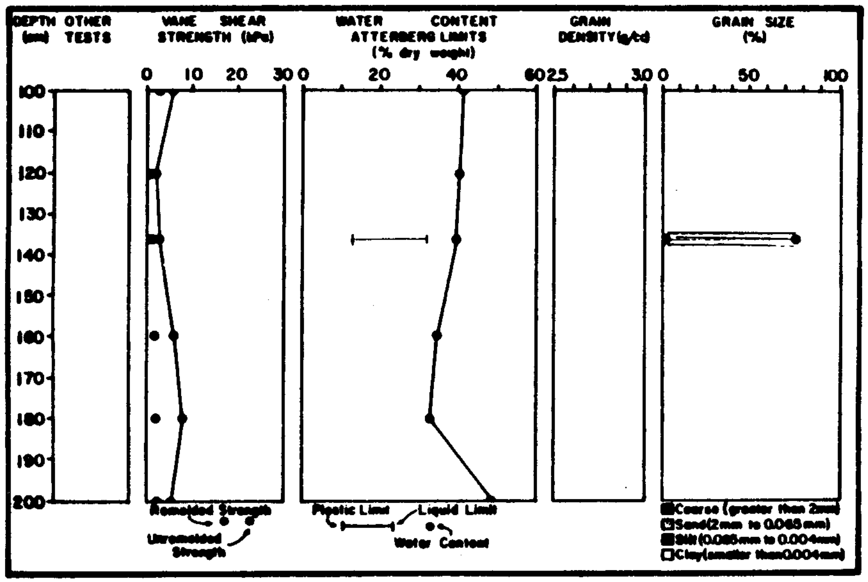

CRUISE: DCI-81-EG CORE: 628G2

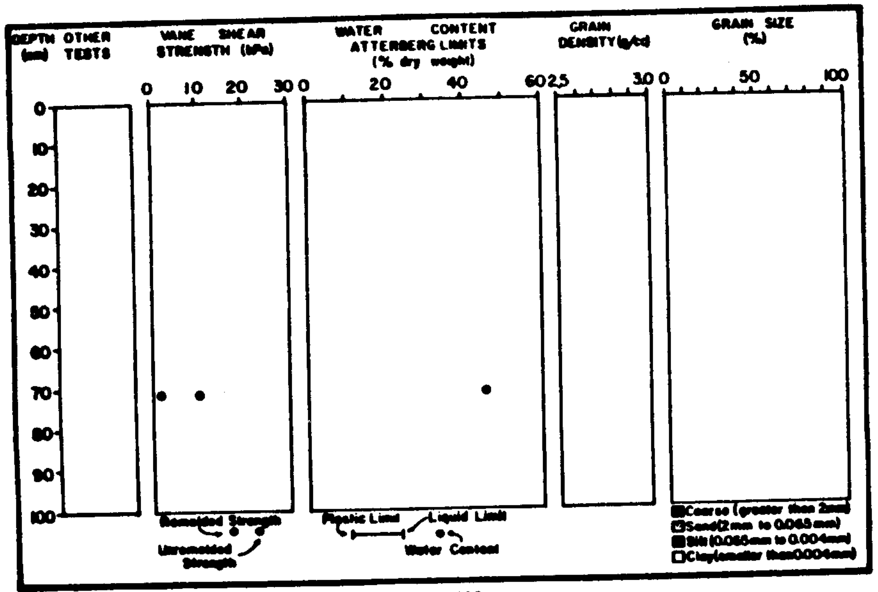

CRUISE: DCI-81-EG CORE: 62803

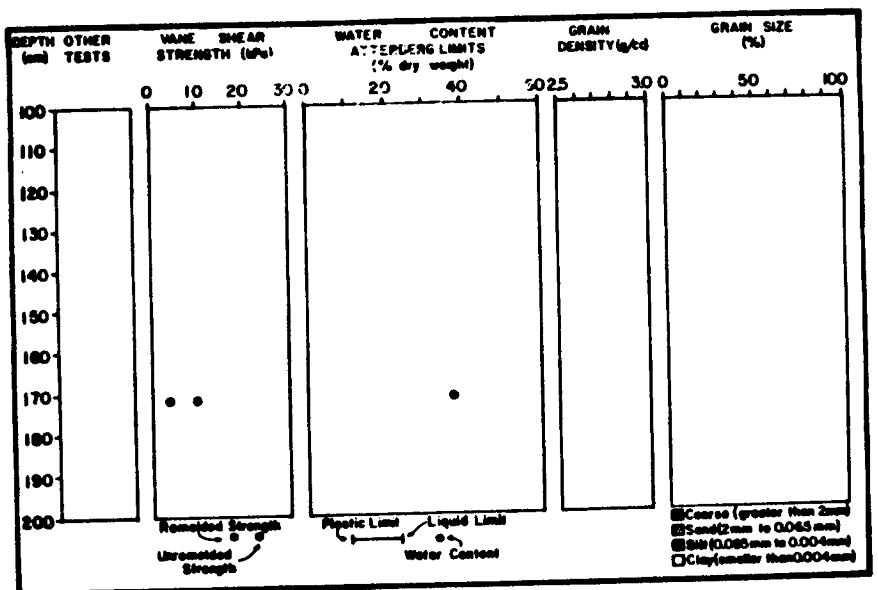

CRUISE: DCI-81-EG CORE: 62803

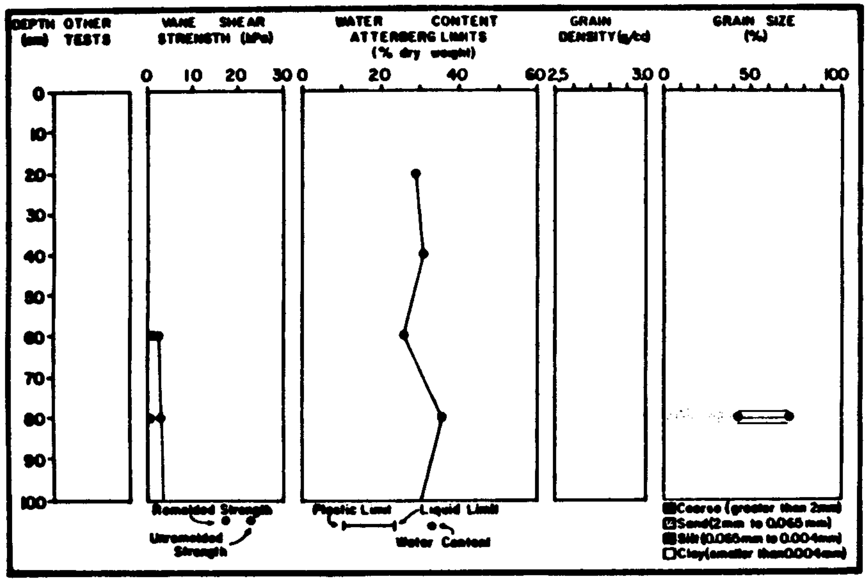

CRUISE: DCI-81-EG CORE: 630A1

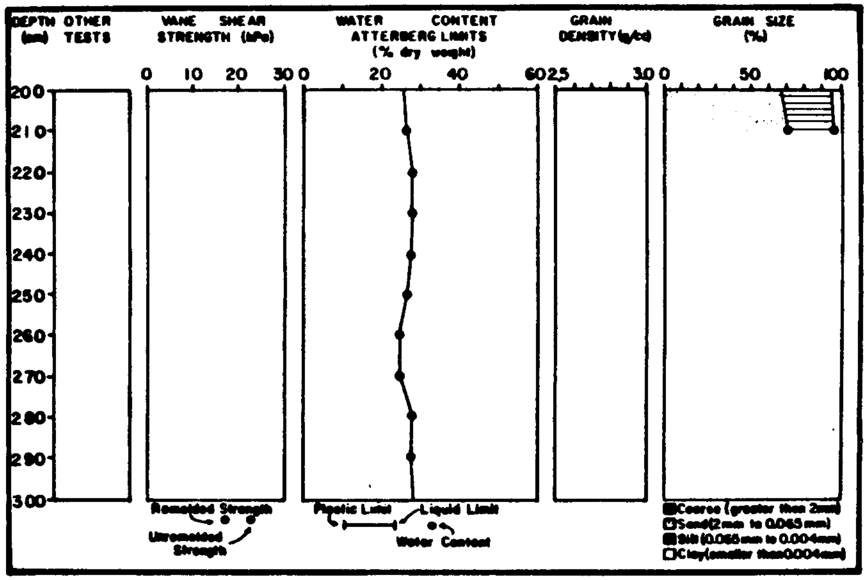

CRUISE: DCI-81-EG CORE: 630A1

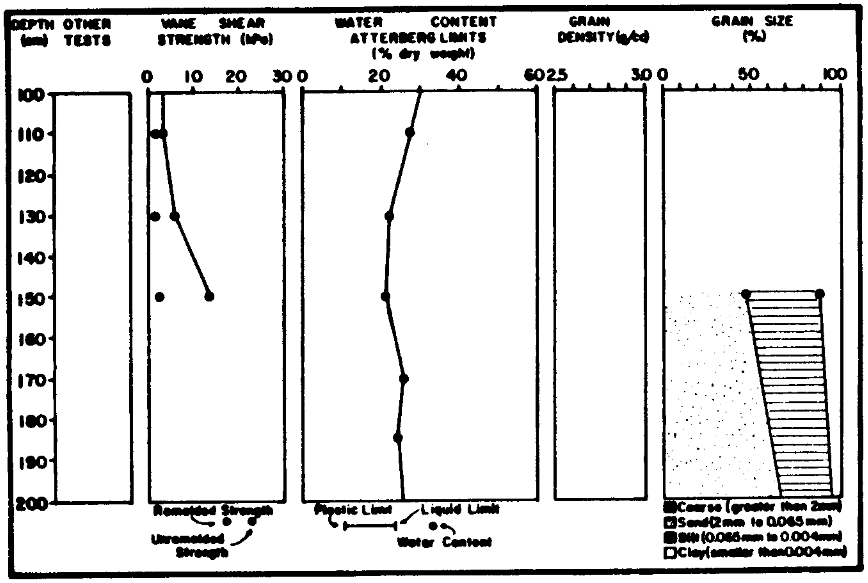

CRUISE: DCI-81-EG CORE: 630A1

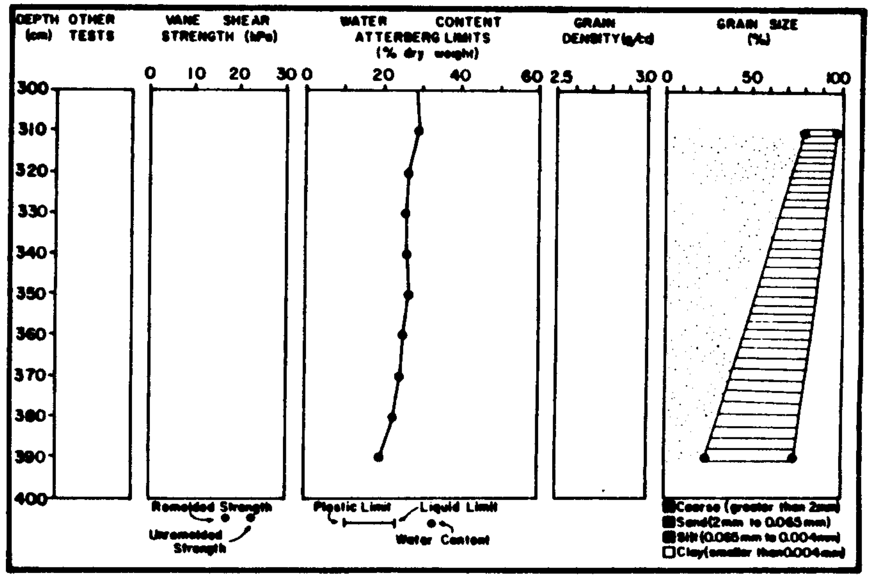

CRUISE: DCI-81-EG CORE: 630A1

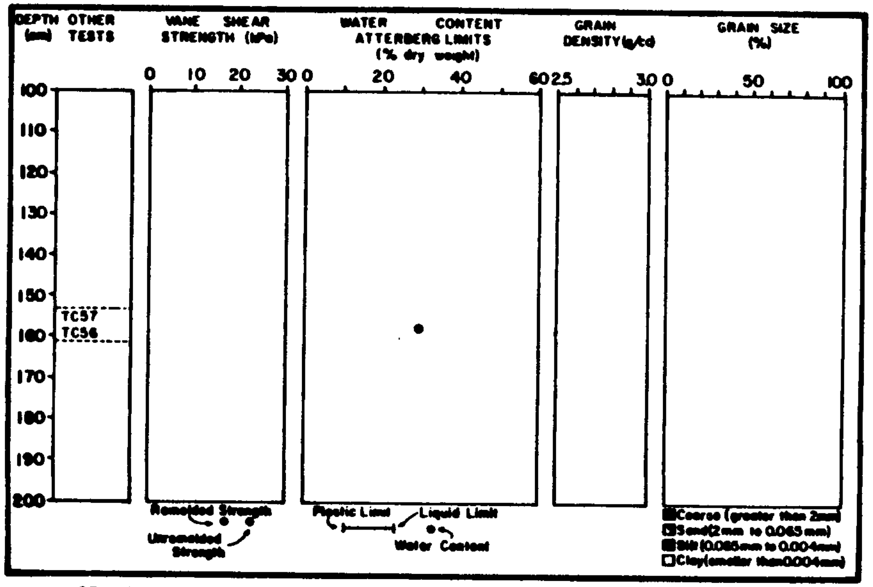

CRUISE: DCI-81-EG CORE: 630A2

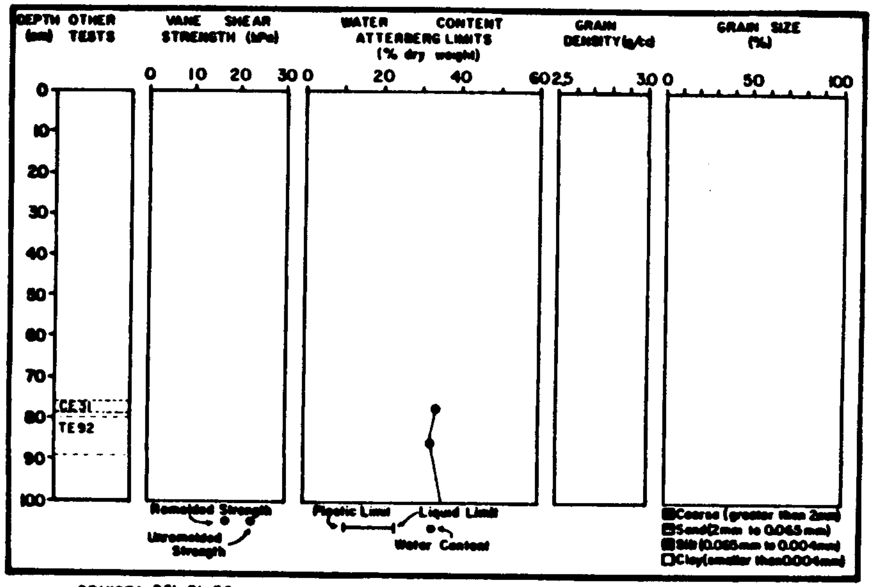

CRUISE: DCI-81-EG CORE: 632G1

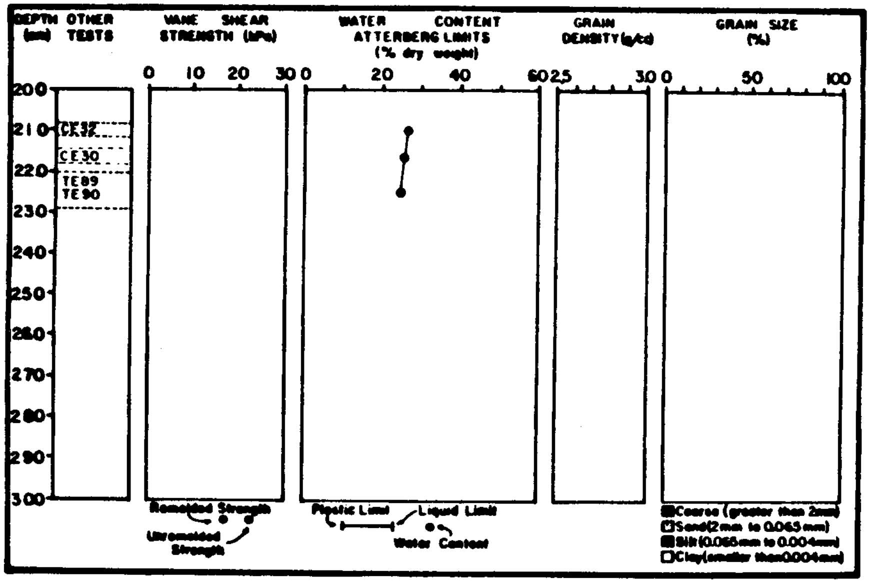

CRUISE: DCI-81-EG CORE: 630A2

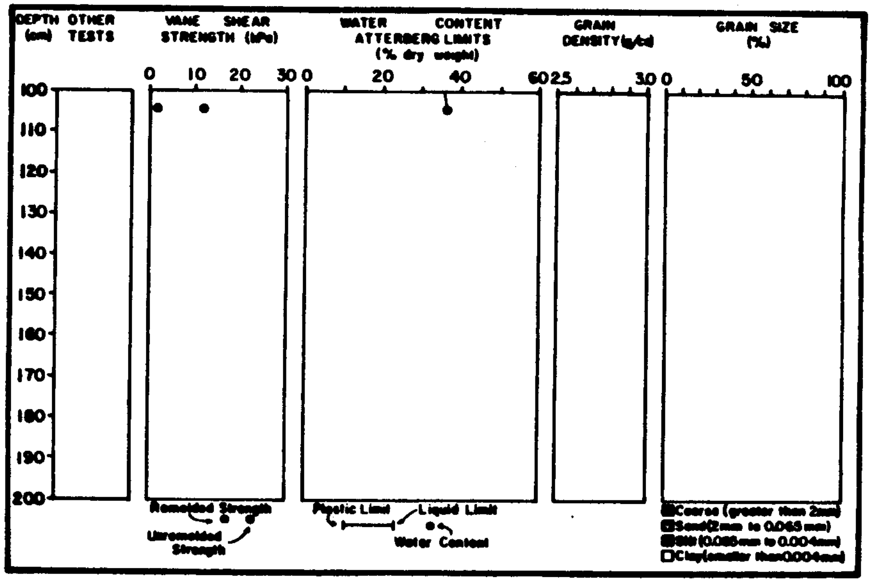

CRUISE: DCI-81-EG CORE: 632G1

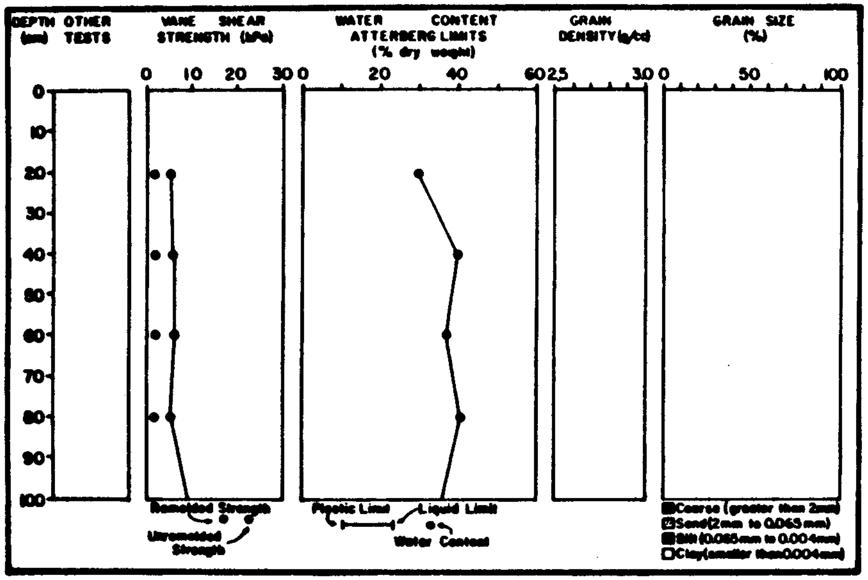

CRUISE: DCI-81-EG CORE: 632G2

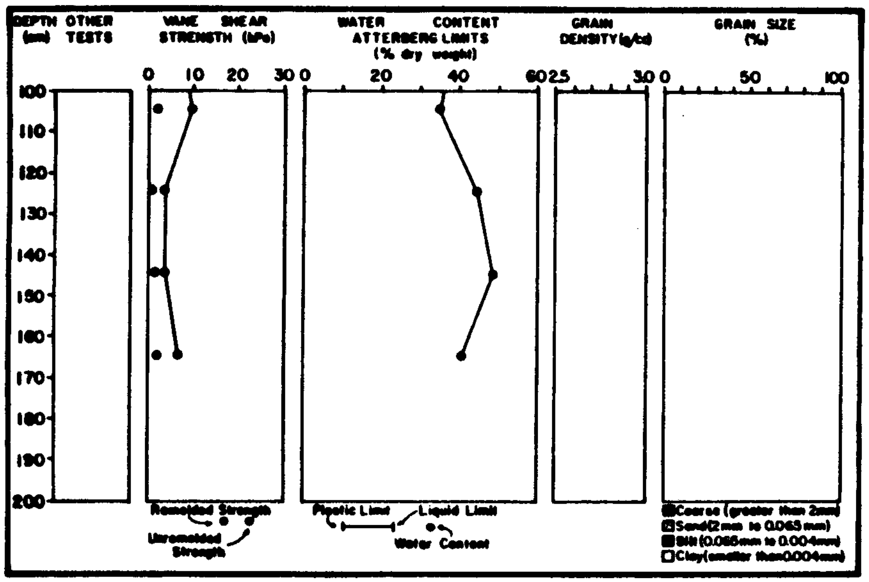

CRUISE: DCI-81-EG CORE: 632G2

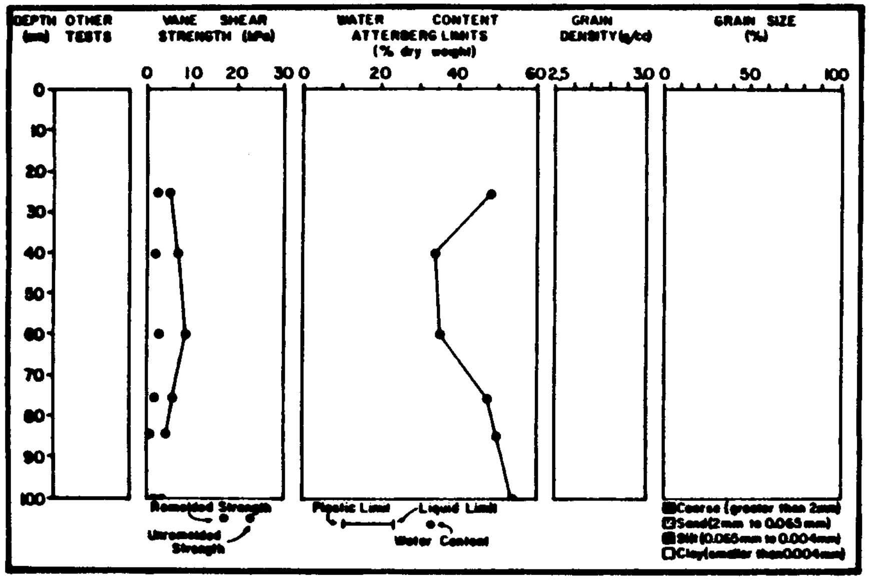

CRUISE: DCI-81-EG CORE: 633G1

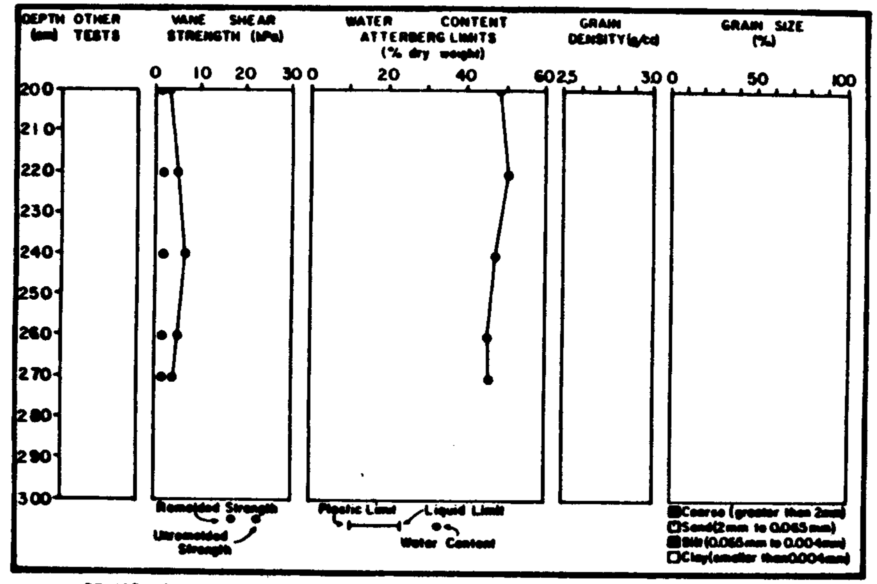

CRUISE: DCI-81-EG CORE: 633G1

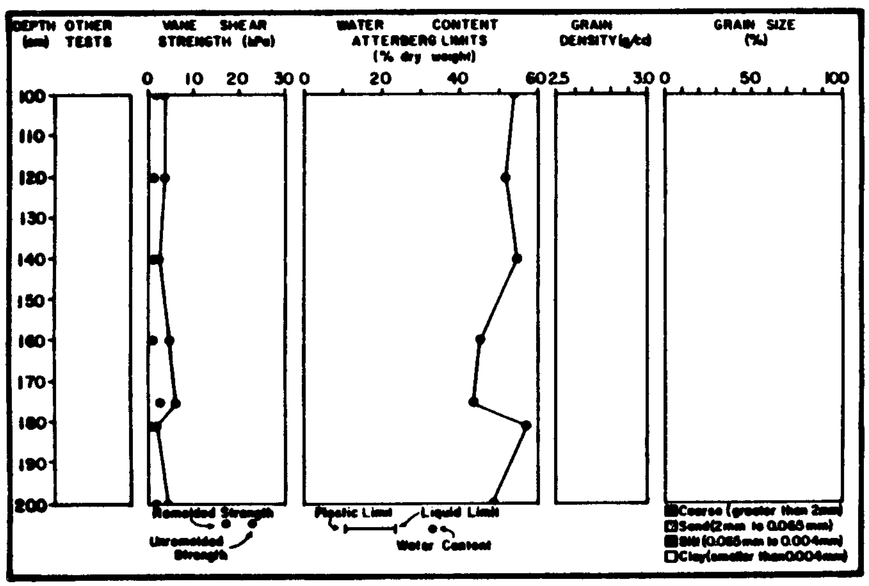

CRUISE: DCI-81-EG CORE: 633G1

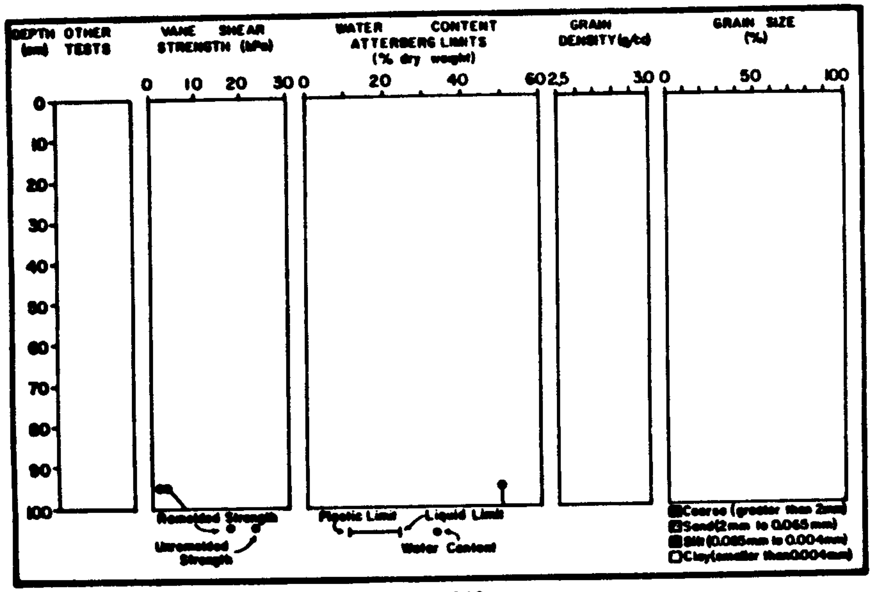

CRUISE: DCI-81-E6 CORE: 633G2

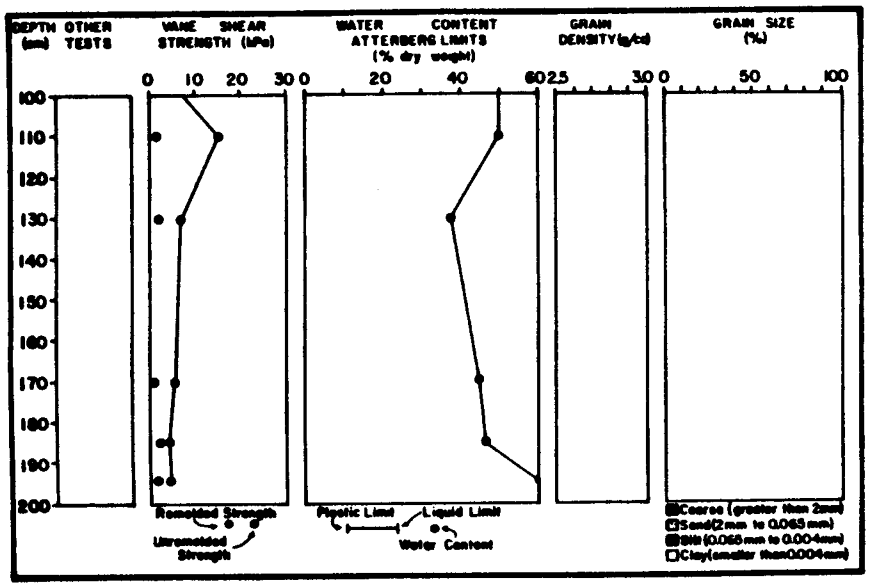

CRUISE: DCI-81-E6 CORE: 633G2

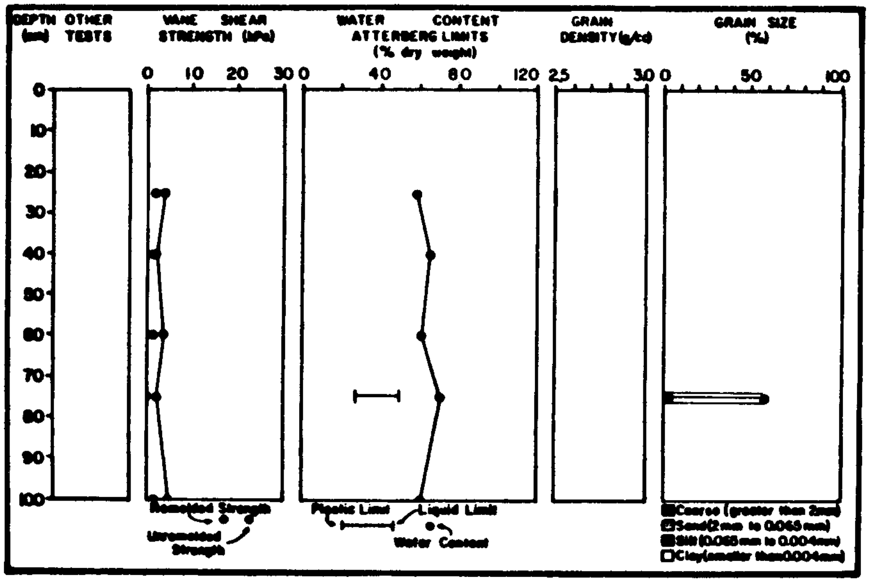

CRUISE: DCI-81-EG CORE: 634G1

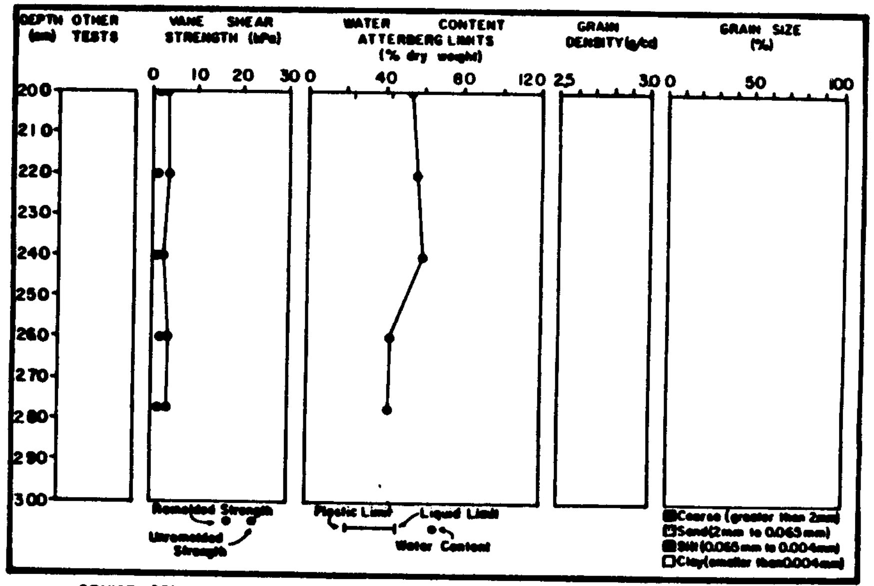

CRUISE: DCI-81-EG CORE: 634G1

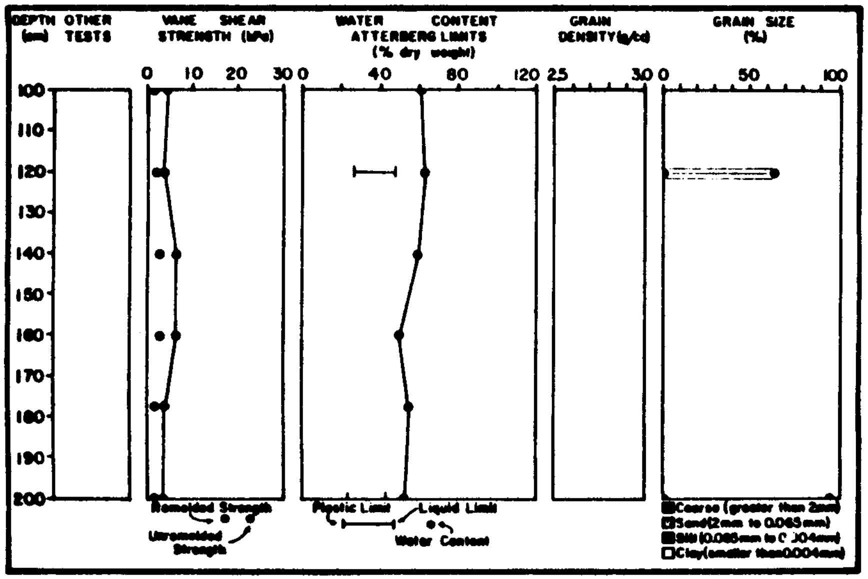

CRUISE: DCI-81-EG CORE: 634G1

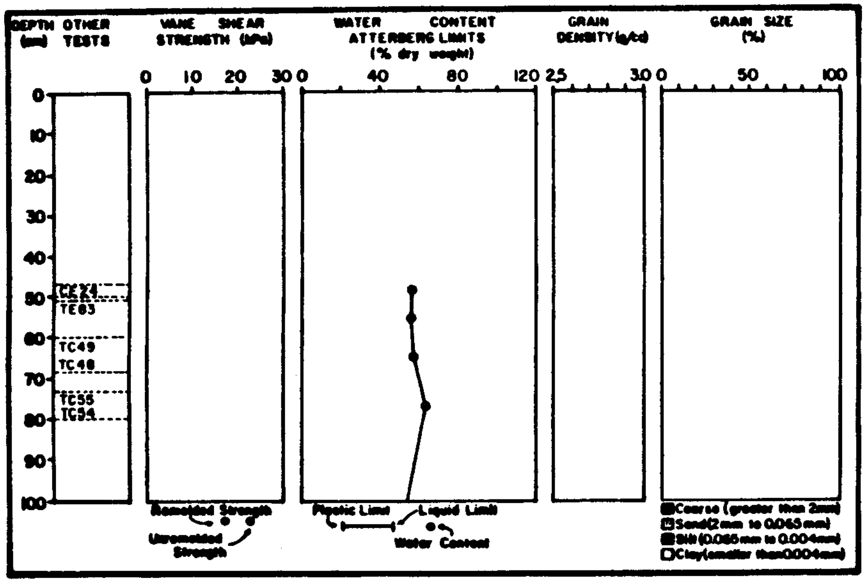

CRUISE: DCI-81-EG CORE: 634G2

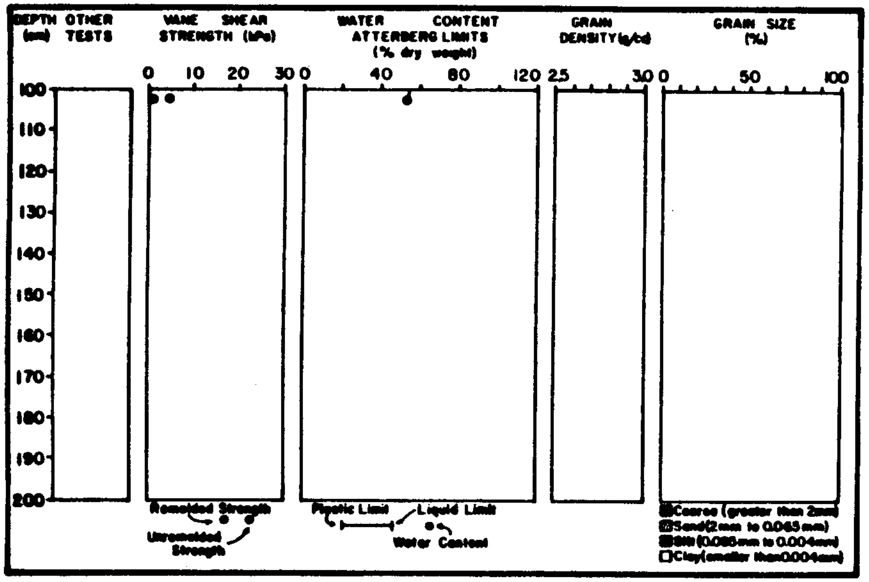

CRUISE: DCI-81-EG CORE: 634G2

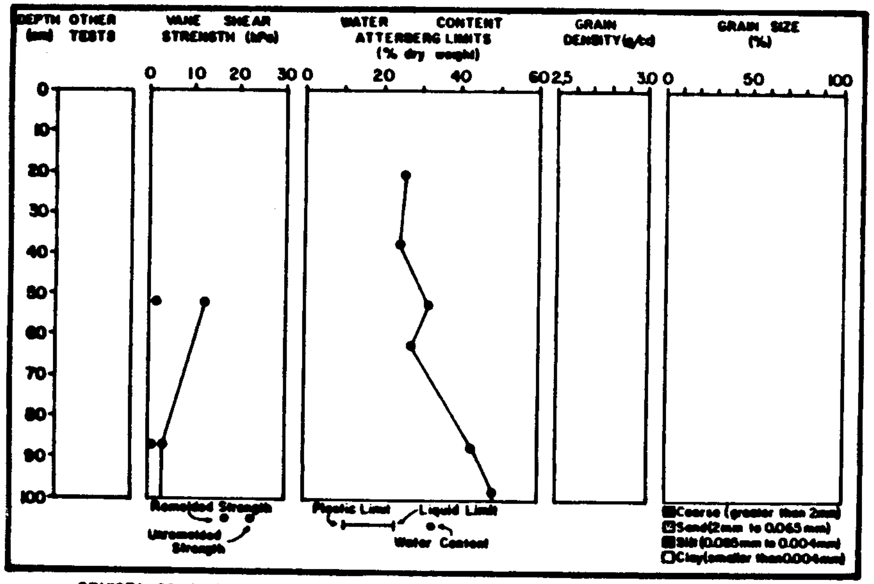

CRUISE: DCI-81-EG CORE: 635A2

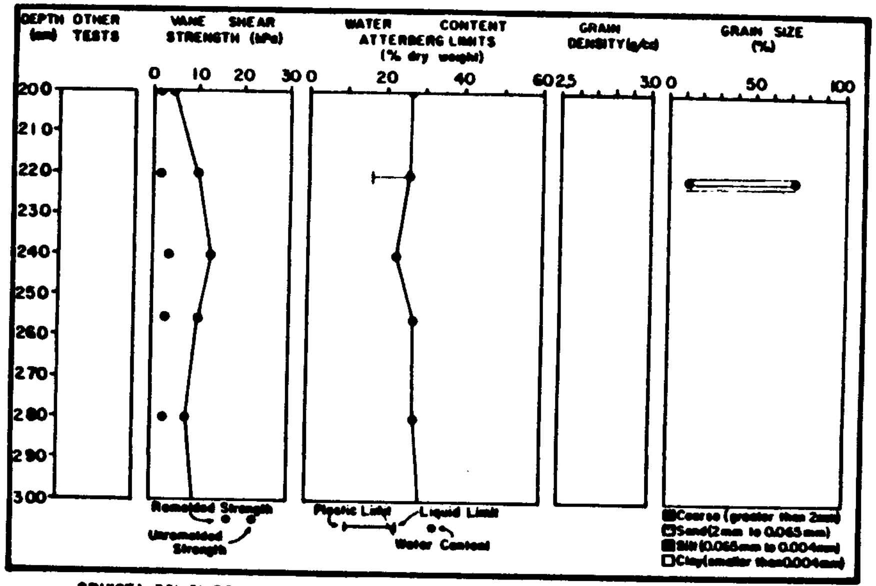

CRUISE: DCI-81-EG CORE: 635A2

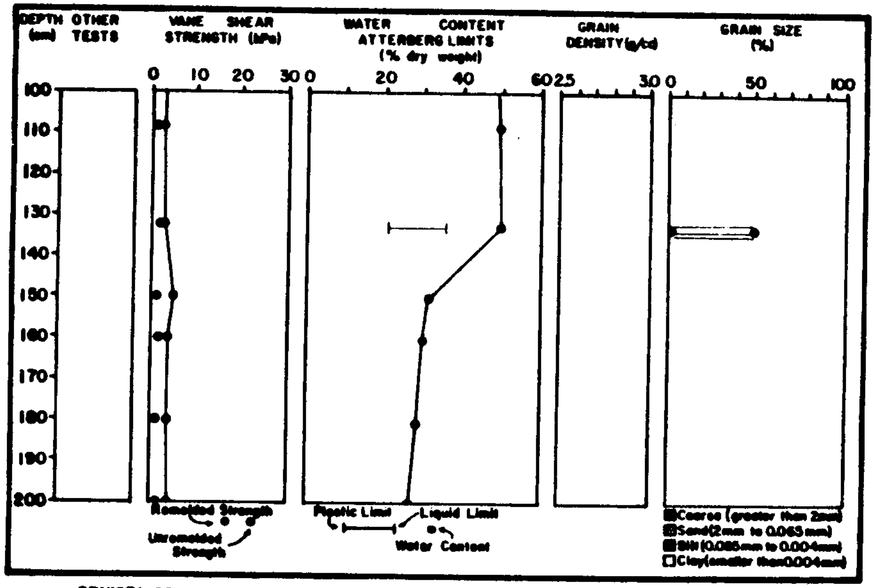

CRUISE: DCI-81-EG CORE: 635A2

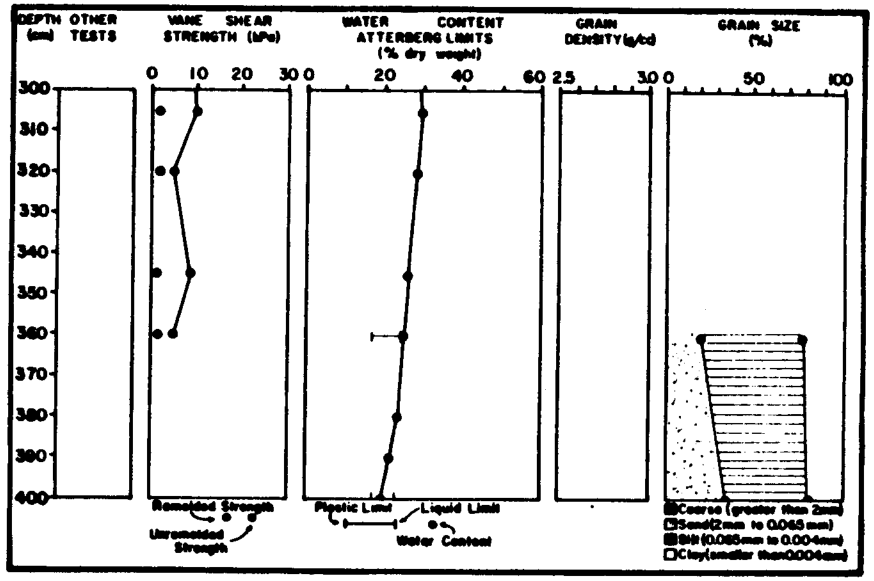

CRUISE: DCI-81-EG CORE: 635A2

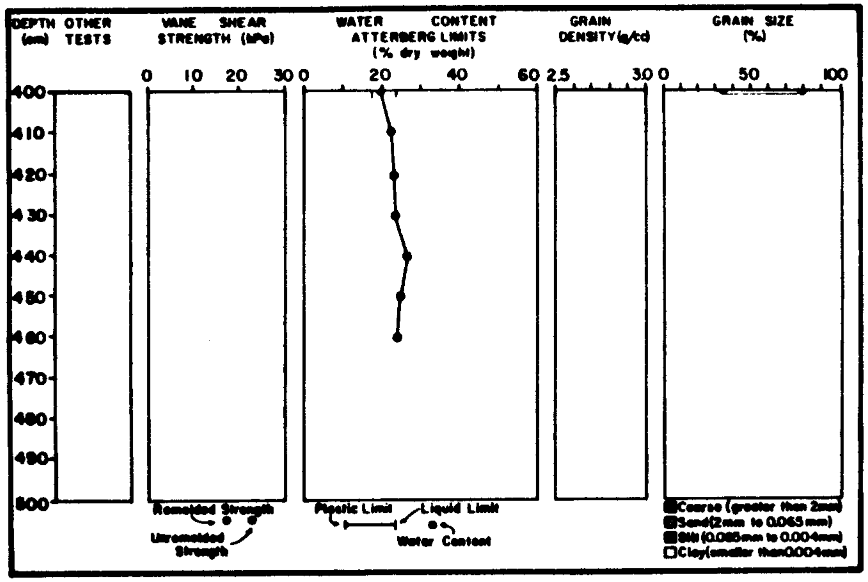

CRUISE: DCI-81-EG CORE: 635A2

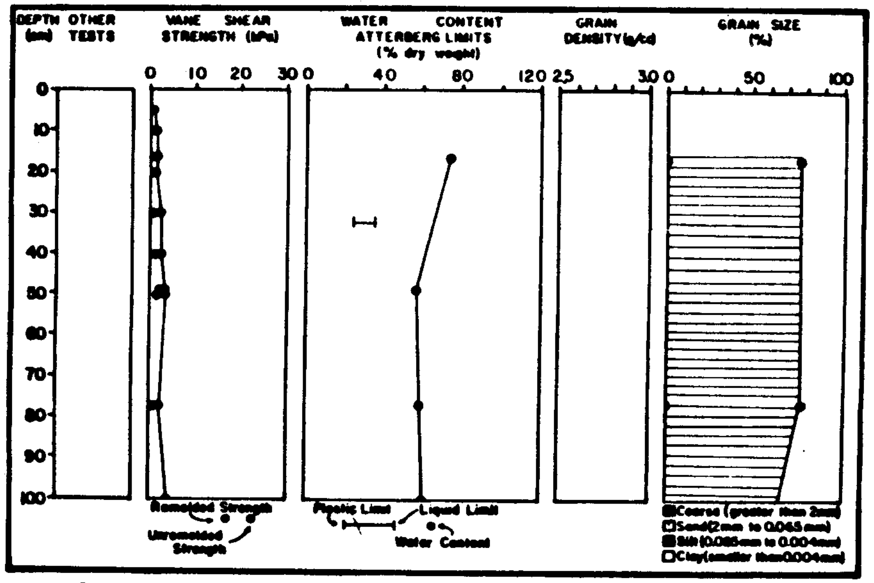

CRUISE: DCI-77-EG CORE: 709B

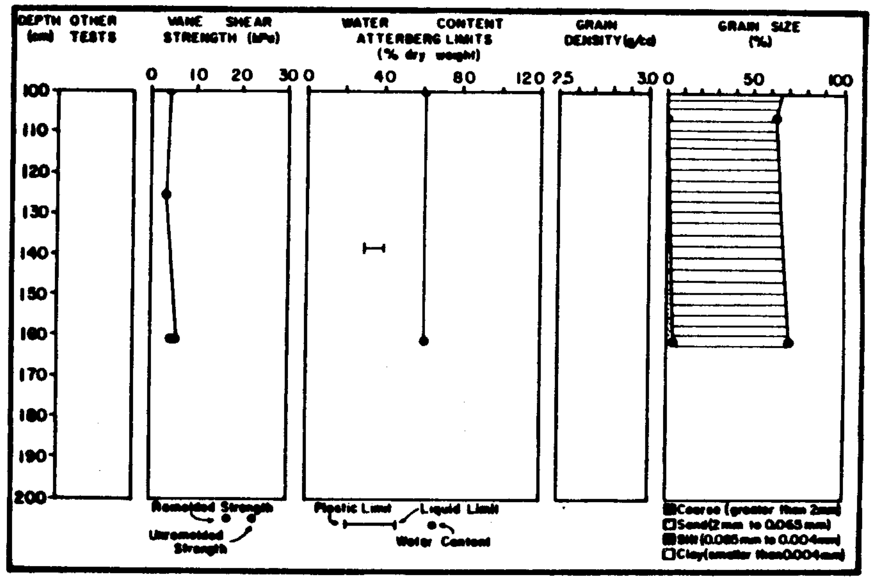

CRUISE: DCI-77-EG CORE: 709B

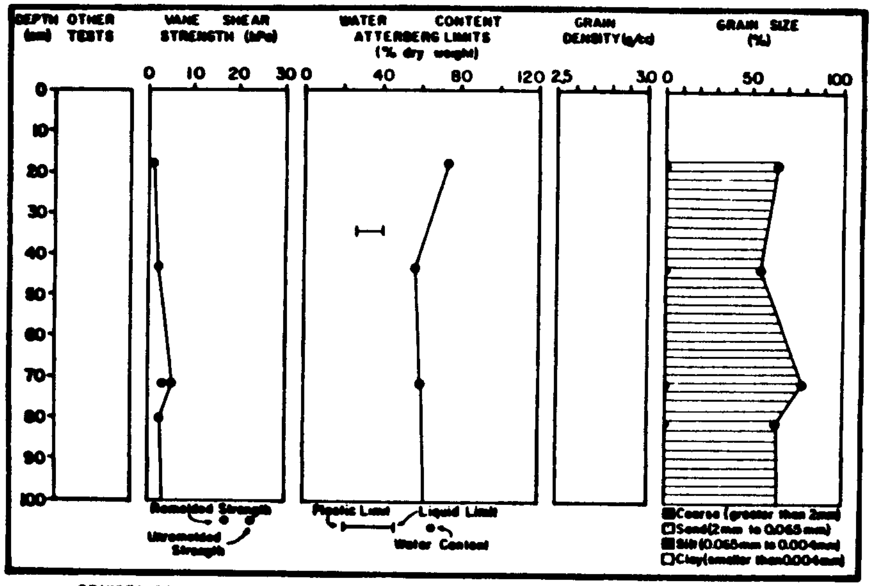

CRUISE: DCI-77-EG CORE: 709C

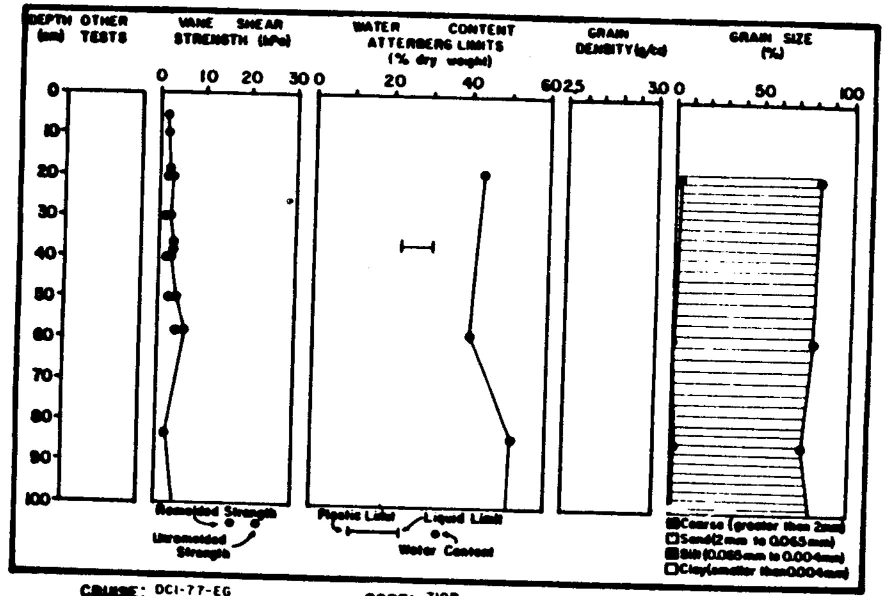

CRUISE: DCI-77-EG CORE: 710B

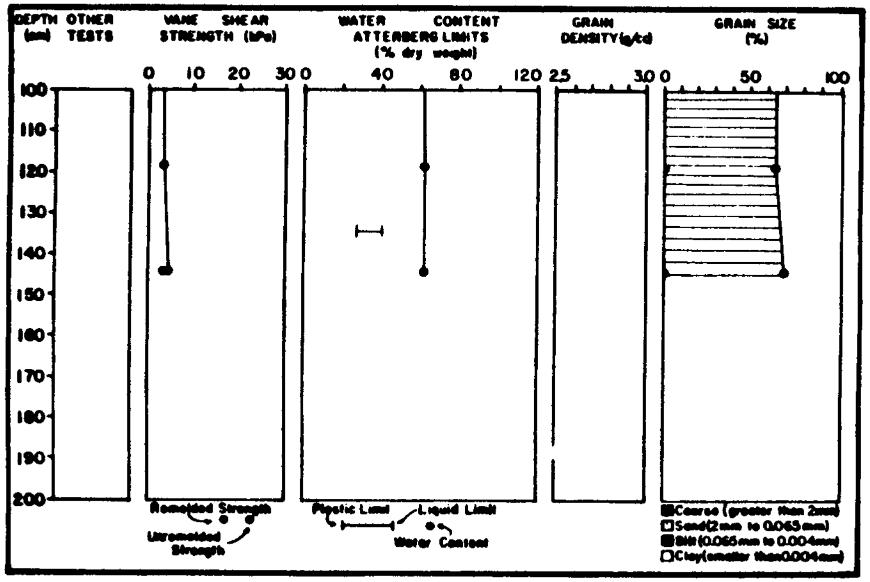

CRUISE: DCI-77-EG CORE: 709C

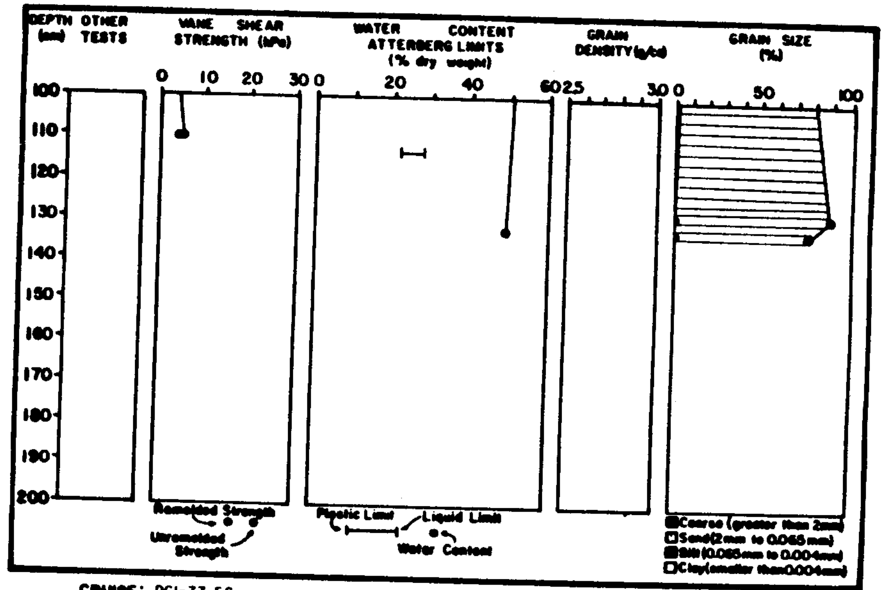

CRUISE: DCI-77-EG CORE: 710B

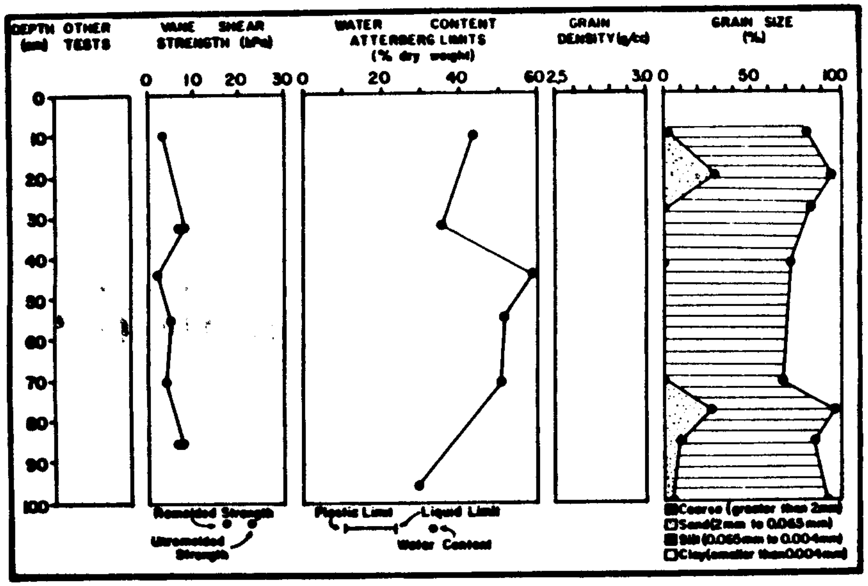

CRUISE: DCI-77-EG CORE: 710C

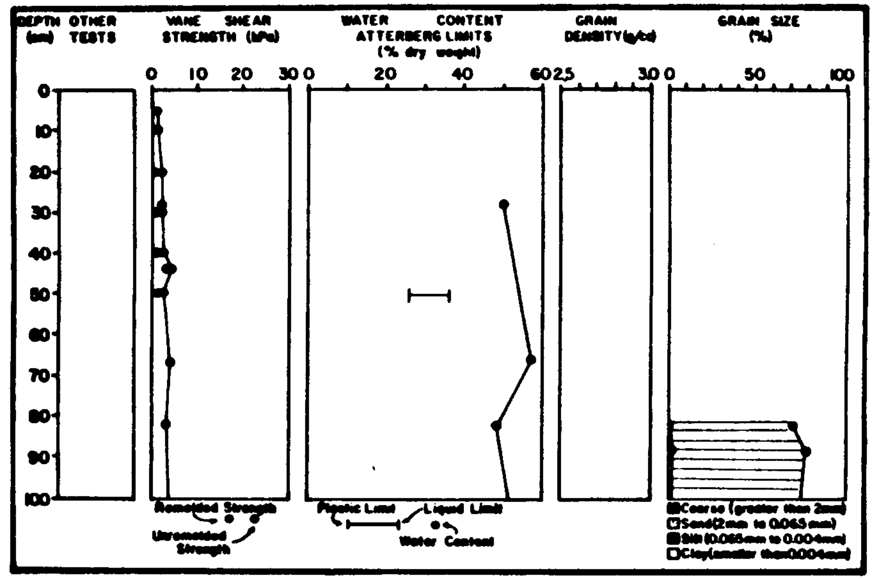

CRUISE: DCI-77-EG CORE: 715B

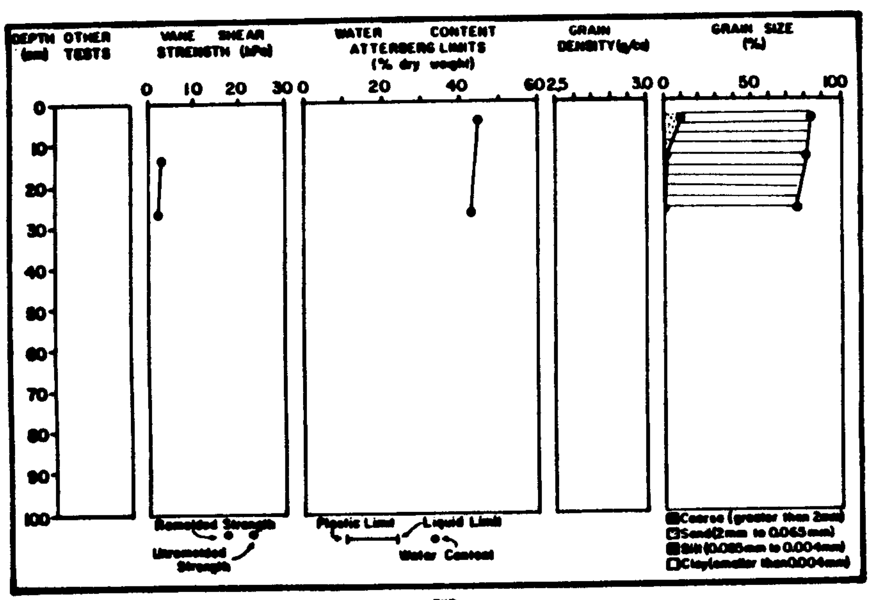

CRUISE: DCI-77-EG CORE: 7HB

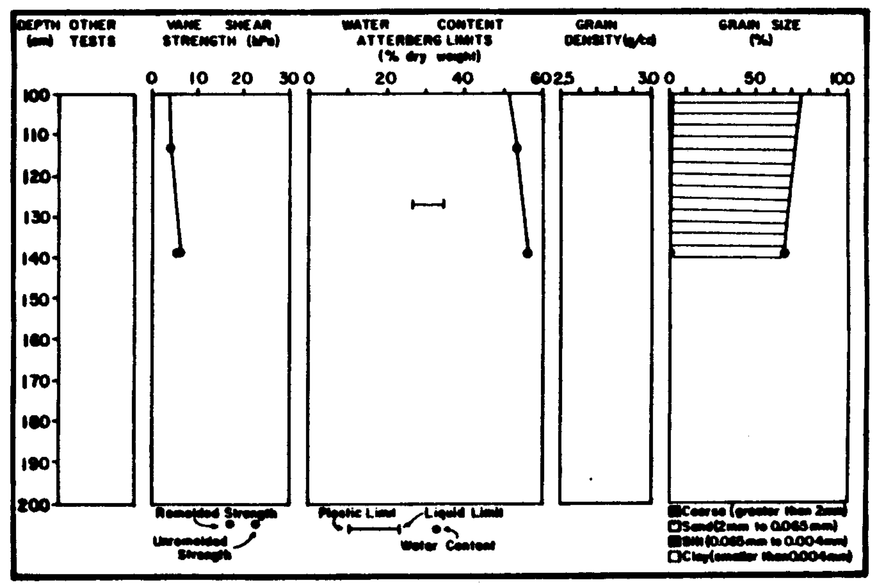

CRUISE: DCI-77-EG CORE: 715B

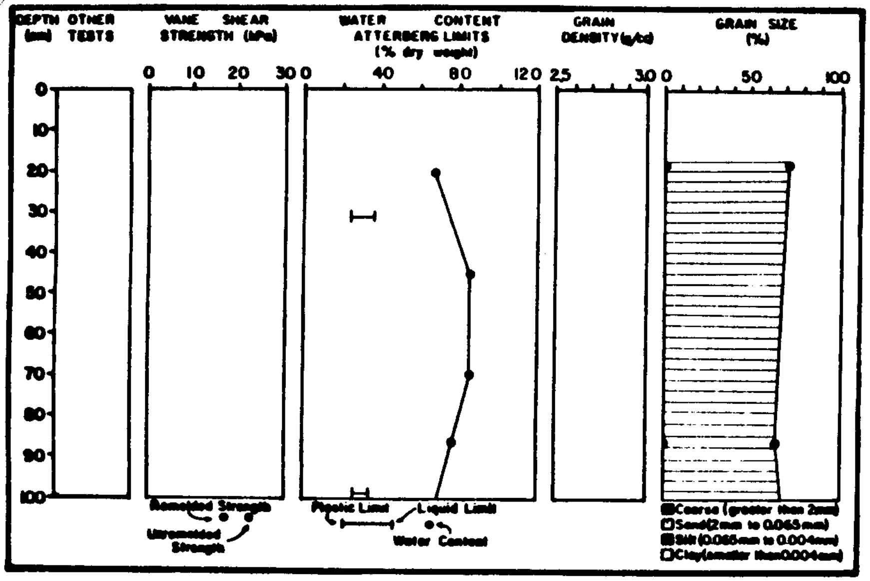

CRUISE: DCI-77-EG CORE: 715C

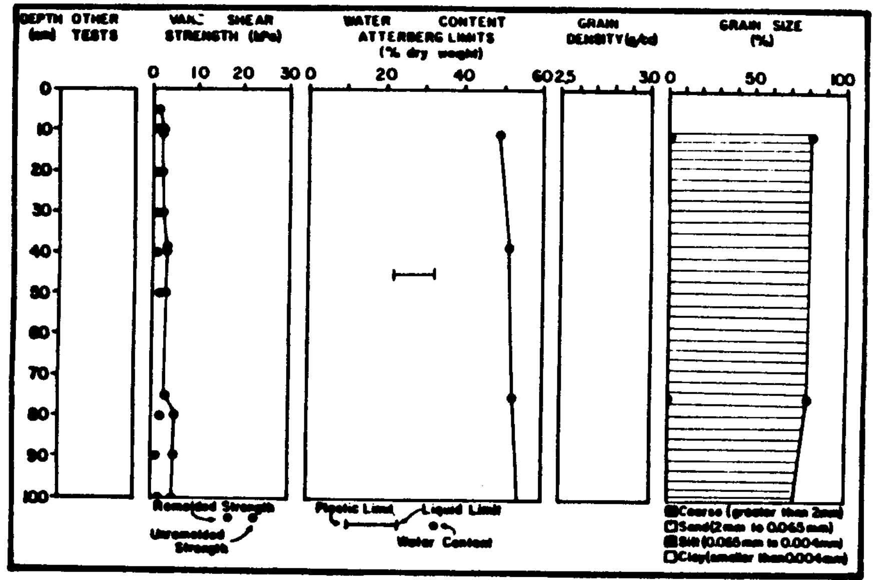

CRUISE: DCI-77-EG CORE: 717B

293

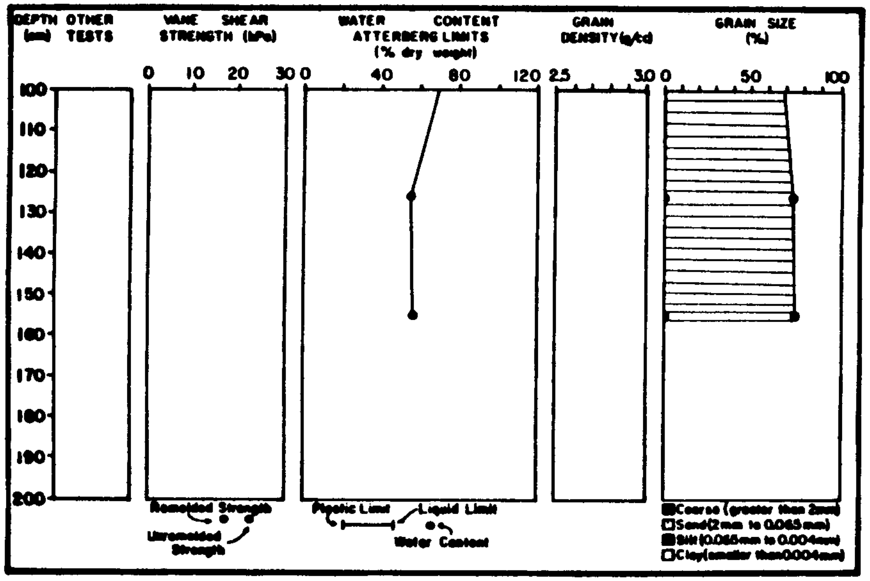

CRUISE: DCI-77-EG CORE: 715C

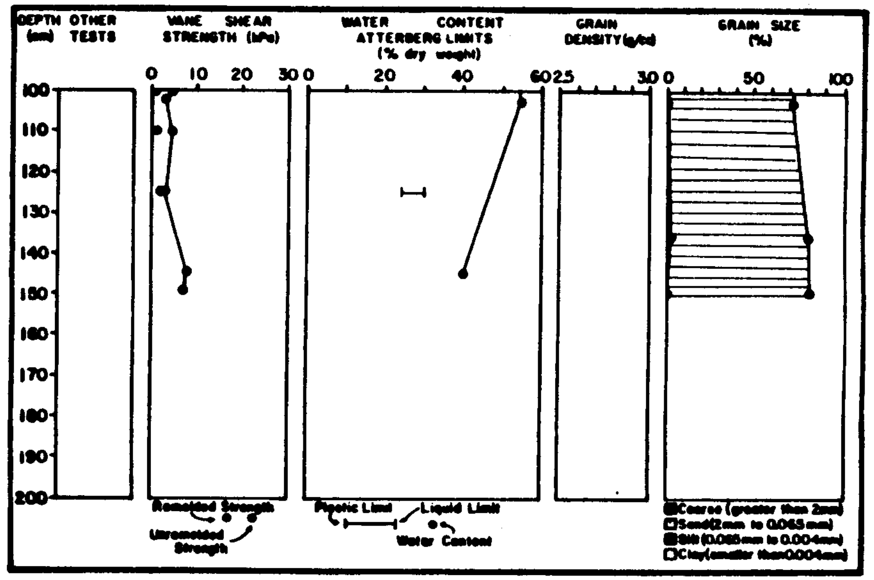

CRUISE: DCI-77-EG CORE: 717B

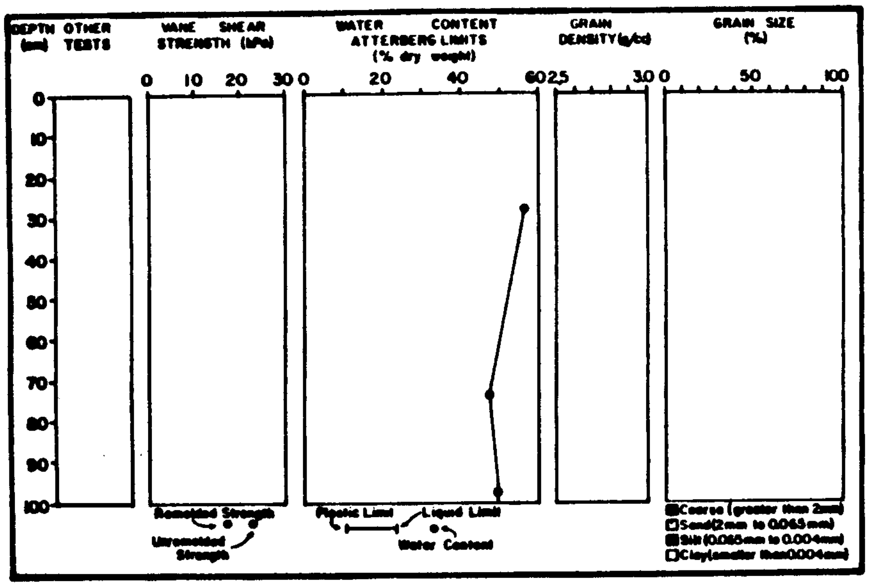

CRUISE: DCI-77-EG CORE: 717C

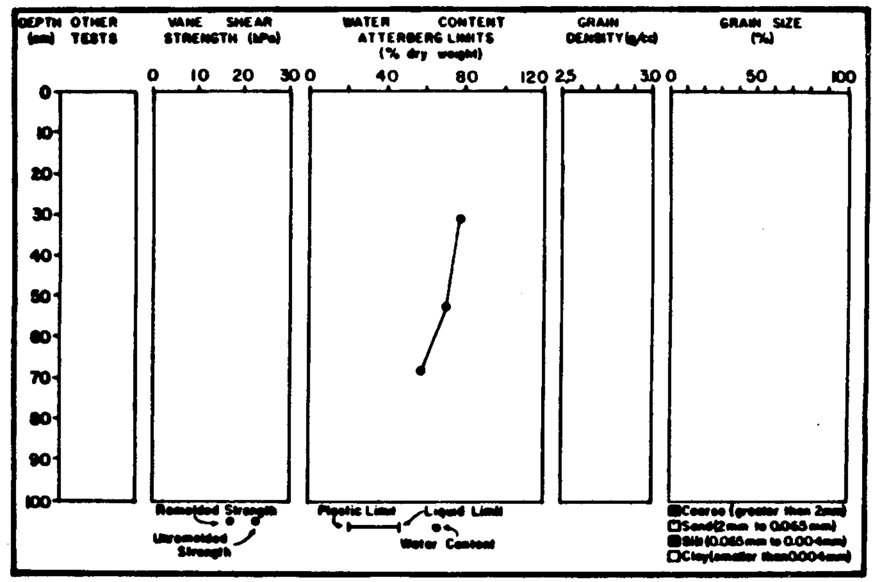

CRUISE: DCI-77-EG CORE: 718B

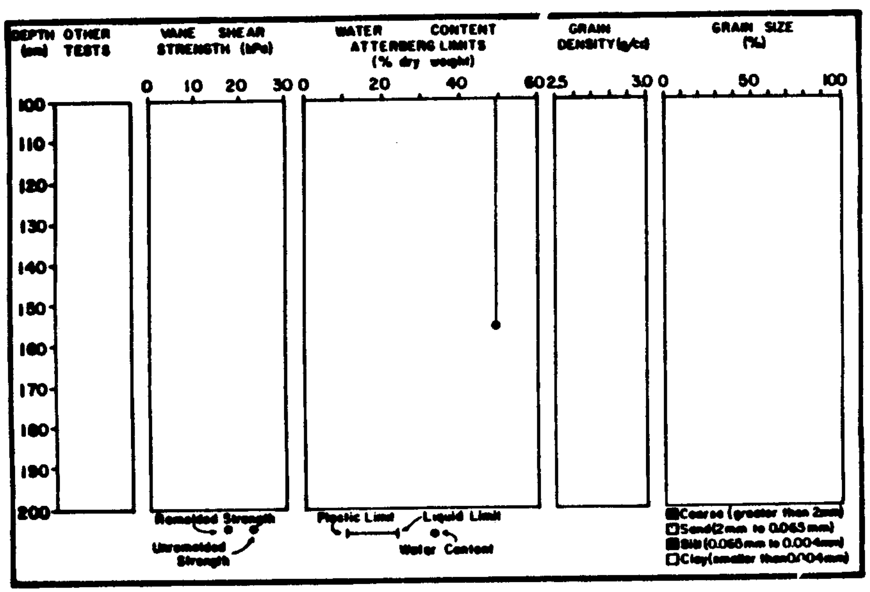

CRUISE: DCI-77-EG CORE: 717C

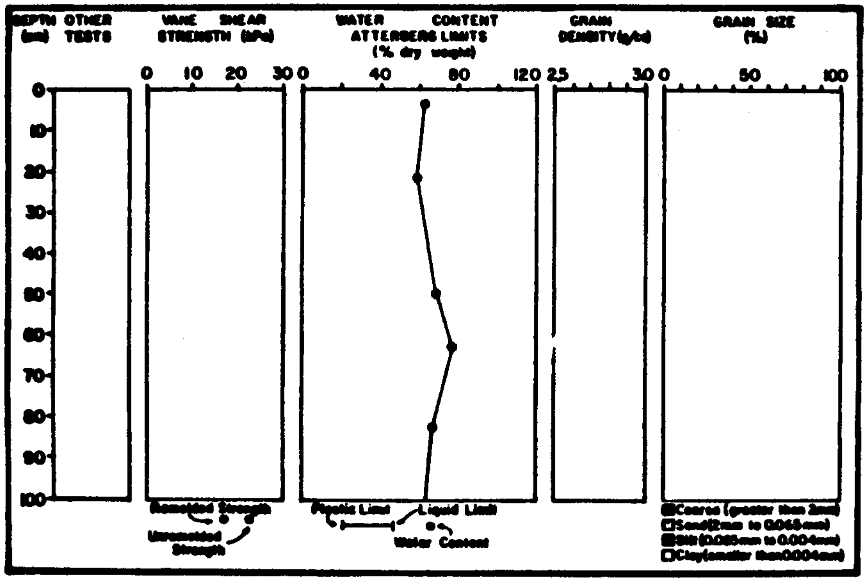

CRUISE: DCI-77-EG CORE: 7198

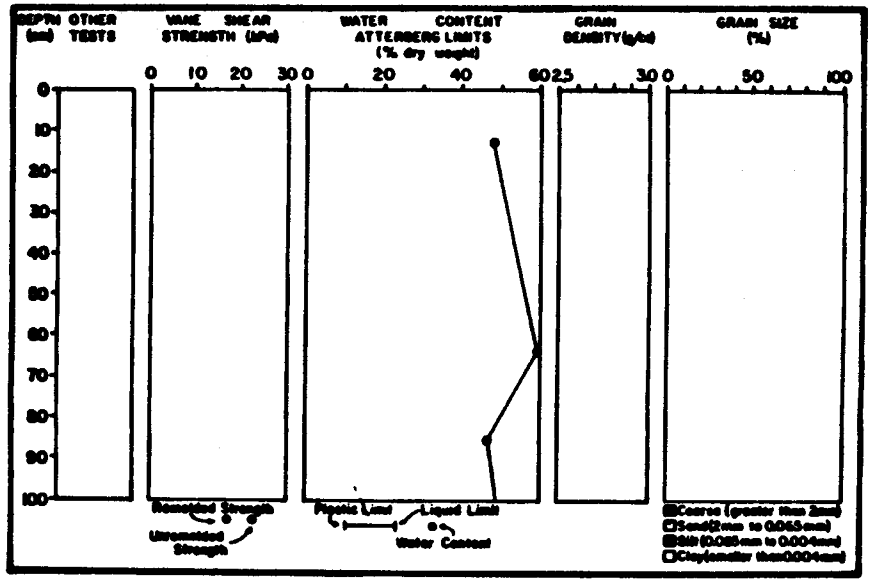

CRUISE: DCI-77-EG CORE: 7208

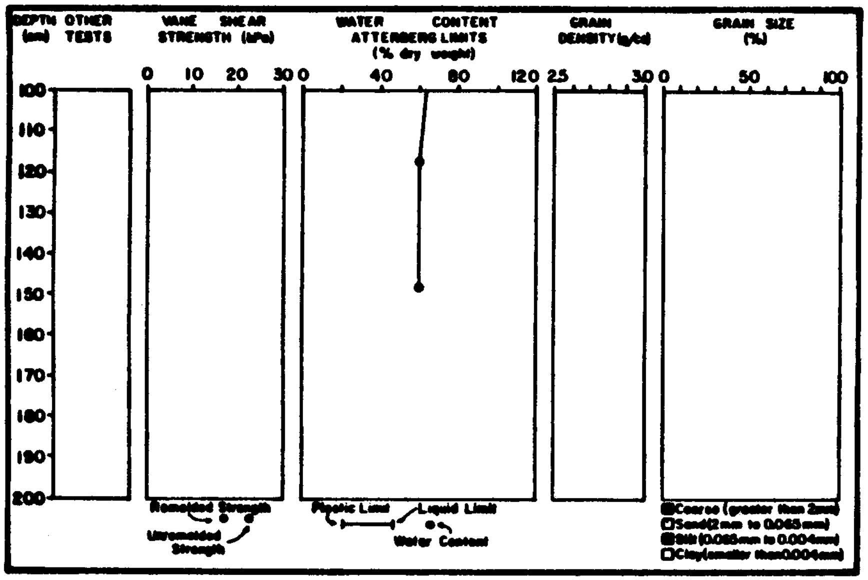

CRUISE: DCI-77-EG CORE: 7198

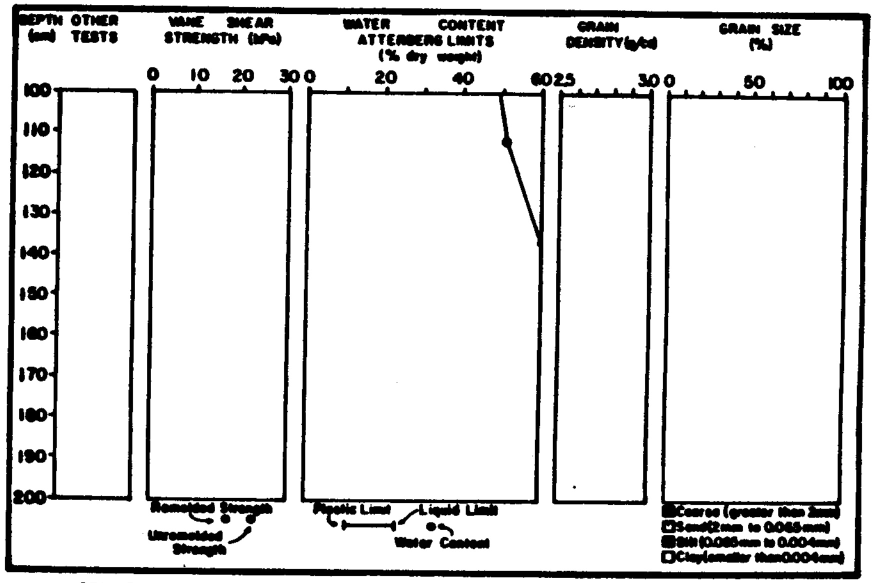

CRUISE: DCI-77-EG CORE: 7208

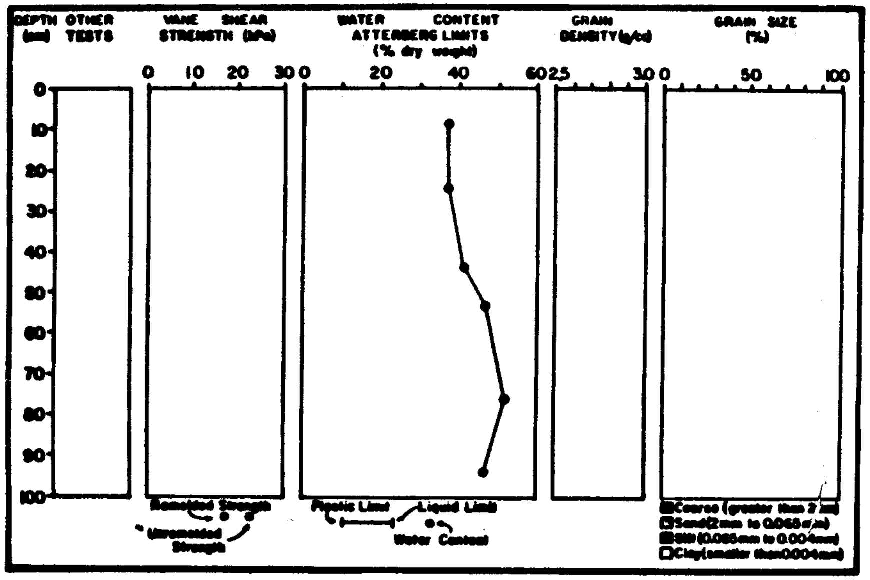

CRUISE: DCI-77-E6 CORE: 721C

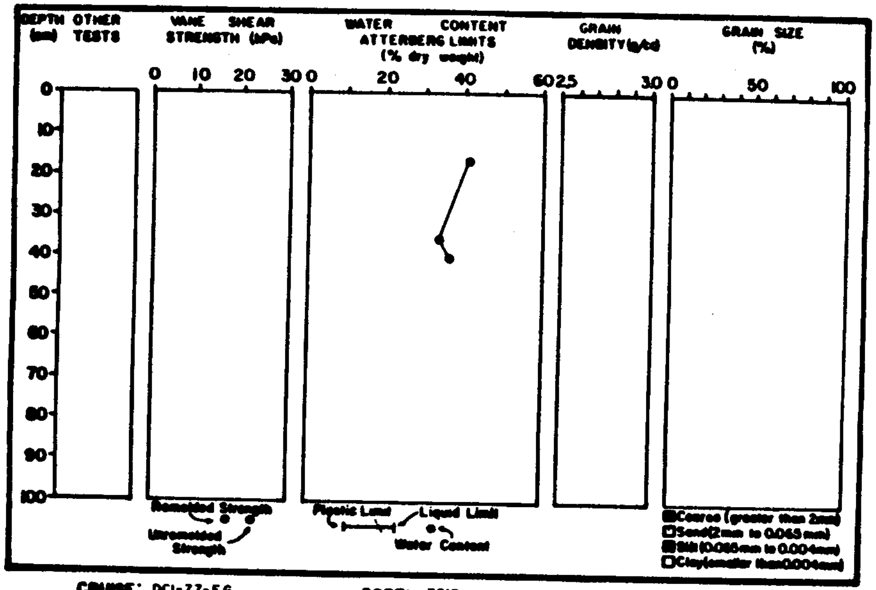

CRUISE: DCI-77-E6 CORE: 721D

ICY BAY STUDY AREA

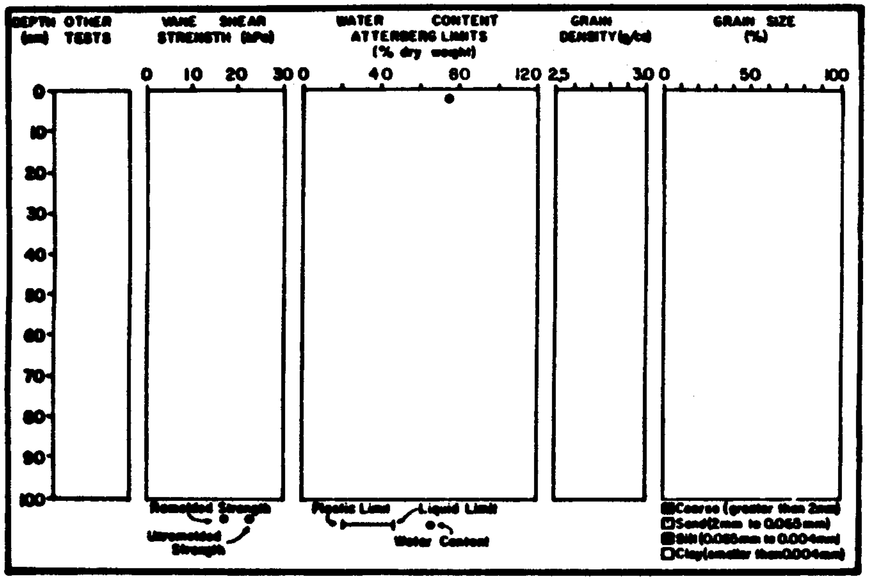

CRUISE: S8-77-EG CORE: 39G

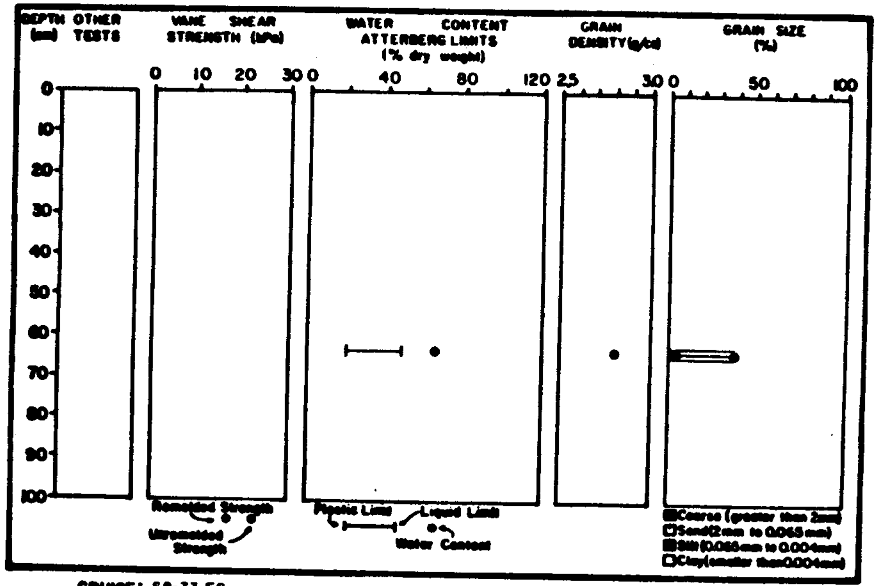

CRUISE: S8-77-EG CORE: 40G

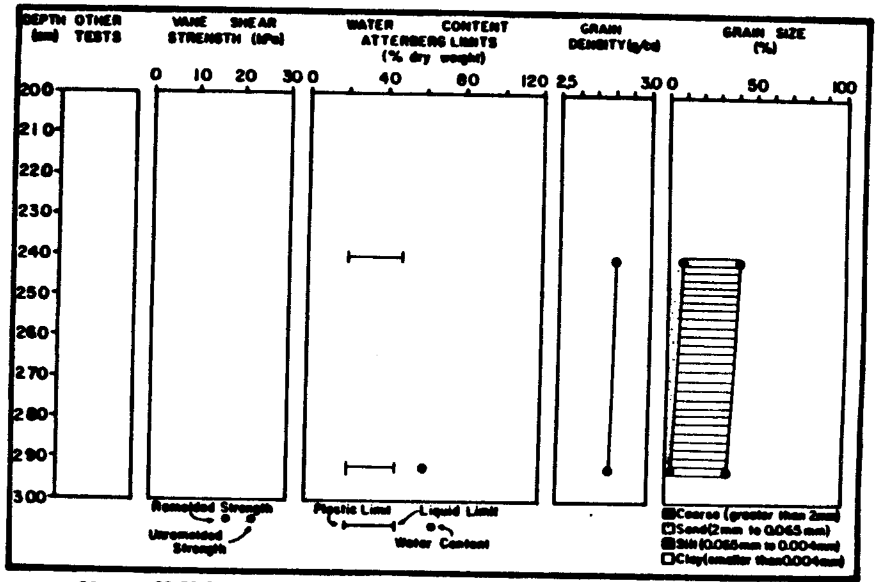

CRUISE: S8-77-EG CORE: 40G

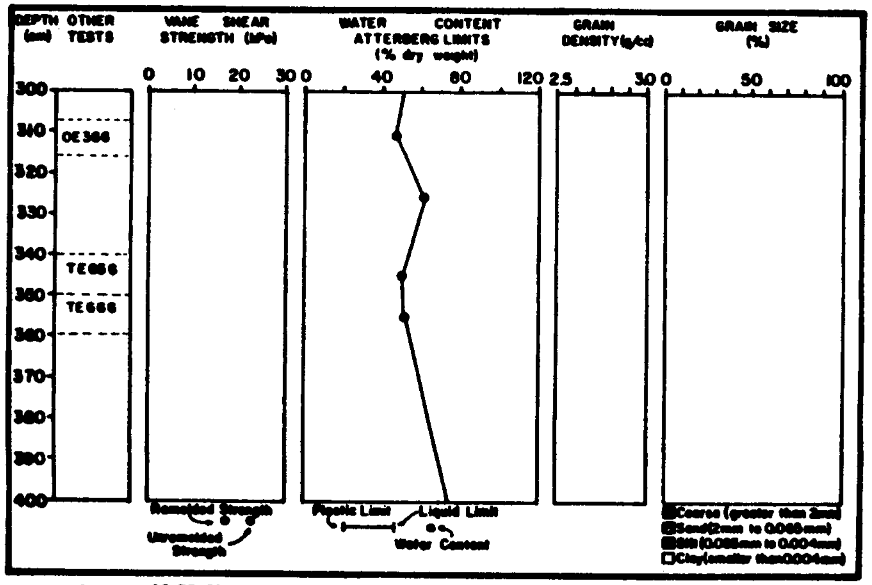

CRUISE: S8-77-EG CORE: 406

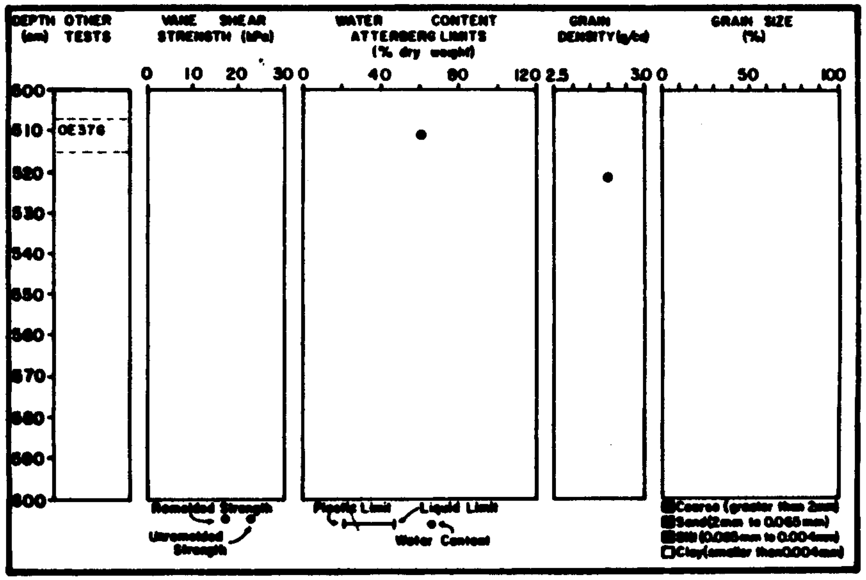

CRUISE: S8-77-EG CORE: 406

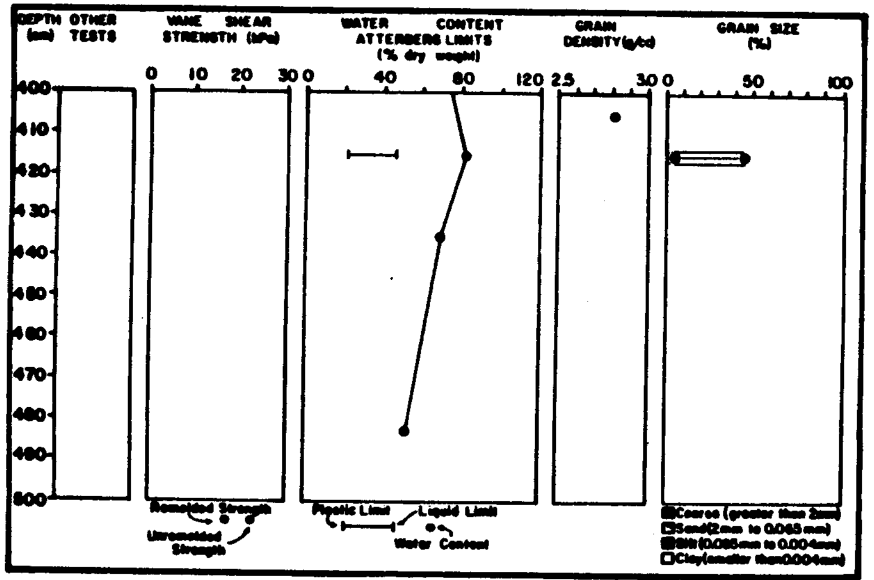

CRUISE: S8-77-EG CORE: 406

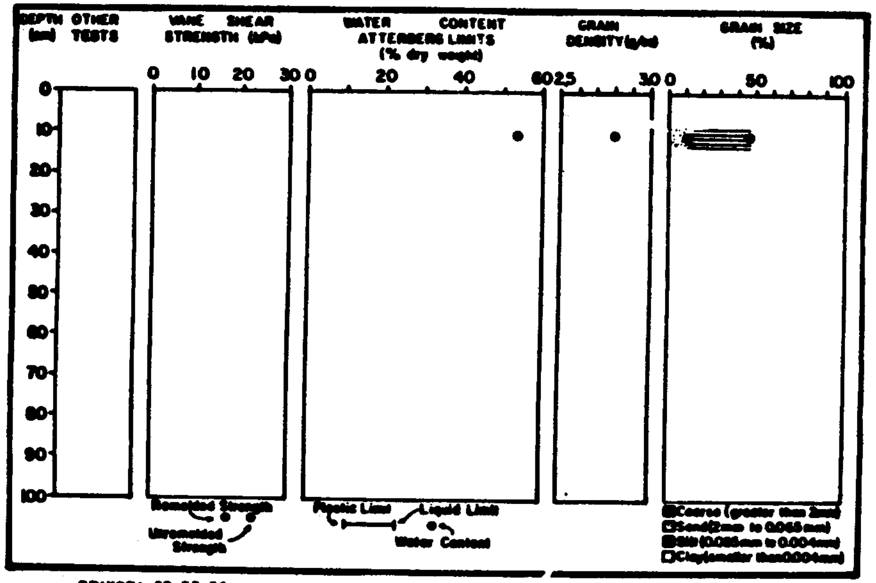

CRUISE: S8-77-EG CORE: 416

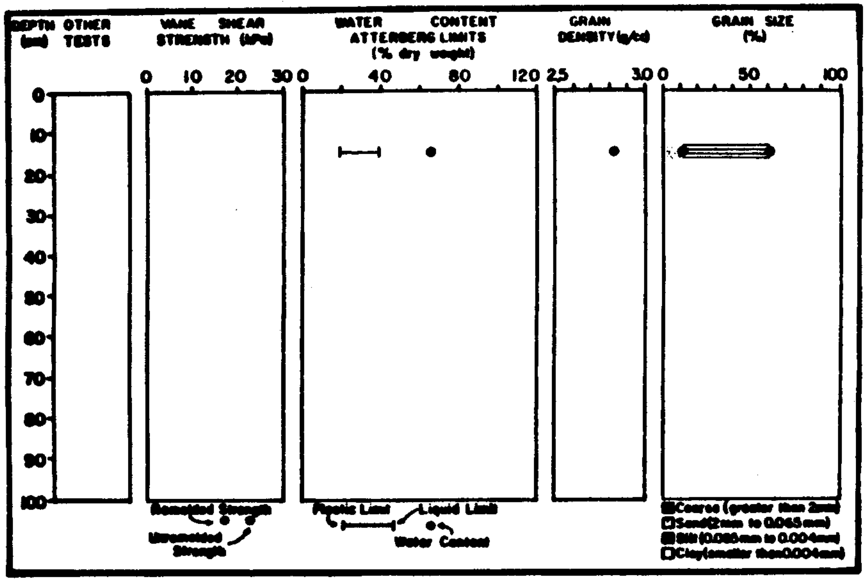

CRUISE: S8-77-EG CORE: 42G

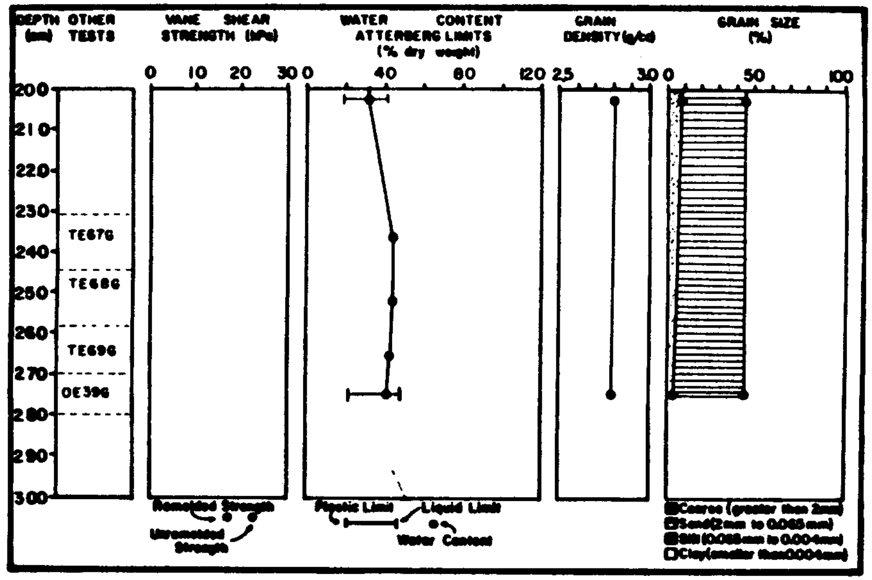

CRUISE: S8-77-EG CORE: 42 G

300

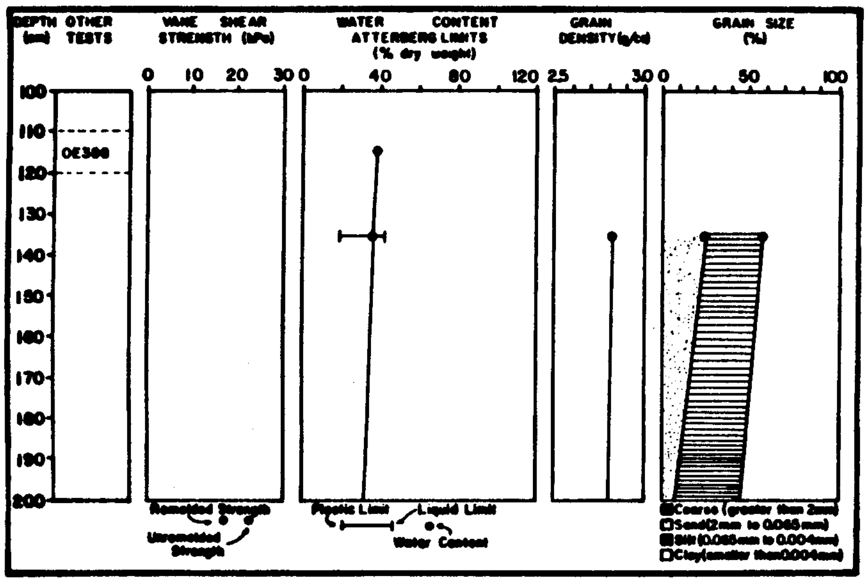

CRUISE: S8-77-EG CORE: 42G

YAKUTAT BAY STUDY AREA

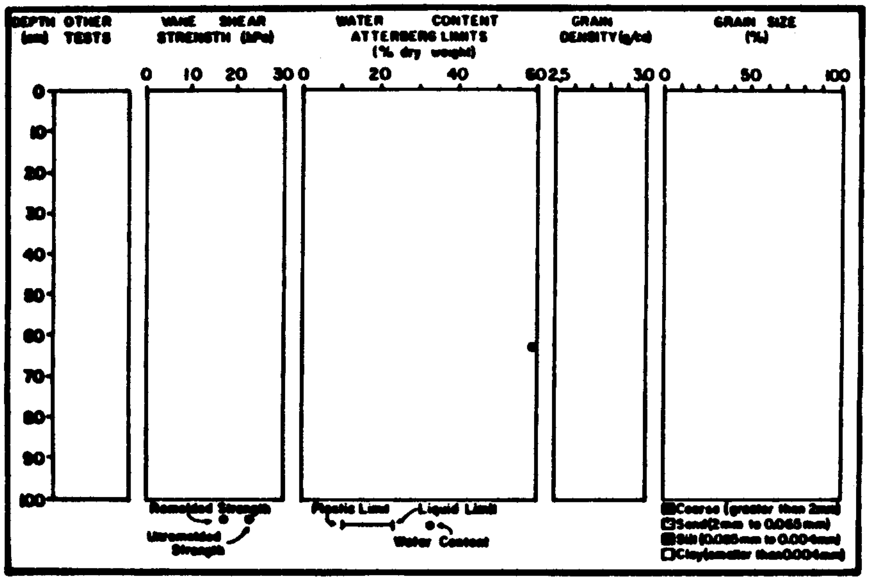

CRUISE: 58-77-EG CORE: 45G

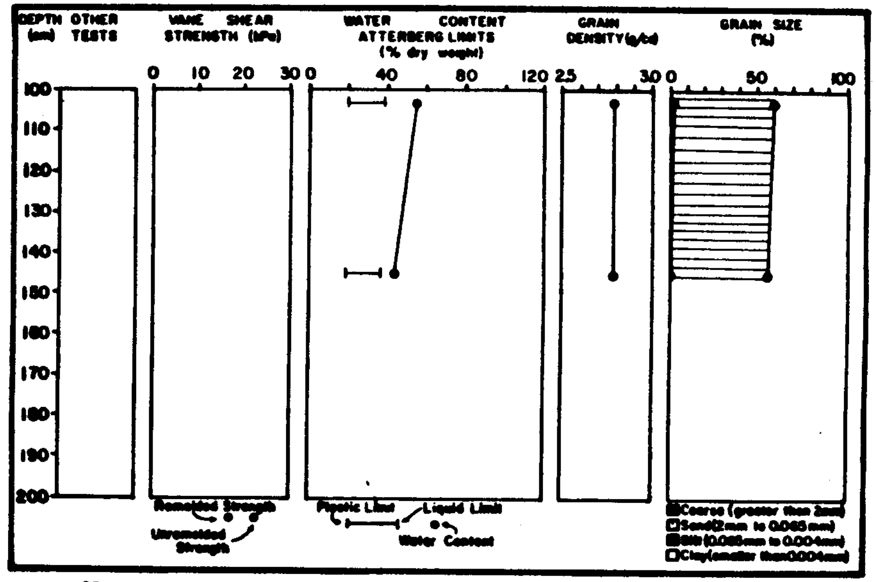

CRUISE: 58-77-EG CORE: 46G

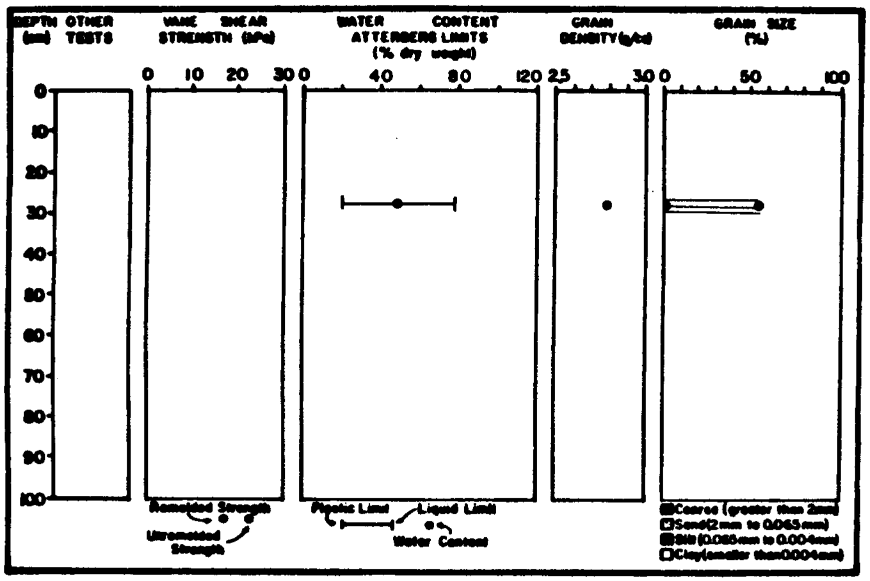

CRUISE: 58-77-EG CORE: 46G

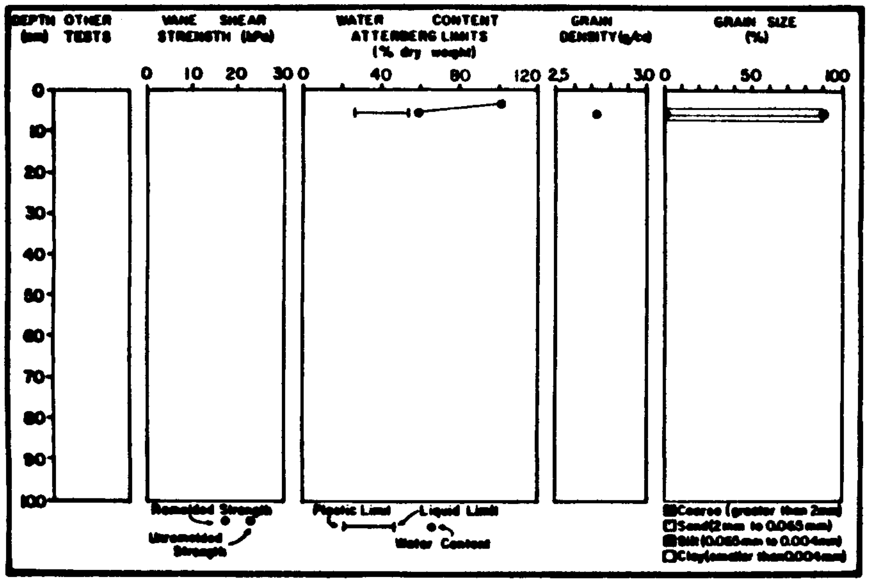

CRUISE: S8-77-EG CORE: 47G

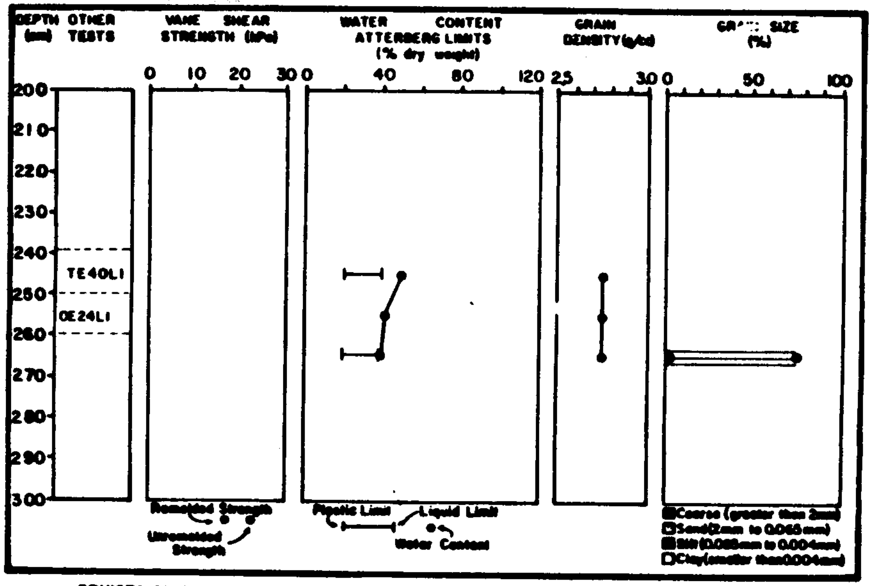

CRUISE: S8-77-EG CORE: 47G

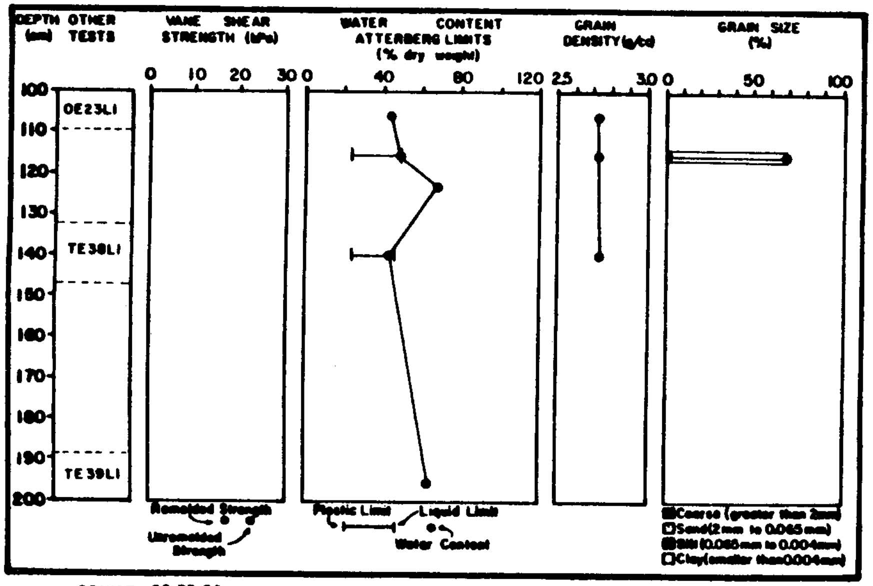

CRUISE: S8-77-EG CORE: 47G

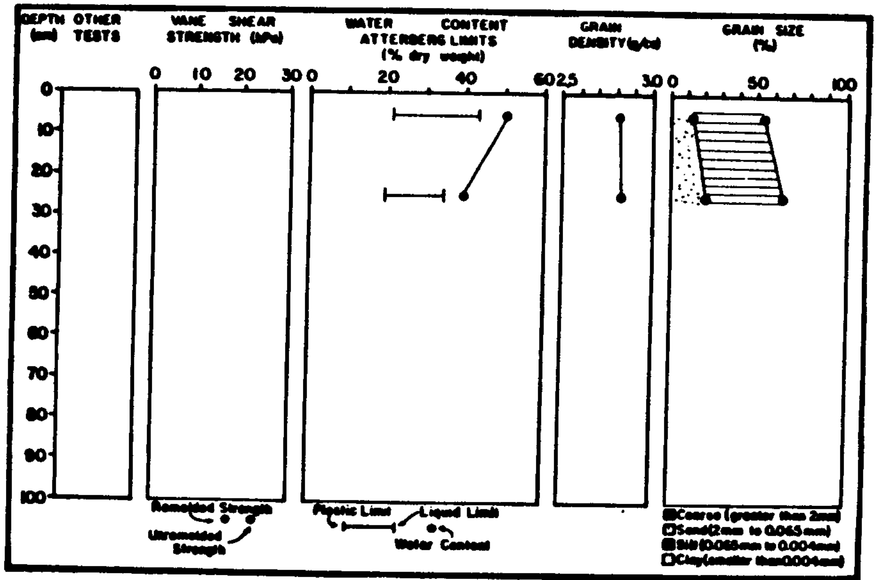

CRUISE: S8-77-EG CORE: 48G

YAKUTAT STUDY AREA

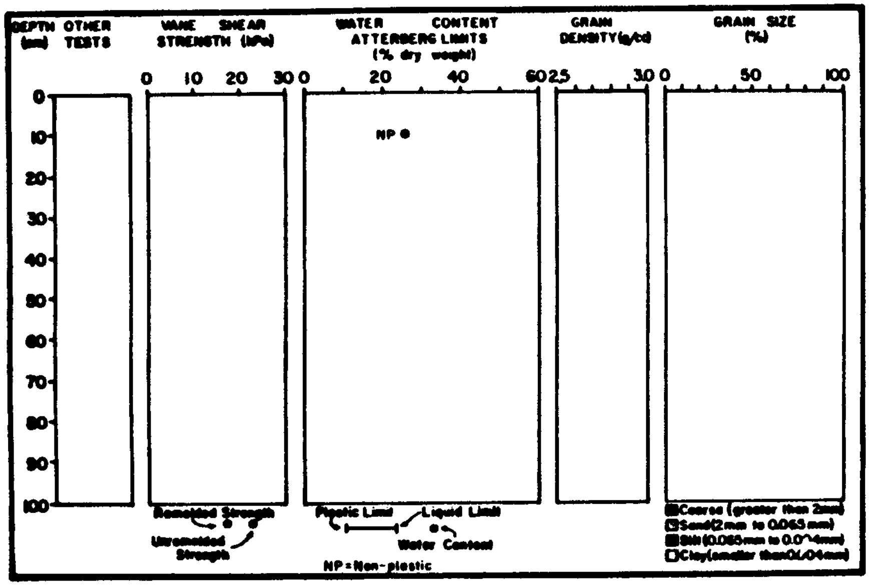

CRUISE: DC2-80-EG CORE: 61G

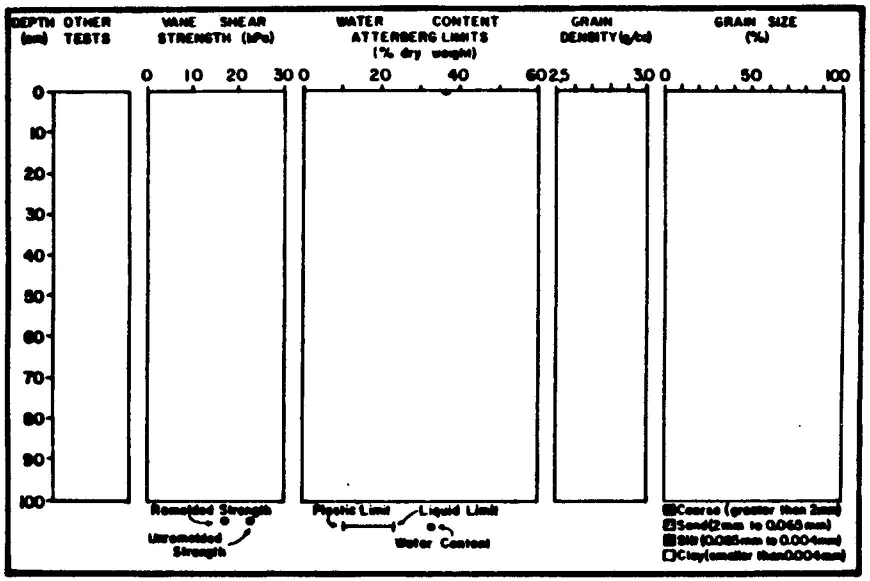

CRUISE: DC2-80-EG CORE: 65G

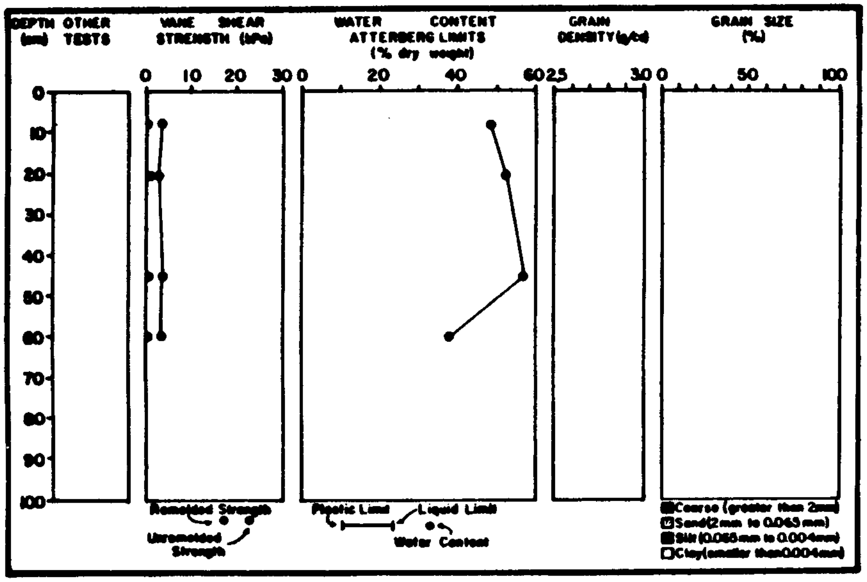

CRUISE: DC2-80-EG CORE: 64G

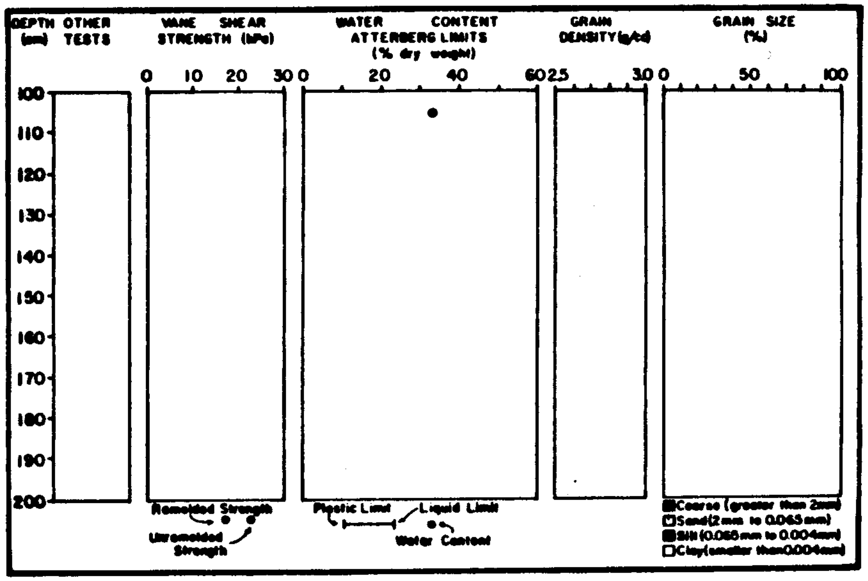

CRUISE: DC2-80-EG CORE: 65G

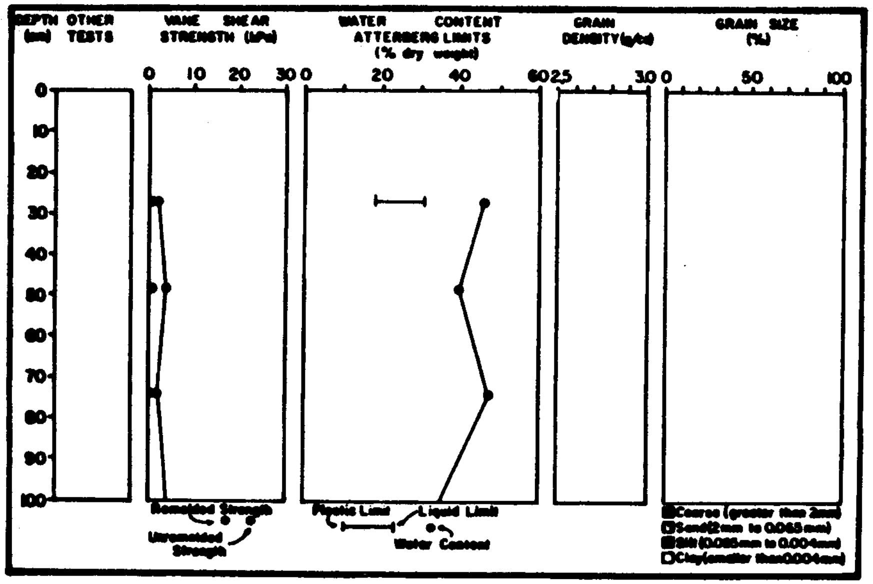

CRUISE: DC2-80-EG CORE: 66G

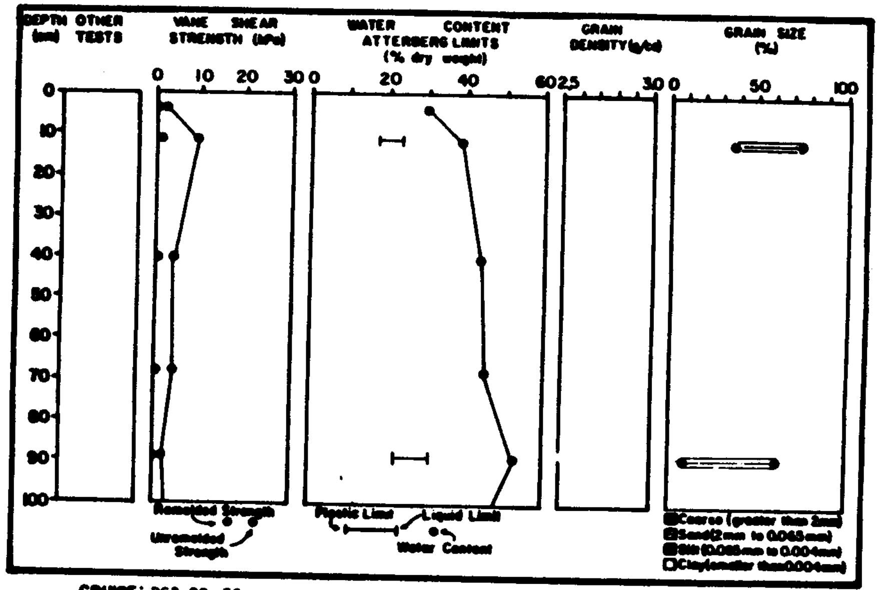

CRUISE: DC2-80-EG CORE: 69G

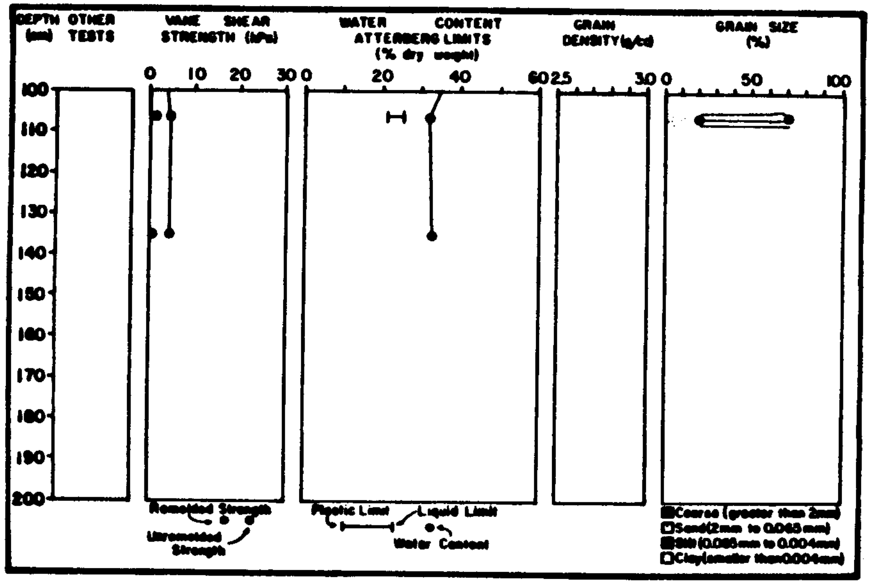

CRUISE: DC2-80-EG CORE: 66G

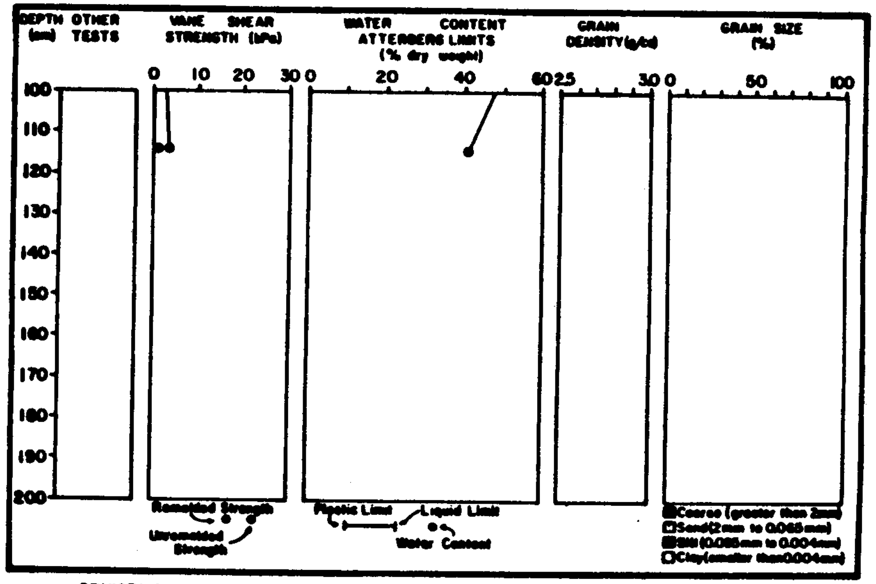

CRUISE: DC2-80-EG CORE: 69G

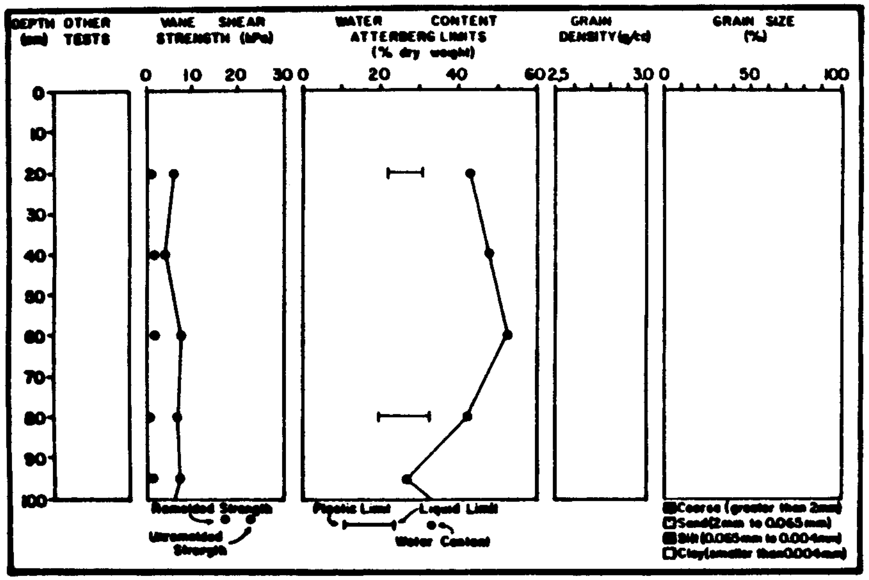

CRUISE: DC2-80-EG CORE: 72G

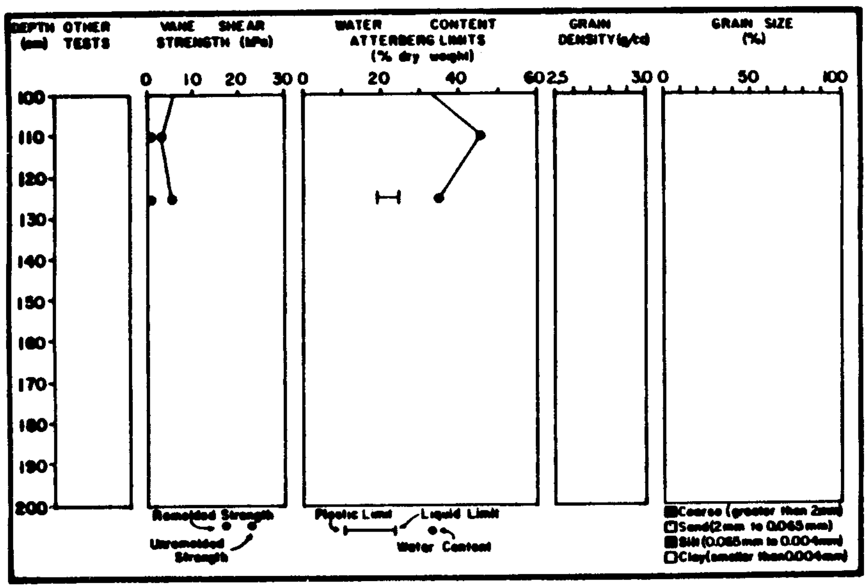

CRUISE: DC2-80-EG CORE: 72G

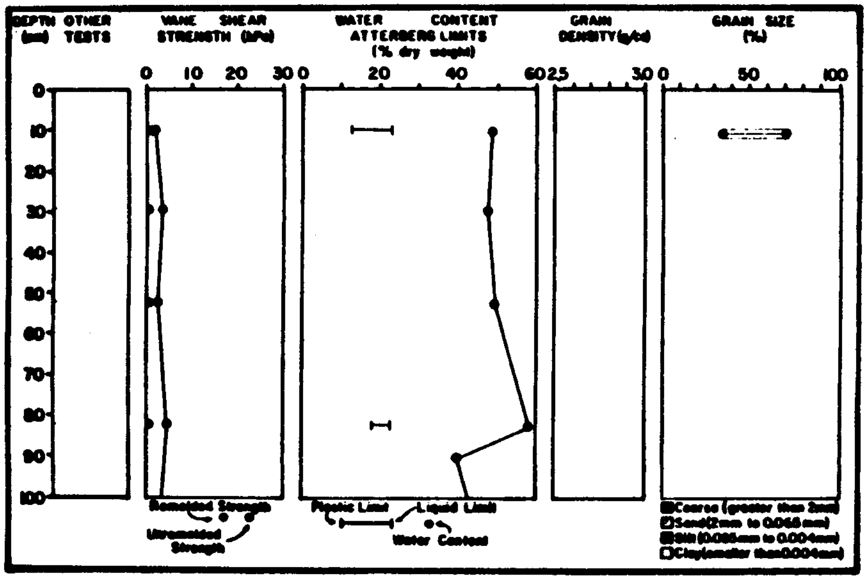

CRUISE: DC2-80-EG CORE: 836

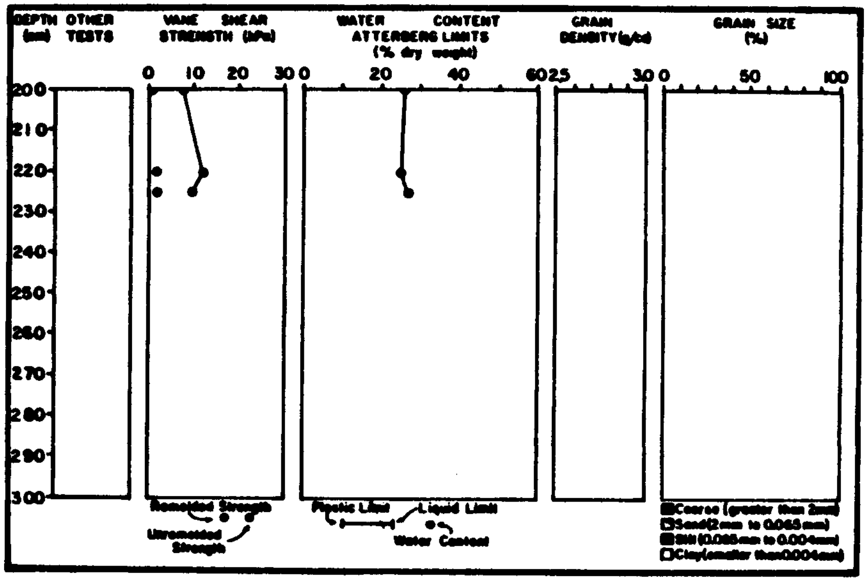

CRUISE: DC2-80-EG CORE: 836

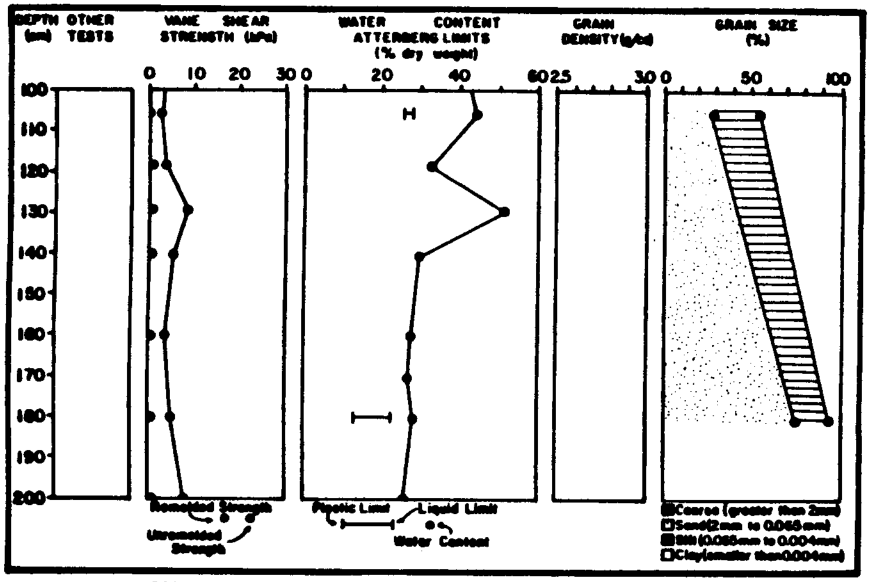

CRUISE: DC2-80-EG CORE: 836

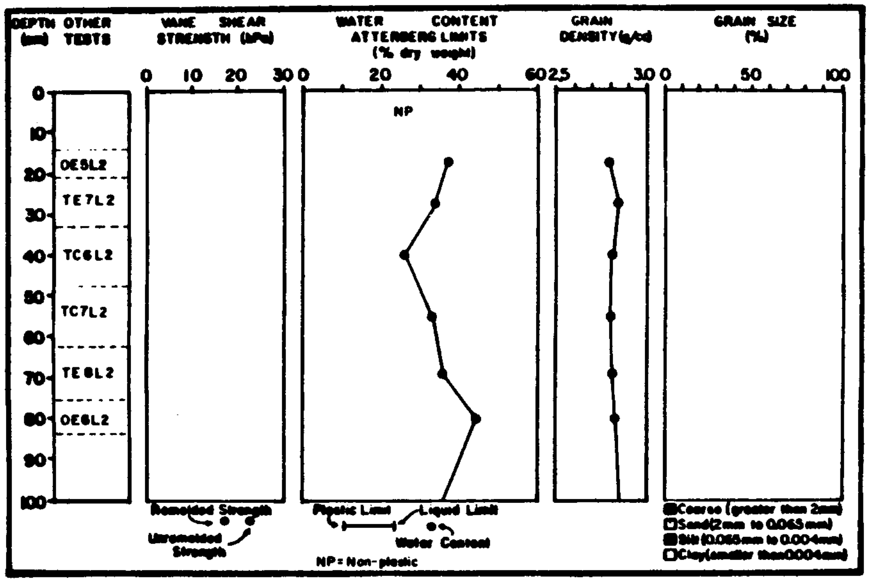

CRUISE: DC2-80-EG CORE: 84G

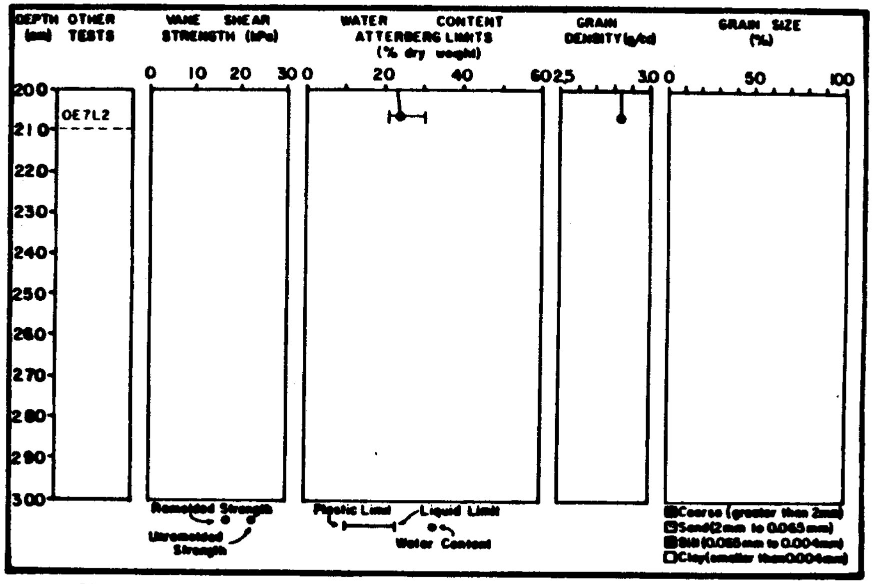

CRUISE: DC2-80-EG CORE: 84G

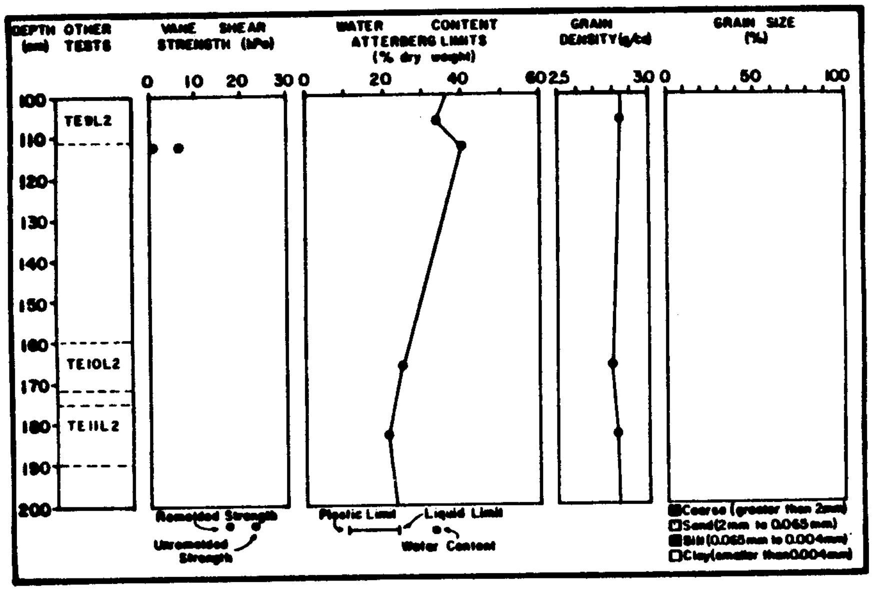

CRUISE: DC2-80-EG CORE: 84G

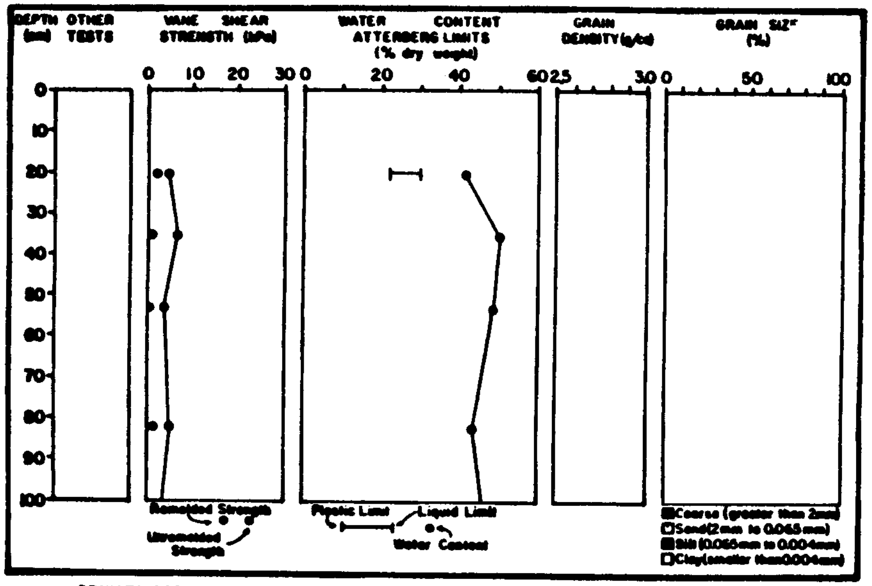

CRUISE: DC2-80-EG CORE: 85G

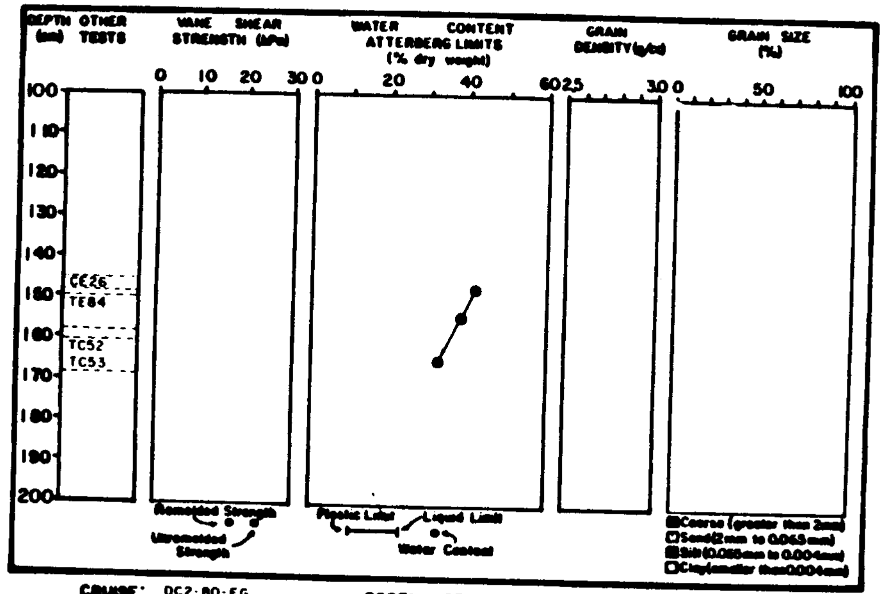

CRUISE: DC2-80-EG CORE: 87G

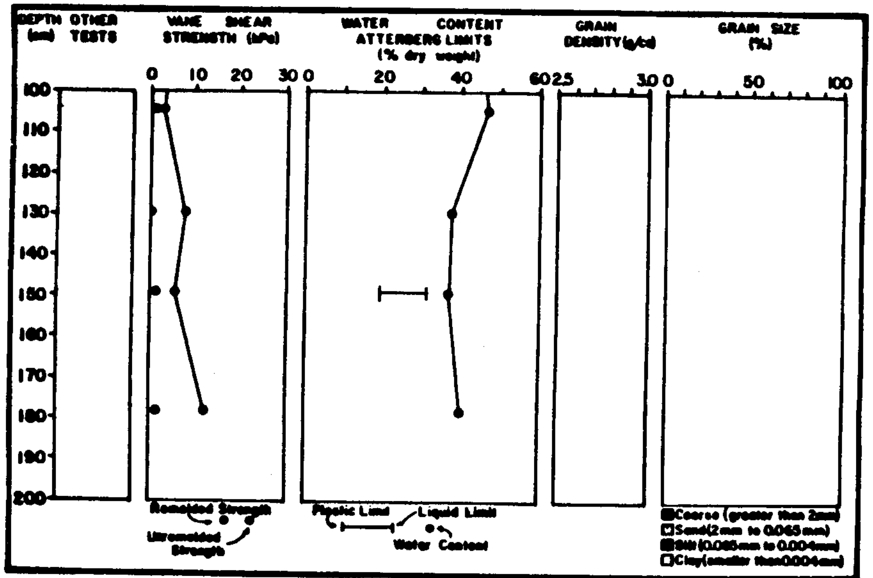

CRUISE: DC2-80-EG CORE: 85G

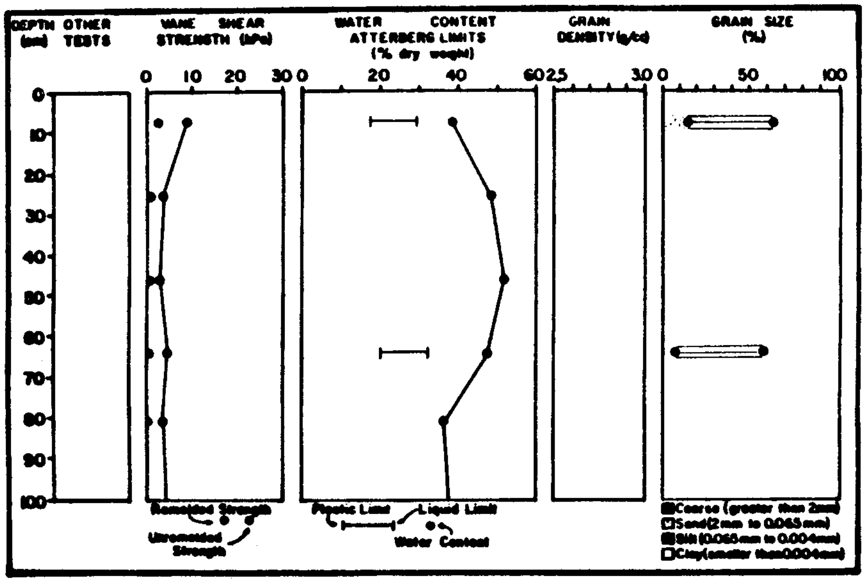

CRUISE: DC2-80-EG CORE: 88G

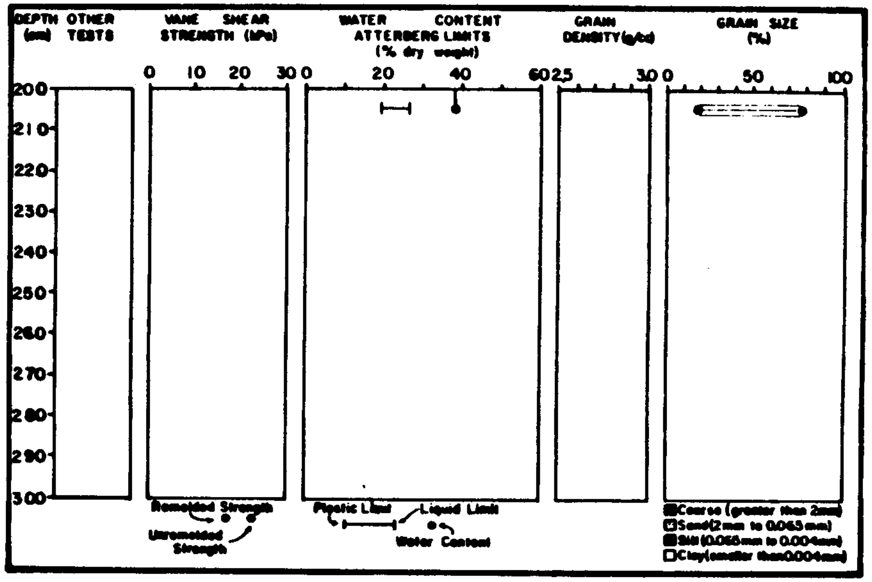

CRUISE: DC2-80-EG CORE: 88G

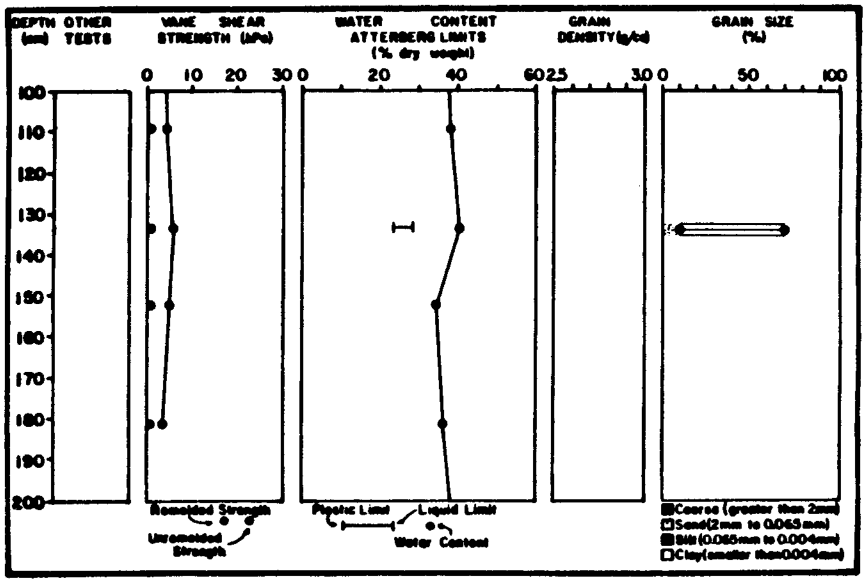

CRUISE: DC2-80-EG CORE: 88G

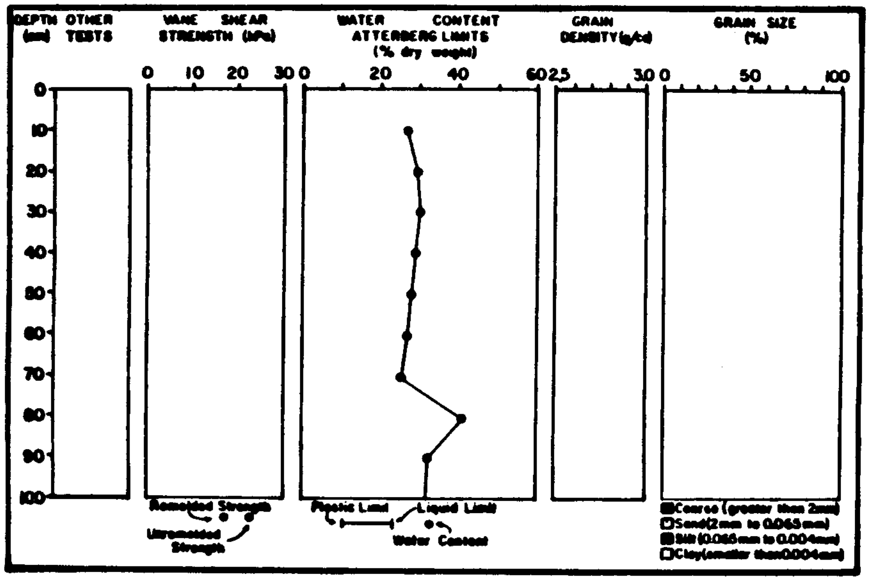

CRUISE: DCI-81-EG CORE: 616A2

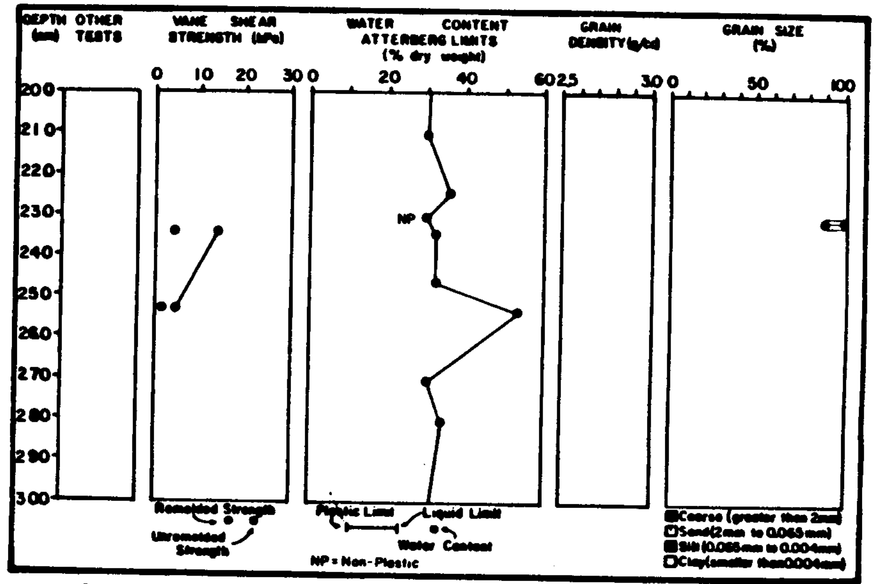

CRUISE: DCI-81-EG CORE: 616A2

313

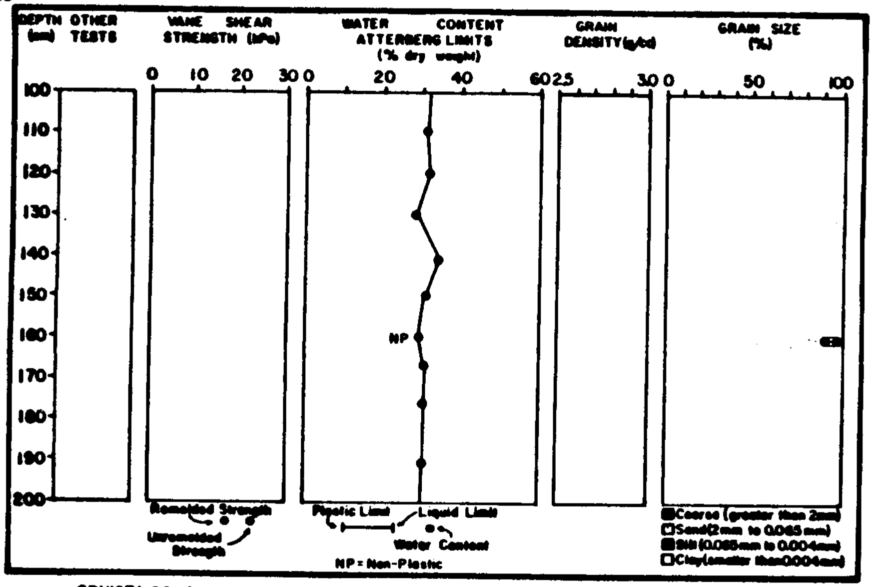

CRUISE: DCI-81-EG CORE: 616A2

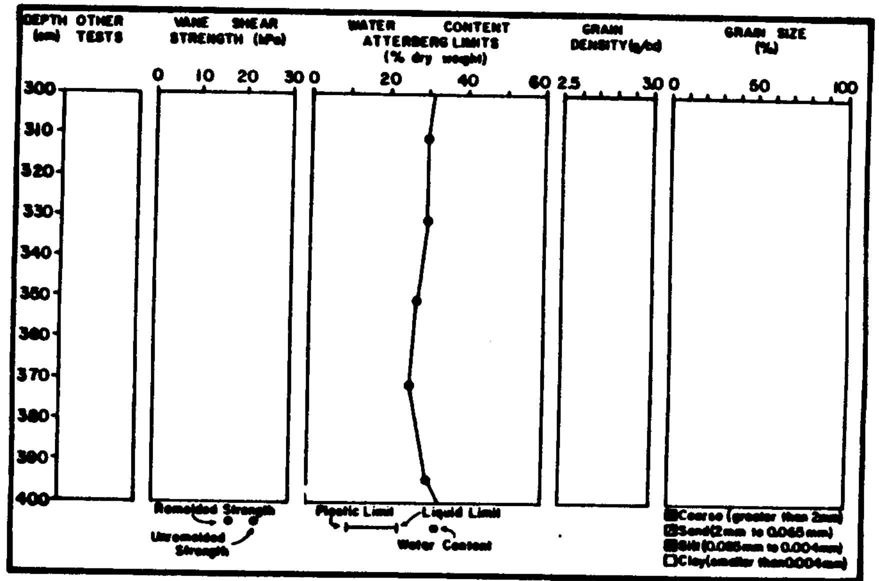

CRUISE: DCI-81-EG CORE: 616A2

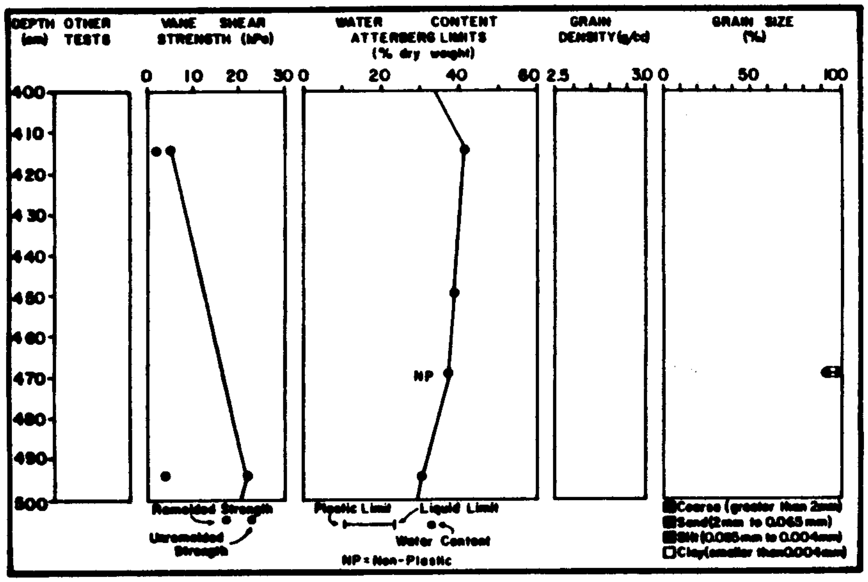

CRUISE: DCI-81-EG CORE: 616A2

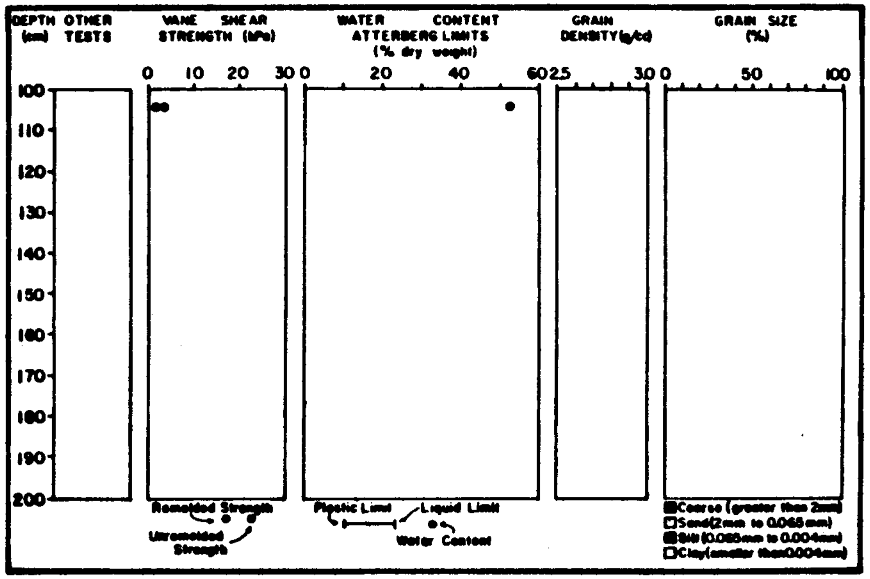

CRUISE: DCI-81-EG CORE: 617G1

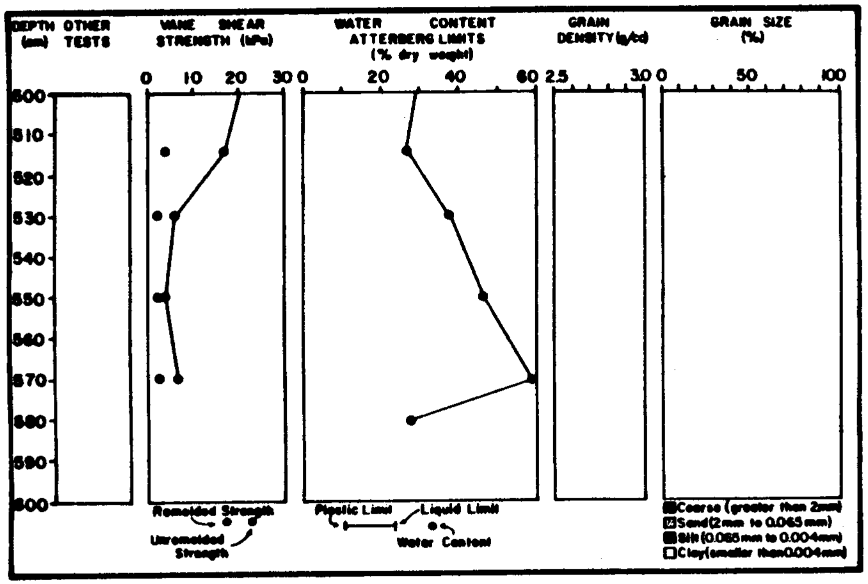

CRUISE: DCI-81-EG CORE: 616A2

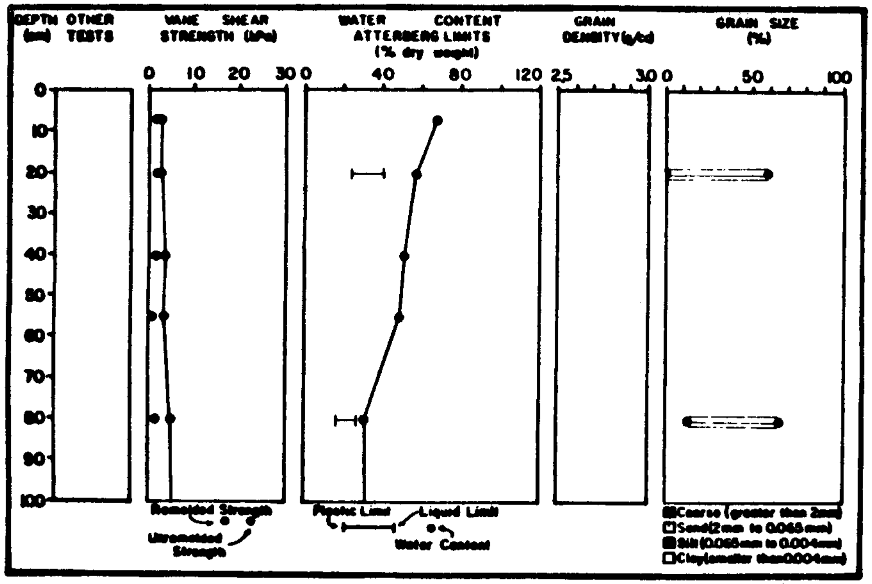

CRUISE: DCI-81-EG CORE: 617G2

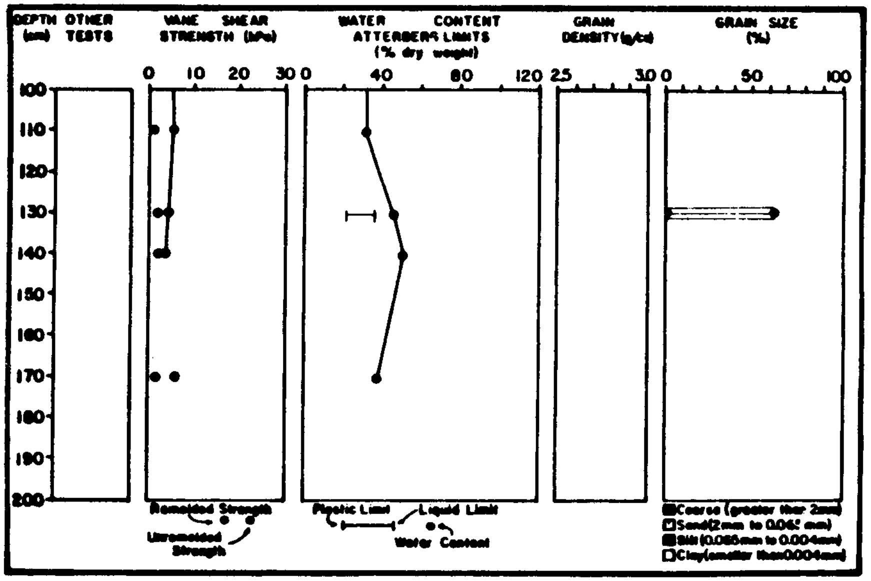

CRUISE: DCI-81-EG CORE: 617G2

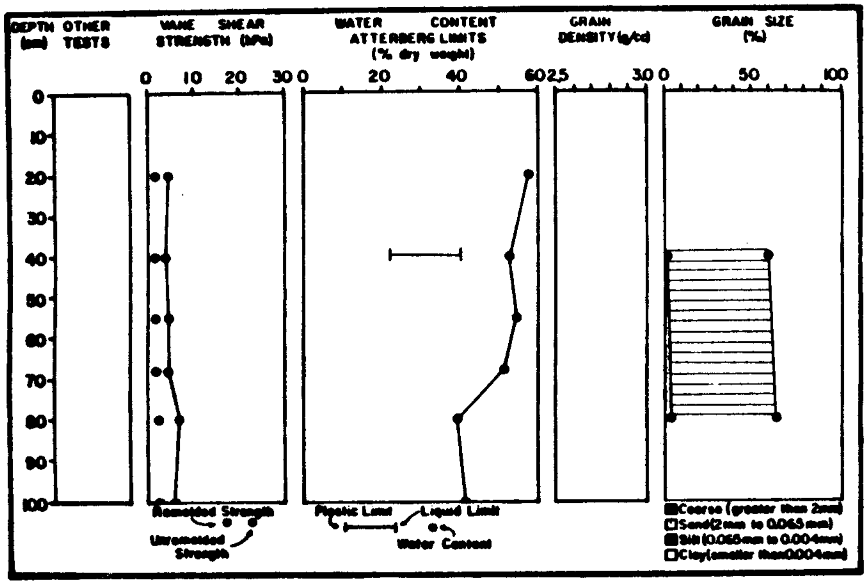

CRUISE: DCI-81-EG CORE: 618G1

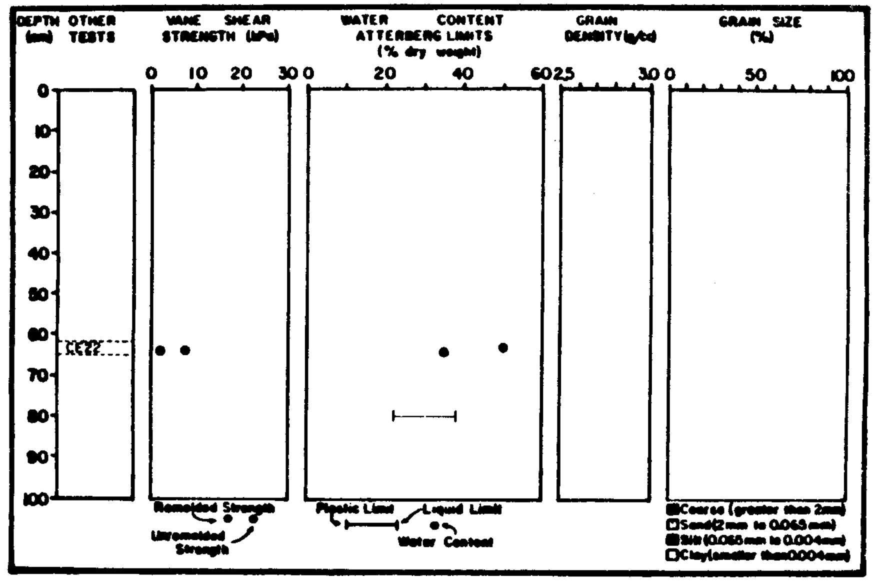

CRUISE: DCI-81-EG CORE: 618G2

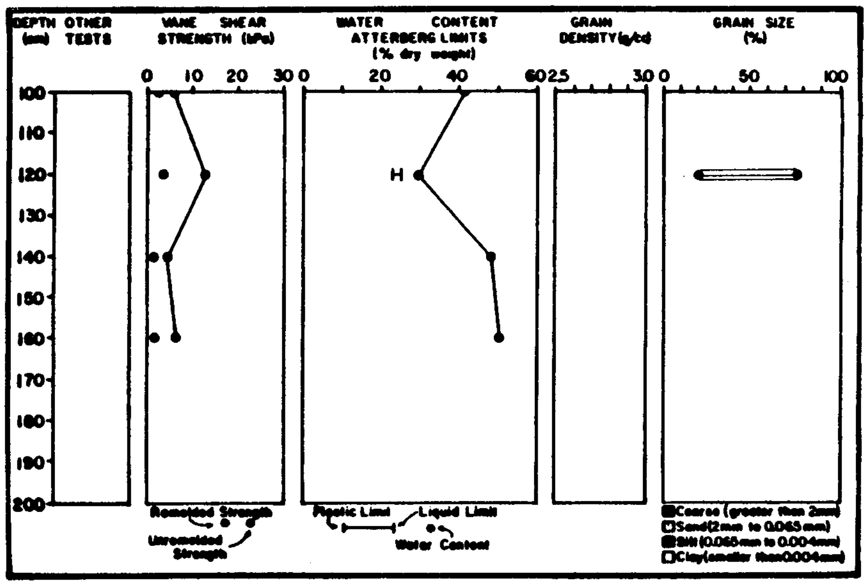

CRUISE: DCI-81-EG CORE: 618G1

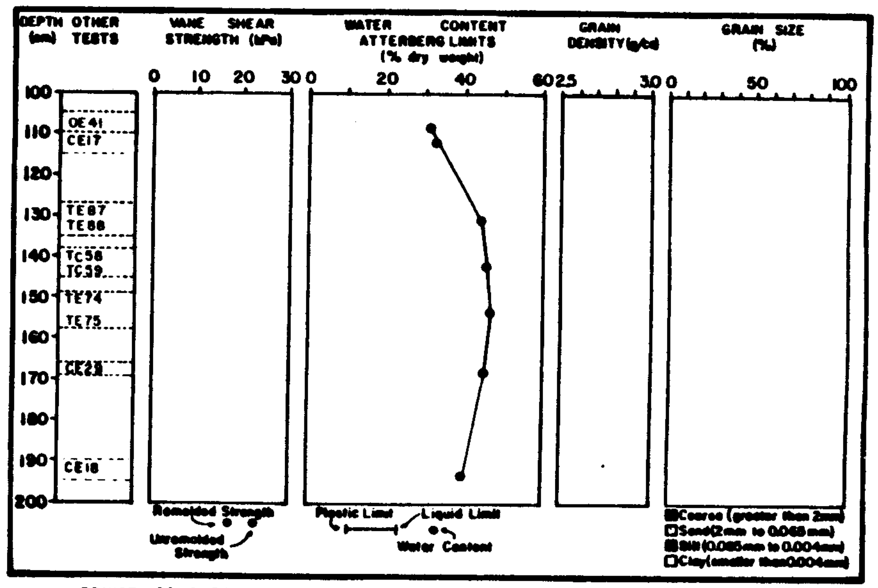

CRUISE: DCI-81-EG CORE: 618G2

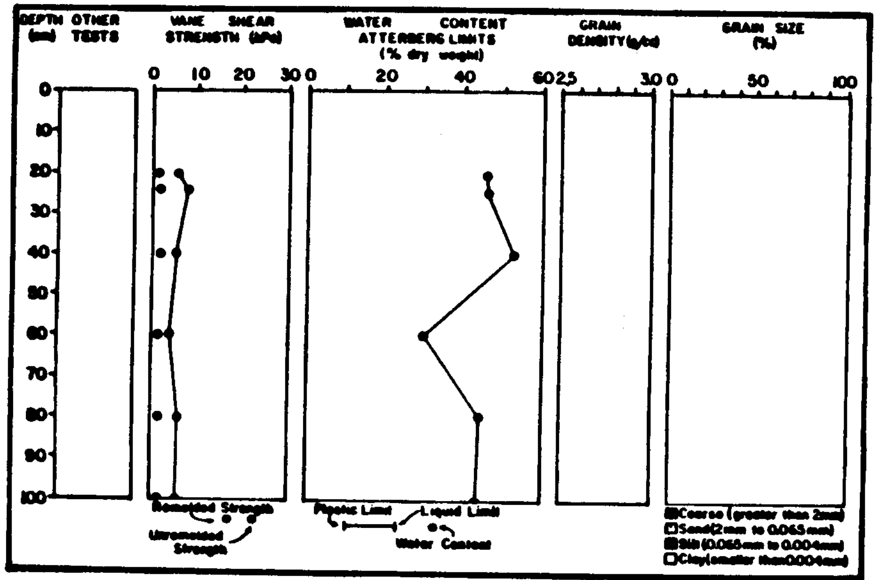

CRUISE: DCI-81-EG CORE: 619GI

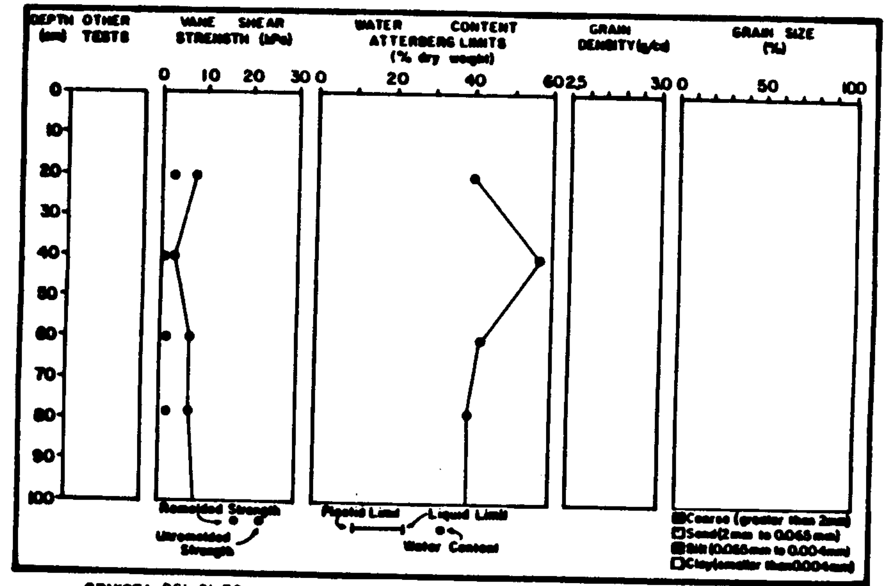

CRUISE: DCI-81-EG CORE: 620GI

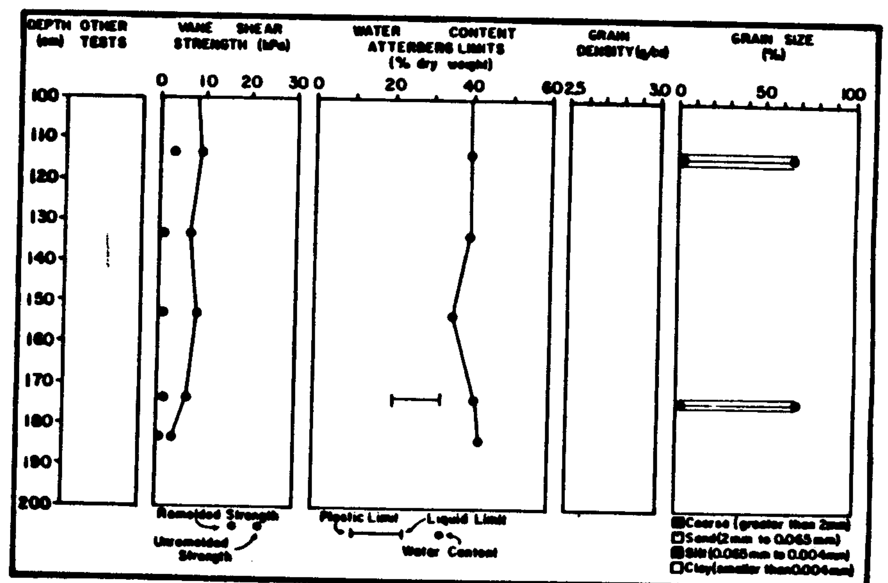

CRUISE: DCI-81-EG CORE: 620GI

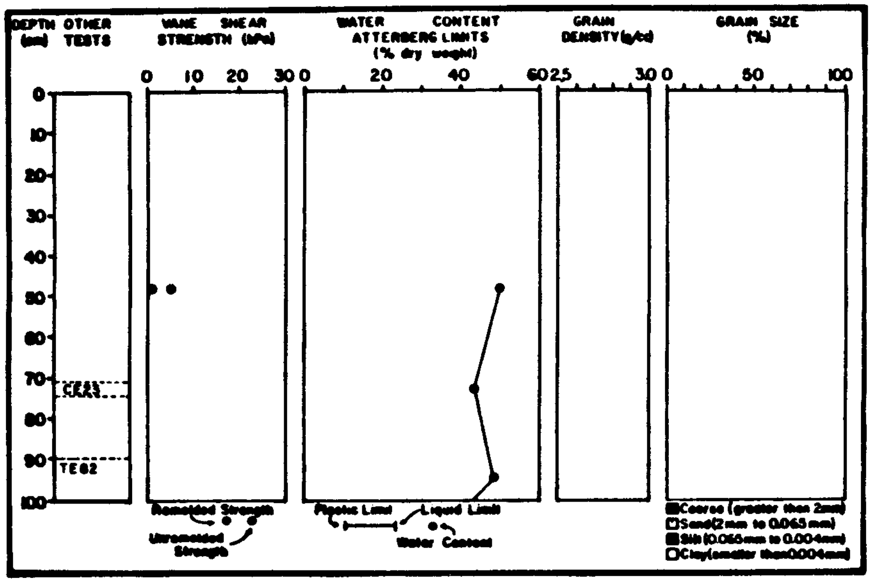

CRUISE: DCI-81-EG CORE: 620G2

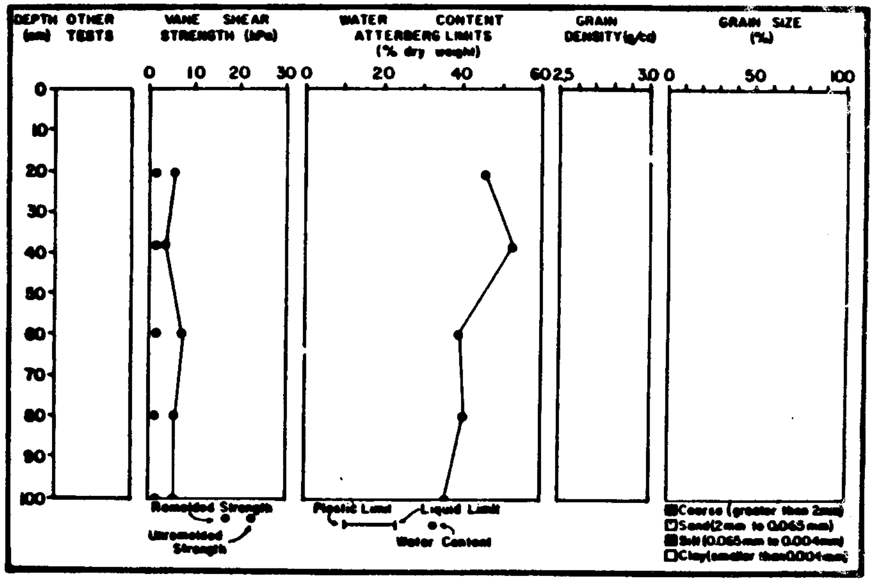

CRUISE: DCI-81-EG CORE: 621G1

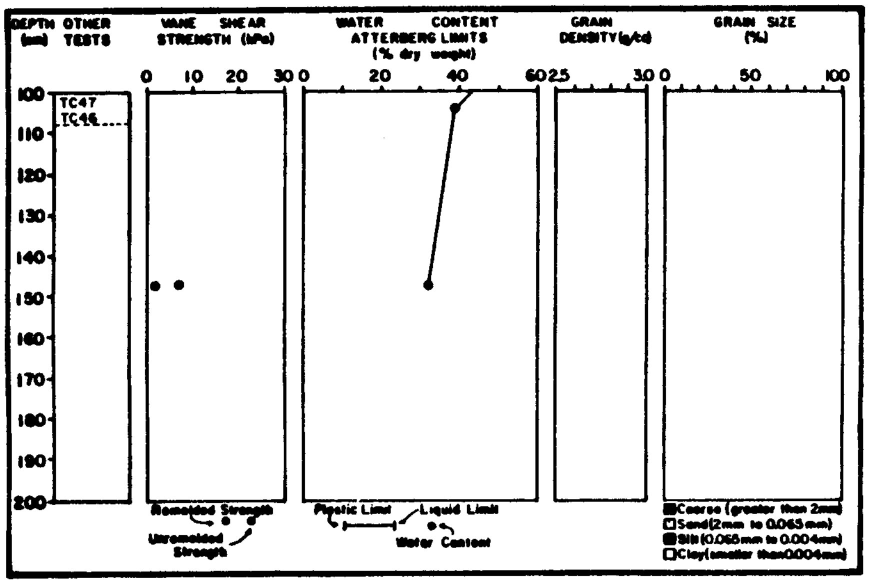

CRUISE: DCI-81-EG CORE: 620G2

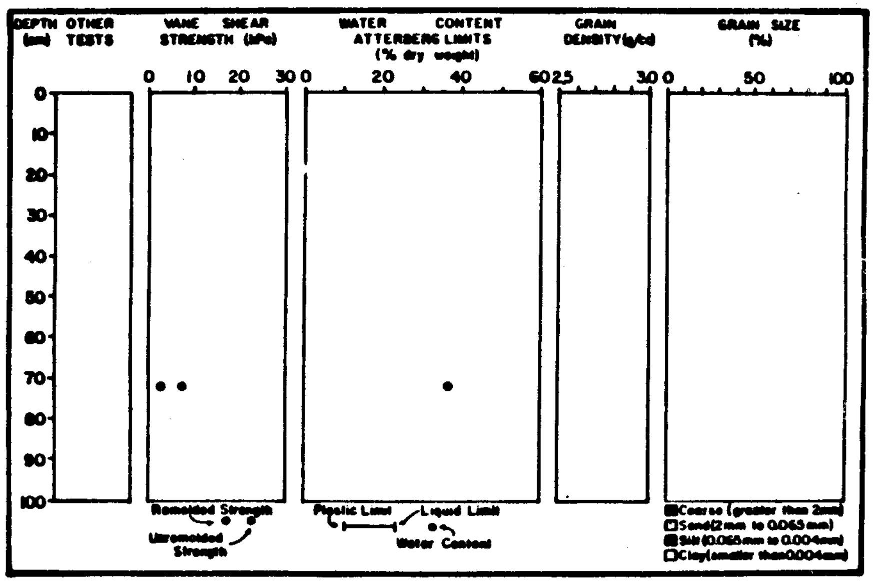

CRUISE: DCI-81-EG CORE: 621G2

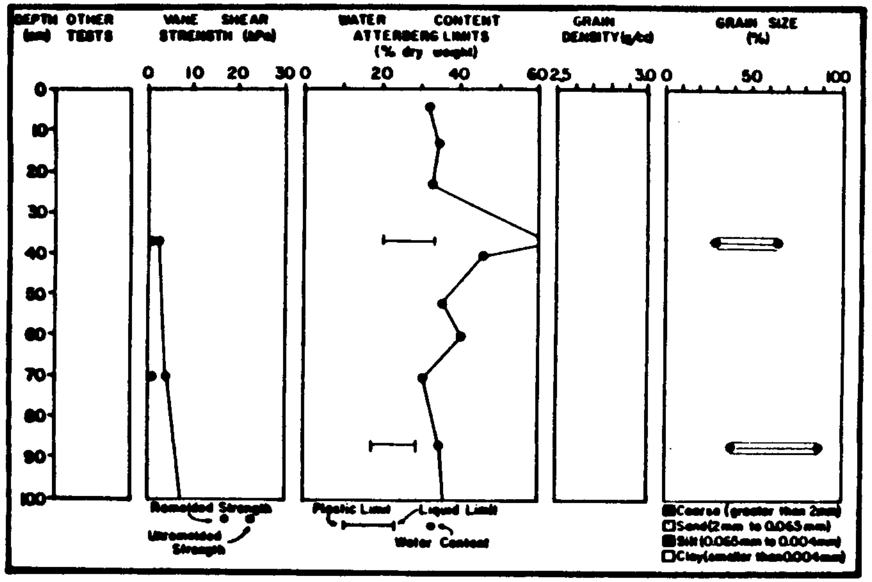

CRUISE: DCI-81-EG CORE: 623A1

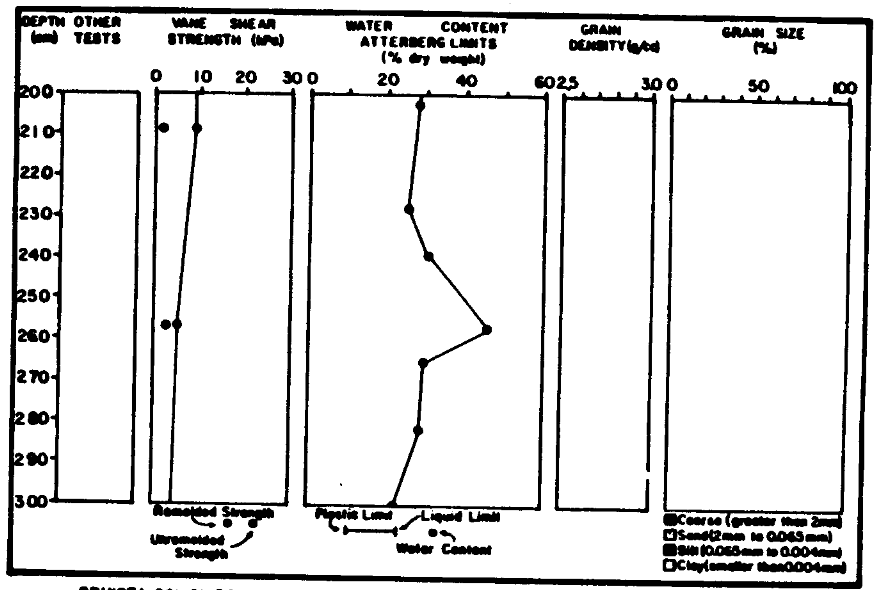

CRUISE: DCI-81-EG CORE: 623A1

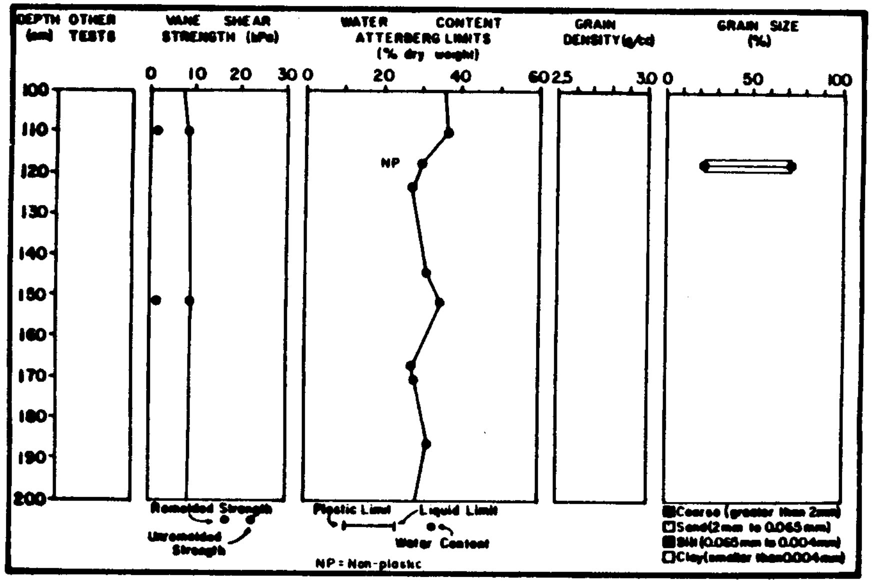

CRUISE: DCI-81-EG CORE: 623A1

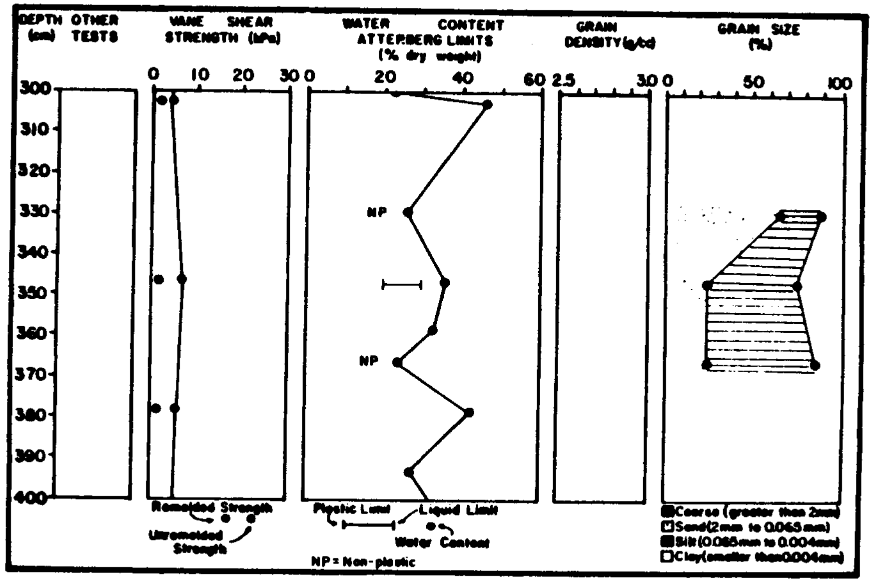

CRUISE: DCI-81-EG . CORE: 623A1

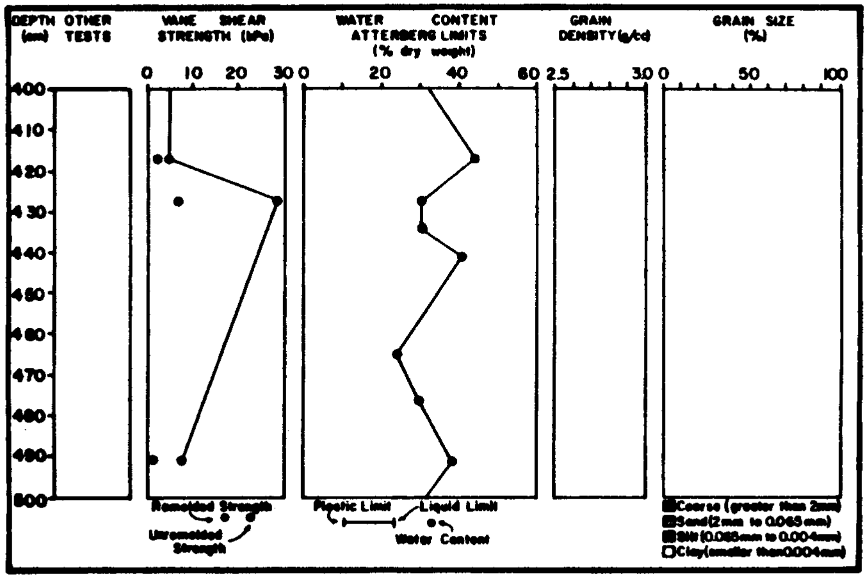

CRUISE: DCI-81-EG CORE: 623A1

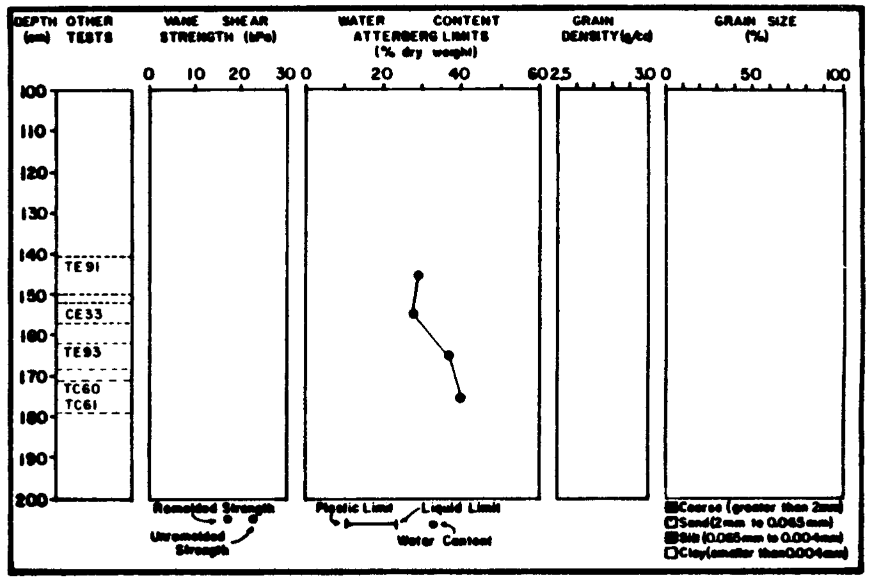

CRUISE: DCI-81-EG CORE: 624A1

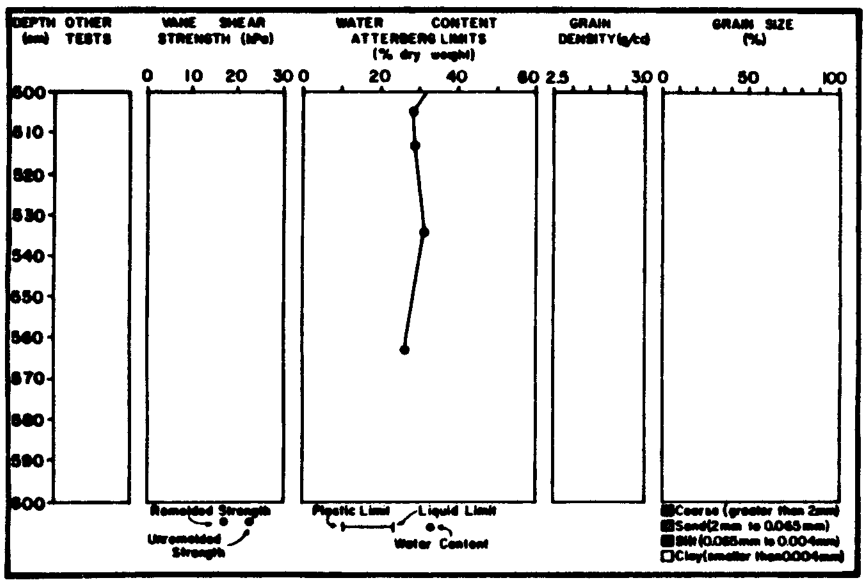

CRUISE: DCI-81-EG CORE: 623A1

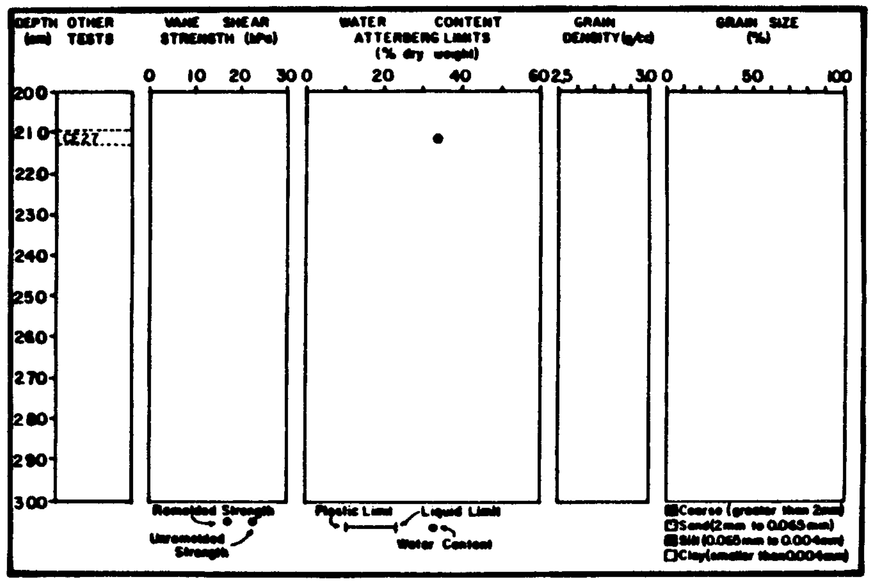

CRUISE: DCI-81-EG CORE: 624A1

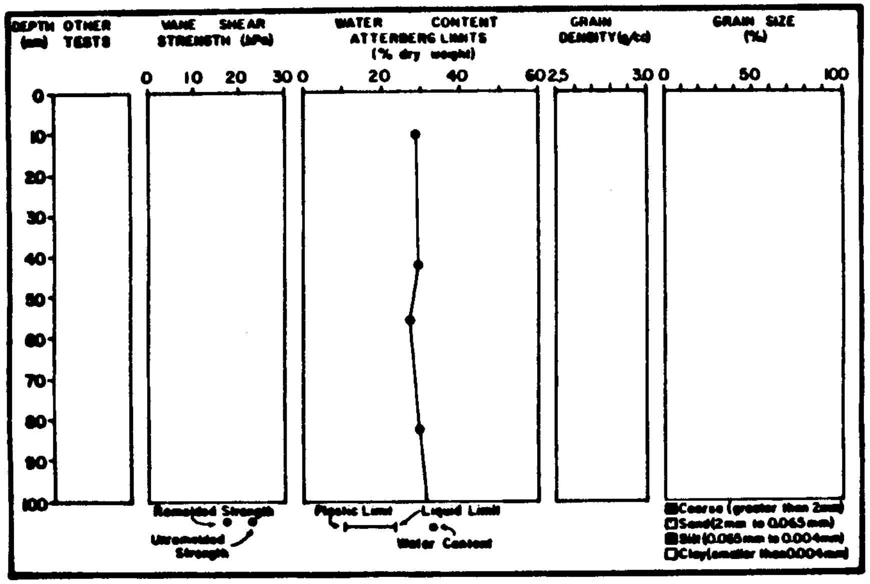

CRUISE: DCI-81-EG CORE: 624A2

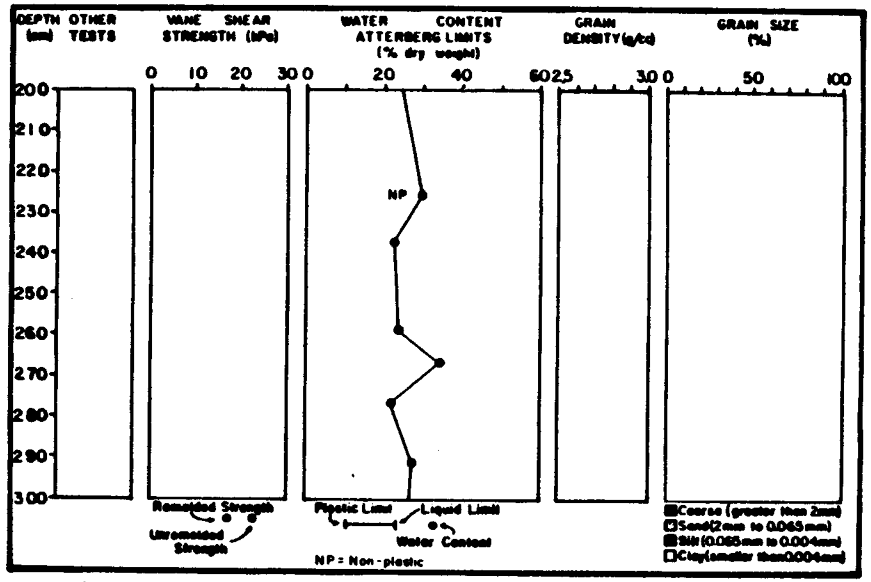

CRUISE: DCI-81-EG CORE: 624A2

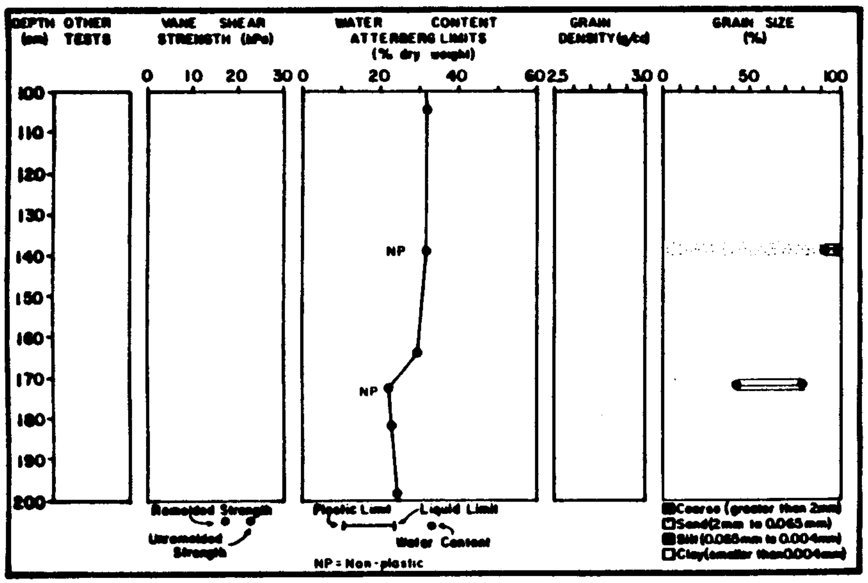

CRUISE: DCI-81-EG CORE: 624A2

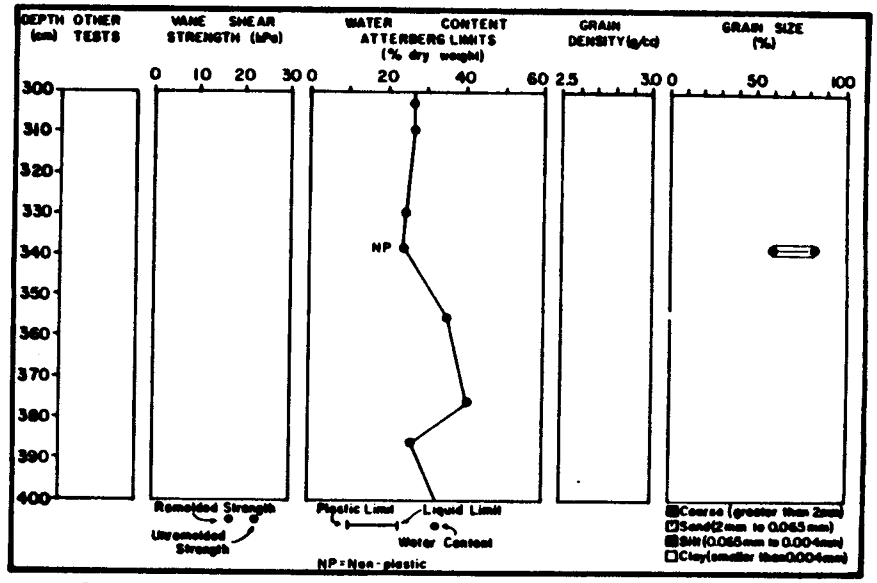

CRUISE: DCI-81-EG CORE: 624A2

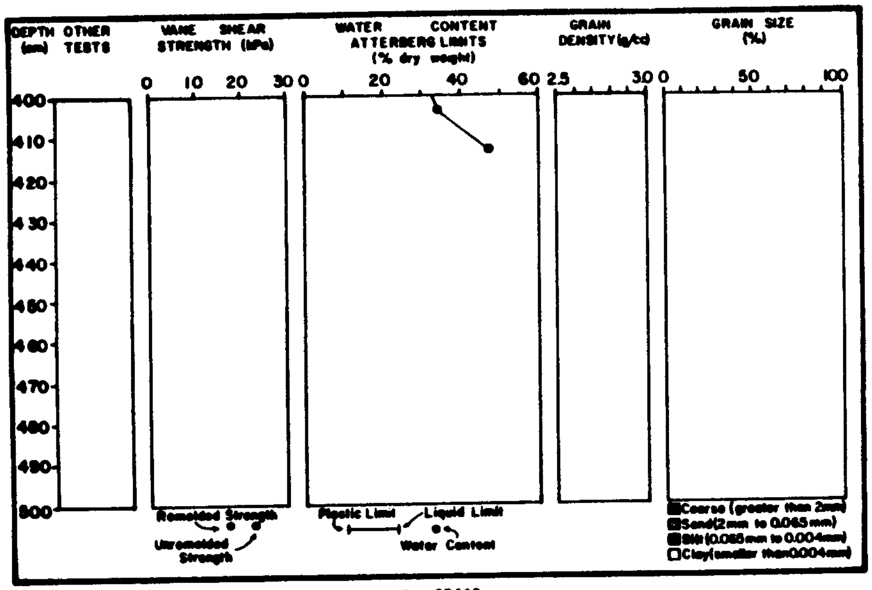

CRUISE: DCI-81-EG CORE: 624A2

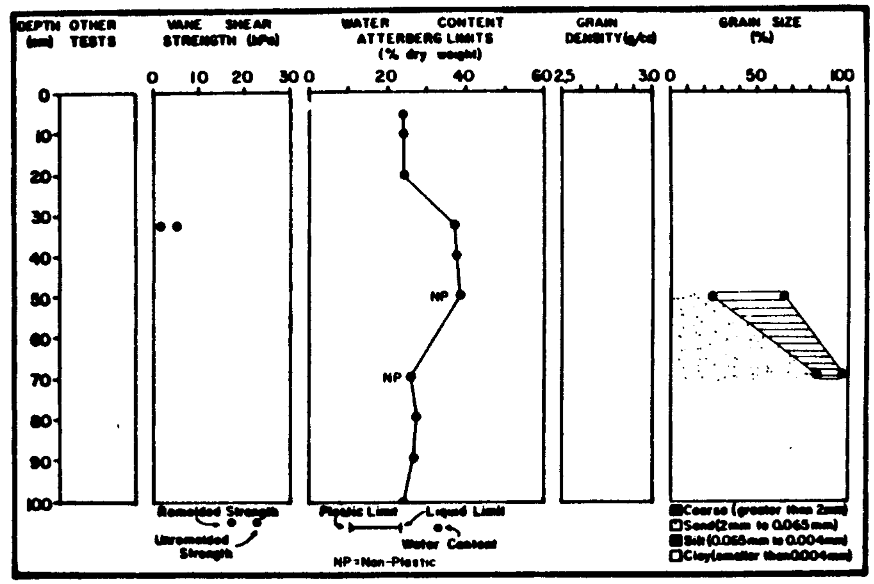

CRUISE: DCI-81-EG CORE: 625A2

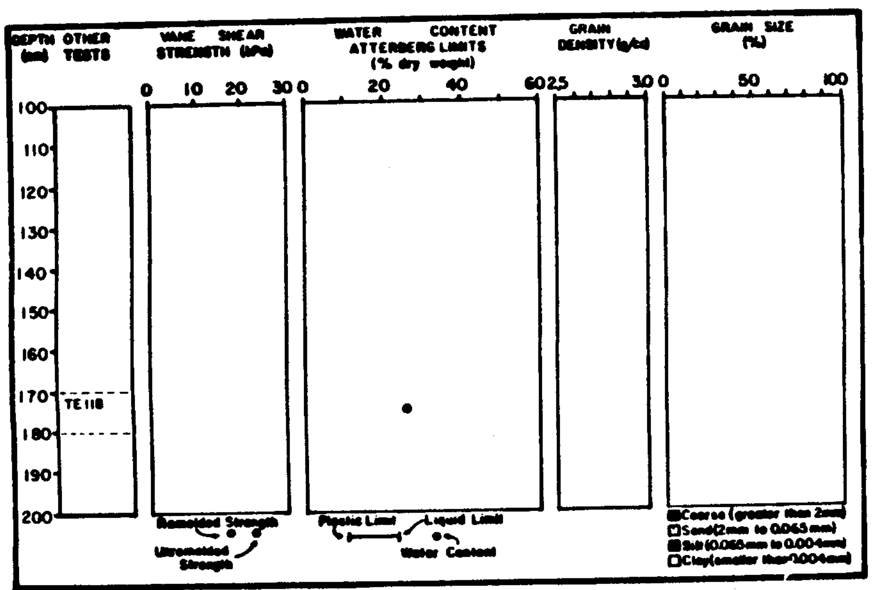

CRUISE: DCI-81-EG CORE: 625A1

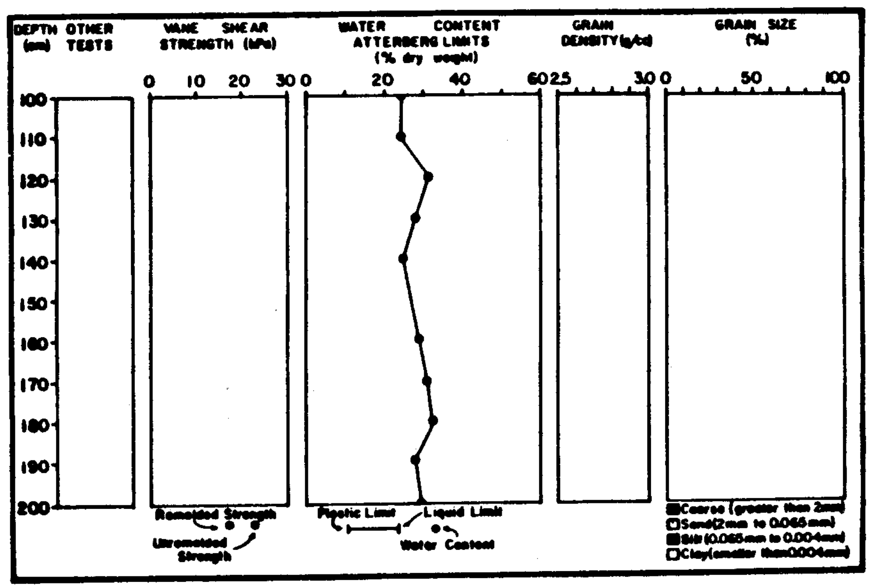

CRUISE: DCI-81-EG CORE: 625A2

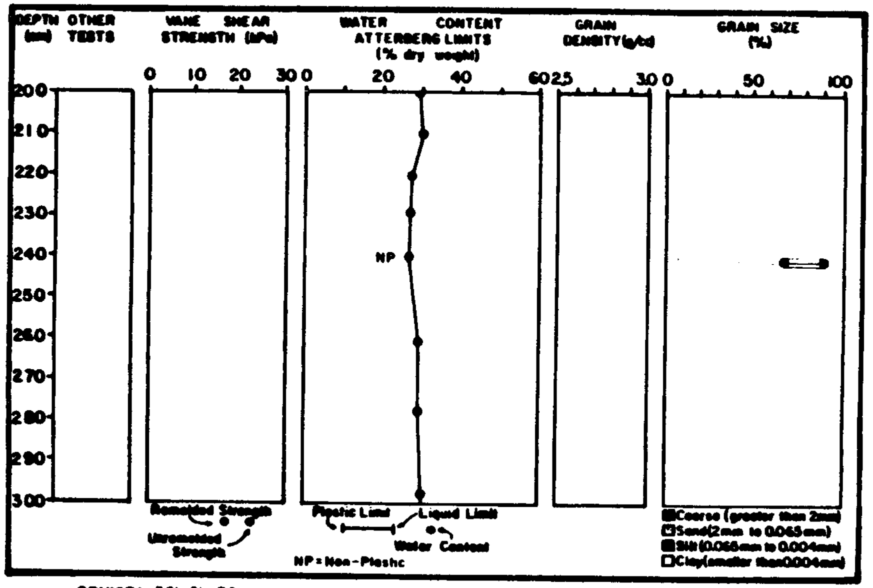

CRUISE: DCI-81-EG CORE: 625A2

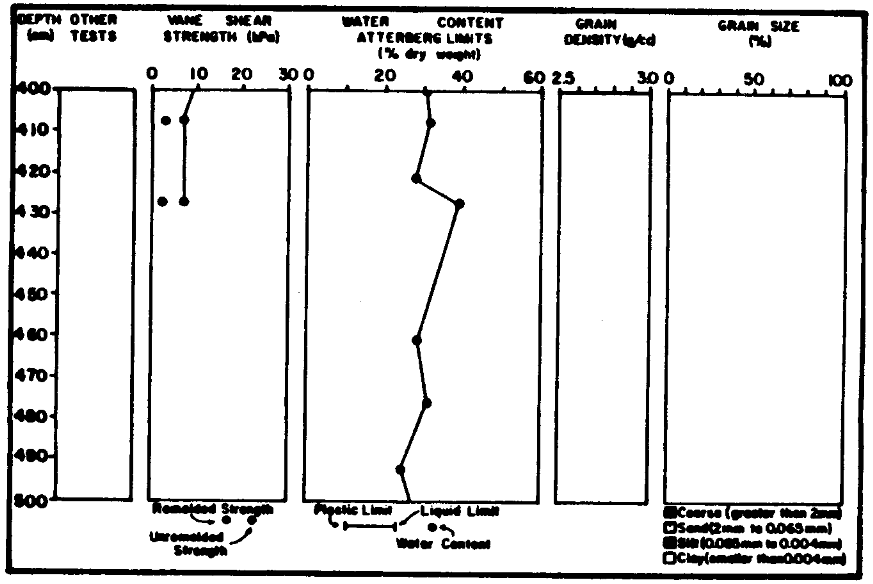

CRUISE: DCI-81-EG CORE: 625A2

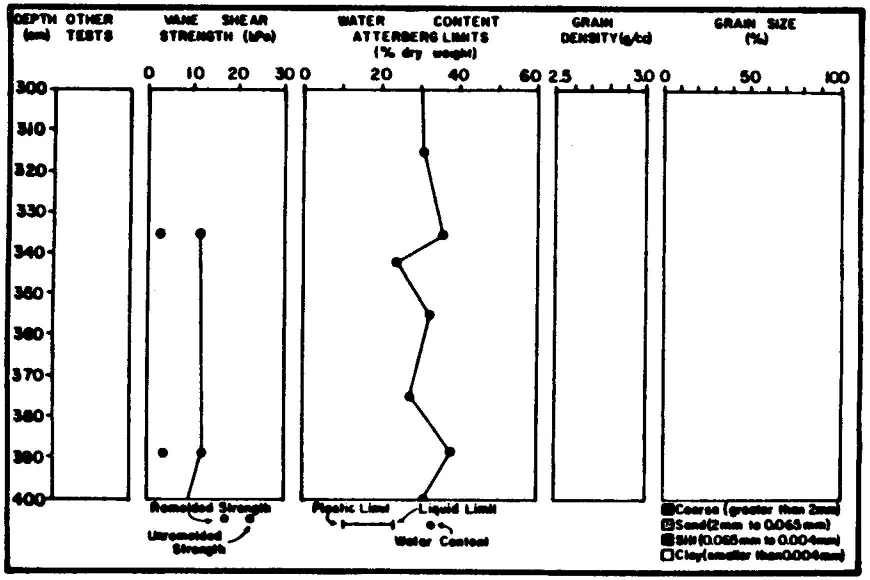

CRUISE: DCI-81-EG CORE: 625A2

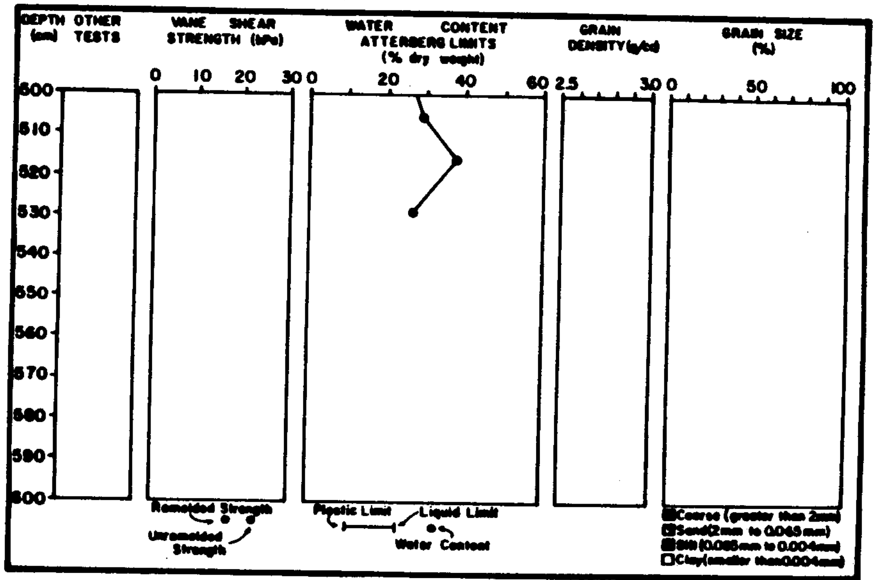

CRUISE: DCI-81-EG CORE: 625A2

ALSEK RIVER STUDY AREA

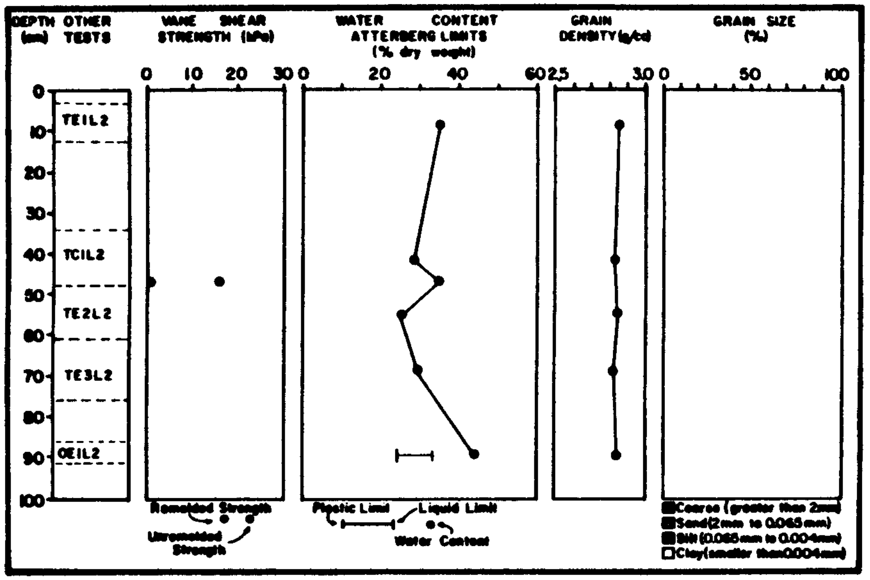

CRUISE: DC2-80-EG CORE: MC3-22

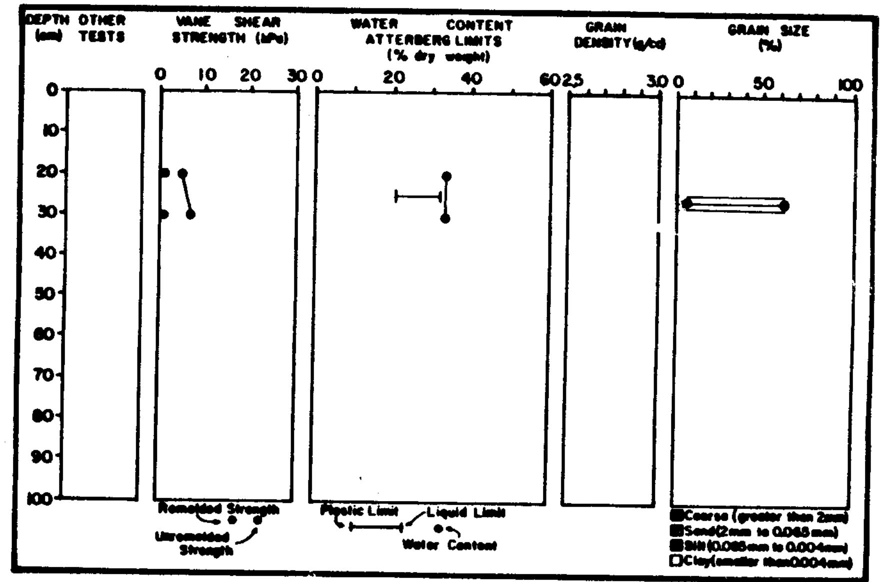

CRUISE: DC2-80-EG CORE: 26G

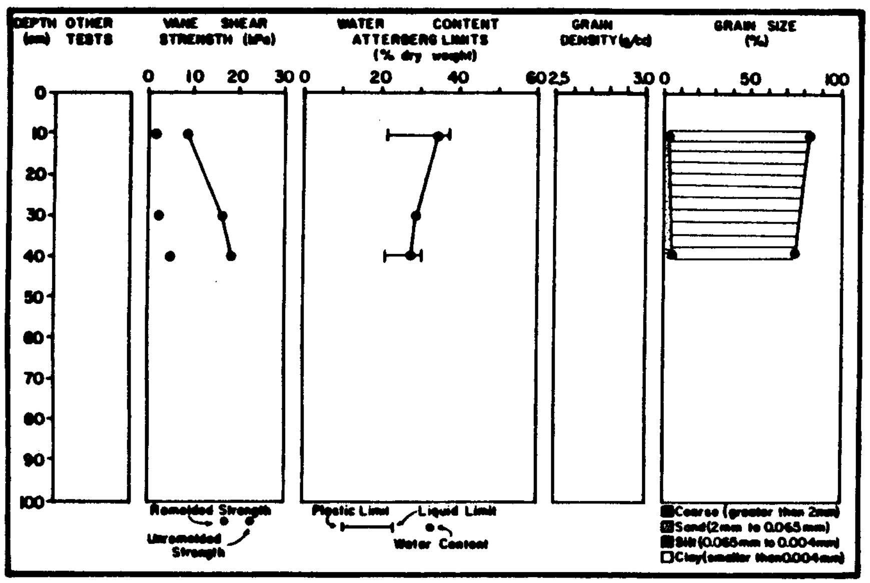

CRUISE: DC2-80-EG CORE: 23G

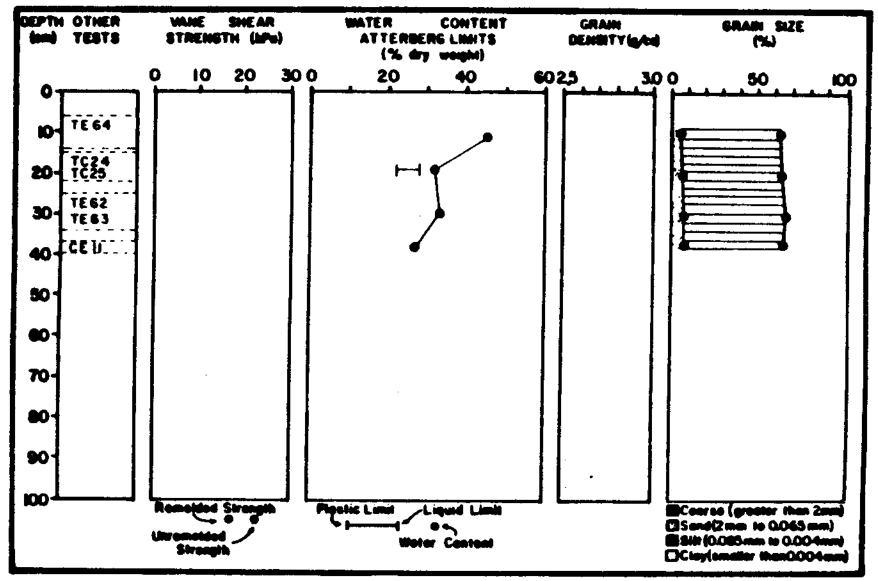

CRUISE: DC2-80-EG CORE: 28G

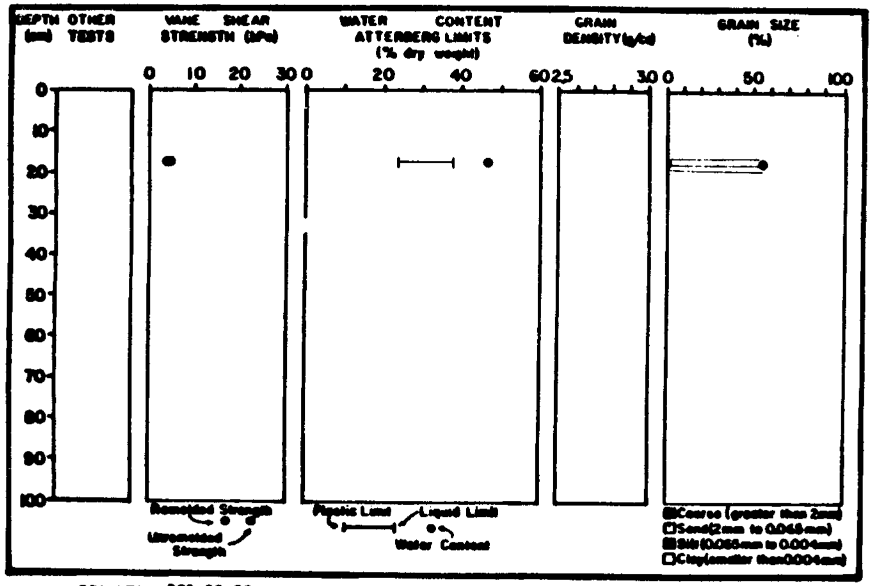

CRUISE: DC2-80-EG CORE: 29G

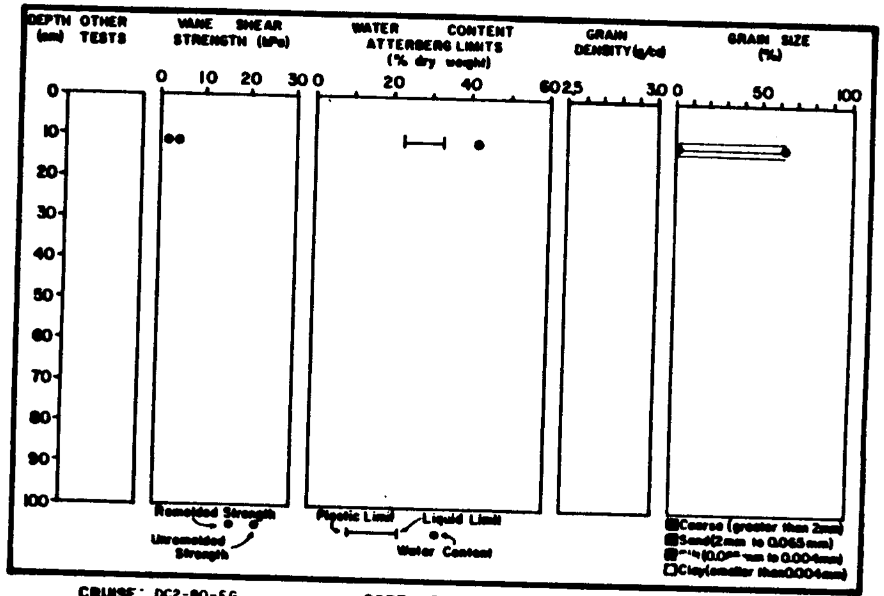

CRUISE: DC2-80-EG CORE: 32G

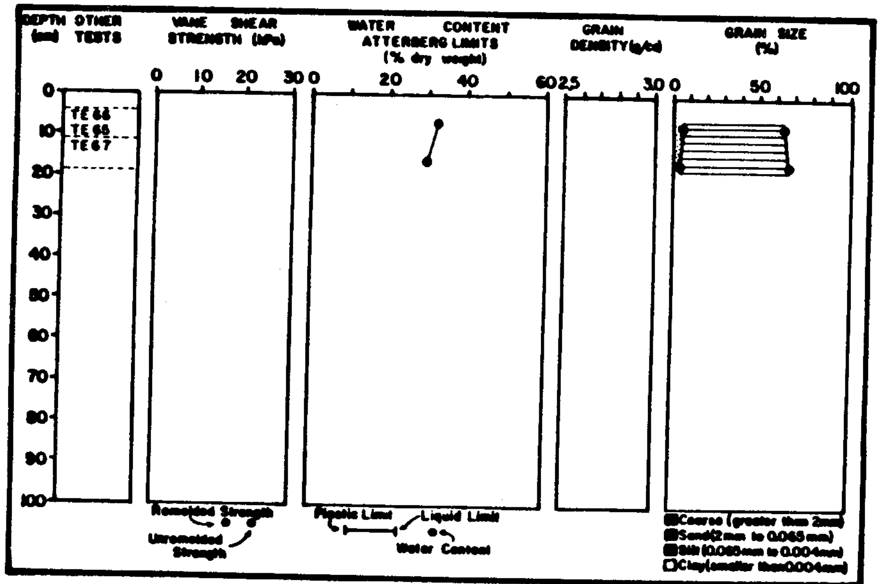

CRUISE: DC2-80-EG CORE: 31G

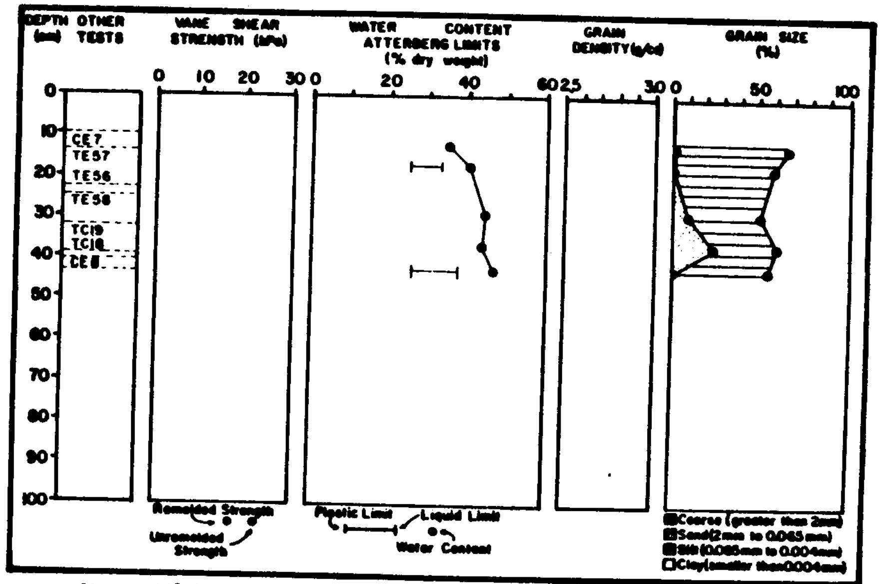

CRUISE: DC2-80-EG CORE: 35G

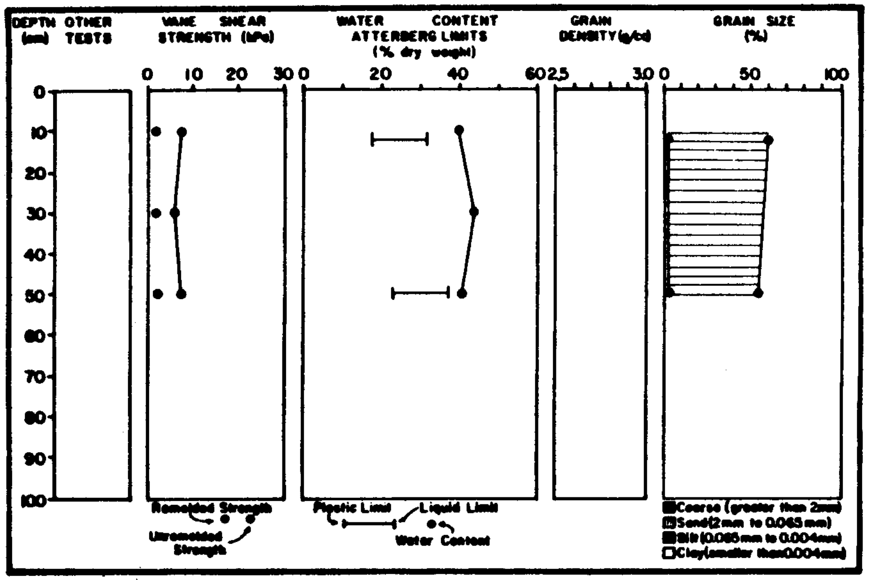

CRUISE: DC2-80-EG CORE: 36G

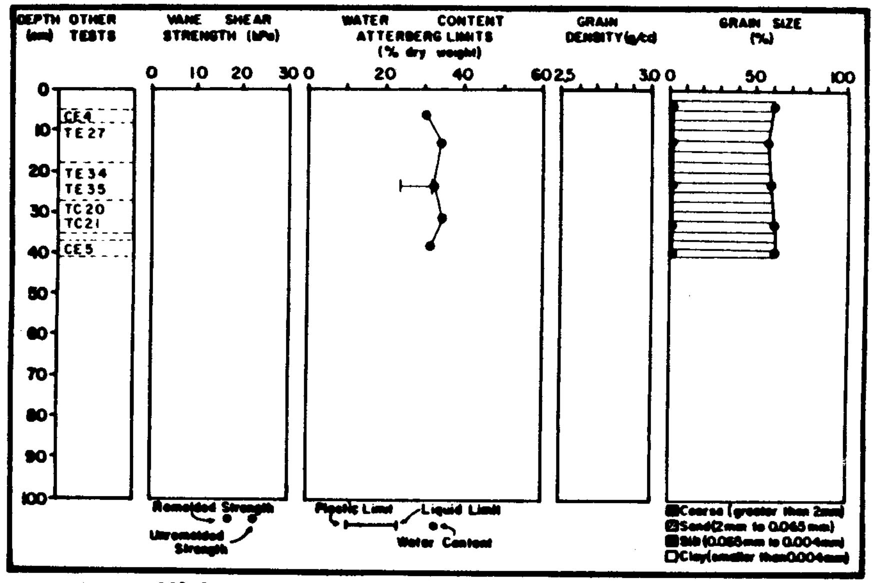

CRUISE: DC2-80-EG CORE: 43G

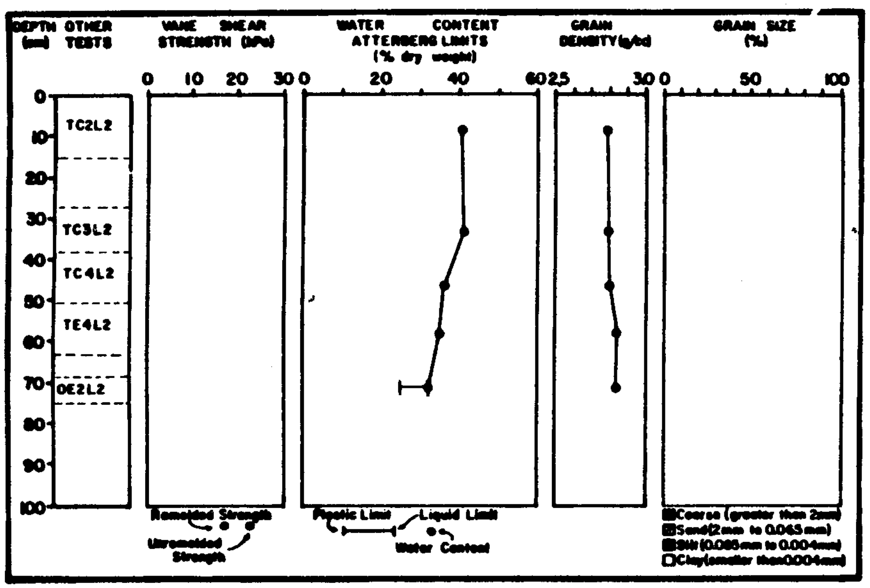

CRUISE: DC2-80-EG CORE: 38G

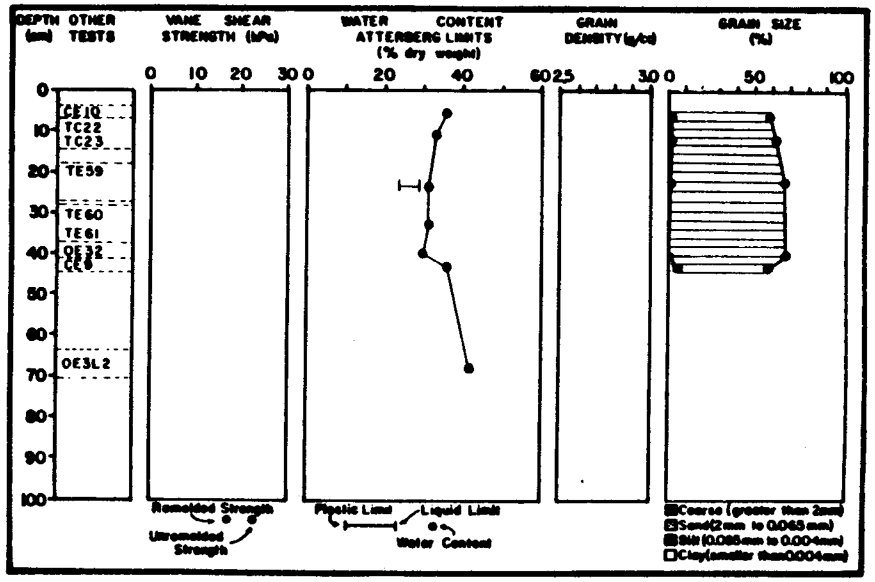

CRUISE: DC2-80-EG CORE: 46G

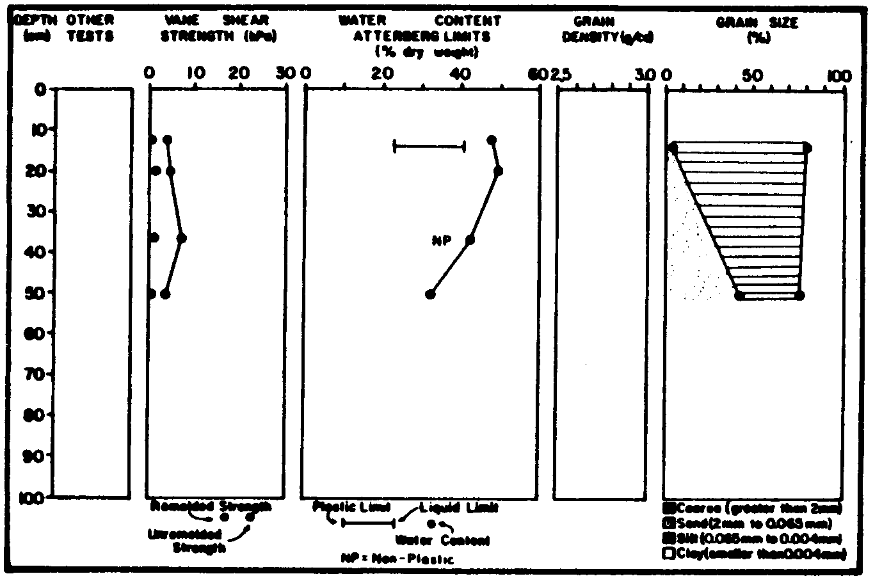

CRUISE: DC2-80-EG CORE: 47G

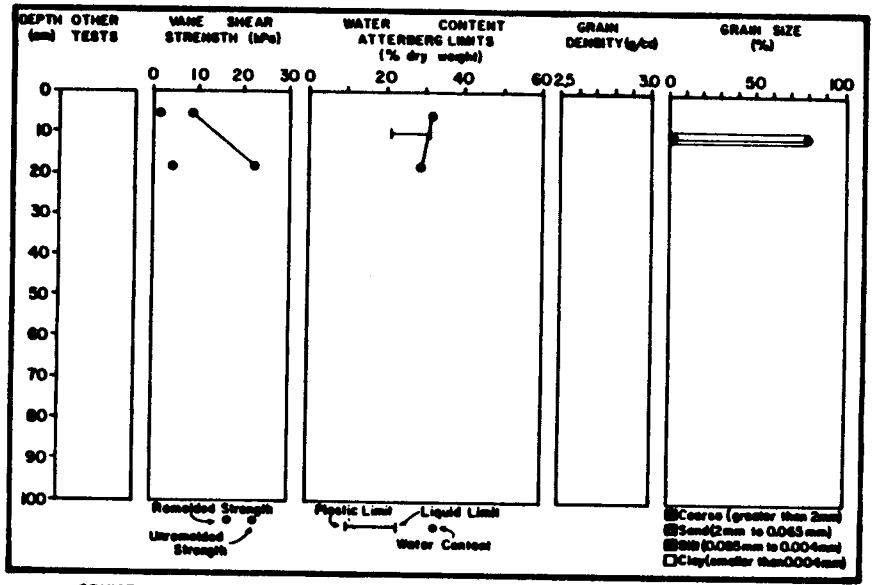

CRUISE: DC2-80-EG CORE: 50G

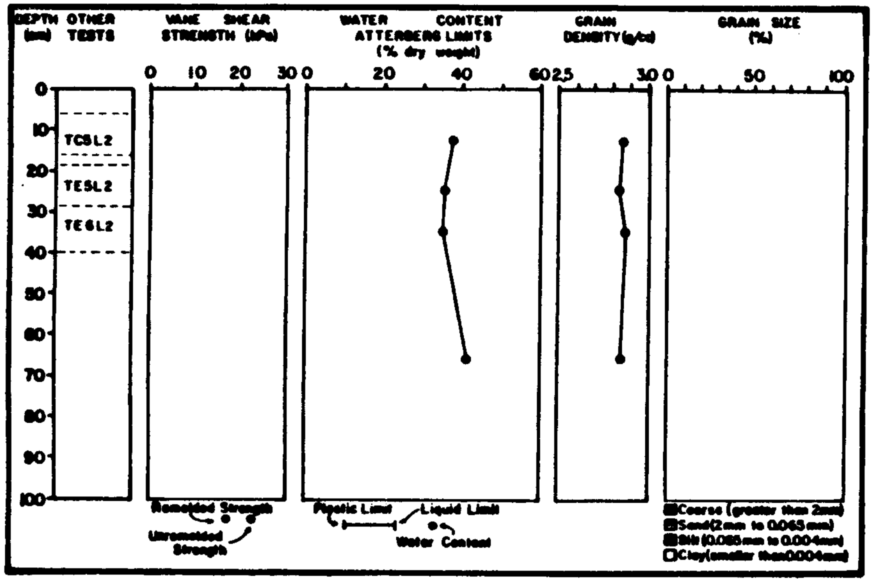

CRUISE: DC2-80-EG CORE: 49G

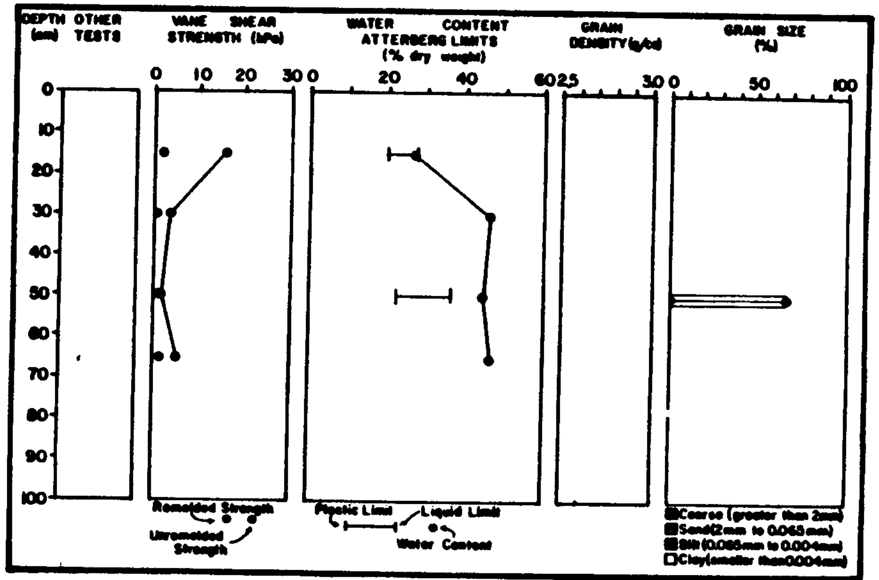

CRUISE: DC2-80-EG CORE: 52G

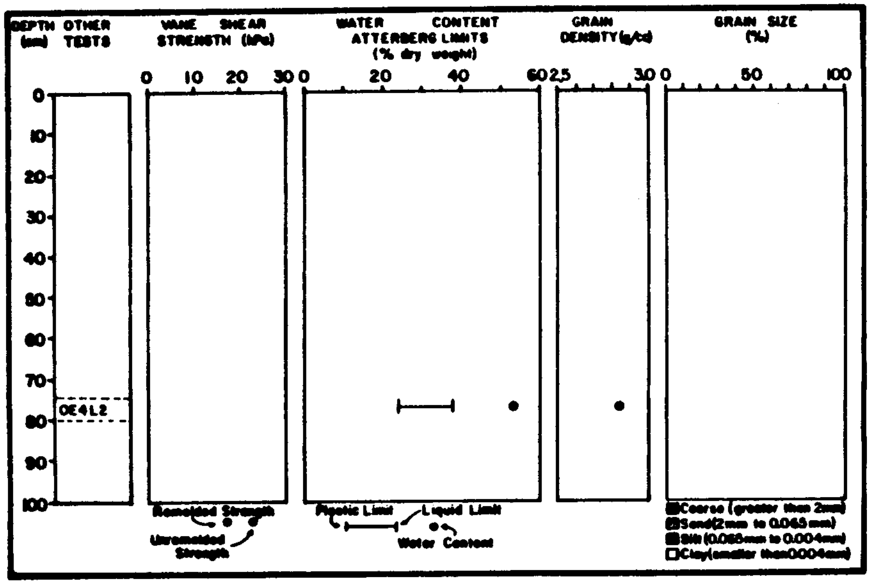

CRUISE: DC2-80-EG CORE: 55G

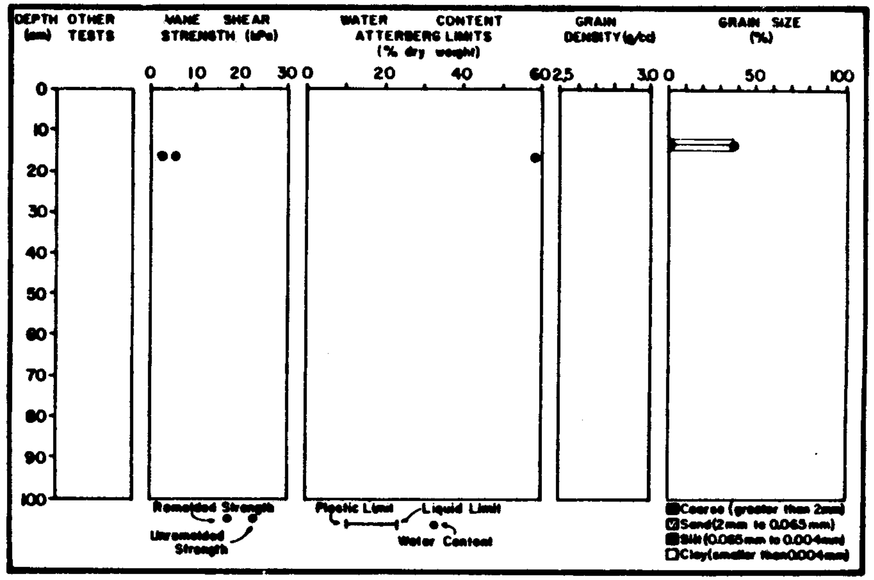

CRUISE: DC1-81-EG CORE: 601G2

330

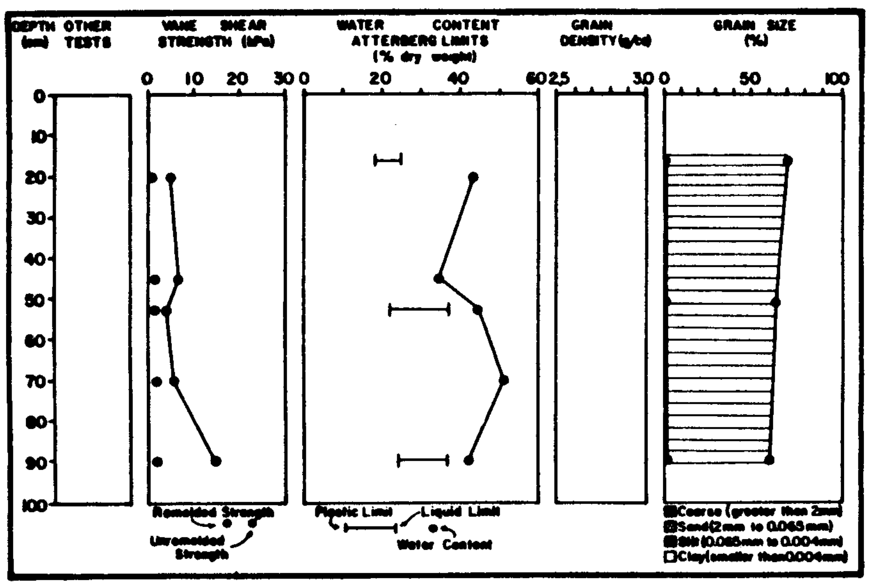

CRUISE: DC2-80-EG CORE: 56G

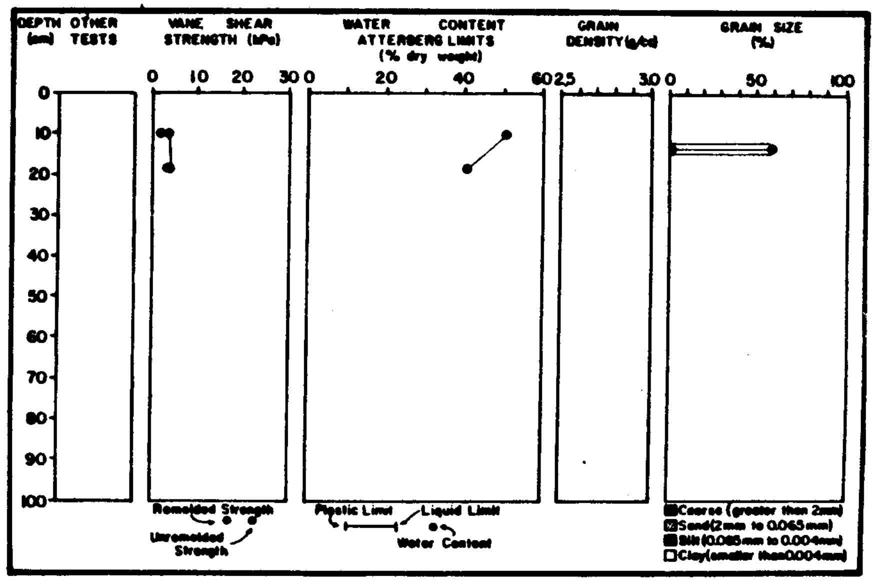

CRUISE: DC1-81-EG CORE: 602G3

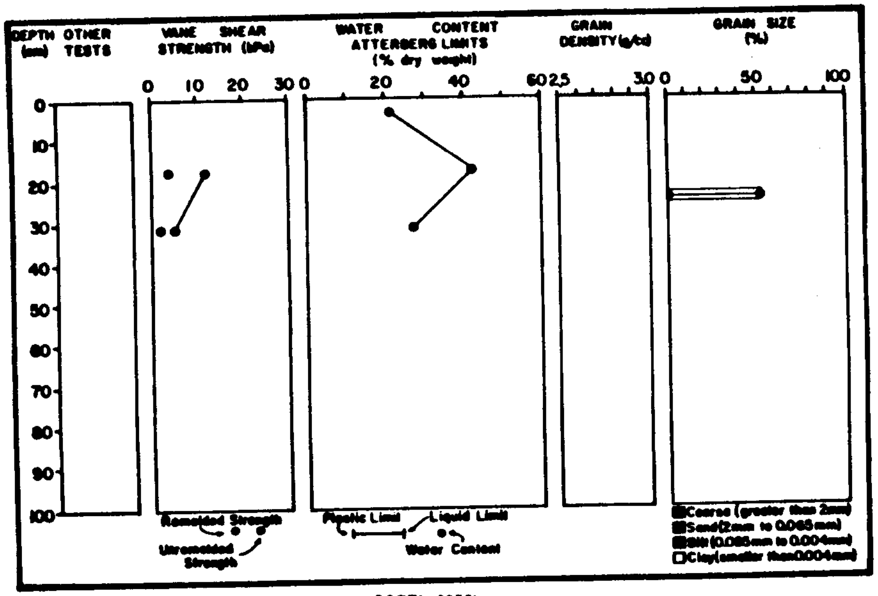

CRUISE: DCI-81-EG CORE: 60361

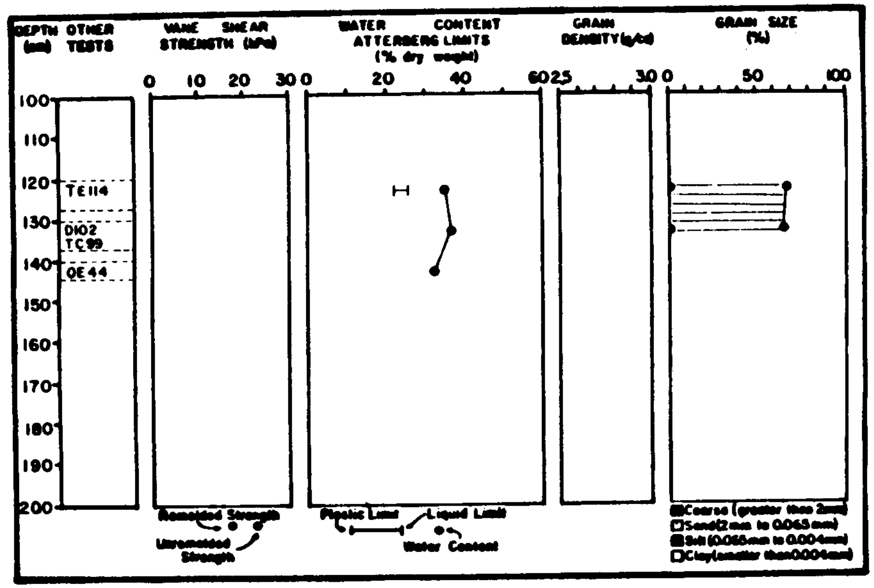

CRUISE: DCI-81-EG CORE: 60463

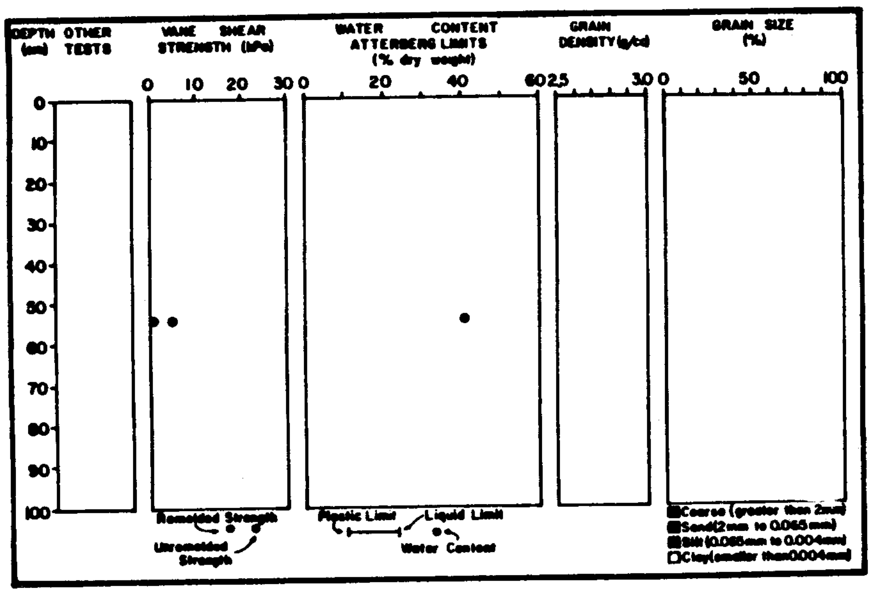

CRUISE: DCI-81-EG CORE: 60463

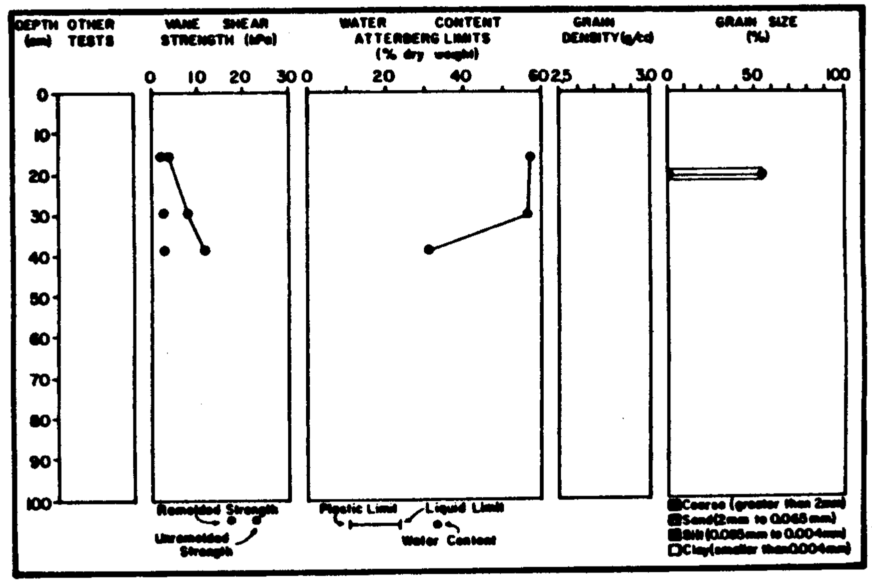

CRUISE: DCI-81-EG CORE: 60464

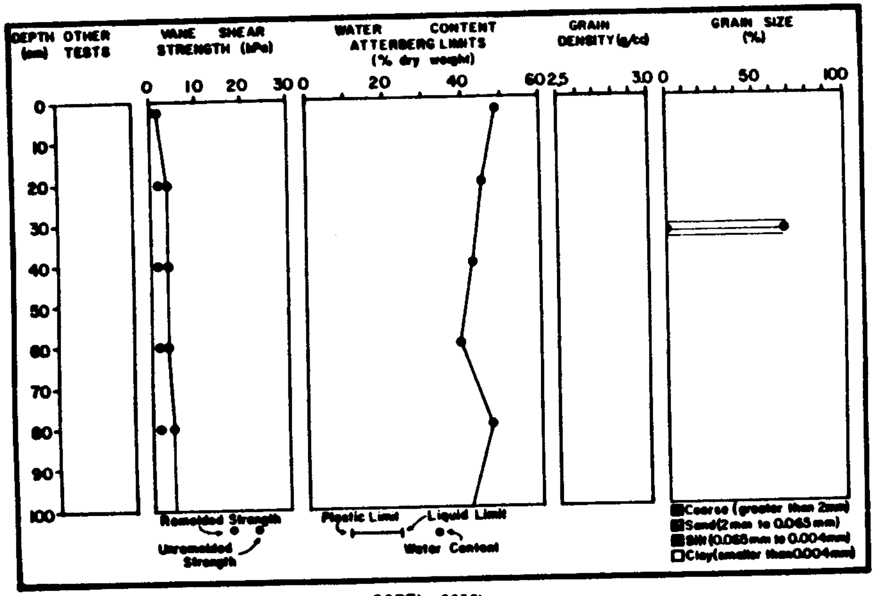

CRUISE: DCI-81-EG CORE: 605G1

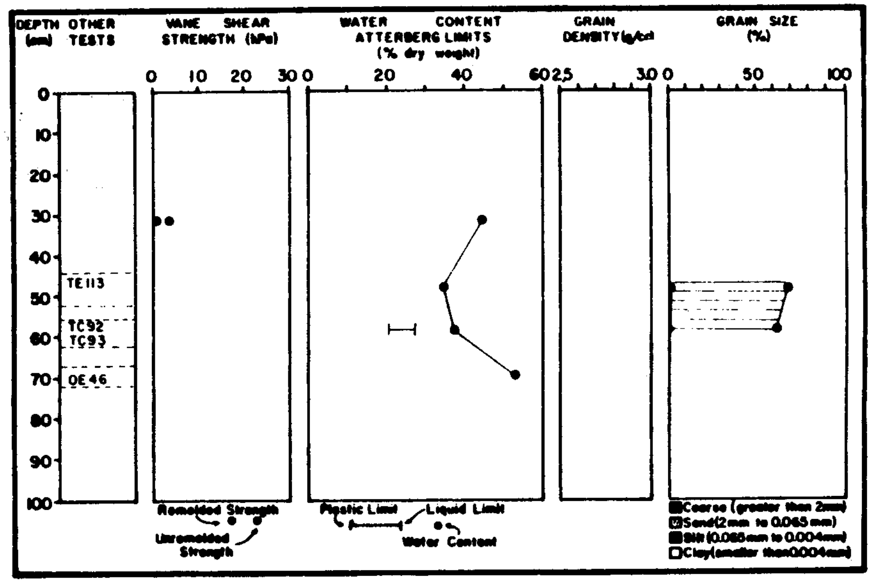

CRUISE: DCI-81-EG CORE: 605G2

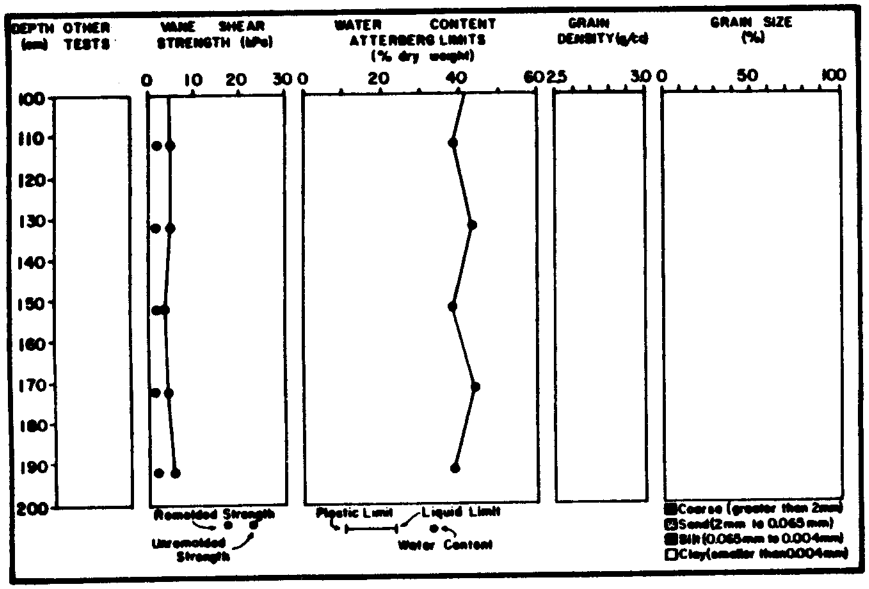

CRUISE: DCI-81-EG CORE: 605G1

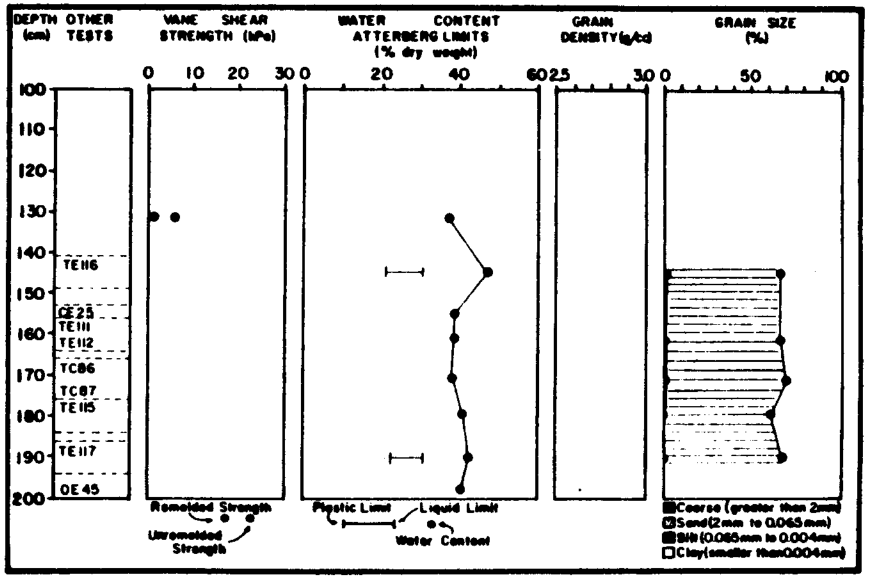

CRUISE: DCI-81-EG CORE: 605G2

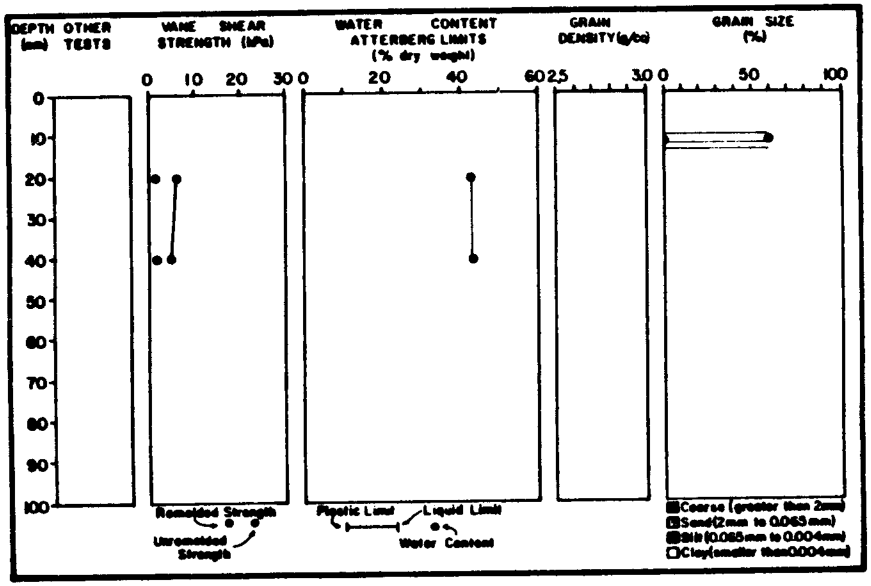

CRUISE: DCI-81-EG CORE: 606G1

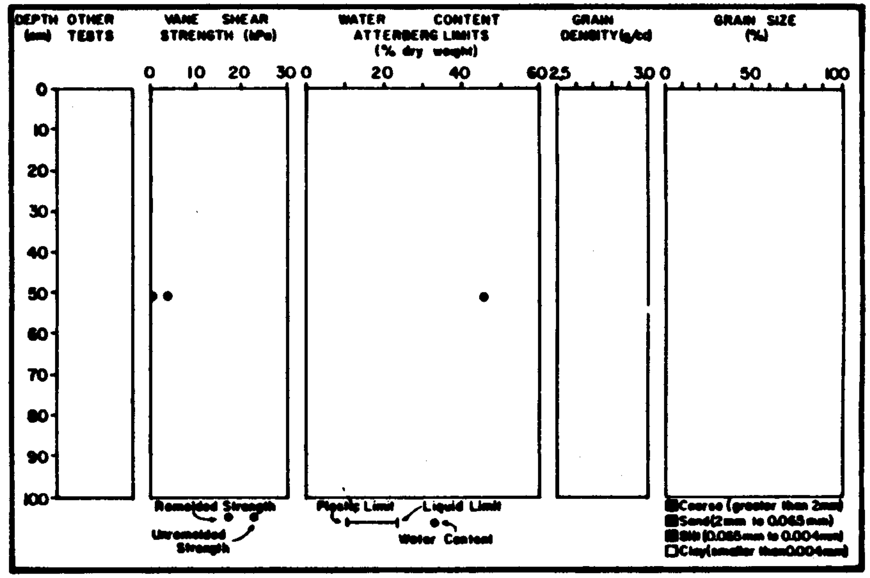

CRUISE: DCI-81-EG CORE: 607A1

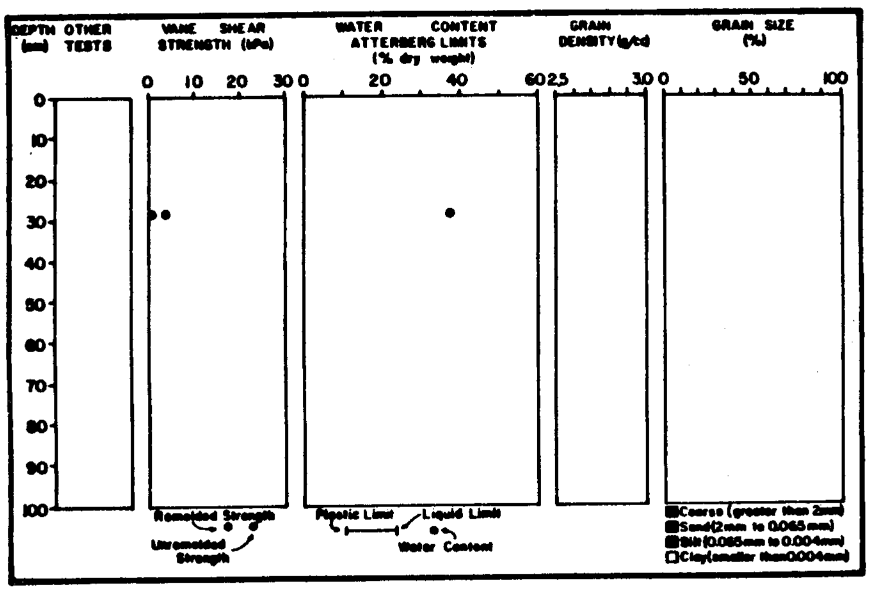

CRUISE: DCI-81-EG CORE: 606G2

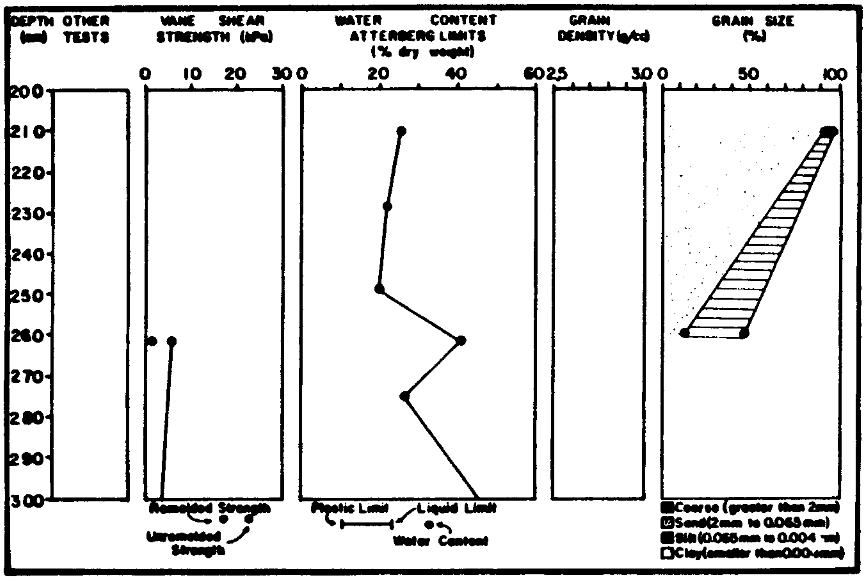

CRUISE: DCI-81-EG CORE: 607A2

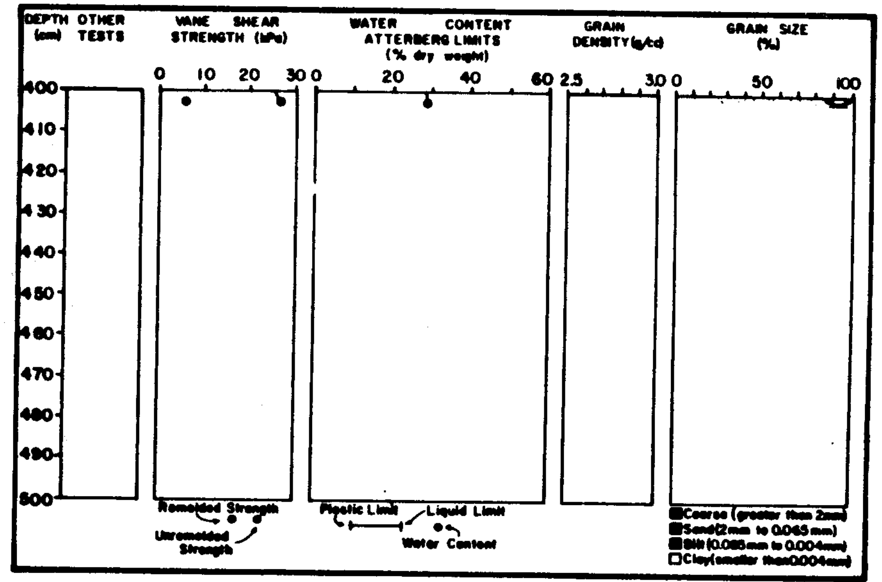

CRUISE: DCI-81-EG CORE: 607A2

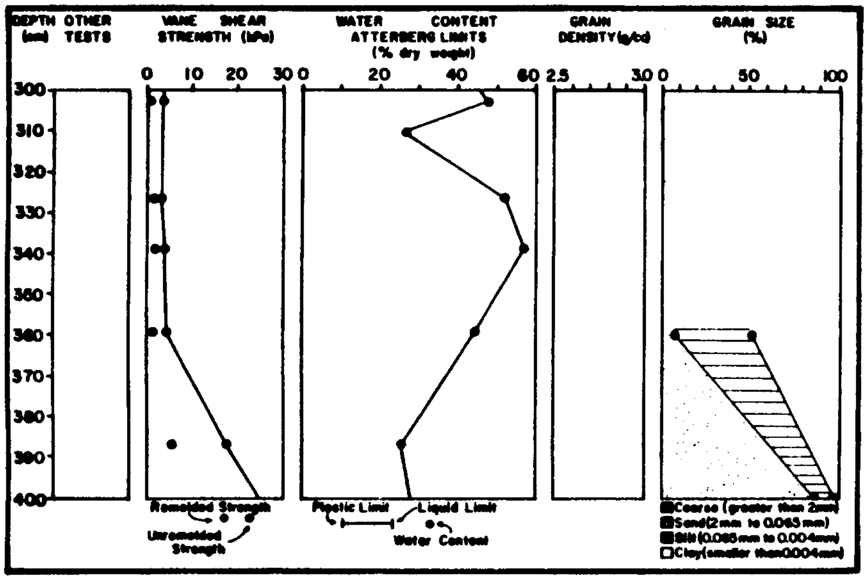

CRUISE: DCI-81-EG CORE: 607A2

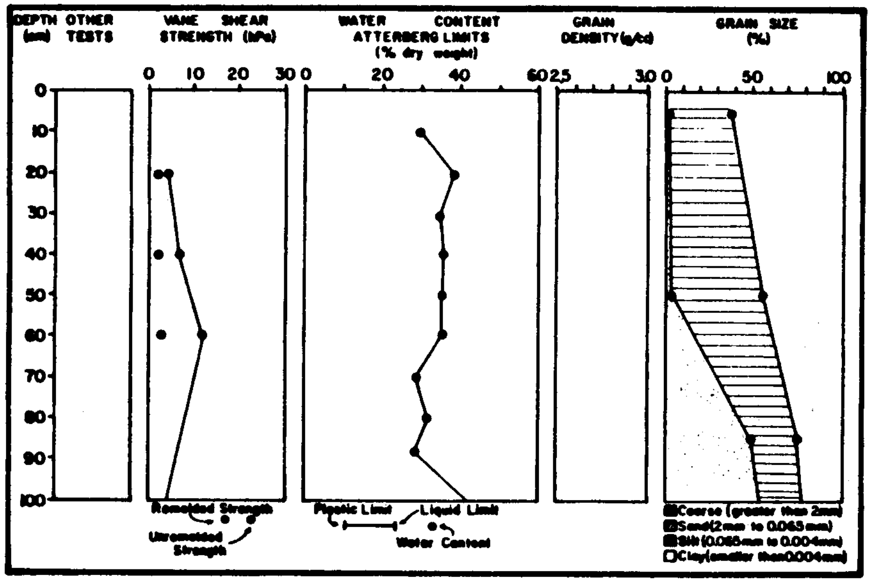

CRUISE: DCI-81-EG CORE: 608A2

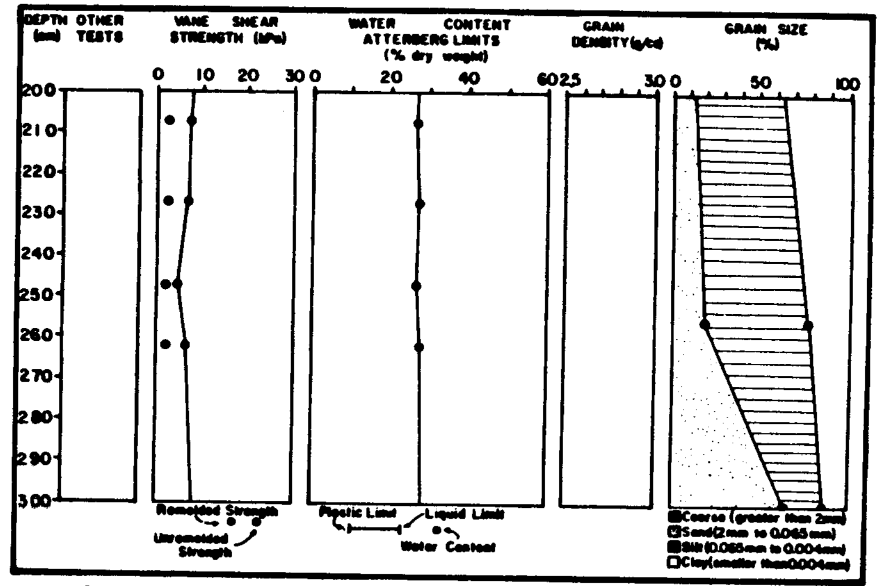

CRUISE: DCI-81-EG CORE: 608A2

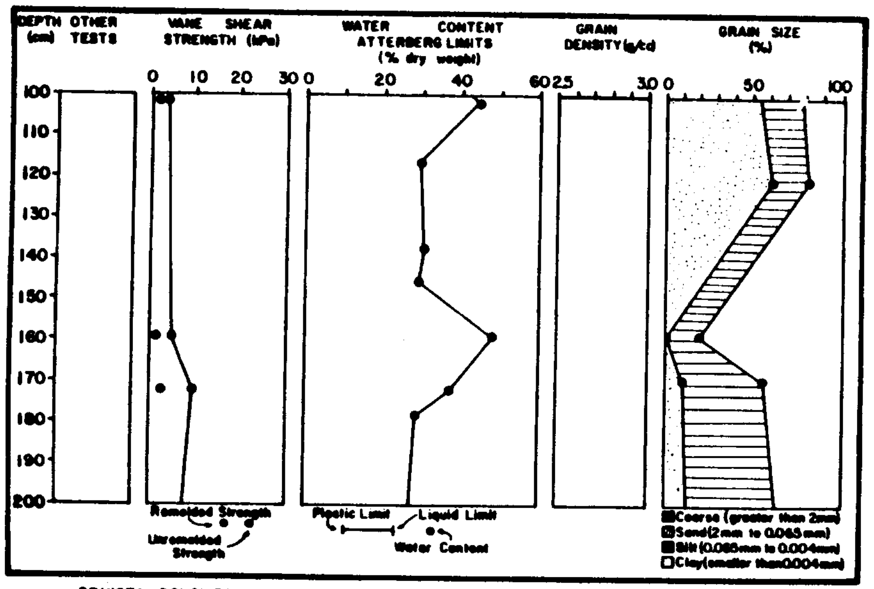

CRUISE: DCI-81-EG CORE: 608A2

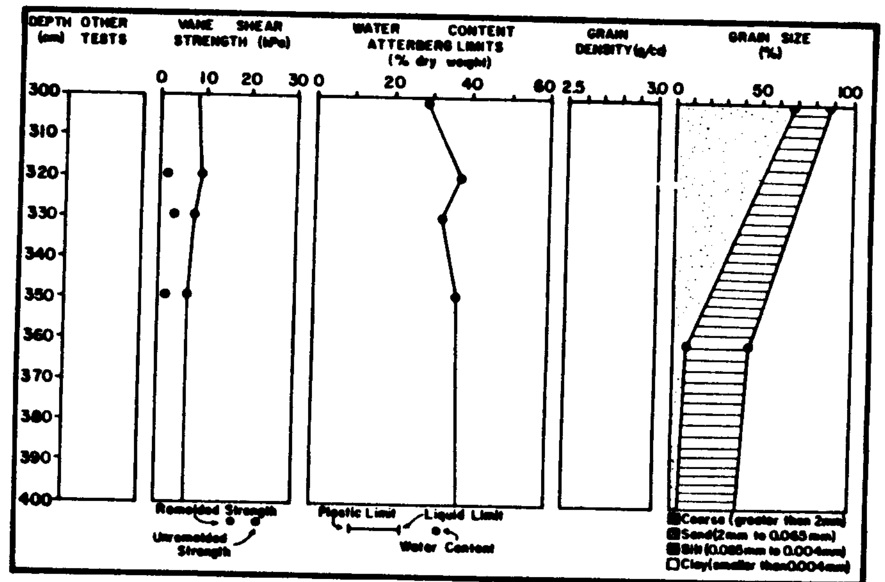

CRUISE: DCI-81-EG CORE: 608A2

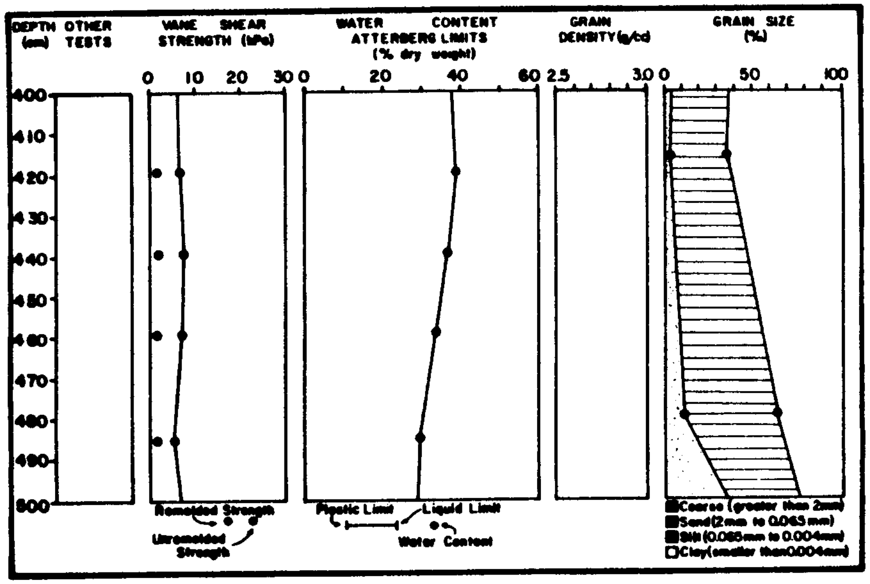

CRUISE: DCI-81-EG CORE: 608A2

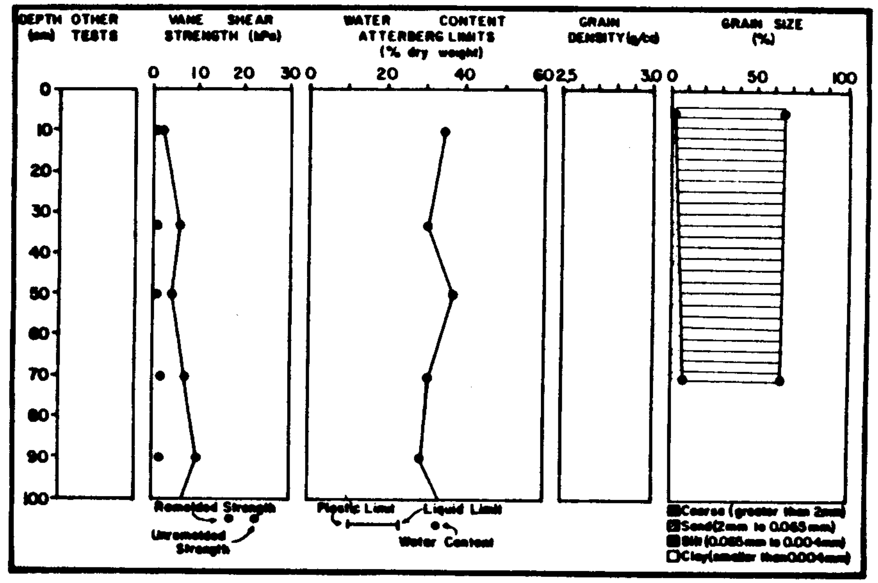

CRUISE: DCI-81-EG CORE: 609A1

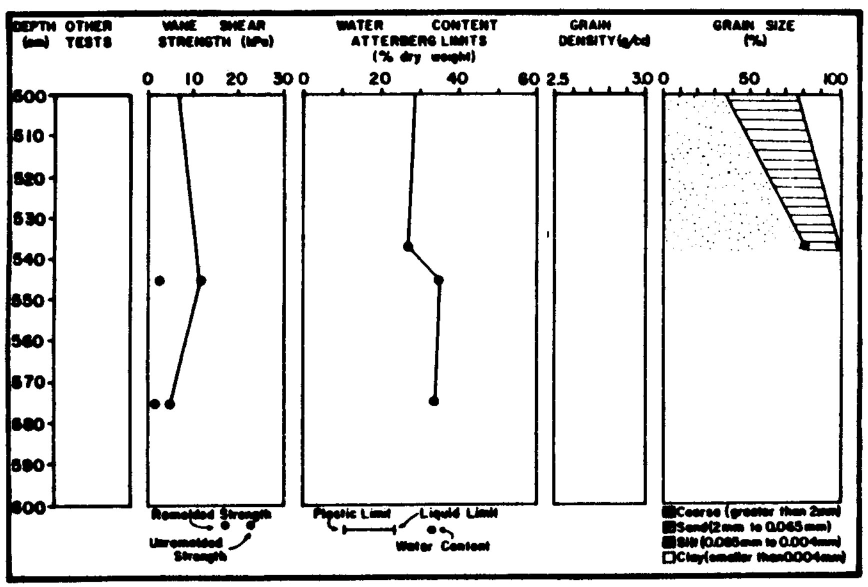

CRUISE: DCI-81-EG CORE: 608A2

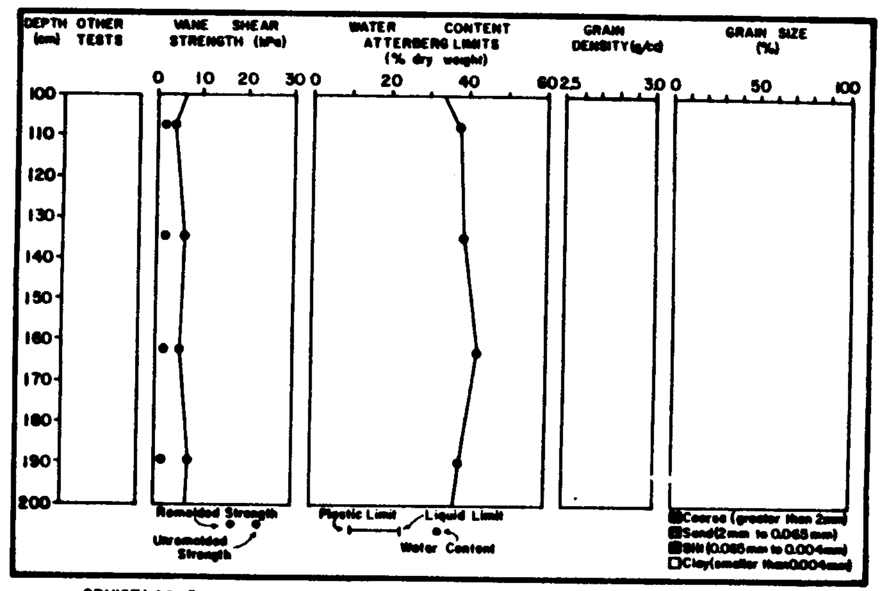

CRUISE: DCI-81-EG CORE: 609A1

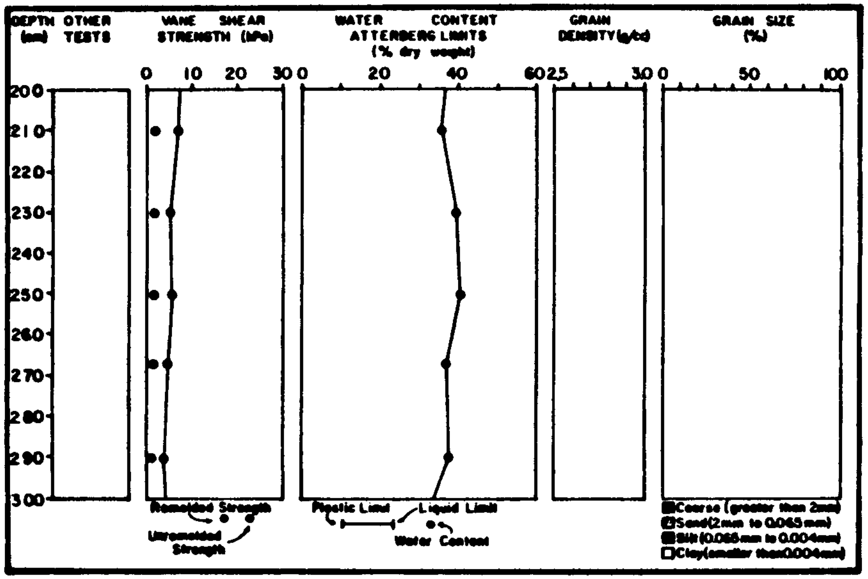

CRUISE: DCI-81-EG CORE: 609A1

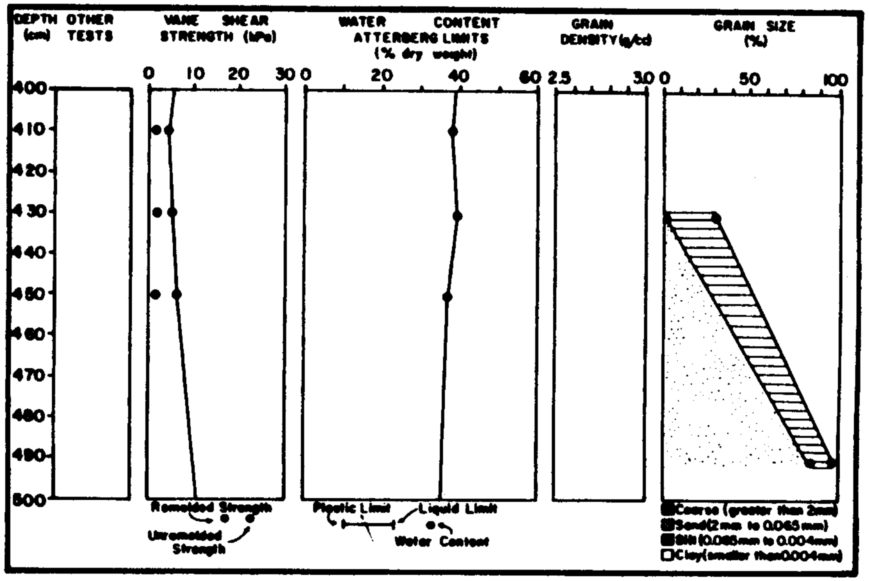

CRUISE: DCI-81-EG CORE: 609A1

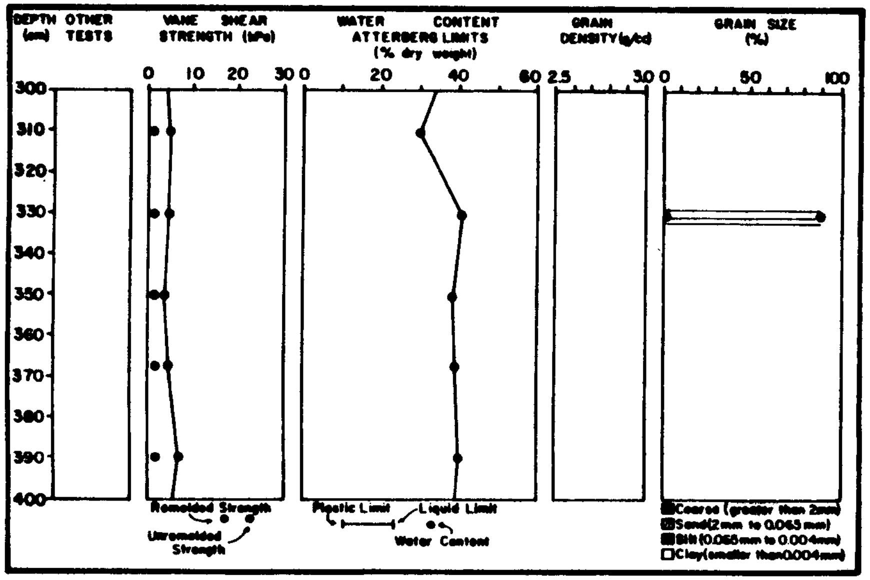

CRUISE: DCI-81-EG CORE: 609A1

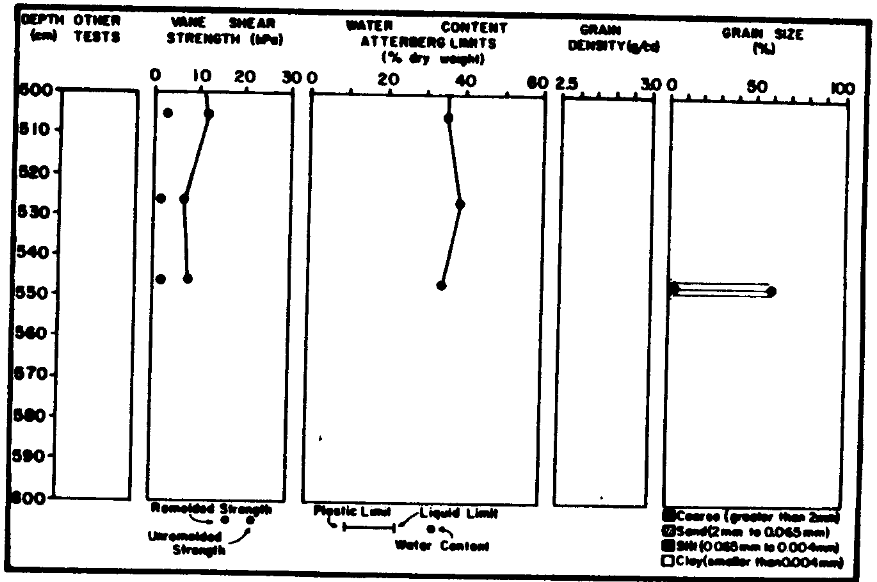

CRUISE: DCI-81-EG CORE: 609A1

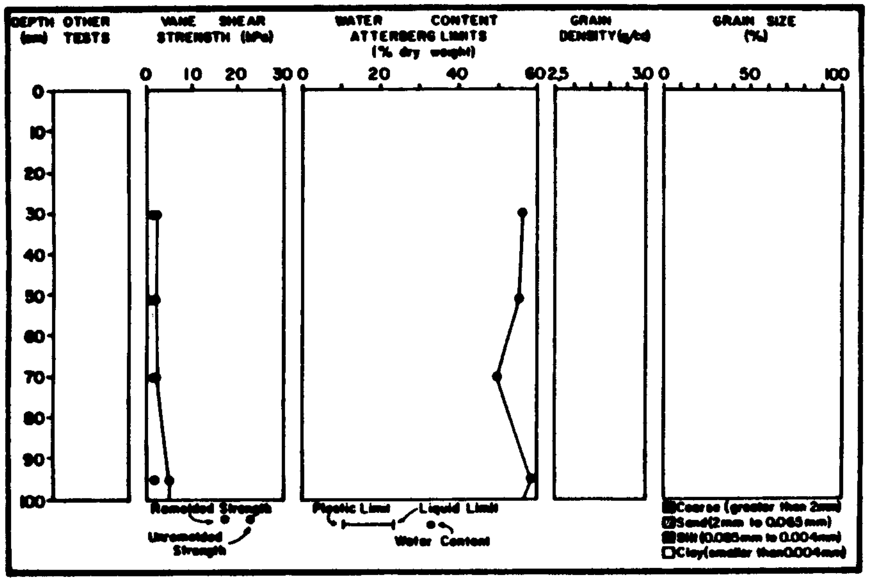

CRUISE: DCI-81-EG CORE: 610A2

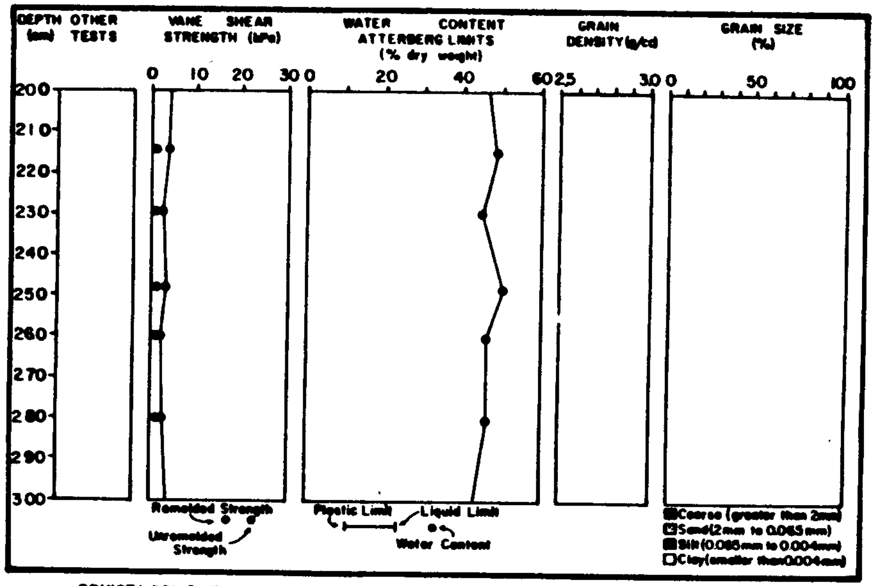

CRUISE: DCI-81-EG CORE: 610A2

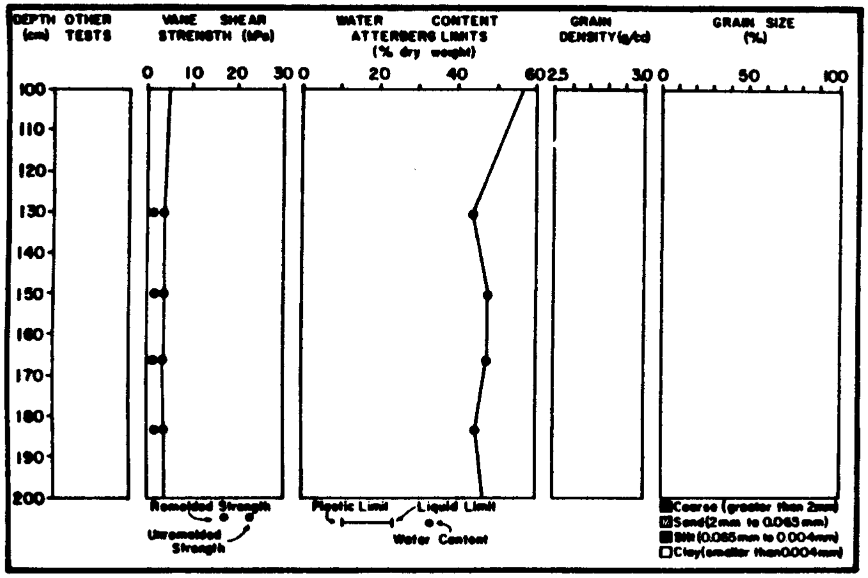

CRUISE: DCI-81-EG CORE: 610A2

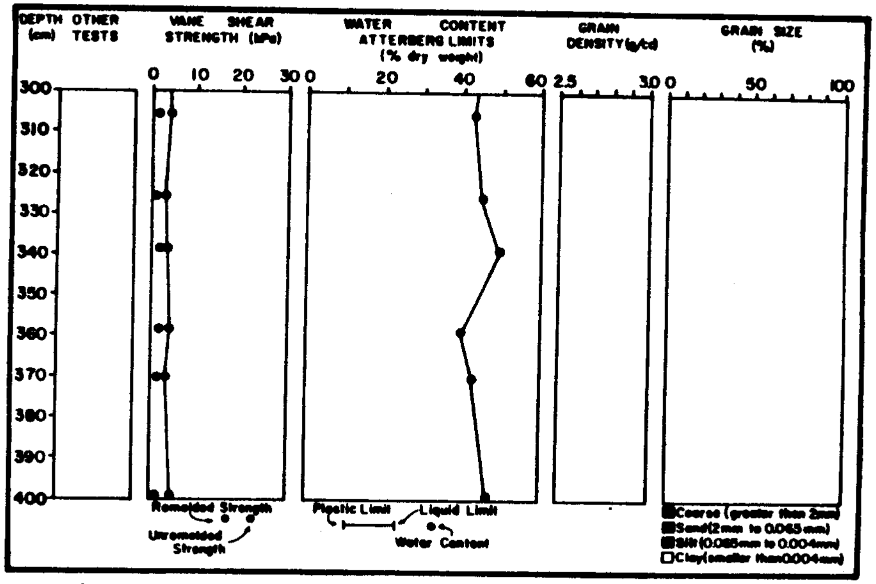

CRUISE: DCI-81-EG CORE: 610A2

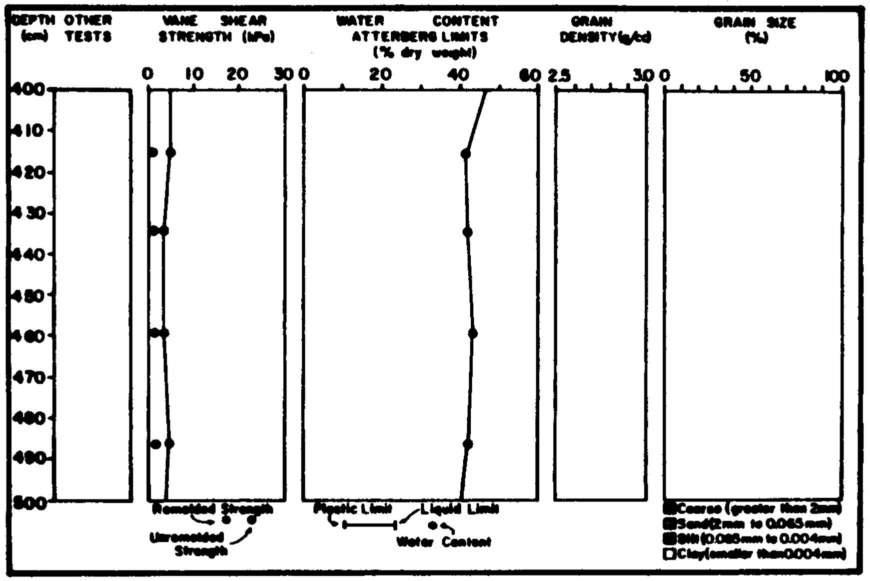

CRUISE: DCI-81-EG CORE: 610A2

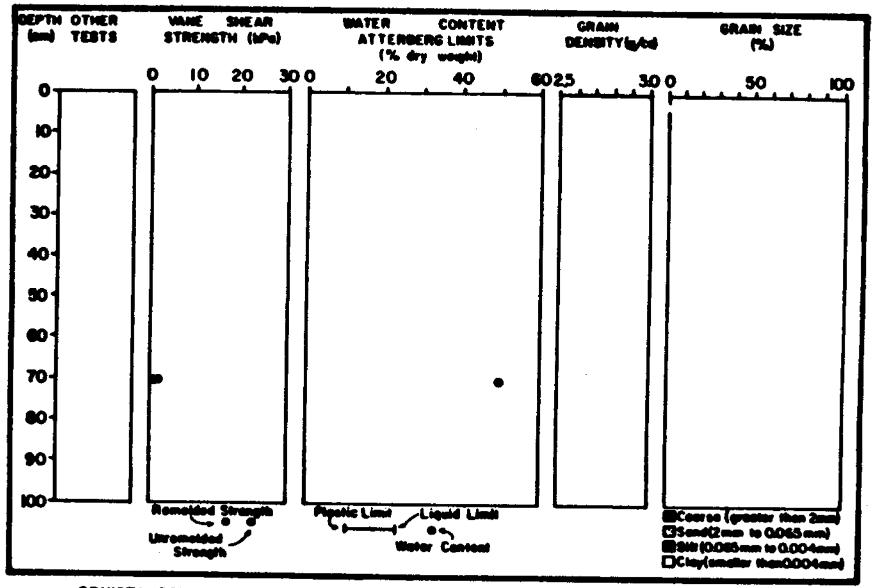

CRUISE: DCI-81-EG CORE: 611G1

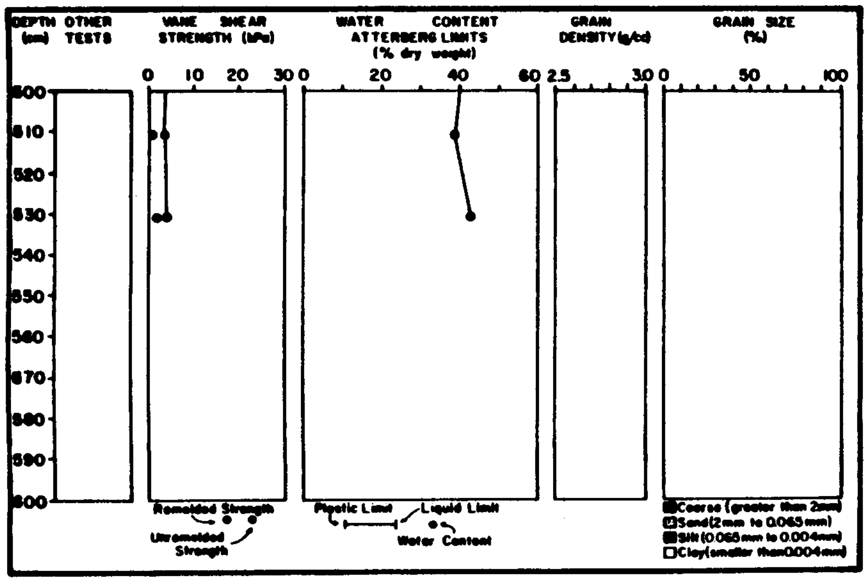

CRUISE: DCI-81-EG CORE: 610A2

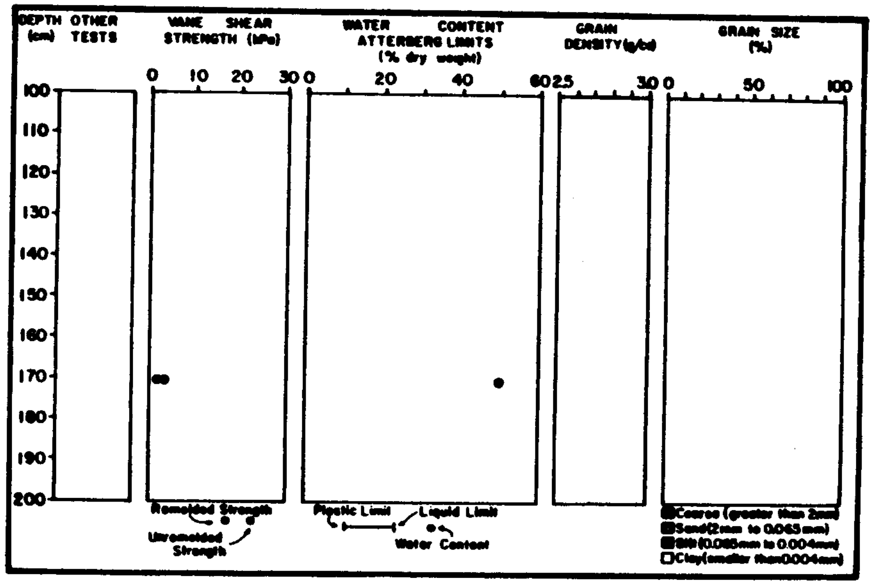

CRUISE: DCI-81-EG CORE: 611G1

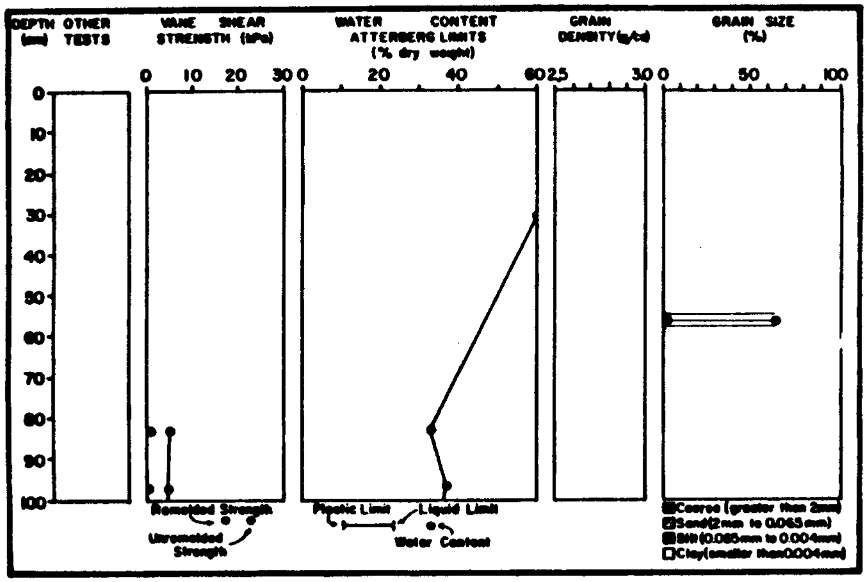

CRUISE: DCI-81-EG   CORE: 611G2

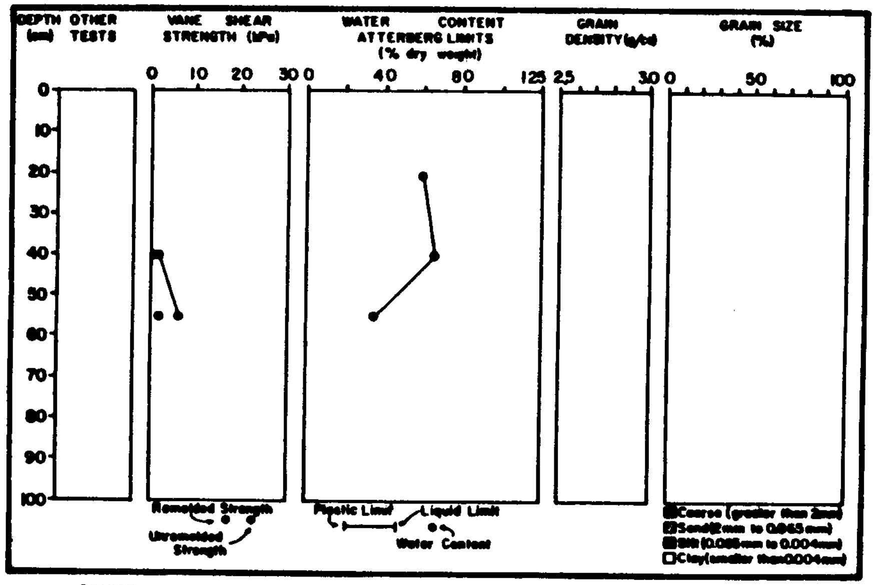

CRUISE: DCI-81-EG   CORE: 612G1

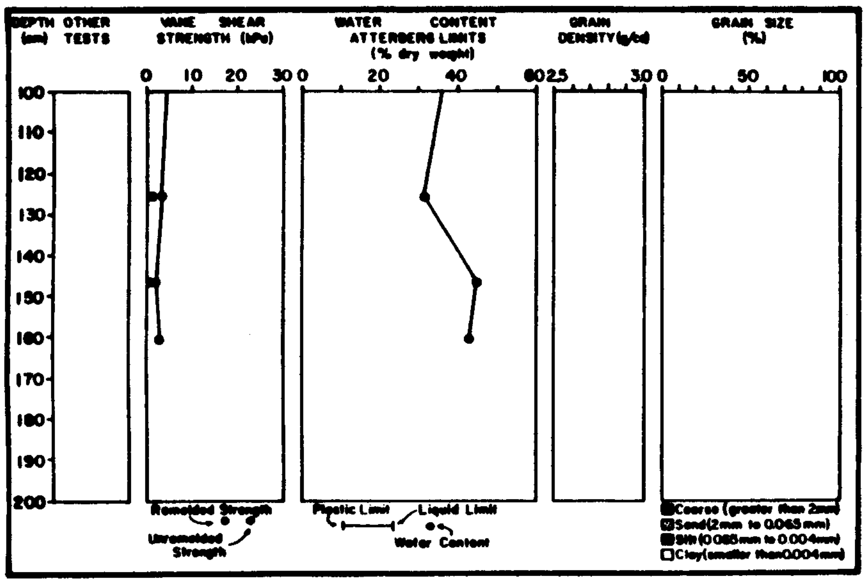

CRUISE: DCI-81-EG   CORE: 611G2

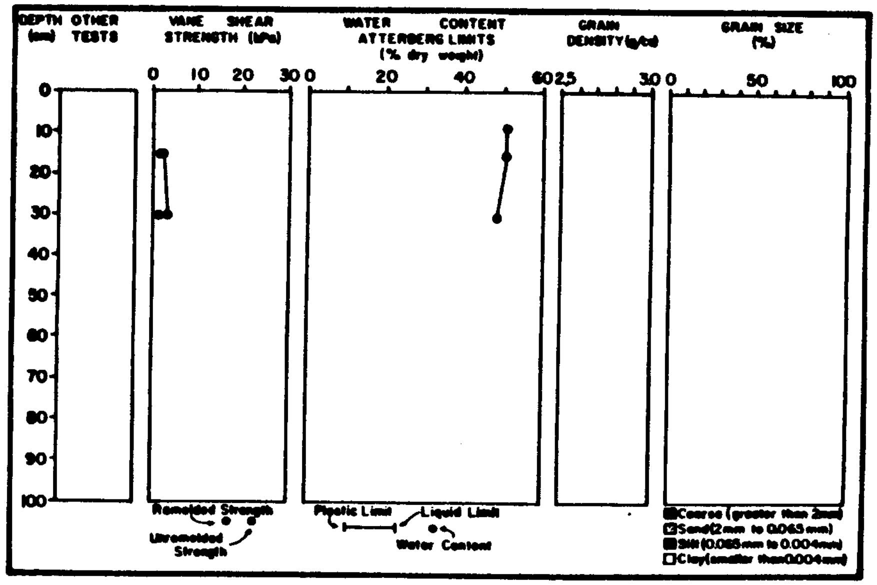

CRUISE: DCI-81-EG   CORE: 613G2

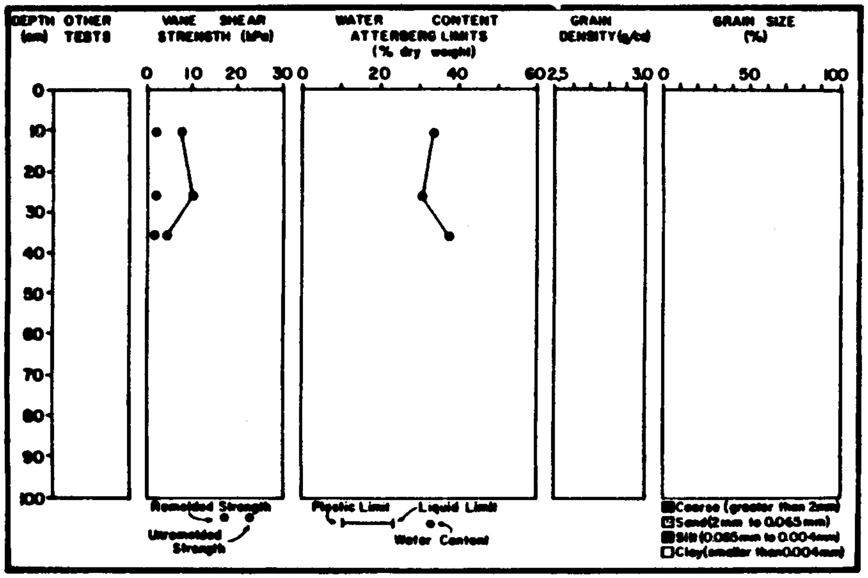

CRUISE: DCI-81-EG CORE: 614G2

OTHER

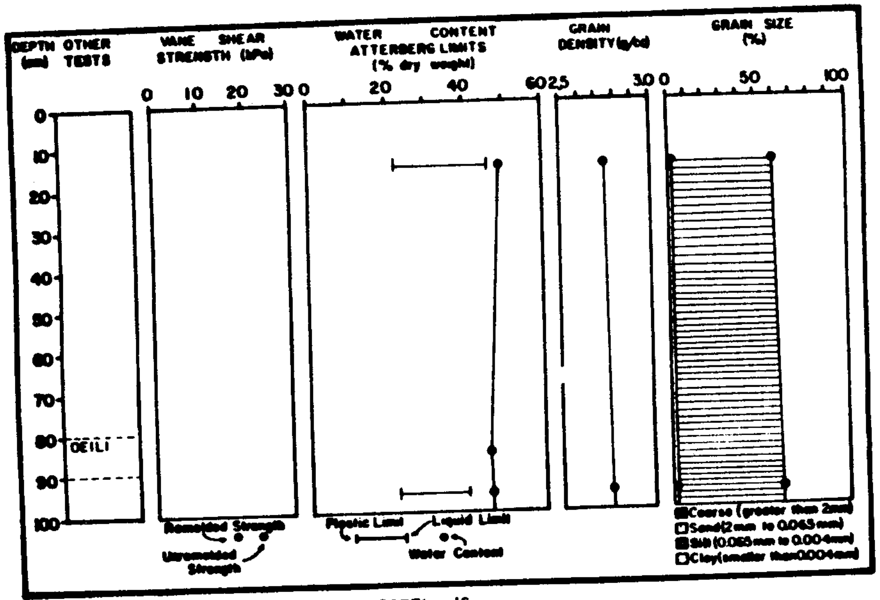

CRUISE: S8-77-EG CORE: 1G

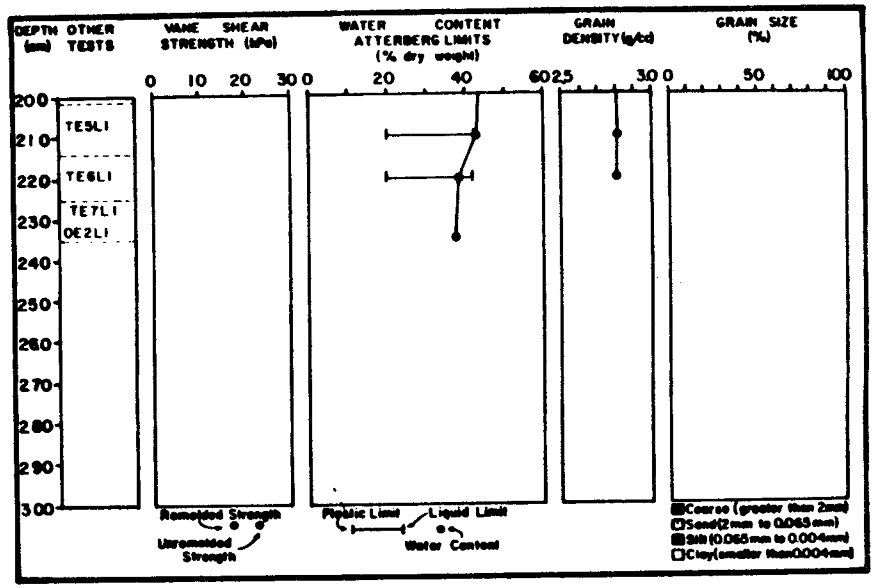

CRUISE: S8-77-EG CORE: 1G

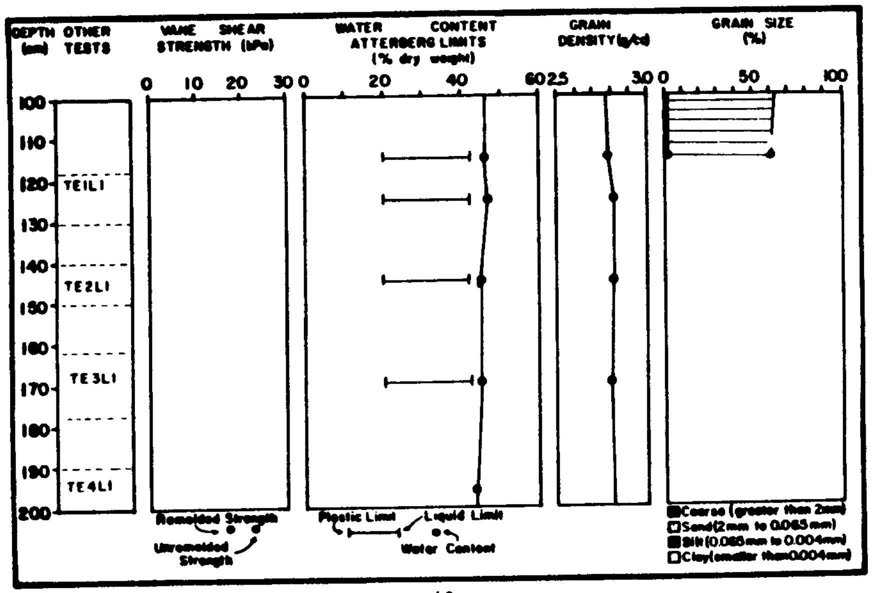

CRUISE: S8-77-EG CORE: 1G

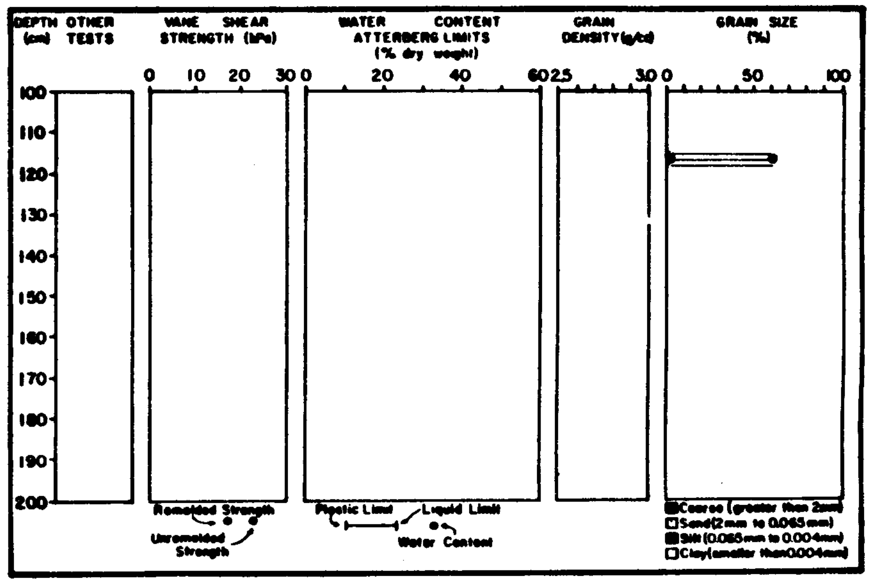

CRUISE: S8-77-EG CORE: 2G

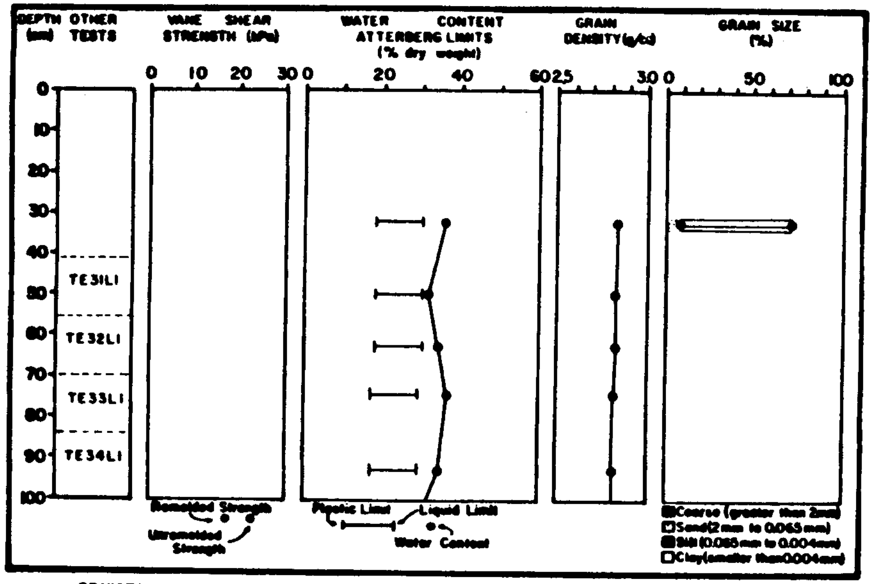

CRUISE: S8-77-EG CORE: 23G

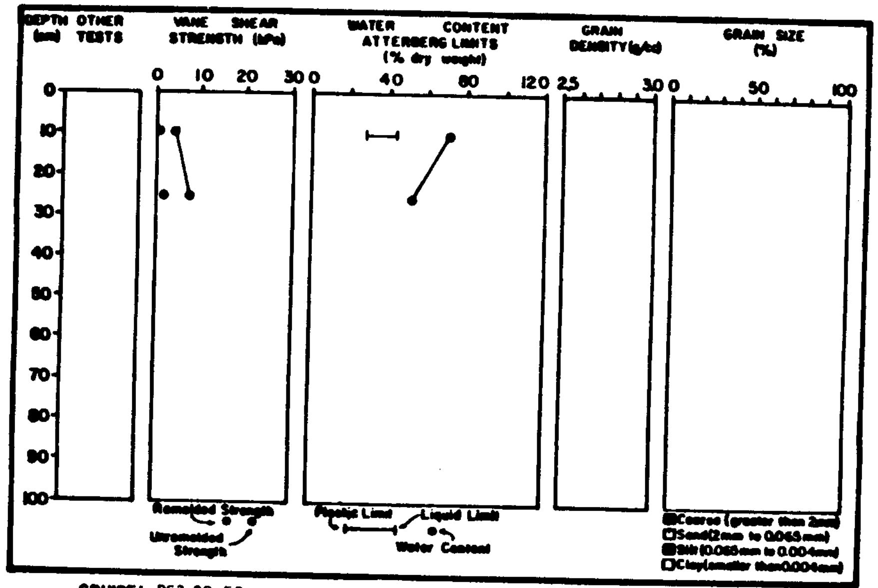

CRUISE: DC2-80-EG CORE: 92G

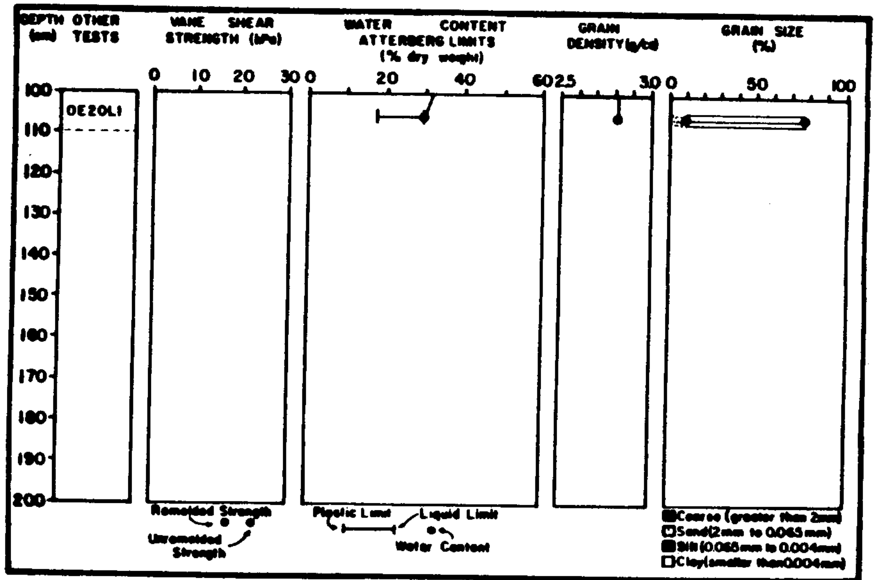

CRUISE: S8-77-EG CORE: 23G

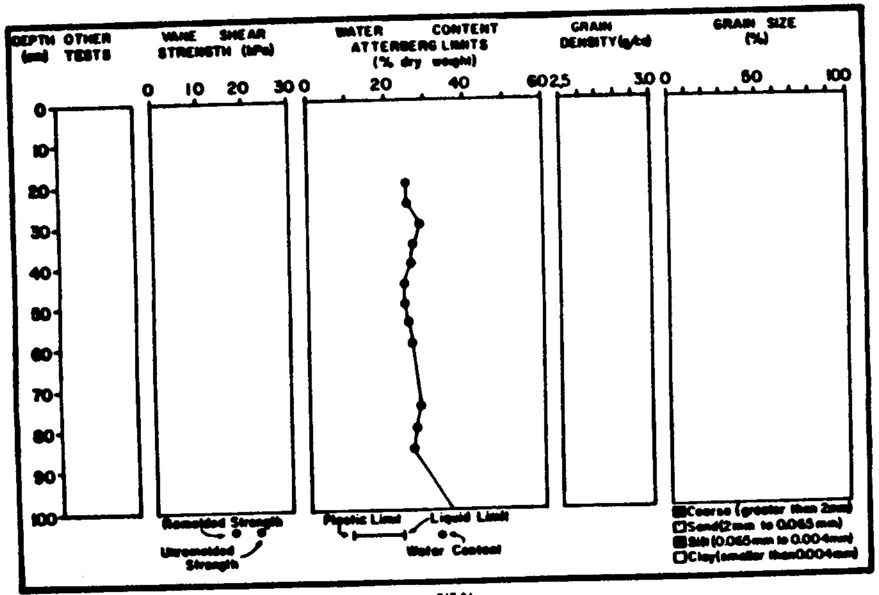

CRUISE: DCI-81-EG CORE: 615A1

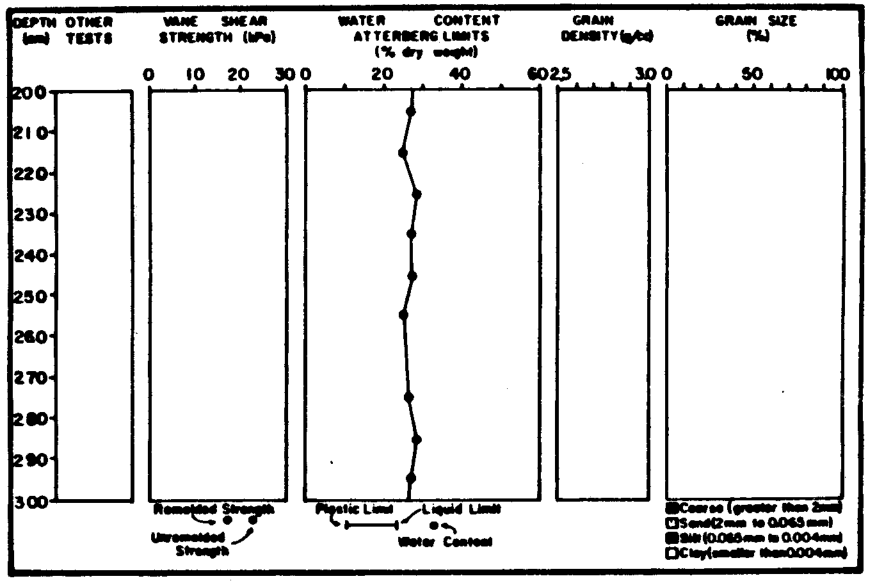

CRUISE: DCI-81-EG CORE: 615A1

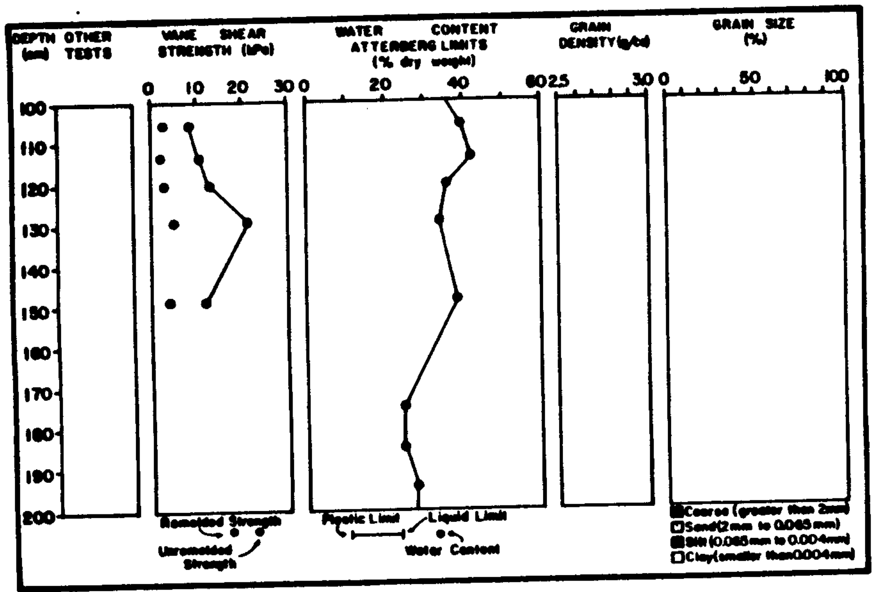

CRUISE: DCI-81-EG CORE: 615A1

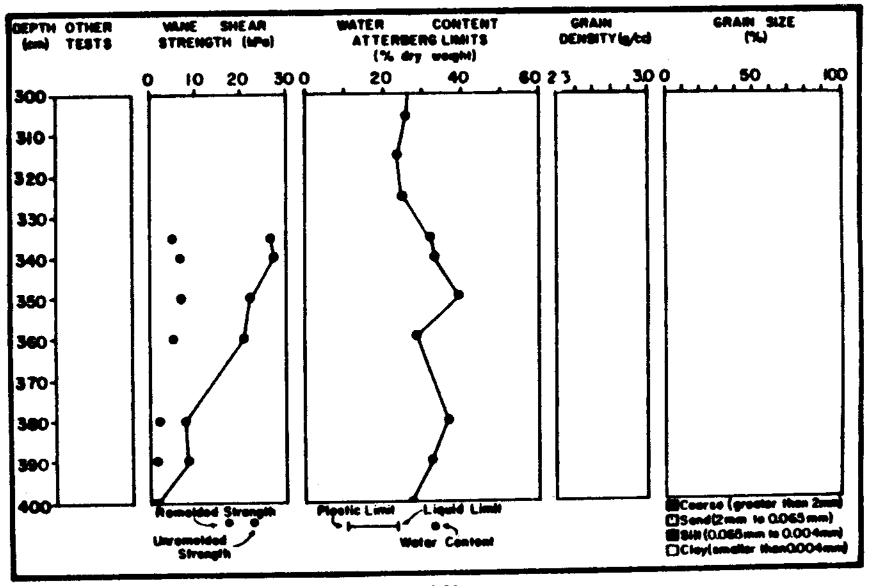

CRUISE: DCI-77-EG CORE: 615A1

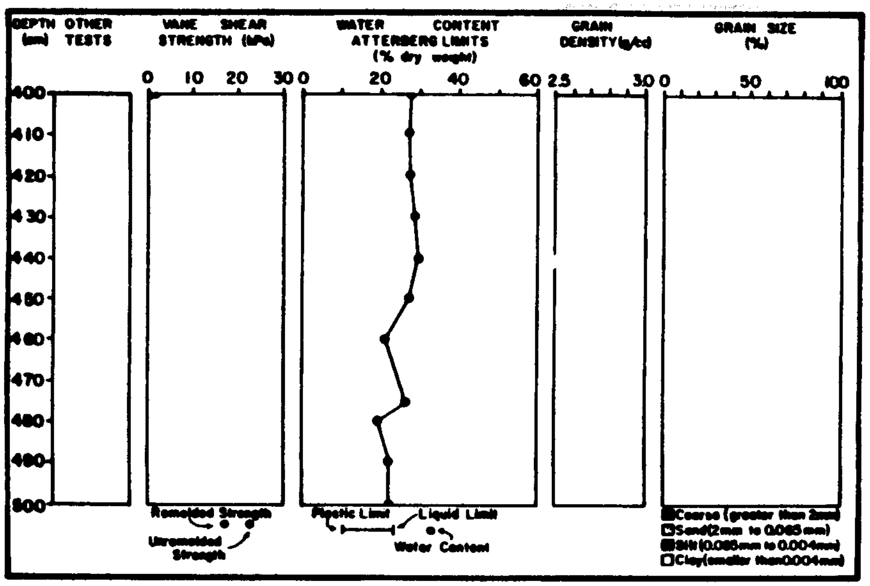

CRUISE: DCI-81-EG CORE: 615A1

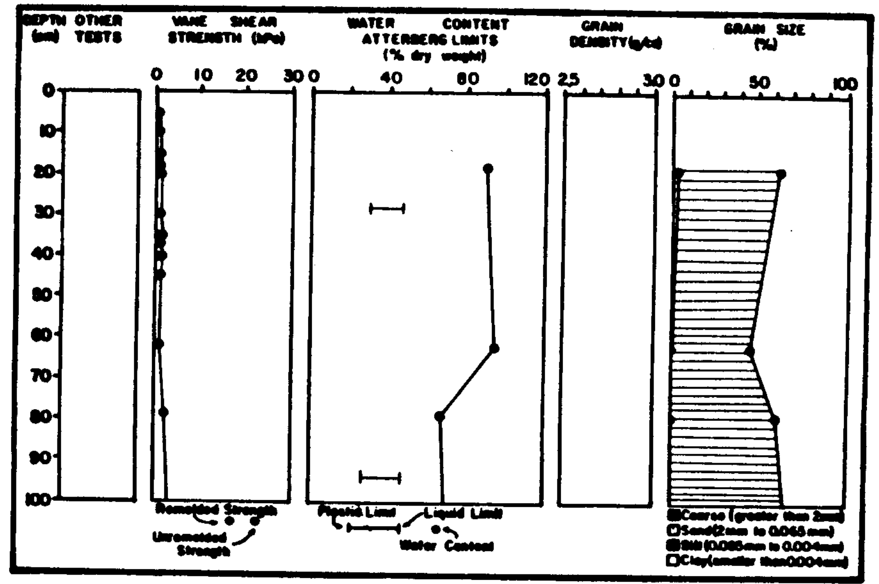

CRUISE: DCI-77-EG CORE: 700B

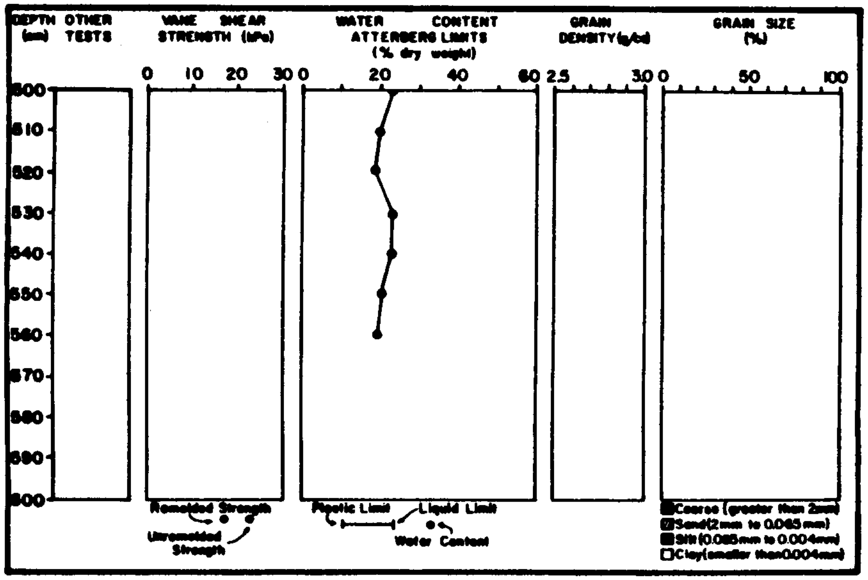

CRUISE: DCI-81-EG CORE: 615A1

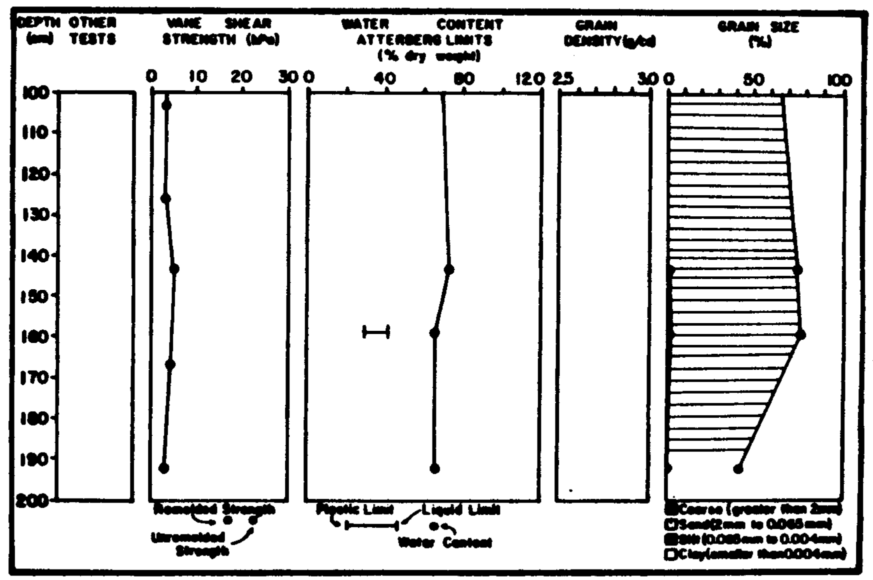

CRUISE: DCI-77-EG CORE: 700B

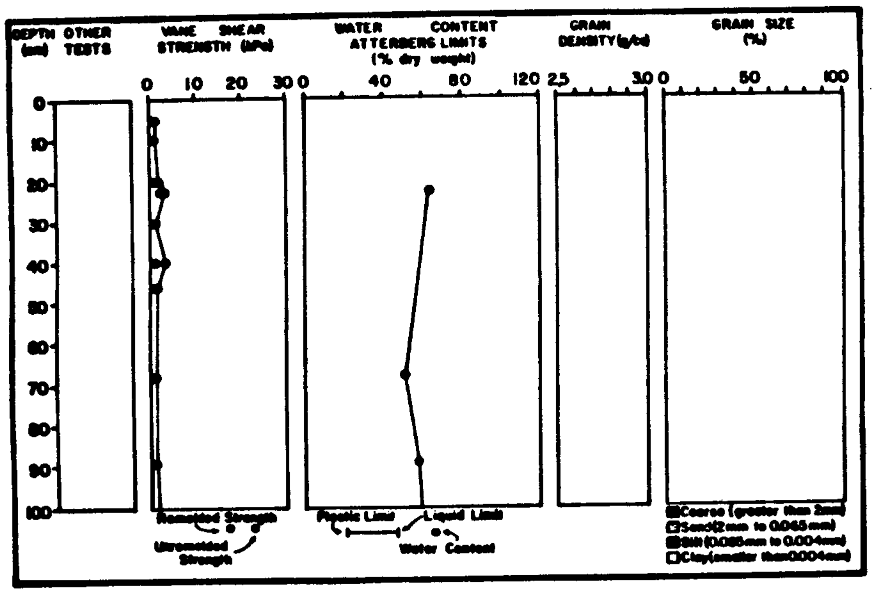

CRUISE: DCI-77-EG CORE: 704B

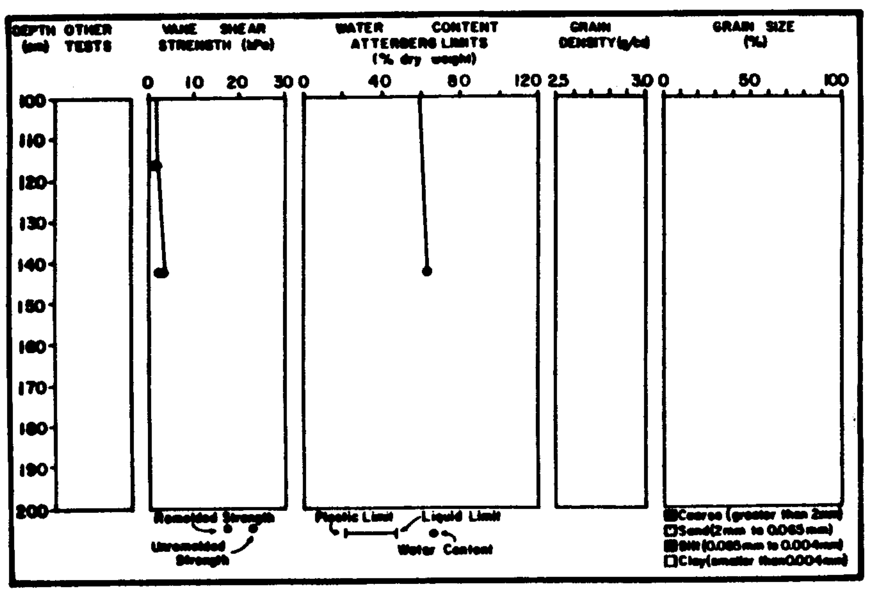

CRUISE: DCI-77-EG CORE: 704B

APPENDIX D

CONSOLIDATION AND TRIAXIAL TEST RESULTS--

LAW ENGINEERING AND TESTING COMPANY (1977 cores)

APPENDIX D. CONSOLIDATION AND TRIAXIAL TEST RESULTS-LAW ENGINEERING AND TESTING COMPANY (1977 cores)

This appendix presents the results of consolidation and static triaxial testing performed by Law Engineering and Testing Company under Contract number 14-08-0001-17356 with the U.S. Geological Survey. Testing was performed under the direction of R.W. Sparrow, P.G. Swanson and R.E. Brown. Core samples were from Cruise S8-77-EG.

All tests in this group have been assigned a test number with L1 as the last two characters. The consolidation tests (first two characters are OE) are presented first and are ordered by test number. Results from a single test are presented on a page in the form of void ratio and calculated coefficient of consolidation (c_v) versus the vertical effective stress given in bars (1 bar=101.3 kPa).

The static triaxial tests (first two characters are TE) are given second and ordered by test number. Results from one to as many as four tests are presented on the same sheet. The uppermost plot is a stress path presented as a plot of deviator stress versus mean normal effective stress. The deviator stress is the vertical effective stress (σ_v') minus the horizontal effective stress (σ_h'). The mean normal effective stress is ($\sigma_v'+2\sigma_h'$)/3. <u>Note: This definition is not the same as that used in the stress paths given in Appendices E, F, and G.</u>

The middle graph is either the deviator stress or Q/σ_c versus the axial strain. The parameter Q is the deviator stress while σ_c is the consolidation stress (or confining pressure). The last graph is the measured excess pore water pressure plotted versus axial strain.

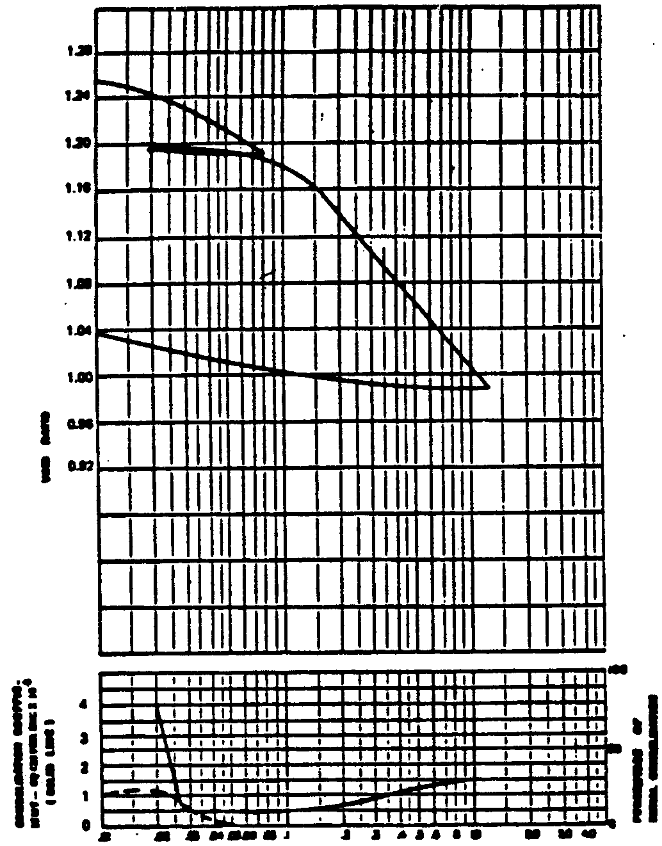

CONSOLIDATION TEST

0.20
1 G
W-6-2087

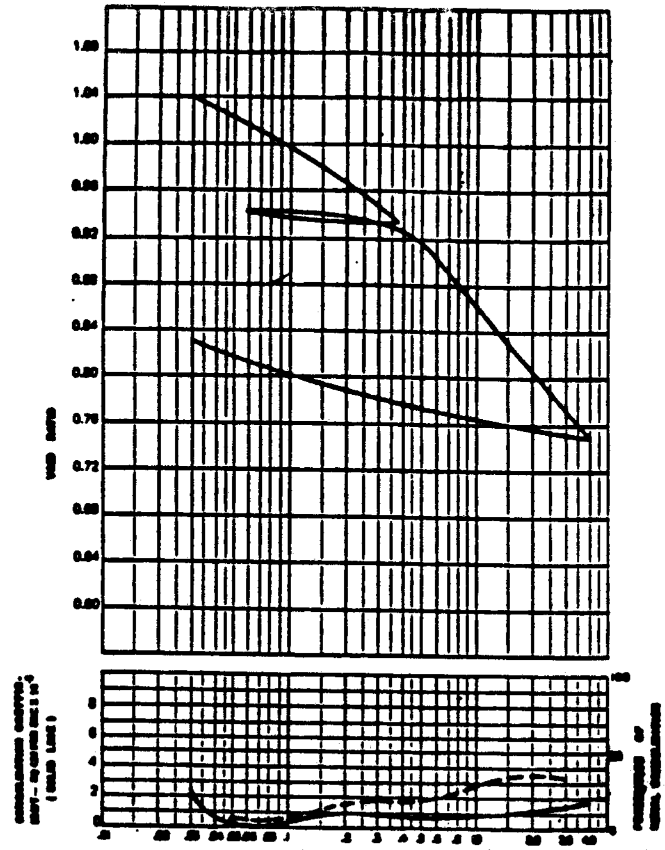

CONSOLIDATION TEST

0.17
10G
W-6-2087

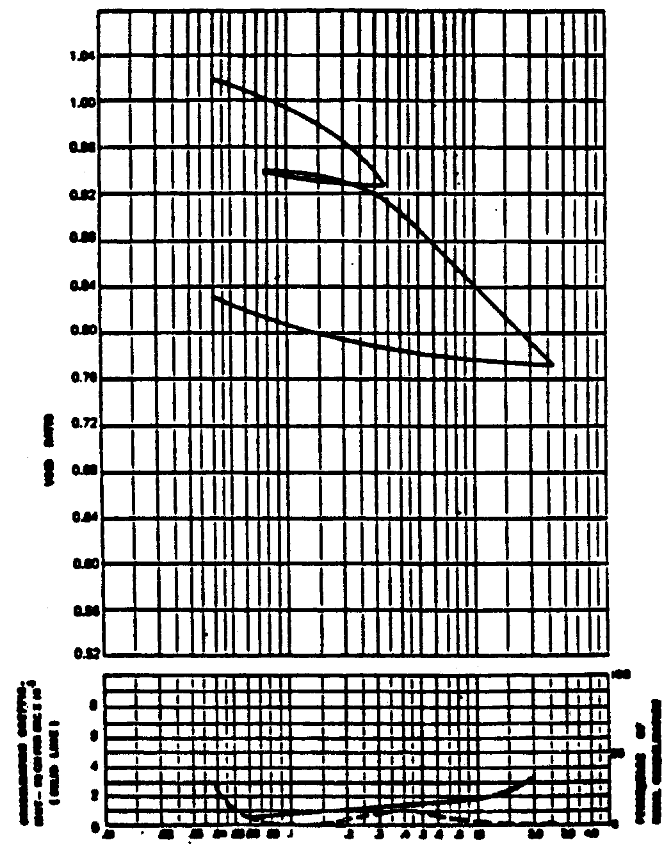

CONSOLIDATION TEST

0.15
1.80 gm/cc
37.9%
10.
W-6-2087

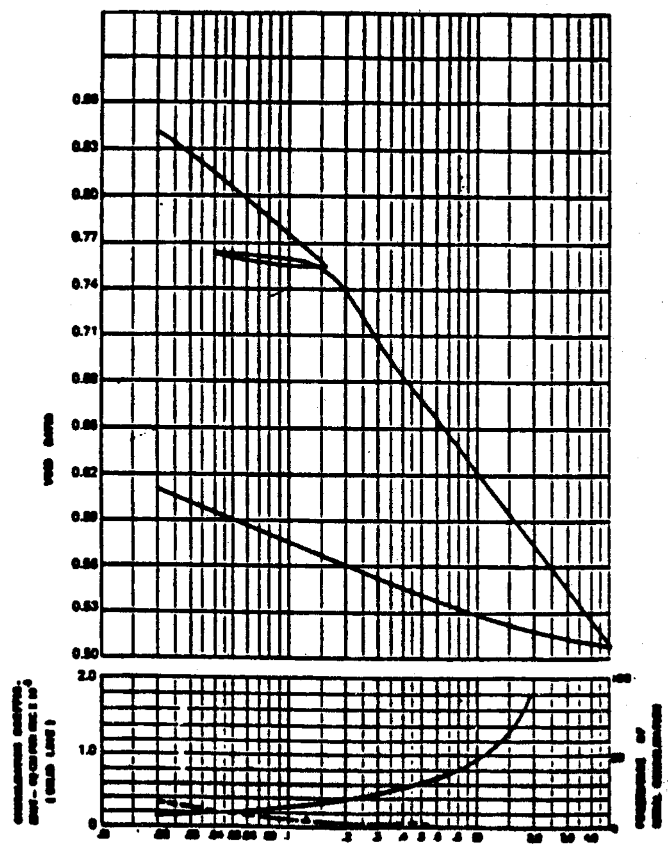

CONSOLIDATION TEST

0.17
11G
115-125 cm
W-6-2087

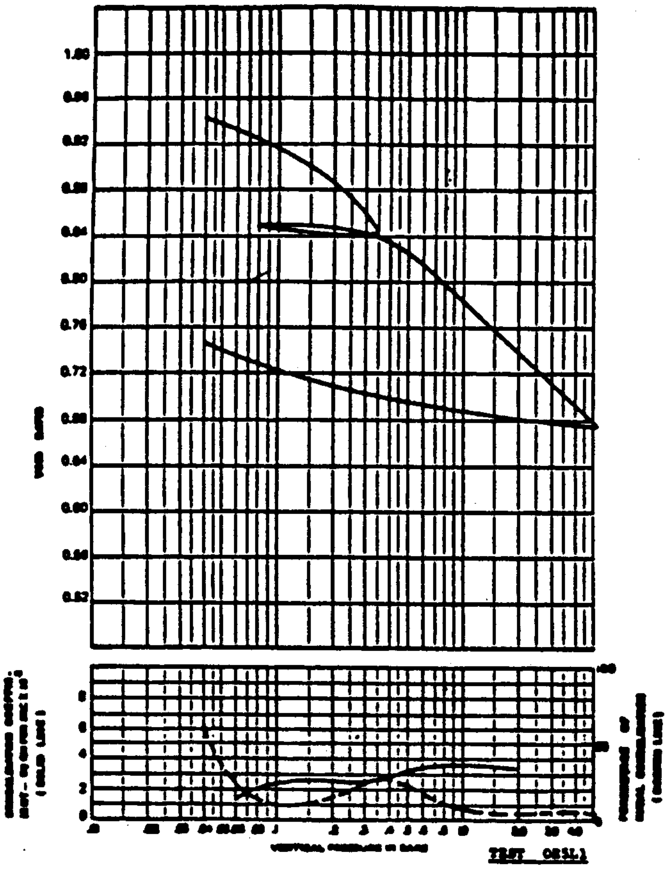

TEST [illegible]

CONSOLIDATION TEST

COMPRESSION INDEX 0.15
UNIT WEIGHT 1.89 gm/cc
WATER CONTENT 28.7%
SATURATION 100%

BORING NO. 28-77. 80 SAMPLE NO. 116
ELEV. OR DEPTH 240-250 cm JOB NO. W-8-2097

LAW ENGINEERING TESTING COMPANY

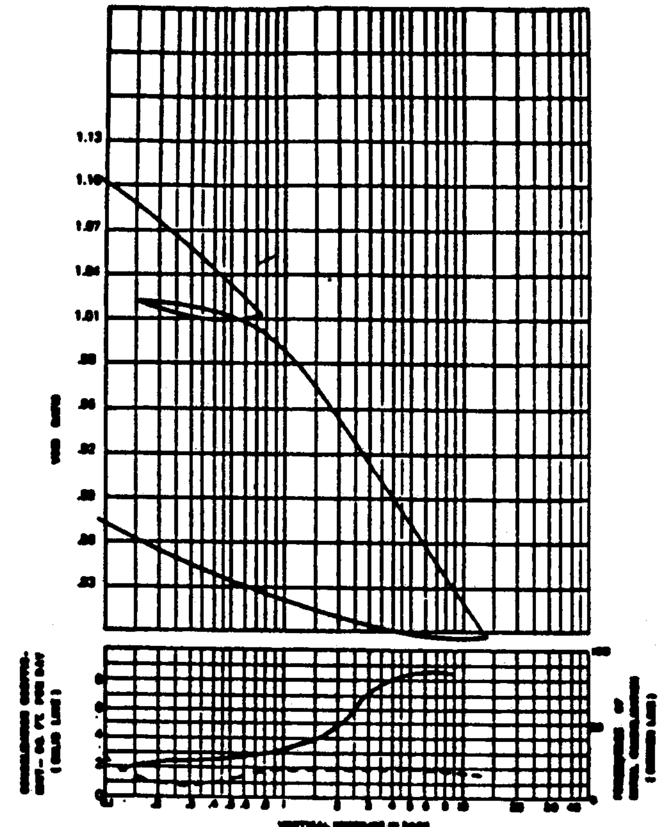

TEST [illegible]

CONSOLIDATION TEST

COMPRESSION INDEX .29
UNIT WEIGHT 1.80 gm/cc
WATER CONTENT 41.7%
SATURATION 97.2%

BORING NO. 28-11. 80 SAMPLE NO. 116
ELEV. OR DEPTH [illegible] JOB NO. W-8-2097

LAW ENGINEERING TESTING COMPANY

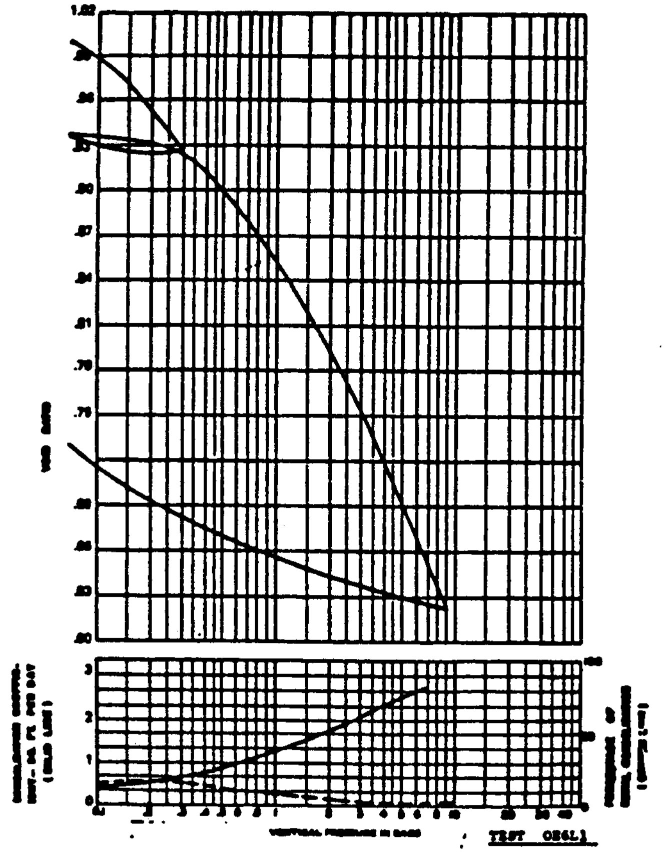

TEST [illegible]

CONSOLIDATION TEST

COMPRESSION INDEX 0.20
UNIT WEIGHT 1.84 gm/cc
WATER CONTENT [illegible]
SATURATION [illegible]

BORING NO. 28-77-80 SAMPLE NO. 110
ELEV. OR DEPTH 380-400 cm JOB NO. W-8-2097

LAW ENGINEERING TESTING COMPANY

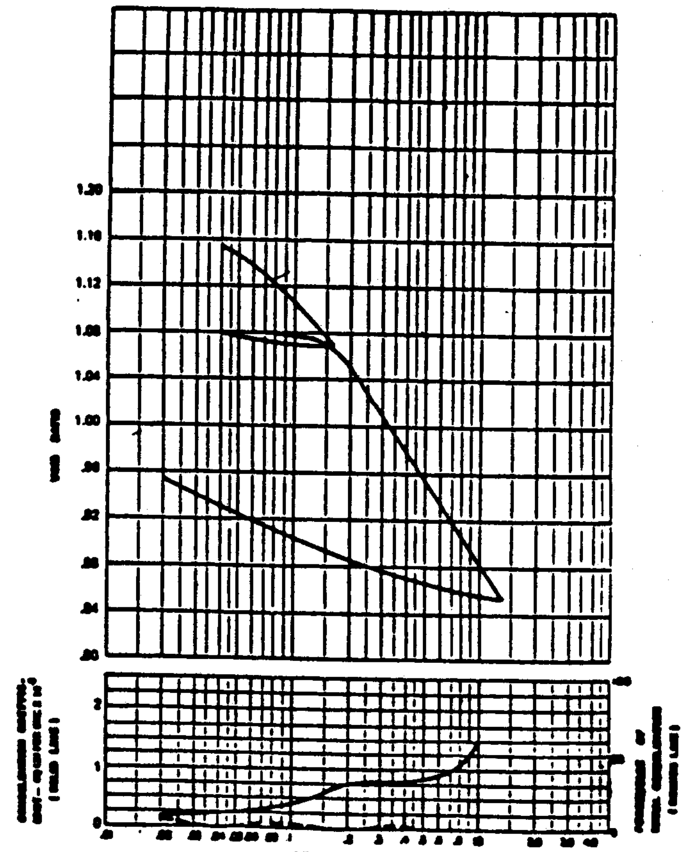

TEST [illegible]

CONSOLIDATION TEST

COMPRESSION INDEX 0.23
UNIT WEIGHT 1.77 gm/cc
WATER CONTENT 42.8%
SATURATION 98.3%

BORING NO. 28-77. 80 SAMPLE NO. 140
ELEV. OR DEPTH 105-110 cm JOB NO. W-8-2097

LAW ENGINEERING TESTING COMPANY

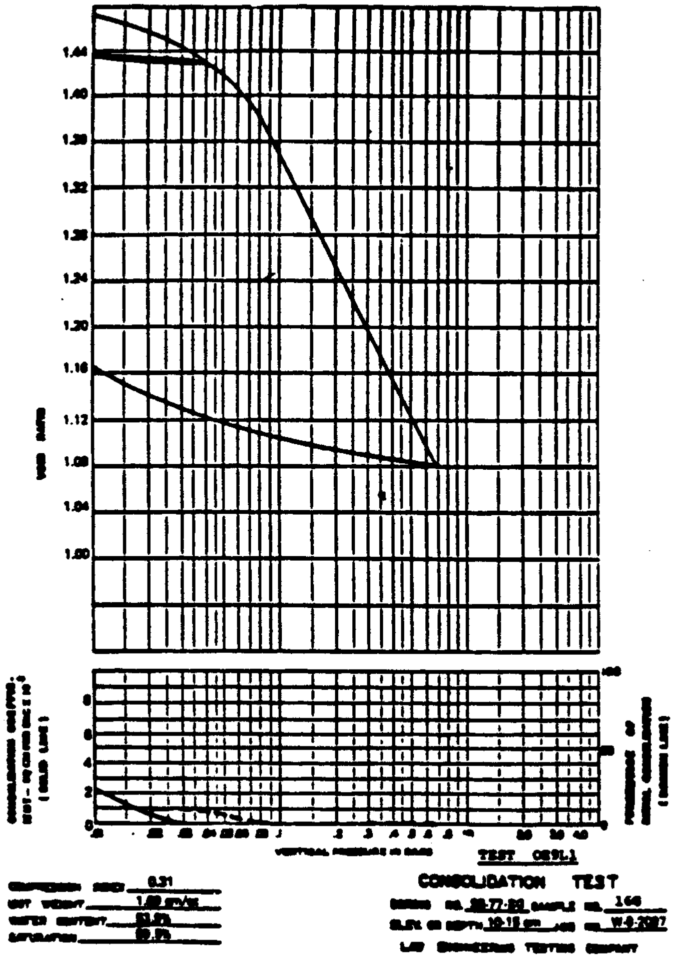
TEST OE9L1
CONSOLIDATION TEST

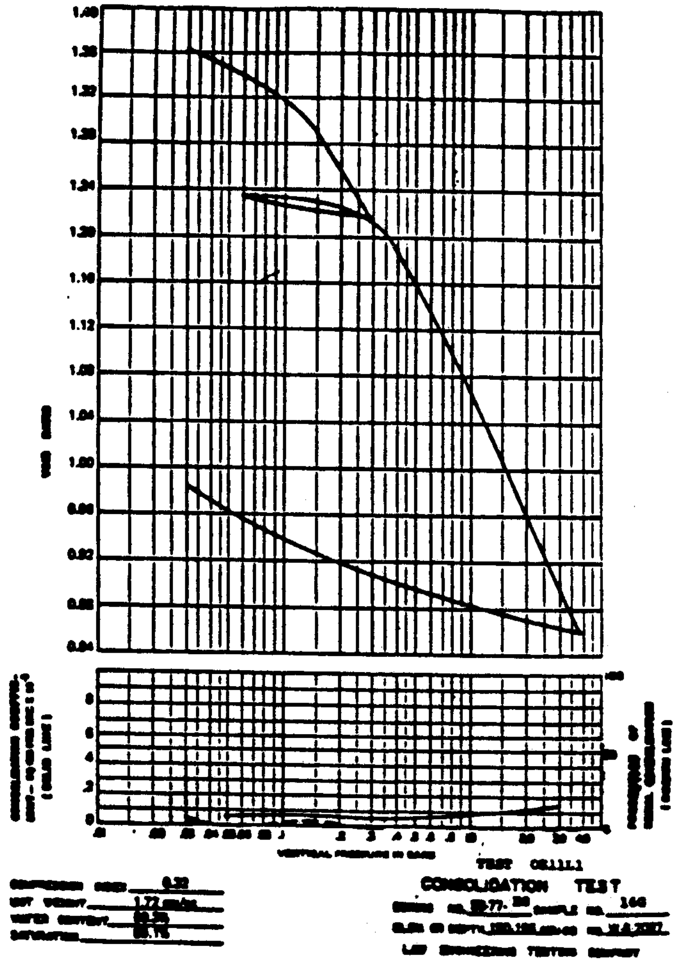
TEST OE11L1
CONSOLIDATION TEST

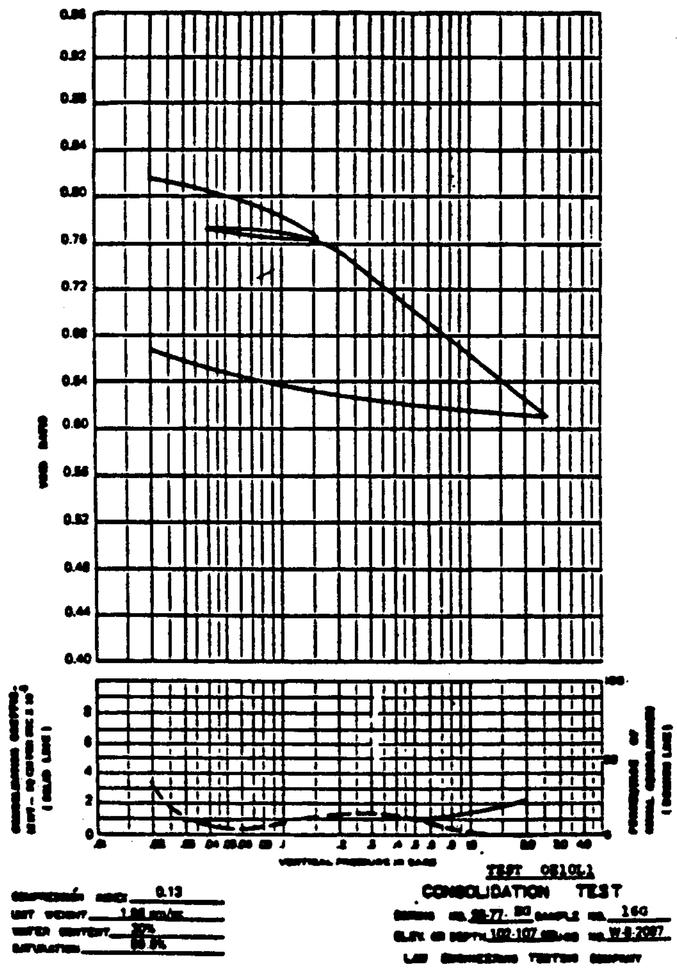
TEST OE10L1
CONSOLIDATION TEST

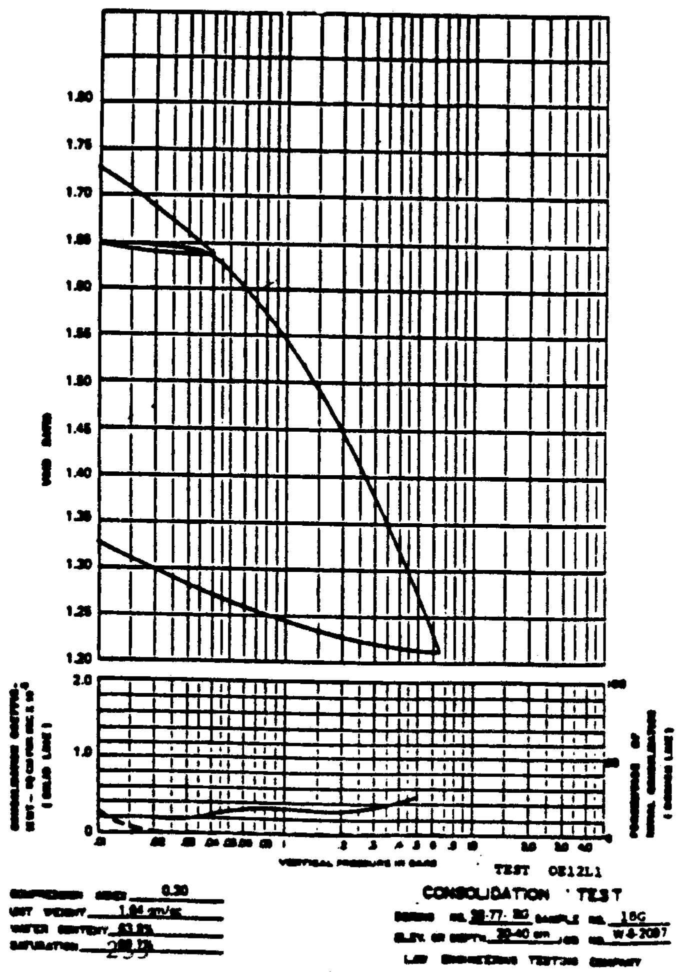
TEST OE12L1
CONSOLIDATION TEST

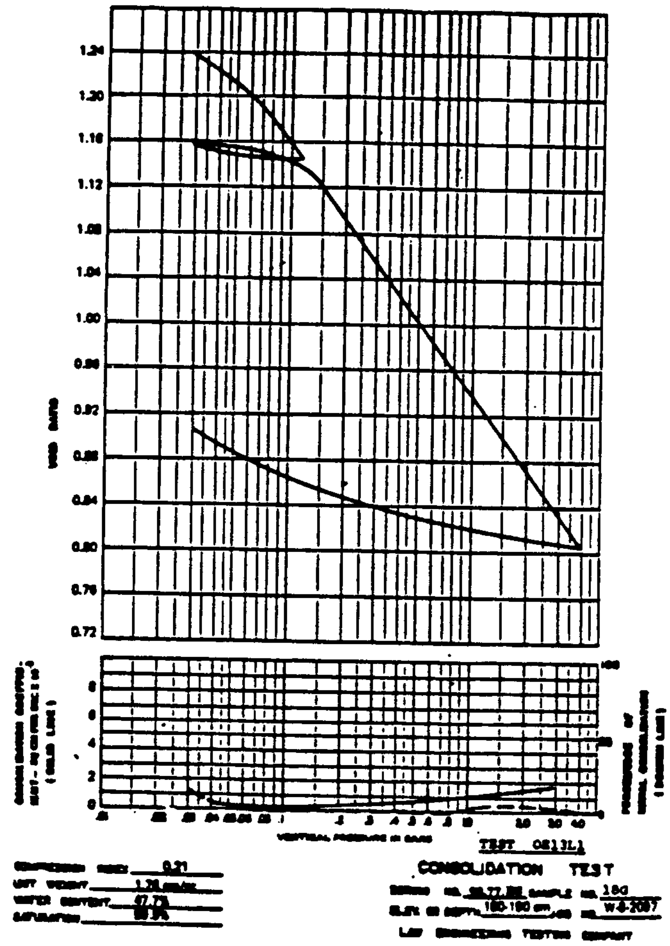
TEST OE13L1
CONSOLIDATION TEST
0.21
47.7%
18G
180-190 cm
W-8-2087

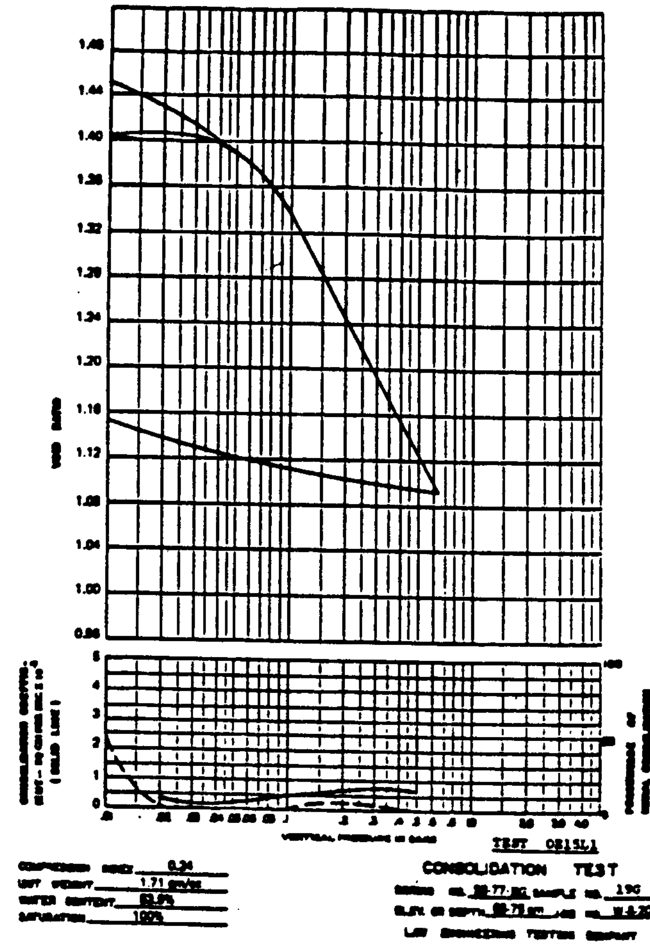
TEST OE15L1
CONSOLIDATION TEST
0.24
1.71 gm/cc
100%
19G

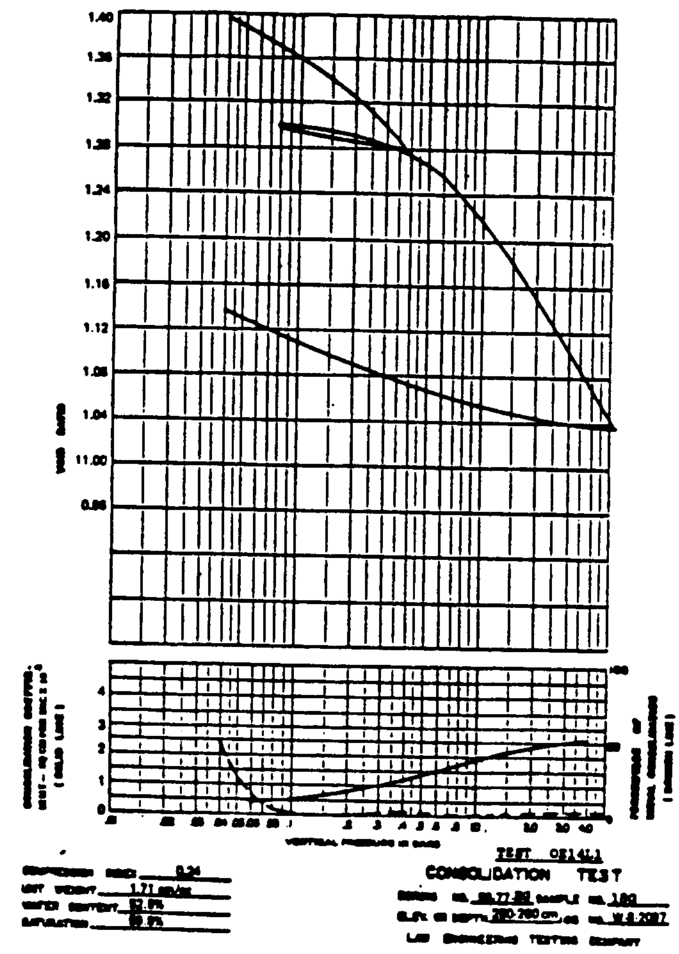
TEST OE14L1
CONSOLIDATION TEST
0.24
1.71 gm/cc
18G

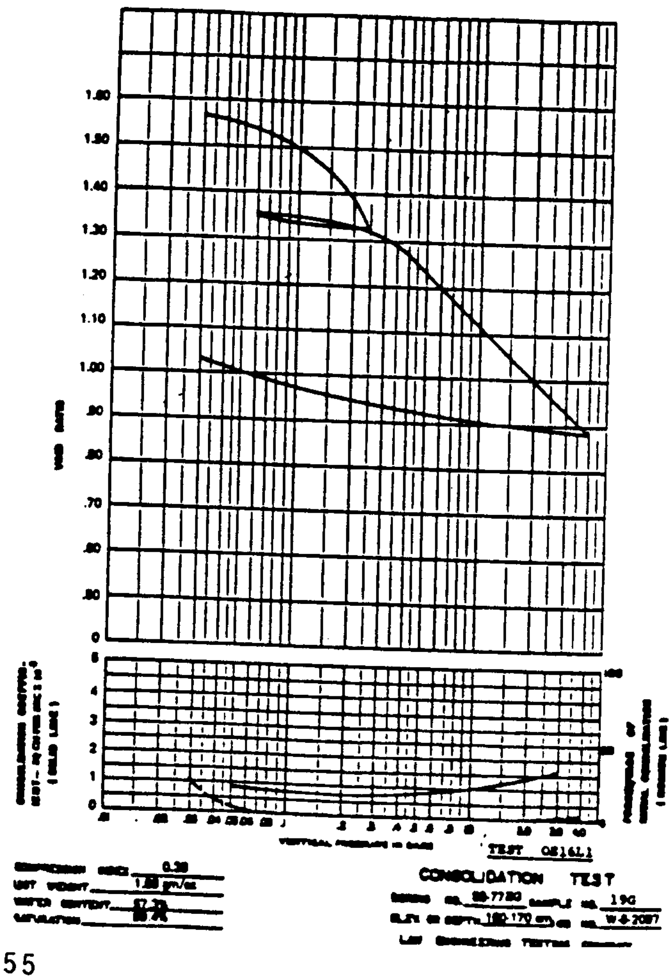
TEST OE16L1
CONSOLIDATION TEST
0.38
19G
180-170 cm

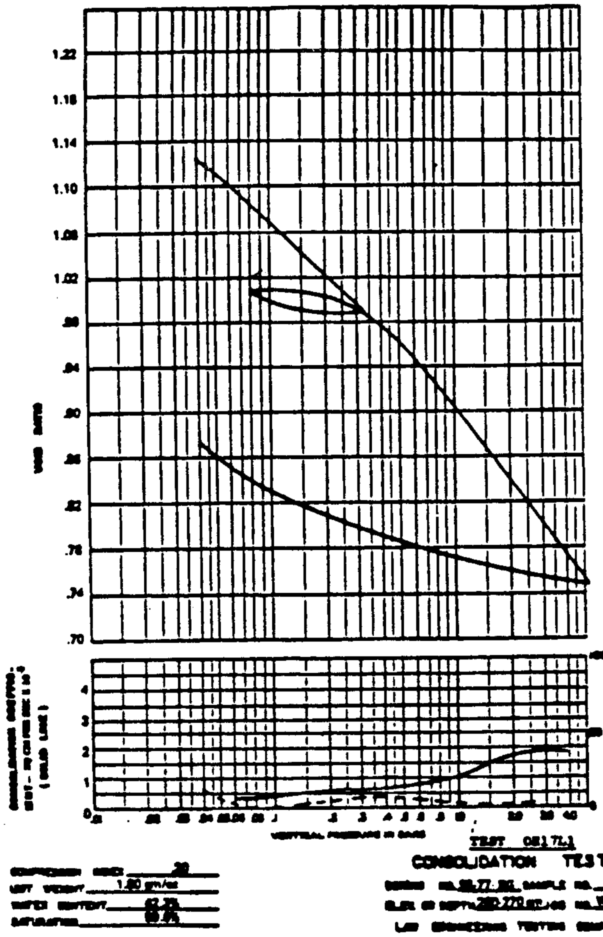
TEST OE17L1
CONSOLIDATION TEST
19G
W-8-2097

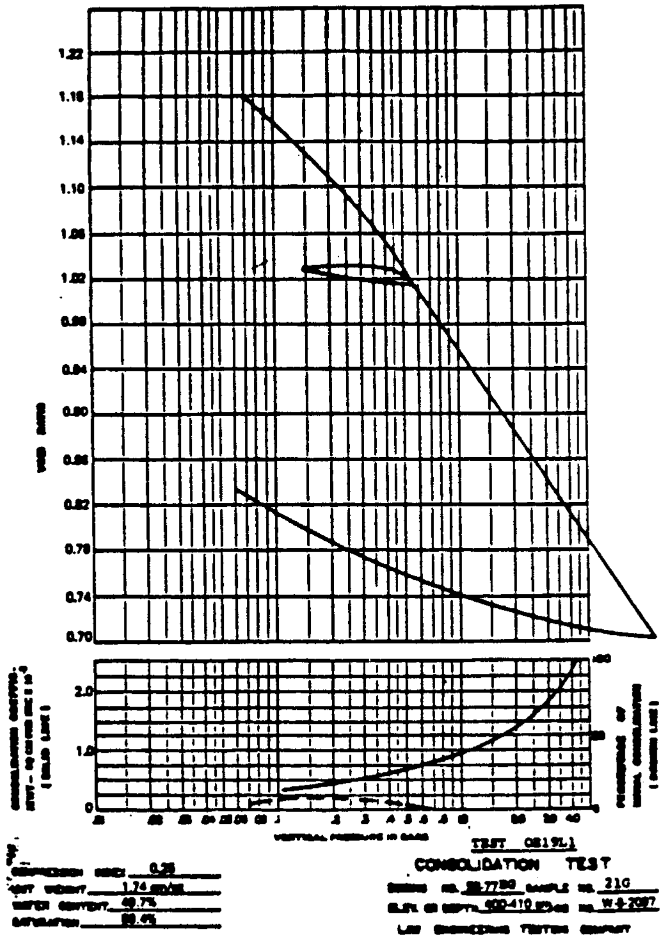
TEST OE19L1
CONSOLIDATION TEST
21G
W-8-2097

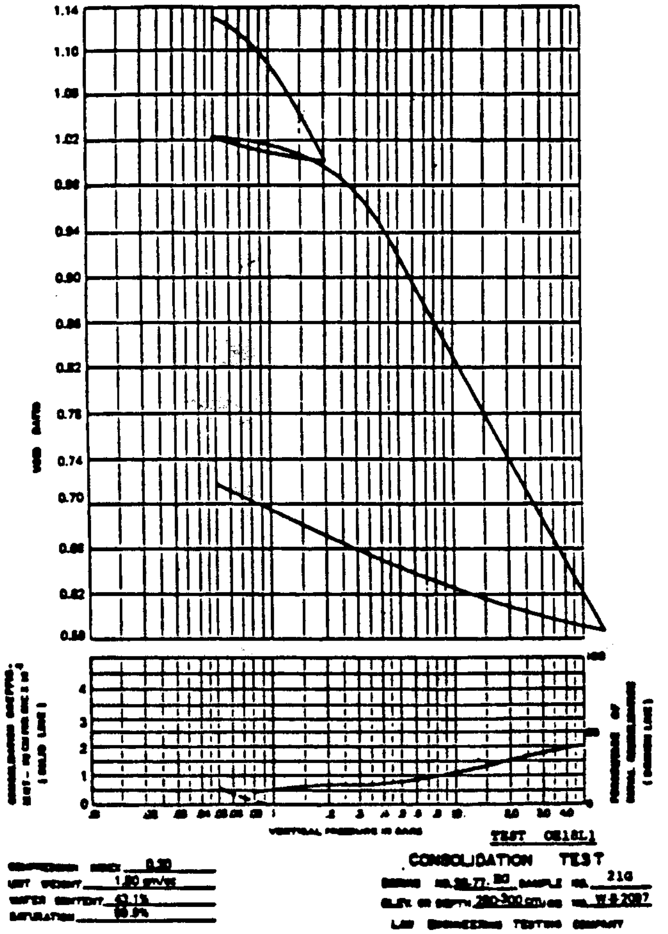
TEST OE18L1
CONSOLIDATION TEST
21G
W-8-2097

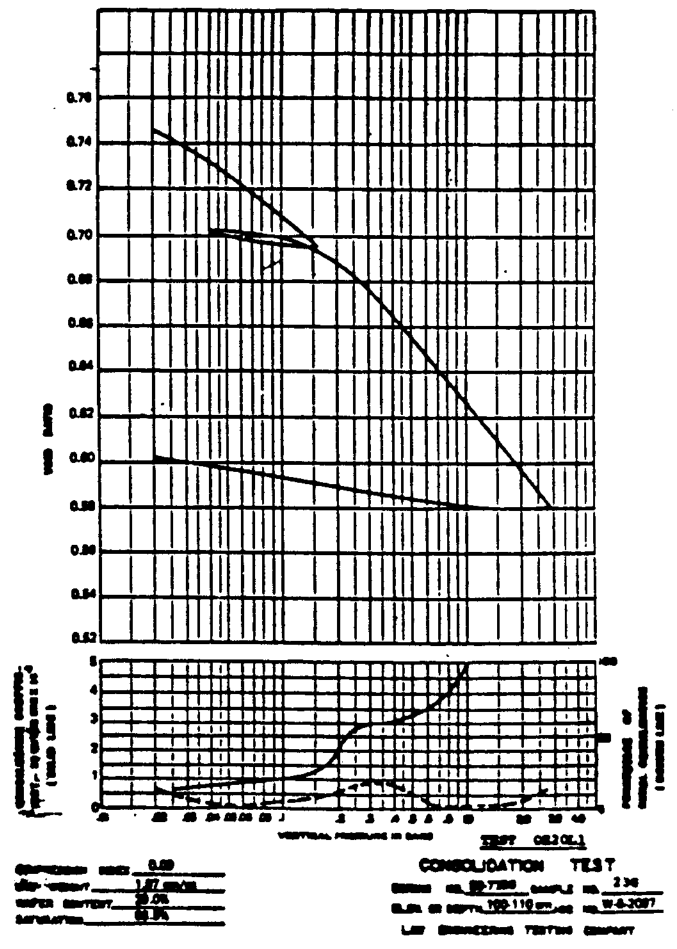
TEST OE20L1
CONSOLIDATION TEST
23G
W-8-2097

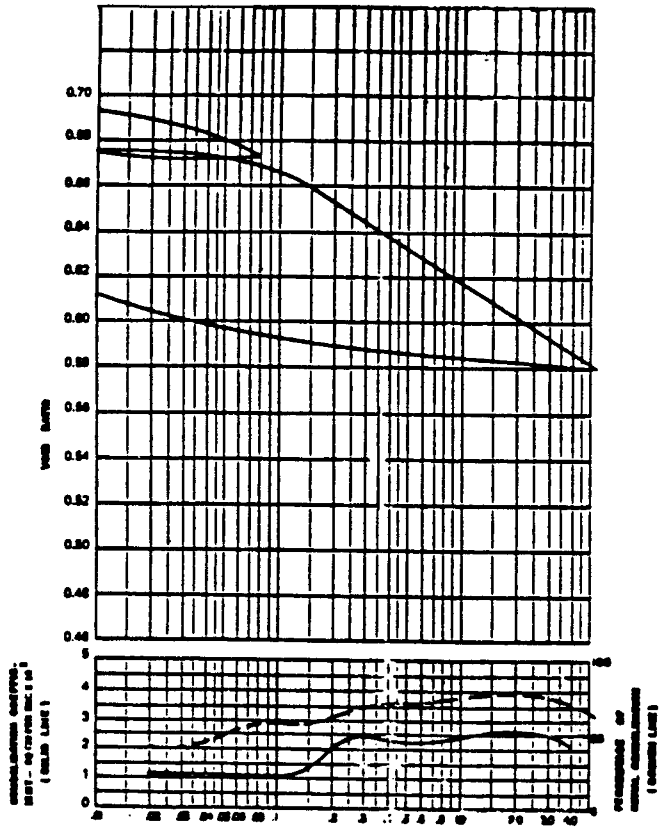

TEST OE21L1

CONSOLIDATION TEST

0.08
2.0 gm/cc
22.0%
81.0%

34G
80-70 cm
W-8-2087

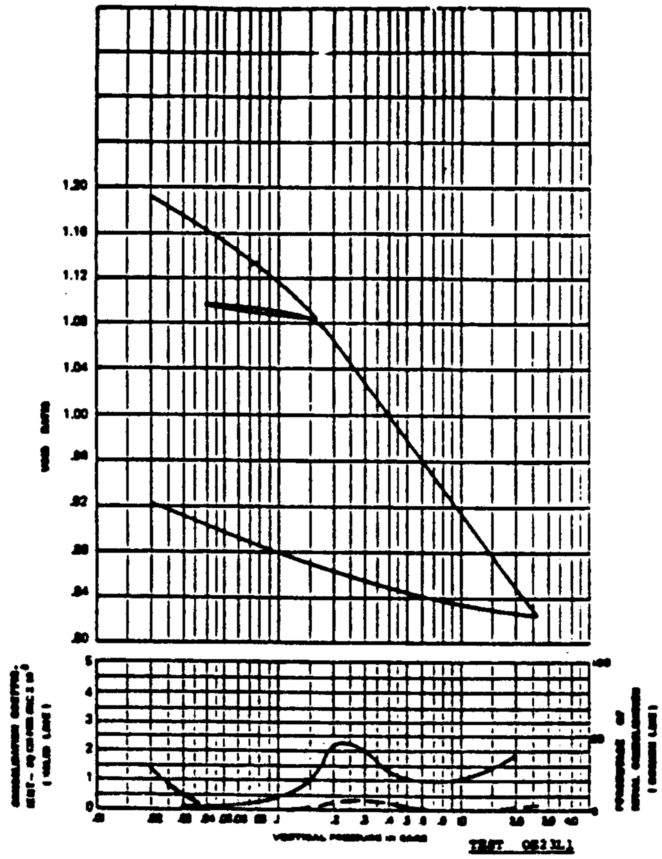

TEST OE23L1

CONSOLIDATION TEST

0.18
1.78 gm/cc
63.8%
97.2%

47G
100-110 cm

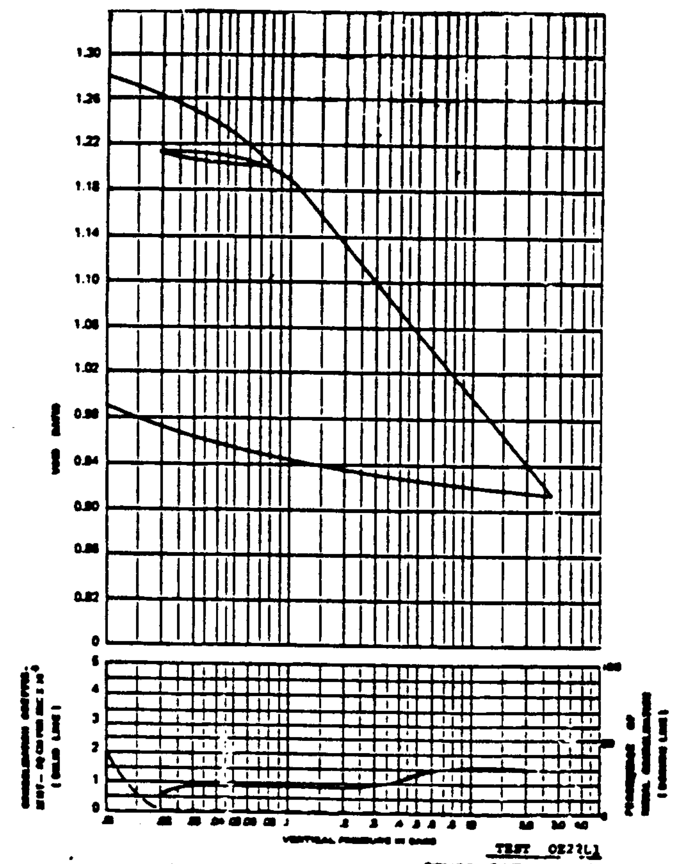

TEST OE22L1

CONSOLIDATION TEST

0.28
1.79 gm/cc
46.9%
99.7%

33G
27-37 cm
W-8-2087

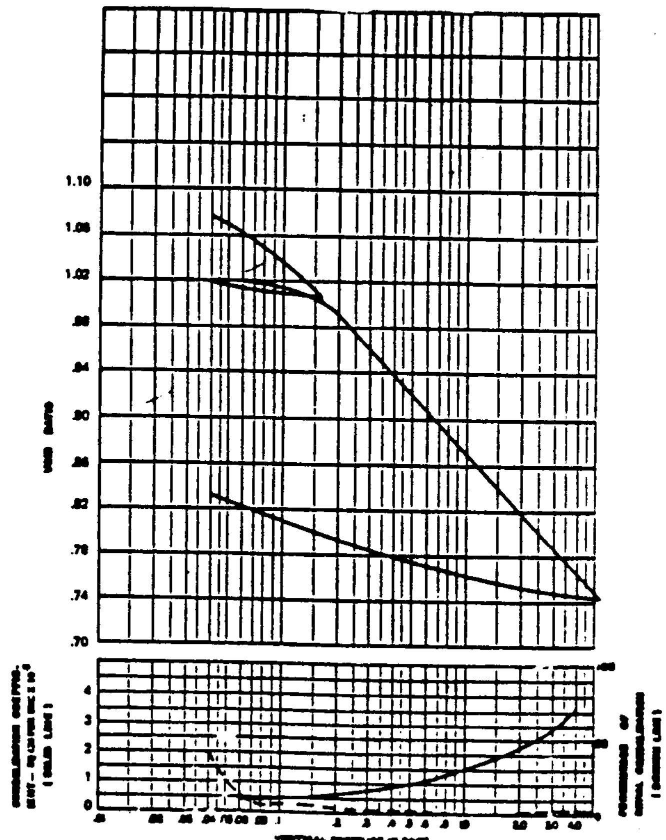

TEST OE24L1

CONSOLIDATION TEST

1.19
1.82 gm/cc
41.1%
99.9%

47G
280-290 cm
W-8-2087

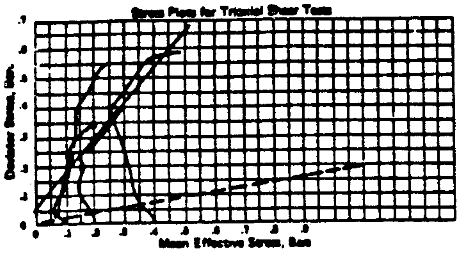

Cohesion, C 0.00 BAR

Angle of Shear Resistance 31.1°

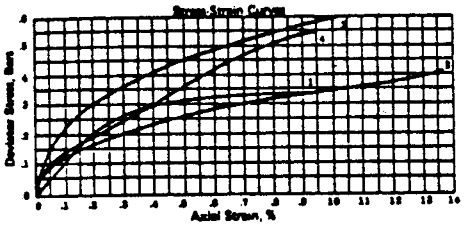

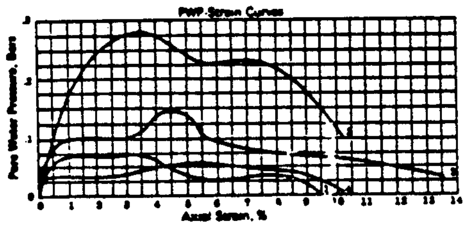

TESTS
(1) TE1L1
(2) TE2L1
(3) TE3L1
(4) TE4L1

* Stress Controlled Test

CURVE NO.	(1)	(2)	(3)	(4)
Confining Pressure Bars	.10	[illegible]	[illegible]	[illegible]
Initial Length, cm	9.9	9.8	9.5	[illegible]
Initial Diameter, cm	6.16	6.13	[illegible]	[illegible]
Wet Unit Weight, gm/cc	1.77	1.76	[illegible]	[illegible]
Moisture Content, %	67.40	[illegible]	[illegible]	[illegible]
Initial Void Ratio	[illegible]	[illegible]	[illegible]	[illegible]
Initial Percent Saturation	[illegible]	[illegible]	[illegible]	[illegible]

Consolidated Undrained Triaxial Shear Test with Pore Pressure Measurements

CORE 1G

CRUISE 88-77-BG

Date [illegible]

Job No. [illegible]

LAW ENGINEERING TESTING COMPANY

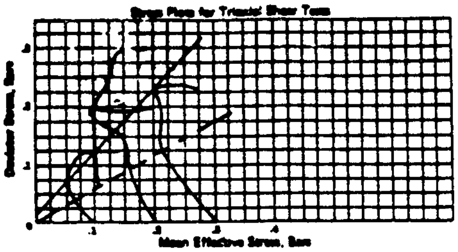

Cohesion, C [illegible]

Angle of Shear Resistance [illegible]

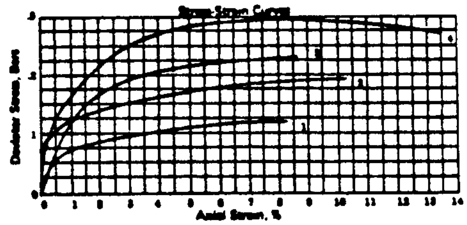

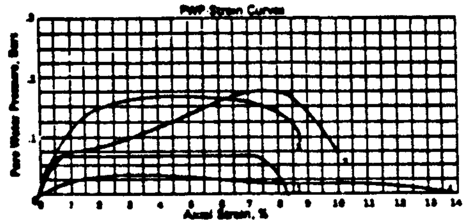

TESTS
(1) TE8L1
(2) TE9L1
(3) TE10L1
(4) TE11L1

Stress Controlled Test

CURVE NO.	(1)	(2) •	(3)	(4) •
Confining Pressure Bars	.10	.20	.20	[illegible]
Initial Length, cm	10.0	9.7	[illegible]	[illegible]
Initial Diameter, cm	[illegible]	[illegible]	[illegible]	[illegible]
Wet Unit Weight, gm/cc	1.77	1.74	1.74	[illegible]
Moisture Content, %	[illegible]	[illegible]	[illegible]	[illegible]
Initial Void Ratio	[illegible]	[illegible]	[illegible]	[illegible]
Initial Percent Saturation	[illegible]	[illegible]	[illegible]	[illegible]

Consolidated Undrained Triaxial Shear Test with Pore Pressure Measurements

CORE 10G

CRUISE 88-77-BG

Date [illegible]

Job No. [illegible]

LAW ENGINEERING TESTING COMPANY

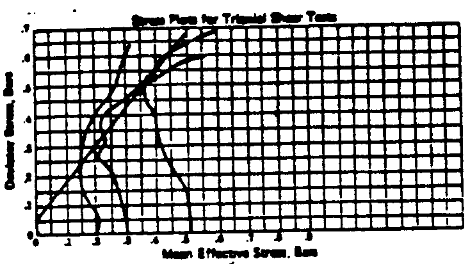

Cohesion, C [illegible]

Angle of Shear Resistance 31.1°

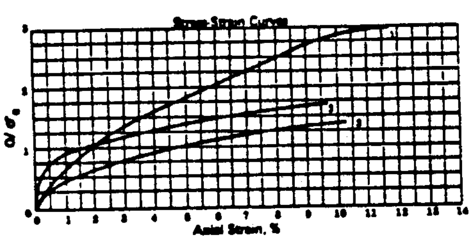

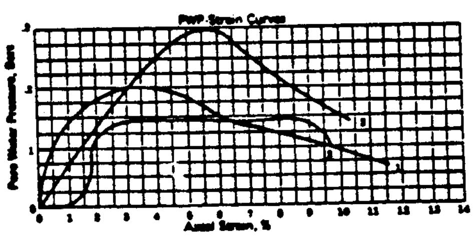

TESTS
(1) TE5L1
(2) TE6L1
(3) TE7L1

* Stress Controlled Test

CURVE NO.	(1)	(2)	(3)	(4)
Confining Pressure Bars	[illegible]	[illegible]	[illegible]	
Initial Length, cm	[illegible]	9.4	[illegible]	
Initial Diameter, cm	[illegible]	6.10	[illegible]	
Wet Unit Weight, gm/cc	[illegible]	[illegible]	[illegible]	
Moisture Content, %	[illegible]	[illegible]	[illegible]	
Initial Void Ratio	[illegible]	[illegible]	[illegible]	
Initial Percent Saturation	[illegible]	[illegible]	[illegible]	

Consolidated Undrained Triaxial Shear Test with Pore Pressure Measurements

CORE 1G

CRUISE 88-77-BG

Date [illegible]

Job No. [illegible]

LAW ENGINEERING TESTING COMPANY

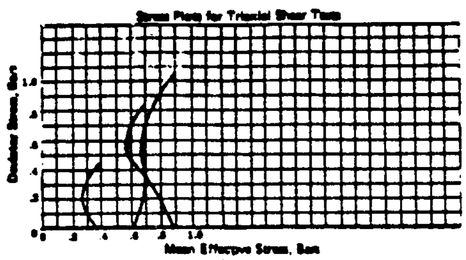

Cohesion, C [illegible]

Angle of Shear Resistance [illegible]

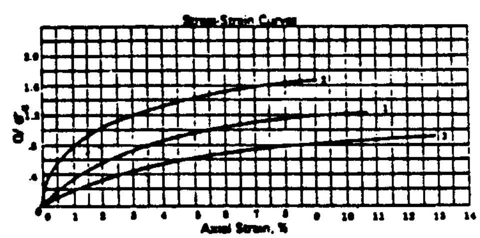

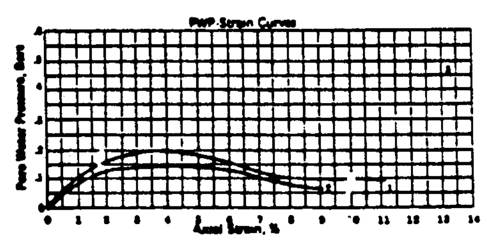

TESTS
(1) TE12L1
(2) TE13L1
(3) TE14L1

* Stress Controlled Test

CURVE NO.	(1)	(2)	(3)	(4)
Confining Pressure Bars	[illegible]	[illegible]	[illegible]	
Initial Length, cm	[illegible]	7.7	10.3	
Initial Diameter, cm	[illegible]	[illegible]	[illegible]	
Wet Unit Weight, gm/cc	[illegible]	[illegible]	[illegible]	
Moisture Content, %	[illegible]	[illegible]	[illegible]	
Initial Void Ratio	[illegible]	[illegible]	[illegible]	
Initial Percent Saturation	[illegible]	[illegible]	[illegible]	

Consolidated Undrained Triaxial Shear Test with Pore Pressure Measurements

CORE [illegible]

CRUISE [illegible]

Date [illegible]

Job No. [illegible]

LAW ENGINEERING TESTING COMPANY

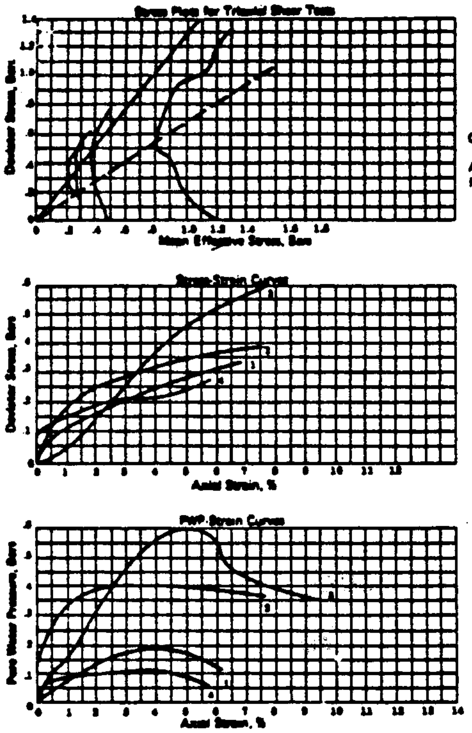

Cohesion, C 0

Angle of Shear Resistance [illegible]°

TESTS
(1) TE15L1
(2) TE16L1
(3) TE17L1
(4) TE18L1

* Stress Controlled Test

CURVE NO.	(1) *	(2) *	(3)	(4) *
Confining Pressure Bars	[illegible]	[illegible]	1.[illegible]	[illegible]
Initial Length, cm	10.2	10.2	9.5	10.7
Initial Diameter, cm	[illegible]	[illegible]	[illegible]	[illegible]
Wet Unit Weight, gm/cc	[illegible]	[illegible]	[illegible]	[illegible]
Moisture Content, %	[illegible]	[illegible]	[illegible]	[illegible]
Initial Void Ratio	[illegible]	[illegible]	[illegible]	[illegible]
Initial Percent Saturation	[illegible]	[illegible]	[illegible]	[illegible]

Consolidated Undrained Triaxial Shear Test with Pore Pressure Measurements

CORE 11G

CRUISE 86-77-BG

Date [illegible]

Job No. [illegible]

LAW ENGINEERING TESTING COMPANY

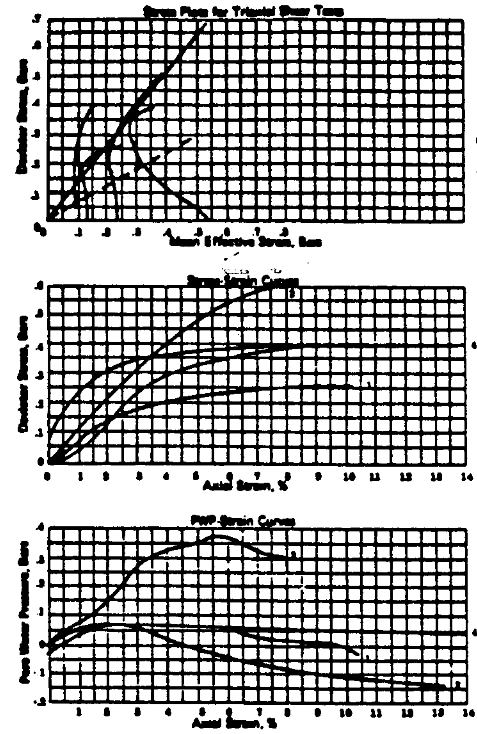

Cohesion, C 0

Angle of Shear Resistance [illegible]°

TESTS
(1) TE22L1
(2) TE23L1
(3) TE24L1
(4) TE25L1

* Stress Controlled Test

CURVE NO.	(1)	(2)	(3)	(4) *
Confining Pressure Bars	.13	[illegible]	[illegible]	[illegible]
Initial Length, cm	9.9	10.3	10.3	7.6
Initial Diameter, cm	[illegible]	[illegible]	[illegible]	[illegible]
Wet Unit Weight, gm/cc	[illegible]	[illegible]	[illegible]	[illegible]
Moisture Content, %	[illegible]	[illegible]	[illegible]	[illegible]
Initial Void Ratio	[illegible]	[illegible]	[illegible]	[illegible]
Initial Percent Saturation	[illegible]	[illegible]	[illegible]	[illegible]

Consolidated Undrained Triaxial Shear Test with Pore Pressure Measurements

CORE 16G

CRUISE 86-77-BG

Date [illegible]

Job No. [illegible]

LAW ENGINEERING TESTING COMPANY

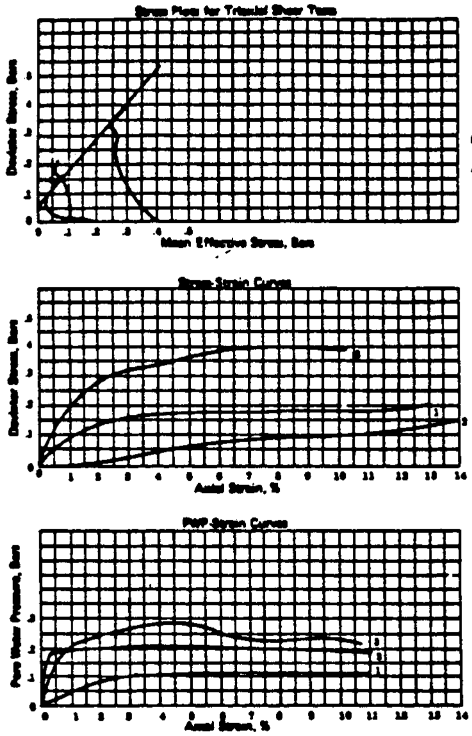

Cohesion, C [illegible] BARS

Angle of Shear Resistance [illegible]°

TESTS
(1) TE19L1
(2) TE20L1
(3) TE21L1

* Stress Controlled Test

CURVE NO.	(1) *	(2) *	(3)	(4)
Confining Pressure Bars	[illegible]	[illegible]	[illegible]	
Initial Length, cm	9.9	9.9	9.7	
Initial Diameter, cm	[illegible]	[illegible]	[illegible]	
Wet Unit Weight, gm/cc	[illegible]	[illegible]	[illegible]	
Moisture Content, %	[illegible]	[illegible]	[illegible]	
Initial Void Ratio	[illegible]	[illegible]	[illegible]	
Initial Percent Saturation	[illegible]	[illegible]	[illegible]	

Consolidated Undrained Triaxial Shear Test with Pore Pressure Measurements

CORE 14G

CRUISE 86-77-BG

Date [illegible]

Job No. [illegible]

LAW ENGINEERING TESTING COMPANY

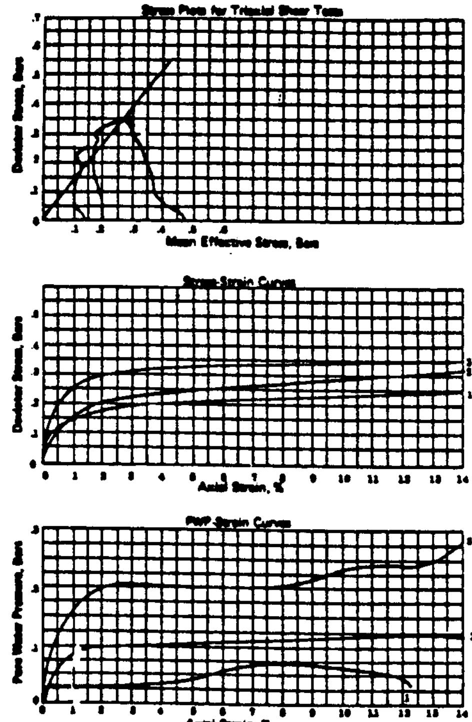

Cohesion, C 0

Angle of Shear Resistance [illegible]°

TESTS
(1) TE26L1
(2) TE27L1
(3) TE28L1

* Stress Controlled Test

CURVE NO.	(1) *	(2) *	(3) *	(4)
Confining Pressure	[illegible]	[illegible]	[illegible]	
Initial Length, cm	[illegible]	10.5	10.4	
Initial Diameter, cm	[illegible]	[illegible]	[illegible]	
Wet Unit Weight, gm/cc	[illegible]	[illegible]	[illegible]	
Moisture Content, %	[illegible]	[illegible]	[illegible]	
Initial Void Ratio	[illegible]	[illegible]	[illegible]	
Initial Percent Saturation	[illegible]	[illegible]	[illegible]	

Consolidated Undrained Triaxial Shear Test with Pore Pressure Measurements

CORE 19G

CRUISE 86-77-BG

Date [illegible]

Job No. [illegible]

LAW ENGINEERING TESTING COMPANY

Stress Paths for Triaxial Shear Tests

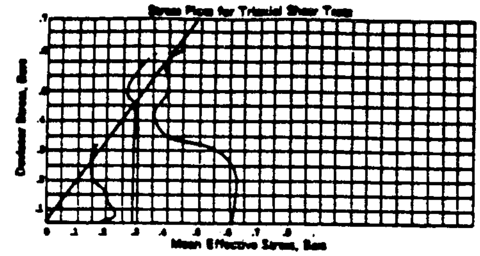

Cohesion, C 0

Angle of Shear Resistance 35.5°

Stress-Strain Curves

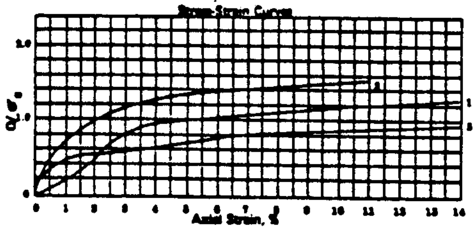

PWP-Strain Curves

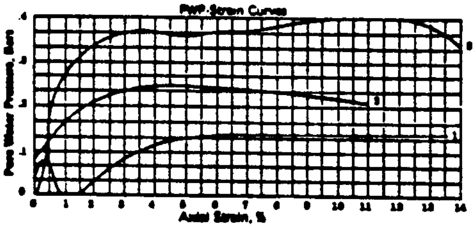

TESTS
(1) TE29L1
(2) TE30L1
(3) TE31L1

* Stress Controlled Test

CURVE NO.	(1)	(2)	(3)	(4)
Confining Pressure Bars	[illegible]	[illegible]	[illegible]	
Initial Length, cm	10.[illegible]	[illegible]	[illegible]	
Initial Diameter, cm	[illegible]	[illegible]	[illegible]	
Wet Unit Weight, gm/cc	[illegible]	1.72	1.72	
Moisture Content, %	[illegible]	[illegible]	[illegible]	
Initial Void Ratio	[illegible]	[illegible]	[illegible]	
Initial Percent Saturation	[illegible]	[illegible]	[illegible]	

Consolidated Undrained Triaxial Shear Test with Pore Pressure Measurements

CORE 21G

CRUISE S8-77-BG

Date [illegible]

Job No. [illegible]

LAW ENGINEERING TESTING COMPANY

Stress Paths for Triaxial Shear Tests

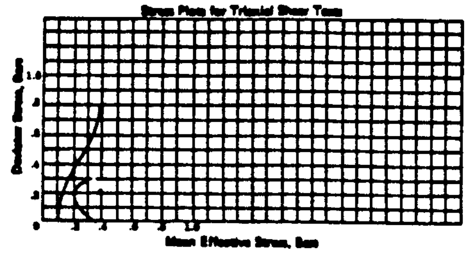

Cohesion, C

Angle of Shear Resistance

Stress-Strain Curves

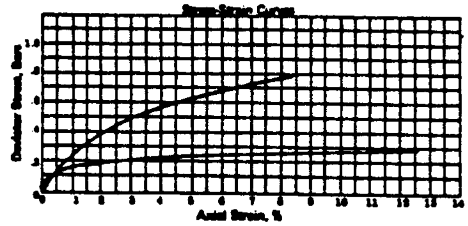

PWP-Strain Curves

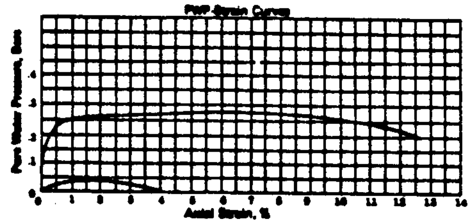

TESTS
(1) TE36L1
(2) TE37L1

* Stress Controlled Test

CURVE NO.	(1) *	(2) *	(3)	(4)
Confining Pressure Bars	0.10	0.40		
Initial Length, cm	[illegible]	10.1		
Initial Diameter, cm	[illegible]	[illegible]		
Wet Unit Weight, gm/cc	[illegible]	[illegible]		
Moisture Content, %	[illegible]	[illegible]		
Initial Void Ratio	[illegible]	[illegible]		
Initial Percent Saturation	[illegible]	[illegible]		

Consolidated Undrained Triaxial Shear Test with Pore Pressure Measurements

CORE 36G

Cruise S8-77-BG

Date [illegible]

Job No. [illegible]

LAW ENGINEERING TESTING COMPANY

Stress Paths for Triaxial Shear Tests

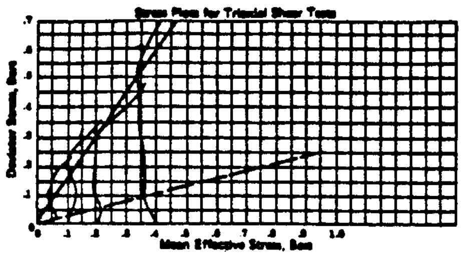

Cohesion, C 0

Angle of Shear Resistance 35.0°

Stress-Strain Curves

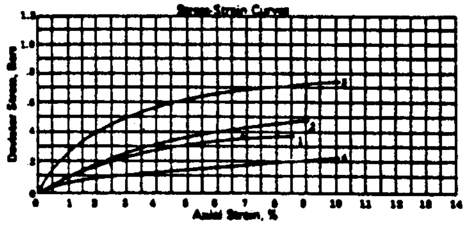

PWP-Strain Curves

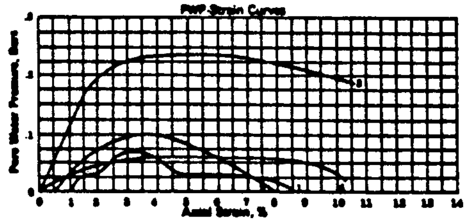

TESTS
(1) TE32L1
(2) TE33L1
(3) TE34L1
(4) TE35L1

* Stress Controlled Test

CURVE NO.	(1) *	(2)	(3) *	(4) *
Confining Pressure Bars	.30	[illegible]	.40	[illegible]
Initial Length, cm	10.4	[illegible]	10.[illegible]	[illegible]
Initial Diameter, cm	[illegible]	[illegible]	[illegible]	[illegible]
Wet Unit Weight, gm/cc	[illegible]	[illegible]	1.64	[illegible]
Moisture Content, %	[illegible]	[illegible]	[illegible]	[illegible]
Initial Void Ratio	[illegible]	[illegible]	[illegible]	[illegible]
Initial Percent Saturation	[illegible]	[illegible]	[illegible]	[illegible]

Consolidated Undrained Triaxial Shear Test with Pore Pressure Measurements

CORE 23G

CRUISE S8-77-BG

Date [illegible]

Job No. [illegible]

LAW ENGINEERING TESTING COMPANY

Stress Paths for Triaxial Shear Tests

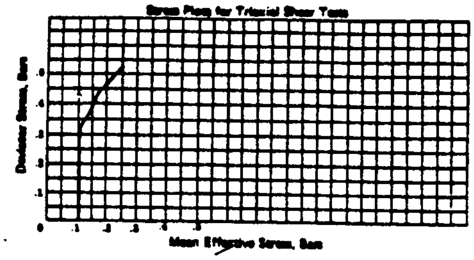

Cohesion, C

Angle of Shear Resistance

Stress-Strain Curves

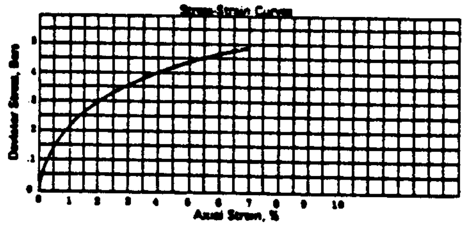

PWP-Strain Curves

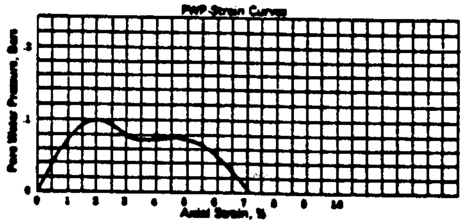

TEST TE38L1

* Stress Controlled Test

CURVE TE37L1	(1) *	(2)	(3)	(4)
Confining Pressure Bars	.10			
Initial Length, cm	[illegible]			
Initial Diameter, cm	[illegible]			
Wet Unit Weight, gm/cc	[illegible]			
Moisture Content, %	[illegible]			
Initial Void Ratio	[illegible]			
Initial Percent Saturation	[illegible]			

Consolidated Undrained Triaxial Shear Test with Pore Pressure Measurements

CORE 38G

CRUISE S8-77-BG

Date [illegible]

Job No. [illegible]

LAW ENGINEERING TESTING COMPANY

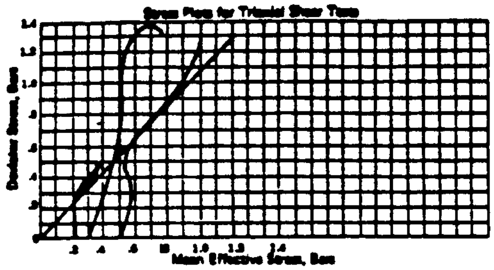

Cohesion, C ___

Angle of Shear Resistance ___

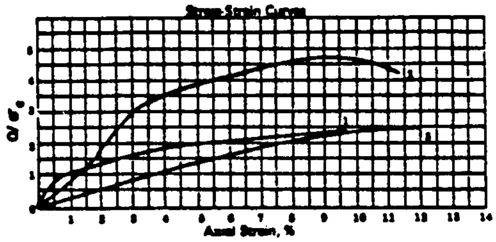

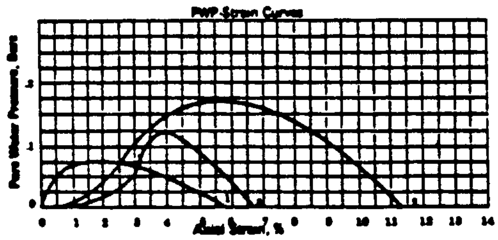

TESTS
(1) TE39L1
(2) TE40L1
(3) TE41L1

* Stress Controlled Test

CURVE NO.	(1)	(2)	(3)	(4)
Confining Pressure Bars	[illegible]	[illegible]	[illegible]	
Initial Length, cm	7.1	8.7	10.1	
Initial Diameter, cm	[illegible]	[illegible]	[illegible]	
Wet Unit Weight, gm/cc	[illegible]	1.75	[illegible]	
Moisture Content, %	[illegible]	[illegible]	[illegible]	
Initial Void Ratio	[illegible]	[illegible]	[illegible]	
Initial Percent Saturation	100	[illegible]	[illegible]	

Consolidated Undrained Triaxial Shear Test with Pore Pressure Measurements

CORE 470

CRUISE 88-77-BG

Date [illegible]

Job No. [illegible]

LAW ENGINEERING TESTING COMPANY

APPENDIX E

CONSOLIDATION AND TRIAXIAL TEST RESULTS--
GEOTECHNICAL ENGINEERS, INCORPORATED (1977 cores)

APPENDIX E. CONSOLIDATION AND TRIAXIAL TEST RESULTS-GEOTECHNICAL ENGINEERS, INCORPORATED (1977 cores)

This appendix presents the results of consolidation and static triaxial tests performed by Geotechnical Engineers, Incorporated under Contract number 14-08-0001-17353 with the U.S. Geological Survey. Testing was performed under the direction of K. Dalenberg and D.P. LaGatta. Cores were from Cruise S8-77-EG.

All tests in this group have been assigned a test number with G as the last character. The consolidation tests (first two characters are OE) are presented first and are ordered by test number. Results from a single test are presented on a page in the form of vertical strain and calculated coefficient of consolidation (c_v) versus the vertical effective stress in kPa (equivalent to kN/m^2).

The static triaxial tests (first two characters are TE) are given second and ordered by test number. Results from a single test are given on a single page. The upper left plot is the maximum shearing stress or $(\sigma_1-\sigma_3)/2$ versus the axial strain. The upper right plot is a stress path presenting the maximum shearing stress versus the normal effective stress on the plane of maximum shearing stress or $(\sigma_1'+\sigma_3')/2$. In Appendices F and G, the stress path plots are defined in the same way but identified as q versus p'. The stress path plots of Appendix D are defined differently. The lower left plot is the excess pore water pressure developed during shear $(u-u_o)$ versus the axial strain.

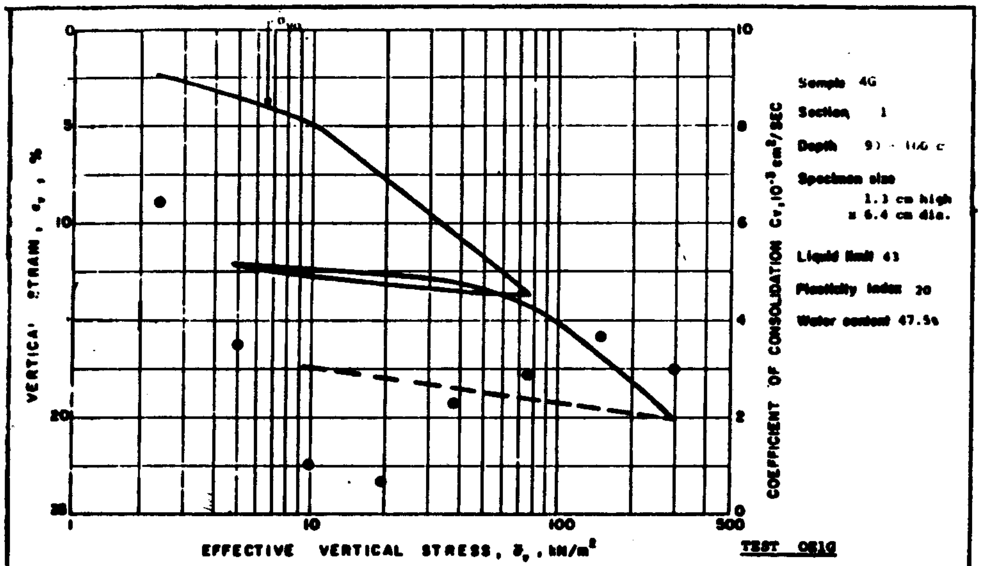

TEST OE1G

CRUISE NO. S8-77-BG

NOTE: SOLID POINTS REFER TO COEFFICIENT OF CONSOLIDATION

U. S. Geological Survey Denver, Colorado	Laboratory Testing of Shallow Sediments Gulf of Alaska	CONSOLIDATION COMPRESSION SAMPLE 4G DEPTH 90 - 100 cm
GEOTECHNICAL ENGINEERS INC. WINCHESTER, MASSACHUSETTS	Project 78466	August, 1978

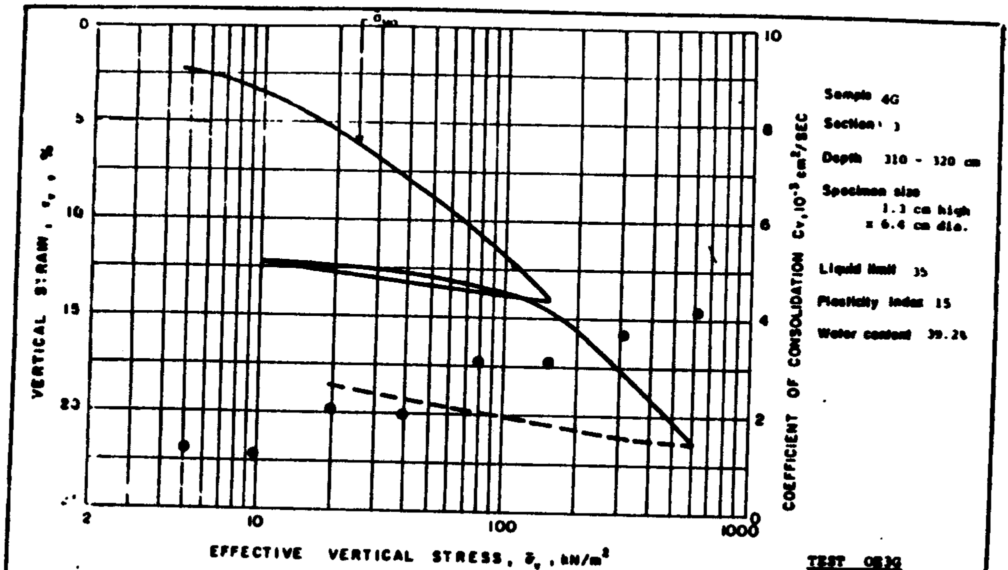

TEST OE3G

CRUISE NO. S8-77-BG

NOTE: SOLID POINTS REFER TO COEFFICIENT OF CONSOLIDATION

U. S. Geological Survey Denver, Colorado	Laboratory Testing of Shallow Sediments Gulf of Alaska	CONSOLIDATION COMPRESSION SAMPLE 4G DEPTH 310-320 cm
GEOTECHNICAL ENGINEERS INC. WINCHESTER, MASSACHUSETTS	Project 78466	August, 1978

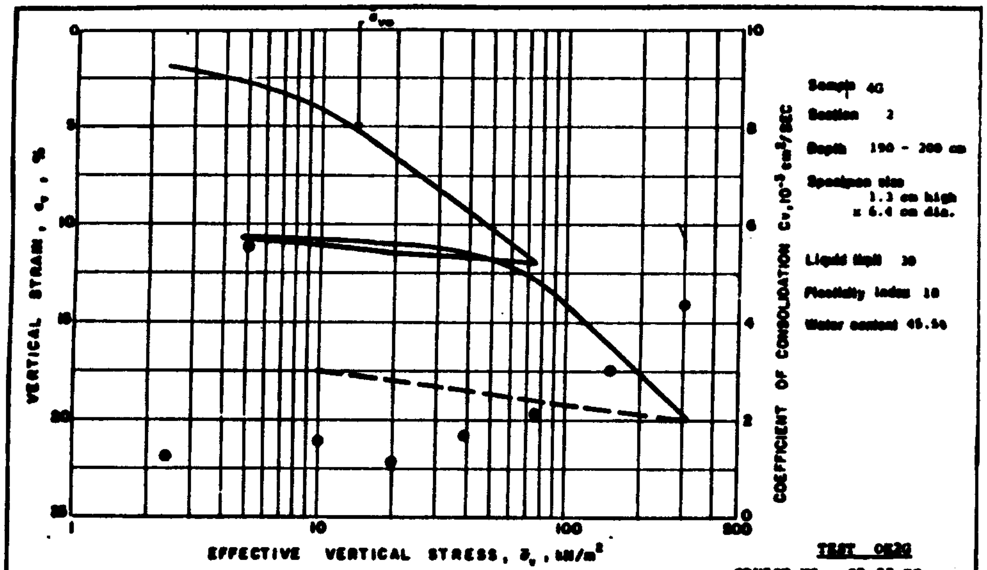

TEST OE2G

CRUISE NO. S8-77-BG

NOTE: SOLID POINTS REFER TO COEFFICIENT OF CONSOLIDATION

U. S. Geological Survey Denver, Colorado	Laboratory Testing of Shallow Sediments Gulf of Alaska	CONSOLIDATION COMPRESSION SAMPLE 4G DEPTH 190 - 200 cm
GEOTECHNICAL ENGINEERS INC. WINCHESTER, MASSACHUSETTS	Project 78466	August, 1978

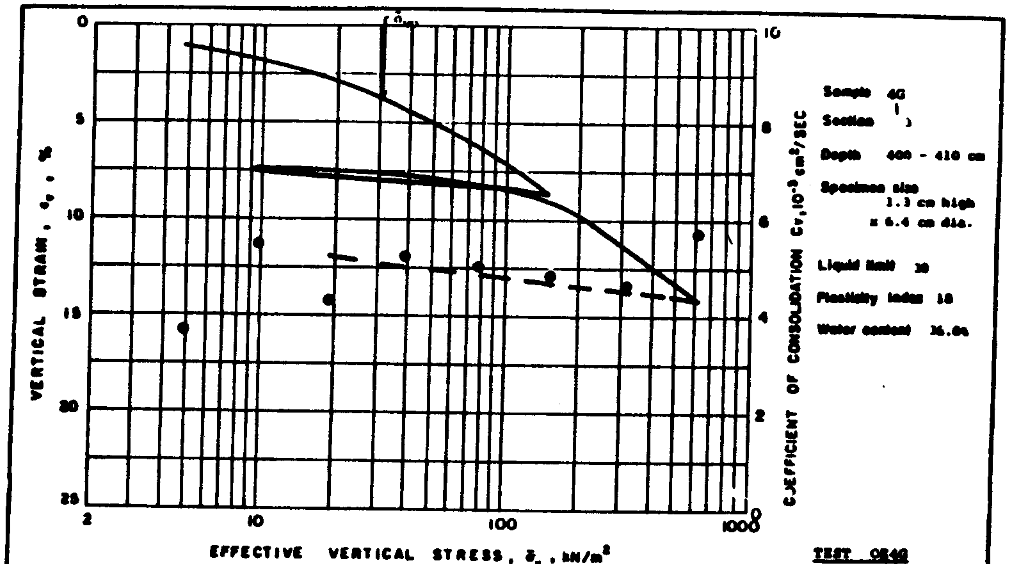

TEST OE4G

CRUISE NO. S8-77-BG

NOTE: SOLID POINTS REFER TO COEFFICIENT OF CONSOLIDATION

U. S. Geological Survey Denver, Colorado	Laboratory Testing of Shallow Sediments Gulf of Alaska	CONSOLIDATION COMPRESSION SAMPLE 4G DEPTH 400 - 410 cm
GEOTECHNICAL ENGINEERS INC. WINCHESTER, MASSACHUSETTS	Project 78466	August, 1978

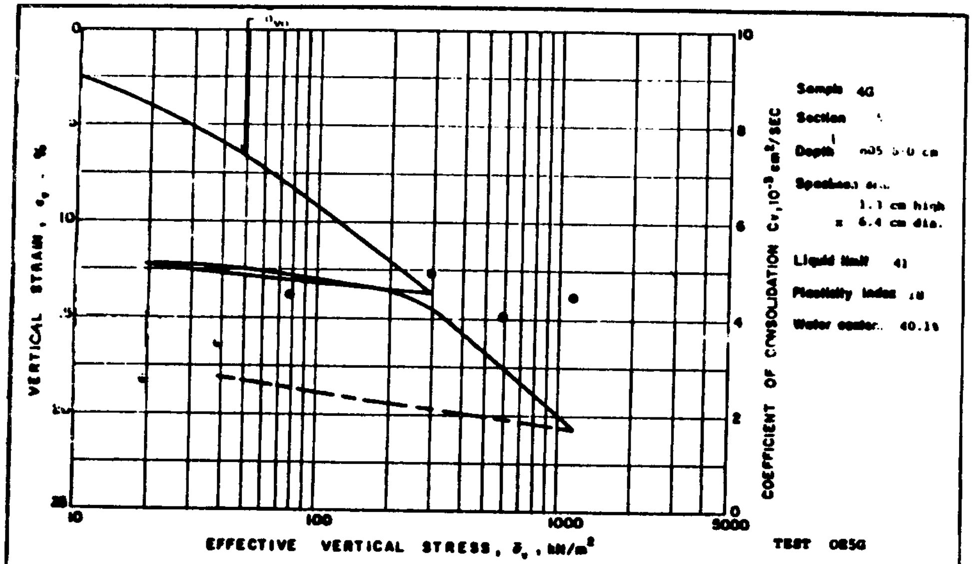

CRUISE NO. S8-77-EG

NOTE: SOLID POINTS REFER TO COEFFICIENT OF CONSOLIDATION

U. S. Geological Survey Denver, Colorado	Laboratory Testing of Shallow Sediments Gulf of Alaska	CONSOLIDATION COMPRESSION SAMPLE 4G DEPTH 605-610 cm
GEOTECHNICAL ENGINEERS INC. WINCHESTER, MASSACHUSETTS	Project 78466	August, 1978

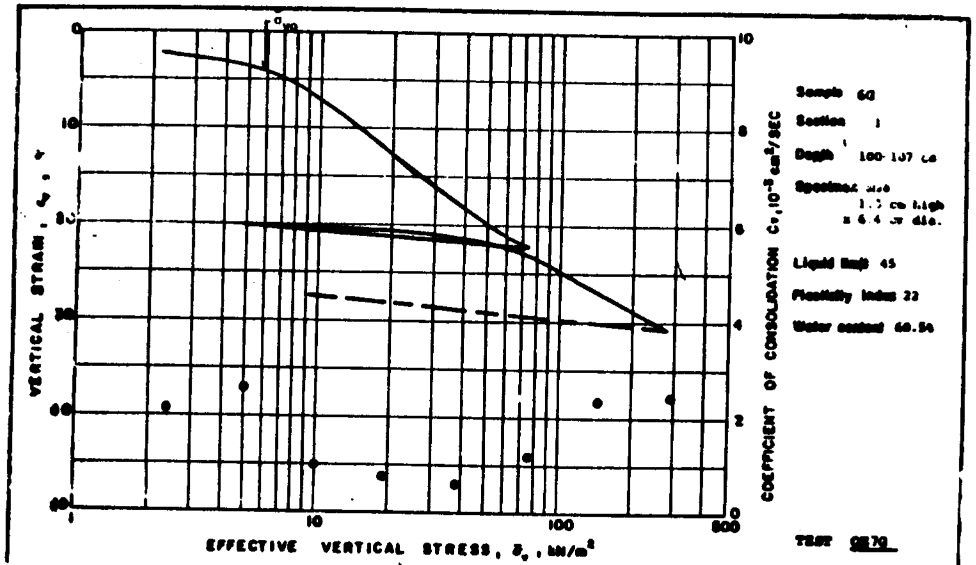

CRUISE NO. S8-77-EG

NOTE: SOLID POINTS REFER TO COEFFICIENT OF CONSOLIDATION

U. S. Geological Survey Denver, Colorado	Laboratory Testing of Shallow Sediments Gulf of Alaska	CONSOLIDATION COMPRESSION SAMPLE 6G DEPTH 100-107 cm
GEOTECHNICAL ENGINEERS INC. WINCHESTER, MASSACHUSETTS	Project 78466	September, 1978

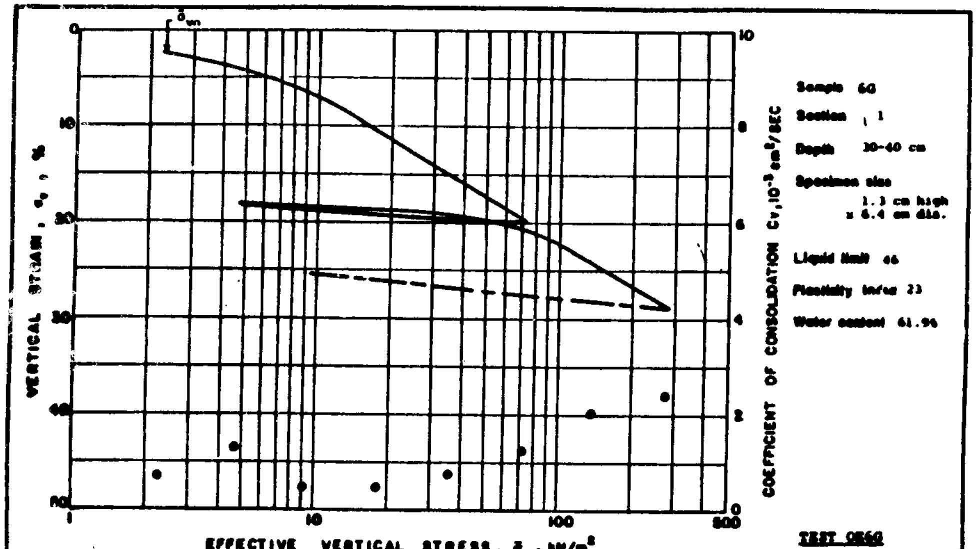

CRUISE NO. S8-77-EG

NOTE: SOLID POINTS REFER TO COEFFICIENT OF CONSOLIDATION

U. S. Geological Survey Denver, Colorado	Laboratory Testing of Shallow Sediments Gulf of Alaska	CONSOLIDATION COMPRESSION SAMPLE 6 G DEPTH 30-40 cm
GEOTECHNICAL ENGINEERS INC. WINCHESTER, MASSACHUSETTS	Project 78466	August, 1978

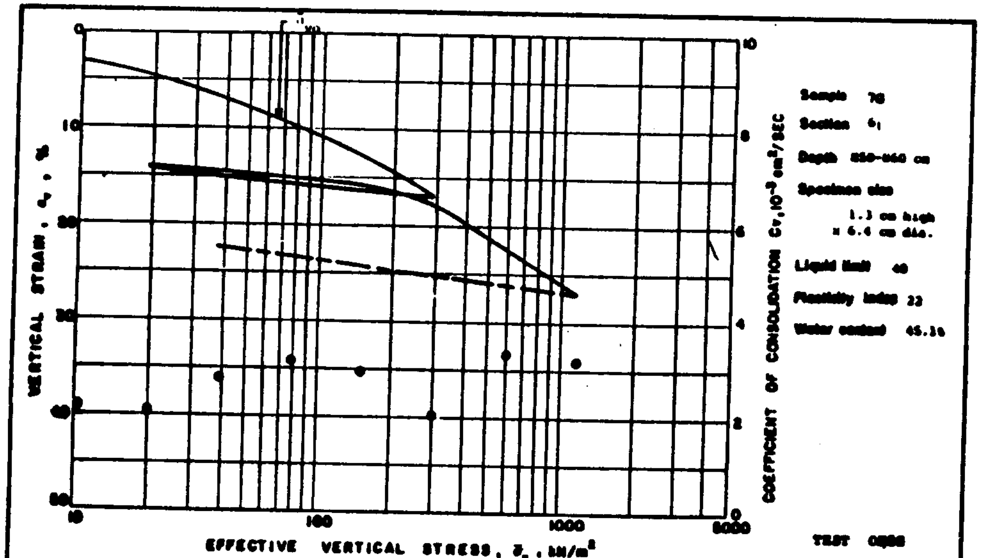

CRUISE NO. S8-77-EG

NOTE: SOLID POINTS REFER TO COEFFICIENT OF CONSOLIDATION

U. S. Geological Survey Denver, Colorado	Laboratory Testing of Shallow Sediments Gulf of Alaska	CONSOLIDATION COMPRESSION SAMPLE 7G DEPTH 850-860 cm
GEOTECHNICAL ENGINEERS INC. WINCHESTER, MASSACHUSETTS	Project 78466	August, 1978

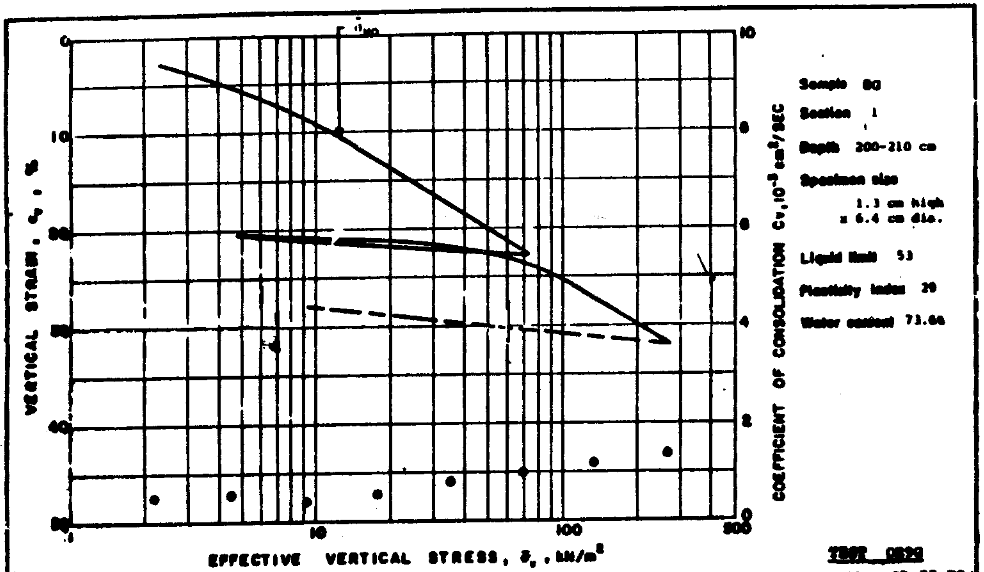

TEST OE9G

CRUISE NO. S8-77-BG

NOTE: SOLID POINTS REFER TO COEFFICIENT OF CONSOLIDATION

U. S. Geological Survey Denver, Colorado	Laboratory Testing of Shallow Sediments Gulf of Alaska	CONSOLIDATION COMPRESSION SAMPLE 8 G DEPTH 200-210 cm
GEOTECHNICAL ENGINEERS INC. WINCHESTER, MASSACHUSETTS	Project 78465	August, 1978

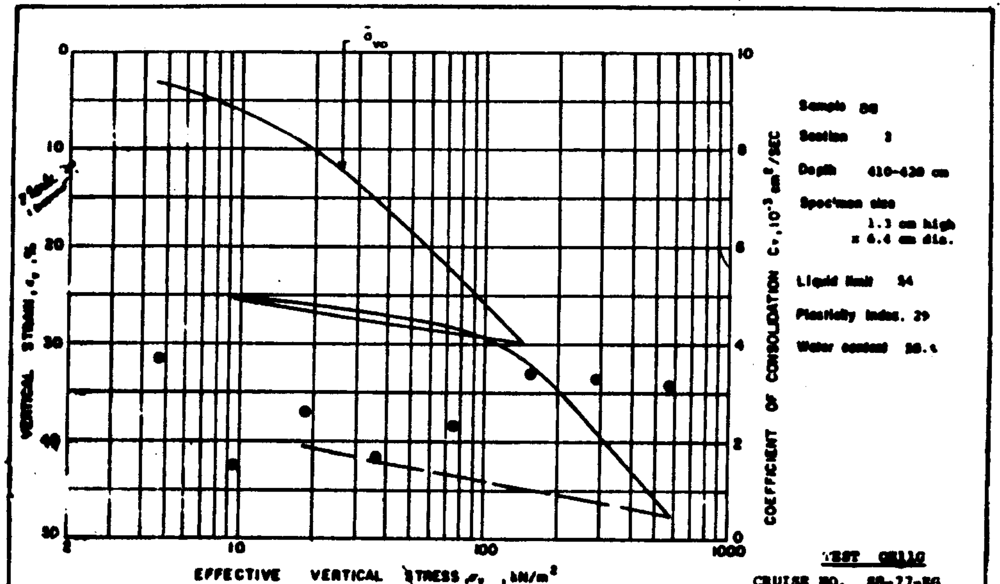

TEST OE11G

CRUISE NO. S8-77-BG

NOTE: SOLID POINTS REFER TO COEFFICIENT OF CONSOLIDATION

U.S. Geological Survey Denver, Colorado	Laboratory Testing of Shallow Sediments Gulf of Alaska	CONSOLIDATION COMPRESSION SAMPLE 8G DEPTH 410-420 cm
Geotechnical Engineers Inc. Winchester, Massachusetts	Project 78465	September, 1978

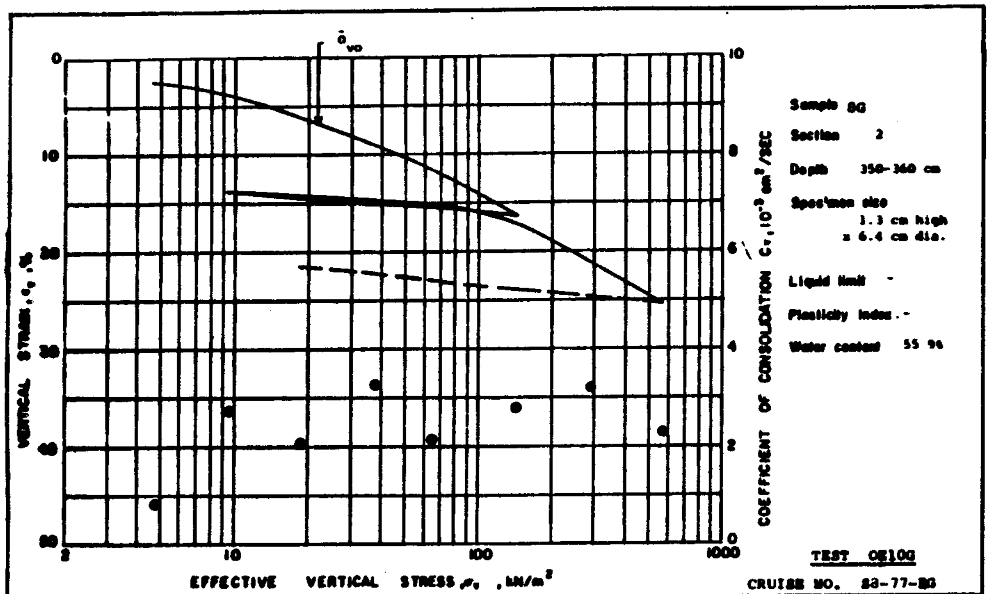

TEST OE10G

CRUISE NO. S8-77-BG

NOTE: SOLID POINTS REFER TO COEFFICIENT OF CONSOLIDATION

U.S. Geological Survey Denver, Colorado	Laboratory Testing of Shallow Sediments Gulf of Alaska	$\bar{\sigma}$ TEST Sample 8G Depth 350-360 cm
Geotechnical Engineers Inc. Winchester, Massachusetts	Project 78465	September, 1978

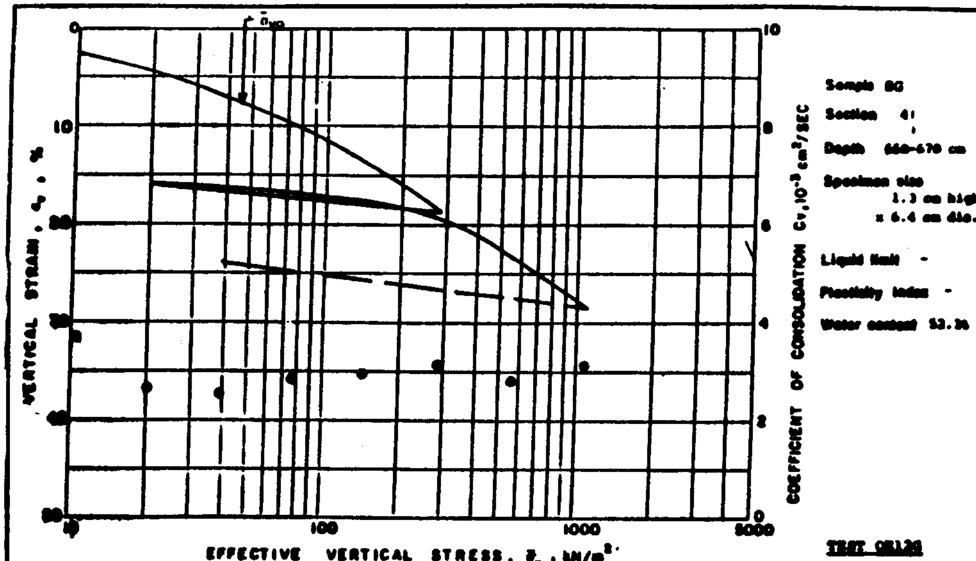

TEST OE12G

CRUISE NO. S8-77-BG

NOTE: SOLID POINTS REFER TO COEFFICIENT OF CONSOLIDATION

U. S. Geological Survey Denver, Colorado	Laboratory Testing of Shallow Sediments Gulf of Alaska	CONSOLIDATION COMPRESSION SAMPLE 8G DEPTH 660-670 cm
GEOTECHNICAL ENGINEERS INC. WINCHESTER, MASSACHUSETTS	Project 78465	September, 1978

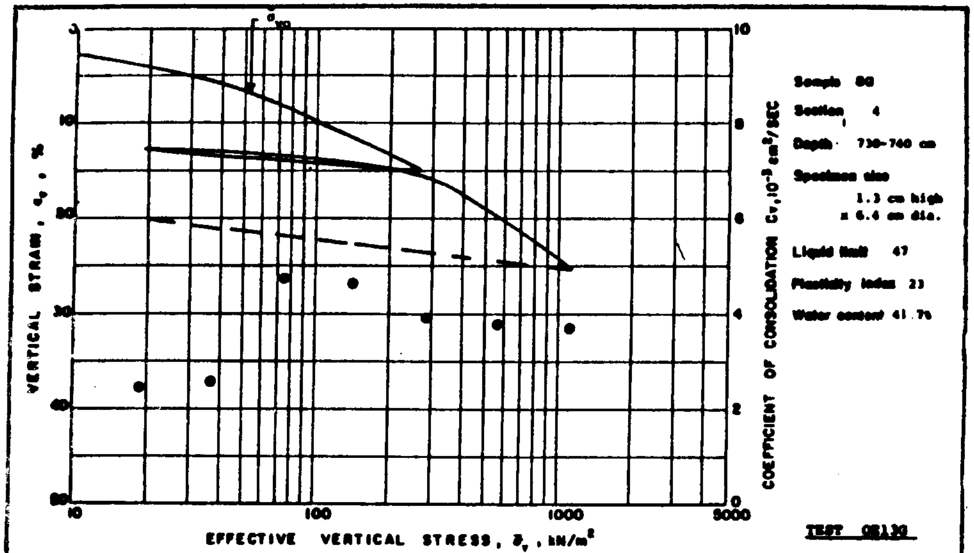

CRUISE NO. S8-77-EG

NOTE: SOLID POINTS REFER TO COEFFICIENT OF CONSOLIDATION

U. S. Geological Survey Denver, Colorado	Laboratory Testing of Shallow Sediments Gulf of Alaska	CONSOLIDATION COMPRESSION SAMPLE 8G DEPTH 730-740 cm
GEOTECHNICAL ENGINEERS INC. WINCHESTER, MASSACHUSETTS	Project 78468	August, 1978

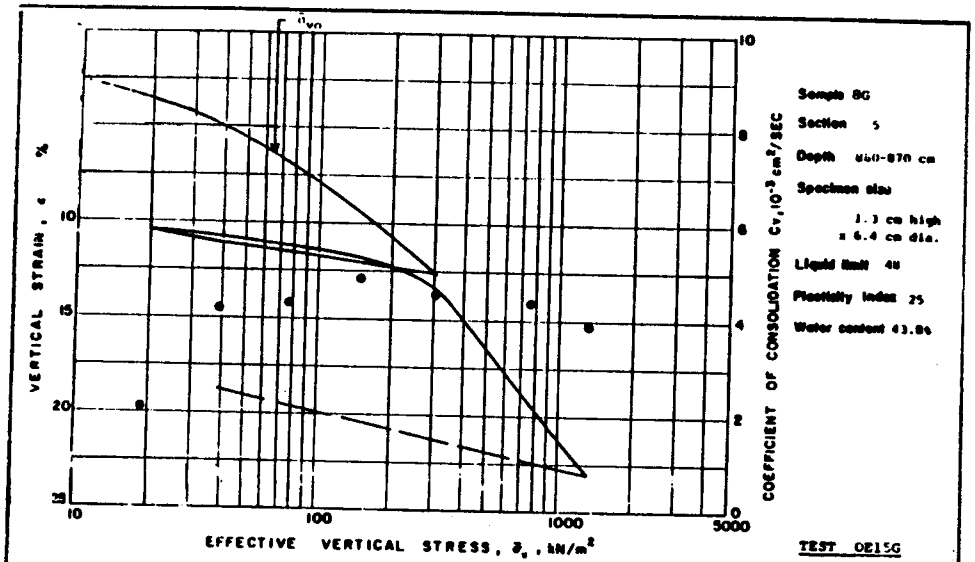

CRUISE NO. S8-77-EG

NOTE: SOLID POINTS REFER TO COEFFICIENT OF CONSOLIDATION

U. S. Geological Survey Denver, Colorado	Laboratory Testing of Shallow Sediments Gulf of Alaska	CONSOLIDATION COMPRESSION SAMPLE 8G DEPTH [illegible] cm
GEOTECHNICAL ENGINEERS INC. WINCHESTER, MASSACHUSETTS	Project 78468	August, 1978

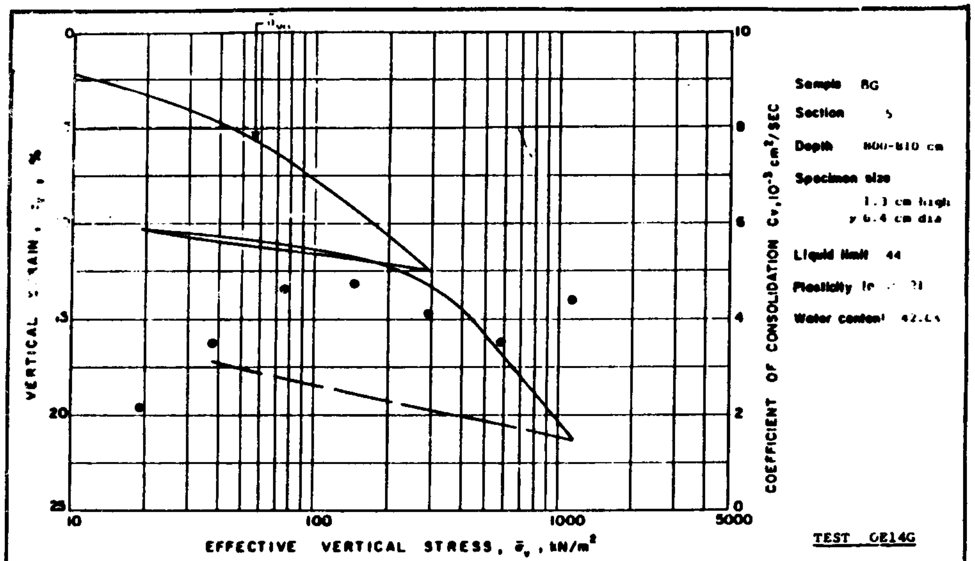

CRUISE NO. S8-77-EG

NOTE: SOLID POINTS REFER TO COEFFICIENT OF CONSOLIDATION

U. S. Geological Survey Denver, Colorado	Laboratory Testing of Shallow Sediments Gulf of Alaska	CONSOLIDATION COMPRESSION SAMPLE 8G DEPTH 800-810 cm
GEOTECHNICAL ENGINEERS INC. WINCHESTER, MASSACHUSETTS	Project 78468	August, 1978

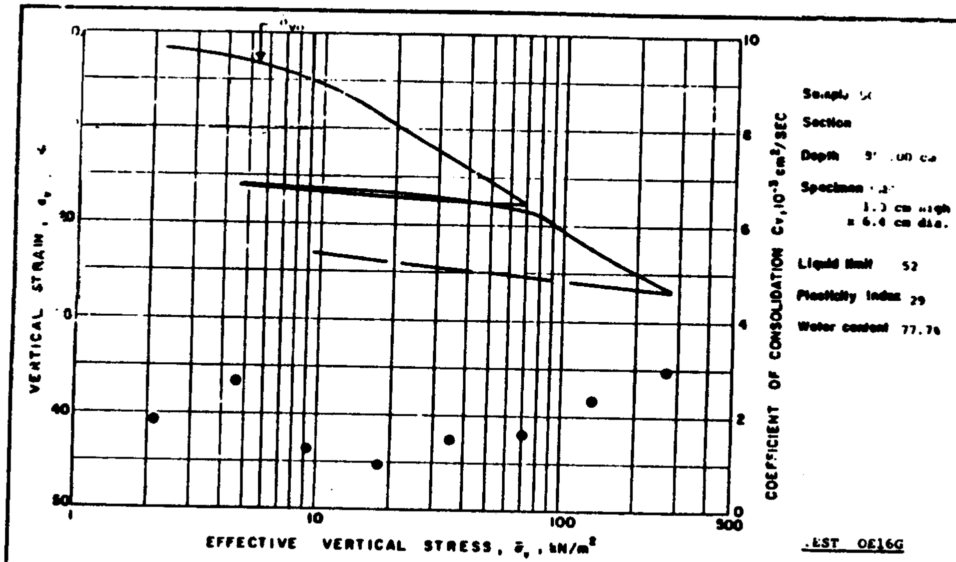

CRUISE NO. S8-77-EG

NOTE: SOLID POINTS REFER TO COEFFICIENT OF CONSOLIDATION

U. S. Geological Survey Denver, Colorado	Laboratory Testing of Shallow Sediments Gulf of Alaska	CONSOLIDATION COMPRESSION SAMPLE 9G DEPTH 85-100 cm
GEOTECHNICAL ENGINEERS INC. WINCHESTER, MASSACHUSETTS	Project 78468	September, 1978

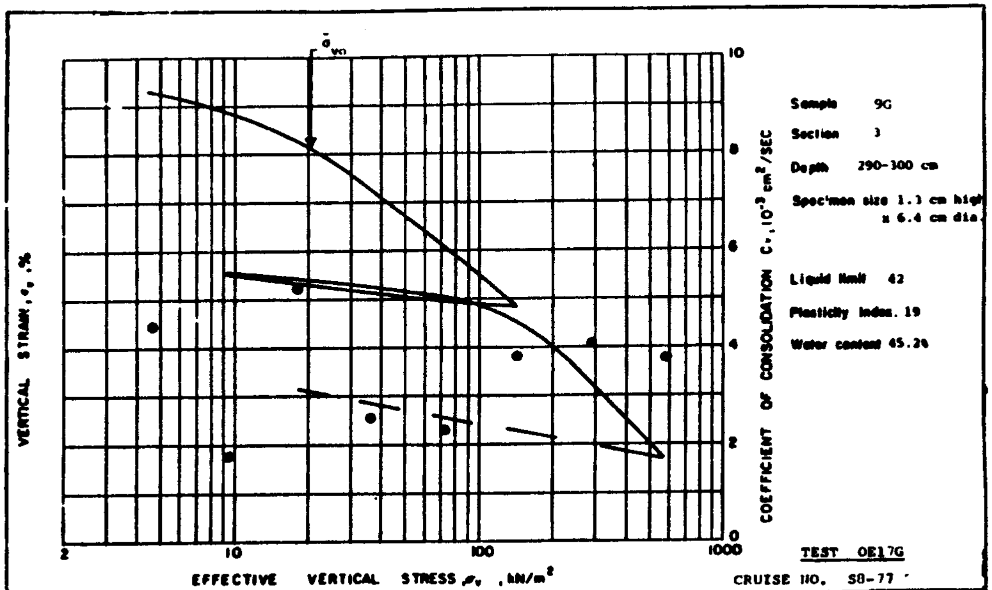

CRUISE NO. S8-77

NOTE: SOLID POINTS REFER TO COEFFICIENT OF CONSOLIDATION

U.S. Geological Survey Denver, Colorado	Laboratory Testing of Shallow Sediments Gulf of Alaska	CONSOLIDATION COMPRESSION SAMPLE DEPTH
Geotechnical Engineers Inc. Winchester, Massachusetts	Project 78465	September, 19

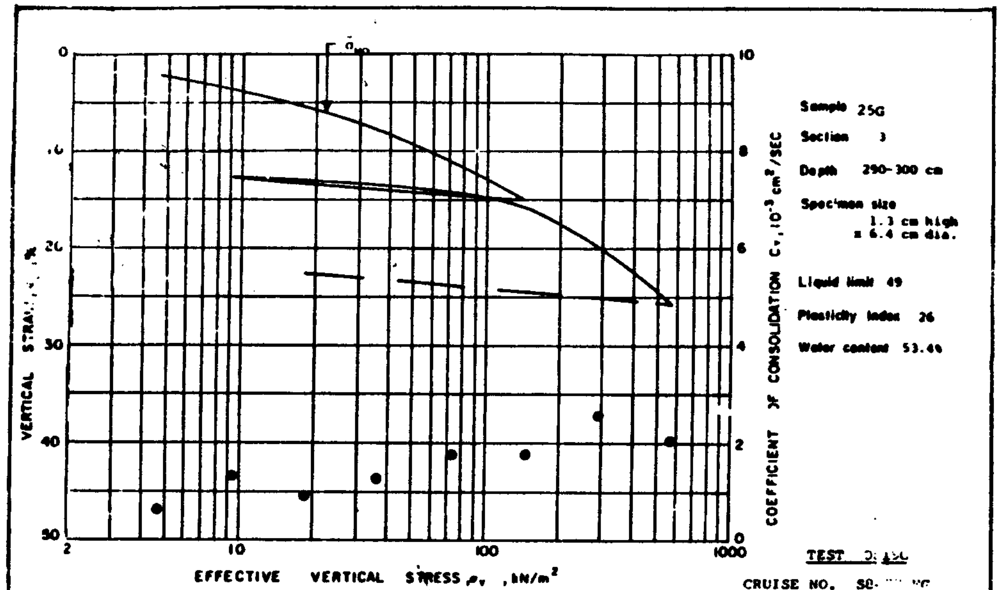

CRUISE NO. S8-

NOTE: SOLID POINTS REFER TO COEFFICIENT OF CONSOLIDATION

U.S. Geological Survey Denver, Colorado	Laboratory Testing of Shallow Sediments Gulf of Alaska	CONSOLIDATION COMPRESSION SAMPLE 25G DEPTH 290-300 cm
Geotechnical Engineers Inc. Winchester, Massachusetts	Project 78465	September, 1978

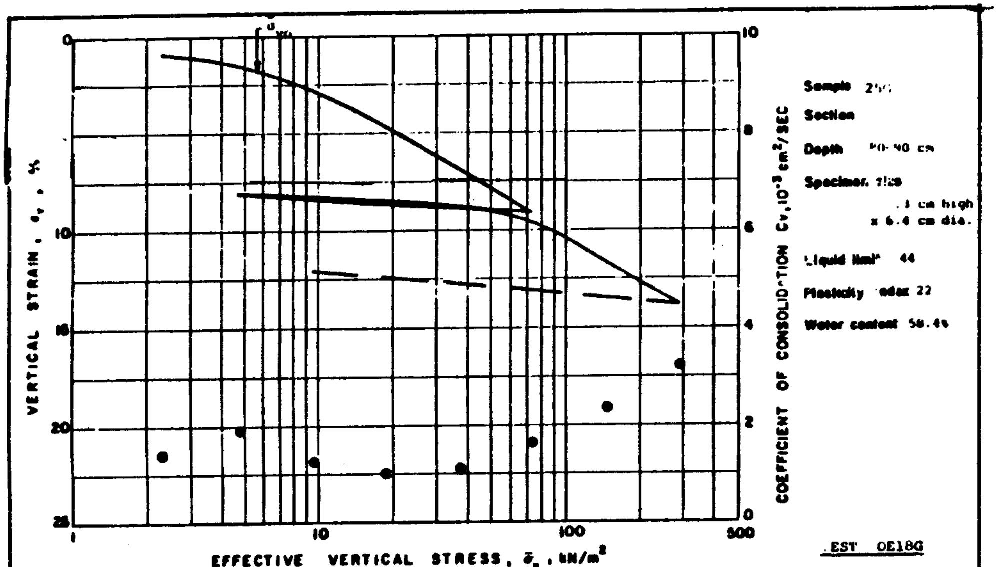

CRUISE NO. S8-77-EG

NOTE: SOLID POINTS REFER TO COEFFICIENT OF CONSOLIDATION

U. S. Geological Survey Denver, Colorado	Laboratory Testing of Shallow Sediments Gulf of Alaska	CONSOLIDATION COMPRESSION SAMPLE SECTION DEPTH 80-
GEOTECHNICAL ENGINEERS INC. WINCHESTER, MASSACHUSETTS	Project 78465	September, 197

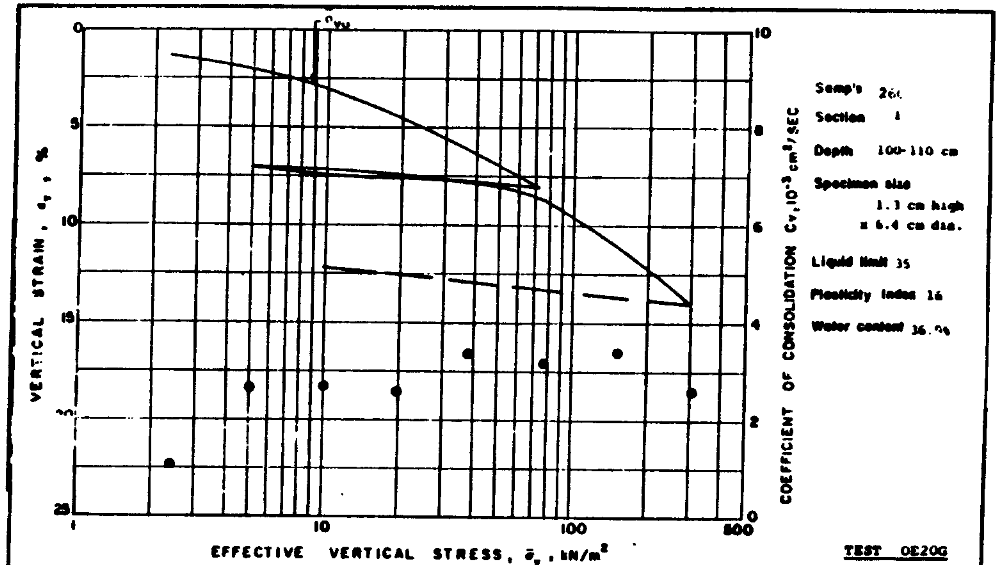

CRUISE NO. S8-77-EG

NOTE: SOLID POINTS REFER TO COEFFICIENT OF CONSOLIDATION

U. S. Geological Survey Denver, Colorado	Laboratory Testing of Shallow Sediments Gulf of Alaska	CONSOLIDATION COMPRESSION SAMPLE 26 G DEPTH 100-110 cm
GEOTECHNICAL ENGINEERS INC. WINCHESTER, MASSACHUSETTS	Project 78465	September, 1978

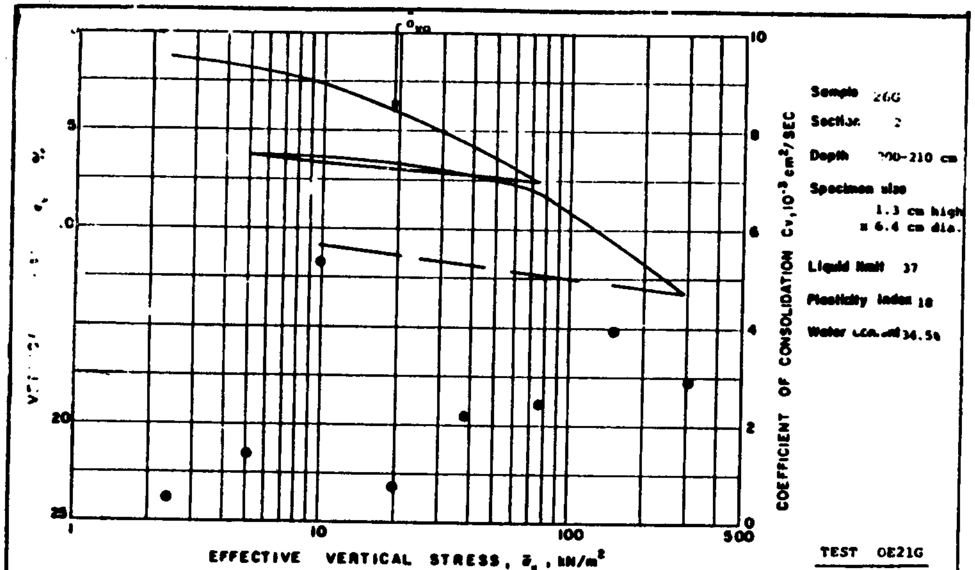

CRUISE NO. S8-77-EG

NOTE: SOLID POINTS REFER TO COEFFICIENT OF CONSOLIDATION

U. S. Geological Survey Denver, Colorado	Laboratory Testing of Shallow Sediments Gulf of Alaska	CONSOLIDATIO. COMPRESSIO SAMPLE 26G DEPTH 200-210 cm
GEOTECHNICAL ENGINEERS INC. WINCHESTER, MASSACHUSETTS	Project 78465	September, 1978

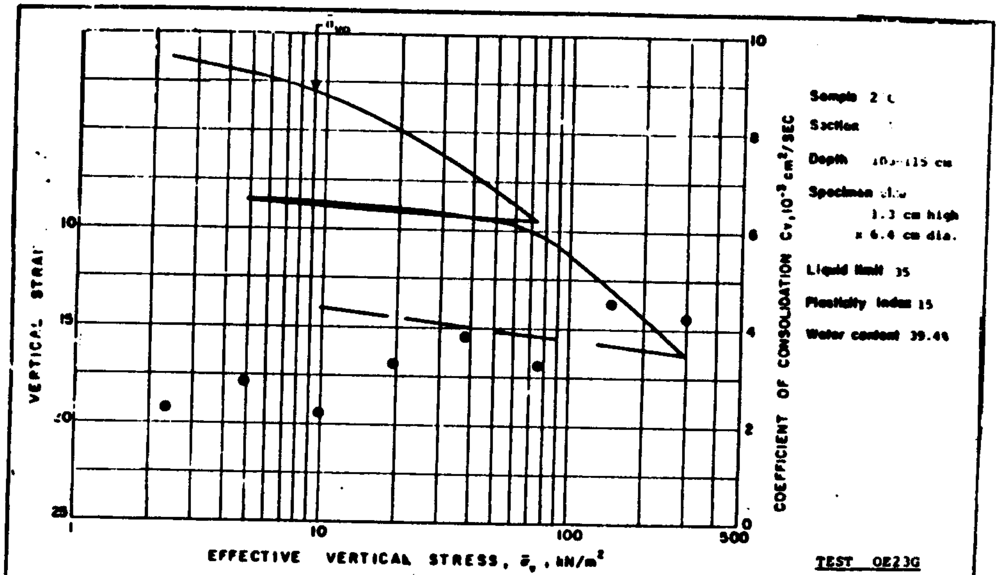

CRUISE NO. S8-77-EG

NOTE: SOLID POINTS REFER TO COEFFICIENT OF CONSOLIDATION

U. S. Geological Survey Denver, Colorado	Laboratory Testing of Shallow Sediments Gulf of Alaska	CONSOLIDATION COMPRESSION SAMPLE 29 G DEPTH 105-115 cm
GEOTECHNICAL ENGINEERS INC. WINCHESTER, MASSACHUSETTS	Project 78465	September, 1978

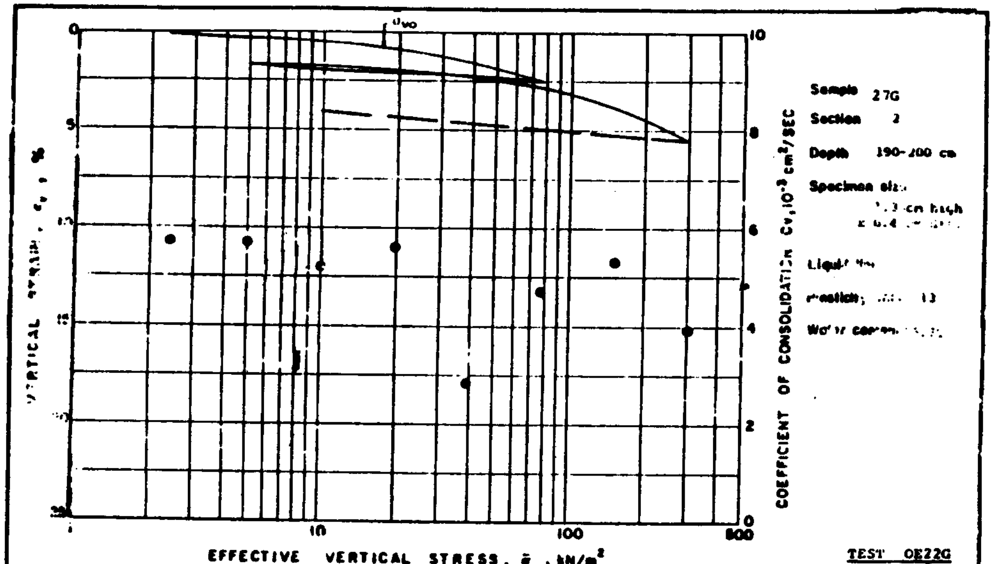

CRUISE NO. S8-77-EG

NOTE: SOLID POINTS REFER TO COEFFICIENT OF CONSOLIDATION

U. S. Geological Survey Denver, Colorado	Laboratory Testing of Shallow Sediments Gulf of Alaska	CONSOLIDATION COMPRESSION SAMPLE 27 G DEPTH 190-200 cm
GEOTECHNICAL ENGINEERS INC. WINCHESTER, MASSACHUSETTS	Project 78465	September, 1978

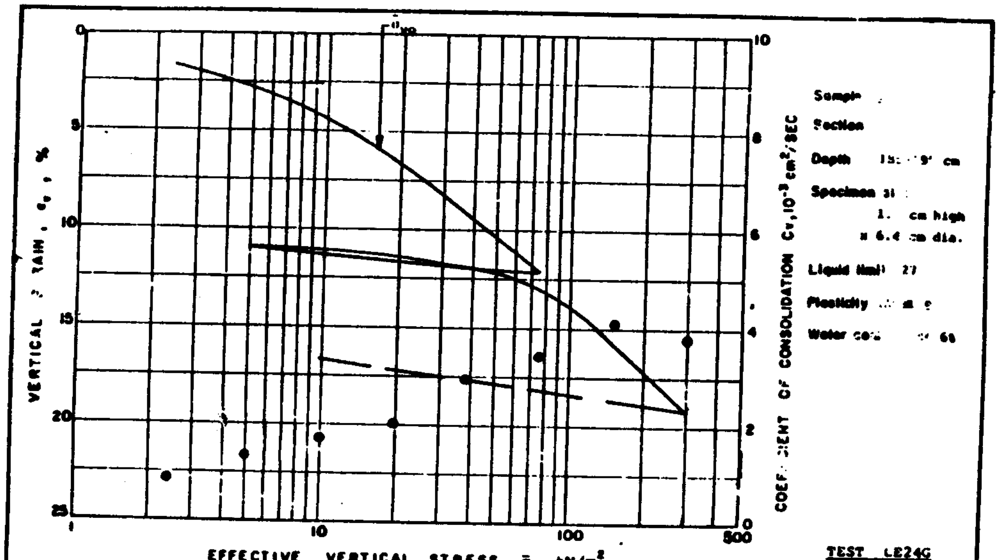

CRUISE NO. S8-77-EG

NOTE: SOLID POINTS REFER TO COEFFICIENT OF CONSOLIDATION

U. S. Geological Survey Denver, Colorado	Laboratory Testing of Shallow Sediments Gulf of Alaska	CONSOLIDATION COMPRESSION SAMPLE 29G DEPTH 185-195 cm
GEOTECHNICAL ENGINEERS INC. WINCHESTER, MASSACHUSETTS	Project 78465	September, 1978

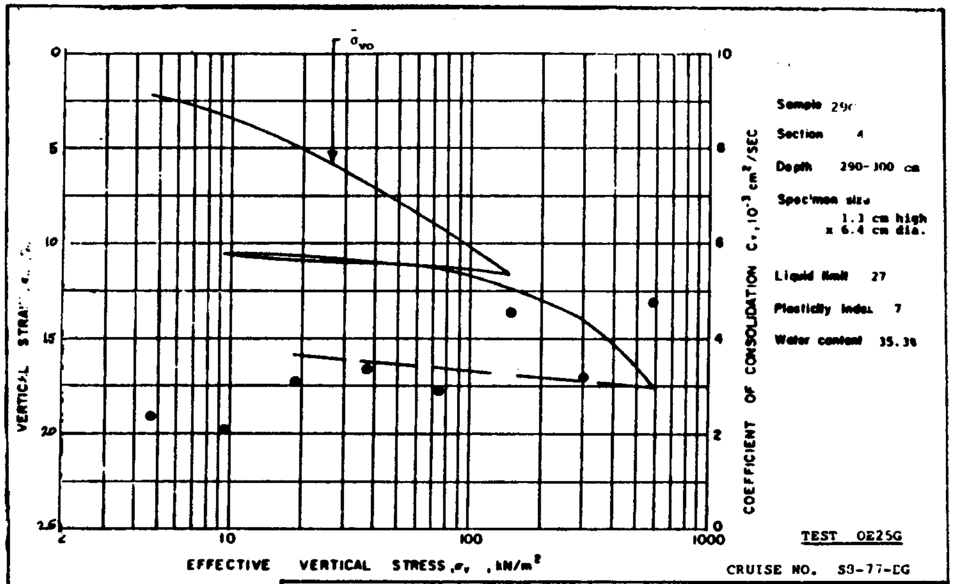

CRUISE NO. S8-77-EG

NOTE: SOLID POINTS REFER TO COEFFICIENT OF CONSOLIDATION

U.S. Geological Survey Denver, Colorado	Laboratory Testing of Shallow Sediments Gulf of Alaska	CONSOLIDATION COMPRESSION SAMPLE 29 G DEPTH 285-295 cm
Geotechnical Engineers Inc. Winchester, Massachusetts	Project 78465	September, 1978

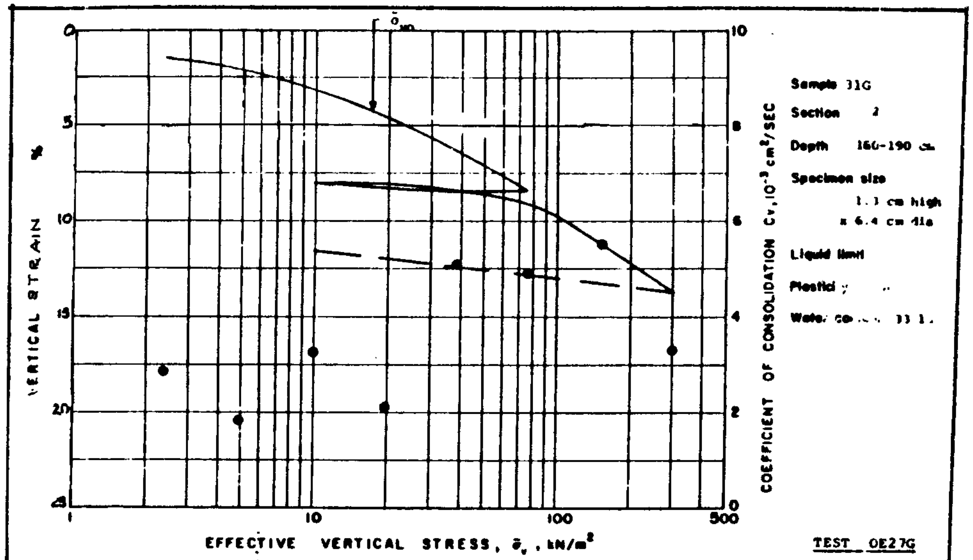

CRUISE NO. S8-77-EG

NOTE: SOLID POINTS REFER TO COEFFICIENT OF CONSOLIDATION

U. S. Geological Survey Denver, Colorado	Laboratory Testing of Shallow Sediments Gulf of Alaska	CONSOLIDATION COMPRESSION SAMPLE 31G DEPTH 180-190 cm
GEOTECHNICAL ENGINEERS INC. WINCHESTER, MASSACHUSETTS	Project 78465	September, 1978

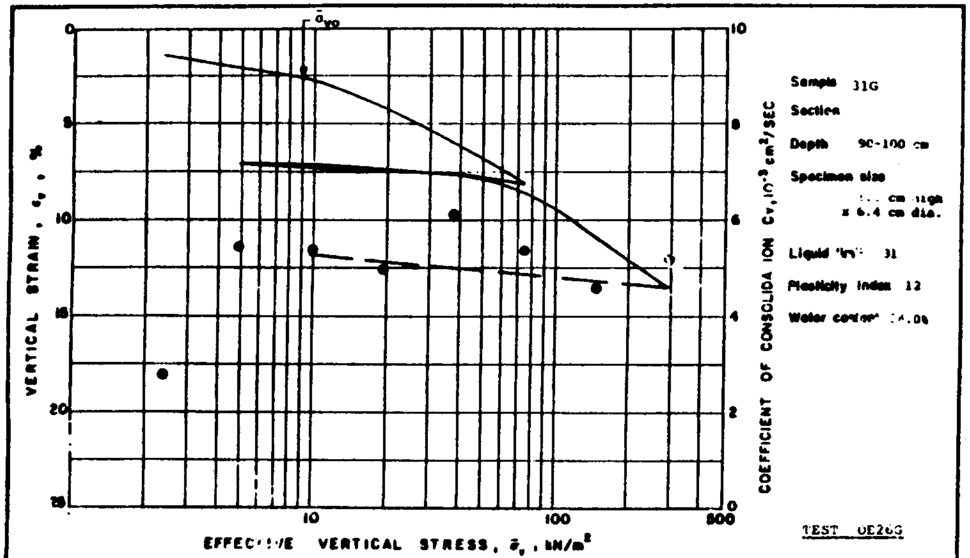

CRUISE NO. S8-77-EG

SOLID POINTS REFER TO COEFFICIENT OF CONSOLIDATION

U. S. Geological Survey Denver, Colorado	Laboratory Testing of Shallow Sediments Gulf of Alaska	CONSOLIDATION COMPRESSION SAMPLE DEPTH 90-100 cm
GEOTECHNICAL ENGINEERS INC. WINCHESTER, MASSACHUSETTS	Project 78465	September, 197[illegible]

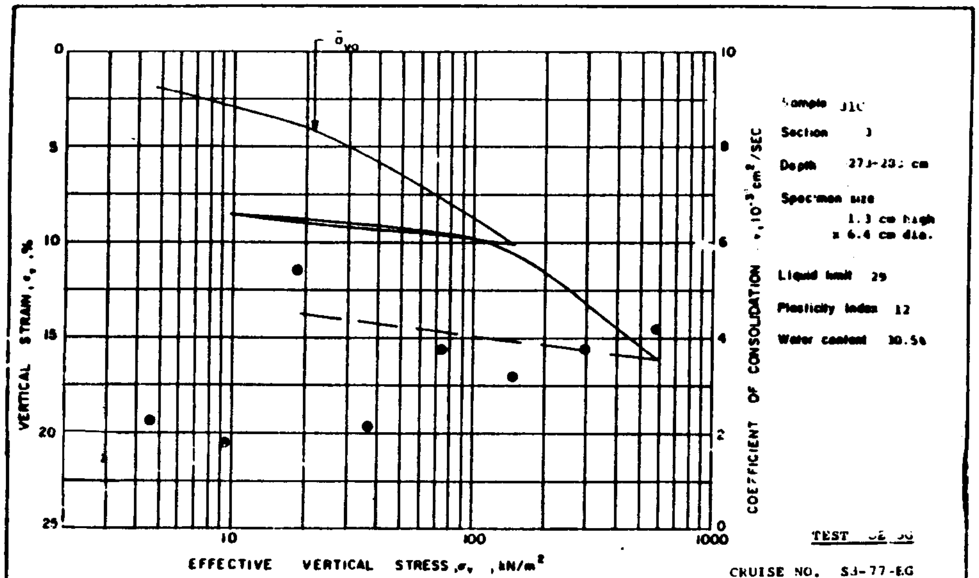

CRUISE NO. S8-77-EG

NOTE: SOLID POINTS REFER TO COEFFICIENT OF CONSOLIDATION

U.S. Geological Survey Denver, Colorado	Laboratory Testing of Shallow Sediments Gulf of Alaska	CONSOLIDATION COMPRESSION SAMPLE DEPTH 273-283 cm
Geotechnical Engineers Inc. Winchester, Massachusetts	Project 78465	September, 1978

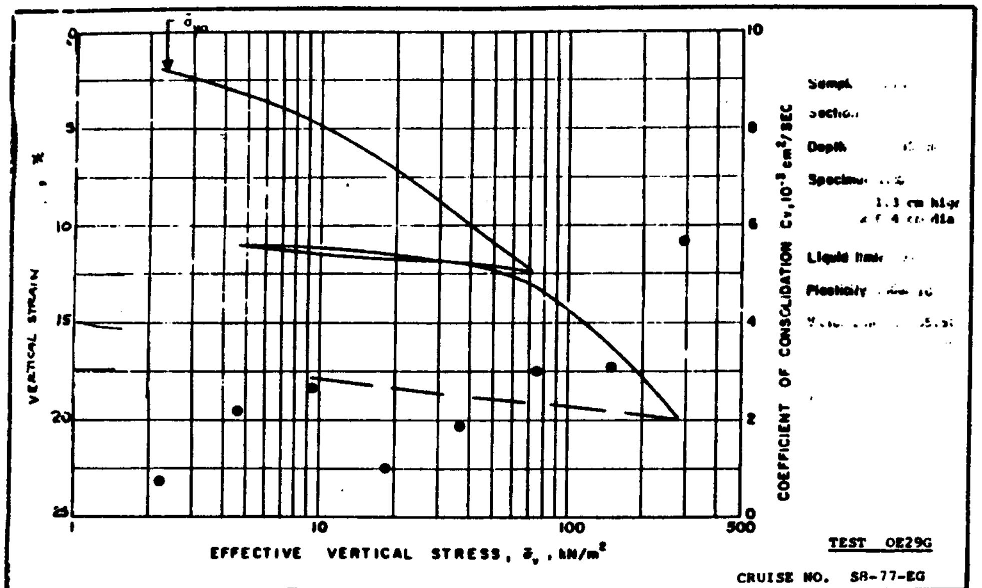

CRUISE NO. S8-77-EG

NOTE: SOLID POINTS REFER TO COEFFICIENT OF CONSOLIDATION

U. S. Geological Survey Denver, Colorado	Laboratory Testing of Shallow Sediments Gulf of Alaska	CONSOLIDATION COMPRESSION SAMPLE 33 G DEPTH 22-30 cm
GEOTECHNICAL ENGINEERS INC. WINCHESTER, MASSACHUSETTS	Project 78465	September, 1978

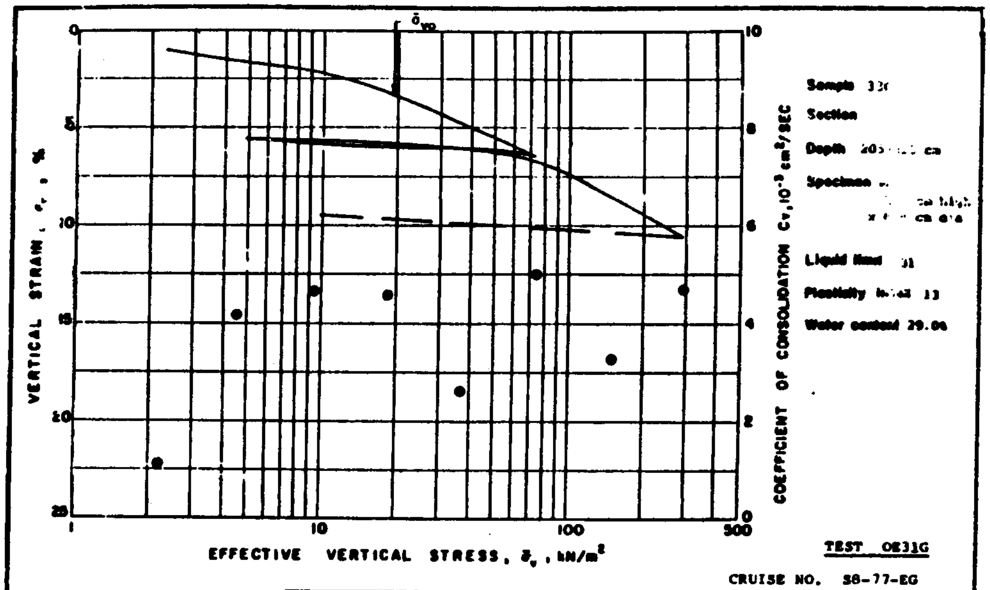

CRUISE NO. S8-77-EG

NOTE: SOLID POINTS REFER TO COEFFICIENT OF CONSOLIDATION

U. S. Geological Survey Denver, Colorado	Laboratory Testing of Shallow Sediments Gulf of Alaska	CONSOLIDATION COMPRESSION SAMPLE 33 G DEPTH 205-216 cm
GEOTECHNICAL ENGINEERS INC. WINCHESTER, MASSACHUSETTS	Project 78465	September, 1978

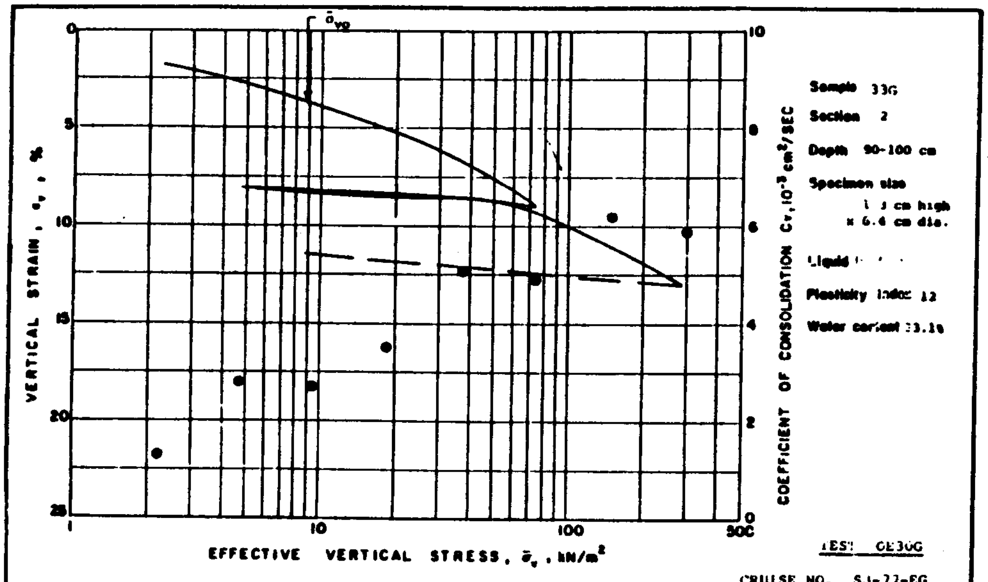

CRUISE NO. S8-77-EG

NOTE: SOLID POINTS REFER TO COEFFICIENT OF CONSOLIDATION

U. S. Geological Survey Denver, Colorado	Laboratory Testing of Shallow Sediments Gulf of Alaska	CONSOLIDATION COMPRESSION SAMPLE 33G DEPTH 90-100 cm
GEOTECHNICAL ENGINEERS INC. WINCHESTER, MASSACHUSETTS	Project 78465	September, 1978

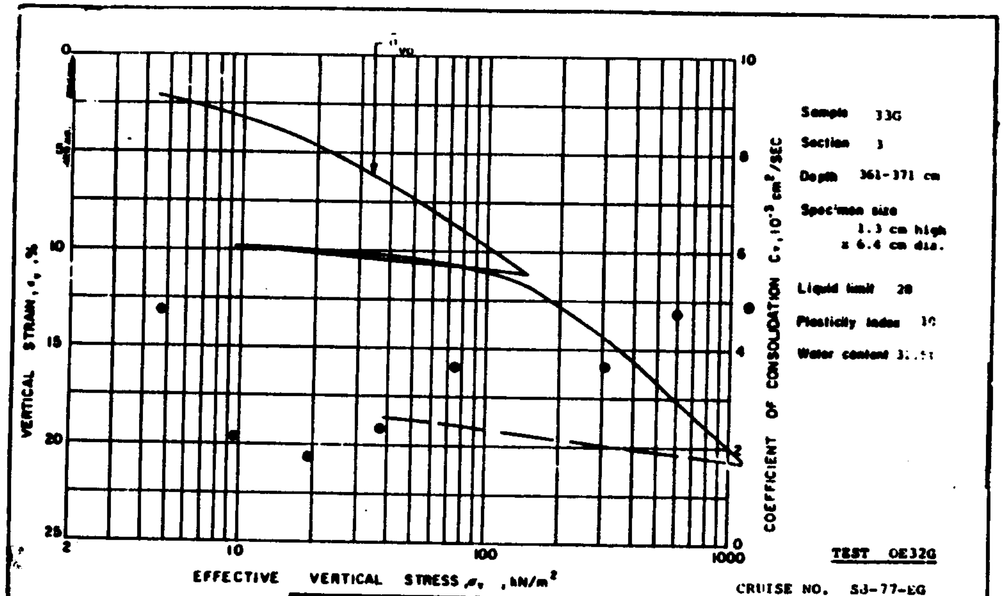

CRUISE NO. S8-77-EG

NOTE: SOLID POINTS REFER TO COEFFICIENT OF CONSOLIDATION.

U.S. Geological Survey Denver, Colorado	Laboratory Testing of Shallow Sediments Gulf of Alaska	CONSOLIDATION COMPRESSION SAMPLE 33G DEPTH 361-371 cm
Geotechnical Engineers Inc. Winchester, Massachusetts	Project 78465	September, 1978

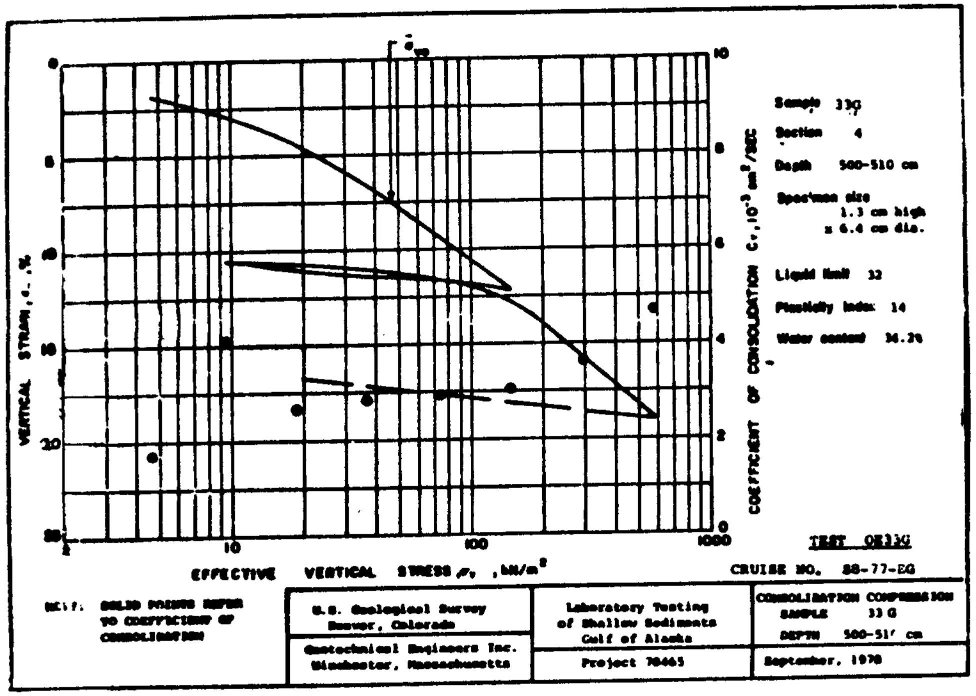
VERTICAL STRAIN, ε, %
COEFFICIENT OF CONSOLIDATION Cv, 10⁻³ cm²/SEC
EFFECTIVE VERTICAL STRESS σ̄v, kN/m²
σ̄vo
Sample 33G
Section 4
Depth 500-510 cm
Specimen size 1.3 cm high x 6.4 cm dia.
Liquid limit 32
Plasticity index 14
Water content 34.3%
TEST OE33G
CRUISE NO. S8-77-EG
NOTE: SOLID POINTS REFER TO COEFFICIENT OF CONSOLIDATION
U.S. Geological Survey Denver, Colorado
Geotechnical Engineers Inc. Winchester, Massachusetts
Laboratory Testing of Shallow Sediments Gulf of Alaska
Project 78465
CONSOLIDATION COMPRESSION SAMPLE 33 G DEPTH 500-510 cm
September, 1978

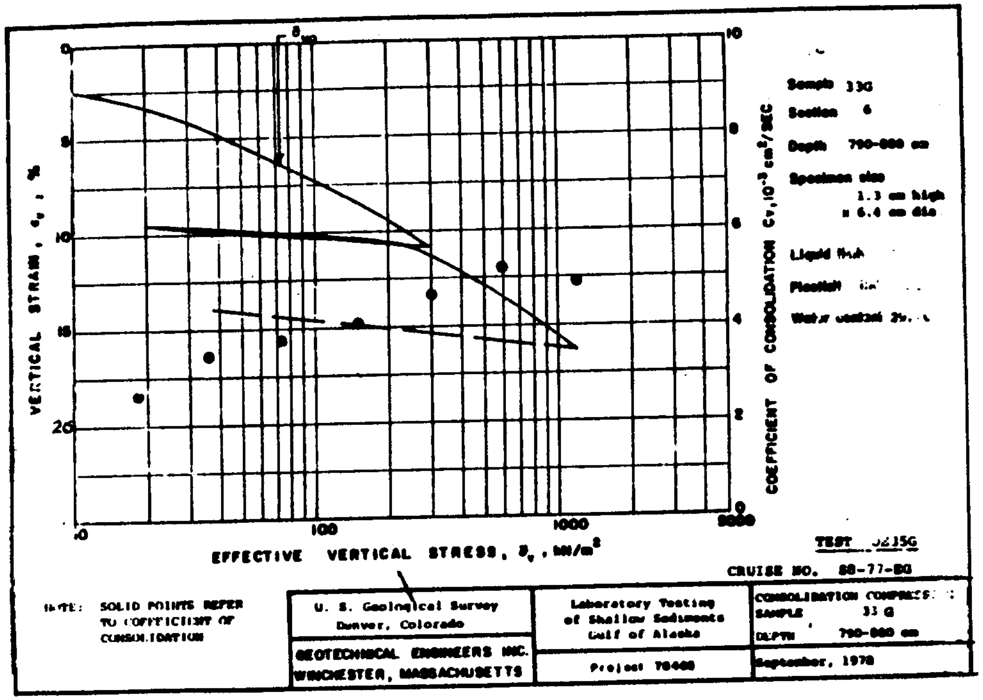
VERTICAL STRAIN, εv, %
COEFFICIENT OF CONSOLIDATION Cv, 10⁻³ cm²/SEC
EFFECTIVE VERTICAL STRESS, σ̄v, kN/m²
σ̄vo
Sample 33G
Section 6
Depth 790-800 cm
Specimen size 1.3 cm high x 6.4 cm dia.
TEST OE35G
CRUISE NO. S8-77-EG
NOTE: SOLID POINTS REFER TO COEFFICIENT OF CONSOLIDATION
U. S. Geological Survey Denver, Colorado
GEOTECHNICAL ENGINEERS INC. WINCHESTER, MASSACHUSETTS
Laboratory Testing of Shallow Sediments Gulf of Alaska
Project 78466
SAMPLE 33 G DEPTH 790-800 cm
September, 1978

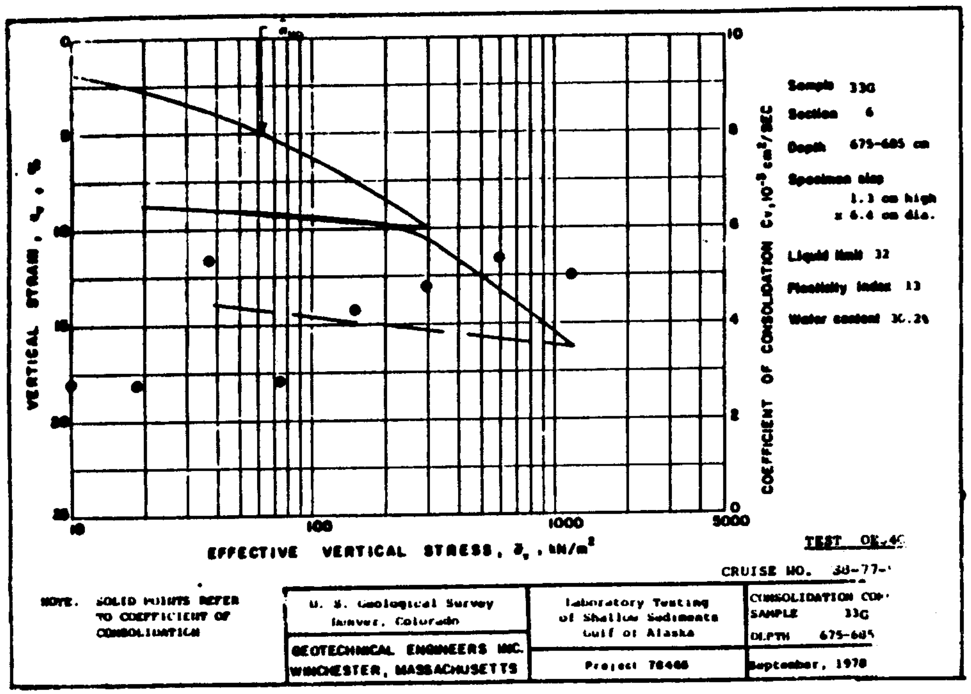
VERTICAL STRAIN, εv, %
COEFFICIENT OF CONSOLIDATION Cv, 10⁻³ cm²/SEC
EFFECTIVE VERTICAL STRESS, σ̄v, kN/m²
σ̄vo
Sample 33G
Section 6
Depth 675-685 cm
Specimen size 1.3 cm high x 6.4 cm dia.
Liquid limit 32
Plasticity index 13
Water content 30.2%
CRUISE NO. S8-77-
NOTE. SOLID POINTS REFER TO COEFFICIENT OF CONSOLIDATION
U. S. Geological Survey Denver, Colorado
GEOTECHNICAL ENGINEERS INC. WINCHESTER, MASSACHUSETTS
Laboratory Testing of Shallow Sediments Gulf of Alaska
Project 78466
SAMPLE 33G DEPTH 675-685
September, 1978

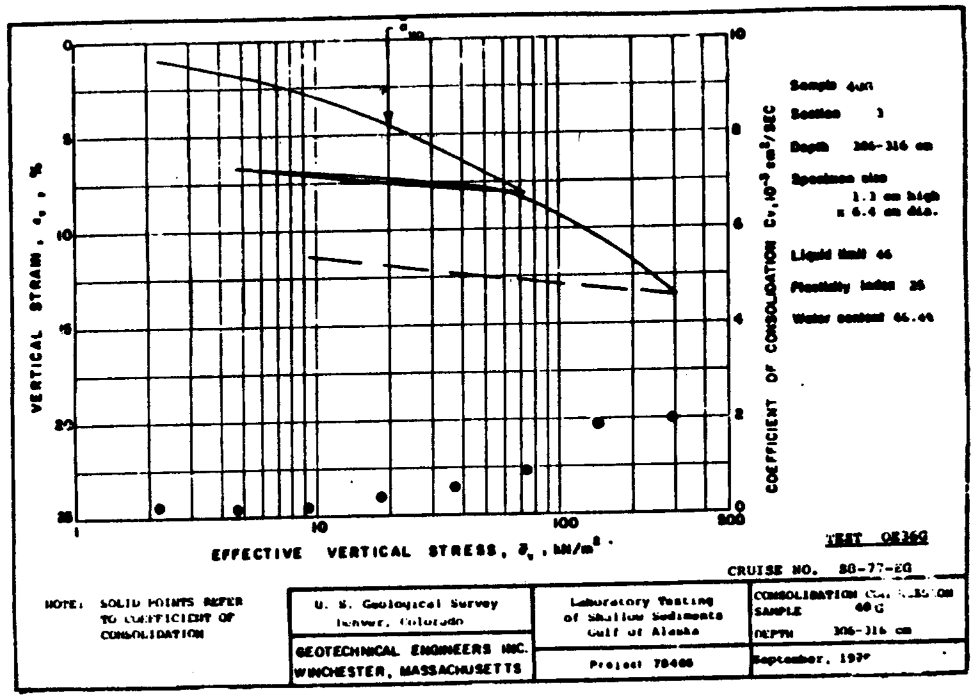
VERTICAL STRAIN, εv, %
COEFFICIENT OF CONSOLIDATION Cv, 10⁻³ cm²/SEC
EFFECTIVE VERTICAL STRESS, σ̄v, kN/m²
σ̄vo
Section 3
Depth 306-316 cm
Specimen size 1.3 cm high x 6.4 cm dia.
Liquid limit 46
Plasticity index 26
Water content 46.4%
TEST OE36G
CRUISE NO. S8-77-EG
NOTE: SOLID POINTS REFER TO COEFFICIENT OF CONSOLIDATION
U. S. Geological Survey Denver, Colorado
GEOTECHNICAL ENGINEERS INC. WINCHESTER, MASSACHUSETTS
Laboratory Testing of Shallow Sediments Gulf of Alaska
Project 78466
SAMPLE 40 G DEPTH 306-316 cm

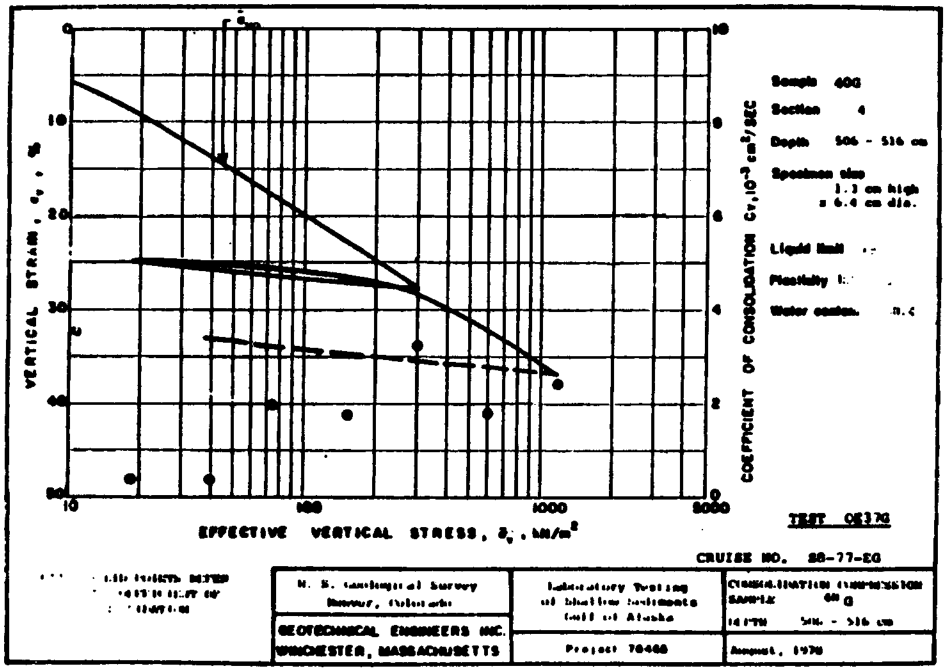

VERTICAL STRAIN, ϵ_v, %
COEFFICIENT OF CONSOLIDATION $C_v, 10^{-3}$ cm^2/SEC
EFFECTIVE VERTICAL STRESS, $\bar{\sigma}_v$, kN/m^2
Sample 40G
Section 4
Depth 506 - 516 cm
Specimen size 1.3 cm high x 6.4 cm dia.
Liquid limit
Plasticity
Water conten.
TEST OE37G
CRUISE NO. S8-77-EG
U. S. Geological Survey Denver, Colorado
Laboratory Testing of Shallow Sediments Gulf of Alaska
CONSOLIDATION COMPRESSION
GEOTECHNICAL ENGINEERS INC. WINCHESTER, MASSACHUSETTS
Project 78468
August, 1978

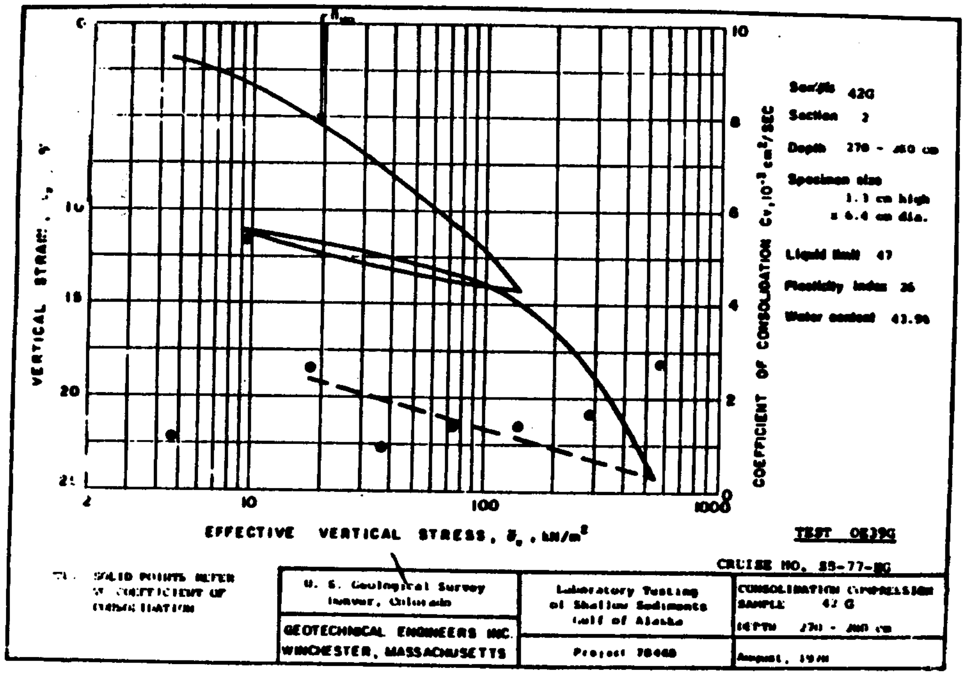

VERTICAL STRAIN
COEFFICIENT OF CONSOLIDATION $C_v, 10^{-3}$ cm^2/SEC
EFFECTIVE VERTICAL STRESS, $\bar{\sigma}_v$, kN/m^2
Sample 42G
Section 2
Depth 270 - 280 cm
Specimen size 1.3 cm high x 6.4 cm dia.
Liquid limit 47
Plasticity index 26
Water content 43.9%
TEST OE39G
CRUISE NO. S8-77-EG
SOLID POINTS REFER TO COEFFICIENT OF CONSOLIDATION
U. S. Geological Survey Denver, Colorado
Laboratory Testing of Shallow Sediments Gulf of Alaska
CONSOLIDATION COMPRESSION SAMPLE 42 G
GEOTECHNICAL ENGINEERS INC. WINCHESTER, MASSACHUSETTS
Project 78468
August, 1978

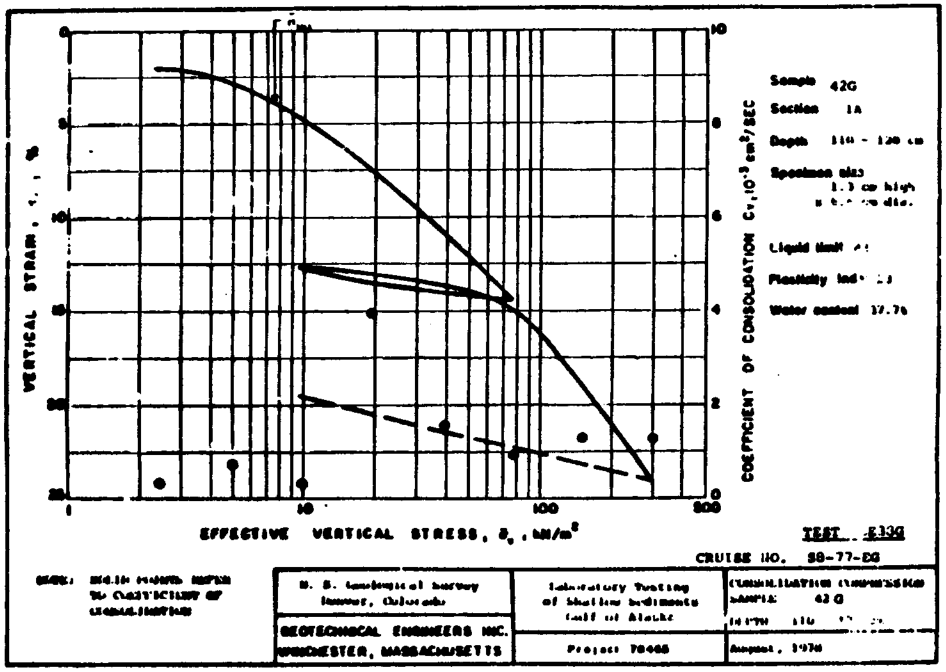

VERTICAL STRAIN, %
COEFFICIENT OF CONSOLIDATION $C_v, 10^{-3}$ cm^2/SEC
EFFECTIVE VERTICAL STRESS, $\bar{\sigma}_v$, kN/m^2
Sample 42G
Section 1A
Depth 110 - 120 cm
Specimen size 1.3 cm high
Liquid limit
Plasticity index
Water content 37.7%
TEST E33G
CRUISE NO. S8-77-EG
NOTE: SOLID POINTS REFER TO COEFFICIENT OF CONSOLIDATION
U. S. Geological Survey Denver, Colorado
Laboratory Testing of Shallow Sediments Gulf of Alaska
CONSOLIDATION COMPRESSION SAMPLE 42 G
GEOTECHNICAL ENGINEERS INC. WINCHESTER, MASSACHUSETTS
Project 78468
August, 1978

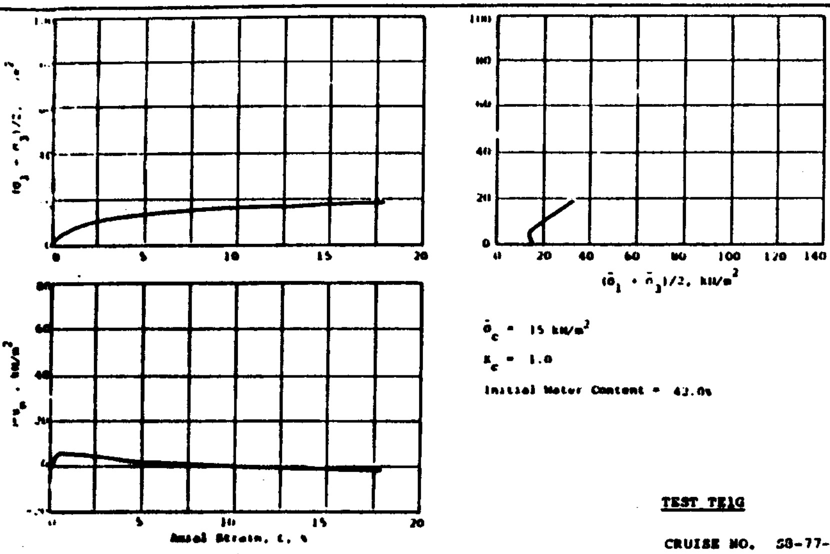

$\bar{\sigma}_c$ = 15 kN/m^2

K_c = 1.0

Initial Water Content = 42.0%

TEST TE1G

CRUISE NO. S8-77-EG

U.S. Geological Survey Denver, Colorado	Laboratory Testing of Shallow Sediments Gulf of Alaska	$\bar{A}$ TEST Sample 4G Depth 210-220 cm
Geotechnical Engineers Inc. Winchester, Massachusetts	Project 78465	August, 1978

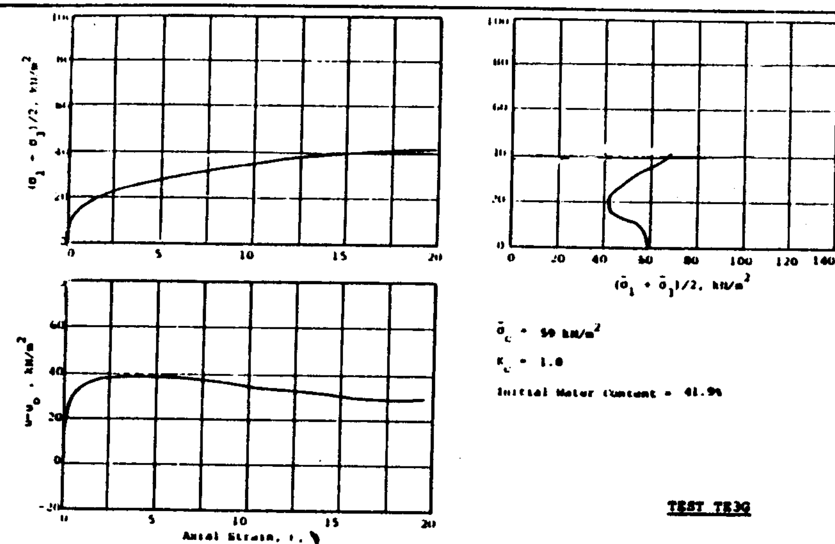

$\bar{\sigma}_c$ = 59 kN/m^2

K_c = 1.0

Initial Water Content = 41.9%

TEST TE3G

CRUISE NO. S8-77-EG

U.S. Geological Survey Denver, Colorado	Laboratory Testing of Shallow Sediments Gulf of Alaska	$\bar{A}$ TEST Sample 4G Depth 230-240 cm
Geotechnical Engineers Inc. Winchester, Massachusetts	Project 78465	August, 1978

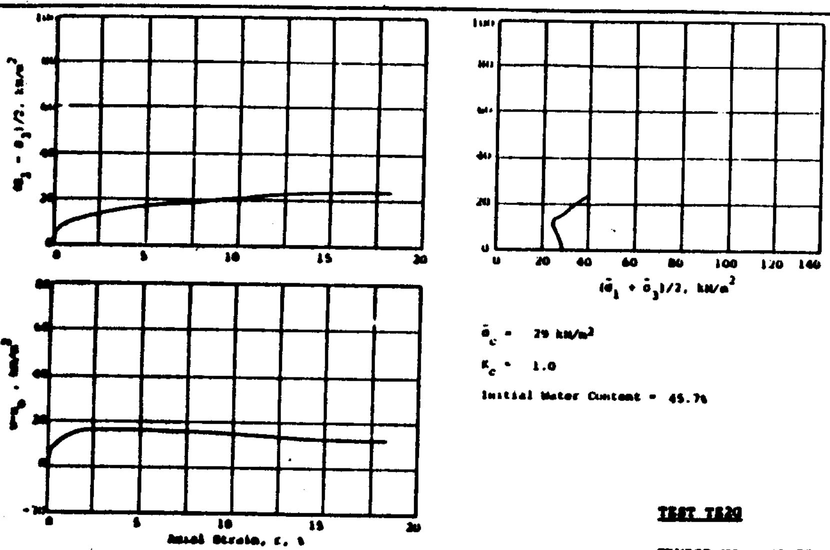

$\bar{\sigma}_c$ = 29 kN/m^2

K_c = 1.0

Initial Water Content = 45.7%

TEST TE2G

CRUISE NO. S8-77-EG

U.S. Geological Survey Denver, Colorado	Laboratory Testing of Shallow Sediments Gulf of Alaska	$\bar{A}$ TEST Sample 4 G Depth 220-230 cm
Geotechnical Engineers Inc. Winchester, Massachusetts	Project 78465	August, 1978

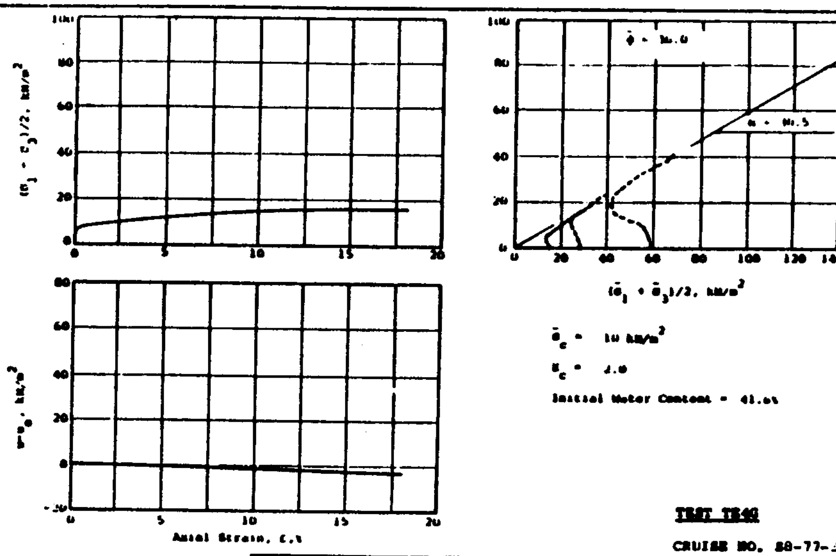

$\bar{\sigma}_c$ = 10 kN/m^2

K_c = 1.0

Initial Water Content = 41.6%

TEST TE4G

CRUISE NO. S8-77-EG

NOTE: Dashed curves taken from tests TE1G, TE2G, and TE3G.

U.S. Geological Survey Denver, Colorado	Laboratory Testing of Shallow Sediments Gulf of Alaska	$\bar{A}$ TEST Sample 4G Depth 240-250 cm
Geotechnical Engineers Inc. Winchester, Massachusetts	Project 78465	August, 1978

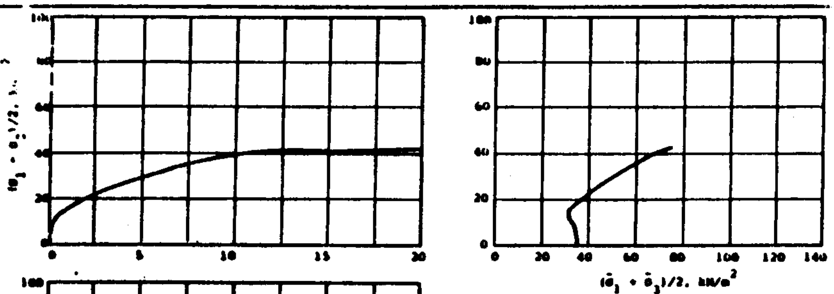

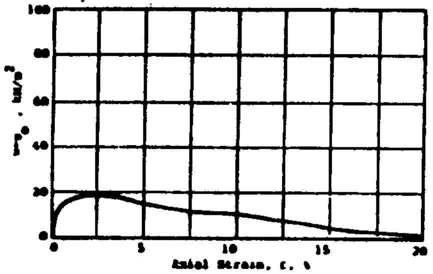

$\bar{\sigma}_c$ = 34

K_c = 1.0

Initial Water Content = 39.2%

TEST TE5G

CRUISE NO. S8-77-EG

U.S. Geological Survey Denver, Colorado	Laboratory Testing of Shallow Sediments Gulf of Alaska	$\bar{R}$ TEST Sample 4 G Depth 630-640 cm
Geotechnical Engineers Inc. Winchester, Massachusetts	Project 78465	August, 1978

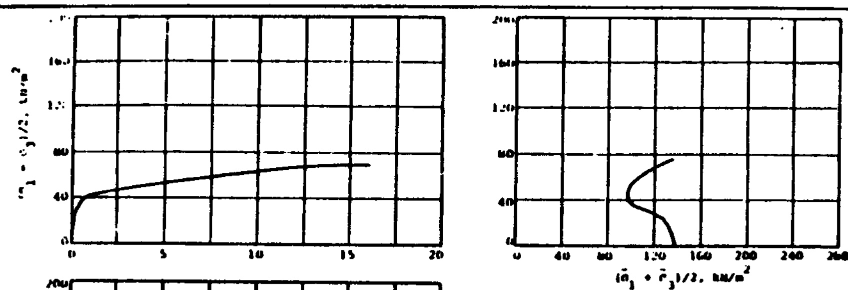

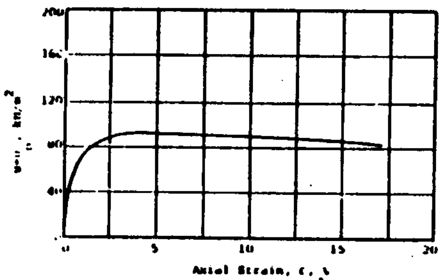

$\bar{\sigma}_c$ = 130 kN/m^2

K_c = 1.0

Initial Water Content = 41.6%

TEST TE7G

CRUISE NO. S8-77-EG

U.S. Geological Survey Denver, Colorado	Laboratory Testing of Shallow Sediments Gulf of Alaska	$\bar{R}$ TEST Sample 4G Depth 650-660 cm
Geotechnical Engineers Inc. Winchester, Massachusetts	Project 78465	August, 1978

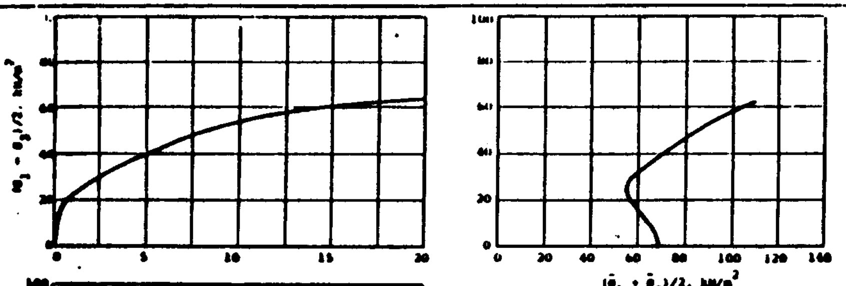

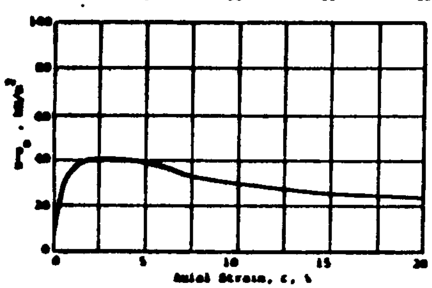

$\bar{\sigma}_c$ = 69 kN/m^2

K_c = 1.0

Initial Water Content = 36.9%

TEST TE6G

CRUISE NO. S8-77-EG

U.S. Geological Survey Denver, Colorado	Laboratory Testing of Shallow Sediments Gulf of Alaska	$\bar{R}$ TEST Sample 4 G Depth 640-650 cm
Geotechnical Engineers Inc. Winchester, Massachusetts	Project 78465	August, 1978

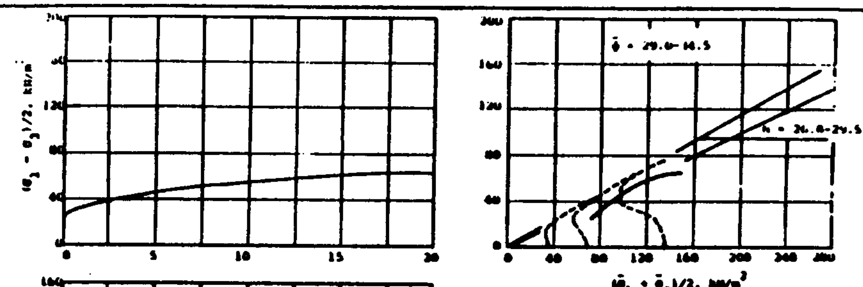

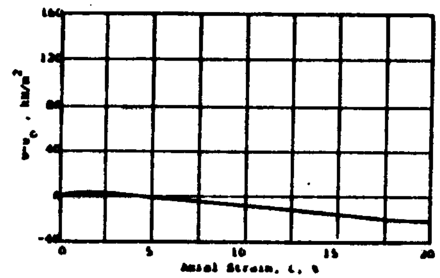

$\bar{\sigma}_c$ = 25 kN/m^2

K_c = 1.0

Initial Water Content = 36.8%

TEST TE8G

CRUISE NO. S8-77-EG

NOTE: Dashed curves are from tests TE5G TE6G, and, TE7G.

U.S. Geological Survey Denver, Colorado	Laboratory Testing of Shallow Sediments Gulf of Alaska	$\bar{R}$ TEST Sample 4G Depth 660-670 cm
Geotechnical Engineers Inc. Winchester, Massachusetts	Project 78465	August, 1978

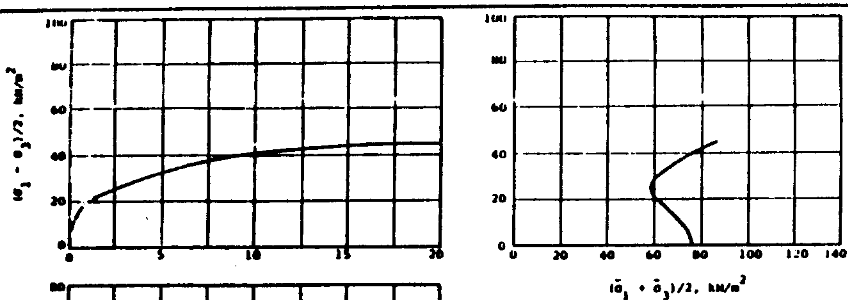

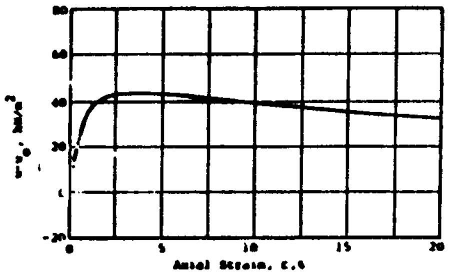

$\bar{\sigma}_c$ = 75 kN/m^2

$\bar{\varepsilon}_c$ = 1.0

Initial Water Content = 40.5%

TEST TE9G

CRUISE NO. S8-77-BG

U.S. Geological Survey Denver, Colorado	Laboratory Testing of Shallow Sediments Gulf of Alaska	$\bar{K}$ TEST Sample 4G Depth 670-680 cm
Geotechnical Engineers Inc. Winchester, Massachusetts	Project 76465	August, 1978

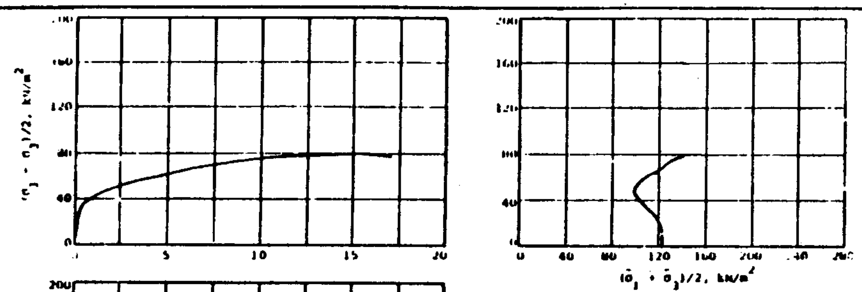

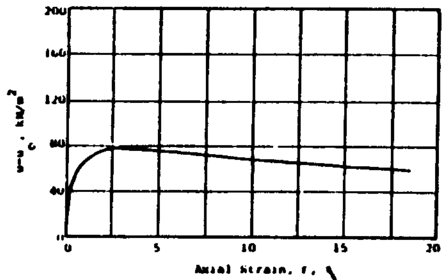

$\bar{\sigma}_c$ = 125 kN/m^2

$\bar{\varepsilon}_c$ = 1.0

Initial Water Content = 36.5%

TEST TE11G

CRUISE NO. S8-77-BG

U.S. Geological Survey Denver, Colorado	Laboratory Testing of Shallow Sediments Gulf of Alaska	$\bar{K}$ TEST Sample 4G Depth 690-700 cm
Geotechnical Engineers Inc. Winchester, Massachusetts	Project 76465	August, 1978

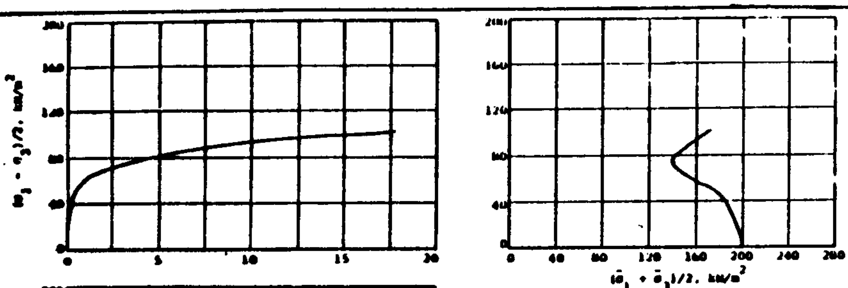

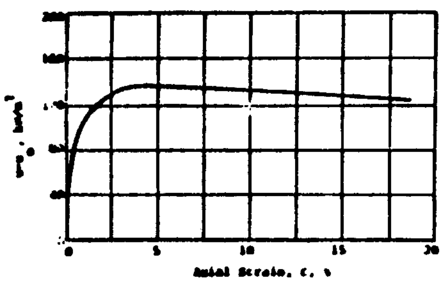

$\bar{\sigma}_c$ = 200 kN/m^2

$\bar{\varepsilon}_c$ = 1.0

Initial Water Content = 37.6%

TEST TE10G

CRUISE NO. S8-77-BG

U.S. Geological Survey Denver, Colorado	Laboratory Testing of Shallow Sediments Gulf of Alaska	$\bar{K}$ TEST Sample 4G Depth 680-690 cm
Geotechnical Engineers Inc. Winchester, Massachusetts	Project 76465	August, 1978

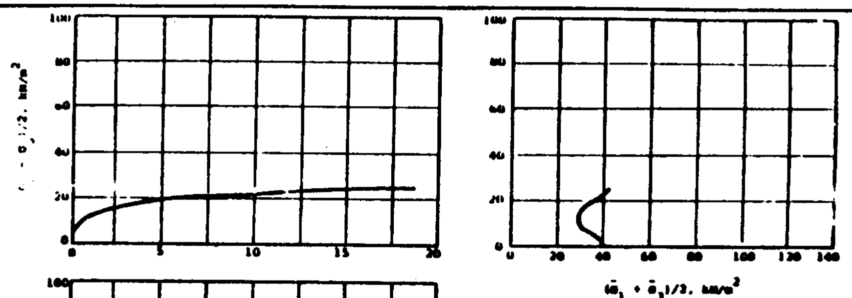

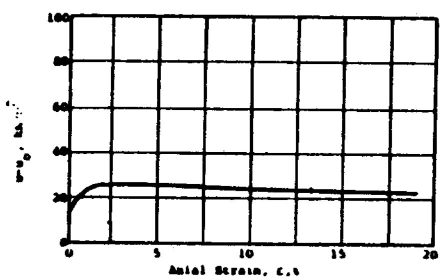

$\bar{\sigma}_c$ = 40 kN/m^2

$\bar{\varepsilon}_c$ = 1.0

Initial Water Content = 47.7%

TEST TE12G

CRUISE NO. S8-77-BG

U.S. Geological Survey Denver, Colorado	Laboratory Testing of Shallow Sediments Gulf of Alaska	$\bar{K}$ TEST Sample 7G Depth 780-790 cm
Geotechnical Engineers Inc. Winchester, Massachusetts	Project 76465	August, 1978

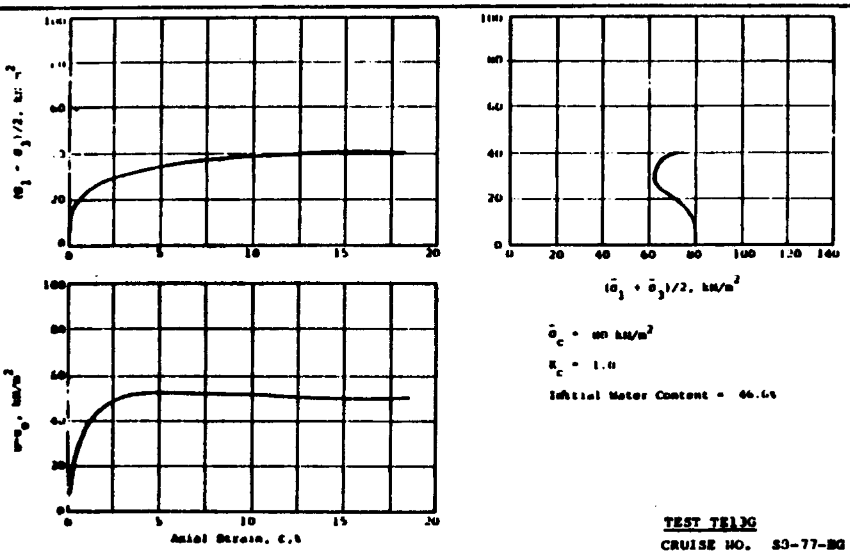

TEST TE13G
CRUISE NO. S8-77-EG

U.S. Geological Survey Denver, Colorado	Laboratory Testing of Shallow Sediments Gulf of Alaska	$\bar{R}$ TEST Sample 7G Depth 790-800 cm
Geotechnical Engineers Inc. Winchester, Massachusetts	Project 78465	August, 1978

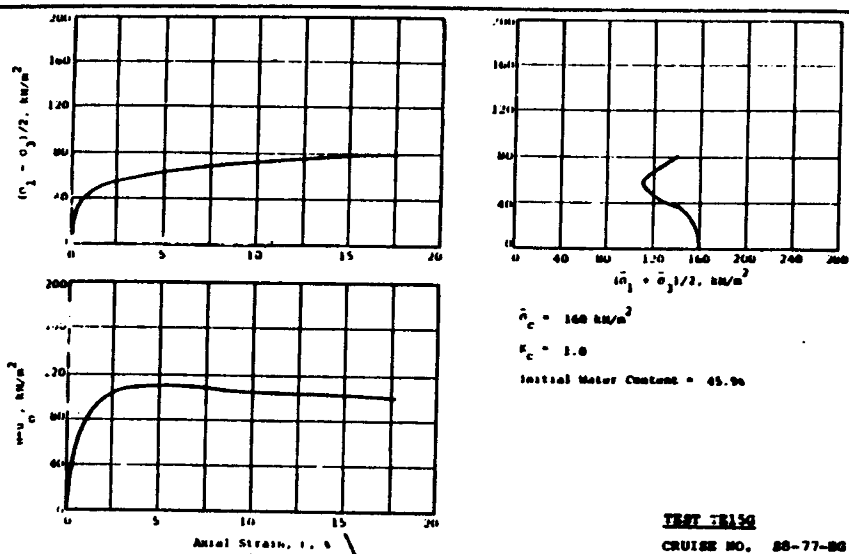

TEST TE15G
CRUISE NO. S8-77-EG

U.S. Geological Survey Denver, Colorado	Laboratory Testing of Shallow Sediments Gulf of Alaska	$\bar{R}$ TEST Sample 7G Depth 810-820 cm
Geotechnical Engineers Inc. Winchester, Massachusetts	Project 78465	August, 1978

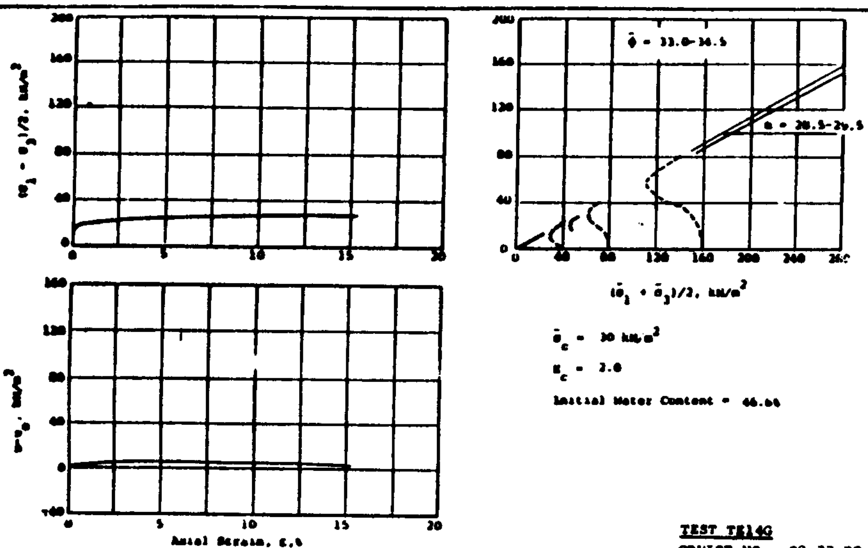

TEST TE14G
CRUISE NO. S8-77-EG

NOTE: Dashed curves are taken from tests TE12G, TE13G, and TE15G.

U.S. Geological Survey Denver, Colorado	Laboratory Testing of Shallow Sediments Gulf of Alaska	$\bar{R}$ TEST Sample 7G Depth 800-810 cm
Geotechnical Engineers Inc. Winchester, Massachusetts	Project 78465	August, 1978

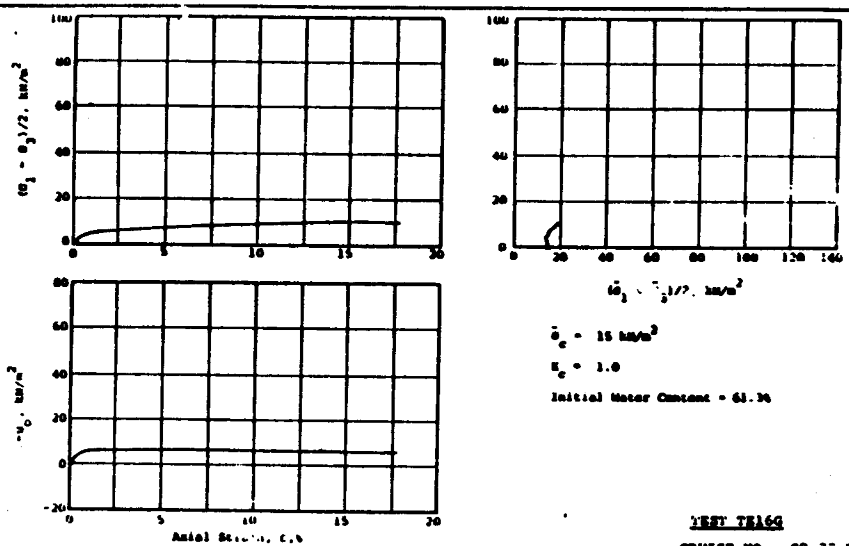

TEST TE16G
CRUISE NO. S8-77-EG

U.S. Geological Survey Denver, Colorado	Laboratory Testing of Shallow Sediments Gulf of Alaska	$\bar{R}$ TEST Sample 8G Depth 230-240
Geotechnical Engineers Inc. Winchester, Massachusetts	Project 78465	September, 1978

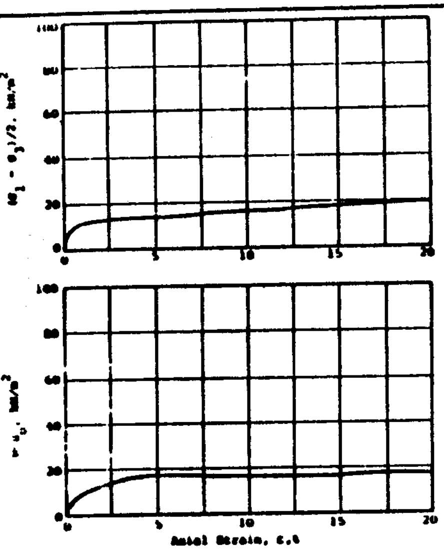

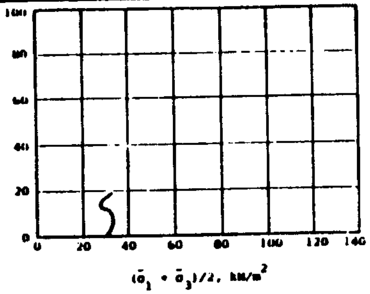

$\bar{\sigma}_c$ = 30 kN/m²

K_c = 1.0

Initial Water Content = 67.8%

TEST TE17G

CRUISE NO. S8-77-BG

U.S. Geological Survey Denver, Colorado	Laboratory Testing of Shallow Sediments Gulf of Alaska	$\bar{R}$ TEST Sample 8 G Depth 240-250 cm
Geotechnical Engineers Inc. Winchester, Massachusetts	Project 78465	August, 1978

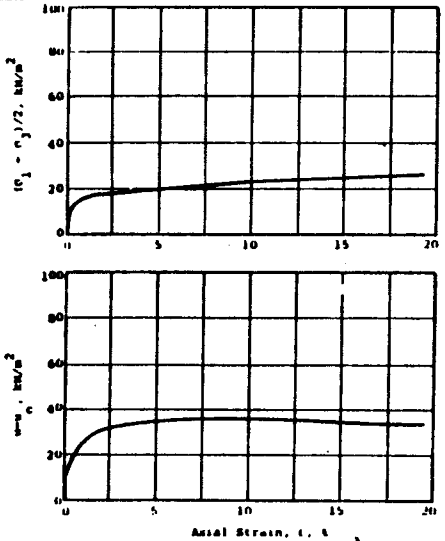

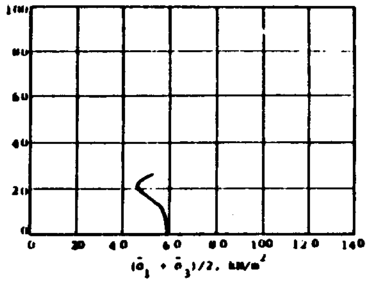

$\bar{\sigma}_c$ = 60 kN/m²

K_c = 1.0

Initial Water Content = 63.3%

TEST TE19G

CRUSIE NO. S8-77-BG

U.S. Geological Survey Denver, Colorado	Laboratory Testing of Shallow Sediments Gulf of Alaska	$\bar{R}$ TEST Sample 8G Depth 260-270 cm
Geotechnical Engineers Inc. Winchester, Massachusetts	Project 78465	August, 1978

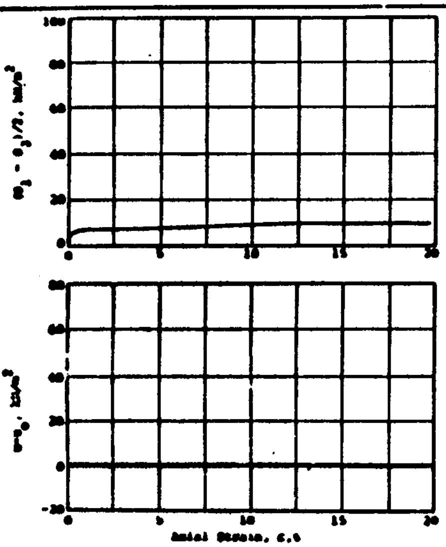

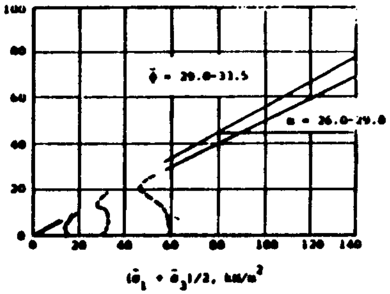

$\bar{\sigma}_c$ = 10 kN/m²

K_c = 2.0

Initial Water Content = 66.0%

TEST TE18G

CRUISE NO. S8-77-BG

NOTE: Dashed curves are taken from tests TE16G, TE17G, and TE19G.

U.S. Geological Survey Denver, Colorado	Laboratory Testing of Shallow Sediments Gulf of Alaska	$\bar{R}$ TEST Sample 8 G Depth 250-260 cm
Geotechnical Engineers Inc. Winchester, Massachusetts	Project 78465	August, 1978

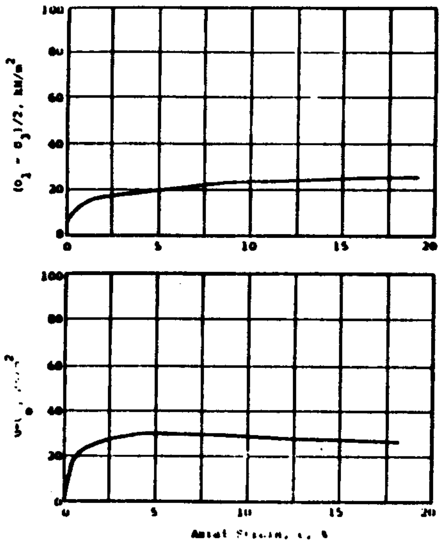

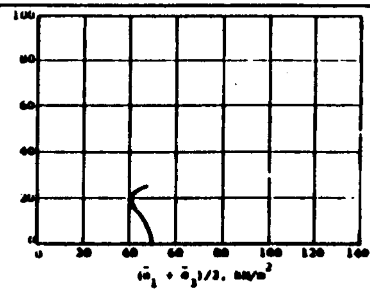

$\bar{\sigma}_c$ = 50 kN/m²

K_c = 1.0

Initial Water Content = 58.4%

TEST TE20G

CRUISE NO. S8-77-BG

U.S. Geological Survey Denver, Colorado	Laboratory Testing of Shallow Sediments Gulf of Alaska	$\bar{R}$ TEST Sample 8G Depth 650-660 cm
Geotechnical Engineers Inc. Winchester, Massachusetts	Project 78465	August, 1978

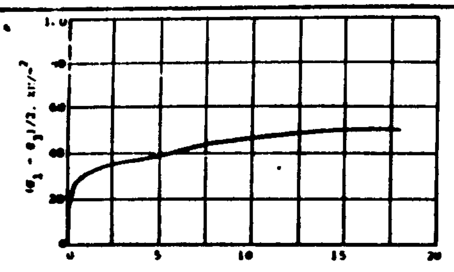
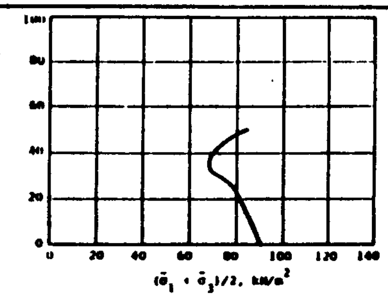
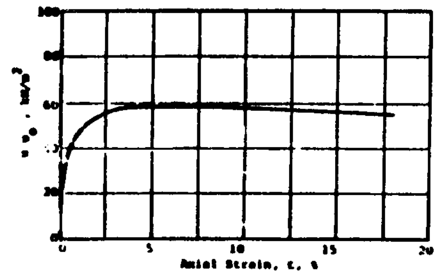

$\bar{\sigma}_c$ = 90 kN/m²

K_c = 1.0

Initial Water Content = 50.3%

TEST TE21G

CRUISE NO. S8-77-EG

U.S. Geological Survey Denver, Colorado	Laboratory Testing of Shallow Sediments Gulf of Alaska	$\bar{R}$ TEST Sample 8G Depth 670-680 cm
Geotechnical Engineers Inc. Winchester, Massachusetts	Project 78465	August, 1978

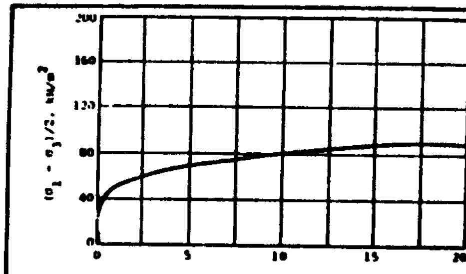
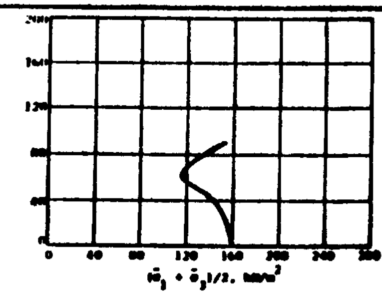
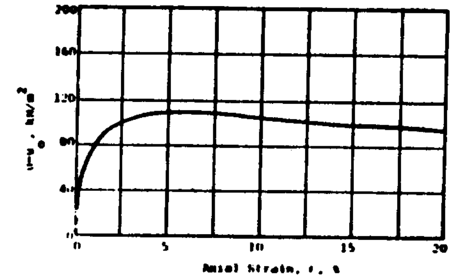

$\bar{\sigma}_c$ = 160 kN/m²

K_c = 1.0

Initial Water Content = 48.4%

TEST TE23G

CRUISE NO. S8-77-EG

U.S. Geological Survey Denver, Colorado	Laboratory Testing of Shallow Sediments Gulf of Alaska	$\bar{R}$ TEST Sample 8G Depth 790-800 cm
Geotechnical Engineers Inc. Winchester, Massachusetts	Project 78465	August, 1978

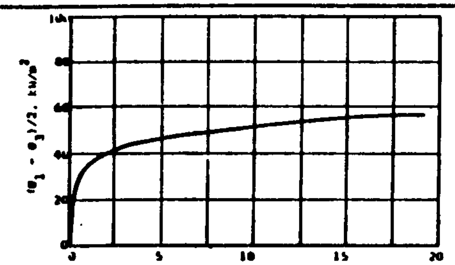
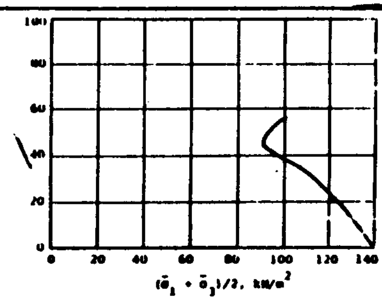
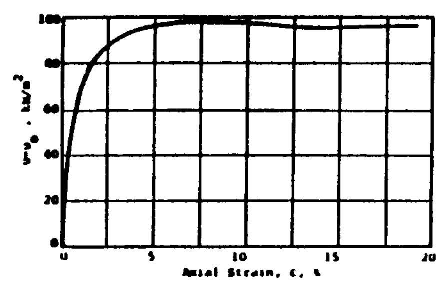

$\bar{\sigma}_c$ = 140 kN/m²

K_c = 1.0

Initial Water Content = 53.7%

TEST TE22G

CRUISE NO. S8-77-EG

U.S. Geological Survey Denver, Colorado	Laboratory Testing of Shallow Sediments Gulf of Alaska	$\bar{R}$ TEST Sample 8G Depth 680-690 cm
Geotechnical Engineers Inc. Winchester, Massachusetts	Project 78465	August, 1978

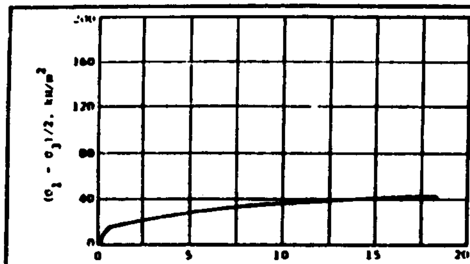
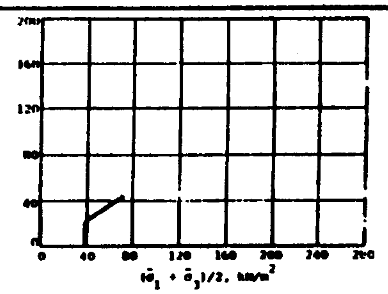
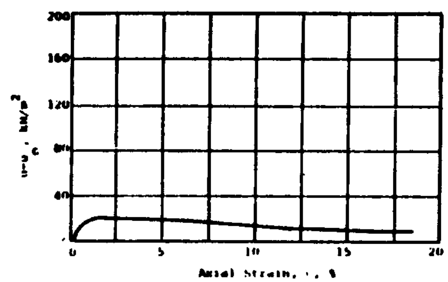

$\bar{\sigma}_c$ = 40 kN/m²

K_c = 1.0

Initial Water Content = 45.7%

TEST TE24G

CRUISE NO. S8-77-EG

U.S. Geological Survey Denver, Colorado	Laboratory Testing of Shallow Sediments Gulf of Alaska	$\bar{R}$ TEST Sample 8G Depth 810-820 cm
Geotechnical Engineers Inc. Winchester, Massachusetts	Project 78465	August, 1978

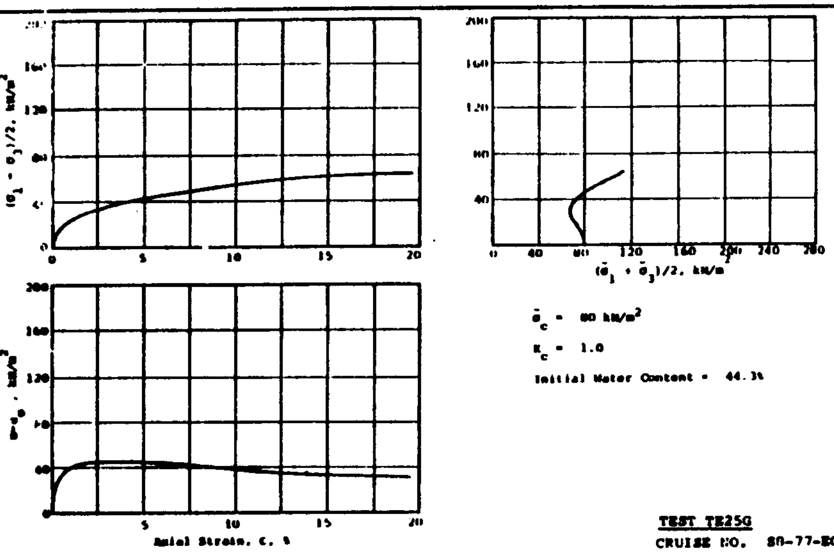

$\bar{\sigma}_c$ = 80 kN/m^2

K_c = 1.0

Initial Water Content = 44.3%

TEST TE25G

CRUISE NO. S8-77-EG

U.S. Geological Survey Denver, Colorado	Laboratory Testing of Shallow Sediments Gulf of Alaska	$\bar{R}$ TEST Sample 8G Depth 820-830 cm
Geotechnical Engineers Inc. Winchester, Massachusetts	Project 78465	August, 1978

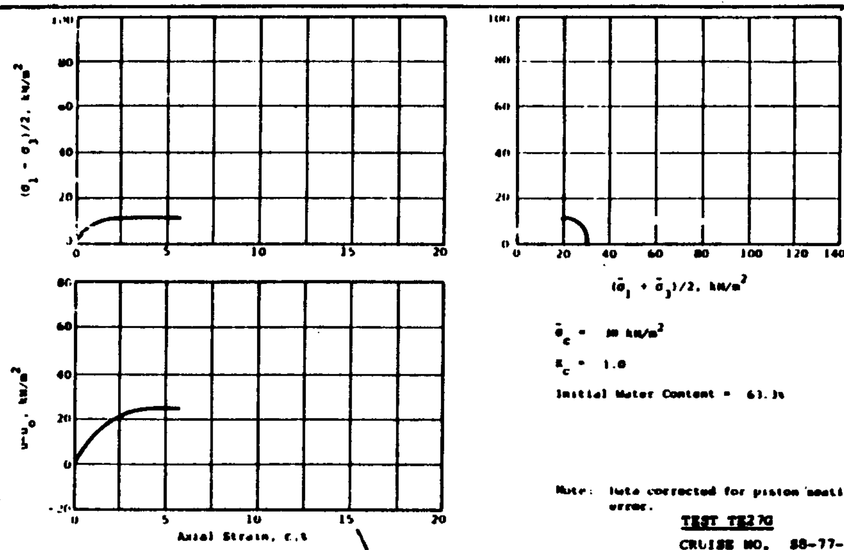

$\bar{\sigma}_c$ = 30 kN/m^2

K_c = 1.0

Initial Water Content = 63.3%

Note: Data corrected for piston seating error.

TEST TE27G

CRUISE NO. S8-77-EG

U.S. Geological Survey Denver, Colorado	Laboratory Testing of Shallow Sediments Gulf of Alaska	$\bar{R}$ TEST Sample 9G Depth 260-270 cm
Geotechnical Engineers Inc. Winchester, Massachusetts	Project 78465	August, 1978

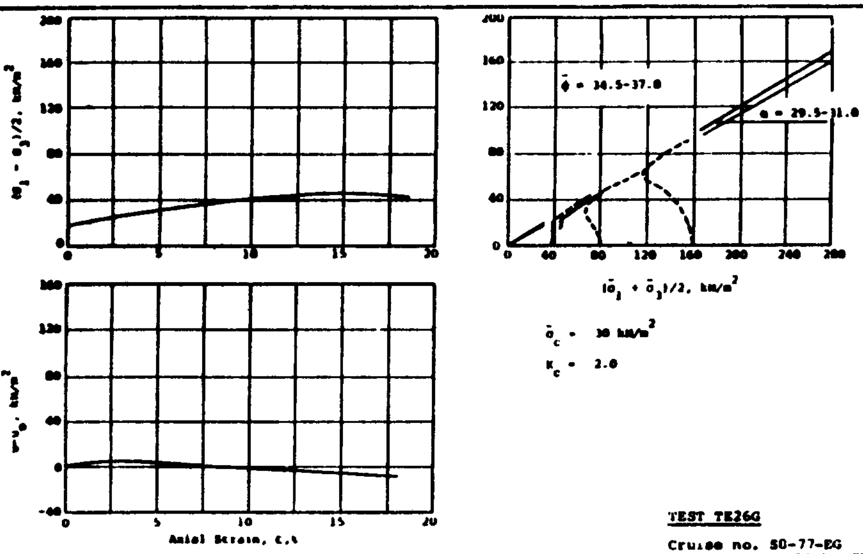

$\bar{\sigma}_c$ = 30 kN/m^2

K_c = 2.0

TEST TE26G

Cruise no. S8-77-EG

NOTE: Dashed curves are taken from tests TE23G, TE24G, and TE25G..

U.S. Geological Survey Denver, Colorado	Laboratory Testing of Shallow Sediments Gulf of Alaska	$\bar{R}$ TEST Sample 8G Depth 830-840 cm
Geotechnical Engineers Inc. Winchester, Massachusetts	Project 78465	August, 1978

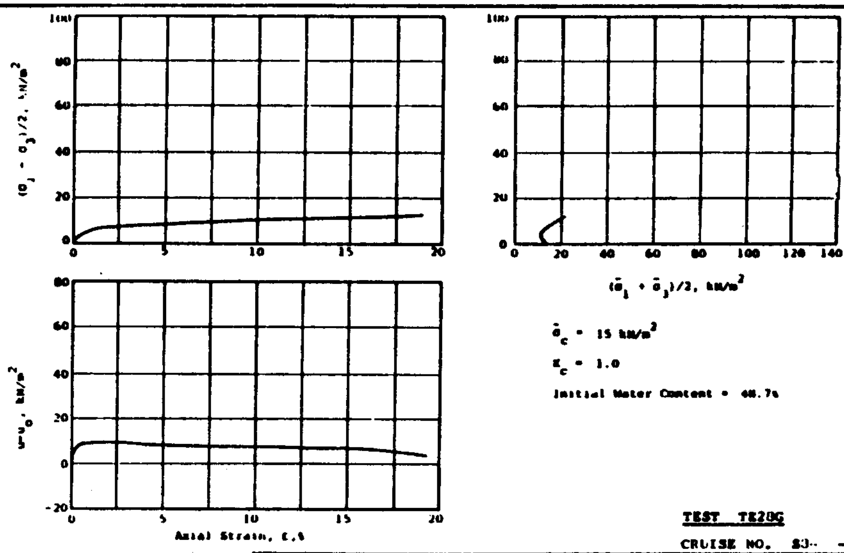

$\bar{\sigma}_c$ = 15 kN/m^2

K_c = 1.0

Initial Water Content = 48.7%

TEST TE28G

CRUISE NO. S8- -EG

U.S. Geological Survey Denver, Colorado	Laboratory Testing of Shallow Sediments Gulf of Alaska	$\bar{R}$ TEST Sample 9G Depth 270-280 cm
Geotechnical Engineers Inc. Winchester, Massachusetts	Project 78465	August, 1978

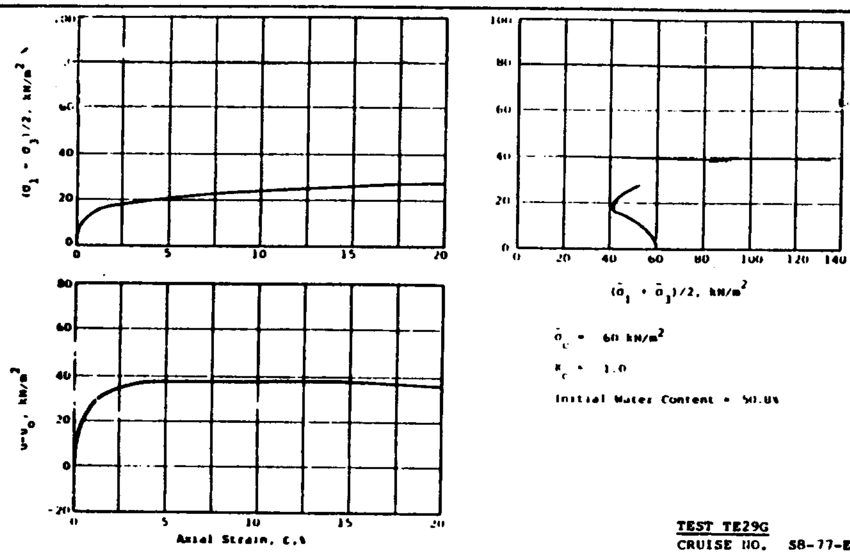

$\bar{\sigma}_c$ = 60 kN/m²

K_c = 1.0

Initial Water Content = 50.8%

TEST TE29G

CRUISE NO. S8-77-EG

U.S. Geological Survey Denver, Colorado	Laboratory Testing of Shallow Sediments Gulf of Alaska	$\bar{R}$ TEST Sample 9 G Depth 270-280
Geotechnical Engineers Inc. Winchester, Massachusetts	Project 78465	August, 1978

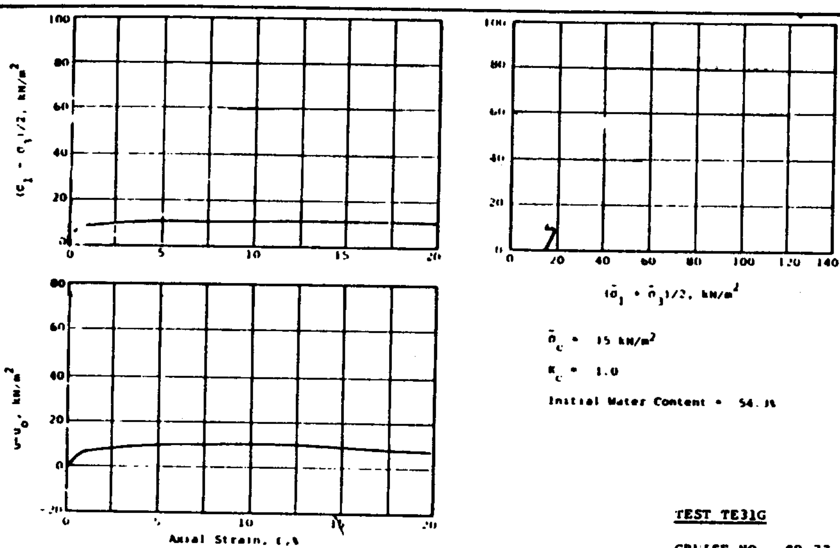

$\bar{\sigma}_c$ = 15 kN/m²

K_c = 1.0

Initial Water Content = 54.1%

TEST TE31G

CRUISE NO. S8-77-EG

U.S. Geological Survey Denver, Colorado	Laboratory Testing of Shallow Sediments Gulf of Alaska	$\bar{R}$ TEST Sample 25G Depth 240-250 cm
Geotechnical Engineers Inc. Winchester, Massachusetts	Project 78465	August, 1978

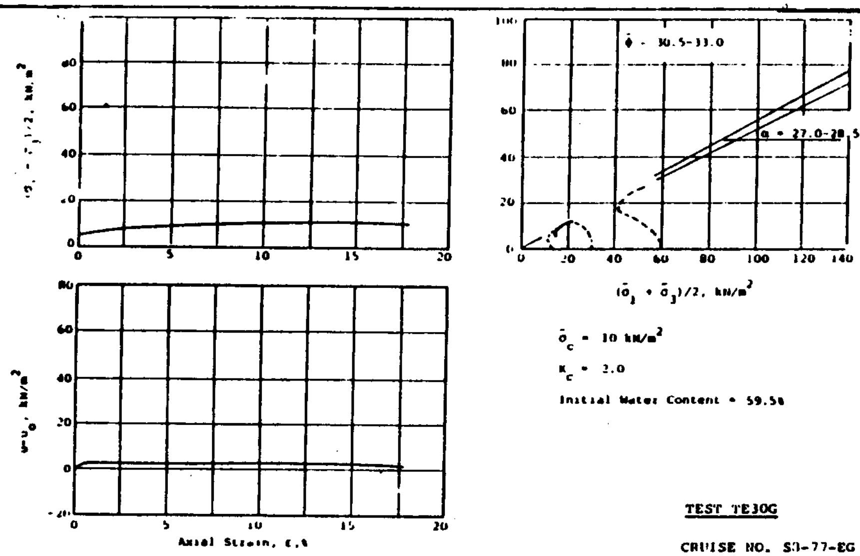

$\bar{\sigma}_c$ = 10 kN/m²

K_c = 2.0

Initial Water Content = 59.5%

TEST TE30G

CRUISE NO. S8-77-EG

NOTE: Dashed curves are taken from tests TE27G, TE28G, and TE29G.

U.S. Geological Survey Denver, Colorado	Laboratory Testing of Shallow Sediments Gulf of Alaska	$\bar{R}$ TEST Sample 9 G Depth 280-290 cm
Geotechnical Engineers Inc. Winchester, Massachusetts	Project 78465	August, 1978

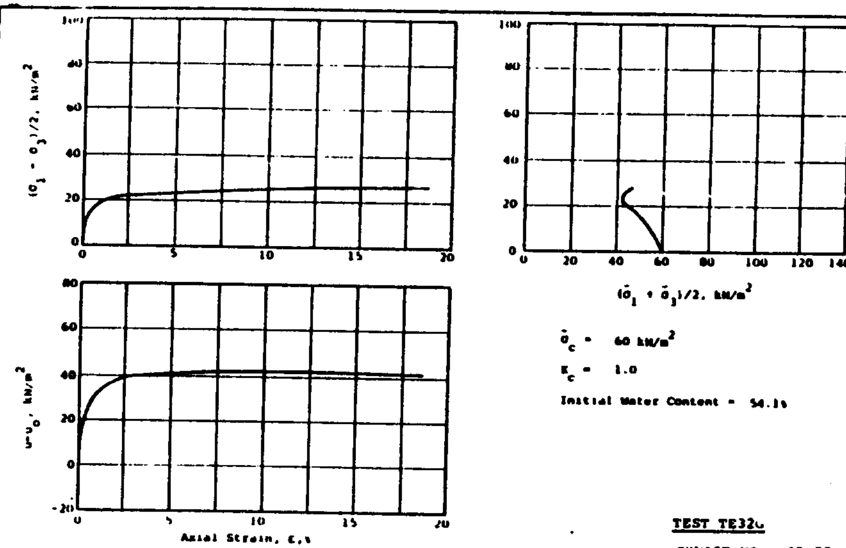

$\bar{\sigma}_c$ = 60 kN/m²

K_c = 1.0

Initial Water Content = 54.1%

TEST TE32G

CRUISE NO. S8-77-EG

U.S. Geological Survey Denver, Colorado	Laboratory Testing of Shallow Sediments Gulf of Alaska	$\bar{R}$ TEST Sample 25G Depth 260-270 cm
Geotechnical Engineers Inc. Winchester, Massachusetts	Project 78465	August, 1978

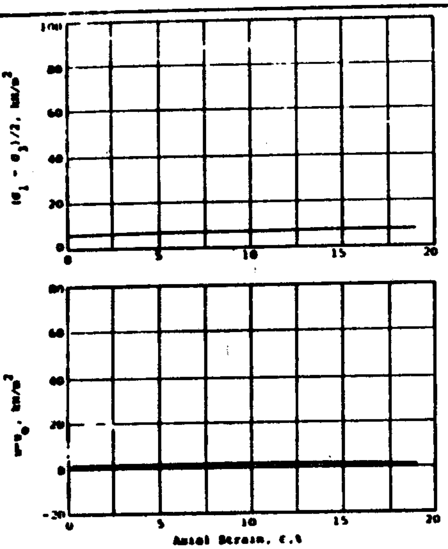

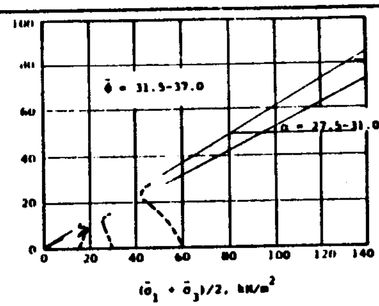

$\bar{\sigma}_c$ = 10 kN/m²

K_c = 2.0

Initial Water Content = 55.5%

TEST TE33G

CRUISE NO. S8-77-EG

NOTE: Dashed curves are taken from tests TE31G, S33G, and TE34G..

U.S. Geological Survey Denver, Colorado	Laboratory Testing of Shallow Sediments Gulf of Alaska	$\bar{K}$ TEST Sample 25 G Depth 270-280 cm
Geotechnical Engineers Inc. Winchester, Massachusetts	Project 78465	August, 1978

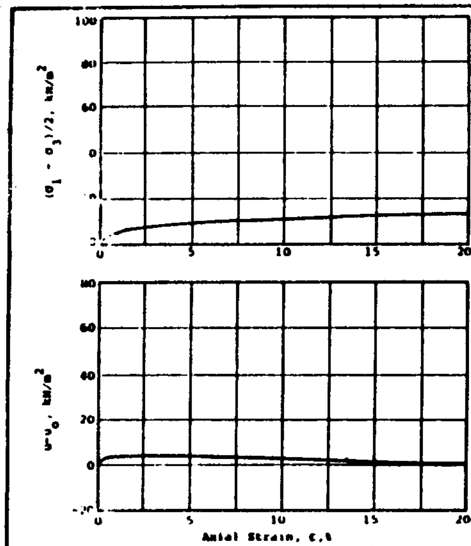

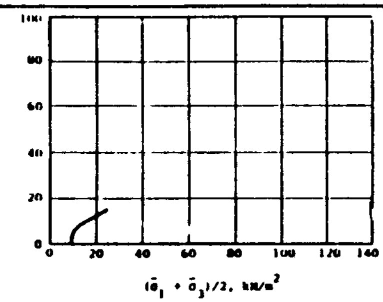

$\bar{\sigma}_c$ = 10 kN/m²

K_c = 1.0

Initial Water Content = 37.6%

TEST TE35G

CRUISE NO. S8-77-EG

U.S. Geological Survey Denver, Colorado	Laboratory Testing of Shallow Sediments Gulf of Alaska	$\bar{K}$ TEST Sample 26 G Depth 90-100 cm
Geotechnical Engineers Inc. Winchester, Massachusetts	Project 78465	August, 1978

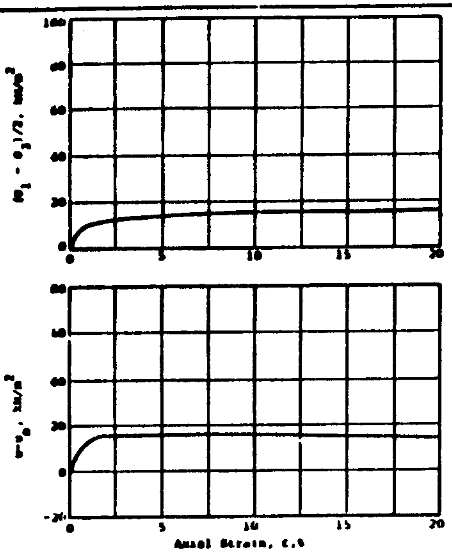

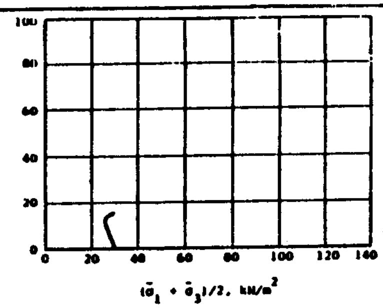

$\bar{\sigma}_c$ = 30 kN/m²

K_c = 1.0

Initial Water Content = 49.7%

TEST TE34G

CRUISE NO. S8-77-EG

U.S. Geological Survey Denver, Colorado	Laboratory Testing of Shallow Sediments Gulf of Alaska	$\bar{K}$ TEST Sample 25 G Depth 280-290 cm
Geotechnical Engineers Inc. Winchester, Massachusetts	Project 78465	August, 1978

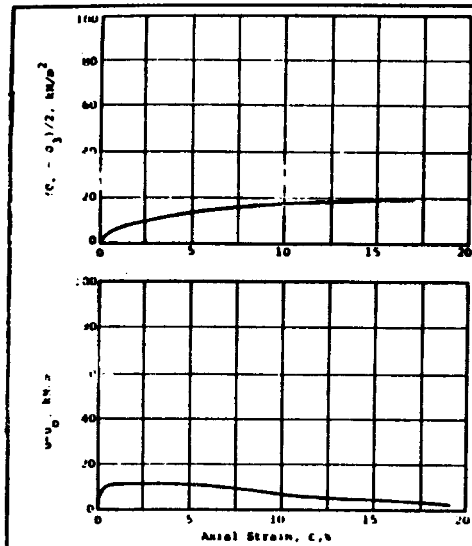

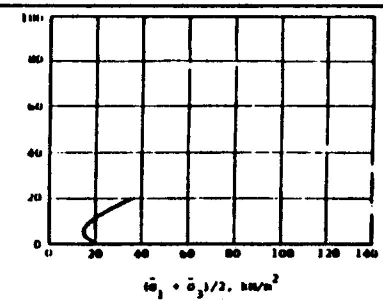

$\bar{\sigma}_c$ = 20 kN/m²

K_c = 1.0

Initial Water Content = 37.0%

TEST TE36G

CRUISE NO. S8-77-EG

U.S. Geological Survey Denver, Colorado	Laboratory Testing of Shallow Sediments Gulf of Alaska	$\bar{K}$ TEST Sample 26 G Depth 160-170 cm
Geotechnical Engineers Inc. Winchester, Massachusetts	Project 78465	August, 1978

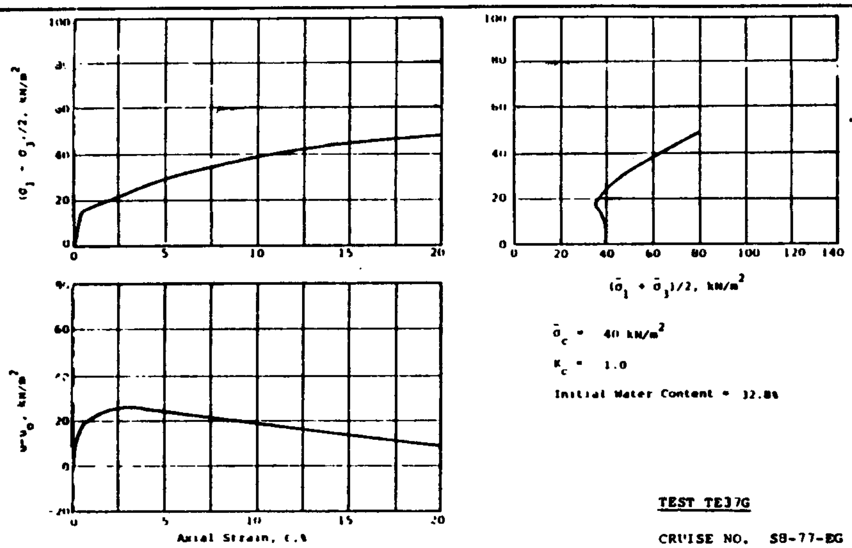

$\bar{\sigma}_c$ = 40 kN/m^2

K_c = 1.0

Initial Water Content = 32.8%

TEST TE37G

CRUISE NO. S8-77-EG

U.S. Geological Survey Denver, Colorado	Laboratory Testing of Shallow Sediments Gulf of Alaska	$\bar{R}$ TEST Sample 26 G Depth 170-180 cm
Geotechnical Engineers Inc Winchester, Massachusetts	Project 78465	August, 1978

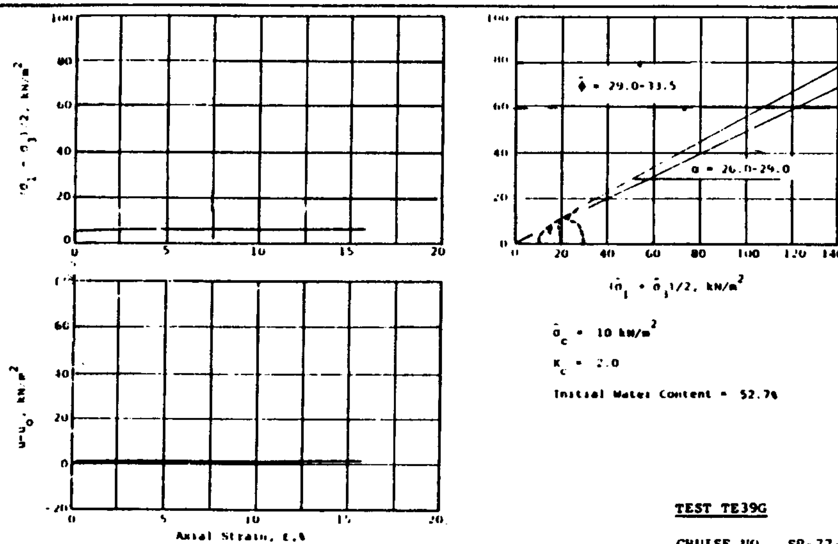

$\bar{\phi}$ = 29.0-33.5

α = 26.0-29.0

$\bar{\sigma}_c$ = 10 kN/m^2

K_c = 2.0

Initial Water Content = 52.7%

TEST TE39G

CRUISE NO. S8-77-EG

Dashed curves are taken from Figs. 4-40, 4-41, and 4-42.

U.S. Geological Survey Denver, Colorado	Laboratory Testing of Shallow Sediments Gulf of Alaska	$\bar{R}$ TEST Sample 27G Depth 50-60 cm
Geotechnical Engineers Inc Winchester, Massachusetts	Project 78465	August, 1978

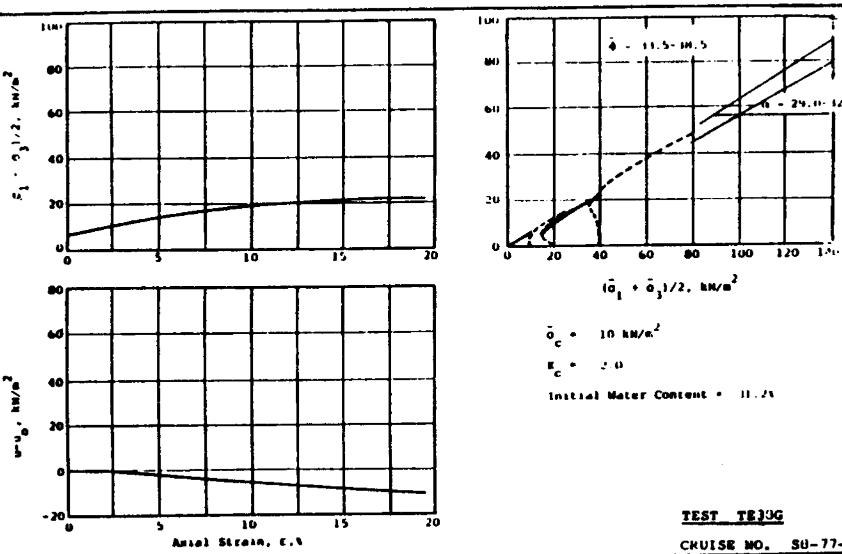

$\bar{\phi}$ = 33.5-38.5

α = 29.0-32.0

$\bar{\sigma}_c$ = 10 kN/m^2

K_c = 2.0

Initial Water Content = 31.2%

TEST TE38G

CRUISE NO. S8-77-EG

NOTE: Dashed curves are taken from tests TE35G, TE36G, and TE37G.

U.S. Geological Survey Denver, Colorado	Laboratory Testing of Shallow Sediments Gulf of Alaska	$\bar{R}$ TEST Sample 26G Depth 180-190 cm
Geotechnical Engineers Inc Winchester, Massachusetts	Project 78465	August, 1978

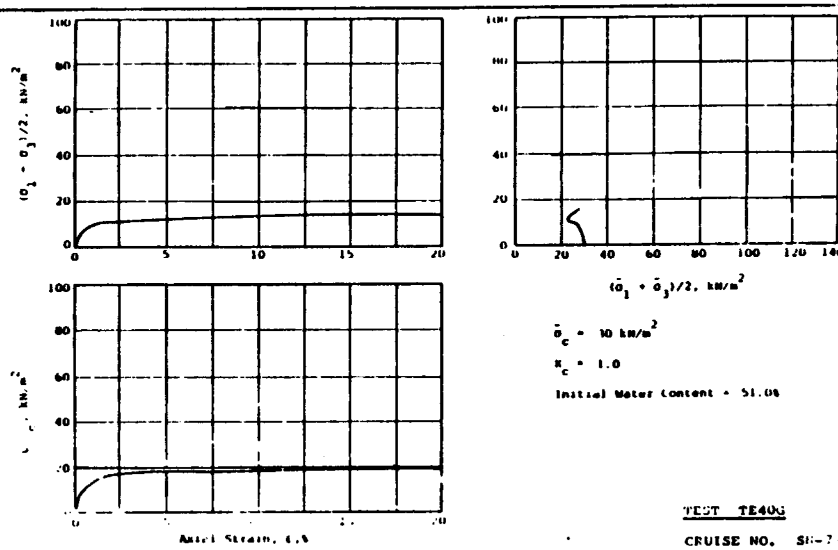

$\bar{\sigma}_c$ = 10 kN/m^2

K_c = 1.0

Initial Water Content = 51.0%

TEST TE40G

CRUISE NO. S8-77-EG

U.S. Geological Survey Denver, Colorado	Laboratory Testing of Shallow Sediments Gulf of Alaska	$\bar{R}$ TEST Sample 27G Depth 60-70 cm
Geotechnical Engineers Inc Winchester, Massachusetts	Project 78465	August, 1978

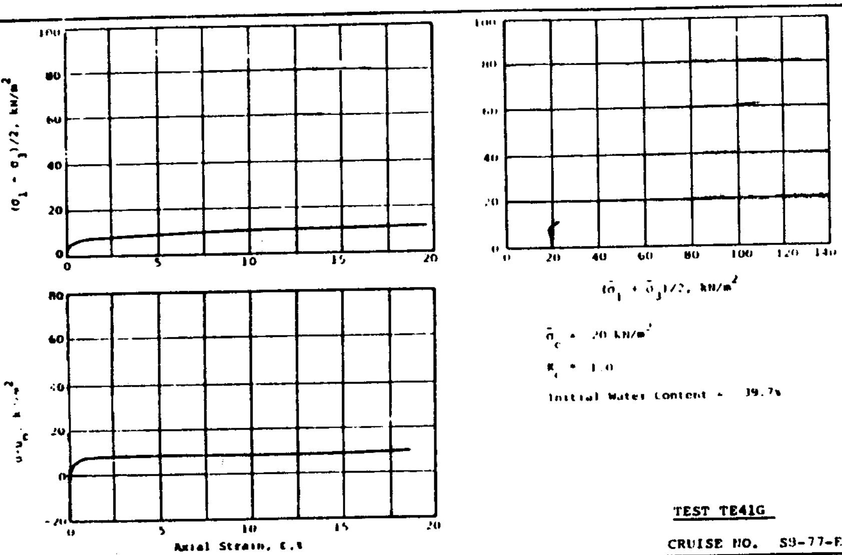

$\bar{\sigma}_c$ = 20 kN/m^2

K_c = 1.0

Initial Water Content = 39.7%

TEST TE41G

CRUISE NO. S9-77-EG

U.S. Geological Survey Denver, Colorado	Laboratory Testing of Shallow Sediments Gulf of Alaska	$\bar{K}$ TEST Sample 27G Depth 80-90 cm
Geotechnical Engineers Inc. Winchester, Massachusetts	Project 78465	August, 1978

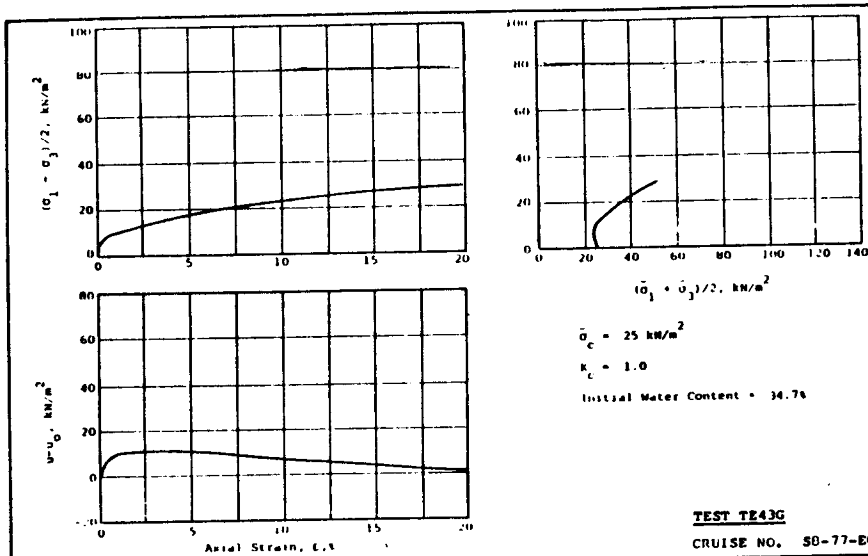

$\bar{\sigma}_c$ = 25 kN/m^2

K_c = 1.0

Initial Water Content = 34.7%

TEST TE43G

CRUISE NO. S8-77-EG

U.S. Geological Survey Denver, Colorado	Laboratory Testing of Shallow Sediments Gulf of Alaska	$\bar{K}$ TEST Sample 27G Depth 140-150 cm
Geotechnical Engineers Inc. Winchester, Massachusetts	Project 78465	August, 1978

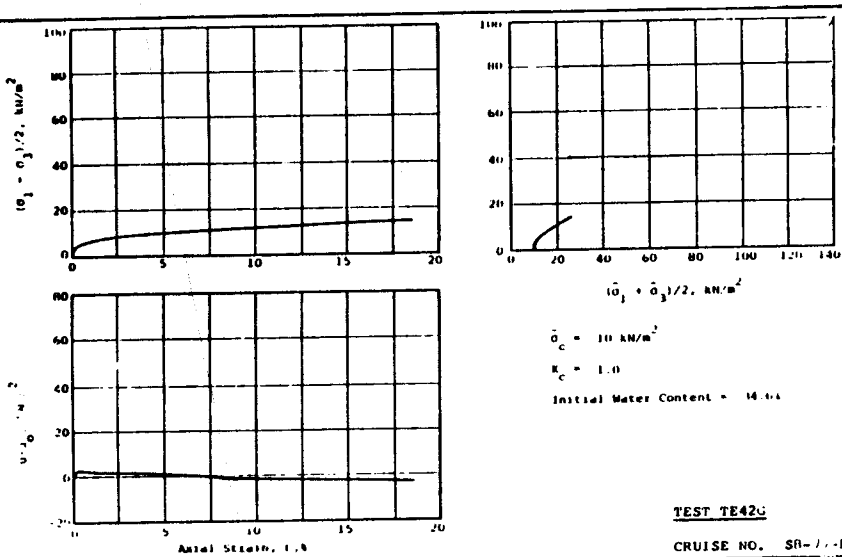

$\bar{\sigma}_c$ = 10 kN/m^2

K_c = 1.0

Initial Water Content = 34.6%

TEST TE42G

CRUISE NO. S8-77-EG

U.S. Geological Survey Denver, Colorado	Laboratory Testing of Shallow Sediments Gulf of Alaska	$\bar{K}$ TEST Sample 27G Depth 90-100 cm
Geotechnical Engineers Inc. Winchester, Massachusetts	Project 78465	August, 1978

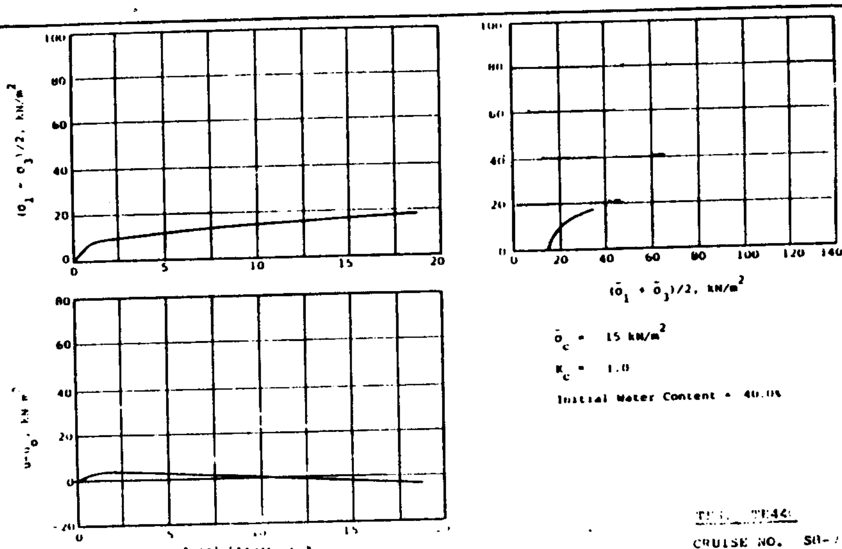

$\bar{\sigma}_c$ = 15 kN/m^2

K_c = 1.0

Initial Water Content = 40.0%

TEST TE44G

CRUISE NO. S8-77-EG

U.S. Geological Survey Denver, Colorado	Laboratory Testing of Shallow Sediments Gulf of Alaska	$\bar{K}$ TEST Sample 27G Depth 150-160 cm
Geotechnical Engineers Inc. Winchester, Massachusetts	Project 78465	August, 1978

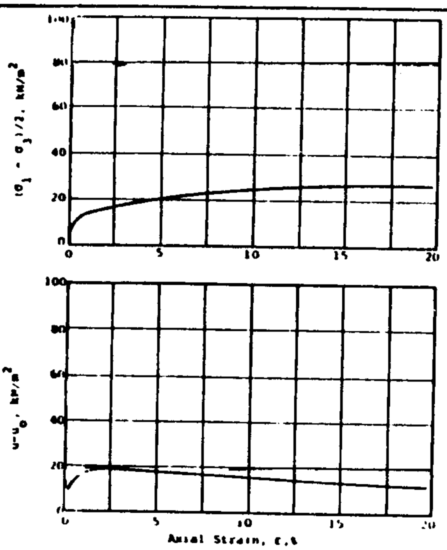

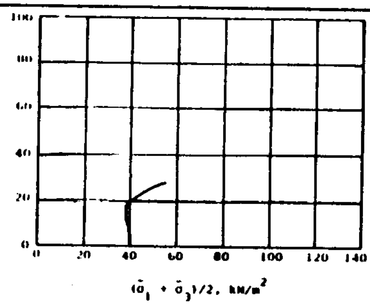

$\bar{\sigma}_c$ = 40 kN/m²

K_c = 1.0

Initial Water Content = 37.7%

TEST TE45G

CRUISE NO. SO-77-EG

U.S. Geological Survey Denver, Colorado	Laboratory Testing of Shallow Sediments Gulf of Alaska	$\bar{R}$ TEST Sample 27G Depth 180-190 cm
Geotechnical Engineers Inc. Winchester, Massachusetts	Project 7846S	August, 1978

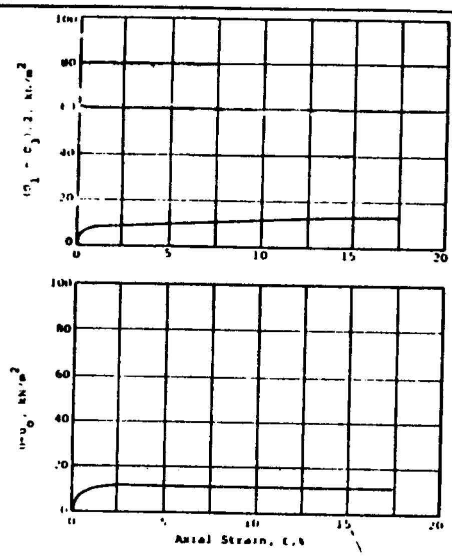

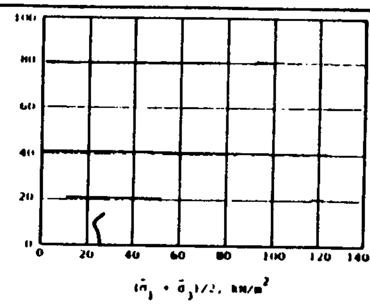

$\bar{\sigma}_c$ = 25 kN/m²

K_c = 1.0

Initial Water Content = 43.9%

TEST TE47G

CRUISE NO. SO-77-EG

U.S. Geological Survey Denver, Colorado	Laboratory Testing of Shallow Sediments Gulf of Alaska	$\bar{R}$ TEST Sample 29 G Depth 145-155 cm
Geotechnical Engineers Inc. Winchester, Massachusetts	Project 7846S	August, 1978

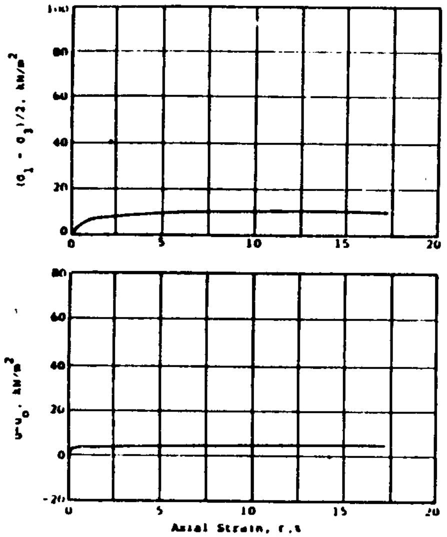

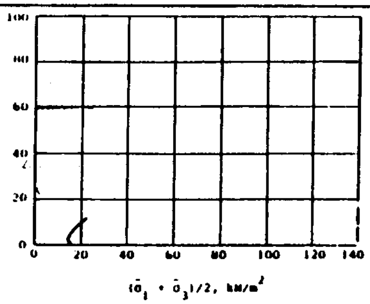

$\bar{\sigma}_c$ = 15 kN/m²

K_c = 1.0

Initial Water Content = 47.2%

TEST TE46G

CRUISE NO. SO-77-EG

U.S. Geological Survey Denver, Colorado	Laboratory Testing of Shallow Sediments Gulf of Alaska	$\bar{R}$ TEST Sample 29G Depth 135-145 cm
Geotechnical Engineers Inc. Winchester, Massachusetts	Project 7846S	August, 1978

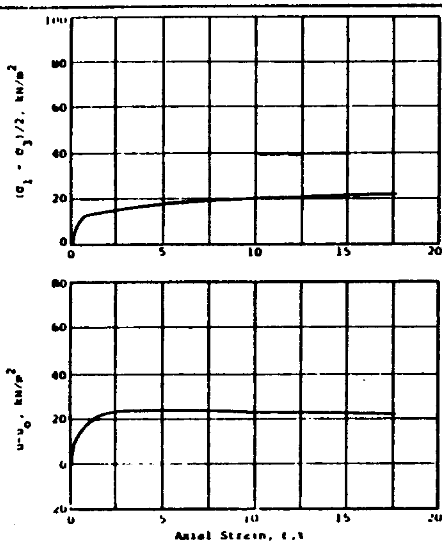

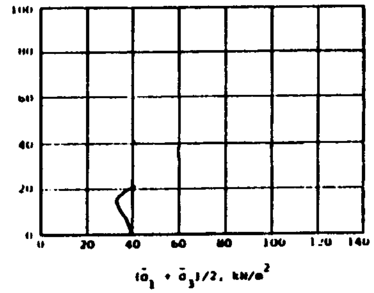

$\bar{\sigma}_c$ = 40 kN/m²

K_c = 1.0

Initial Water Content = 39.4%

TEST TE48G

CRUISE NO. SO-77-EG

U.S. Geological Survey Denver, Colorado	Laboratory Testing of Shallow Sediments Gulf of Alaska	$\bar{R}$ TEST Sample 29 G Depth 155-165 cm
Geotechnical Engineers Inc. Winchester, Massachusetts	Project 7846S	August, 1978

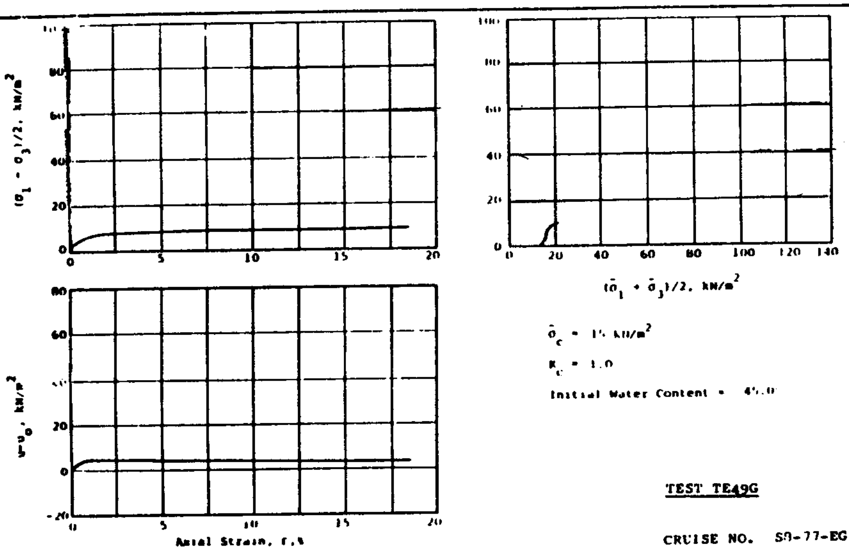

$\bar{\sigma}_c$ = 15 kN/m²

K_c = 1.0

Initial Water Content = 45.0

TEST TE49G

CRUISE NO. S8-77-EG

U.S. Geological Survey Denver, Colorado	Laboratory Testing of Shallow Sediments Gulf of Alaska	$\bar{K}$ TEST Sample 29G Depth [illegible] cm
Geotechnical Engineers Inc. Winchester, Massachusetts	Project 78465	August, 1978

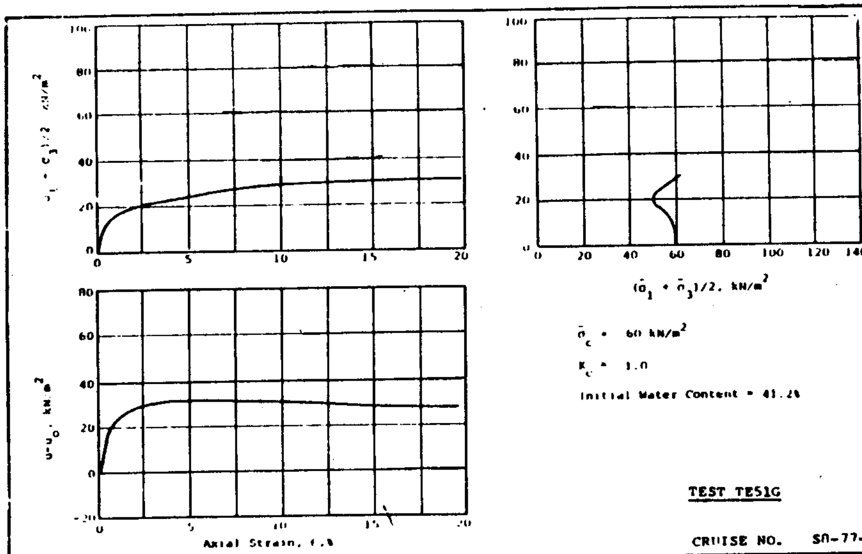

$\bar{\sigma}_c$ = 60 kN/m²

K_c = 1.0

Initial Water Content = 41.2%

TEST TE51G

CRUISE NO. S8-77-EG

U.S. Geological Survey Denver, Colorado	Laboratory Testing of Shallow Sediments Gulf of Alaska	$\bar{K}$ TEST Sample 29G Depth 340-350 cm
Geotechnical Engineers Inc. Winchester, Massachusetts	Project 78465	August, 1978

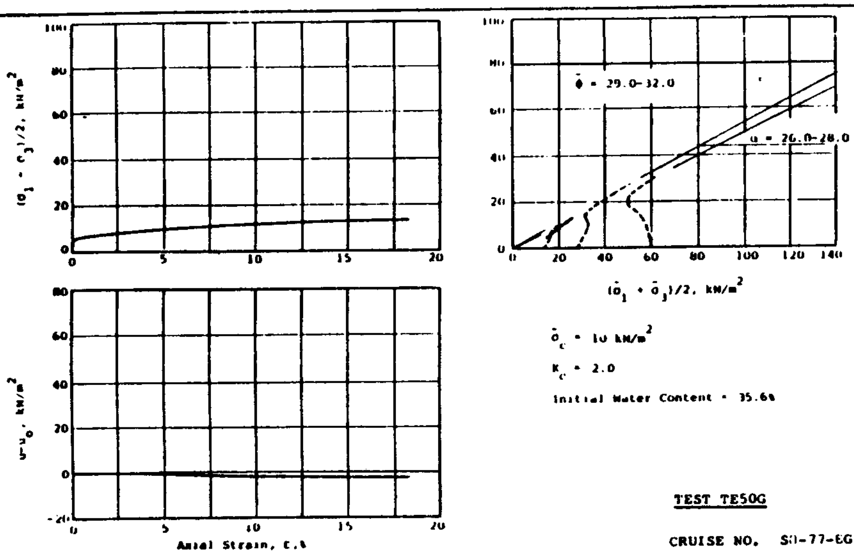

$\bar{\sigma}_c$ = 10 kN/m²

K_c = 2.0

Initial Water Content = 35.6%

TEST TE50G

CRUISE NO. S8-77-EG

NOTE: Dashed curves are taken from tests TE49G, TE51G, and TE52G.

U.S. Geological Survey Denver, Colorado	Laboratory Testing of Shallow Sediments Gulf of Alaska	$\bar{K}$ TEST Sample 29G Depth 330-340 cm
Geotechnical Engineers Inc. Winchester, Massachusetts	Project 78465	August, 1978

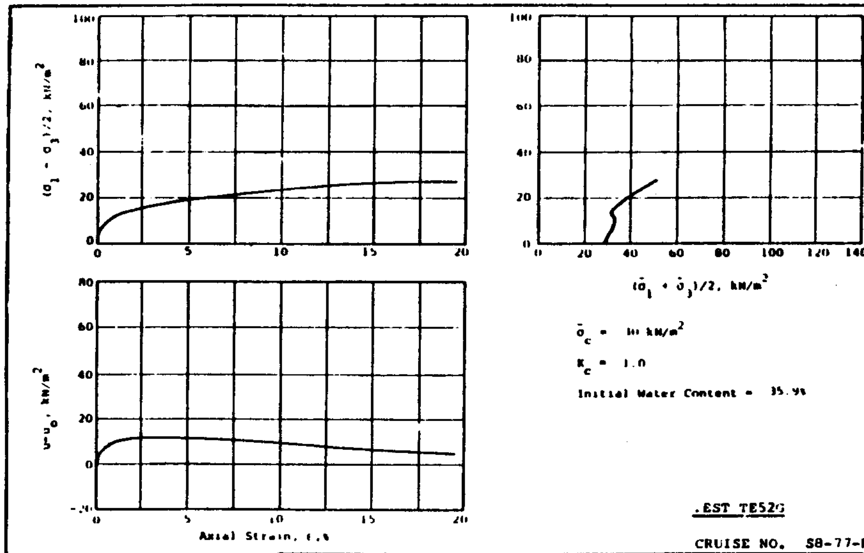

$\bar{\sigma}_c$ = 30 kN/m²

K_c = 1.0

Initial Water Content = 35.9%

TEST TE52G

CRUISE NO. S8-77-EG

U.S. Geological Survey Denver, Colorado	Laboratory Testing of Shallow Sediments Gulf of Alaska	$\bar{K}$ TEST Sample 29G Depth 350-360 cm
Geotechnical Engineers Inc. Winchester, Massachusetts	Project 78465	August, 1978

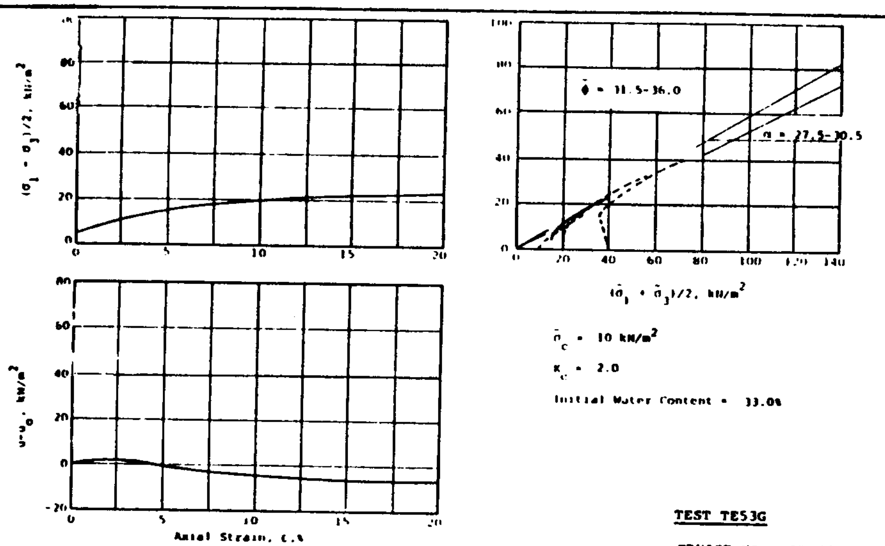

TEST TE53G

CRUISE NO. S8-77-EG

NOTE: Dashed curves are taken from Figs. 4-54, 4-55, and 4-56.

U.S. Geological Survey Denver, Colorado	Laboratory Testing of Shallow Sediments Gulf of Alaska	$\bar{R}$ TEST Sample 31 G Depth 150-160 cm
Geotechnical Engineers Inc. Winchester, Massachusetts	Project 78465	August, 1978

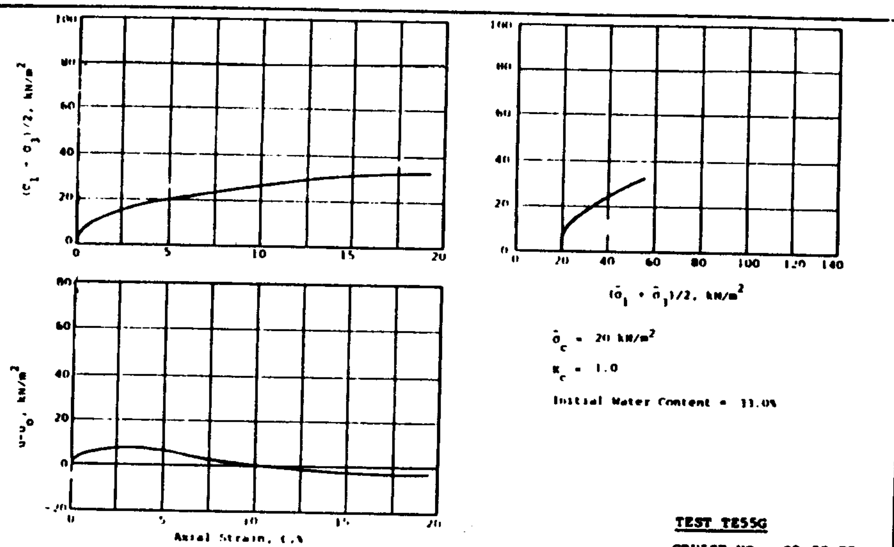

TEST TE55G

CRUISE NO. S8-77-EG

U.S. Geological Survey Denver, Colorado	Laboratory Testing of Shallow Sediments Gulf of Alaska	$\bar{R}$ TEST Sample 31 G Depth 170-180 cm
Geotechnical Engineers Inc. Winchester, Massachusetts	Project 78465	August, 1978

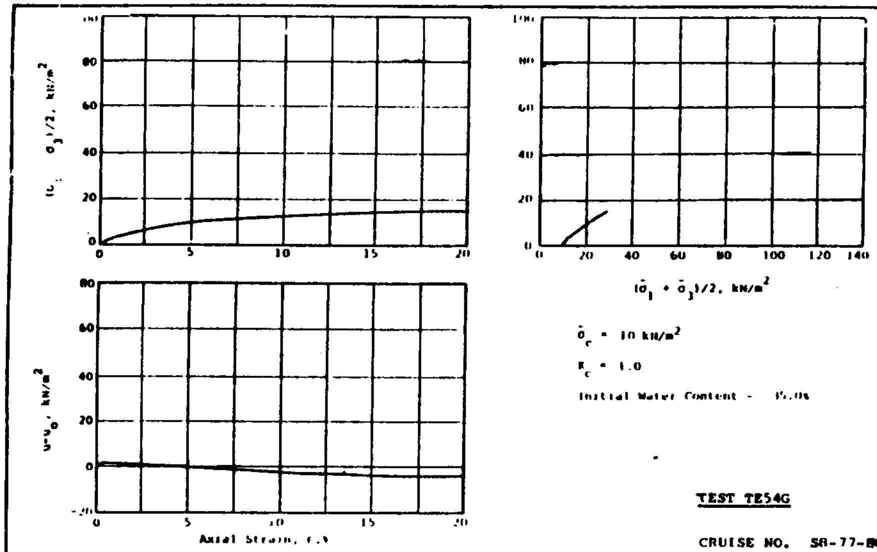

TEST TE54G

CRUISE NO. S8-77-EG

U.S. Geological Survey Denver, Colorado	Laboratory Testing of Shallow Sediments Gulf of Alaska	$\bar{R}$ TEST Sample 31 G Depth 160-170 cm
Geotechnical Engineers Inc. Winchester, Massachusetts	Project 78465	August, 1978

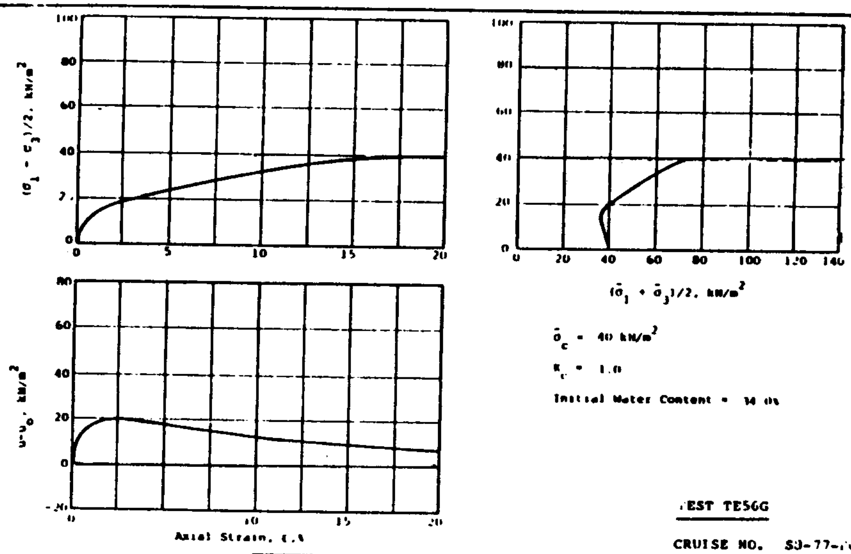

TEST TE56G

CRUISE NO. S8-77-EG

U.S. Geological Survey Denver, Colorado	Laboratory Testing of Shallow Sediments Gulf of Alaska	$\bar{R}$ TEST Sample 31 G Depth 190-200 cm
Geotechnical Engineers Inc. Winchester, Massachusetts	Project 78465	August, 1978

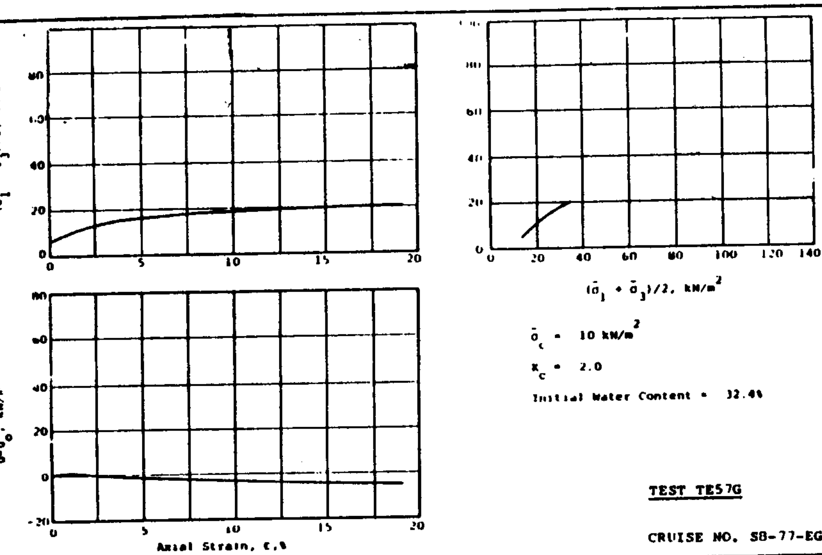

$\bar{\sigma}_c$ = 10 kN/m²

K_c = 2.0

Initial Water Content = 32.4%

TEST TE57G

CRUISE NO. S8-77-EG

U.S. Geological Survey Denver, Colorado	Laboratory Testing of Shallow Sediments Gulf of Alaska	$\bar{R}$ TEST Sample 33G Depth 290-300 cm
Geotechnical Engineers Inc. Winchester, Massachusetts	Project 78465	August, 1978

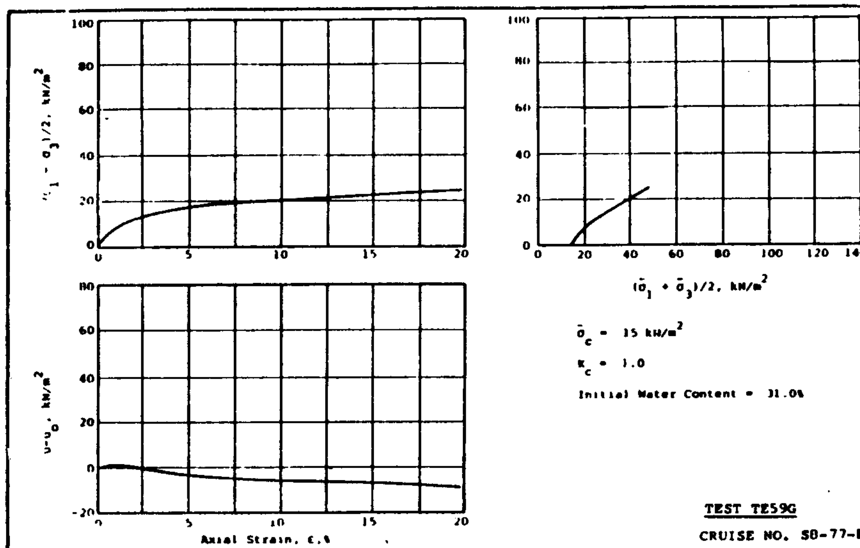

$\bar{\sigma}_c$ = 15 kN/m²

K_c = 1.0

Initial Water Content = 31.0%

TEST TE59G

CRUISE NO. S8-77-EG

U.S. Geological Survey Denver, Colorado	Laboratory Testing of Shallow Sediments Gulf of Alaska	$\bar{R}$ TEST Sample 33 G Depth 331-341 cm
Geotechnical Engineers Inc. Winchester, Massachusetts	Project 78465	August, 1978

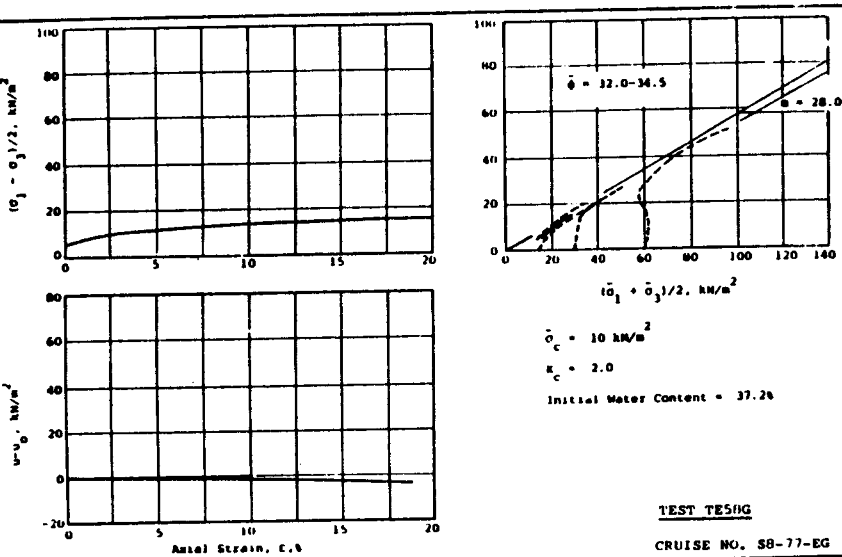

$\bar{\sigma}_c$ = 10 kN/m²

K_c = 2.0

Initial Water Content = 37.2%

TEST TE58G

CRUISE NO. S8-77-EG

NOTE: Dashed curves are taken from tests TE57G, TE59G, TE60G and TE61G.

U.S. Geological Survey Denver, Colorado	Laboratory Testing of Shallow Sediments Gulf of Alaska	$\bar{R}$ TEST Sample 33 G Depth 321-331 cm
Geotechnical Engineers Inc. Winchester, Massachusetts	Project 78465	August, 1978

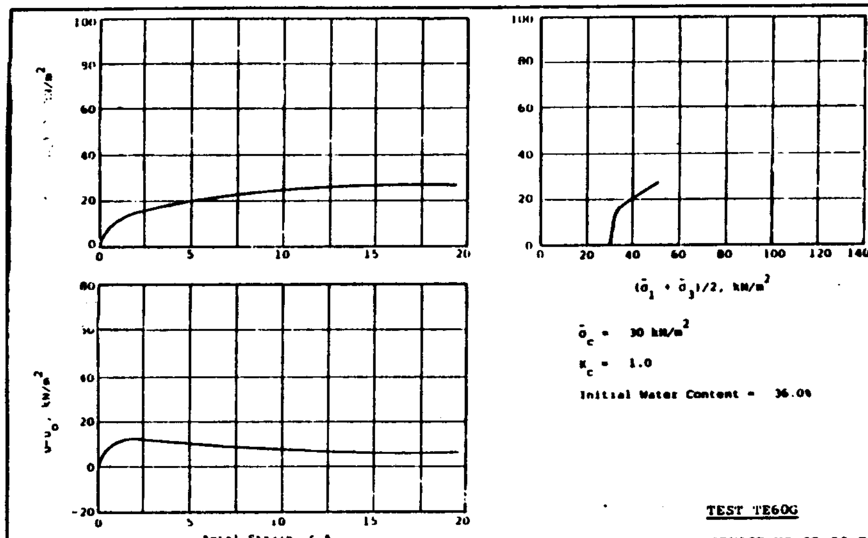

$\bar{\sigma}_c$ = 30 kN/m²

K_c = 1.0

Initial Water Content = 36.0%

TEST TE60G

CRUISE NO. S8-77-EG

U.S. Geological Survey Denver, Colorado	Laboratory Testing of Shallow Sediments Gulf of Alaska	$\bar{R}$ TEST Sample 33 G Depth 341-351 cm
Geotechnical Engineers Inc. Winchester, Massachusetts	Project 78465	August, 1978

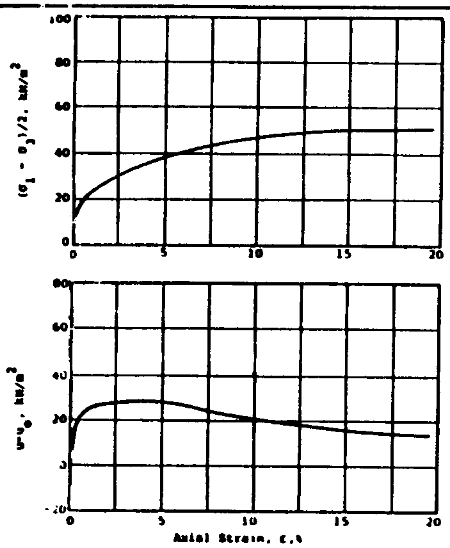

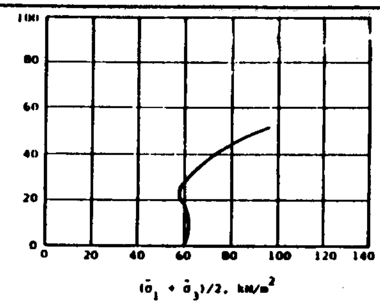

$\bar{\sigma}_c$ = 60 kN/m^2

K_c = 1.0

Initial Water Content = 33.3%

TEST TE61G

CRUISE NO. S0-77-EG

U.S. Geological Survey Denver, Colorado	Laboratory Testing of Shallow Sediments Gulf of Alaska	$\bar{R}$ TEST Sample 33G Depth 351-361 cm
Geotechnical Engineers Inc. Winchester, Massachusetts	Project 78465	August, 1978

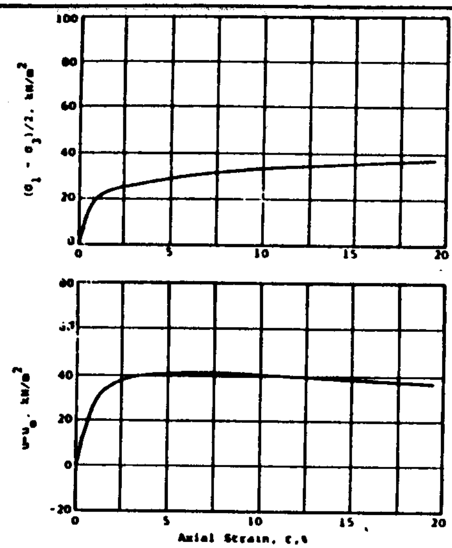

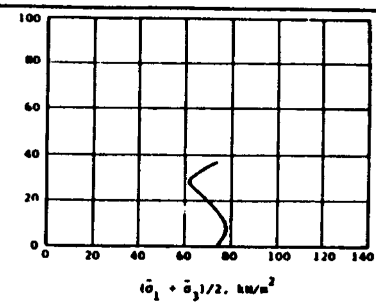

$\bar{\sigma}_c$ = 75 kN/m^2

K_c = 1.0

Initial Water Content = 43.8%

TEST TE63G

CRUISE NO. S0-77-EG

U.S. Geological Survey Denver, Colorado	Laboratory Testing of Shallow Sediments Gulf of Alaska	$\bar{R}$ TEST Sample 33G Depth 480-490 cm
Geotechnical Engineers Inc. Winchester, Massachusetts	Project 78465	August, 1978

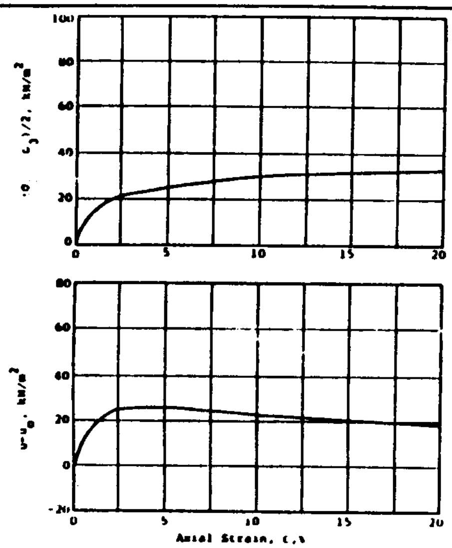

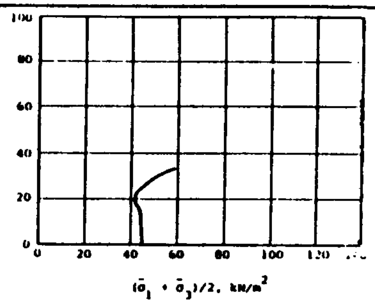

$\bar{\sigma}_c$ = 45.0 kN/m^2

K_c = 1.0

Initial Water Content = 37.5%

TEST TE62G

CRUISE NO. S0-77-EG

U.S. Geological Survey Denver, Colorado	Laboratory Testing of Shallow Sediments Gulf of Alaska	$\bar{R}$ TEST Sample 33G Depth 470-480 cm
Geotechnical Engineers Inc. Winchester, Massachusetts	Project 78465	August, 1978

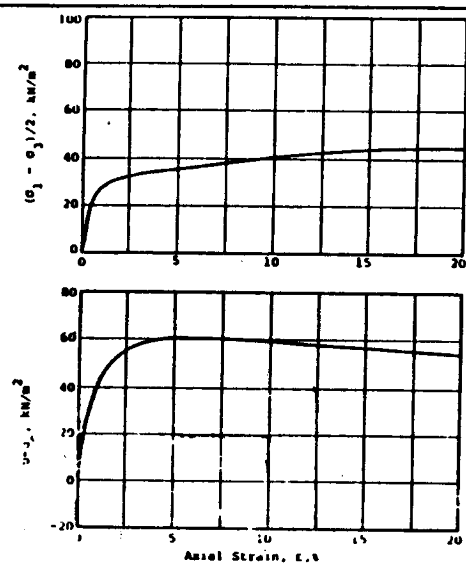

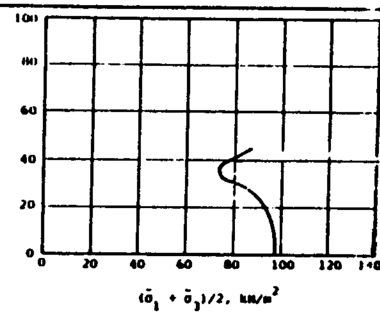

$\bar{\sigma}_c$ = 98 kN/m^2

K_c = 1.0

Initial Water Content = 40.0%

EST TE64G

CRUISE NO. S0-77-EG

U.S. Geological Survey Denver, Colorado	Laboratory Testing of Shallow Sediments Gulf of Alaska	$\bar{R}$ TEST Sample 33G Depth 490-500 cm
Geotechnical Engineers Inc. Winchester, Massachusetts	Project 78465	August, 1978

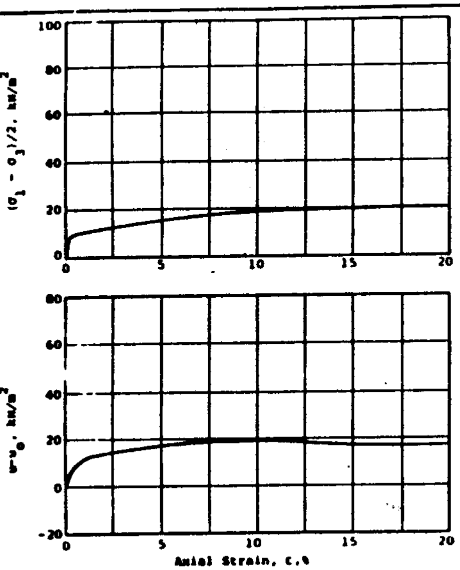

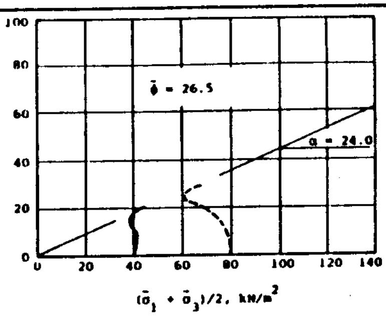

$\bar{\sigma}_c$ = 40 kN/m^2

K_c = 1.0

Initial Water Content = 49.3%

NOTE: Dashed curve is taken from test TE66G.

TEST TE65G

CRUISE NO. SB-77-EG

U.S. Geological Survey Denver, Colorado	Laboratory Testing of Shallow Sediments Gulf of Alaska	$\bar{R}$ TEST Sample 40G Depth 340-350 cm
Geotechnical Engineers Inc. Winchester, Massachusetts	Project 78465	August, 1978

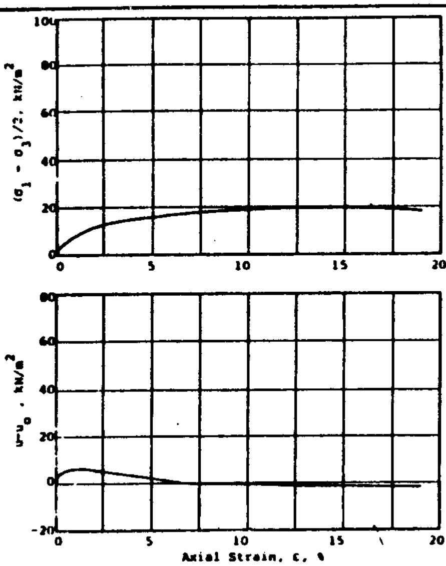

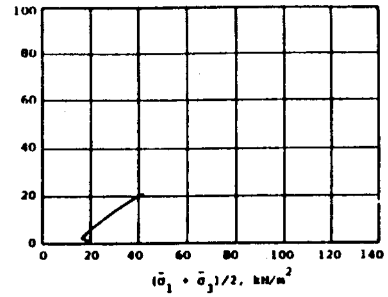

$\bar{\sigma}_c$ = 20 kN/m^2

K_c = 1.0

Initial Water Content = 41.6%

TEST TE67G

CRUISE NO. SB-77-EG

U.S. Geological Survey Denver, Colorado	Laboratory Testing of Shallow Sediments Gulf of Alaska	$\bar{R}$ TEST Sample 42 G Depth 231-245 cm
Geotechnical Engineers Inc. Winchester, Massachusetts	Project 78465	August, 1978

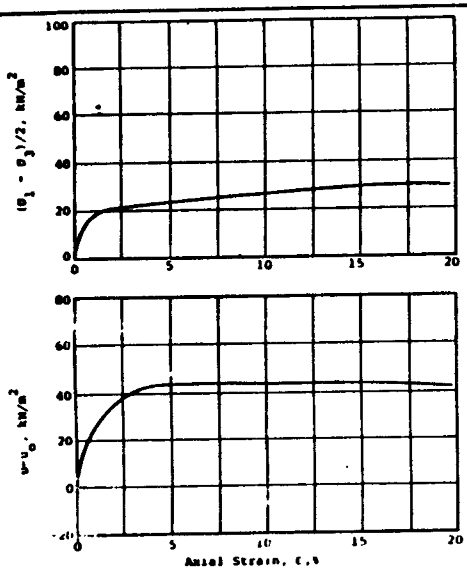

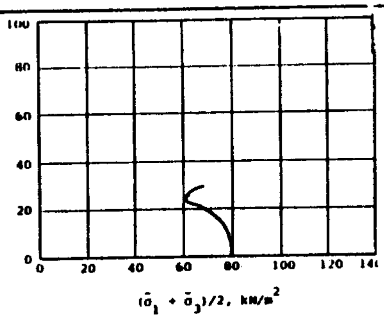

$\bar{\sigma}_c$ = 80 kN/m^2

K_c = 1.0

Initial Water Content = 51.8%

TEST TE66G

CRUISE NO. SB-77-EG

U.S. Geological Survey Denver, Colorado	Laboratory Testing of Shallow Sediments Gulf of Alaska	$\bar{R}$ TEST Sample 40G Depth 350-360 cm
Geotechnical Engineers Inc. Winchester, Massachusetts	Project 78465	August, 1978

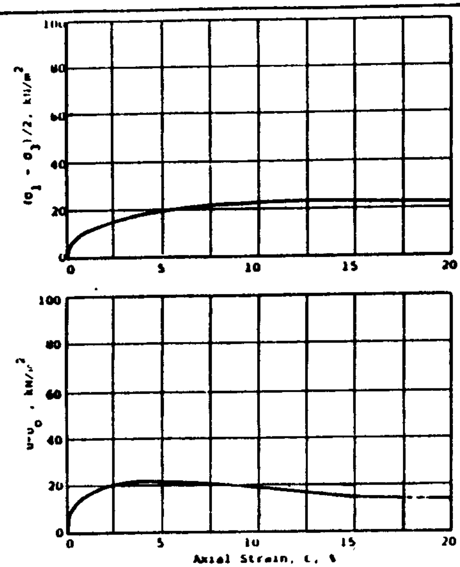

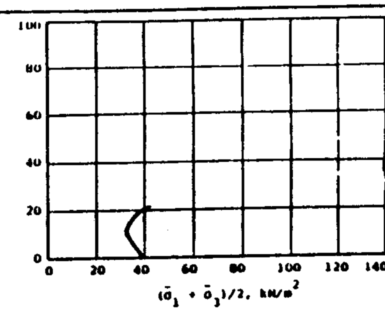

$\bar{\sigma}_c$ = 39 kN/m^2

K_c = 1.0

Initial Water Content = 43.1%

TEST TE6[illegible]G

CRUISE NO. S[illegible]7-EG

U.S. Geological Survey Denver, Colorado	Laboratory Testing of Shallow Sediments Gulf of Alaska	$\bar{R}$ TEST Sample 42 G Depth 245-250 cm
Geotechnical Engineers Inc. Winchester, Massachusetts	Project 78465	August, 1978

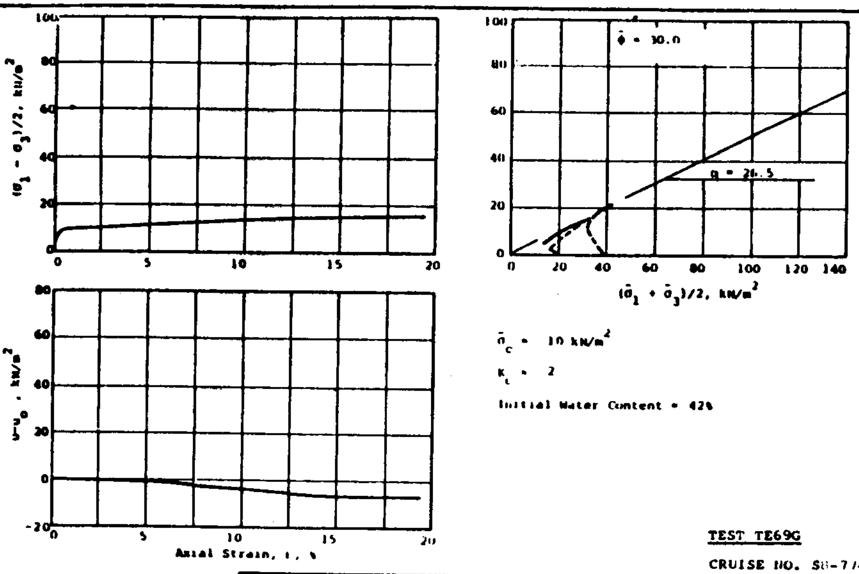

$\bar{\sigma}_c$ = 10 kN/m^2

K_c = 2

Initial Water Content = 42%

TEST TE69G

CRUISE NO. S8-77-EG

NOTE: Dashed curves are taken from tests TE67G and TE68G.

U.S. Geological Survey Denver, Colorado	Laboratory Testing of Shallow Sediments Gulf of Alaska	$\bar{R}$ TEST Sample 42 G Depth 250-270 cm
Geotechnical Engineers Inc. Winchester, Massachusetts	Project 78465	August, 1978

APPENDIX F

CONSOLIDATION AND TRIAXIAL TEST RESULTS--

LAW ENGINEERING AND TESTING COMPANY (1980 cores)

APPENDIX F. CONSOLIDATION AND TRIAXIAL TEST RESULTS-LAW ENGINEERING AND TESTING COMPANY (1980 cores)

This appendix presents the results of consolidation and triaxial testing performed by Law Engineering and Testing Company under Contract number 4-08-0001-19241 with the U.S. Geological Survey. Testing was performed under the direction of R.G. Hamadock, P.G. Swanson and P.W. Mayne. Core samples were from DC2-80-EG.

All tests in this group have been assigned a test number with L2 as the last two characters. The consolidation tests (first two characters are OE) are presented first and are ordered by test number. Results from a single test are presented on a page in the form of void ratio versus the vertical effective stress.

The static triaxial tests (first two characters are TE) are given second and ordered by test number. Results from one to as many as four tests are presented on the same sheet. The upper left plot is a stress path presented as a plot of maximum shear stress (q) versus the normal effective stress on the plane of maximum shear (p'). <u>The stress paths of Appendix D are defined differently</u>. The upper right plot is the maximum shearing stress versus the axial strain. The lower left plot is the measured excess pore water pressure plotted versus axial strain.

The cyclic triaxial tests (first two characters are TC) are given third and ordered by test number. Results from one to three tests are presented on two sheets. The first sheet includes p'-q stress path, shear stress-axial strain and excess pore pressure-axial strain plots that are analogous to the plots given for static triaxial tests. However, the plots are given for only a few selected cycles to illustrate how the response changes as the number of cycles increases. Numbers on the plots correspond to cycle number.

The second sheet shows several parameters plotted versus cycle number. The upper left graph shows the cyclic stress level normalized by the static strength (obtained from a nearby sample-Method I of the main text) versus the number of cycles to achieve a given double amplitude strain level. Lines are drawn connecting points corresponding to the same strain level. The upper right graph shows the excess pore pressure generated as a function of the cycle number. The lower right graph shows the double amplitude axial strain as a function of cycle number.

CONSOLIDATION TEST

TEST OE1L2

COMPRESSION INDEX 0.197

SWELLING INDEX 0.023

MAXIMUM PRECONSOLIDATION STRESS 22

INITIAL VOID RATIO 1.192

INITIAL WATER CONTENT 43.8

INITIAL SATURATION 100.0

DENSITY (kN/m³) 18.27

EFFECTIVE OVERBURDEN (kPa) 7.6

SAMPLE IDENTIFICATION

CRUISE NO. DC2-80-EG

CORE NO. MC3-22

DEPTH (cm) 88-02

U.S.G.S. ALASKAN CORES
CONTRACT NO. 14-08-0001-19241
LETCO PROJECT NO. W-8-2010

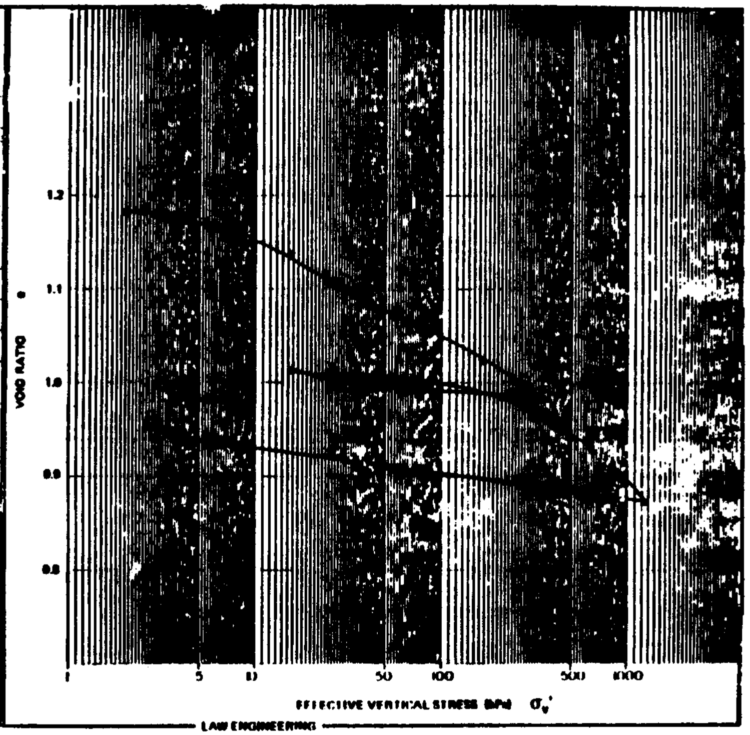

CONSOLIDATION TEST

TEST OE3L2

COMPRESSION INDEX 0.158

SWELLING INDEX 0.037

MAXIMUM PRECONSOLIDATION STRESS 30

INITIAL VOID RATIO 1.104

INITIAL WATER CONTENT 41.4

INITIAL SATURATION 100.0

DENSITY (kN/m³) 18.26

EFFECTIVE OVERBURDEN (kPa) 5.6

SAMPLE IDENTIFICATION

CRUISE NO. DC1-80 EG

CORE NO. 40 G

DEPTH (cm) 84-71

U.S.G.S. ALASKAN CORES
CONTRACT NO. 14-08-0001-19241
LETCO PROJECT NO. W-8-2010

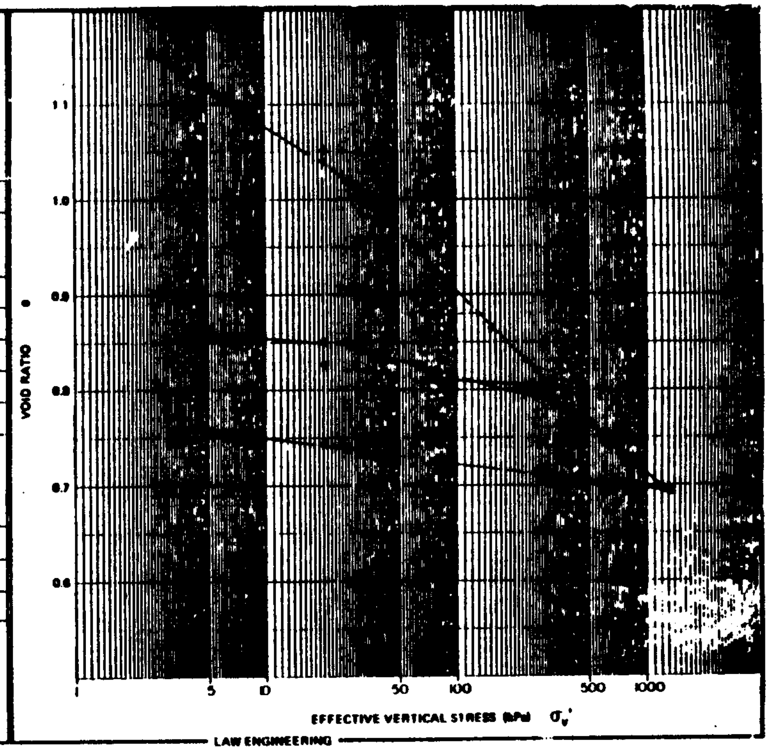

CONSOLIDATION TEST

TEST OE2L2

COMPRESSION INDEX 0.202

SWELLING INDEX 0.021

MAXIMUM PRECONSOLIDATION STRESS 22

INITIAL VOID RATIO 0.985

INITIAL WATER CONTENT 31.6

INITIAL SATURATION 91.0

DENSITY (kN/m³) 18.44

EFFECTIVE OVERBURDEN (kPa) 6.0

SAMPLE IDENTIFICATION

CRUISE NO. DC2-80 EG

CORE NO. 30 G

DEPTH (cm) 88-74

U.S.G.S. ALASKAN CORES
CONTRACT NO. 14-08-0001-19241
LETCO PROJECT NO. W-8-2010

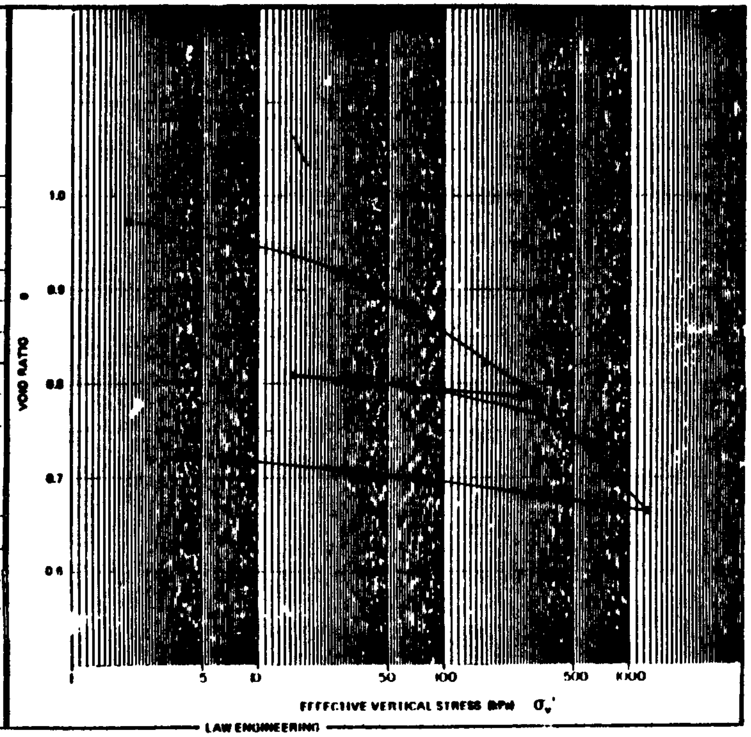

CONSOLIDATION TEST

TEST OE4L2

COMPRESSION INDEX 0.268

SWELLING INDEX 0.028

MAXIMUM PRECONSOLIDATION STRESS 26

INITIAL VOID RATIO 1.434

INITIAL WATER CONTENT 53.1

INITIAL SATURATION 100.0

DENSITY (kN/m³) 17.63

EFFECTIVE OVERBURDEN (kPa) 6.2

SAMPLE IDENTIFICATION

CRUISE NO. DC2-80EG

CORE NO. 66 G

DEPTH (cm) 74-80

U.S.G.S. ALASKAN CORES
CONTRACT NO. 14-08-0001-19241
LETCO PROJECT NO. W-8-2010

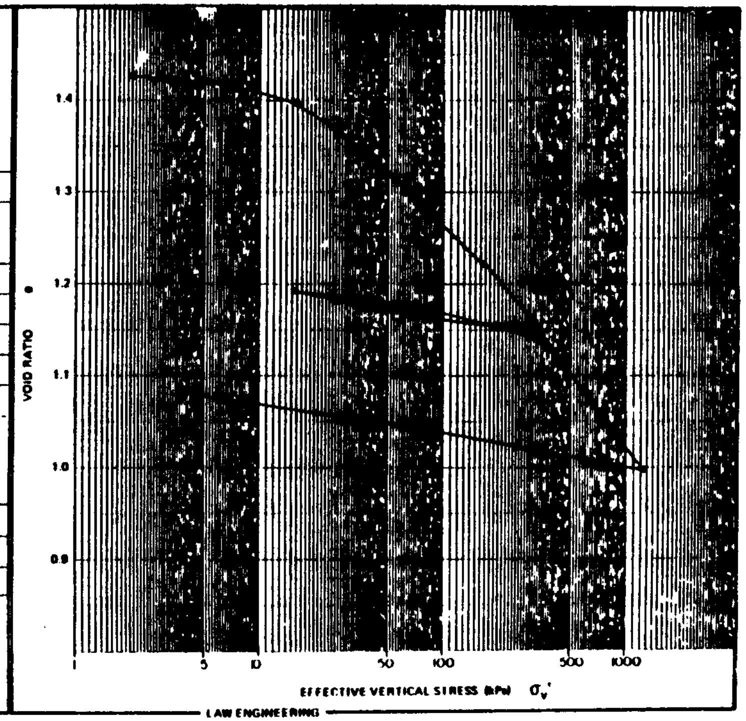

CONSOLIDATION TEST

TEST OE5L2

COMPRESSION INDEX 0.108

SWELLING INDEX 0.017

MAXIMUM PRECONSOLIDATION STRESS

INITIAL VOID RATIO 0.835

INITIAL WATER CONTENT 29.6

INITIAL SATURATION 98.9

DENSITY (kN/m³) 19.45

EFFECTIVE OVERBURDEN (kPa) 0.0

SAMPLE IDENTIFICATION

CRUISE NO. DC2-80EG

CORE NO. 84 G

DEPTH (cm) 14-21

U.S.G.S. ALASKAN CORES
CONTRACT NO. 14-08-0001-19241
LETCO PROJECT NO. W-0-2010

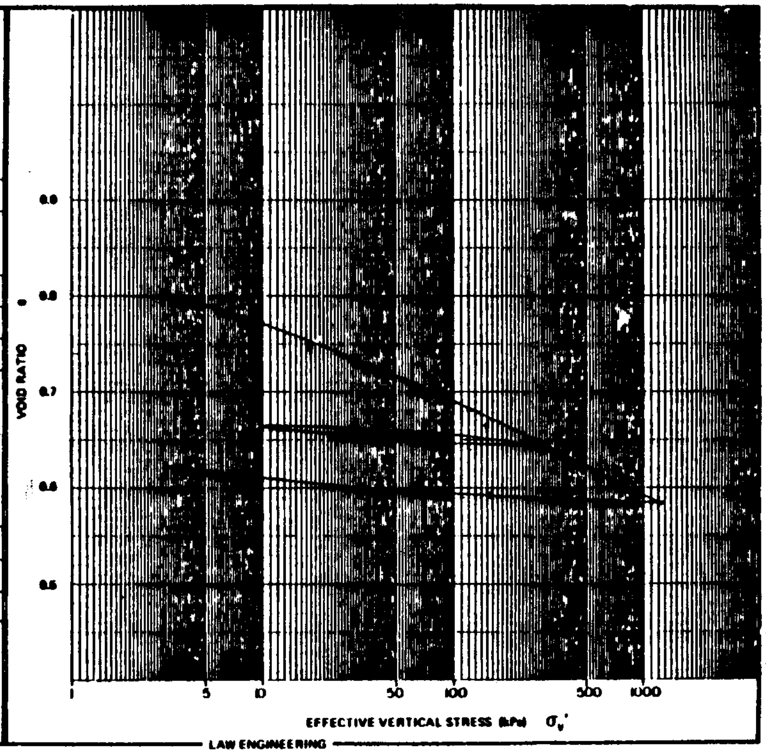

CONSOLIDATION TEST

TEST OE7L2

COMPRESSION INDEX 0.086

SWELLING INDEX 0.016

MAXIMUM PRECONSOLIDATION STRESS 60

INITIAL VOID RATIO 0.710

INITIAL WATER CONTENT 23.8

INITIAL SATURATION 86.3

DENSITY (kN/m³) 20.17

EFFECTIVE OVERBURDEN (kPa) 14.4

SAMPLE IDENTIFICATION

CRUISE NO. DC2-80EG

CORE NO. 84 G

DEPTH (cm) 200-210

U.S.G.S. ALASKAN CORES
CONTRACT NO. 14-08-0001-19241
LETCO PROJECT NO. W-0-2010

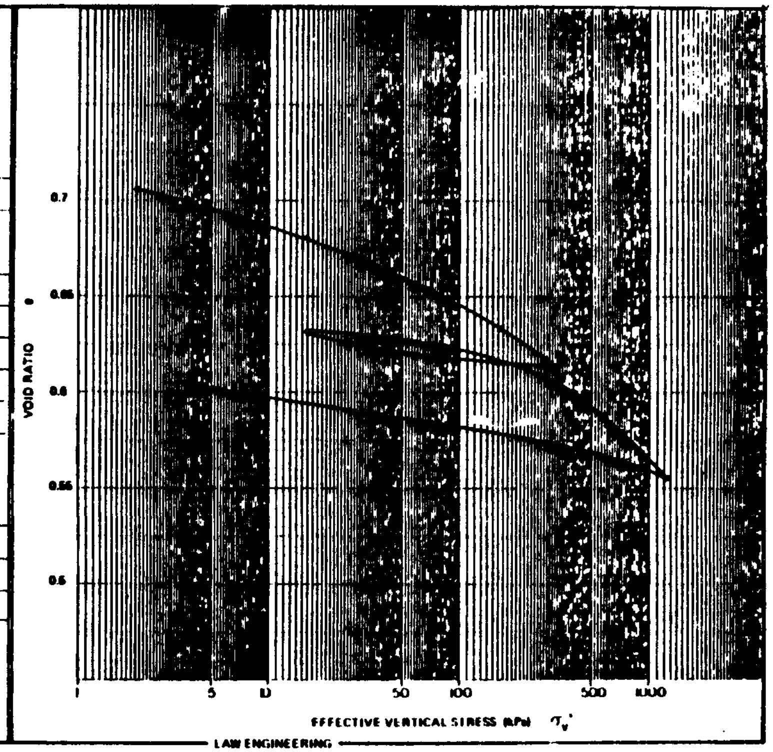

CONSOLIDATION TEST

TEST OE6L2

COMPRESSION INDEX 0.220

SWELLING INDEX 0.030

MAXIMUM PRECONSOLIDATION STRESS 20.0

INITIAL VOID RATIO 1.240

INITIAL WATER CONTENT 44.0

INITIAL SATURATION 100.0

DENSITY (kN/m³) 17.70

EFFECTIVE OVERBURDEN (kPa) 6.00

SAMPLE IDENTIFICATION

CRUISE NO. DC2-80EG

CORE NO. 84 G

DEPTH (cm) 76-84

U.S.G.S. ALASKAN CORES
CONTRACT NO. 14-08-0001-19241
LETCO PROJECT NO. W-0-2010

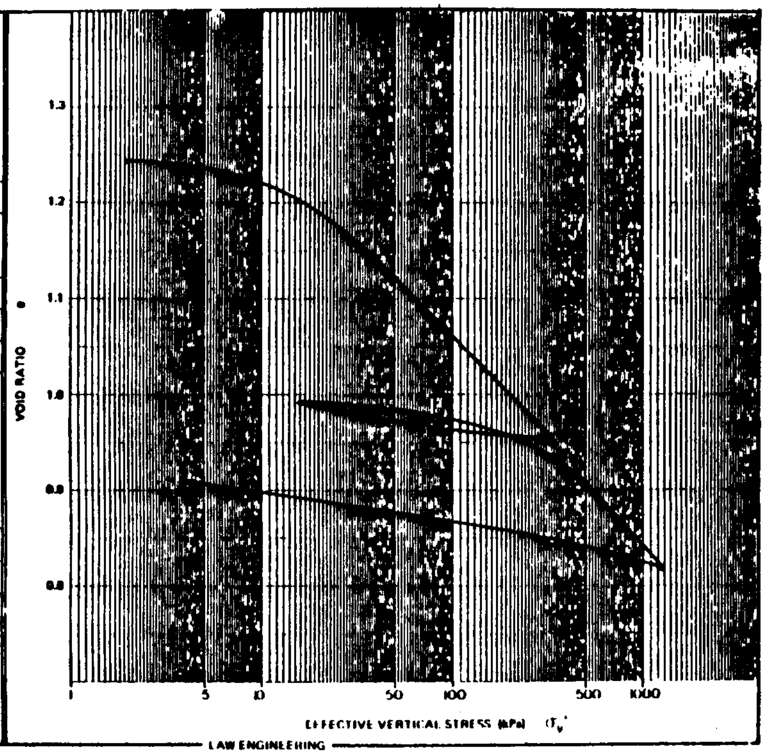

CONSOLIDATION TEST

TEST OE8L2

COMPRESSION INDEX 0.186

SWELLING INDEX 0.053

MAXIMUM PRECONSOLIDATION STRESS 10.0

INITIAL VOID RATIO 1.122

INITIAL WATER CONTENT 39.3

INITIAL SATURATION 98.0

DENSITY (kN/m³) 17.80

EFFECTIVE OVERBURDEN (kPa) 7.4

SAMPLE IDENTIFICATION

CRUISE NO. DC2-80EG

CORE NO. 86 G

DEPTH (cm) 80-86

U.S.G.S. ALASKAN CORES
CONTRACT NO. 14-08-0001-19241
LETCO PROJECT NO. W-0-2010

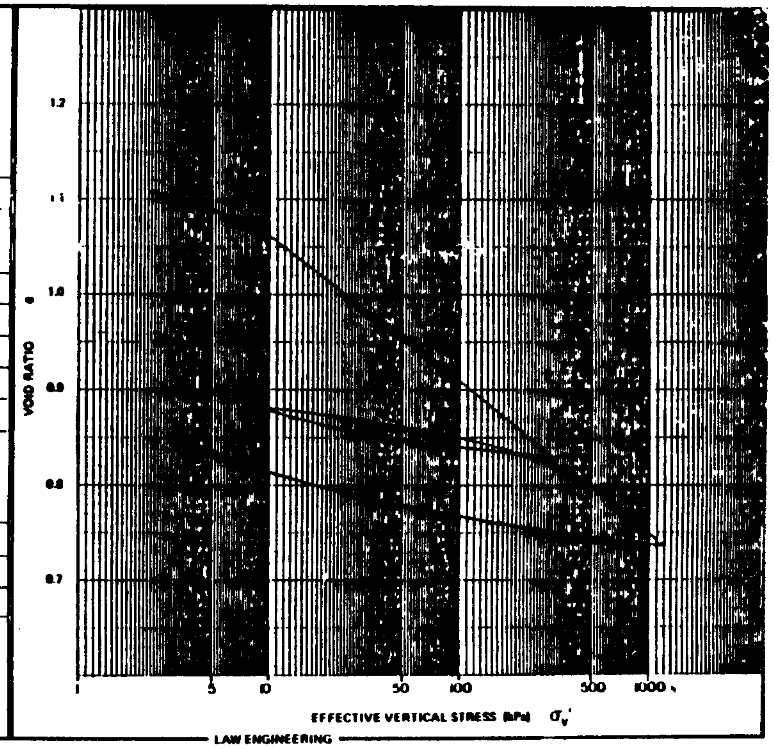

CONSOLIDATION TEST

TEST OE9L2

COMPRESSION INDEX	0.127
SWELLING INDEX	0.016
MAXIMUM PRECONSOLIDATION STRESS	120
INITIAL VOID RATIO	0.810
INITIAL WATER CONTENT	28.0
INITIAL SATURATION	88.5
DENSITY (kN/m³)	18.56
EFFECTIVE OVERBURDEN (kPa)	27.0

SAMPLE IDENTIFICATION

CRUISE NO.	DC2-80-EG
CORE NO.	86 G
DEPTH (cm)	263-271

U.S.G.S. ALASKAN CORES
CONTRACT NO. 14-08-0001-19041
LETCO PROJECT NO. W-0-2010

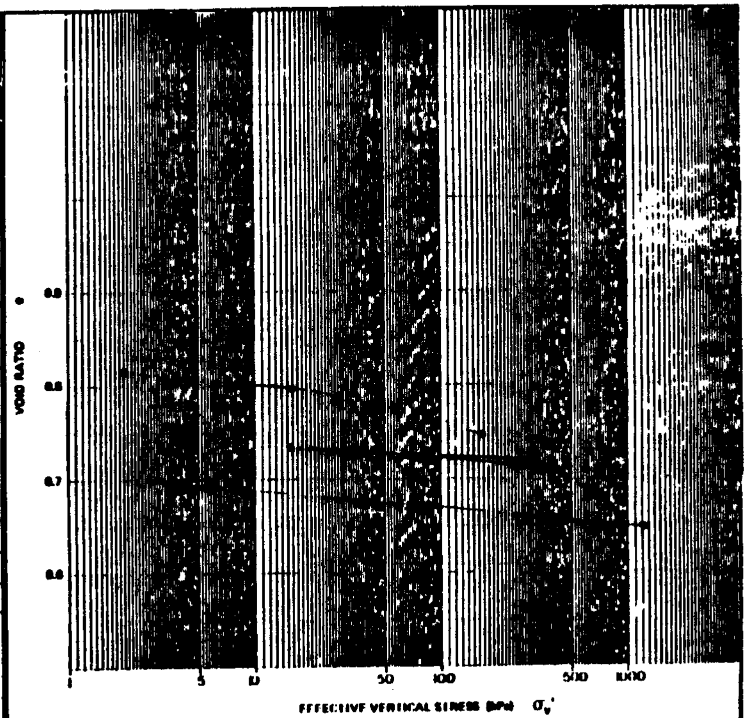

LAW ENGINEERING

CONSOLIDATION TEST

TEST OE11L2

COMPRESSION INDEX	0.135
SWELLING INDEX	0.037
MAXIMUM PRECONSOLIDATION STRESS	40.0
INITIAL VOID RATIO	1.047
INITIAL WATER CONTENT	38.0
INITIAL SATURATION	100.0
DENSITY (kN/m³)	16.[illegible]
EFFECTIVE OVERBURDEN (kPa)	[illegible]

SAMPLE IDENTIFICATION

CRUISE NO.	DC2-80EG
CORE NO.	86 G
DEPTH (cm)	375-381

U.S.G.S. ALASKAN CORES
CONTRACT NO. 14-08-0001-19041
LETCO PROJECT NO. W-0-2010

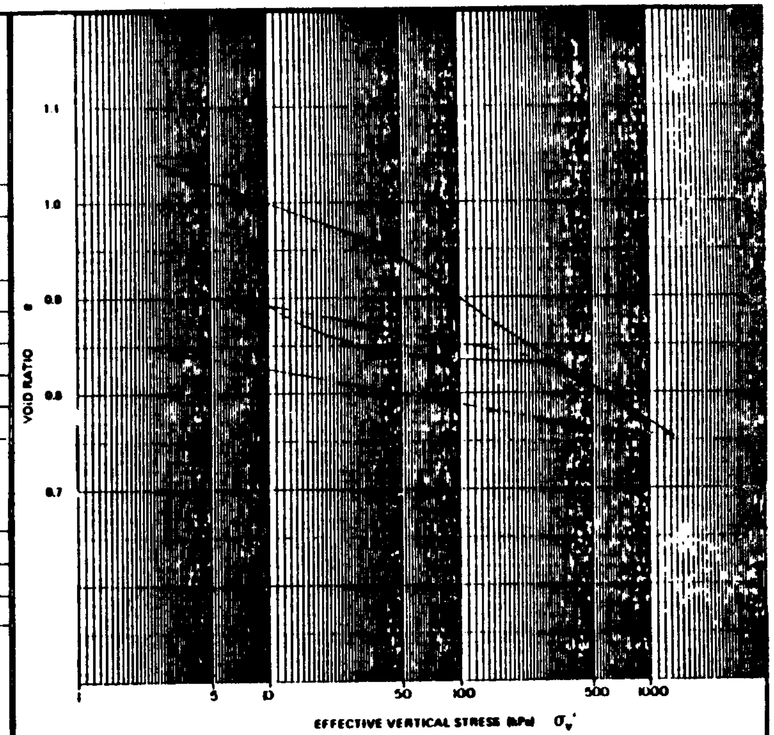

LAW ENGINEERING

CONSOLIDATION TEST

TEST OE10L2

COMPRESSION INDEX	0.171
SWELLING INDEX	0.022
MAXIMUM PRECONSOLIDATION STRESS	31.0
INITIAL VOID RATIO	0.864
INITIAL WATER CONTENT	32.7
INITIAL SATURATION	98.8
DENSITY (kN/m³)	18.82
EFFECTIVE OVERBURDEN (kPa)	30.0

SAMPLE IDENTIFICATION

CRUISE NO.	DC2-80EG
CORE NO.	86 G
DEPTH (cm)	354-361

U.S.G.S. ALASKAN CORES
CONTRACT NO. 14-08-0001-19041
LETCO PROJECT NO. W-0-2010

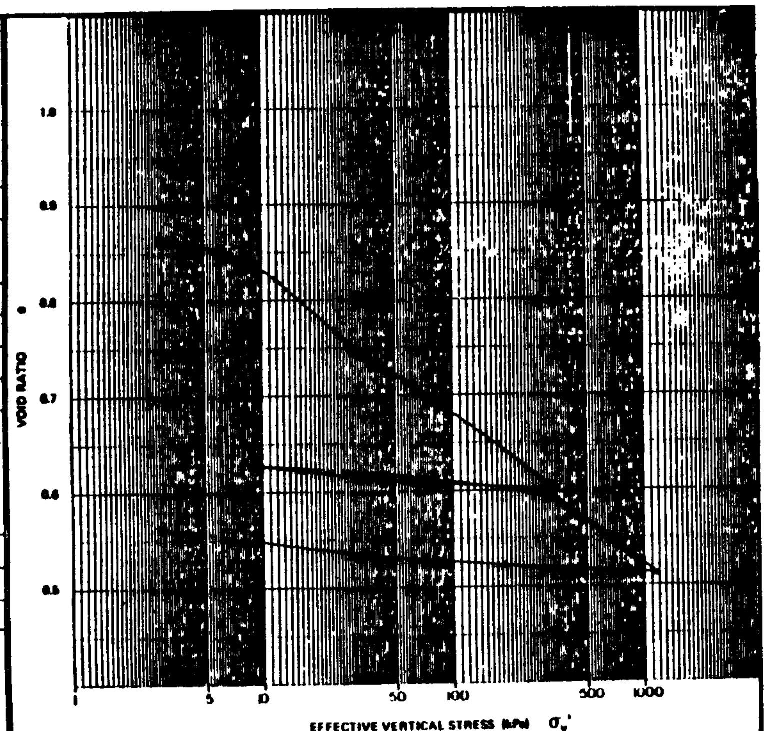

LAW ENGINEERING

CONSOLIDATION TEST

TEST OE12L2

COMPRESSION INDEX	0.186
SWELLING INDEX	0.017
MAXIMUM PRECONSOLIDATION STRESS	70
INITIAL VOID RATIO	0.934
INITIAL WATER CONTENT	31.48
INITIAL SATURATION	86.3
DENSITY (kN/m³)	18.86
EFFECTIVE OVERBURDEN (kPa)	3.2

SAMPLE IDENTIFICATION

CRUISE NO.	DC2-80-EG
CORE NO.	190 G
DEPTH (cm)	30-38

U.S.G.S. ALASKAN CORES
CONTRACT NO. 14-08-0001-19041
LETCO PROJECT NO. W-0-2010

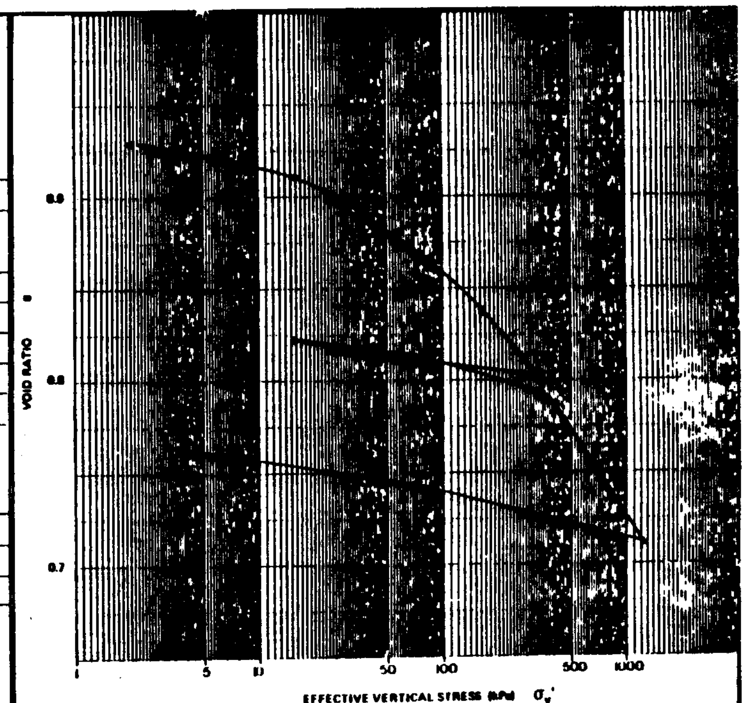

LAW ENGINEERING

CONSOLIDATION TEST

TEST OE13L2

COMPRESSION INDEX 0.206
SWELLING INDEX 0.028
MAXIMUM PRECONSOLIDATION STRESS 46.0
INITIAL VOID RATIO 1.052
INITIAL WATER CONTENT 40.7
INITIAL SATURATION 100.0
DENSITY (kN/m³) 18.22
EFFECTIVE OVERBURDEN (kPa) 18.8

SAMPLE IDENTIFICATION

CRUISE NO. DC-2-80EG
CORE NO. 190 G
DEPTH (cm) 220-227

U.S.G.S. ALASKAN CORES
CONTRACT NO. 14-08-0001-19041
LETCO PROJECT NO. W-0-2010

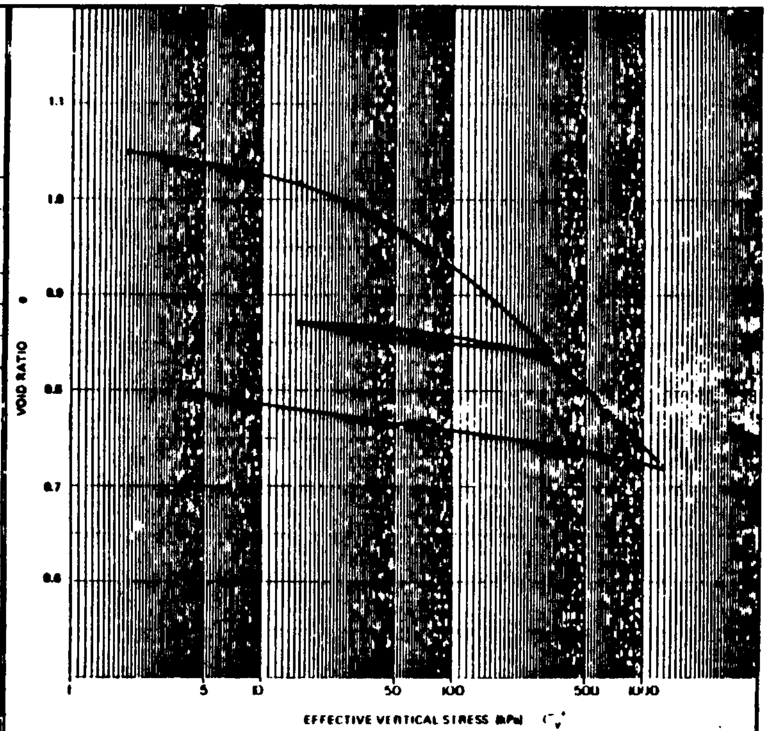

CONSOLIDATION TEST

TEST OE15L2

COMPRESSION INDEX 0.103
SWELLING INDEX 0.031
MAXIMUM PRECONSOLIDATION STRESS 23.0
INITIAL VOID RATIO 0.779
INITIAL WATER CONTENT 28.6
INITIAL SATURATION 100.0
DENSITY (kN/m³) 19.96
EFFECTIVE OVERBURDEN (kPa) 14.2

SAMPLE IDENTIFICATION

CRUISE NO. DC2-80EG
CORE NO. 196 G
DEPTH (cm) 142-148

U.S.G.S. ALASKAN CORES
CONTRACT NO. 14-08-0001-19041
LETCO PROJECT NO. W-0-2010

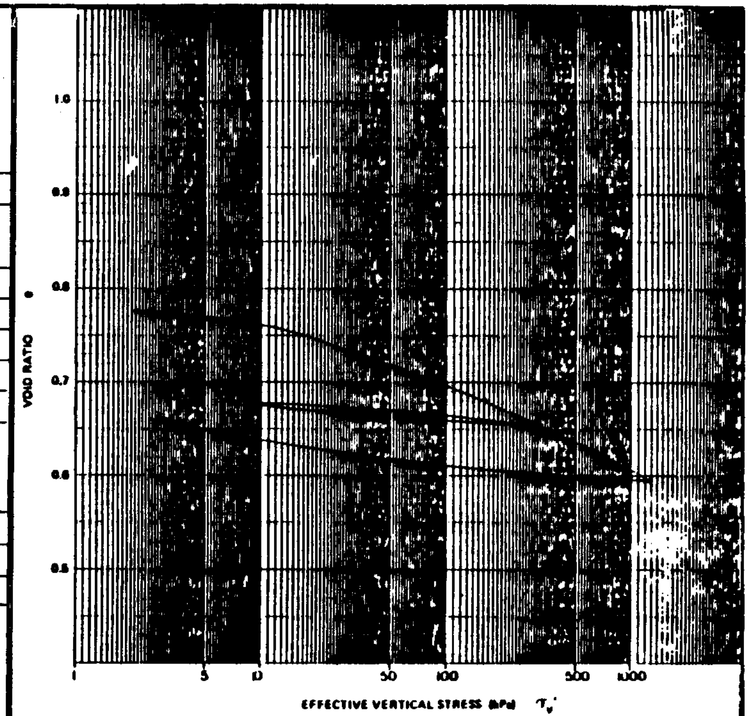

CONSOLIDATION TEST

TEST OE14L2

COMPRESSION INDEX 0.211
SWELLING INDEX 0.064
MAXIMUM PRECONSOLIDATION STRESS 50.0
INITIAL VOID RATIO 1.071
INITIAL WATER CONTENT 38.0
INITIAL SATURATION 97.6
DENSITY (kN/m³) 17.98
EFFECTIVE OVERBURDEN (kPa) 23.2

SAMPLE IDENTIFICATION

CRUISE NO. DC2-80EG
CORE NO. 190 G
DEPTH (cm) 281-288

U.S.G.S. ALASKAN CORES
CONTRACT NO. 14-08-0001-19041
LETCO PROJECT NO. W-0-2010

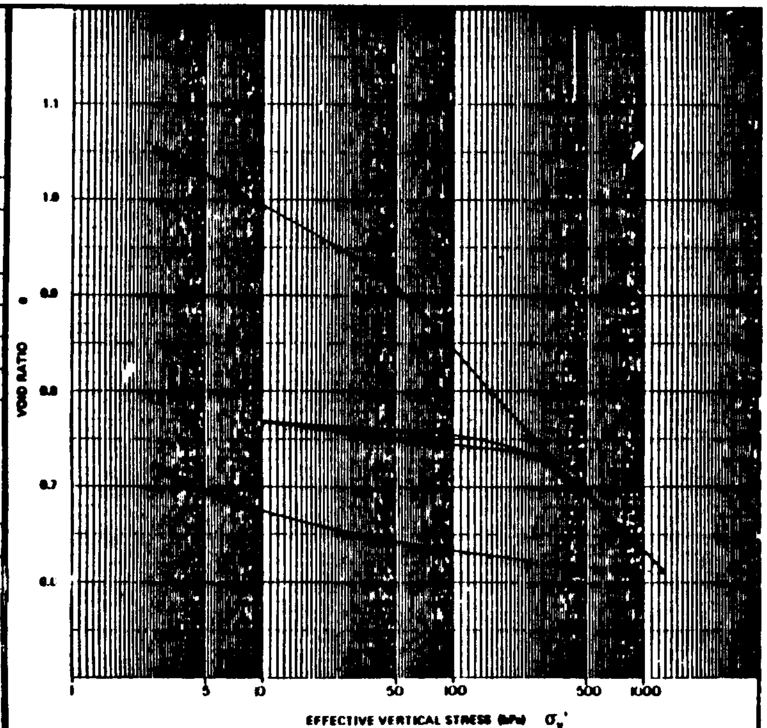

CONSOLIDATION TEST

TEST OE16L2

COMPRESSION INDEX 0.120
SWELLING INDEX 0.021
MAXIMUM PRECONSOLIDATION STRESS 140
INITIAL VOID RATIO 0.701
INITIAL WATER CONTENT 26.7
INITIAL SATURATION 100.0
DENSITY (kN/m³) 18.80
EFFECTIVE OVERBURDEN (kPa) 25.2

SAMPLE IDENTIFICATION

CRUISE NO. DC2-80EG
CORE NO. 196 G
DEPTH (cm) 248-256

U.S.G.S. ALASKAN CORES
CONTRACT NO. 14-08-0001-19041
LETCO PROJECT NO. W-0-2010

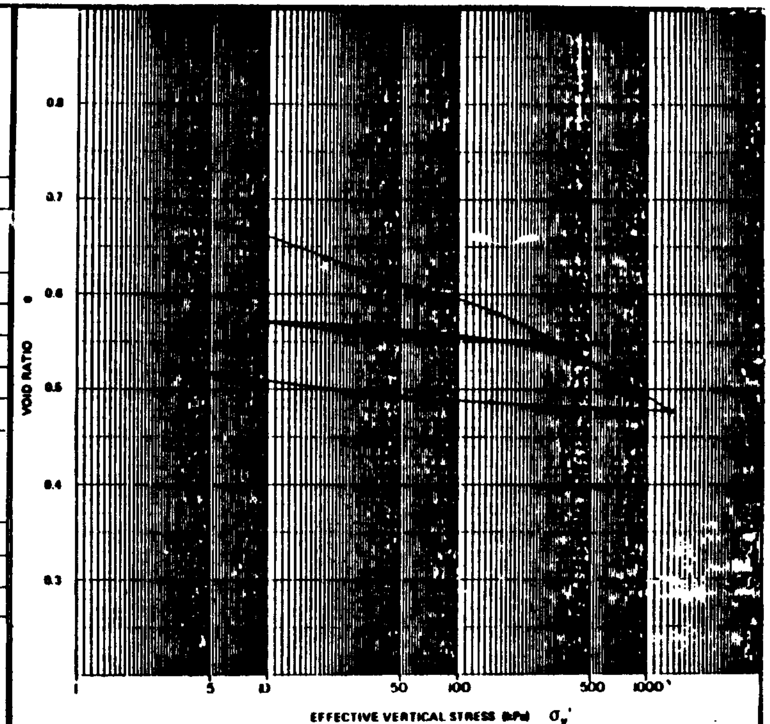

CONSOLIDATION TEST

TEST OE17L2

COMPRESSION INDEX	0.100
SWELLING INDEX	0.027
MAXIMUM PRECONSOLIDATION STRESS	120.0
INITIAL VOID RATIO	0.682
INITIAL WATER CONTENT	21.9
INITIAL SATURATION	91.4
DENSITY (kN/m³)	20.20
EFFECTIVE OVERBURDEN (kPa)	46.8

SAMPLE IDENTIFICATION

CRUISE NO.	DC2 80EG
CORE NO.	196 G
DEPTH (cm)	436-439

U.S.G.S. ALASKAN CORES
CONTRACT NO. 14-08-0001-19001
LETCO PROJECT NO. W-0-2010

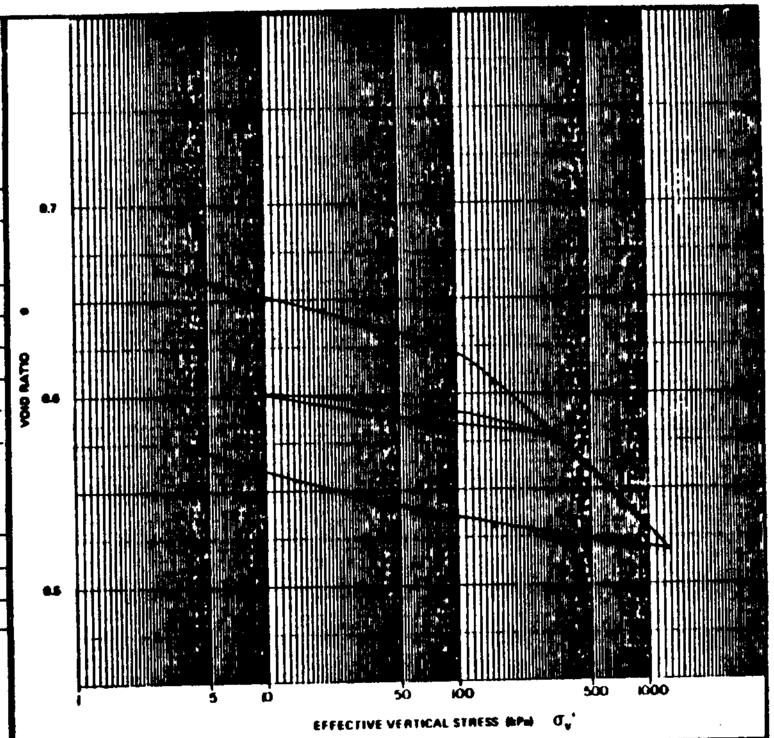

LAW ENGINEERING

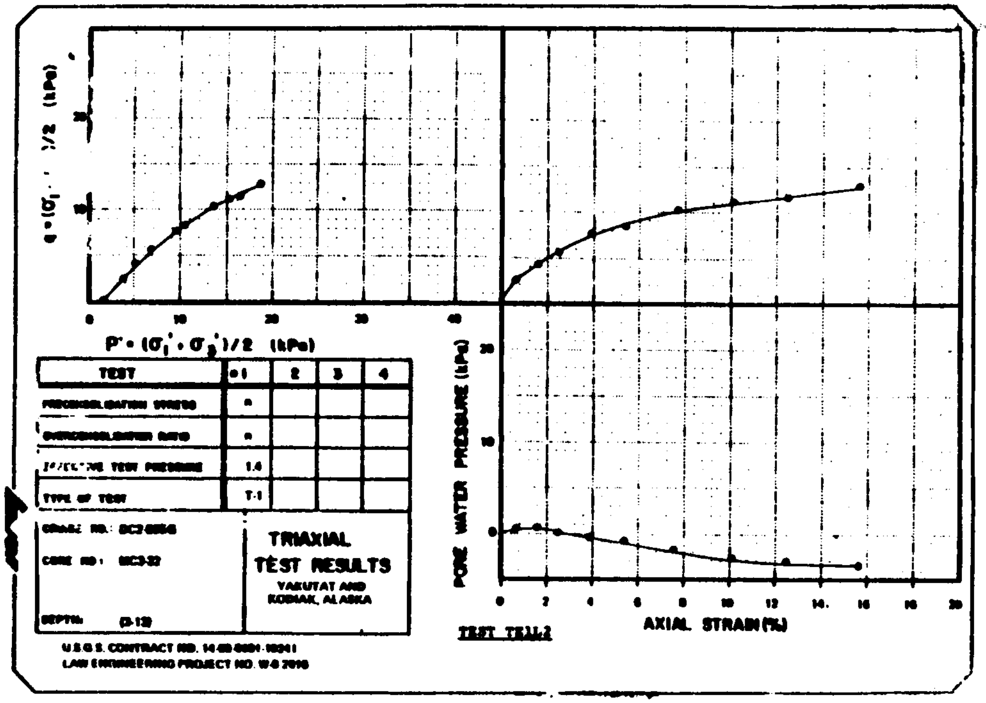

TEST	●1	2	3	4
PRECONSOLIDATION STRESS	n			
OVERCONSOLIDATION RATIO	n			
EFFECTIVE TEST PRESSURE	1.4			
TYPE OF TEST	T-1			

CRUISE NO.: DC2-80EG
CORE NO.: MC3-22
DEPTH: (3-13)

TRIAXIAL TEST RESULTS
YAKUTAT AND KODIAK, ALASKA

U.S.G.S. CONTRACT NO. 14-08-0001-18241
LAW ENGINEERING PROJECT NO. W-8 2010

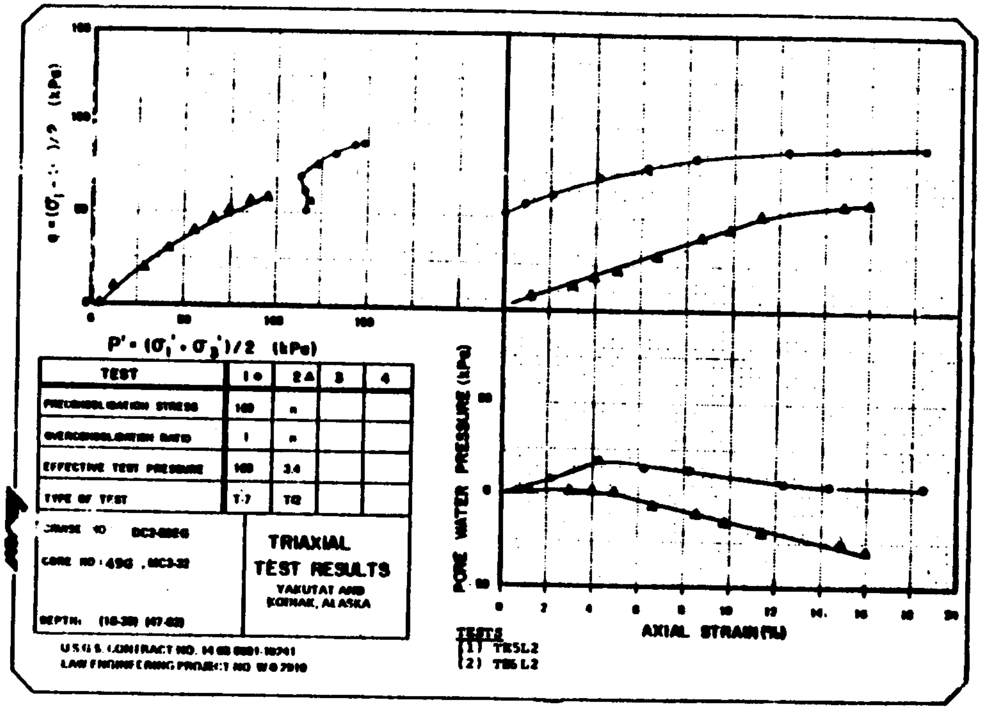

TEST	1●	2▲	3	4
PRECONSOLIDATION STRESS	100	n		
OVERCONSOLIDATION RATIO	1	n		
EFFECTIVE TEST PRESSURE	100	3.4		
TYPE OF TEST	T-7	T12		

CRUISE NO. DC2-80EG
CORE NO: 49G, MC3-22
DEPTH: (10-20) (47-60)

TRIAXIAL TEST RESULTS
YAKUTAT AND KODIAK, ALASKA

U.S.G.S. CONTRACT NO. 14-08-0001-18241
LAW ENGINEERING PROJECT NO. W-8 2010

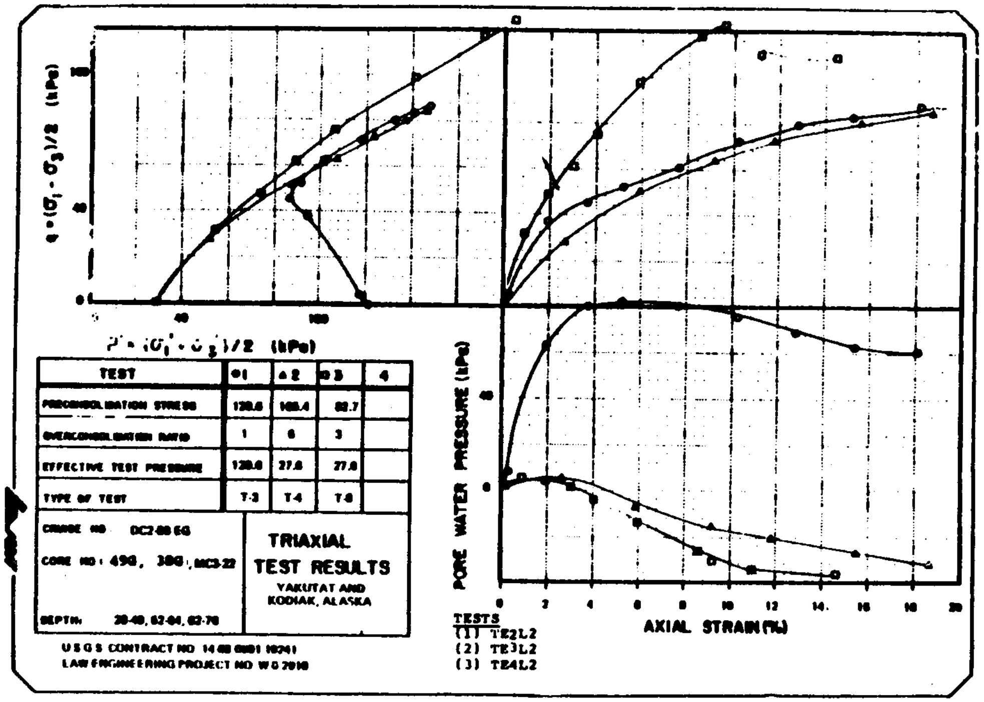

TEST	●1	▲2	▫3	4
PRECONSOLIDATION STRESS	120.6	100.4	82.7	
OVERCONSOLIDATION RATIO	1	6	3	
EFFECTIVE TEST PRESSURE	120.6	27.6	27.6	
TYPE OF TEST	T-3	T-4	T-6	

CRUISE NO. DC2-80EG
CORE NO: 49G, 38G, MC3-22
DEPTH: 20-40, 62-64, 62-70

TRIAXIAL TEST RESULTS
YAKUTAT AND KODIAK, ALASKA

U.S.G.S. CONTRACT NO. 14-08-0001-18241
LAW ENGINEERING PROJECT NO. W-8 2010

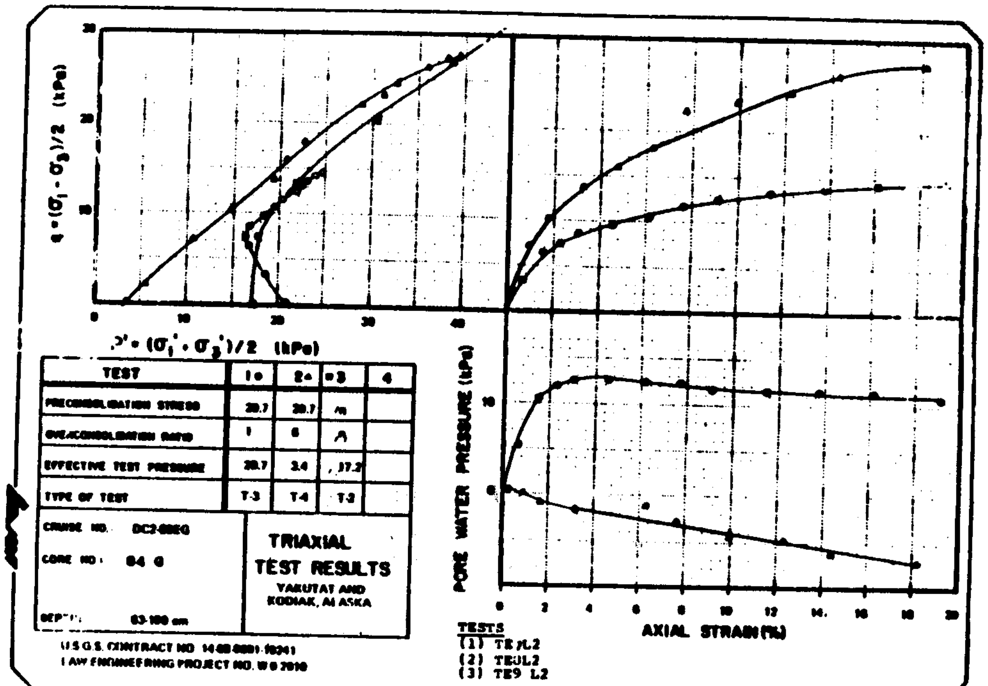

TEST	1●	2▲	▫3	4
PRECONSOLIDATION STRESS	20.7	20.7	n	
OVERCONSOLIDATION RATIO	1	6	n	
EFFECTIVE TEST PRESSURE	20.7	3.4	37.2	
TYPE OF TEST	T-3	T-4	T-2	

CRUISE NO. DC2-80EG
CORE NO: 84 G
DEPTH: 83-100 cm

TRIAXIAL TEST RESULTS
YAKUTAT AND KODIAK, ALASKA

U.S.G.S. CONTRACT NO. 14-08-0001-18241
LAW ENGINEERING PROJECT NO. W-8 2010

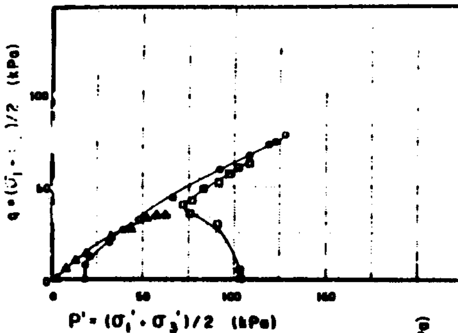

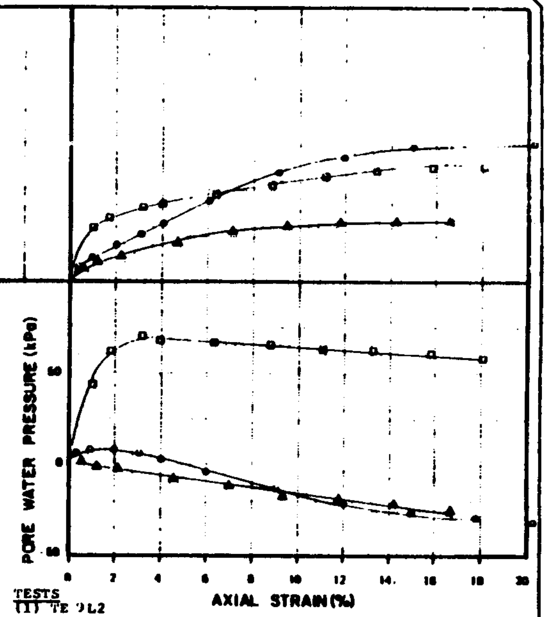

TEST	○ 1	△ 2	□ 3	4
PRECONSOLIDATION STRESS	n	n	103.3	
OVERCONSOLIDATION RATIO	n	n	1	
EFFECTIVE TEST PRESSURE	17.2	1.4	103.3	
TYPE OF TEST	T-2	T-1	T-3b	

CRUISE NO. DC2-80EG
CORE NO: 84 G
DEPTH: (100 100) (21-33 cm)

TRIAXIAL TEST RESULTS
YAKUTAT AND KODIAK, ALASKA

TESTS
(1) TE9L2
(2) TE10L2
(3) TE11L2

U.S.G.S. CONTRACT NO. 14-08-0001-19241
LAW ENGINEERING PROJECT NO. W-0-2010

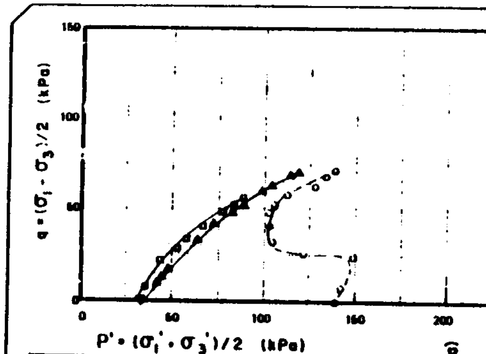

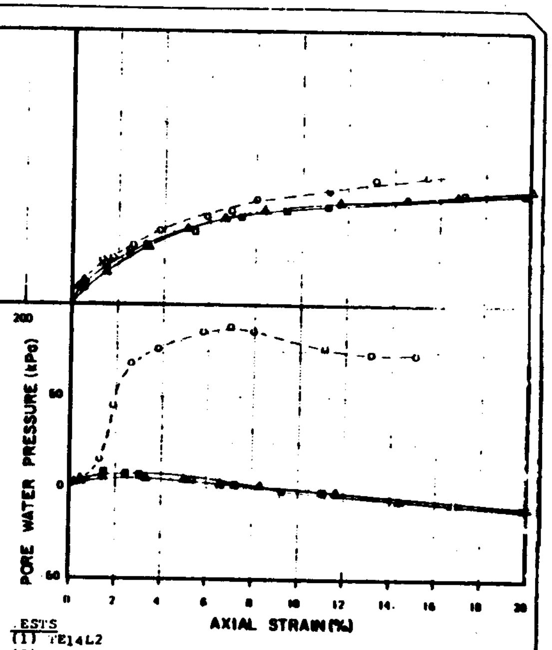

TEST	○ 1	△ 2	□ 3	4
PRECONSOLIDATION STRESS	139.8	139.8	90.9	
OVERCONSOLIDATION RATIO	1	4	3	
EFFECTIVE TEST PRESSURE	139.8	34.8	30.3	
TYPE OF TEST	T-3	T-4	T-6	

CRUISE NO. DC2-80EG
CORE NO: 96 G
DEPTH: (198-212) (303-374)

TRIAXIAL TEST RESULTS
YAKUTAT AND KODIAK, ALASKA

TESTS
(1) TE14L2
(2) TE15L2
(3) TE16L2

U.S.G.S. CONTRACT NO. 14-08-0001-19241
LAW ENGINEERING PROJECT NO. W-0-2010

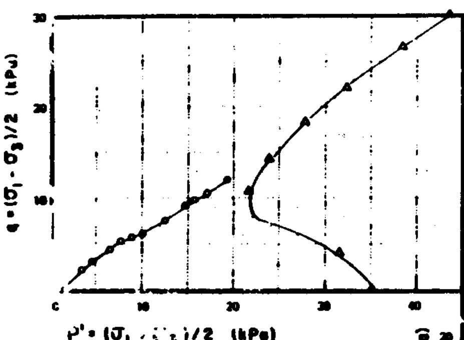

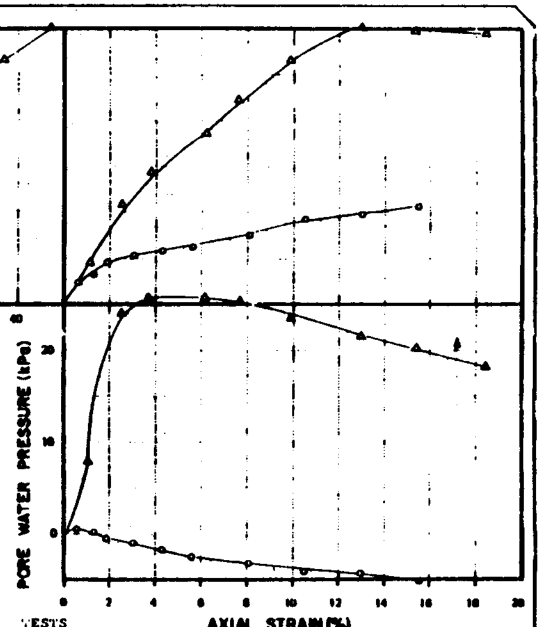

TEST	○ 1	△ 2	3	4
PRECONSOLIDATION STRESS	n	n		
OVERCONSOLIDATION RATIO	n	n		
EFFECTIVE TEST PRESSURE	1.4	35.1		
TYPE OF TEST	T-1	T-2		

CRUISE NO. DC2-80EG
CORE NO: 96 G
DEPTH: 166-183 cm

TRIAXIAL TEST RESULTS
YAKUTAT AND KODIAK, ALASKA

TESTS
(1) TE12L2
(2) TE13L2

U.S.G.S. CONTRACT NO. 14-08-0001-19241
LAW ENGINEERING PROJECT NO. W-0-2010

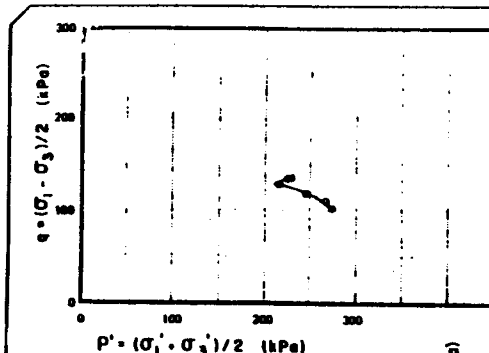

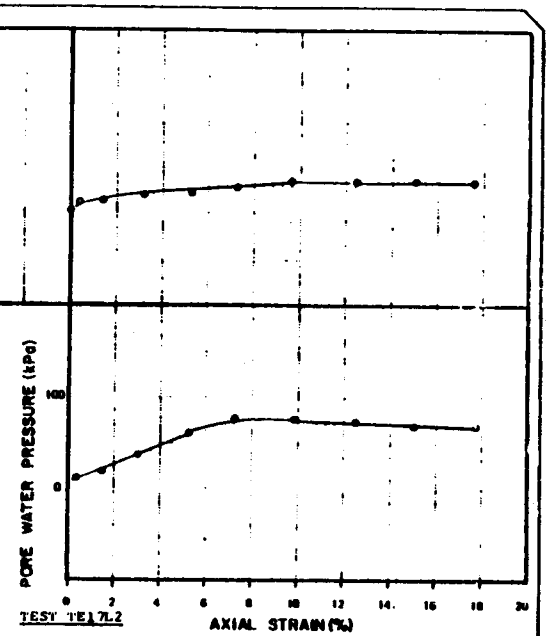

TEST	1 ●	2	3	4
PRECONSOLIDATION STRESS	370			
OVERCONSOLIDATION RATIO	1			
EFFECTIVE TEST PRESSURE	370			
TYPE OF TEST	T-7			

CRUISE NO. DC2-80EG
CORE NO: 96 G
DEPTH: 108-124

TRIAXIAL TEST RESULTS
YAKUTAT AND KODIAK, ALASKA

TEST TE17L2

U.S.G.S. CONTRACT NO. 14-08-0001-19241
LAW ENGINEERING PROJECT NO. W-0-2010

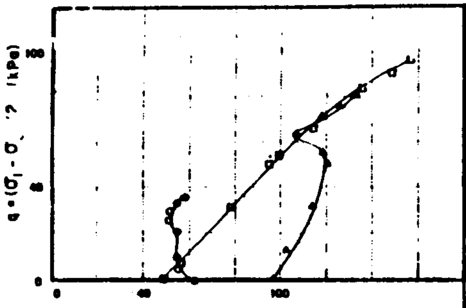

$P' = (\sigma_1' + \sigma_3')/2$ (kPa)

TEST	○ 1	▲ 2	□ 3	4
PRECONSOLIDATION STRESS	62	280	280	
OVERCONSOLIDATION RATIO	1	3	6	
EFFECTIVE TEST PRESSURE	62	96.5	46.2	
TYPE OF TEST	T-3	T-6	T-4	

CRUISE NO DC2-80-EG

CORE NO: 190 G

DEPTH: 94-126

TRIAXIAL TEST RESULTS

YAKUTAT AND KODIAK, ALASKA

U.S.G.S CONTRACT NO. 14-08-0001-19241

LAW ENGINEERING PROJECT NO. W-0-7910

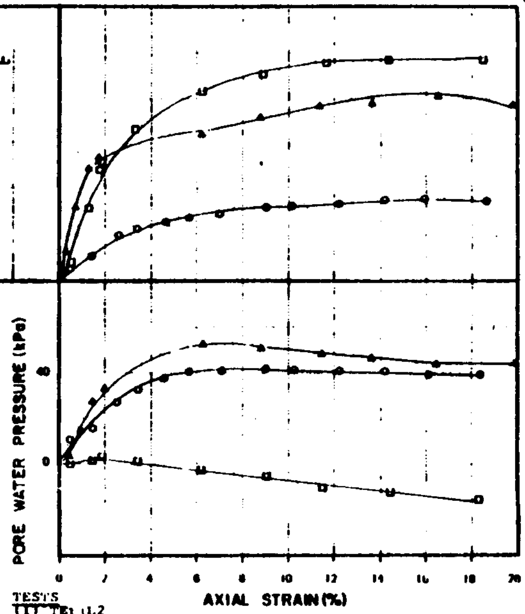

TESTS
(1) TE18L2
(2) TE19L2
(3) TE20L2

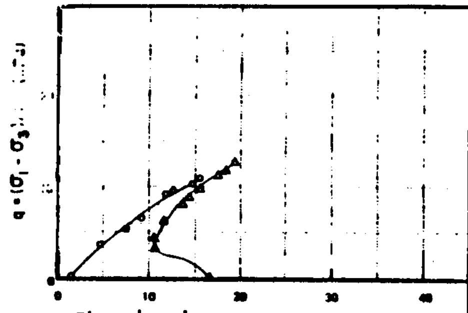

$P' = (\sigma_1' + \sigma_3')/2$ (kPa)

TEST	○ 1	▲ 2	3	4
PRECONSOLIDATION STRESS	n	n		
OVERCONSOLIDATION RATIO	n	n		
EFFECTIVE TEST PRESSURE	1.4	16.5		
TYPE OF TEST	T-1	T-2		

CRUISE NO. DC2-80EG

CORE NO: 190 G

DEPTH: 201-224 cm

TRIAXIAL TEST RESULTS

YAKUTAT AND KODIAK, ALASKA

U.S.G.S CONTRACT NO. 14-08-0001-19241

LAW ENGINEERING PROJECT NO. W-0-7910

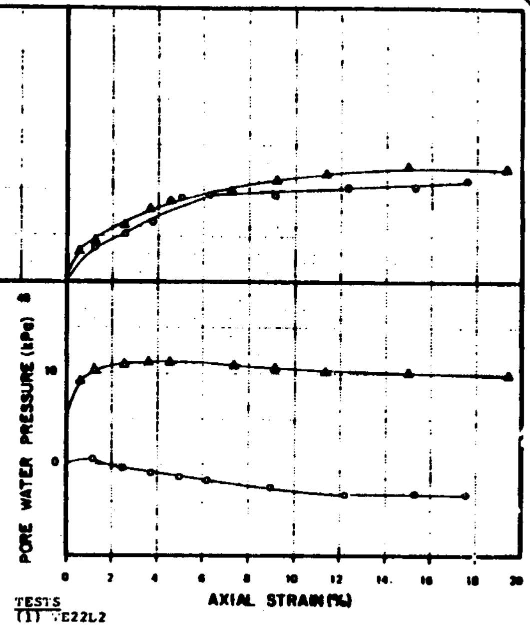

TESTS
(1) TE22L2
(2) TE23L2

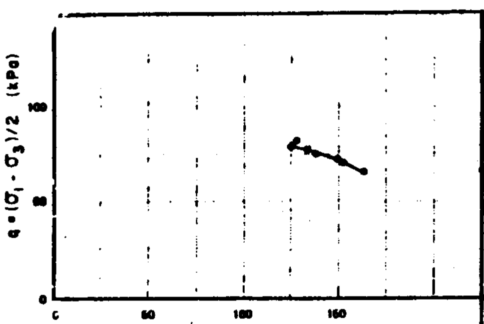

$P' = (\sigma_1' + \sigma_3')/2$ (kPa)

TEST	1 ●	2	3	4
PRECONSOLIDATION STRESS	231			
OVERCONSOLIDATION RATIO	1			
EFFECTIVE TEST PRESSURE	231			
TYPE OF TEST	T-7			

CRUISE NO DC2-80EG

CORE NO: 190 G

DEPTH: 176-188

TRIAXIAL TEST RESULTS

YAKUTAT AND KODIAK, ALASKA

U.S.G.S CONTRACT NO. 14-08-0001-19241

LAW ENGINEERING PROJECT NO. W-0-7910

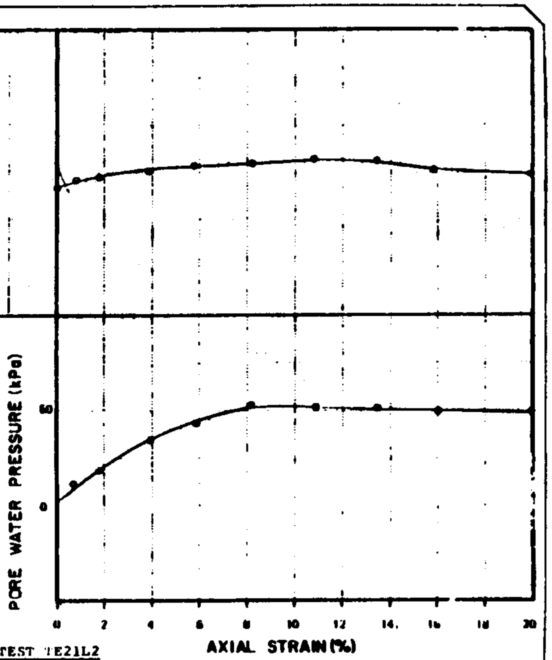

TEST TE21L2

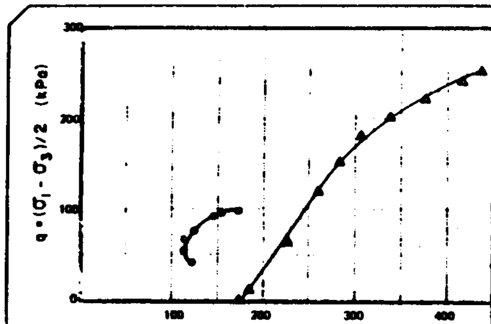

$P' = (\sigma_1' + \sigma_3')/2$ (kPa)

TEST	1 ●	2 ▲	3	4
PRECONSOLIDATION STRESS	165	517		
OVERCONSOLIDATION RATIO	1	3		
EFFECTIVE TEST PRESSURE	165	172		
TYPE OF TEST	T-7	T-8		

CRUISE NO DC2-80EG

CORE NO. 196 G

DEPTH: (100-173) (274-288)

TRIAXIAL TEST RESULTS

YAKUTAT AND KODIAK, ALASKA

U.S.G.S CONTRACT NO. 14-08-0001-19241

LAW ENGINEERING PROJECT NO. W-0-7910

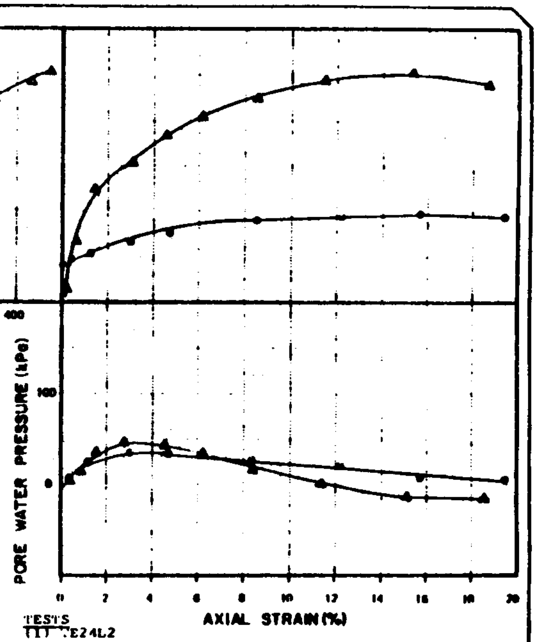

TESTS
(1) TE24L2
(2) TE25L2

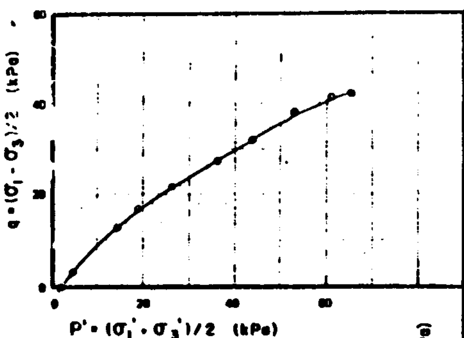

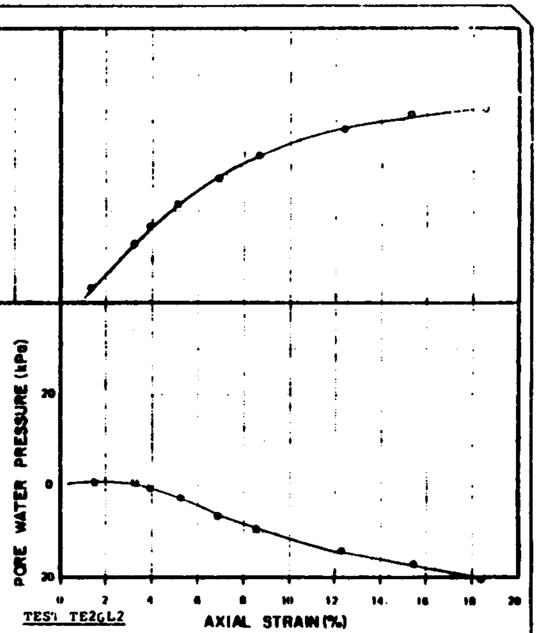

TEST TE26L2

TEST	1 o	2	3	4
PRECONSOLIDATION STRESS	1.4			
OVERCONSOLIDATION RATIO	n			
EFFECTIVE TEST PRESSURE	1.4			
TYPE OF TEST	T-1			

CRUISE NO. DC2-80 EG
CORE NO.: 196 G
DEPTH: 200-208 cm

TRIAXIAL TEST RESULTS
YAKUTAT AND KODIAK, ALASKA

U.S.G.S. CONTRACT NO. 14 08 0001 19241
LAW ENGINEERING PROJECT NO. W 0 2910

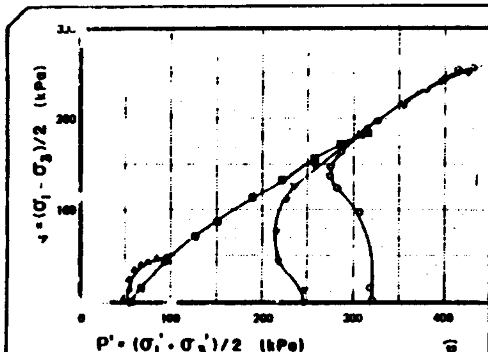

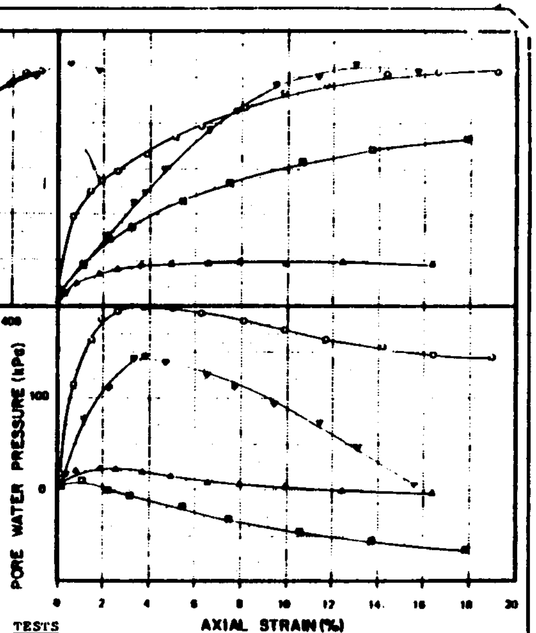

TEST	1 o	2 ▲	3 ■	4 ▼
PRECONSOLIDATION STRESS	320.4	n	330.7	248.1
OVERCONSOLIDATION RATIO	1.0	n	6	1.0
EFFECTIVE TEST PRESSURE	320.4	48.2	56.1	248.1
TYPE OF TEST	T-3a	T-2	T-4	T-3b

CRUISE NO. DC2-80EG
CORE NO.: 196 G
DEPTH: (234-240) (386-422)

TRIAXIAL TEST RESULTS
YAKUTAT AND KODIAK, ALASKA

U.S.G.S. CONTRACT NO. 14 08 0001 19241
LAW ENGINEERING PROJECT NO. W 0 2910

TESTS
(1) TE27L2
(2) TE28L2
(3) TE29L2
(4) TE30L2

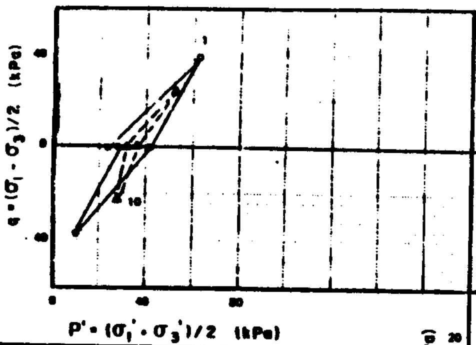

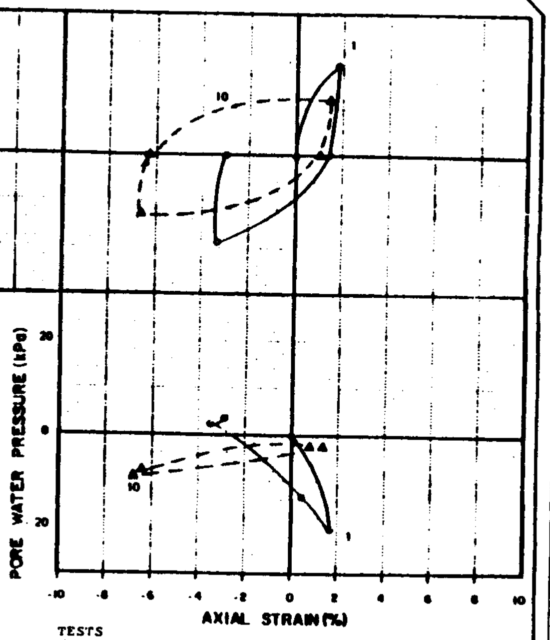

TEST	1 ●	2 ▲	3	4
PRECONSOLIDATION STRESS	165	165		
OVERCONSOLIDATION RATIO	6	6		
EFFECTIVE TEST PRESSURE	27.6	27.6		
TYPE OF TEST	T-8	T-10		

CRUISE NO. DC2-80EG
CORE NO.: 38G, MC3-22
DEPTH: 1-16, 35-47

TRIAXIAL TEST RESULTS
YAKUTAT AND KODIAK, ALASKA

U.S.G.S. CONTRACT NO. 14-08-0001-19241
LAW ENGINEERING PROJECT NO. W-0-2910

TESTS
(1) TC1L2
(2) TC2L2

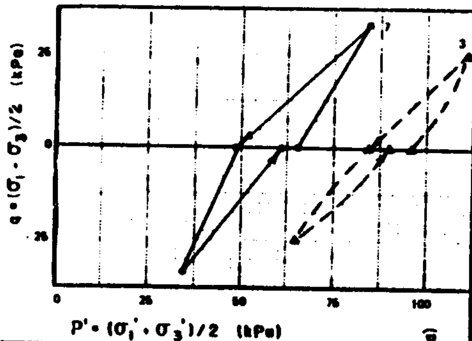

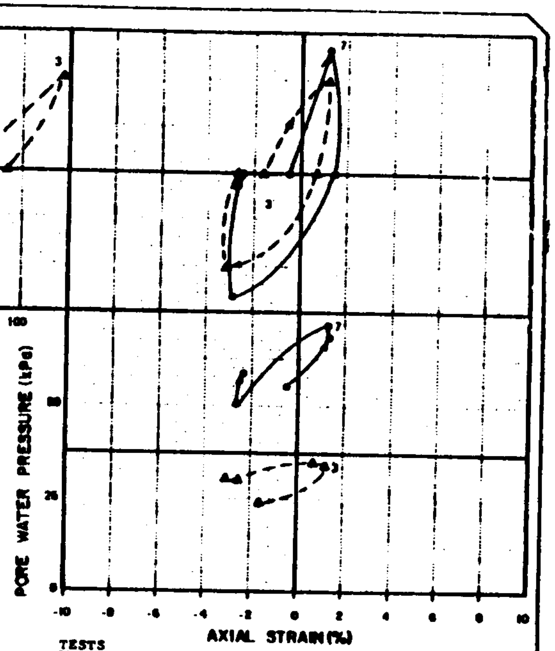

TEST	1 ●	2 ▲	3	4
PRECONSOLIDATION STRESS	120	120		
OVERCONSOLIDATION RATIO	1	1		
EFFECTIVE TEST PRESSURE	120	120		
TYPE OF TEST	T-6	T-6		

CRUISE NO.: DC-2-80EG
CORE NO.: 38 G
DEPTH: 27-62 cm

TRIAXIAL TEST RESULTS
YAKUTAT AND KODIAK, ALASKA

U.S.G.S. CONTRACT NO. 14-08-0001-19241
LAW ENGINEERING PROJECT NO. W-0-2910

TESTS
(1) TC3L2
(2) TC4L2

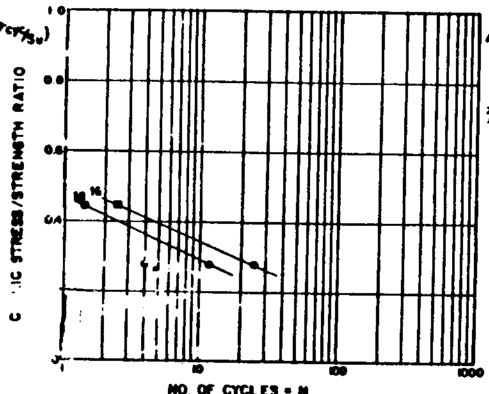

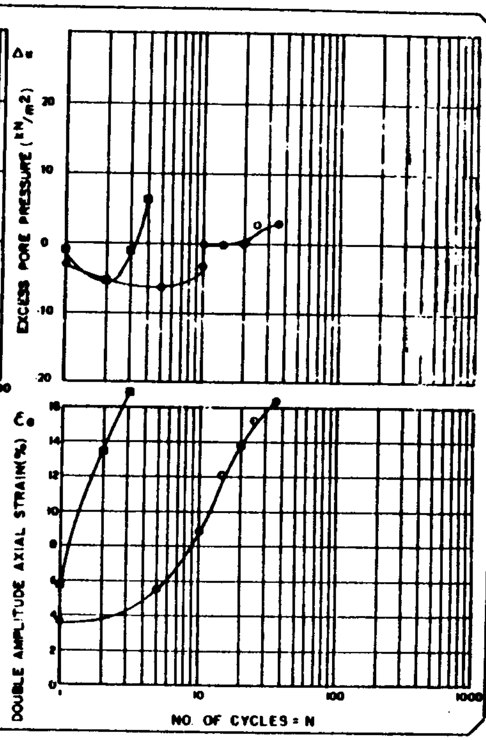

TEST	○ 1	▲ 2		
CYCLIC DEVIATOR STRESS (kN/m²)	47.5	76.1		
STRESS/STRENGTH RATIO	0.276	0.442		
STATIC BIAS	0.0	0.0		
PRECONSOLIDATION STRESS (kN/m²)	165.4	165.4		
OVERCONSOLIDATION RATIO	6.0	6.0		
EFFECTIVE TEST PRESSURE (kN/m²)	27.6	27.6		
TYPE OF TEST	T 10	T 8		

CRUISE NO. DC2 80 EG
CORE NO. MC3 22; 38 G

CYCLIC TRIAXIAL TEST RESULTS
YAKUTAT AND KODIAK, ALASKA

U.S.G.S. CONTRACT NO 14-08-0001-19241
LAW ENGINEERING NO W-0-2910

TESTS
(1) TC2L2
(2) TC1L2

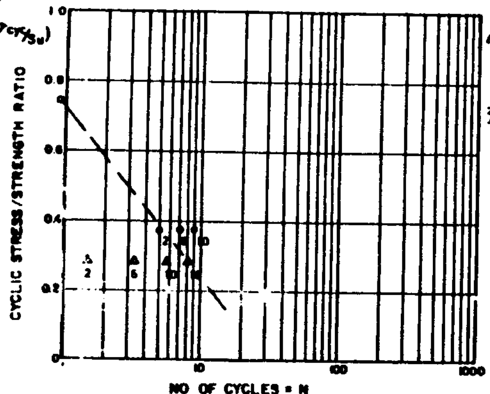

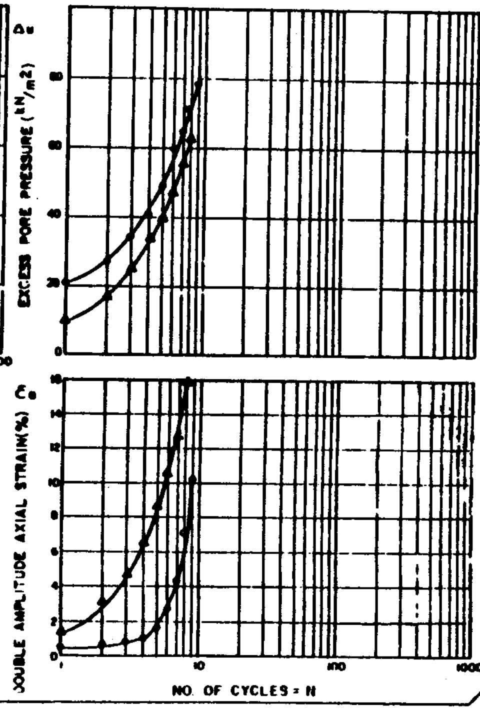

TEST	■ 1	● 1	▲ 2	
CYCLIC DEVIATOR STRESS (kN/m²)	130.7	66.3	49.9	
STRESS/STRENGTH RATIO	0.746	0.378	0.284	
STATIC BIAS	0.0	0.0	0.0	
PRECONSOLIDATION STRESS (kN/m²)	120.6	120.6	120.6	
OVERCONSOLIDATION RATIO	1	1	1	
EFFECTIVE TEST PRESSURE (kN/m²)	120.6	120.6	120.6	
TYPE OF TEST	T 6b	T 6b	T 6	

CRUISE NO. DC2-80EG
CORE NO. 38G, 49G

CYCLIC TRIAXIAL TEST RESULTS
YAKUTAT AND KODIAK, ALASKA

U.S.G.S. CONTRACT NO 14-08-0001-19241
LAW ENGINEERING NO W-0-2910

TESTS
(1) TC3L2
(2) TC4L2
(3) TC5L2

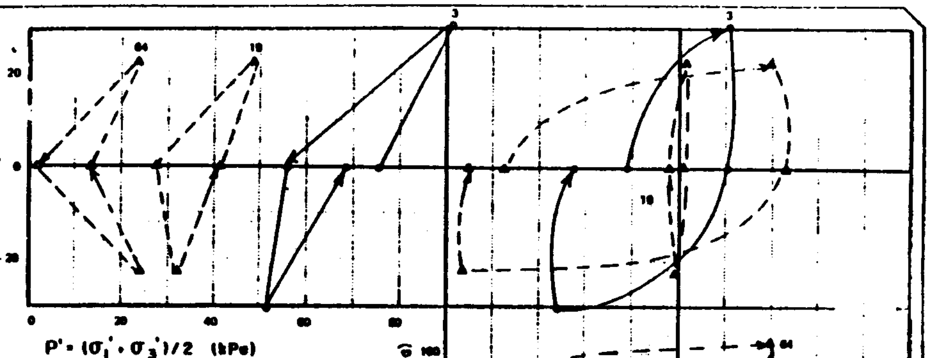

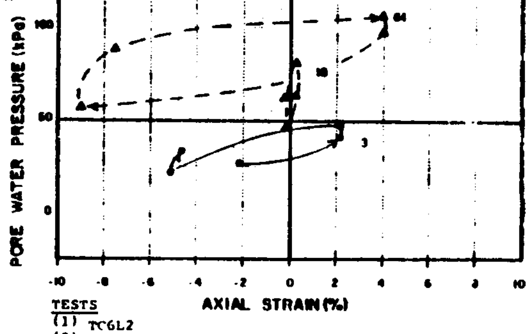

TEST	1 ●	2 ▲	3	4
PRECONSOLIDATION STRESS	103	103		
[illegible] RATIO	1	1		
[illegible] TEST PRESSURE	103	103		
TYPE OF TEST	T-6	T-6		

CRUISE NO: DC2-80EG
CORE NO: 84 G
DEPTH: 31-83 cm

TRIAXIAL TEST RESULTS
YAKUTAT AND KODIAK, ALASKA

U.S.G.S. CONTRACT NO. 14-08-0001-19241
LAW ENGINEERING PROJECT NO. W-D 2910

TESTS
(1) TC6L2
(2) TC7L2

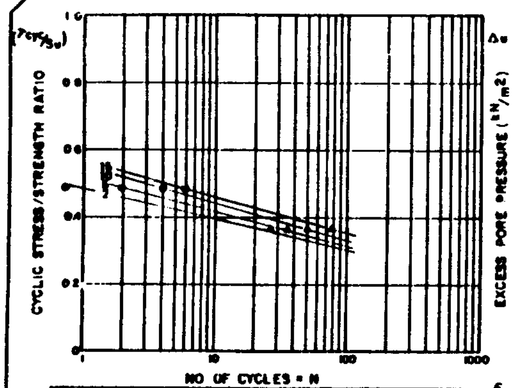

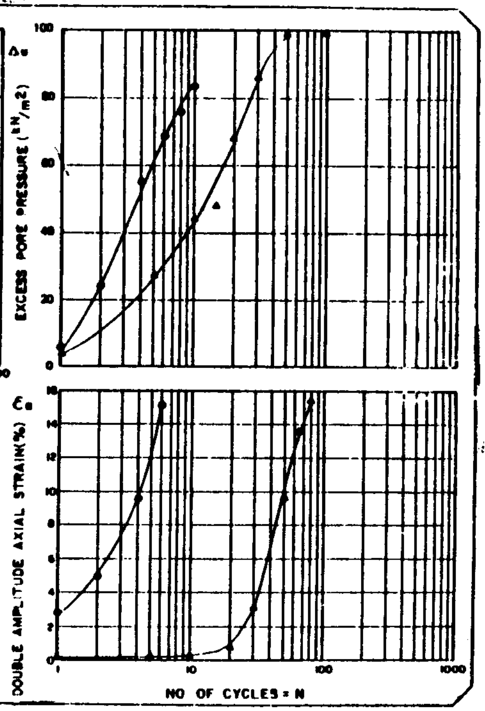

TEST	● 1	▲ 2		
CYCLIC DEVIATOR STRESS (kN/m^2)	62.9	47.8		
STRESS/STRENGTH RATIO	0.488	0.372		
STATIC BIAS	0	0		
PRECONSOLIDATION STRESS (kN/m^2)	103	103		
OVERCONSOLIDATION RATIO	1	1		
EFFECTIVE TEST PRESSURE (kN/m^2)	103	103		
TYPE OF TEST	T-6	T-6		

CRUISE NO: DC2-80EG
CORE NO: 8 4 G

CYCLIC TRIAXIAL TEST RESULTS
YAKUTAT AND KODIAK, ALASKA

U.S.G.S. CONTRACT NO. 14-08-0001-19241
LAW ENGINEERING NO. W-D-2910

TESTS (1) TC6L2
(2) TC7L2

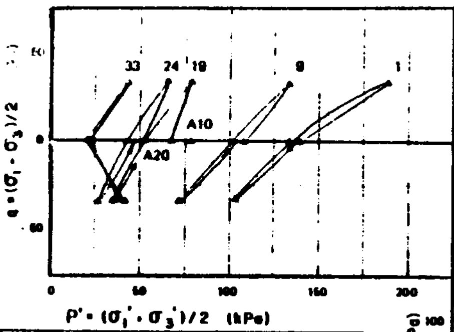

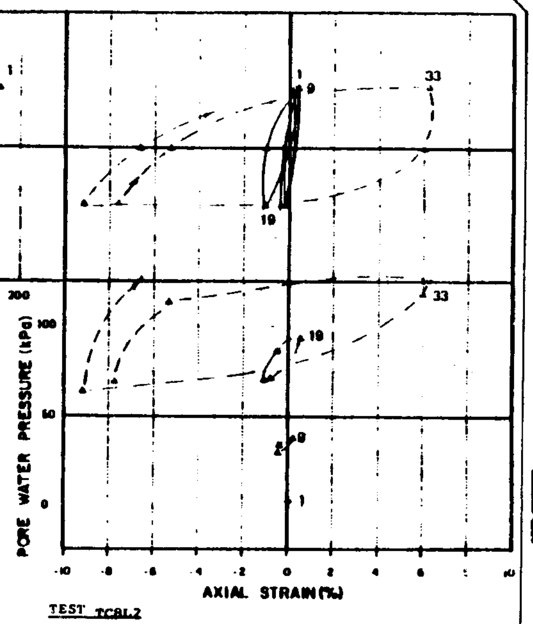

TEST	▲1	2	3	4
PRECONSOLIDATION STRESS	137.7			
OVERCONSOLIDATION RATIO	1			
EFFECTIVE TEST PRESSURE	137.7			
TYPE OF TEST	T-6			

CRUISE NO DC2-80-EG

CORE NO: 96 G

DEPTH: 226-237 cm

TRIAXIAL TEST RESULTS

YAKUTAT AND KODIAK, ALASKA

U.S.G.S. CONTRACT NO 14-08-0001-19241
LAW ENGINEERING PROJECT NO W-0-2910

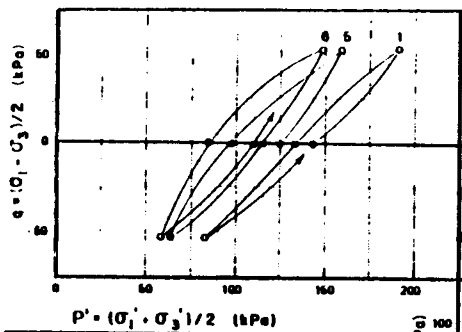

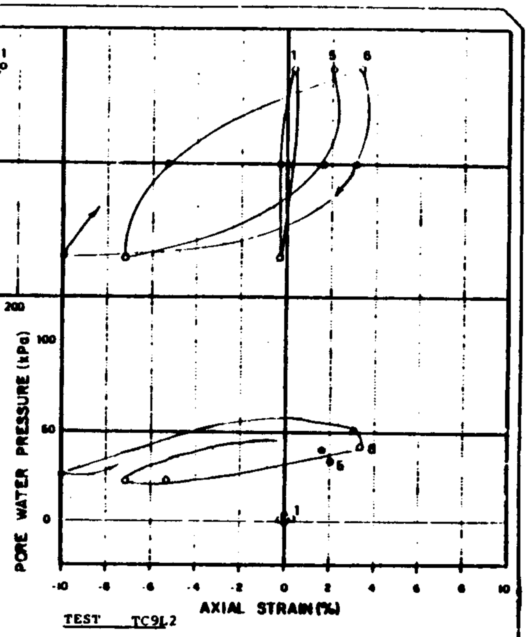

TEST	o1	2	3	4
PRECONSOLIDATION STRESS	137.7			
OVERCONSOLIDATION RATIO	1			
EFFECTIVE TEST PRESSURE	137.7			
TYPE OF TEST	T6			

CRUISE NO DC2-80-EG

CORE NO: 96 G

DEPTH: 331-343 cm

TRIAXIAL TEST RESULTS

YAKUTAT AND KODIAK, ALASKA

U.S.G.S. CONTRACT NO 14-08-0001-19241
LAW ENGINEERING PROJECT NO W-0-2910

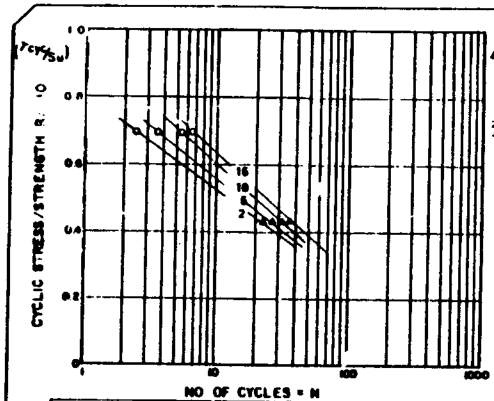

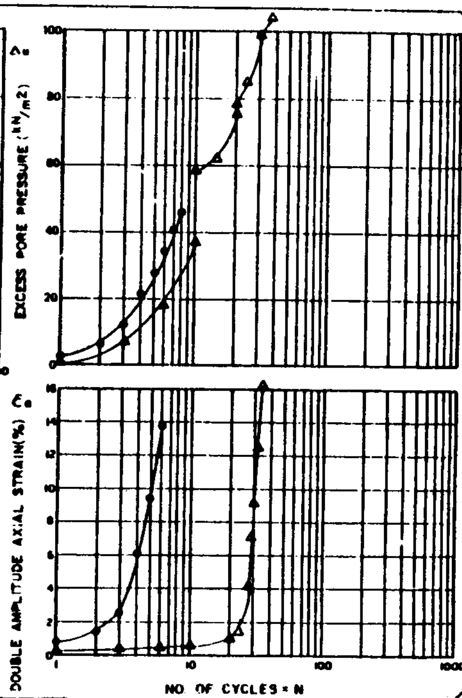

TEST	o 2	▲ 1		
CYCLIC DEVIATOR STRESS (kN/m^2)	109.6	88.2		
STRESS/STRENGTH RATIO	0.763	0.425		
STATIC BIAS	0.0	0.0		
PRECONSOLIDATION STRESS (kN/m^2)	137.8	137.8		
OVERCONSOLIDATION RATIO	1.0	1.0		
EFFECTIVE TEST PRESSURE (kN/m^2)	137.8	137.8		
TYPE OF TEST	T6	T6		

CRUISE NO DC2-80EG

CORE NO 96 G

CYCLIC TRIAXIAL TEST RESULTS

YAKUTAT AND KODIAK, ALASKA

U.S.G.S. CONTRACT NO 14-08-0001-19241
LAW ENGINEERING NO W-0-2910

TESTS (1) TC8L2
(2) TC9L2

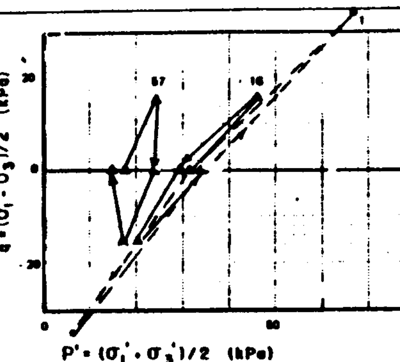

TEST	1▲	2●	3	4
PRECONSOLIDATION STRESS	140	138		
OVERCONSOLIDATION RATIO	4	4		
EFFECTIVE TEST PRESSURE	35	34.6		
TYPE OF TEST	T-10	T-9		

CRUISE NO: DC2-80EG
CORE NO: 96G
DEPTH: 208-332

TRIAXIAL TEST RESULTS
YAKUTAT AND KODIAK, ALASKA

U.S.G.S. CONTRACT NO. 14-08-0001-19241
LAW ENGINEERING PROJECT NO. W-0-2910

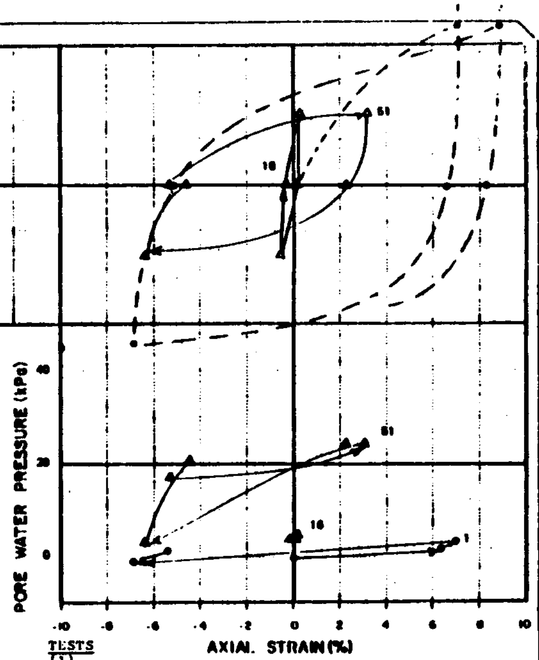

TESTS
(1) TC10L2
(2) TC11L2

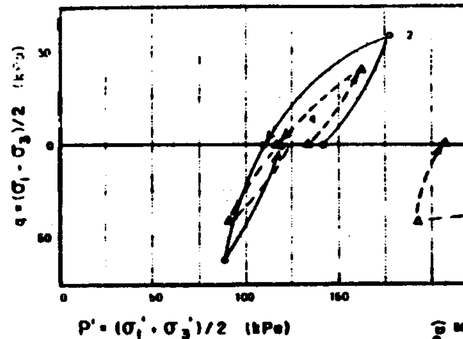

TEST	1●	2▲	3	4
PRECONSOLIDATION STRESS	162	162		
OVERCONSOLIDATION RATIO	1	1		
EFFECTIVE TEST PRESSURE	162	162		
TYPE OF TEST	T-6	T-6		

CRUISE NO: DC2-80EG
CORE NO: 190 G
DEPTH: 88-87

TRIAXIAL TEST RESULTS
YAKUTAT AND KODIAK, ALASKA

U.S.G.S. CONTRACT NO. 14-08-0001-19241
LAW ENGINEERING PROJECT NO. W-0-2910

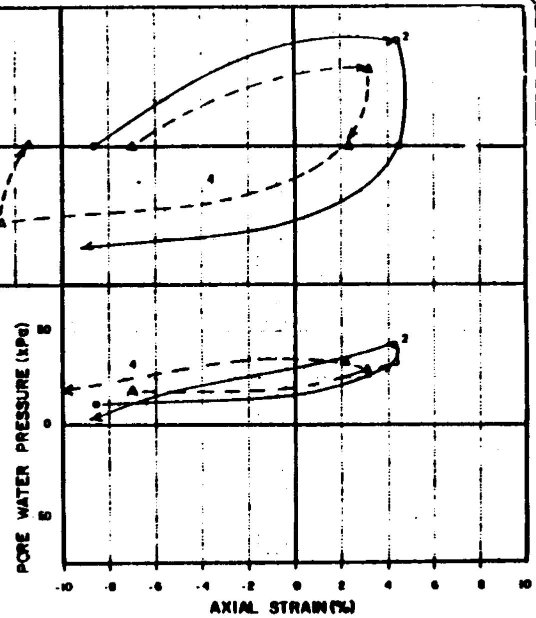

TESTS
(1) TC12L2
(2) TC13L2

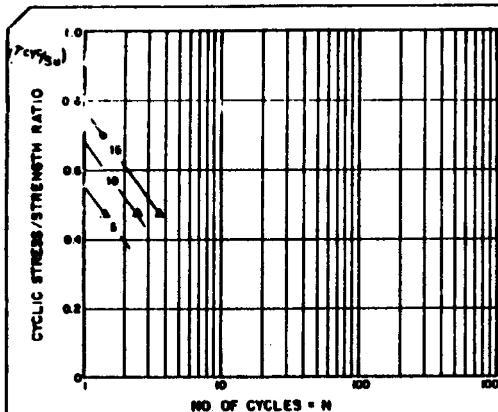

TEST	● 1	▲ 2		
CYCLIC DEVIATOR STRESS (kN/m^2)	124	81		
STRESS/STRENGTH RATIO	0.704	0.460		
STATIC BIAS	0	0		
PRECONSOLIDATION STRESS (kN/m^2)	162	162		
OVERCONSOLIDATION RATIO	1	1		
EFFECTIVE TEST PRESSURE (kN/m^2)	162	162		
TYPE OF TEST	T-6	T-6		

CRUISE NO DC2-80EG
CORE NO 190 G

CYCLIC TRIAXIAL TEST RESULTS
YAKUTAT AND KODIAK, ALASKA

U.S.G.S. CONTRACT NO 14-08-0001-19241
LAW ENGINEERING NO W-0-2910

TESTS (1) TC12L2
(2) TC13L2

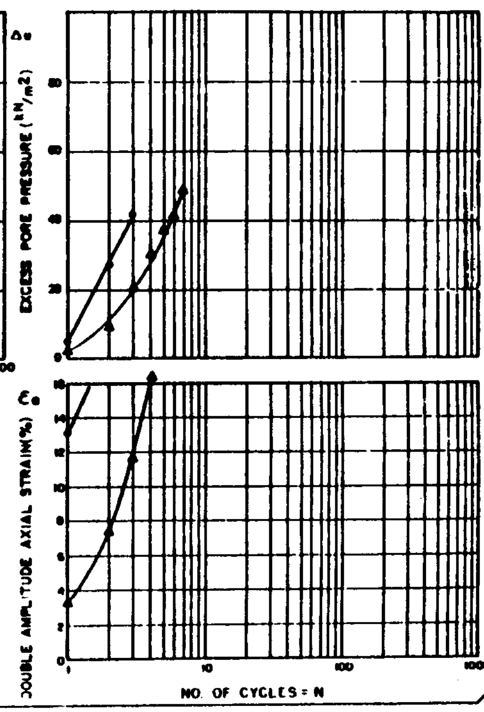

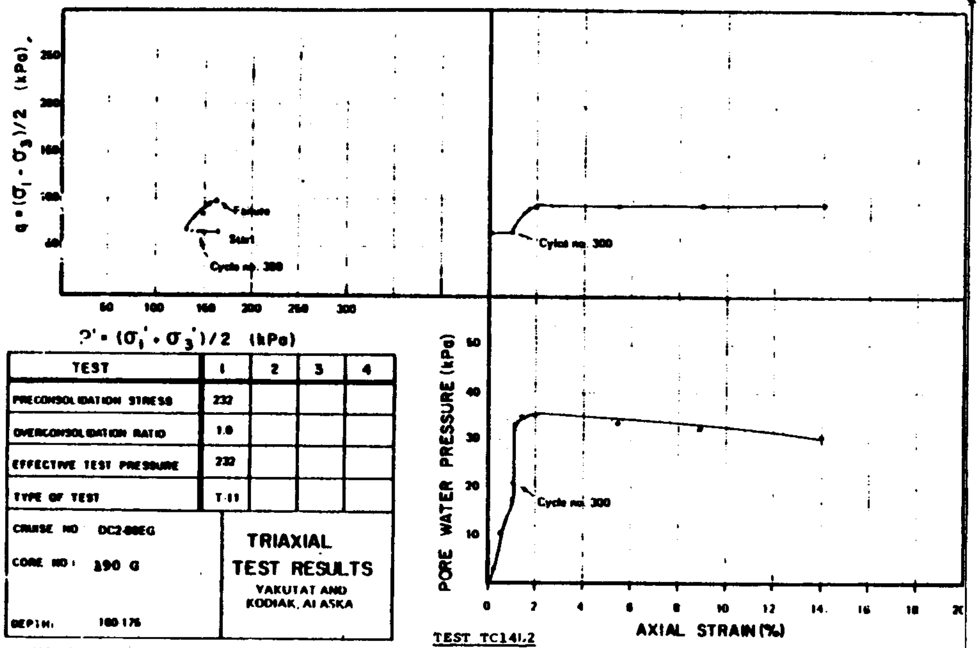

TEST	1	2	3	4
PRECONSOLIDATION STRESS	232			
OVERCONSOLIDATION RATIO	1.0			
EFFECTIVE TEST PRESSURE	232			
TYPE OF TEST	T-11			

CRUISE NO DC2-80EG
CORE NO: 190 G
DEPTH: 100-176

TRIAXIAL TEST RESULTS
YAKUTAT AND KODIAK, ALASKA

TEST TC14L2

U.S.G.S CONTRACT NO 14-08-0001-19241
LAW ENGINEERING PROJECT NO. W-0-2910

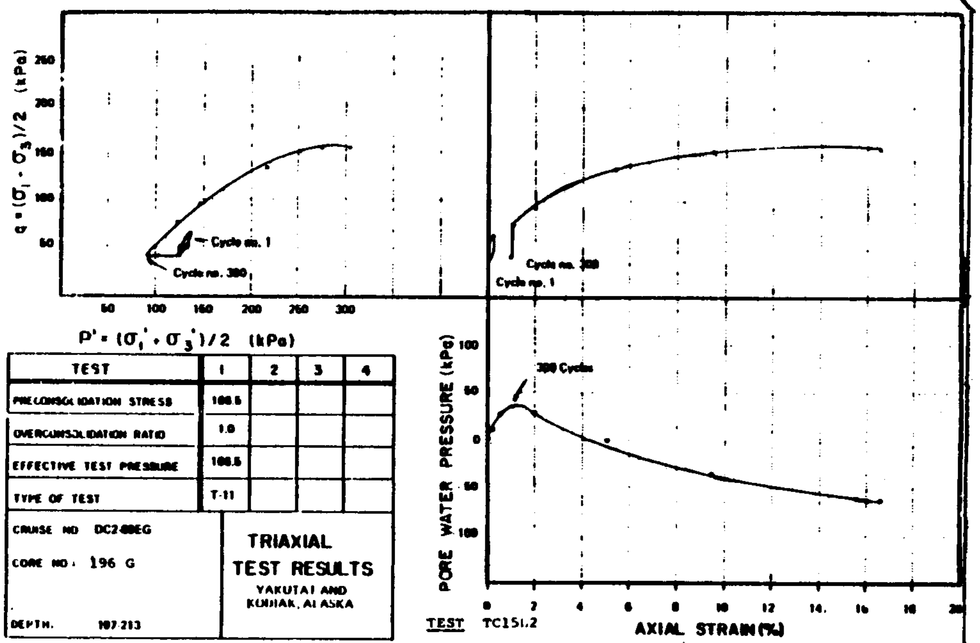

TEST	1	2	3	4
PRECONSOLIDATION STRESS	108.5			
OVERCONSOLIDATION RATIO	1.0			
EFFECTIVE TEST PRESSURE	108.5			
TYPE OF TEST	T-11			

CRUISE NO DC2-80EG
CORE NO: 196 G
DEPTH: 107-213

TRIAXIAL TEST RESULTS
YAKUTAT AND KODIAK, ALASKA

TEST TC15L2

U.S.G.S CONTRACT NO 14-08-0001-19241
LAW ENGINEERING PROJECT NO W-0-2910

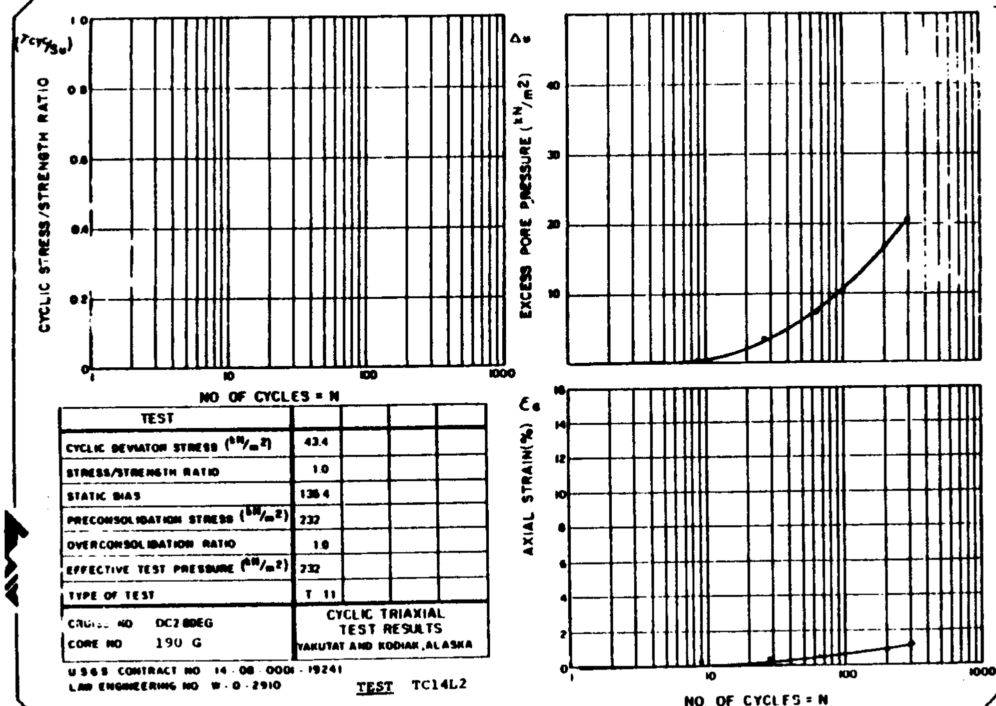

TEST	1			
CYCLIC DEVIATOR STRESS (kN/m^2)	43.4			
STRESS/STRENGTH RATIO	1.0			
STATIC BIAS	135.4			
PRECONSOLIDATION STRESS (kN/m^2)	232			
OVERCONSOLIDATION RATIO	1.0			
EFFECTIVE TEST PRESSURE (kN/m^2)	232			
TYPE OF TEST	T-11			

CRUISE NO DC2-80EG
CORE NO 190 G

CYCLIC TRIAXIAL TEST RESULTS
YAKUTAT AND KODIAK, ALASKA

U.S.G.S. CONTRACT NO 14-08-0001-19241
LAW ENGINEERING NO W-0-2910

TEST TC14L2

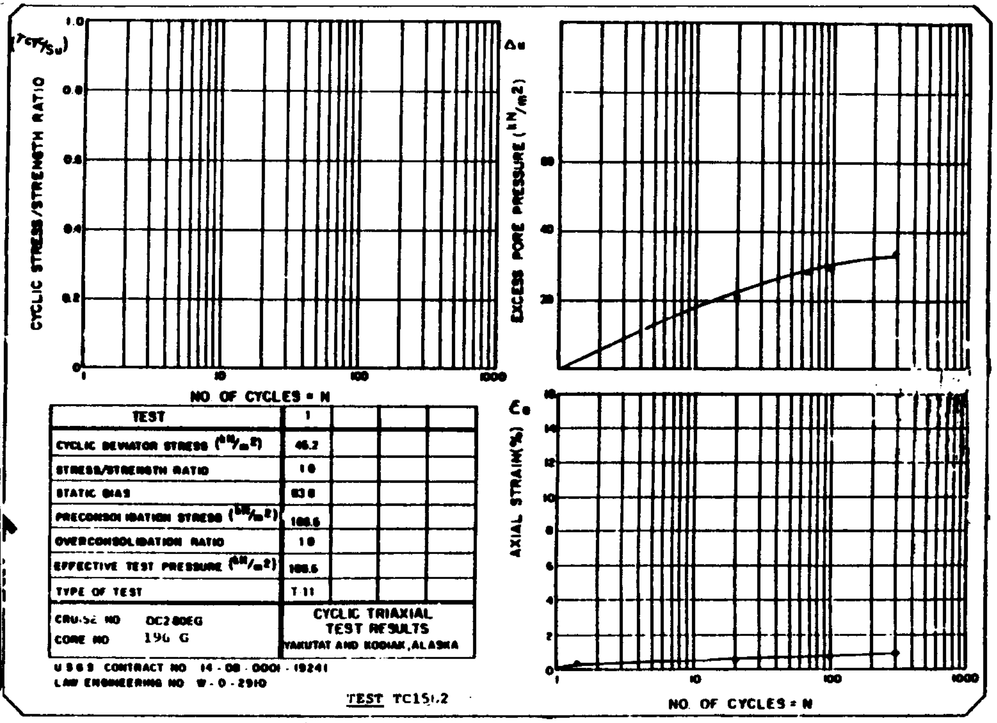

TEST	1			
CYCLIC DEVIATOR STRESS (kN/m^2)	46.2			
STRESS/STRENGTH RATIO	1.0			
STATIC BIAS	63.6			
PRECONSOLIDATION STRESS (kN/m^2)	108.5			
OVERCONSOLIDATION RATIO	1.0			
EFFECTIVE TEST PRESSURE (kN/m^2)	108.5			
TYPE OF TEST	T-11			

CRUISE NO DC2-80EG
CORE NO 196 G

CYCLIC TRIAXIAL TEST RESULTS
YAKUTAT AND KODIAK, ALASKA

U.S.G.S. CONTRACT NO 14-08-0001-19241
LAW ENGINEERING NO W-0-2910

TEST TC15L2

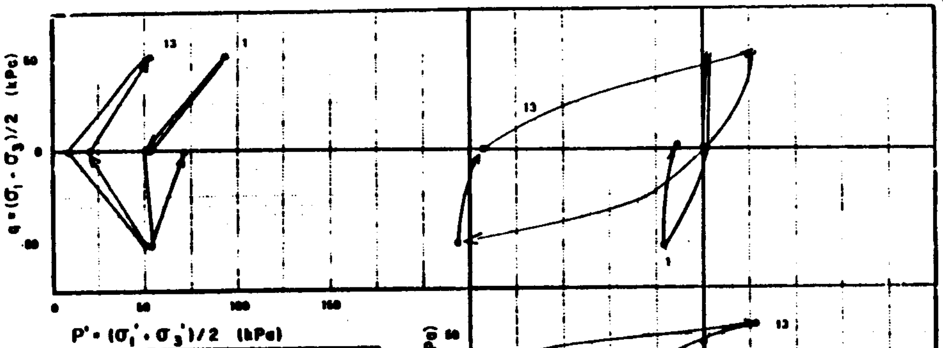

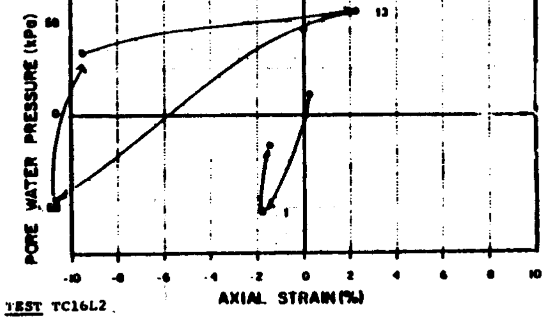

TEST	1 ●	2	3	4
PRECONSOLIDATION STRESS	320			
OV-RCL-A"-DATION RATIO	6			
EFFECTIVE TEST PRESSURE	63			
TYPE OF TEST	T-8			

CRUISE NO. DC2-80EG

CORE NO. 196 G

DEPTH: 312-326

TRIAXIAL TEST RESULTS

YAKUTAT AND KODIAK, ALASKA

TEST TC16L2

U.S.G.S. CONTRACT NO. 14-08-0001-19241

LAW ENGINEERING PROJECT NO. W.O 2010

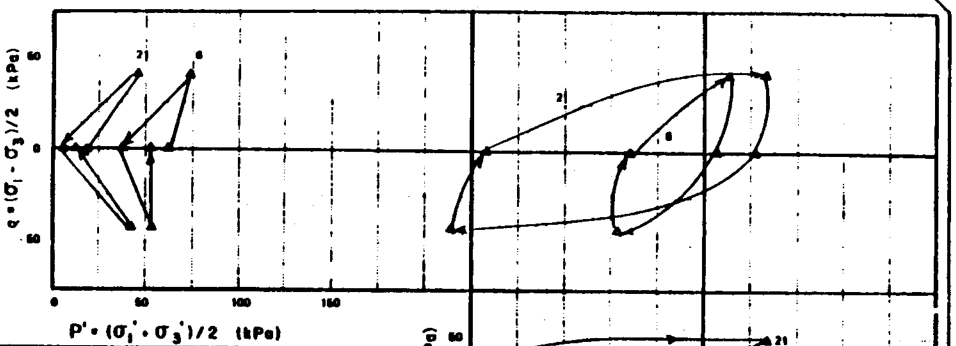

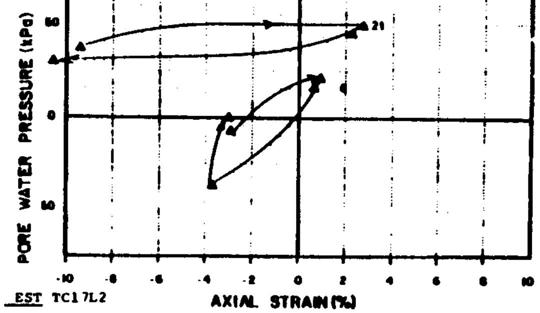

TEST	1 ▲	2	3	4
PRECONSOLIDATION STRESS	320			
OVERCONSOLIDATION RATIO	6			
EFFECTIVE TEST PRESSURE	63			
TYPE OF TEST	T-10			

CRUISE NO DC2-80EG

CORE NO. 196 G

DEPTH: 326-340

TRIAXIAL TEST RESULTS

YAKUTAT AND KODIAK, ALASKA

TEST TC17L2

U.S.G.S. CONTRACT NO. 14-08-0001-19241

LAW ENGINEERING PROJECT NO. W.O 2010

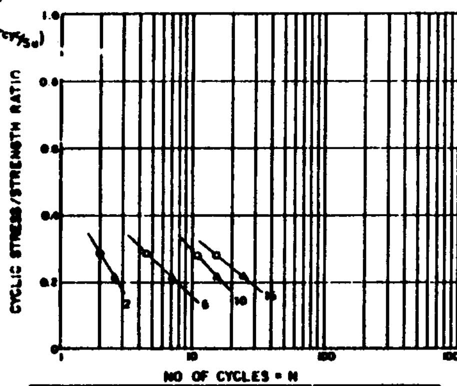

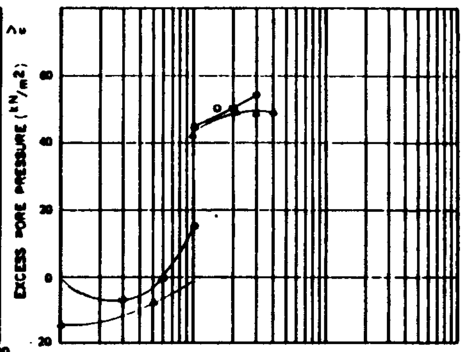

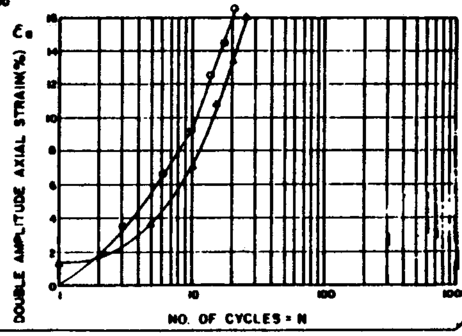

TEST	○ 1	▲ 2		
CYCLIC DEVIATOR STRESS (kN/m^2)	102	83		
STRESS/STRENGTH RATIO	0.277	0.224		
STATIC BIAS	0	0		
PRECONSOLIDATION STRESS (kN/m^2)	320	320		
OVERCONSOLIDATION RATIO	6	6		
EFFECTIVE TEST PRESSURE (kN/m^2)	63	63		
TYPE OF TEST	T-8	T-10		

CRUISE NO. DC2-80EG

CORE NO. 196 G

CYCLIC TRIAXIAL TEST RESULTS

YAKUTAT AND KODIAK, ALASKA

U.S.G.S. CONTRACT NO. 14-08-0001-19241

LAW ENGINEERING NO. W-0-2010

TESTS (1) TC16L2
(2) TC17L2

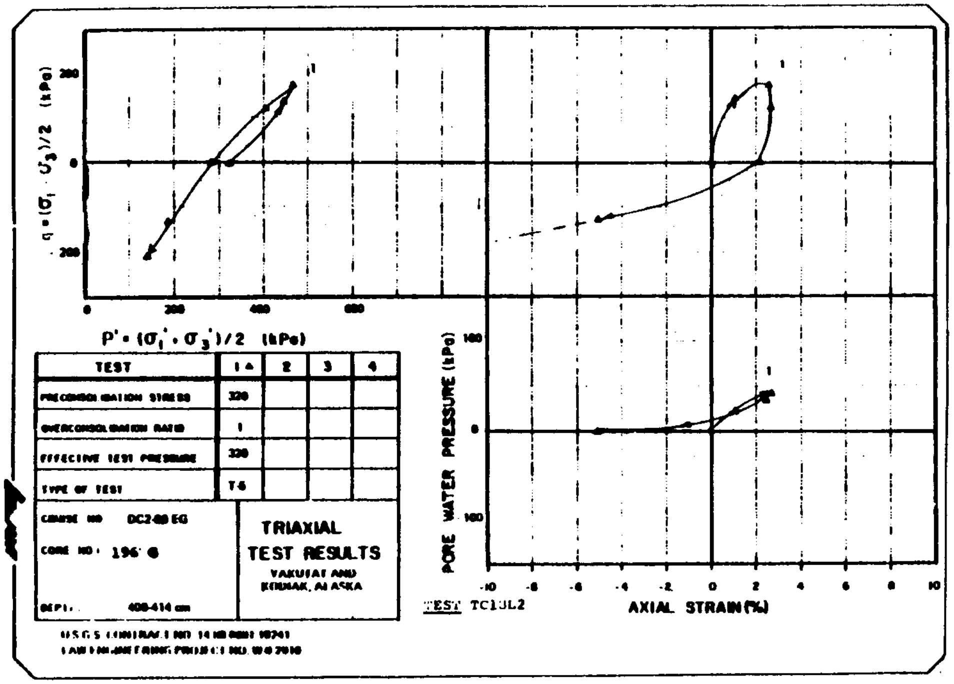
q = (σ1 - σ3)/2 (kPa)
P' = (σ1' + σ3')/2 (kPa)
PORE WATER PRESSURE (kPa)
AXIAL STRAIN (%)
TEST | 1A | 2 | 3 | 4
PRECONSOLIDATION STRESS | 320
OVERCONSOLIDATION RATIO | 1
EFFECTIVE TEST PRESSURE | 320
TYPE OF TEST | T6
CRUISE NO DC2-80 EG
CORE NO: 196 G
DEPTH 408-414 cm
TRIAXIAL TEST RESULTS
YAKUTAT AND KODIAK, ALASKA
U.S.G.S. CONTRACT NO. 14-08-0001-19241
LAW ENGINEERING PROJECT NO. W-O-2910
TEST TC10L2
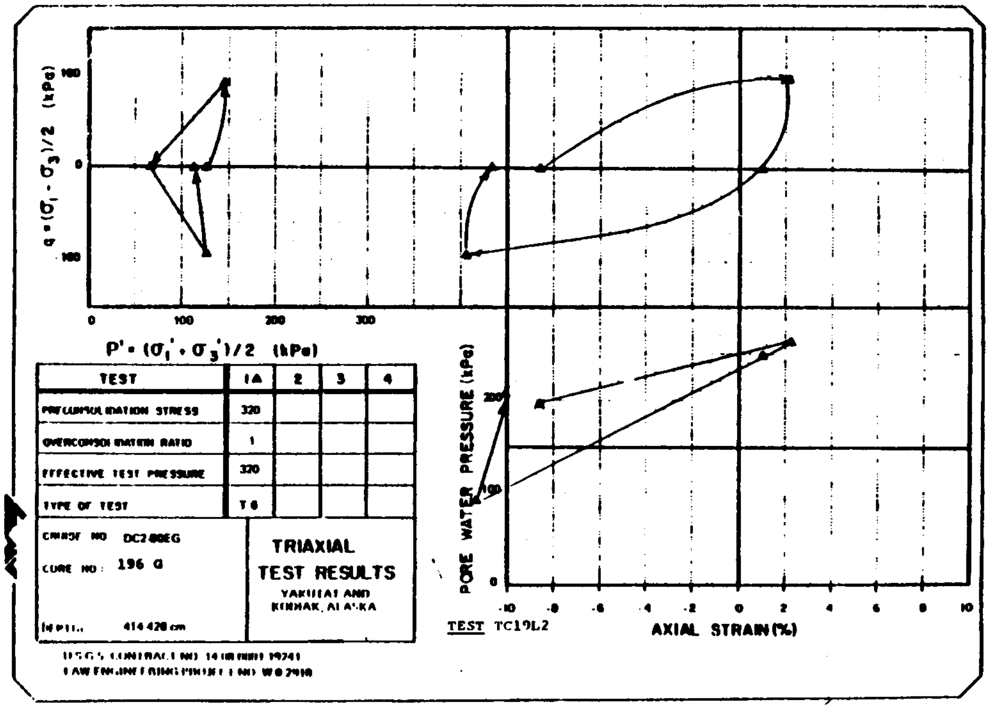
q = (σ1 - σ3)/2 (kPa)
P' = (σ1' + σ3')/2 (kPa)
PORE WATER PRESSURE (kPa)
AXIAL STRAIN (%)
TEST | 1A | 2 | 3 | 4
PRECONSOLIDATION STRESS | 320
OVERCONSOLIDATION RATIO | 1
EFFECTIVE TEST PRESSURE | 320
TYPE OF TEST | T6
CRUISE NO DC2-80EG
CORE NO: 196 G
DEPTH 414-420 cm
TRIAXIAL TEST RESULTS
YAKUTAT AND KODIAK, ALASKA
U.S.G.S. CONTRACT NO. 14-08-0001-19241
LAW ENGINEERING PROJECT NO. W-O-2910
TEST TC19L2
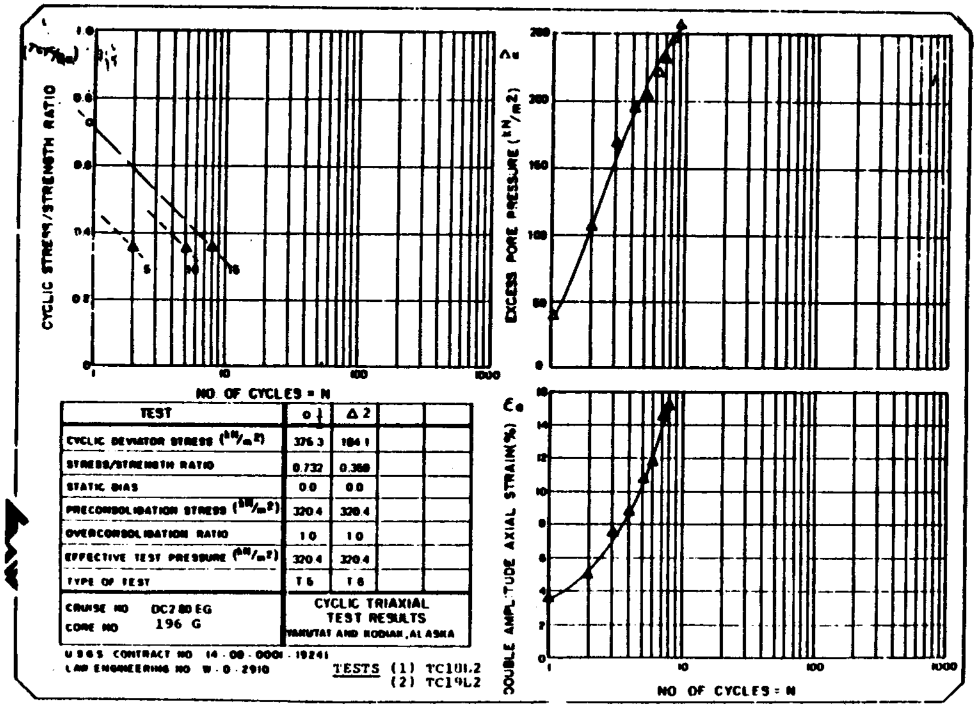
CYCLIC STRESS/STRENGTH RATIO
EXCESS PORE PRESSURE (kN/m2)
DOUBLE AMPLITUDE AXIAL STRAIN (%)
NO. OF CYCLES = N
TEST | o 1 | Δ 2
CYCLIC DEVIATOR STRESS (kN/m2) | 376.3 | 184.1
STRESS/STRENGTH RATIO | 0.732 | 0.360
STATIC BIAS | 0.0 | 0.0
PRECONSOLIDATION STRESS (kN/m2) | 320.4 | 320.4
OVERCONSOLIDATION RATIO | 1.0 | 1.0
EFFECTIVE TEST PRESSURE (kN/m2) | 320.4 | 320.4
TYPE OF TEST | T6 | T6
CRUISE NO DC2-80 EG
CORE NO 196 G
CYCLIC TRIAXIAL TEST RESULTS
YAKUTAT AND KODIAK, ALASKA
U.S.G.S. CONTRACT NO. 14-08-0001-19241
LAW ENGINEERING NO. W-O-2910
TESTS (1) TC10L2
(2) TC19L2

APPENDIX G

CONSOLIDATION AND TRIAXIAL TEST RESULTS--

U.S. GEOLOGICAL SURVEY (1980 AND 1981 cores)

APPENDIX G. CONSOLIDATION AND TRIAXIAL TEST RESULTS-U.S. GEOLOGICAL SURVEY (1980 and 1981 cores)

This appendix presents the results of consolidation and triaxial testing performed at the U.S. Geological Survey's marine geotechnical laboratory. Core samples were from cruises DC2-80-EG and DC1-81-EG. Results were automatically recorded, reduced and plotted.

The tests in this group do not have trailing characters in their test numbers. The consolidation tests (first characters are CE for constant rate of strain, CRS, tests and OE for oedometer tests) are presented first and are ordered by test number. Results from a single test are presented on a single page in the form of void ratio and calculated coefficient of consolidation (c_v) versus the vertical effective stress (identified as STRESS). Some of the plots for CRS tests are irregular as a result of transducer drift.

Static triaxial tests (first two characters are TE) are given second and ordered by test number. The upper left graph is a stress path presented as a plot of maximum shear stress (q) versus the normal effective stress on the plane of maximum shear (p'). The stress path plots of Appendix D are defined differently. The upper right plot is the maximum shearing stress versus strain. The lower right plot is the measured excess pore water pressure (DELTAu) versus axial strain. The title block gives SIG1c' and SIG3' which are the vertical and horizontal consolidation stresses, respectively. The induced OCR is the overconsolidation ratio forced on the sample in the triaxial cell. A value of 1.0 may or may not correspond to true overconsolidation because the triaxial cell consolidation stress may be less than the maximum past stress the sample experienced in place.

The cyclic triaxial tests (first two characters are TC) are given third and ordered by test number. Results from one test are presented on two sheets. The first sheet includes deviator stress (DEV STRESS or 2 times the shear stress)-axial strain and p'-q stress paths that are analogous to the graphs given for static triaxial tests. However, the plots are given for only a few selected cycles of loading to illustrate how the response changes as the number of cycles increases. Numbers on the plots correspond to cycle number.

The second sheet shows several parameters plotted versus cycle number. The upper left plot shows peak single amplitude strain (positive in compression) versus cycle number. Lower left and lower right plots show calculated damping and Young's modulus (E) versus number of cycles,respectively. The upper right plot shows the minimum and maximum excess pore water pressure (DELU) measured during a cycle. In some plots a dashed line in both the strain and pore pressure plots shows an equilibrium value established between bursts of cyclic stress applications.

The title blocks for both figures show a static qf or estimated static shearing strength. The value was obtained from a test on a nearby sample (Method I of the main text). The average maximum q (AVG MAX q) is the average peak compressive shearing strength for all of the cycles. The percentage value that follows in parentheses represents the percentage of the estimated (Method I) static shearing strength. The "AVG MIN q" is the same as the average maximum q except it represents values in tension.

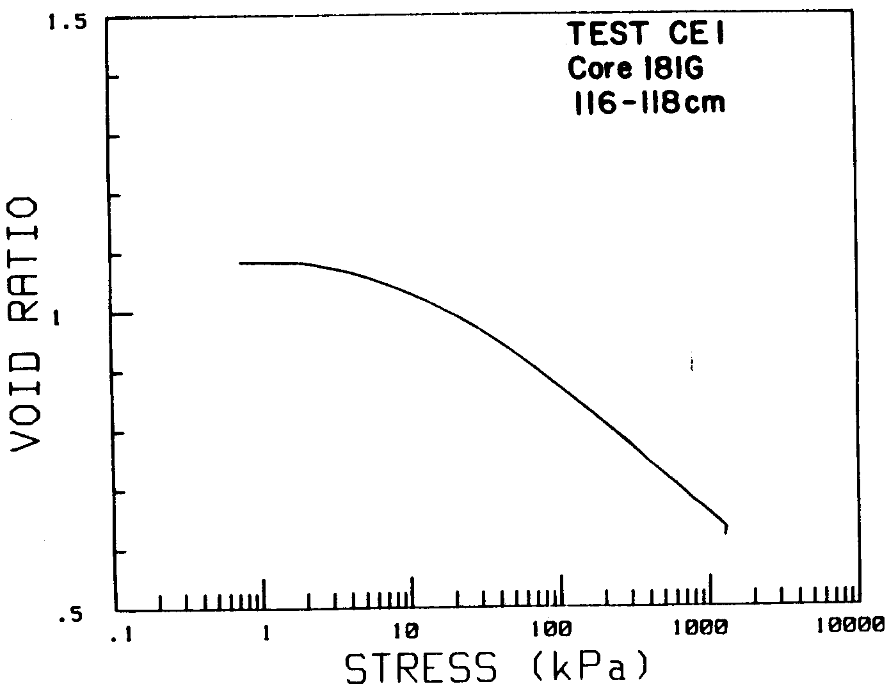

TEST CE1
Core 181G
116-118cm
VOID RATIO
STRESS (kPa)
1.5
1
.5
.1
1
10
100
1000
10000

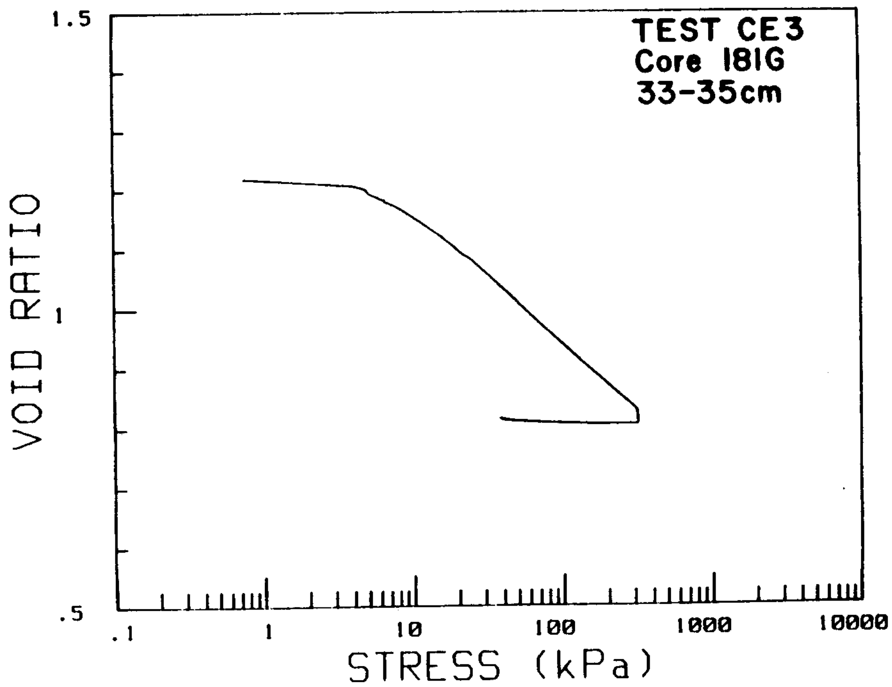

TEST CE3
Core 181G
33-35cm
VOID RATIO
STRESS (kPa)
1.5
1
.5
.1
1
10
100
1000
10000

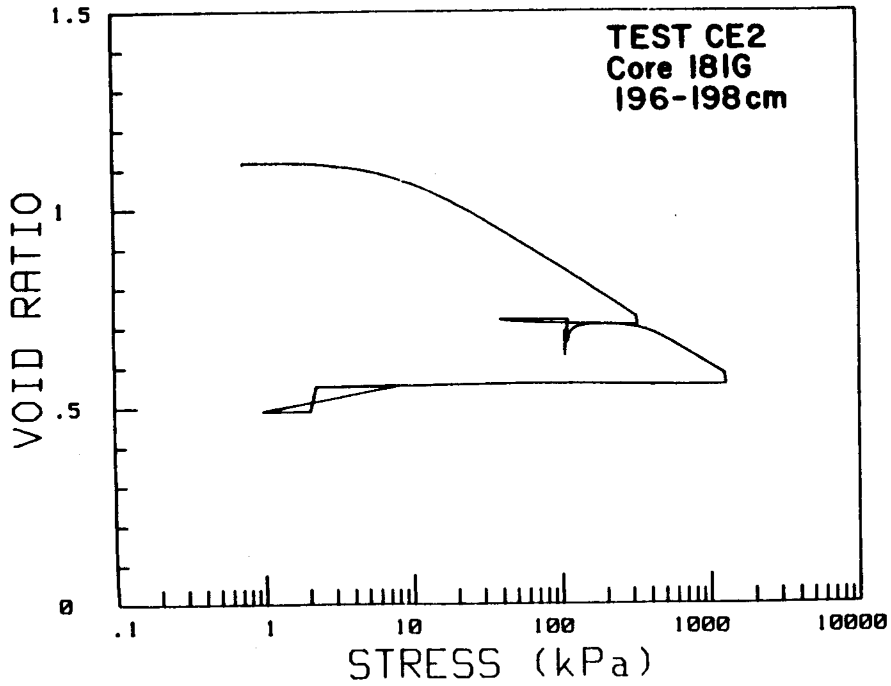

TEST CE2
Core 181G
196-198cm
VOID RATIO
STRESS (kPa)
1.5
1
.5
0
.1
1
10
100
1000
10000

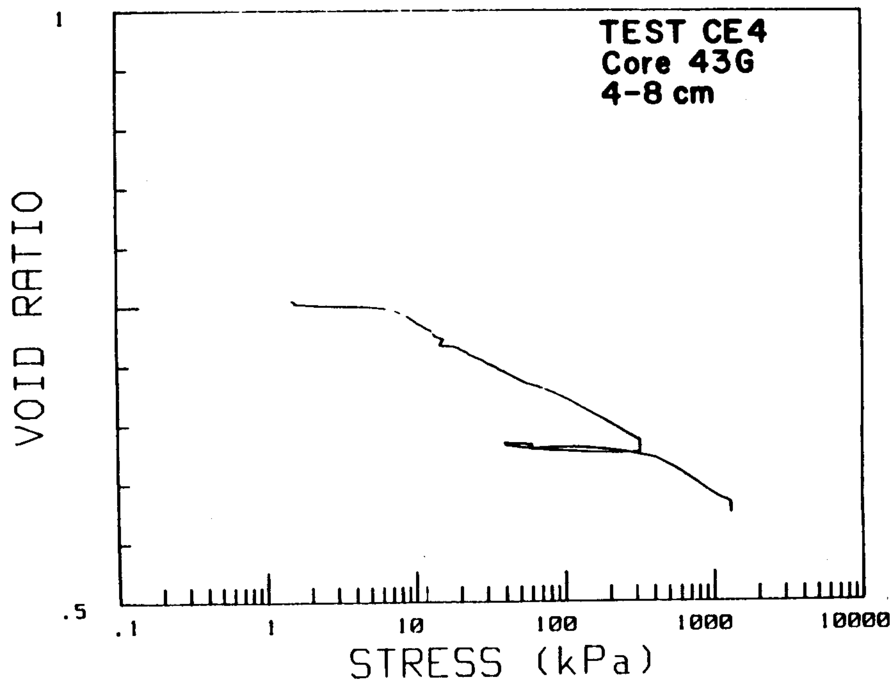

TEST CE4
Core 43G
4-8 cm
VOID RATIO
STRESS (kPa)
1
.5
.1
1
10
100
1000
10000

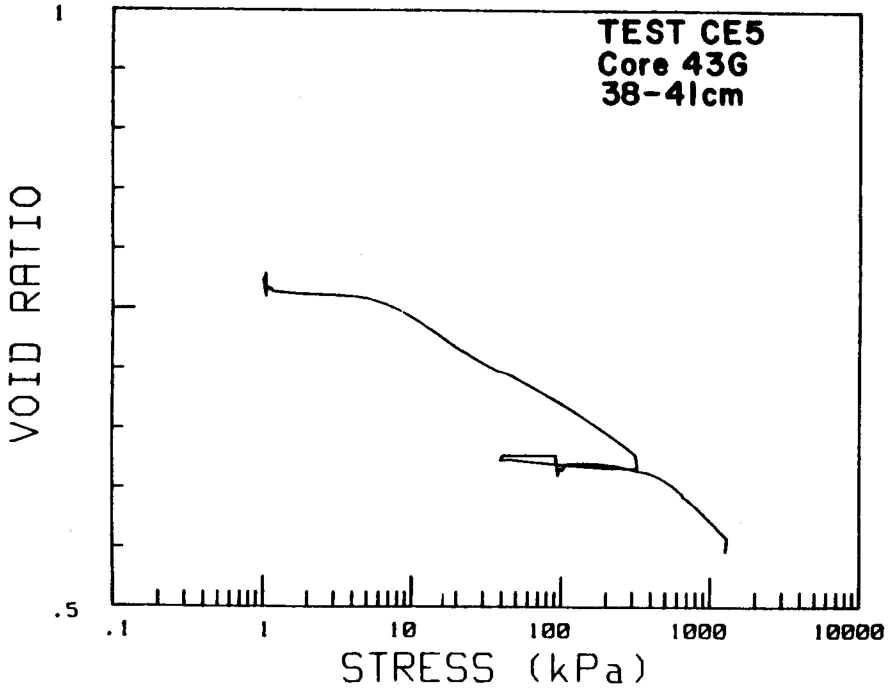
TEST CE5
Core 43G
38-41cm
VOID RATIO
STRESS (kPa)
1
.5
.1
1
10
100
1000
10000

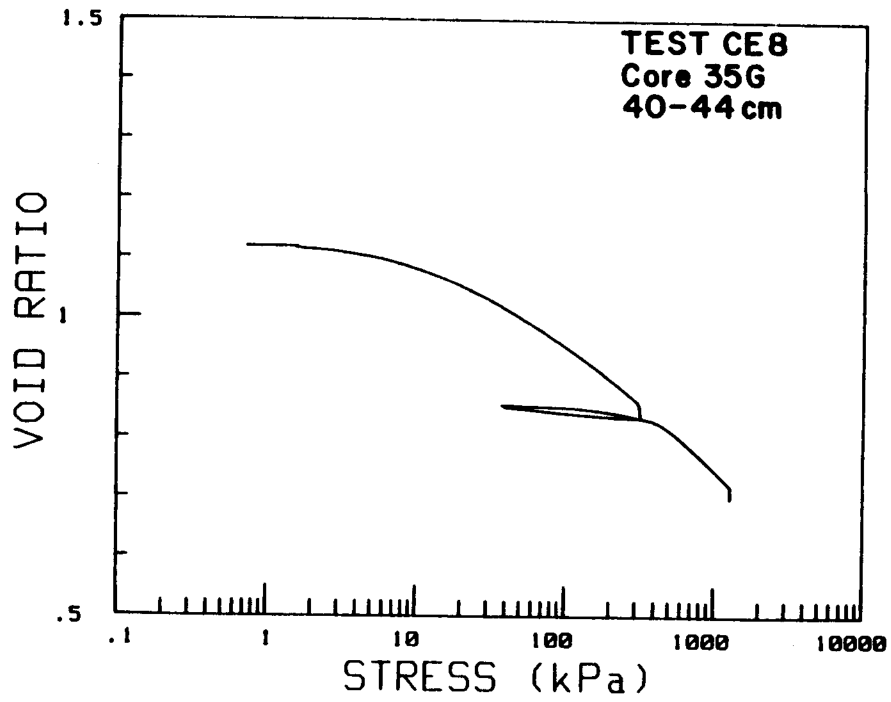
TEST CE8
Core 35G
40-44 cm
VOID RATIO
STRESS (kPa)
1.5
1
.5
.1
1
10
100
1000
10000

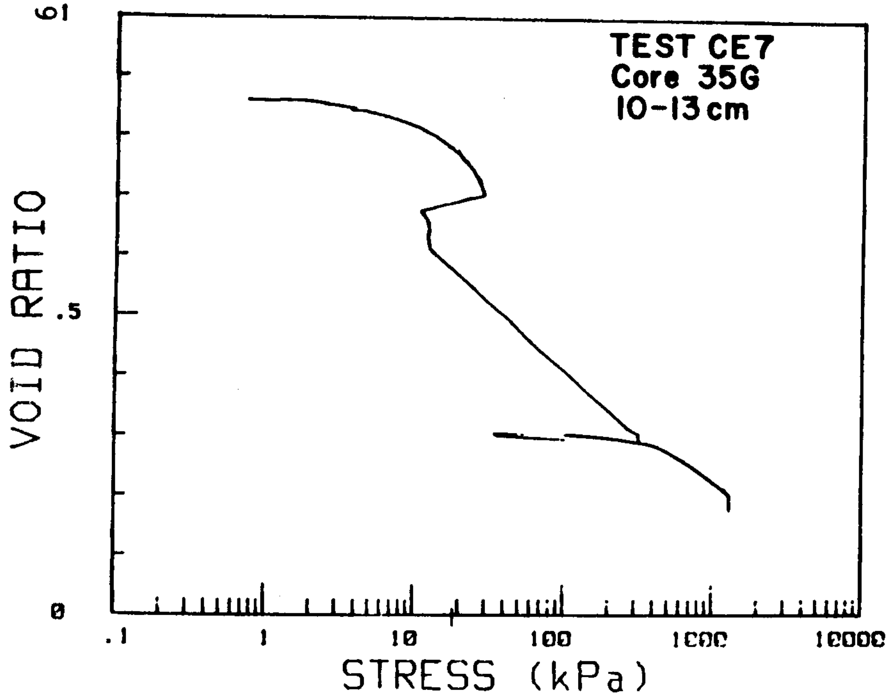
TEST CE7
Core 35G
10-13 cm
VOID RATIO
STRESS (kPa)
1
.5
0
.1
1
10
100
1000
10000

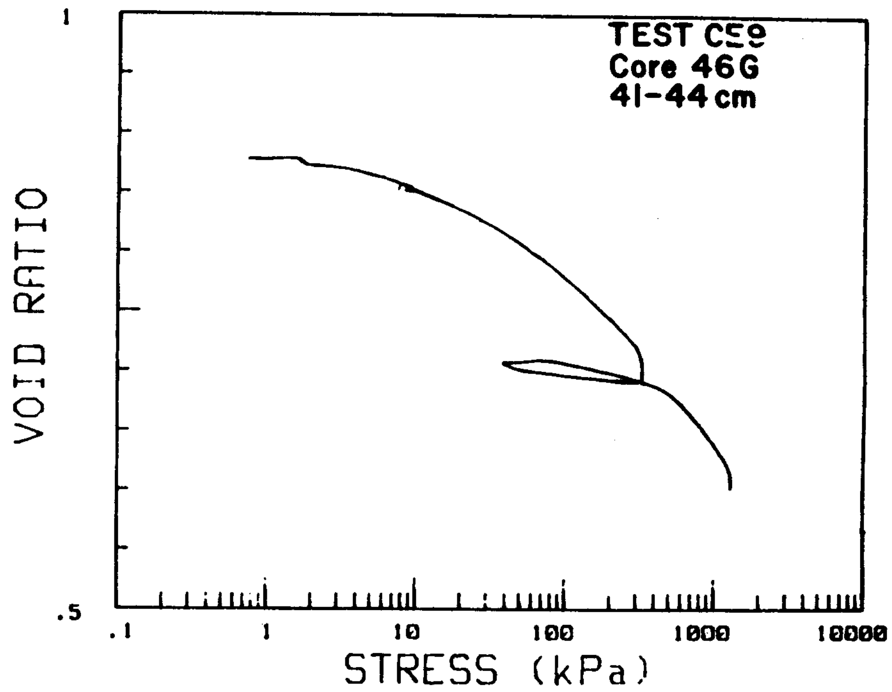
TEST CE9
Core 46G
41-44 cm
VOID RATIO
STRESS (kPa)
1
.5
.1
1
10
100
1000
10000

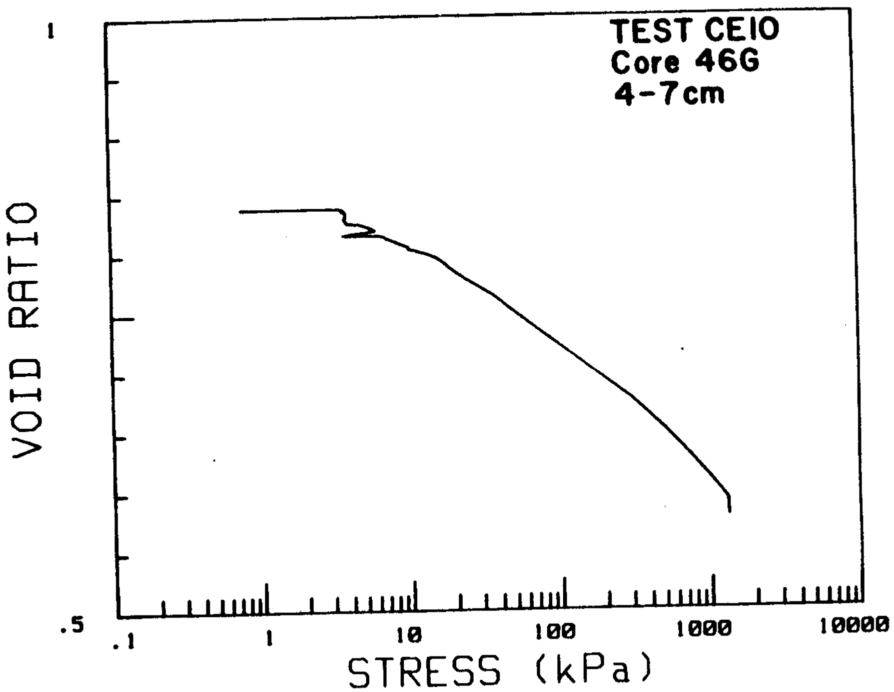
TEST CE10
Core 46G
4-7cm
VOID RATIO
1
.5
.1
1
10
100
1000
10000
STRESS (kPa)

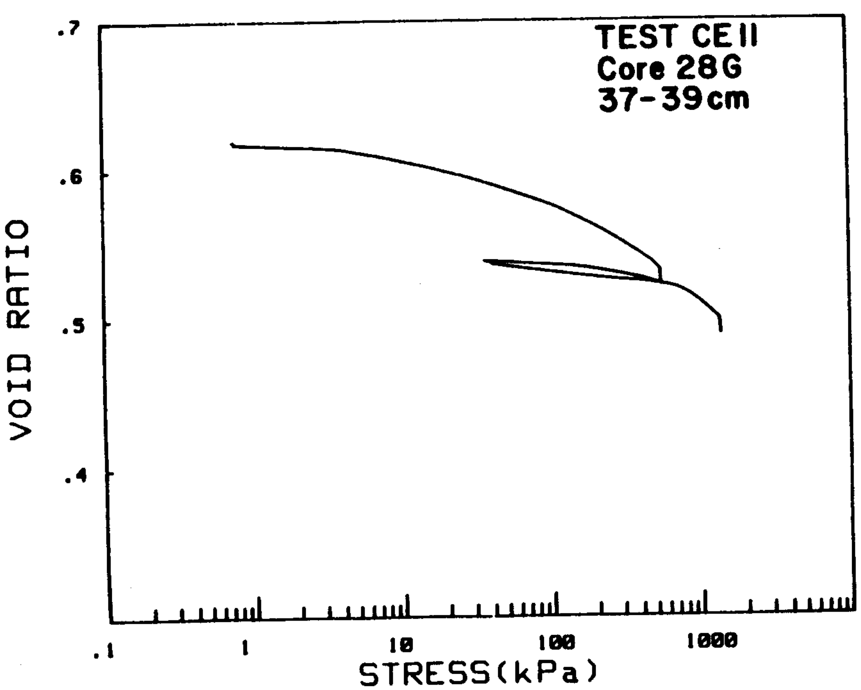
TEST CE11
Core 28G
37-39cm
VOID RATIO
.7
.6
.5
.4
.1
1
10
100
1000
STRESS(kPa)

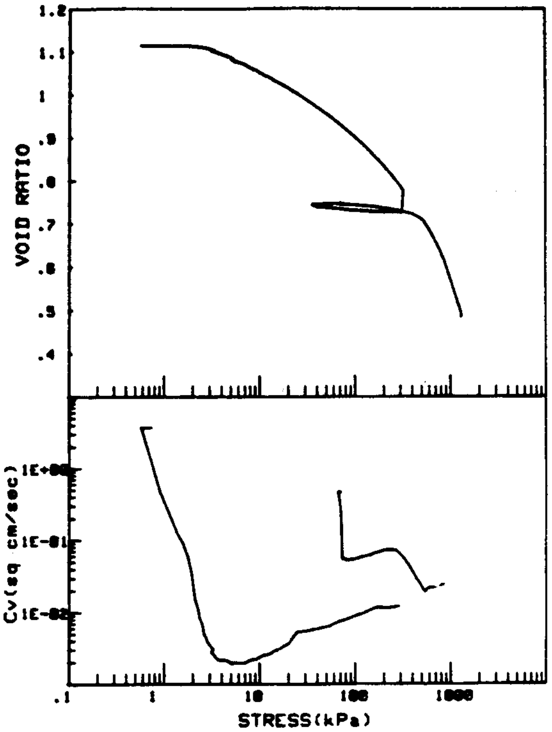

CRUISE DC1-81-EG	INCREMENT (cm)	116-118
CORE NO. 827G2	TEST NO.	CE13

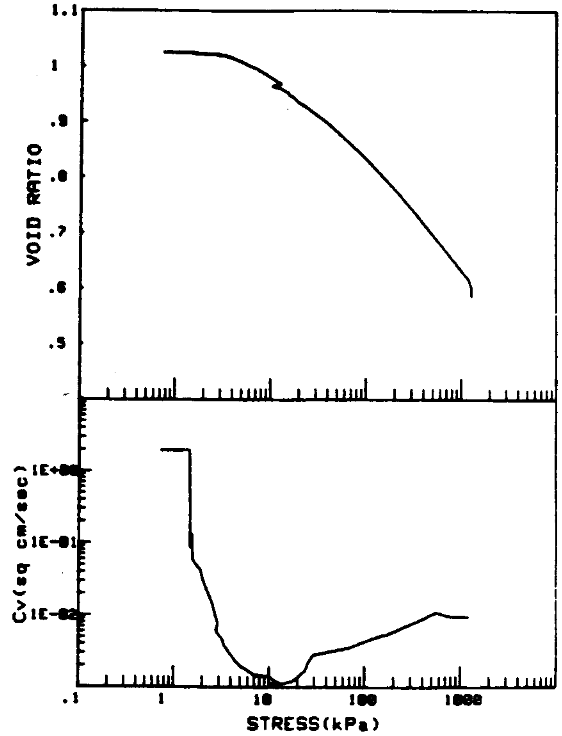

CRUISE DC1-81-EG	INCREMENT (cm)	222-224
CORE NO. 827G2	TEST NO.	CE15

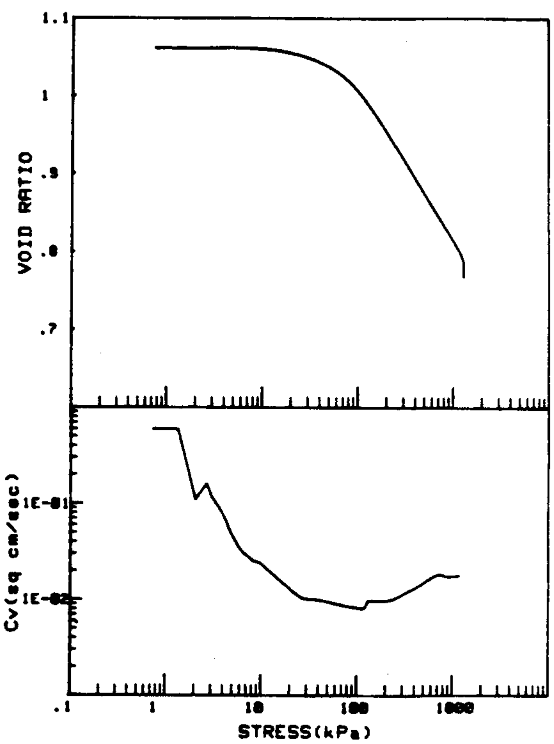

CRUISE DC1-81-EG	INCREMENT (cm)	32-34
CORE NO. 827G2	TEST NO.	CE14

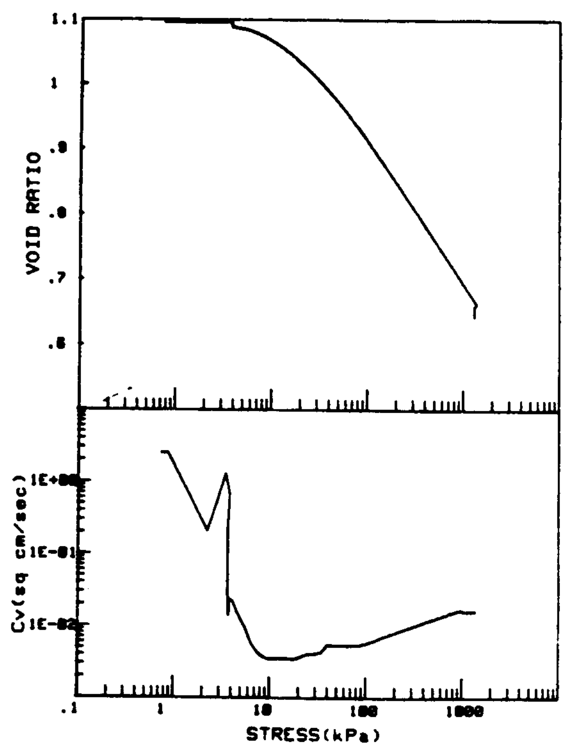

CRUISE DC1-81-EG	INCREMENT (cm)	26-28
CORE NO. 827G2	TEST NO.	CE16

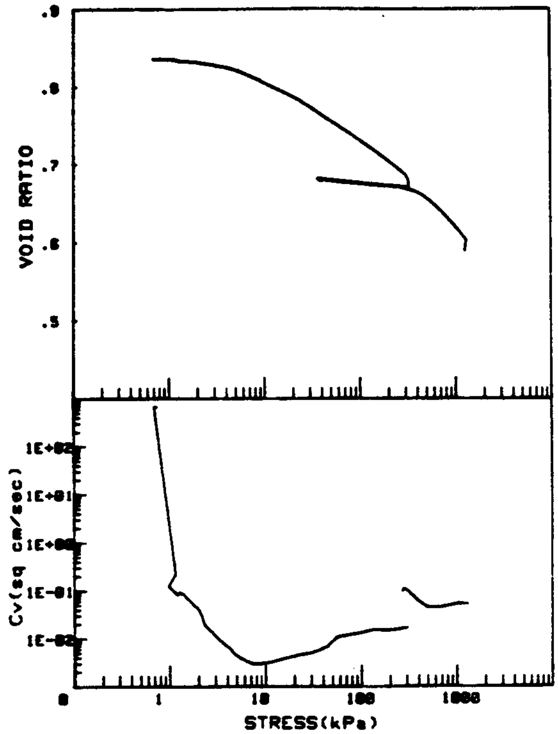

CRUISE DC1-81-EG INCREMENT (cm) 110-115
CORE NO. 610G2 TEST NO. CE17

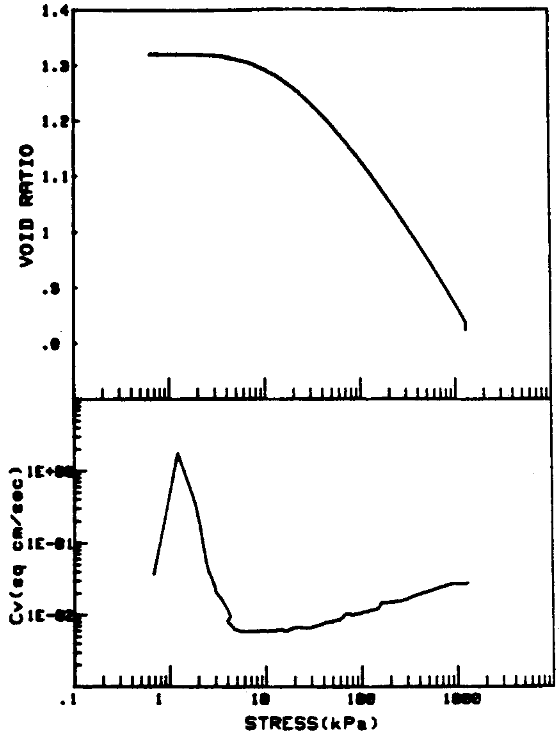

CRUISE DC1-81-EG INCREMENT (cm) 82-84
CORE NO. 610G2 TEST NO. CE22

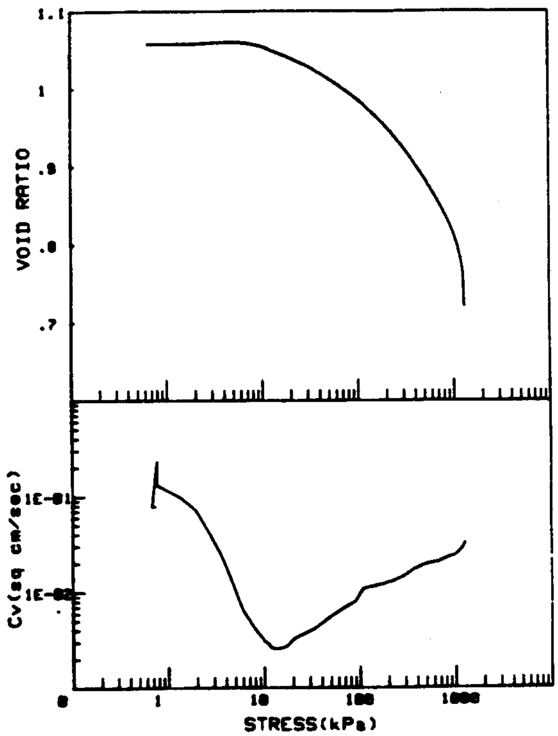

CRUISE DC1-81-EG INCREMENT (cm) 190-195
CORE NO. 610G2 TEST NO. CE18

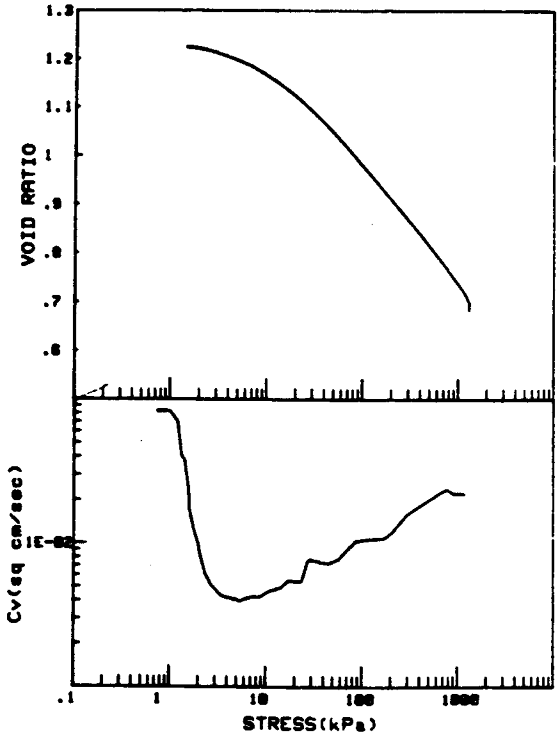

CRUISE DC1-81-EG INCREMENT (cm) 71-73
CORE NO. 620G2 TEST NO. CE23

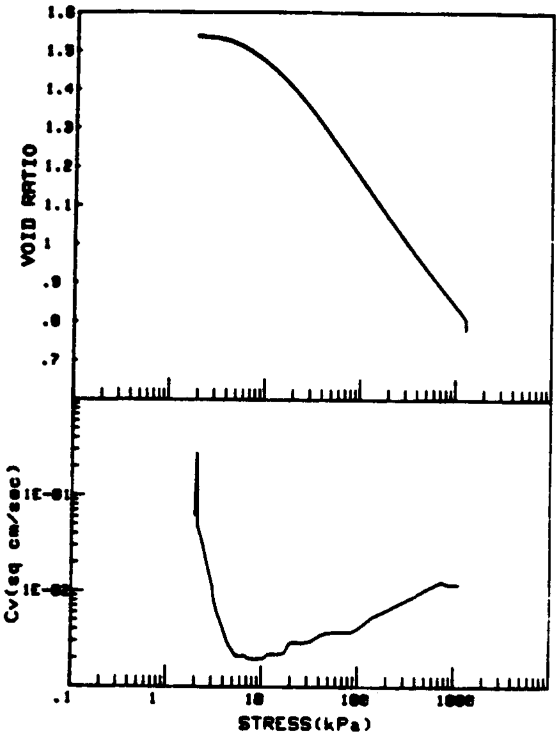

CRUISE DC1-81-EG		INCREMENT (cm)	47-49
CORE NO.	834G2	TEST NO.	CE24

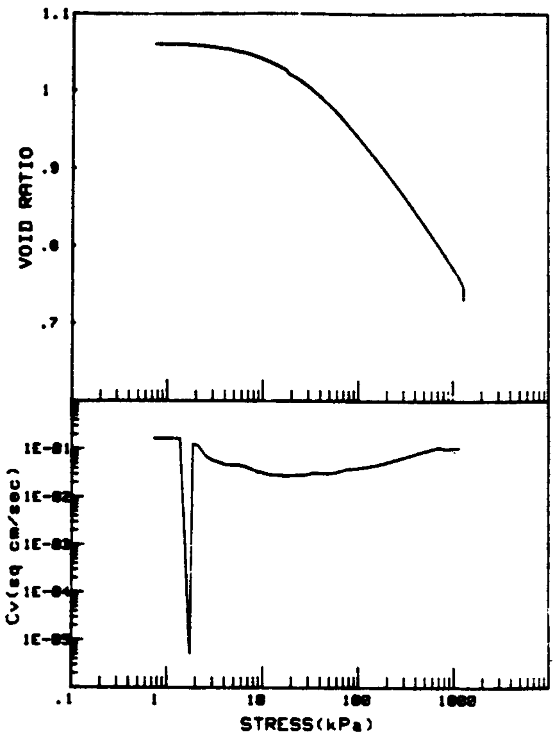

CRUISE DC2-80-EG		INCREMENT (cm)	146-148
CORE NO.	07G	TEST NO.	CE26

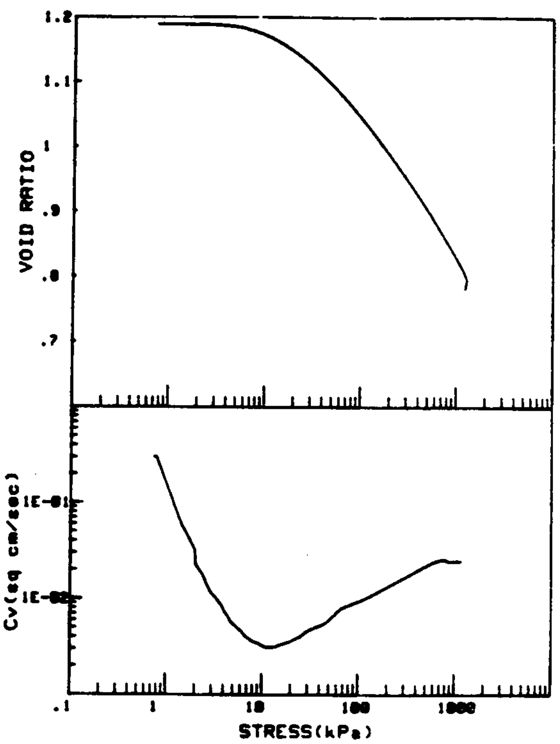

CRUISE DC1-81-EG		INCREMENT (cm)	153-155
CORE NO.	805G2	TEST NO.	CE25

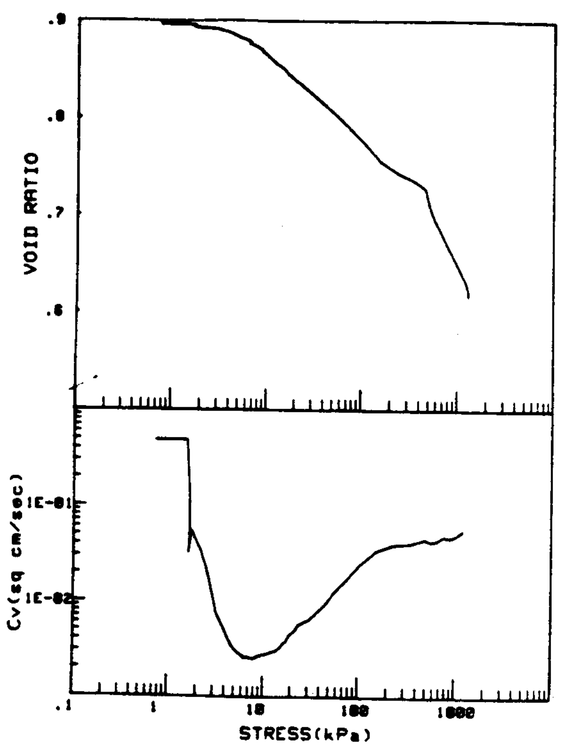

CRUISE DC1-81-EG		INCREMENT (cm)	210-212
CORE NO.	824R1	TEST NO.	CE27

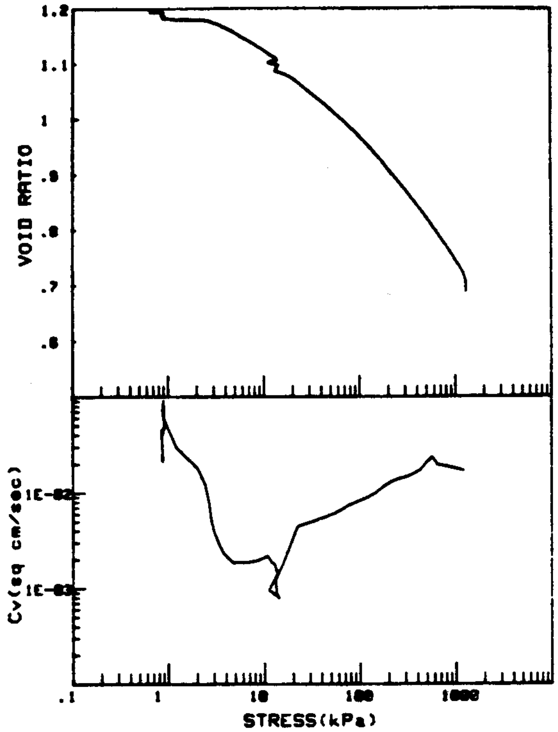

CRUISE DC1-81-EG		INCREMENT (cm)	106-108
CORE NO.	810G2	TEST NO.	CE29

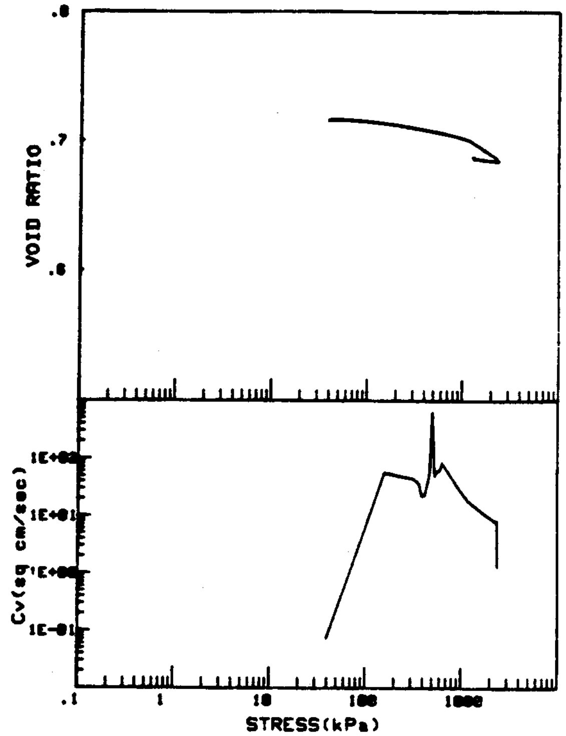

CRUISE DC1-81-EG		INCREMENT (cm)	208-211
CORE NO.	830R2	TEST NO.	CE32

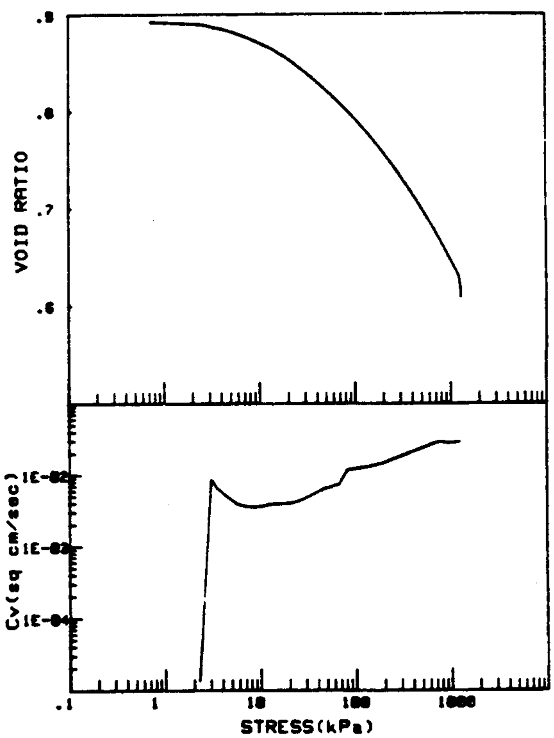

CRUISE DC1-81-EG		INCREMENT (cm)	76-78
CORE NO.	832G1	TEST NO.	CE31

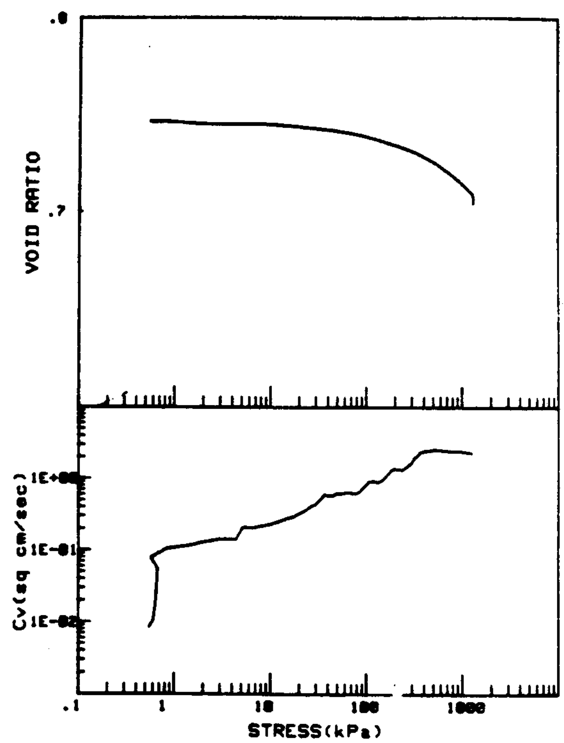

CRUISE DC1-81-EG		INCREMENT (cm)	152-157
CORE NO.	824R1	TEST NO.	CE33

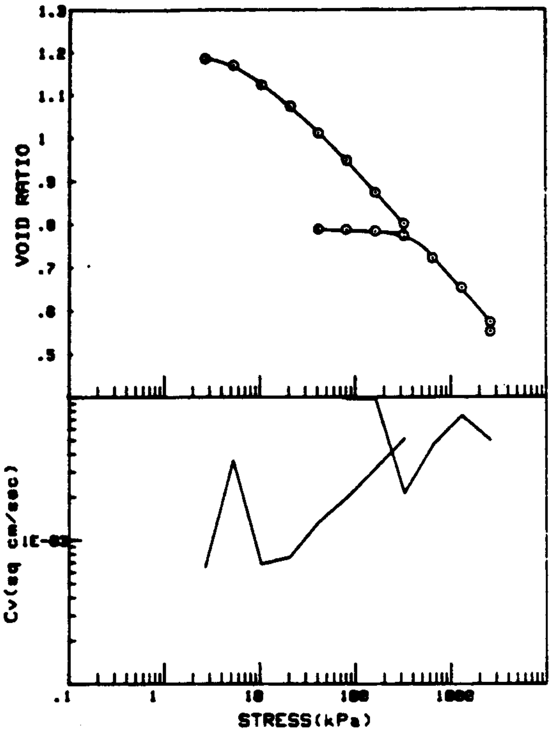

CRUISE DC1-81-EG	INCREMENT (cm) 122-124
CORE NO. 027G2	TEST NO. 0E40

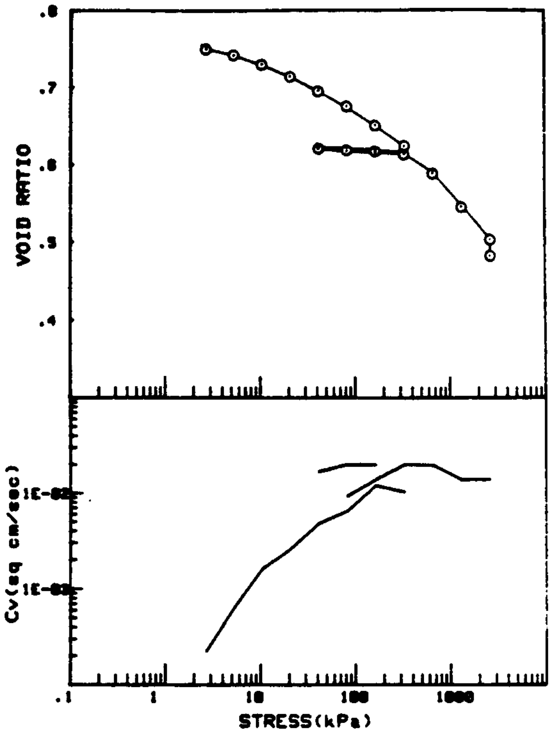

CRUISE DC1-81-EG	INCREMENT (cm) 140-144
CORE NO. 004G1	TEST NO. 0E44

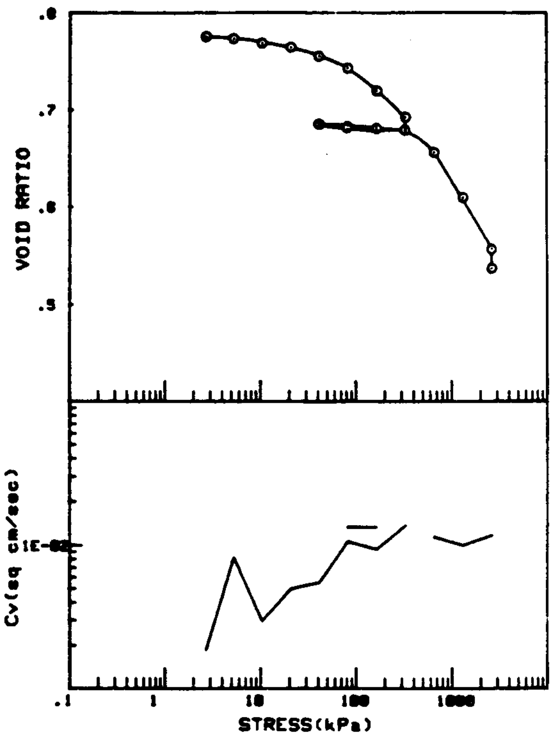

CRUISE DC1-81-EG	INCREMENT (cm) 106-108
CORE NO. 010G2	TEST NO. 0E41

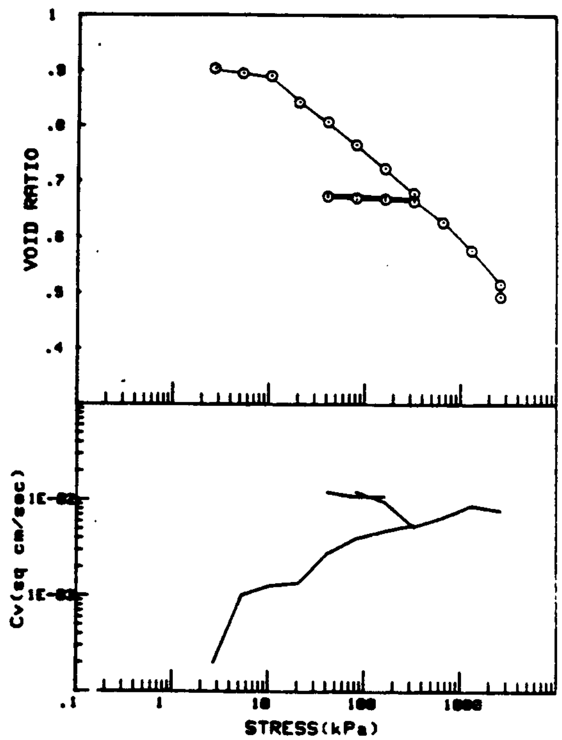

CRUISE DC1-81-EG	INCREMENT (cm) 196-200
CORE NO. 005G2	TEST NO. 0E45

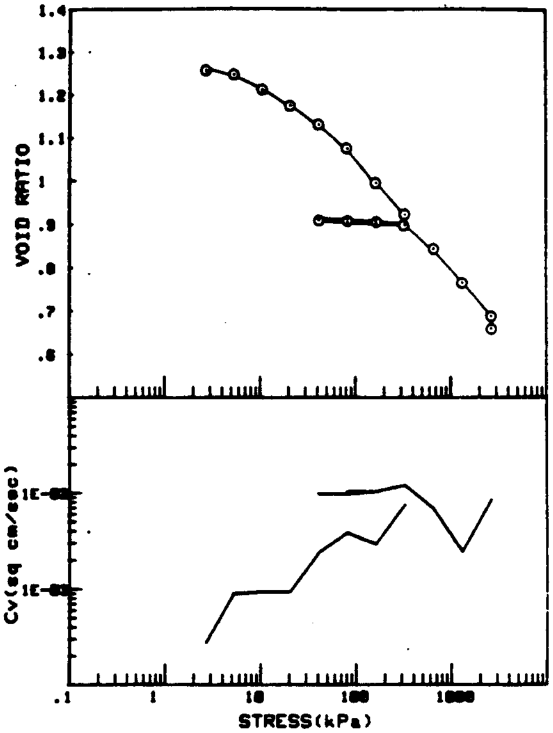

CRUISE DC1-81-EG		INCREMENT (cm)	67-72
CORE NO.	085G1	TEST NO.	0E46

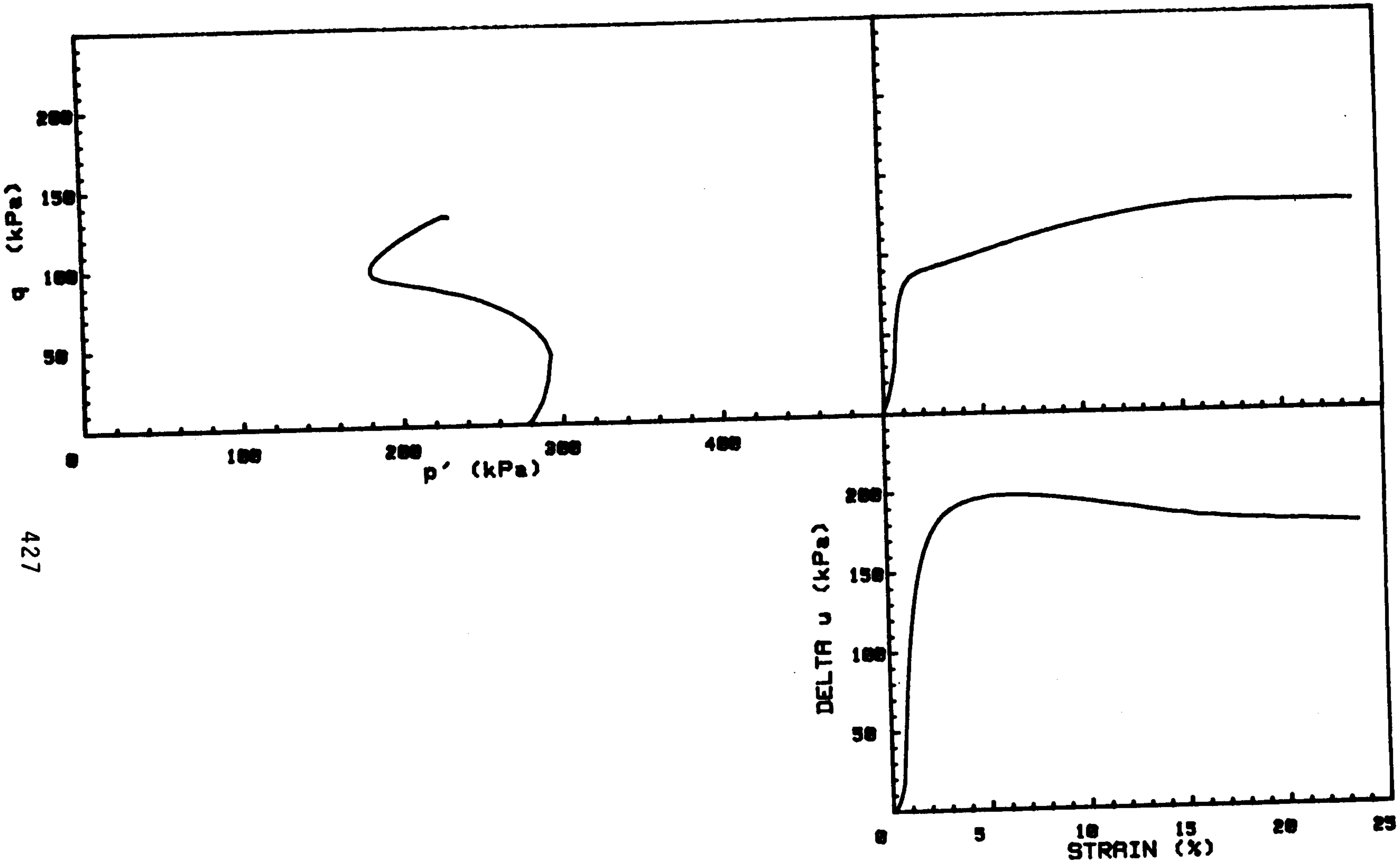

CRUISE	DC2-80-EG	INCREMENT (cm)	5-15
CORE NO.	G181	TEST NO.	TE15

SIG1c'(kPa) 277.7
SIG3c'(kPa) 277.7
INDUCED OCR 1.0

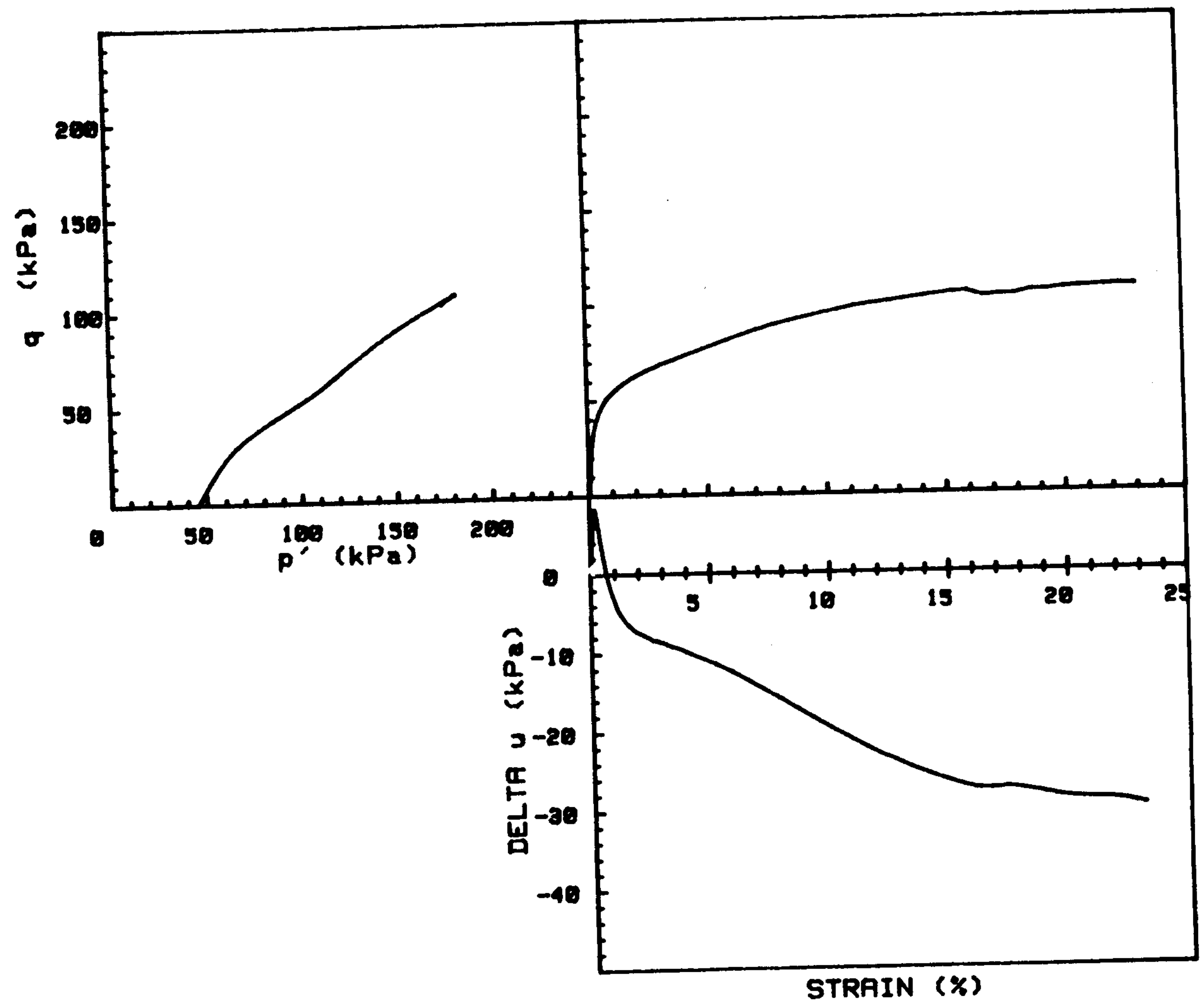

CRUISE DC2-80-EG		INCREMENT (cm)	5-14
CORE NO.	G181	TEST NO.	TE16
SIG1c′(kPa)	45.0		
SIG3c′(kPa)	45.0		
INDUCED OCR	6.1		

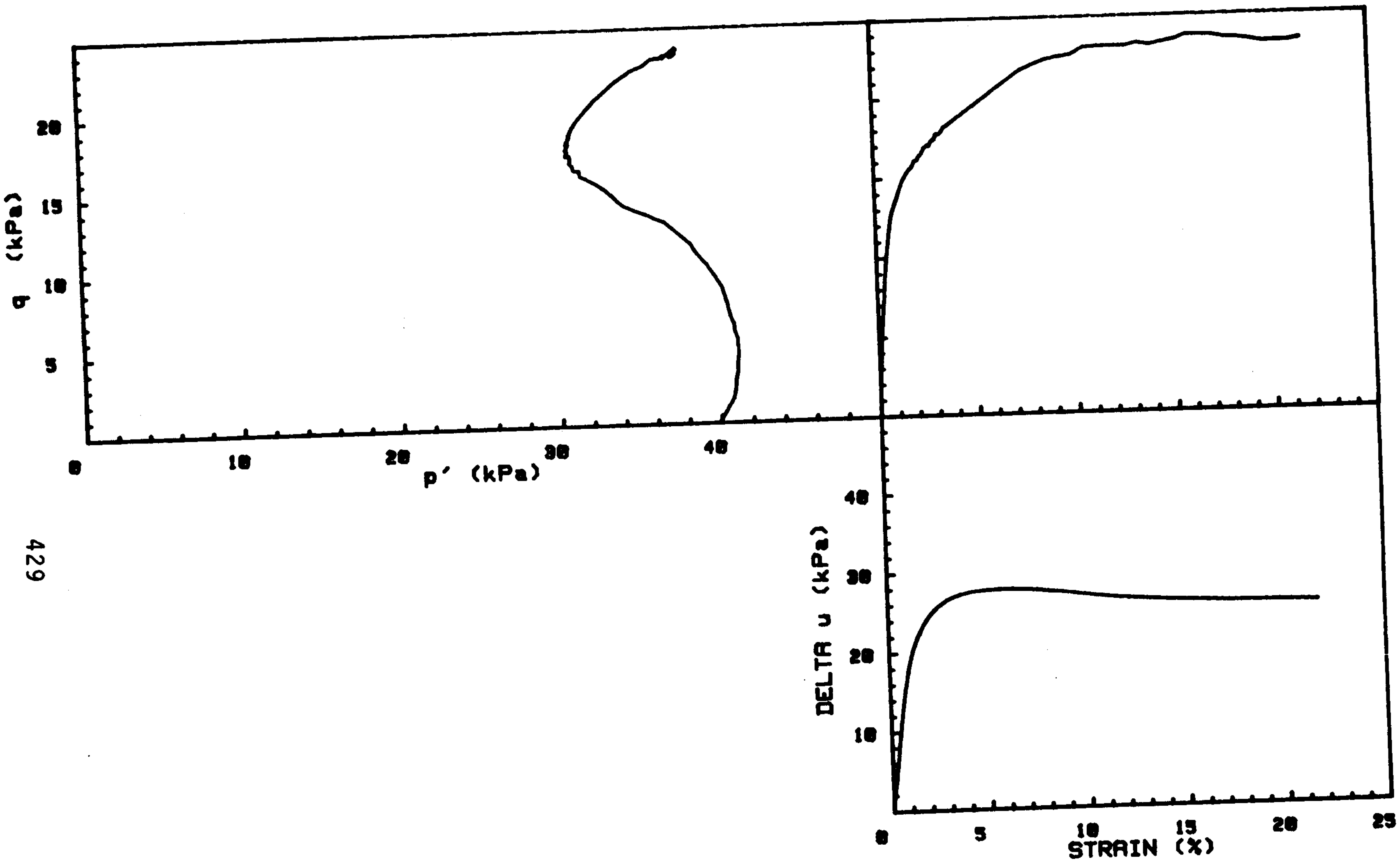

CRUISE DC2-80-EG		INCREMENT (cm)	71-81
CORE NO.	G181	TEST NO.	TE18
SIG1c′(kPa)	39.9		
SIG3c′(kPa)	39.9		
INDUCED OCR	1.0		

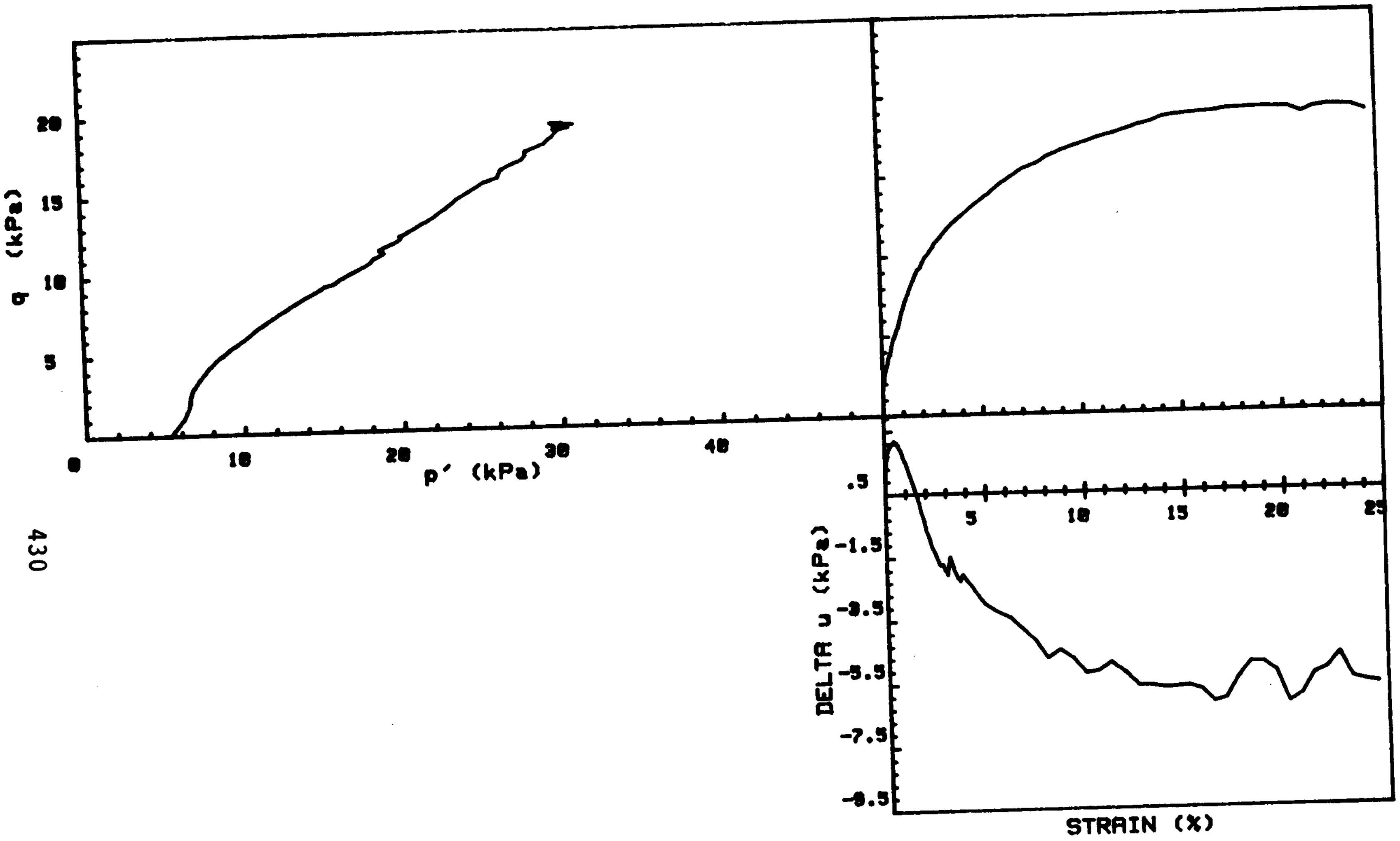

CRUISE DC2-80-EG		INCREMENT (cm)	71-80
CORE NO.	G181	TEST NO.	TE19
SIG1c′(kPa)	5.3		
SIG3c′(kPa)	5.3		
INDUCED OCR	7.3		

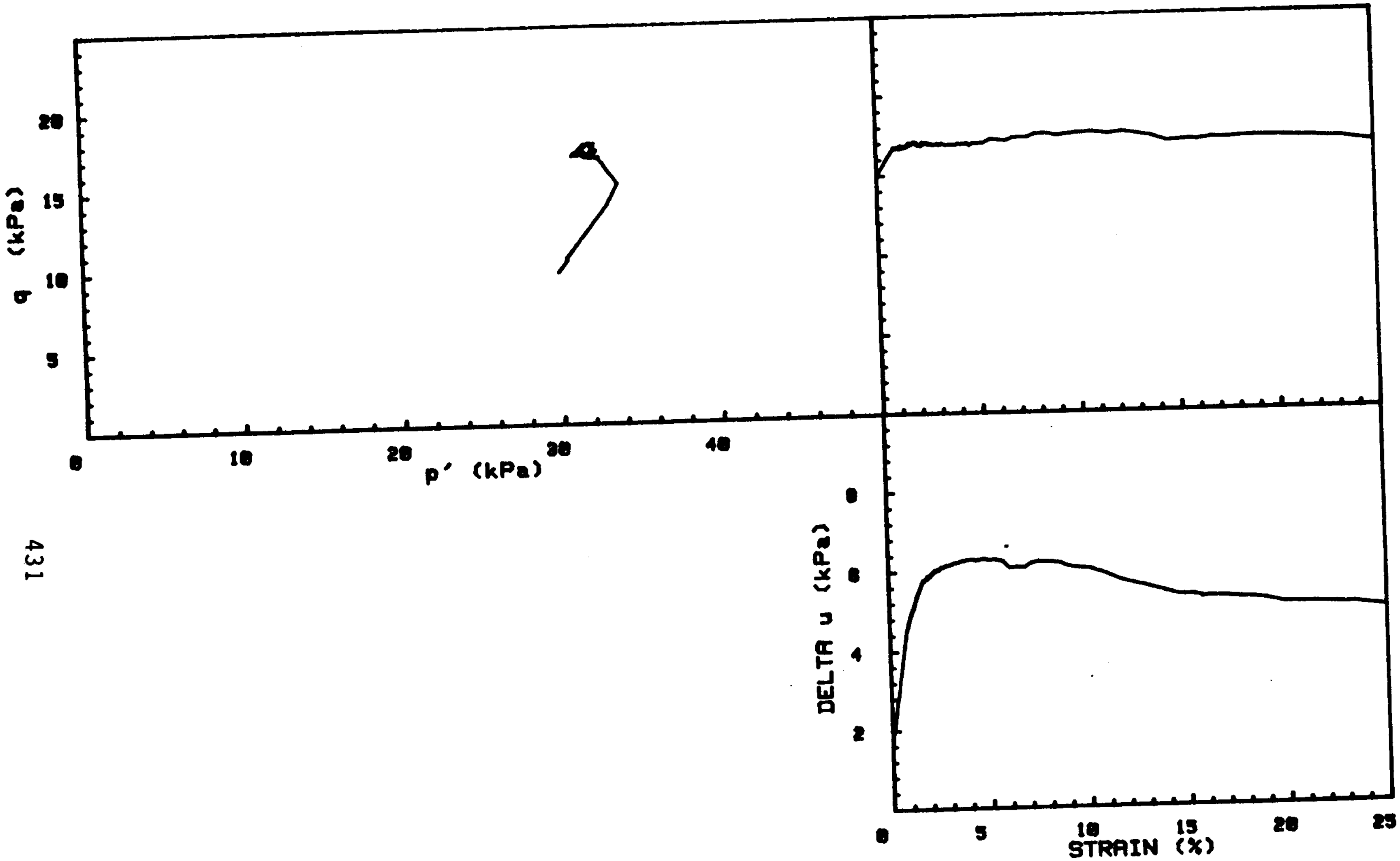

CRUISE DC2-80-EG		INCREMENT (cm)	100-109
CORE NO.	G181	TEST NO.	TE20
SIG1c′(kPa)	39.4		
SIG3c′(kPa)	20.3		
INDUCED OCR	1.0		

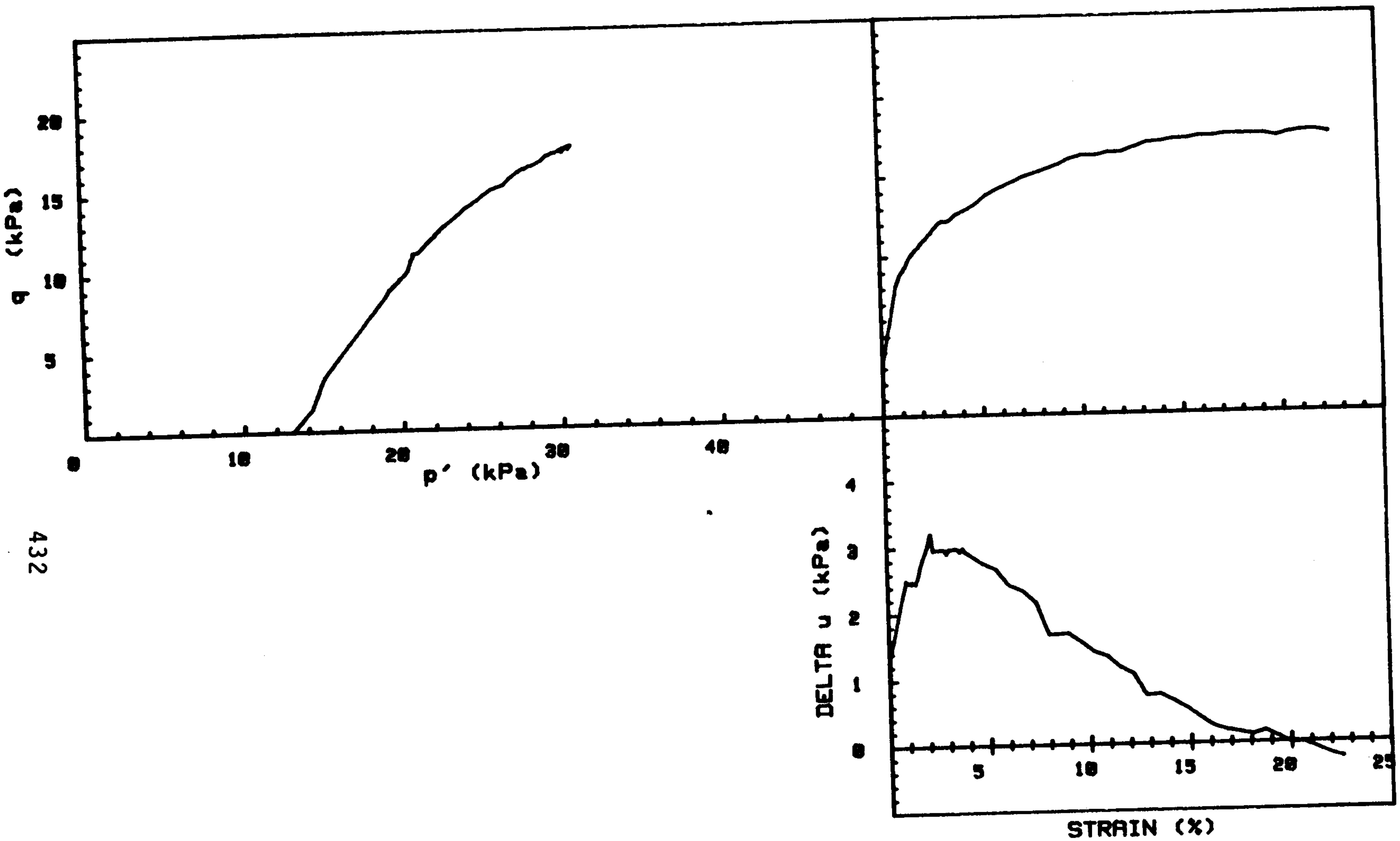

CRUISE DC2-80-EG		INCREMENT (cm)	100-110
CORE NO.	G101	TEST NO.	TE21
SIG1c′(kPa)	13.1		
SIG3c′(kPa)	13.1		
INDUCED OCR	3.0		

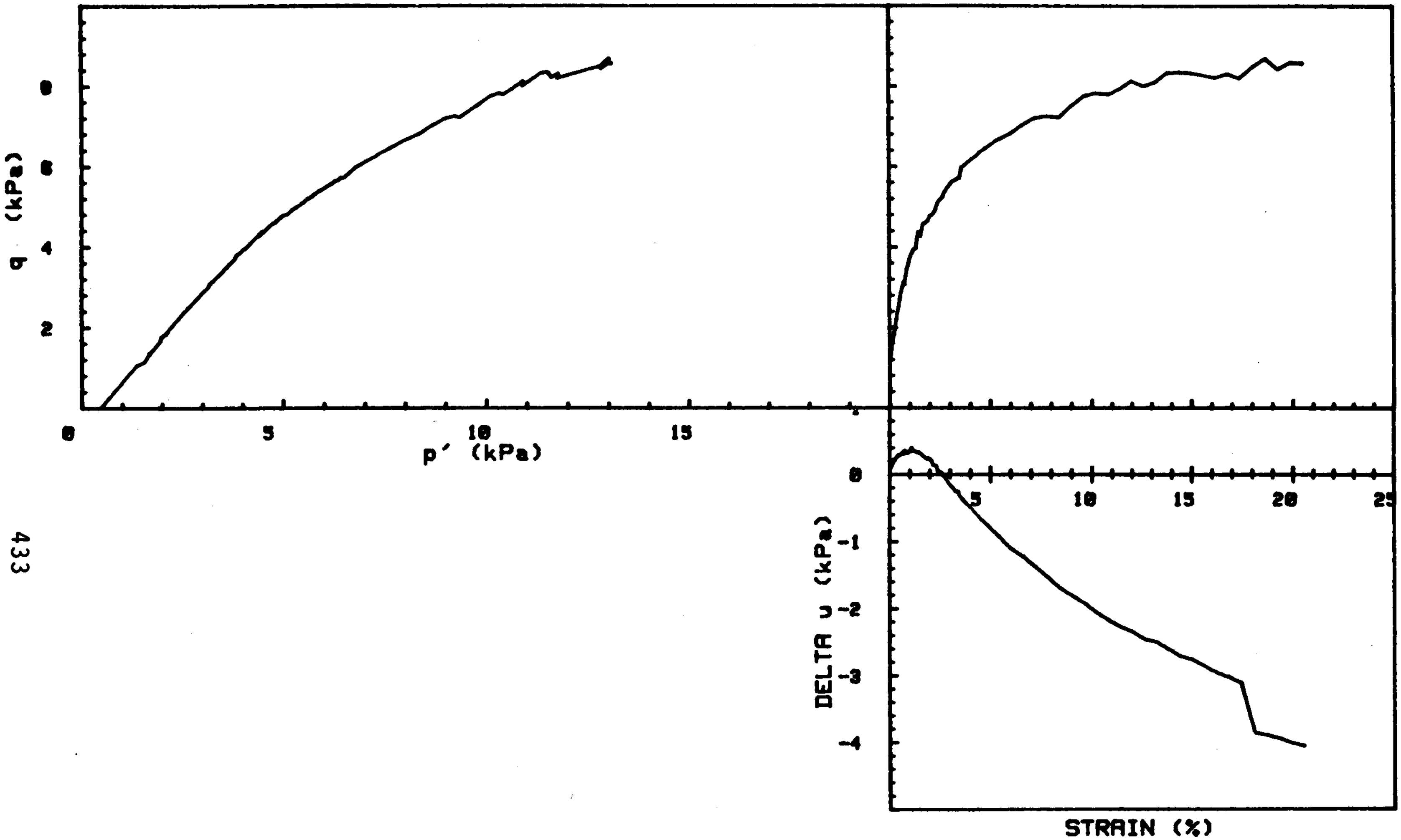

CRUISE DC2-80-EG		INCREMENT (cm)	120-130
CORE NO.	G181	TEST NO.	TE22

SIG1c′(kPa) .5
SIG3c′(kPa) .5
INDUCED OCR 1.0

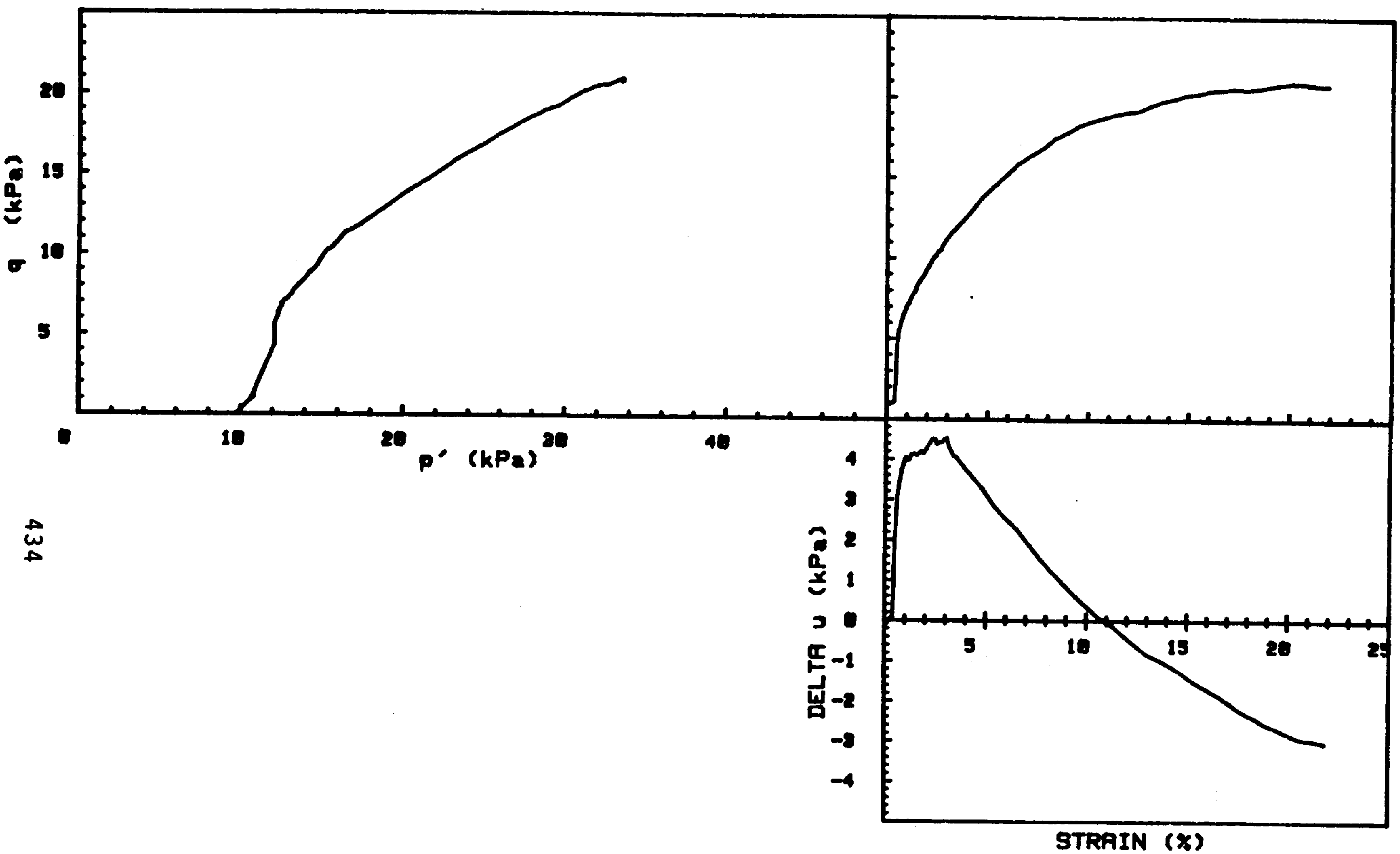

CRUISE	DC2-80-EG	INCREMENT (cm)	120-130
CORE NO.	G181	TEST NO.	TE23
SIG1c′(kPa)	9.7		
SIG3c′(kPa)	9.7		
INDUCED OCR	1.0		

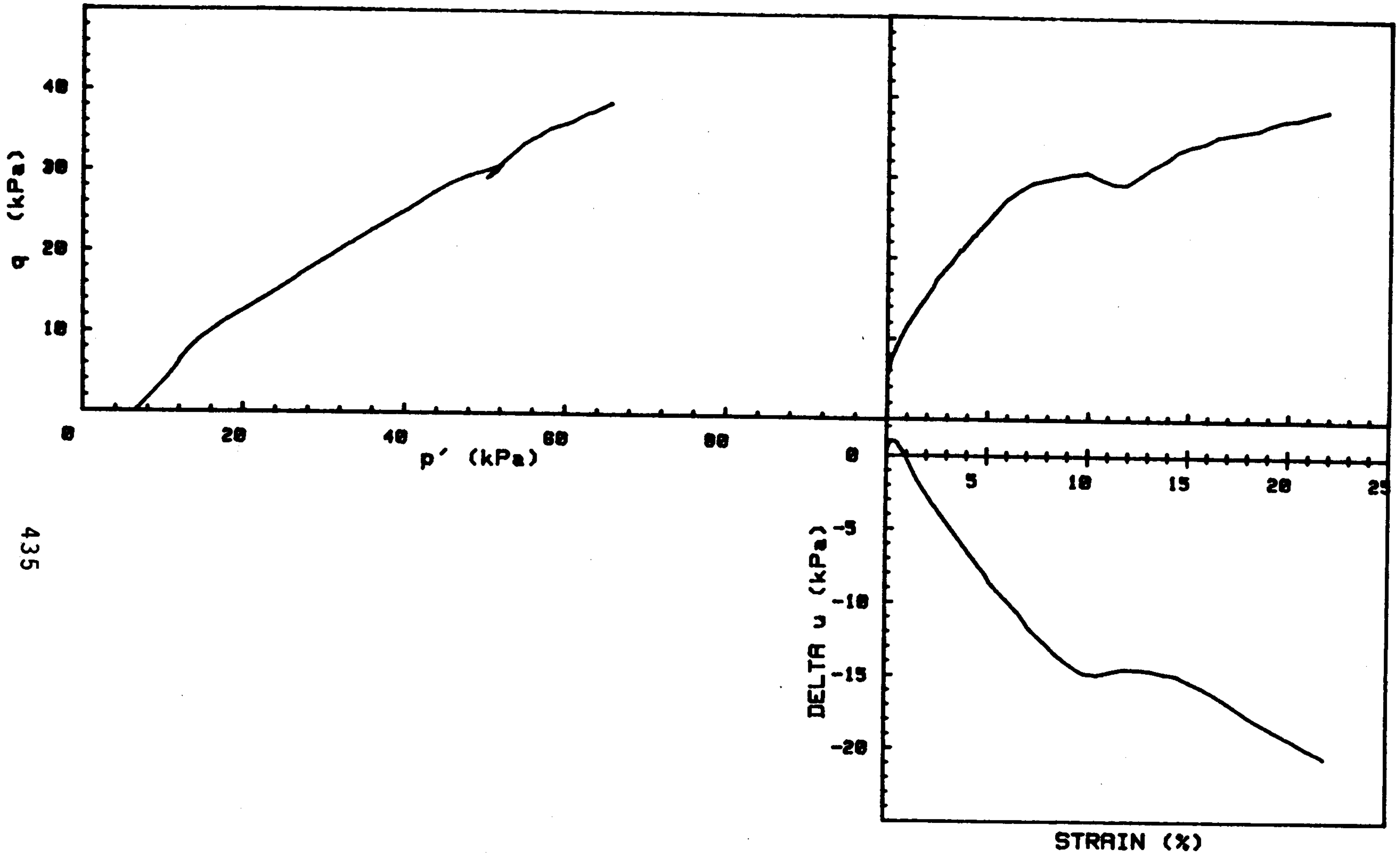

CRUISE DC2-80-EG		INCREMENT (cm)	8-17
CORE NO.	43G	TEST NO.	TE27
SIG1c′(kPa)	6.5		
SIG3c′(kPa)	6.5		
INDUCED OCR	5.0		

435

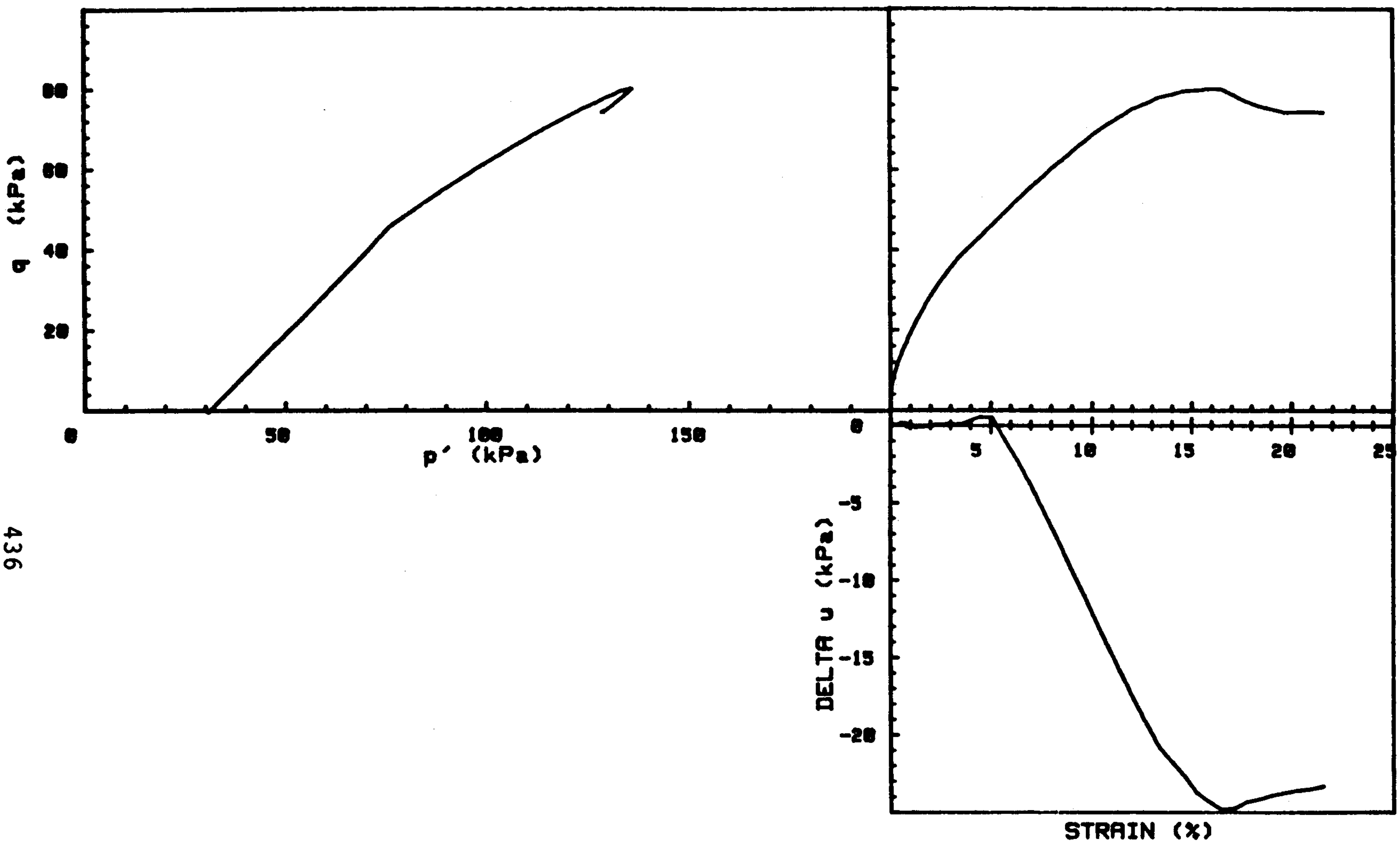

CRUISE DC2-80-EG		INCREMENT (cm)	18-27
CORE NO.	43G	TEST NO.	TE34

SIG1c′(kPa) 31.3
SIG3c′(kPa) 31.3
INDUCED OCR 1.0

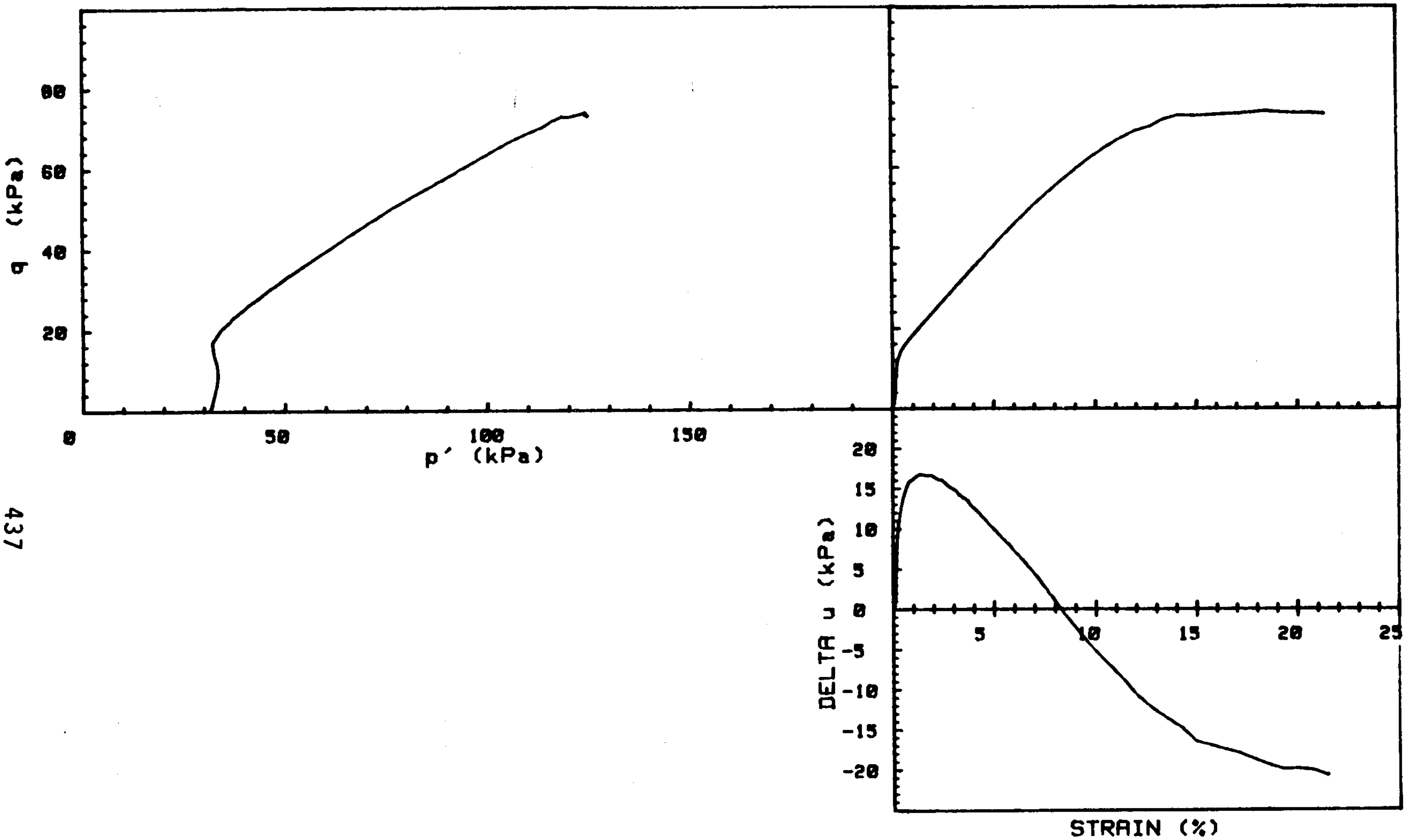

CRUISE DC2-80-EG		INCREMENT (cm)	18-27
CORE NO.	43G	TEST NO.	TE35
SIG1c′(kPa)	31.1		
SIG3c′(kPa)	31.1		
INDUCED OCR	1.0		

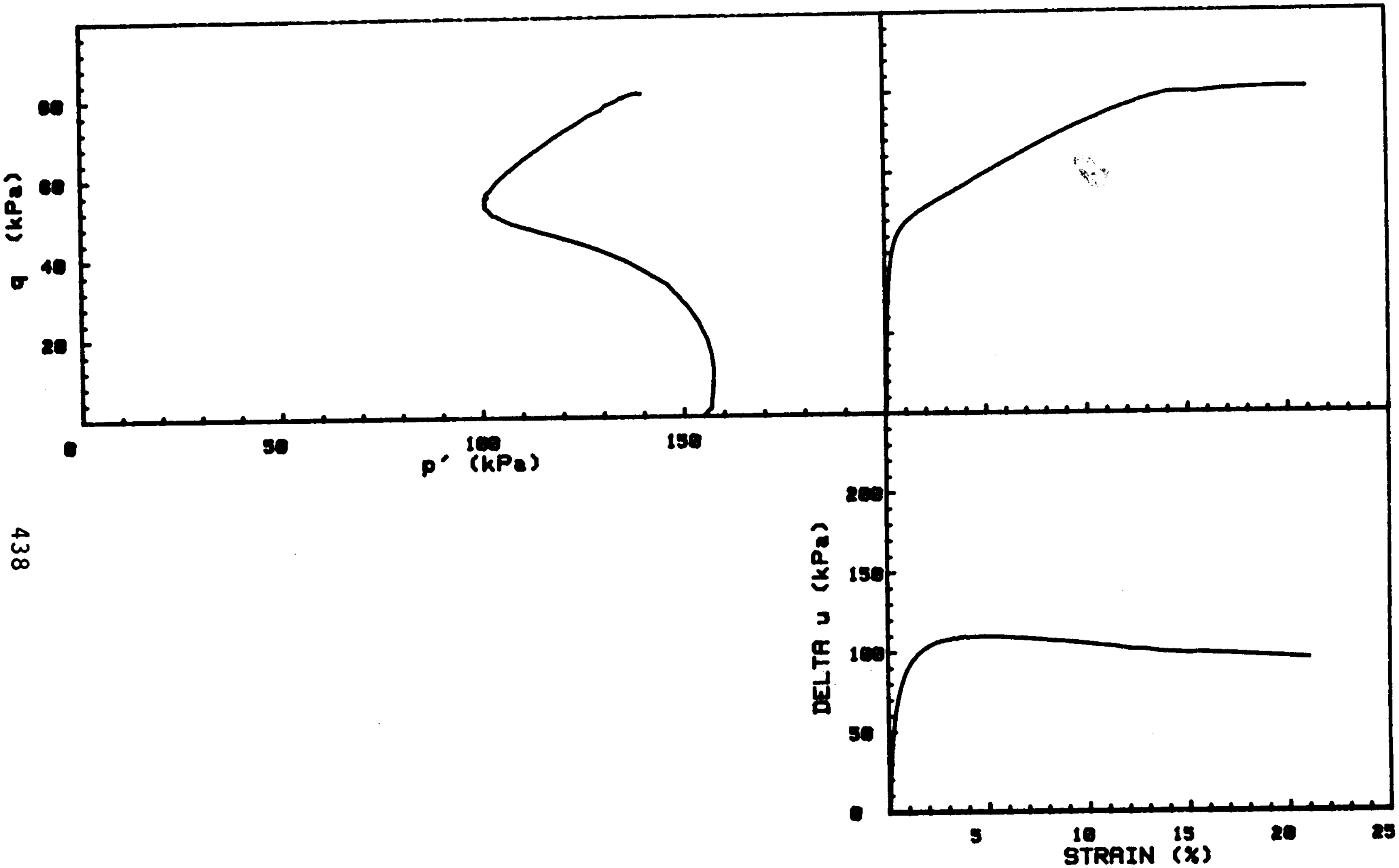

CRUISE DC2-80-EG		INCREMENT (cm)	13-22
CORE NO.	35G	TEST NO.	TE56
SIG1c'(kPa)	154.8		
SIG3c'(kPa)	154.8		
INDUCED OCR	1.0		

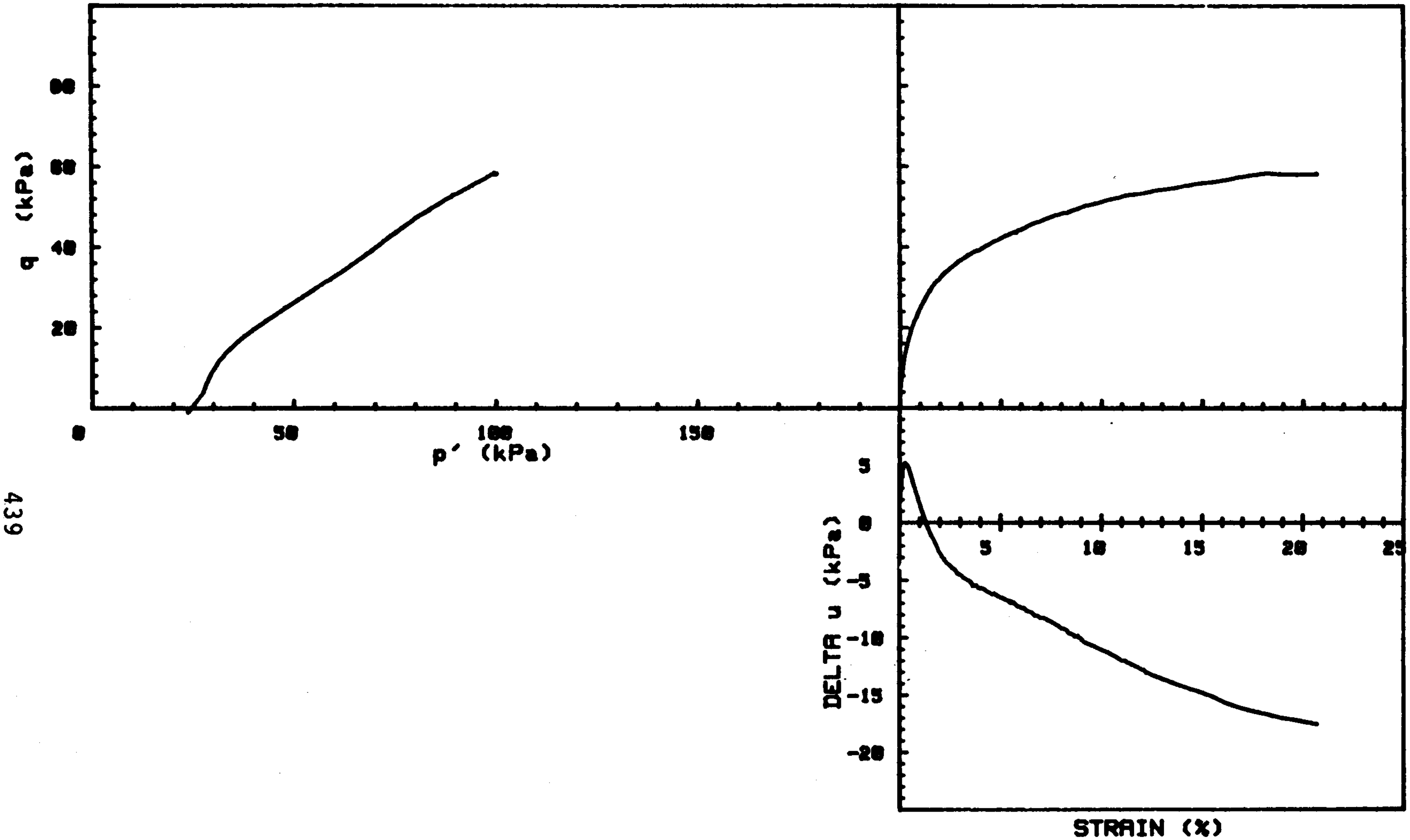

CRUISE	DC2-80-EG	INCREMENT (cm)	13-25
CORE NO.	35G	TEST NO.	TE57

SIG1c'(kPa) 24.7
SIG3c'(kPa) 24.7
INDUCED OCR 6.0

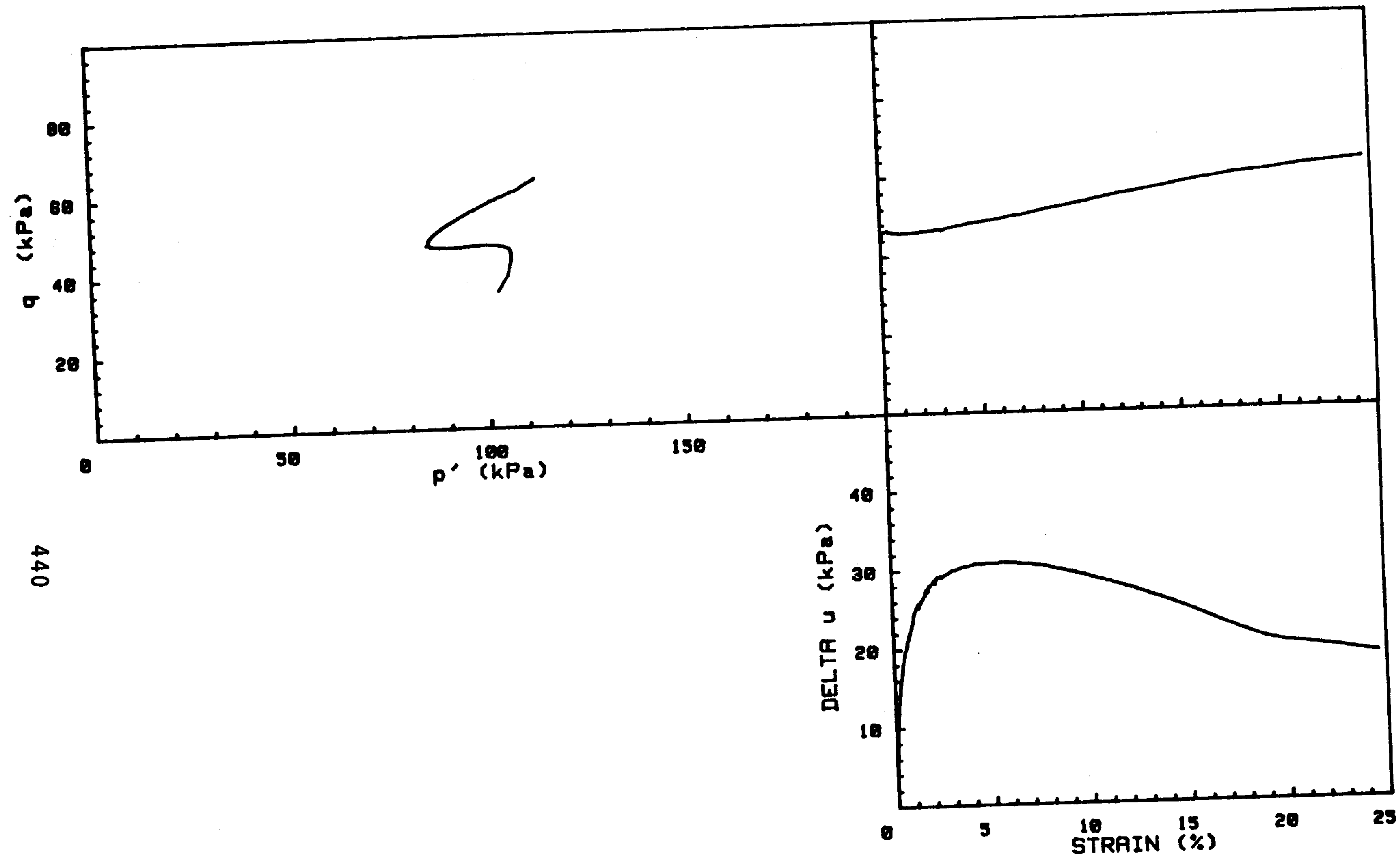

CRUISE DC2-80-EG		INCREMENT (cm)	25-32
CORE NO.	35G	TEST NO.	TE58
SIG1c′(kPa)	137.6		
SIG3c′(kPa)	68.5		
INDUCED OCR	1.0		

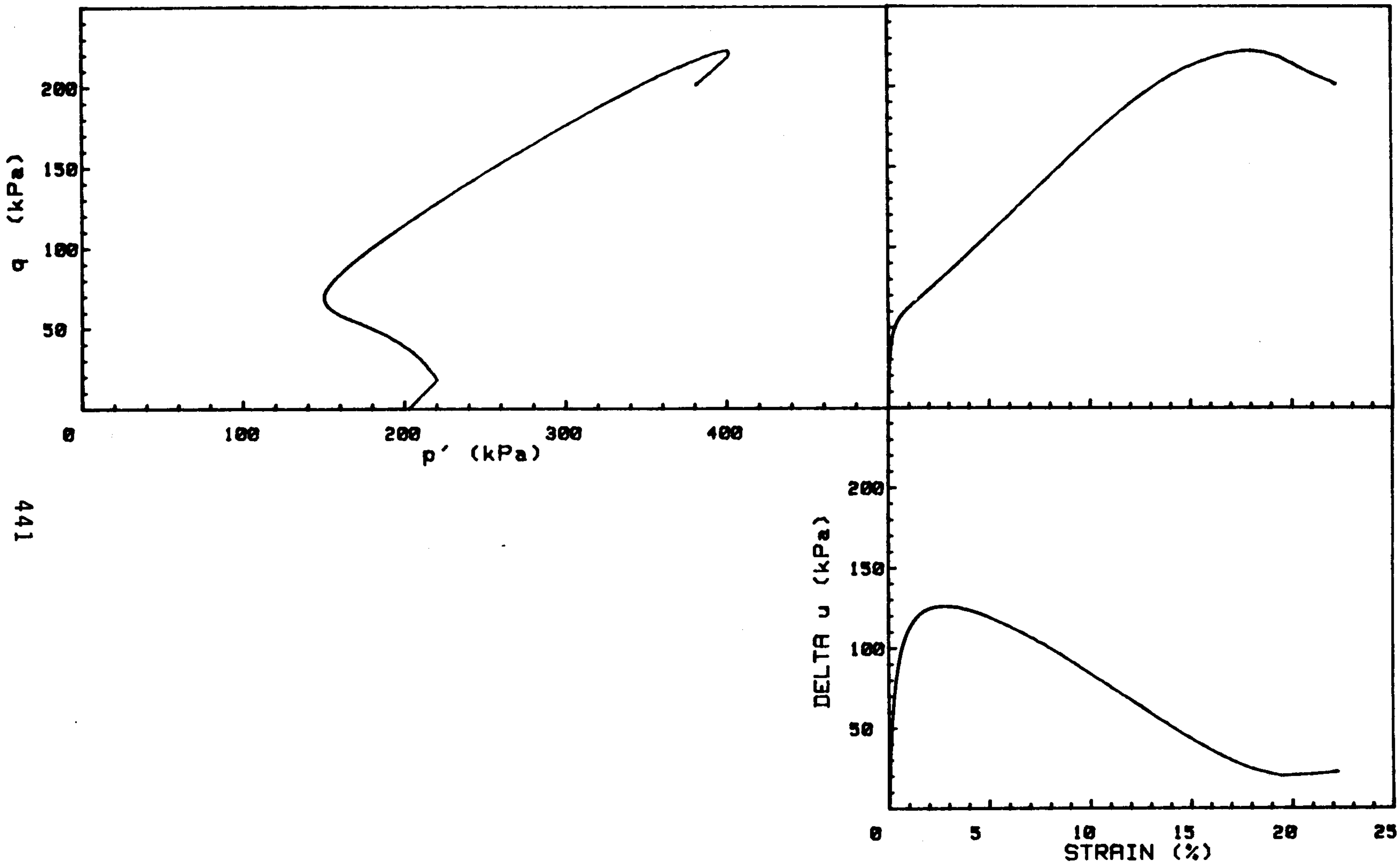

CRUISE DC2-80-EG		INCREMENT (cm)	17-28
CORE NO.	46G	TEST NO.	TE59
SIG1c′(kPa)	203.1		
SIG3c′(kPa)	203.1		
INDUCED OCR	1.0		

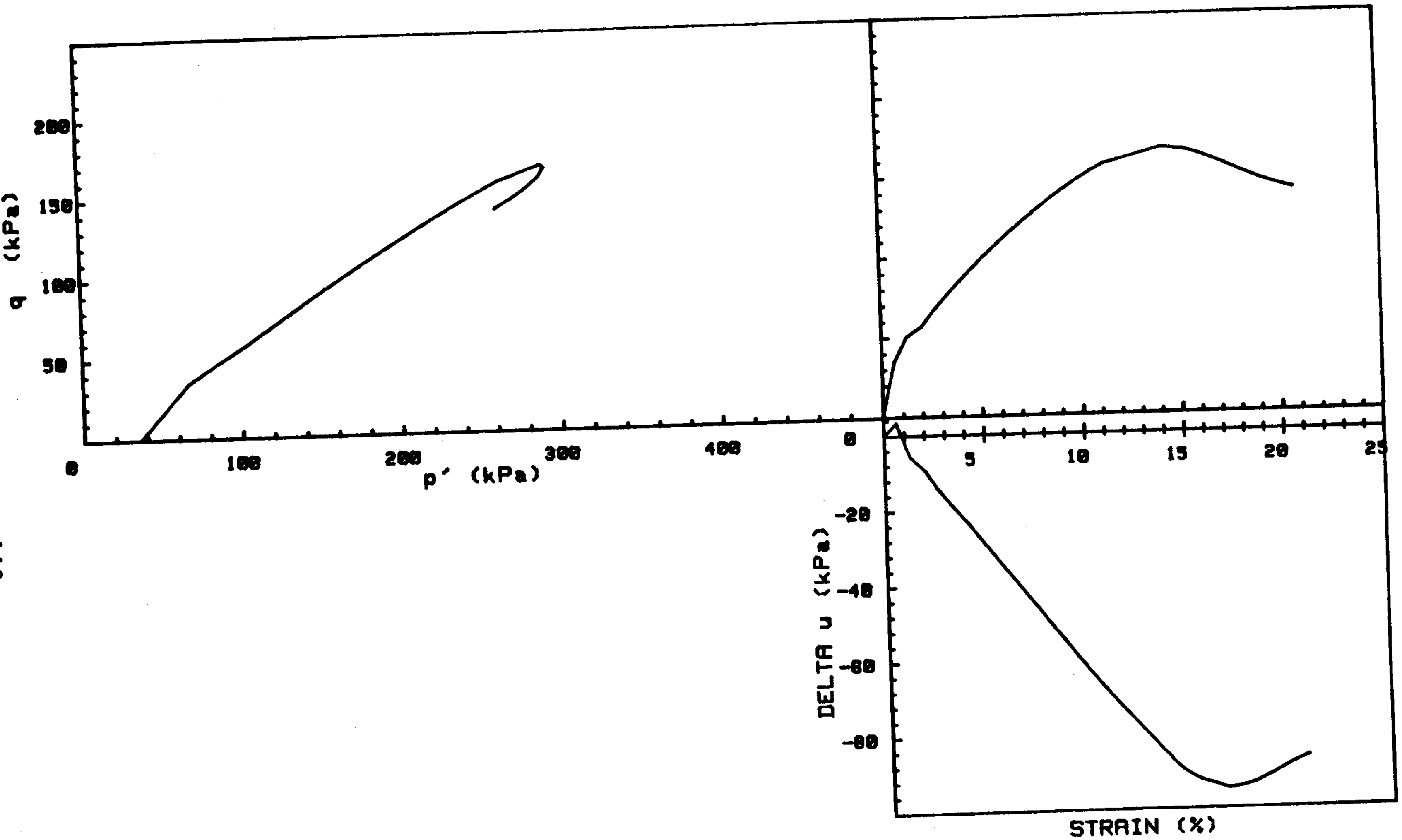

CRUISE DC2-80-EG		INCREMENT (cm)	28-37
CORE NO.	46G	TEST NO.	TE60
SIG1c′(kPa)	35.7		
SIG3c′(kPa)	35.7		
INDUCED OCR	6.0		

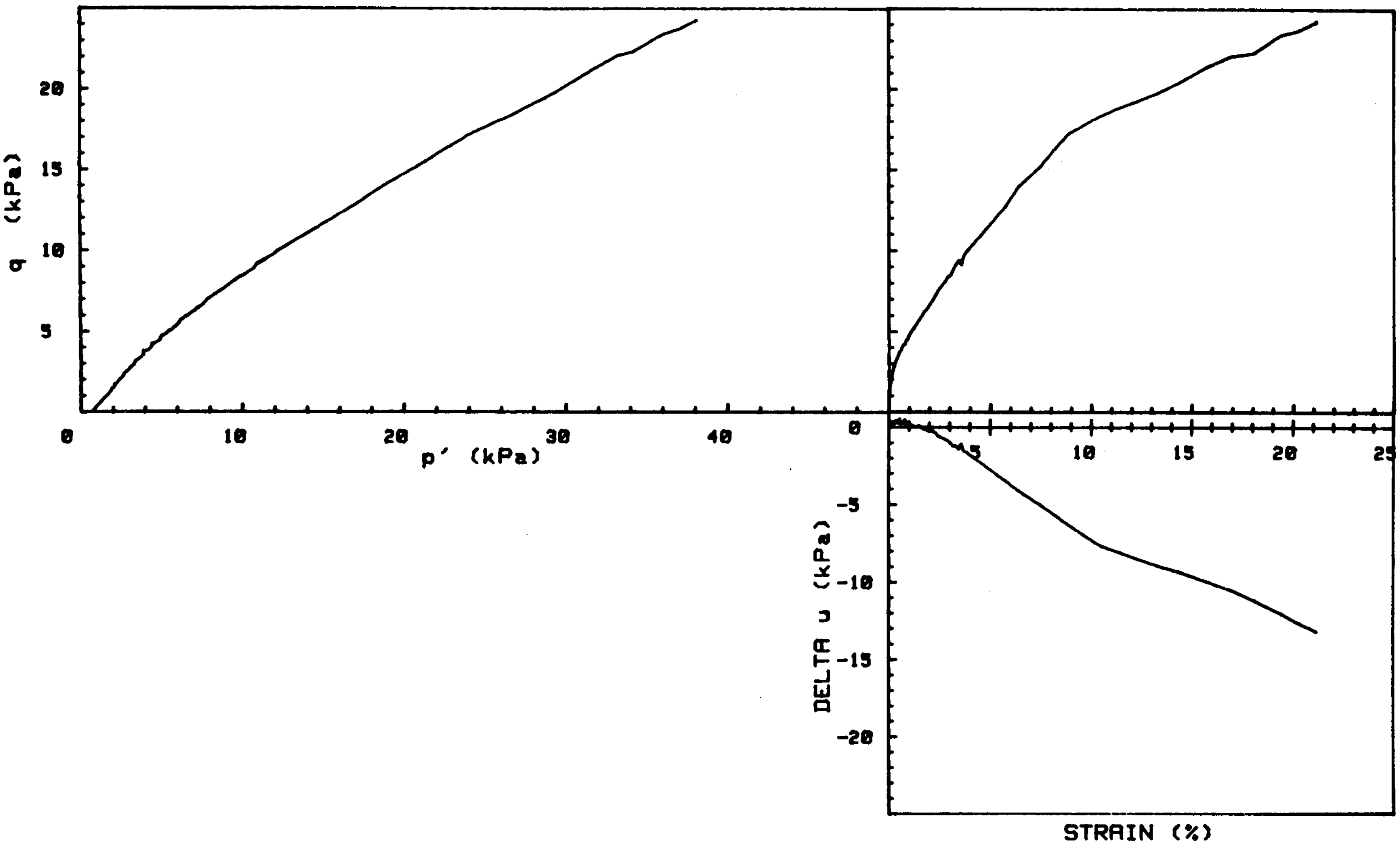

CRUISE	DC2-80-EG	INCREMENT (cm)	28-37
CORE NO.	46G	TEST NO.	TE61

SIG1c′(kPa) .7
SIG3c′(kPa) .7
INDUCED OCR 1.0

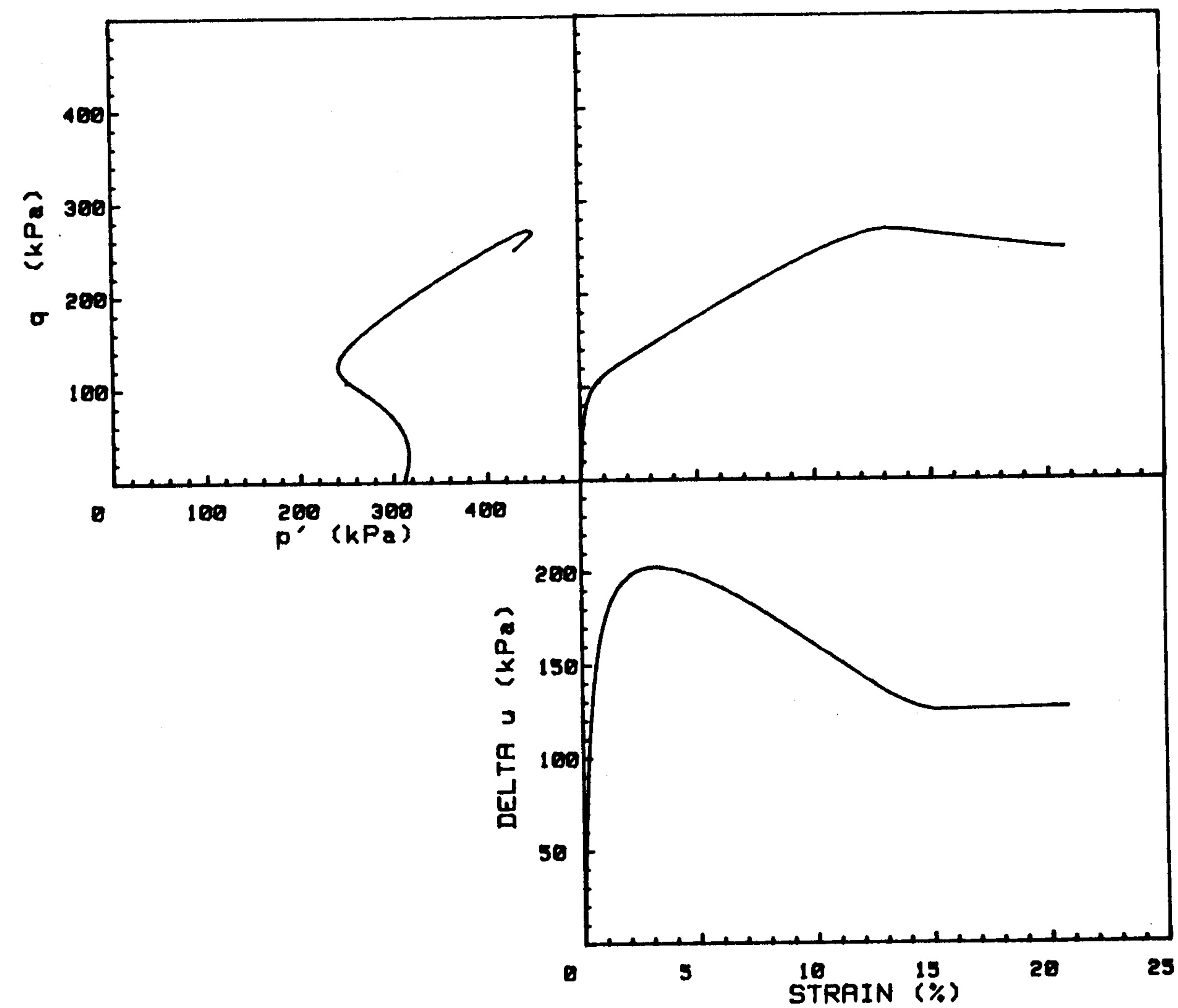

CRUISE DC2-80-EG		INCREMENT (cm)	26-35
CORE NO.	28G	TEST NO.	TE62
SIG1c′(kPa)	310.7		
SIG3c′(kPa)	310.7		
INDUCED OCR	1.0		

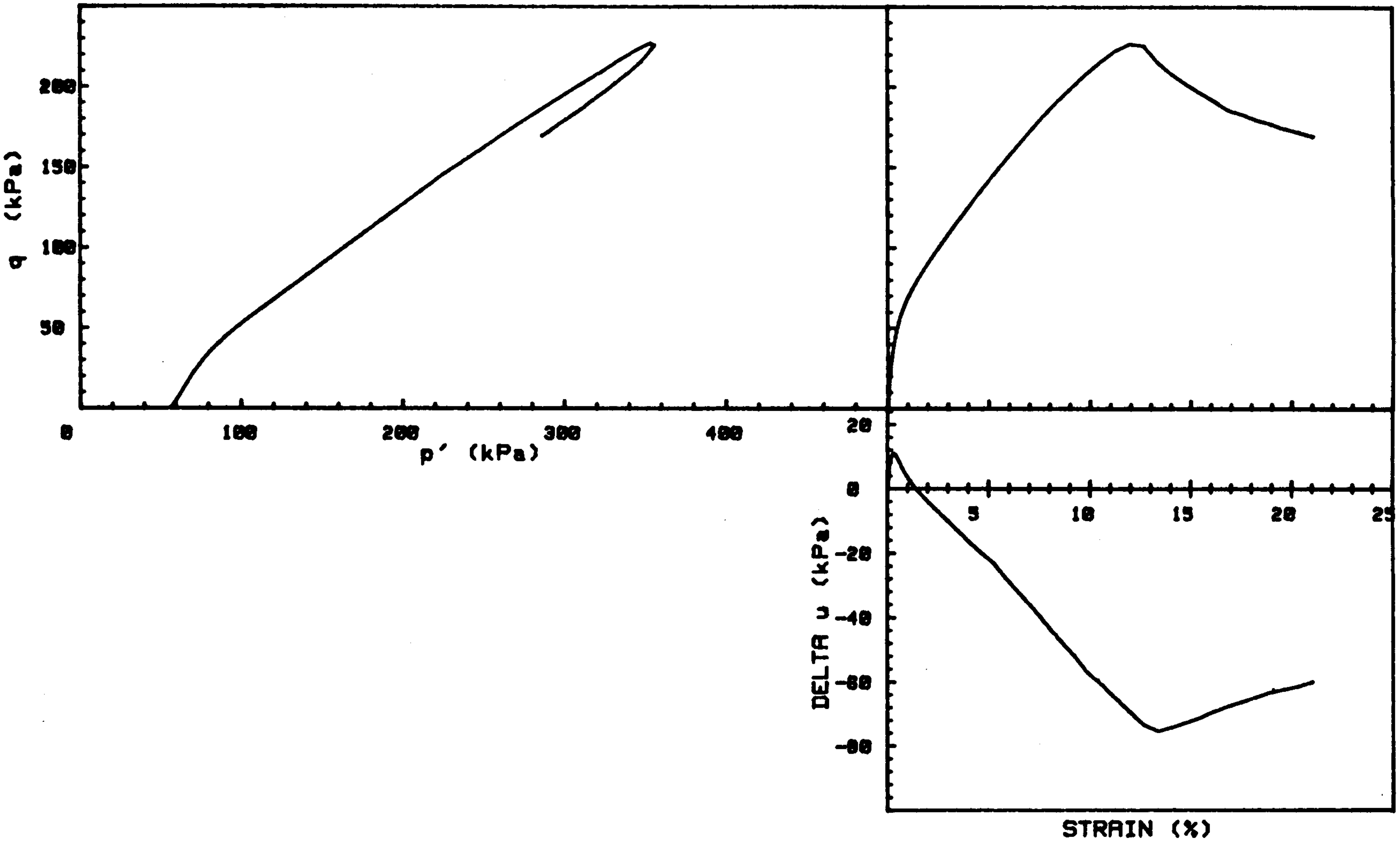

CRUISE DC-2-80 EG		INCREMENT (cm)	26.5-35.1
CORE NO.	28G	TEST NO.	TE63
SIG1c′(kPa)	56.9		
SIG3c′(kPa)	56.9		
INDUCED OCR	6.0		

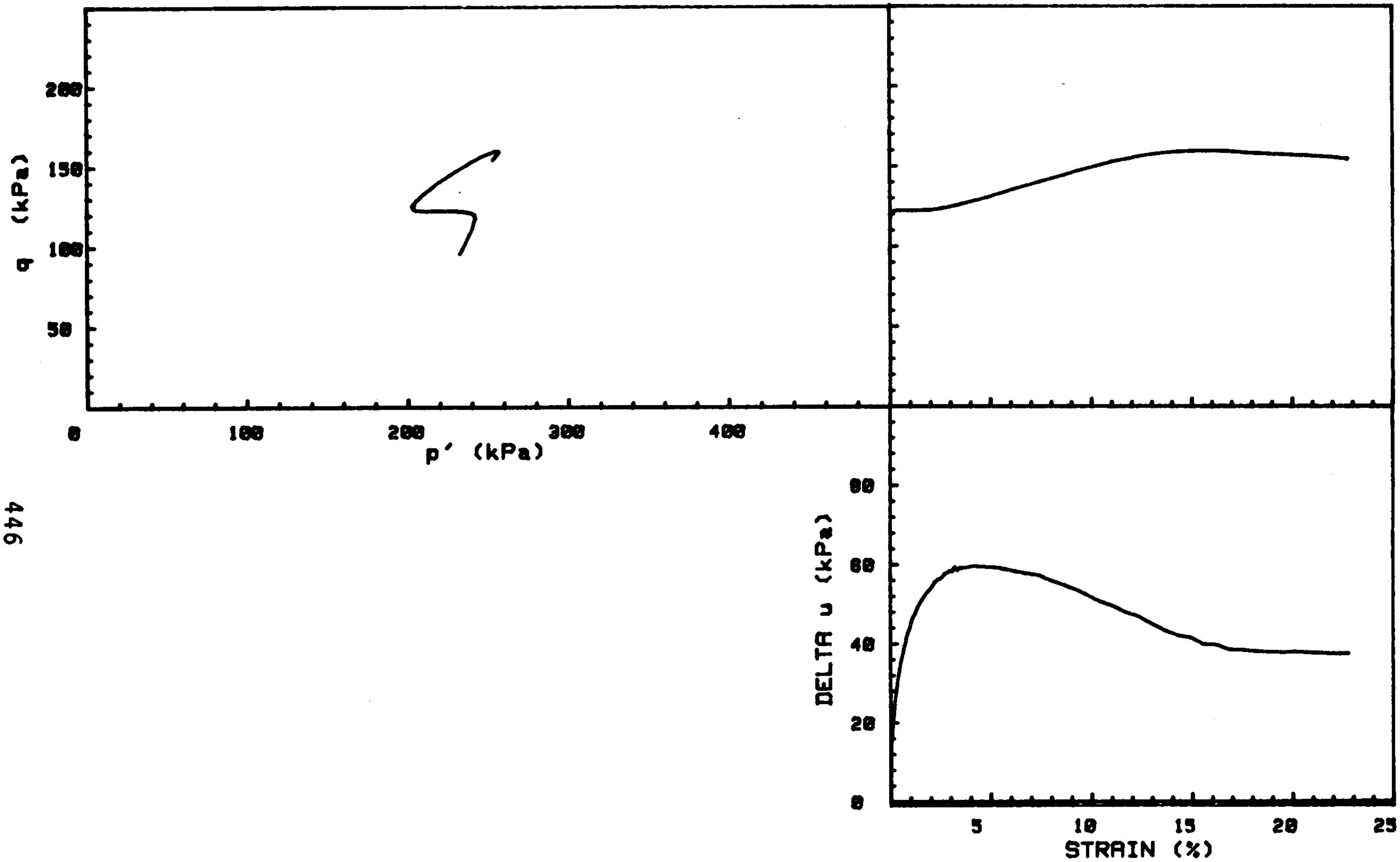

CRUISE DC2-80-EG		INCREMENT (cm)	6.8-15.2
CORE NO.	28G	TEST NO.	TE64
SIG1c′(kPa)	328.5		
SIG3c′(kPa)	136.8		
INDUCED OCR	1.0		

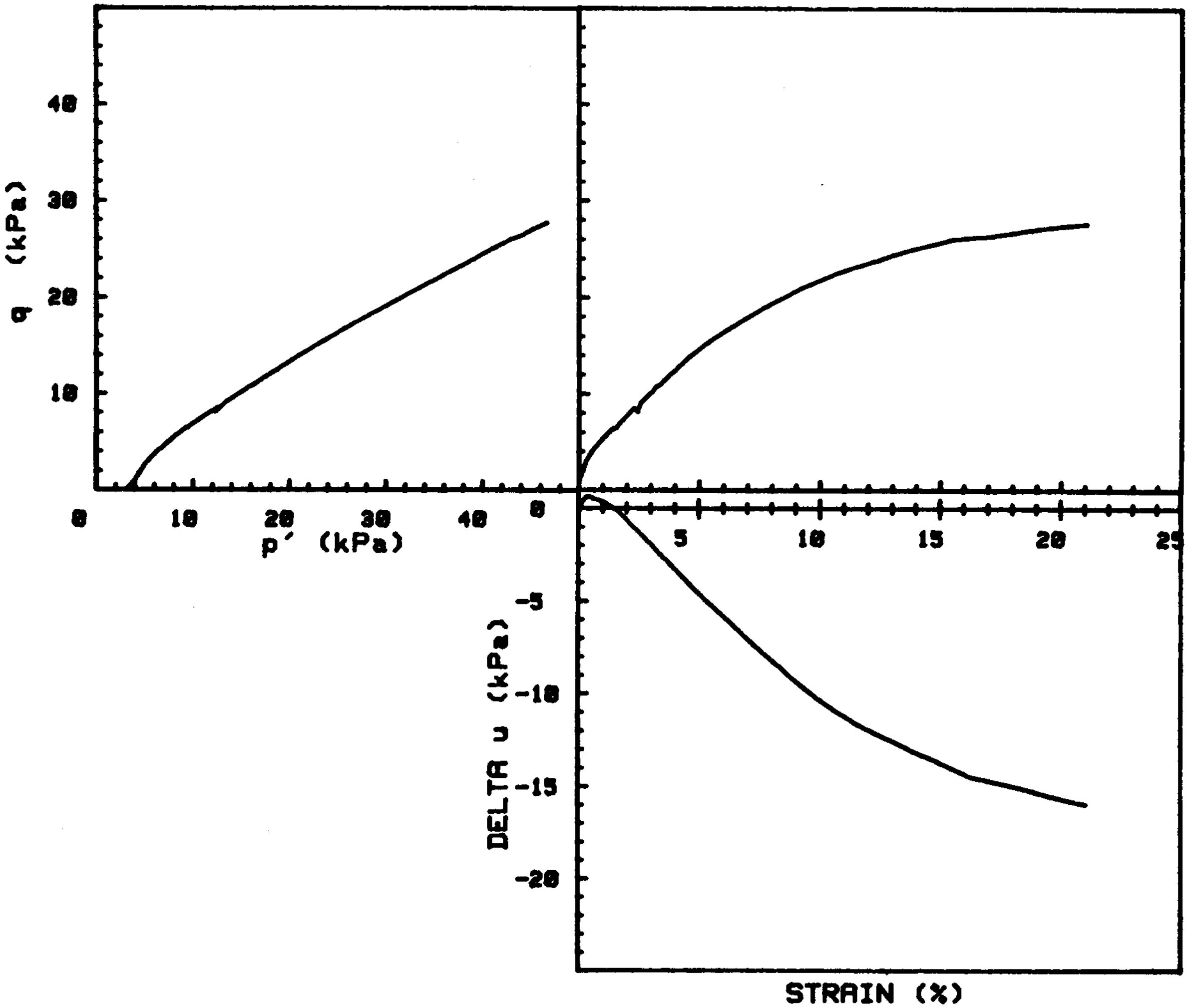

CRUISE DC2-80-EG		INCREMENT (cm)	4-11
CORE NO.	31G	TEST NO.	TE65
SIG1c′(kPa)	3.0		
SIG3c′(kPa)	3.0		
INDUCED OCR	1.0		

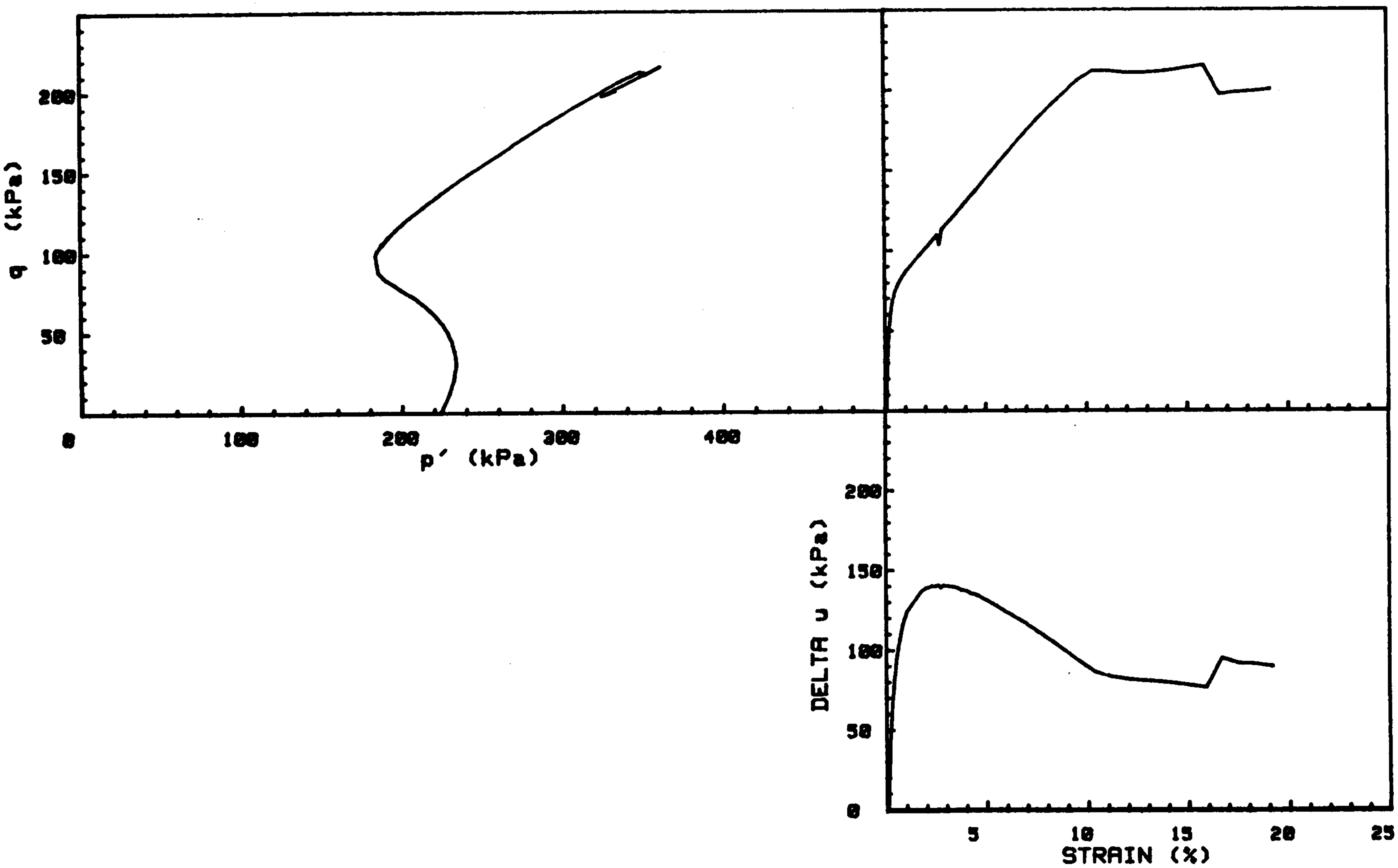

CRUISE DC2-80-EG		INCREMENT (cm)	4-11
CORE NO.	31G	TEST NO.	TE66
SIG1c′(kPa)	223.2		
SIG3c′(kPa)	223.2		
INDUCED OCR	1.0		

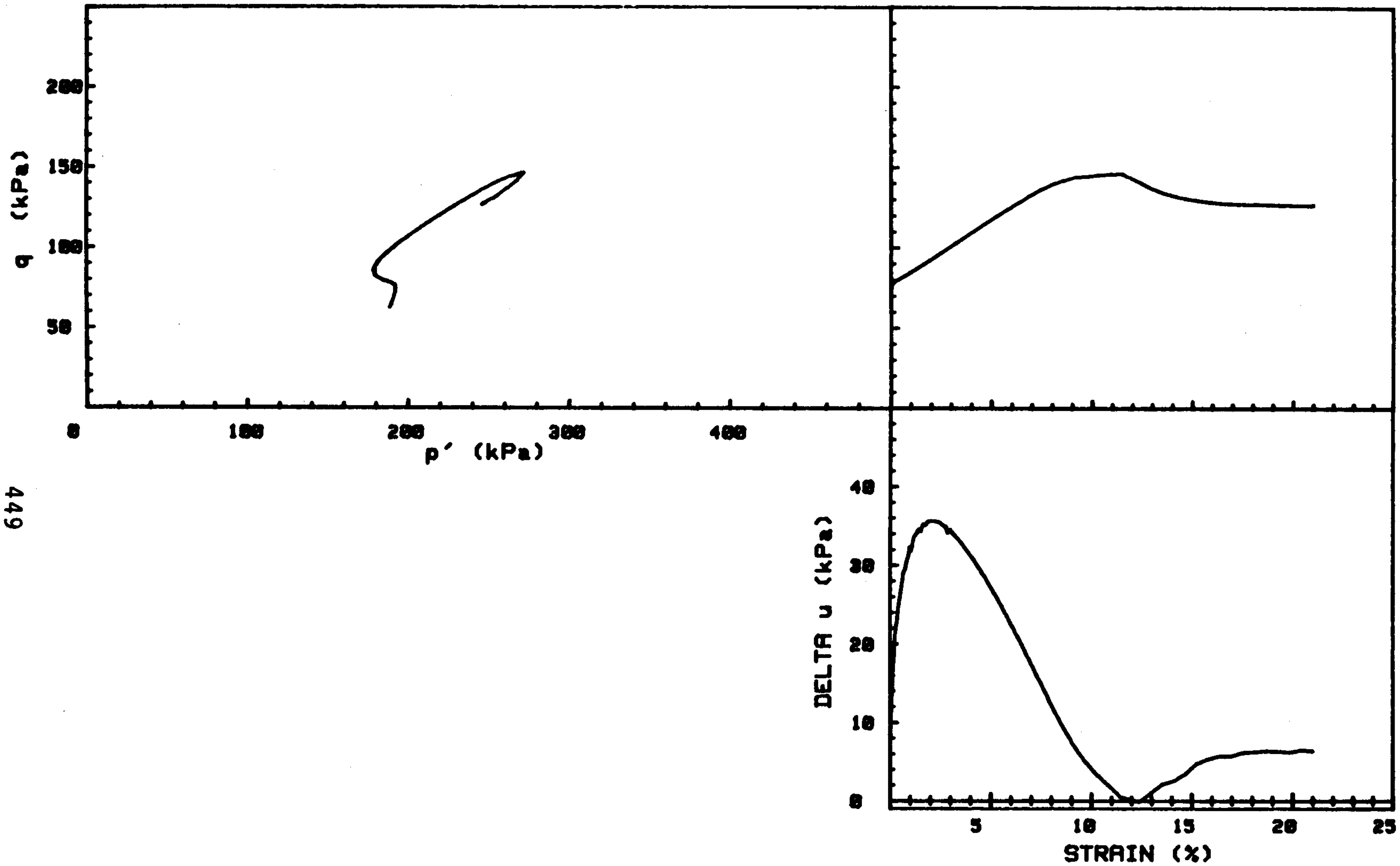

CRUISE	DC2-80-EG	INCREMENT (cm)	12.1-19.9
CORE NO.	31G	TEST NO.	TE67
SIG1c′(kPa)	251.2		
SIG3c′(kPa)	126.1		
INDUCED OCR	1.0		

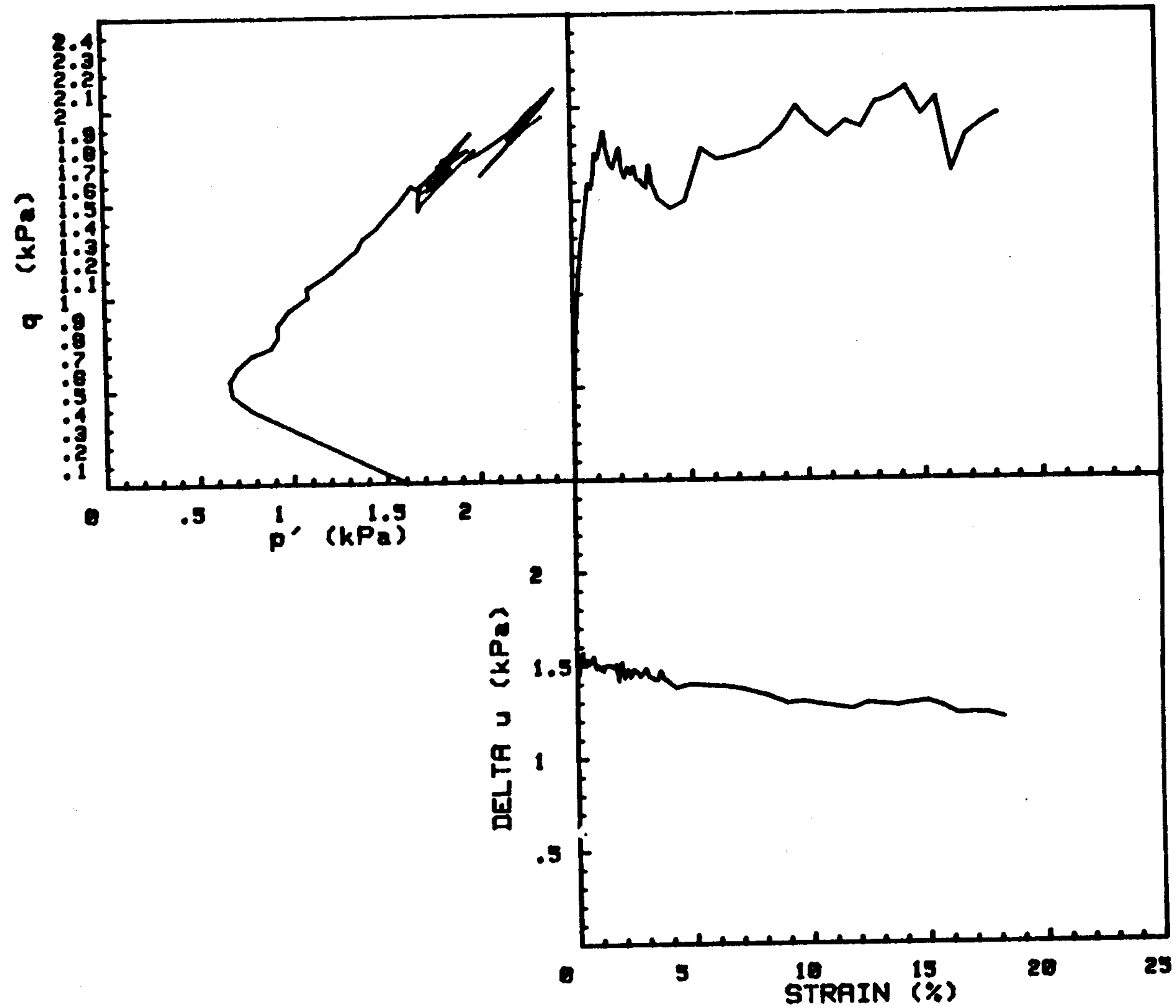

CRUISE DC1-81-EG		INCREMENT (cm)	105-113
CORE NO.	627G2	TEST NO.	TE68
SIG1c′(kPa)	1.6		
SIG3c′(kPa)	1.6		
INDUCED OCR	1.0		

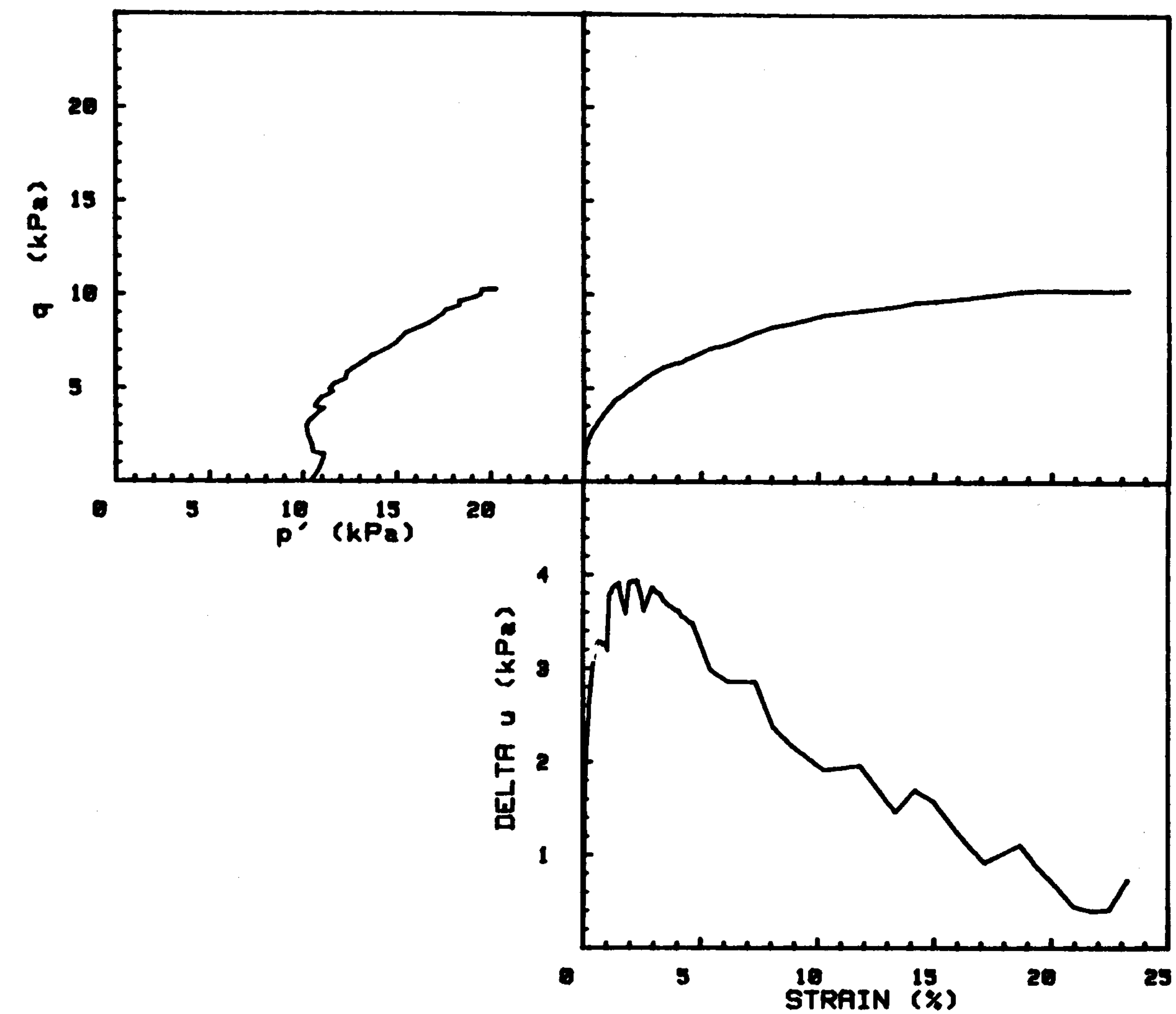

CRUISE DC1-81-EG		INCREMENT (cm)	105.5-113.7
CORE NO.	627G2	TEST NO.	TE69
SIG1c'(kPa)	10.4		
SIG3c'(kPa)	10.4		
INDUCED OCR	1.0		

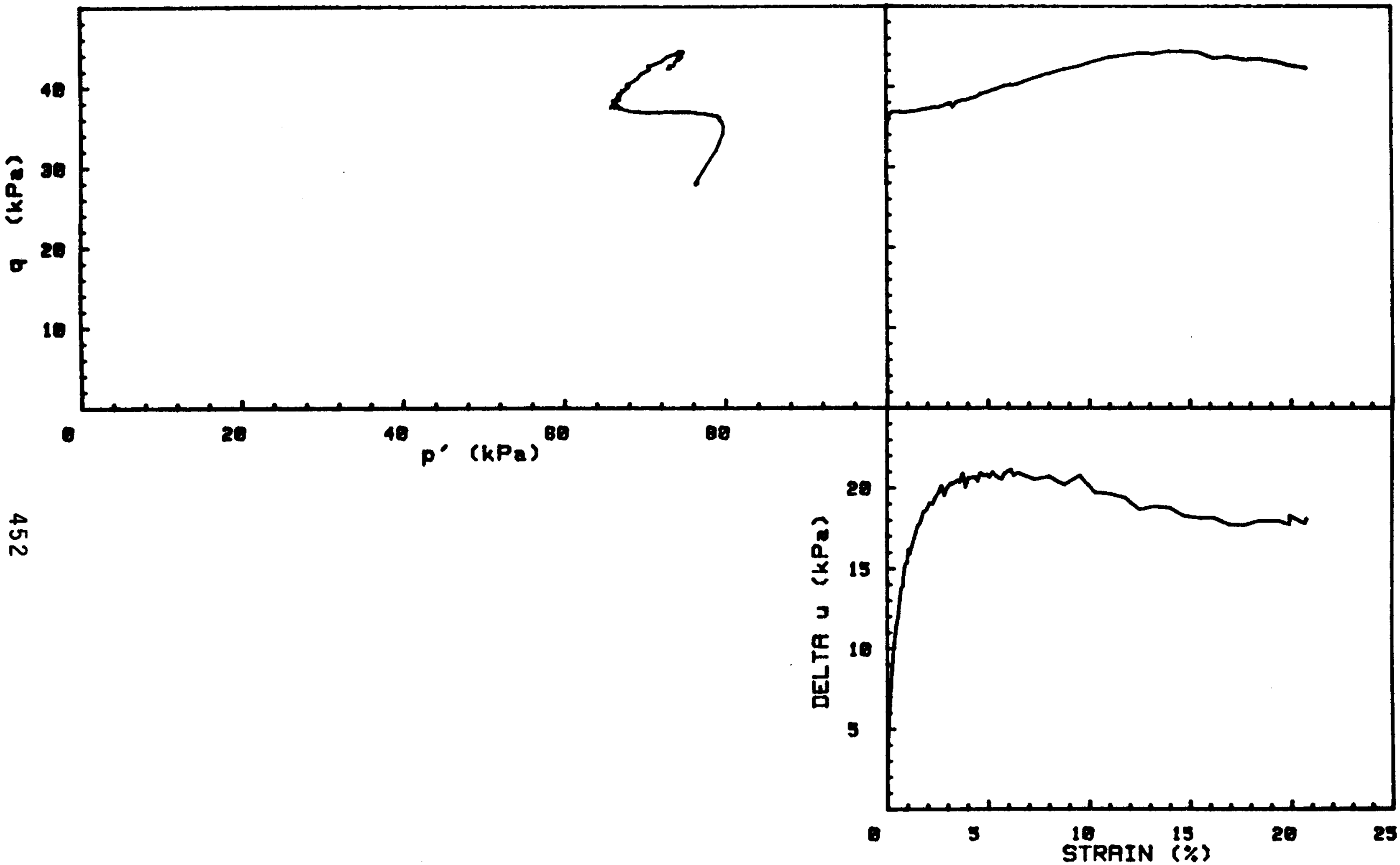

CRUISE	DC1-81-EG	INCREMENT (cm)	82-93
CORE NO.	627G2	TEST NO.	TE70
SIG1c′(kPa)	104.7		
SIG3c′(kPa)	48.7		
INDUCED OCR	1.0		

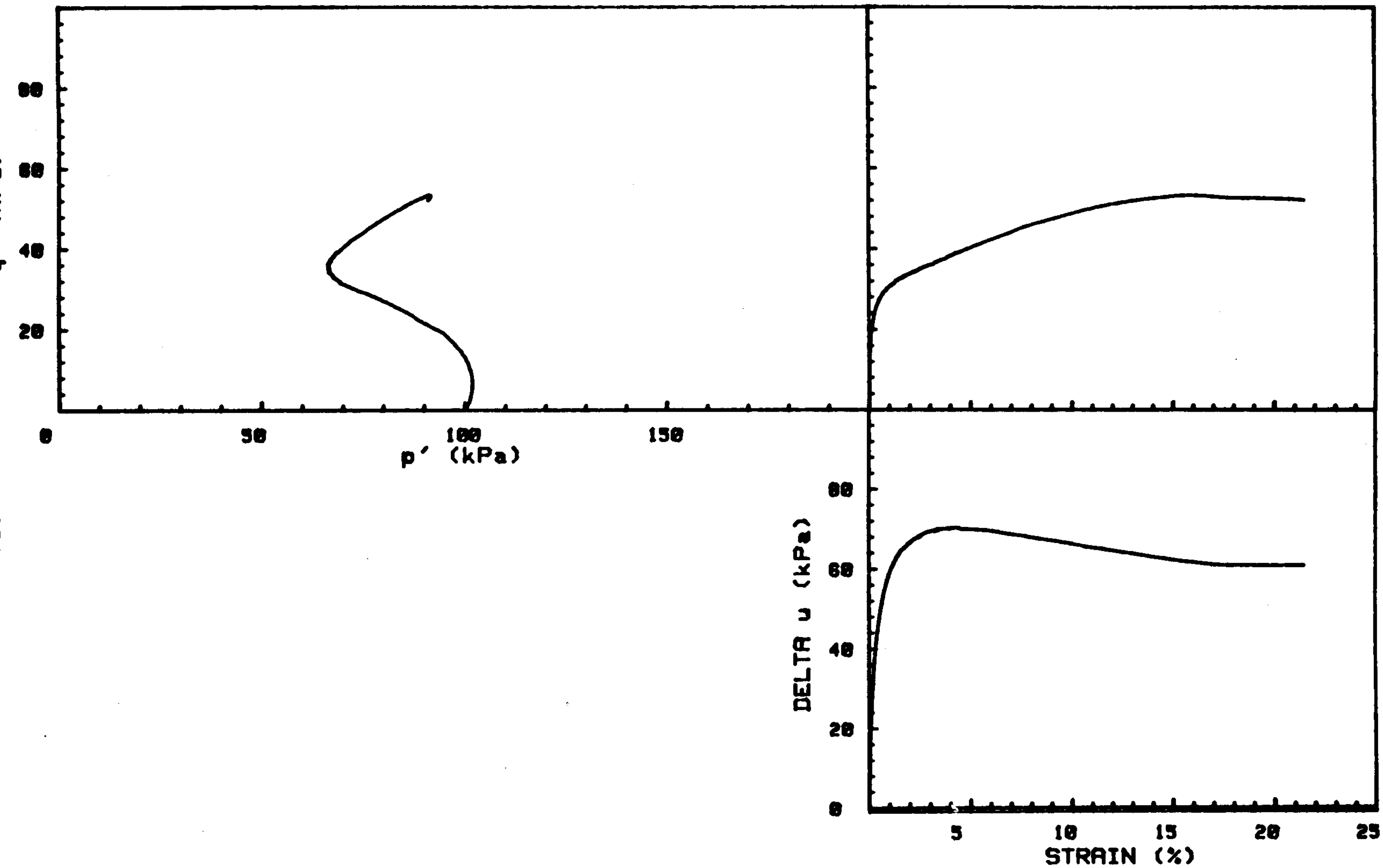

CRUISE	DC1-81-EG	INCREMENT (cm)	82-93
CORE NO.	627G2	TEST NO.	TE71
SIG1c'(kPa)	100.1		
SIG3c'(kPa)	100.1		
INDUCED OCR	1.0		

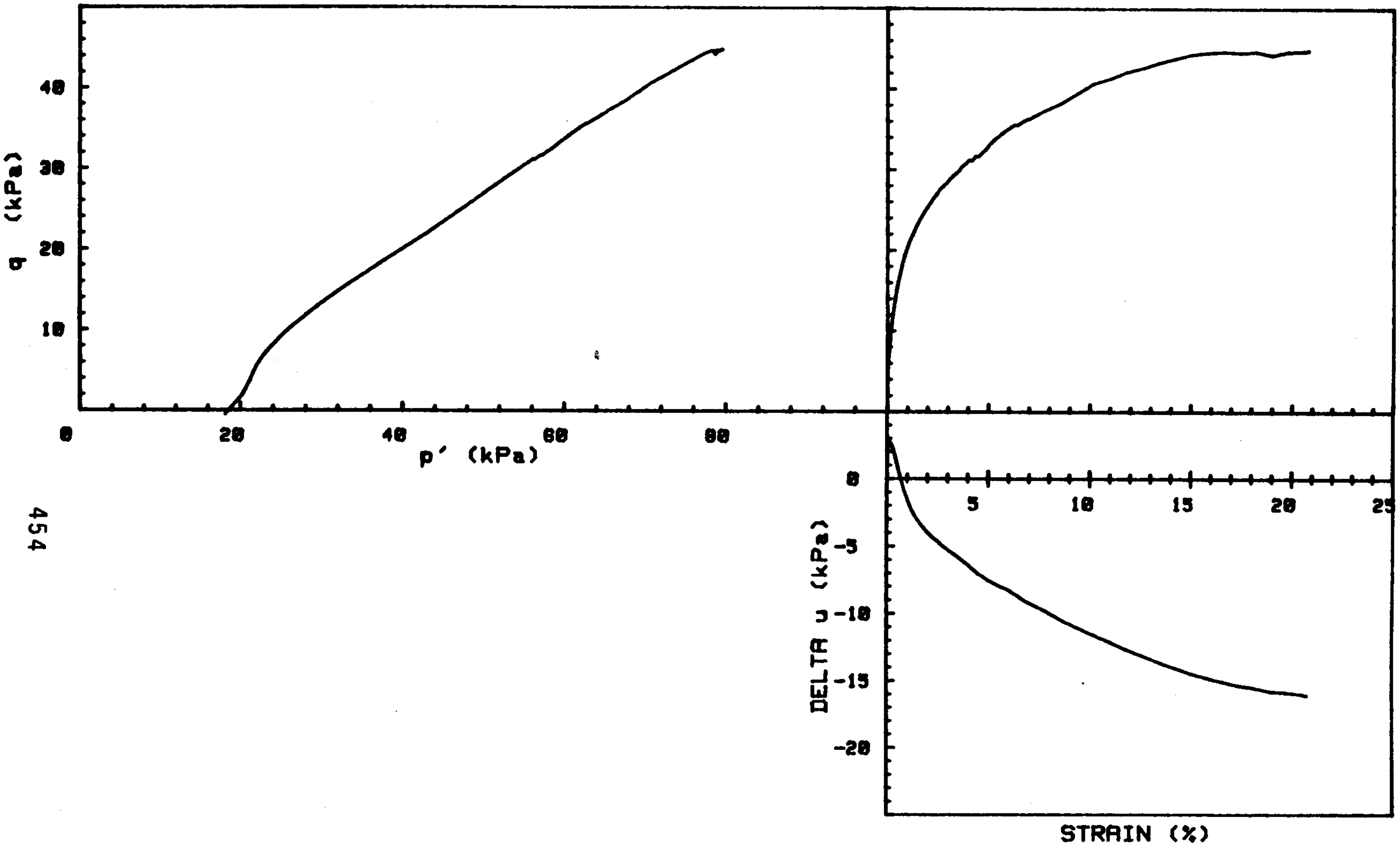

CRUISE DC1-81-EG		INCREMENT (cm)	71-82
CORE NO.	627G2	TEST NO.	TE72
SIG1c'(kPa)	18.6		
SIG3c'(kPa)	18.6		
INDUCED OCR	6.0		

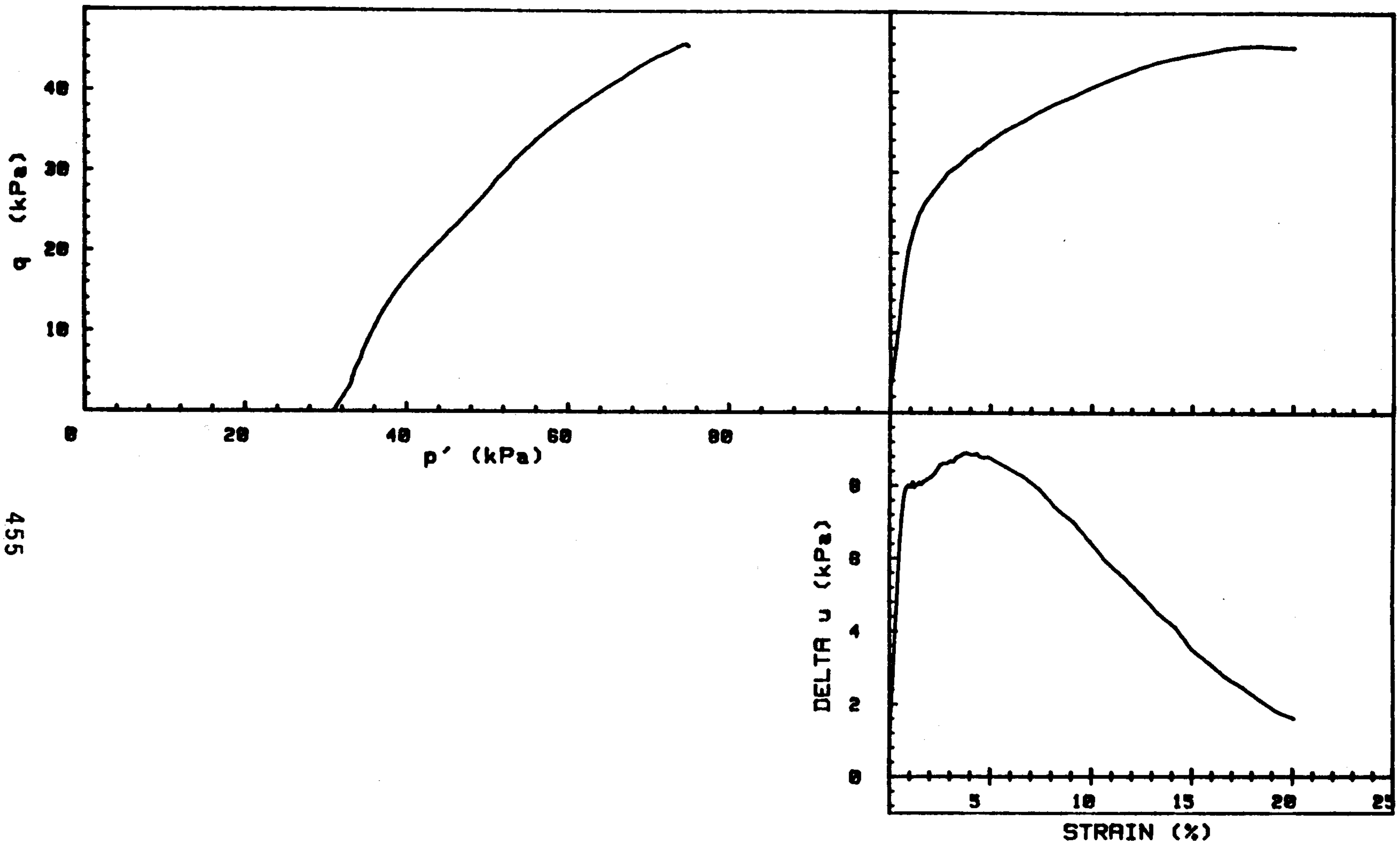

CRUISE DC1-81-EG		INCREMENT (cm)	71-82
CORE NO.	627G2	TEST NO.	TE73

SIG1c′(kPa) 31.0
SIG3c′(kPa) 31.0
INDUCED OCR 3.0

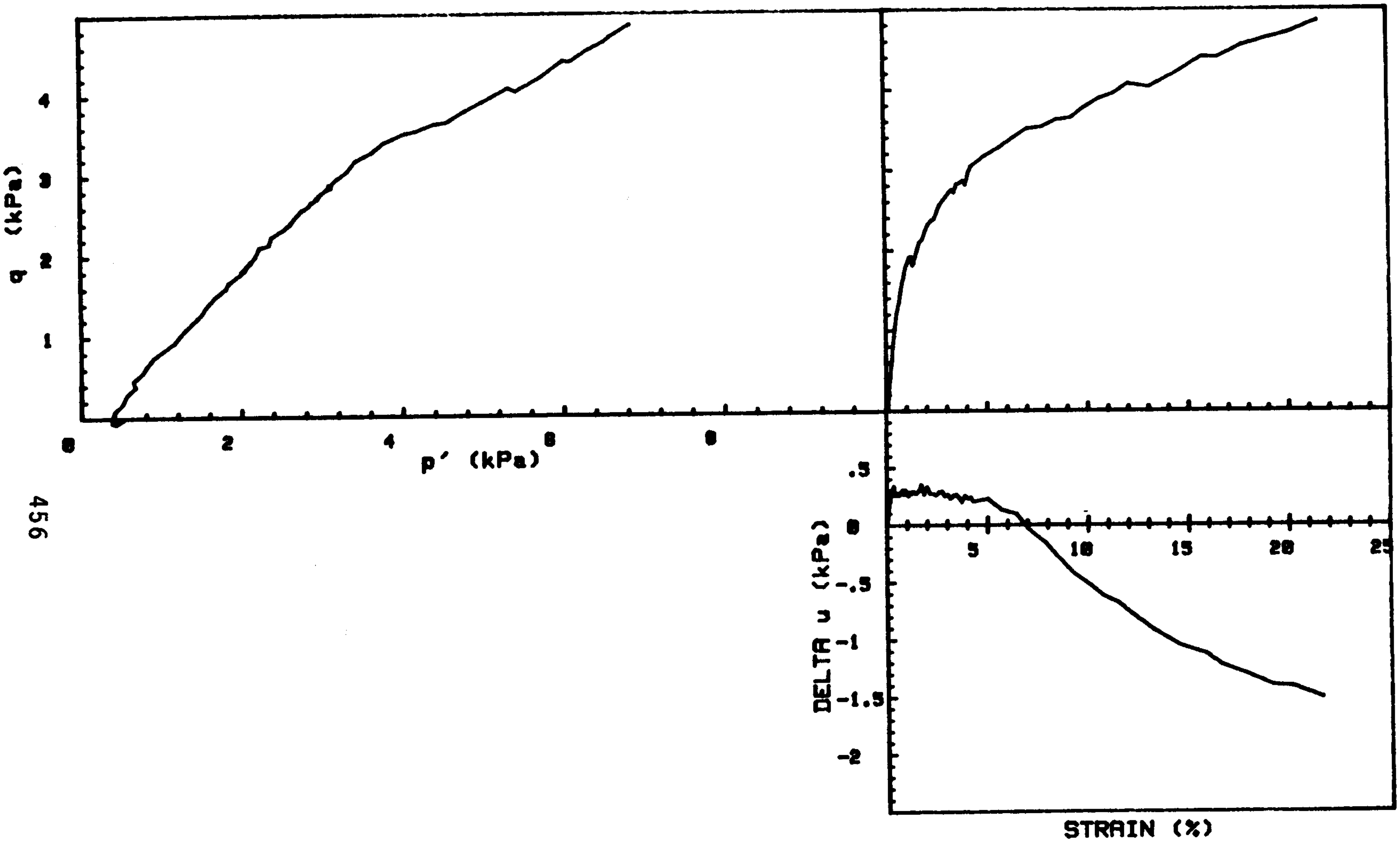

CRUISE DC1-81-EG		INCREMENT (cm)	149-160
CORE NO.	618G2	TEST NO.	TE74
SIG1c′(kPa)	.5		
SIG3c′(kPa)	.5		
INDUCED OCR	1.0		

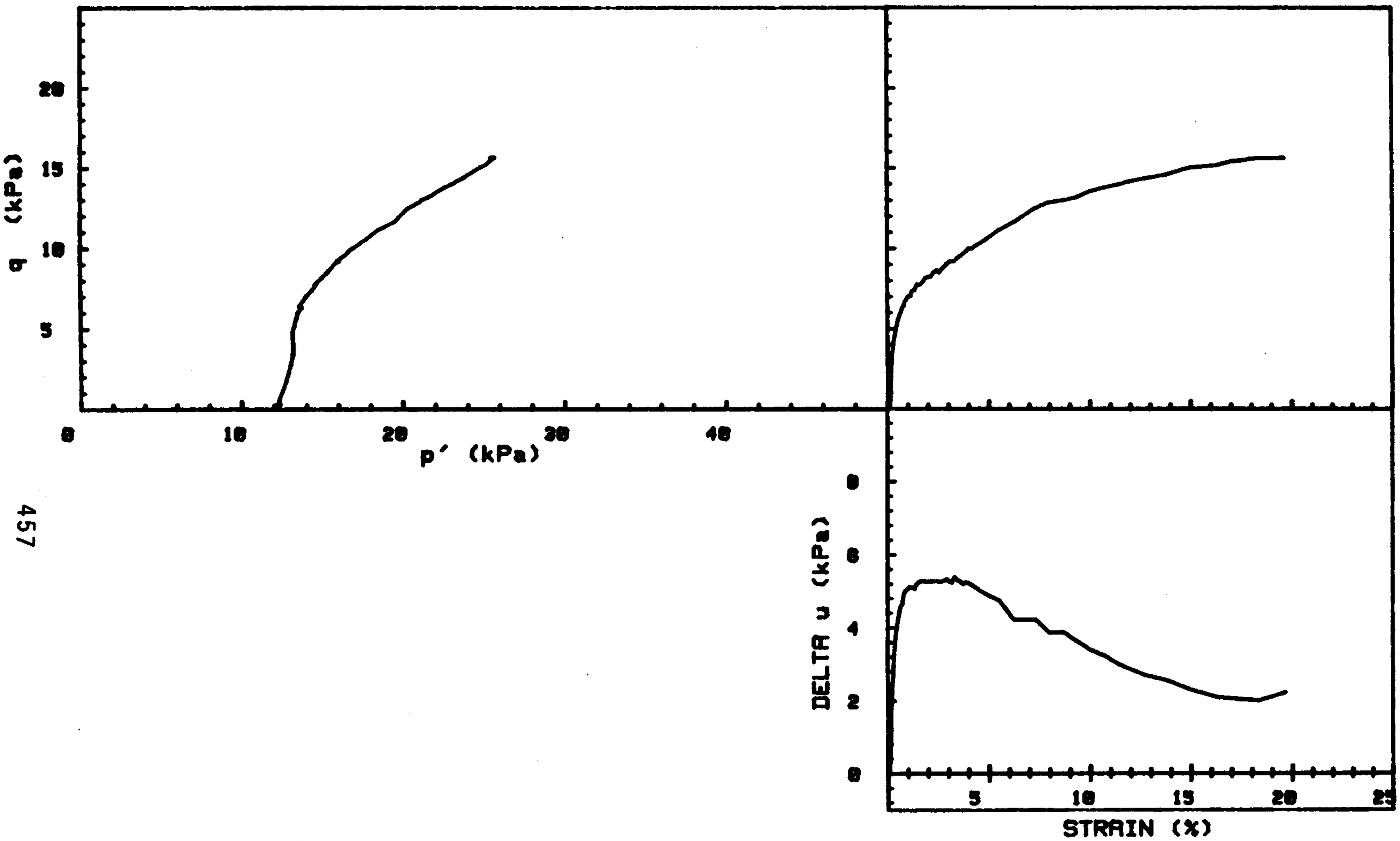

CRUISE DC1-81-EG		INCREMENT (cm)	149-160
CORE NO.	610G2	TEST NO.	TE75
SIG1c′(kPa)	12.1		
SIG3c′(kPa)	12.1		
INDUCED OCR	1.0		

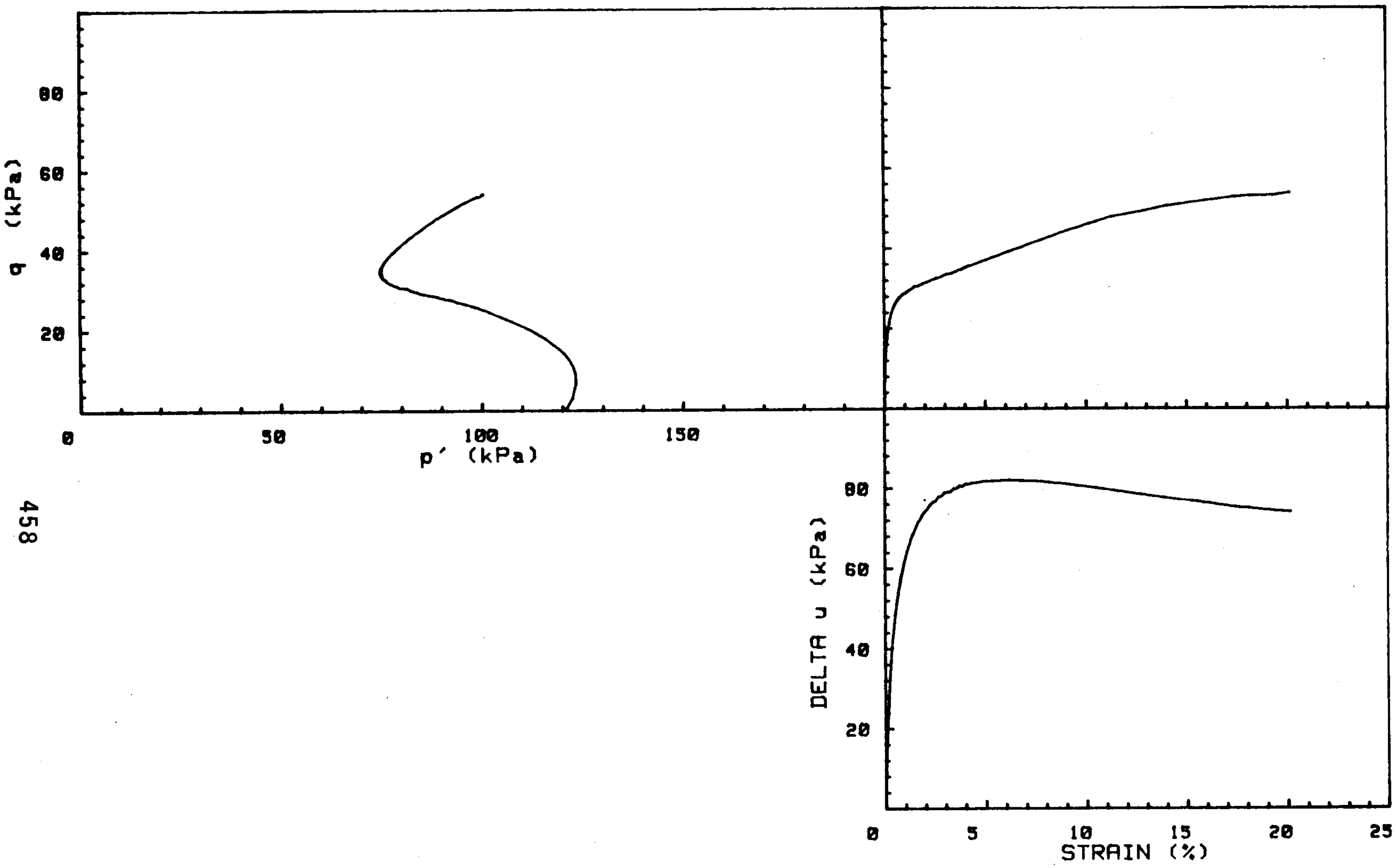

CRUISE DC1-81-EG   INCREMENT (cm)   90-99
CORE NO.   620G2   TEST NO.   TE82

SIG1c′(kPa) 120.8
SIG3c′(kPa) 120.8
INDUCED OCR 1.0

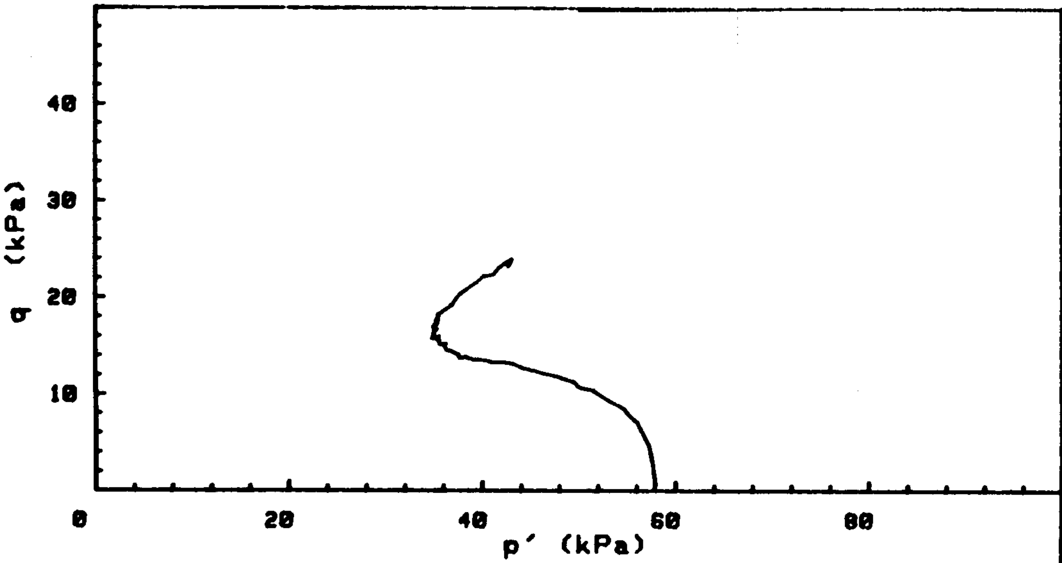

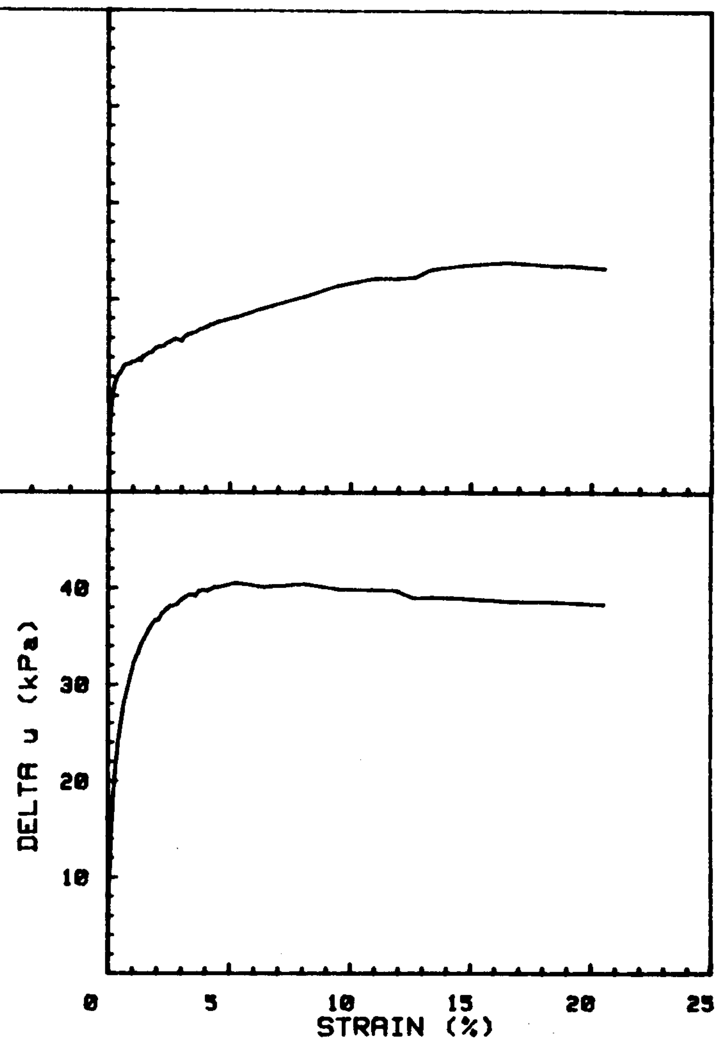

CRUISE	DC1-81-EG	INCREMENT (cm)	51-60
CORE NO.	634G2	TEST NO.	TE83

SIG1c′(kPa) 57.9
SIG3c′(kPa) 57.9
INDUCED OCR 1.0

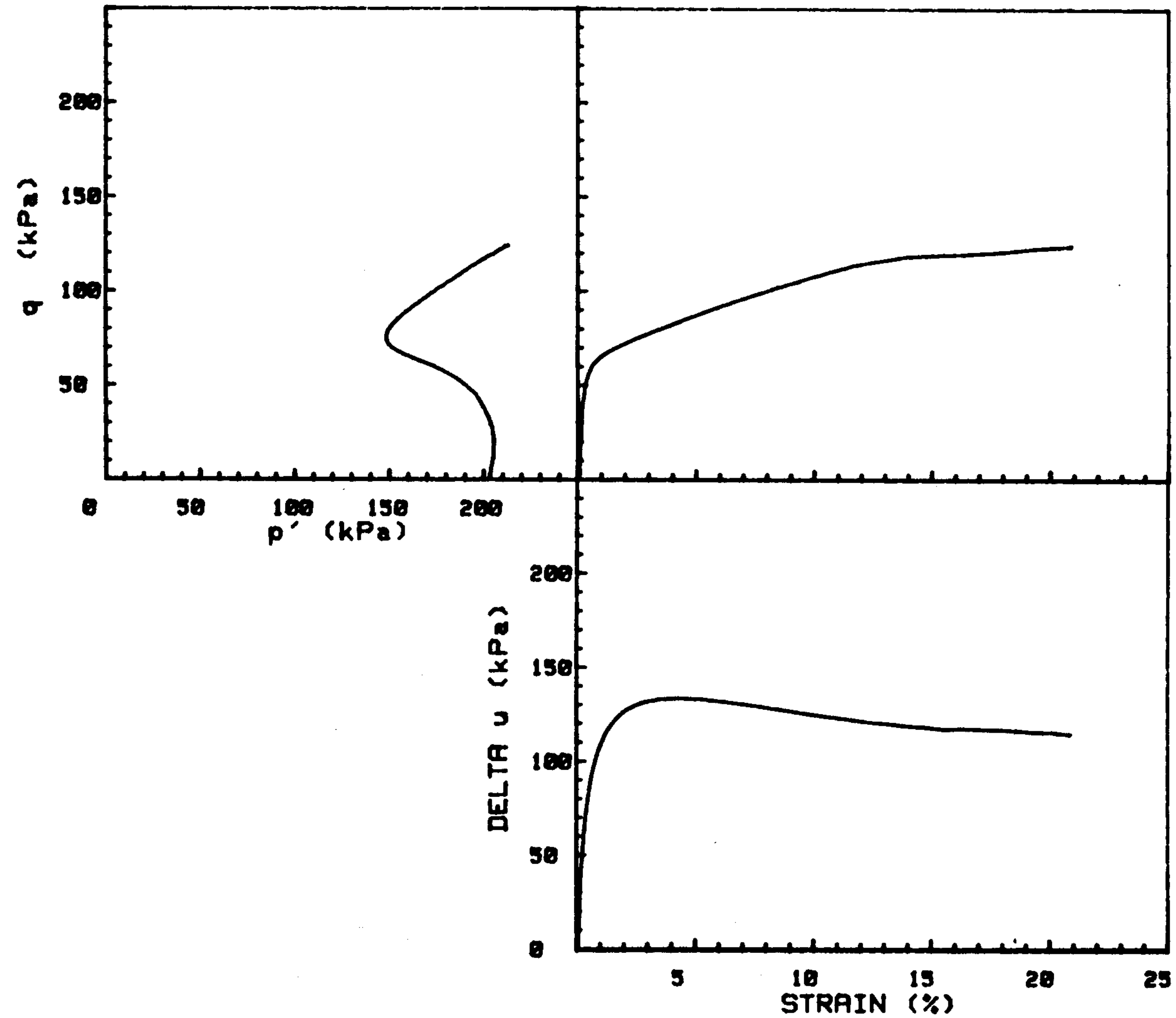

CRUISE DC2-80-EG		INCREMENT (cm)	150-158
CORE NO.	87G	TEST NO.	TE84
SIG1c′(kPa)	203.1		
SIG3c′(kPa)	203.1		
INDUCED OCR	1.0		

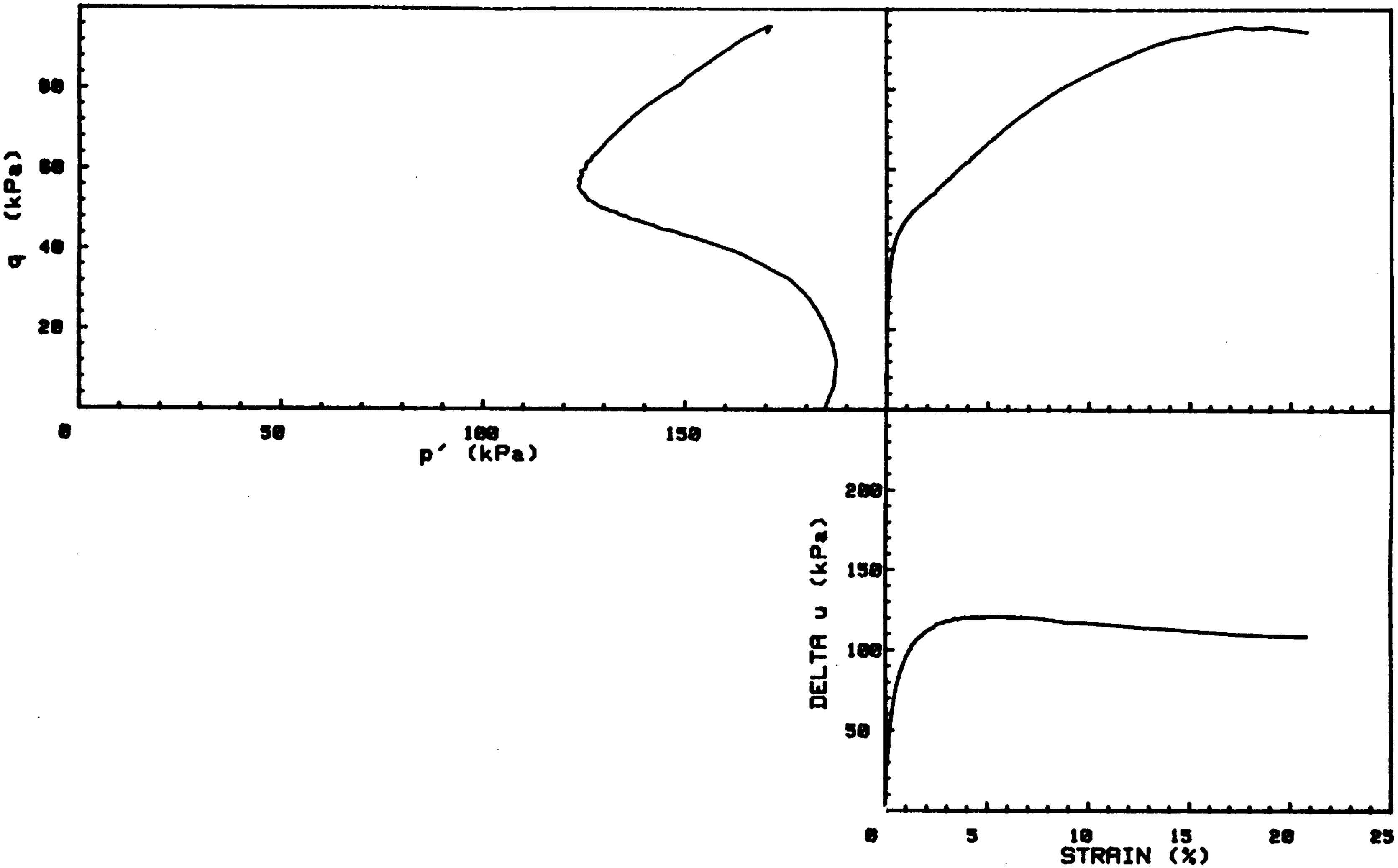

CRUISE DC1-81-EG		INCREMENT (cm)	127-138
CORE NO.	618G2	TEST NO.	TE87
SIG1c′(kPa)	184.7		
SIG3c′(kPa)	184.7		
INDUCED OCR	1.0		

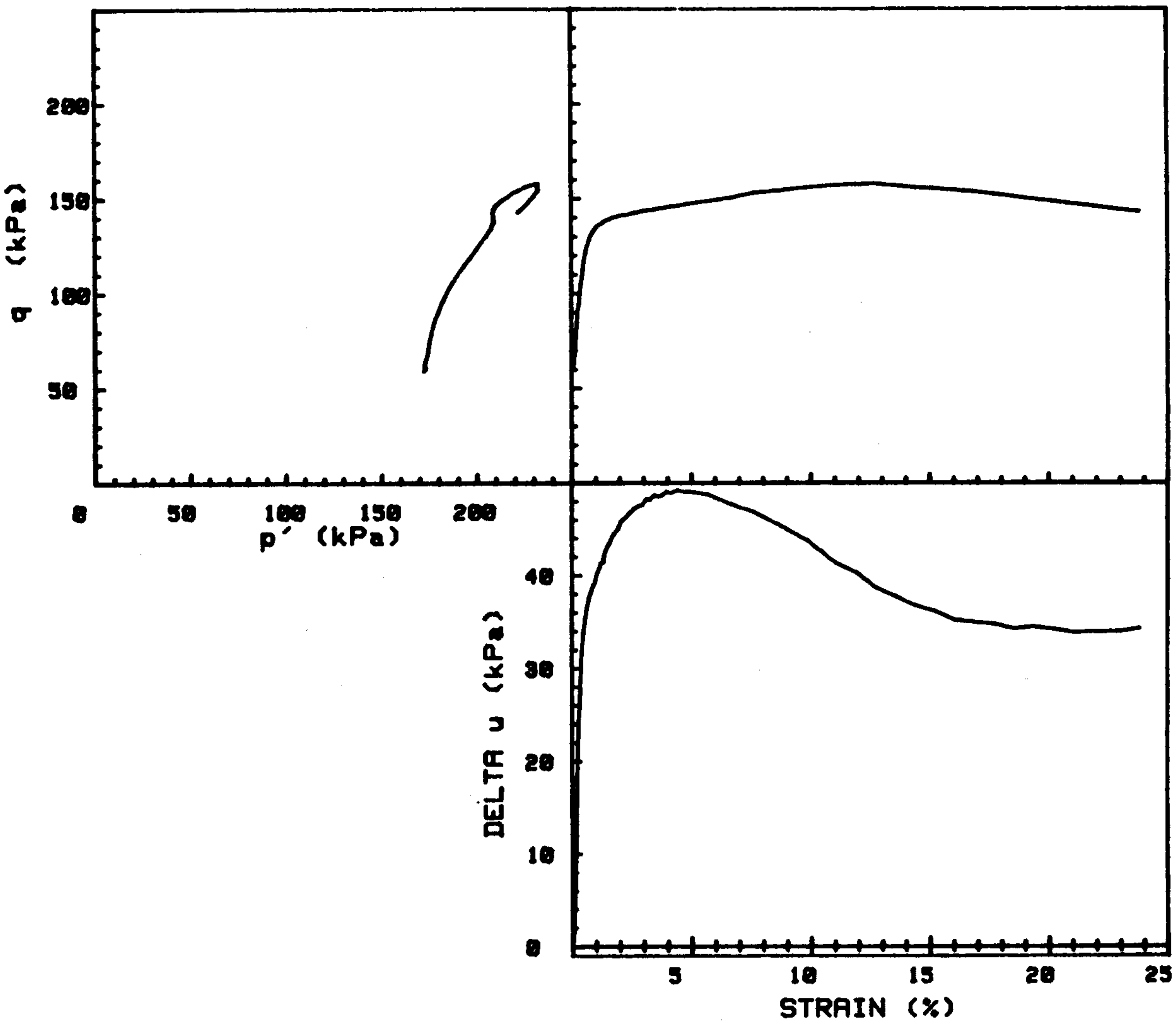

CRUISE DC1-81-EG INCREMENT (cm) 127-138
CORE NO. 618G2 TEST NO. TE88

SIG1c′(kPa) 231.5
SIG3c′(kPa) 113.6
INDUCED OCR 1.0

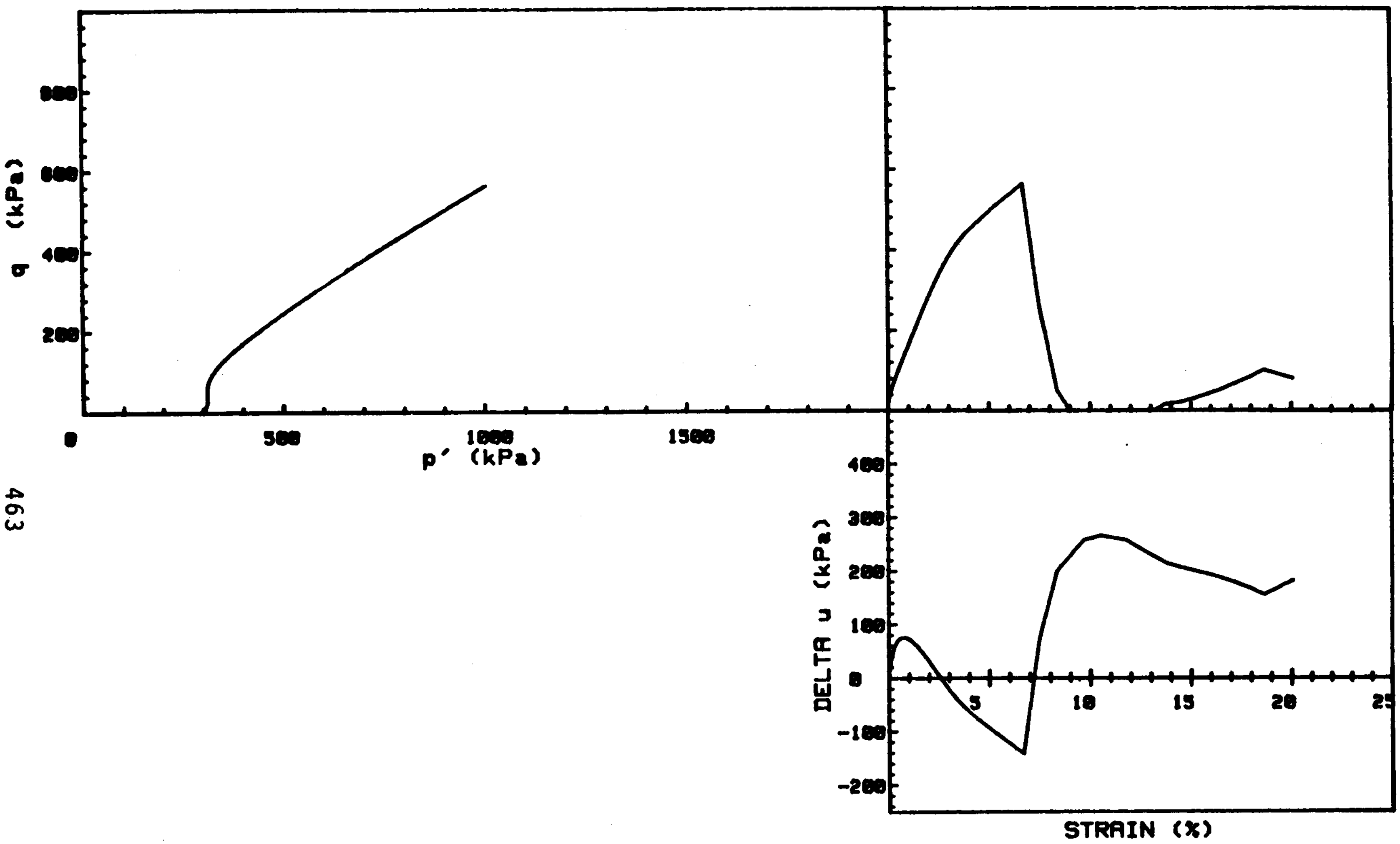

CRUISE DC1-81-EG		INCREMENT (cm)	220-230
CORE NO.	630A2	TEST NO.	TE89
SIG1c′(kPa)	299.9		
SIG3c′(kPa)	299.9		
INDUCED OCR	1.0		

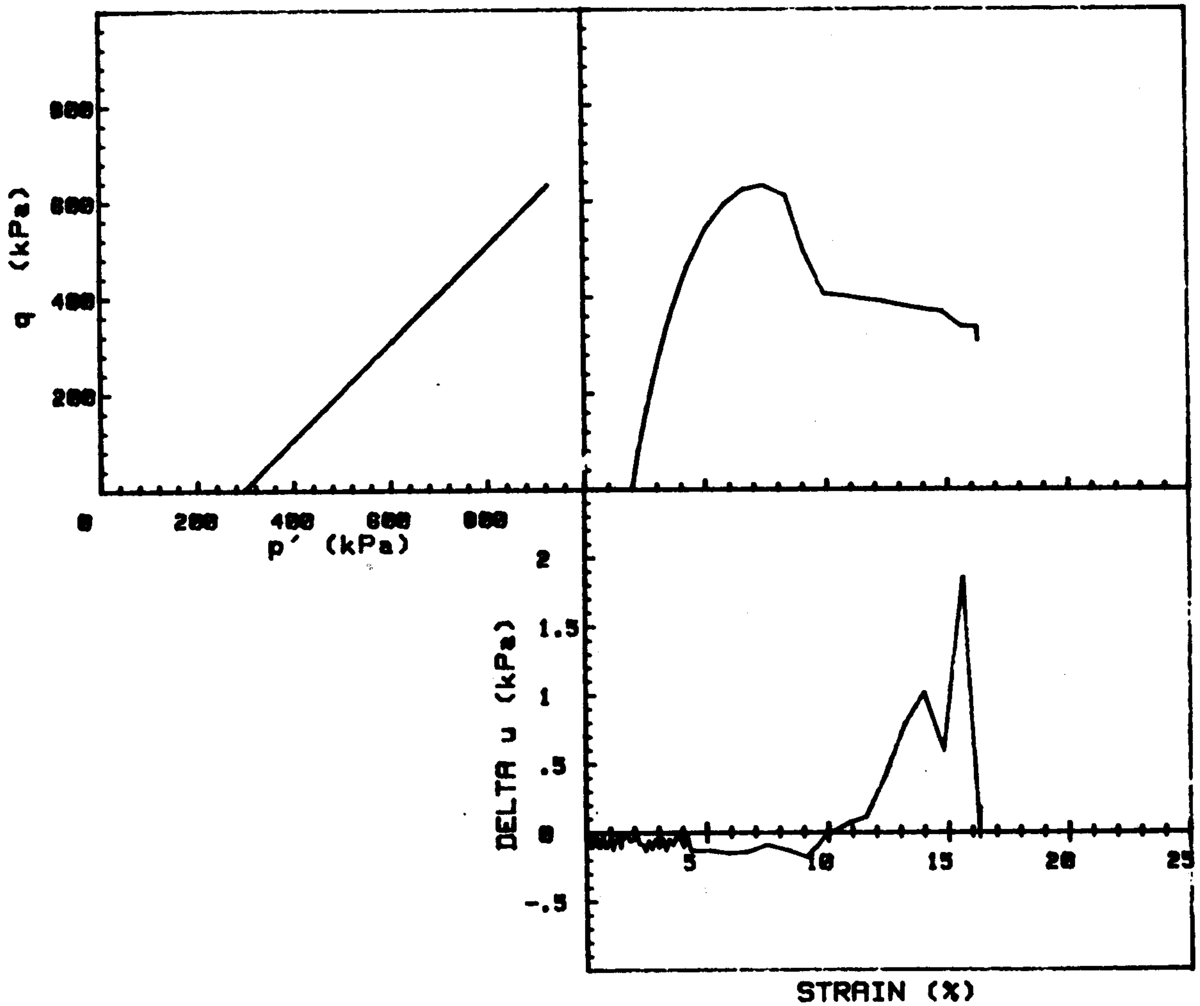

CRUISE DC1-81-EG		INCREMENT (cm)	220-229
CORE NO.	630A2	TEST NO.	TE90

SIG1c′(kPa) 295.5
SIG3c′(kPa) 295.5
INDUCED OCR 1.0

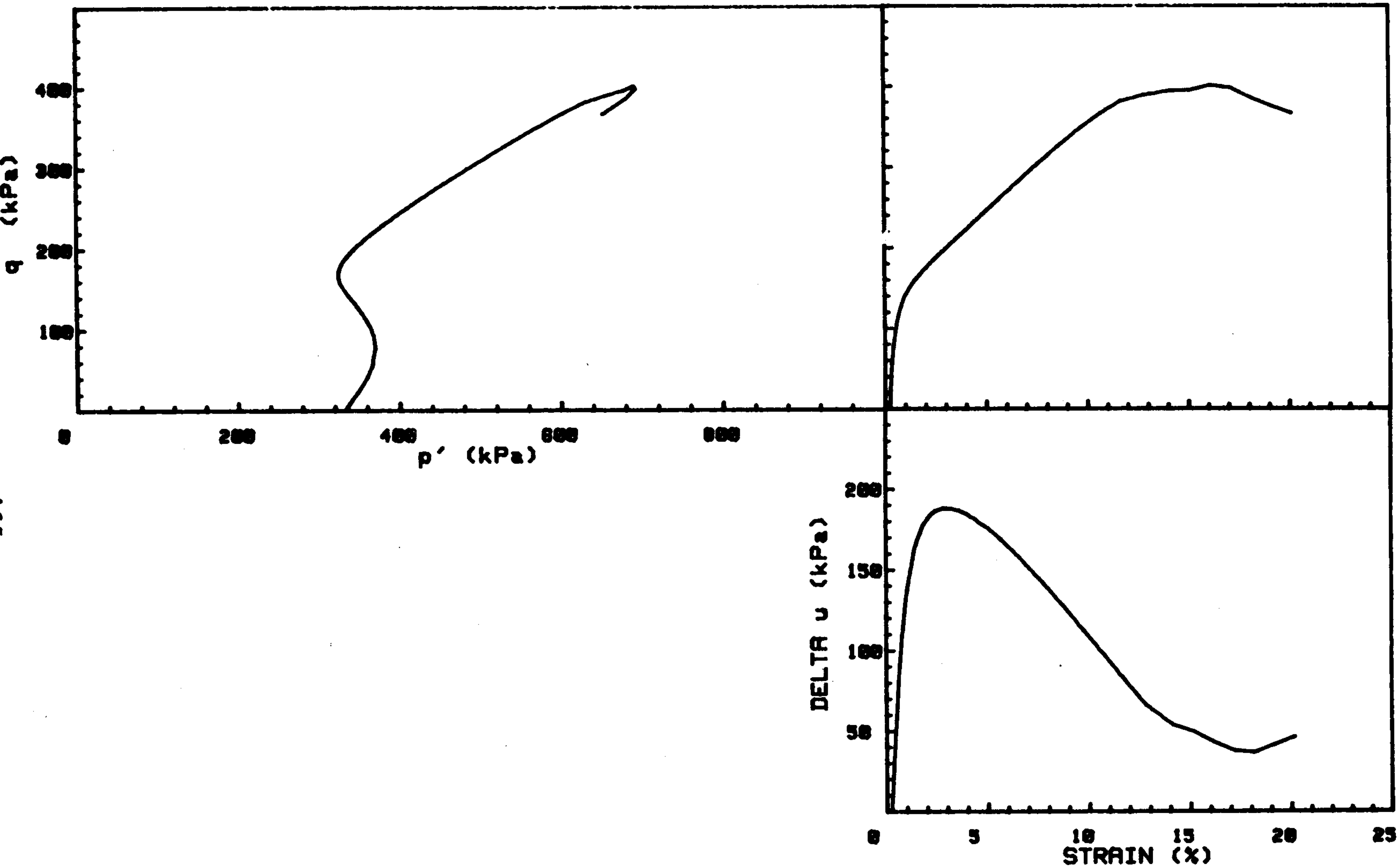

CRUISE DC1-81-EG		INCREMENT (cm)	141-150
CORE NO.	624A1	TEST NO.	TE91
SIG1c′(kPa)	333.1		
SIG3c′(kPa)	333.1		
INDUCED OCR	1.0		

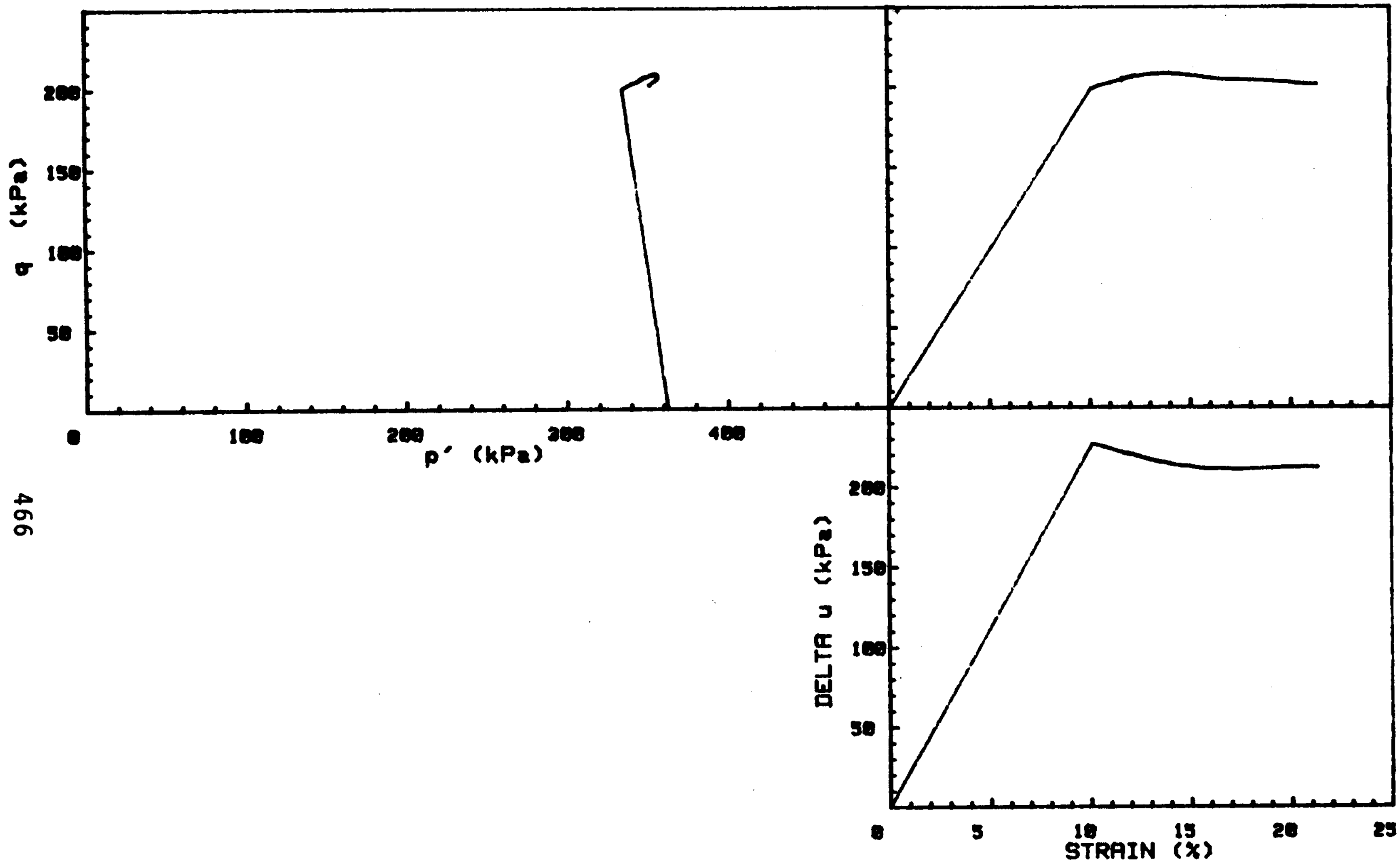

CRUISE DC1-81-EG	INCREMENT (cm) 80-89
CORE NO. 632G1	TEST NO. TE92

SIG1c′(kPa) 362.8
SIG3c′(kPa) 362.8
INDUCED OCR 1.0

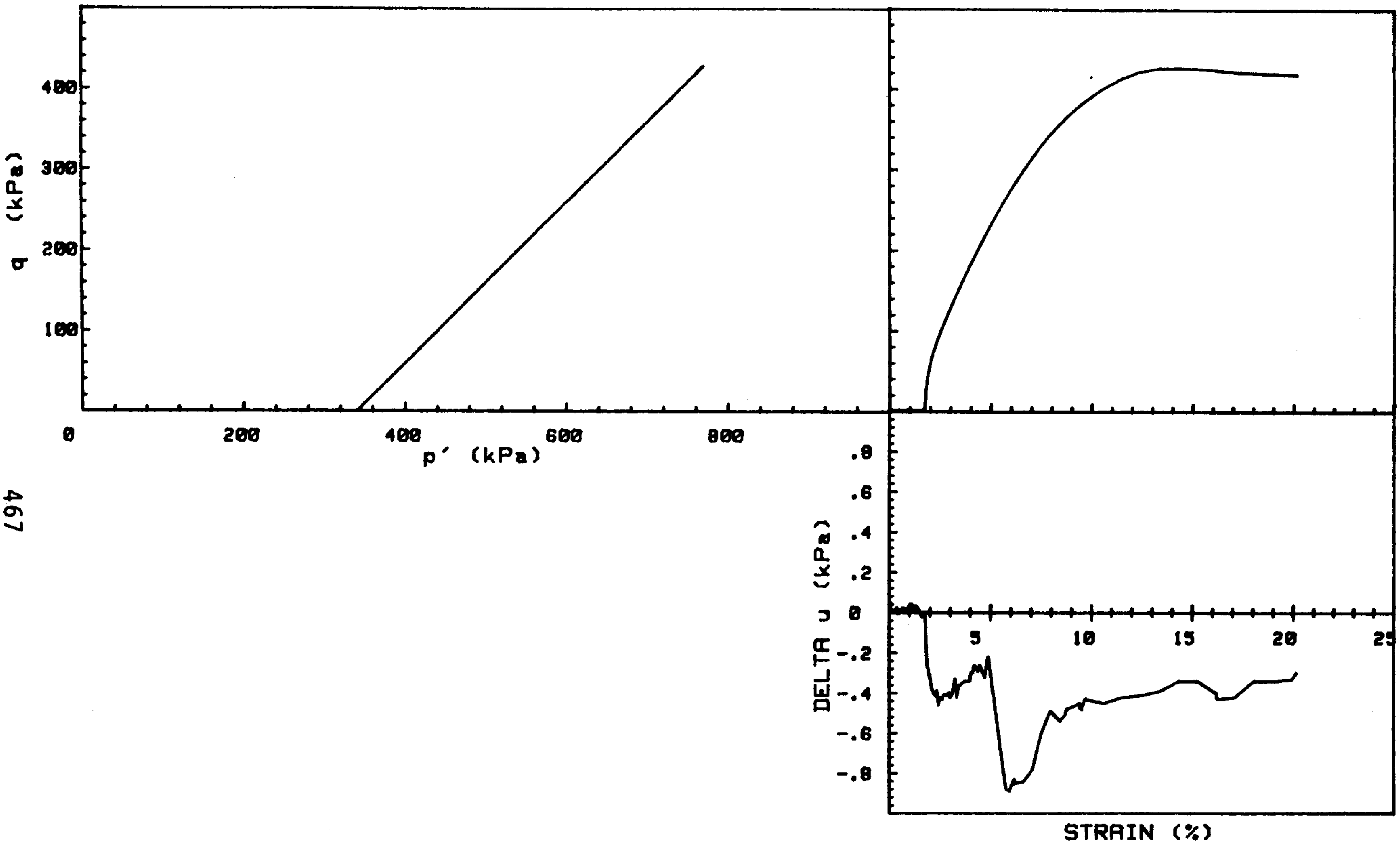

CRUISE DC1-81-EG		INCREMENT (cm)	162-168
CORE NO.	624A1	TEST NO.	TE93
SIG1c´(kPa)	341.5		
SIG3c´(kPa)	341.5		
INDUCED OCR	1.0		

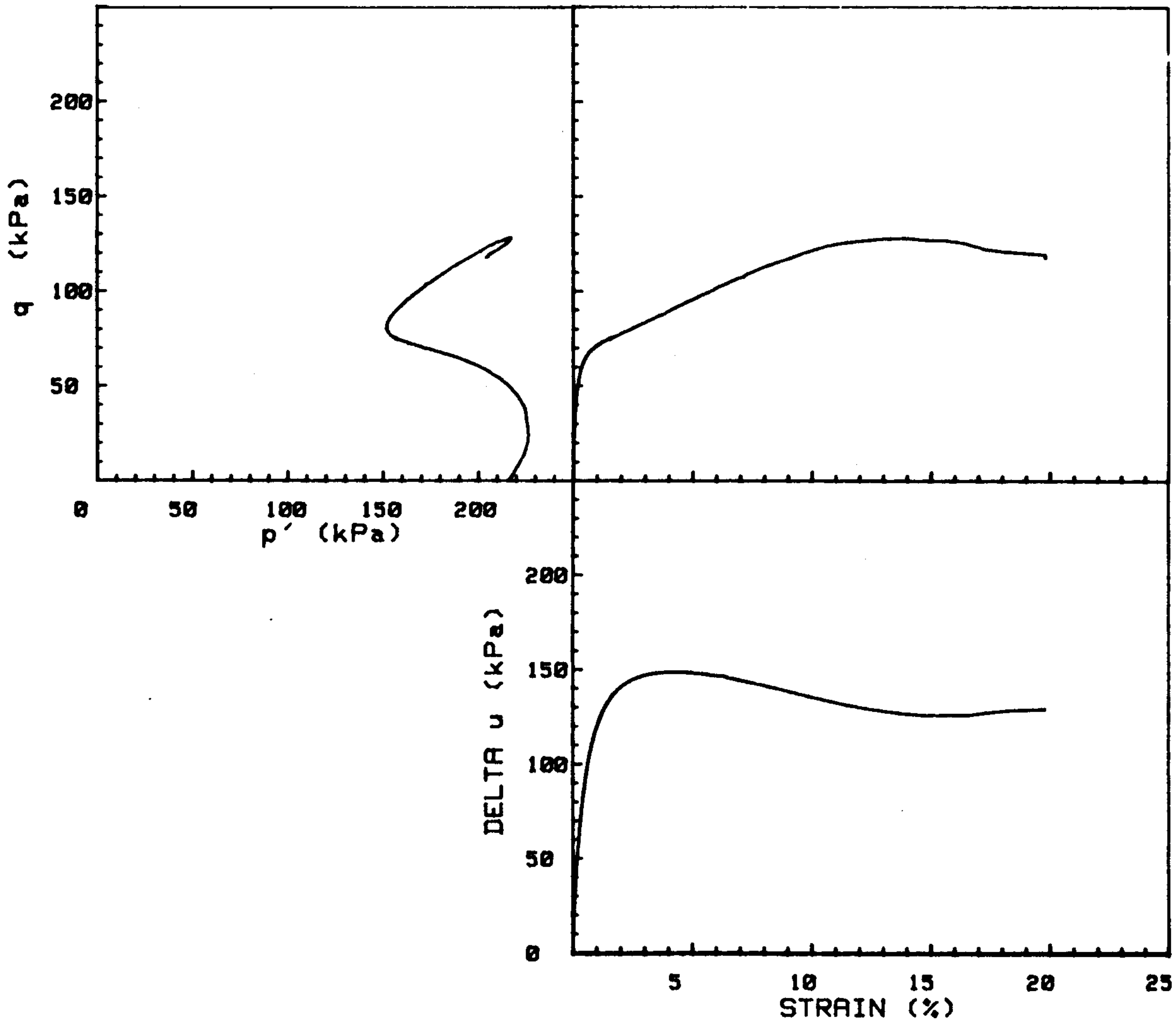

CRUISE DC1-81-EG		INCREMENT (cm)	157-165
CORE NO.	605G2	TEST NO.	TE111

SIG1c′(kPa) 216.1
SIG3c′(kPa) 216.1
INDUCED OCR 1.0

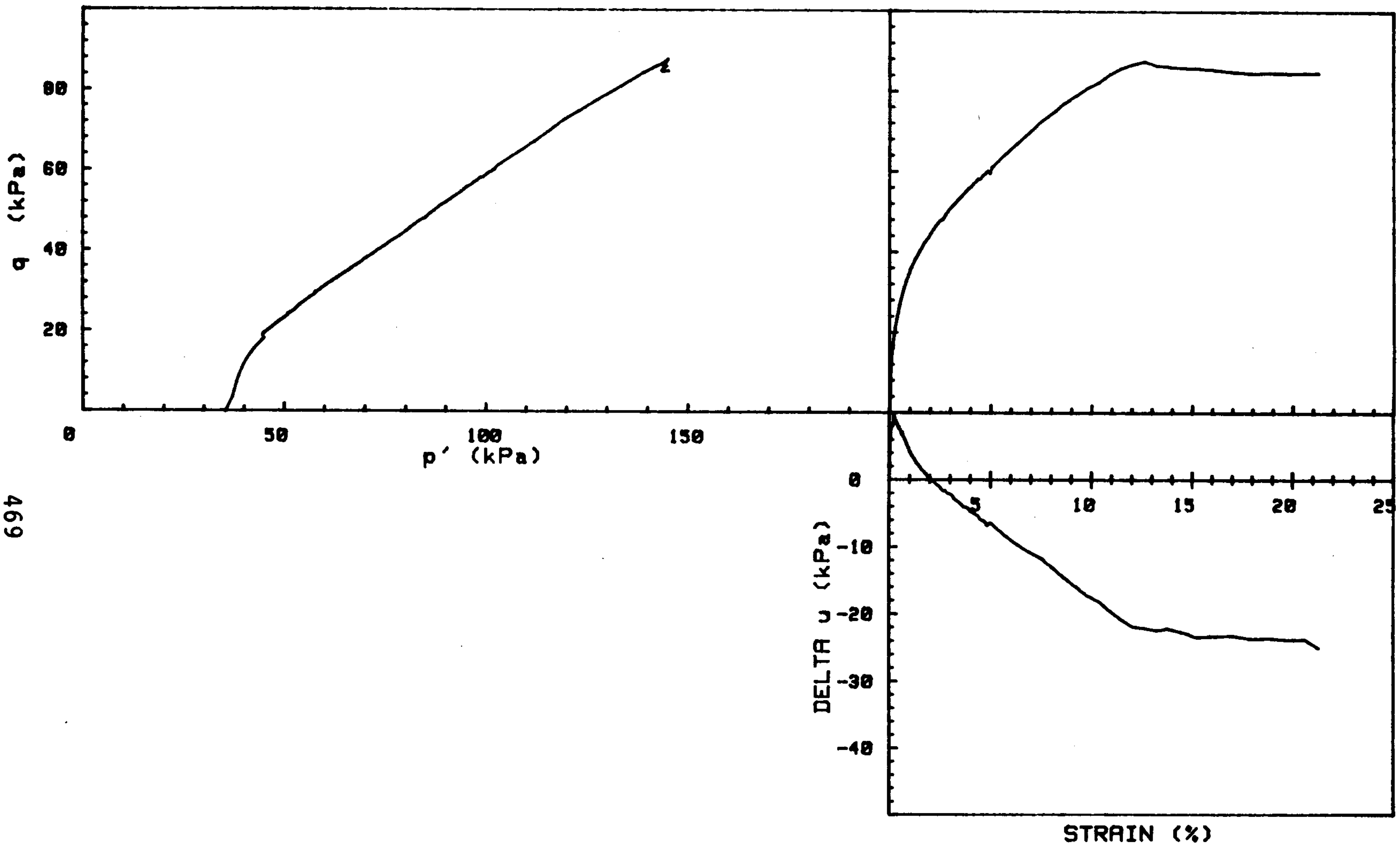

CRUISE DC1-81-EG		INCREMENT (cm)	156-164
CORE NO.	605G2	TEST NO.	TE112
SIG1c′(kPa)	35.3		
SIG3c′(kPa)	35.3		
INDUCED OCR	6.0		

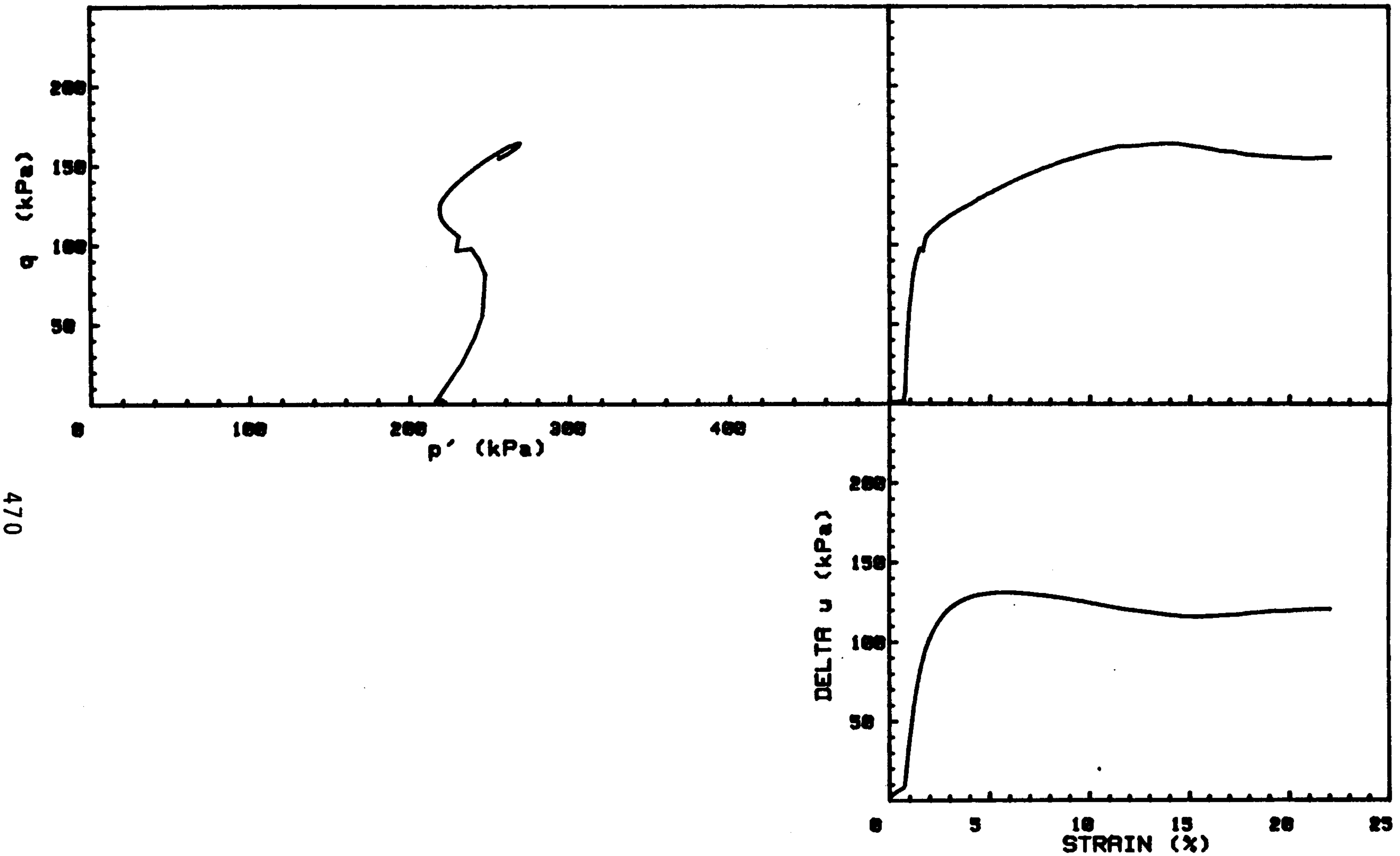

CRUISE DC1-81-EG INCREMENT (cm) 45-53
CORE NO. 605G2 TEST NO. TE113

SIG1c′(kPa) 222.2
SIG3c′(kPa) 222.2
INDUCED OCR 1.0

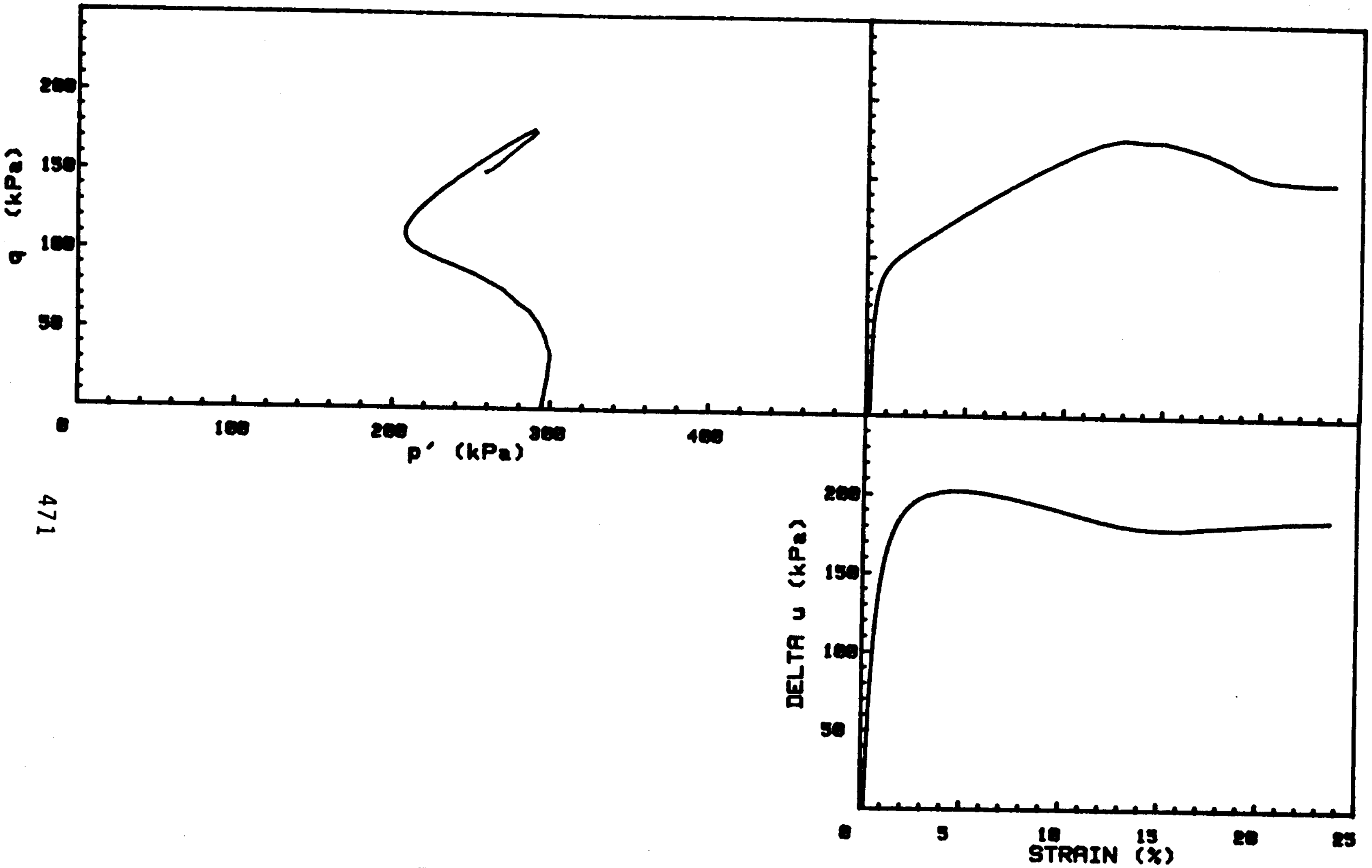

CRUISE DC1-81-EG		INCREMENT (cm)	121-129
CORE NO.	604G3	TEST NO.	TE114
SIG1c′(kPa)	293.4		
SIG3c′(kPa)	293.4		
INDUCED OCR	1.0		

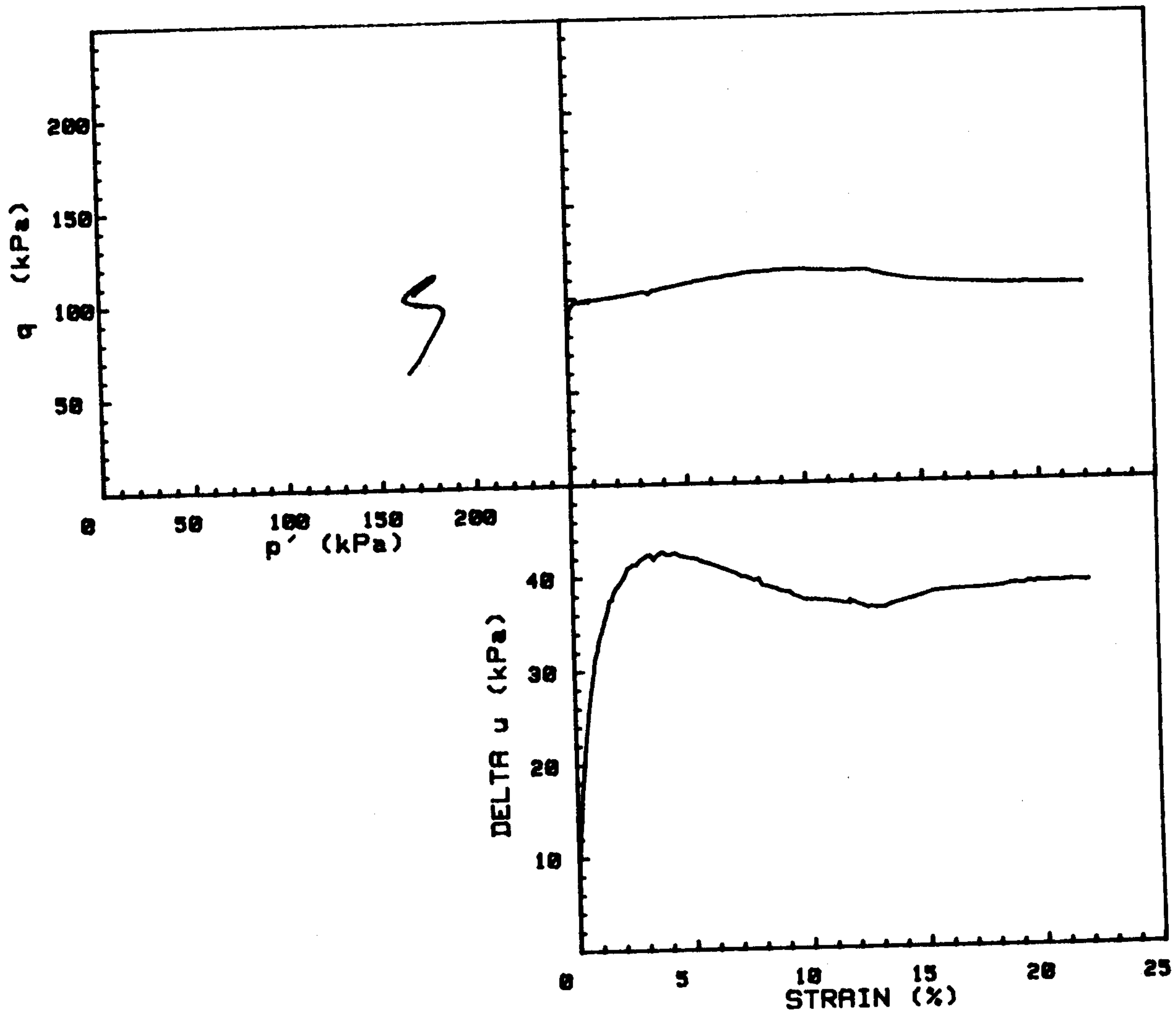

CRUISE DC1-81-EG		INCREMENT (cm)	176-184
CORE NO.	605G2	TEST NO.	TE115

SIG1c′(kPa) 227.9
SIG3c′(kPa) 102.9
INDUCED OCR 1.0

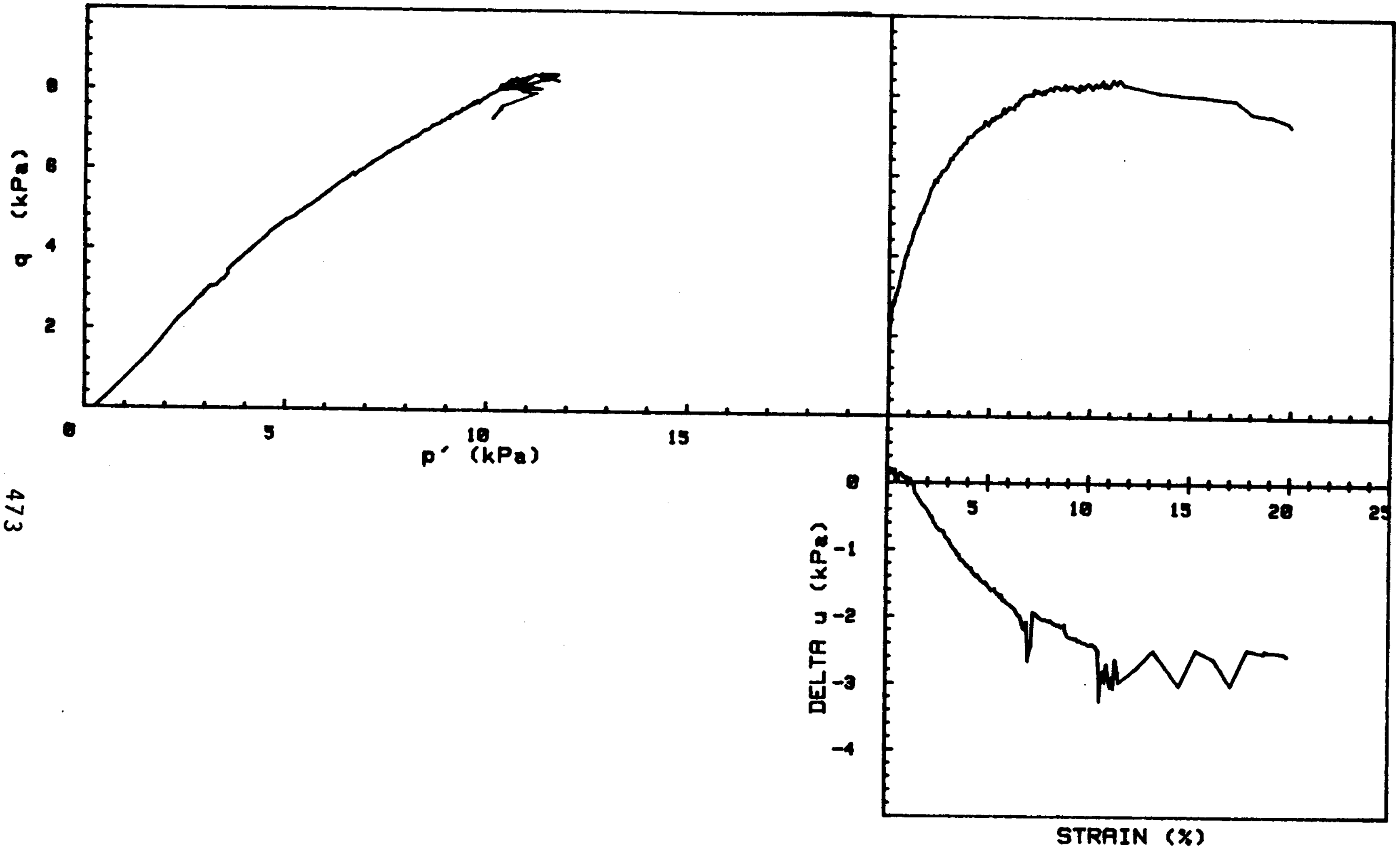

CRUISE	DC1-81-EG	INCREMENT (cm)	141-149
CORE NO.	605G2	TEST NO.	TE116
SIG1c′(kPa)	.3		
SIG3c′(kPa)	.3		
INDUCED OCR	1.0		

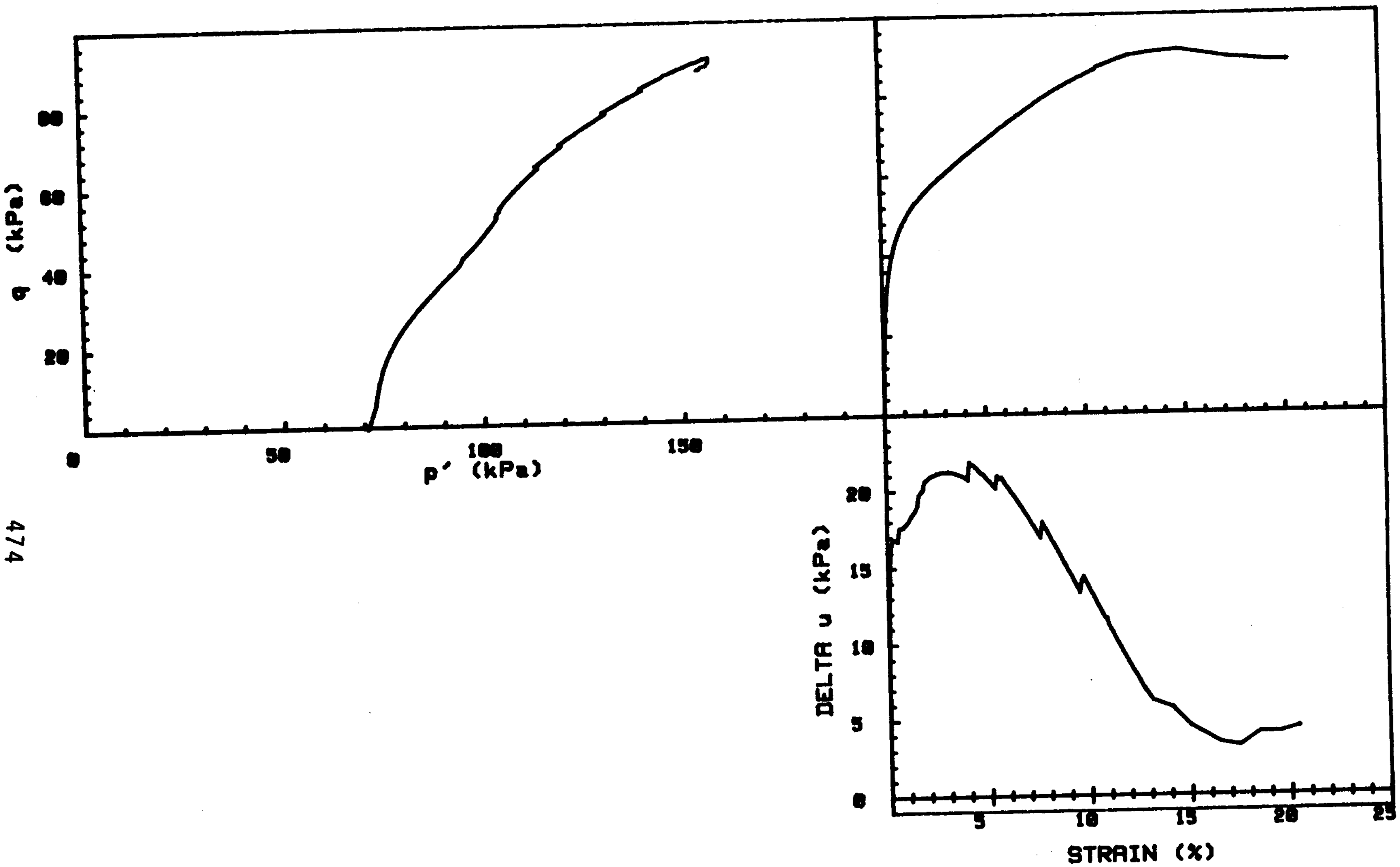

CRUISE DC1-81-EG   INCREMENT (cm)   186-194
CORE NO.   605G2   TEST NO.   TE117

SIG1c'(kPa) 71.3
SIG3c'(kPa) 71.3
INDUCED OCR 6.0

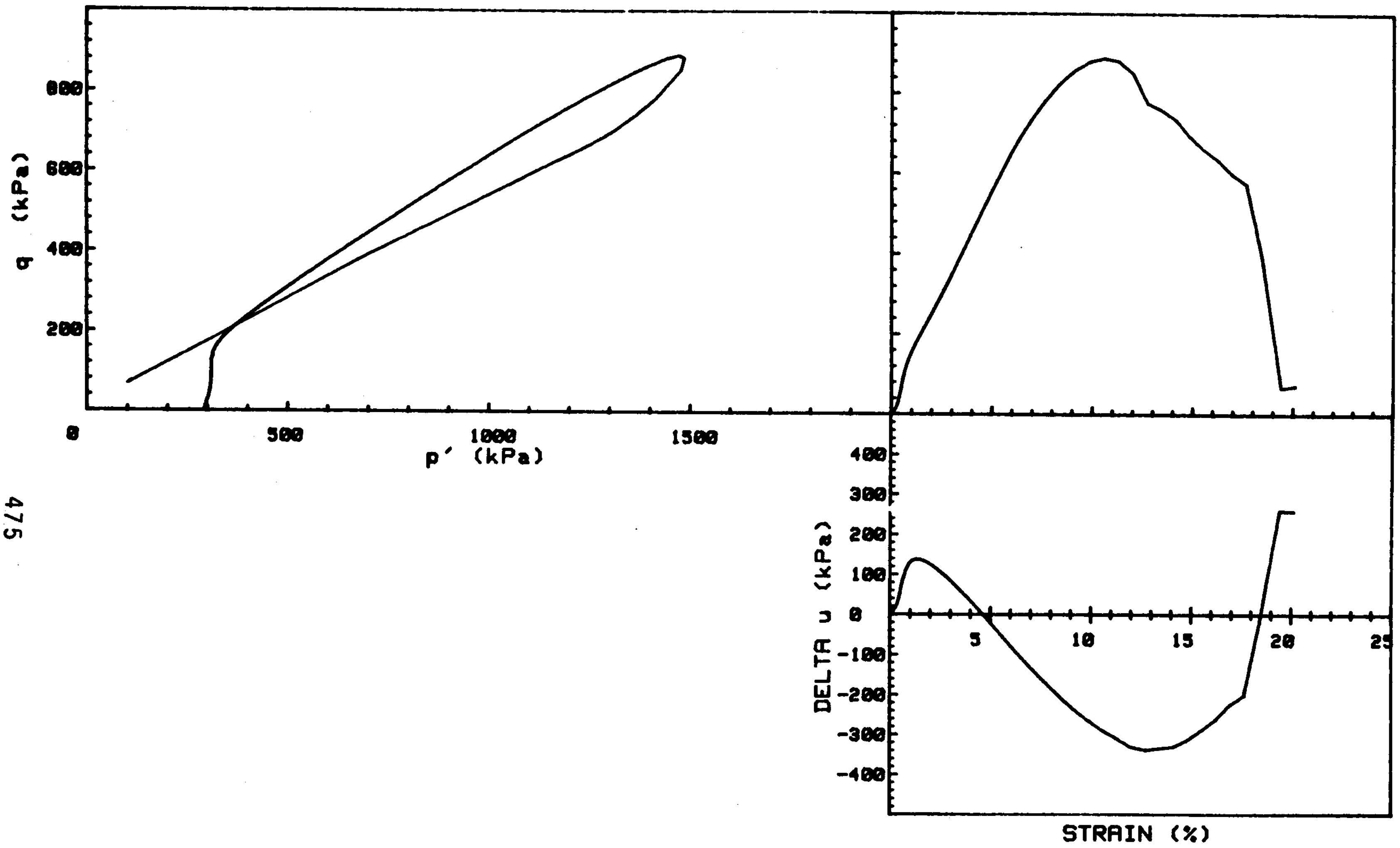

CRUISE DC1-81-EG		INCREMENT (cm)	170-180
CORE NO.	625A1	TEST NO.	TE118
SIG1c′(kPa)	293.3		
SIG3c′(kPa)	293.3		
INDUCED OCR	1.0		

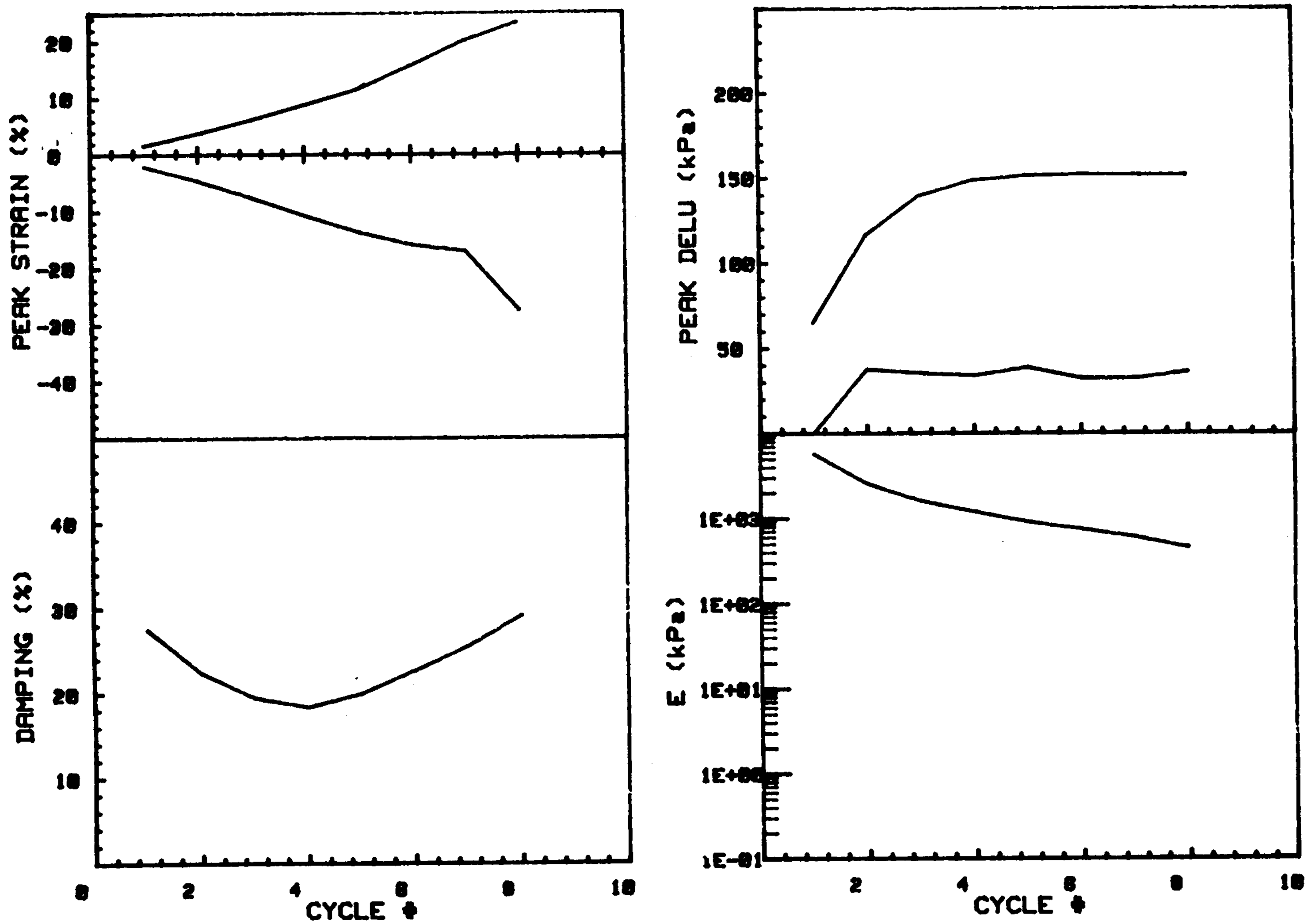

CRUISE DC2-80-EG		INCREMENT (cm)	32-39
CORE NO.	35G	TEST NO.	TC18
SIG1c′(kPa)	160.3	STATIC qf (kPa)	80.8
SIG3c′(kPa)	160.3	AVG MAX q (kPa)	54.9 (67.9%)
INDUCED OCR	1.0	AVG MIN q (kPa)	-49.9 (61.8%)

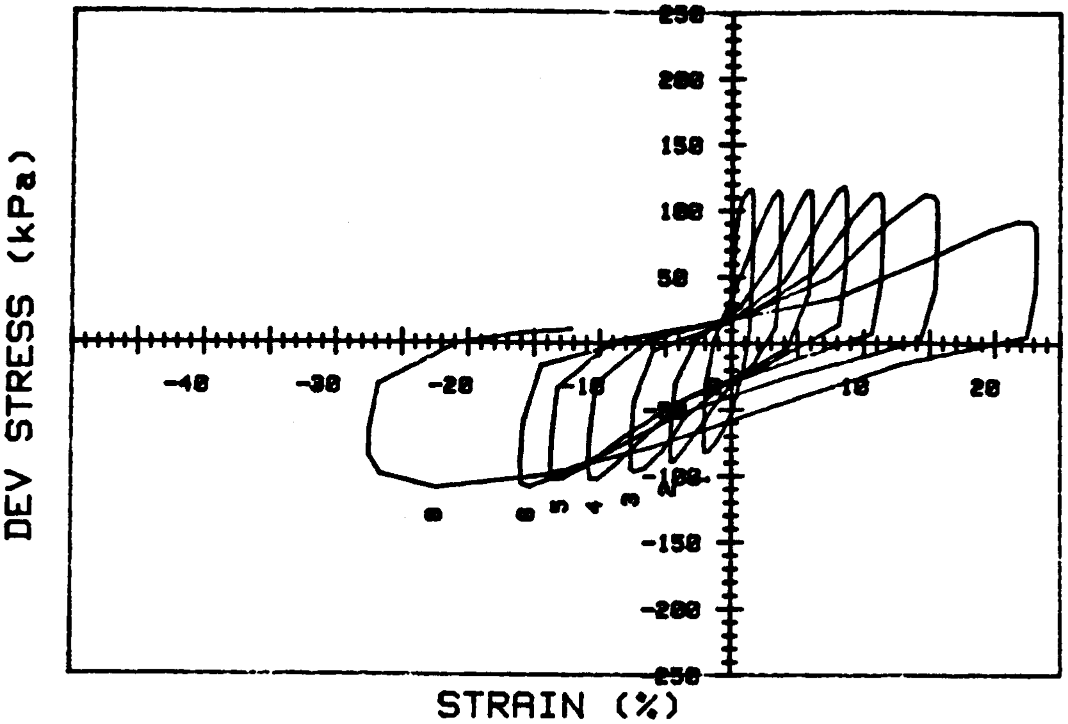

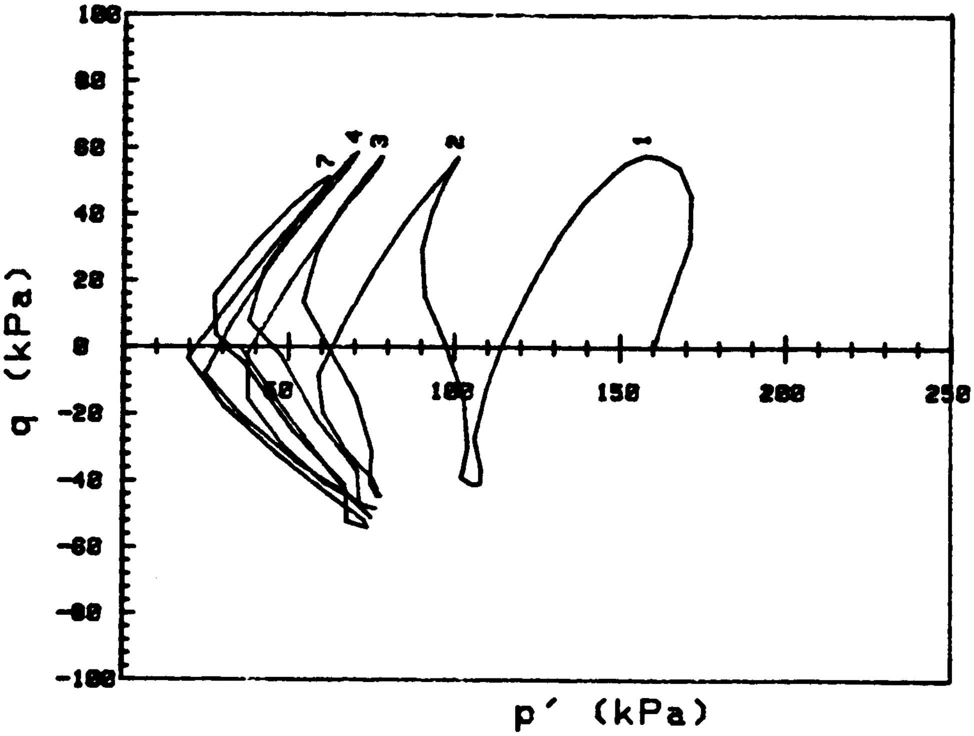

CRUISE DC2-80-EG		INCREMENT (cm)	32-39
CORE NO.	35G	TEST NO.	TC18
SIG1c′(kPa)	160.3	STATIC qf (kPa)	80.8
SIG3c′(kPa)	160.3	AVG MAX q (kPa)	54.9 (67.9%)
INDUCED OCR	1.0	AVG MIN q (kPa)	-49.9 (61.8%)

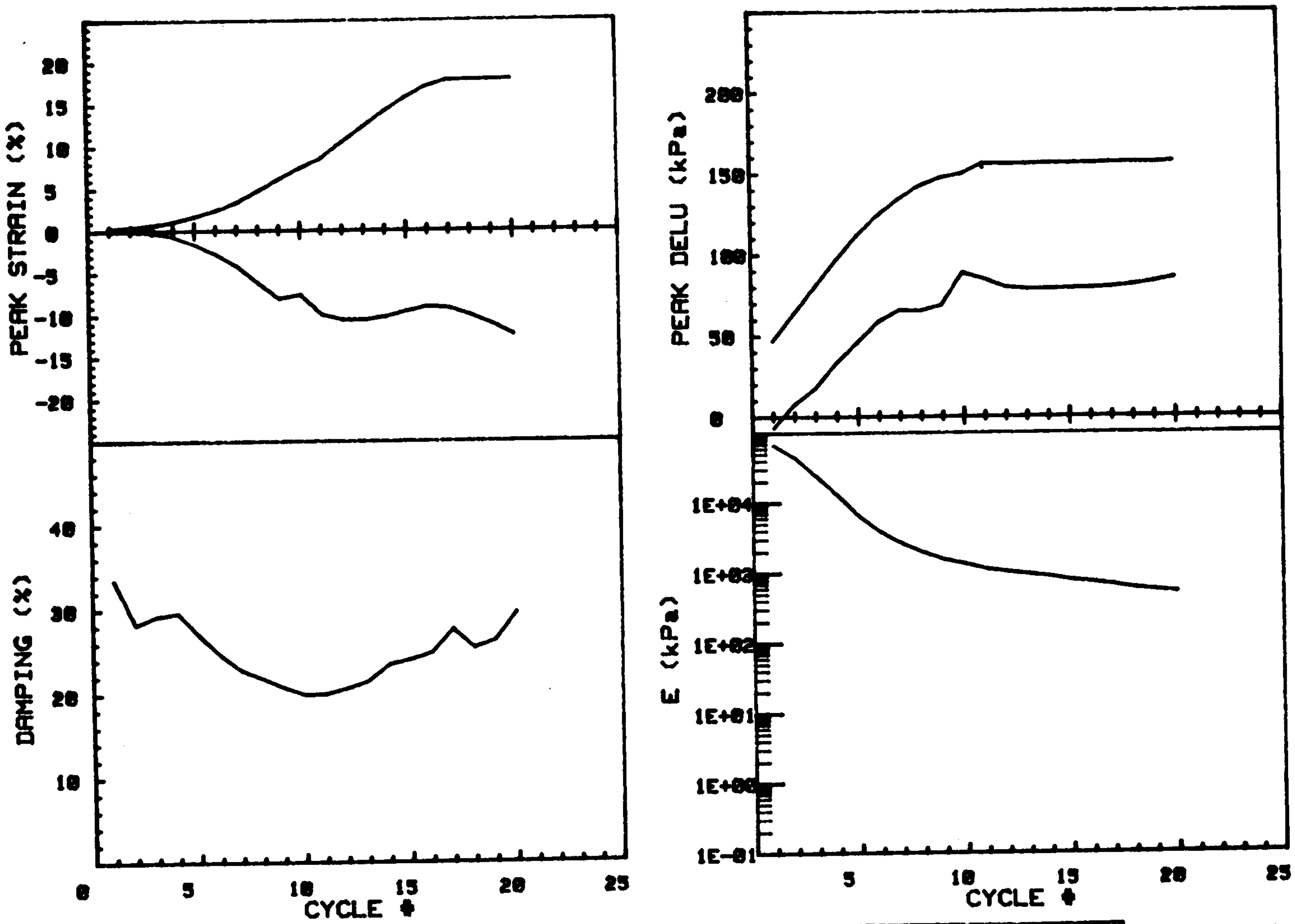

CRUISE DC2-80-EG		INCREMENT (cm)	32-39
CORE NO.	35G	TEST NO.	TC19
SIG1c'(kPa)	154.6	STATIC qf (kPa)	80.8
SIG3c'(kPa)	154.6	AVG MAX q (kPa)	51.6 (63.9%)
INDUCED OCR	1.0	AVG MIN q (kPa)	-43.5 (53.8%)

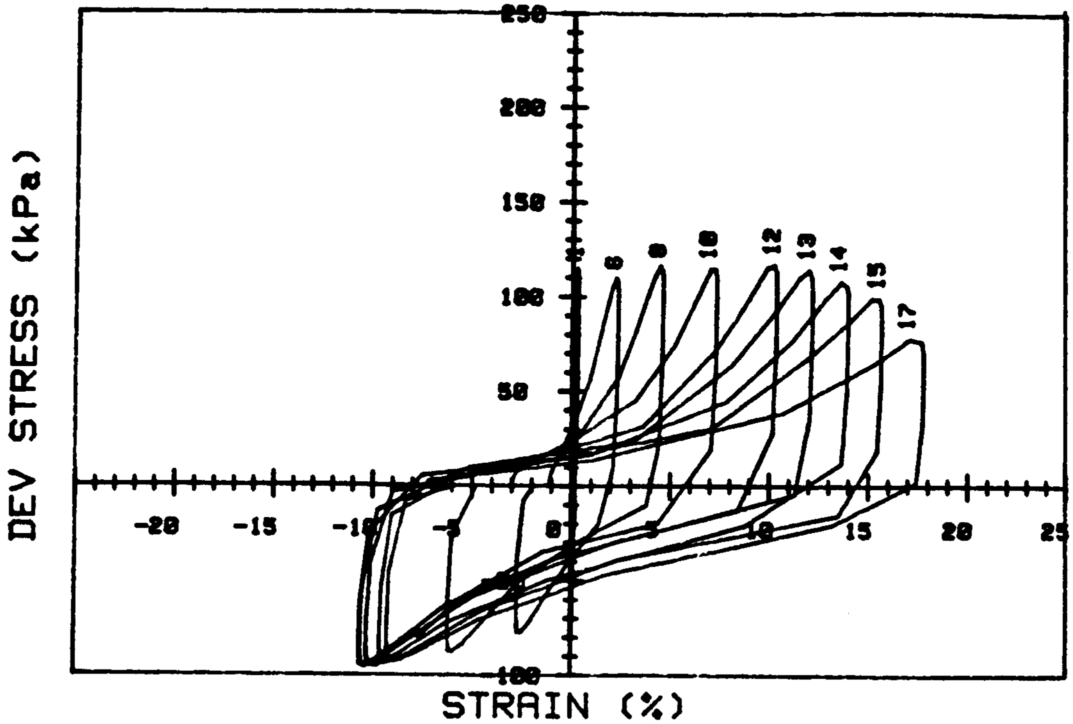

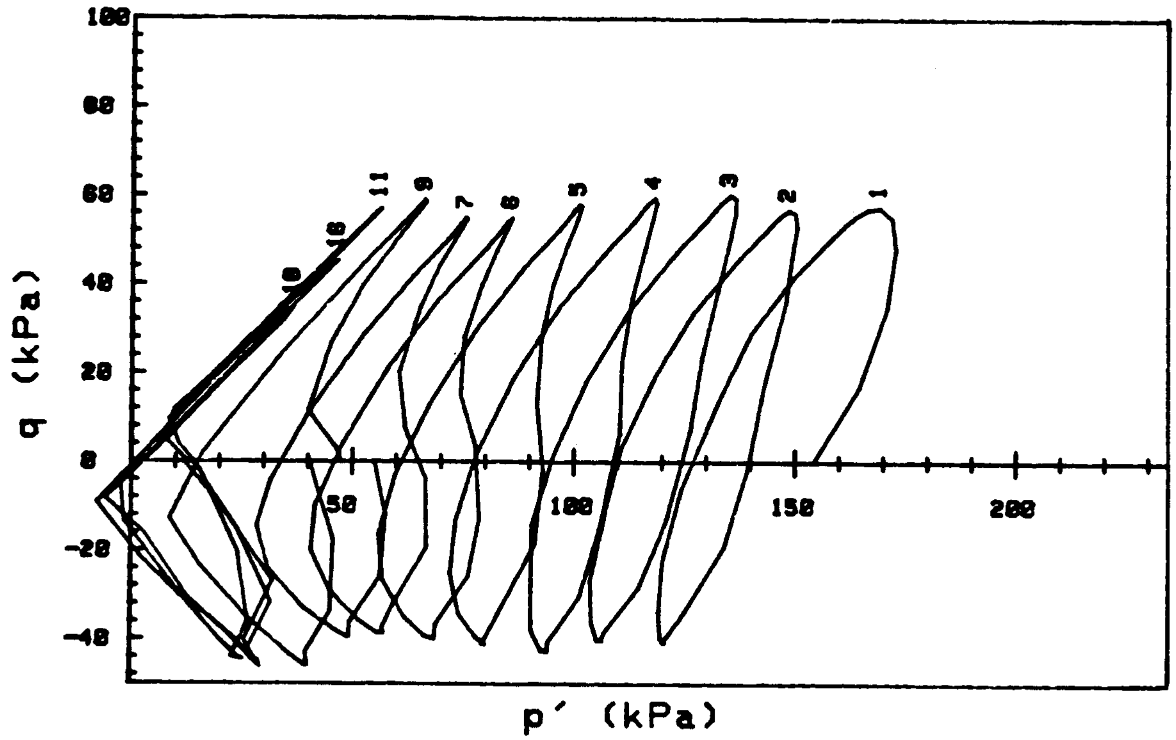

CRUISE DC2-80-EG		INCREMENT (cm)	32-39
CORE NO.	35G	TEST NO.	TC19
SIG1c′(kPa)	154.6	STATIC qf (kPa)	80.8
SIG3c′(kPa)	154.6	AVG MAX q (kPa)	51.6 (63.9%)
INDUCED OCR	1.0	AVG MIN q (kPa)	-43.5 (53.8%)

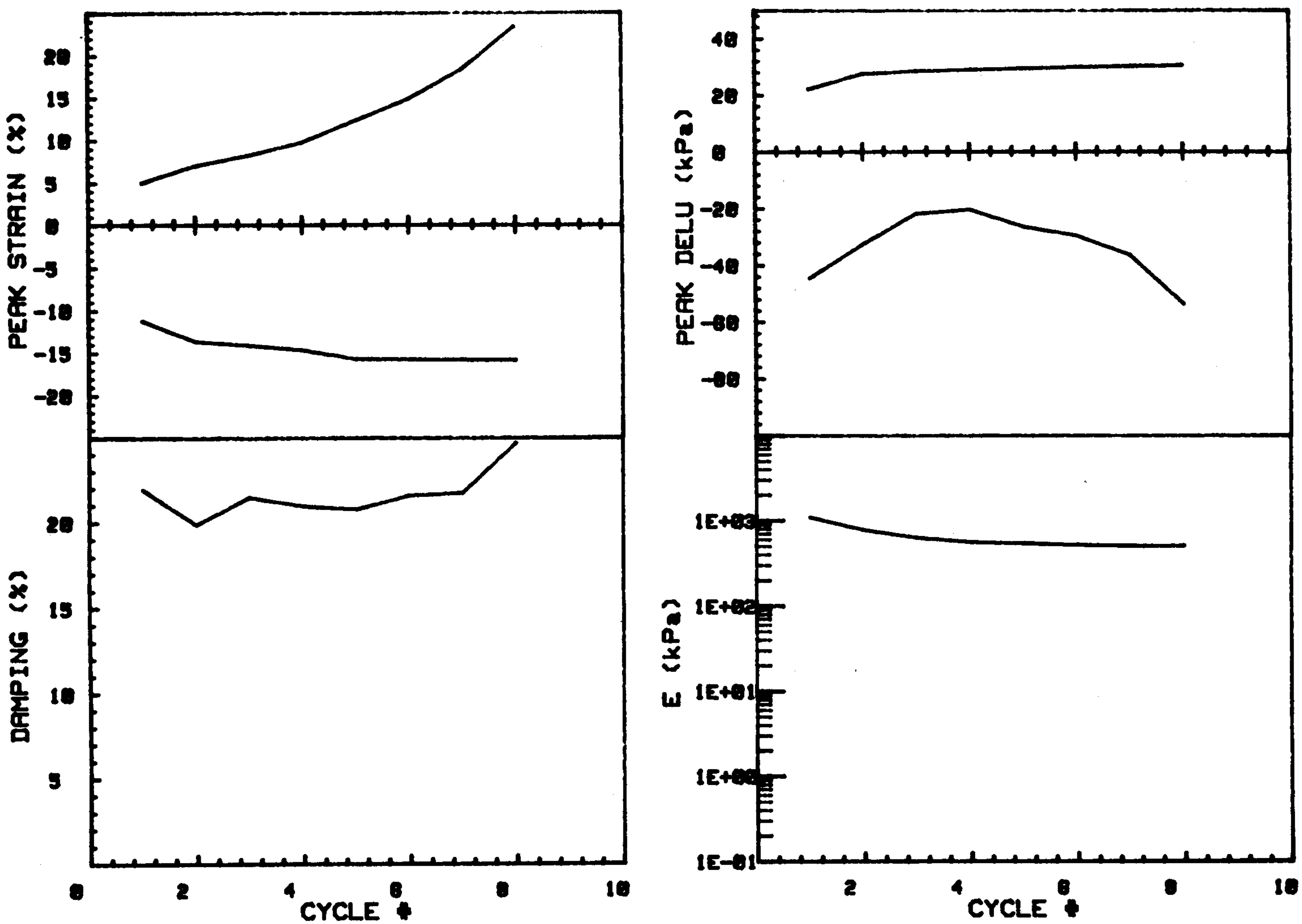

CRUISE DC2-80-EG		INCREMENT (cm)	27-35
CORE NO.	43G	TEST NO.	TC20
SIG1c'(kPa)	28.3	STATIC qf (kPa)	73.9
SIG3c'(kPa)	28.3	AVG MAX q (kPa)	43.2 (58.5%)
INDUCED OCR	1.0	AVG MIN q (kPa)	-34.5 (46.7%)

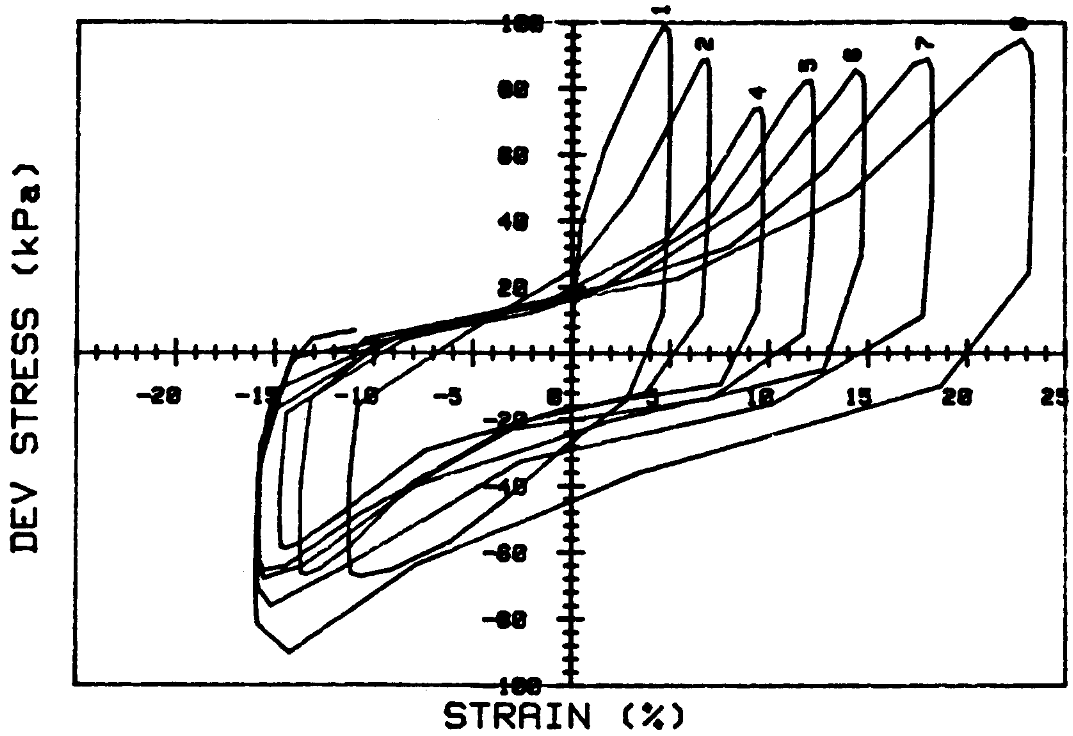

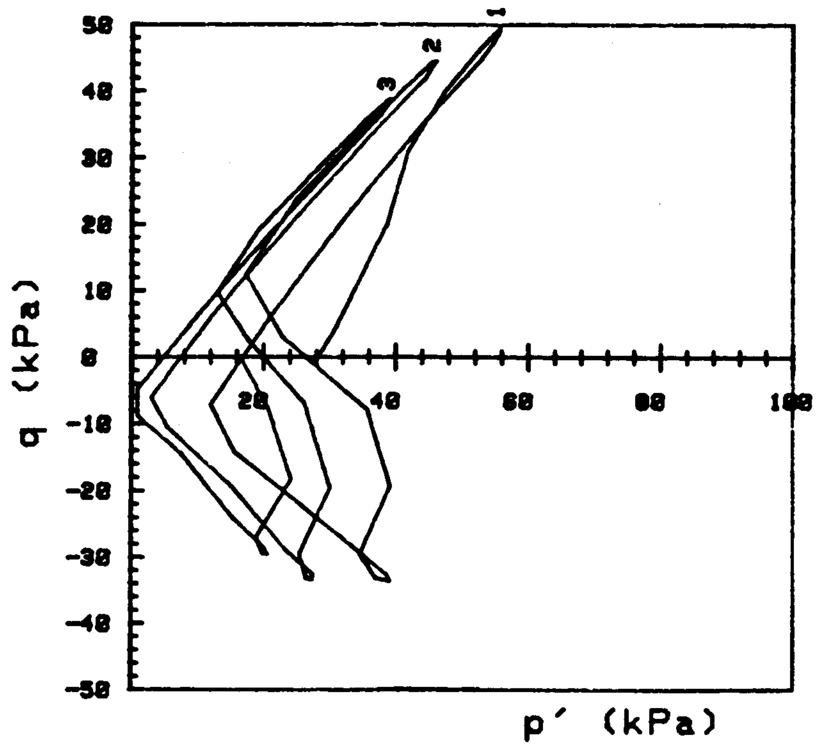

CRUISE DC2-80-EG		INCREMENT (cm)	27-35
CORE NO.	43G	TEST NO.	TC20
SIG1c′(kPa)	28.3	STATIC qf (kPa)	73.9
SIG3c′(kPa)	28.3	AVG MAX q (kPa)	43.2 (58.5%)
INDUCED OCR	1.0	AVG MIN q (kPa)	-34.5 (46.7%)

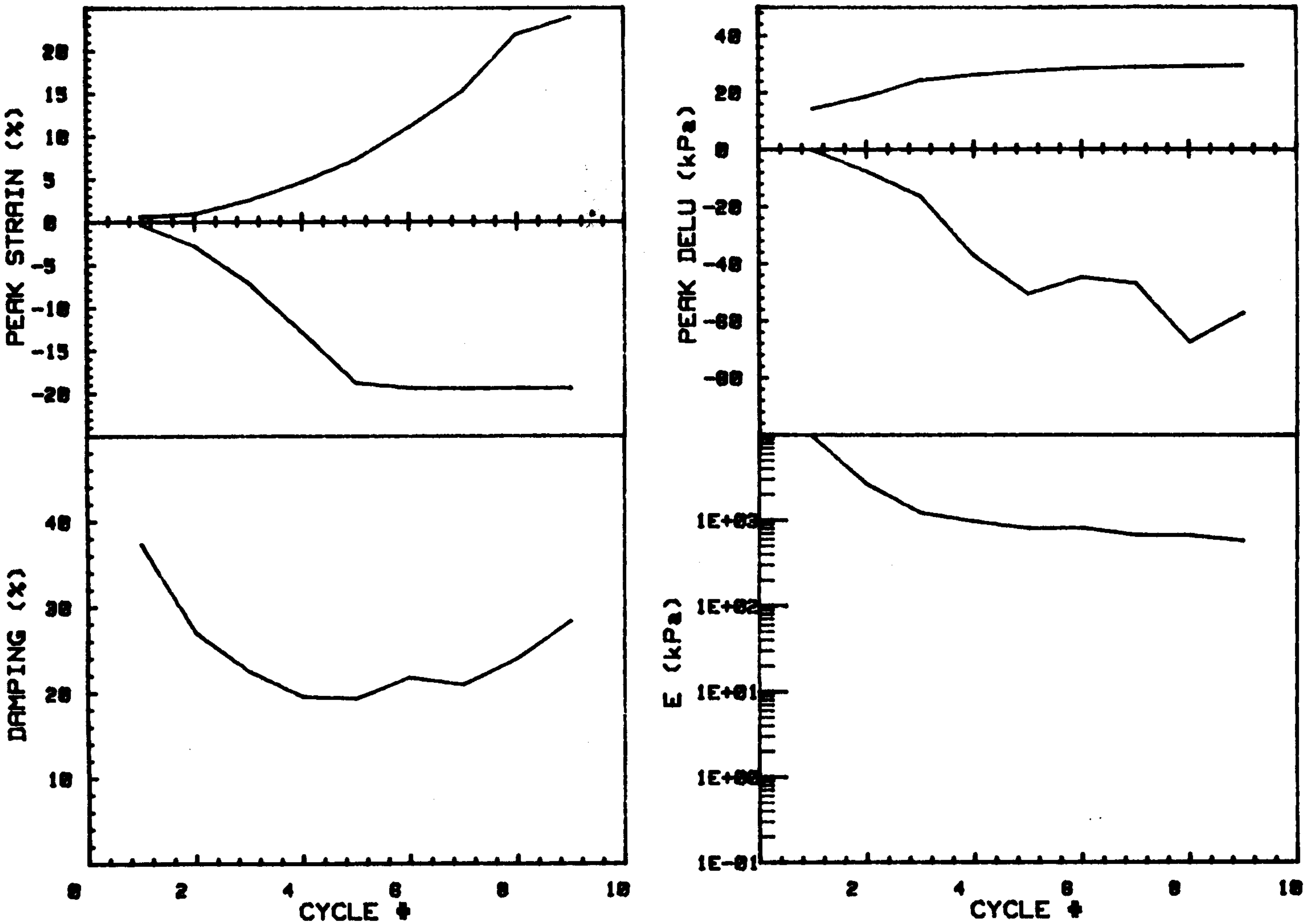

CRUISE DC2-80-EG		INCREMENT (cm)	27-35
CORE NO.	43G	TEST NO.	TC21
SIG1c'(kPa)	27.2	STATIC qf (kPa)	73.9
SIG3c'(kPa)	27.2	AVG MAX q (kPa)	45.7 (61.8%)
INDUCED OCR	1.0	AVG MIN q (kPa)	-42.0 (56.8%)

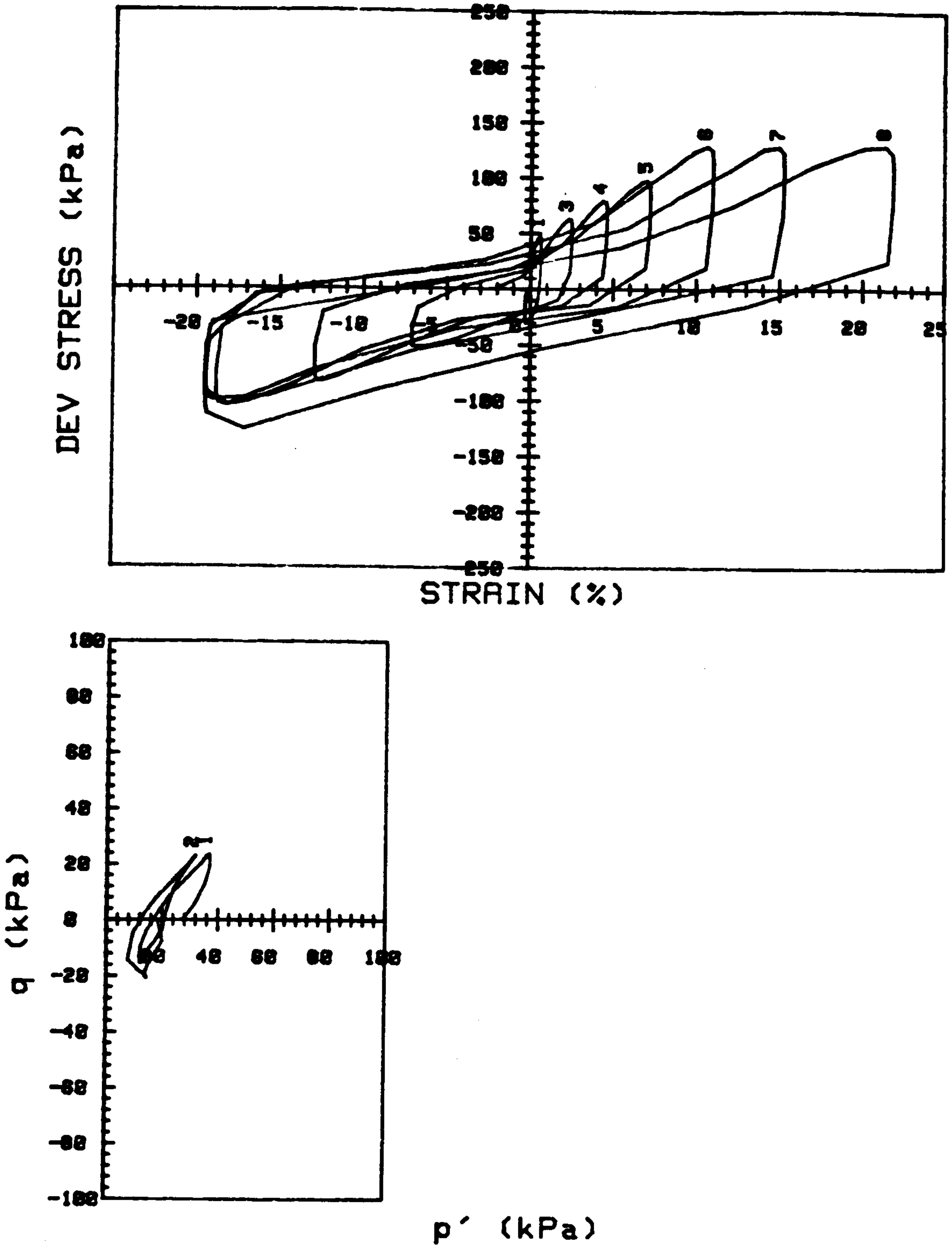

CRUISE DC2-80-EG		INCREMENT (cm)	27-35
CORE NO.	43G	TEST NO.	TC21
SIG1c'(kPa)	27.2	STATIC qf (kPa)	73.9
SIG3c'(kPa)	27.2	AVG MAX q (kPa)	45.7 (61.8%)
INDUCED OCR	1.0	AVG MIN q (kPa)	-42.0 (56.8%)

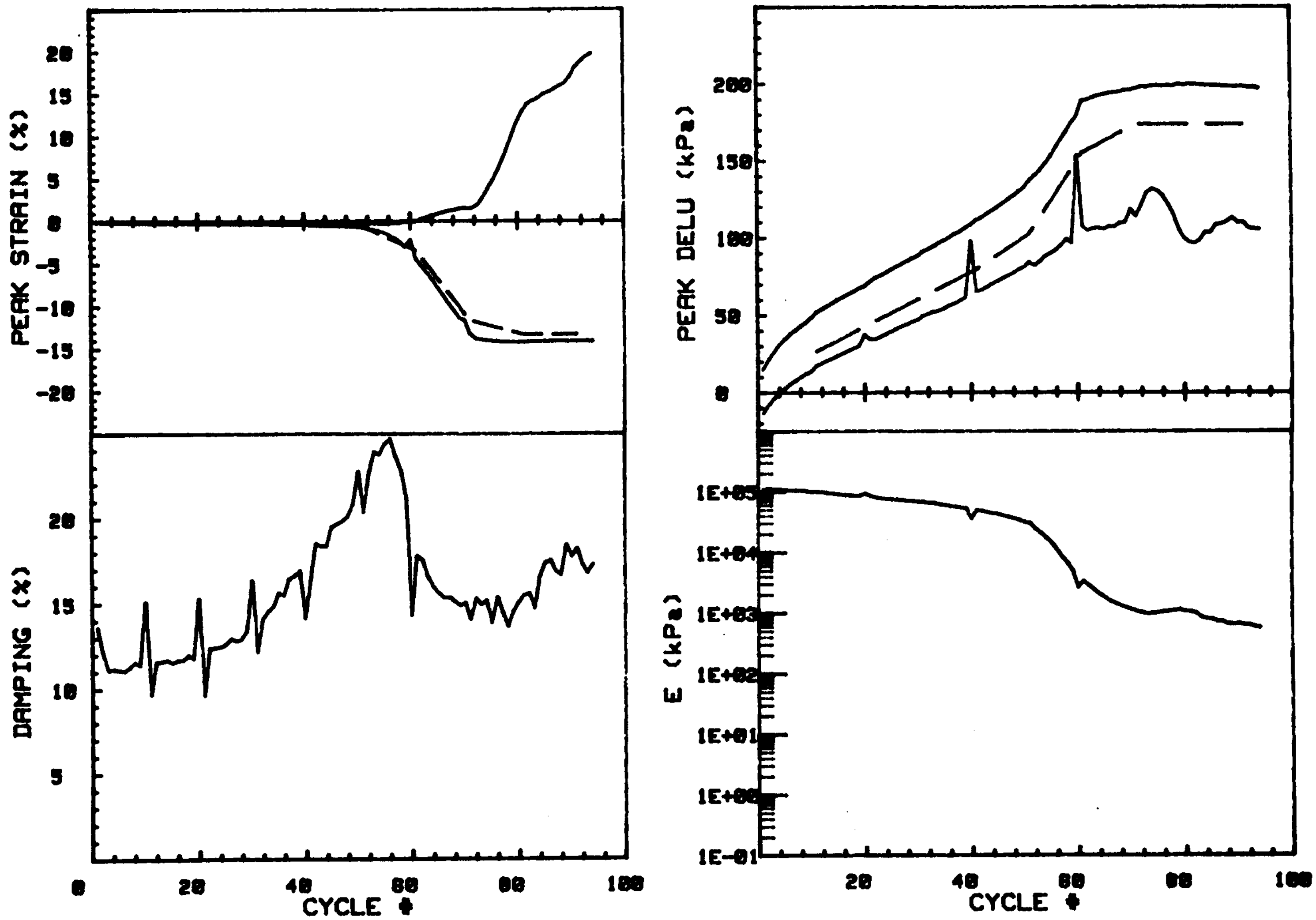

CRUISE DC2-80-EG		INCREMENT (cm)	7-15
CORE NO.	46G	TEST NO.	TC22
SIG1c'(kPa)	196.2	STATIC qf (kPa)	222.4
SIG3c'(kPa)	196.2	AVG MAX q (kPa)	33.5 (15.1%)
INDUCED OCR	1.0	AVG MIN q (kPa)	-42.4 (19.1%)

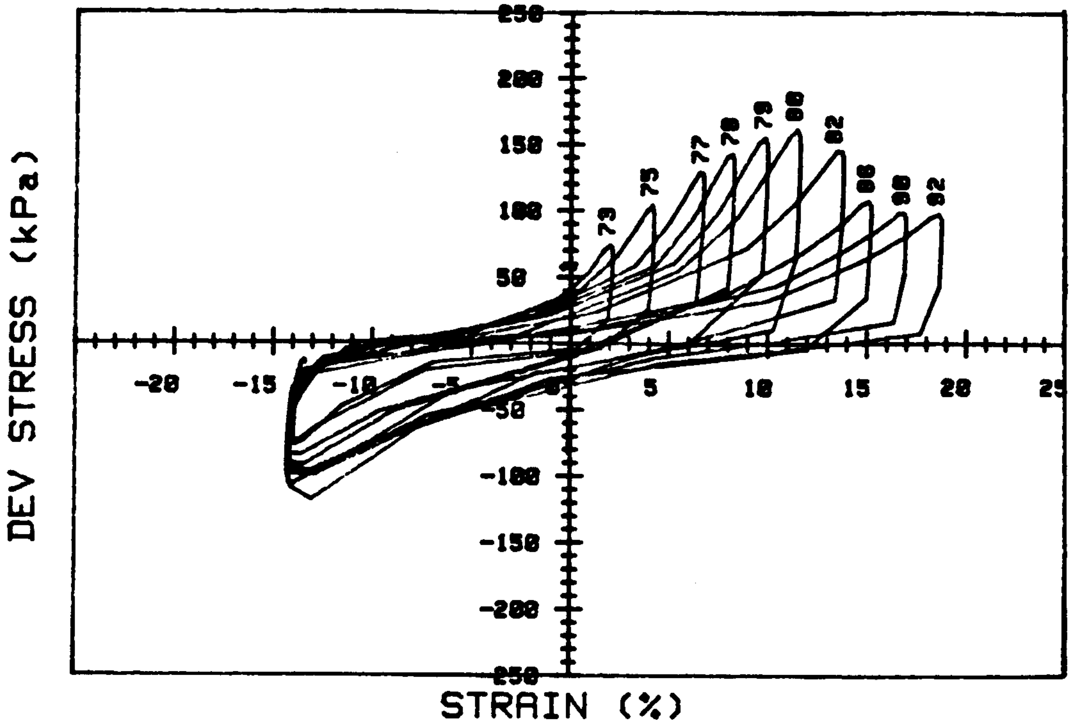

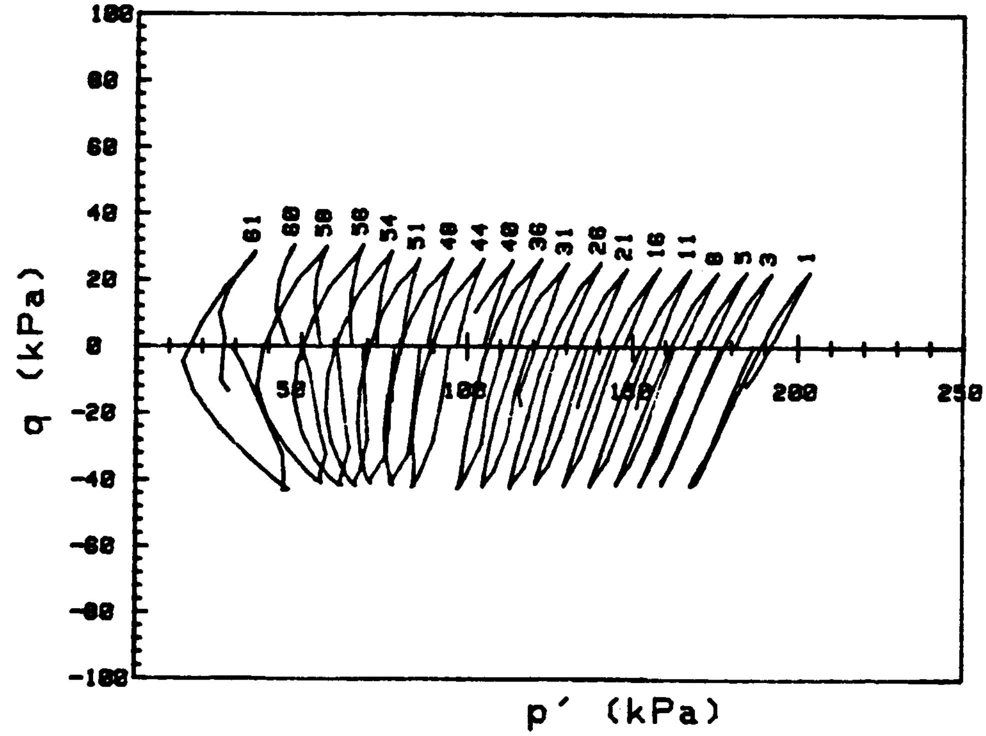

CRUISE DC2-80-EG		INCREMENT (cm)	7-15
CORE NO.	46G	TEST NO.	TC22
SIG1c′(kPa)	196.2	STATIC qf (kPa)	222.4
SIG3c′(kPa)	196.2	AVG MAX q (kPa)	33.5 (15.1%)
INDUCED OCR	1.0	AVG MIN q (kPa)	-42.4 (19.1%)

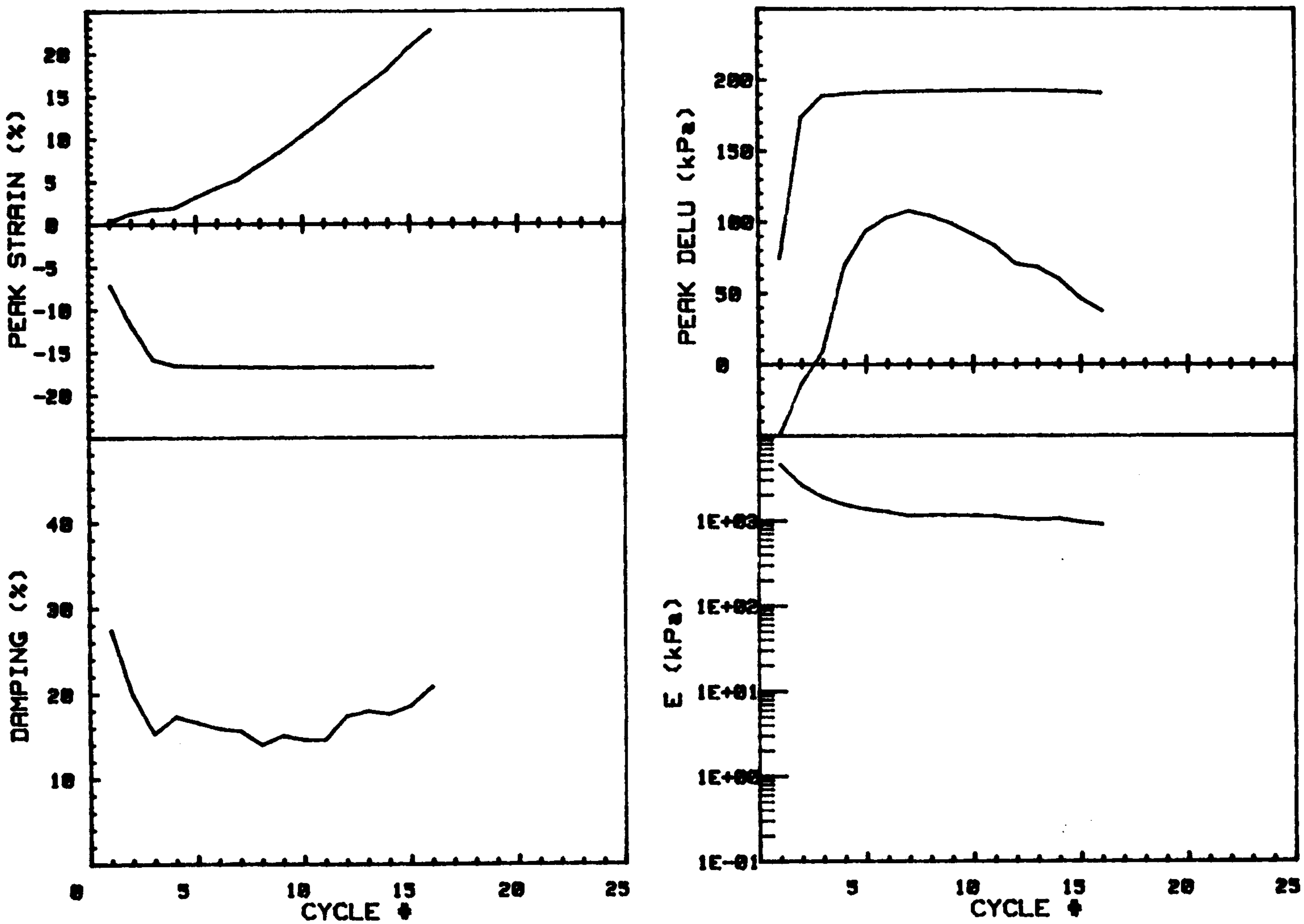

CRUISE DC2-80-EG		INCREMENT (cm)	7-15
CORE NO.	46G	TEST NO.	TC23
SIG1c'(kPa)	192.6	STATIC qf (kPa)	222.4
SIG3c'(kPa)	192.6	AVG MAX q (kPa)	79.0 (35.5%)
INDUCED OCR	1.0	AVG MIN q (kPa)	-71.8 (32.3%)

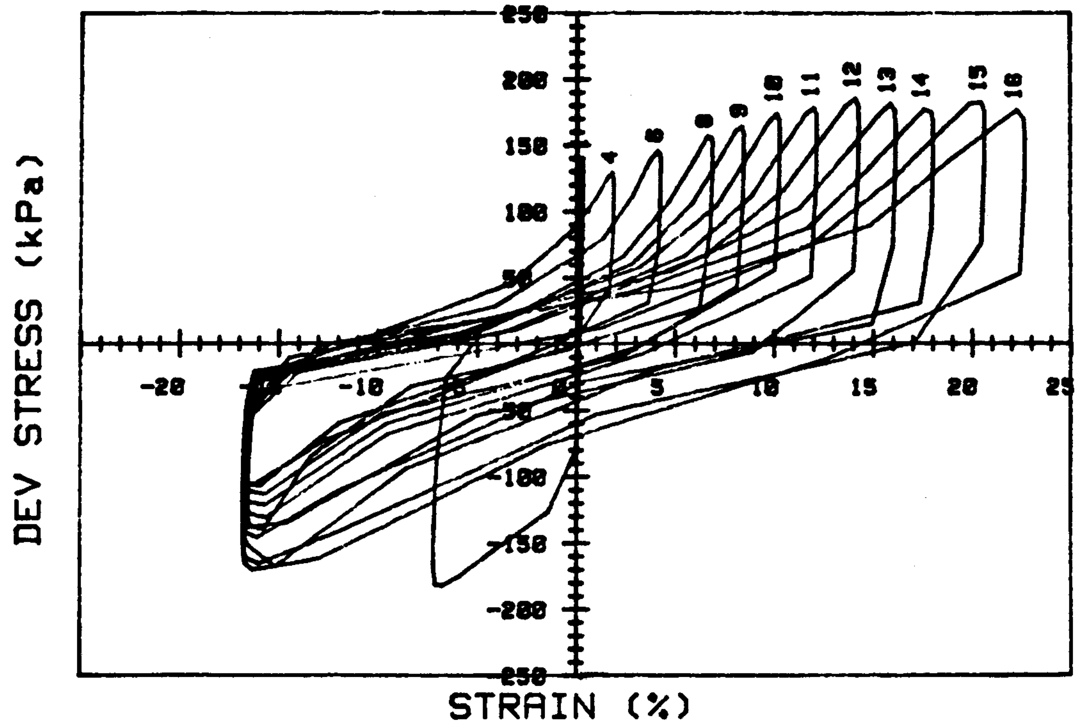

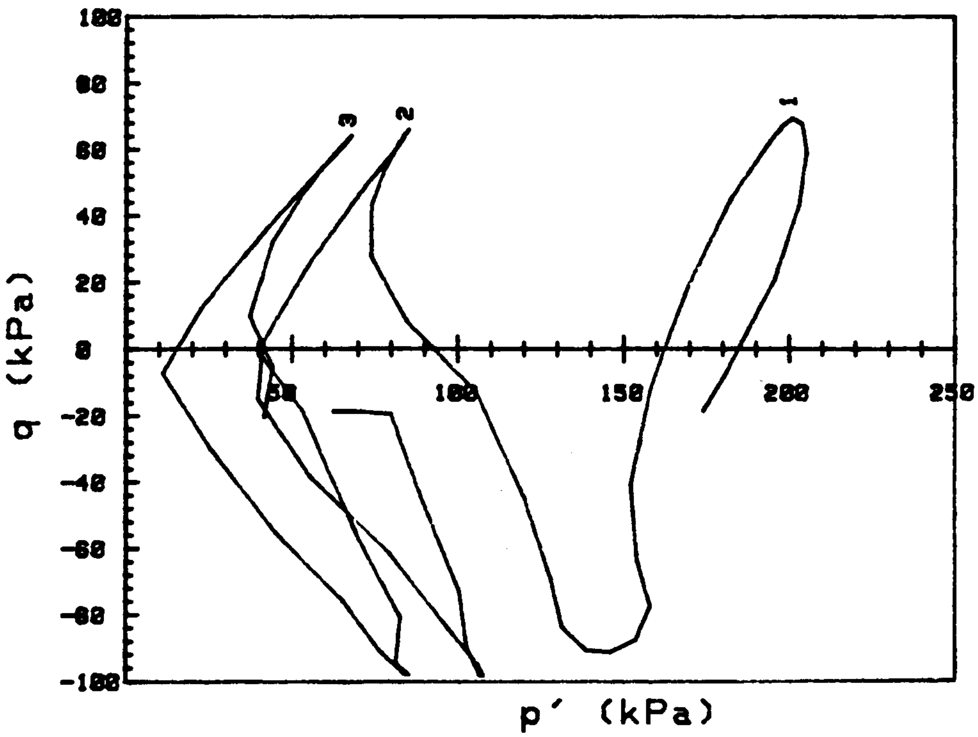

CRUISE DC2-80-EG		INCREMENT (cm)	7-15
CORE NO.	46G	TEST NO.	TC23
SIG1c′(kPa)	192.6	STATIC qf (kPa)	222.4
SIG3c′(kPa)	192.6	AVG MAX q (kPa)	79.0 (35.5%)
INDUCED OCR	1.0	AVG MIN q (kPa)	-71.8 (32.3%)

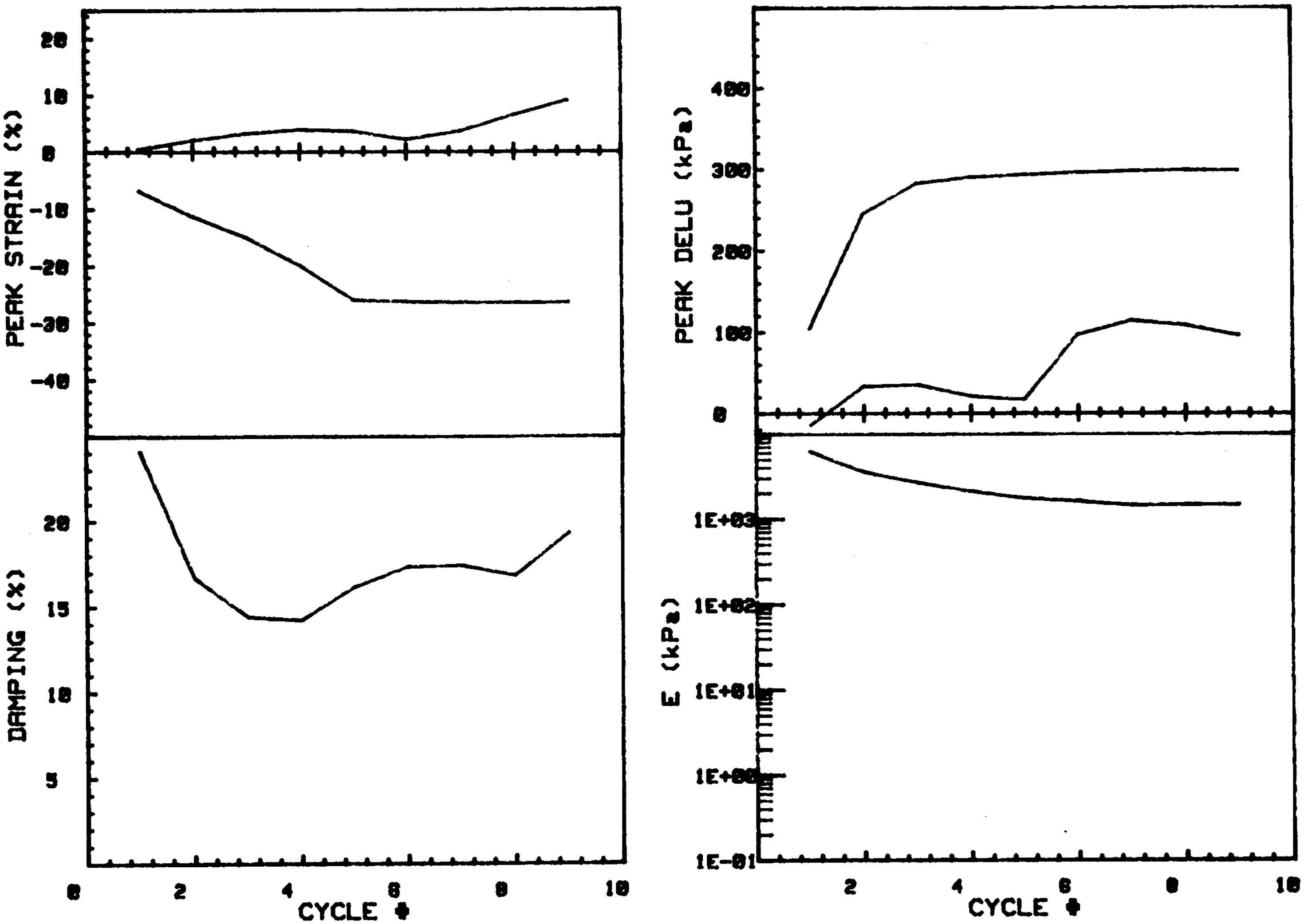

CRUISE DC2-80-EG		INCREMENT (cm)	15-22
CORE NO.	28G	TEST NO.	TC24
SIG1c'(kPa)	302.6	STATIC qf (kPa)	268.9
SIG3c'(kPa)	302.6	AVG MAX q (kPa)	115.6 (43.0%)
INDUCED OCR	1.0	AVG MIN q (kPa)	-100.5 (37.4%)

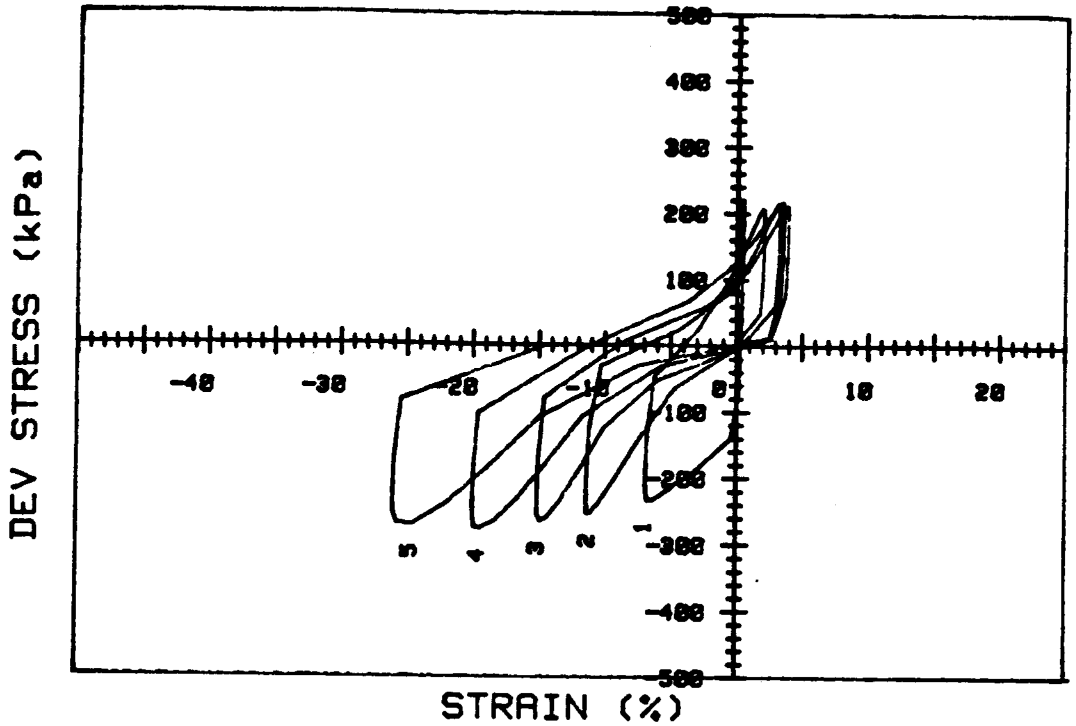

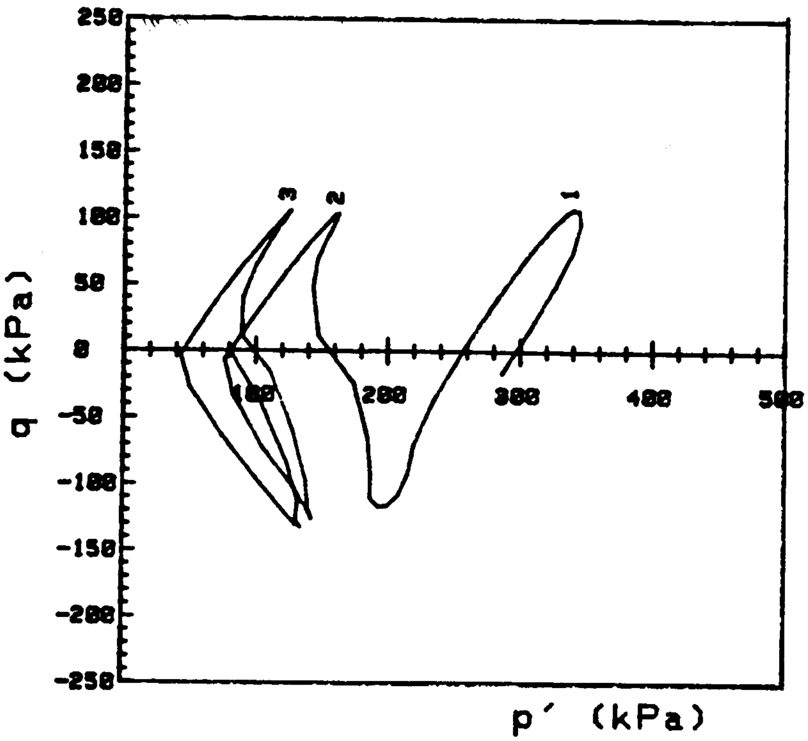

CRUISE DC2-80-EG		INCREMENT (cm)	15-22
CORE NO.	28G	TEST NO.	TC24
SIG1c′(kPa)	302.6	STATIC qf (kPa)	268.9
SIG3c′(kPa)	302.6	AVG MAX q (kPa)	115.6 (43.0%)
INDUCED OCR	1.0	AVG MIN q (kPa)	-100.5 (37.4%)

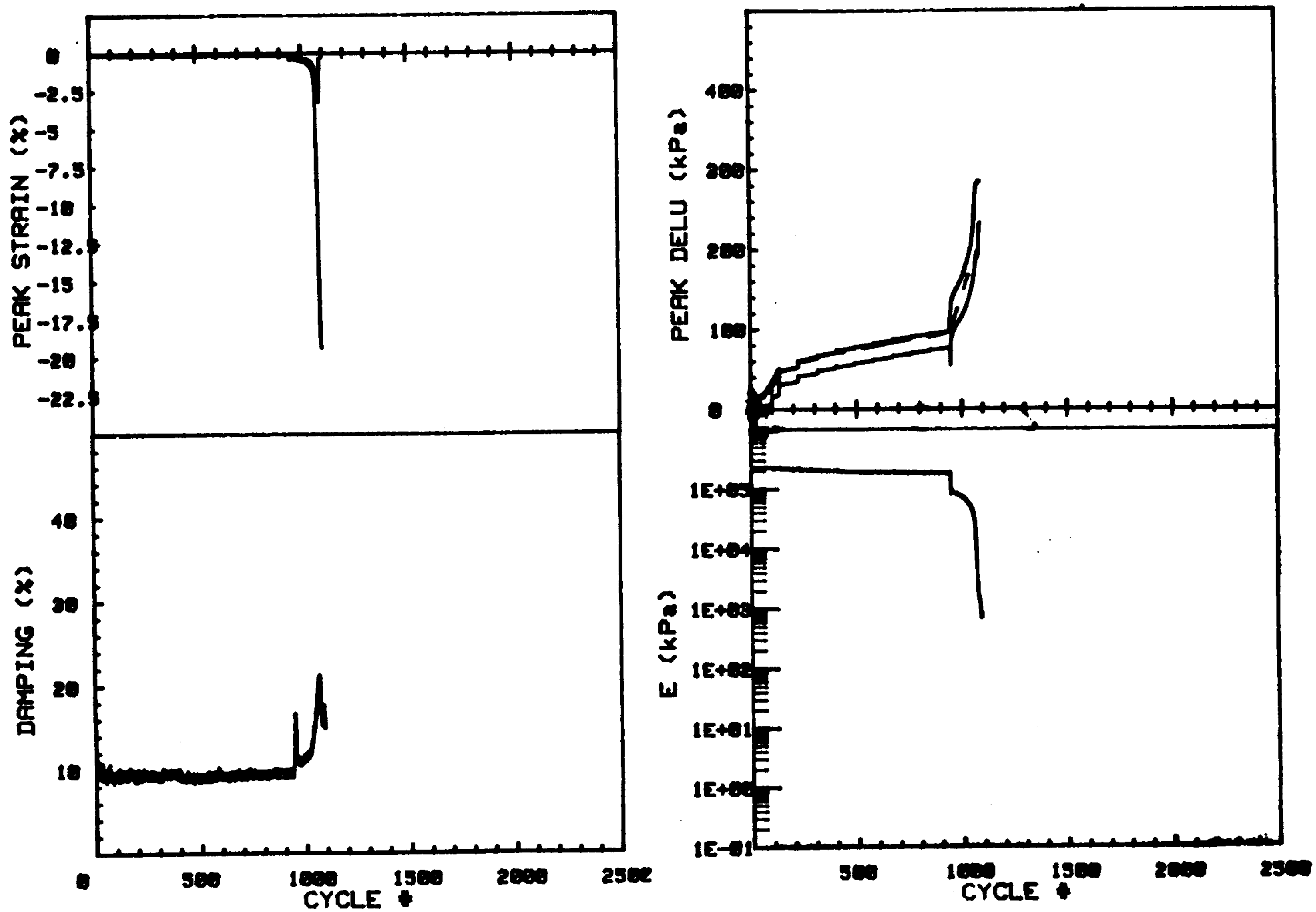

CRUISE DC2-80-EG		INCREMENT (cm)	15-22.4
CORE NO.	28G	TEST NO.	TC25
SIG1c'(kPa)	297.9	STATIC qf (kPa)	270.0
SIG3c'(kPa)	297.9	AVG MAX q (kPa)	21.1 (7.8%)
INDUCED OCR	1.0	AVG MIN q (kPa)	-16.6 (6.1%)

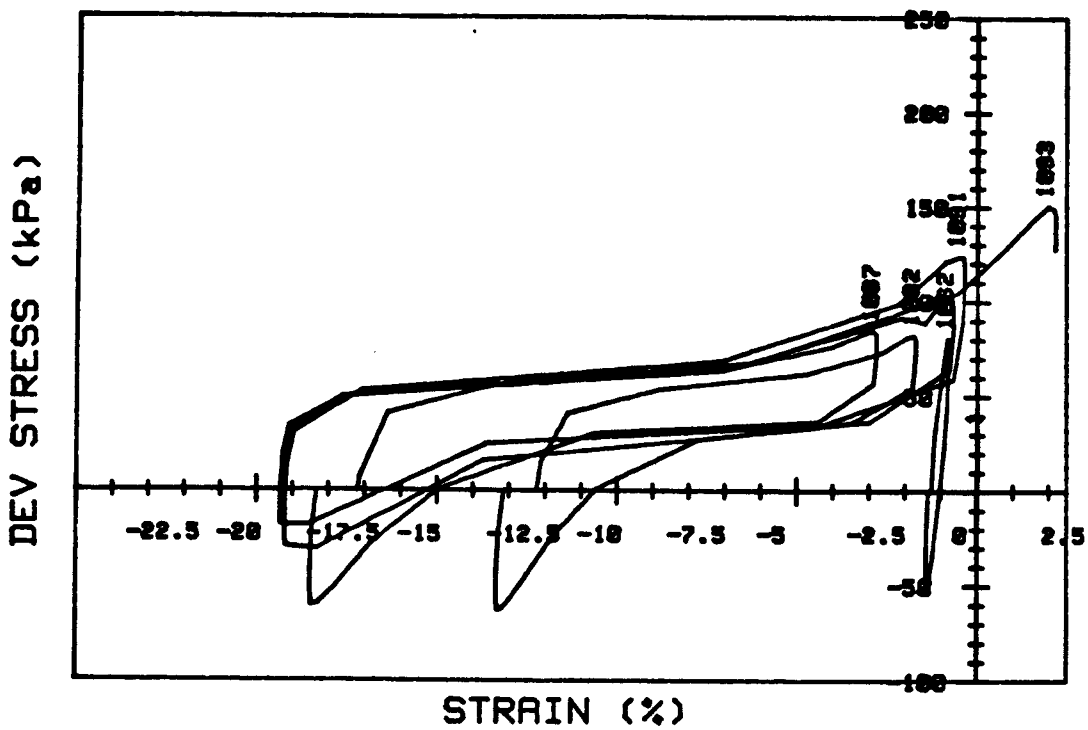

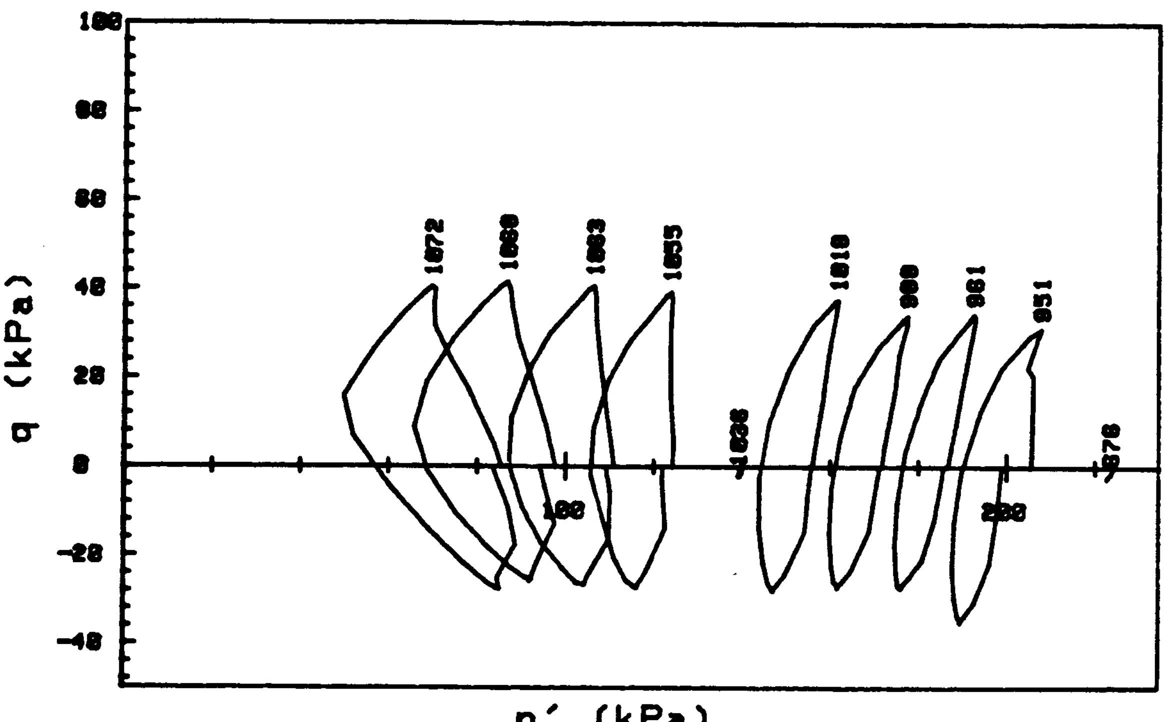

CRUISE DC2-80-EG		INCREMENT (cm)	15-22.4
CORE NO.	28G	TEST NO.	TC25
SIG1c′(kPa)	297.9	STATIC qf (kPa)	270.0
SIG3c′(kPa)	297.9	AVG MAX q (kPa)	21.1 (7.8%)
INDUCED OCR	1.0	AVG MIN q (kPa)	-16.6 (6.1%)

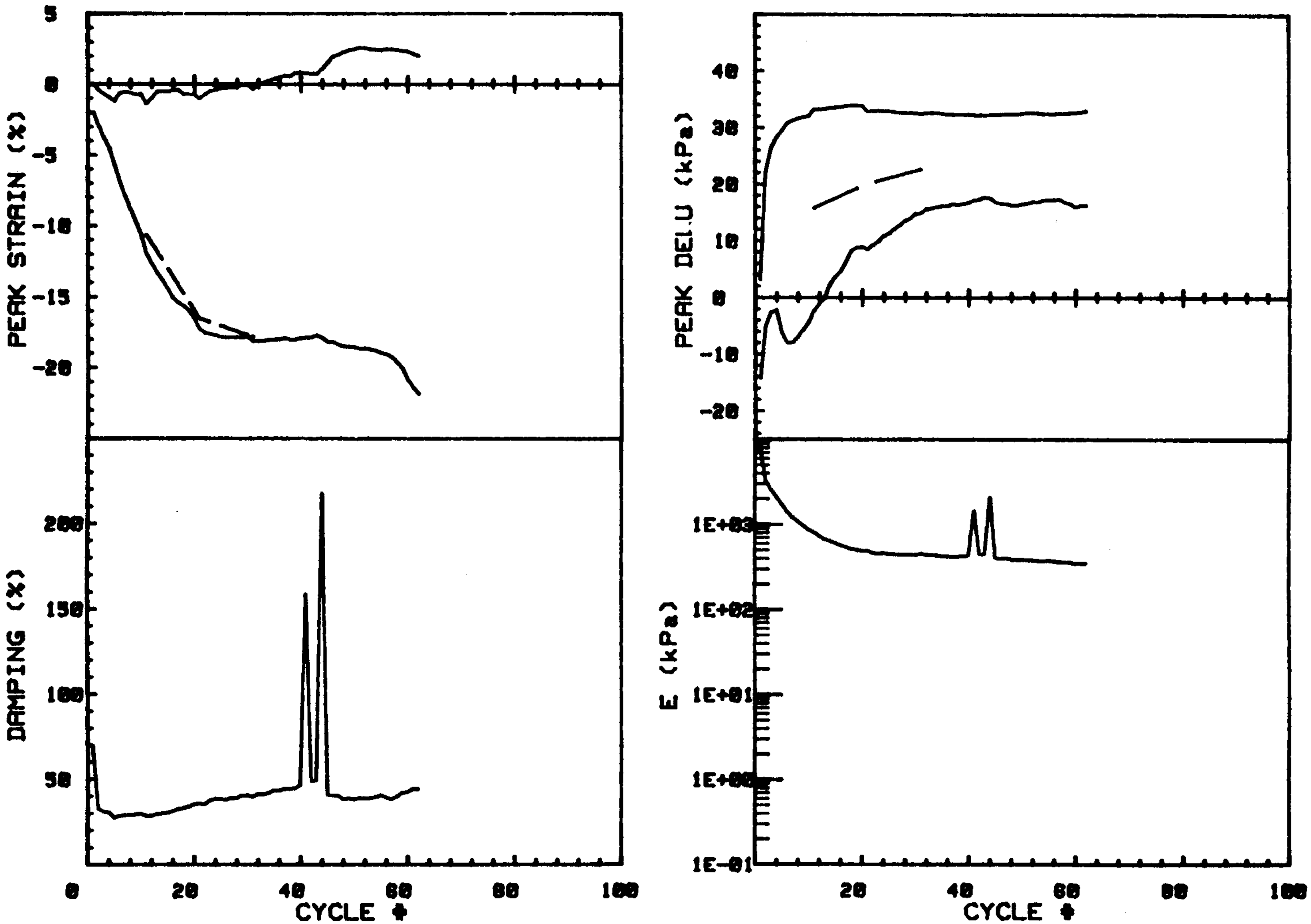

CRUISE DC2-80-EG		INCREMENT (cm)	61-71
CORE NO.	181G	TEST NO.	TC30
SIG1c'(kPa)	30.3	STATIC qf (kPa)	23.7
SIG3c'(kPa)	30.3	AVG MAX q (kPa)	14.3 (60.3%)
INDUCED OCR	1.0	AVG MIN q (kPa)	-25.0 (105.5%)

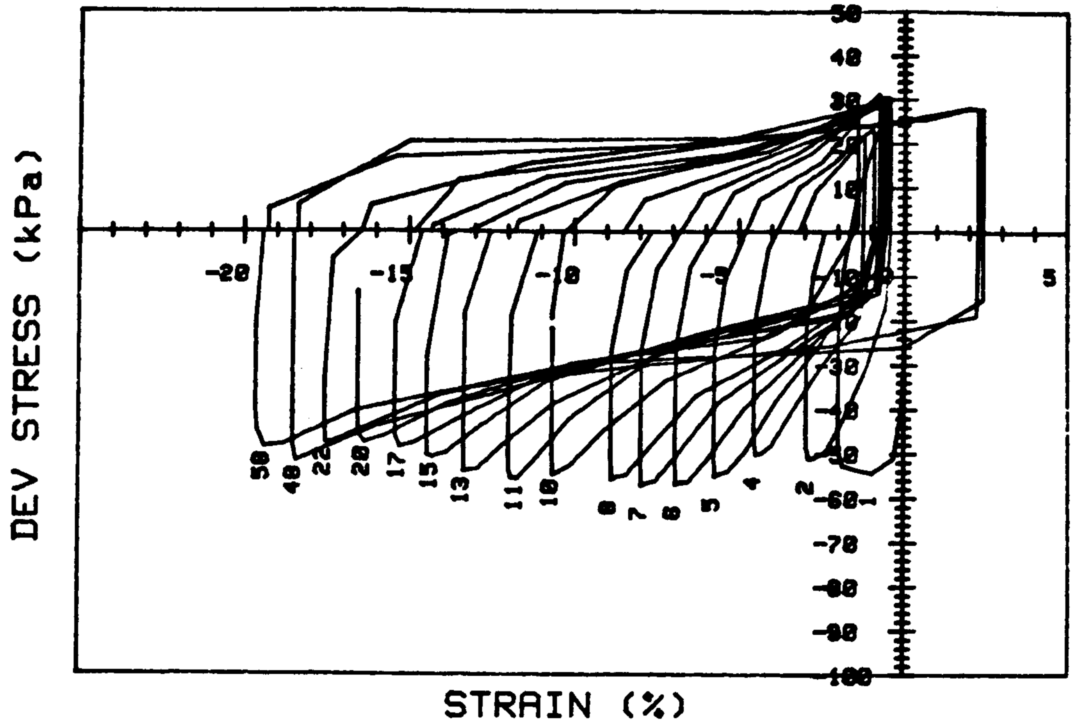

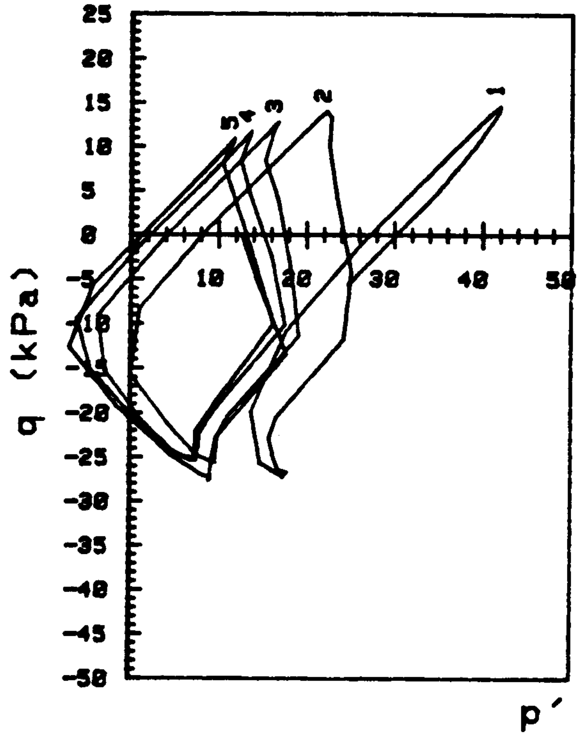

CRUISE DC2-80-EG		INCREMENT (cm)	61-71
CORE NO.	181G	TEST NO.	TC30
SIG1c'(kPa)	30.3	STATIC qf (kPa)	23.7
SIG3c'(kPa)	30.3	AVG MAX q (kPa)	14.3 (60.3%)
INDUCED OCR	1.0	AVG MIN q (kPa)	-25.0 (105.5%)

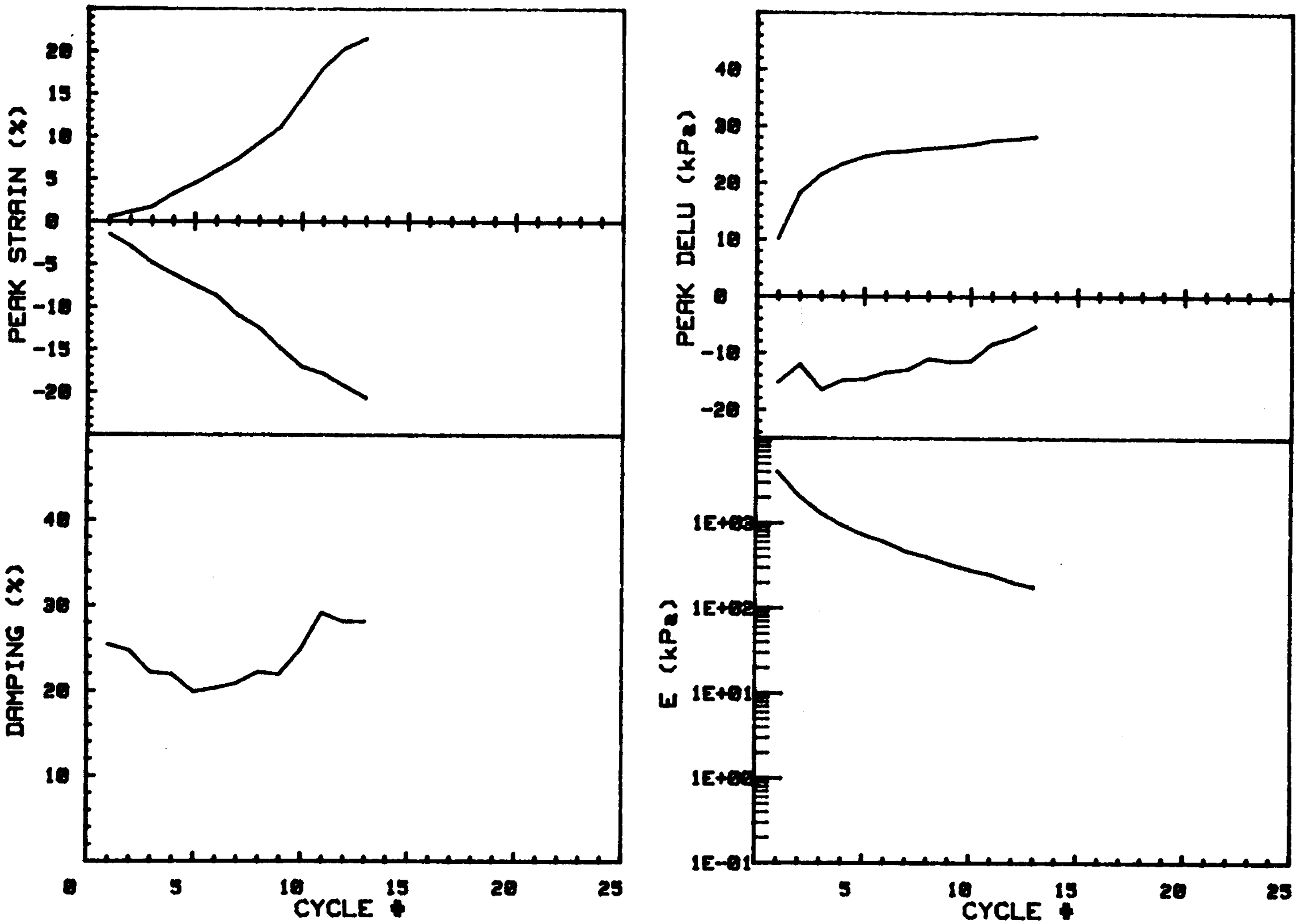

CRUISE DC2-80-EG		INCREMENT (cm)	61-71
CORE NO.	181G	TEST NO.	TC31
SIG1c'(kPa)	24.2	STATIC qf (kPa)	23.7
SIG3c'(kPa)	24.2	AVG MAX q (kPa)	17.2 (72.6%)
INDUCED OCR	1.0	AVG MIN q (kPa)	-23.8 (100.4%)

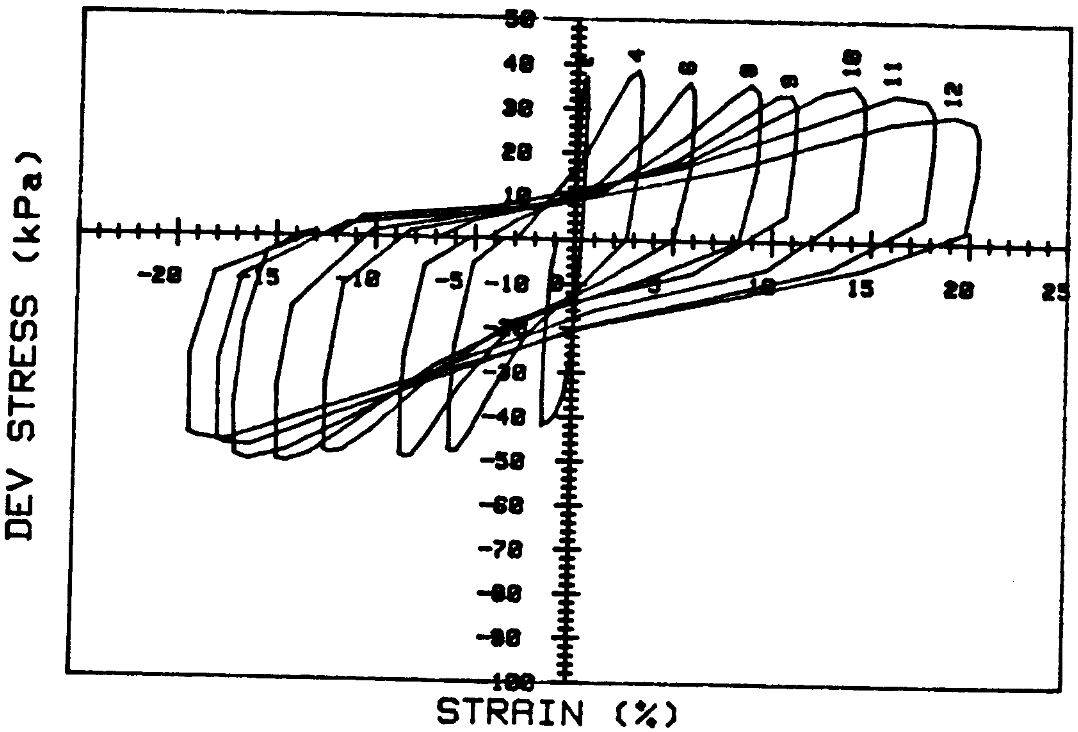

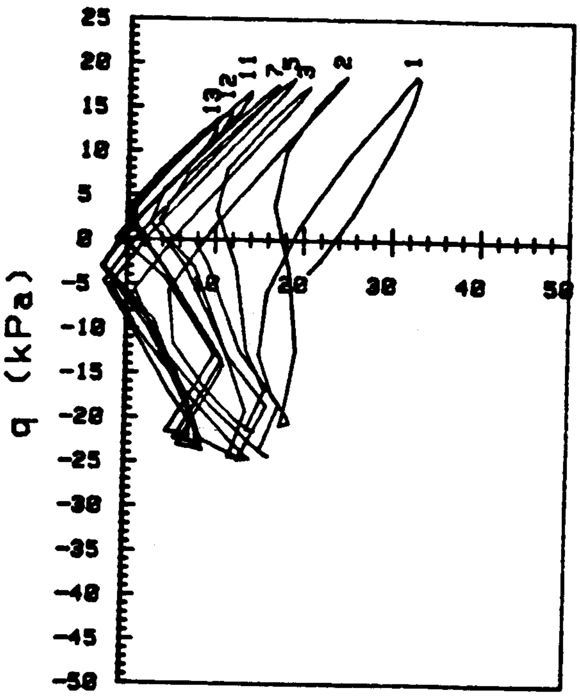

CRUISE DC2-80-EG		INCREMENT (cm)	61-71
CORE NO.	181G	TEST NO.	TC31
SIG1c′(kPa)	24.2	STATIC qf (kPa)	23.7
SIG3c′(kPa)	24.2	AVG MAX q (kPa)	17.2 (72.6%)
INDUCED OCR	1.0	AVG MIN q (kPa)	-23.8 (100.4%)

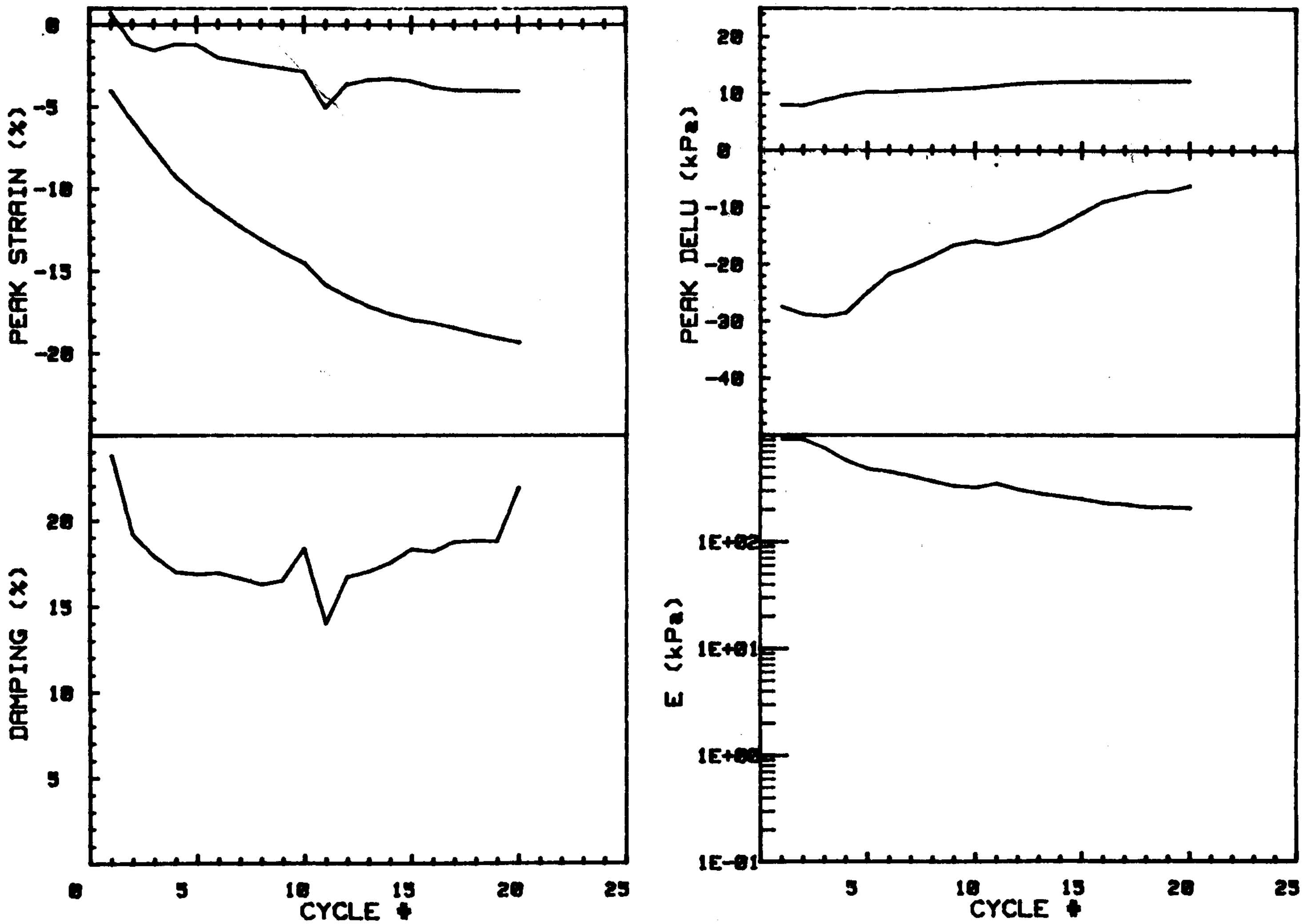

CRUISE DC2-80-EG		INCREMENT (cm)	85-95
CORE NO.	101G	TEST NO.	TC32
SIG1c'(kPa)	10.4	STATIC qf (kPa)	19.0
SIG3c'(kPa)	10.4	AVG MAX q (kPa)	3.7 (19.5%)
INDUCED OCR	3.5	AVG MIN q (kPa)	-15.0 (78.9%)

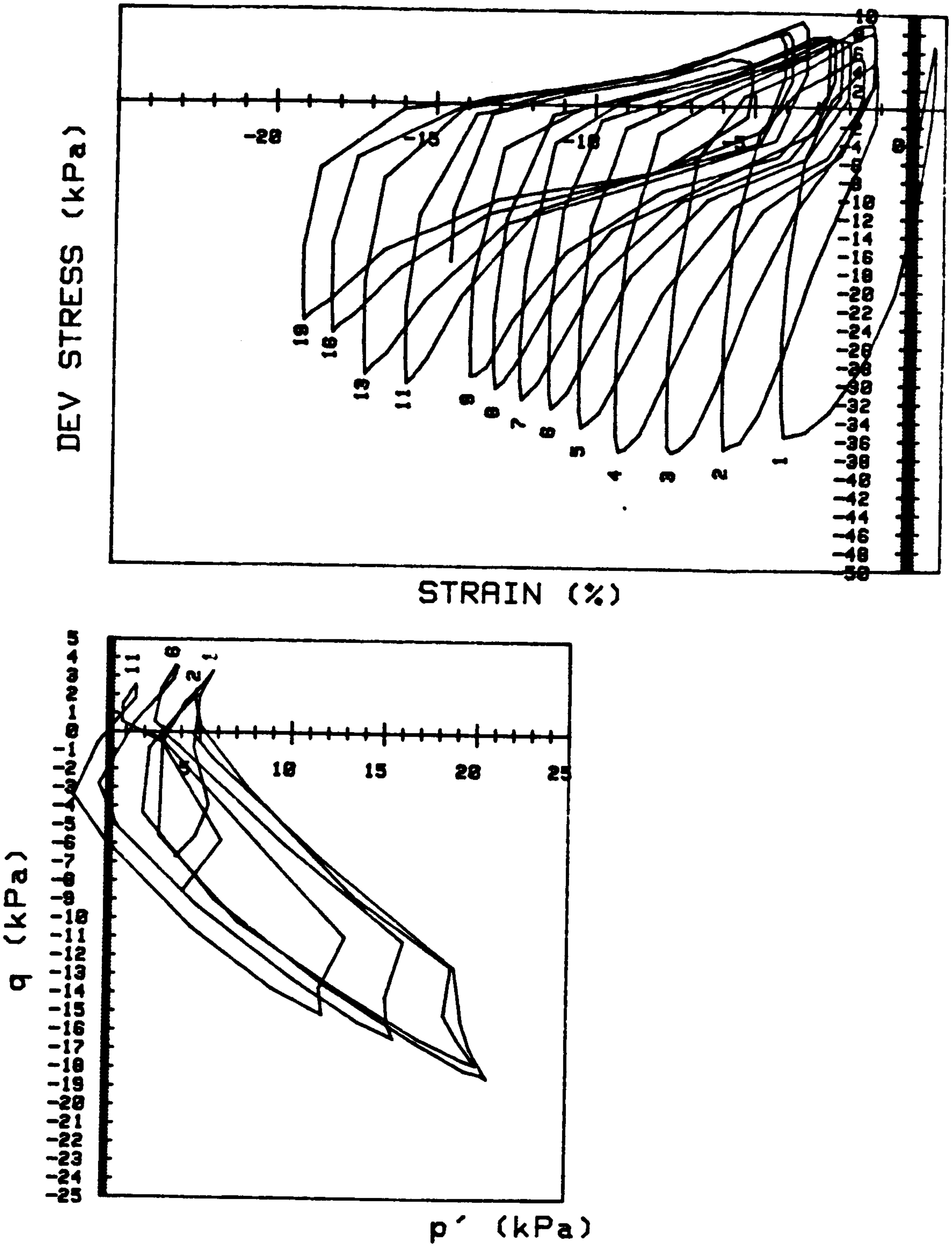

CRUISE DC2-80-EG		INCREMENT (cm)	85-95
CORE NO.	181G	TEST NO.	TC32
SIG1c′(kPa)	10.4	STATIC qf (kPa)	19.0
SIG3c′(kPa)	10.4	AVG MAX q (kPa)	3.7 (19.5%)
INDUCED OCR	3.5	AVG MIN q (kPa)	-15.0 (78.9%)

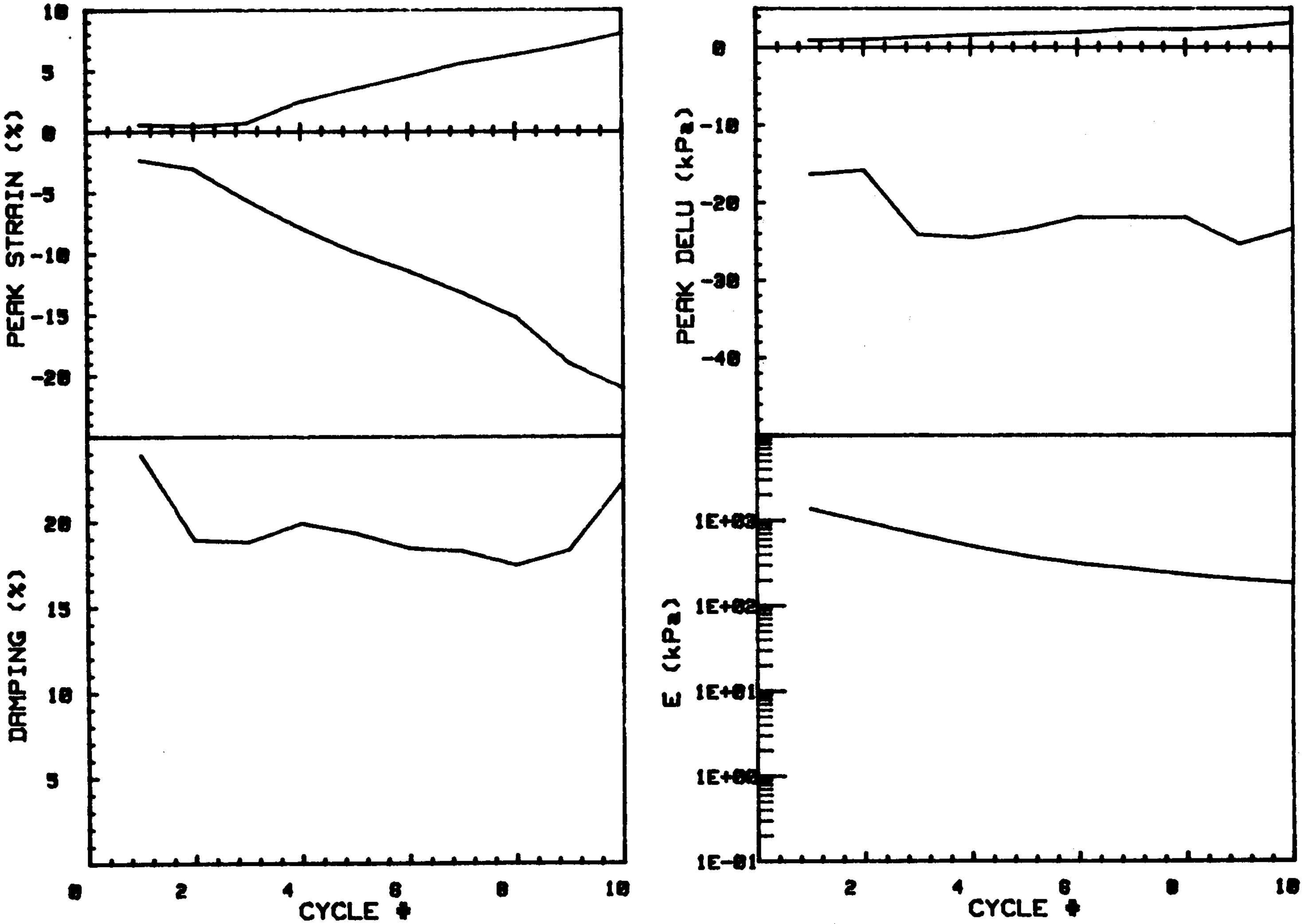

CRUISE DC2-80-EG		INCREMENT (cm)	85-95
CORE NO.	181G	TEST NO.	TC33
SIG1c'(kPa)	2.5	STATIC qf (kPa)	19.0
SIG3c'(kPa)	2.5	AVG MAX q (kPa)	7.2 (37.9%)
INDUCED OCR	14.4	AVG MIN q (kPa)	-15.9 (83.7%)

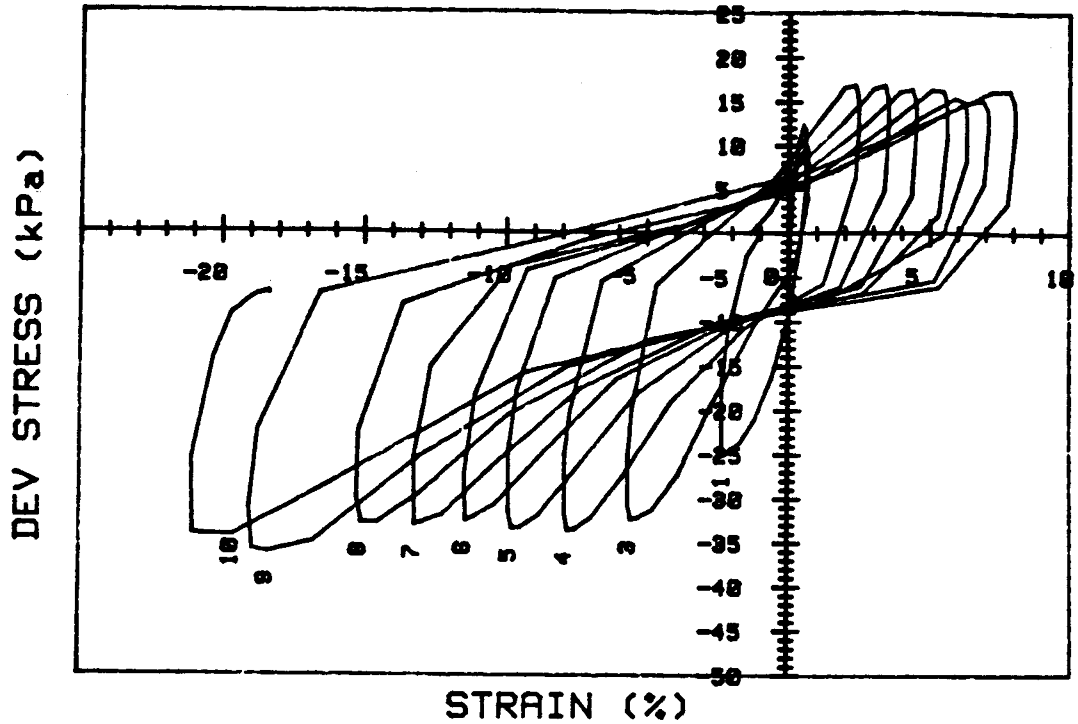

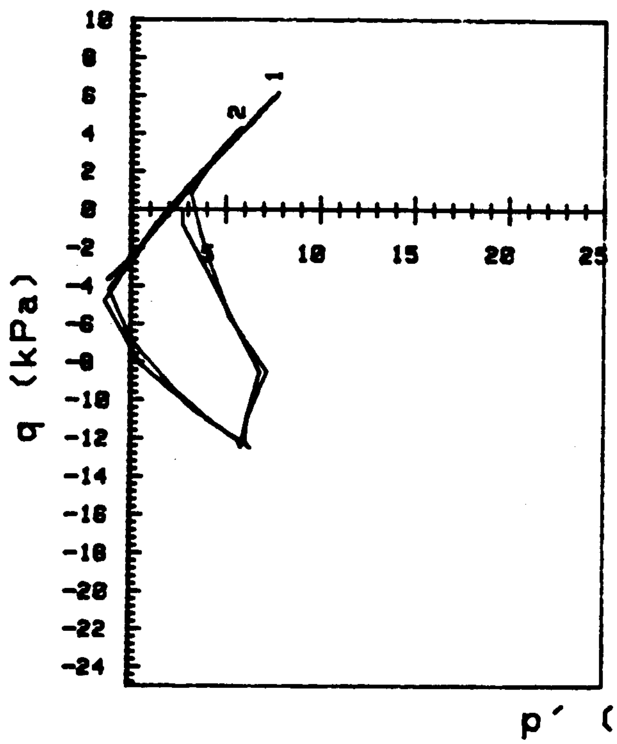

CRUISE DC2-80-EG		INCREMENT (cm)	85-95
CORE NO.	181G	TEST NO.	TC33
SIG1c′(kPa)	2.5	STATIC qf (kPa)	19.0
SIG3c′(kPa)	2.5	AVG MAX q (kPa)	7.2 (37.9%)
INDUCED OCR	14.4	AVG MIN q (kPa)	-15.9 (83.7%)

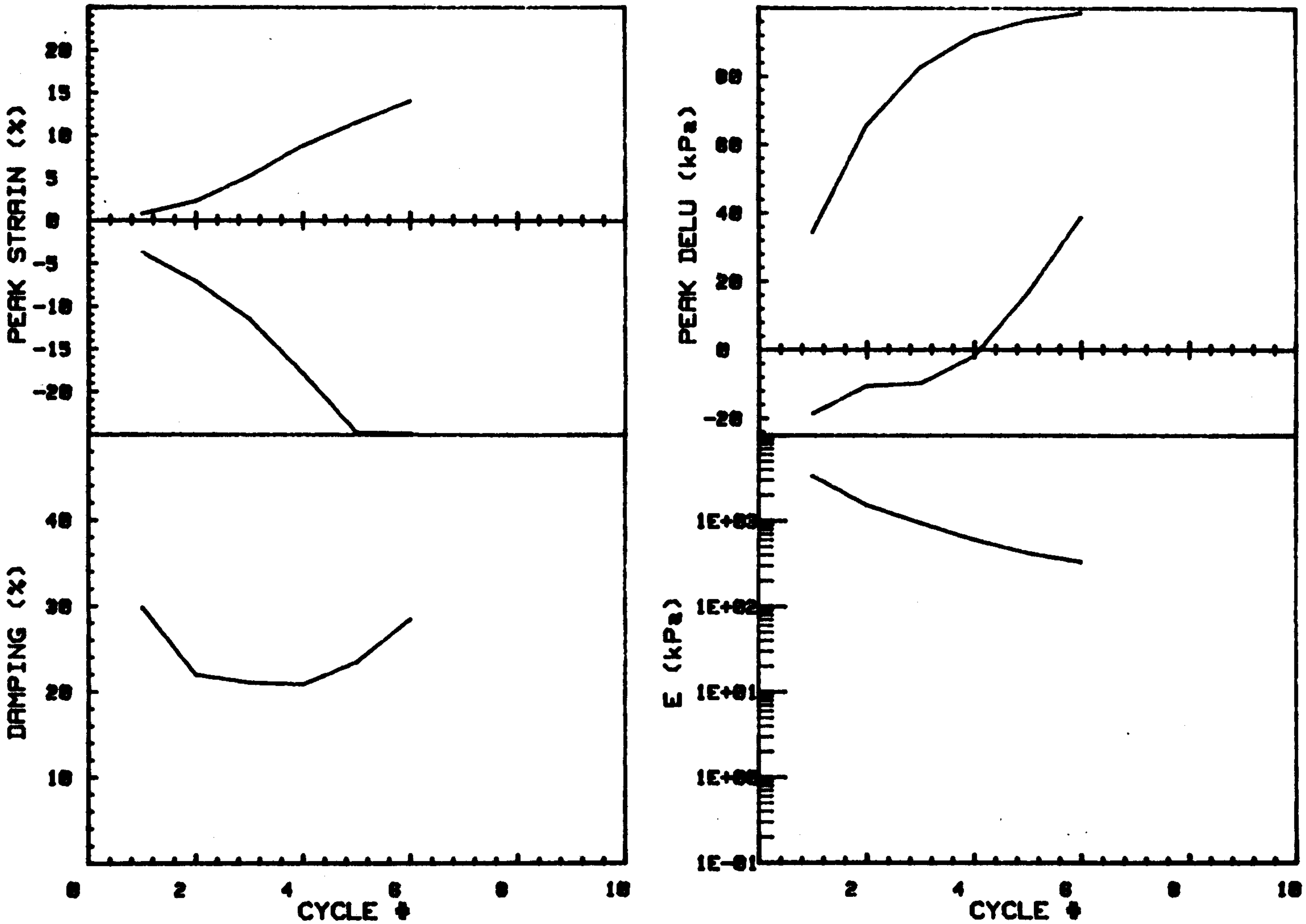

CRUISE DC1-81-EG		INCREMENT (cm)	93-104
CORE NO.	627G2	TEST NO.	TC34
SIG1c'(kPa)	100.7	STATIC qf (kPa)	53.2
SIG3c'(kPa)	100.7	AVG MAX q (kPa)	28.6 (53.8%)
INDUCED OCR	1.0	AVG MIN q (kPa)	-39.4 (74.1%)

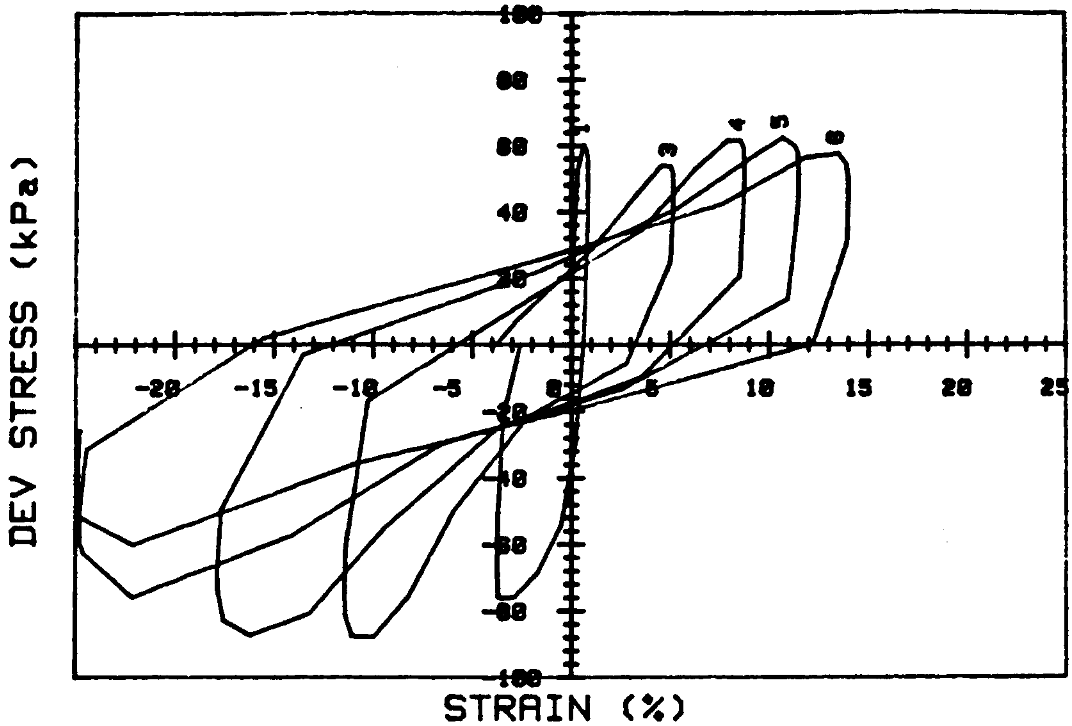

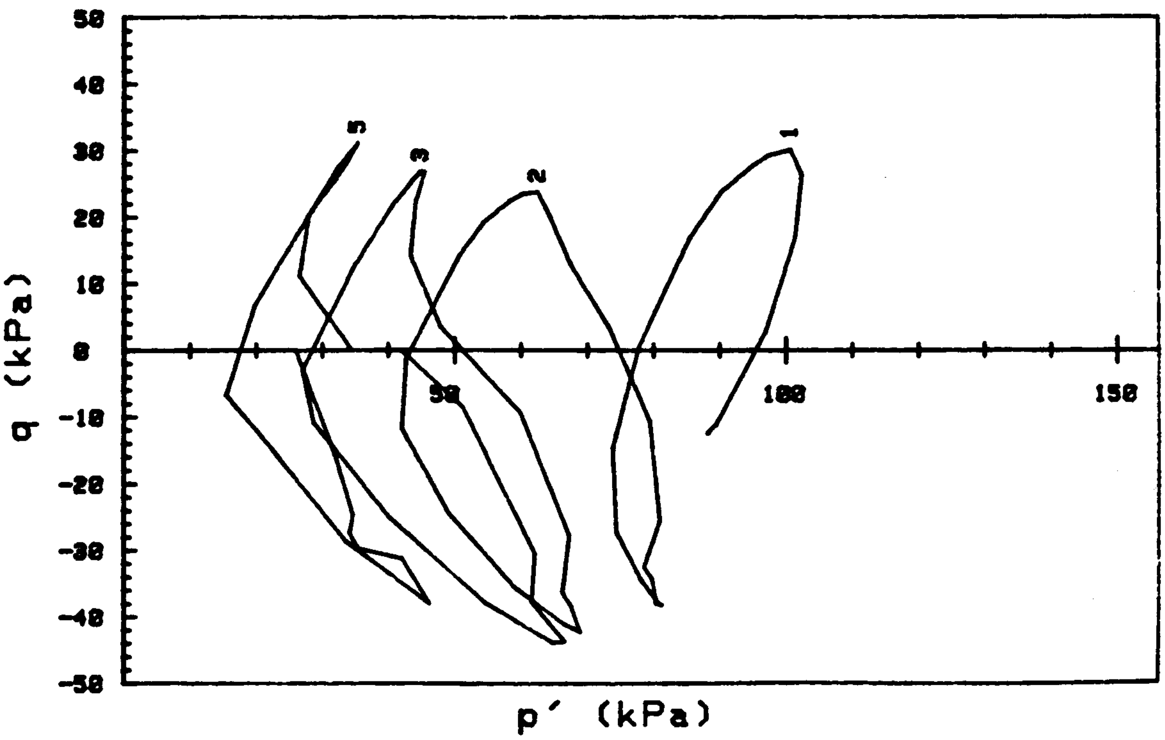

CRUISE DC1-81-EG		INCREMENT (cm)	93-104
CORE NO.	627G2	TEST NO.	TC34
SIG1c′(kPa)	100.7	STATIC qf (kPa)	53.2
SIG3c′(kPa)	100.7	AVG MAX q (kPa)	28.6 (53.8%)
INDUCED OCR	1.0	AVG MIN q (kPa)	-39.4 (74.1%)

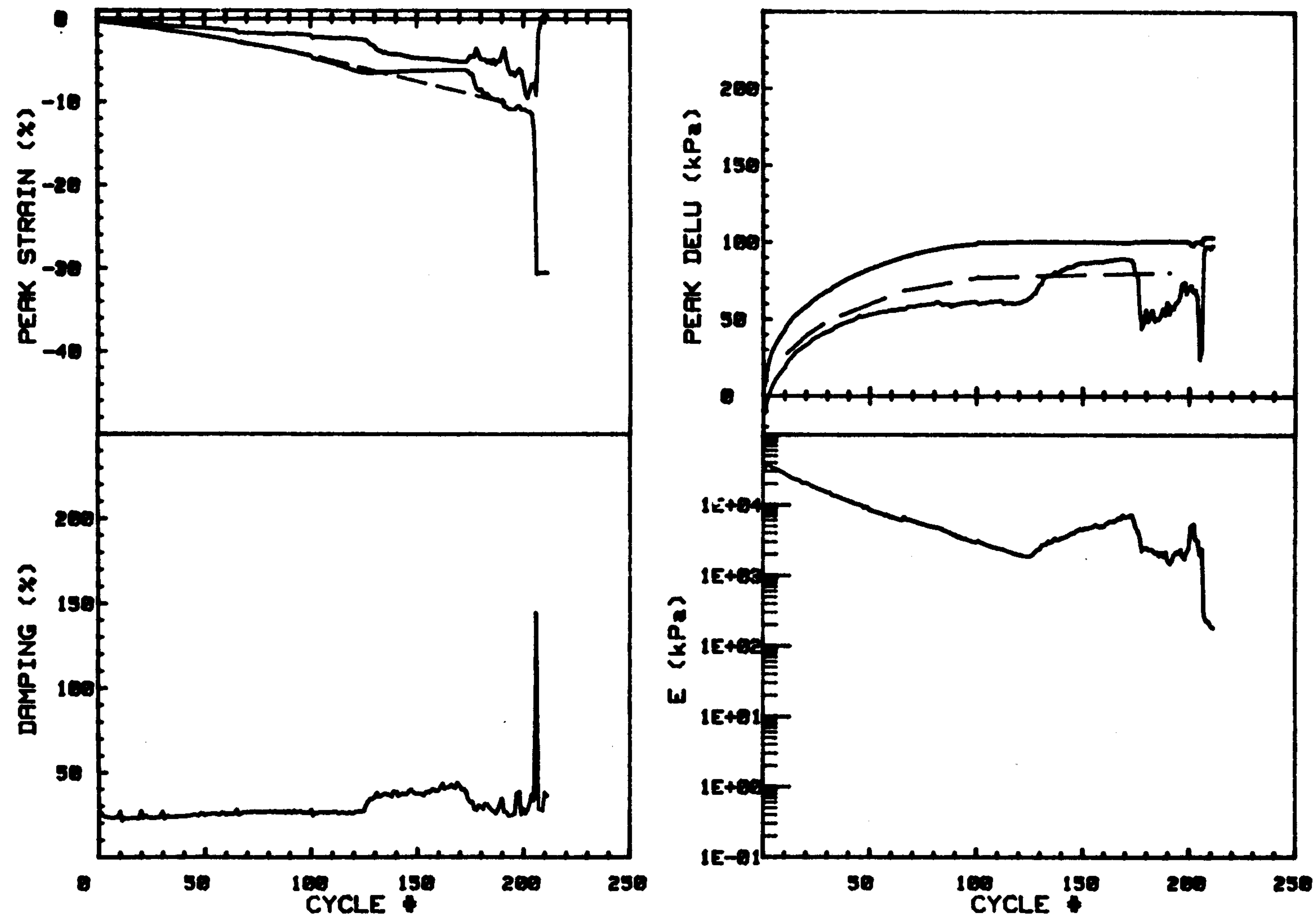

CRUISE	DC1-81-EG	INCREMENT (cm)	93-104
CORE NO.	627G2	TEST NO.	TC35
SIG1c'(kPa)	99.5	STATIC qf (kPa)	53.2
SIG3c'(kPa)	99.5	AVG MAX q (kPa)	11.9 (22.4%)
INDUCED OCR	1.0	AVG MIN q (kPa)	-26.4 (49.6%)

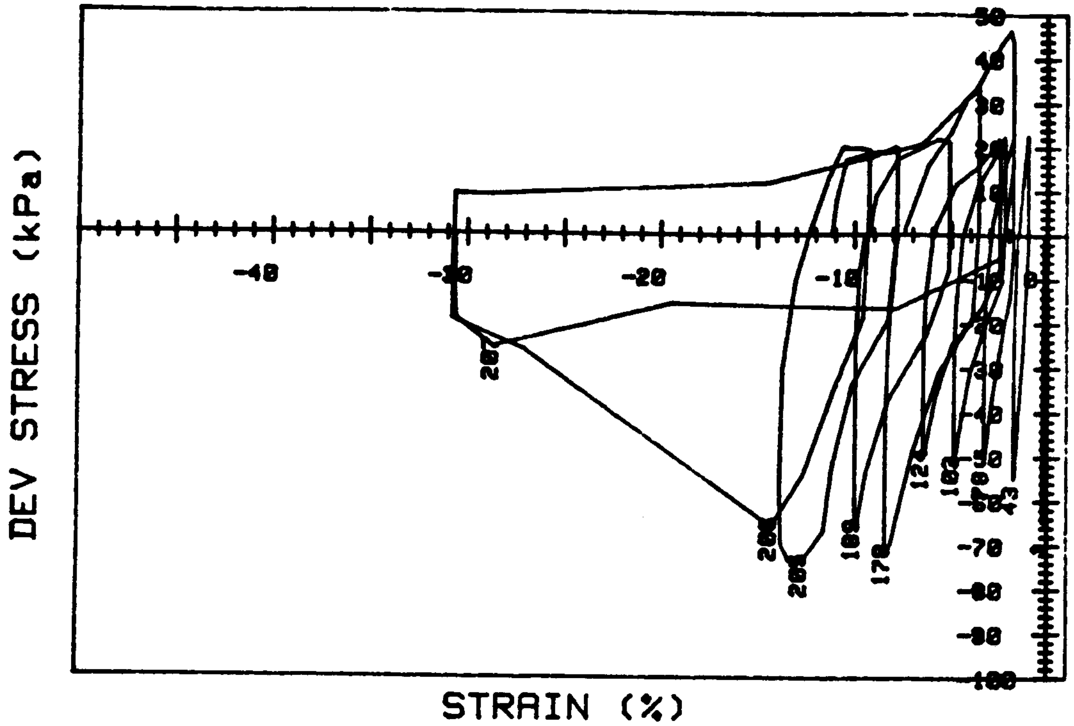

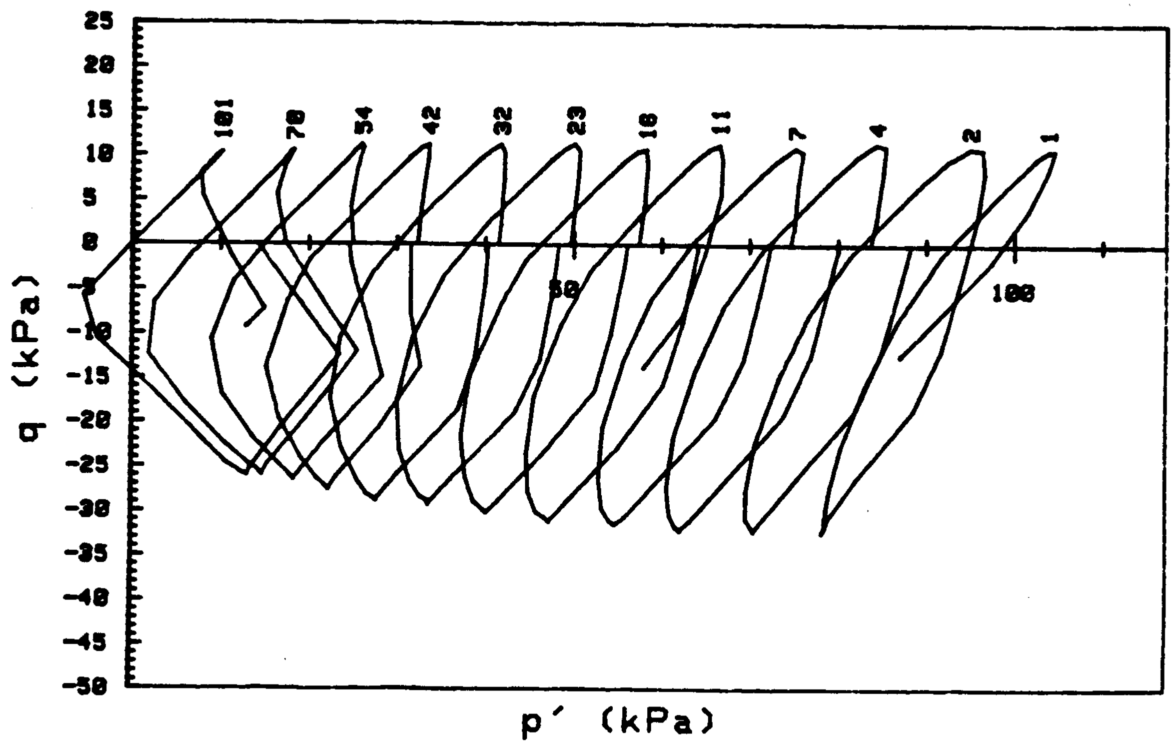

CRUISE DC1-81-EG		INCREMENT (cm)	93-104
CORE NO.	627G2	TEST NO.	TC35
SIG1c´(kPa)	99.5	STATIC qf (kPa)	53.2
SIG3c´(kPa)	99.5	AVG MAX q (kPa)	11.9 (22.4%)
INDUCED OCR	1.0	AVG MIN q (kPa)	-26.4 (49.6%)

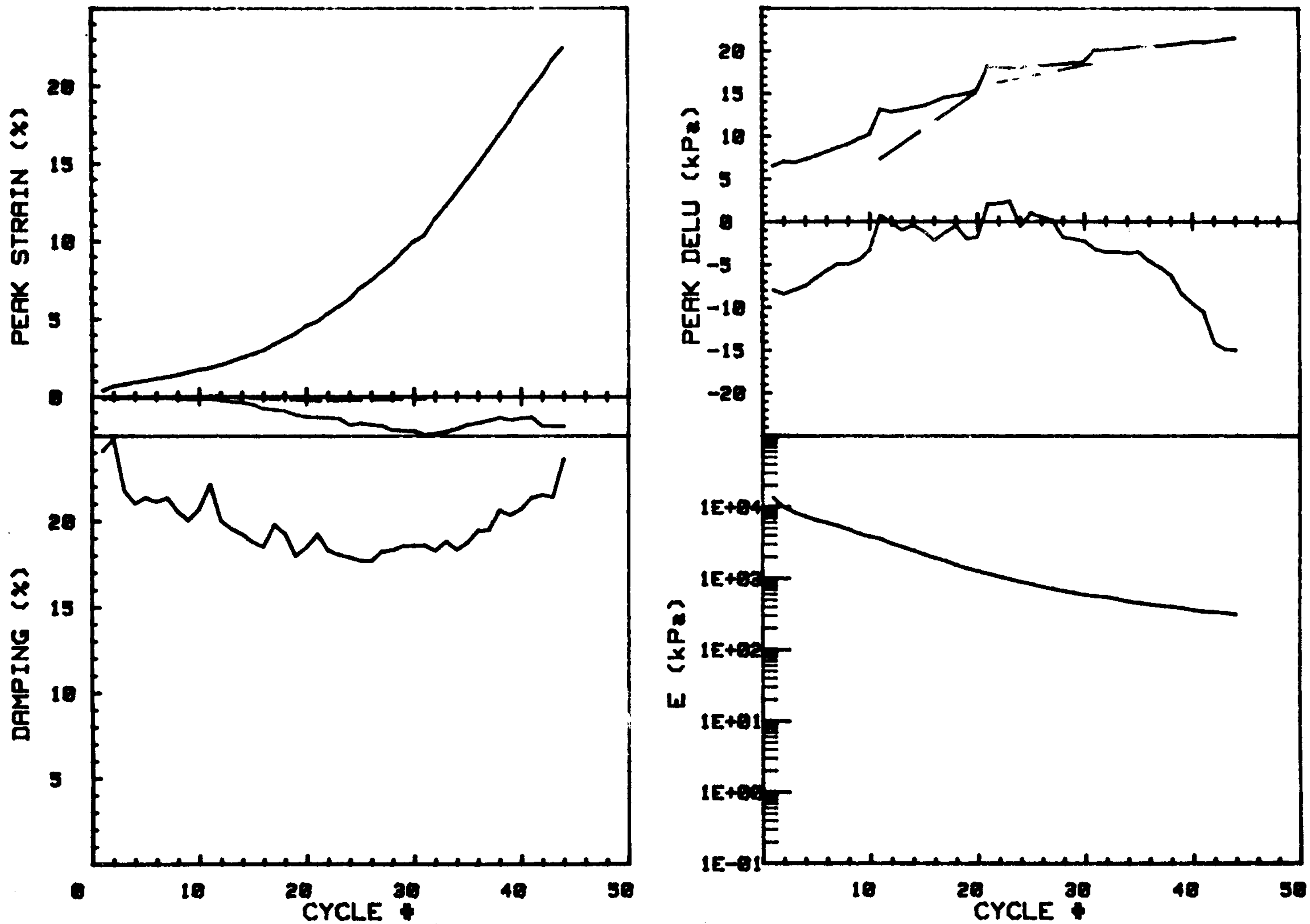

CRUISE DC1-81-EG		INCREMENT (cm)	60-71
CORE NO.	627G2	TEST NO.	TC36
SIG1c'(kPa)	18.3	STATIC qf (kPa)	44.7
SIG3c'(kPa)	18.3	AVG MAX q (kPa)	21.5 (48.1%)
INDUCED OCR	5.5	AVG MIN q (kPa)	-14.0 (31.3%)

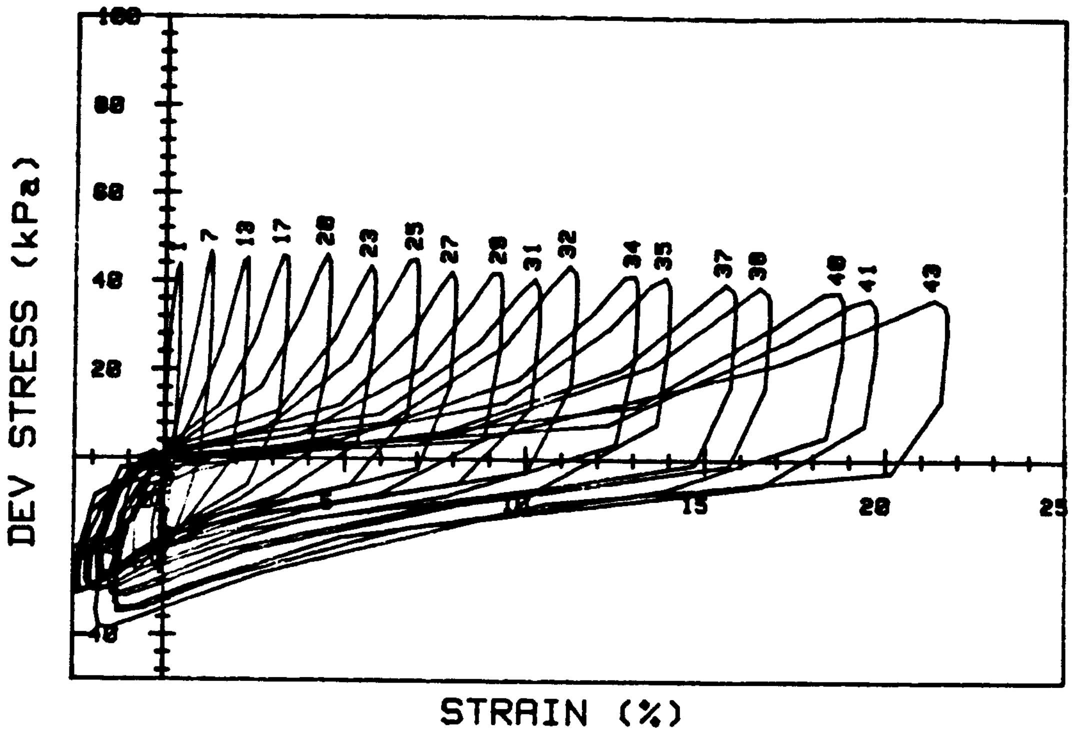

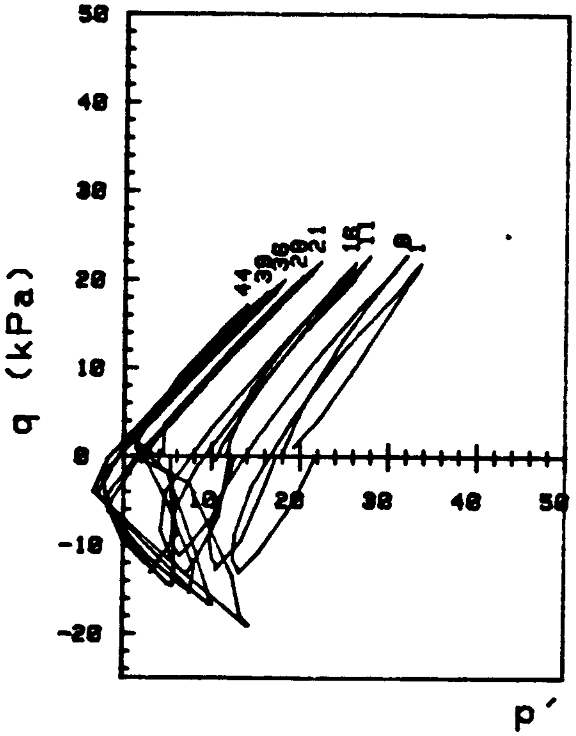

CRUISE DC1-81-EG		INCREMENT (cm)	60-71
CORE NO.	627G2	TEST NO.	TC36
SIG1c′(kPa)	18.3	STATIC qf (kPa)	44.7
SIG3c′(kPa)	18.3	AVG MAX q (kPa)	21.5 (48.1%)
INDUCED OCR	5.5	AVG MIN q (kPa)	-14.0 (31.3%)

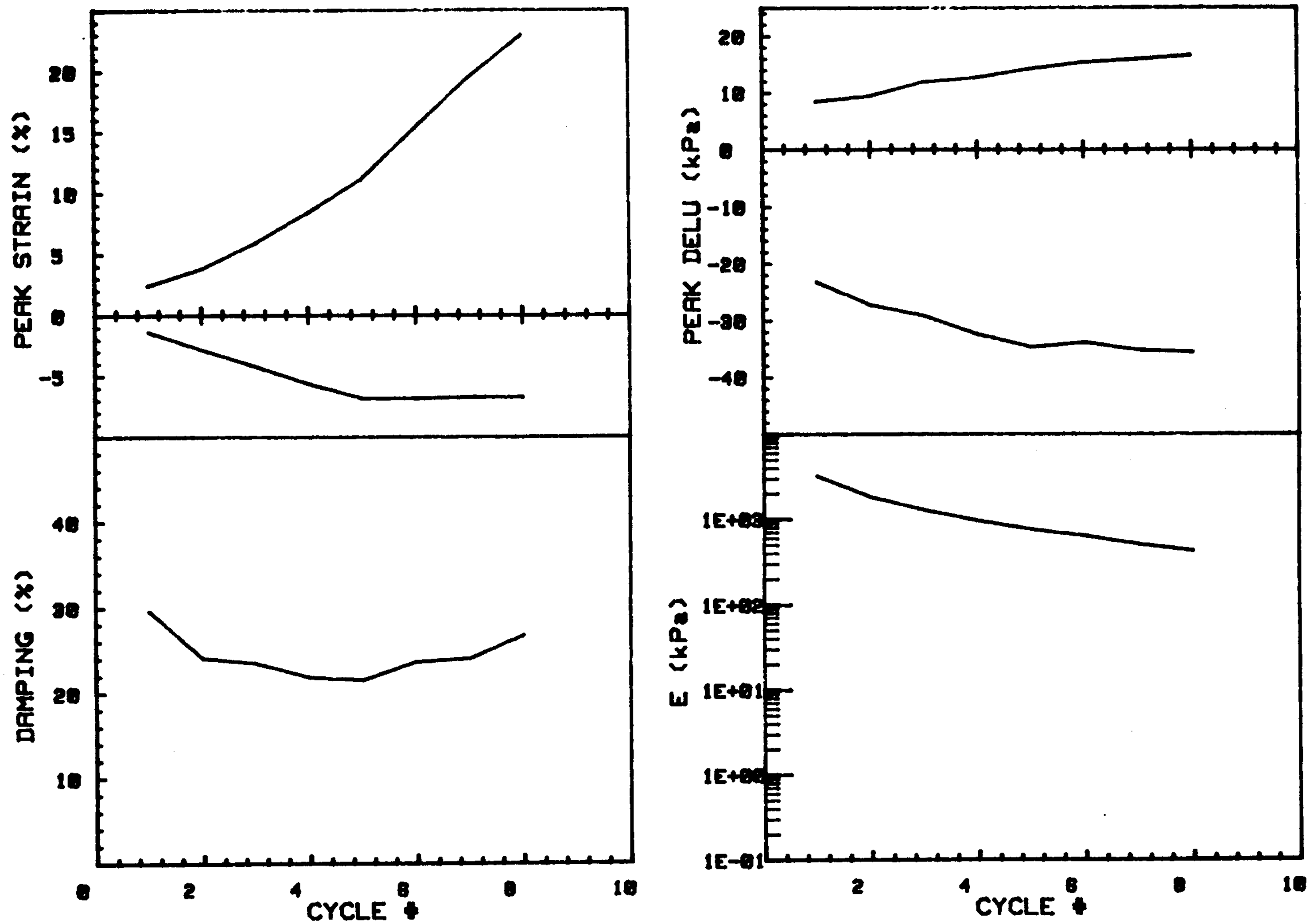

CRUISE DC1-81-EG		INCREMENT (cm)	60-71
CORE NO.	627G2	TEST NO.	TC37
SIG1c′(kPa)	17.3	STATIC qf (kPa)	44.7
SIG3c′(kPa)	17.3	AVG MAX q (kPa)	34.7 (77.6%)
INDUCED OCR	5.8	AVG MIN q (kPa)	-27.2 (60.9%)

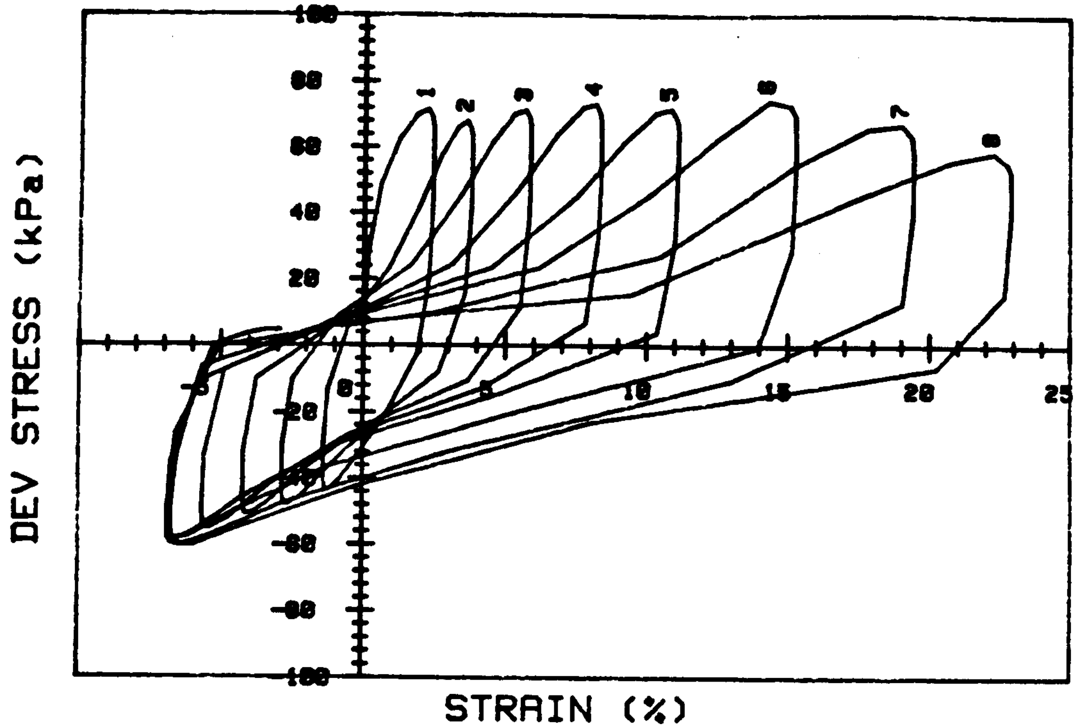

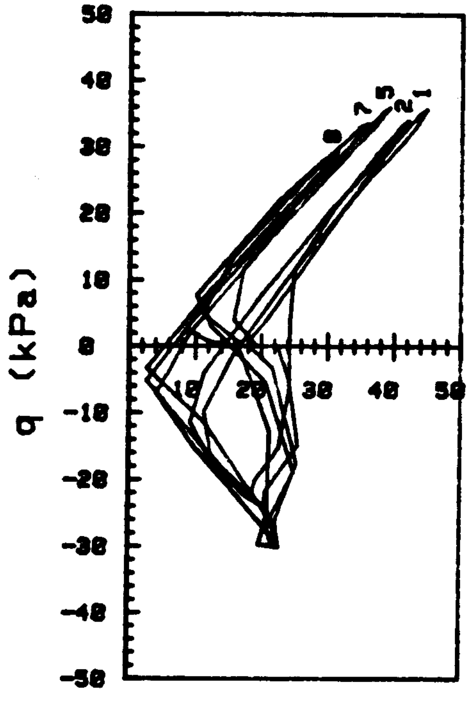

CRUISE DC1-81-EG		INCREMENT (cm)	60-71
CORE NO.	627G2	TEST NO.	TC37
SIG1c′(kPa)	17.3	STATIC qf (kPa)	44.7
SIG3c′(kPa)	17.3	AVG MAX q (kPa)	34.7 (77.6%)
INDUCED OCR	5.8	AVG MIN q (kPa)	-27.2 (60.9%)

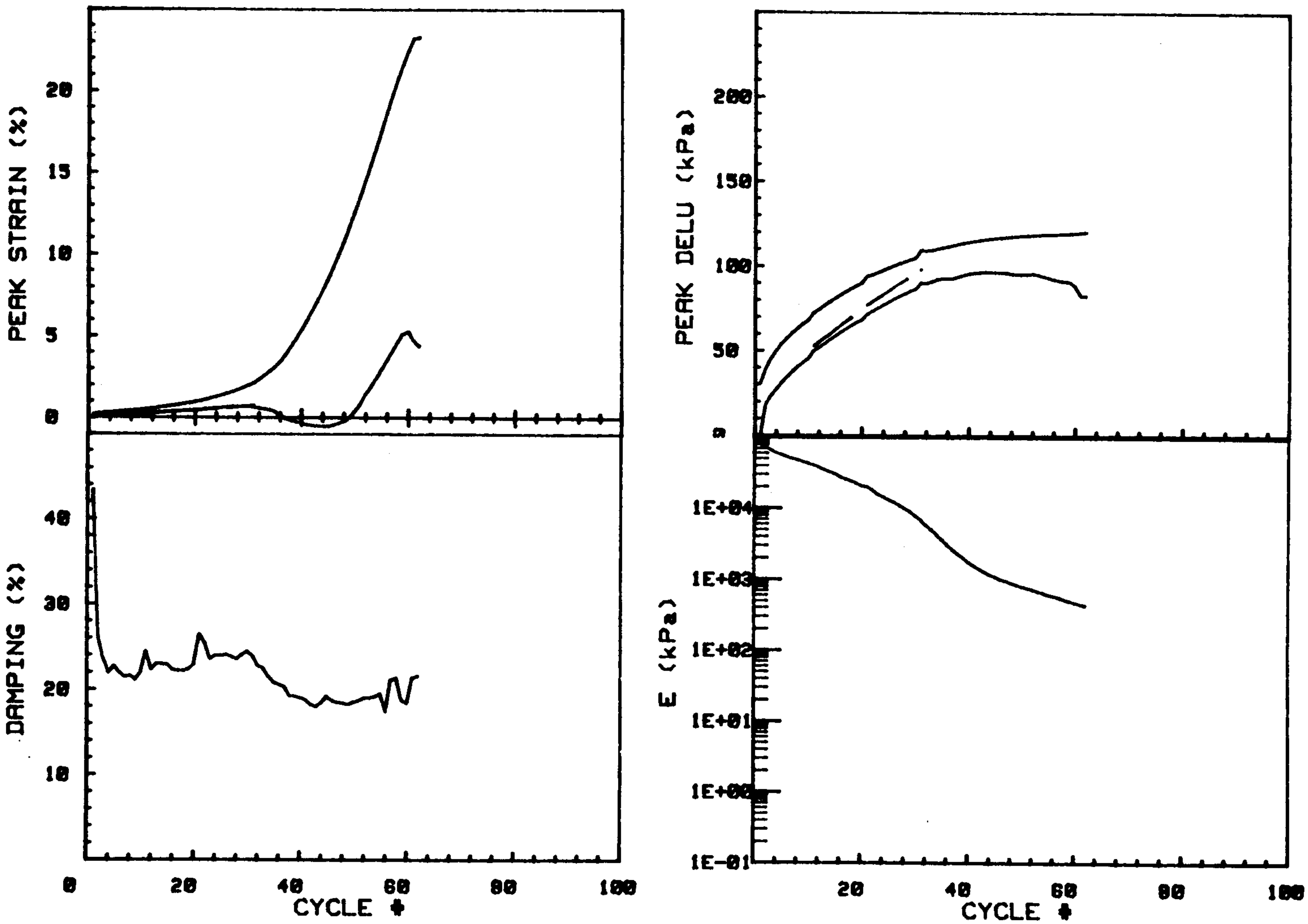

CRUISE DC1-81-EG		INCREMENT (cm)	100-108
CORE NO.	620G2	TEST NO.	TC46
SIG1c'(kPa)	121.8	STATIC qf (kPa)	53.2
SIG3c'(kPa)	121.8	AVG MAX q (kPa)	31.0 (58.3%)
INDUCED OCR	1.0	AVG MIN q (kPa)	-16.4 (30.8%)

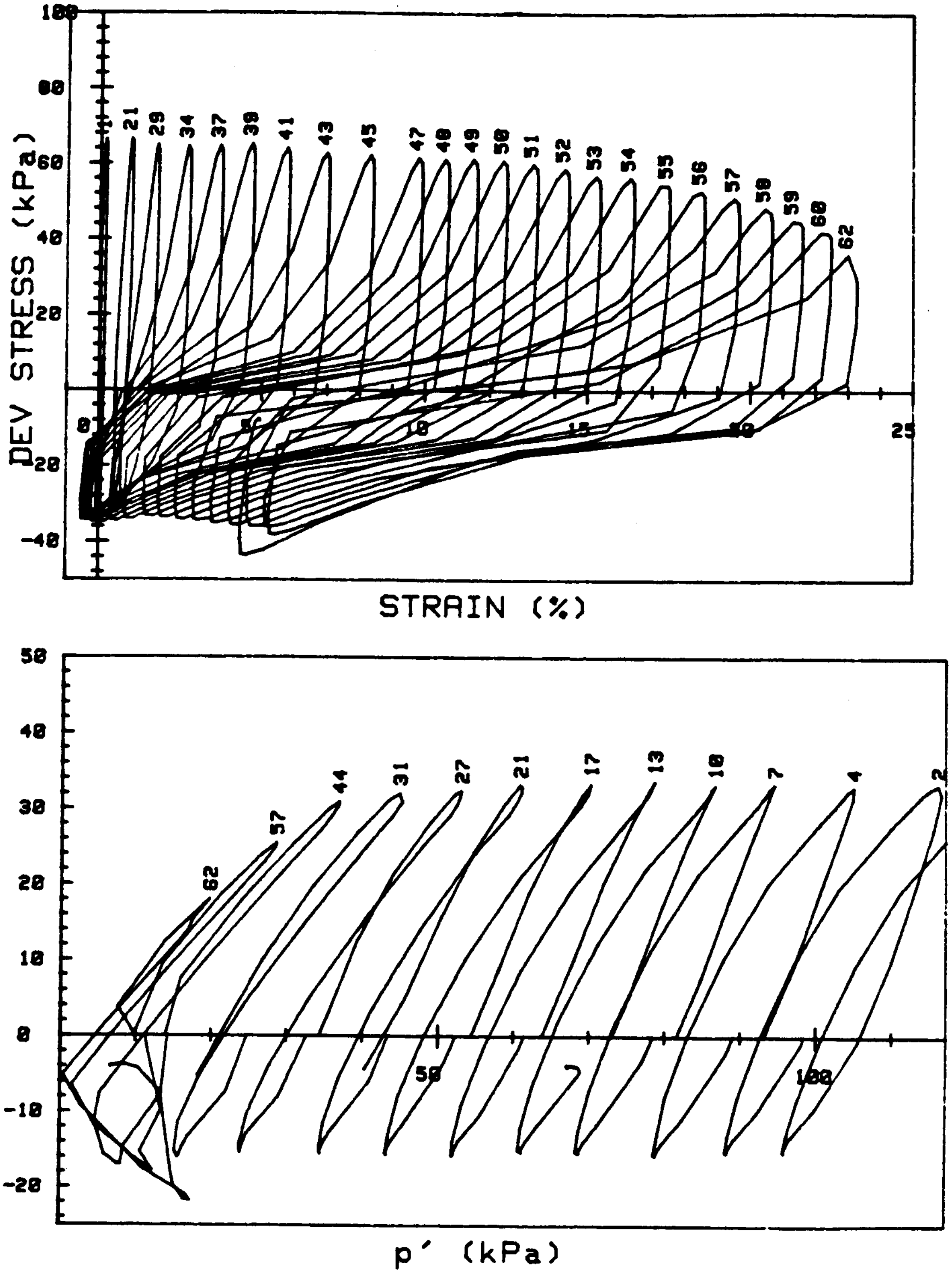

CRUISE DC1-81-EG		INCREMENT (cm)	100-108
CORE NO.	620G2	TEST NO.	TC46
SIG1c′(kPa)	121.8	STATIC qf (kPa)	53.2
SIG3c′(kPa)	121.8	AVG MAX q (kPa)	31.0 (58.3%)
INDUCED OCR	1.0	AVG MIN q (kPa)	-16.4 (30.8%)

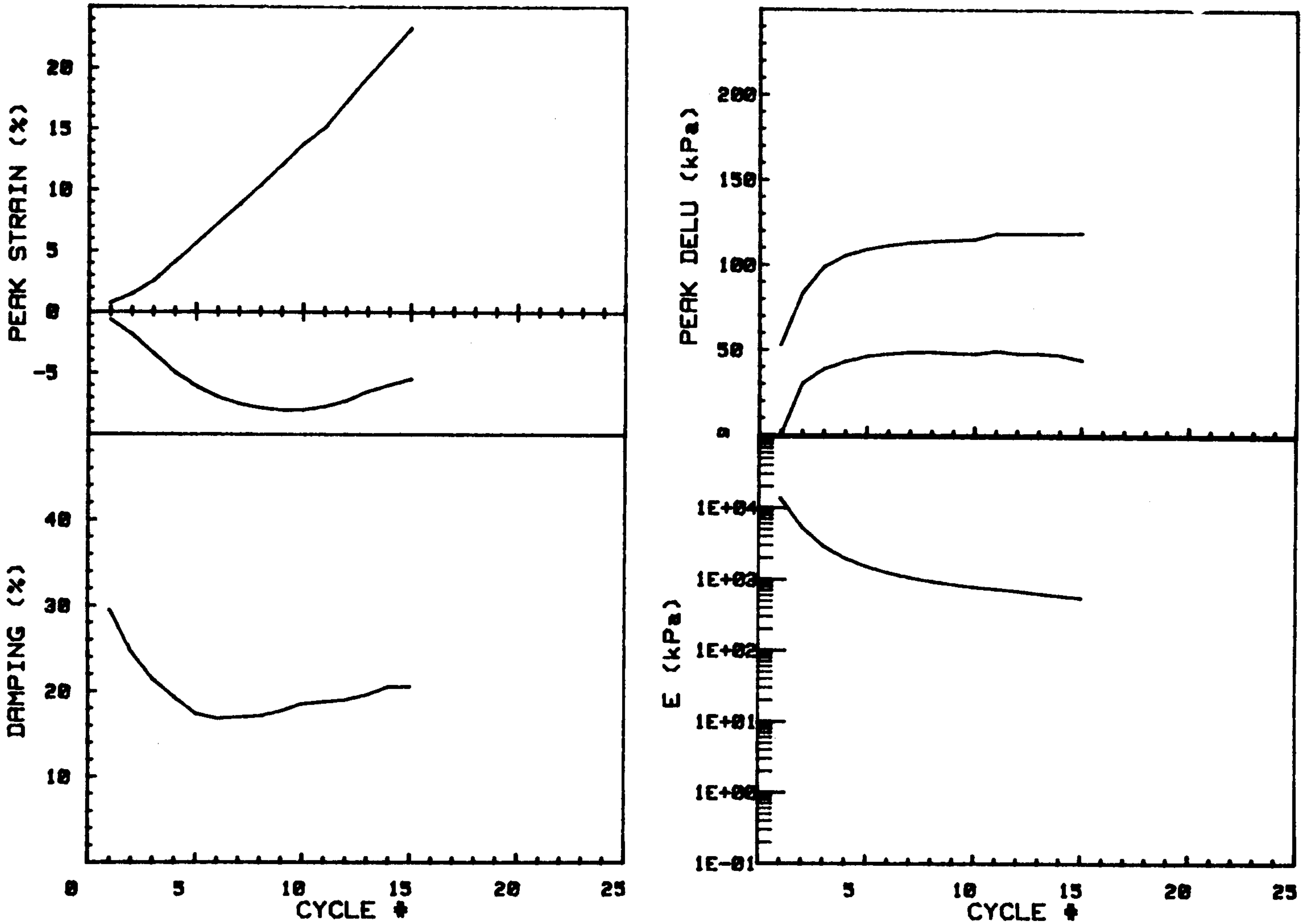

CRUISE DC1-81-EG		INCREMENT (cm)	100-108
CORE NO.	620G2	TEST NO.	TC47
SIG1c'(kPa)	117.6	STATIC qf (kPa)	53.2
SIG3c'(kPa)	117.6	AVG MAX q (kPa)	46.1 (86.7%)
INDUCED OCR	1.0	AVG MIN q (kPa)	-36.4 (68.4%)

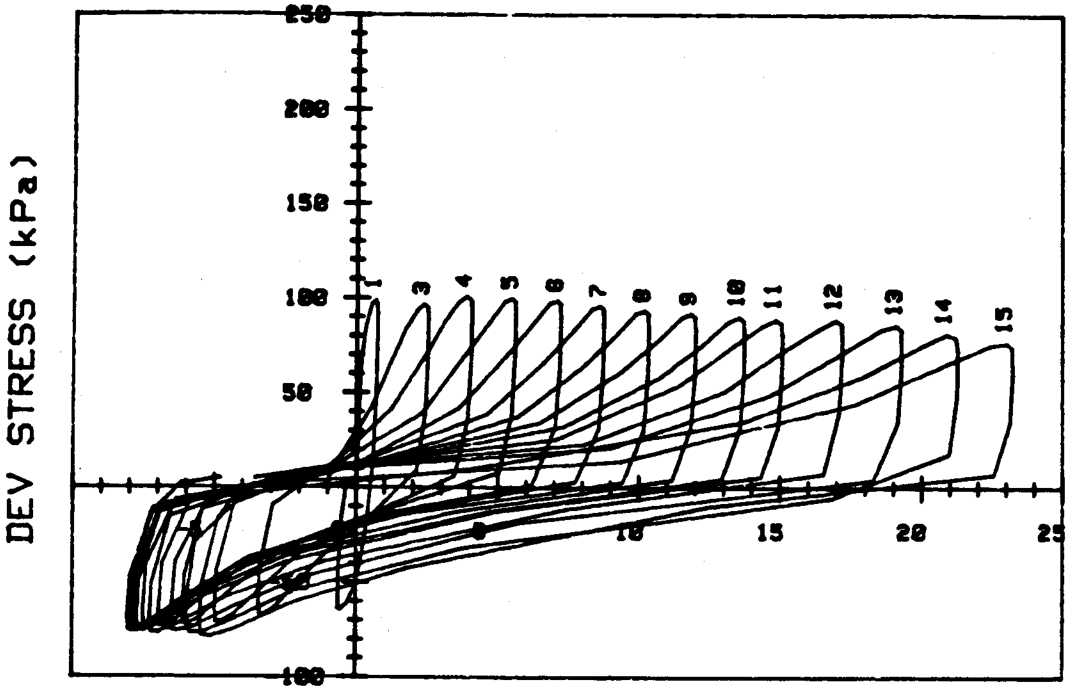

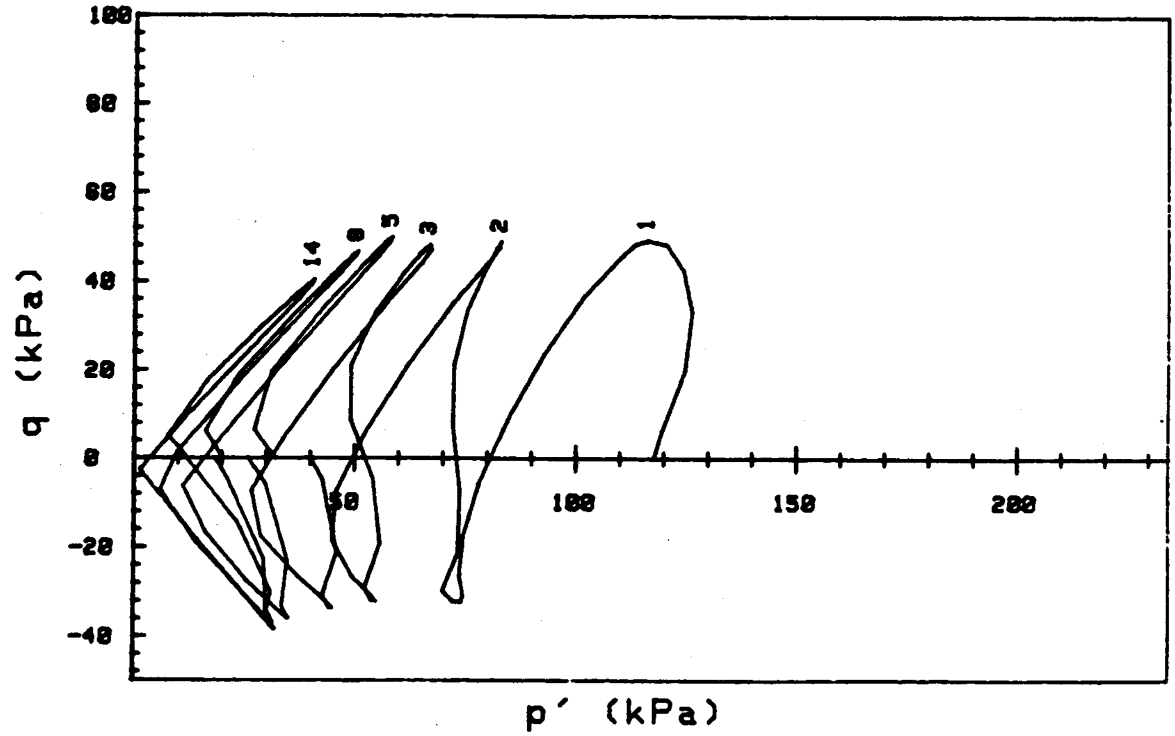

CRUISE DC1-81-EG		INCREMENT (cm)	100-108
CORE NO.	620G2	TEST NO.	TC47
SIG1c′(kPa)	117.6	STATIC qf (kPa)	53.2
SIG3c′(kPa)	117.6	AVG MAX q (kPa)	46.1 (86.7%)
INDUCED OCR	1.0	AVG MIN q (kPa)	-36.4 (68.4%)

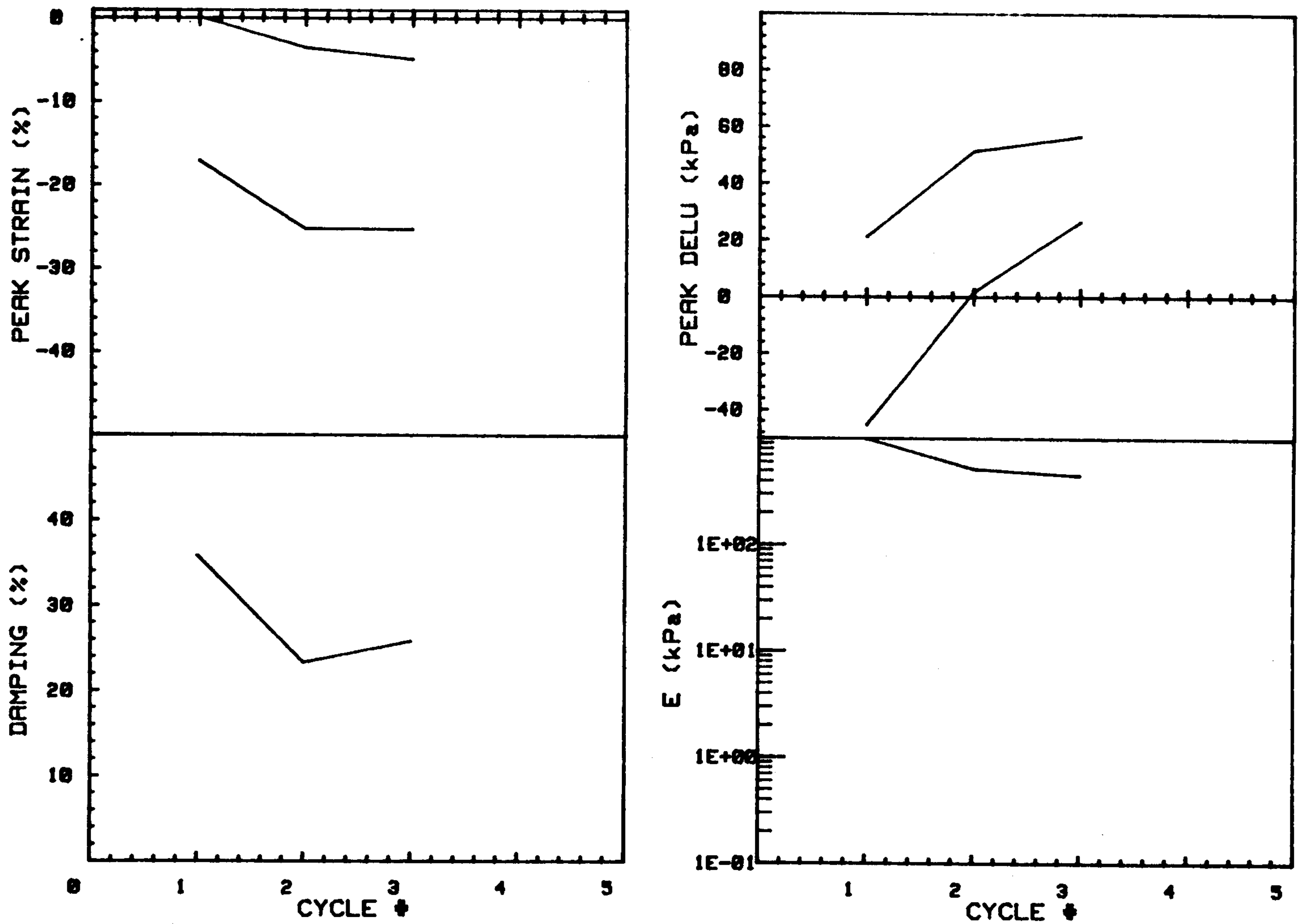

CRUISE	DC1-81-EG	INCREMENT (cm)	61-69
CORE NO.	634G2	TEST NO.	TC48
SIG1c'(kPa)	60.3	STATIC qf (kPa)	23.9
SIG3c'(kPa)	60.3	AVG MAX q (kPa)	14.9 (62.3%)
INDUCED OCR	1.0	AVG MIN q (kPa)	-40.6 (169.9%)

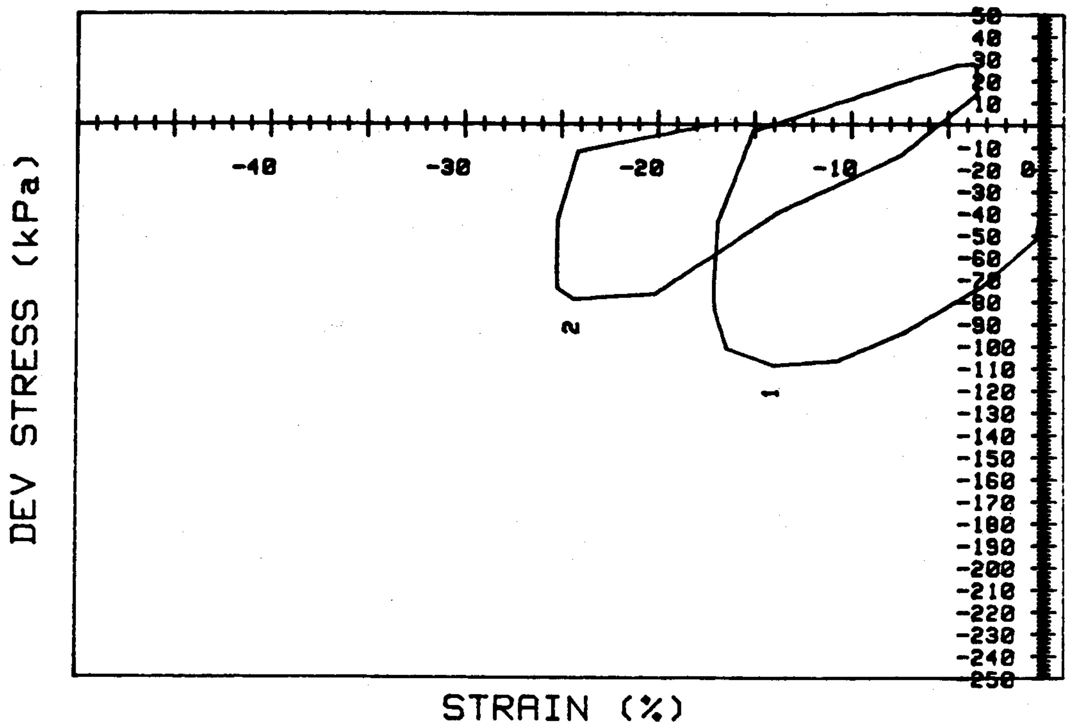

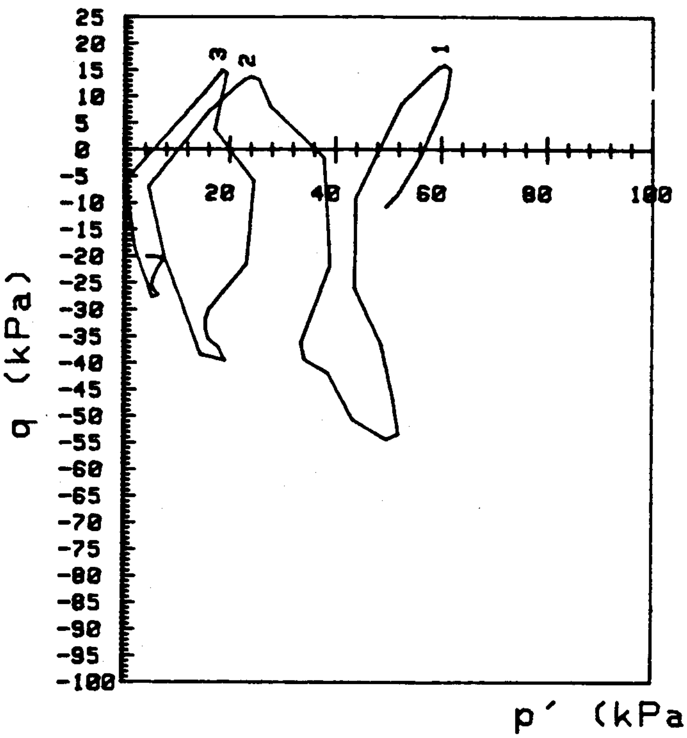

CRUISE DC1-81-EG		INCREMENT (cm)	61-69
CORE NO.	634G2	TEST NO.	TC48
SIG1c′(kPa)	60.3	STATIC qf (kPa)	23.9
SIG3c′(kPa)	60.3	AVG MAX q (kPa)	14.9 (62.3%)
INDUCED OCR	1.0	AVG MIN q (kPa)	-40.6 (169.9%)

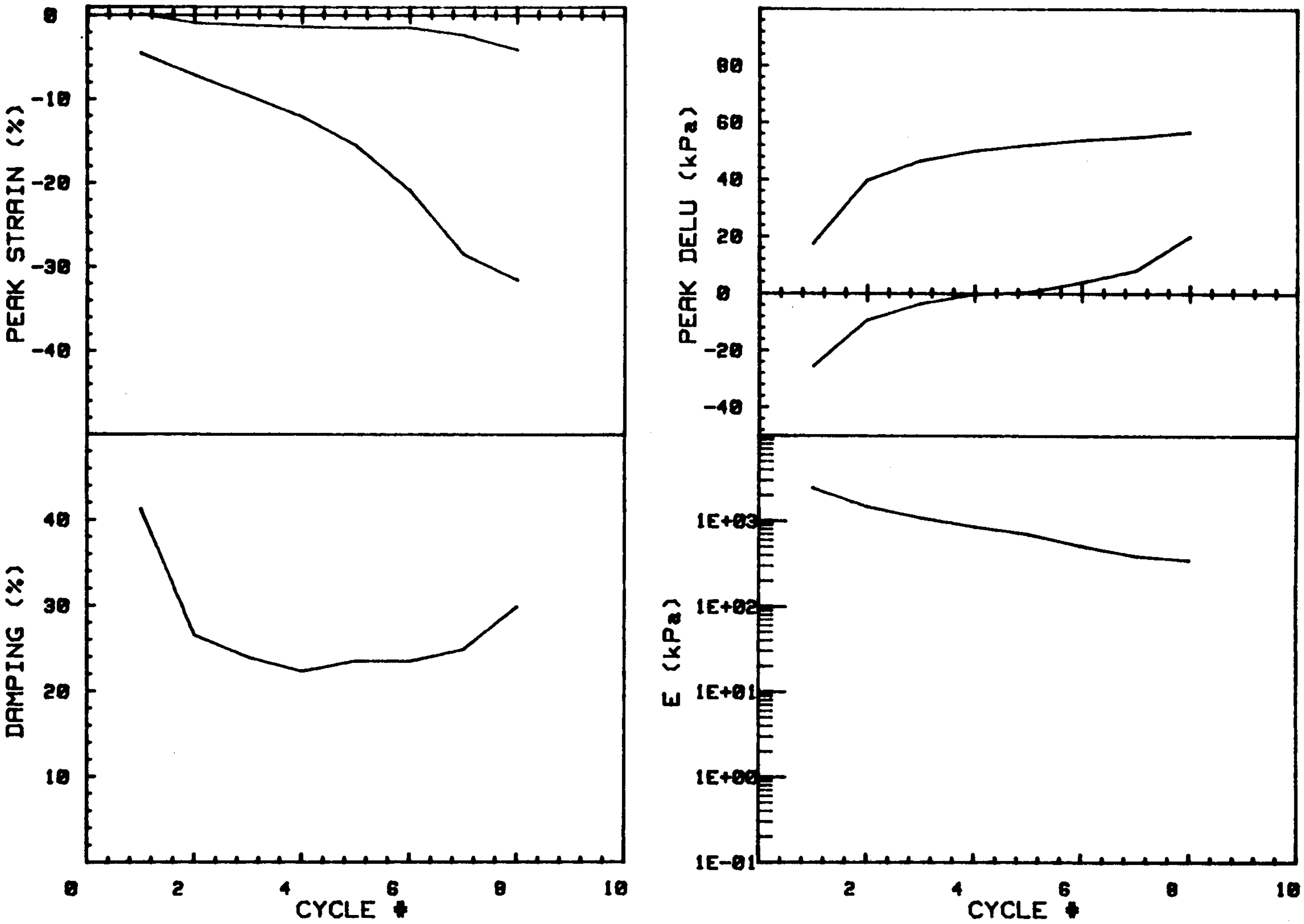

CRUISE DC1-81-EG		INCREMENT (cm)	61-68
CORE NO.	634G2	TEST NO.	TC49
SIG1c'(kPa)	58.1	STATIC qf (kPa)	23.9
SIG3c'(kPa)	58.1	AVG MAX q (kPa)	12.7 (53.1%)
INDUCED OCR	1.0	AVG MIN q (kPa)	-31.8 (133.1%)

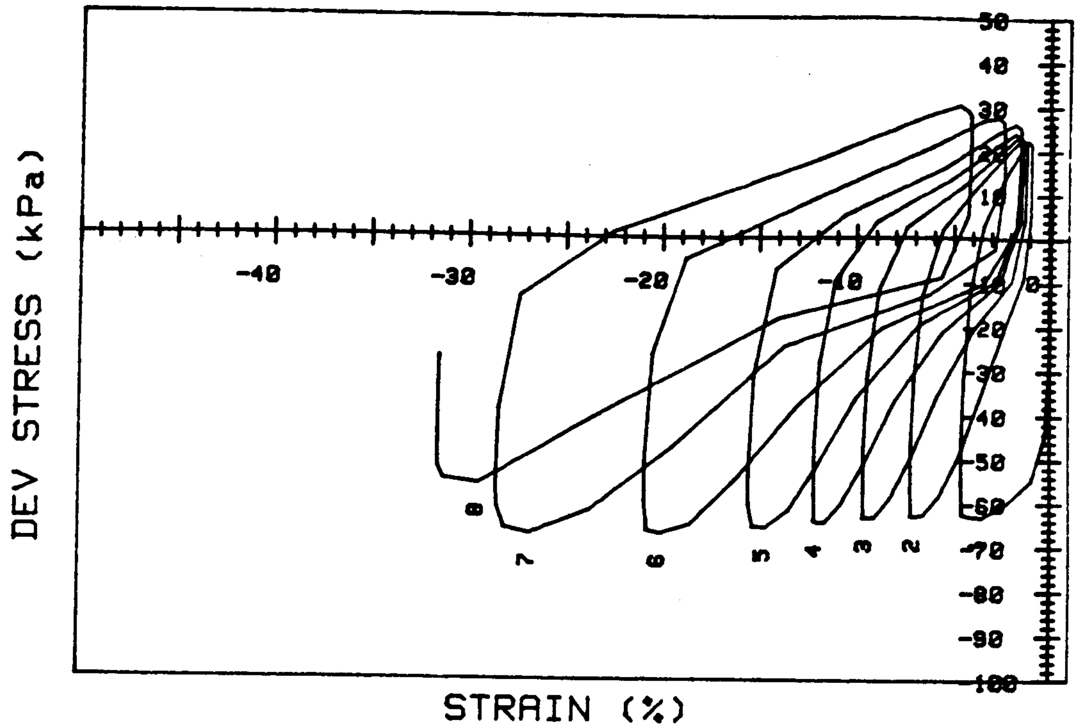

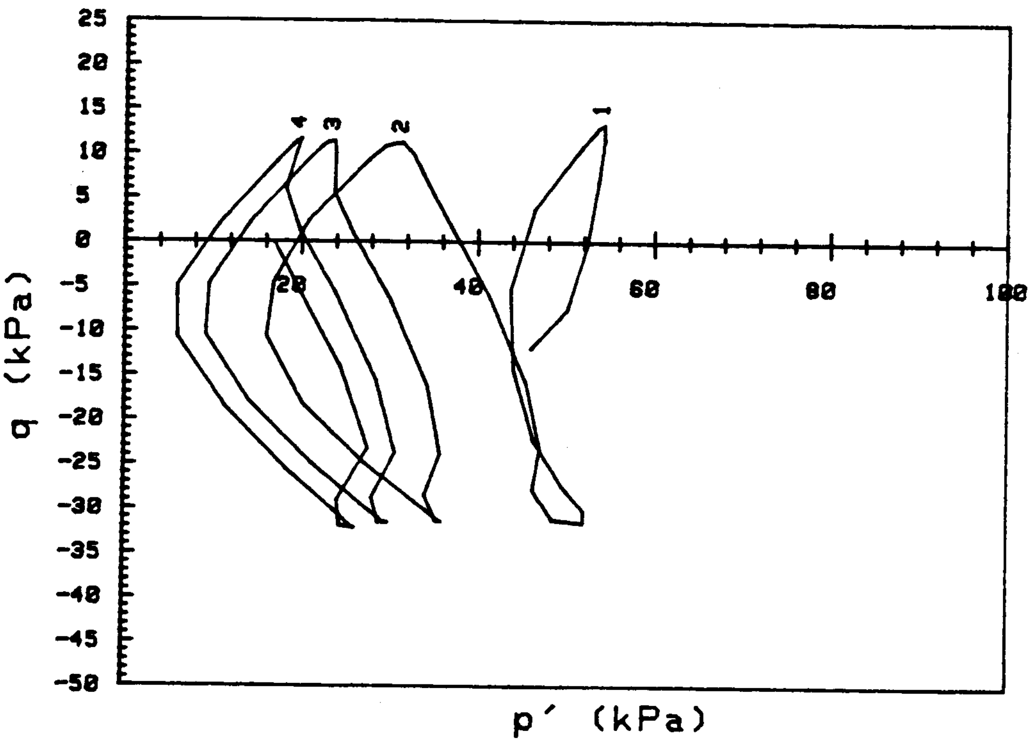

CRUISE DC1-81-EG		INCREMENT (cm)	61-68
CORE NO.	634G2	TEST NO.	TC49
SIG1c′(kPa)	58.1	STATIC qf (kPa)	23.9
SIG3c′(kPa)	58.1	AVG MAX q (kPa)	12.7 (53.1%)
INDUCED OCR	1.0	AVG MIN q (kPa)	-31.8 (133.1%)

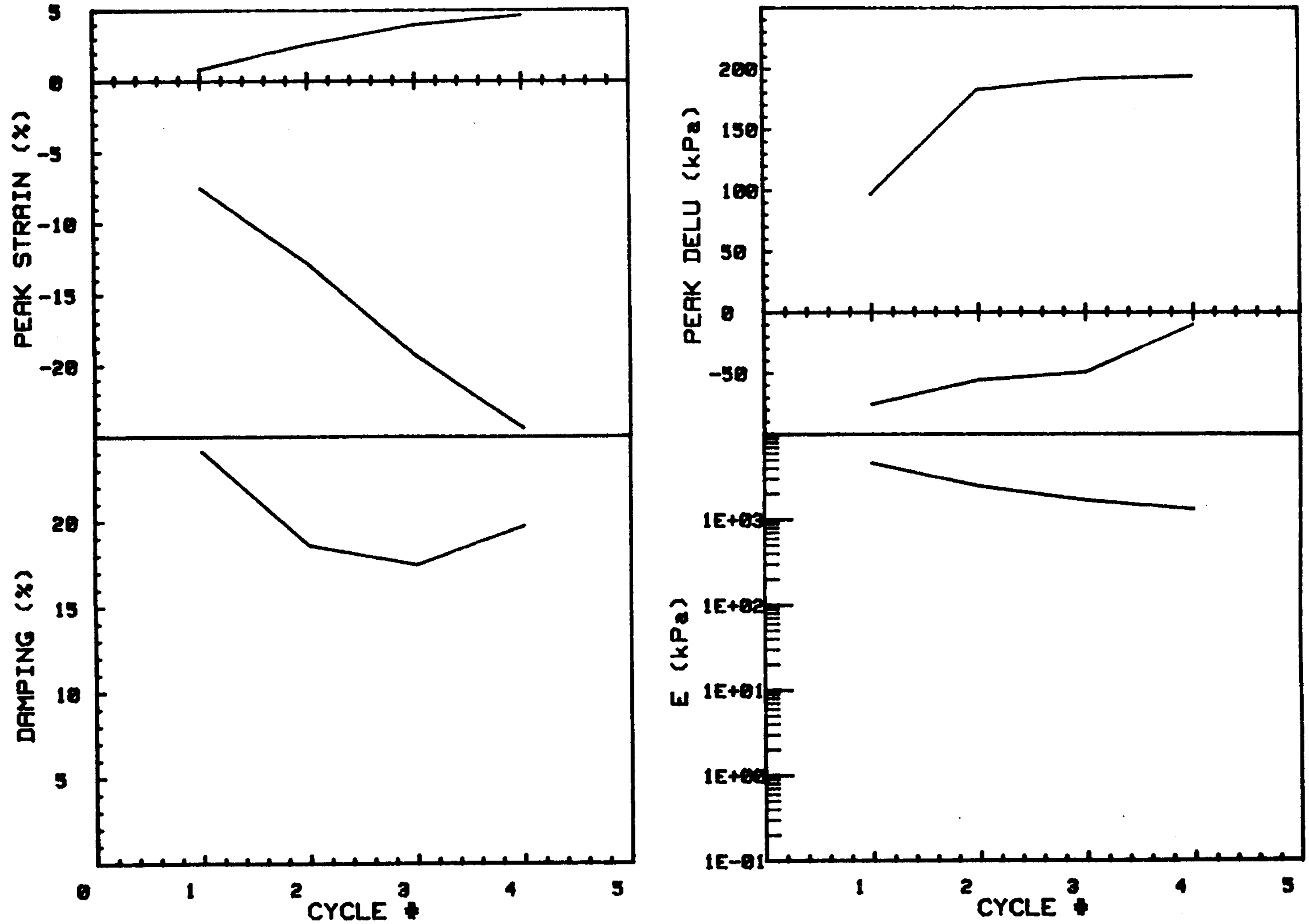

CRUISE DC2-80-EG		INCREMENT (cm)	161-172
CORE NO.	87G	TEST NO.	TC52
SIG1c'(kPa)	200.9	STATIC qf (kPa)	122.8
SIG3c'(kPa)	200.9	AVG MAX q (kPa)	76.8 (62.5%)
INDUCED OCR	1.0	AVG MIN q (kPa)	-106.3 (86.6%)

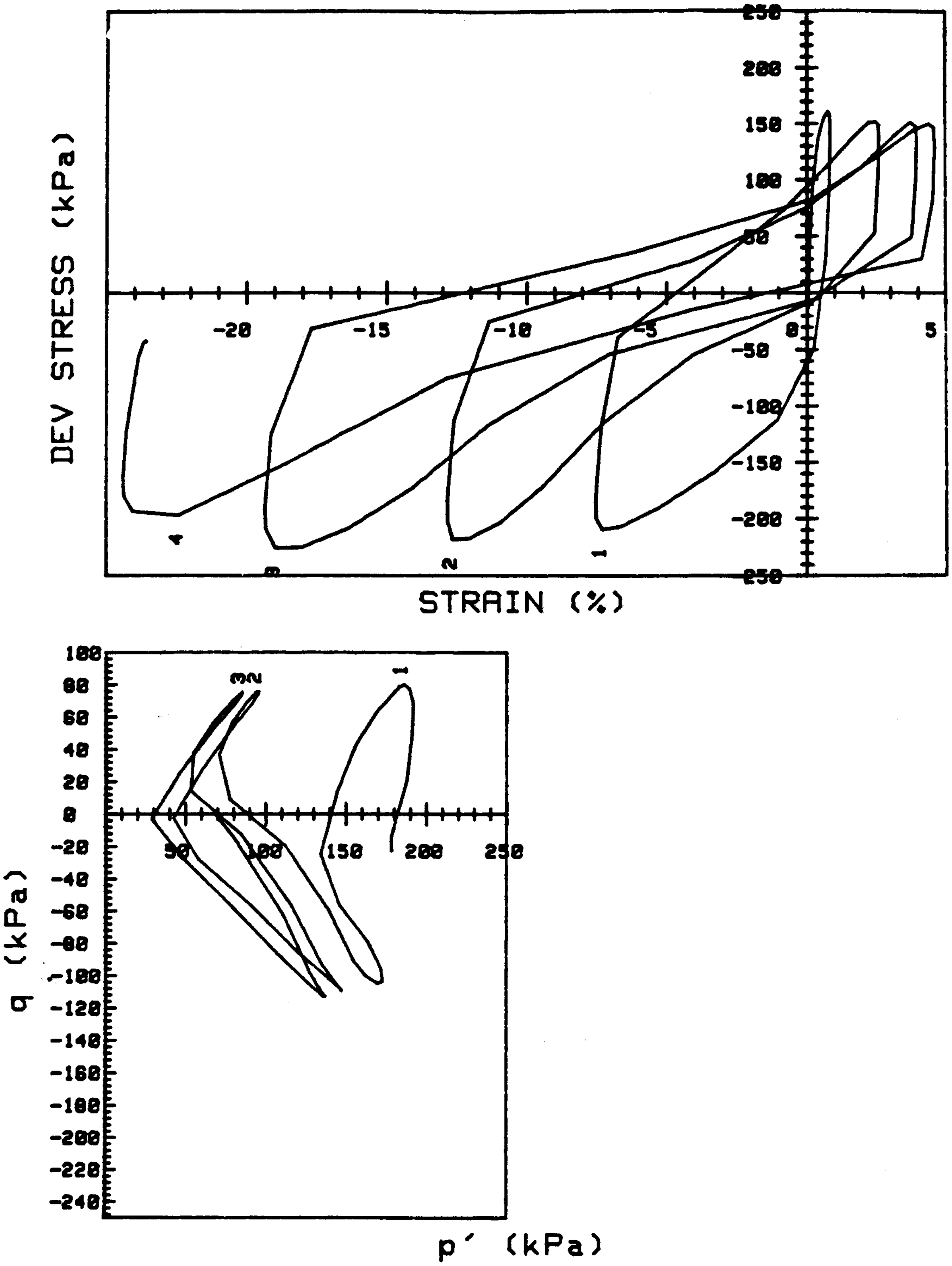

CRUISE DC2-80-EG		INCREMENT (cm)	161-172
CORE NO.	87G	TEST NO.	TC52
SIG1c′(kPa)	200.9	STATIC qf (kPa)	122.8
SIG3c′(kPa)	200.9	AVG MAX q (kPa)	76.8 (62.5%)
INDUCED OCR	1.0	AVG MIN q (kPa)	-106.3 (86.6%)

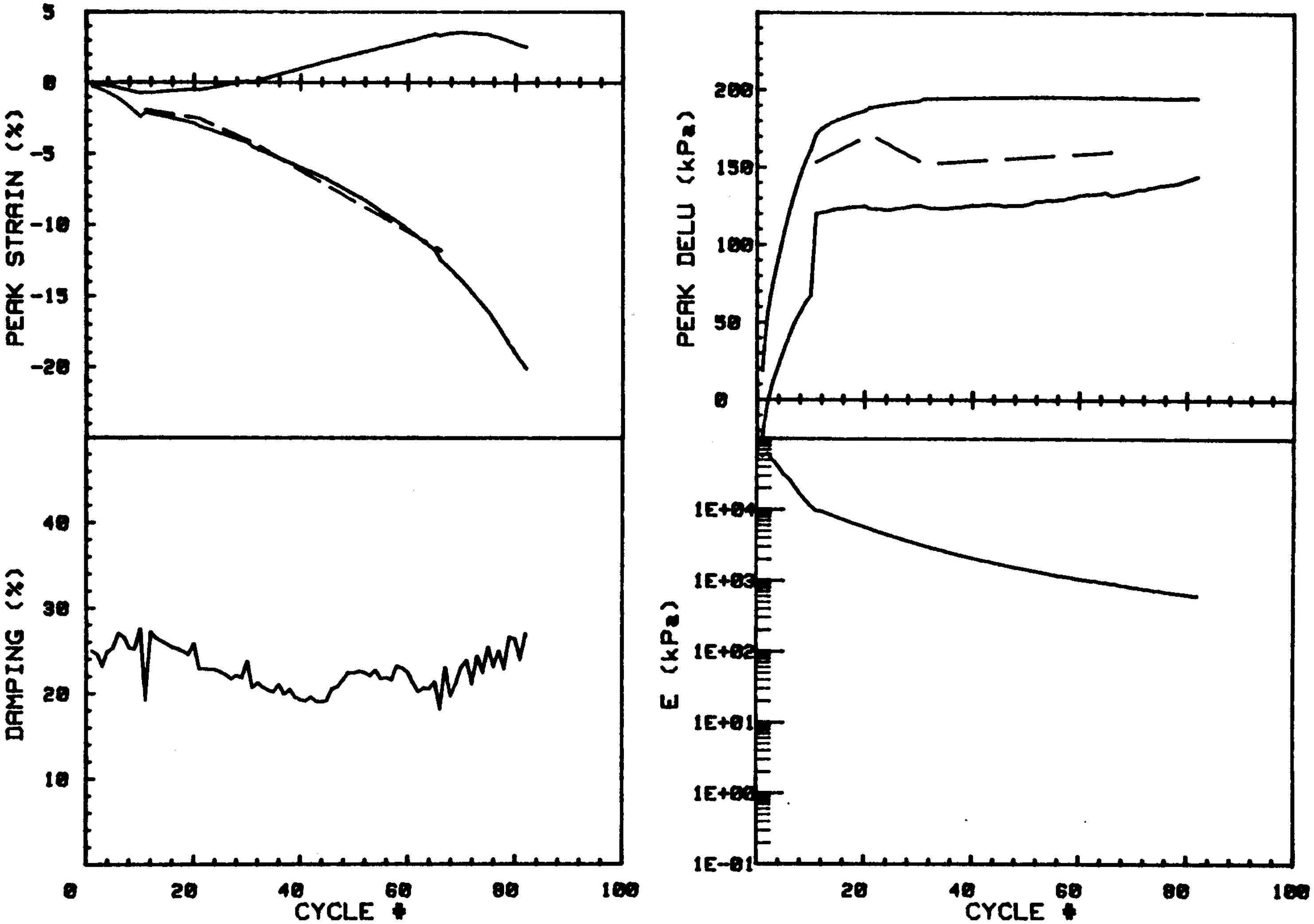

CRUISE DC2-80-EG		INCREMENT (cm)	161-172
CORE NO.	87G	TEST NO.	TC53
SIG1c′(kPa)	194.3	STATIC qf (kPa)	122.8
SIG3c′(kPa)	194.3	AVG MAX q (kPa)	26.4 (21.5%)
INDUCED OCR	1.0	AVG MIN q (kPa)	-45.5 (37.1%)

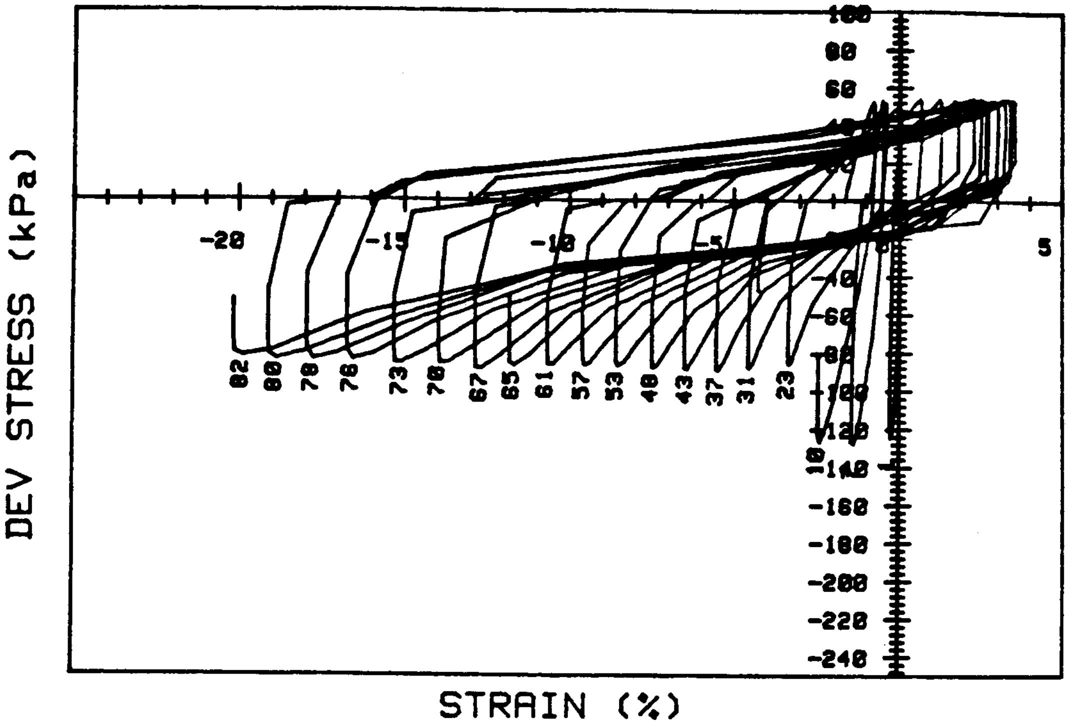

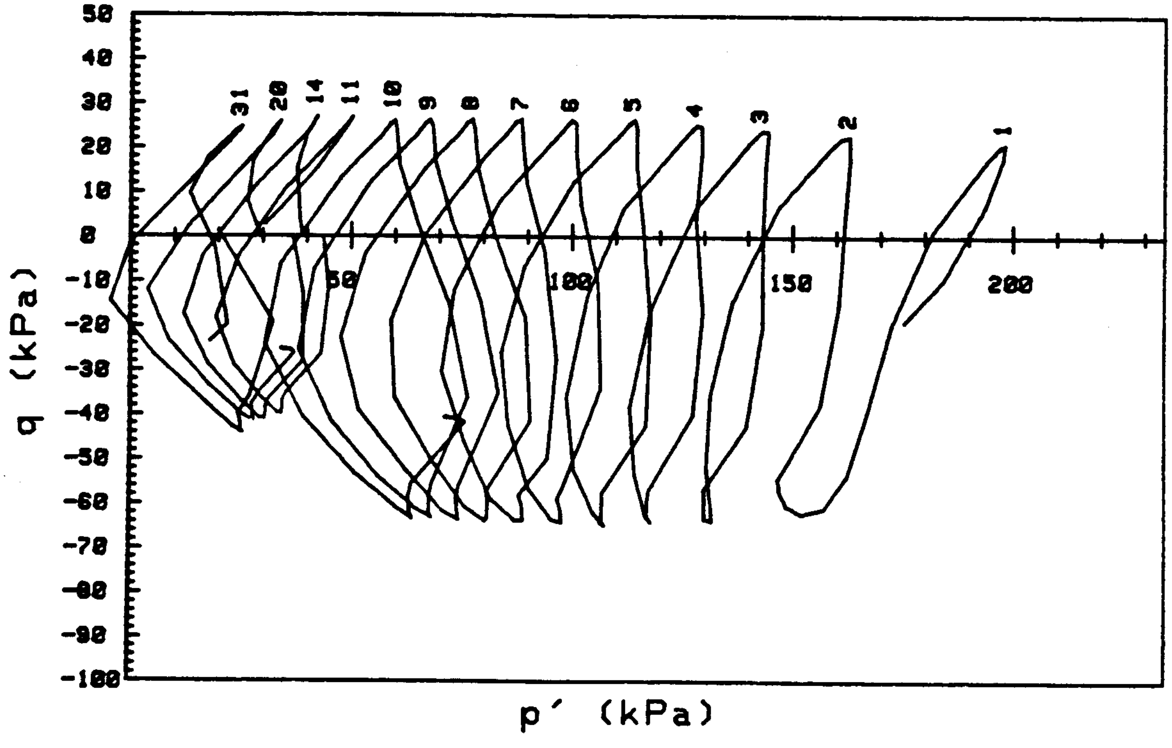

CRUISE DC2-80-EG		INCREMENT (cm)	161-172
CORE NO.	87G	TEST NO.	TC53
SIG1c′(kPa)	194.3	STATIC qf (kPa)	122.8
SIG3c′(kPa)	194.3	AVG MAX q (kPa)	26.4 (21.5%)
INDUCED OCR	1.0	AVG MIN q (kPa)	-45.5 (37.1%)

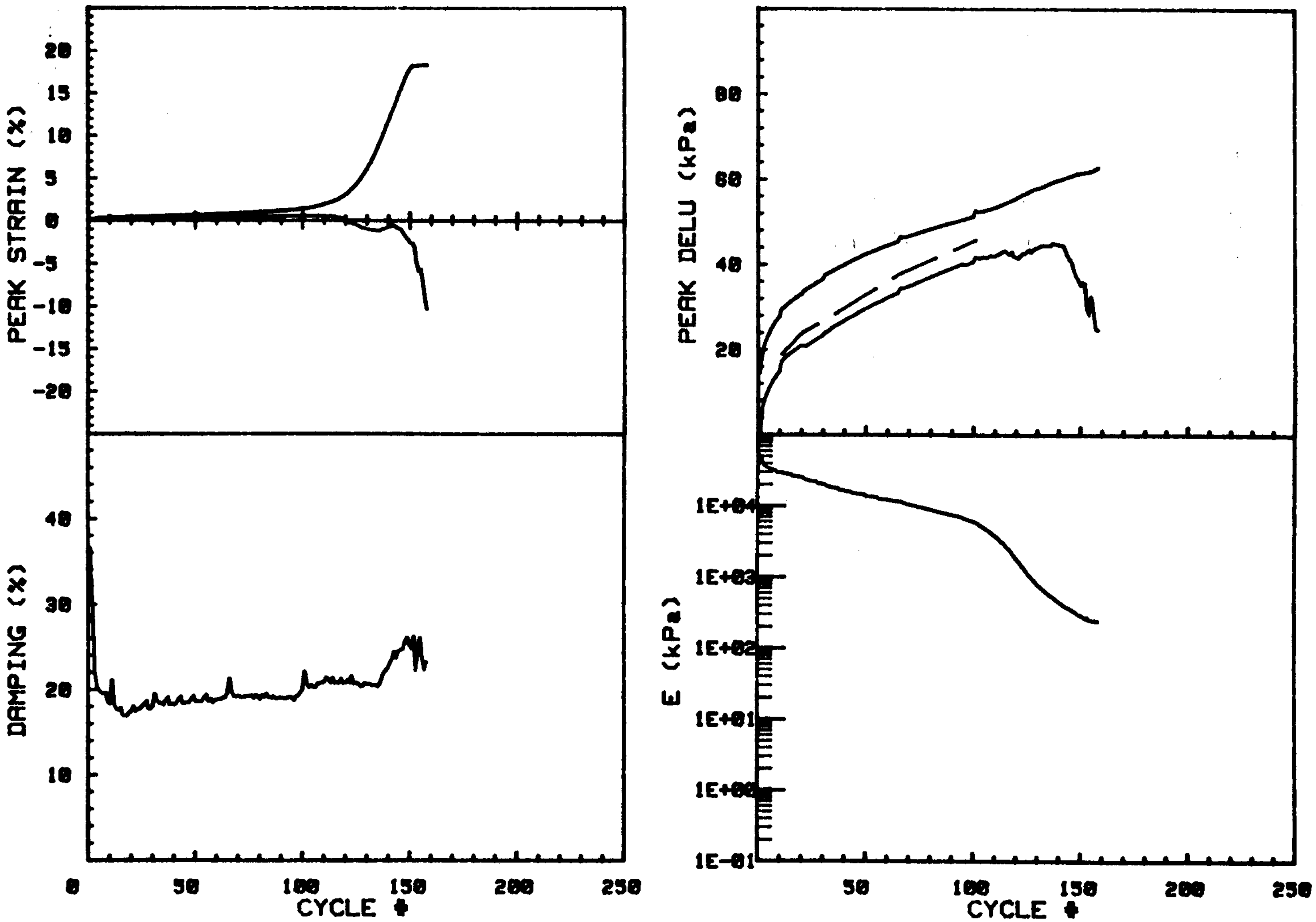

CRUISE DC1-81-EG		INCREMENT (cm)	72-82
CORE NO.	634G2	TEST NO.	TC54
SIG1c′(kPa)	61.9	STATIC qf (kPa)	23.9
SIG3c′(kPa)	61.9	AVG MAX q (kPa)	17.6 (73.6%)
INDUCED OCR	1.0	AVG MIN q (kPa)	-8.8 (36.8%)

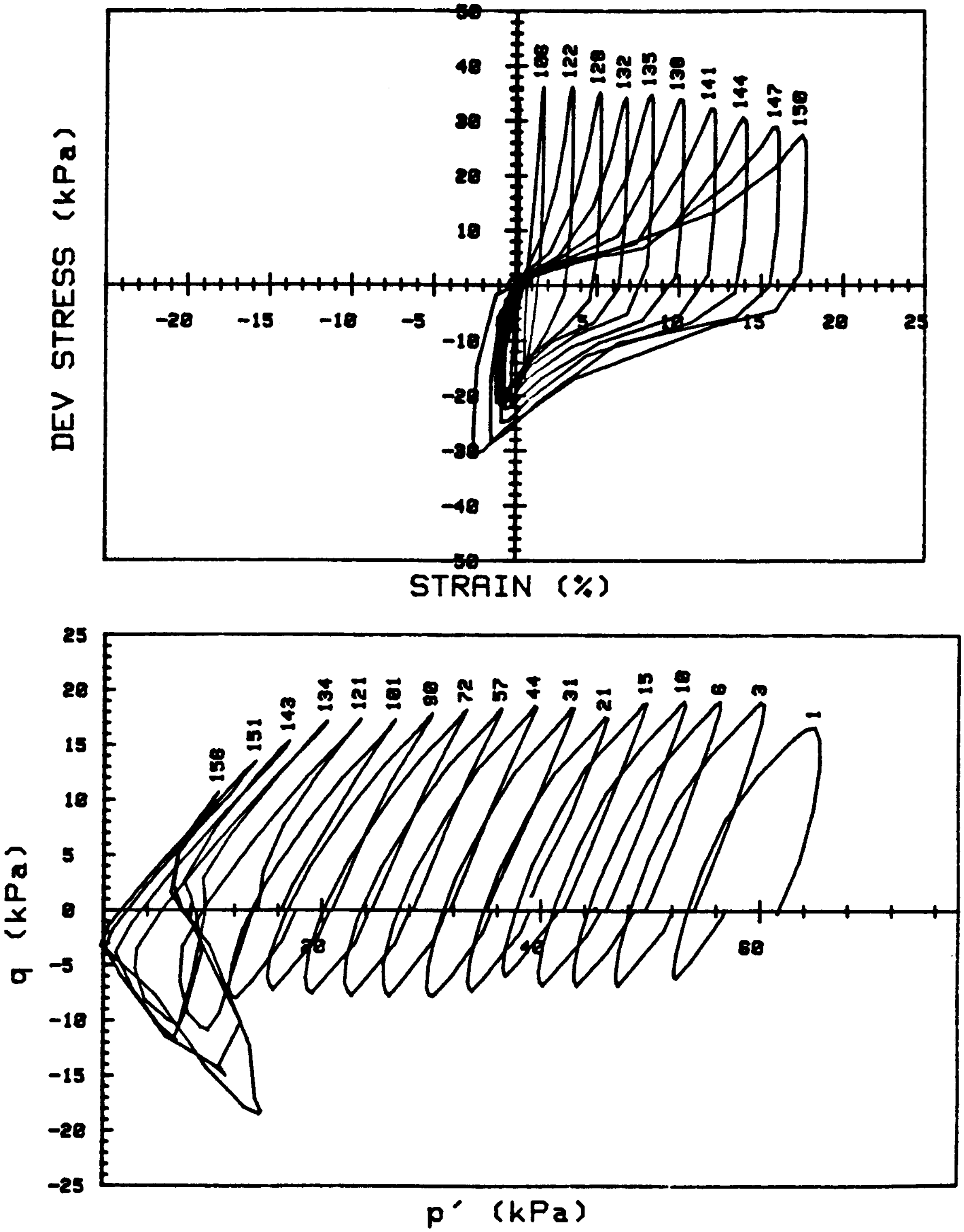

CRUISE DC1-81-EG		INCREMENT (cm)	72-82
CORE NO.	634G2	TEST NO.	TC54
SIG1c′(kPa)	61.9	STATIC qf (kPa)	23.9
SIG3c′(kPa)	61.9	AVG MAX q (kPa)	17.6 (73.6%)
INDUCED OCR	1.0	AVG MIN q (kPa)	-8.8 (36.8%)

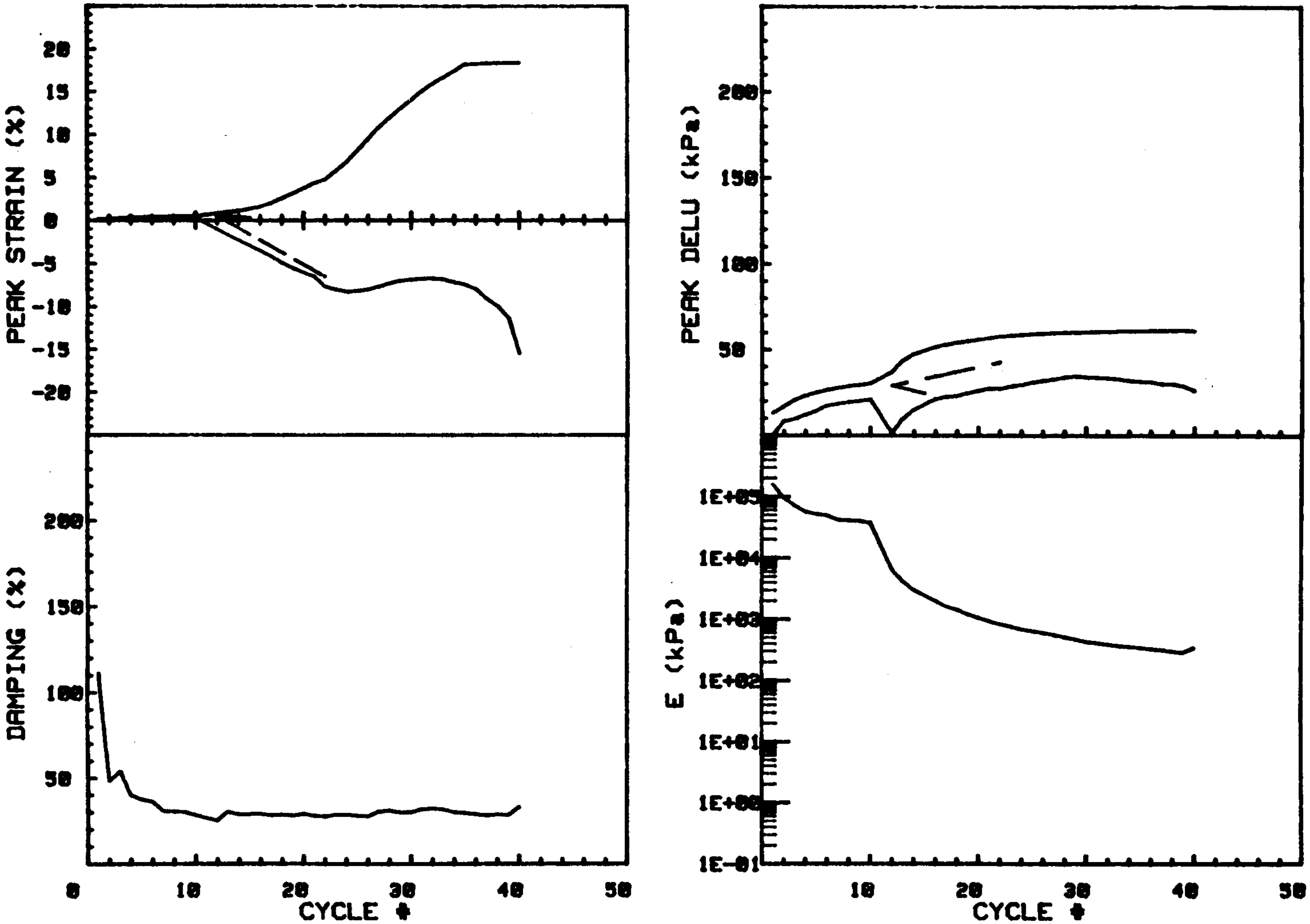

CRUISE DC1-81-EG		INCREMENT (cm)	72-82
CORE NO.	634G2	TEST NO.	TC55
SIG1c′(kPa)	59.3	STATIC qf (kPa)	23.9
SIG3c′(kPa)	59.3	AVG MAX q (kPa)	22.2 (92.9%)
INDUCED OCR	1.0	AVG MIN q (kPa)	-19.9 (83.3%)

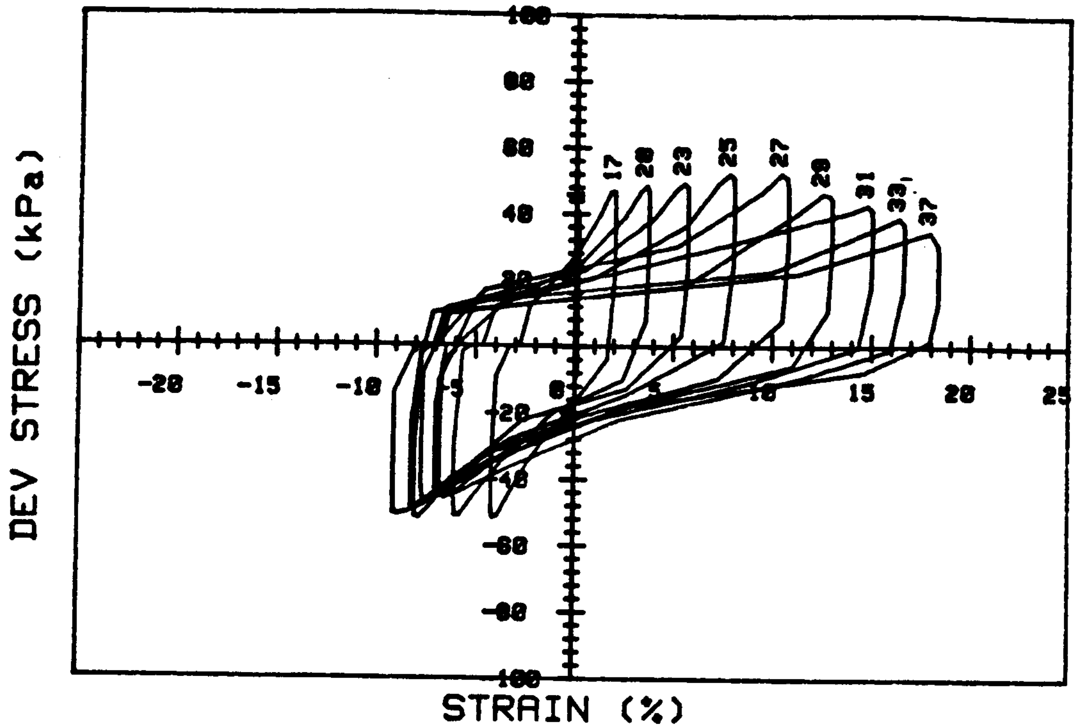

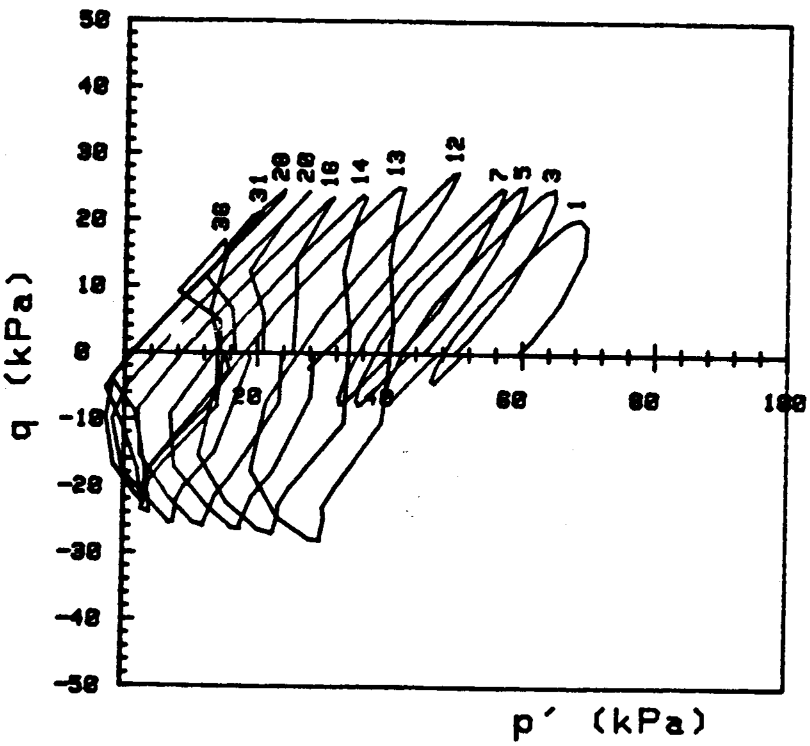

CRUISE DC1-81-EG		INCREMENT (cm)	72-82
CORE NO.	634G2	TEST NO.	TC55
SIG1c′(kPa)	59.3	STATIC qf (kPa)	23.9
SIG3c′(kPa)	59.3	AVG MAX q (kPa)	22.2 (92.9%)
INDUCED OCR	1.0	AVG MIN q (kPa)	-19.9 (83.3%)

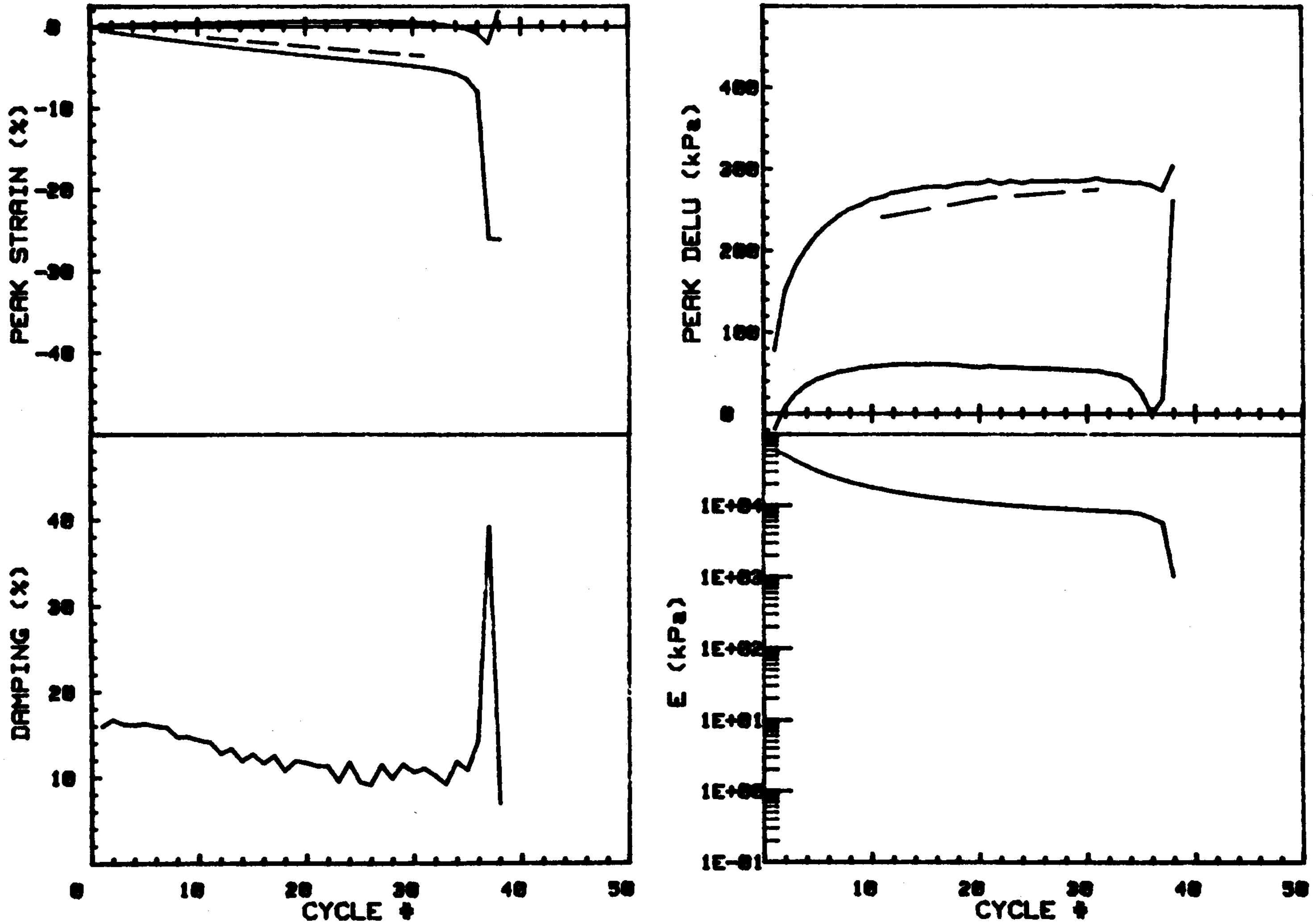

CRUISE DC1-81-EG		INCREMENT (cm)	153-161
CORE NO.	630A2	TEST NO.	TC56
SIG1c'(kPa)	301.0	STATIC qf (kPa)	562.0
SIG3c'(kPa)	301.0	AVG MAX q (kPa)	120.2 (21.4%)
INDUCED OCR	1.0	AVG MIN q (kPa)	-98.8 (17.6%)

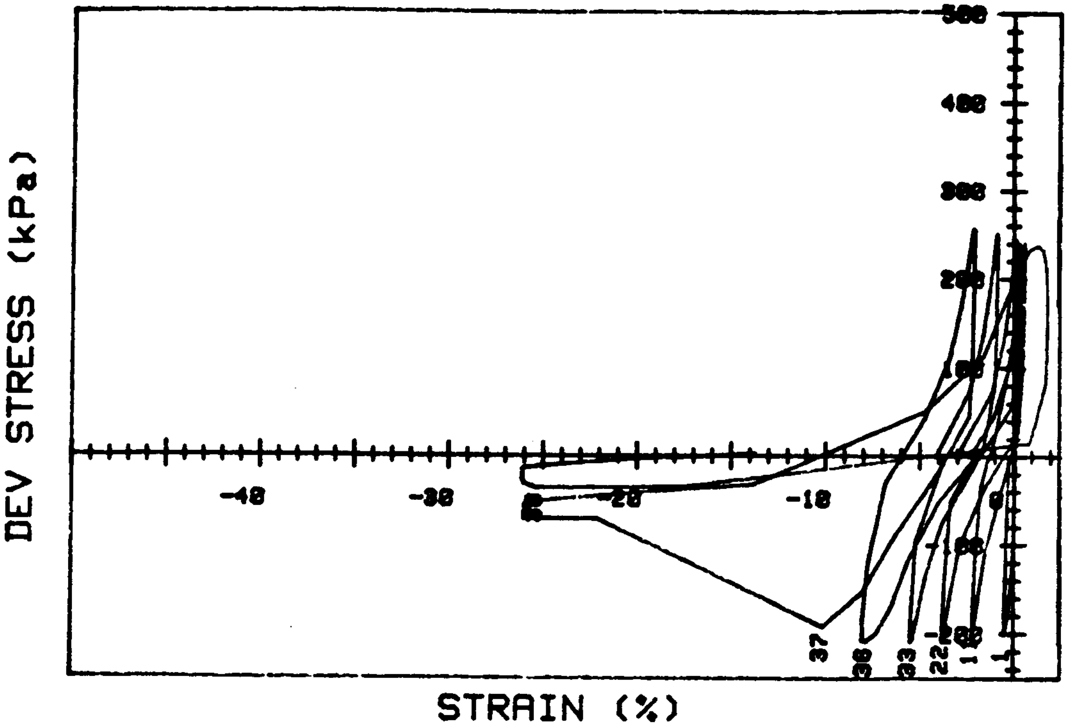

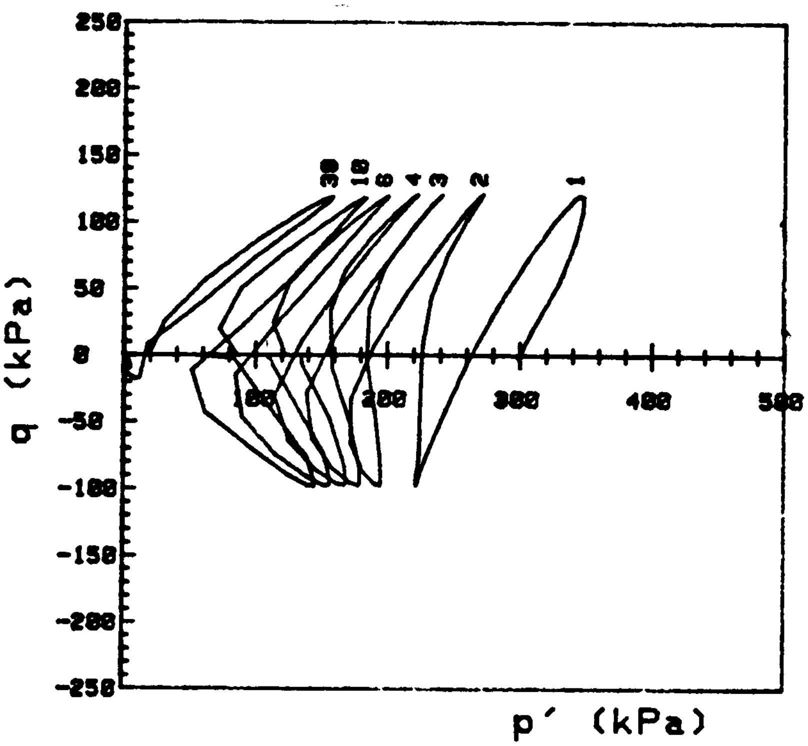

CRUISE DC1-81-EG		INCREMENT (cm)	153-161
CORE NO.	630A2	TEST NO.	TC56
SIG1c'(kPa)	301.0	STATIC qf (kPa)	562.0
SIG3c'(kPa)	301.0	AVG MAX q (kPa)	120.2 (21.4%)
INDUCED OCR	1.0	AVG MIN q (kPa)	-98.8 (17.6%)

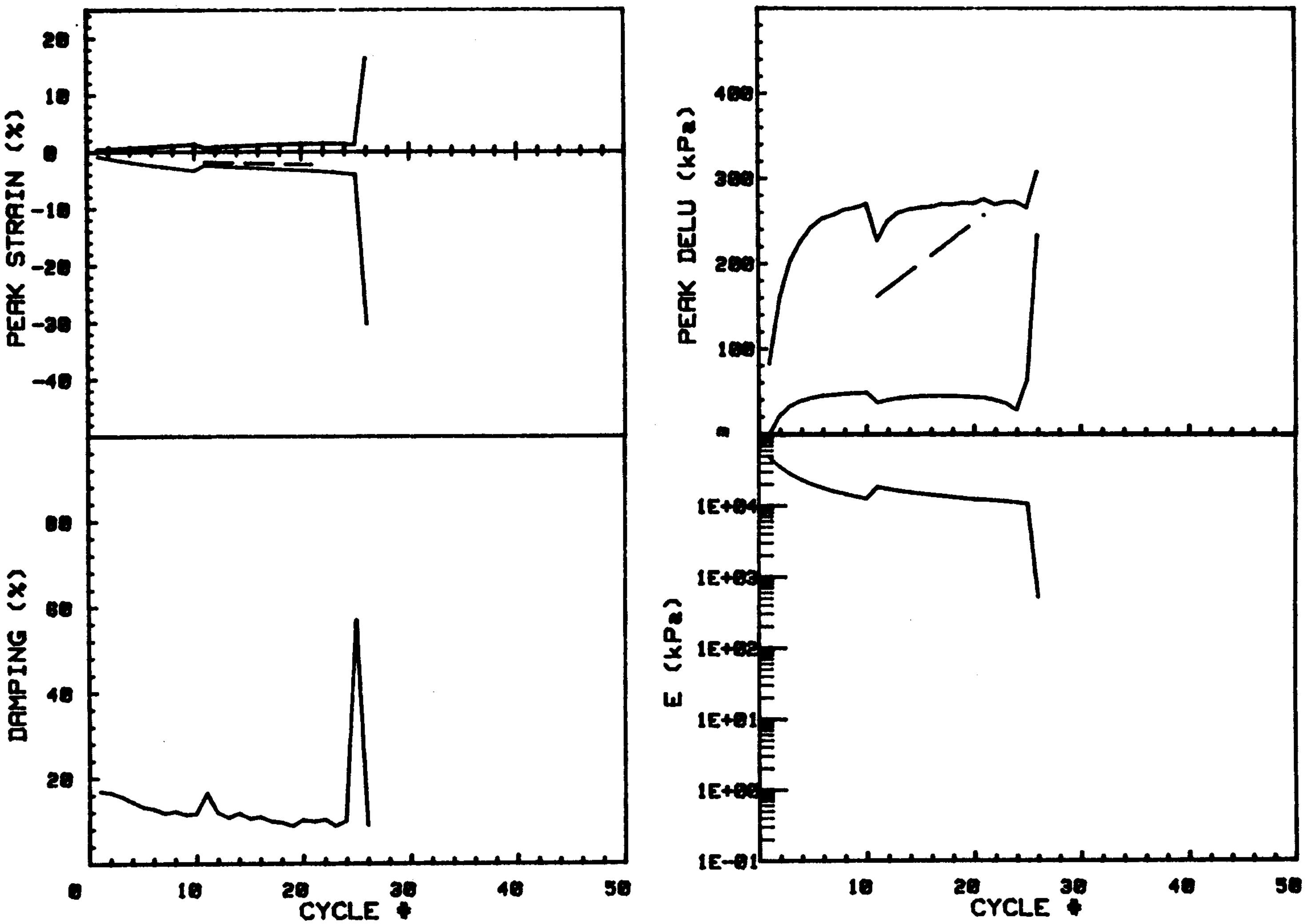

CRUISE DC1-81-EG		INCREMENT (cm)	153-160.5
CORE NO.	630A2	TEST NO.	TC57
SIG1c'(kPa)	297.9	STATIC qf (kPa)	562.0
SIG3c'(kPa)	297.9	AVG MAX q (kPa)	162.9 (29.0%)
INDUCED OCR	1.0	AVG MIN q (kPa)	-115.1 (20.5%)

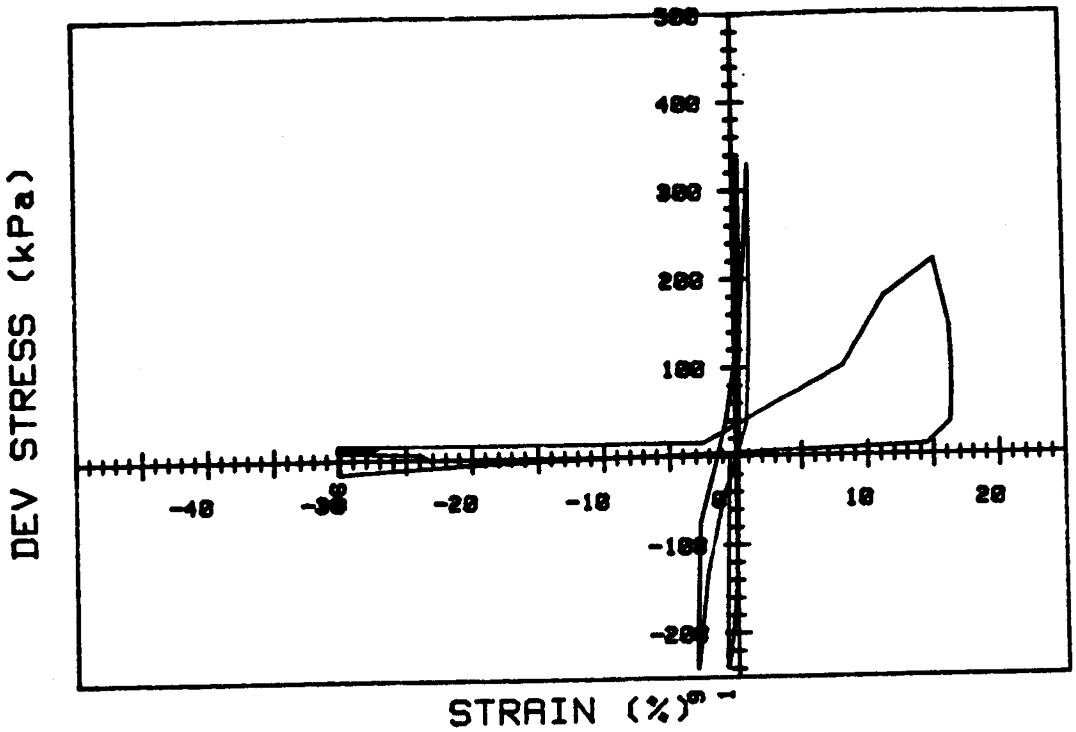

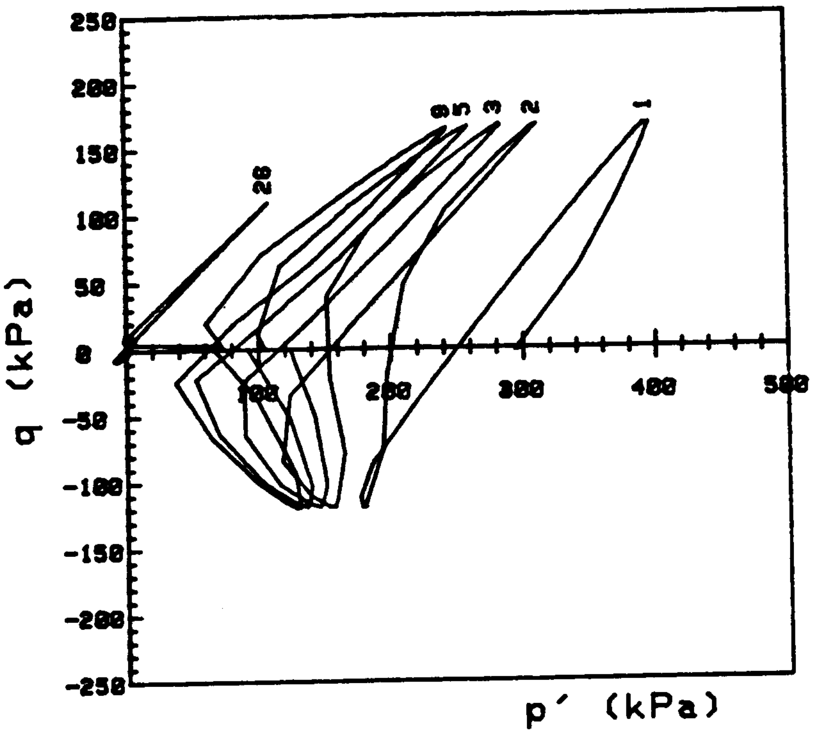

CRUISE DC1-81-EG		INCREMENT (cm)	153-160.5
CORE NO.	630A2	TEST NO.	TC57
SIG1c′(kPa)	297.9	STATIC qf (kPa)	562.0
SIG3c′(kPa)	297.9	AVG MAX q (kPa)	162.9 (29.0%)
INDUCED OCR	1.0	AVG MIN q (kPa)	-115.1 (20.5%)

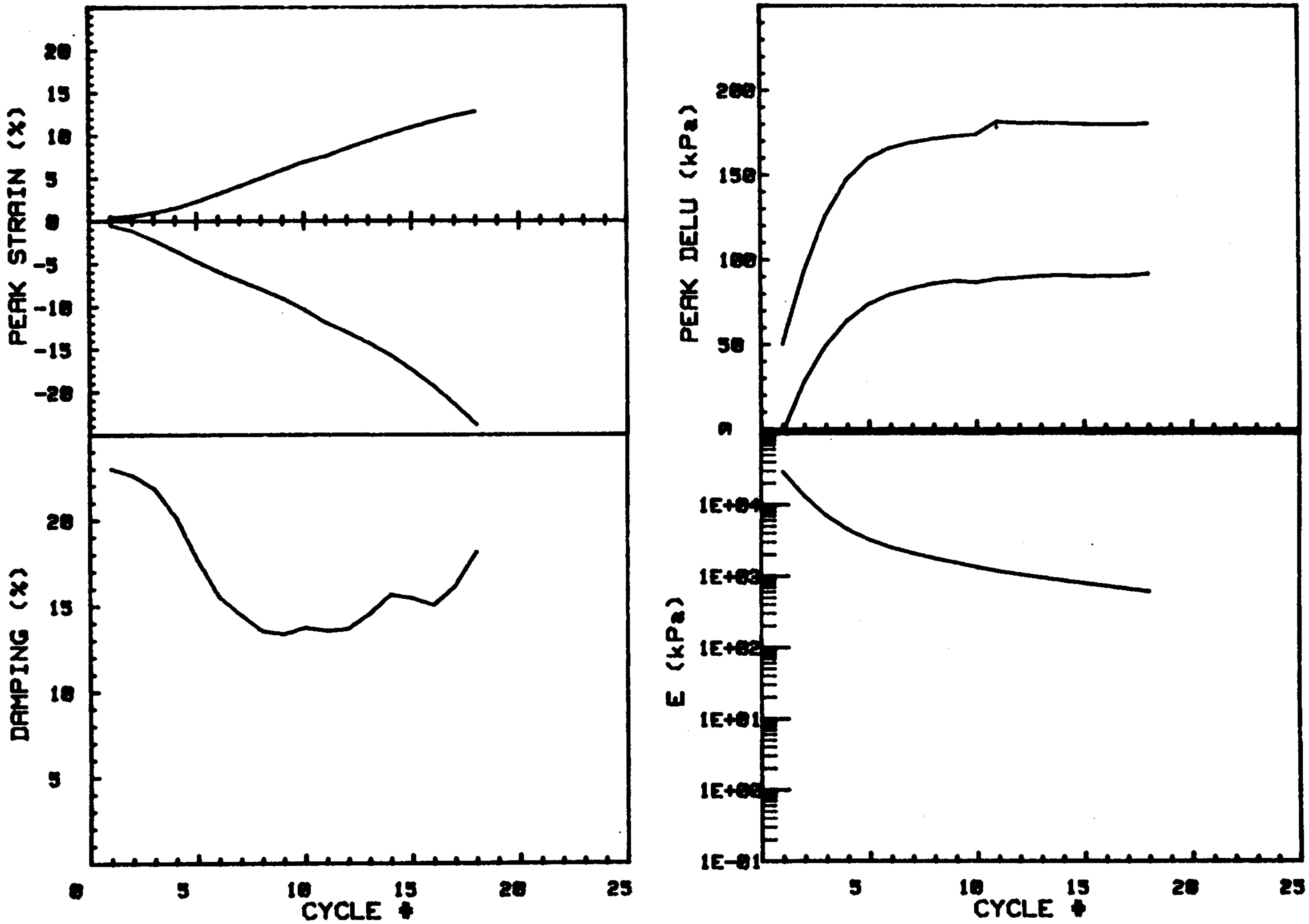

CRUISE DC1-81-EG		INCREMENT (cm)	138-149
CORE NO.	618G2	TEST NO.	TC58
SIG1c'(kPa)	184.8	STATIC qf (kPa)	95.6
SIG3c'(kPa)	184.8	AVG MAX q (kPa)	56.2 (58.8%)
INDUCED OCR	1.0	AVG MIN q (kPa)	-53.5 (56.0%)

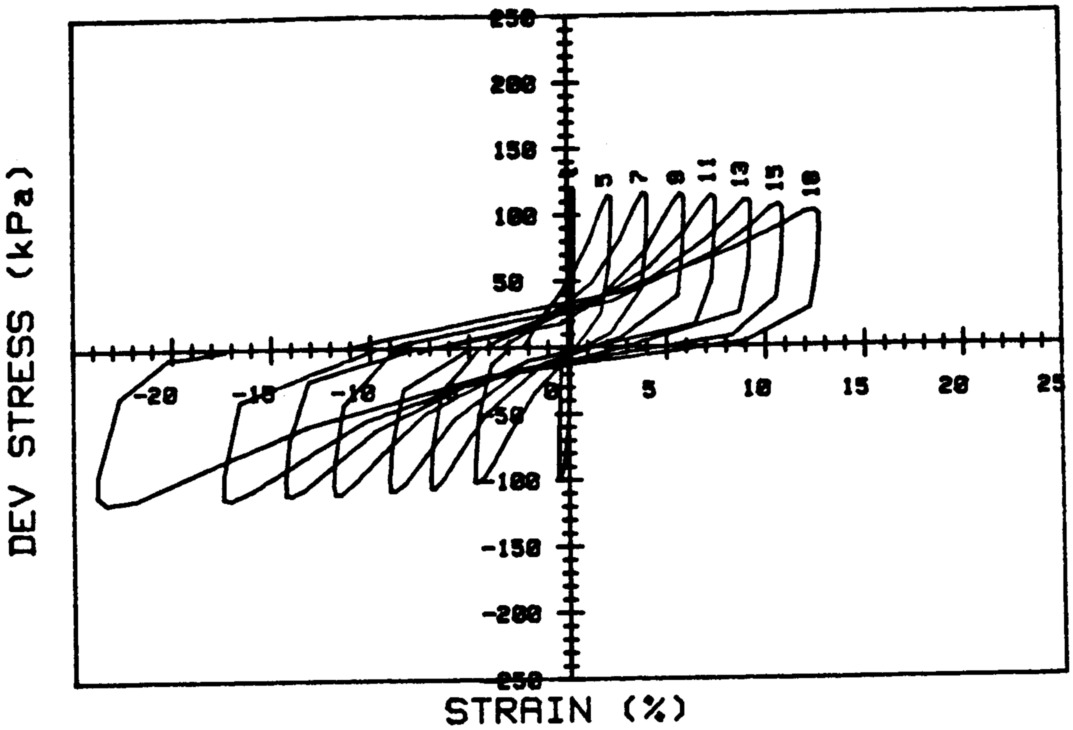

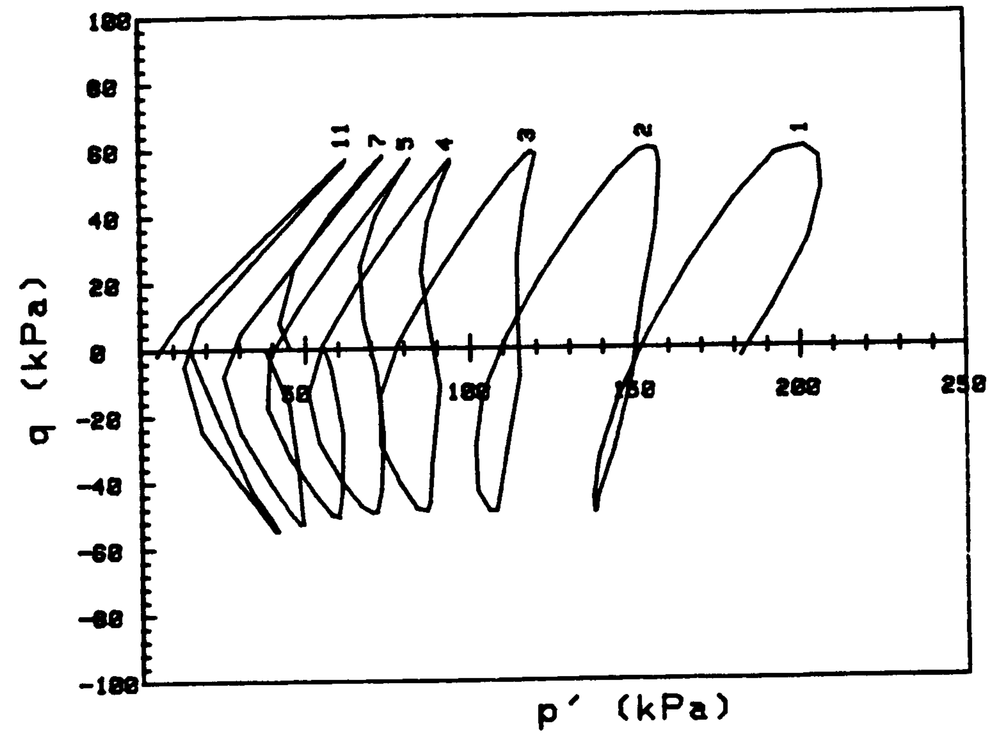

CRUISE	DC1-81-EG	INCREMENT (cm)	138-149
CORE NO.	618G2	TEST NO.	TC58
SIG1c′(kPa)	184.8	STATIC qf (kPa)	95.6
SIG3c′(kPa)	184.8	AVG MAX q (kPa)	56.2 (58.8%)
INDUCED OCR	1.0	AVG MIN q (kPa)	-53.5 (56.0%)

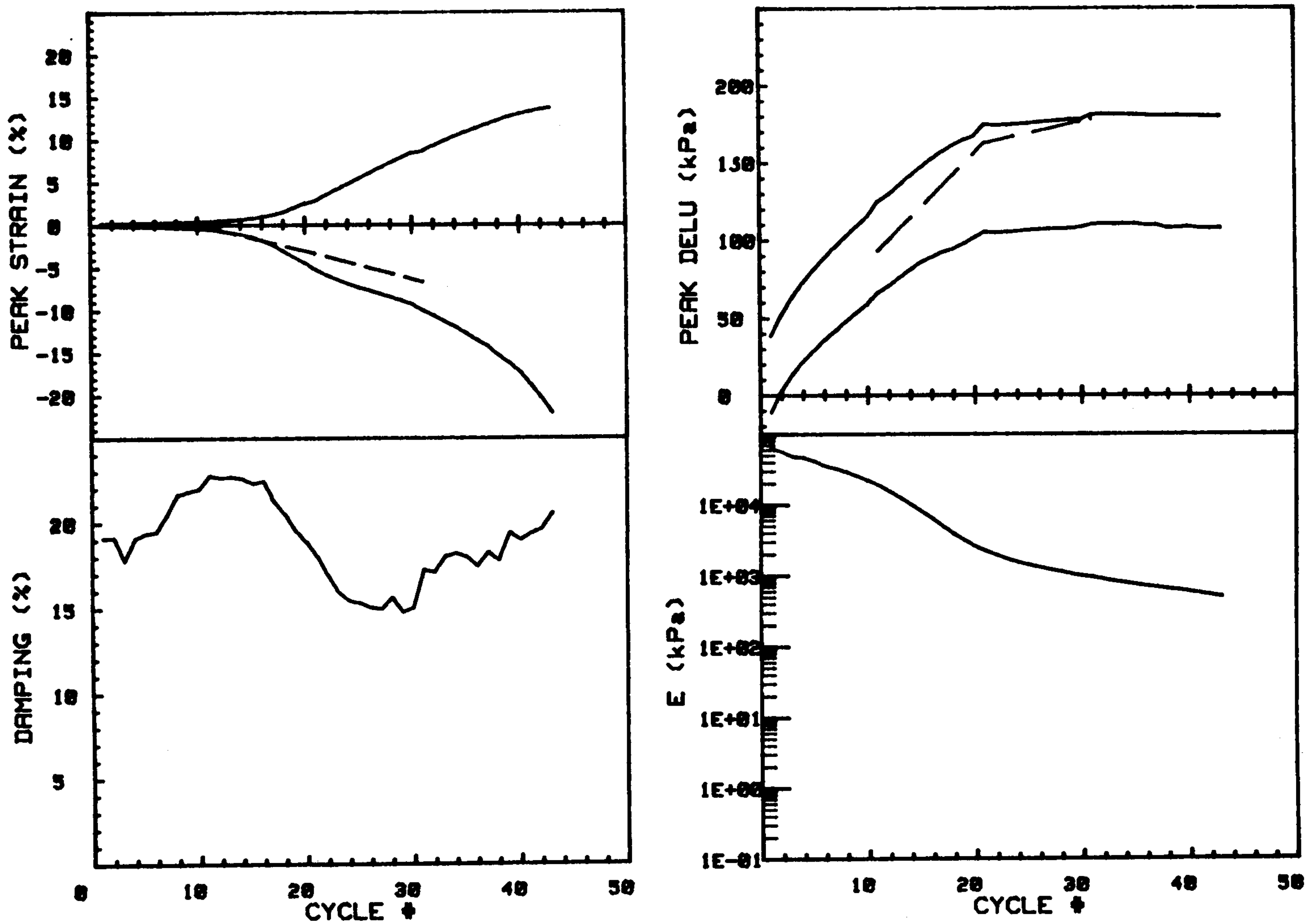

CRUISE DC1-81-EG		INCREMENT (cm)	138-149
CORE NO.	618G2	TEST NO.	TC59
SIG1c'(kPa)	183.9	STATIC qf (kPa)	95.6
SIG3c'(kPa)	183.9	AVG MAX q (kPa)	44.6 (46.7%)
INDUCED OCR	1.0	AVG MIN q (kPa)	-41.2 (43.1%)

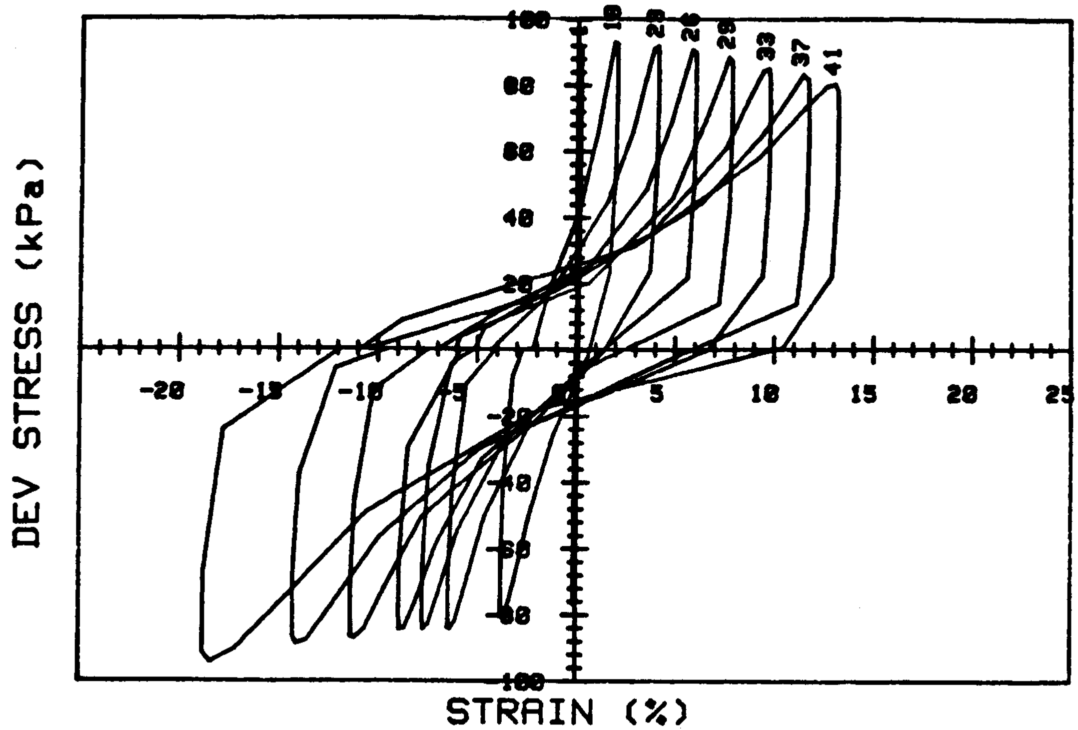

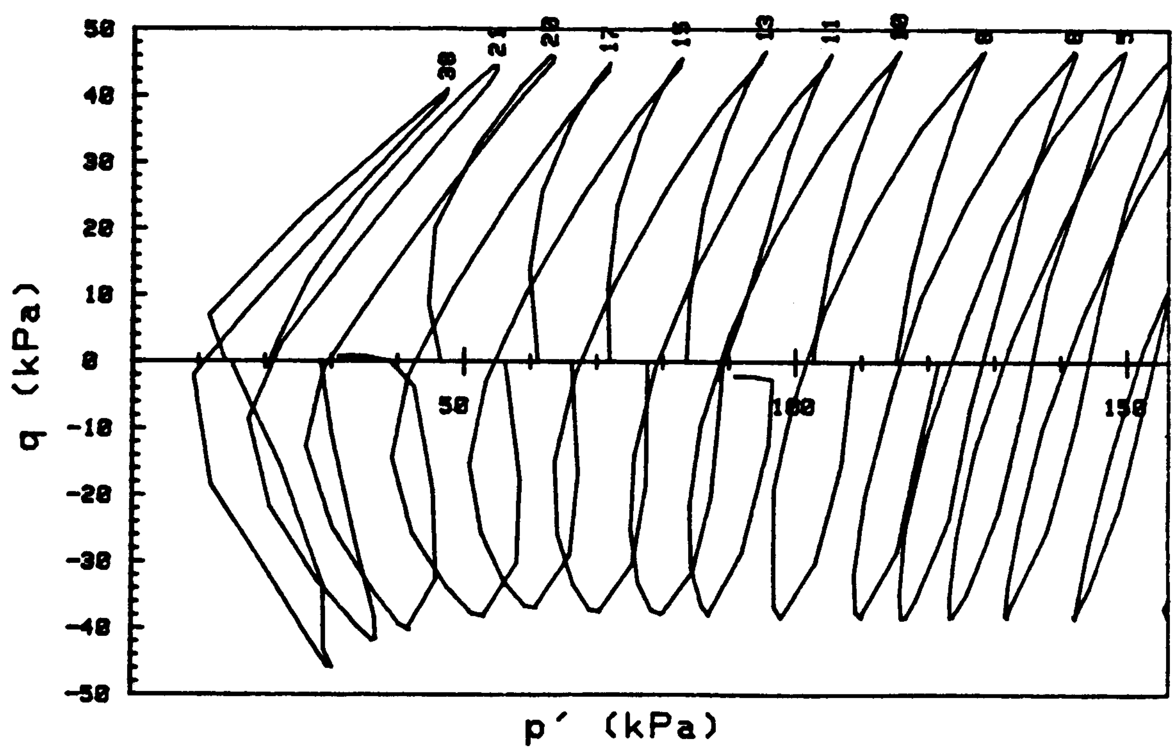

CRUISE DC1-81-EG		INCREMENT (cm)	138-149
CORE NO.	618G2	TEST NO.	TC59
SIG1c′(kPa)	183.9	STATIC qf (kPa)	95.6
SIG3c′(kPa)	183.9	AVG MAX q (kPa)	44.6 (46.7%)
INDUCED OCR	1.0	AVG MIN q (kPa)	-41.2 (43.1%)

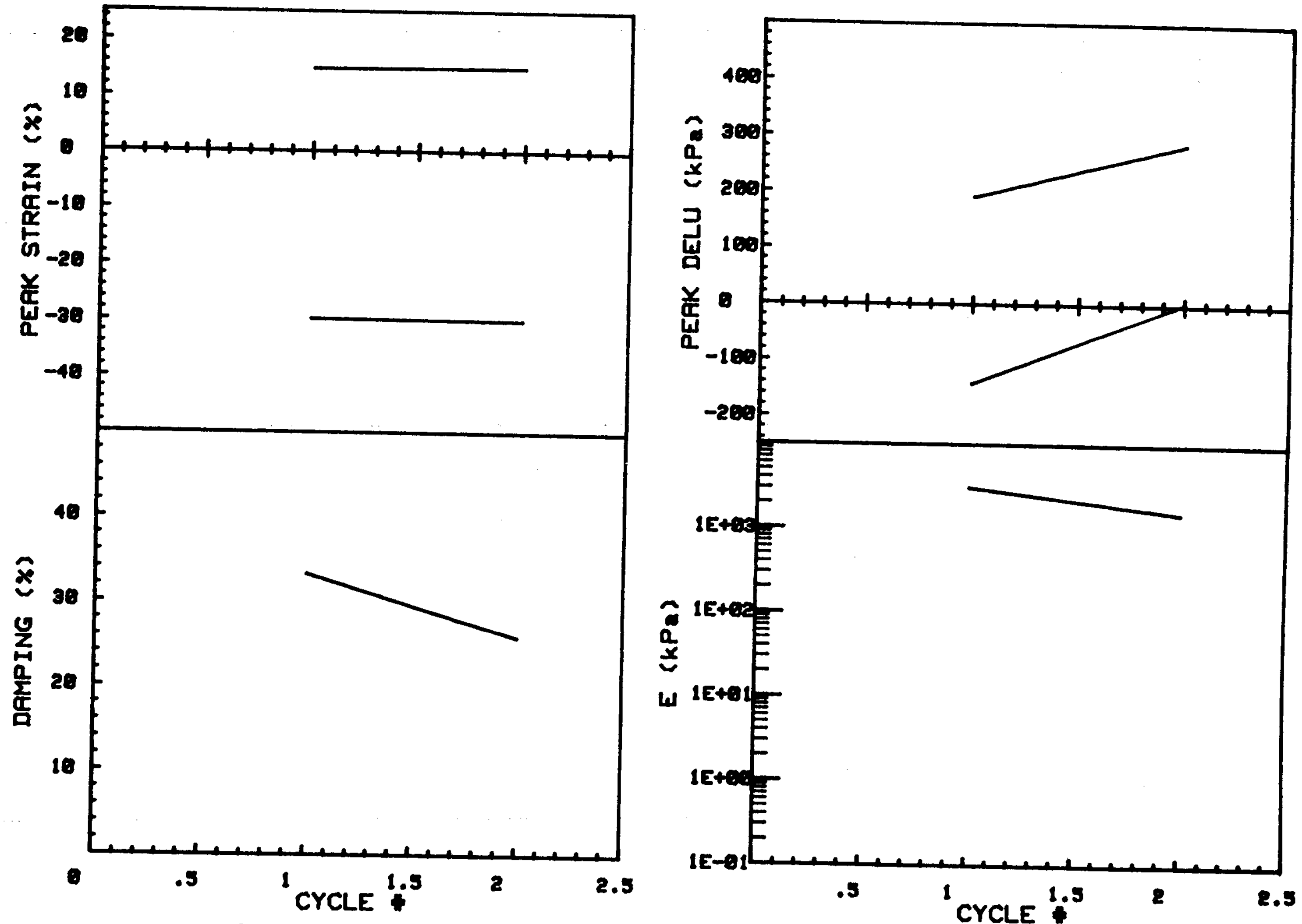

CRUISE DC1-81-EG		INCREMENT (cm)	174-181
CORE NO.	624A1	TEST NO.	TC60
SIG1c'(kPa)	338.9	STATIC qf (kPa)	401.3
SIG3c'(kPa)	338.9	AVG MAX q (kPa)	206.6 (51.5%)
INDUCED OCR	1.0	AVG MIN q (kPa)	-184.9 (46.1%)

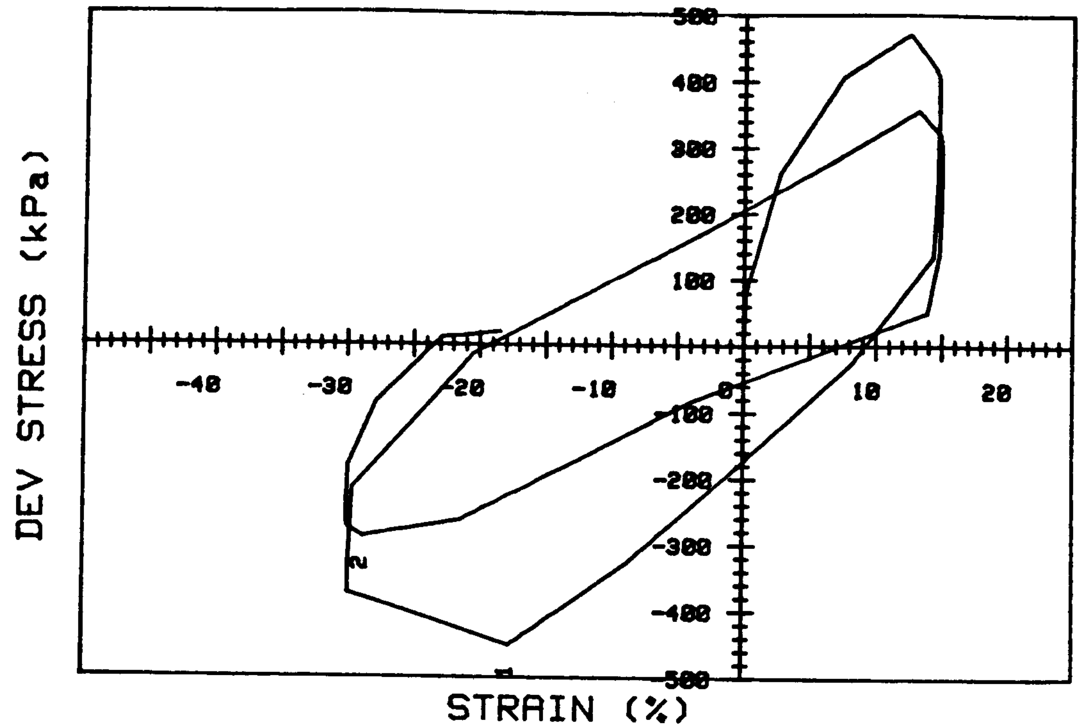

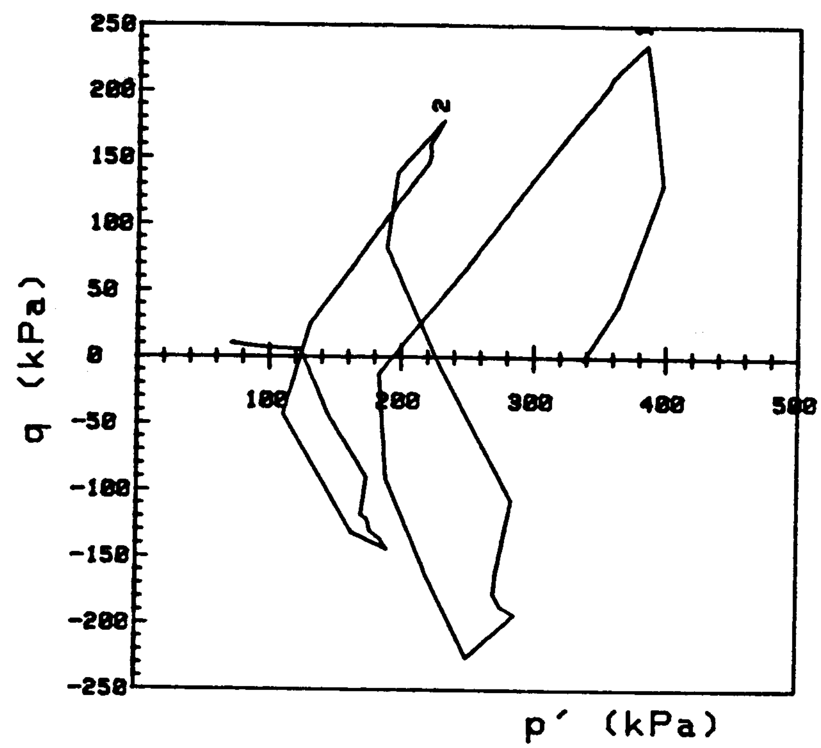

CRUISE DC1-81-EG		INCREMENT (cm)	174-181
CORE NO.	624A1	TEST NO.	TC60
SIG1c′(kPa)	338.9	STATIC qf (kPa)	401.3
SIG3c′(kPa)	338.9	AVG MAX q (kPa)	206.6 (51.5%)
INDUCED OCR	1.0	AVG MIN q (kPa)	-184.9 (46.1%)

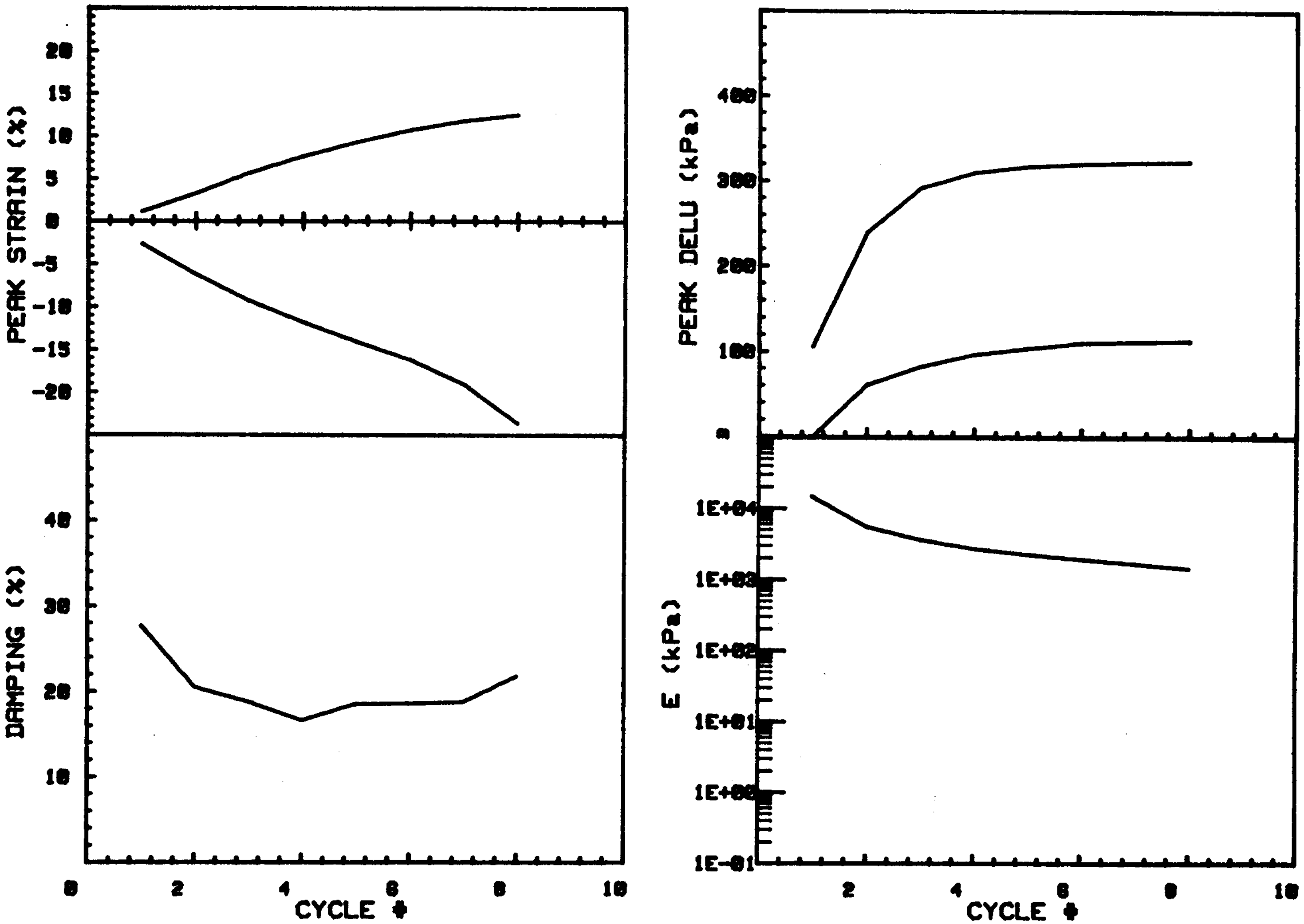

CRUISE DC1-81-EG		INCREMENT (cm)	174-181
CORE NO.	624A1	TEST NO.	TC61
SIG1c'(kPa)	344.7	STATIC qf (kPa)	401.3
SIG3c'(kPa)	344.7	AVG MAX q (kPa)	121.8 (30.4%)
INDUCED OCR	1.0	AVG MIN q (kPa)	-134.6 (33.5%)

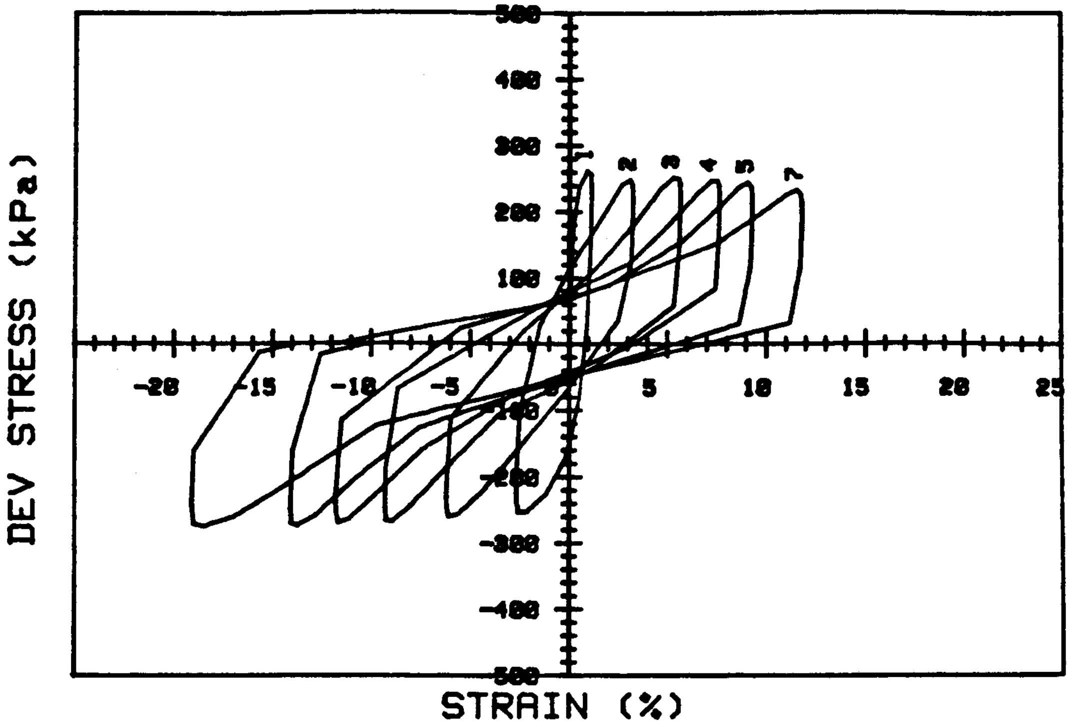

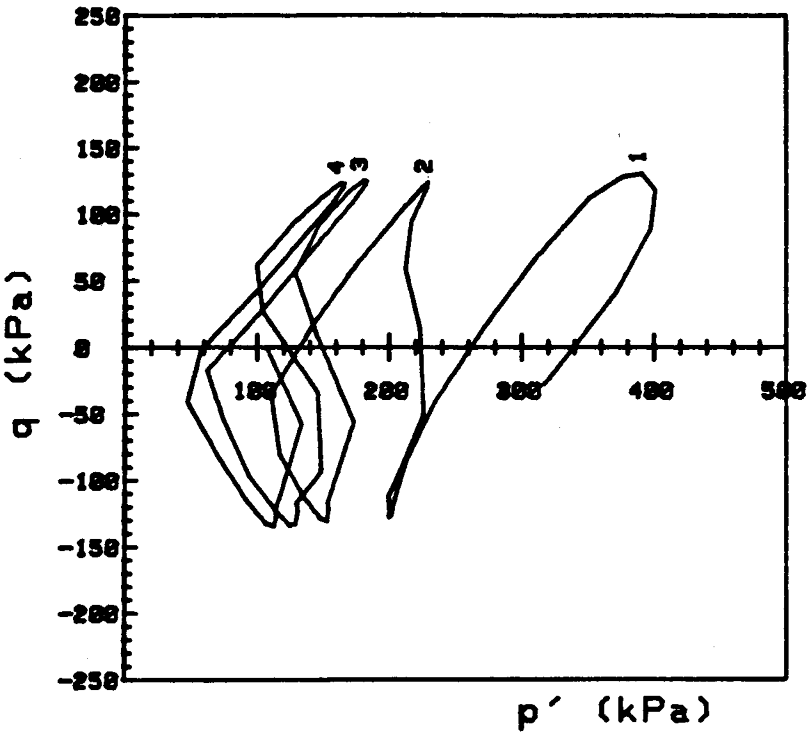

CRUISE DC1-81-EG		INCREMENT (cm)	174-181
CORE NO.	624A1	TEST NO.	TC61
SIG1c′(kPa)	344.7	STATIC qf (kPa)	401.3
SIG3c′(kPa)	344.7	AVG MAX q (kPa)	121.8 (30.4%)
INDUCED OCR	1.0	AVG MIN q (kPa)	-134.6 (33.5%)

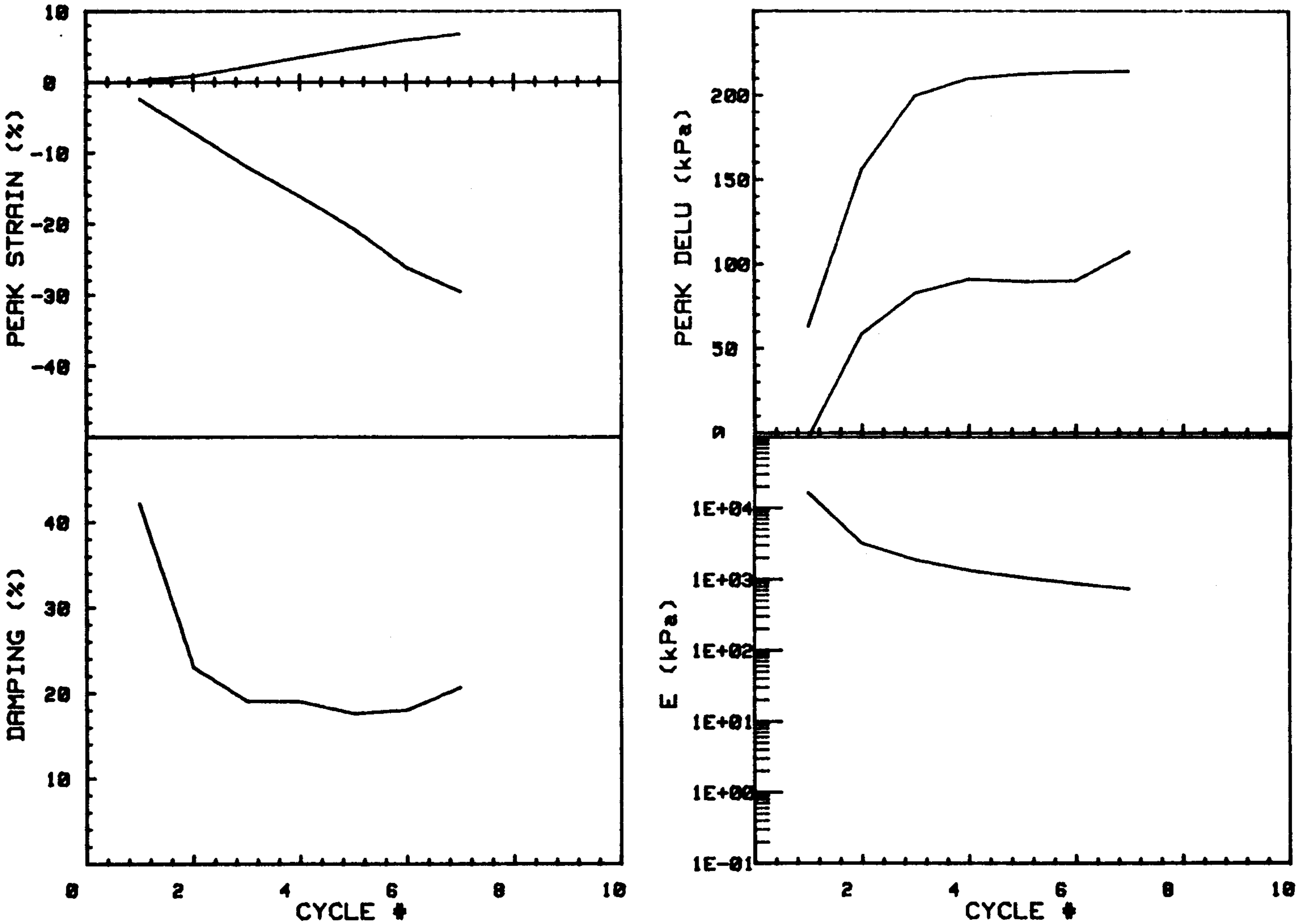

CRUISE DC1-81-EG		INCREMENT (cm)	166-173
CORE NO.	605G2	TEST NO.	TC86
SIG1c'(kPa)	216.3	STATIC qf (kPa)	127.9
SIG3c'(kPa)	216.3	AVG MAX q (kPa)	62.6 (48.9%)
INDUCED OCR	1.0	AVG MIN q (kPa)	-66.5 (52.0%)

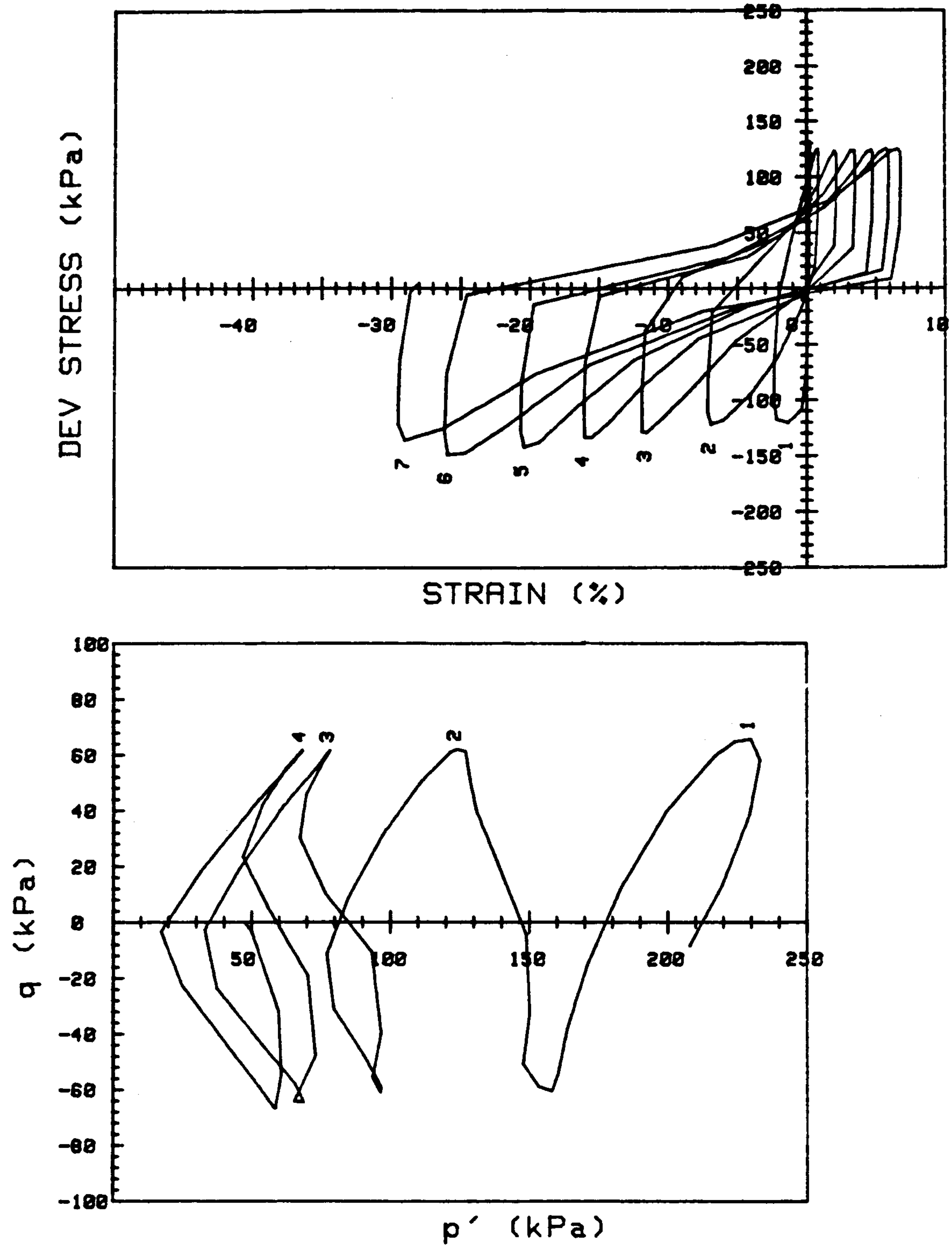

CRUISE DC1-81-EG		INCREMENT (cm)	166-173
CORE NO.	605G2	TEST NO.	TC86
SIG1c′(kPa)	216.3	STATIC qf (kPa)	127.9
SIG3c′(kPa)	216.3	AVG MAX q (kPa)	62.6 (48.9%)
INDUCED OCR	1.0	AVG MIN q (kPa)	-66.5 (52.0%)

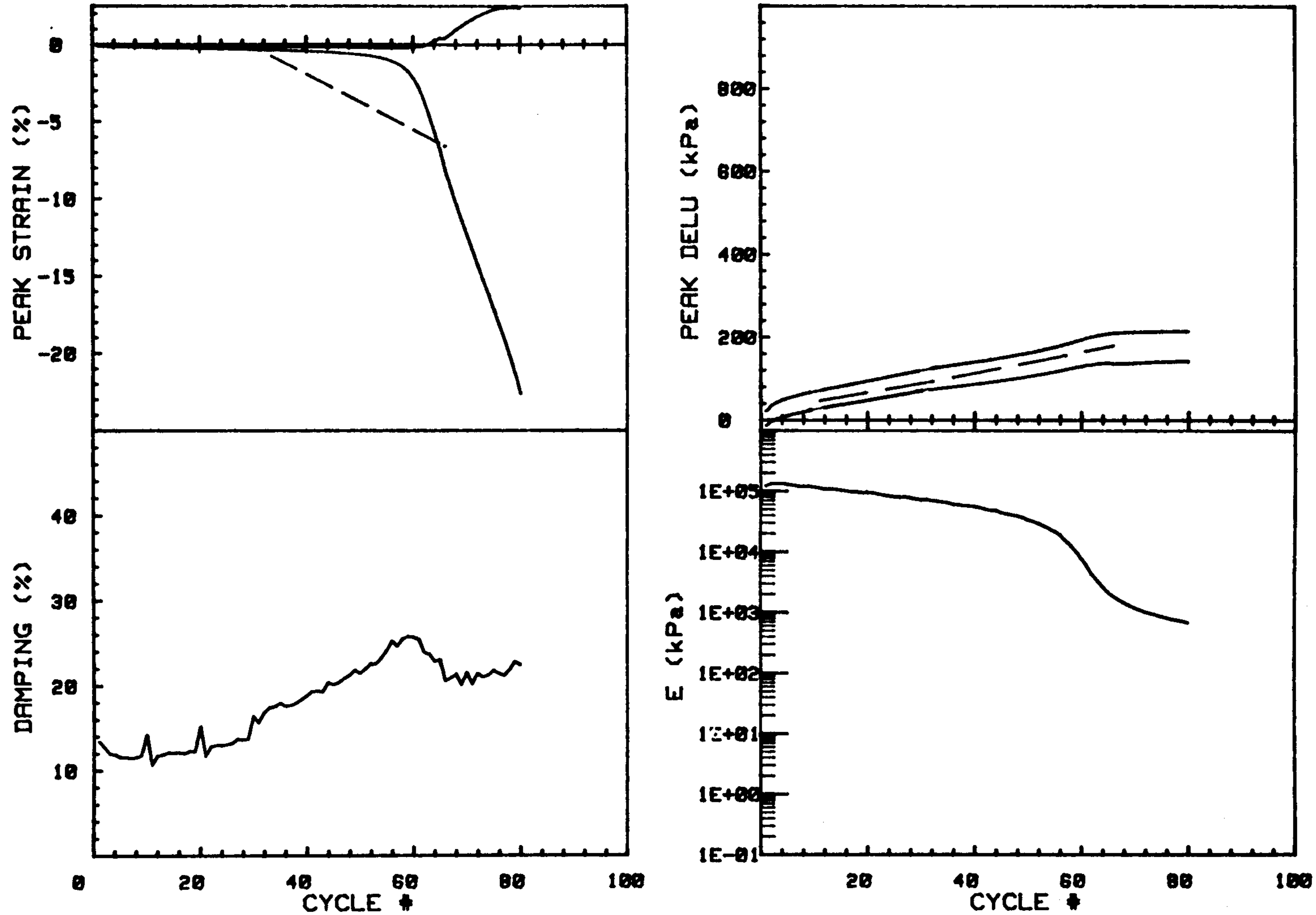

CRUISE DC1-81-EG		INCREMENT (cm)	166-173
CORE NO.	605G2	TEST NO.	TC87
SIG1c'(kPa)	215.1	STATIC qf (kPa)	127.9
SIG3c'(kPa)	215.1	AVG MAX q (kPa)	35.5 (27.8%)
INDUCED OCR	1.0	AVG MIN q (kPa)	-41.8 (32.7%)

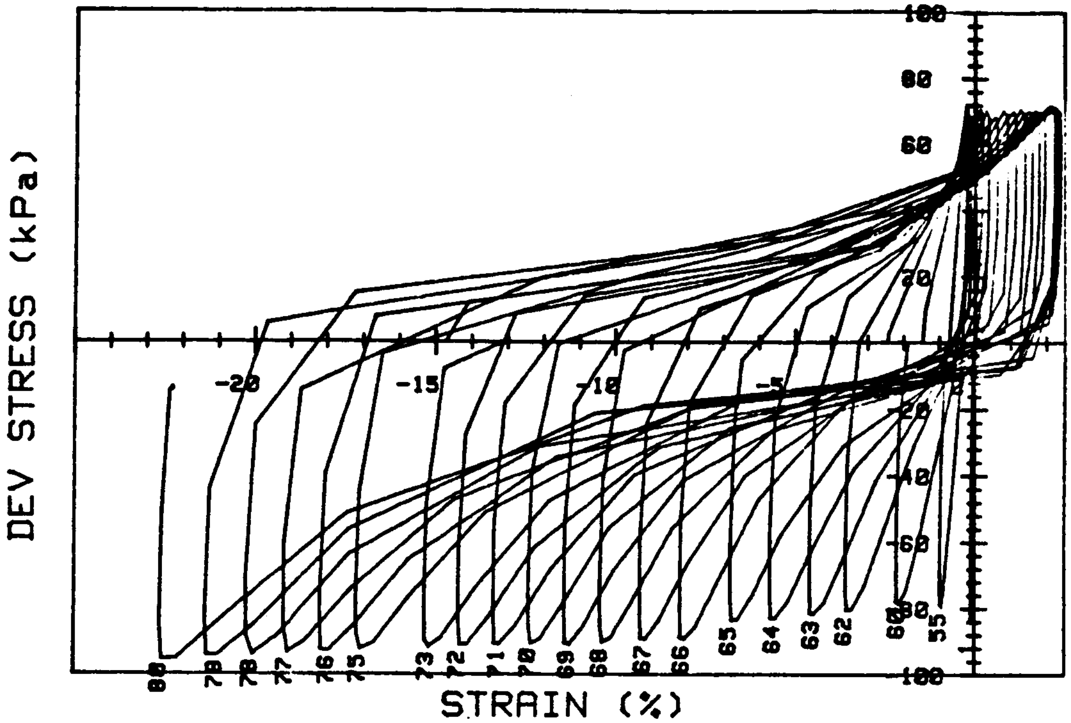

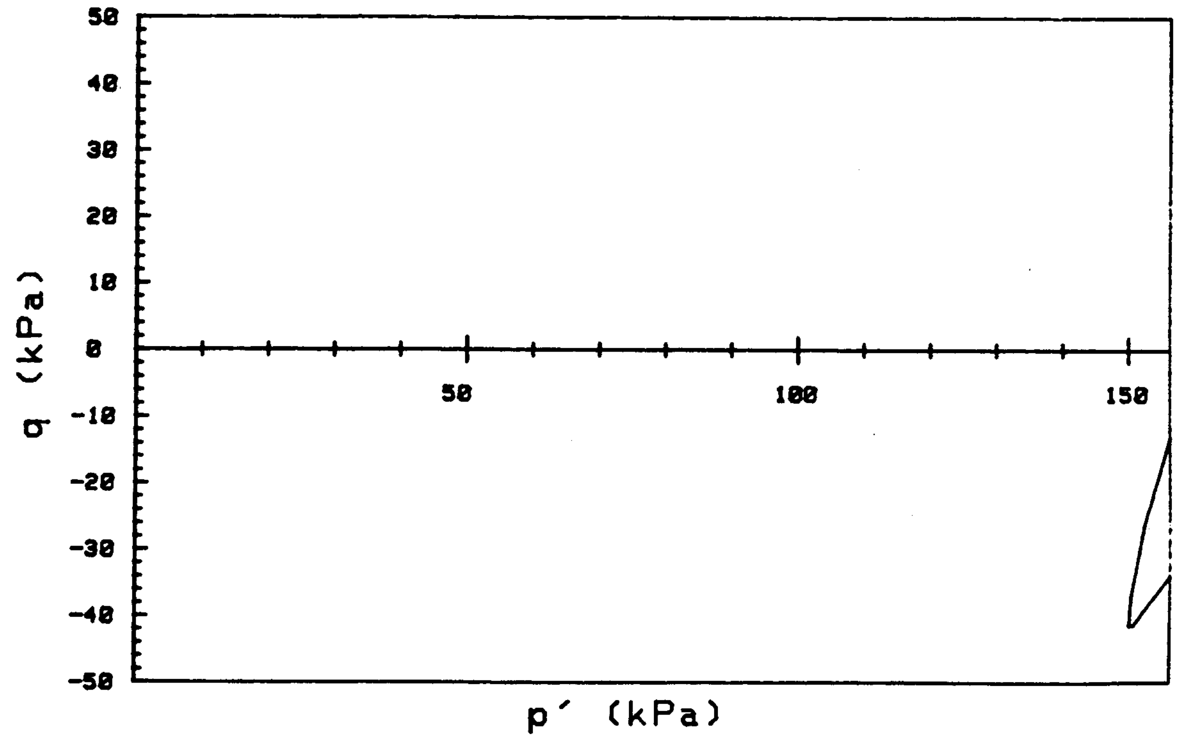

CRUISE	DC1-81-EG	INCREMENT (cm)		166-173	
CORE NO.	605G2	TEST NO.		TC87	
SIG1c′(kPa)	215.1	STATIC qf (kPa)		127.9	
SIG3c′(kPa)	215.1	AVG MAX q (kPa)		35.5	(27.8%)
INDUCED OCR	1.0	AVG MIN q (kPa)		-41.8	(32.7%)

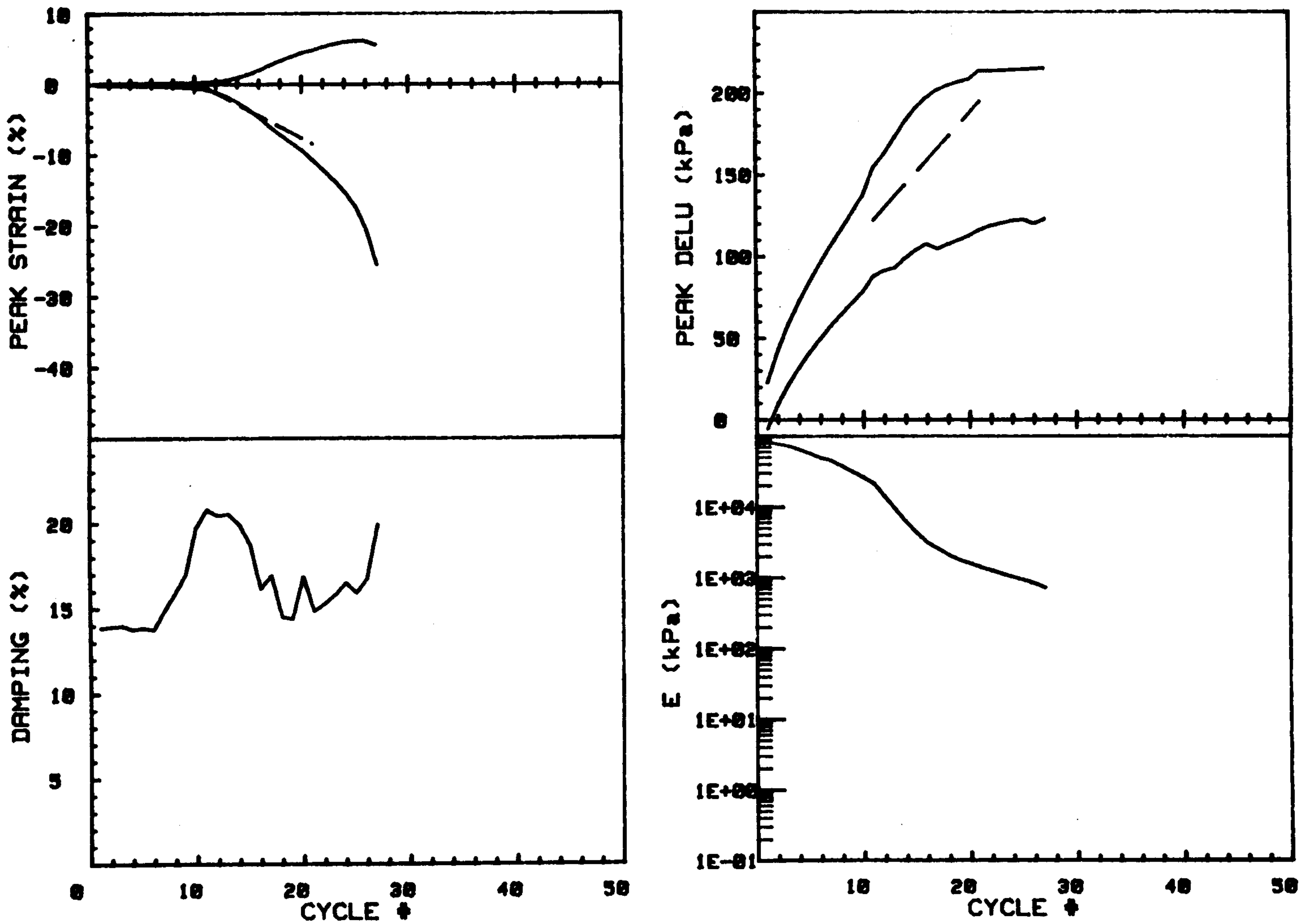

CRUISE DC1-81-EG		INCREMENT (cm)	54-61
CORE NO.	605G2	TEST NO.	TC92
SIG1c'(kPa)	215.9	STATIC qf (kPa)	163.8
SIG3c'(kPa)	215.9	AVG MAX q (kPa)	47.9 (29.2%)
INDUCED OCR	1.0	AVG MIN q (kPa)	-55.7 (34.0%)

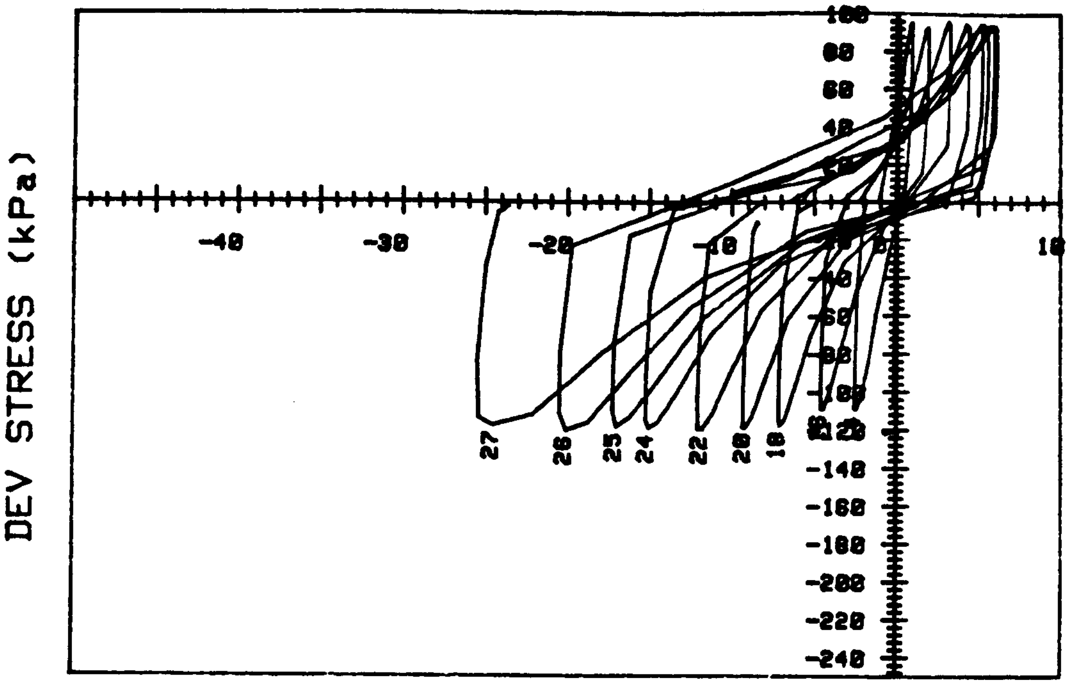

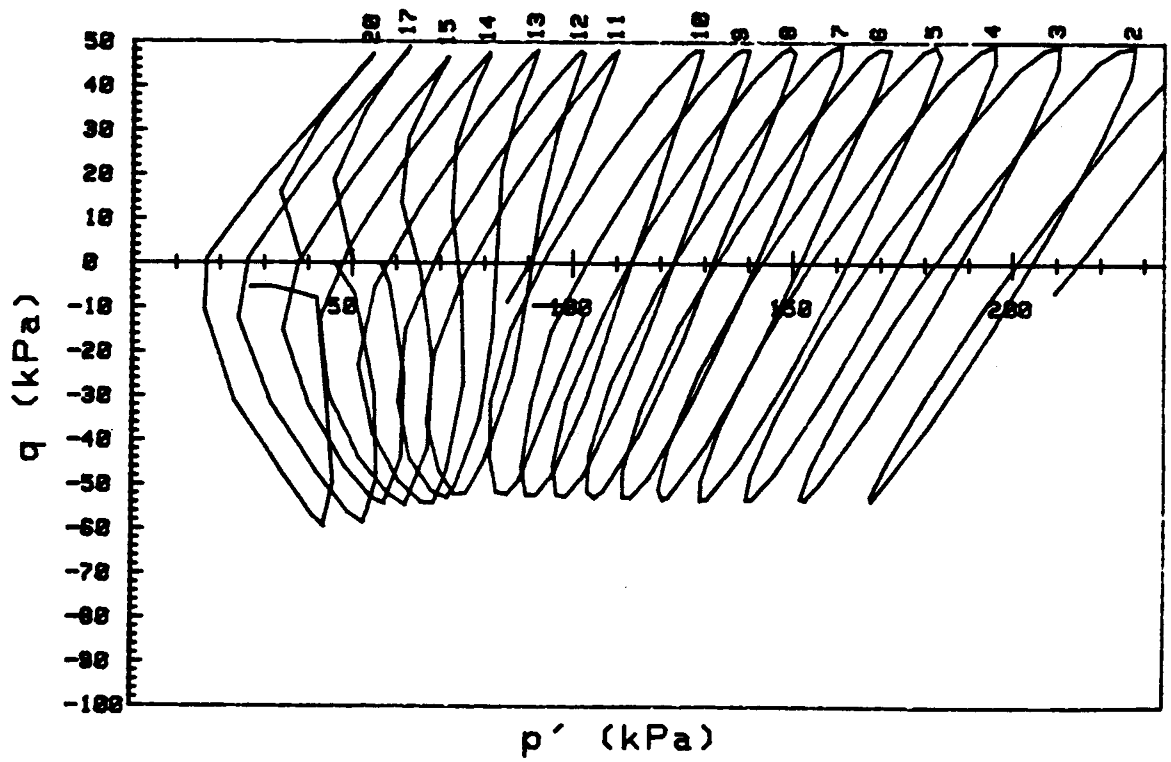

CRUISE DC1-81-EG		INCREMENT (cm)	54-61
CORE NO.	605G2	TEST NO.	TC92
SIG1c′(kPa)	215.9	STATIC qf (kPa)	163.8
SIG3c′(kPa)	215.9	AVG MAX q (kPa)	47.9 (29.2%)
INDUCED OCR	1.0	AVG MIN q (kPa)	-55.7 (34.0%)

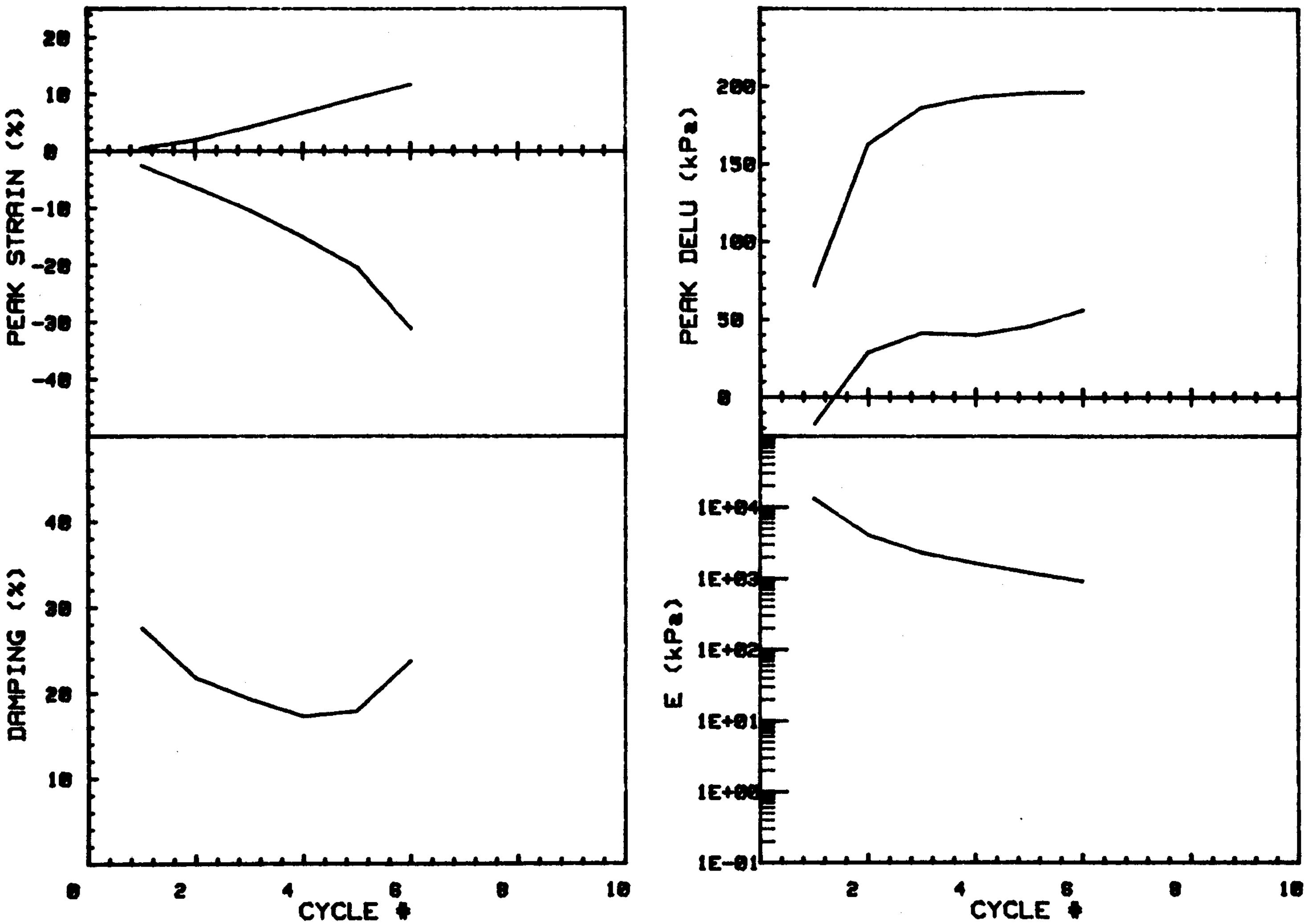

CRUISE DC1-81-EG		INCREMENT (cm)	54-60
CORE NO.	605G2	TEST NO.	TC93
SIG1c'(kPa)	204.8	STATIC qf (kPa)	163.8
SIG3c'(kPa)	204.8	AVG MAX q (kPa)	83.3 (50.9%)
INDUCED OCR	1.0	AVG MIN q (kPa)	-84.1 (51.3%)

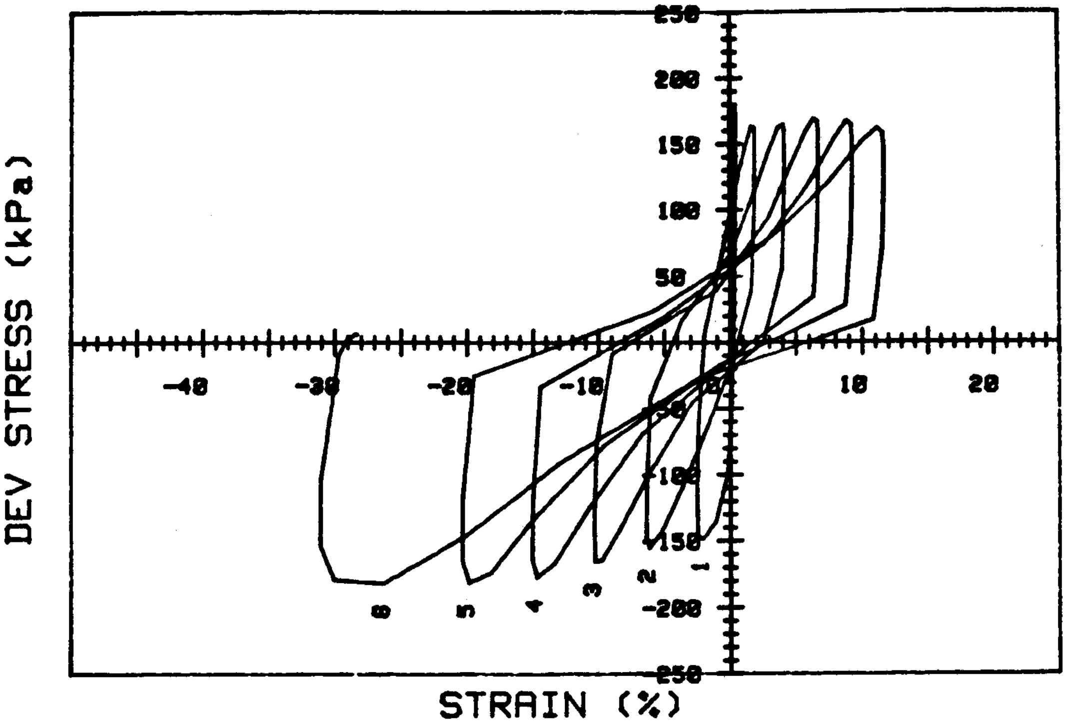

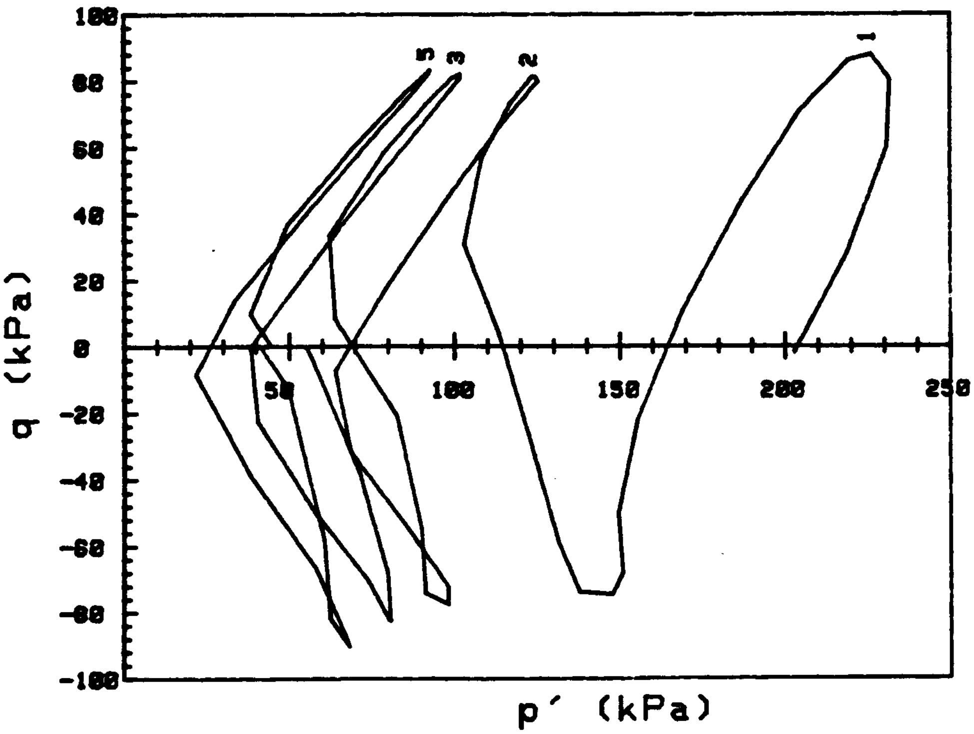

CRUISE DC1-81-EG		INCREMENT (cm)	54-60
CORE NO.	605G2	TEST NO.	TC93
SIG1c′(kPa)	204.8	STATIC qf (kPa)	163.8
SIG3c′(kPa)	204.8	AVG MAX q (kPa)	83.3 (50.9%)
INDUCED OCR	1.0	AVG MIN q (kPa)	-84.1 (51.3%)

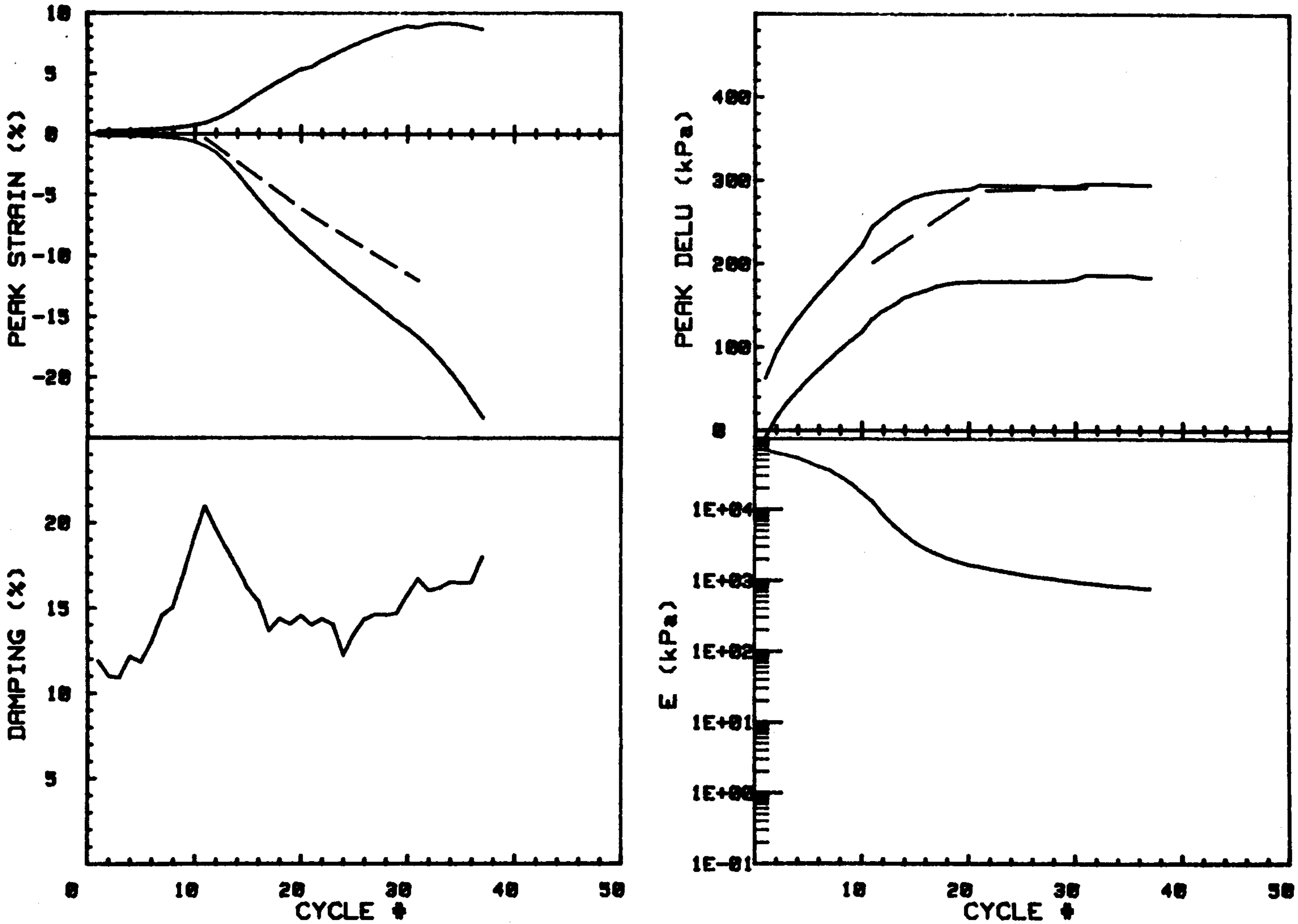

CRUISE DC1-81-EG		INCREMENT (cm)	130-137
CORE NO.	604G3	TEST NO.	TC99
SIG1c'(kPa)	297.1	STATIC qf (kPa)	176.6
SIG3c'(kPa)	297.1	AVG MAX q (kPa)	61.5 (34.8%)
INDUCED OCR	1.0	AVG MIN q (kPa)	-56.2 (31.8%)

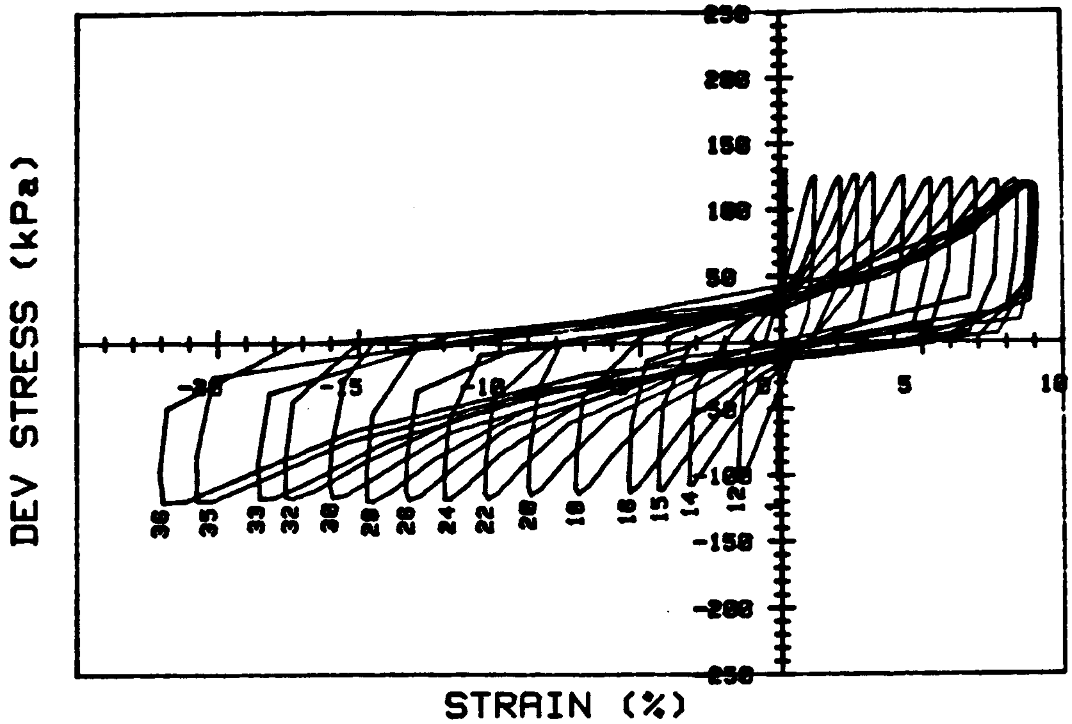

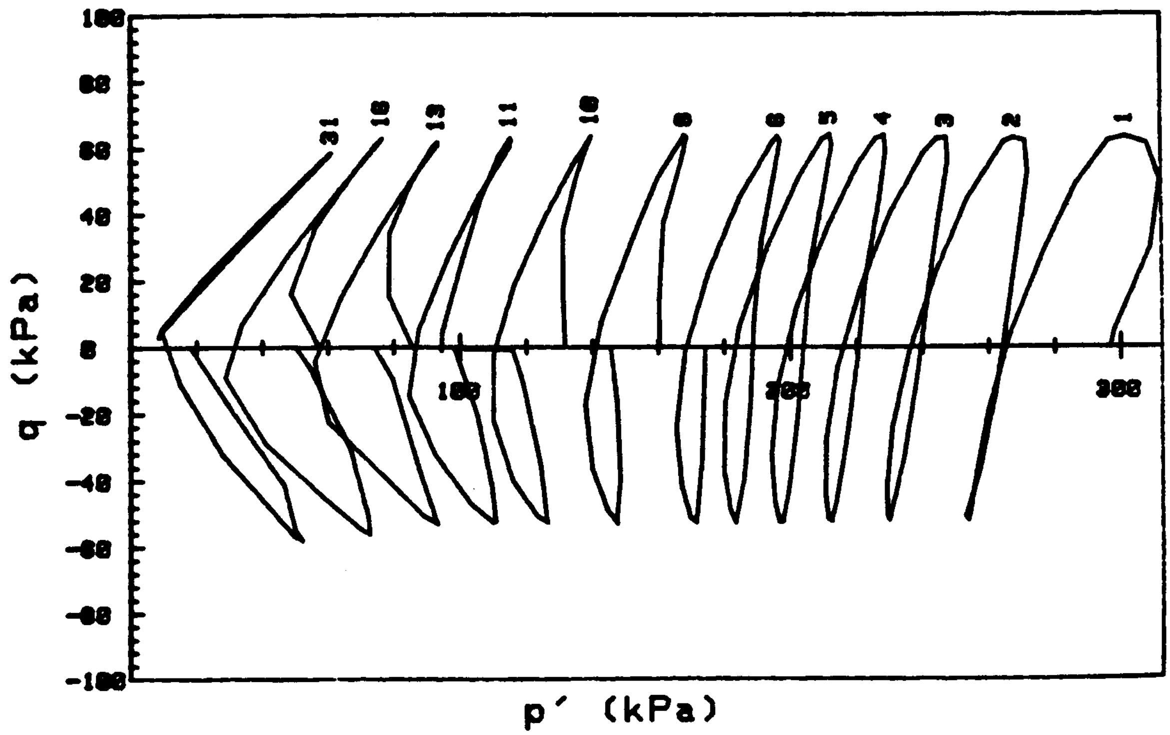

CRUISE DC1-81-EG		INCREMENT (cm)	130-137
CORE NO.	604G3	TEST NO.	TC99
SIG1c′(kPa)	297.1	STATIC qf (kPa)	176.6
SIG3c′(kPa)	297.1	AVG MAX q (kPa)	61.5 (34.8%)
INDUCED OCR	1.0	AVG MIN q (kPa)	-56.2 (31.8%)

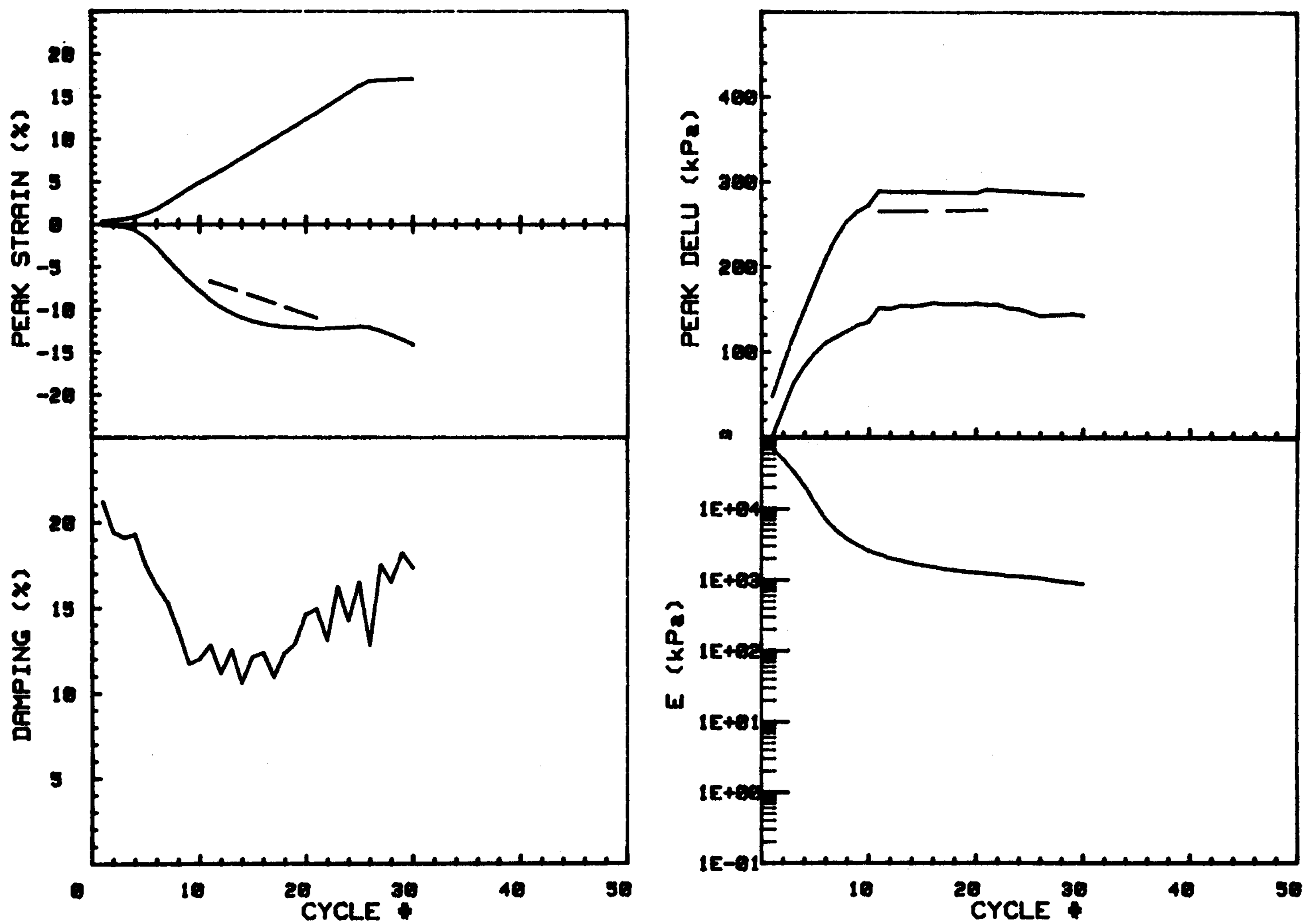

CRUISE DC1-81-EG		INCREMENT (cm)	130-137
CORE NO.	604G3	TEST NO.	D102
SIG1c'(kPa)	290.4	STATIC qf (kPa)	176.6
SIG3c'(kPa)	290.4	AVG MAX q (kPa)	86.5 (49.0%)
INDUCED OCR	1.0	AVG MIN q (kPa)	-68.0 (38.5%)

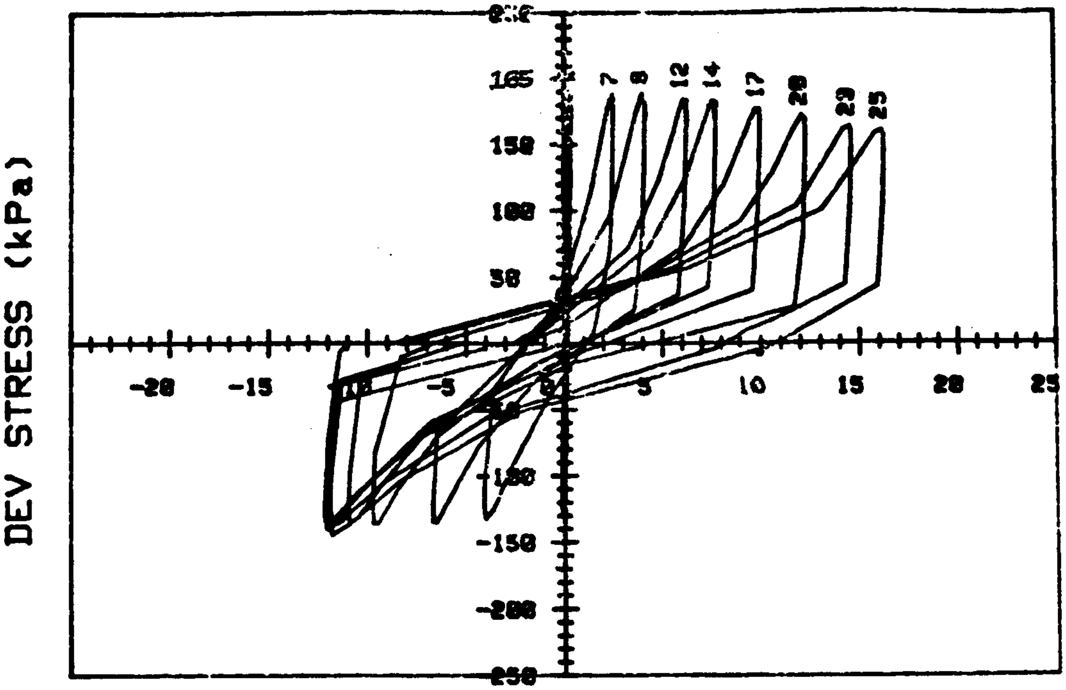

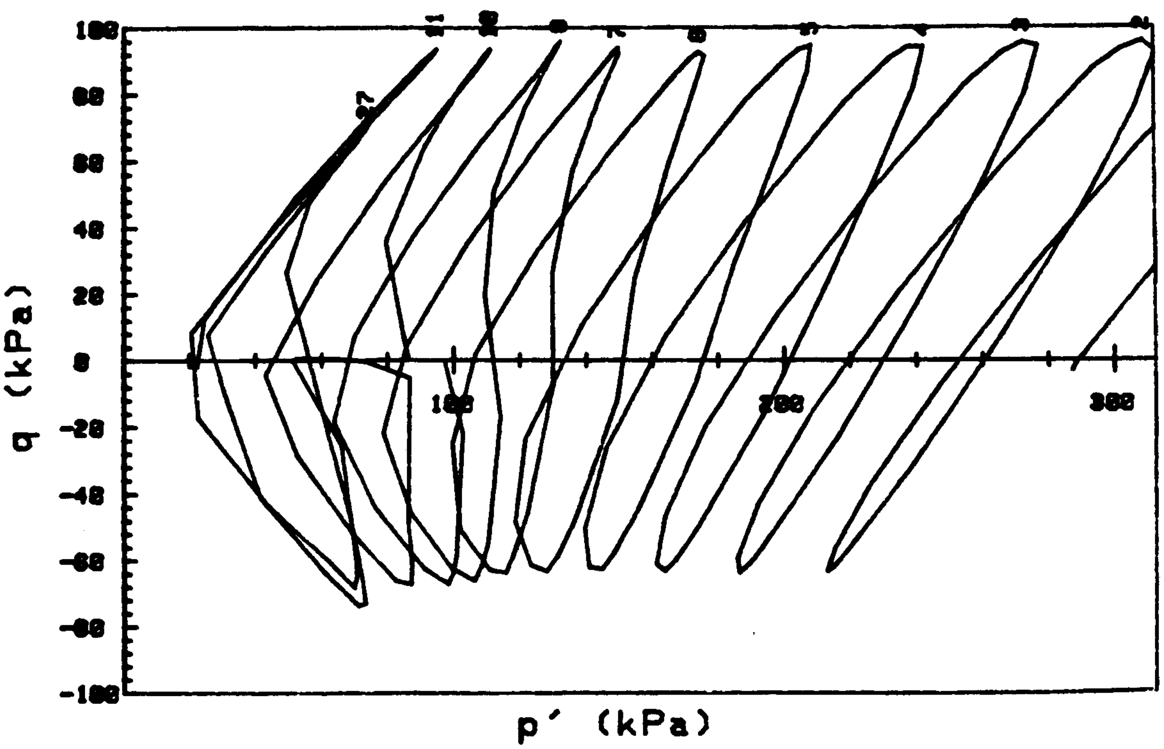

CRUISE DC1-81-EG		INCREMENT (cm)	130-137
CORE NO.	604G3	TEST NO.	D102
SIG1c′(kPa)	290.4	STATIC qf (kPa)	176.6
SIG3c′(kPa)	290.4	AVG MAX q (kPa)	86.5 (49.0%)
INDUCED OCR	1.0	AVG MIN q (kPa)	-68.0 (38.5%)